CURRENT EVENTS IN HYDRAULIC ENGINEERING

Editors:
Jerzy M. Sawicki
Piotr Zima

Gdańsk 2011

PRZEWODNICZĄCY KOMITETU REDAKCYJNEGO
WYDAWNICTWA POLITECHNIKI GDAŃSKIEJ
Romuald Szymkiewicz

REDAKTOR PUBLIKACJI NAUKOWYCH
Janusz T. Cieśliński

RECENZENCI
Romuald Szymkiewicz
Marek Mitosek

PROJEKT OKŁADKI
Miriam Artichowicz

Wydano za zgodą
Rektora Politechniki Gdańskiej

Oferta wydawnicza Politechniki Gdańskiej jest dostępna pod adresem
http://www.pg.gda.pl/WydawnictwoPG

ISBN 978–83–7348–375–0

WYDAWNICTWO POLITECHNIKI GDAŃSKIEJ

Wydanie I. Ark. wyd. 19,2, ark. druku 18,75, 104/668

Druk i oprawa: *EXPOL* P. Rybiński, J. Dąbek, Sp. Jawna
ul. Brzeska 4, 87-800 Włocławek, tel. 54 232 37 23

CONTENTS

1 Drainage and Infiltration Resistance of Rivers – Element of Interaction Between Surface – and Groundwater

Dana Baroková, Andrej Šoltész (Slovak University of Technology in Bratislava, Faculty of Civil Engineering)

1.1. Introduction

Properly defined interaction between surface water and groundwater is a complicated process which requires the use of hydrodynamic and water-balance equations. Study of the interaction between surface water and groundwater is of great importance in both theoretical and applied investigations. Quantitative assessment of the interaction can be performed using Cauchy-type boundary conditions with different resistances for discharge or recharge. Cauchy boundary condition is needed to properly represent surface waters alternatively losing water through the bottom (high resistance) or gaining water mostly near the water surface (low resistance). Groundwater simulation package TRIWACO [2, 7, 11] is a program which enables the representation of a Cauchy-type boundary condition with different resistances for discharge or recharge conditions presented in the paper.

1.2. Materials and Methods

The problem of the resistance of river bottom sediment layer (drainage and infiltration resistance) is closely connected with the interaction of surface- and groundwater as well through a clogging river bed. Generally, the drainage or infiltration resistance of the river bed is dependent on hydraulic conductivity and the thickness of clogged layer. It is very complicated to determine the hydraulic conductivity and the thickness of the clogged layer separately [5, 7]. Mostly, the bottom layer resistance is a model parameter used as an estimative one. It is determined by calibration process.

Many natural processes and human activities are influenced by interaction of surface- and groundwater interaction [9]. For better understanding of interaction processes between surface- and groundwater [3, 4] it is necessary to know the relation between the water level in the river and groundwater level. Infiltration (percolation of surface water into groundwater) or drainage (water flow from the aquifer into the river) is given by hydraulic gradient between the surface and groundwater. Distribution of river bed sediment permeability and thickness of sediment material is called clogging of the river bed [10], i.e. clogging means a certain degree of reduction of the water flow through the river bottom.

The problem of the interaction between the surface- and groundwater flow is solvable only when boundary conditions as well as initial conditions (unsteady flow) are given. Three types of boundary conditions can in such a case appear (Fig. 1) [2, 7]:

— Dirichlet (stable) boundary condition. It determines on the part of the boundary Γ_1 directly the value of the searched function (piezometric head) h

$$h = h_0(x, y) \quad \text{on} \quad \Gamma_1 \tag{1}$$

— Neumann (unstable) boundary condition. It determines on part of the boundary Γ_2 the derivation of the searched function in the direction of the external normal $\boldsymbol{n}(n_x, n_y)$

$$\boldsymbol{n}\left(\boldsymbol{k}\nabla_{xy}h\right) + q_0(x, y) = 0 \quad \text{on} \quad \Gamma_2, \tag{2}$$

where q_0 is a specific discharge through defined part of the boundary. If the solved region Γ is anisotropic and anisotropy axes are parallel to coordinate axes, the condition can be written as

$$k_x \frac{\partial h}{\partial x} n_x + k_y \frac{\partial h}{\partial y} n_y + q_0(x, y) = 0, \tag{3}$$

where n_x and n_y are directional cosines to external normal line to the boundary part Γ_2.

— Cauchy (combined) boundary condition. It determines on part of the boundary Γ_3 the derivation of the searched function (piezometric head) depending on its value

$$\boldsymbol{n}\left(\boldsymbol{k}\nabla_{xy}h\right) = \alpha\left(h - h_0\right) \quad \text{on} \quad \Gamma_3, \tag{4}$$

where $\alpha = k_0/b_0$ is the characteristics of the clogged layer, i.e. the ratio called by [5] as induced bank infiltration, k_0 is the permeability of the clogged layer on the river bed bottom ($m \cdot s^{-1}$) and b_0 is the thickness of the clogged layer on the river bed bottom (m). The reciprocal value of parameter α can be determined as the resistance of the layer $c_r = 1/\alpha$.

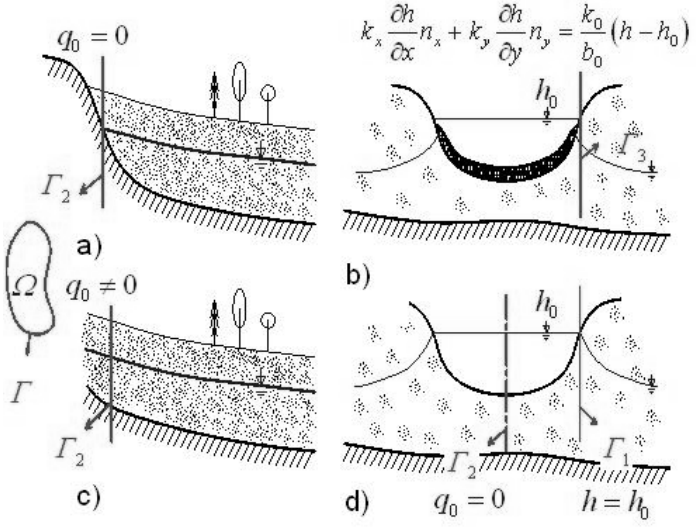

Fig. 1. Examples of boundary conditions [2, 7] on Γ_i, i = 1, 2, 3: a) Neumann condition (homogeneous), b) Cauchy condition, c) Neumann condition (non-homogeneous), d) Dirichlet condition

1.2.1. Modelling and Practical Solution of the Interaction

Rivers and drainage channels are linear sources generally located in the upper aquifer. Putting them into a numerical groundwater modelling system mostly they are substituted by sink/source nodal points defining the water level course. Similarly as in previous text was mentioned the recharge into the river can be defined in two ways:

— by means of water level in the river and the water flow will be calculated,
— water flow (infiltration, drainage) is given and subsequently the water level (piezometric head) in river nodes will be calculated.

For each river node the inflow value is calculated according to the relation:

$$Q_r = A_r \frac{(h_r - h)}{c_r}, \tag{5}$$

Where: Q_r – is infiltration from (drainage to) river node of the mesh ($m^3 s^{-1}$),
A_r – area belonging to the river node (m^2) given by conjunction of the wetted perimeter and relevant length between two river nodes.
h – groundwater level (*m a.s.l.*) (unknown value –calculated using modelling),
h_r – water level in the surface flow (*m a.s.l.*),
c_r – infiltration ($c_r = CI$) or drainage (($c_r = CD$) resistance of the river bed bottom is determined in (*s*) or in (day).

Values of the resistance c_r differ in the nature depending on the relation between the surface water level and groundwater level. In case of infiltration $h_r > h$ and for the drainage $h_r < h$. Numerical models mostly offer the possibility to define different values of the resistance for infiltration and drainage processes (CI and CD). Determination of river bed (channel) bottom resistance is the matter of model calibration. Investigation of k_0 and b_0 parameters separately [5] is very complicated. There are no relevant river bed resistance values in the available literature recommended for the modelling purposes. The drainage resistance values $c_r = b_0/k_0$ can be determined from the following diagram (Fig. 2) and is mostly given in days.

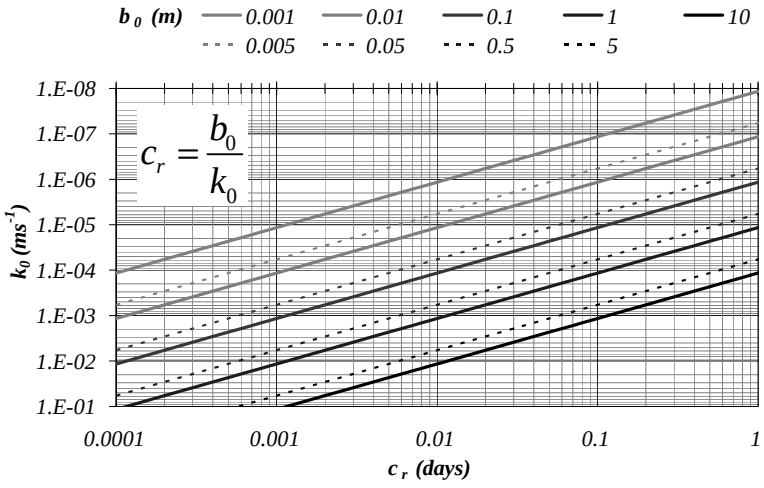

Fig. 2. Diagram for determination of the drainage resistance value for permeability k_0 in ms^{-1} and thickness b_0 in *m* [2]

1.3. Results and Discussion

The groundwater modelling system TRIWACO [11] has been used for solving interaction processes of surface- and groundwater flow according to the proposed methodology. The chosen territory for the modelling research was a locality where a water structure with a small hydropower plant is assumed to be built in the vicinity of the Hron River – the tributary river of the Danube River (Fig. 3).

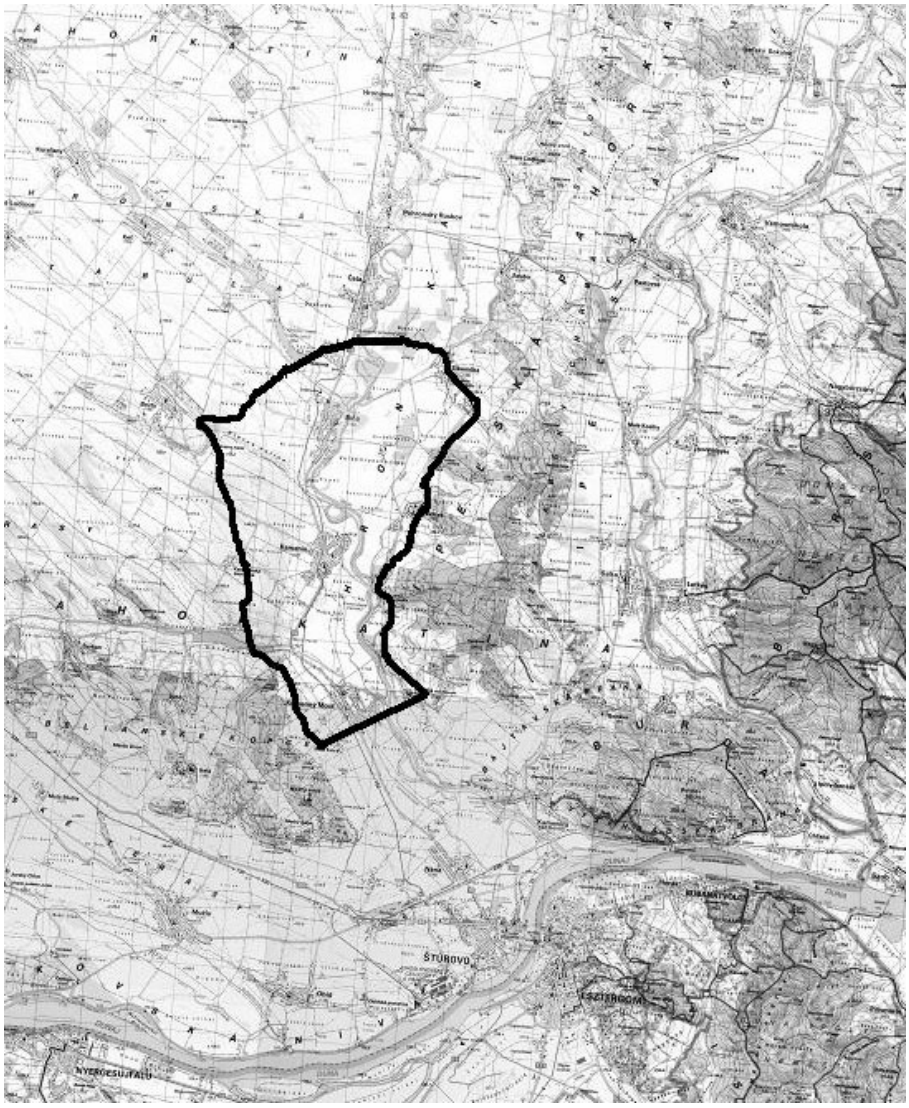

Fig. 3. Location of interest with the definition of the boundaries [1]

All necessary hydrologic, hydro-geological and morphological data were available for definition of a solved locality. Missing data have been accomplished by geodetic measurements. As boundary conditions the surface water levels in the Hron River as well as water levels in adjacent boreholes of Slovak hydro-meteorological institute have been taken into account, i.e. Dirichlet boundary condition has been used for the groundwater numerical modelling.

2-D numerical modelling by means of finite element method has been used for determination of the groundwater level course in steady as well as unsteady conditions. Piezometric head contour map in Fig.4 is one of the output results of the groundwater level numerical modelling. The groundwater modelling process was supplemented by simulation for several CD and CI values. The CD (CI) values were changing from 0.02 d, 0.2 d, 2d and 20 days. The general finding was that if the CD or CI value was higher the groundwater level changes were smaller and slower.

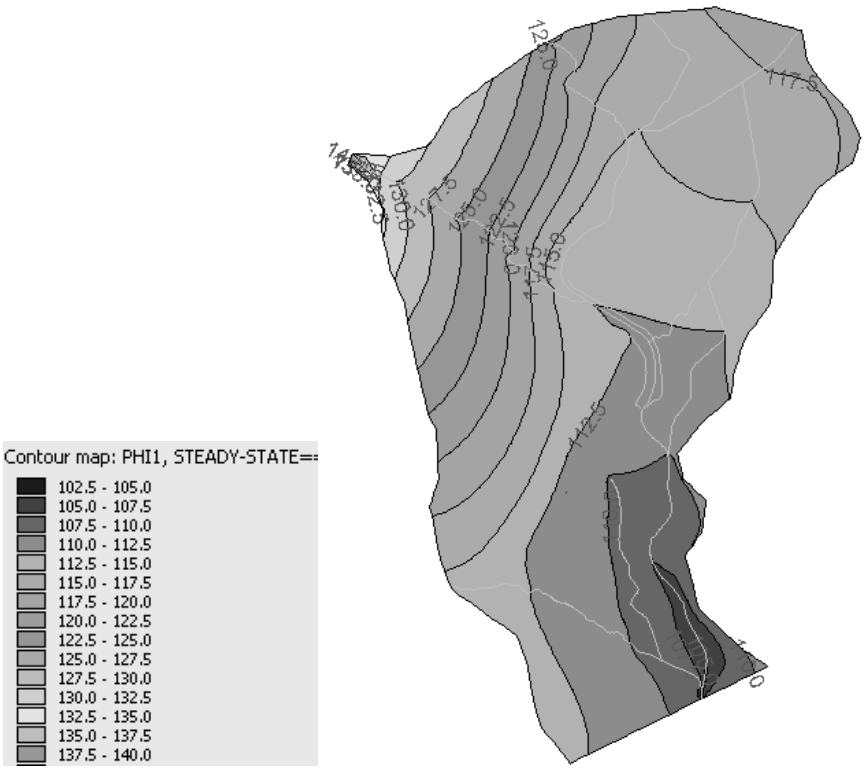

Fig. 4. Piezometric head isolines course – TRIWACO modelling system output [1]

On base of given outputs the modelling process has been précised for a particular chronological interval from March 2005 to June 2005. For this time period consequent calibration has been performed for more precise comparison of modelled and measured groundwater level values. Results of such a calibration are illustrated in the Fig. 5.

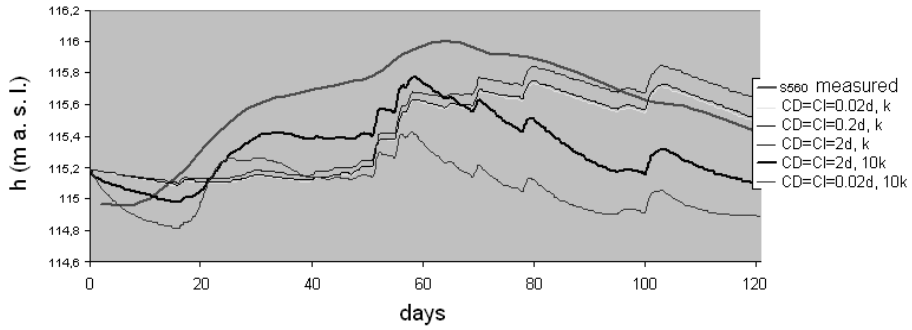

Fig. 5. Comparison of measured and modelled groundwater level in the borehole 560

1.4. Conclusion

An enhanced numerical modelling of surface- and groundwater interaction has been analysed for illustration of the influence of the river bed bottom resistance on groundwater level course. The proposed numerical analysis compared with measured groundwater level data is a good basis for obtaining an overview about the problem of clogged layer in the bottom of the river bed. For more precise investigation a coupling of detailed laboratory research [6, 10] and numerical modelling would be the correct direction of the future research.

References

[1] Andrássy T.: Influence of the river bed resistance on groundwater regime. Diploma thesis, SVF-5378-26922, STU in Bratislava, Faculty of Civil Engineering, 49, 2010.

[2] Baroková D.: Determination of influence of the water structure on groundwater level regime and possibilities of its control. Edition of scientific papers, No. 33, ISBN80-227-2367-3. STU Bratislava, 152, 2006.

[3] Burger F.: Characteristics of the groundwater in the riverine area at flood water level of the Danube and Váh River. Acta Hydrologica Slovaca, Vol.11, No. 2, ISSN 1335-6291, 234–245, 2010.

[4] Gomboš M., Pavelková D.: Estimation and planar presentation of forecasted changes of soil water storage by the climate changes. Növénytermelés, ISSN 0546-8191, 353–356, 2011.

[5] Mucha I., Šestakov V.: Groundwater hydraulics. Bratislava: Alfa 1987, 342.

[6] Pařílková J., Ševčík R.: The physical substance of the method of electrical impedance spectrometry. Proc. of EUREKA 2010 Conference, Brno University of Technology, 23–43, 2010.

[7] Šlezingr M., Synková J., Foltýnová L., Uhmanová H.: Possibility of Utilization Directing Structures in River Revitalization, Slovak Journal of Civil Engineering. - ISSN 1210-3896. - Vol. 18, No. 3, 33–36, 2010.

[8] Šoltész A., Baroková D.: Hydrodynamics of groundwater flow. Life-long learning course in Civil Engineering, ISBN 80-227-2558-7, 162, 2006.

[9] Veličković B.: Colmation as one of the process in interaction between the ground water and surface water, FACTA UNIVERSITATIS, Series: Architecture and Civil Engineering, Vol. 3, No. 2, 165–172, 2005.

[10] Velísková Y., Dulovičová R.: Variability of bed sediments in channel network of Rye Island (Slovakia), Proc. of XXIV Conference of the Danubian Countries. IOP Conference Series: Earth and Environmental Science, Vol. 4, IOP Publishing 012044, 1–7, 2008.
[11] http://www.triwaco.com/

Acknowledgements

This paper was supported by the Grant agency VEGA under contract No.1/0894/10.

2 Safety of Hydraulic Structures Affected by Natural Environment

Emília Bednárová, Danka Grambličková, Marian Minárik (Slovak University of Technology in Bratislava, Faculty of Civil Engineering)

2.1. Introduction

Safety and reliability of hydraulic structures is in considerable manner dependent on factors of natural environment as hydrological, hydrogeological, geological, geotechnical, climatic conditions, etc. Because these factors create input data of hydraulic structures design, their reliability is extraordinary important. Moreover, during operation of hydraulic structures these factors can be more or less changed. For example in geological environment in the subsoil of flood dikes can occur after long term operation changes in structure caused by hidden piping. In dam's subsoil such changes of natural environment also cannot be excluded. These aspects can be in the design stage considered by variability in input data, which can be suitably applied in numerical modelling of given task. Monitoring has important position by solving safety of hydraulic structures during operation. Its part is also special methods of measurements as for example geophysical measurements of filtration velocities in the boreholes. Statistical methods of processing of the measured data can by also suitably applied. In this paper are presented some lessons learned and experiences gained from reviewing safety of the hydraulic structures.

2.2. Utilising Numerical Methods by Optimisation of the Treatment on the Flood Dyke Under HPP Gabčíkovo

Changes in hydrological conditions (Q_{100}, water level in tailrace channel and duration of flood discharge) invoked necessity of reviewing the filtration stability and construction stability of existing left bank flood dyke. Dyke is 8.1 km long and approximately 3 – 4 m high. It is constructed from local materials – silty gravels or gravels with additions of fine particles. Inclination of dyke's slopes range from 1:2 to 1:7 near downstream toe. Besides quality of dyke itself and duration of food discharges safety of dyke is affected by geological composition of subsoil and morphology. The subsoil of dyke is composed of gravel materials with various percentages of sand fractions. Generally, on the surface are situated lowly permeable silty soils with variable thickness. In some sections of dyke were in surface layers recorded silty sands, locally the gravel soils ascend to the ground surface. Morphology of scoped region – altitude of terrain near downstream toe of dyke varies from 114 m a.s.l. to 116.5 m a.s.l. (Fig.1).

In recent years were during flood discharges in river Danube observed several risk factors which threatened its safety as outflows on the downstream toe, local outflows in adjacent area, loading of the overburden by uplift and planar wetting of the downstream

toe of the slope. Danube gravels are also susceptible to piping. Therefore it was necessary to design appropriate treatment.

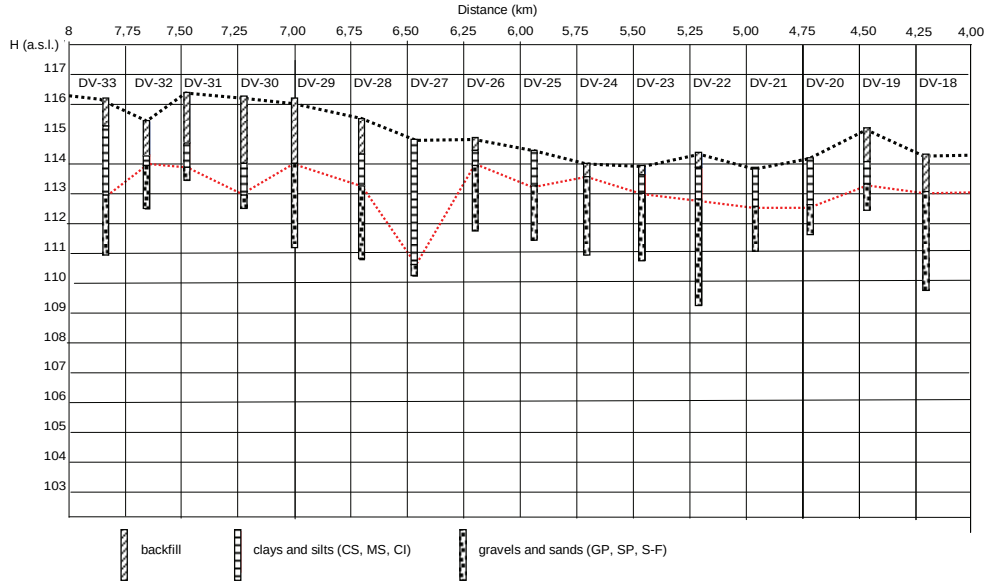

Fig. 1. Variability of subsoil geology and morphology in km 4 – 8 of flood dyke

Due to good experiences gained from realization treatment on left bank flood dyke below Sap it was decided to design equal measures. Sealing of upstream slope with PVC foil with protective backfill was designed for elimination seepages through the body of dyke and suspended cut-off wall (COW) for reduction loading of subsoil by seeping water (Fig. 2).

Fig. 2. Realization of the sealing of the upstream slope of flood dyke (Photo: Sabo J.)

Estimation of the optimal depth of COW and necessity of additional treatment on the toe of flood dyke slope was investigated. The optimal depth of COW was due to wide variability of input parameters estimated by parametric study. In this parametric study, it was necessary to regard assorted morphology along downstream toe of dyke, variable geological composition of subsoil, expected anisotropy of gravels in its subsoil, variable composition and thickness of overburden and various depth of cut-off wall. Natural environment variability and various depth of COW which were used for optimization of treatment are documented on Fig. 3. Finite element method (FEM) was applied for analysing flow through the body and subsoil of dyke; software SEFTRANS, where it is possible to simulate transient flow tasks.

Estimating of hydraulic criteria, e.g. critical values of hydraulic gradients in the subsoil of dyke was necessary for elimination of piping. Respecting theoretical knowledge and lessons learned from designing treatment on Danube, Moravia and Latorica flood dykes were on flood dykes of HPP Gabčíkovo applied criteria graded by depth. In the region of foundation base were adopted the most strict criteria of Istomina and Hálek, i_{crit} = 0.2. In the depth around bottom ending of COW (10 m under terrain) where can be expected short term concentration of filtration flow with increased values of hydraulic gradients were adopted moderate criteria of Busch, Luckner, etc. – i_{crit} = 0.75.

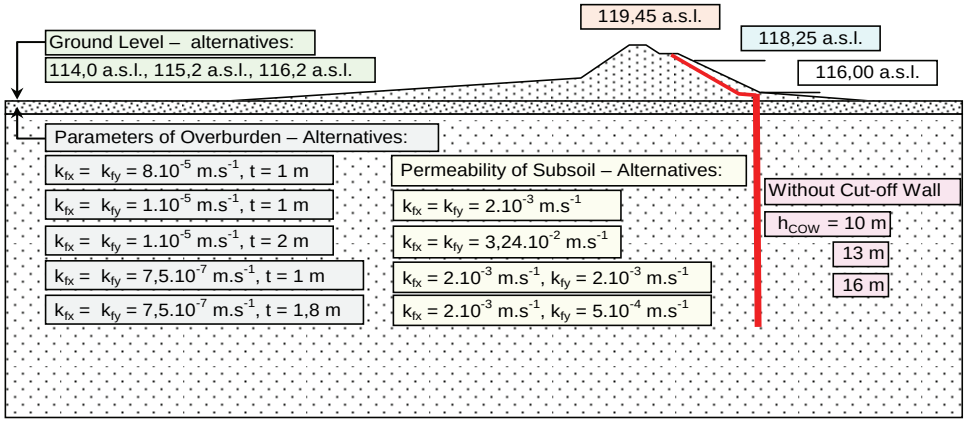

Fig. 3. Natural environment variability of the flood dyke of tailrace channel of HPP Gabčíkovo

Suspended COW is needful for prevention of the risk factors in the subsoil. By optimal prolongation of seepage path can be eliminated occurrence of outflows on the downstream toe of flood dyke, minimized wetting of adjacent area along downstream toe of the dyke, partially reduced uplifts on overburden, excluded risk of origin of the internal erosion of gravel materials in the subsoil of dyke, concentrated maximal intensity of filtration flow in the subsoil to the deeper parts under bottom ending of COW and partially reduced seepages through the subsoil of a dyke.

From the calculation executed as parametric study resulted depth of COW 13 m. Its efficiency is sufficient in section of flood dyke which is equipped with lightening drainage system. In section where was not constructed lightening drainage system it was essential to confirm or disconfirm necessity of supplement treatment for elimination risk of the breakage of the overburden. From the analysis results, that to eliminate risks of breakage of

the overburden is in some sections of flood dyke besides designed treatment (sealing of upstream slope of flood dyke with PVC foil and COW in the subsoil of dyke) necessary additional treatment. Stabilizing backfills on the toe of downstream slopes of flood dyke were designed in these sections

2.3. Geophysical Measurements of Filtration Velocities on Dams

Use of special measurements of filtration velocities in observation objects has its substantiation. Measurement of water levels, uplifts, seepages or pore water pressures may not be for detecting real filtration flow regime sufficient. As an example can be mentioned reviewing filtration stability of soils and joints in rock mass. Common monitoring cannot sufficiently solve this task, it is necessary to identify intensity of underground and seeping water flow in observed area. By systematic measurements of filtration velocities on dams we obtain knowledge on trends of development. From the trends of development of average and maximal values it is possible to estimate if the filtration flow is consolidated or there is a rising trend signalling risk of the occurrence of piping. As an example can be mentioned dam Klenovec (Fig. 4), where was through the medium of measurements of filtration velocities detected these risks in the left abutment. After retightening of grouting curtain intensity of filtration flow decreased (Fig. 5).

Fig. 4. Dam Klenovec (Photo: Panenka P.)

Good explanatory ability provides distribution functions of filtration velocities. Through the medium of them it is possible to estimate medians of filtration velocities, probability of occurrence of average filtration velocities, eventually review risk of exceeding critical velocities and trends in filtration flow development. In Fig. 6 are presented distribution functions of filtration velocities on dam Veľká Domaša (Fig. 7). It is evident, that here the filtration regime is consolidated.

Geophysical measurement of filtration velocities in boreholes is suitable method for clarification anomalies in water level regime on water structures. As an example can be mentioned dam Rozgrund (Fig. 8).

Dam Rozgrund, constructed in 1744, belongs to a water management system of a historic value. In the boreholes inbuilt to the body of dam from the dam's crest were recorded sudden changes in water levels, signalising existence of preferred seepage paths. To find reasons for the mentioned anomalies geophysical measurements of filtration velocities were performed by an artificial increase of the water levels (Fig. 9). High

filtration velocities in the depths approximately from 2.5 to 5 m under terrain confirmed existence of permeable horizon.

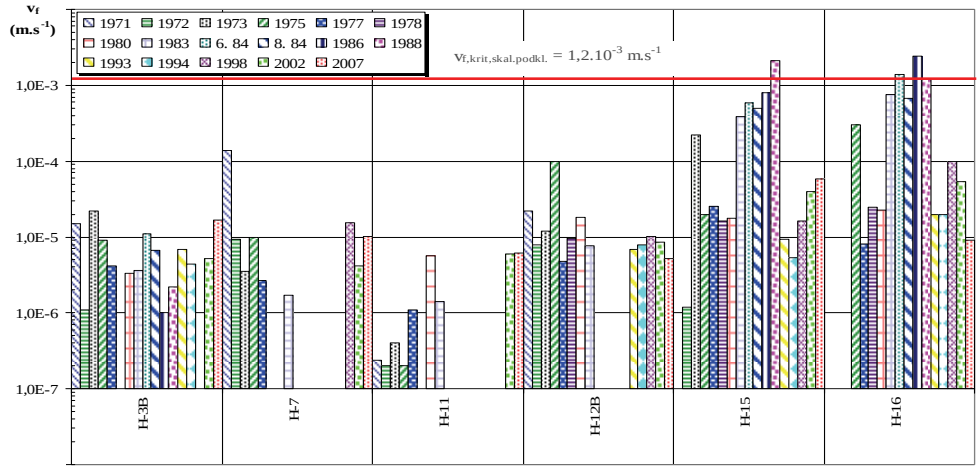

Fig. 5. Development of maximal filtration velocities in the rock subsoil of dam Klenovec

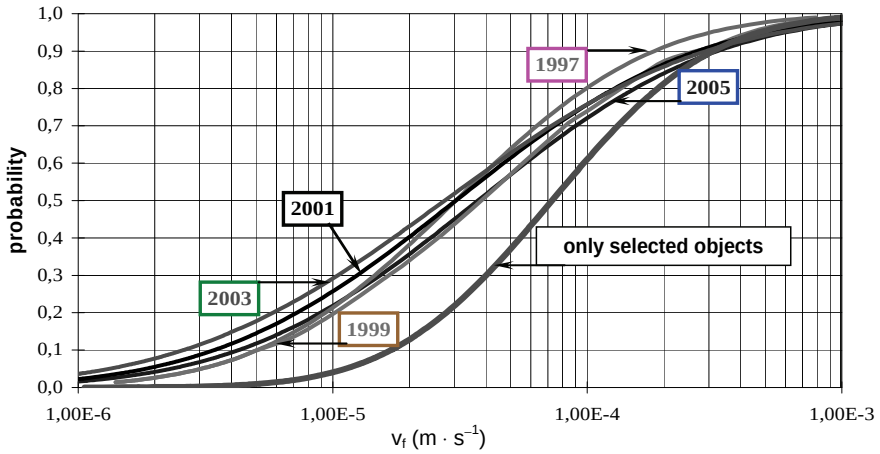

Fig. 6. Development of the distribution functions of filtration velocities under dam Veľká Domaša

Measurements directly inside the grouting curtain represent another example of the utilizing of special measurements of the filtration velocities. Their goal is to observe regime of filtration flow in grouted subsoil of dam and consequently review permeability of grouting curtain. Measurements are usually performed by open and closed uplift boreholes. Better results are obtained from closed boreholes. Presence of permeable horizons in grouting curtain can be estimated from trend of the vertical flow of water in the borehole and corresponding filtration velocities.

Fig. 7. Dam Veľká Domaša (Photo: Uhorščák Ľ.)

Fig. 8. Dam Rozgrund during reconstruction of bottom outlet (Photo: Bednárová E.)

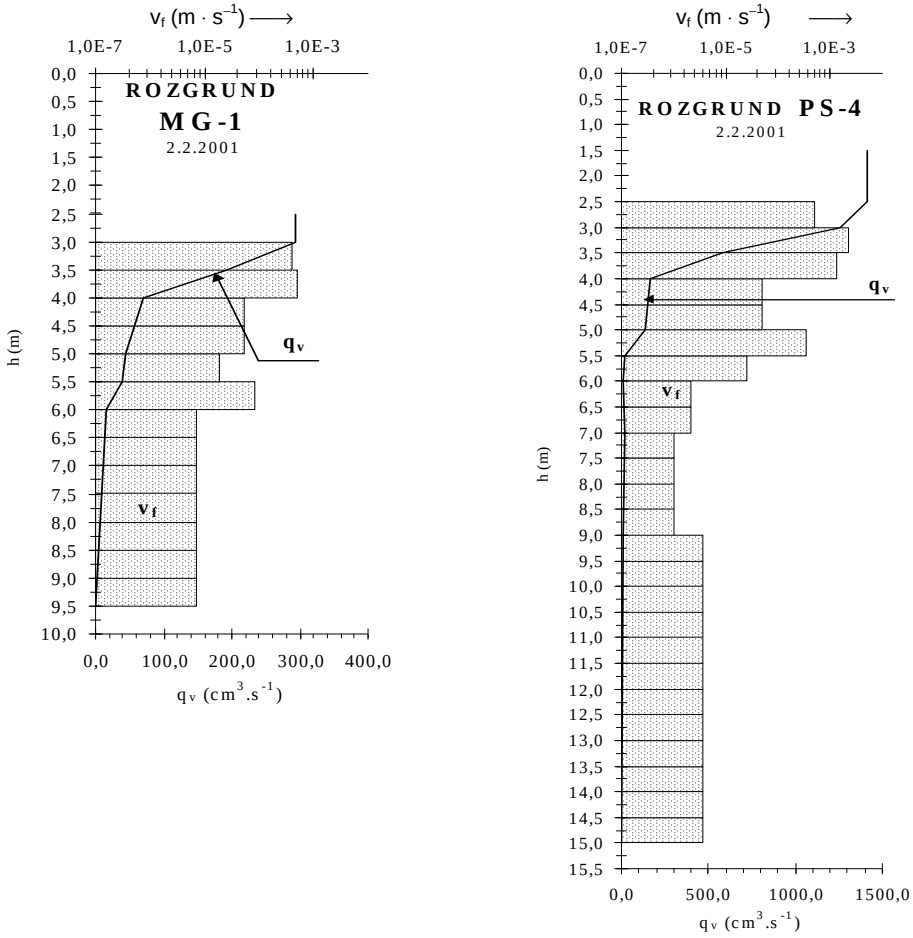

Fig. 9. Application of geophysical measurements of filtration velocities by detecting the occurrence of preferred seepage paths in the body of the dam Rozgrund

2.4. Application of Statistic by Reviewing the Safety of Starina Dam

Existence of seepages in the abutments can be confirmed or disconfirmed by in situ measurements of water levels, uplifts and in some places also seepages. In some cases such review is not possible, because e.g. boreholes on the downstream side show nought values, drainage system does not distinguish water from slope etc. Therefore, when analyzing such problems any method that will help to clarify them is suitable (seepages through the abutments). Above mentioned problem is characteristic for hydraulic structure Starina (Fig. 10). Construction of the Starina dam was completed in 1987. It is a 50 m high earth-fill heterogeneous dam with internal silt sealing. Morphology of the territory and the occurrence of tectonic failures in the subsoil predestine seepages to the left abutment of the dam (Fig. 11).

Fig. 10. Dam Starina (Photo: Uhorščák, Ľ.)

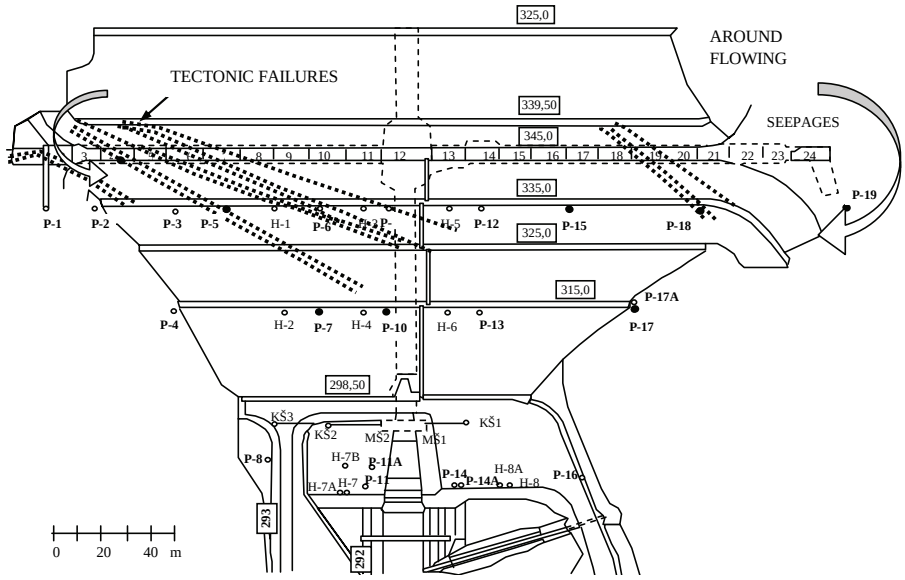

Fig. 11. Dam Starina – situation of monitoring objects

After first impoundment of reservoir were in the boreholes situated on the left side of dam recorded high increases of water levels from 7 to 15 m. Because during construction of dam were in this region discovered springs, it was not clear if the increases are caused by them or by the water flowing from reservoir through the abutment. Large dataset of in situ measurements was processed for clarification of these anomalies. These effects can be specified by means of analysis of correlation coefficients between water levels in boreholes and the water level in the reservoir. In the boreholes situated in the left abutment the correlation relations were significant (Fig. 12 – P19). In boreholes situated in the right abutment were correlation coefficients minor. Therefore it is possible to mention that in the region of the left abutment the water is flowing around the dam. But the measurements of filtration velocities are not signalling risk of failures in filtration stability. Trend in development of water levels and seepages is here consolidated. In the region of the right abutment is flowing of water around the dam improbable. The presented example demonstrates that results of a statistical assessment have important position in water structure surveillance.

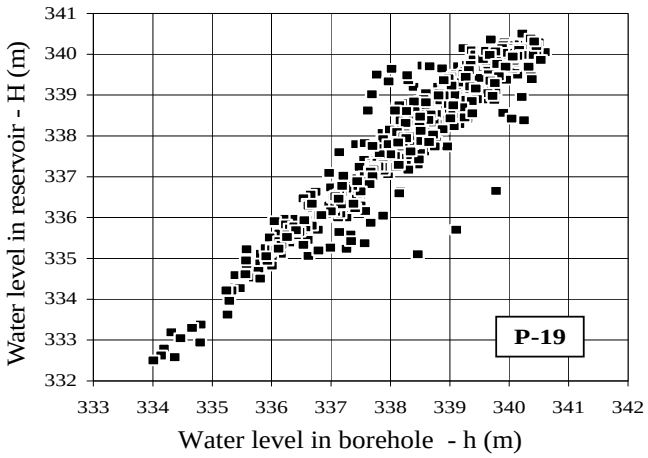

Fig. 12. Correlation relations between water level in borehole and water level in reservoir

2.5. Conclusion

Hydraulic structures – dams, polders, flood dykes are for human society irreplaceable. More than 7000 year history of their construction confirms their importance. Nowadays, the global warming and extremes of weather is very topical. In this context can be expected increased importance of these structures in the future. During the drought reservoirs may create storage of water for drinking, industry, agriculture purposes and so on. During flood period are reservoirs, polders and flood dykes often critical technical measures, without which the consequences of floods will be disastrous. Besides these positive effects of water works for the society it is extremely important to maintain their safety and reliability of operation. Therefore, any methodology that can reduce the risk of breakdown or accident – from the traditional in situ measurements, via special geophysical measurements, using numerical and statistical methods – should be taken positively. Some lessons learned and experiences gained from application of these methods in Slovakia demonstrate it.

References

[1] Bednárová E., Minárik M.: The role of measurements of flow velocities by evaluation the safety of dams. In: 14. German Dam Symposium, Freising near Munich, Germany 2007, 21–27.

[2] Bednárová E., Minárik M., Grambličková D., Marikovičová A.: Using of geophysics and statistics by monitoring of dams. In.: 76th Annual Meeting of ICOLD, Symposium Operation, Rehabilitation and U–P Grading of Dams, Session II, rap. 2–46, 9.

Acknowledgements

This paper was supported by grant project VEGA No. 1/0704/09.

3 Fajerov Mlin SHPP on the Glina River, Croatia

Boris Beraković, Eva Ocvirk (University of Zagreb, Faculty of Civil Engineering, Croatia)

3.1. Introduction

3.1.1. Harnessing Water Power and Energy – an Overview

In ancient times, man had only used power and energy of his mussels. Gradually, he developed tools and devices to facilitate use of the than only available form of energy. The man started using animals and their power and energy for carrying out necessary and useful work. The need for power and energy was growing on a daily basis, so the man tried to find ways to use energy available from the nature. The next step was a discovery that it is possible to harness power and energy of wind and water. Energy available from nature (primary energy) is usually not suitable for use in its natural form, so it is transformed (energy conversion) into a useful form of energy (e.g. mechanical energy), which is used directly. Wind energy was used for navigation but also to drive wind mills, and water energy to run water mills – wind and water energy being converted into the mechanical energy. Mills have been used since the Roman times to turn mill stones and grind grains. All tools and facilities, including the mills, improved with time. A particularly intensive development happened in 19^{th} century with creation of waterwheels and turbines for harnessing larger powers and energy of water streams. The water energy is also used to operate sawmills, blacksmith shops and textile mills. The mills were built along the water streams, particularly on their steeper stretches and in points of higher heads. In Croatian karst, the mills are located by springs and sink holes. The mills were also built on larger rivers to harness water motion energy (kinetic energy) only. Once alternative current was adopted as one of significant forms of primary energy conversion into a useful energy form, the door was open to a considerable exploitation of available water wave power and energy. Twentieth century is characterized by development of large turbines and construction of hydroelectric power plants for production of electric energy. Such development gradually resulted in phasing out of direct water use for driving of mills, sawmills, blacksmiths' and textile mills and its replacement with electricity. Today, water stream power and energy is used almost exclusively in production of electricity, while other forms of water use disappeared for practical reasons. A small number of mills remaining in Croatia are mostly used in tourism and as protected cultural heritage, many have became derelict, and some left no trace of their existence.

The below photographs are from [1].

Fig. 1. Kocijanova vodenica mill near Varaždin from 1961 (Living by the Drava –Past and Present, Varaždin 2004, p. 45)

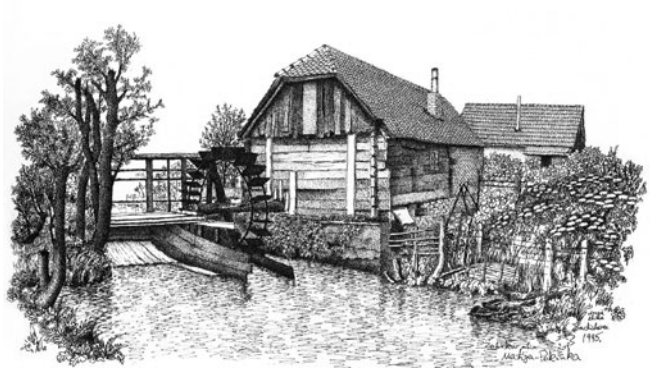

Fig. 2. Žabekova vodenica mill (undershot wheel) in Ladislavec near Zlatar (M. Pokrivka, Croatian Mills, Zagreb 2004, p. 129)

Fig. 3. Watermill in Torčec under reconstruction, 2007 (photo: Ivan Zvijerac)

3.1.2. History of Mills In Croatia

The mills have played an important role in the Croatian economy. They developed during the industrial age (18–20th century), but watermills had already been built on the European brooks and rivers since 12th century. Croatia had between three and five thousand watermills. The mills were run by free-of charge energy harmless for the nature, and sites became oases of greenery, fish ponds, and the like which made brooks and rivers more accessible to the people. The first mill census for Croatia was carried out during the rule of the empress Maria Theresia (1740–1780). The census was regional, conducted by counties. One of the reasons for such an approach was that river training and development schemes were prepared at the time for the navigable rivers (Danube, Sava, Drava and Kupa) with a large number of mills, so it was necessary to undertake measures for their demolition or removal to new sites to enable normal navigation. At the time, these were mostly gristmills used for food production, i.e. to grind grain. Tab. 1 shows number of mills/waterwheels at the Zagreb County territory based on the available data.

Table 1

Mills/waterwheels at the Zagreb County in 18th Century

Zagreb County	Sava	153/154
	Kupa	107/123
	Odra	10/15
	Dobra	17/29
	Other	607/679
	Total	894/1000

Similar but less detailed and not easily accessible censuses exist for other Croatian regions. At approximately the same time, 827 mills were recorded along the Drava River in Varaždin County. In the Croatian Military Border region, census was conducted on several occasions in early 19th century. According to the first census from 1806, 792 mills were recorded of which 21 on the Danube, 125 on the Sava, and 546 on brooks. In the Petrinja area about 400 mills were recorded, and on the Slunj, Glina and Lika territory the number of mills varied between 300 and 500.

All the above confirms that the potential of rivers and brooks was recognized early, as well as benefit of its use which has been slowly vanishing both in Croatia and in entire Europe during the last century. However, in times of very high energy demand, when the non-renewable energy resources are being depleted at a fast pace, the developed societies have created new possibilities for use of renewable energy resources. This approach should rely on historical experience, and use this experience as grounds for new concepts more suited to the present situation. Harnessing of water energy and power, particularly at small hydroelectric power plants, has direct reference to the watermills. Many sites are still suitable for development, particularly considering water course maintenance, land-use planning an environmental acceptability and cost-efficiency. There is certainly a number of former mill sites which are no more attractive. The present paper describes an example of how a suitable mill site in Croatia could be used for the purpose.

3.2. Fajerov Mlin SHPP

3.2.1. Concept Description

Fajerov Mlin mill was operating as a gristmill and for electricity production until 1995. Fajerov Mlin is located at the r.h. bank of the Glina River. A concrete sill had been built in the riverbed to diverts water towards the mill. The existing fixed sill causes sedimentation downstream from the sill, and since it is positioned at an angle it contributes to erosion of the left bank and demands its intensive maintenance. A sill with moving equipment has numerous advantages compared to this concept, and it also enables more efficient use of available water energy of the Glina River at the site under consideration. The mill became derelict because both the mill itself and the concrete sill have not been maintained, and the sill is considerably damaged (Fig. 4). An exceptionally poor conditions of the existing sill demand that a new drop structure be built immediately upstream from the present Fajerov Mlin mill site.

Fig. 4. Fajerov mlin – present state

A new water drop structure would maintain the same water level permanently, with possibility that the level be decreased automatically in case of floods. At the same time, this headwater would enable operation of the Fajerov Mlin SHPP at flow rate of 20 m^3/s (minimum flow rate 3 m^3/s). The Fajerov Mlin SHPP power house with new intake and outlet structures is planned to be located at the r.h. bank. It is also necessary to build the spillway and bottom outlet stilling basin. (Fig. 5 and 6).

New concrete drop structure is planned for construction upstream from the existing derelict sill. A flap gate would maintain water level at 108.50 m a.s.l. at lower flow rates, and a fixed sill at elevation 105.85 m a.s.l., and the bottom outlet for discharge of the upstream section at elevation 104.50 m a.s.l. will be built. During construction, the bottom outlet would be used as a diversion canal for water discharge off the construction site. In the event of floods, the flap gate would be lowered automatically to allow the flood water discharge.

A vertical Kaplan turbine is selected for Fajerov Mlin SHPP, with rated discharge of 20 m^3/s and four-blade rotor diameter of 2 240 mm.

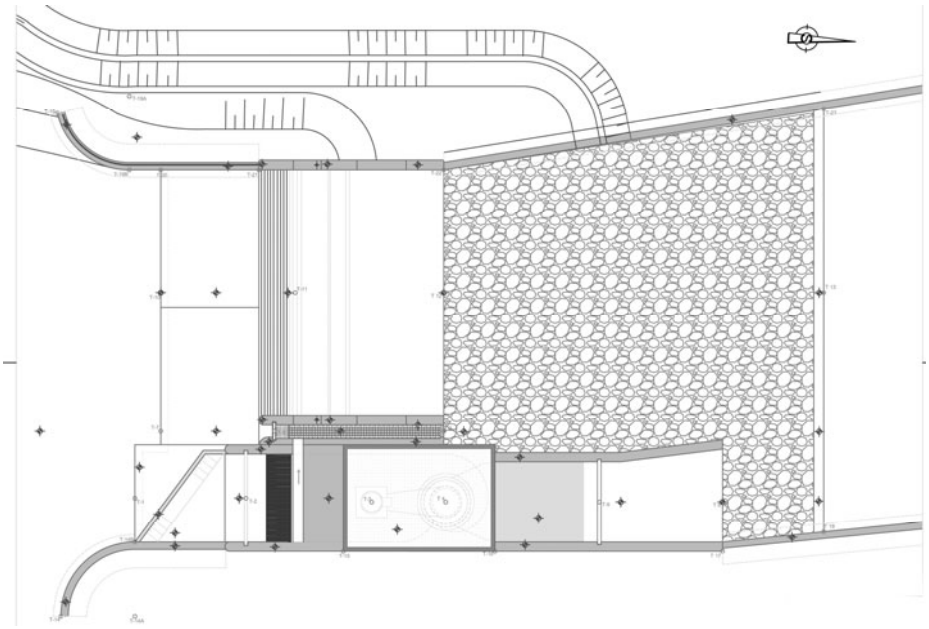

Fig. 5. Layout

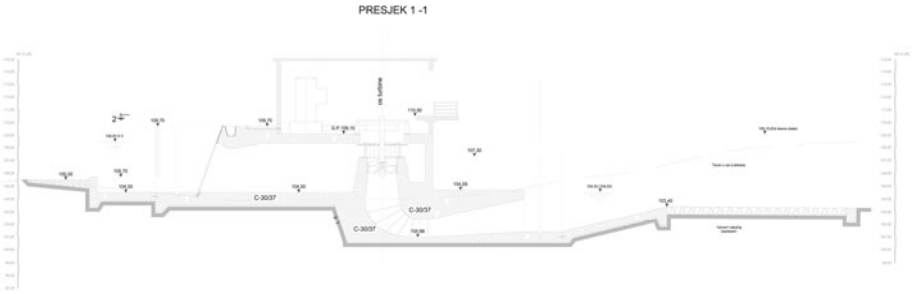

Fig. 6. Cross-section

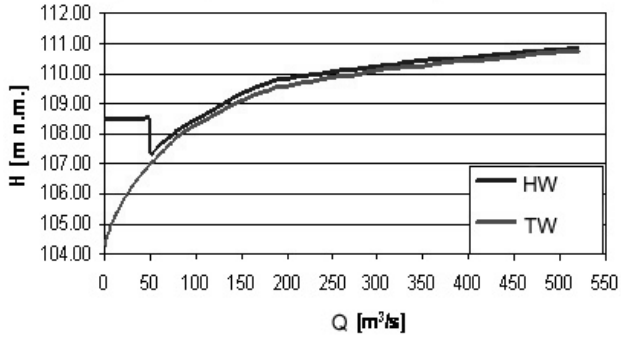

Fig. 7. Headwater (HW) and tailwater (TW)

Headwater (HW) and tailwater (TW) are determined by mathematical model HEC-RAS, and results are given in Fig. 7.

An average annual flow duration curve (Fig. 8) was used to define maximum capacity of 0.432 MW at flow rate of 20 m^3/s and total annual output of 2.0 MWh (Tab. 2).

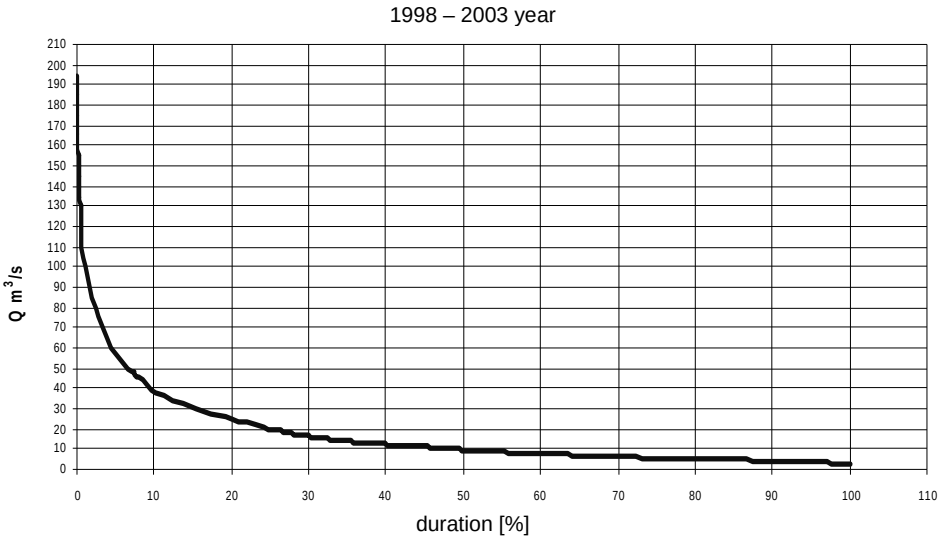

Fig. 8. An average annual flow duration curve

Table 2

Total annual output for $Q_i = 20$ m^3/s

Q [m^3/s]	Q_R [m^3/s]	H_n [m]	n [%]	P [kW]	P_{sred} [kW]	T [%]	ΔT [h/yr]	ΔT [MWh/yr]
3.00	3.00	3.94	55	64		99.0		
3.45	3.45	3.45	60	79	71.5	95.5	306.6	21.9
5.00	5.00	3.77	72	133	106.2	82.5	1138.8	120.9
8.00	8.00	3.50	81	222	177.8	58.0	2146.2	381.6
10.00	10.00	3.34	83	272	247.2	48.5	832.2	205.7
12.00	12.00	3.19	84	315	293.7	41.0	657.0	193.0
15.00	15.00	2.99	84	370	342.5	32.8	718.3	246.0
16.00	16.00	2.52	84	332	350.9	30.5	201.5	70.7
18.50	18.50	2.11	83	318	325.0	27.0	306.6	99.7
20.00	20.00	2.68	82	431	374.5	25.5	131.4	49.2
30.00	30.00	2.20	82	354	392.6	15.5	876.0	343.9
50.00	50.00	1.44	82	232	292.8	6.5	788.4	230.9
						W[GWH/yr]		2.0

3.2.2. Fajerov Mlin SHPP Economic Characteristics

Economic characteristics of the Fajerov Mlin SHPP are shown by an internal rate of return (IRR) where benefit-cost ratio equals 1, and net benefit 0. The gross benefit here includes all the benefits created during the economic lifetime, and the costs are all the costs incurred to realized the expected benefits. The gross benefits and costs are expressed as an average annual value. Gross benefit is evaluated on the basis of an average annual electricity output and unit price that could be achieved in Croatia. For analyses, an equal value was adopted for interest and discount rate. Annual maintenance costs are evaluated at 3% of construction costs. It is expected that a small hydro power plant construction period is 2 years, and its economic lifetime is set up at 30 years. Results are given in Fig. 9a and 9b.

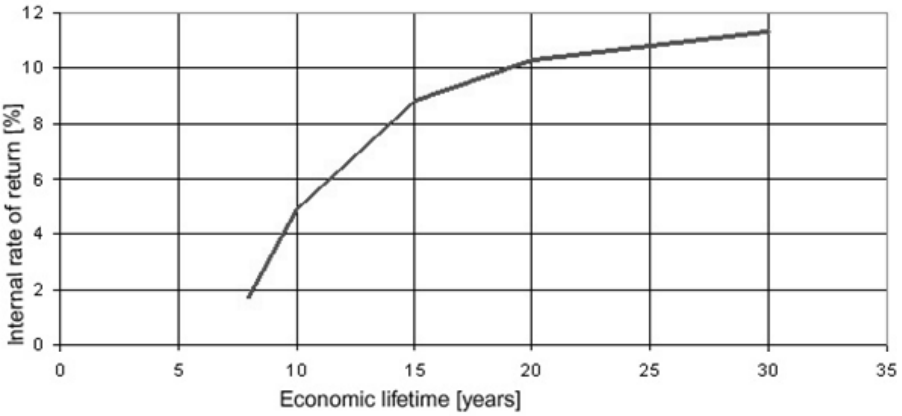

Fig. 9a. Internal rate of return

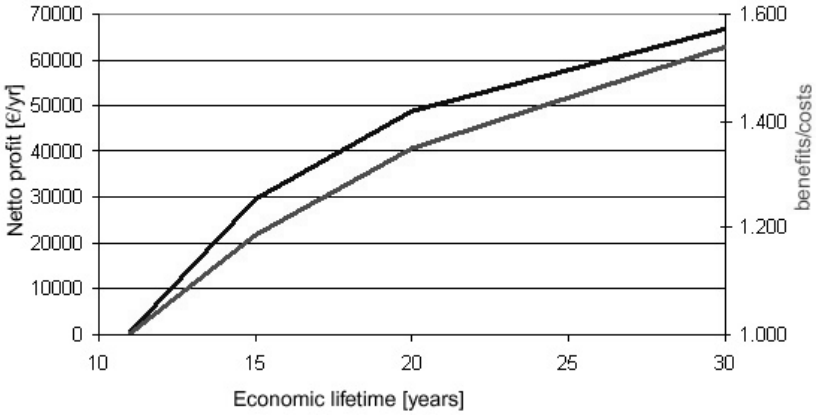

Fig. 9b. Netto profit and cost-benefit ratio for 6% interest rate

The results indicate that capital payback period for Fajerov Mlin SHPP construction could be 15 years at 8.5% interest rate. Therefore, the analyses confirm that the project is feasible.

3.3. Conclusion

The paper describes vast experience with harnessing the water energy and power. Smaller power was considered adequate in the past, when the needs were lower and methods of water use different. The present demand is considerably higher and the methods of water use have been changing. With a focus on small hydro power plants, the sites of abandoned water mills are certainly the first prospective sites to be considered. Although use of renewable energy resources has been getting support and encouragement, not a single small hydro project has been implemented recently (12 years) for different reasons. Use of abandoned watermills could result in making the licensing procedure more efficient (feasibility, land-use plans), and water course training and development would result in savings for the local authorities. The affirmative example of the Fajerov Mlin SHPP described in this paper is the only project that has been approved licenses and permissions for work continuation (Location Permit).

References

[1] Kolar-Dimitrijević M., Wagner E.: Watermills in Croatia (18^{th} – 20^{th} Century) an Example of Relation People had with Rivers/Streams. Ekonomika i ekohistorija, Research Journal for Economic and Environmental History, Volume III / Issue 3, Zagreb, 2007.

[2] Fajerov Mlin SHPP, Preliminary Design. Faculty of Civil Engineering, University of Zagreb, 2008.

4 Functional Relation Between Representative Wave Periods Based on Wave Spectra and Autocorrelation Function

Mateja Blažević, Marko Pršić, Dalibor Carević (University of Zagreb, Faculty of Civil Engineering, Croatia)

4.1. Introduction

Real sea waves generated by wind are characterized by irregularities as to direction, amplitude and frequency. Wave field may be considered a random process which is denoted with a random function $\hat{\eta}(\vec{r},t)$. Waves are observed by a fixed wave staff as a realization of the random function $\hat{\eta}(\vec{r},t)$, i.e. the wave record $\eta(t)$ is obtained as a function of physical sea surface elevation in time. Such wave records may be analysed in the probability domain yielding statistical representative paremeters of the wave profile, in the frequency domain using spectral analysis or in the time domain yielding autocorrelation function.

Statistical processing of individual wave heights within the studied wave record is used to obtain representative wave heights: $\overline{H}$, H_s=$H_{1/3}$, $H_{1/10}$,$H_{1/100}$, $H_{\max}$, where:

$$H_{1/n} = \frac{1}{N_0/n} \sum_{i=1}^{N_0/n} H_i^{desc} \tag{1}$$

It is theoretically proved [4] that the distribution of random wave height variable follows the probability distribution function of the Rayleigh type. Representative wave periods are determined from the periods associated to wave heights used for determination of representative wave heights. Such periods are to be obtained from the wave record by applying the method of zero-upcrossing or zero-downcrossing.

$$T_{1/n} = \frac{1}{N_0/n} \sum_{i=1}^{N_0/n} T\left(H_i^{desc}\right) \tag{2}$$

In addition to statistical method of wave description, spectral method is also developed, based on dividing a complex physical phenomenon such as the wave process, into individual components with respect to frequencies [3]. Unidirectional (local) wave spectrum represents mathematical description of wave energy distribution considering the frequencies.

Longuet-Higgins [4] defined the spectrum width parameter as:

$$\varepsilon_4 = \sqrt{1 - \frac{m_2^2}{m_0 m_4}} \tag{3}$$

where:

$$m_n = \int_0^\infty f^n S_{\eta\eta}(f) df \tag{4}$$

Regarding the narrow-band spectra ($\varepsilon_4 \to 0$) the wave height distribution follows the Rayleigh distribution, while in the case of wideband spectra ($\varepsilon_4 \to 1$), the wave height distribution approaches the Gaussian distribution function. The theoretical relation between the significant wave height H_s and the zeroth spectral moment m_0 reads as follows:

$$H_s = 4\sqrt{m_0} \tag{5}$$

For spectral widths that occur in reality ($\varepsilon_4 < 1$), it has been shown that the connection between the important wave height and the zeroth spectral moment differs from the theoretical [2], and therefore it is more appropriate to use the coefficient 3.7–3.8 instead of 4.

The spectral peak period T_p corresponds to the reciprocal value of peak frequency f_p:

$$T_p = \frac{1}{f_p} \tag{6}$$

Spectral moments are used to define periods $T_{0,1}$ and $T_{0,2}$:

$$T_{0,1} = \frac{m_0}{m_1} \tag{7}$$

$$T_{0,2} = \sqrt{\frac{m_0}{m_2}} \tag{8}$$

Spectral period $T_{0,2}$ is theoretically identical to the statistically defined mean period $\overline{T}_0$ [1], and it is noticed that $T_{0,1}$ corresponds very well with $\overline{T}_0$ [6].

The autocorrelation function (ACF) is a measure of correlation of the random process variable values in successive time intervals and is used for description of random, but frequent signals. According to the Wiener-Khinchin theorem, the power spectral density of a wide-sense stationary random process is the Fourier transform of the corresponding autocorrelation function:

$$S_{\eta\eta}(f) = \int_{-\infty}^{\infty} R_{\eta\eta}(\tau) e^{-i2\pi f\tau} d\tau \tag{9}$$

where

$$R_{\eta\eta}(\tau) = E\left[\eta(t)\overline{\eta}(t+\tau)\right] \tag{10}$$

The autocorrelation function of the periodical function is also periodical, having the same period as the initial function. For a discrete case such as the wave record, the Eq. (9)

turns into:

$$S_{\eta\eta}(f) = \sum_{k=-\infty}^{\infty} R_{\eta\eta}(k) e^{-2\pi i f k} \tag{11}$$

4.2. Wave Sample

For the purposes of analysis the wave records used were taken from the Panon wave recorder station in the northern Adriatic (Fig. 1) for the period from 1978 to 1986. The sample consists of 202 wave records of 5 minute duration recorded through 21 wave situations. The wave records were selected by the criterion that the significant wave height H_s exceeds 1.5 m in order to analyze high sea states which are interesting from the engineering point of view. The wave situations include two typical Adriatic winds: the Bora (NE) and the Sirocco (SE). The wave records were digitalized at 1 s intervals for the purpose of the planned analyses.

Statistical analysis was used to obtain the representative wave heights $\overline{H}$, H_s, H_{max} and the representative wave periods $\overline{T}_0$ and T_s. The analysis of wave spectra was used to obtain the spectral periods $T_{0,1}$ and $T_{0,2}$ as well as the peak period T_p. From the autocorrelation function of each record the first period T_{1af} (first "wave on the ACF) was defined as well as the mean period of the first quarter of autocorrelation function T_{af}.

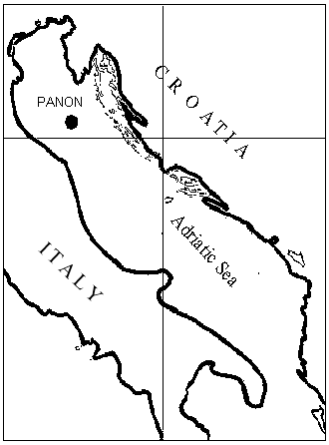

Fig. 1. Location of data collection: oil platform Panon, depth 50 m (taken from [6])

The basic characteristics of the sample are given in the Tab. 1, while the typical form of the wave record, the spectral density function and the autocorrelation function are shown in Fig. 2.

Initial verification of the applied mathematical apparatus was made for the relationship between statistically and spectrally defined significant wave height H_s. Spectral widths of observed sample wave processes range in the interval between $0.55 < \varepsilon_4 < 0.85$ (Fig. 3). The significant wave height *Hs* for the observed sample can be determined from the zeroth spectral moment m_0 according to:

$$H_s = 3{,}7\sqrt{m_0} \tag{12}$$

which corresponds to the results for real wave spectra in the Adriatic Sea [5].

Table 1

Sample characteristics of wave records from the Panon station

Sample characteristics	Value	Unit
Wave situations	21	[1°]
Wave records	202	[1°]
Average H_s	2.67	[m]
Highest H_{max}	8.50	[m]
Average T_0	6.11	[s]
Average T_s	6.61	[s]
Average $T_{0,1}$	5.88	[s]
Average $T_{0,2}$	5.47	[s]
Average T_p	7.10	[s]
Average T_{af}	7.16	[s]
Average $\overline{T}_{af}$	6.86	[s]
Average spectral peak energy	11.69	[m^2/s]

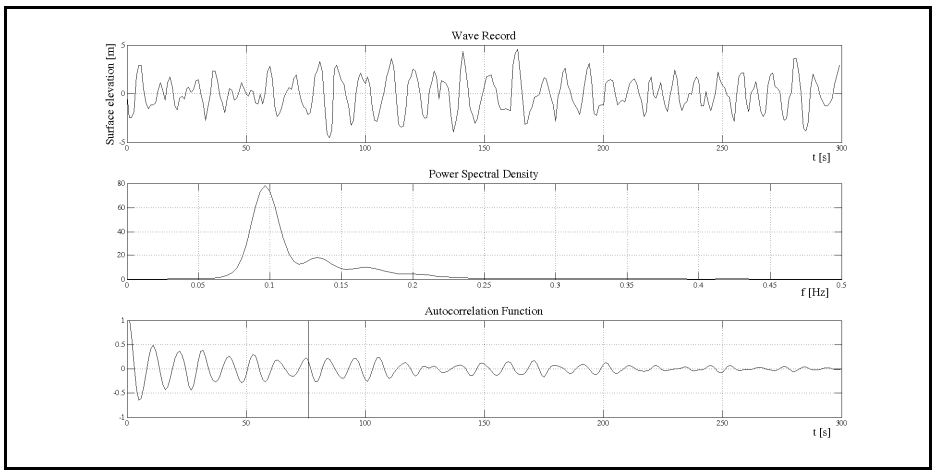

Fig. 2. Wave record from the Panon wave recorder station, 21 Dec, 1979 from 10:00 to 10 : 05 h, spectral density function and autocorrelation function

4.3. Relationship Between Statistical, Spectral and Autocorrelation Periods

Further analyses were focused on wave periods. As it has been presented in the Introduction, the spectral equivalent of the mean period $\overline{T}_0$ is the period $T_{0,2}$. However, the conducted analyses showed that the spectral period $T_{0,1}$ corresponds better with the mean period $\overline{T}_0$ (Fig. 4).

$$\overline{T}_0 = 1{,}038 \cdot T_{0,1} \tag{13}$$

$$\overline{T}_0 = 1{,}117 \cdot T_{0,2} \tag{14}$$

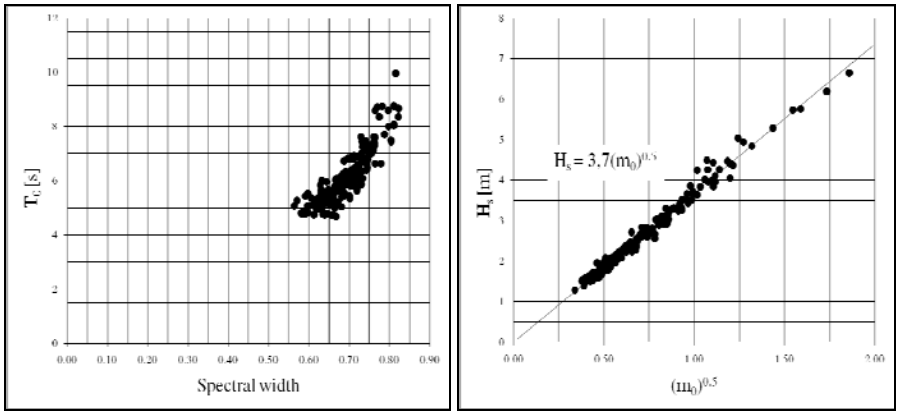

Fig. 3. Spectral widths of the analysed sample (left) and the relationship of statistically defined H_s and the root of zeroth spectral moment (right)

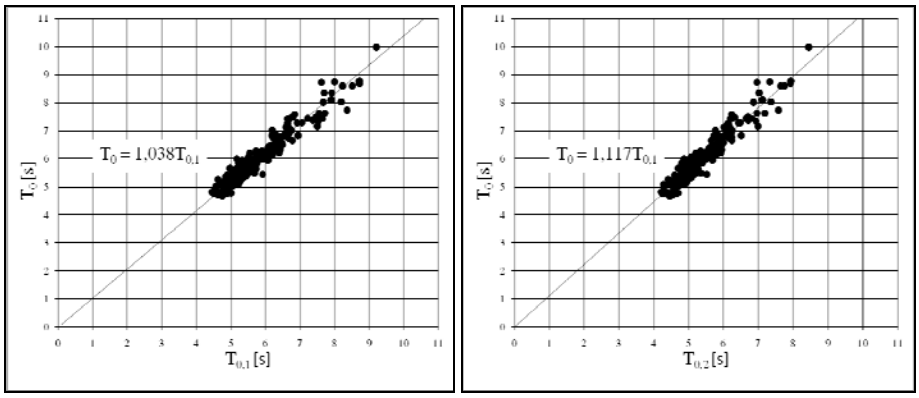

Fig. 4. Relationship of the statistically determined mean period T_0 and spectral periods $T_{0,1}$ (left) and $T_{0,2}$ (right)

It may be observed from (13) and (14) that it is better to use the relationship $\overline{T}_0 = T_{0,1}$ since the theoretical relationship $\overline{T}_0 = T_{0,2}$ generates 10% error in the mean period calculation. The analysis of the relationship of the significant wave period T_s and the mean period $\overline{T}_0$ results in the following relationship:

$$\overline{T}_0 = 0.9 \cdot T_s \tag{15}$$

For the observed wave records a linear relationship between the peak period of the wave spectrum and the significant wave period determined by statistical methods was established (Fig. 5):

$$T_s = 0.928 \cdot T_p \tag{16}$$

The largest deviation from the relationship (16) occurs during the Sirocco blowing (SE), especially in the phase of sea state increase.

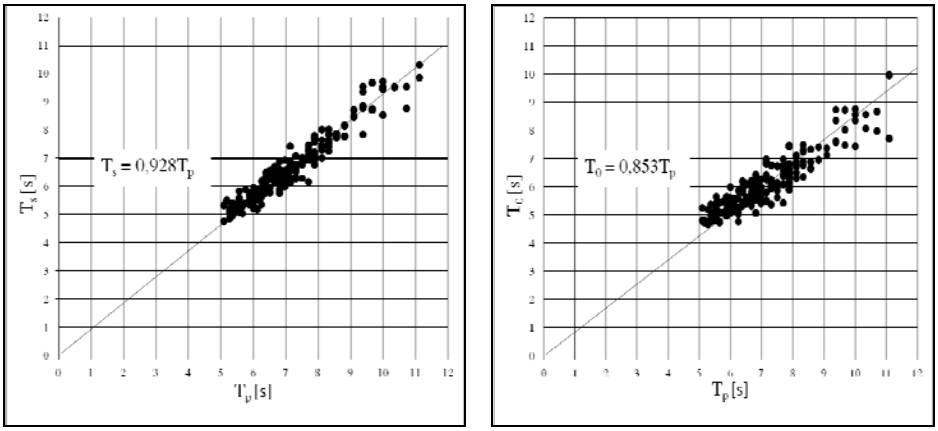

Fig. 5. Relationship of the peak period T_p and statistical periods T_s(left) and $\overline{T}_0$ (right)

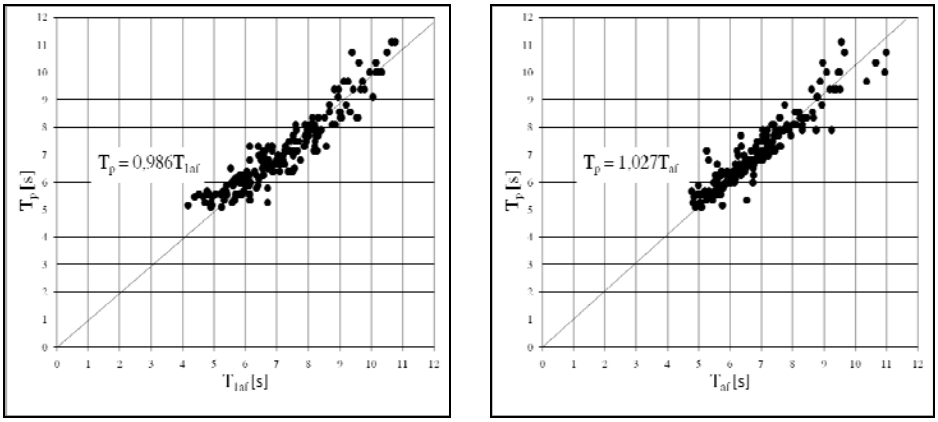

Fig. 6. Relationship between the spectral peak period T_p and autocorrelation function period T_{1af} (left) and T_{af} (right)

The peak period T_p relationship towards the mean period $\overline{T}_0$ shows a much wider dispersion than the relationship of T_p towards the significant period T_s (Fig. 5).

$$\overline{T}_0 = 0{,}853T_p \tag{17}$$

The periodicity analysis of autocorrelation functions of wave recordings showed that the first ACF period T_{1af} is on average larger than the mean ACF period T_{af} by 4%. As it is shown in Fig. 6, the spectral peak period T_p may be well approximated with autocorrelation function periods T_{1af} and T_{af}:

$$T_p = 0{,}986 \cdot T_{1af} \tag{18}$$

$$T_p = 1{,}027 \cdot T_{af} \tag{19}$$

The greatest deviations still occur during the Sirocco storm (SE).

As per the definition, the autocorrelation function of periodical function should also be periodical having the same period. It was established by the analysis of wave situations in the Adriatic Sea that the relationship between the significant wave period T_s and the mean period of autocorrelation function T_{af} is linear.

$$T_s = 0{,}957 \cdot T_{af} \tag{20}$$

The mean period of the autocorrelation function T_{af} on average exceeds the values of the significant wave period T_s by 4%, as it is shown in Fig. 7. The greatest deviations occurred for the situation between 21–23 Dec, 1979 during the Sirocco storm, when the maximum wave heights were recorded.

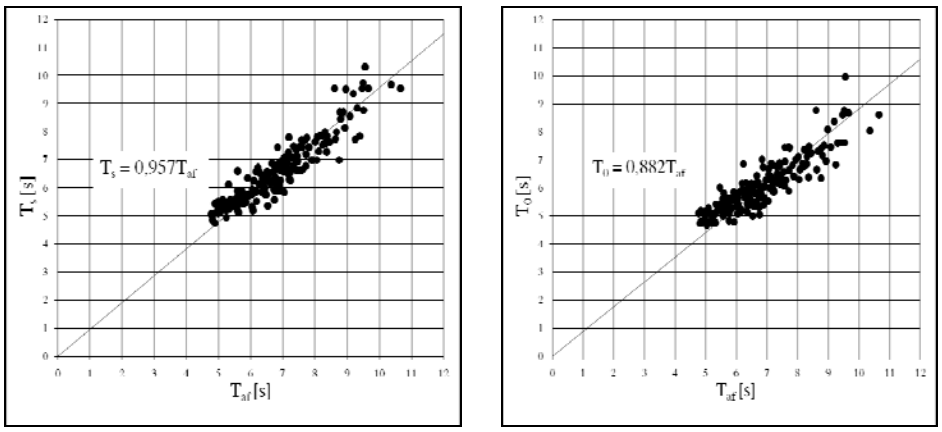

Fig. 7. Relationship between the mean period of the autocorrelation function T_{af} and and statistical periods T_s (left) and $\overline{T}_0$ (right)

Relationship between mean period $\overline{T}_0$ and mean ACF period T_{af} is also linear (Fig. 7).

$$\overline{T}_0 = 0.882 \cdot T_{af} \tag{21}$$

4.4. Conclusion

The Tab. 2 provides a review of defined relationships between the statistical and spectral periods and the autocorrelation function periods along with the standard deviations and maximum departures.

For the observed Adriatic high sea states, it was established that the statistical mean period $\overline{T}_0$ may be approximated with the spectral period $T_{0,1}$ better than with the spectral period $T_{0,2}$. The spectral peak period T_p is approximately equal to the initial and mean period of autocorrelation function T_{1af} and T_{af}. The mean wave period $\overline{T}_0$ is by 10% shorter

than the significant wave period T_s. Statistically significant wave period T_s may be defined through the peak period T_p and the average period of autocorrelation function T_{af} using (16) and (20), and in practice it may be taken that the significant wave period T_s is by 5% shorter than the spectral peak period T_p and the mean period of autocorrelation function T_{af}.

It is recommended to use the Eq. (13), (15), (16), (19) and (20) for relations between statistical, ACF and spectral wave periods for Adriatic high sea states.

Table 2

Review of defined functional relationships between the representative periods

Eq		σ_T [s]	$\sigma_T/\overline{Ti}$ [%]	ΔT_{min} [s]	ΔT_{max} [s]
(13)	$T_0 = 1{,}038 \cdot T_{0,1}$	0.26	0.04	–0.81	0.95
(14)	$T_0 = 1{,}117 \cdot T_{0,2}$	0.27	0.04	–0.95	0.76
(15)	$T_0 = 0{,}9 \cdot T_s$	0.32	0.05	–0.97	1.15
(16)	$T_s = 0{,}928 \cdot T_p$	0.33	0.05	–0.84	1.19
(18)	$T_p = 0{,}986 \cdot T_{1af}$	0.50	0.07	–1.14	1.33
(19)	$T_p = 1{,}027 \cdot T_{af}$	0.43	0.06	–1.16	1.46
(20)	$T_s = 0{,}957 \cdot T_{af}$	0.45	0.07	–1.21	1.28

References

[1] Goda Y.: Random Seas and Design of Maritime Structures, Advanced Series on Ocean Engineering – Vol.15, World Scientific Publishing Co, Singapore 2000.

[2] Goda Y: Estimation of Wave Statistics from Spectral Information. Waves '74, Int. Symp vol. 1. New Orleans, New York, ASCE 1974, 320–337, 1974.

[3] Liu Z. Frigaard P.: Generation and Analysis of Random Waves, Laboratoriet for Hydraulik og Havnebygning, Instituttet for Vand, Jord og Miljoteknik, Aalborg Universitet, Aalborg 2001.

[4] Longuet-Higgins M. S: The Statistical Analysis of a Random Moving Surface: Proceedings of Royal Society (UK) Series A (1957), 321–387.

[5] Pršić M.: Optimization of Rouble Mound Breakwater in the Conditions of the Adriatic Wave Spectrum: Doctoral dissertation, University of Zagreb, Faculty of Civil Engineering, Zagreb 1987.

[6] Pršić M., Smirčić A., Leder N.: Adriatic High Sea State Characteristics, Wind and Wave Climate '99 – Proceedings of the International MEDCOAST Conference on Wind and Wave Climate of the Mediterranean and Black Sea, Antalya, Turky, 277–293, 199.

5 Comparison of Erosion and Erosion Control Works in Macedonia, Serbia and Bulgaria

Ivan Blinkov (Ss Cyril and Methodius University, Faculty of Forestry, Skopje, Macedonia), Stanimir Kostadinov (University of Belgrade, Faculty of Forestry, Serbia), Ivan Marinov (Bulgarian Academy of Science, Institute of Forestry, Sofia, Bulgaria)

5.1. Introduction

Soil erosion is a natural process, occurring over geological time, and most concerns about erosion are related to accelerated erosion, where the natural rate has been significantly increased by human action. Slope sediment transport processes are of two very broad types, first the weathering and second the transport of the regolith. Within each of these types, there are a number of separate processes, which may be classified by their particular mechanisms into groups, although many of these processes occur in combination. Soil erosion is regarded as the major and most widespread form of soil degradation, and as such, poses severe limitations to sustainable agricultural land use. Soil can be eroded away by wind and water. High winds can blow away loose soils from flat or hilly terrain. Erosion by water occurs due to the energy of water as or when it falls toward the earth and flows over the surface. Most slope processes are greatly assisted by the presence of water, which helps chemical reactions, makes masses slide more easily, carries debris as it flows and supports the growth of plants and animals. For both weathering and transport, the processes can conveniently be distinguished as chemical, physical and biological [6]. Erosion damages are classified in 2 basic groups as follow:

1 – **"on-site" damages** (loss of topsoil and nutrients, disturbance of the hydrological regime, landscape changes) and

2 – **"off-site" damages** ((flash flooding, siltation of the reservoirs and land in the downstream sections, soil halomorphism, chemical pollution of water with pesticides, fertilizers, and other pollutants connected to the suspended sediment that deposed in the downstream sections and reservoirs).

Water erosion is the most spread problem of land degradation in Europe. European Council report got through the GLASOD data method [18, 22] enable overview of land degradation processes in Europe. Region of South and Southeast Europe is significantly prone to erosion process. In parts of the region, erosion has reached a stage of irreversibility and in some places erosion has practically ceased because there is no more soil left. With a very slow rate of soil formation, any soil loss of more than 1 t/ha/yr can be considered as irreversible within a time span of 50–100 years Losses of 20 to 40 t/ha in individual storms, that may happen once every two or three years, are measured regularly in Europe with losses of more than 100 t/ha in extreme events [16]. It may take some time before the effects of such erosion become noticeable, especially in areas with the deepest and most fertile soils or on heavily fertilized land. However, this is all the more dangerous because, once the effects have become obvious, it is usually too late to do anything about it.

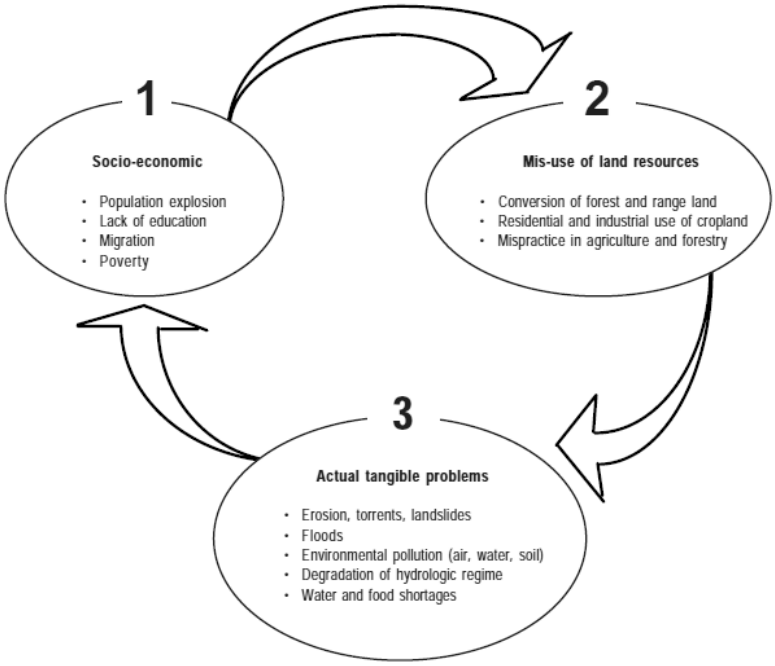

Fig 1. Interconnectivity of the groups of factors active in degradation of watershed resources in a vicious circle [17]

The **erosion control concept** depends on:

— status, role and importance of the object,
— natural (ecological) characteristics generally and partially,
— erosion intensity and erosion forms on the slopes and into the drainage network,
— state and functionality of existed biological ameliorative (silvicultural and agro-meliorative) measures, hydraulic and other measures and activities,
— soc-economic characteristics in the area and region.

Erosion control concept, depends on a scale of activity, could be understand as: single (on a small field) or on a scale of watershed. Single concept is in use just to solve single problem especially to minimize any single on-site effect (raindrop erosion, erosion from agricultural parcel, erosion on construction sites etc.). On a scale of watershed, erosion control is a part of a whole watershed management planning.

Erosion control measures are classified in the following groups: technical – ameliorative measures; biological – ameliorative measures (silvicultural and agro-meliorative); hydraulic structures; administrative measures and educative measures [19].

The purposes of technical ameliorative works are: reducing surface water runoff, storing water, reducing erosion on the hills, enabling preconditions for biological works (afforestation and grassing as well as agriculture production) on steep slopes, rehabilitation of small gullies etc. In the group of technical – ameliorative works belong: contour ditches, contour walls (made by various material), furrows and terraces (various dimension, form etc). These structures could be built by different material as: soil, stone, wood, concrete, armature concrete etc. and semi-structures as: single and double wattles, fascines, gabions.

The choice of material, semi-structure, form, and dimension should be defined with detail – final designs. Usually in the areas, where there is a large quantity of stone, stone structures or gabions structures are fully recommended. In other areas could be used wood structures or to be used wattles of fascines. During the process of preparation final design an attention should be paid on the following: selection of species for planting (drilling), selection of planting (drilling) season, selection of appropriate techniques and approaches for planting (drilling), selection method for land treatment and maintenance of the new plantation etc. Species that enable the fastest and best protection from erosion in the edaphically conditions of location have and advantage in a process of selection. Domestic species should be selected in advance. Usually, the nature shows the most appropriate species because the present species show their adjustment on various conditions. Habitus of the species is very important. Species with laid low habitus are recommended for steep slopes especially on the road slopes. Productive capacities of the species are absolutely secondary in a case of erosion control especially in erosion control. In closed areas to the reservoirs should be paid attention on horticultural values. For silviluctural works on the extreme locations, species should have wide ecological valence. Selection of method for land treatment depends on the needed effect for decrease of tangential pressure on the soil, water retention and erosion reducing in general. Maintenance of the plantations should be in accordance with their erosion control character, the habitat conditions, as well as the current legislation. On a rocky terrains setting turfs is usual measure.

All cross hydraulic constructions: check dams, cascades, thresholds combined with the, longitudinal construction: dikes, channels etc., have multiply role: reducing fluvial erosion and rehabilitation the previous damages, stream bank stabilization, improve of the water regime, retention of large quantity of sediment even stabilization of landslides. On a slopes where there are rock falls could be used appropriate retardation walls made by gabions or should be used protective wire.

5.2. Aims, Objectives and Methods

The main aim of this paper is to present specific erosion control measures and structure used in Macedonia, Bulgaria and Serbia as well as to show their effects.

The objectives of this study are:

— to present current erosion intensity,
— to analyze and present historical overview of erosion control in different, country,
— to extract and present the most specific erosion control measures and structures, per country,
— to evaluate and present their effectiveness.

Qualitative method – text analyze method was used for these study.

As a base for comparative analyses were used significant of studies, country reports related to the topic by countries and various available papers.

5.3. Study Areas Characteristics

Study area is located on the Balkan Peninsula. It encompassed territory of the following countries: Republic of Macedonia (RM), Republic of Serbia (SR) and Republic of Bulgaria (BG).

All three groups of erosion factors-energy, resistance and protection [15] – promote the soil erosion in the study area. The energy group includes the ability of rainfall and runoff to cause erosion. The relief in the southern part of Serbia is characterized by relatively steep slopes, which directly influence the power of the erosive agents. About 80% of the territory of RM belong to hilly and hilly-mountainous and mountainous region where slopes are very steep. Significant part of the territory of Bulgaria belongs to mountain region too.

Fig. 2. Study area

Considering the resistance factors, the significant erodibility of the soil and geological substrata should be mentioned. The geological structure of the major part of the considered area consists of rocks of high erodibility (conglomerates, schists, etc.) which contribute to the denudation processes. Resistant rocks (granites, andezites, etc.) are present in a smaller area of this region.

Fig. 3. Relief map of Europe

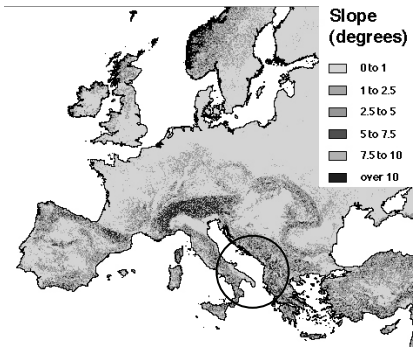

Fig. 4. Slope distribution in Europe

The protection group of erosion factors is related to the population density and land use. The average population density in Serbia is moderate — about 100 inhabitants per km^2, 87 inhabitants per km^2 in Macedonia and. 67 in Bulgaria.

During the history, this region has been settled permanently. Inadequate land treatment and intensive forest cut contributed to high intensity erosion processes. In the period of Ottoman Empire for forest was proclaimed “res nullius” that means nobody is owner of forest and everybody can cut for fulfilling own needs. Result of this was conversed significant part of the region from forest to bare land. It rapidly increased erosion processes and torrential flows.

Because of all natural and socioeconomic conditions, this region is highly vulnerable to erosion processes.

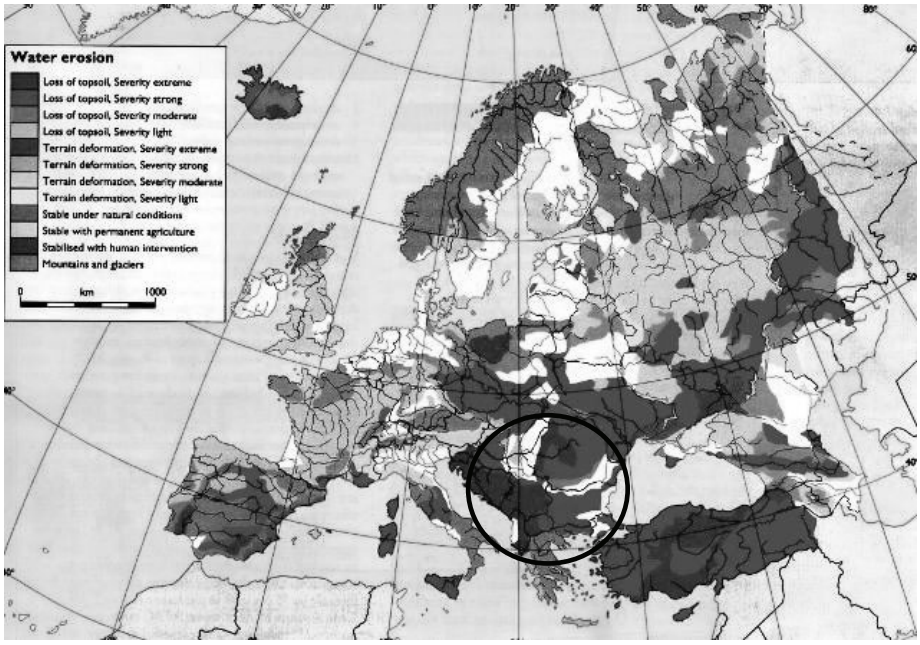

Fig. 5. Water Erosion Map of Europe (EEA, 1993)
(http://www.eea.europa.eu/data-and-maps/figures/water-erosion-in-europe-1993)

According to the European Environment Agency (1993) [26], Macedonia, together with Albania, Serbia and Bosnia perform so-called “red zone” of water erosion in Europe.

5.4. Results

5.4.1. Erosion Intensity

Related to the watershed management need, the EPM is the most comprehensive erosion risk assesment method (ERAM) because it gave solution to almost all tasks as follow: evaluation of various ERAM depend on fulfilling various tasks, evaluation of various ERAM depend on the scale, evaluation of various ERAM depend on solving

various erosion types, evaluation of various ERAM depend on the sector [4]. According to the sam reserach, for the Balkan territory, the EPM method is the most appropriate for hilly-mountain and mountain region, but use of USLE for agricultural area (hilly and valley) is limited because of absence of data (Macedonia, Serbia, Bosnia, Montenegro).

However, various methodologies are used for erosion mapping. While in Macedonia and Serbia "Erosion Potential Model" by Gavrilovic is in use, Bulgaria use USLE methodology. Data and maps between counries could be compared if data would be conversed from t/h to $m^3 \cdot km^{-2} \cdot y^{-1}$.

5.4.1.1. Erosion intensity in Macedonia

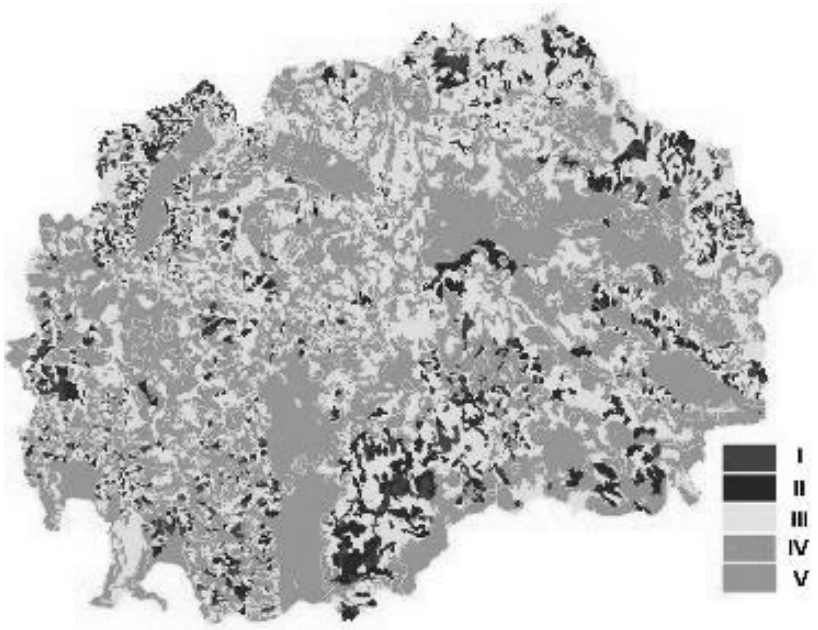

Fig. 6. Erosion map of the Republic of Macedonia

Table 1

Erosion distribution in MAcedonia (by EPM methodology)

Degradation category (erosion processess)		Area (km^2)	Percent (%)	Erosion intensity ($m^3\ km^2\ y^{-1}$)
I	extremely high	698	2.77	> 3000
II	high	1 832	7.38	1500 – 3000
III	medium	6 893	27.78	1000 – 1500
IV	low	7 936	31.98	500 – 1000
V	very low	7 463	30.09	70 – 500
		25 713	**100.00**	

According to the Erosion map of Macedonia [23], 96% of the total area is affected by

processes of erosion. An amount 9423 km^2 or 36.65% of the total state territory is in the highest categories (I – III). The total annual production of erosive material on the whole territory is about 17×10^6 $m^3 y^{-1}$ or 685 $m^3 km^{-2} \cdot y^{-1}$, which of 7.5×10^6 $m^3 y^{-1}$ or 303 $m^3 km^{-2} \cdot y^{-1}$ are carried away. Significant part of these deposits, about 3×10^6 m^3 y^{-1} is not carried through the downstream sections of the rivers to the exit of the state territory, but deposed in nature lakes and reservoirs. For example, the rates of annual sediment yield in the biggest reservoirs in Macedonia are: Tikves ($1.3 \cdot 10^6$ m^3 or 497 m^3/km^2), Kalimanci (0.42×10^6 m^3 or 970 m^3/km^2). Typical for these reservoirs is that great part of the eroded material was deposed in the so called "useful storage of the reservoir", so it decreases water resources of the reservoir.

5.4.1.2. Erosion intensity in Serbia

Erosion map was made in 1973 using EPM methodology. This map shows that the total area of Serbia is endangered by erosion processes (mean 86.00%) of various intensity: Vojvodina 72.29%, Kosovo and Metohija 94.82%.

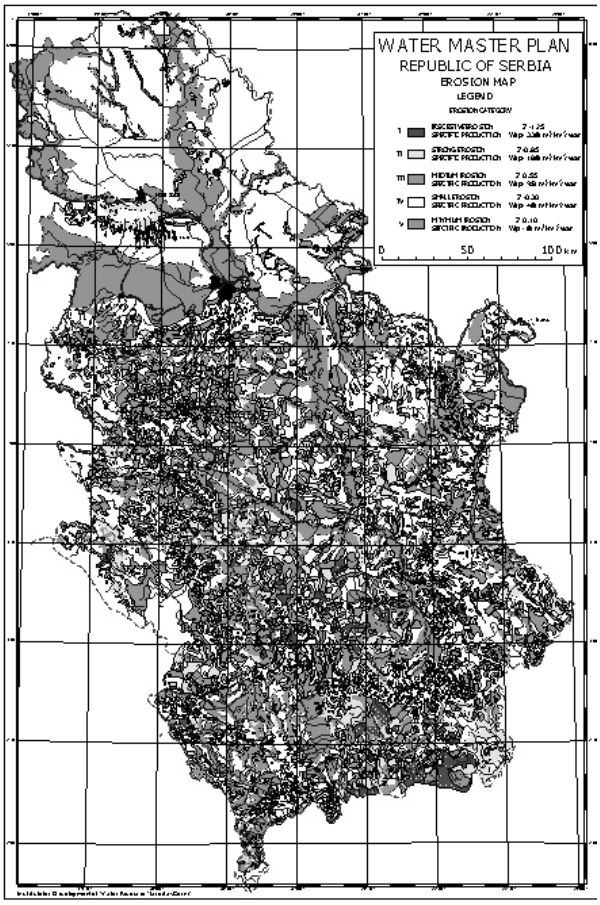

Fig. 7. Erosion map of Serbia

A new map of erosion was produced in 1984, but there were no essential differences compared to the map in 1973. Total average annual gross erosion in Serbia amounts is 37 249 975 $m^3 \cdot y^{-1}$, specific annual gross erosion amounts to 421.57 $m^3 \cdot km^{-2} \cdot y^{-1}$, annual sediment transport is 9 350 765 $m^3 \cdot y^{-1}$, specific annual sediment transport is 105.80 $m^3 \cdot km^{-2} \cdot y^{-1}$.

Permanent soil loss in Serbia is 487.86 $m^3 \cdot km^{-2} \cdot y^{-1}$, Kosovo and Metohija 248.98 $m^3 \cdot km^{-2} \cdot y^{-1}$. In the normal erosion, which is a positive process, soil loss is 0.1 mm, i.e. up to 100 $m^3 \cdot km^{-2} \cdot y^{-1}$.

The most endangered region in Serbia is Southeast part of the country that is closed to Macedonia and Bulgaria borders.

5.4.1.3. Erosion intensity in Bulgaria

Studies concerning land resources status in Bulgaria showed that over 80% of the arable lands and 15% of the forest lands are subjected to water erosion, while 37% are subjected to wind erosion [12]. The irrigation erosion potentially can affect 0.5×10^6 ha, which represents 50% from the irrigated land in the country. It was established that the erosion is observed at territories with slopes steeper than 2% at gravitational irrigation and at sprinkling irrigation at 8% slopes. The total mean annual lose as a result of erosion, according Krasteva V. [11] are 15×10^6 m^3 and 100×10^6 m^3 irrigation water, which was not absorbed in the soil but was lost with the runoff. The mean annual loses of soil due to water erosion was 170 $t \cdot km^{-2}$, which is 1.5 times higher as compared to the average intensity of the Global surface erosion [1].

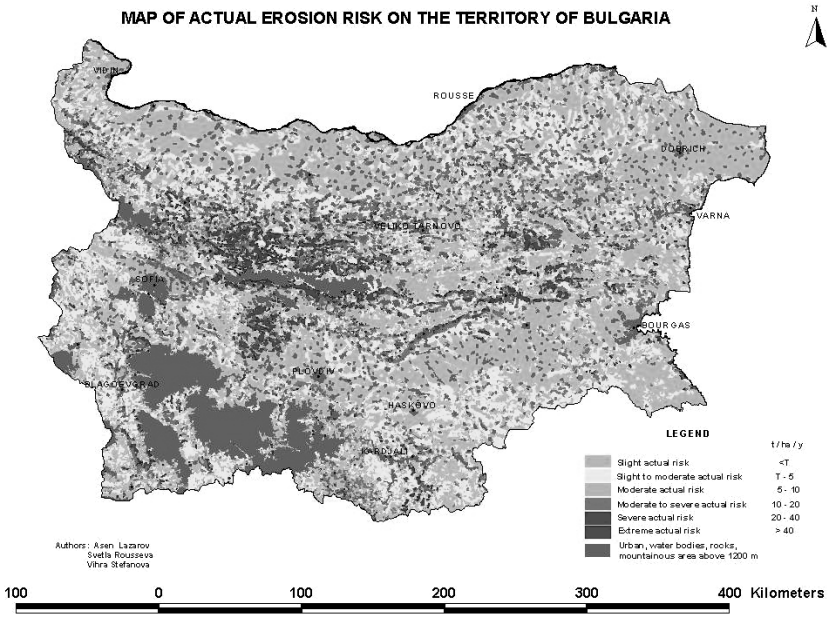

Fig. 8. Erosion risk map of Bulgaria [21]

Erosion on agricultural land is significant. Percentage distribution according to the degree of water erosion risk of the area of different types of land use considering field crop rotations with 50:50% proportion of row to cover crop shows that about 1/3 of the agricultural land, including 65.3% of the area of perennials, 34.9% of the area of rangeland and 23.3% of the cropland are with a risk of erosion exceeding 3 $t \cdot ha^{-1} \cdot y^{-1}$. The average annual and 4.76 $ha^{-1} \cdot y^{-1}$ for the cropland, to 12.65 $ha^{-1} \cdot y^{-1}$ for the perennials. Average annual soil loss estimate amounts to about 32 000 000 tones, over 2/3 of which are formed from the cropland area.

5.4.2. Erosion Control

5.4.2.1. Erosion control in Macedonia

Measures to control erosion were initiated in the early 1900's, aimed mostly at protecting rivers and reservoirs. Following passage of the Law on Financing Melioration Systems (1958), these measures were strengthened, and as of 1985, 285 torrents were regulated. The water management projections anticipate continuing this work

Measures to control erosion on deforested barren lands have also been under way since 1945, when restrictions were placed on nomadic breeding of goats and sheep in forests. This measure, though unpopular, led to a recovery of degraded forest and shrub land.

There were few acts directly related to erosion control in past: The Act for afforestation of bare land (1951), Act of erosion control on steep slopes (1952), Act of steep slopes protection and torrent control (1957). Later, these acts were suspended.

As part of the erosion control programme an “Afforestation Fund” was established in 1970 and it exist till 1990.

Until 1990, erosion control measures and activities were on “higher level” and institutional support was higher. There were sections for erosion control in all regional water management enterprises. There were parts of the budget aimed at erosion control.

Now, the situation is the opposite. Unfortunately, erosion is one the biggest environmental and economic problems in Macedonia, but there are no special

In the period 50’s–70’s, classical stone barrages were made usually. Then building of concrete barrages started. All these structures were made by water management enterprises, where in past existed sector for erosion and torrent control. Now water management is in transformation period. Realization of the plans is partially. About 65% of hydraulic structures was built, but only 25% of planed afforestation are realized.

5.4.2.2. Erosion control in Serbia

The erosion and torrent control works (ETCW) on the territory of Serbia started by the end of XIX^{th} century, but the organized work started in 1907.

The first works refer to torrent control and channel training in the zones of intersections with railway, aiming at railroad protection.

There were works in the torrents of the Grdelička Klisura gorge in the South-East of Serbia, where the international railway line Belgrade-Skopje -Athens passes.

During the period of almost 100 year in Serbia mostly were applied Classical European French and Prof. Rosić’s System torrent control. In the field of erosion and torrent control in Serbia, especially after the Second World War (period 1946–1989) significant results have been achieves. Many roads and railways, settlements, industry, agricultural soil and storage reservoirs have been protected (fully or partially), from sedimentation and from torrent floods.

Still, this is not enough, considering the present conditions and requirements. In last 15 years intensifying of erosion processes. For almost 100 years of ETCW in Serbia, it is characteristic that erosion control works were not performed on farmland on the slopes, except in the period 1955–1966 when there was a small extent of these works.

5.4.2.3. Erosion control in Bulgaria

The incidentally erosion and torrent control works (ETCW) on the territory of Bulgaria started near the end of XIXth century (1878) when the first erosion control plantations (Knazevo. Dupnica, Kustendil, park "Aiazmoto") were carried out. The organized work started in 1905 when the "Bureau for protection of forest and afforestation in Kazanlak" has been established. Felix Vozli is founder of organized erosion control in Bulgaria. In those period were afforested 500 ha bare lands, 3 400 m^3 barrages are built too.

Significant influence on erosion control in Builgari has legal base because from 1878 are proclaimed 7 laws on forest (where erosion and torrent control are appointed), separate law on torrent control and afforestation (1942) and secondary legislation.

National long-term programme for erosion control has been in charge from 1982. Up to 1990, 80 erosion control projects for reservoir watershed, irrigation schemes and other are carried out. For the more then 100 hundred years organized erosion control, were afforested more then 2 300 000 ha, on 820 000 ha, various technical – ameliorative works are launched, more then 600 000 m^3 barrages and thresholds are built, about 600 000 m^3 cleyonages are constructed, 395 000 m^3 rocky thresholds, 428 000 m stream protective wattles were built.

5.4.3. Comparision of Erosion Intensity Between Countries

Table 2

Erosion intensity per counutry

Country	Erosion intensity		Methodology
	$m^3\ y^{-1}$	$m^3\ km^{-2}\ y^{-1}$	
Macedonia	$17 * 10^6$	680	EPM
Serbia	$37 * 10^6$	622	EPM
Bulgaria	$15 * 10^6$	170 t km^{-2}	USLE

Data from Serbia and Macedonian is done using the same methodology – Erosion Potential Model and is easy to be compared while data from Bulgaria is diffrent. Values for erosion intensity in Bulgaria are low. It is a result of used methodology.

USLE methodlogy only predicts the amount of soil loss that results from sheet or rill erosion on a single slope and does not account for additional soil losses that might occur from gully, wind or tillage erosion.

5.4.4. Comparison of Erosion Control Works Between Countries

5.4.4.1. Quantity of erosion control works

Bulgaria paid significant attention to affoirstation of bare lands and other erosive land. Regarding the percentage of the afforested territory (7,39%), Bulgaria is one of leaders in

Europe. Macedonia paid significant attention to affoirstation also. Percentage of afforsted territory of the total counutrea area is high too (4,67%).

Table 3

Erosion control works per country

Country	Afforestation		Hydraulic structures	
	ha	% of territory	m^3	m^3/km^2
Macedonia	120 000	4.67	100 000 (taxative)	3.89
Serbia	114 000	1.20	1 486 167	16.82
Bulgaria	820 000	7.39	617 000	5.56

On the other hand, Serbia paid more attention on building of hydraulic structures in the toront beds. Value of 16.82 m^3/km^2 is between the highest in Europe.

5.4.4.2. Dynamic of erosion control works

Common characteristics for all three countries is that during the sociualism, erosion control was much higher intensive. In the period after fail of old socialistic system, erosion control decrease rapidly.

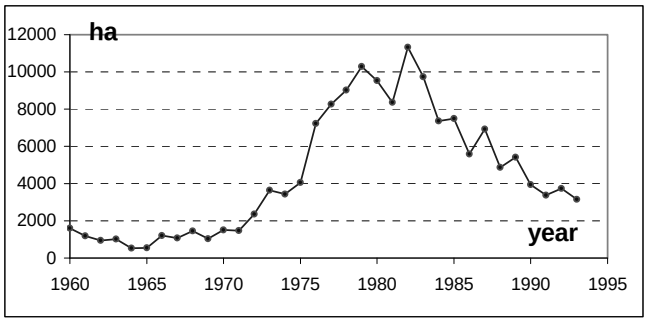

Fig. 9. Dynamic of afforestation in Macedonia per year

Afforestation in Macedoina were the highest intesive in the period 1975–1990. Later there was a rapid decrease of this activity. In the latest 5 years, this activity increase and the average intensity of afforestation in last 5 years (2005–2010) was about 5000 ha.

Related to the hydraulic structures, there is no data available, but due to the collapse of and transformation of water maanagemnt in the counutrey, trend of decrease continue.

Common characteristics for all three countries is that period from 1945–1990 is the "golden period" of erosion control works.

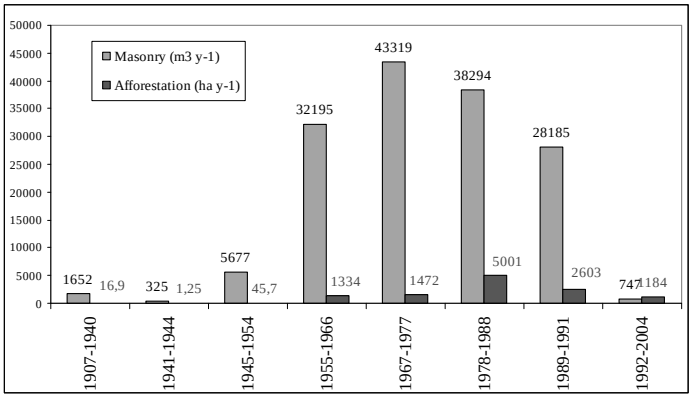

Fig. 10. Dynamic of erosion control works in Serbia

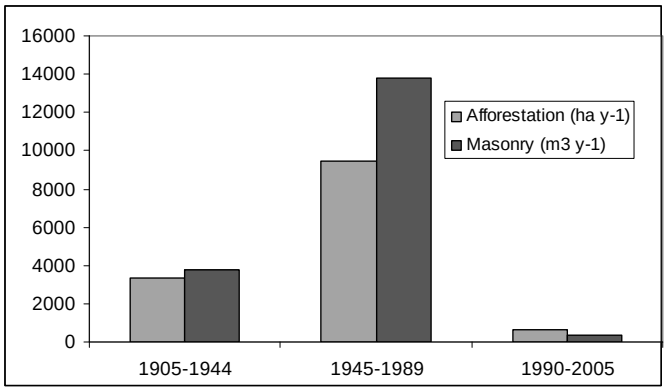

Fig. 11. Dynamic of erosion control works in Bulgaria

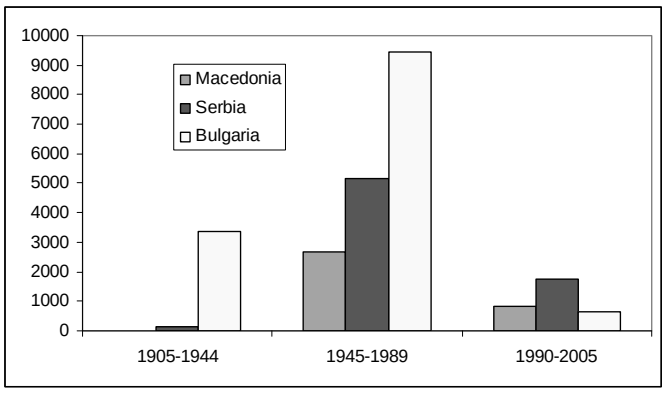

Fig. 12. Comparison of dynamic of annual intensity of afforestation

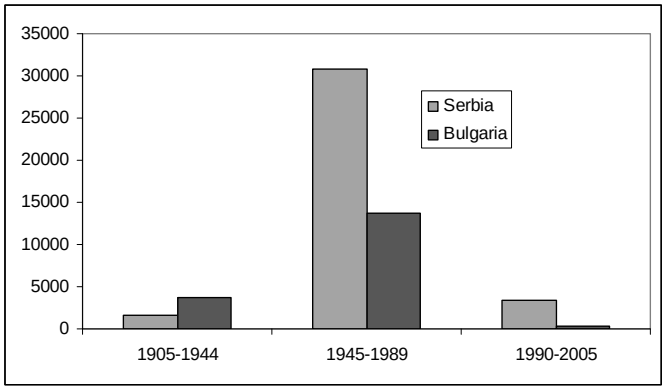

Fig. 13. Comparison of dynamic of annual intensity of building hydraulic structures

5.4.5. Specific Erosion Control Works

Various erosion control works are done in all countries, but there are some specific works that are per country that are not usual for other two countries.

5.4.5.1. Specific erosion control works in Macedonia

The most specific hydraulic structure in Macedonia is screw check dams – Herheulidze type. These structures are built in western part of Macedonia where confirmation type is Alpine type. Erosion intensity is very high, weathering is significant and it result in rock particles with huge dimension. This type of check-dams was built in few torrents in western part of the country.

Fig. 14. Screw chack-dam (barrage) type Herheulidze (torrent Arvati and torrent Pena)

Central part of Macedonia is semiarid area where total annual sum of precipitation is less then 500 even the absolute measured minimal annual sum of precipitation in this area was 195 mm. This region is vulnerable to desertification processes. Various types of afforestation were carried out in this region using various tree species.

Fig. 15. Afforestation in arid region in Macedonia (plantation in holes and in furrows)

5.4.5.2. Specific erosion control works in Serbia

Erosion control expert in Serbia used various types of check dams but the most specific are Rosic – type of barrages.

Fig. 16. Specific checkdamss in Serbia – Rosic type

Fig. 17. Orchardes on teraces in Serbia

Regarding biological works, besid clasical afforestation, the specific of Serbia is plantation of orchardas on erosive land on the hilly – mountainous region.

While in Bulgaria and Macedonia the greates parts of erosive land is state owned, in Serbia significant part of this erosive land is in prvate property. Private owners interest not only to protect land from erosion but to get income from it.

It was the main reasons for forcing orchard production on erosive land in hilly mountain regions in Serbia.

5.4.5.3. Specific erosion control works in Bulgaria

While new trend in stream restoration in Europe is “ecological stream restoration”, it was carried out in Bulgaria long time ago.

Fig. 18. Regulation of river Perperek

Typical example is river Perperek

For restoration of river Perperek were used only natural materails, wood and stone. Structures. In Fig. 17 are presented photoses from differnt period (begining of restoration and after few decades. Now this stream looks very naturaly.

Regrading the biological woorks, it was mentioned that Bulgaria is one of leaders in Europe related to this.

The most specific part of Bulgaria is region of Krdjali where former “rocky desert” through intensive work was transformed to good forest.

5.5. Conclusions

Erosion intensity in Macedonia, Serbia and Bulgaria is between the highest in Europe ant erosion is assigned as one of the most important ecological and economic problems.
Faced with problems with erosion, organized erosion control started in the beginning of the XX century.

The "golden period" of erosion control was period of 1945–1990. After this period is noticed significant decrease of erosion control activities.

Serbia paid more attention to hydraulic structures building. Intensity of 16.82 m^3/km^2 is between the highest in Europe. On the other hand, Bulgaria paid significant attention to afforestation – and was afforested 7.39% of the total area of the country which is the highest in Europe.
Specific hydraulic structures are built in Macedonia – screw check-dams Herheulidze type. Beside it specific for Macedonia is afforestation in extreme arid conditions.

Specific Rosic type check dams are characteristic for Serbia. Beside it, plantation of orchards on terraces in hilly – mountain region is specific.

Beside mass afforestation one of the most specific of erosion control Bulgaria is "ecological river restoration" principle using natural materials: wood and stone that has been using from 50's of the XX century.

References

[1] Biolchev A., Kitin B., Kerenski S., Ochev N., Pimpirev P., Stanev I., Georgiev G., Dimitrov S., Tsvetkov Ts., Kasov D., Tsvetkov M.: Methodology foDeveloping a National Long-term Erosion Control Programme in bulgaria. Ministry of Agriculture, Food Production and Forestry, Sofia, 1977.

[2] Blinkov I., Trendafilov A.: Erosion control works in the Republic of Macedonia – country report International Conference "100 years erosion control in Bulgaria, 18–21 may 2005 Krdjali, Bulgaria.

[3] Blinkov I., Trendafilov A., Andonoska B.: Comparison of the state of the erosion in some Balkan countries, l III Congress of ecologists of Macedonia with international participation 6–9 October 2007, Struga / Macedonia.

[4] Blinkov I., Kostadinov S.: Applicability of various erosion risk assessment methods for engineering purposes, BALWOIS conference, Ohrid 25–29.05.2010.

[5] Daskalov Y.: 90 years soil erosion control in Bulgaria. Sofia, 8–12, 1995.

[6] Gobin A., Campling P., Govers G. [Katholieke Univeriteit Leuven]; Kirkby M. J. [University of Leeds]; Kosmas C. [Agricultural University of Athens]; Jones R. J. A. [Environment Institute, DG-JRC]: Assesment and reporting on soil erosion (Draft background document for the soil erosion workshop at EFA, Copenhagen), KU Leuven, 2001.

[7] Kostadinov S.: Soil Erosion and Sediment Transport in the Torrents of Serbia. XX Conference of the Danubian Countries on "Hydrological Forecasting and Hydrological Bases of Water Management", Bratislava, Slovakia, 4–8 September 2000. Papers on CD. Abstract Book, 76, 2000.

[8] Kostadinov S.: Erosion and Torrent Control in Mountainous Regions of Serbia; Proceedings,Keynote paper; International Year of Mountainous Conference: "Natural and Socio-Economic Effects of Erosion Control in Mountainous Regions; Edited by: M. Zlatić, S. Kostadinov, N. Dragović; Belgrade/Vrujci Spa, Dec.10–13, 2002, 33–56, 2002.

[9] Kostadinov S., Dragovic N.: Eerosion and torrent control in Serbia: experiences and perspectives. International Conference: 100 years erosion control in Bulgaria, 18–21 may 2005 Krdjali, Bulgaria.

[10] Kostadinov S., Markovic S.: Soil erosion and effects of erosion control works in the torrential drainage basins of southeast Serbia Erosion and Sediment Yield: Global and Regional Perspectives (Proceedings of the Exeter Symposium, July 1996). IAHS Publ. no. 236, 321–332, 1996.
[11] Krasteva V.: Soil erosion control under spray irrigation in Bulgaria. Sofia, v. 1, 211, 1984.
[12] Kroumov V., Dochev G.: Soil Erosion Control under Conditions of Private Agriculture in Bulgaria, Lutte contre l'érosion du sol après réforme agraire en Bulgarie http://natres.psu.ac.th/Link/SoilCongress/bdd/symp31/2613-t.pdf (15.04.2011).
[13] Marinov I.: Losses and damgaes fro torrnetial floods, International Conference: 100 years erosion control in Bulgaria, 18–21 may 2005 Krdjali, Bulgaria.
[14] Ministry for agriculture and forestry – Department for forests: Soil erosiin in Bulgaria – state and measures, national report, International Conference: 100 years erosion control in Bulgaria, 18–21 may 2005 Krdjali, Bulgaria.
[15] Morgan R. P. C.: Soil Erosion and Conservation. Longman Scientific and Technical, London, 1986.
[16] Morgan R. P. C.: Soil Erosion in the Northern Countries of the European Community. EIW Workshop: Elaboration of a Framework of a Code of Good Agricultural Practices, Brussels, 21–22 May 1992.
[17] Necdet Özyuvacú 1, Süleyman Özhan 1, ErtuXrul GörcelioXlu 2: Integrated watershed management for sustainable development of renewable natural resources, 263, http://www.fao.org/forestry/docrep/wfcxi/PUBLI/PDF/V2E_T9.PDF (22.04.2011).
[18] Oldeman L. R., Hakkeling R. T. A., Sombroek W. G.: Word Map of the status of human-induced soil degradation, and explanatory notes, Global Assessment of Soil Degradation (GLASOD), ISRIC, Wageningen, The Netherlands, 1991.
[19] Petkovic S., Dragovic N., Markovic S.,: Erosion and sedimentation problems in Serbia, Hydrological Sciences Journal des Sciences Hydrologiques, 44(1) February 1999.
[20] Regional departmet of forest – Krdjali – Eroison control in Krdjali region, International Conference: 100 years erosion control in Bulgaria, 18–21 may 2005 Krdjali, Bulgaria.
[21] Rouseva S., Lazarov A., Stefanova V., Malinov I.: Soil Erosion Risk Assessments in Bulgaria, BALWOIS conference, Ohrid 25–29.05. 2008.
[22] Van Lynden G. W. J.: European Soil Resources. Current Status of Soil Degradation, Causes, Impact and Need for Action. Council of Europe Press. Nature and Environment, No 71, Strasbourg, France, 1995.
[23] WDI – Water Development Institute of Macedonia, Erosion Map of the Republic of Macedonia 1993.
[24] http://eros.usgs.gov/#/Find_Data/Products_and_Data_Available/gtopo30/hydro/europe
[25] http://eros.usgs.gov/#/Find_Data/Products_and_Data_Available/gtopo30/hydro/europe
[26] (http://www.eea.europa.eu/data-and-maps/figures/water-erosion-in-europe-1993)

APPENDIX – Effects of afforestation

Serbia

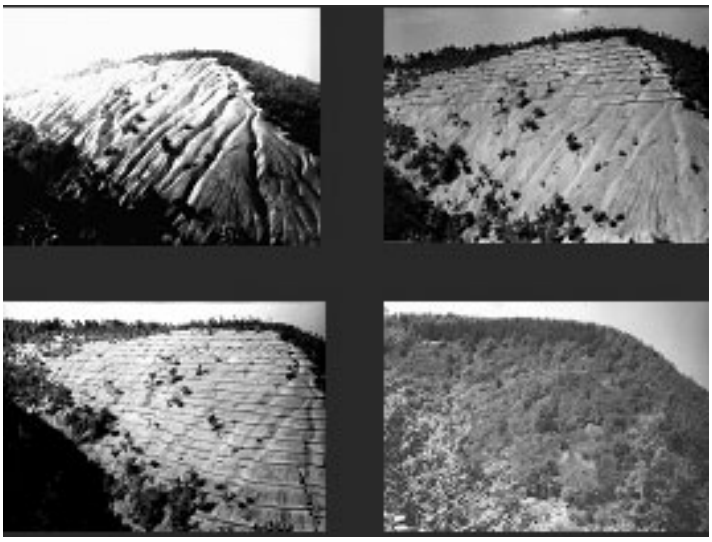

1958 2005

Serbia

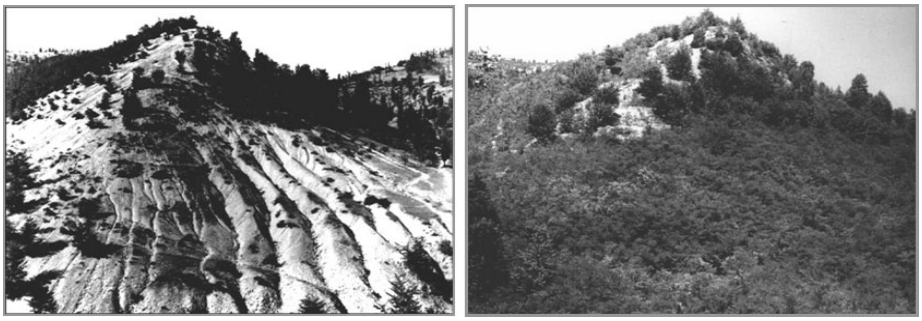

1958 2003

Bulgaria

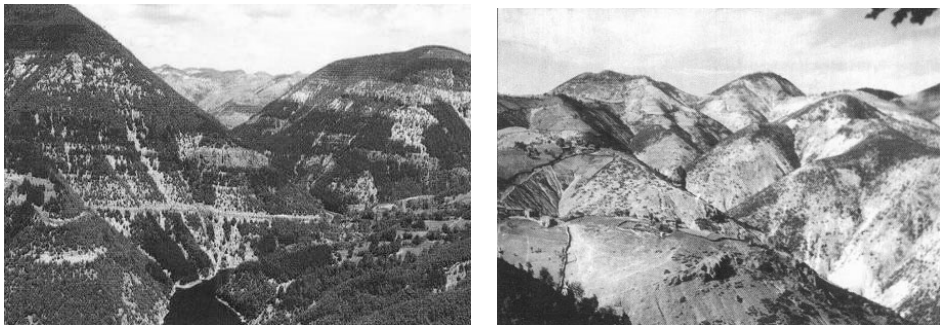

1995 2005

6 An Easy to Use Calculation Method of Weir Operations in Controlled Drainage Systems

Barbara Bohne, Isidor Storchenegger (Universität Rostock, 18059 Rostock, Germany), Peter Widmoser (Christian-Albrecht-Universität, 24098 Kiel, Germany)

6.1. Introduction

To support local and regional authorities, agencies and engineers in charge with rural water management we developed a model to simulate unsteady discharge and recharge of land drainage systems controlled by weirs or orifices.
To avoid the integration of partial differential equations we considered a system consisting of three reservoirs: the reservoir recipient (S_R), the reservoir saturated soil (groundwater S_{GW}) and the reservoir unsaturated soil (capillary water S_C).Since storage S of reservoirs only varies with time t a set of ordinary differential equations is adequate to simulate dropping and rising of water tables in ditches and soil.

6.2. Reference Layout of a Controlled Drainage System

A simple layout of a land drainage system serves as a reference system to illustrate the mode of operation, the models underlying the simulation, and the effectiveness of a management of controlled drainage systems.

The reference system consists of a ditch of 1000 m length as recipient and laterals on either side of the ditch with a length of 200 m. The drain spacing may be varied to study its effect. The slope of the ditch is 0.005 while the laterals are supposed to be horizontal. The roughness coefficient of the ditch is taken according to the chosen maintenance schedule.

6.3. Reservoirs and Their Equations

The storage equation is used to describe the unsteady process in the reservoirs mentioned above. That means: The difference between inflow $Q_I(t)$ and outflow $Q_O(t)$ equals the derivative of the storage S with respect to time t. The storage equation is commonly transformed to establish a relation between a representative water table elevation z and the time t:

$$\frac{dS(z(t))}{dt} = Q_I(z(t)) - Q_O(z(t)) = \frac{dS}{dz}\frac{dz}{dt} \quad \rightarrow \quad \frac{dz}{dt} = \frac{= Q_{in}(z(t)) - Q_{out}(z(t))}{\frac{dS}{dz}} \tag{1}$$

6.3.1. The Reservoir “Soil”

The storage of the reservoir “soil” (Fig. 1) is obtained from

$$S = 2l_L \cdot l_R \cdot \left(\theta_s \cdot \left(z_{GW} - z_{Barr}\right) + \int_{hp=0}^{hp=zG-zGW} \theta\left(h_p = z - z_{GW}\right) \cdot dh_p \right)$$

Whereas soil water content Θ in the saturated zone is constant Θ_S, it decreases in the unsaturated zone with increasing elevation from groundwater table (6). Assuming hydrostatic equilibrium between soil water pressure and elevation above groundwater table, soil water content reflects the soil water retention characteristic $\Theta(h_P)$ [1].

Midpoint Elevation. Assuming the curvature of the groundwater table to be of elliptic shape during drainage [2] as well as during imbibition [3] and assuming the major axis of ellipse to be located at the level z_{WR} of the water table in ditch, then the average elevation of groundwater z_{GW} is positioned at $\pi/4$ of the distance between the ellipse axis and the elevation z_M of the most distant point of the curvature (Fig. 1). With $c_F = \pi/4$ the relation between recipient water table z_{WR}, groundwater table z_{GW}, and the groundwater midpoint elevation z_M can be written as

$$z_{GW} = z_{WR} + c_F \cdot \left(z_M - z_{WR}\right) \quad \Rightarrow \quad z_M = \frac{1}{c_F} \cdot z_{GW}(t) - \frac{1 - c_F}{c_F} \cdot z_{WR} \tag{2}$$

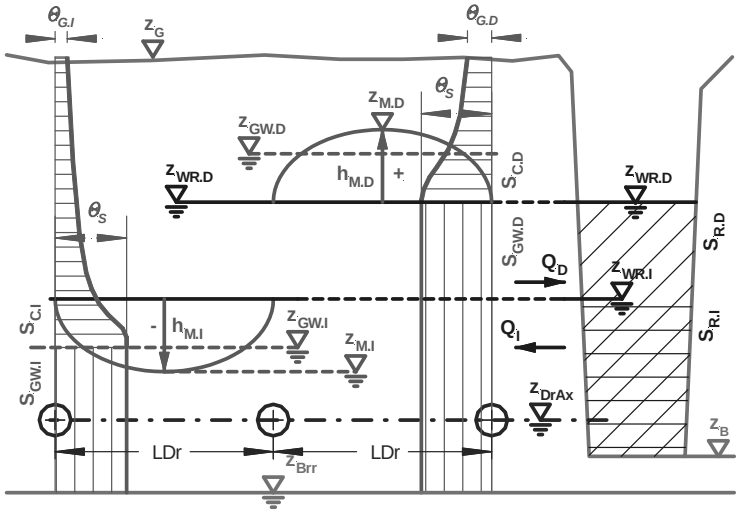

Fig. 1. Cross sections with groundwater table between drains during imbibition (left) and drainage (middle), related to the water table in the ditch (right) – not to scale

The midpoint elevation z_M drives discharge and recharge of the drain field. Its derivative with respect to time serves to define the initial conditions more precisely and helps moreover to stabilize the numerical integration.

$$dz_M = \frac{\partial z_M}{\partial z_{GW}} \cdot \frac{\partial z_{GW}}{\partial t} \cdot dt + \frac{\partial z_M}{\partial z_{WR}} \cdot \frac{\partial z_{WR}}{\partial t} \cdot dt \quad \Rightarrow \quad \frac{dz_M}{dt} = \frac{1}{c_F} \cdot \frac{dz_{GW}}{dt} - \frac{1 - c_F}{c_F} \frac{dz_{WR}}{dt} \tag{3}$$

Storage Equation of Groundwater. The storage $S_{GW}(z_{GW})$ of groundwater in a drain system may be written as

$$S_{GW} = 2l_L \cdot l_R \cdot \theta_S \cdot \left(z_{GW} - z_{Brr}\right) = 2l_L \cdot l_R \cdot \theta_S \cdot \left(c_F \cdot z_M + \left(1 - c_F\right) \cdot z_{WR} - z_{Brr}\right) \tag{4}$$

The derivatives of the storage with respect to average groundwater elevation z_{GW} and the midpoint elevation z_M are given as

$$\frac{\partial S_{GW}}{\partial z_{GW}} = 2l_L \cdot l_R \cdot \theta_S \; ; \qquad \frac{\partial S_{GW}}{\partial z_M} = \underbrace{2l_L \cdot l_R}_{A_E} \cdot \theta_S \cdot c_F \tag{5}$$

Storage Equation of Soil Moisture. The storage S_C of capillary water is assumed to change with the average groundwater table z_{GW}. According to the above mentioned equilibrium assumption, it is governed by the water retention curve, which relates the soil water content to the capillary pressure head h_P. Hence the capillary pressure head h_P in the vadose zone equals the distance to the averaged water table.

$$S_C = \int_{hp=0}^{hp=zG-zGW} \theta\left(h_p = z - z_{GW}\right) \cdot dh_p = \int_{hp=0}^{hp=zG-zGW} \left(\theta_r + \frac{\theta_S - \theta_r}{\left(1 + \left(\alpha \cdot \left|h_P\right|\right)^{ng}\right)^m} \right) \cdot dh_p \tag{6}$$

The area of the cross section is given by the integral with respect to the capillary pressure head h_P from zero to the distance from the ground surface z_G to the groundwater table.

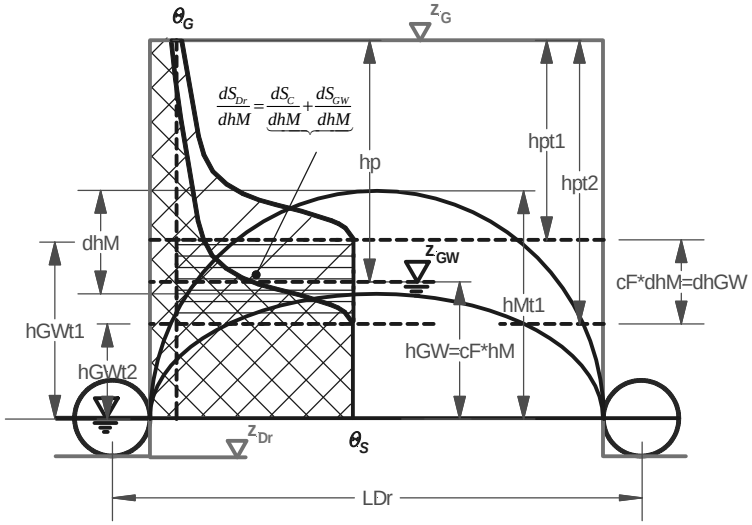

Fig. 2. Groundwater and soil moisture in a drained field showing the meaning of storage equation: the closer the groundwater table to the ground surface, the less precipitation is needed to fill it totally and to start surface runoff– not to scale

Due to the transformation given in Eq. (1), not the integral but its derivative is needed, what at any instant equals the value of the water retention curve at the surface z_G.

$$\frac{\partial S_C}{\partial z_{GW}} = \frac{\partial\left(A_E \cdot \int_{hp=0}^{hp=zG-zGW} \theta(h_p)\cdot dh_p\right)}{\partial z_{GW}} = 2l_L \cdot l_R \cdot \theta(z_G - z_{GW}(t)) \cdot \underbrace{\frac{\partial h_p}{\partial z_{GW}}}_{-1} \tag{7}$$

In conformance with Eq. (1) the storage equation for the soil may be deduced from

$$\frac{d[S_{GW}(z_{GW}) + S_C(z_{GW})]}{dt} = \frac{dz_{GW}}{dt}\left[\frac{dS_{GW}}{dz_{GW}} + \frac{dS_C}{dz_{GW}}\right] = \frac{dz_{GW}}{dt} \cdot A_E \cdot [\theta_S - \theta(z_G - z_{GW})] \tag{8}$$

leading to

$$\frac{dz_{GW}}{dt} = \frac{Q_{In}(z(t)) - Q_{Out}(z(t))}{A_E \cdot [\theta_S - \theta(z_G - z_{GW})]} = \frac{q_I \cdot A_E - q_{Dr}(z_{WR}, z_{GW}) \cdot A_E}{A_E \cdot [\theta_S - \theta(z_G - z_{GW})]} = \frac{q_I - q_{Dr}(z_{WR}, z_{GW})}{[\theta_S - \theta(z_G - z_{GW})]} \tag{9}$$

Inflow and outflow. Both parts of the soil reservoirs are mainly discharged and recharged by underdrains. The flow between ditch and drained field is driven by the difference between the elevation of the water table in the ditch z_{WR} and the midpoint elevation z_M of groundwater in the drain field. Discharge Q_{Dr} is given by the Hooghoudt-Equation [5] (Eq. (10)) and recharge $\boldsymbol{Q_{Irr}}$ is given by the Ernst-Equation [3] (Eq. (11)),

$$Q_{Dr} = A_E \cdot q_{Dr}; \quad q_{Dr} = \frac{4[z_M(t) - z_{WR}(t)]}{l_{Dr}^2} \cdot [2k_{DU} \cdot d + k_{DL} \cdot (z_M(t) - z_{WR}(t))] \tag{10}$$

$$Q_{Irr} = A_E \cdot q_{IDr}; \quad q_{Irr} = \frac{4[z_M(t) - z_{WR}(t)]}{l_{Dr}^2} \cdot \left[2k_{DU} \cdot d + k_{DL}\frac{d}{h_{Du}} \cdot (z_M(t) - z_{WR}(t))\right] \tag{11}$$

where q_{Dr} is the drainage rate with the same units like the permeability k_{Du} of the upper layer and k_{DL} of the lower layer of drained soil and d is the thickness of a compensatory layer. q_{Irr} is the recharge rate in case of subirrigation.

Beside the recharge by the drain system the inflow q_I may also result from infiltration. The solution of Eq. (9) has been compared with reliable numerical solutions and yielded good results [4].

6.3.2. The Reservoir "Ditch"

Storage equation. Since the ditch is considered as a prismatic channel, its storage is given by the cross-sectional area $A_R(z_{WR})$ multiplied by the ditch length l_R. The cross-sectional area is the integral of the water table width b_{WR} with respect to the water depth $h_R = z_{WR} - z_B$ from zero to $z_{WR} - z_B$. In conformance with Eq. (1) the storage equation and its transformation may be written as

$$S_R(z_{WR}) = l_R \cdot \int_{z=zB}^{z=zWR} b_{WR}(z)\cdot dz \;\rightarrow\; \frac{dS_R}{dz_{WR}} = \frac{d\left(l_R \cdot \int_{z=zR}^{z=zWR} b(z)\cdot dz\right)}{dz_{WR}} = b_{WR}(z_{WR}) \cdot l_R \tag{12}$$

and the equation for water table routing in the ditch becomes

$$\frac{dz_{WR}}{dt} = \frac{Q_{IR}(t) - Q_{OR}(z_R(t))}{b_{WR}(z_{WR}(t)) \cdot l_R} \tag{13}$$

Inflow. Inflow Q_{IR} to the recipient may occur as drainage discharge Q_{Dr} (Eq. (10)). Upstream tributaries may also contribute. Vice versa outflow may occur as recharge Q_{Irr} (Eq. (11)) by subirrigation and as outflow Q_{OR} through the outlet structure.

Outflow. Various types of gates are suitable to control the water table in a ditch in order to control discharge and recharge of land drainage system or to keep the groundwater table at a distinct level in the steady state. Hence a combination of vertical lift gates and hook gates is widely used (Fig. 3). The calculation of the outflow is directed by the hydraulics of weir flow and orifice flow.

Weir flow is governed by the weir equation [6] of Darcy-Weisbach (Eq. (14)), which in a simpler form is known as Poléni-Equation,

$$Q_{O.Weir} = \xi \cdot \frac{2}{3} \cdot \mu \cdot \sqrt{2g} \cdot l_{Cr.} \cdot \left[\underbrace{\left(h_{Weir} + \frac{v_R^2}{2g} \right)^{\frac{3}{2}}}_{hER} - \left(\frac{v_R^2}{2g} \right)^{\frac{3}{2}} \right] \approx \xi \cdot \frac{2}{3} \mu \cdot l_{Cr.} \cdot \sqrt{2g} \cdot h_{Weir}^{\frac{3}{2}} \tag{14}$$

where $Q_{O.Weir}$ is discharge over a gate as a weir, g is acceleration of gravity, $h_{Weir} \approx (z_{WR} - z_{Cr})$ is the weir head, z_{Cr} is the elevation and l_{Cr} is the length of crest. The weir coefficient μ accounts for influences of the weir type (Eq.15) and can be affected by the height of the weir $h_d = z_{Cr} - z_B$. And the submergence factor ξ (Eq. (16)) corrects for submerged flow (Fig. 4).

If the elevation of tailwater rises sufficiently over the weir crest or over the issuing jet of an orifice, the discharge rate of both, weir and orifice is affected by submergence (Fig. 3, Fig. 4). If the flow in the ditch cannot fill the orifice (Fig. 4) nonuniform open channel flow will occur.

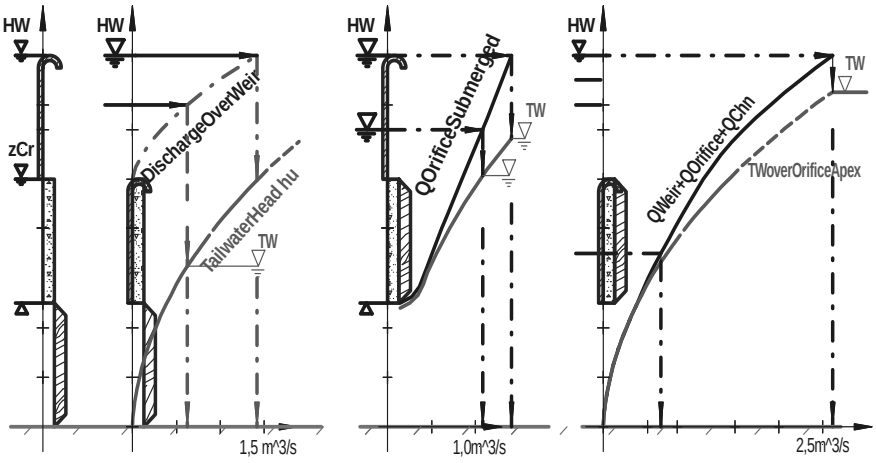

Fig. 3. Outlet structure combining a vertical hook gate and a leaf gate showing different gate positions and their outflow-characteristics

For gates which are usually installed in recipients, the weir coefficient μ (Eq. (15)) of beveled stop logs [6] and the submergence factor ξ (Eq. (16)) of the standard weir [7] seems to be adequate.

$$\mu_{SL} = 0.6035 + 0.0813\frac{h_{Weir}}{h_d}\left(1 - 0.20\exp\left(-0.60\left(\frac{h_{Weir}}{d_{Cr}}\right)^{3.06}\right)\right)\cdot 1.1\exp\left(-0.037\left(\frac{h_{Weir}}{d_{Cr}}\right)^{0.6}\right) \quad (15)$$

$$\xi = 1 - 0.1273\cdot\left(\frac{h_{Weir.TW}}{h_{Weir}}\right)^{0.6}\exp\left(1.6866\frac{h_{Weir.TW}}{h_{Weir}}\right) \quad (16)$$

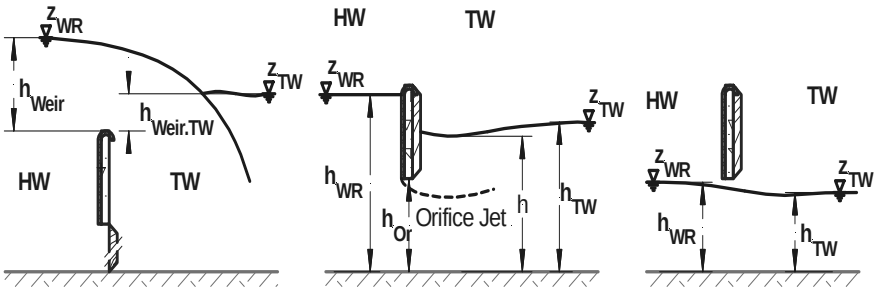

Fig. 4. Definition sketch illustrating different flow conditions at outlet structure

Orifice flow is calculated by an improved Toricelli-Equation which reads

$$Q_{O.Or}(z_{WR}) = \psi \cdot h_{Or} \cdot b_{Or} \cdot \sqrt{\frac{2g \cdot h_R(z_{WR})}{\frac{h_R(z_{WR}) + \psi \cdot h_{Or}}{h_R(z_{WR})}}} \quad (17)$$

where $Q_{O.Or}$ is the discharge through gated openings, which is similar to the flow through an orifice, ψ represents design variables of the gate, h_{Or} and b_{Or} are height and width of the opening, and $h_R(z_{WR})$ is the water depth in the recipient close to the opening [2].

While the submergence factor reduces the discharge over a weir, submerged orifice flow is described by different formulas.

If the bottom elevation z_B is taken constant next to the outlet structure and water depth h_{TW} is the difference between tailwater elevation z_{TW}, and bottom z_B, then the tailwater depth h close to the orifice is given by

$$h = \frac{2\mu \cdot h_{Or}}{h_{TW}} \cdot (h_{TW} - h_{Or}) + \sqrt{\left(\frac{2\mu \cdot h_{Or}}{h_{TW}} \cdot (h_{TW} - h_{Or})\right)^2 + h_{TW}^2 - \frac{4\mu \cdot h_{Or}}{h_{TW}} \cdot (h_{TW} - h_{Or}) \cdot h_R(z_{WR})} \quad (18)$$

Then the discharge through a submerged orifice becomes:

$$Q_{O.Or}(z_{WR}, z_{TW}) = \mu \cdot h_{Or} \cdot b_{Or} \cdot \sqrt{2g \cdot (h_R(z_{WR}) - h(z_{TW}))} \quad (19)$$

Discharge through the outlet structure is affected by the downstream water depth which is calculated for the reference system by the continuity equation (Eq. (20)) based on uniform channel flow, where A_{TW} is the cross-sectional area, n_M is Manning's roughness coefficient and r_{TW} is the hydraulic radius.

$$Q_{O.Weir}(z_{WR}, z_{TW}) + Q_{O.Or}(z_{WR}, z_{TW}) - A_{TW} \cdot \frac{1}{n_M} \cdot r_{TW}^{\frac{2}{3}} \cdot I_B^{\frac{1}{2}} = 0 \tag{20}$$

The water table elevation z_{WR} in the recipient results from the integration procedure of Eq. (13). According to the analysis above, weir flow $Q_{O.Weir}$ (Eqs. (14), (15), (16)) and orifice flow $Q_{O.Or}$ (Eqs. (17), (18), (19)) are functions of z_{WR} as well as of the tailwater table z_{WT}. Substituting these functions in Eq. (20) the continuity equation Eq. (20) is solved to get z_{WT} leading to the values of $Q_{O.Weir}$ and $Q_{O.Or}$.

The relationship between $Q_{O.Weir}$ and $Q_{O.Or}$ on the one hand and z_{WR} and z_{WT} on the other hand is to establish before integrating Eqs. (3), (9) and (13).

Nonuniform flow. If the headwater is lower than the orifice apex, nonuniform open channel flow through the outlet structure occurs. Assuming uniform flow in the downstream the continuity equation leads to an expression for the discharge $Q_{OR}(z_{TW})$ through the structure, which has to satisfy the Bernoulli-Equation of nonuniform flow, where h_L is the total loss of head, ζ_E stands for entrance losses, ζ_A for enlargement losses and β is the angel between the wingwalls of the outlet structure and flow direction.

$$\begin{aligned}
&\left(z_{WR} + \frac{v_R^2}{2g}\right) - \left(z_{TW} + \frac{v_{TW}^2}{2g}\right) - h_L = 0; \qquad z_{Or} = \frac{z_{WR} - z_{TW}}{2};\\
&Q = A_{TW} \cdot \frac{1}{n_M} \cdot r_{TW}^{\frac{2}{3}} \cdot I_B^{\frac{1}{2}};\\
&z_{WR} - z_{TW} + \frac{Q^2}{2g} \cdot\\
&\cdot \left[\left(\frac{1}{A_R^2(z_{WR})} - \frac{1}{A_{TW}^2(z_{TW})}\right) - \left(\frac{1}{\zeta_E} - 1\right)\frac{1}{A_{Or}^2(z_{Or})} - \frac{\xi_A}{A_{Or}^2(z_{Or})}\left(1 - \frac{A_{Or}(z_{Or})}{A_{TW}(z_{TW})}\right)^2\right] = 0\\
&\zeta_E\left(\frac{A_R}{A_{Or}}\right) = 0{,}5905 + 0{,}3126\frac{A_R}{A_{Or}} - 0{,}7831\left(\frac{A_R}{A_{Or}}\right)^2 + 0{,}8746\left(\frac{A_R}{A_{Or}}\right)^3;\\
&\text{for } \beta > 60°: \ \zeta_O(\beta) = 1
\end{aligned} \tag{21}$$

Due to the short way through the structure friction in the contraction is neglected.

6.4. Numerical Solution

To support local agencies and practicing engineers we implemented a solution in EXCEL assuming that everybody is familiar with this package.

EXCEL offers the possibility to solve nonlinear equations like Eq. (20) and Eq. (21) but routines for interpolation and for integration of ordinary differential equations are missing.

A cubic polynomial regression has been applied to obtain the best-fit head-discharge relationship between upstream water table elevation and downstream elevation (e.g. curves of Fig. 3). The water table elevations in the ditch are given by fixed levels. If a change of the configuration of the gates leads to a change of the tailwater elevations EXCEL's RGP-routine automatically redefines the regression parameters.

The numerical solution of Eqs. (3), (9) and (13) is done by the predictor-corrector method of HEUN. Disadvantage of the implicit method is that a change in input data leads

to a sudden change of the entire solution, while the explicit method calls for macros for a stepwise solution of implicit equations. The implicit method is handicapped by the disability of EXCEL to start the SOLVER by macros.

A programmer would prefer to implement the equations in Mathlab or Octave. These packages contain comfortable routines for interpolation, solving instantaneous equations and integration of ordinary differential equations, but these tools are rarely used among engineers.

Despite of all its limitations the EXEL-program enables practicing engineers familiar with EXCEL to tackle unsteady discharge and recharge of controlled drainage systems, a matter that so far was done by researchers exclusively.

Furthermore, it helps to solve many others problems of nowadays rural water resources engineering:

— Answering the question, which land drainage system is favorable for distinct goals of rural water management
— deducing operation rules for outlet structures
— decision making on daily operation of controlled drainage and subirrigation
— decision making on hazard fighting
— planning land drainage systems according to new design criteria
— data acquisition of the hydraulic cycle in order to supply storage routing and flood routing in larger catchment areas.

6.5. Problems to Cope With

In the last two decades Europe's large river systems like Rhine river, Oder/Odra river and Elbe river carried extreme floods and became a hazard to all activities along their banks. As in the decades before many structural measures have been undertaken to mitigate flood damage, hydrologists gained the understanding, that appropriate rural water management may reduce flood runoff. Therefore Germany runs a program „Wasserwirtschaft in der Fläche", i.e. water management on the catchment scale.

On the other hand the HELCOM Baltic Sea Action Plan aspires "to restore the good ecological status of the Baltic marine environment by 2021". It forces the adjoining coastal states to reduce their phosphorus and nitrogen input to the Baltic.

We recognized controlled drainage systems as appropriate facilities to mitigate flood as well as to reduce phosphorus and nitrogen leakage [8]. Controlled land drainage systems will become an important feature in order to manage rural water resources which comprise the major part of all large scale water management systems.

Our mathematical program may be useful to evaluate suitable drainage systems, to operate weirs (preferably remote controlled) based on weather forecast in order to store precipitation thereby mitigating floods, reducing erosion and controlling nutrient leakage as well as providing for optimal water supply for agricultural production and for distinct habitat conditions.

6.5.1. Decision Making on Evaluating Suitable Systems

Drainage systems in the plains adjacent to the southern coast of the Baltic are preferably eligible for controlled drainage. Though, not all are appropriate either physically or economically. A widely held belief recognizes peat land preferable for flood mitigation.

We compared the effectiveness of controlled drainage in a mineral soil and in an organic soil [9] assuming both were designed according the German Standards for land

drainage [10]. Fig. 5 and Fig 6 illustrate the results of our calculations. It is assumed that in the beginning both soils are saturated up to the surface.

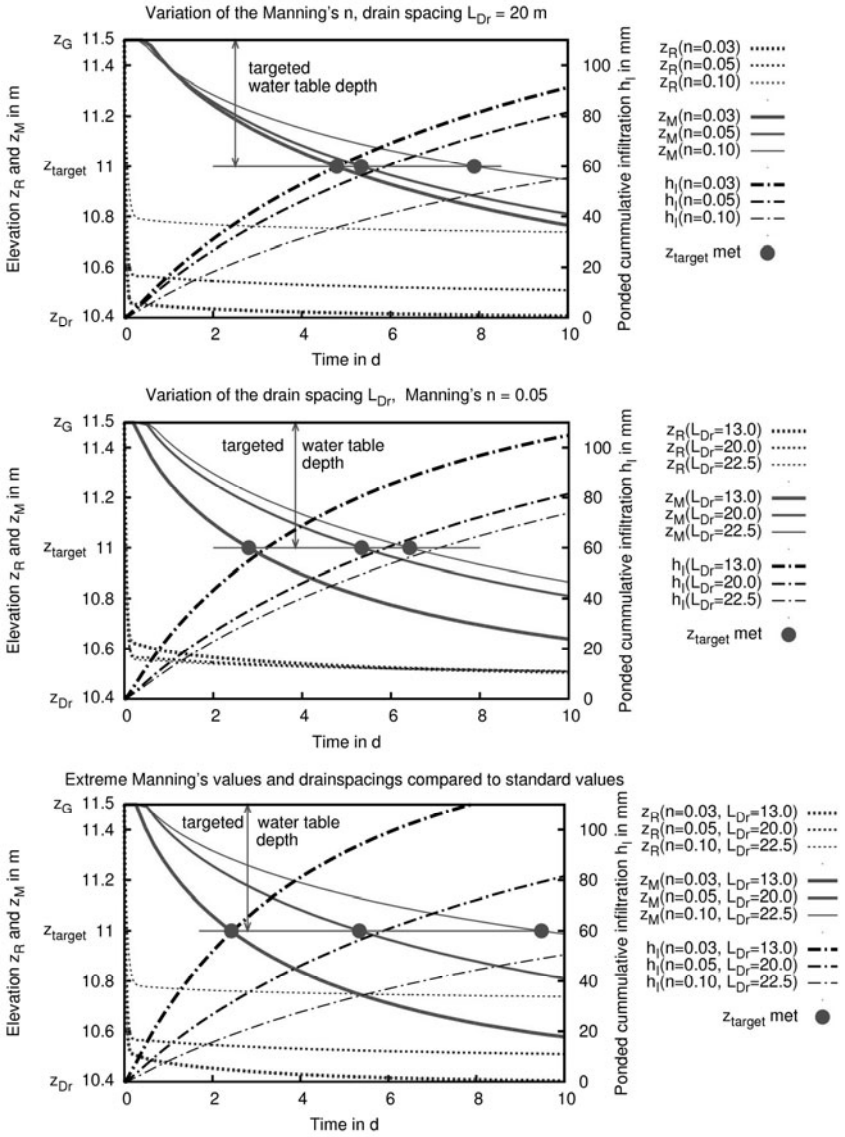

Fig. 5. Calculated drawdown of water table in a mineral soil: Diagrams showing the effect of drain spacing and roughness coefficient by controlling drainage for arable land. A drainage system of arable land designed according to German standards is gentle affected by a bad maintenance of ditches. A 10% larger spacing nearly doubles the time need to reach the target elevation. Reducing the drain spacing doesn't reduce the time lag a lot. Dropping the water table to the target elevation provides an infiltration capacity of nearly 60mm. Only the smallest drain spacing creates that capacity within the forecast horizon of 3 days

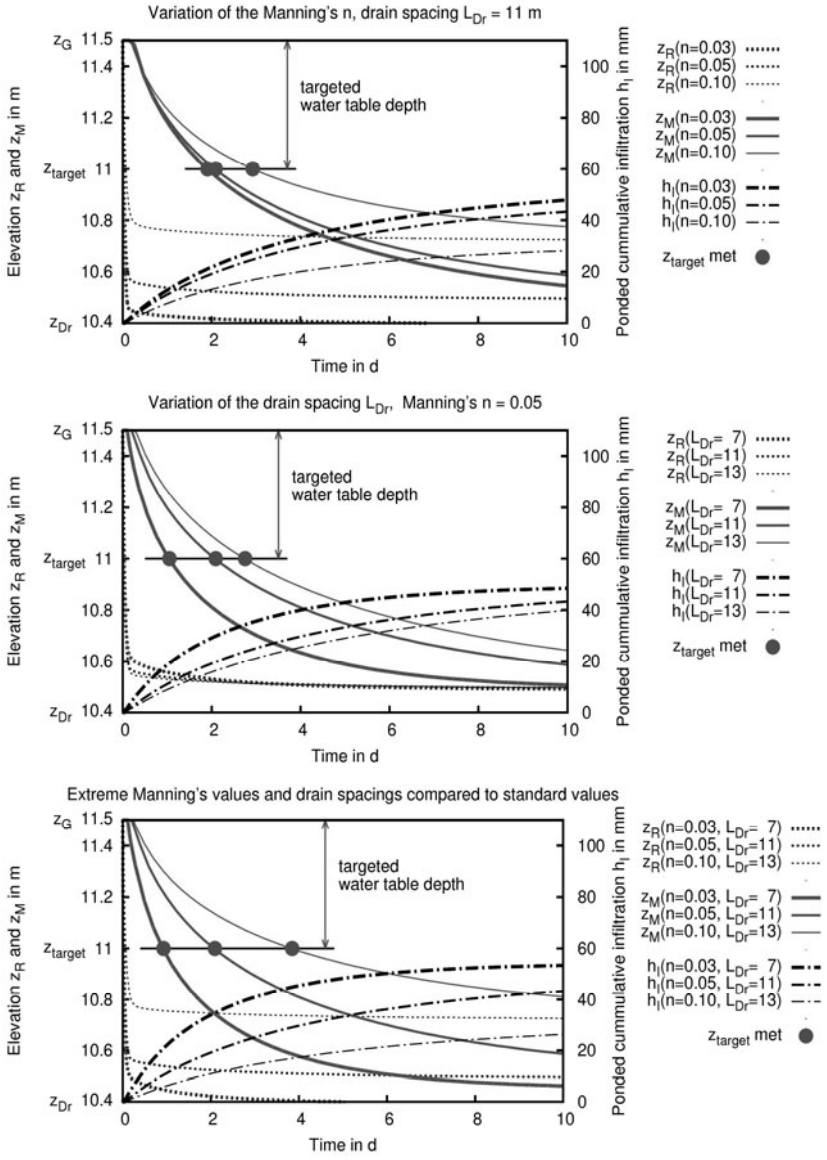

Fig. 6. Calculated drawdown of water table in an organic soil: Diagrams showing the effect of drain spacing and roughness coefficient by controlling drainage of peat land. The top elevation of groundwater drops quickly to the targeted elevation but infiltration capacity created within the forecast horizon of 3 days is less than that of mineral soil. Maximum infiltration capacity of 50mm provides a drain spacing of 7m and a well maintained ditch

Tough the midpoint groundwater elevation drops quick below the permissible maximum level according to German Standards, due to the soil properties of peat land, less infiltration capacity is caused after discharging during the forecast horizon of 3 days. It follows that cultivated organic soils are not favorable for flood mitigation.

Furthermore the diagrams prove that neglected maintenance (only once a year) affects the time lag for dropping appreciably. To avoid phosphorus leakage caused by surface runoff, an adequate infiltration capacity should be maintained by drainage. A hydraulic gradient into the soil reduces seepage failure (“micro soil heaves”, “micro blowups”), the main cause of erosion.

6.5.2. Deducing Operation Rules for Controlled Drainage Systems

Different adjacent land uses are often the cause conflicts. Such conflicts suggest to elaborate and to implement operation rules of controlled drainage systems. Pressure groups have to be satisfied by demonstrating how their interests are affected by different ways of operating.

Peat land should be kept saturated as long as possible in spring. An adjacent farmer wants the field to be ready for tillage operations as early as possible in the spring. If the simulation assures him of draining the field within 3 to 5 days, he may agree.

Supposed the main target of controlled drainage would be flood mitigation and drain spacing is 20m, then in discussion with pressure groups we could offer the following:

If for saving nutrients the water table is at ground surface, then within the forecast horizon of 3 days the system could prepare the soil for a precipitation of 35mm during winter time and also in summer provided the ditch is well maintained. The latter may evoke resistance of conservationists. It’s to argument how much interferences are needed to create an acceptable infiltration capacity and to avoid harmful disturbance of a habitat.

6.5.3. Decision Making on Daily Operating

Daily operating has to be in accordance with the operating rules and the weather forecast and meet the needs of agricultural production as well as those of habitat conditions.

6.5.4. Decision Making on Hazard Fighting

If a hazard occurs to a recipient and if the recipient is well partitioned by controlling structures, the pollutants may be kept in the reach between the control structures. In order to prevent recharge to avoid contamination through the drainage system the calculation has to answer the question: At which elevation the water table should be kept to guarantee drainage discharge at that amount that might be pumped away by disaster control.

6.5.5. Data Acquisition and Remote Controlled Drainage

Remote controlled weirs require data transfer between weir and operator. Data logging of upstream and downstream water level permit the operator to control the gates in order to achieve levels and discharges according to agreed guidelines. If the operations and water levels are recorded the weir equations of the calculation programs serve to determine a quite accurate runoff hydrograph. Additionally recorded meteorological data in the catchment area may be used to balance the water cycle and to determine evapotranspiration.

For this purpose Eqs. (14), (17) or (21), respectively, have to be modified in such a way that the discharges $Q_{O.Weir}$ and $Q_{O.Or}$ are the unknowns to be found by solving the equations. Yet in Eq. (21) discharge Q_{OR} is not to be substituted by the Manning formula.

6.5.6. New Design Criteria for Land Drainage

In addition to support decision making in operating facilities the program may serve to design or redesign devices as weirs, ditches and land drainage systems in accordance with new design criteria.

The design criteria for land drainage in use are deduced from the objective to remove a certain amount of excess water of the soil in a reasonable time. This requires calculations of unsteady drainage. An engineer with his earlier modest tools couldn't do that. Thus standards simplified the basic goal. A drainage modulus or drainage coefficient, the amount of water that should be removed during a distinct duration or at a groundwater level at a distinct elevation became the design criterion. The amount of water to be removed by drainage usually is related to a precipitation rate.

We propose to request that drainage systems lowers the groundwater table within 1 to 3 days in agreement with agricultural requirements – or for other land uses of interest, e.g. sport (e.g. to a level at which the water content provides sufficient consistence for targeted use).

6.6. Suitable Outlet Works

In order to face the nowadays problems of water-resources the authors propose a water management based on modern, comfortable software and appropriate facilities such as:

— remote operated weirs equipped with fish passes and designed with respect to agreed management rules,
— renewed and improved drainage systems with drain spacing according to water management objectives of the region.

The offered software enables local agencies and engineering enterprises to cope with these tasks and to contribute to flood mitigation and to pollutant control.

Notations

A_E – catchment area
$A_{Or/R/TW}$ – cross-sectional area in gate opening / recipient / tailwater
b_{Or} – width of gate opening
b_{WR} – water table width
c_F – shape factor
d – equivalent thickness
d_{Cr} – width of crest in longitudinal section
g – acceleration of gravity
α – van-Genuchten parameter of water retention curve
h_P – capillary pressure head
h_L – total loss of head
$h_{R/TW}$ – water depth of ditch / tailwater
$h_{Weir/Or}$ – upstream head on weir / head on gate opening
I_B – bottom slope
$k_{Du/DL}$ – permeability of upper / lower soil layer
l_{Cr} – width of crest in cross section

$l_{L/R}$ – length of laterals / recipient
m – van-Genuchten parameter of water retention curve
n_g – van-Genuchten parameter of water retention curve
n_M – Manning's roughness coefficient
$Q_{I/In}$ – Inflow
$Q_{O,Out}$ – Outflow
Q_{Irr}/q_{Irr} – recharge / recharge rate (subirrigation)
Q_{Dr}/q_{dr} – discharge / discharge rate (drainage)
r/r_{TW} – hydraulic radius in ditch / tailwater
$S_{GW/C}$ – water storage of saturated zone (groundwater) / vadose zone
t – time
v – velocity of flow
$z_{G/GW/Barr}$ – elevation of ground surface / mean groundwater level / impervious barrier
α – van-Genuchten parameter of water retention curve
β – angle of enlargement
μ – weir coefficient
ψ – orifice coefficient
θ – volumetric water content
θ_r – van-Genuchten parameter of water retention curve
θ_s – volumetric water content of saturated soil
$\zeta_{E/O}$ – coefficient of velocity head for losses of entrance / enlargement
ξ – weir submergence factor

References

[1] van Genuchten M.Th.: A closed form equation for predicting the hydraulic conductivity of unsaturated soils. Soil Sci. Soc. Am. J., 44, 892–898.
[2] Dracos T.: Hydraulik – Vorlesungsunterlagen. Wiesbaden: vdf Verlag der Fachvereine Zürich 1990.
[3] Ernst F. L.: Formulae for the groundwater flow in areas with sub-irrigation by means of open conduits with a raised water level. Archiwum Hydrotechniki, 22, H.1, 4–30, 1975.
[4] Storchenegger I., Bohne B.: A New Solution to Non-steady Drain Discharge. In: Proceedings ICID 21st European Regional Conference on Integrated Land and Water Resources Management: Towards Sustainable Rural Development 2005.
[5] Hooghoudt S.: Algemene beschouwing van het probleem van de detailontwatering en de infiltratie door middel van parallel loopende drains, greppels, slooten en kanalen. Bodemkundig Instituut te Groningen, No. 7 (in Dutch) 1940.
[6] Peter G.: Überfälle und Wehre – Grundlagen und Berechnungsbeispiele. Wiesbaden: Vieweg Verlag 2005.
[7] Schmidt M.: Die Berechnung unvollkommener Überfälle. Wasserwirtschaft, 47, 174–178 (in German) 1957.
[8] Storchenegger I.: Erarbeitung von Wehrreglementen zur Steuerung des Bodenwasser-haushaltes. In: Kulturtechnik-Tagung 21./22. Nov. 2007: Ostseeverschmutzung und Flächenentwässerung, Bd 6. Universität Rostock ISBN 978-3-86009-018-3, 2007.
[9] Storchenegger I., Bohne B., Widmoser P.: Ein praktisches Berechnungsverfahren zur Regelung von Dränsystemen durch Kulturstauen. Wasserwirtschaft 3, 2011.
[10] Widmoser P.: Kap. 10 „Be- und Entwässerung" in Lecher, K. et al.: Taschenbuch der Wasserwirtschaft. Berlin: Parey Verlag 2001.

7 Navigation Objects on Small Water Structures

Roman Cabadaj (Slovak University of Technology in Bratislava, Faculty of Civil Engineering)

7.1. Introduction

The steady growth in popularity of sports and recreational navigation in Slovakia, entails the need for addressing this problem, which is still unresolved in Slovakia and not enough attention is paid to it. The absence of objects, necessary to overcome the many locks, steps, sills, complicates the navigation of small pleasure crafts and often gives rise to situations that threaten the safety and lives of people enjoying the water tourism. It is therefore appropriate to try to incorporate, into the object composition of new water works, also the objects for pleasure boating. It is clear that the investors of water structures, whose intention is to reduce the investment costs, especially for those objects which are not directly connected with the main purpose of the water structure, are not the only one responsible for this situation. The state administration bodies, which approve of the project documentation and issue permits for the realization of a construction project are to blame for the existing insufficiencies together with the gaps in the legislation, which tolerates the absence of sports water structures.

7.2. Vessels for Recreational and Sporting Navigation

For the purposes of sport and recreation area, Act no. 338/2000 Coll., on inland navigation, as amended, defines, in its Article 2 section 1 point f), the small vessel as a vessel with a length of the hull up to 20 m, which is designed to carry a maximum of 12 passengers and the vessel, designed solely for sports and leisure purposes, regardless of the means of its propulsion, with a length of the hull from 2.5 m to 24 m, with the exception of vessels built or designed for pushing or towing or driving in laterally tie-up convoy of vessels, which are not small vessels, ferries and sailing machines. This definition of the vessel, designed for recreational or sporting purposes, sets out useful proportions, to be used for the design of the objects of water structures, enabling them to be overcome these water structures. Before the draft of the technical measures to overcome the existing navigation obstacle it is necessary to carry out a survey or analysis of the vessels found on the respective waterway and to make use of the collected data, when drafting a concrete technical solution.

7.3. Objects Used to Overcome Small Water Structures

The most visited descent rivers with water tourists in Slovakia are: Morava, Malý Dunaj, Hron, Orava, Horný Váh, Dunajec and Bodrog. Therefore, the following section of the contribution will be devoted to, in particular, technical measures designed to overcome the existing or planned water structures on these rivers. The objects for non-powered small vessels on descent rivers should create conditions for landing, getting off a shore, lifting and a carrying down the vessels or possibly for overcoming the built weirs and small water structures (Fig. 1). The simplest technical solutions are:

— simple reinforcing of the bank in a length from 10 to 20 m created by a more moderate incline of the slope,
— sloping ramps, appropriate to be built as concrete, in at an incline ranging from 1:5 to 1:8, with a width from 5 to 8 m, ranging from 0.5 to 0.8 m below the water-level and with the side slopes with stone pavement or stone packing. This solution also enables the launching or lifting of smaller motor boats.-stairs, built at an incline of the slope as concrete or stone. It is appropriate to build the respective steps in a width of minimum 4 m or possibly to build a pair of stairs with a width of about 1 m, with an axial distance of 4 m.

Fig. 1. Carrying of the vessel

Technical objects solving the problems of overcoming of weirs and water structures result from the character of the river and the expected types of sport and recreational vessels.

The mainly used are:

— small navigation chambers for sport boats or small ship railways or small high – lift locks, which may be attractive for water tourists, however, this substantially increases the investment costs,
— slip-ways, boats passes for small sport vessels,
— ship lift.

Ship lift consists of a loading ramp, snub bridge in the upper and lower water and the connecting road. Loading ramp is built on the upstream side so that even at the lowest water levels it would allow the boat cart to enter the floating ship. The snub bridge is located on the bank side to reach the loading ramp above the maximum water level. Water-side is of soft and durable material. The snub bridge has a length from 12.0 to 20.0 m by stable water level. The mooring equipment is located every 5.0 m. By the inclination of the landing ramp of 1:12 and less the snug bridge can have the same inclination as the ramp but it has to be higher by 0.8 m. By the inclination greater than 1:12 water structures with a minimum length of 0.5 m are built instead of the snug bridge and water structures with a minimum length of 7.5 m are built from the inclination of 1:8. Boat cart is sturdy, lightweight frame, equipped with a safety brake. Load capacity for small boats is 1.5 kN, for lightweight sailing boats and motor boats is 3.0 kN. Storage space is curved and superficially modified so that it would not damage the hull. During transport, care should be taken of the secure storage of the vessel. On steep gradients and big weights of vessels the impeller with a rope winch is used for towing of boat carts. All types of sport crafts, except large sailboats and motor boats may be carried, with the help of slips. They are built separately or in combination with the lock chamber.

Slip-way enables to overcome the water structure in a short time and without interruption of the navigation. It is designed for small boats and rowboats with a width of up to 2.1 m (Fig. 2). For a given time it passes through the water structure more vessels with crew and cargo than the ship lift and lock chamber. For safety reasons it is necessary to consider, together with a slip-way, also a path for pedestrians. Children and less able individuals can overcome the critical section on foot.

Slip-way consists of inlet, inlet sill, own slip-way and outlet. It is led directly or curved. The radius of curvature (r) depends on the light width of the slip (b). For b = 1.3 m r is > 150 m for b = 2.3 m r is > 300 m.

The inlet to slip-way is open or locked. The locked slip-way has, on the inlet still, a lock construction (hinged-leaf gate, hydrostatic bag gate with automatic filling), which can regulate the flow. Open slip-way has an unregulated flow, whose minimum value varies according to the width of the slip-way from 1.5 to 2.5 $m^3 \cdot s^{-1}$. Dispositionally, the slip-way is located to the banks. In combination with a navigation chamber the slip-way is situated to the bank and the navigation chamber between the slip-way and the weir. In case of water structure with hydro power plant the slip-way is designed to the opposite bank as a hydro power plant.

The slip-way itself has a rectangular cross section with a constant width of 2.3 or 1.3 m. For a slip-way with a width of 2.3 m the optimum longitudinal inclination is 1:20. If the gradient is greater than 4 m the slip-way can start with an inclination of 1:15 and in the bottom part it continues with an inclination of 1:20. For slip-way with a width of 1.3 m the recommended maximum inclination is of 1:8, with a gradual transition to an inclination of 1:20. The point of the last modification of the inclination must lie 0.4 m below the maximum water level.

To increase the water depth and to create a cross-flow, which keeps the vessel at the centre of the slip-way, retarding elements in the shape of V with the tip against the flow of water and with an deflection angle of 20° from the vertical axis of slip-way are placed at the bottom of the slip-way. From a psychological point of view and for a smooth passage of boats it is appropriate to design the side walls of the slip-way as low. The surface is smooth and without projections [3].

At the present time, a new type of a fishway, a so called **brush-furnished fishway** (Borstenfischpass") which can also be applied as **a slip-way for pleasure craft**, appears increasingly. The nature of the cross-section is similar to the slit technical fishway, but its brushes increase the roughness (flow resistance), similarly to the fishway stones and accompanying vegetation in the bio-corridor. Fishways bed is covered with a layer of gravel, which is the habitat of the bottom organisms (benthos). In addition to this, the proposed fishway is suitable also for recreational pleasure crafts since the brushes are able to regulate the flow of the water and the brushes are also flexible enough not to damage and overturn the vessels. The functionality of this system in practice has been demonstrated on a pilot project Hydro power plant Au-Schönenberg on the river Thur [1]. Flexible and permeable brush elements are replacement for the used concrete partitions. Brush elements are composed of individual bundles, firmly anchored in the basic concrete bottom plate of the slip-way. Their deployment ensures the meandering of the jet stream and the creation of the stream shadows, which provide refuge and relax for fishes. The bottom of the slip-way is filled with coarse-grained substrate (gravel), which makes the brush-furnished fishway suitable for bottom organisms.

Disposition and installation of rough brush elements depends on the local situation of a specific water structure (flow rate, flow, slope and the expected quantity of fishes). A width of the brush-furnished fishway and the depth of water in it, do not affect the flow velocity, so the constant velocity is provided at constant slope of brush-furnished fishway. The laboratory tests with live fishes have also showed that the brush-furnished fishway does not operate selective and it is crossable for all fishes from both sides.

Advantages of the brush-furnished fishway:

— transformation of energy takes place on a short section with low turbulence due to bundles of bristles which increase the roughness,
— flow velocity among the bristles is dependent only on difference of the height among rows of bristles and it is less than 1.2 ms^{-1}, in a slope of the riverbed of fishway from 8% to 10%,
— idle places beyond the bristles (with a maximum speed 0.3 ms^{-1}) are used by fish as resting places (called refuges),
— hydraulic properties are mostly independent from type and line of the slip-way,
— the flow impact on the coarse-grained substrate covered floor is negligible due to low flow velocity among the bristle elements due to the slip-way is crossable for the bottom organisms [2].

By small depth of water in the river-basin under the weir it is possible to leave the outlet from the slip-way non-extended with arch or coin modification of lower gridiron of weir. In case of insufficient water depth it is possible to deepen the floor of the river under the slip-way. In greater depths it is appropriate to funnelled extend the outlet or build a horizontal plate submerged below lower water level, which ensures a navigation depth in the outlet as its own slip-way. A water cylinder cannot be created in the outlet.

Navigation Chamber (NC) is designed in water structure, where we expect heavy traffic of large pleasure craft (yachts, sailboats and motor boats). NC consists of its own chamber, upper and lower gates, gridiron, roadstead and gear (Fig. 3).

The useful length of the chamber is 20.0 m, a width is 4.0 or 4.5 m. By heavy traffic it is possible to design the chamber with a width of 7.0 m. Safe distance from the upper and lower gates depends on the filling and emptying system. A minimum distance from the upper gate is 1.0 m and from the lower gate is 0.5 m. Freeboard of NC over the maximum

water level is at least 0.75 m and recommended is 1.0 m. The minimum depth of the water in the chamber and the roadstead is 1.2 m. A filling and emptying system is designed as a direct or by long by-pass.

Fig. 2. Detail of the brush elements in the slip-way and slip-way with retarding elements

Fig. 3. Navigation Chamber for the sports and recreational vessels

Equipment of the NC includes on both sides at least two ladders, two tether rods and two niches with a series of bollards. The bollards are placed over the tether rods, in the niche or on the platform of NC. Mobile tether facilities come into consideration by higher chambers. The chamber is lighted, edges of niches and pillars of the NC are armoured.

In the roadstead of the NC there is ensured safety mooring of vessels in all water stages where the NC operates. The width of roadstead consists of fairway width of 7.5 m, a minimum width of NC 4.0 (4.5) m and a safety distance of 0.5 m. The minimum overall width of the roadstead is 12.0 m. A length of holding area of the roadstead is at least 1.5

times of the effective length of the NC. The mooring bridge is located on side of holding area which a minimum length is 7.0 m and a width is 3.0 m. The tether facilities are located every 2 m. The remaining length of holding area is equipped every 5 m with vertical tether rods, bollards or tether piles.

The NC is designed as a self-service. An operation must be simple, safe and comfortable. Operating instructions and safety measures against wrong operation in multiple languages have to be placed near the operating equipment. A machine drive is equipped with a manual crank facility for an emergency operation. Particular phases of filling and emptying are controlled automatically. Due to security it is allowed to stop immediately or drop back every phase. Traffic can be controlled by light signals which are operated automatically. Additional equipment with main features and rescue accessories in the NC – lifebuoy, boat hooks, throw bags and etc. may be placed directly in the chamber to increase the security.

7.4. Conclusion

It is necessary to design appropriate navigation objects for sports and recreational navigation according to the local conditions and typical parameters for each site.

Slip-way for powerless vessels (kayaks, canoes, prams) is considered suitable. Slip-way is the object that requires small investment costs (in comparison to the total costs for the whole water structure) it will help to increase the safety to overcome the slope on the water structure and it also contributes to the attractiveness of the navigation.

It is now possible to observe the growing trend of spending leisure time in sports and recreational navigation. For these activities it is necessary to create also the appropriate conditions through not only by objects to overcome the water structures but also by building of ports, camps and restful areas with appropriate equipment.

References

[1] Hintermann M.: Borstenfischpass als neuartige Fischaufstiegshilfe Pilotanlage Kraftwerk Au-Schönenberg. listed in: http://www.vol.be.ch/site/borstenfischpass-2.pdf, 2007.

[2] Šulek P., Čubanová L.: Rybie priechody, Inžinierske stavby 1/2010, ISSN 1335-0846, JAGA Group, s.r.o., 2010.

[3] Hodák T., Možiešik Ľ.: (1994) Sklz pre nesamohybné plavidlá do 300 kg medzi zdržou a starým korytom Dunaja pri Čunove – štúdia, Bratislava 2004.

8 Reduction of Wave Load on the Perforated Seawall Defended by the Submerged Breakwater

Dalibor Carevic, Ocvirk Eva, Prsic Marko (University of Zagreb, Faculty of Civil Engineering, Croatia)

8.1. Introduction

In this work, the perforated seawall loading defended by the smooth low crested structure (LCS) is analyzed.

The perforated seawall structure is a coastal defense structure of vertical wall type containing some kind of perforations (circular, rectangular, longitudinal vertical, longitudinal horizontal, etc.). The water flow through the perforations causes the dissipation of wave energy, which results in smaller reflected wave heights. Regardless of their construction complexity and increased price as related to solid vertical seawalls, the perforated types are more and more popular as internal port antireflective structures or as breakwaters of perforated caisson type. The advantages of the perforated structures are characterized by the fact that they reduce the reflection, overtopping, the erosion of the construction toe, and the force affecting the structure. Their advantages can be also recognized in the fact that they do not occupy a lot of space as related to the classical antireflective structure of rubble mound type. As structural and functional parts they can be installed in various port structures that are not intended primarily for the wave defense, as e.g.: pier or jetty. The example of the perforated breakwater with one perforated wall on the stone dike is presented on Fig. 1. The reflection characteristics of perforated structures are relatively well investigated and described in the works [1, 2, 3, 4, 5, 6]. The load calculation of perforated structures has been elaborated in the works [7, 8, 9, 10]. In this work a calculation model for the pressure exerted on the perforated structure from the work [9] is used that is based on the load calculation for the solid coastal wall according to the Goda's procedure [12], so that the calculation model of the solid wall is corrected by means of correction coefficients.

LCS is the type of rubble mound structure with emerged, submerged or zero freeboard causing the wave breaking and the dissipation of wave energy. There are LCS-s with rubble mound armour usually used and their functional characteristics (transmission and reflection) are described in the works [14, 15, 16, 17, 18, 19]. This paper deals with LCS with smooth armour, the type of structure rarely used. The possibility of generalizing the results of this work to be applied for rubble mound structures is explained in the chapter 8.2.2. The theoretical model for calculation of the transmission of wave heights by means of smooth LCS used in this work has been taken over from [20].

The seawall failures are mainly caused by extreme wave actions, through displacement of the entire structure, or progressive failure starting from locally weak point, or through overall foundation failures, or through overtopping and toe erosion. The need for force

reduction on these structures to increase the life span has resulted in different force reduction techniques like the introduction of porosity at the front face of the caisson, construction of low-crested caissons, defense with offshore low crested structures etc. The combination of smooth low crested structure and perforated seawall is the main objective of this paper, respectively, the reduction of wave load on the perforated seawall defended by the submerged breakwater.

The defence of rubble mound breakwater with low crested structure was investigated in paper [21], where the authors concluded that the run up and run down for the breakwater defenced by submerged LCS are reduced up to 30 and 60%, respectively, compared to single breakwater not defenced by LCS. The damage of the optimally defenced breakwater is reduced by 40–100% compared to a non-defenced (single) breakwater.

In the papers [22] and [23] the authors deal with the reduction of wave load on the solid seawall defended by the submerged LCS. They concluded that the relative height of the LCS (construction height/water depth) associated with the formation of standing wave and resonant conditions between the structures are found to be important parameters for the oscillatory behavior of the force ratios, which also depends on wave period. The amplitudes of the forces decrease with the increase in relative LCS height. For submerged LCS-s the reduction of horizontal forces on solid seawall is 30–60% depending on wave parameters and LCS relative height, for zero freeboard reduction it is 65–80% and for emerged 65–95%. The influence of the pool length on the reduction of forces is observed to be small (to the order of 5–10%) for two different ranges studied.

The research in this paper is based on the results obtained from the measurement of the pressures on physical model of perforated structure (chapter 8.3) and the results obtained by means of the proposed theoretical model (chapter 8.2). First, the pressures were measured on the perforated structure (Fig. 1), without LCS (experiment inter 0). After that, the LCS was placed in front of the perforated structure, and the distance of the LCS from the perforated structure, as well as the LCS crest submergence (experiments inter 1÷6) were variated. The chapter 8.4 presents the raw measurement results, and the chapter 8.5 contains the analysis and the comments on measurement results.

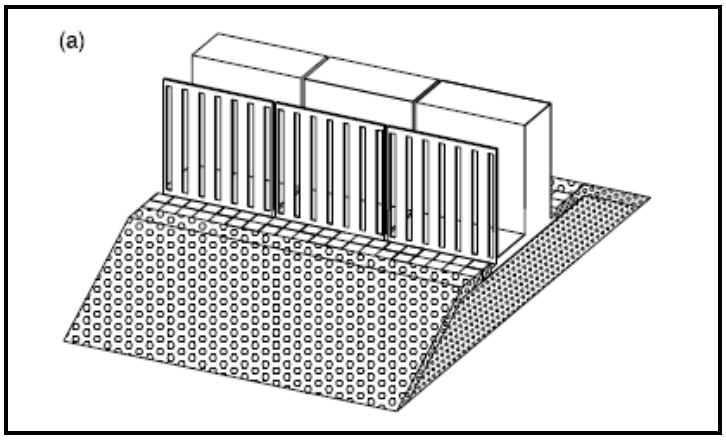

Fig. 1. Example of perforated breakwater with one perforated wall on rubble mound foundation without ceiling

This paper has the following research objectives: 1. to investigate the influence of LCS, depending on its position and submergence, on the force by which the waves, after passing over LCS, affect the perforated structure (chapters (8.5.2 and 8.5.3), 2. to compare the measured forces on the perforated structure with the forces obtained by the proposed theoretical model (chapter 8.5.5).

8.2. Theoretical Model for the Calculation of Forces on Perforated Seawall Defended by Smooth Submerged Low Crested Structure (LCS)

The hydraulic interaction of the submerged LCS and the perforated seawall through the aspect of wave load implies the following: 1. the influence of LCS on the load of perforated seawall, and 2. the influence of the perforated seawall on the load (stability) of LCS. The influence of the perforated seawall on the load of LCS has not been investigated.

Part of wave energy is transmitted over the seawall in the form of significant transmitted wave height H_{st} (Fig. 2). The waves of significant wave height H_{st} move to the perforated seawall and cause the pressures on the construction as it is presented on the figure below. When the wave crest comes across the perforated wall, it loads it with the pressure diagram (red) in the moment t_1, the wave crest travels further to the rear solid wall and loads it with the pressure diagram (green) in the moment t_2. Then the reflection of the wave crest occurs and the path of the wave crest traveling is in the direction of LCS. When it comes across the perforated wall again, it loads it with the pressure diagram (blue) in the moment t_3, but in the opposite direction. The maximal load of the seawall develops at the moment when the vector sum of resulting forces of pressure diagrams (Fig. 2) is maximal. If we continue to monitor the movement of the wave crest that is now traveling towards LCS, then it is partly reflected from LCS in a complex interaction with the incidental waves. The influence of the re-reflection in such a complex interaction is an insufficiently researched phenomenon. In this paper the small influence of the re-reflection will be presumed and it will be neglected.

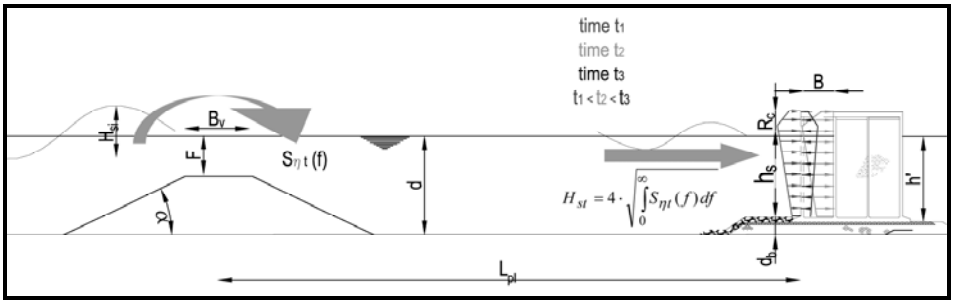

Fig. 2. Definition sketch of smooth submerged LCS and perforated seawall interaction

8.2.1. Theoretical Model for Perforated Seawall Forces Calculation

The method of the force reducing that is based on Goda‘s procedure intended for the

calculation of solid seawalls [12]. The Goda's procedure was used by Takahashi [13], for the purpose of calculating the perforated structures. Takahashi's procedure has been improved by Tabet-Aoul and Belorgey [9] and it has been used in this paper as well. The calculation model for the solid seawall is corrected by the correction coefficients that depend on the geometry of perforated structure and incoming wave parameters. The calculation model yields maximal diagram of the pressure acting on the front perforated and the rear solid seawall, as well as the maximal force acting on the whole structure. The model is presented further in the text [9]:

Procedure is valid for $B/L < 0.35$.

$$\eta^* = 0.75(1+\cos\beta)\lambda_{i1}H_D$$

where: H_D – project wave height in front of wall [m].

According to Goda:

$$H_D = H_{1/250} = 1.8\ H_s,$$

where: H_s – significant wave height at the seawall toe without reflection from wall,
l_{i1} – multiplication factors. For front perforated wall $l_{i1} = 0.42$, and for rear solid wall $l_{i1} = (0.7 - B/L)^2$,
b – incident wave angle [°].

Calculation of pressures:

$$\alpha_1 = 0.6 + 0.5\left(\frac{\frac{4\pi d}{L_s}}{\sin h\left(\frac{4\pi d}{L_s}\right)}\right)^2 \tag{1}$$

$$\alpha_2 = \min\left(\frac{\left(1-\frac{h_s}{d_b}\right)\left(\frac{H_D}{h_s}\right)^2}{3}, \frac{2h_s}{H_D}\right)^2 \tag{2}$$

$$\alpha_3 = 1-\left(\frac{h'}{d}\right)\left(1-\frac{1}{\cos h\left(\frac{2\pi d}{L_s}\right)}\right) \tag{3}$$

$$\alpha_4 = 1-\frac{R_c^*}{\eta^*} \tag{4}$$

$$R_c^* = \min(R_c, \eta^*),$$

$$\alpha^* = \max(\alpha_1, \alpha_2),$$

where (Fig. 2): L_p – peak wave length at the toe [m],
h_s – water depth from the berm to the water surface [m],
d_b – water depth at the location at a distance 5 H_s from the seawall [m],

d – water depth in front of the wall [m],
h' – submerged height of the wall [m],
r – density of the sea water [kg/m^3].

Pressure diagrams for the front perforated wall (Fig. 3):

$$p_{p1} = 0.5(1+\cos\beta)\left(0.42\alpha_1 + (B/2L_s)(1+\alpha^*)\cos^2\beta\right)\rho g H_D \tag{5}$$

$$p_{p3} = \alpha_3 p_{p1} \tag{6}$$

$$p_{p4} = \alpha_4 p_{p1} \tag{7}$$

Pressure diagrams for the rear solid wall:

$$p_{r1} = 0.5(1+\cos\beta)\left((0.7 - B/L_s)^2\alpha_1 + (0.43 - B/L_s)\left(1+\alpha^*\right)\cos^2\beta\right)\rho g H_D \tag{8}$$

$$p_{r3} = \alpha_3 p_{r1} \tag{9}$$

$$p_{r4} = \alpha_4 p_{r1} \tag{10}$$

Horizontal force on the front perforated wall:

$$F_p = \left[(p_{p1} + p_{p3})\frac{h_s}{2} + (p_{p1} + p_{p4})\frac{R_C^*}{2}\right](1-p) \tag{11}$$

where: p – perforated wall porosity.

Horizontal force on the rear solid wall:

$$F_r = \left[(p_{r1} + p_{r3})\frac{h_s}{2} + (p_{r1} + p_{r4})\frac{R_C^*}{2}\right] \tag{12}$$

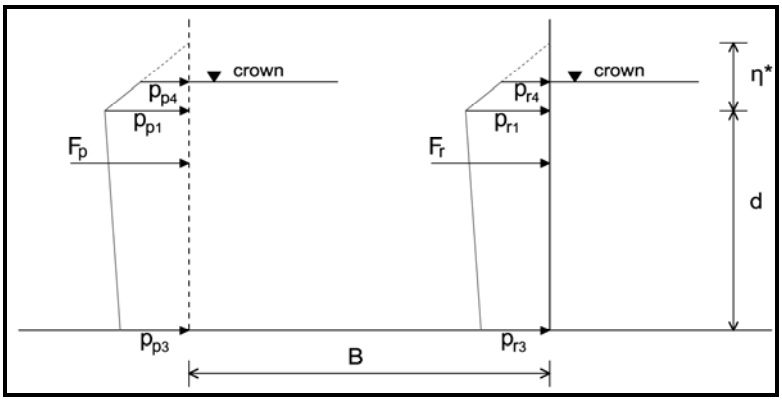

Fig. 3. Scheme of pressure diagrams calculated by means of model [9]

8.2.2. Theoretical Model for Calculation of Transmission Coefficients Over Smooth LCSs

LCS need not be necessarily covered with rock fill. Sometimes smooth and impermeable LCS can be covered with asphalt or concrete armour. The slopes of these LCSs are sometimes more gentle (1:3 or 1:4) than it is the case with the LCS with the stone armour, mostly due to construction reasons.

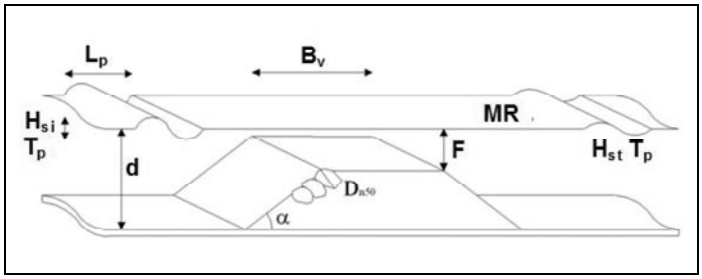

Fig. 4. Definition of symbols for smooth LCS theoretical model: F – water depth at the crown [m], H_{si} significant wave height in front of LCS (recommendation $H_{si} = 4\sqrt{m_0}$) [m], ξ – Irribaren number, $\xi = \text{tg}\ \alpha/(s_{op})^{0.5}$, $s_{op} = 2\pi H_{si}/(gT_p^2)$, B_v – crown width [m]

The asphalt and concrete LCSs are mostly built in dray conditions, and not under the water. The presence of tides enables the building of such structure in dry conditions.

Since the smooth LCSs are different in the process of hydraulic functioning than the seawalls covered with rock fill, there are different formulas for the transmission coefficient.

The wave transmission can be calculated according to the paper [20]:

$$K_T = [-0.3\ F/H_{si} + 0.75[1 - \exp(-0.5\xi)]]\cos^{2/3}\beta \tag{13}$$

with the minimum $K_T = 0.075$ and the maximum $K_T = 0.8$, and with the following limitations: $1 < \xi < 3$, $0° \leq \beta \leq 70°$, $1 < B_v/H_{si} < 4$. The symbols are defined on Fig. 4. Eq. (13) takes the angle wave transmission into consideration by means of the expression $\cos^{2/3}\beta$.

It can be realistically expected that LCSs with the stone armour, as related to those with smooth armour (concrete, asphalt) are mostly used. In the experimental research related to this paper the LCSs with smooth armour are used. The smooth armour was chosen because the laboratory equipment and the experiment methodology require many relocations of LCSs, which would need a significant amount of work and significantly increased experiment costs.

Since the smooth armour has been selected, one should know whether there is a possibility of generalizing the results of the experiment done with smooth LCS and apply them for LCS with stone armour. For this purpose there was a theoretical research carried out previously by means of empirical formulas for the transmission calculation for LCS with smooth armour (Eq. (13)) and for LCS with stone armour the equation from the work [24]. The research was needed to find out how much the transmission coefficients for the LCS of certain geometry with the stone and with the smooth armour differ. There were the following parameters used in the comparison: $F/H_{si} = -0.5 \div -0.05$; $H_{si}/L_{si} = 1/10 \div 1/30$, $B_v/H_{si} = 1 \div 4$, $a = 1 : 2$ (symbols according to Fig. 4). The comparison leads to the conclusion that the

smooth armour transmits more energy than the stone armour. The transmission coefficient K_T is up to 25% smaller for submerged LCS with rough armour as related to the smooth armour. This difference at LSCs with zero-board submergence is even larger, up to 40%.

At the same time the question of the difference in transmitted wave spectrum for smooth and stone armour is raised. Namely, the transmitted spectra are different from incident spectra. In the process of the transmission over the submerged LCS there are two or more generated waves on the side behind the LCS in the process of wave transmission. It results in more energy on higher frequencies of wave spectrum than it is the case with incident spectra. Generally speaking, the peak period is very close to incident period, and mean period is reduced. First analysis could be found in the work [18], but the process itself has not bee sufficiently researched and theoretically supported. In the paper [25] there are the descriptive differences of the form of transmitted spectrum for smooth and stone LCS given, and it can be concluded that additional research is needed in this area.

On the basis of the above mentioned it is obvious that LCSs with smooth armour as related to LCS with stone armour transmits larger amount of wave energy for the same geometric and wave parameters, and yield different transmitted mean wave periods (spectra). The generalization of the research results from this paper is possible only if all above-mentioned differences are taken into account.

8.3. Physical Model

8.3.1. Wave Channel and Measurement Equipment

The experimental research was made in the Laboratory of the Faculty of Civil Engineering in Zagreb. The wave channel width was 1m, the height was 1.1 m, and the depth of water in the channel was d = 0.5 m.

The measuring equipment includes the piston wave generator with the installed AWACS system, and the data collection system (sampling frequency 40 Hz) produced by DHI (Horsholm, Denmark). Capacitive gauges (DHI) G1–G8 (Fig. 6) were used for measuring the surface elevation. The analysis of the collected data was made by means of the system DHI Wave Synthesizer. The incident wave parameters in front of LCS were determined in the spectral domain by means of the WS Wave Reflection Analysis. The spectral analyses were performed with the following parameters: size of FFT block: 512, overlap: 0.667, Number of subseries: 68, lower cut-off frequency: 0.0 Hz, higher cut-off frequency: 20.0 Hz, Data window: Hanning method, frequency step: 0.078 Hz.

The differential pressure gauges RS216-6253 having the following characteristics: the range of measured pressure from 0 to 0.1psi, output voltage of 14.7 to 18.7 mV, sensitivity 16.7 mV/phi, sampling frequency 60 ms, were installed onto the model of perforated seawall. The measured pressure values were recorded in the computer by means of ADAM program.

8.3.1.1. Physical model of the perforated seawall (inter 0)

A wooden model of the perforated seawall was placed into the wave channel at the distance of 15.7 m from the wave generator (Fig. 5, Fig. 6). The model of the perforated seawall was made of wood with the porosity of p = 30% (p-ratio of the opening and the total surface of the wall) and with vertical longitudinal openings, and with the width of

dissipation chamber of B = 0.18 m. There were altogether eight pressure gauges (T1–T8), placed on the model, four of them were placed on the front chamber wall (the perforated), and the other four on the rear (solid) wall. The pressure gauges were used to measure the pressure every 60 ms, and thus, the pressure time series was obtained for every pressure gauge (T1–T8).

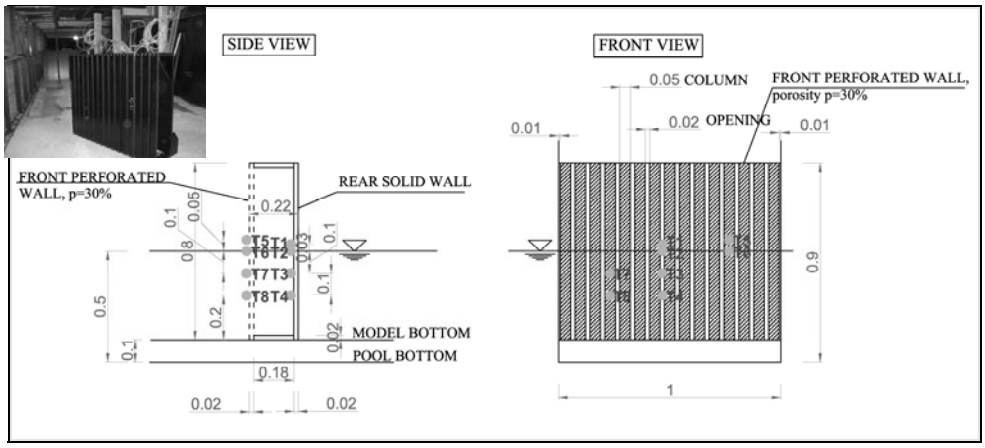

Fig. 5. Model of perforated seawall with pressure gauges scheme (T1−T8), p-porosity of the perforated wall

In front of the model there were five capacitive gauges (G_3–G_7) placed, needed to measure the oscillations of the water surface (Fig. 6). The separation of the incident and reflecting spectra recorded by the capacitive gauges G_3–G_7 was created by means of the method defined in the paper [26]. From the separated incident and reflected spectra it is possible to obtain the incident H_{si} and reflected significant wave height H_{sr}.

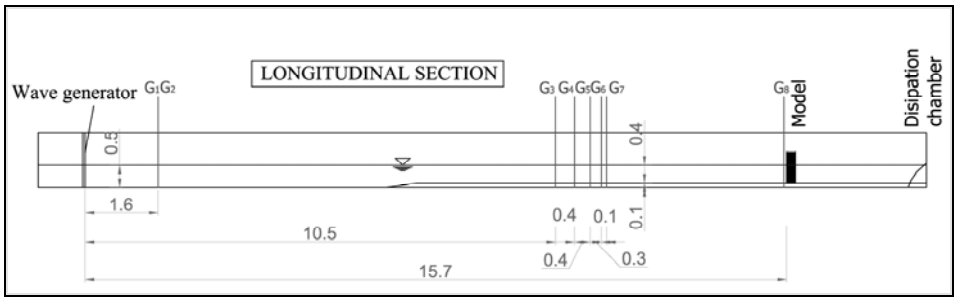

Fig. 6. Longitudinal section of wave channel with capacitive gauges (G1−G8) and perforated seawall (Model) positions (Inter 0)

The gauges G_1 and G_2 were used for the measurement of incident waves generated by the wave generator. The gauge G_8 was used as control gauge for the elevation in front of the perforated wall. The time duration for an experiment amounts to ~5 min., which is approx. three hundred waves per an experiment, pursuant to the recommendations from the paper [27]. There were altogether 9 testing procedures conducted according to the Tab. 1.

Table 1

Wave parameters used in experiments without LCS (inter 0) and with LCS (inter 1–6)

JONSWAP; γ= 3.3, σ_1 = 0.07, σ_2 = 0.09				
Test	T_p [s]	H_s [m]	L_p [m]	L_p/H_s
1	0.68	0.06	0.72	12
2	0.81	0.06	1.02	17
3	1.01	0.06	1.50	25
4	0.89	0.10	1.20	12
5	1.10	0.10	1.70	17
6	1.45	0.10	2.50	25
7	0.99	0.12	1.44	12
8	1.24	0.12	2.04	17
9	1.68	0.12	3.00	25

8.3.1.2. Physical model of the perforated seawall and submerged smooth LCS interaction (Inter 1–6)

The model of the seawall was made of wood with the crown width of B_v = 0.16 m, the slopes of 1:2 and the possibility to change the submergence depth so that two depths 0.055 m and 0.101m can be achieved (Fig. 7).

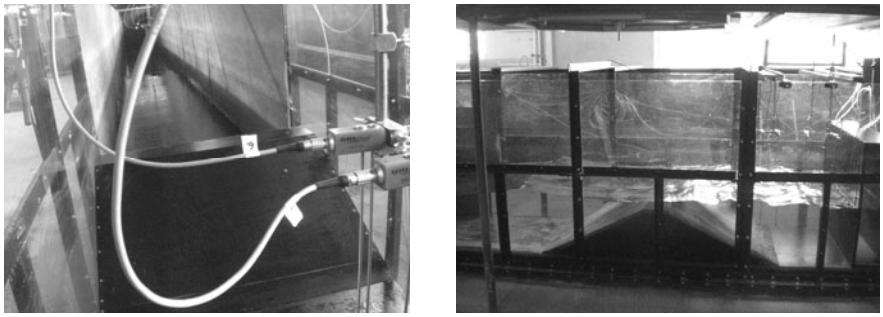

Fig. 7. Photographs of submerged low crested structure (LCS) positioned in channel for crown submergence F = 0.055 m

During the testing the distance of the LCS from the perforated seawall L_{p1} and seawall submergence F varied. There were three distances of the breakwater from the seawall L_{p1} = 1.2 m, 2.4 m and 6.2 m used, as well as two submergences F = 0.055 m and F = 0.101 m. In this way the total of 6 combinations was obtained. The combinations are called inter1, inter2, inter3, inter4, inter5 and inter6 (Fig. 8).

The wave parameters used to perform experimental testing for each single interaction, (inter1÷6), are defined in Tab. 1. Thus, altoghether 54 testing procedures were conducted.

The gauges G_2–G_4 were used to measure the oscillations of the water surface. The separation of incident and reflected spectra from the records on the gauges G_2–G_4 was undertaken by means of the method defined in the paper [26]. The incident H_{si} significant wave height can be obtained from the incident and reflected spectra.

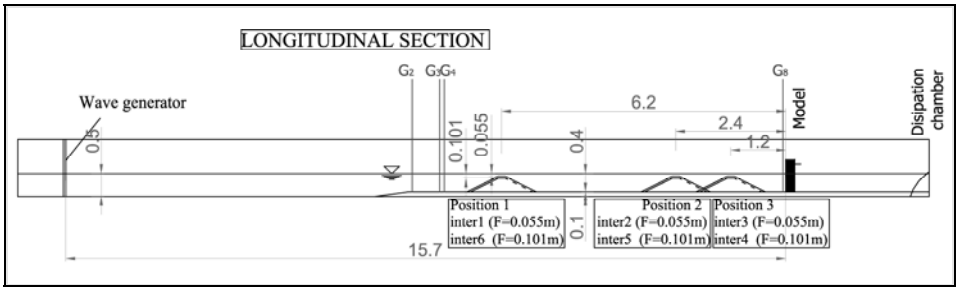

Fig. 8. Longitudinal section of wave channel with the positions of submerged LCS and perforated seawall for three different pool distances, L_{pl} = 1.2 m, 2.4 m and 6.2 m and two LCS submergence F = 0.055 m and F = 0.101 m (inter1÷6)

8.4. Pressure Measurement Results

8.4.1. Processing of the Measured Pressures

There were altogether 54 testing procedures made for the wave parameters from the Tab. 1, for inter1÷6 (with LCS), and 9 testing procedures from the Tab. 1 for inter 0 (without LCS). There were 4 to 5 thousand data about the pressure obtained for each single pressure gauge (T1–T8) in one measurement. The example of the measured pressures (for inter 6, H_s = 0.12 m, T_p = 1.68 s) is presented in Fig. 9.

The calculation of the value of hydrodynamic pressure P_{hd} out of raw measured pressures is obtained separately for the pressure gauges T1, T2, T5 and T6 and the pressure gauges T3, T4, T7 and T8. For the pressure gauges T1, T2, T5 and T6 the values of hydrodynamic pressure P_{hd} are equal to the value of maximal measured pressure $P_{\max}$, taking into consideration that these are the pressure gauges on and above water surface (P_{hd} = $P_{\max}$). Since they are above and on the water surface, the minimal values of the measured pressure are 0 (Fig. 9).

For the pressure gauges T3, T4, T7 and T8 the values of hydrodynamic pressure P_{hd} are equal to the difference of the measured maximal pressure $P_{\max}$ and the mean pressure P_{mean} ($P_{hd} = P_{\max} - P_{mean}$). Such calculation was used because it was found out that the mean value of the pressure P_{mean} calculated as an integral average of the measured pressures (on T3, T4, T7 and T8) during every single measurement, is equal to the hydrostatic pressure.

Fig. 10 shows a characteristic form of the hydrodynamic pressure produced by the wave activity on the vertical wall. There were altogether 63 graphic presentations for such results made. The results are not shown here, since the paper needs to be concise.

8.4.2. Calculation of Wave Hydrodynamic Horizontal Force F_{meas} from Measured Pressures P_{hd}

The horizontal resultant force F_{meas} is obtained by the integration of the surface below the diagram of the measured hydrodynamic pressure P_{hd} (Fig. 10), especially for the perforated wall and especially for rear wall. In this way the measured horizontal resultant force F_{meas} is obtained for the part of the front wall from the pressure gauge T5 (level +0.05 m) to the pressure gauge T8 (level –0.2 m) and for the part of the rear wall from the

pressure gauge T1 (level +0.03 m) to the pressure gauge T4 (level –0.2 m). Thus, calculated force F_{meas} on the perforated wall is also multiplied by the coefficient (1–p) since the force acts only on the columns of the perforated wall with its share in the total surface of the front wall (1–p) (Eq. (11)).

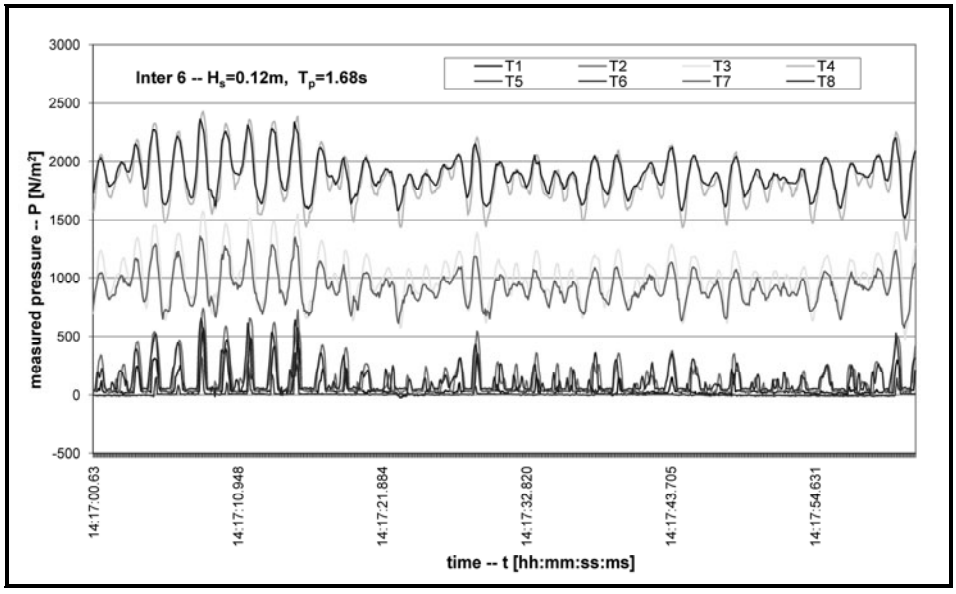

Fig. 9. Example of measured pressures on pressure gauges T1÷T8 for inter 6 (H_s = 0.12 m, T_p = 1.24 s)

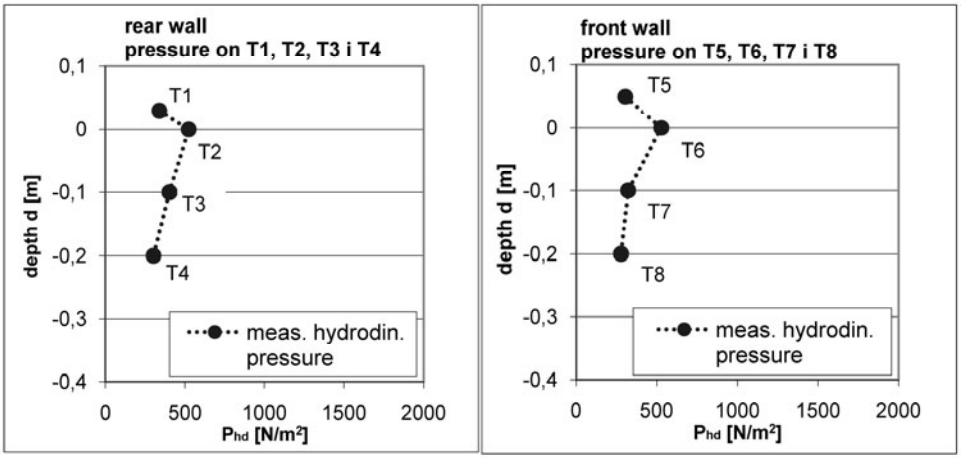

Fig. 10. Example of calculated hydrodynamic pressures P_{hd} on rear solid and front perforated wall for inter 6, H_s = 0.12 m and T_p = 0.99 s

8.5. Analysis of Measurements

8.5.1. Comparison of Measured $(F_{inter0})_{meas}$ and Theoretical $(F_{inter0})_{theor}$ Horizontal Force on Perforated Seawall Undefended by LCS

Fig. 11 shows that larger forces are occured on the rear wall as related to the front wall. This difference occurs because of the relaxation of the part of loading on the front perforated wall when the water flows through the openings. It can also be seen that the calculated forces $(F_{inter0})_{theor}$ are larger even by ≈ 50% than $(F_{inter0})_{meas}$ in the area of higher measured values. For the purpose of explaining such disproportion, the results of the model [9] verification were used (from paper [28]). In the paper [28] the results of the theoretical model were compared with a series of experimental and "in situ" measurements. It was found out that the model [9] is conservative and that it overestimates the measured results ≈ 30–40%, which is very similar to the results on Fig. 11. For the verification in [28] the mean value F_{meas}/F_{theor} for individual measurements was used. The obtained mean value of the parameter F_{meas}/F_{theor} for all measurements is 0.9, and the standard deviation is from 0.086 to 0.21 depending on the source of measured results. For the results on the Fig. 11 the mean value 0.95 and the standard deviation 0.3 were calculated. High standard deviation shows somewhat larger data dispersion around the mean value, but the mean value and the conservative trend of the model are similar.

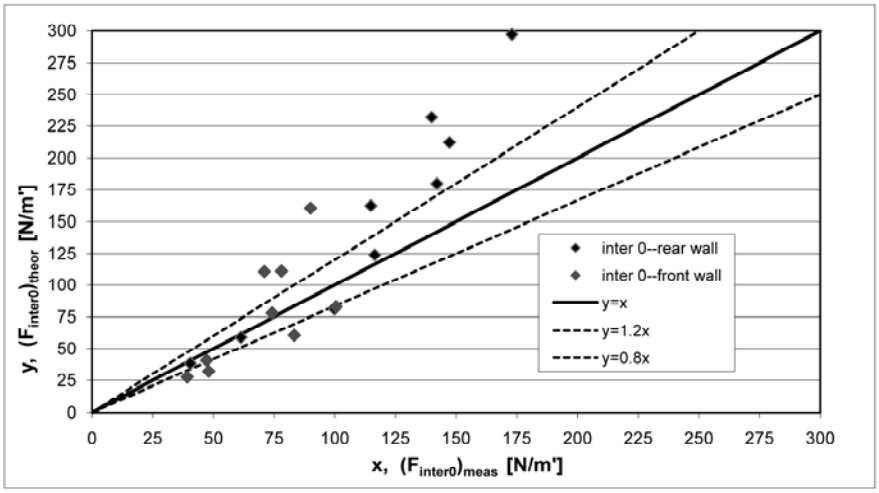

Fig. 11. Comparison of measured force $(F_{inter0})_{meas}$ and calculated by theoretical model [9] $(F_{inter0})_{theor}$, for perforated seawall unprotected with LCS (inter 0), for front and rear wall

8.5.2. Comparison of Measured Horizontal Force $F_{(inter1\div6)meas}$ on Perforated Seawall Defended by Submerged LCS

Fig. 12 and Fig. 13 show the influence that the LCS, depending on its position and the water depth on the crown, has on the measured horizontal force $F_{(inter1\div6)meas}$ as related to the measured horizontal force on the perforated seawall without LCS $F_{(inter0)meas.}$

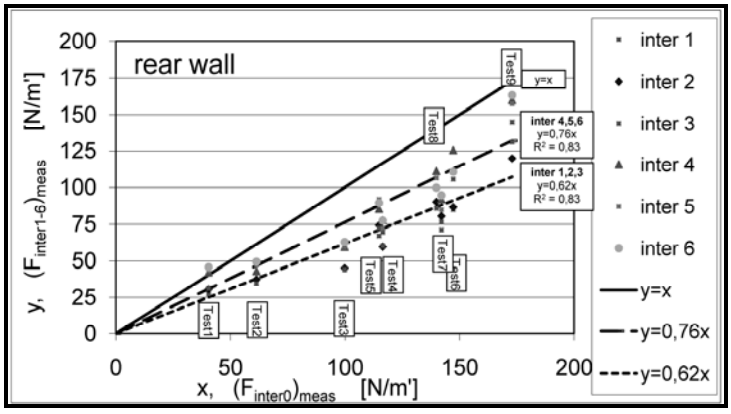

Fig. 12. Dependence of measured horizontal force on perforated seawall defended by LCS ($F_{(inter1–6)meas}$) and measured force without LCS ($F_{(inter0)meas}$), for rear wall. The measured values are approximated with linear functions (least square method) for inter1–3 (F = 5.5 cm) and inter4–6 (F = 10.1 cm), F – submergence

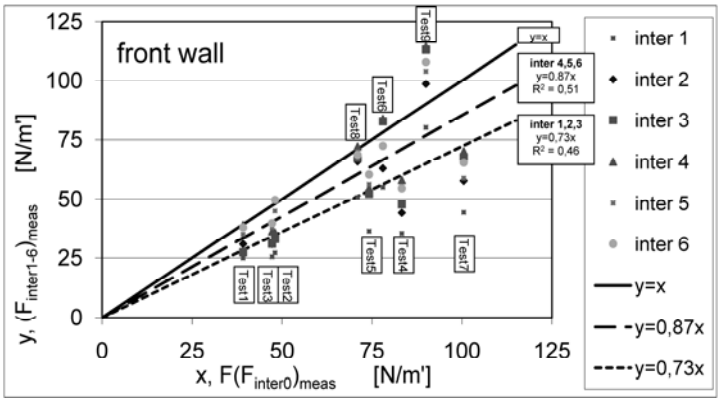

Fig. 13. Dependence of measured horizontal force on perforated seawall defended by LCS ($F_{(inter1–6)meas}$) and measured force without LCS ($F_{(inter0)meas}$), for front wall. The measured values are approximated with linear functions (least square method) for inter1–3 (F = 5.5 cm) and inter4–6 (F = 10.1 cm), F – submergence

Most of the measurements in Fig. 12 and Fig. 13 are placed below the straight-line $y = x$ which indicates obvious reduction of the measured forces under the activity of LCS. This reduction is larger on the rear wall and makes 38% (for inter 1, 2, 3) and 24% (for inter 4, 5, 6), regarding the straight lines by which the measured data have been approximated. For the front wall the reduction makes 27% (for inter 1, 2, 3) and 13% (for inter 4, 5, 6). The reduction of forces for inter 1, 2, 3 is larger since the submergence F is smaller than for inter 4, 5, 6, and the wave heights that appear behind LCS are smaller causing smaller loading. On the front wall one can notice even larger forces for individual tests (Test 9 and Test 6) under the influence of LCS. This phenomenon is explained in more details in the chapter 8.5.3.

8.5.3. Influence of Pool Length L_{pl} on Perforated Seawall Forces

Fig. 14 and Fig. 15 show the measured forces $F_{(inter1\div6)meas}$ and $F_{(inter0)meas}$ on the seawall for various wave parameters (Test 1÷9) and for various distances of LCS from the wall (inter1÷6), and for the situation without LCS (inter 0). The forces on the rear wall are the largest for inter 0, except for the Test 1 (inter 4, 5 and 6) where the waves, because of their small height, pass without being broken over LCS, so that LCS has almost no effect.

Inter 1–3 (rear wall) for various wave situations (Test 1÷9) have approximately equal forces $F_{(inter1\div3)meas}$ which shows that there is no significant influence of the distance (L_{pl}) on the loading of the rear wall. The same pattern can be used also for inter 4÷6 for the rear wall.

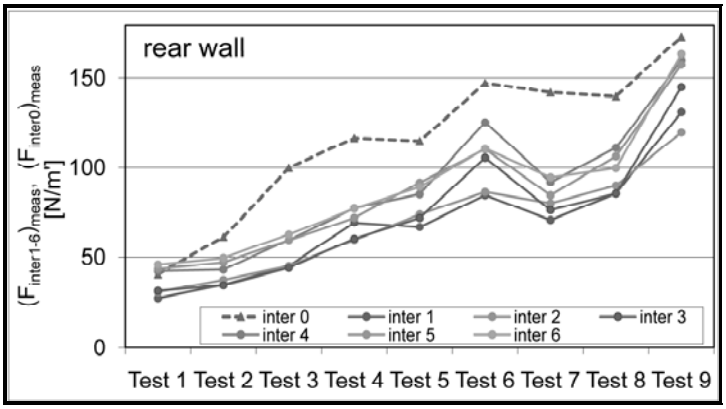

Fig. 14. Measured forces $F_{(inter1–6)meas}$ and $F_{(inter0)meas}$ on perforated seawall for different wave situations (Test 1–9, Tab. 1) and pool lengths L_{pl} (inter 1–6) (Fig. 8), for rear wall

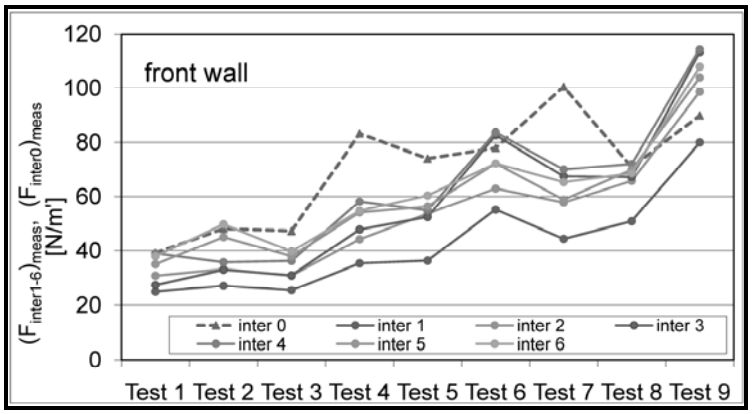

Fig. 15. Measured force $F_{(inter1–6)meas}$ and $F_{(inter0)meas}$ on perforated seawall for different wave situations (Test 1–9, Tab. 1) and pool lengths L_{pl} (inter 1–6), (Fig. 8), for front wall

The forces on the front wall for inter 0 are not the largest for individual test situations. For the Test 1 the waves pass over LCS without being broken, and LCS has no positive effect. Similar conclusions can be made for the Test 2.

In the Test 9 (rear and front wall) one can notice generally the smallest force reduction for all interactions, and in the case of the front wall even the forces for inter 2÷6 are larger than the forces for inter 0. This phenomenon is explained in the Fig. 16 and Fig. 17.

Fig. 16 and Fig. 17 present the influence of the parameter L_{pl}/L_{si} on the loading of the coastal wall, i.e. on the parameter $(F_{(inter1\div6)}/F_{(inter0)})_{meas}$. The tests where the wave breaking doesn't appears, i.e. where LCS has no effect (Test 1 – inter 4, 5, 6), were eliminated from the figures. It is obvious in Fig. 16 (on the left) that larger forces on the coastal wall are occured along with the reduction of the parameter L_{pl}/L_{si}. When long waves appear in the combination with the small distance L_{pl}, the wave jet is formed during the wave breaking on the crown of LCS causing the larger forces on the front wall. This growth is especially noticeable for the values $L_{pl}/L_{si} < 1$ for inter 3 and 2. In this area the values of the recorded forces $F_{(inter1\div6)}$ are larger than $F_{(inter0)}$. Similar pattern appears in Fig. 16 (on the right) as well, although the point that corresponds inter6- Test 9 (final left green point) is not in favor.

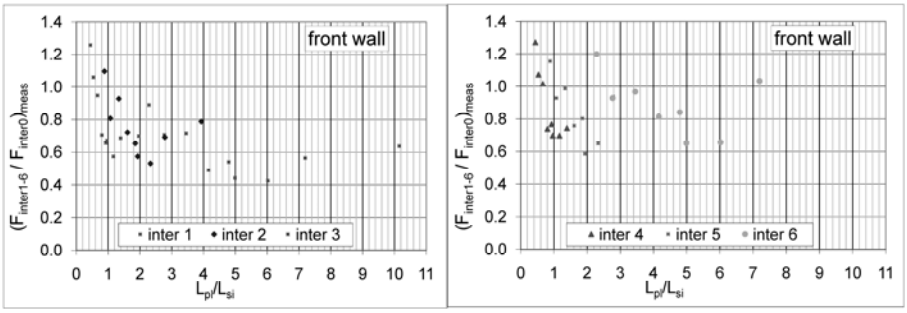

Fig. 16. Influence of the distance between structures (L_{pl}) on perforated seawall forces for front wall, (L_{pl} – distance between LCS and perf. seawall, L_{si} incoming significant wave length in front of the LCS)

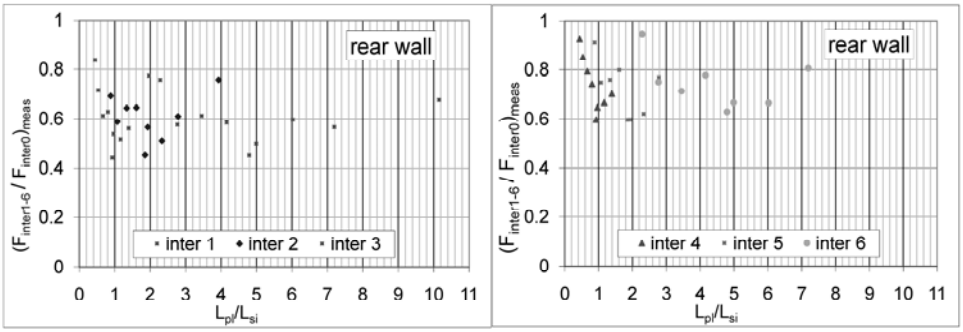

Fig. 17. The influence of the distance between LCS and the perforated seawall L_{pl} on the loading of the perforated seawall for the rear wall, (L_{pl} – the distance between LCS and seawall, L_{si} incoming significant wave height in front of the breakwater)

This effect is less expressed in Fig. 17 because we are dealing with the rear wall here that is partly protected by the front wall so that the influence of the parameter L_{pl}/L_{si} is less

expressed. For all values is valid: $(F_{(inter1–6)}/F_{(inter0)})_{meas}$ <1, which is not the case with the front wall.

On the other hand, the measuring accuracy for the Test 9 and 8 (inter 0) can be questioned for the front wall (Fig. 15) because there are extraordinary small measured values $(F_{inter0})_{meas}$ obtained in relation to the theoretical values according to the model [9]. It is also noticed that the trend for the Test 9 and 8 (inter 0) for the front wall is decreasing unlike the same tests made on the rear wall, where it is mostly growing. Taking everything above presented into consideration, the conclusion given should be considered with a reserve.

8.5.4. Comparison of Measured and Theoretical Hydrodynamic Pressure on Seawall

Proposed theoretical model required to obtain theoretical hydrodynamic pressure on the perforated wall protected by LCS is presented in the Chapter 8.2. An example of measured and theoretical hydrodynamic pressure is given in Fig. 18.

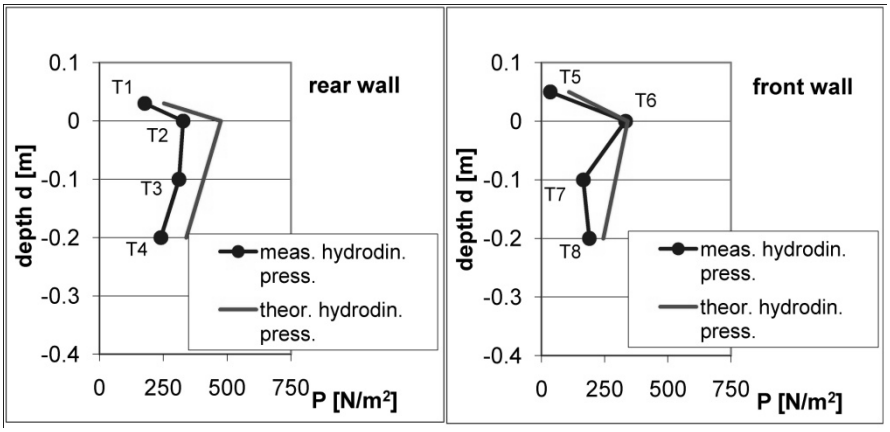

Fig. 18. Hydrodynamic pressures P_{hd} measured and calculated with theoretical model from chapter 8.2, for Test5: H_s = 0.1 m and T_p = 1.1 s, inter1

The example of comparison between measured and theoretical pressures (Fig. 18) points out the fact that the theoretical model relatively well describes the changes of hydrodynamic measured pressure by depth, but generally overestimates measured results. All calculated hydrodynamic pressures point out at the same conclusion, but are not shown here due to limited space.

8.5.5. Comparison of Measured $(F_{inter1\div6})_{meas}$ and Theoretical $(F_{inter1\div6})_{theor}$ Hydrodynamic Force on the Seawall

Fig. 19 gives the comparison between theoretical horizontal resultant force $(F_{inter1\div6})_{theor}$ calculated according to proposed model (Chapter 8.2) and measured horizontal resultant force $(F_{inter1\div6})_{meas}$ for inter1÷6.

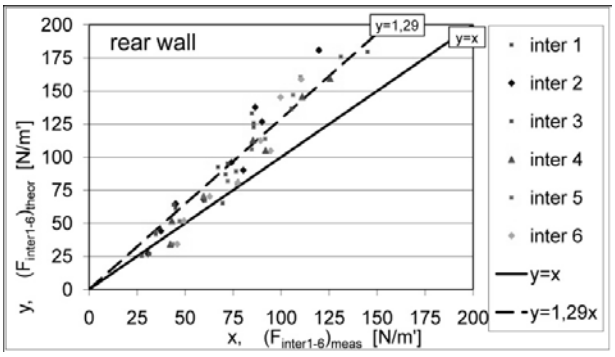

Fig. 19. Comparison of theoretical $(F_{inter1\div6})_{theor}$ and measured $(F_{inter1\div6})_{meas}$ horizontal force on rear wall of perforated seawall protected by submerged LCS. Values are approximated with linear functions (least square method)

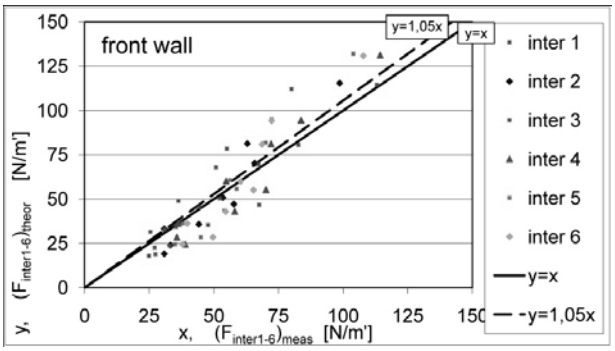

Fig. 20. Comparison of theoretical $(F_{inter1–6})_{theor}$ and measured $(F_{inter1–6})_{meas}$ horizontal force on the front wall of perforated seawall protected by submerged LCS. Values are approximated with linear functions (least square method)

For the rear wall it can be concluded that the theoretical values of the horizontal force $(F_{inter1\div6})_{theor}$ are larger for ≈29% than the measure values of the force $(F_{inter1–6})_{meas}$, and for the front wall the difference is ≈5% according to approximation lines. This comparison indicates that the proposed theoretical model of the resultant force calculation on the perforated seawall overestimates measured data, and is on the safe side.

8.6. Conclusion

The paper confirms that the theoretical model [9] for the perforated seawall load calculation is conservative providing larger values than the measured ones up to ≈50%.
It was concluded that by implementing smooth submerged LCS for the protection of the perforated seawall the force on the perforated seawall decreases depending on the water depth over LCS's crest. This decrease is ≈25–40% for the rear wall, and ≈15–25% for the front wall, depending on the depth of crest's submergence. Obtained results point to the fact

that the depth reduction above the LCS's crest causes the decrease of force values on the perforated coastal structure.

There is also the phenomenon of the negative effect of LCS manifested by larger forces on the perforated front wall than in the case when the perforated seawall is not being protected by LCS. When the LCS is quite close to the perforated seawall, i.e. when the distance ratio between the structures and the incoming significant wave length is $L_{pl}/L_{si} < 1$ larger forces are occurring than when the perforated seawall is not being protected by LCS. When long waves combined with short distance L_{pl} occur, the wave jet develops during the wave break on the crest of LCS causing increased force on the front wall. This phenomenon is insufficiently supported in this paper, so additional research is needed to be undertaken.

It can be concluded on the basis of obtained comparison between measured pressures and pressures of the proposed theoretical model that the theoretical model relatively well describes the changes of measured hydrodynamic pressure by depth. However it overestimates generally measured results. It can be summed up that the forces value obtained by the theoretical model is larger for ≈ 5% for the front wall and ≈ 30% for the rear wall than the measured values. The theoretical model for the force calculation for the perforated and the rear wall is conservative.

References

[1] Marks M., Jarlan G. E.: Experimental study on a fixed perforated breakwater. Proc. 11th Coastal Engineering Conference, III, ASCE, 1121–1140, 1968.

[2] Sawaragi T., Iwata, K.: Irregular wave attenuation due to a vertical barrier with air chamber. Coastal Structures 79, ASCE, 29–47, 1979.

[3] Allsop N. W. H., Hettiarachichi S. S. L.: Wave reflections in harbours: design, construction and performance of wave absorbing structures. Report OD 89, HR Wallingford, 1989.

[4] Fugazza M.; Natale L.: Hydraulic design of perforated breakwaters. Journal of Waterway, Port, Coastal, and Ocean Engineering, Vol. 118, No. 1, 1992.

[5] Park W. S., Chun I. S., Lee D. S.: Hydraulic experiments for the reflection characteristics of perforated breakwaters. Journal of Korean Society of Coastal and Ocean Engineers 5 (3); 198–203 (in Korean, with English abstract), 1993.

[6] Suh Kyumg-Duck, Park Jae Kil, Park Woo Sun: Wave reflection from partially perforated-wall caisson breakwater. Ocean Engineering 33 264–280, 2006.

[7] Takahashi S., Tanimoto K., Shimosako K.: A proposal of impulsive pressure coefficient for the design of composite breakwaters. Proceedings International Conference on Hydro-Technical Engineering for Port and Harbour Construction (Hydro-Port), Yokosuka, Japan, vol. 1, Part 1, 489–504, 1994.

[8] Requejo S., Vidal C., Losada I. J.: Modeling of wave loads and hydraulic performance of vertical permeable structures. Coastal Engineering 46, 249–276, 2002.

[9] Tabet-Aoul Lamber: Tentative new formula for maximum horizontal wave forces acting on perforated caisson. Journal of Waterway, Port, Coastal and Ocean Engineering, January-February, 2003.

[10] Chen X., Li Y., Wang D., Liu Y., Ma B., Jiang J.: Study for the horizontal wave forces and their overturning moment on perforated caissons with upper structure. Proceedings of the Seventh 2006 ISOPE Pacific/Asia Offshore Mechanics Symposium, ISOPE PACOMS 2006, 282–287, 2006.

[11] Chen X., Li, Y., Teng, B.: Numerical and simplified methods for the calculation of the total horizontal wave force on a perforated caisson with a top cover. Coastal Engineering, Volume 54, Issue 1, 67–75, 2007.

[12] Goda Y.: Random seas and design of maritime structures. 2nd edn. World Scientific, Singapore, 443, 2000.

[13] Takahashi S. Tanimoto K. Miyanaga S.: Uplift wave forces due to compression of enclosed air layer and their similitude law. Coastal Engineering Journal, Volume 28, 191–206, 1985.
[14] D'Angremond K., Van der Meer de Jong R. J.: Wave transsmision at low-crested structures. ASCE, Proc. ICCE, Orlando, Florida, 3305–3318, 1996.
[15] Seabrook S. R., Hall K. R.: Wave transsmision at submerged rubble mound breakwaters"; Proc. 26TH Int. Conf. on Coast. Engineering, ASCE, 2000–2013, 1998.
[16] Buccino M., Calabrese M.: Conceptual approach for prediction of wave transmission at low-crested breakwaters. Journal of Waterway, Port, Coastal, and Ocean Engineering, ASCE, May/June 2007.
[17] Van der Meer J. W., Wang B., Wolters A., Zanuttigh B., Kramer M.: Oblique wave transmission over low-crested structures. ASCE, Proc. Coastal Structures, Portland, Oregon, 2003.
[18] Van der Meer, J. W., Regeling H. J., de Waal J. P.: Wave transmission: spectral changes and its effect on run-up and overtopping. ASCE, Proc.ICCE, Sydney, Australia, 2156–2168, 2000.
[19] Briganti R., Van der Meer J. W., Buccino M., Calabrese M.: Wave transmission behind low crested structures. ASCE, Proc. Coastal Structures, Portland, Oregon 2003.
[20] Van der Meer J. W., Wang B., Wolters A., Zanuttigh B., Kramer M.: Oblique wave transmission over low-crested structures. ASCE, Proc. Coastal Structures, Portland, Oregon 2003.
[21] Shirlal K. G., Rao S., Ganesh V., Manu: Stability of breakwater defencedby a seaward submerged reef. Ocean Engineering, 33, 829–846, 2006.
[22] Muni Reddy M. G., Neelamani S.: Hydrodynamic studies on vertical seawall defenced by low-crested breakater. Ocean Engineering 32, 747–764, 2005.
[23] Muni Reddy M. G., Sannasiraj S. A., Natarajan R.: Numerical investigation on the dynamics of a vertical wall defenced by an offshore breakwater. Ocean Engineering 34, 790-798, 2007.
[24] D'Angremond, K., Van der Meer, de Jong, R.J.: Wave transsmision at low-crested structures. ASCE, Proc. ICCE, Orlando, Florida, 3305–3318, 1996.
[25] Van der Meer, Briganti R., Zanuttigh B. Wang B.: Wave Transmission and Reflection at Low-crested Structures: Design Formulae, Oblique Wave Attack and Spectral change. Coastal Engineering 50, 915–929, 2005.
[26] Zelt J. A., Skjelbreia J. E.: "Estimating incident and reflected wave fields using an arbitrary number of wave gauges". Coastal Engineering, 2002.
[27] Journée J. M. J., Massie W. W.: Offshore Hydromechanics. First Edition, Delft University of Technology, http://www.shipmotions.nl, 5–43, 2001.
[28] Oumeraci H., Kortenhaus A., Allsop W., De Groot M., Crouch R., Vrijling H., Voortman H.: Probabilistic design tools for vertical breakwaters. A. A. Balkema Publishers, February 134–156, 2001.
[29] Yip T. L., Sahoo T., Chwang A. T.: Trapping of surface waves by porous and flexible structures. J. Wave Motion 35, 41–54, 2002.
[30] Suh Kyung Doug, Choi Jae Chun, Kim Bum Hyoung, Park Woo Sun, Lee Kil Seong: Reflection of irregular waves from perforated-wall caisson breakwaters. Coastal Engineering 44, 141–151, 2001.

9 Application of Flood Mapping Methods on Failure Wave Modelling

Katarína Cipovová, Radomil Květon (Slovac University of Technology in Bratislava, Faculty of Civil Engineering)

9.1. Introduction

Following the Directive of The Ministry of Environment No. 1/2007 – 1.5 [1], the aim of this paper is to present the project of calculation the failure wave from Liptovská Mara water scheme and to emphasize the difference between 1D and 2D modelling of such a flood wave. This project also contains demolition effects evaluation.

In 2010 our department participated in calculation of Liptovská Mara failure wave. A failure wave is a specific type of a flood wave caused by failure or crash of a water structure. Its characteristics are rapid increase of an extreme discharge and relatively short duration. The Directive of The Ministry of Environment from 30th April 2007 No. 1/2007 – 1.5 determinates the calculation methods of failure wave calculation.

Whole directive is predominantly 1D oriented. It allows application of 2D model in plane areas but for valleys with uniform flow direction it predetermines branch 1D model. At a time when the Directive had been formed this approach was chosen because of limited application of 2D models. Because of high computing demandingness 2D modelling was applied only on relatively small areas.

Modern modelling tools and efficient computer-assisted techniques enable accurate 2D modelling of water flow on large areas and long river stretches.

This paper also contains recommendations for 2D model results interpretation and elaboration of results from MIKE 21 FM is described.

A very calculation was realized together with DHI Slovakia Company using MIKE 21 FM software with flexible computation mesh.

Submitted paper sufficiently demonstrates the necessity to modify the Directive for failure wave calculation so that modern computing systems could be used and more accurately results should be obtained.

This paper also contains application of Loss Curves for evaluation of damages caused by a flood wave.

9.2. Basic Information

The hydraulic system Liptovská Mara-Bešeňová lies in the North Slovakia on the longest Slovak river – the Váh River (Fig.1). Liptovská Mara Reservoir is the largest Slovak reservoir; it belongs to dams registered by the ICOLD. The purpose of this hydraulic structure is to use the hydro power potential of the Váh River, to supply the flow of water under the dam and to protect the area from floods. Besides its important water

management effects as the production of peak electric energy, water supply of industry and agriculture and flood protection, it also influences positively the use of the hydro potential of the Váh all along the Váh Cascade. [10]

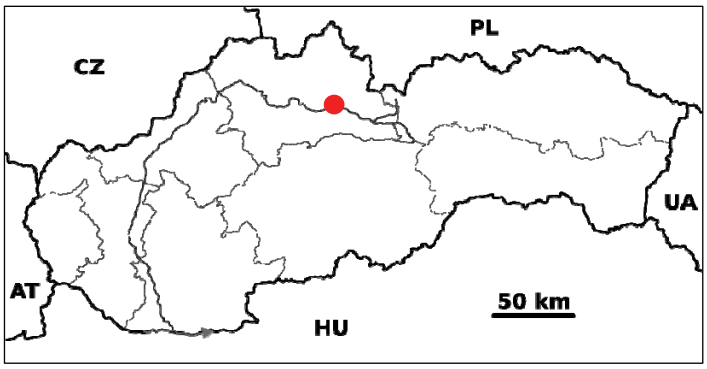

Fig. 1. River Váh catchment and the location of Liptovská Mara water structure

Construction:	1967 – 1975
Chainage of a dam cross section:	338.40 km
Height of a dam above the terrain:	45.0 m
H. of a dam above the foundations:	52.5 m
Level of the dam crest:	567.59 m a.s.l.
Length of a dam crest:	1225 m
Volume of the reservoir:	361.9 mil. m^3
Volume of the dam:	1.80 mil. m^3
Power plant:	$2 \times$ Kaplan turbines ($2 \times 140\ m^3 \cdot s^{-1}$)
	2 reversible turbines ($2 \times 130\ m^3 \cdot s^{-1}$)

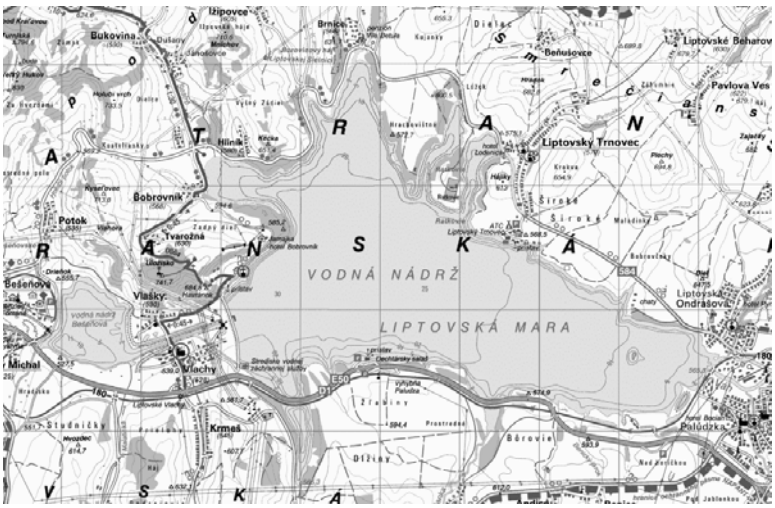

Fig. 2. Liptovská Mara reservoir

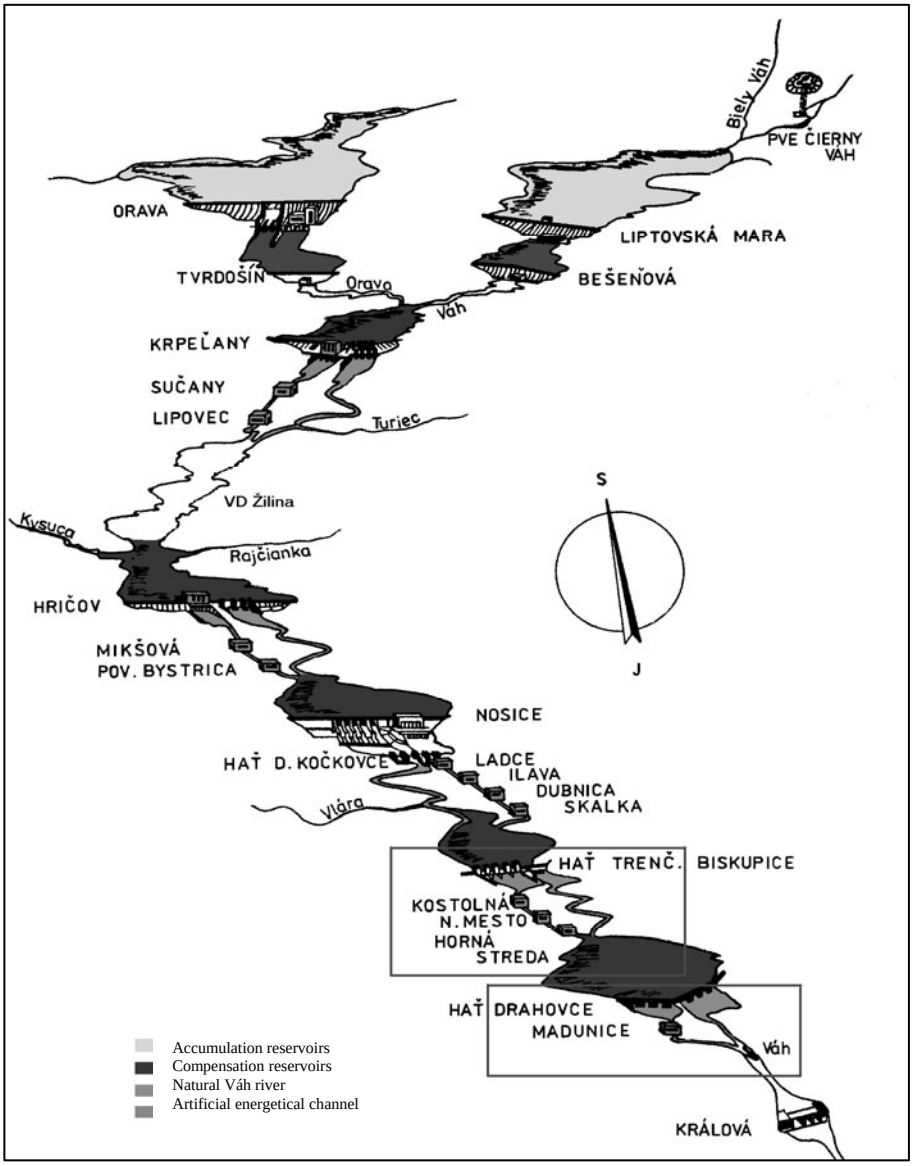

Fig. 3. The scheme of a Váh Cascade – two model areas Trenčianske Biskupice – Drahovce and Drahovce – Kráľová; are in red rectangles

9.2.1. Model Area

Our task was to calculate and model the failure wave of Liptovská Mara dam and to draw the flood line into the maps. Upper part Liptovská Mara – Trenčianske Biskupice had been calculated in 2004 by Hydroconsult, Bratislava using 1 – dimensional MIKE 11 software [2]. We continued the calculation according to their results, but using 2 – dimensional MIKE 21 FM software. We divided the area into two parts, Trenčianske

Biskupice–Drahovce and Drahovce-Kráľová (Fig. 3). The whole length of the simulated area is approximately 99 km.

9.2.2. Input Data

An initial discharge for a simulation was given 145 $m^3 \cdot s^{-1}$; what is an average annual discharge Q_a. This value was divided into derivation channel (50 $m^3 \cdot s^{-1}$) and natural Váh channel (95 $m^3 \cdot s^{-1}$). According to high value of hundred year discharge in Trenčianske Biskupice cross section (Q_{100}>2000 $m^3 \cdot s^{-1}$), Q_a of the other tributaries have been neglected.

Digital terrain model was provided by © EUROSENSE, s.r.o. [3], and improved where necessary according to handling regulations of single water structures.

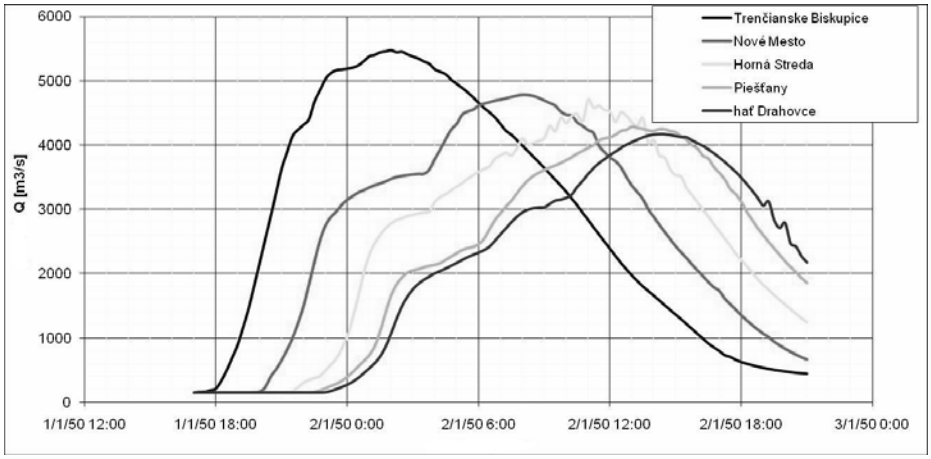

Fig. 4. Flood waves in cross sections: Trenčianske Biskupice, Nové Mesto, Horná Streda, Piešťany and weir in Drahovce

9.2.3. Simulation

A very calculation was realized with MIKE 21 FM software with flexible triangular computation mesh, which enables compressing the computation mesh at important objects, line structures or water-courses. MIKE 21 FM is two-dimensional mathematical model of unsteady flow based on a flexible mesh approach and it has been developed for applications within oceanographic, coastal and estuarine environments, but it may also be applied for studies of overland flooding. The system is based on the numerical solution of the two-dimensional incompressible Reynolds averaged Navier-Stokes equations invoking the assumptions of Boussinesq and of hydrostatic pressure. The spatial discretization of the basic equations is performed using a cell-centred finite volume method. The spatial domain is discretized by subdivision of the continuum into non-overlapping triangular or quadrilateral elements (cells). [9] The FM version is particularly well suited for modelling large complex areas that, at the same time, require a detailed resolution of specific features. The result from MIKE 21 FM is water level, flow direction and flow vectors in **X** and **Y** direction for the points in simulated area for appropriate time steps, water depths and specific discharges. Everything can be shown in map, graphical or numerical form. The

output provides real view on hydraulic conditions during the flood. Simulation of a failure wave has to be performed that far until its maximum discharge is lower than Q_{max100}. In case of plane areas simulation is performed till failure wave elevation falls to 0.5 m over existing ground. Correctly simulation should end not till the discharge falls under Q_a (average year discharge) or isolated water masses originate.

The result of that simulation is water depth or water level and mean cross section velocity in every element of the triangular computation mesh (Fig. 5).

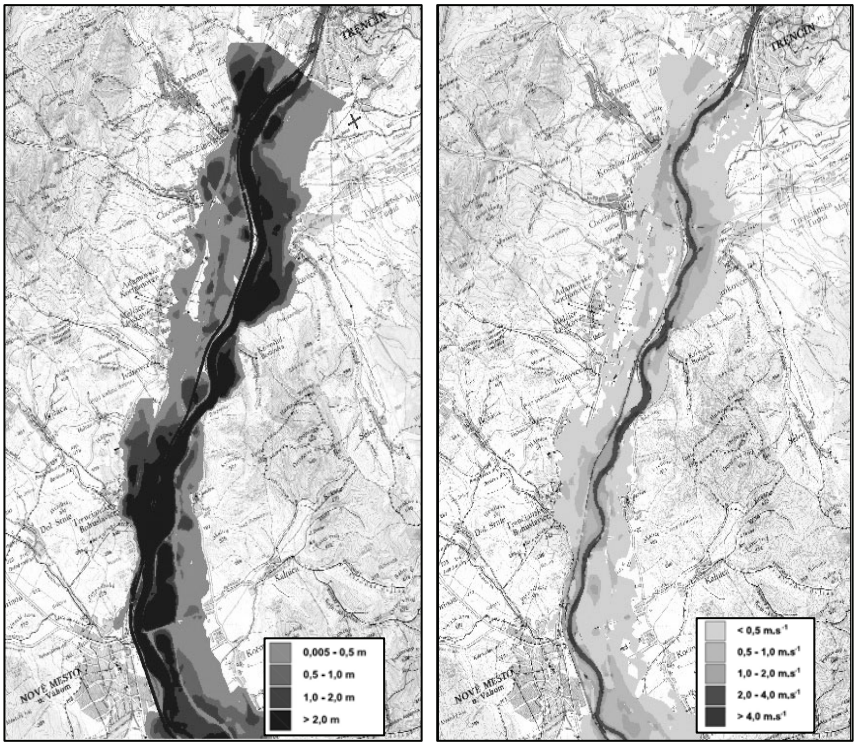

Fig. 5. Maps of maximum water depth (left) and velocities (right) in Trenčianske Biskupice – Nové Mesto part – graphic variant of the results.

9.3. Directive 1/2007 – 1.5. from the 30th April 2007 for Calculation of a Failure Wave from a Water Structure

According to this directive [1], project documentation of calculation of a failure wave must contain:

— technical report,
— general scheme of a model area in 1:50 000 scale,
— numeric values of calculated parameters elaborated in table form,
— graphic-elaborated parameters,
— evaluation of damages caused by a failure wave,

— flood lines in each endangered municipality must be drawn in into cadastral map,
— flood lines must be drawn in maps 1:10 000.

Because of delimited usage of 2D mathematical models in time of issuing this directive it is preliminary 1D oriented [6]. It allows application of 2D model in flat areas, but for simulations in valleys with explicit direction of a flow it predetermines the usage of a branch-1D mathematical model. It is also caused by high computation demandingness of 2D model as well as high data storage demandingness. Quantity of results (much bigger from 2D than from 1D) as well as their modification from section to local; force us to change not only the method of presenting the results, but also to provide tools for precise gathering of maximum and instant values in defined time step in each asked locality. Working with 2D model results poses high claims on the user and obligatory project documentation should conform to that, for example by creating functional user documentation.

9.4. Demolition Effects Evaluation

The directive [1] orders to process the demolition effects evaluation in a table form (like Tab. 1). For every endangered municipality, highway, bridge or railway there must be defined: chainage (or distance of an object from the dam, time when the wave decreases under Q_{max100} and the level of damage/destruction of an object.

Table 1

Demolition effects evaluation – appendix municipalities

Town		Chainage	Max. Height of a wave in a town		Max. Velocity of wave	Time of entry of the wave to the town		Time of culmination of the wave in a town		Time of decrease of the wave under Q_{max100}		Demolition effects evaluation
			level	depth	max							
		(rkm)	(m a.s.l)	(m)	(m · s^{-1})	(HH:MM)	date	(HH:MM)	date	(HH:MM)	date	
1	Sokolovce	112.975	154.64	1.98	1.19	9:45	2.1.	15:15	2.1	–		flooded 50%
2	Drahovce	108.475	152.50	3.34	1.79	11:15	2.1.	16:30	2.1	20:30	2.1.	flooded 100%
3	Jalšowé	109.625	151.52	1.07	0.17	11:00	2.1.	15:45	2.1	–		flooded boarders
4	Madunice	104.775	147.72	2.26	0.71	13:30	2.1.	19:45	2.1	–		flooded 60%
...	...	...										...

It seems to be convenient to use the results from the risk analysis of flooded areas, which has been developed within the framework of flood modelling. The intensity of the failure wave should be defined similarly to the intensity of the flood wave (IP), according to the water depth h and velocity v:

$IP=h$ *for* $h>0$ *and* $v<1\ m \cdot s^{-1}$ *zone of predominant hydrostatic effect*
$IP=h \cdot v$ *for* $h>0$ *and* $v>1\ m \cdot s^{-1}$ *zone of predominant hydrodynamic effect*

following by its division to zones with low, medium and high failure wave intensity (Tab. 2) [7].

Table 2

Categories of flood intensity effects evaluation – appendix municipalities

Category of IP [m^2/s]	Effects
IP<0,5 low (green)	people and animals are little endangered small damages to buildings are possible
0,5<IP<2 medium (yellow)	people and animals are little endangered outside the building (inside just little) bigger damages to buildings are possible (not destruction)
IP>2 high (red)	people and animals are endangered destroying of buildings is possible

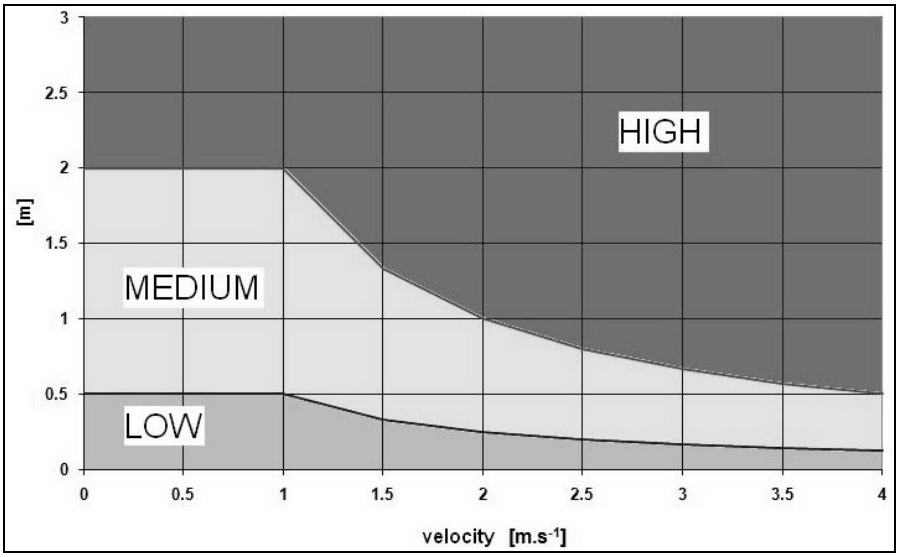

Fig. 6. Categories of flood intensity (IP)

Assuming velocities outside the channel (in the urban areas) $v < 1\ \mathrm{m} \cdot \mathrm{s}^{-1}$, it's possible to put IP = water depth *h*. Following this assumption the map of flood intensities has been created.

9.5. Using the Loss Curves

The loss curve represents the functional reliance of the degree of the damage on the flood progress attributes. Loss curves have been developed for more types of representatives of objects (like family houses, buildings in general, halls, blocks of flats, etc.) after floods on south Moravia in 2006 [8]. Following the information about the flood damage in Czech Republic those curves has been verified in 2002. The basic parameter for

creating graphic loss curves was the water depth and the duration of the flood.

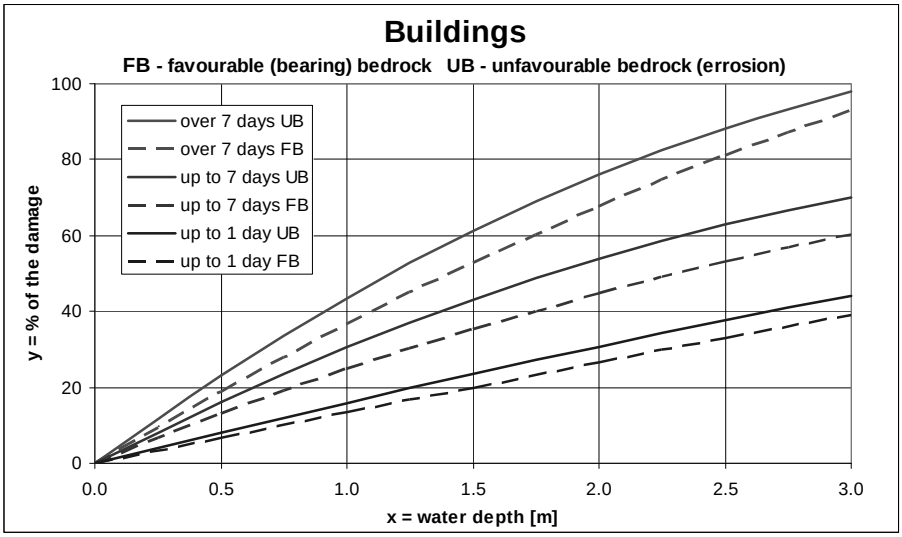

Fig. 7. Loss curves in flooded area according to the properties of a bedrock and the duration of the flood (Buildings for management and administration, shopping and catering, standard blocks of flats, untypical blocks of flats)

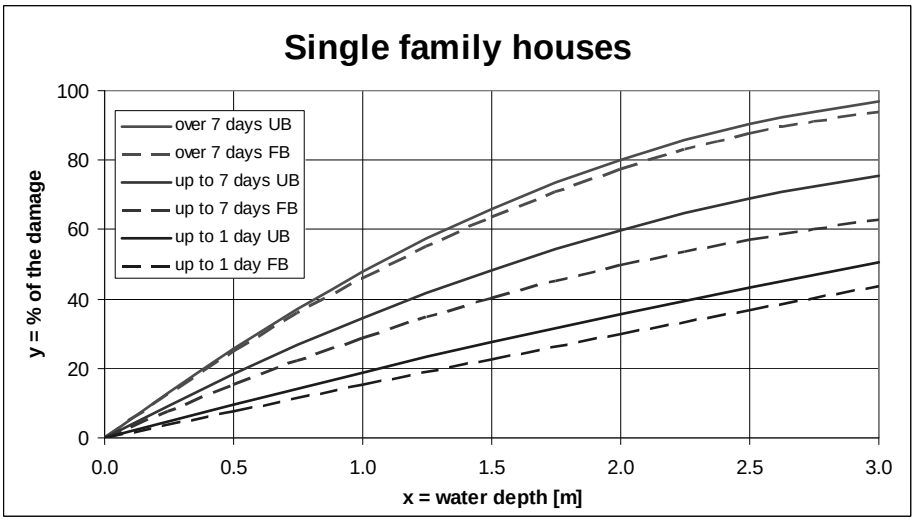

Fig. 8. Loss curves in flooded area according to the properties of a bedrock and the duration of the flood (single one-flat family houses)

Next were the properties of the bedrock (favourable/unfavourable), contamination and sediment transport. However, in [8], there is no velocity factor being considered, e.g. hydrodynamic effects are neglected. In the case of Liptovská Mara failure wave, we take

into account the blue curves (flood with duration less than 24 hours), whereas the whole flood caused by a failure wave lasts approximately one day.

Those pictures (Fig. 7 – Fig. 10) show the influence of the duration of the flood and the properties of the bedrock on the % of the damage of the object. For example, during the flood lasting less than one day it doesn't matter what bedrock is under a hall. It behaves the same up to 1.5 m water depth (Fig. 10).

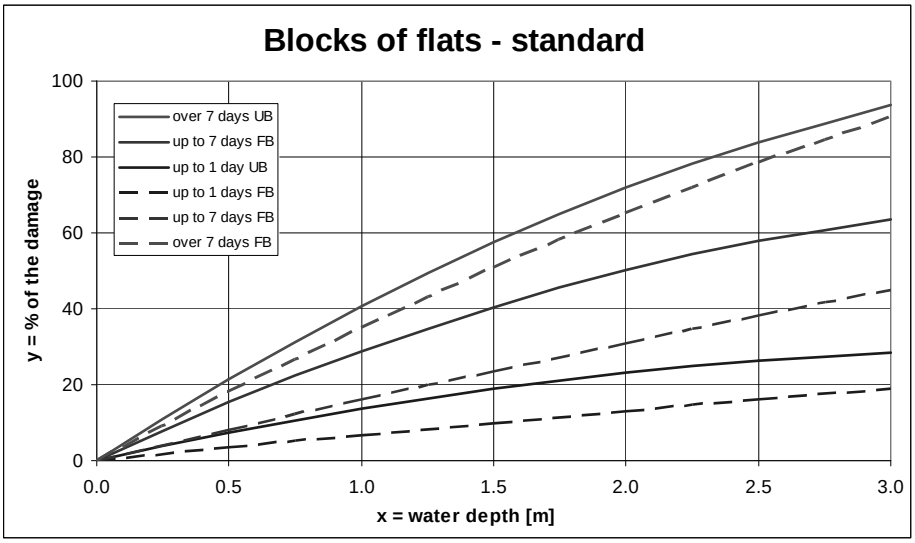

Fig. 9. Loss curves in flooded area according to the properties of a bedrock and the duration of the flood (blocks of flats with national unitized construction system)

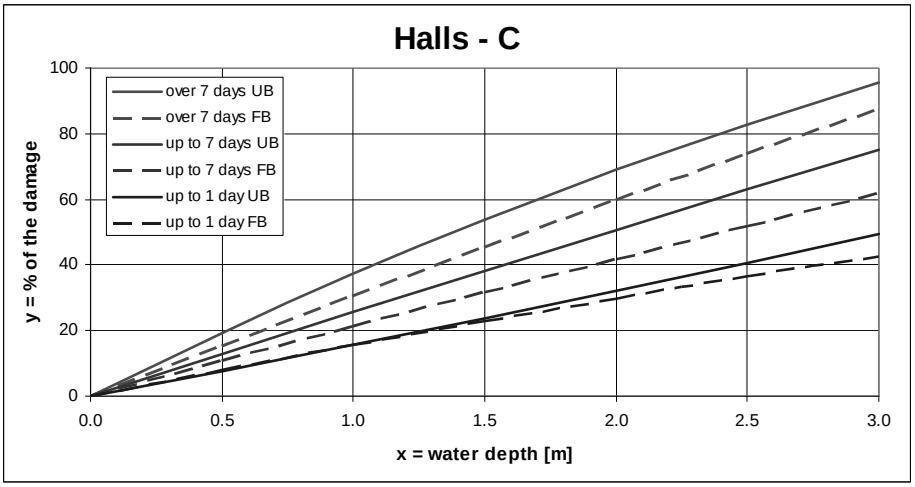

Fig. 10. Loss curves in flooded area according to the properties of a bedrock and the duration of the flood (halls for civic amenities, halls for production and services, component halls)

Fig. 11. Planar evaluation of the % of the damage of the object for the Opatovce locality (buildings in general)

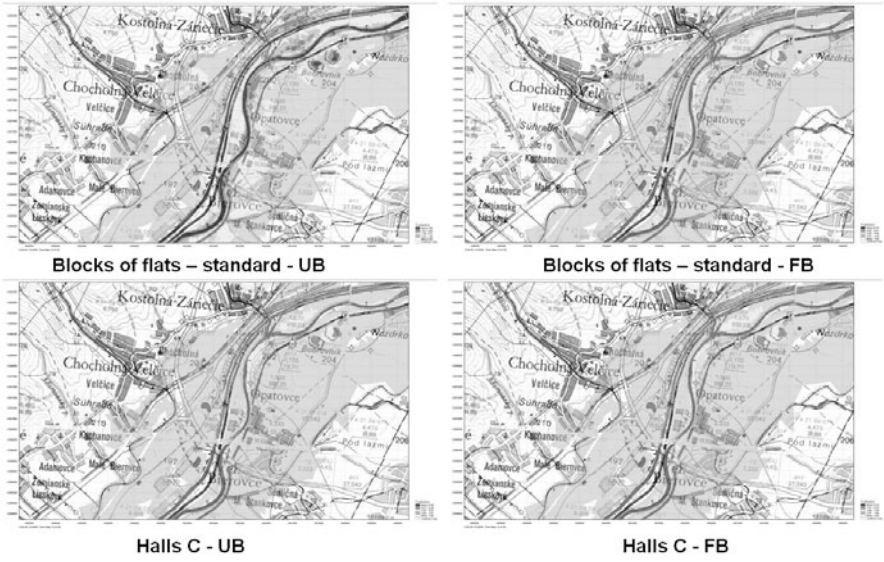

Fig. 12. Planar evaluation of the % of the damage of the object for the Opatovce locality (different types of buildings)

From those loss curves we deduced the ranges for graphic evaluation of damages according to the water depth (Fig. 11).

9.6. Conclusions

Following all those facts and data; submitted paper sufficiently demonstrates the necessity to modify the Directive for failure wave calculation so that modern computing systems could be used and more accurate results should be obtained.
Using of the loss curves in our conditions is convenient and desirable, but it should be very useful to adjust them also for the zones with predominant hydrodynamic effects.

References

[1] Smernica Ministerstva životného prostredia Slovenskej republiky z 30.apríla 2007 č.1/2007 – 1.5. pre výpočet prielomovej vlny z vodnej stavby.
[2] VD Liptovská Mara – Kompletná dokumentácia výpočtu prielomovej vlny, Dopočet od hate Trenčianske Biskupice, SvF STU v Bratislave, 08/2010.
[3] Digitálny model terénu dotknutej oblasti © EUROSENSE, s.r.o., www.eurosense.sk.
[4] VD Liptovská Mara, Kompletná dokumentácia výpočtu prielomovej vlny, Hydroconsult Bratislava, 11/2004.
[5] Mišík M., Kučera M., Květon R., Šulek P.: Modelovanie prielomových vĺn v údolí riek pomocou 2D matematického modelu, Medzinárodná odborná konferencia o bezpečnosti vodných stavieb pri príležitosti 35. výročia činnosti TBD, Bratislava, 2010.
[6] Květon R., Šulek P., Orfánus M., Mišík M., Kučera M.: Smernica pre výpočet prielomovej vlny z vodnej stavby a 2D matematické modelovanie, Medzinárodná odborná konferencia o bezpečnosti vodných stavieb pri príležitosti 35. výročia činnosti TBD, Bratislava, 2010.
[7] Dráb A.: Riziková analýza záplavových území s podporou GIS, habilitačná práca, VUT Brno, 2009.
[8] Korytárová J. a kol.: Povodně a nemovitý majetek v území, FAST VUT Brno 2007.
[9] DHI, 2009b. MIKE 21 & MIKE 3 FLOW MODEL FM, Hydrodynamic and Transport Module, Scientific Documentation.
[10] Bednárová E. et al.: Priehradné staviteľstvo na Slovensku. KUSKUS, Bratislava, 2010, ISBN 978-80-970428-0-6.

Acknowledgements

This paper was supported by the Grant agency VEGA under contract No. 1/0578/11 and No. 1/0281/10 and the Slovak Research and Development Agency under contract No.APVV-0680-10.

10 Methods of Modeling of Leachate from the Landfill

Kristína Galbová, Ivona Škultétyová (Slovak University of Technology in Bratislava, Faculty of Civil Engineering)

10.1. Introduction

Protection of groundwater quality is a primary performance goal for all waste containment systems, including final cover systems. The potential adverse impact to groundwater quality results from the release of leachate generated in landfills or other waste disposal units such as surface impoundments. The rate of leachate generation (and potential impact on groundwater) can be minimized by keeping liquids out of a landfill or contaminated source area of a remediation site. As a result, the function of minimizing percolation becomes a key performance criterion for a final cover system (EPA 1991) [37].

The basic law governing the responsibilities for waste management in the Slovak Republic Act no. 223/2001 Z. z. on waste and amending certain laws as amended.

The Landfill Directive requires the prevention or reduction of negative impacts of landfills on the environment, including groundwater. Landfill Directive, as the IPPC Directive lays down provisions for issuing permits based on a range of conditions, including impact assessment studies and is part of the main provisions of the Water Framework Directive (WFD). In order to ensure consistent protection of groundwater has been drawn up of the European Parliament and the Council 2006/118/EC of 12 December 2006 on protection of groundwater against pollution and deterioration.

10.2. The Leachate

Leachate is liquid that penetrated deposited waste and emitted from landfills or remain detained in a landfill [7]. Leachate is the main medium for the transport of contaminants from the landfill to groundwater and surface water. Landfill leachate is formed from the infiltration and passage of water through solid waste which results in a combination of physical, chemical and microbial processes that transfers pollutants from waste materials to the water [15, 16].

Under normal conditions, leachate is found at the bottom of the landfill and moves through the underlying strata. Although, some lateral movement may also occur, depending on the characteristics of the surrounding material, leachate percolates through the underlying strata and many of its chemical and biological constituents will be removed by filtering and absorptive action of the material composing the strata [29]. In general, the extent of this action depends on the characteristics of the soil. The exact volume of the produced leachate cannot be easily estimated as it depends on groundwater infiltration and waste composition.

The hydrometeorological conditions in the area of the landfill and its surroundings are of high importance as they affect the hydrogeological status of the area, leachate production and subsequently the risk of contamination [29].

10.2.1. Leachate Production

Leachates arise from infiltration of rain water body landfill. Occurs while the dissolution of large amounts of substances that are trapped in it. This water may be contaminated with inorganic salts, heavy metals and a high proportion of organic matter [7].

The volume of leachate depends principally on the area of the landfill, the meteorological and hydrogeological factors and the effectiveness of the capping. It is essential that the volume of leachate generated be kept to a minimum. The design and operation of the landfill should ensure that the ingress of groundwater and surface water is minimized and controlled [31].

10.2.2. Leachate Composition

The organic strength of landfill leachate can be greater than 20 to 100 times the strength of raw sewage. Landfill leachate is potentially a potent polluter of soil and groundwater [31]. The composition of leachate depends on many factors, such as the nature of the waste, the hydrological conditions, climate, season, age of the landfill, the amount of landfilled waste and landfill waste moisture penetration [7].

Many factors influence the leachate composition including composition of solid wastes, moisture content, the degree of compaction , hydrology of the site, pH of water, climate, age of the fill and other site-specific conditions including landfill design and type of liners used, if any [5, 17]. The leachate consists of many different organic and inorganic compounds that may either dissolve or suspended. Leachate from municipal landfills is a combination of BOD_5, COD_{Mn}, COD_{Cr}, suspended solids, chlorides, sulfates, sulfides, fluoride, dissolved substances, manganese, iron, aluminum, etc ... [31].

10.2.3. Quantity Leachate

The amount of leachate generated from landfills over long time periods (e.g. years) can be predicted quite well using available water balance models (e.g. HELP [31]).

Their quantity is influenced by the intensity of rainfall, the surface runoff, evaporation and the ability to accumulate the landfill body water [7]. They calculate leachate discharge equal to the difference between precipitation and the sum of actual evapotranspiration, runoff, and water storage within the waste body, whereby the later one is determined on the concept of field capacity (no water flow until the soil or waste reaches certain water content). However, the variation of the leachate discharge rate over time is much more difficult to describe, since it requires an understanding of the water flow processes inside the landfill [25].

Despite the need for obtaining information on the quantity of leachate from the landfill, they have so far not been sufficiently addressed. Process water balance for the landfill is more complex than the water balance of natural origin, because in addition to natural conditions affect the quantity water and bio-chemical processes inside a landfill [25]. Informative Annex A – STN 83 810 Landfilling, waste leachate from landfills describes the calculation of the amount of landfill leachate. It states that quantity leachate can be determined by water balance of landfill, which is generally expressed as follows:

$$Q = Z - P - V + W \pm U + R \quad (1)$$

where: Q – is the quantity leachate collected for landfill sealing system,
Z – rainfall,
P – surface runoff,
V – evaporation,
W – moisture content of the waste deposited,
U – water consumed by or underlying the ongoing march of the landfill,
R – retention capacity of landfill.

Getting quality input data is determined by several factors: the complexity of relationships in a landfill, the availability of necessary information, financial capabilities and etc.. To balance modelling of existing landfills is appropriate equation to calculate the quantities of leachate (1) modified [22].

10.3. Model Flow of Leachate

All over the world, about 70% of waste disposal is by landfilling, especially in the underdeveloped and developing countries [29]. The main environmental impacts of such landfills, containing high amounts of biodegradable organic matter, are caused by emissions of liquid effluents and landfill gas. With no collection and treatment, leachates from landfills pollute groundwater and soils locally [2, 8], while landfill derived methane contribute to climate change on a global level [11].

As water plays a key role in landfills, knowledge about its distribution and transport is fundamental for understanding the behavior of the landfill reactor [1, 2, 9].

In recent decades several water flow models for landfills have been developed. However, their application was almost exclusively limited to laboratory experiments. Comprehensive simulations of leachate flow and its generation rate using data from full scale landfills are very rare [14, 19].

10.3.1. Evaluation of Existing Modelling Approaches

To determine the internal structure of the landfill body and distribution of individual types of landfilled materials, as well as defining the areas of active exothermic reactions is used for this purpose geophysical method of measuring the spontaneous polarization (SP).

The results of the measurement method (SP) can be drawn map of the natural stationary electric field, which shows the movement of groundwater in the landfill body (Fig. 1) [13].

According to the geotechnical methods can identify and evaluate the state of landfills, which may cause transfer of liquids from the body of the landfill and assess the degree of potential risk to groundwater leachate from the landfill [13].

Based on scientific studies was detected that the prevailing approach for modeling water flow processes in solid waste media is based on the assumption of a homogenous porous media [28].

Over the years, a few authors [3, 23, 32] and [20] who accounted for the heterogeneous character of MSW landfills. Authors of studies in their models, waste is not considered to be a homogenous media. The landfilled waste is either divided into two domains of diverse hydraulic characteristics (a channel domain with rapid water flow, and a

surrounding matrix domain with slow water movement), or different local hydraulic conductivities of the waste are specified by probability density functions [20].

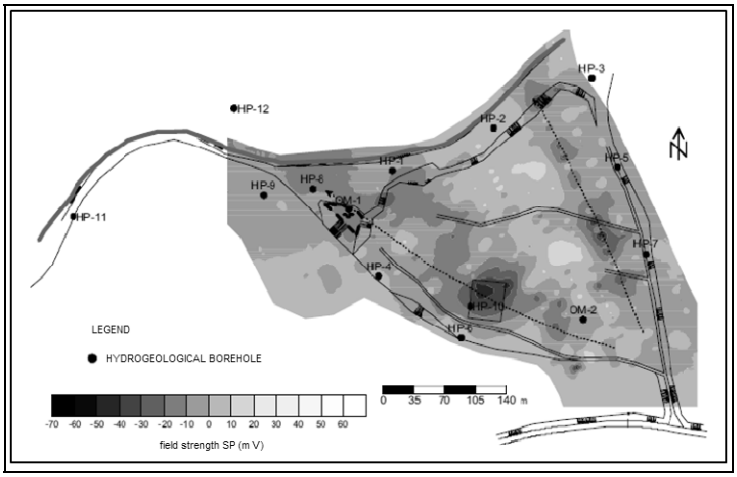

Fig. 1. Map of natural stationary electric field produced by the method of SP

In addition to the work of [20] stochastic approaches describing the heterogeneous character of water flow through waste have, for instance, been applied by [27] and [36]. The concepts for describing the water flow in the two domains are mathematically different. Uguccioni and Zeiss (1997) used the model PREFLO [34] to simulate the moisture movement. This model assumes that the rapid flow in the channel domain follows Poiseuille's Law and the lateral moisture transfer from the channels to the matrix occurs according to Richard's Law. Bendz et al. (1998) used another assumption for describing fast water flow in channels: they used a power function (kinetic wave model), proposed by Beven and Germann (1981) for describing water flows in macrospores soils, to determine the channel flow in landfills.

While the basic premise that is the similarity between water flow in landfills and in soils – has been neither proven nor discussed as a hypothesis yet. Consequently, the water flow pattern in landfills is investigated on a macroscopic level and is compared with non-uniform water flows in soils.

The hydraulic behaviour of single waste components ranges from highly water adsorbent (hydrophilic) to water repellent (lipophilic), from impermeable to readily permeable materials. Nevertheless, it is possible to determine hydraulic parameters for landfilled waste [26], if the investigated volume is big enough to truly represent the mixture of waste materials. The larger the sample, the higher the heterogeneity: If the aim is to consider the whole landfill body, the degree of heterogeneity cannot be described by investigating smaller volumes. Parameters determined at a small scale are not appropriate for characterizing entire landfills [11]. In particular construction elements (e.g., gas wells, daily cover layers), areas with low or high mechanical compaction, and border areas are responsible for enhancing heterogeneity. Furthermore, landfilling and compaction of waste in layers leads to horizontal stratification within the landfill. Consequently, permeability in the horizontal direction is potentially greater than permeability in the vertical direction [18]; [26]. Additionally, anisotropic behaviour is increased due to the orientation of impermeable

materials (such as plastic sheets) perpendicular to the compaction efforts (horizontal stratification of waste layers). Thus, a major part of the water flow in landfills occurs horizontally [6].

Water retention of the barrier layers by this mechanism is associated with a horizontal flow of water towards the vertical channel. This is repeated within the landfill many times, water is funnelled in preferential path ways with increasing depth.

As a consequence water flow becomes more non-uniform towards the landfill bottom. This hypothesis is in agreement with observations of several authors (Wiemer, 1982; Gabr and Valero, 1995; Öman et al., 1999; Yuen et al., 2001), who noted higher spatial differences in the water content towards the landfill bottom. Moreover tracer investigations at a pilot scale landfill [24] indicate that the velocity of solute transport increases with landfill depth.

Contrariwise the hydraulic conductivity of the waste decreases with depth [26], which implies that the waste volume participating in water flow significantly decreases with landfill depth.

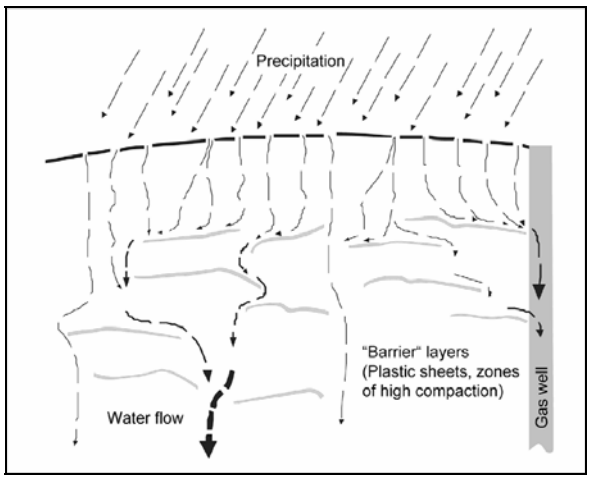

Fig. 2. Water flow pattern in MSW landfills (modified after [21])

The picture is taken from work [21], who first pointed out the importance of an impermeable layer of water movement. Ask compared the water transport inside landfills with the water flow from roofs. The structure indicated in Fig. 2 inevitably leads to a funnelling of water flow towards the bottom of a landfill [11].

The fraction of channel flow and matrix flow is not only dependent on the landfill (structure of the waste body), but also on the water application rate. New flow channels may develop or can be accessed during periods with high infiltration rates due to higher water retention above impermeable surfaces [15].

Even during dry periods (no water infiltration at the landfill surface) water flow is presumably redirected by impermeable layers (e.g., plastic sheets) towards preferential pathways. In soils preferential flow can be caused by the presence of macro-pores and other structural features, water repellence, and funnelling of flow due to the presence of sloping soil layers [30]. The latter phenomenon is most similar with the water flow pattern

observable in landfills. However, landfill models for simulating non-uniform water flow using a 2-domain approach [3, 23, 32] have been exclusively based on models for macro-pore soils.

This implies that most landfill models disregard limitations to vertical flows as a consequence of impermeable horizontal layers. Moreover the water application rate largely determines water movement and its distribution between preferential pathways and the soil matrix. During dry periods water transport is limited to the soil matrix, whereas under wet conditions (during or shortly after water infiltration events) water moves downward mainly through macro-pores. The soil matrix sorbs some water bypassing in preferential pathways due to the capillary forces in micro-pores. The rate of this lateral water movement (water infiltrating from macro-pores into the matrix) mainly depends on the water content (in the strict sense on the matrix potential) of the micro-pores.

10.4. Conclusions

The flow of water through Municipal solid waste (MSW) landfill is highly fragmented and dominated by preferential routes. Therefore, the concepts required to simulate the behaviour that was achieved the desired heterogeneous aqueous system dumps.

The latest models are based on 2-domain approach, distinguishing domain channel with high permeability, and matrix domain with the slow movement of water with high water retention capacity. These models focus on the mathematical description of the rapid flow of water in the channel domain. This work emphasizes the importance of water exchange between the two domains, and extends the 1-dimensional, 2-domain model of flow that into account water flows in two dimensions. Jet array consisting of the vertical path, surrounded by the waste mass is defined by HYDRUS-2D software. When the new model is calibrated using data from the MSW-landfill leachate expected also corresponds with the observed leachate discharge [11].

References

[1] Augenstein D., Pacey J.: Modeling landfill methane generation. In: Christensen, T.H., Cossu, R., Stegmann, R. (Eds.), Proceedings Sardinia 1991, Third International Waste Management and Landfill Symposium. CISA, S. Margherita di Pula, 115–148, 1991.

[2] Beaven R., Knox K., Croft B.: Operation of leachate recirculation trial in a landfill test cell. In: Christensen, T.H., Cossu, R., Stegmann, R. (Eds.), Sardinia 2001, Eighth International Waste Management and Landfill Symposium, Cagliari Sardinia, 595–604, 2001.

[3] Bendz D.: Generation of leachate and the flow regime in landfills. AFR-report 191, Lund, 27 s., 1998.

[4] Beven K., Germann P.: Water flow in soil macropores – a combined flow model. Journal of Soil Science 32, 15–29, 1981.

[5] Blight G. E., Fourie A. B., Shamrock J., Mbande C., Morris J. W. F.: "The effect of waste composition on leachate and gas quality: a study in South Africa", Waste Manage Res., vol 17, 124–140, 1999.

[6] Burrows M. R., Joseph J. B., Mather J. D.: The hydraulic properties of in situ landfilled waste. In: Christensen, T. H., Cossu R., Stegmann R. (Eds.), Proceedings Sardinia 1997, Sixth International Waste Management and Landfill Symposium. CISA, S. Margherita di Pula, 73–83, 1997.

[7] Derco J., Mencáková A., Almásiová B.: Utilization of Ozone for Treatment of Landfill Leachate, In: Chemické listy – ISSN 1213-7103 – Vol. 103, č. (7), 581–588, 2009.

[8] Ehrig H.-J.: Quality and quantity of sanitary landfill leachate. Waste Management and Research 1, 53–68, 1983.
[9] El-Fadel M., Findikakis A. N., Leckie J. O.: 1997b. Modelling leachate generation and transport in solid waste landfills. Environmental Technology 18, 669–686, 1997.
[10] El-Fadel M., Findikakis A. N., Leckie J. O.: 1997a. Environmental impacts of solid waste landfilling. Journal of Environmental Management 50 (1), 1–25, 1997.
[11] Fellner J., Brunner P. H.: Modeling of leachate generation from MSW landfills by a 2-dimensional 2-domain approach, Waste Management, Volume 30, Issue 11, November 2010, 2084–2095.
[12] Gabr M. A., Valero S. N.: Geotechnical properties of municipal solid waste. Geotechnical Testing Journal 18 (2), 241–251, 1995.
[13] Gajdoš V., Rozimant K.: Sstaré environmentálne záťaže a ich charakterizácia na základe geofyzikálnych meraní, In: Acta environmentalica universitatis comenianae, Bratislava, Vol. 14, 2(2006): 41–48 ISSN 1335–0285.
[14] García de Cortázar A. L., Tejero Monzón I.: Application of simulation models to the diagnosis ofMSWlandfills: an example. Waste Management 27 (5), 691–703, 2007.
[15] Jasper S. E., Atwater J. W., Mavinic D. S.: "Leachate production and characteristics as a function of water input and landfill configuration", Water Pollution Research Journal of Canada, vol. 20, 43–56, 1985.
[16] Kjeldsen P., Barlaz M. A., Rooker A. P., Baun A., Ledin A., Christensen T. H.: "Present and long-term composition of MSW landfill leachate: a review". Critical Reviews in Environmental Science and Technology, vol. 32, 297–336, 2002.
[17] Kouzeli-Katsiri A., Bodogianni A., Christoulas D.: "Prediction of leachate quality from sanitary landfills", J Environ Eng Div., 125 (EE10), 950–957, 1999.
[18] Landva A. O., Pelkey S. G., Valsangkar A. J.: Coefficient of permeability of municipal refuse. In: Proceedings of the 3rd International Congress on Environmental Geotechnics, Lisbon, 63–68, 1998.
[19] Lobo A., Muñoz J., Sánchez M. M., Tejero I.: Comparative analysis of three hydrological landfill models through a practical application (MODUELO 2, HELP and MODUELO 1. In: Christensen, C.A.S. (Ed.), Proceedings of the Ninth International Landfill Symposium, Sardinia 2003. CISA, Cagliari, Italy, 2003.
[20] McCreanor P. T., Reinhart D. R.: Mathematical modeling of leachate routing in a leachate recirculating landfill. Water Research 34 (4), 1285–1295, 2000.
[21] Mesu E. J.: Einflussfaktoren auf den Wasserhaushalt von Hausmülldeponien (in German: Factors determining the water balance of MSW landfills), Gas und Wasserhaushalt von Mülldeponien, Internationale Fachtagung 29.9 – 1.10.1982. Institut für Stadtbauwesen, Braunschweig, 271–288, 1982.
[22] Mikita S., Horvát O.: Využitie bilančného hydrologického modelovania pri štúdiu režimu kontaminačných prejavov zo skládok údolného typu, In: Podzemná voda 2008 – ISSN 1335-1052, XIV, 2/2008, 185–190, 2008.
[23] Obermann I.: Modellierung des Wasserhaushaltes von Deponien vorbehandelter Siedlungsabfälle (in German: Modeling the waster balance of landfills containing pre-treated waste). Ph.D. Thesis, Technische Universität Darmstadt, 1999.
[24] Öman C., Bengtsson Å., Rosqvist H.: Changes with depth and with time of leachates from a pilot-scale landfill. In: Christensen, T.H., Cossu, R., Stegmann, R. (Eds.), Proceedings Sardinia 1999, Seventh International Waste Management and Landfill Symposium. CISA, S. Margherita di Pula, 1999.
[25] Pelikán V.: Ochrana podzemních vod. Vyd. Praha, SNTL 1983, 324.
[26] Powrie W., Beaven R. P.: Hydraulic properties of household waste and implications for liquid flow in landfills. Proceedings of the Institution of Civil Engineers, Geotechnical Engineering 137, 235–247, 1999.
[27] Rosqvist H.: Water Flow and Solute Transport in Landfills. Ph.D. Thesis, Royal Institute of Technology, Stockholm, 40, 1999. `

[28] Schroeder P. R., Morgan J. M., Walski T. M., Gibson A. C.: The hydrologic evaluation of landfill performance (HELP) model, volume I, user's guide for version 1. Technical Resource Document EPA/530-SW-84-009, US Environmental Protection Agency, Cincinnati, 1984.
[29] Shao-gang Dong, Zhong-hua Tang, Bai-wei Liu: Numerical modeling of the environment impact of landfill leachate leakage on groundwater quality-A field application, 2009 International Conference on Environmental Science and Information Application Technology, 565-568, 2009.
[30] Šimunek J., Šejna M., van Genuchten M. T.: The HYDRUS_2D Software Package for Simulating Water Flow and Solute Transport in Two-Dimensional Variably Saturated Media. Version 1.0.. US Department of Agriculture Riverside, California, 1996.
[31] Škultétyová I.: Water source protection from landfills leachate, In: WMHE 2009.Vol.I.: Eleventh International Symposium on Water Management and Hydralic Engineering. Ohrid, Macedonia, 1.-5.9. 2009. Skopje: University Ss.Cyril and Methodius, 2009 – ISBN 978-9989-2469-6-8, 523–532.
[32] Uguccioni M., Zeiss C.: Comparison of two approaches to modelling moisture movement through municipal solid waste. Journal Environmental Systems 25 (1), 41–63, 1997.
[33] Wiemer, K.: Messung des Wassergehaltes und der Dichte von ungestörten Müllproben (in German: Measurement of water content and density at undisturbed waste samples), Gas und Wasserhaushalt von Mülldeponien, Internationale Fachtagung 29.9 – 1.10.1982. Institut für Stadtbauwesen, Braunschweig, 289–300, 1982.
[34] Workman S., Skaggs, R.: PREFLOW: A water management model capable of simulating preferential flow. Transaction of the American Society of Agricultural Engineerings 33 (6), 1939–1965, 1990.
[35] Yuen S. T. S., Wang Q. J., Styles J. R., McMahon T. A.: Water balance comparison between a dry and a wet landfill – a full-scale experiment. Journal of Hydrology 251 (1–2), 29–48, 2001.
[36] Zacharof A. I., Butler A. P.: Stochastic modelling of landfill leachate and biogas production incorporating waste heterogeneity. Model formulation and uncertainty analysis. Waste Management 24 (5), 453–462, 2004.
[37] http://www.epa.gov/superfund/accomp/news/pdfs/evapo.pdf

Acknowledgements

The article is supported by the Scientific Grant Agency and the Cultural and Educational Grant Agency of the Ministry of Education – VEGA Project No. 1/0559/10 dealt with at the Department of Sanitary and Environmental Engineering, Faculty of Civil Engineering, Slovak University of Technology in Bratislava.

11 Impact of Morphodynamical Changes on the Bridge Stability: Case Study of Jakuševac Bridge in Zagreb

Gordon Gilja, Neven Kuspilić, Damir Bekić (University of Zagreb, Faculty of Civil Engineering, Croatia)

11.1. Introduction

When watercourses are regulated, riverbed morphology changes in comparison to the natural state of the watercourse; it is shortened and, therefore, causes greater longitudinal slope and concentration of the river flow energy. Due to greater longitudinal slope, river velocity as well as riverbed shear force are locally higher causing changes in the riverbed morphology. When hydrodynamic force reaches its critical value and disrupts the balance of forces keeping the particles on the river bottom in place, the particles are lifted from the bottom and transported downstream. After a while they settle again thus influencing the morphological development of the riverbed.

Under critical flow velocity conditions in riverbeds with movable bottoms, rivers and channels adapt their riverbed shape to the boundary conditions and mold a natural flow and bed-load transport [13]. The shape of a river valley is a result of fluvial erosion and is influenced by hydrodynamic forces which act on non-coherent material in riverbeds. The stability of a river channel is dependent on the regime of sediment load discharge. If the natural balance of sediment discharge is disrupted, the result is deepening of the riverbed (global erosion), river bank erosion and even discharge profile obstruction can occur. In addition to global erosion, local scour can occur in places where the flow pattern is disrupted due to the influence of a submerged structure like a bridge pier. A significant hydraulic structure in the river usually reduces the local discharge profile, causing backwater effects and disruption of the flow pattern. The flow lines are elongated and concentrated along the solid contour, resulting in increased velocity and unit discharge, as well as increase in local shear stress. Aided by high turbulence, this can result in intensive scouring of material from the channel bed. Although structures may be inherently strong enough to withstand water forces their stability may be endangered by transportation of the material in the channel. The process of channel deepening in the zone influenced by the structure is finalized when equilibrium conditions are established, i.e. when the quantity of sediment entering the scour hole and sediment removed from the scour hole become equal $(Q_s)_{in} = (Q_s)_{out}$. Most investigations of the local erosion phenomenon were conducted to determine the effect on bridge piers.

In hydrotechnical engineering, the need to evaluate river behavior in altered conditions, caused primarily by anthropogenic influence, is extensive. The occurrence of such influences must be foreseen, and their possible impact on the river channel must be estimated, followed by the design of appropriate measures to protect the structure or ensure the stability of the river channel. Considering bed-load transport is never exactly determined and depends on

hydrological and hydraulic flow parameters, the amount of transported bed-load as well as transport distance cannot be precisely defined. While selecting methodology for the sediment discharge estimation, care must be taken with regard to the appropriate theoretical equations, and verification by on-site measurements is required. The most accurate methods in determining the creation and movement of riverbed bed-load in a watercourse are in-situ bed-load and hydrological-hydraulic flow parameter measurements. Modern devices, based on satellite positioning system and acoustic measuring devices are used to collect high quality information for forecasting the stability of the river channel.

11.2. Case Study: Sava Jakuševac Bridge

Intensive riverbed degradation over many years causes damage to structures built in riverbeds. Every structure is designed to withstand conditions relevant at the time of construction, with appropriate safety factor. When the conditions change, the balance of forces affecting the structure is disrupted. The balance can be affected by changes in the hydrological regime of the river, global erosion and local erosion around the structure or a combination of these changes. Flood events cause greatest damage and disruption of the stability of the bridges spanning over rivers. Harmful effects to the structures are various, the most significant being the local washing away of the riverbed material in the area around bridge foundations (abutment and pier foundation erosion). Loss of bridge stability due to erosion is considered to be the result of inadequate criteria used during bridge design and insufficient field analysis of erosion on the built structures. Influence of flow forces is more emphasized when the riverbed is not oversaturated with bed-load. Degradation of river bed in the upper reaches, including the Sava River in the area of Jakuševac is a natural phenomenon. However, the gradient of changes is heavily influenced by a human factor. More specifically, the following parameters have caused the acceleration of the process: reduction of sediment inflow due to construction of dams and weirs in upstream reaches; increased tractive force due to increased longitudinal slopes as a result of shortening of the river course by regulation works; increase of water depth during flood waves due to flow concentration in the channel, without natural floodplains and gravel excavation from the riverbed.

At the end of 1981, on the reach of the Sava River between the stations of HEPP Podsused and Zagreb, significant problems appeared regarding continuous and reliable supply of the necessary amount of cooling water to the thermal power plant 'Termoelektrana – Toplana Zagreb' (TE-TO Zagreb) (rkm 696+400). That was the first time the TE-TO Zagreb plant needed to be shut down due to the low Sava River water level and inability to supply the necessary amounts of cooling water. This incident announced the existence of significant changes in the hydrological regime of the Sava River. Extremely low water levels of the Sava River at the pumping station, causing shut downs of the TE-TO Zagreb plant during 1982, became increasingly frequent and urgent improvements had to be made in order to ensure the necessary amounts of cooling water during low water periods. Research results showed a submerged weir in the riverbed, functioning as a temporary barrier, to be the best solution to the problem of ensuring necessary water level for unhindered functioning of water pumps and stabilization of the riverbed upstream from the barrier weir cross-section. First submerged weir in the Sava riverbed was built in 1983.

Part of the Srednje Posavlje flood protection system, designed and partially constructed after the 1964 Zagreb flood, is the Sava-Odra flood relief canal. The Jankomir overflow located at rkm 710+100, acting as the flood relief canal's starting point was designed to activate when the river discharge reaches 1900 m^3/s. However, in the period from its construction in 1979 until 2000, lowering of the Sava riverbed on the overflow location amounted to 2m [6] and additional 70cm in the last 10 years. Under these new circumstances, the overflow activates only when the river discharge reaches 2350 m^3/s and not 1900 m^3/s, which was originally the maximum allowed discharge. The downstream reach of the river is therefore exposed to influences which dramatically exacerbate the already negative riverbed erosion process. According to the discharge measurements conducted by the DHMZ (Croatian Meteorological and Hydrological Service), the overflow should have been activated 9 times in the period between 1979 and 2006. In fact, it was activated only 5 times: twice in 1979 and once in years 1980, 1990 and 1998 [10].

In everyday practice there are numerous examples of problems caused by the deepening of the riverbed. Case study chosen to illustrate the type of technical problems that can occur is the significant tilting of a pier of the Jakuševac bridge near Mičevec in Zagreb, Croatia (rkm 693+100). The railway bridge Jakuševac is an example of a loss of bridge stability caused by global and local erosion, aided by extreme hydraulic conditions. On March 30, 2009, during the passing of a flood wave in the Sava channel when a freight train was crossing the bridge, the bearing structure of the bridge lost its stability and resulted in a deformation of the bridge structure and tracks. Tilting of the pier was caused by the superposition of two influences: disruption of the global riverbed stability leading to considerable lowering of the riverbed compared with the time the bridge was designed and constructed, and the appearance local scour in area around the bridge pier.

This paper presents the effects of anthropogenic influences on the morphological development of the Sava River, based on the observed characteristic stages collected from the Zagreb and Bundek gauging stations over a number of years. Field surveys have been conducted to monitor development of scour hole with respect to time after bridge collapsed. Analyses of theoretical estimation of scour depth have been made and compared with actual development of scour hole measured through field surveys for verification purposes.

11.3. Hydrological Indicators of Morphological Changes

The Sava River stage and discharge readings at the Zagreb gauging station, situated at rkm 702+800, and the Bundek gauging station, situated at rkm 699+700 were used in this paper. Available data was collected and originally processed by the DHMZ. Annual mean stage and discharge values were calculated for low, mean and high waters, depending on the duration curve. This type of measurements has been available since 1926 for the Zagreb GS and for the Bundek GS since 1967.

The time line is divided into two periods: one spanning over the 1925-82 period and the other covering the period between 1983 until today. These two periods were chosen for two reasons, both having a great impact on the hydrological regime of the Sava River. One reason was the afore mentioned construction of the weir at the TE-TO Zagreb location (rkm 696+400) in 1983, and the other was the occurrence of a long dry period on the territory of the Republic of Croatia after 1980 [14]. In 1983 a unique limit was accepted since dry years added to the first time period could not significantly affect the homogeneity of the data [10].

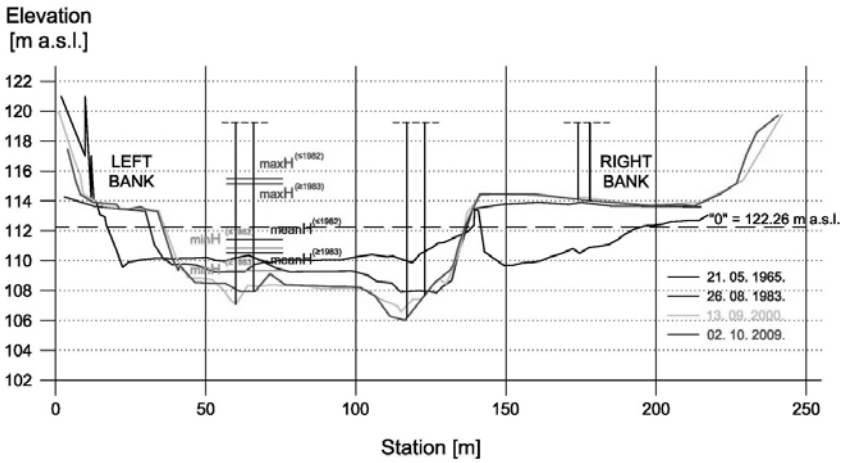

Fig. 1. Cross section of Sava riverbed at Zagreb GS with characteristic stages

Beside measurements of morphological changes and hydraulic flow parameters in a control profile, lowest annual stage trend is the best indicator of morphological changes. Observing stage and discharge values at river profiles over a number of years provides an insight into the trends of hydrological parameters as well as the ground for drawing conclusions on the morphological development of the riverbed on the observed river reach. The following figures show trends in annual maximum, minimum and mean stages at the Zagreb GS and Bundek GS.

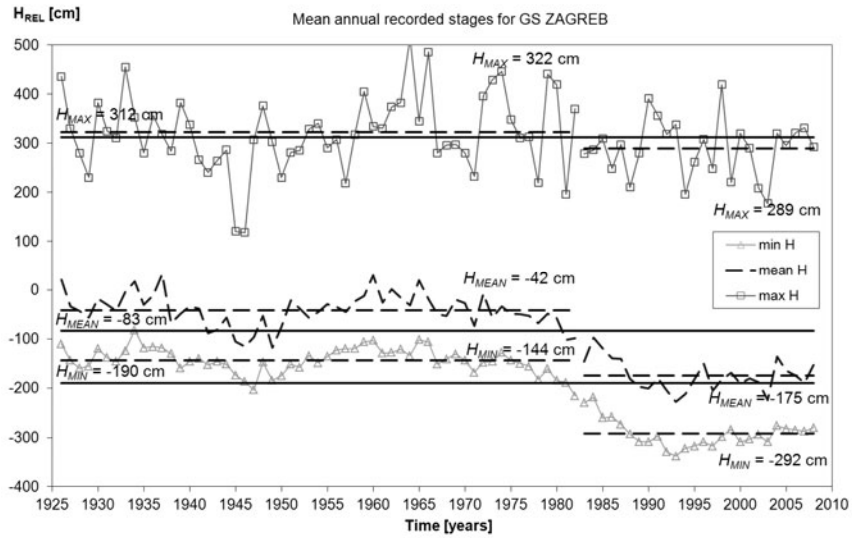

Fig. 2. Characteristic measured stages for the Zagreb GS

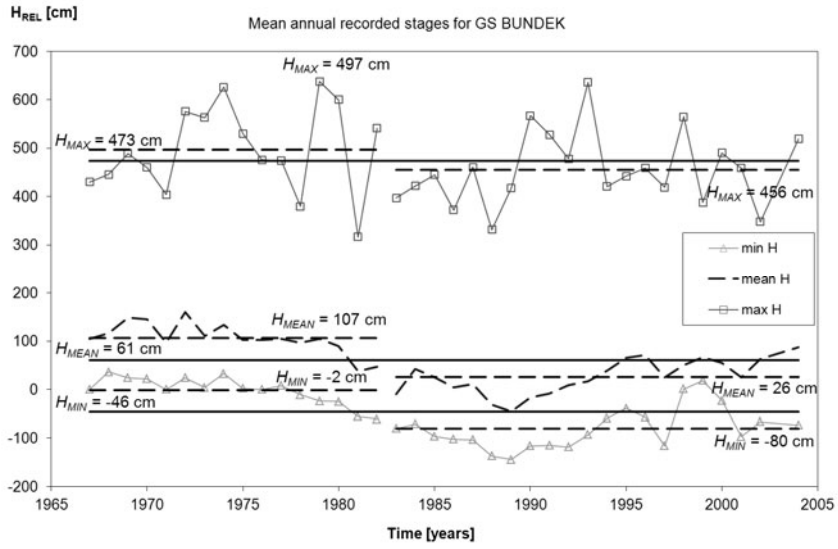

Fig. 3. Characteristic measured stages for the Bundek GS

Fig. 2 and Fig. 3 show two main stage trends: one that lasted until 1983 and is characterized by equable values of mean annual stage for minimum, medium and maximum stages, and the other, which started in 1983 and is still present today. There was an abrupt decline in characteristic annual stages in the period between 1982 and 1986, followed by a period of stage stabilization. Stabilization of the hydrological regime was accomplished by construction and continuous maintenance of the weir at the TE-TO Zagreb location on the Sava River. There was a significant decline predominantly in minimum and mean annual stages caused by riverbed degradation (Fig. 1). The decline in minimum and mean stages amounted to approximately 140cm at the Zagreb GS, whereas at the Bundek GS the stages lowered for approximately 80cm. Riverbed degradation did not significantly affect the regime of annual maximum stages which lowered for 40cm at both stations. The effect of riverbed degradation would probably have been more visible had the weir not been built. The average value of the annual mean stages in the period following the weir construction is 31cm lower than the mean value of the annual minimum stages before building the weir and, therefore, shows significant changes in the hydrological regime.

Although characteristic mean stage values are a good indicator of morphological riverbed changes, they are not sufficient to complete the picture of the Sava River hydrological regime. This would require constant observations of changes in discharge regime. Right before the weir construction a dry period started [15], which manifested itself in lower discharge of the Sava River (Fig. 4). Annual mean discharge for the period after 1983 fell by 15%, from 325 m^3/s to 275 m^3/s, whereas the mean value of the annual minimum discharge fell by 21%, from 87 m^3/s to 69 m^3/s.

The analyses show riverbed degradation not to be the only cause of a declining trend in characteristic stages. Although deepening of the riverbed is cause of concern, declines in characteristic discharges of the Sava River in Zagreb are equally important. Measures for erosion protection exist and can be implemented as required, but on the other hand, there can be no influence on natural forces which supply the discharge and that should be also

taken into consideration. Analyses of hydrological indicators show that they cannot be only indicator for reliable representation of riverbed degradation, because they don't include discharge information. Continuous stage measurements have to be supplemented with periodic bathymetry survey of riverbed, and detailed survey around submerged structures.

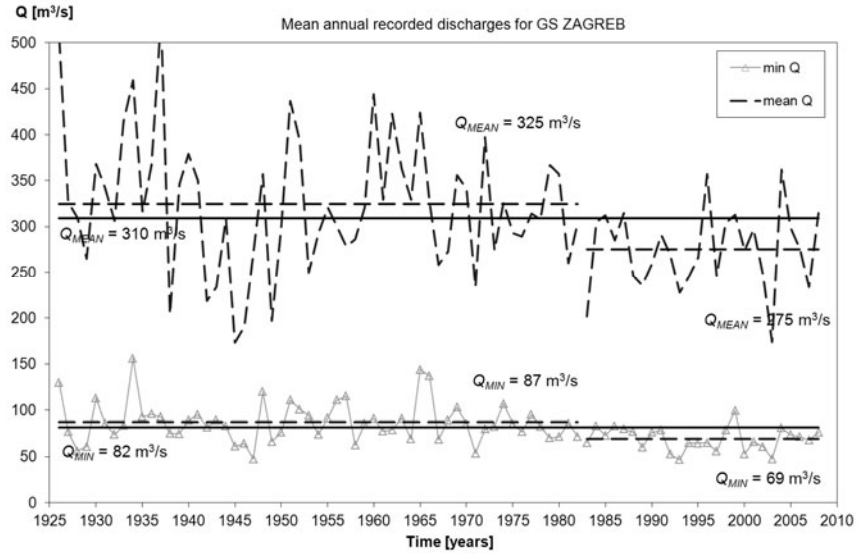

Fig. 4. Characteristic discharges at the Zagreb GS

11.4. Bathymetry Survey

Degradation of river bed in the upper reaches, including the Sava River in the area of Mičevec is a natural phenomenon. However, these changes are greatly influenced by the human factors which accelerated the degradation process: (a) reduction of sediment inflow due to construction of dams and weirs in upstream reaches; (b) increased tractive force due to increased longitudinal slopes as a result of shortening of the river course by regulation works; (c) Increase of water depth during flood waves due to flow concentration in the channel, without natural floodplains; (d) gravel excavation from the riverbed.

Due to advanced global erosion of the channel, the riverbed was considerably lower in relation to the level at the time of bridge design and construction: in the period between 1985 and 2009, the riverbed lowered by about 5–6 m (Fig. 5). The position of the bridge piers in the river channel caused additional bed lowering due to local erosion directly along the upstream walls of the piers, resulting in further river channel deepening by additional 5m. This local scour caused the removal of a part of the foundations under bridge piers and the stability of the bridge was severely reduced, as total scour in the area around the pier compared with the time the bridge was designed was approximately 10 m.

During 2009, in the period between April and October, The Faculty of Civil Engineering in Zagreb (Water Research Department) in collaboration with the Faculty of Geodesy (Department of Hydrography), conducted hydrographic surveys of the Sava River bathymetry. Geodetic and hydrographic surveys included monitoring of the morphologic

changes measurements collected and processed by the Hydrosweep integrated module for the processing of the multibeam echo sounder data. The area covered by hydrographic measurements stretches over 2 ha and encompasses the area to the north and south of the Jakuševac bridge, totaling 200 m in length, including the river bank and the Sava River inundation area. Measurements were conducted at six control cross-sections, three upstream and three downstream from the bridge. The following parameters were measured at each profile: flow velocity profile, flow area, free flow width, stages and discharge.

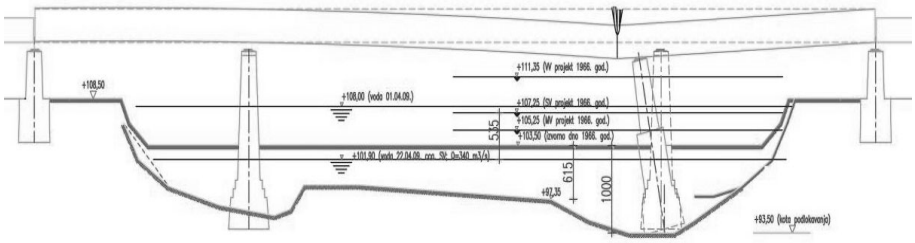

Fig. 5. Influence of global and local scour in the Sava riverbed on the Jakuševac bridge profile over a 20-year period

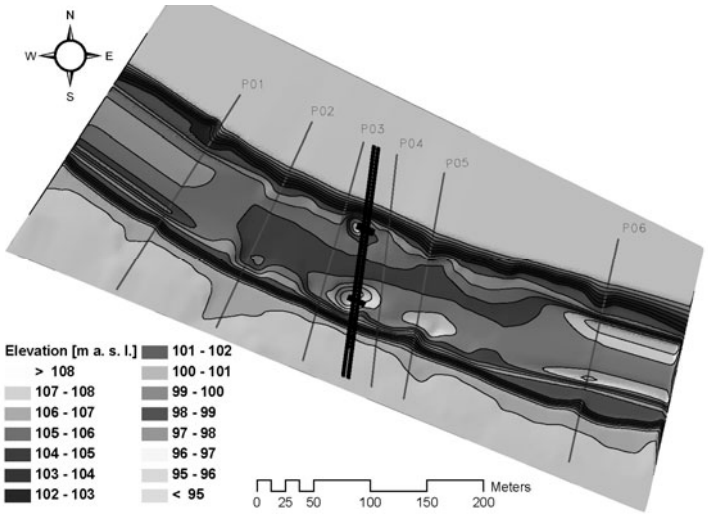

Fig. 6. Measured bathymetry in the bridge zone

It may be seen that the depth of the scour hole formed in the pier zone is greater than 4 m in relation to the mean level of the channel bed at both piers, and that the hole is more or less uniform. This means that, at this stage, local erosion has reached its maximum, and that it is in the state of temporary equilibrium until the entire river channel is additionally deepened under the influence of global erosion. The flow velocity field in the observed section of the river and around the bridge piers was obtained by monitoring velocity profiles. As the bridge is positioned on the river bend, flow velocities are higher on the concave side, i.e. on the side of the south pier and the unit sediment discharge and riverbed erosion are more emphasized on this side (Fig. 6, Fig. 7).

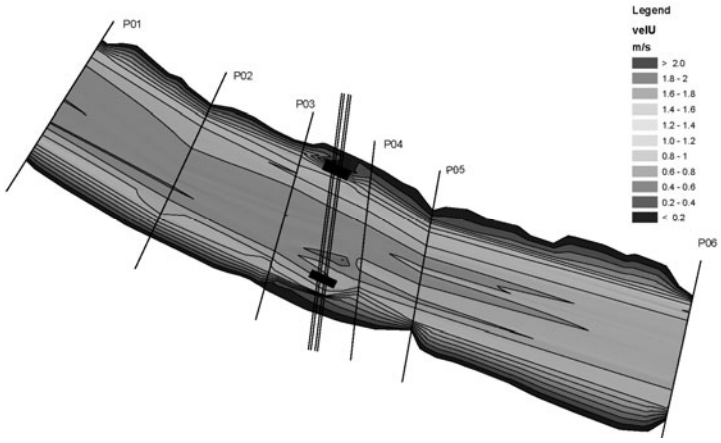

Fig. 7. Measured flow velocity field in the bridge zone

a) April 22, 2009 b) May 7, 2009

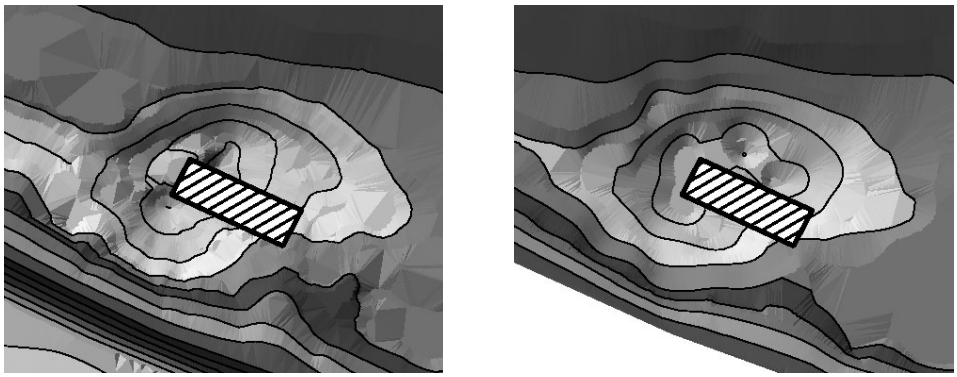

c) September 28, 2009 d) October 26, 2009

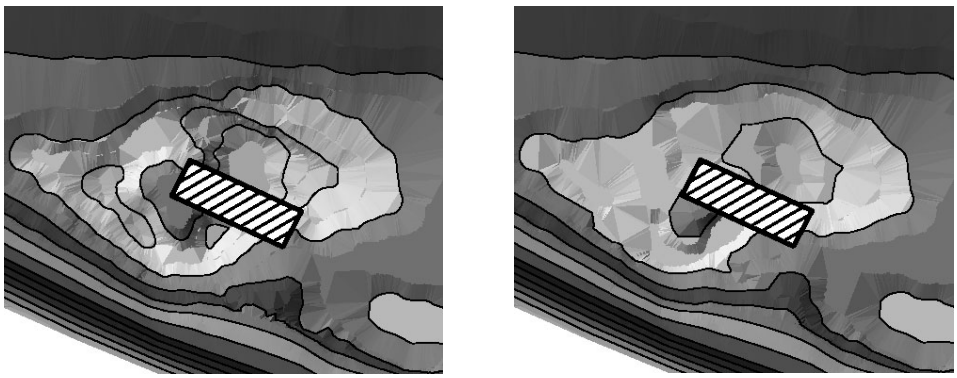

Fig. 8. Development of scour hole under south pier

Field surveys were conducted four times during the monitoring of scour hole development following the bridge collapse: on April 22 and on May 7. As a consequence of tilting of the pier into scour hole, stability of bridge was endangered. In order to temporary slow down scouring process under the pier, railway authorities decided to fill scour hole with bags of gravel. Field surveys were conducted during and after filling of scour hole, on September 28 and October 26, respectively (Fig. 8).

11.5. Theoretical Estimation of Scour Depth

The estimate of the final depth of local scour around the pier is given by empirical equations derived by a number of authors. To get a good quality estimate of scour depth, the methodology of the following authors were utilised: Melville, Larras, Laursen, Breusers, Shen, Coleman, Ansari & Qadar, Hancu and Jain.

Parameters influencing the scour depth d_s may be written as:

$$d_S = f\left[\begin{matrix}\text{Flood flow}\left(\rho,\nu,V,y,G,g\right),\ \text{Bed sediment}\left(d_{50},\sigma_g,\rho_s,V_c\right),\\ \text{Bridge geometry}\left(B,b\right),\ \ \text{Time}\left(t\right)\end{matrix}\right] \tag{1}$$

where: ρ – water density,
v – kinematic viscosity,
V – mean flow velocity,
y – mean flow depth,
G – parameter describing the influence of transversal flow distribution and form of channel cross-section,
g – gravity acceleration,
d_{50} – mean particle size of the riverbed material,
σ_g – standard deviation of particles distribution in the channel,
p_s – sediment density,
V_c – critical flow velocity for moving of channel bed particles,
B – foundation width,
b – width of pier.

In the calculation, hydrological values measured on the observed section were used, as well as empirical coefficients dependent on the pier geometry. Empirical equations gave the values of local scour depth ds around the pier in the range from 3.86 to 8.40 m (Fig. 9). The empirical equations used were subjected to sensitivity analyses for two most influential parameters, i.e. mean flow depth y and pier width b.

It may be seen that the increase if local scour depth with unit increase of pier width is approximately the same for all equations. This is an important fact because erosion of the channel bed in the zone of the bridge caused uncovering of the caisson, which is wider than the pier, and consequently the erosion potential was increased at this point. It may be seen from the graph (Fig. 10) that some of the equations do not take into consideration the flow depth at all, assuming that for a given pier width there is a final local scour depth which will be achieved regardless of the conditions in the river.

It is also apparent that the equations fall into two groups; one group for actual conditions in the observed section of the Sava river gives the mean value of local scour depth d_s = 4.7 m, and the other group gives d_s = 7.7 m. The total mean value of local scour depth of all equations gives the value of d_s = 6.0 m, which corresponds to actual measured

depth of the scour hole at the southern pier of the Jakuševac bridge (Fig. 5, Fig. 6).

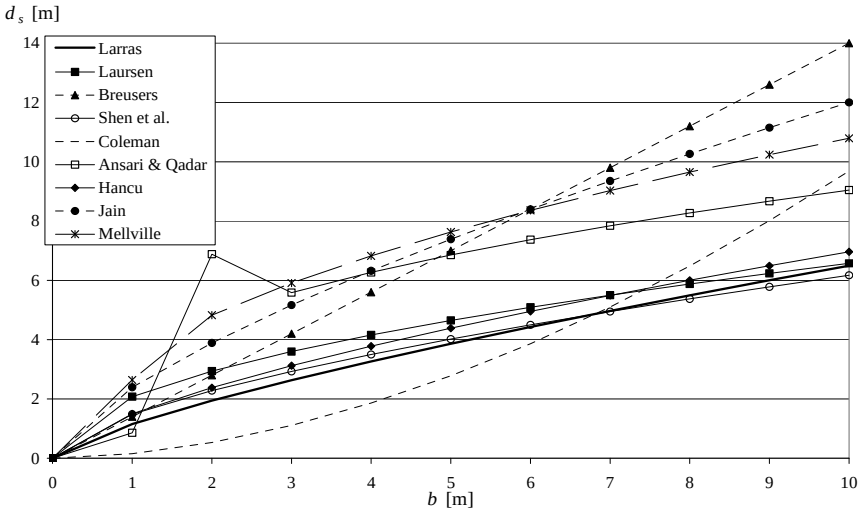

Fig. 9. Dependence of local scour depth d_s on change of pier width b at constant water depth

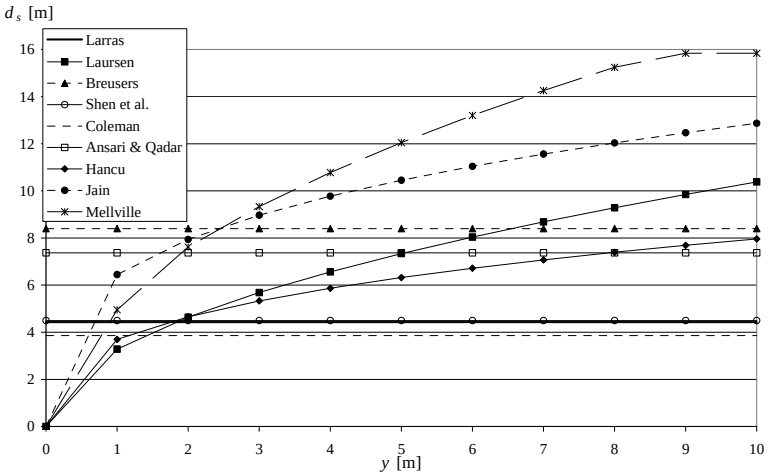

Fig. 10. Dependence of local scour depth d_s on change of water depth y with constant pier width

11.6. Conclusion

To become aware of natural events, one often needs to suffer their consequences, and they are usually of catastrophic proportions, causing human losses and material damage. In order to react on time and undertake improvements or reconstructions of the endangered structure, continuous surveys of physical phenomena trends in nature are needed. In this paper, as in the ones done by other authors in the past, annual minimum and mean stage

trends at gauging stations in the Zagreb area of the Sava River have been analyzed. Although stages are a good indicator of the changes in the riverbed morphology, they are not an independent physical value since they directly depend on the amount of discharge coming from the upstream catchment area. Conclusions based solely on stage measurements are not accurate and it is necessary to concurrently conduct discharge measurements as well. Lack of monitoring causes lower awareness about the problems relating to structures in riverbeds, which in turn may lead to grave consequences, such as the accident at the Jakuševac railway bridge in Zagreb. Advances in information technology, particularly in the field of acoustic equipment which operates on the basis of Doppler effect, simplify and speed up the methodology of measuring stream flow and riverbed bathymetry. In accordance with this, monitoring of hydrological parameters at more important river sections, where there are bridges and other building structures, should be completed with discharge measurements and cross-section profile geometry.

References

[1] Beraković M.: Radovi na rijeci Savi. Hrvatska Vodoprivreda 190–191, 16–20. (Waterworks on the Sava River, Hrvatska Vodoprivreda 190–191, 16–20), 2009.
[2] Biondić, D.: Erozijski proces u savskom koritu kod Zagreba, Zbornik radova: Hidrologija i vodni resursi Save u novim uvjetima, Slavonski brod. (Erosion of the Sava riverbed in the Zagreb area, Conference report: Hydrology and the Sava water resources in new conditions, Slavonski Brod) 2000.
[3] Brkić B.: Tehničko rješenje uređenja hidrotehničkog čvora Jankomir, Zbornik radova: Hidrologija i vodni resursi Save u novim uvjetima, Slavonski brod. (Technical solutions for the organization of the Jankomir hydrotechnical knot, Conference report: Hydrology and the Sava water resources in new conditions, Slavonski Brod) 2000.
[4] Elektroprojekt Zagreb: Prethodna studija izvodljivosti uređenja i korištenja rijeke Save od granice s Republikom Slovenijom do Rugvice. (Preliminary feasibility study of organization and exploitation of the Sava River from the Slovenian-Croatian border to Rugvica) 2004.
[5] Hamill L., Understanding Hydraulics, 2nd Edition, Published by Palgrave 2001.
[6] Kratofil L.: Promjene vodnog režima Save uzrokovane ljudskom djelatnošću, Zbornik radova: Hidrologija i vodni resursi Save u novim uvjetima, Slavonski brod. (Changes in the Sava River water regime caused by anthropogenic activities, Conference report; Hydrology and the Sava water resources in new conditions, Slavonski Brod), 2000.
[7] Melville B. W., Coleman S. E.: Bridge scour. Water Resources Publications, 2000.
[8] Petan S., Horvat A., Padežnik M., Mikoš M., Globevnik L., Brilly M.: Gravel barsampling along Sava River, Proceedings of the XXIVth Conference of the Danubian Countries, Bled, Slovenia, 2008.
[9] Samoupravna vodoprivredna interesna zajednica grada Zagreba: Vodoprivreda Zagreba 1980–1990, Artjus, 1990. (Water management in Zagreb 1980-1990, Artjus, 1990)
[10] Trninić D., Bošnjak T.: Karakteristični protoci Save kod Zagreba. Hrvatske vode 67/70, 257–268. (Characteristic discharges of the Sava River in the Zagreb area, Hrvatske vode 67/70, 257–268), 2009.
[11] Tomczak M., Godfrey J.S.: Regional Oceanography: an Introduction, Pergamon, Oxford, 1994. Also available at http://www.es.flinders.edu.au/~mattom/
[12] Yalin, M.S.; River Mechanics, Pergamon Press, 1992.
[13] Zanke U.: Grundlagen der Sedimentbewegung, Berlin, Heidelberg, New York: Springer-Verlag, 1982.
[14] Žugaj R., Plantić K.: Dotoci na karakterističnim vodotocima u Hrvatskoj. Hrvatske vode 45, 401–416, 2003

12 Comparison of Flow Velocity Vectors Collected by Using RTK-GPS and Bottom-Tracking as a Reference on a Boat Mounted ADCP

Gordon Gilja, Damir Bekić, Neven Kuspilić (University of Zagreb, Faculty of Civil Engineering, Croatia)

12.1. Introduction

The survey of current velocities in the ocean and riverine environment has been greatly improved with the appearance of acoustic Doppler current profilers (ADCPs) which became standard survey equipment for flow measurements in natural streams and artificial canals. ADCP is highly efficient and reliable instrument for flow measurements and is particularly useful for discharge measurement under different flow conditions that cannot be adequately measured by conventional current meters. Two of the most relevant advantages of ADCP application relative to traditional current meters are that ADCP measurements can be made in much less time, and that they provide three-dimensional velocity information [1, 8]. In hydrometry, their primary use is the measurement of river discharge and channel bed survey from a moving boat [19].

The acoustic Doppler current profiler (ADCP) is a device capable of making continuous current measurements at more than one depth from a moving ship. This instrument consists of four transducers set at an angle of 20° in a concave ("Janus") configuration, which transmits acoustic pulses and receives echoes from small particles such as zooplankton, sediments, or other solid particles. Using the Doppler frequency shift measured by the transducer, ADCP can compute the component of vector of the water's velocity along the beam direction and describe a profile of the current throughout the water column [6]. For measuring three velocity components ADCP utilizes four beams pointing in different directions [10]. The current and emerging applications of ADCPs have prompted the need for identifying sources of measurement errors, assessing the impact of these errors on the quality and reliability of the measurements, and developing good measurement practices. Estimates of total ADCP measurement uncertainty are necessary to properly report ADCP discharge data collected for the calibration of water control structures used for indirect real-time flow monitoring [9]. ADCPs mounted on moving vessels measure the velocity of the water relative to the velocity of the instrument. To obtain absolute water velocity, velocity of the instrument (boat speed and course) must be measured and subtracted from the measured relative water velocity:

$$\vec{v}_{water(ABS)} = \vec{v}_{water(REL)} - \vec{v}_{boat} \quad [\mathrm{m/s}] \tag{1}$$

where: $v_{water\ (ABS)}$ – absolute water velocity [m/s],
$v_{water\ (REL)}$ – relative water velocity [m/s],
v_{boat} – ship speed [m/s].

Boat velocity v_{boat} can be acquired either by using the built-in bottom track option or by using external navigation data (GPS). Bottom track data can be used by ADCP to determine its velocity relative to the streambed using the Doppler Effect under assumption that the riverbed is motionless [17]. Apparent movement of the bottom measured this way equals negative vector of the boat velocity. This procedure is effective and convenient because there is no need for an external device (GPS), which could introduce an error [16].

12.2. Sources of Errors in Boat Speed Estimation

Flow currents deduced from shipboard ADCP data contain errors from three main sources: (a) the relative motion of water in relation to ADCP transducers, (b) the movement of the boat during transect and (c) instrument heading [11]. In this paper will be analyzed boat course and instrument heading, as well as their mutual interaction.

12.2.1. Influence of Sediment Transport on Measurements

Sediment transport is a fundamental aspect of natural river flows. The spatiotemporal distribution of bed material transport through a river reach determines river morphology. Sediment transport along and near the streambed can introduce bias in bottom track measurement method. If an ADCP is held stationary in a stream and the streambed is moving, the ADCP will interpret this condition as upstream movement of the ADCP. The underestimation of measured velocity and discharge by ADCP discharge measurements attributed to the movement of sediment near the streambed is an issue widely acknowledged by the scientific community [13]. Error in measured discharge using vessel-mounted ADCPs biased by bed load transport is referred to as moving bed error.

The integration of a global positioning system GPS to measure the speed of the boat has been shown to alleviate the errors associated with a moving bed. The method assumes that GPS provides an accurate and precise measure of boat speed. Errors in GPS are transferred directly as errors in absolute water velocity [18]. When GPS data is used as reference for boat speed it is determined from the difference between two GPS position fixes. This method produces boat speed vector between two measured position fixes. In this way calculated boat course actually represents boat's bearing between two points in given time interval Δt, and not course. Bottom track method measures instantaneous data of boat course and more accurately descripts boat movement. Boat speed and course acquired by bottom track is instantaneous and synchronized in time with related water velocity data. Boat speed and course acquired from GPS data are not synchronized with water velocity data. For given measurements 1 Hz RTK GPS was used so on three water velocity ensembles acquired through ADCP in 1 second comes one data on boat speed and course.

12.2.2. True Earth and ADCP Coordinate System

Bottom tracking's biggest advantage over external devices is that many of its largest errors are matched by exactly the same errors in the current profile. These common-mode errors then cancel exactly when bottom track velocity is subtracted from the current profile data. Major common-mode errors include compass errors and velocity biases caused by beam pointing errors. This advantage arises from the fact that bottom tracking and current profiling use the same coordinate system. In contrast; boat's navigation and current

profiling share no common-mode errors. Using GPS with ADCPs eliminates the effect of a moving bed on the velocity measurements but introduces several sources of potential error. Understanding how GPS operates and how it is used with ADCPs is important for collecting high-quality ADCP measurements when using GPS data as the boat-velocity reference.

The orientation of the ship fore relative to true North is needed to project the relative velocity components into geographic ones (Fig. 1). Any misalignment angle is known from installation and corroborated through compass calibration, because if not spurious current velocities will appear. ADCPs are equipped with internal tilt sensors to measure pitch and roll, and an internal compass to measure heading. Instrument heading errors propagate through the transformation from ship to true earth coordinates for data collected with ADCP. Compass errors due to incorrect magnetic declination do not effect ADCP discharge measurements by bottom tracking. However, errors in compass calibration bias ADCP discharge measurements by GPS tracking [9].

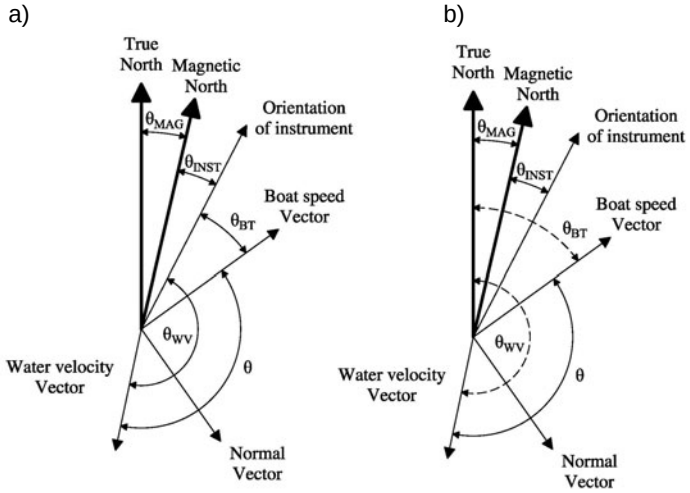

Fig. 1. Boat speed vectors reference by (a) bottom tracking and (b) GPS (adapted from Mueller, 2002)

When bottom tracking is used, the direction of the boat velocity vector as measured by bottom tracking (θ_{BT}) and water velocity vector (θ_{WV}) are referenced to the ADCP (Fig. 1a). The ADCP has an internal fluxgate compass to measure the orientation of the instrument (θ_{Inst}) relative to the magnetic north. The water velocity vector can be easily referenced to magnetic north by rotating the vector based on the measured θI_{nst} and to true north by again rotating the vector by a user-specified magnetic variation (θ_{Mag}). The magnitude of the water velocity is unaffected by any errors in the measurement of θI_{nst} or entry of θ_{Mag} when bottom tracking is used as the boat-velocity reference [14].

To compute the discharge, only the angle between the water velocity and the boat-velocity vectors is needed [19]:

$$Q = \int_0^T \int_0^D \left|\overrightarrow{v_w}\right| \left|\overrightarrow{v_b}\right| \sin\theta \cdot dzdt \tag{2}$$

where: Q – total discharge [m^3/s],
T – total time for which data were collected [s],
D – total depth [m],
$|\vec{v}_w|$ – semi-instantaneous water velocity vector [m/s],
$|\vec{v}_b|$ – boat speed vector [m/s],
θ – angle between the water velocity and boat speed vectors [°] (Fig. 1),
dz – vertical differential depth,
dt – differential time.

When GPS is used to determine the boat speed vector, this vector is referenced to true north as determined from the GPS data (Fig. 1b). The orientation of the instrument relative to true north must be determined to put the boat speed vector and the relative water velocity vector in the same coordinate system and allow for the computation of the water velocity vector and θ. The errors associated with θ_{Inst} can cause errors in the measured discharge that are proportional to the speed of the boat [14].

12.2.3. Compass Calibration

An error in the compass reading can be caused by distortion in the earth's magnetic field because of local objects on the boat, and displacement of the compass out of the horizontal position. The amount of distortion of the magnetic field by objects near a compass depends on the shape, material content, and proximity of the object to the compass. Objects that distort the magnetic field are commonly classified as hard iron and soft iron. Hard iron can be permanent magnets, and soft iron is material that, when placed in a magnetic field, will become magnetized. For ADCPs, hard iron and soft iron consist of the boat, instrument mount, objects on the boat, or structures near the measurement section such as bridges [15]. Errors associated with fluxgate-compass measurements caused by environmental conditions can be classified as one- and two-cycle errors. One-cycle errors are caused by permanent magnets and current-carrying conductors; two cycle errors are caused by iron and magnetically permeable material. ADCPs manufactured by TRDI for making discharge measurements from a moving boat have firmware routines to allow the calibration of the compasses in place to compensate for environmental conditions [14]. The result of the distortion of the magnetic field on compass heading is typically not constant and varies with heading. Compass errors caused by hard iron and soft iron vary with heading and can be modeled as sine and cosine curves. The general equation for compass error for a compass mounted on a boat is [15]:

$$\varepsilon = A + B\sin(\theta) + C\cos(\theta) + D\sin(2\theta) + E\cos(2\theta) \tag{3}$$

where: ε – compass error,
θ – compass heading [°],
A – coefficient that accounts for compass alignment,
B – coefficient that accounts for the fore-aft permanent magnetic field across the compass and a resultant asymmetrical vertical induced effect,
C – coefficient that accounts for the port-starboard permanent magnetic field across the compass, and a resultant asymmetrical vertical induced effect,
D – coefficient that accounts for symmetrical arrangements of horizontal soft iron and
E – coefficient that accounts for asymmetrical arrangements of horizontal soft iron [13].

A hypothetical compass error curve is shown in the following figure (Fig. 2).

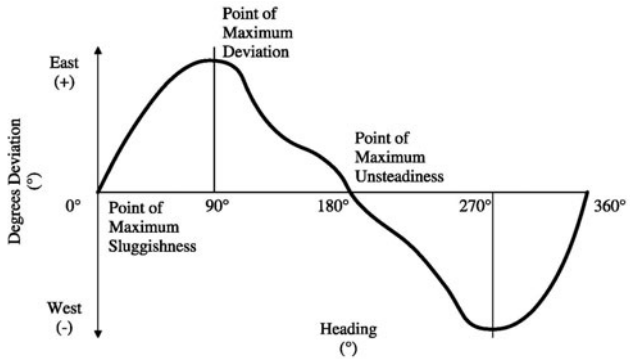

Fig. 2. Hypothetical uncompensated deviation curve as introduced by National Geospatial-Intelligence Agency [15]

Proper setup and calibration of the ADCP's internal compass, determination of the local magnetic variation, and a slow boat speed are critical to quality discharge measurements made by using GPS data as the boat speed reference.

12.2.4. Aim and Scope of This Paper

In this paper it will be analyzed survey data collected with ADCP on 5 independent measurements. The aim is to determine how much uncorrected or poorly corrected ADCP compass can influence discharge measurements. Analyses will include measurements in motionless riverbed conditions and during occurrence of moving riverbed.

12.3. Available Flow Measurements

Analyzed flow velocity measurements analyzed were collected on the Drava River on three locations: Nemetin, Osijek and Koprivnica. The average annual discharge of the Drava River is 522 m^3/s and the river width on given reach varies from 150 – 200 m [7, 12]. The ADCP used for discharge measurements is 1200 kHz broadband with transducer beams at angle of 20 degrees. For location Nemetin were conducted three measurements in year 2010: measurement *m*24 on April 30, *m*25 on July 19 and *m*26 on September 1 [2, 3, 4, 5]. Discharge was collected on 24 transects for each measurement under motionless riverbed conditions. For location Koprivnica was conducted one measurement, *m*01 on April 12, 2011. Discharge was collected on 7 transects under motionless riverbed conditions. For location Osijek was conducted one measurement, *m*02 on May 4, 2011. Discharge was collected on 6 transects under moving bottom conditions.

Flow velocity measurements *m*01, *m*24, *m*25 and *m*26 were conducted in conditions without moving bottom which could introduce bias in water velocity calculation [1]. On each location multiple transects were made to assure that wide angle of ADCP heading is covered. For location Nemetin measurements covered heading between 170 and 50°N (clockwise orientation). For location Koprivnica measurements covered heading between 200 and 310°N. For location Osijek measurements covered heading between 200 and 300°N. Measurements *m*24, *m*25 and *m*26 were conducted using uncorrected compass,

while measurement *m*01 was conducted with corrected compass. Measurement *m*02 was conducted both with corrected and uncorrected compass.

12.4. Results and Discussion

In this paper are first shown results from measurements on location Nemetin. Results are shown for discharge measured on 24 transects in three independent measurements; *m*24, *m*25 and *m*26. Discharges are collected with uncorrected compass and are represented as relative ratio ΔQ_{REL} between discharge collected with GPS as boat reference (GGA) and one collected with bottom track as a boat reference (BT):

$$\Delta Q_{REL} = \frac{Q_{GGA} - Q_{BT}}{Q_{BT}} \cdot 100\,[\%] \tag{4}$$

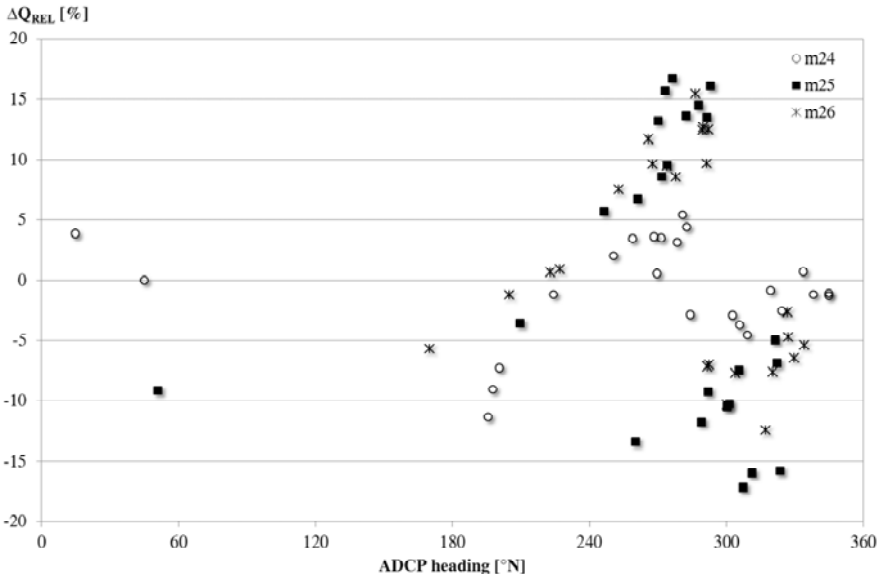

Fig. 3. Scatter plot of relative difference between measured discharges ΔQ_{REL} and instrument heading for location Nemetin

Measured discharge for measurement *m*24 varied from 408 to 457 m^3/s when BT was used as boat reference and from 383 to 465 m^3/s when GGA was used as boat reference; for measurement *m*25 varied from 391 to 448 m^3/s (BT) and from 349 to 509 m^3/s (GGA); for measurement *m*26 varied from 482 to 640 m^3/s (BT) and from 474 to 688 m^3/s (GGA). Below is given table (Tab. 1) with collected data from measurement *m*25. Data is averaged across cross-section and depth for each transect, and contains information about instrument heading, water velocity and direction, boat speed and course and discharge. Data is shown for both ship references, BT and GGA. Fig. 3 gives scatter plot of relative difference between measured discharges ΔQ_{REL} for all transects and all measurements on location Nemetin. Data is displayed in relation to ADCP heading.

Table 1

Data collected on measurement *m*25

Transect	Heading	Reference: BT					Reference: GGA					ΔQ_{REL}
		Q	Vel_{WATER}	Dir_{WATER}	Vel_{BOAT}	Crs_{BOAT}	Q	Vel_{WATER}	Dir_{WATER}	Vel_{BOAT}	Crs_{BOAT}	
	[°N]	[m^3/s]	[m/s]	[°N]	[m/s]	[°N]	[m^3/s]	[m/s]	[°N]	[m/s]	[°N]	[%]
0	260	442	0.75	139	1.00	39	383	0.68	140	1.00	35	–13
1	51	444	0.79	152	0.99	50	403	0.74	154	0.98	46	–9
2	293	433	0.77	155	0.93	255	503	0.87	156	0.94	248	16
3	273	436	0.62	158	1.09	246	504	0.70	162	1.08	241	16
4	291	448	0.79	152	0.83	251	509	0.88	153	0.83	244	13
5	288	443	0.81	145	0.90	248	507	0.91	146	0.90	242	14
6	276	394	0.87	125	0.89	242	460	0.98	127	0.88	231	17
7	282	431	0.83	138	0.82	239	489	0.93	139	0.82	233	14
8	305	424	0.83	137	0.86	48	393	0.79	139	0.86	46	–7
9	270	391	0.88	124	0.92	229	442	0.96	125	0.90	221	13
10	274	434	0.84	127	0.71	224	475	0.92	127	0.71	217	10
11	272	421	1.14	122	0.83	216	458	1.25	122	0.82	208	9
12	322	401	0.97	119	0.49	20	374	0.94	120	0.49	25	–7
13	321	412	0.92	118	0.53	32	392	0.89	118	0.52	20	–5
14	261	443	0.87	112	0.68	210	473	0.94	112	0.67	204	7
15	246	423	0.80	102	0.83	203	447	0.84	102	0.83	200	6
16	324	428	0.65	114	0.69	142	361	0.60	120	0.69	176	–16
17	311	427	0.68	100	0.65	306	359	0.62	103	0.65	326	–16
18	301	422	0.70	89	0.55	275	379	0.65	90	0.54	328	–10
19	307	421	0.69	92	0.78	334	349	0.61	95	0.78	340	–17
20	300	428	0.72	86	0.62	293	383	0.67	87	0.61	340	–10
21	210	420	0.78	72	0.73	160	405	0.76	72	0.73	162	–4
22	292	420	0.76	77	0.71	316	381	0.70	77	0.71	330	–9
23	289	423	0.70	69	0.80	330	373	0.63	71	0.80	326	–12

From given scatter plot (Fig. 3) it is visible that there is no unambiguous relation of discharge collected with GGA and BT as boat reference. For some transects Q_{GGA} is greater than Q_{BT}, and on some is smaller, and relative difference ΔQ_{REL} ranges between −20 and +20%. However, there is visible trend for heading under 230°N and over 290°N which shows that Q_{GGA} is smaller than Q_{BT}, and that for heading between 230°N and 290°N Q_{GGA} is greater than Q_{BT}.

As mentioned before, only difference between discharge calculation in relation to boat reference is in transformation between different coordinate systems. When bottom track option is used there is no need for transformations between coordinate systems as there is only one, which is oriented relative to ADCP beam configuration. When GPS is used as reference collected flow data, as well as boat speed data, are transformed into true earth (N–E) coordinate system. Boat speed is calculated and transformed from raw GPS data

through Ellipsoid transformation, while flow velocity data are transformed into true earth coordinates through utilization of compass integrated in ADCP unit. Different values in discharges acquired by BT and GGA mode are result of different boat course measurement. Figure (Fig. 4) shows one spatial distribution of boat speed and course data collected on one transect from *m*25.

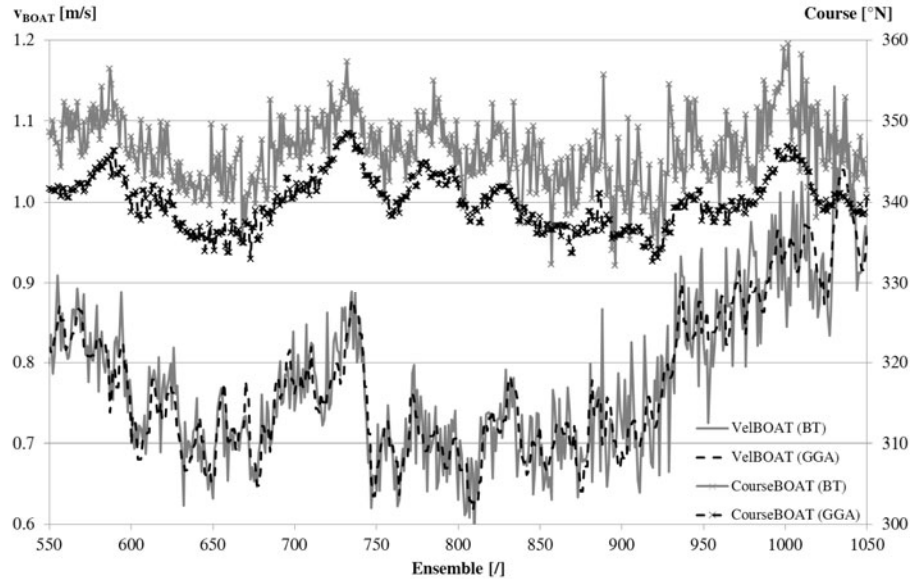

Fig. 4. Spatial distribution of boat speed and course data for transect 19 measured on *m*25

Fig. 4 shows greater fluctuations in both boat speed and course acquired with bottom track method. Average boat speed for given transects is approximately the same when BT and GGA are used as reference. However, there are significant differences between boat course along the transect. Influence of compass error due to non-existing calibration is visible through difference in boat course, $Course_{BOAT}$ (*BT*) and $Course_{BOAT}$ (*GGA*), which is 6.2°, averaged for given transect. Since boat course collected via BT is influenced by lack of compass calibration, data about boat course collected this way are not accurate. Magnitude of boat speed data projected in true earth coordinates is directly affected by erroneous boat course data. Although boat speed calculated from bottom tracking and GPS have same magnitude, different boat course significantly influences calculation of absolute water velocity and discharge, respectively (Tab. 1).

In order to quantify error introduced by compass miscalibration results are shown for measurement *m*01 on location Koprivnica. Flow measurements were conducted on 14 transects after compass calibration was conducted. Procedure used was “Method 3” outlined in WinRiver User’s Guide [20] which uses Rio Grande’s built-in function for one-cycle deviation errors correction of internal flux-gate compass. Hydrologic and hydraulic conditions on given location prevented successful implementation of compass calibration procedure. Namely, water velocity magnitude was over 2.5 m/s on area near to the concave bank, and extremely low depths were present on 30% of river (under 1m). These conditions resulted in high values of standard deviation of instrument’s pitch and roll, which are

unsatisfactory. Average pitch during calibration procedure was 1.60° with pitch standard deviation of 0.68°. Average roll during calibration procedure was 4.84° with roll standard deviation of 1.40°. RD Instruments recommend that standard deviation of pitch and roll should be lower than 1° [20]. Results of measurement *m*01 are given in Tab. 2.

Table 2

Data collected on measurement *m*01

Transect	Heading	Reference: BT					Reference: GGA					ΔQ_{REL}
		Q	Vel_{WATER}	Dir_{WATER}	Vel_{BOAT}	Crs_{BOAT}	Q	Vel_{WATER}	Dir_{WATER}	Vel_{BOAT}	Crs_{BOAT}	
	[°N]	[m³/s]	[m/s]	[°N]	[m/s]	[°N]	[m³/s]	[m/s]	[°N]	[m/s]	[°N]	[%]
1	263	407	1.21	149	1.00	62	409	1.25	148	1.06	64	1
2	282	387	1.35	145	0.96	239	372	1.32	145	0.95	240	–4
3	286	386	1.24	154	1.07	59	396	1.26	153	1.08	60	3
4	285	400	1.41	153	1.12	240	390	1.38	153	1.12	242	–3
5	281	357	1.32	158	1.26	250	349	1.29	159	1.28	251	–2
6	214	345	1.16	158	0.99	64	348	1.20	158	1.05	70	1
7	289	373	1.53	164	1.39	245	363	1.49	165	1.38	247	–3
8	218	389	1.49	163	0.84	64	393	1.50	162	0.86	65	1
9	308	396	1.38	165	0.82	266	387	1.35	164	0.81	268	–2
10	249	394	1.57	168	0.77	75	399	1.59	168	0.78	78	1
11	293	392	1.37	167	1.24	250	373	1.32	167	1.22	253	–5
12	198	411	1.39	162	0.96	68	414	1.41	162	0.96	73	1
13	298	385	1.62	161	1.09	244	375	1.58	161	1.10	245	–3
14	270	387	1.66	159	0.85	76	395	1.67	160	0.86	77	2

Fig. 5 gives scatter plot of relative difference between measured discharges ΔQ_{REL} for all transects and all measurements on location Koprivnica. Data is displayed in relation to ADCP heading.

Fig. 5 shows significant improvement of correlation between Q_{BT} and Q_{GGA}. Maximum relative difference is less than ±5%. There is no consistency in discharge difference, and for one heading Q_{GGA} can be both greater and lower than Q_{BT}. Results show that miscalibration of compass still significantly influences discharge measurements. In order to quantify error introduced by compass miscalibration, or lack of it, on location Osijek were conducted flow measurements on 6 transects before and after compass calibration. When compass calibration was conducted, results for compass correction obtained were: One Cycle K = 0.029 and One Cycle Offset = 65.807°. Average pitch during calibration procedure was 5.02° with pitch standard deviation of 0.43°. Average roll during calibration procedure was −1.78° with roll standard deviation of 0.65°. These values fall in range of recommend values by RD Instruments. Results of measurement *m*02 are given in Tab. 3.

Results show that for uncorrected compass there is no strong correlation between Q_{BT} and Q_{GGA}. For headings between 200 and 210°N Q_{GGA} is greater than Q_{BT} and for headings between 290 and 310°N Q_{GGA} is smaller than Q_{BT} (Fig. 6). These results are very similar to those collected at location Nemetin. When compass correction was applied, for all transects measured discharge Q_{GGA} was greater than Q_{BT}. For averaged values of all transects this difference was 5%. This positive difference in discharge is expected for moving bottom conditions as moving bottom introduces bias that reflects itself in apparent upstream movement of the boat. Results show that discharge measurements are less dispersed after compass calibration, i.e. standard deviation of ΔQ between Q_{GGA} and Q_{BT} was reduced from 9.7 to 8.2 m³/s (Tab. 3).

Table 3

Data collected on measurement *m*02

Compass	Transect	ADCP	Reference: BT					Reference: GGA					ΔQ_{REL}
		Heading	Q	Vel_{WATER}	Dir_{WATER}	Vel_{BOAT}	Crs_{BOAT}	Q	Vel_{WATER}	Dir_{WATER}	Vel_{BOAT}	Crs_{BOAT}	
		[°N]	[m^3/s]	[m/s]	[°N]	[m/s]	[°N]	[m^3/s]	[m/s]	[°N]	[m/s]	[°N]	[%]
Uncorrected	1	199	393	0.93	61	1.17	166	396	0.94	61	1.17	166	1
	2	297	381	0.86	65	1.20	343	373	0.86	64	1.21	343	–2
	3	303	382	0.82	73	1.12	276	376	0.81	74	1.12	271	–1
	4	202	379	0.79	74	1.01	164	383	0.80	74	1.01	164	1
	5	306	394	0.80	80	1.26	340	371	0.78	80	1.26	339	–6
	6	207	387	0.78	81	1.03	168	386	0.80	79	1.02	167	0
Corrected	1	207	400	0.94	64	0.93	171	414	1.01	64	0.91	171	3
	2	292	392	0.92	63	1.16	340	400	0.96	63	1.16	341	2
	3	300	371	0.80	76	1.08	320	391	0.84	74	1.08	307	5
	4	205	385	0.81	74	0.99	167	411	0.87	75	1.00	163	7
	5	302	382	0.75	76	0.94	331	394	0.78	78	0.93	324	3
	6	216	389	0.81	82	0.94	181	418	0.88	82	0.94	177	7

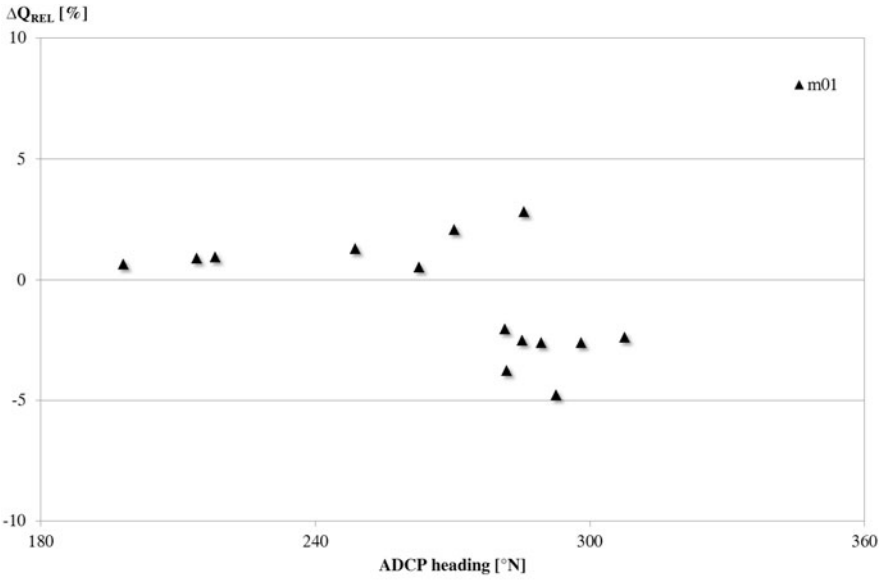

Fig. 5. Scatter plot of relative difference between measured discharges ΔQ_{REL} and instrument heading for location Koprivnica

Next figure (Fig. 7) shows one spatial distribution of boat speed and course data collected on one transect after compass calibration. There is visible better coincidence between boat courses from bottom track and GPS than between ones from uncorrected compass

measurements (Fig. 3). This coincidence is greater in areas pertaining to left and right riverbanks than in middle area of river transect. This is another indicator that there is occurrence of moving bottom on given location, which introduces bias in bottom tracking operation.

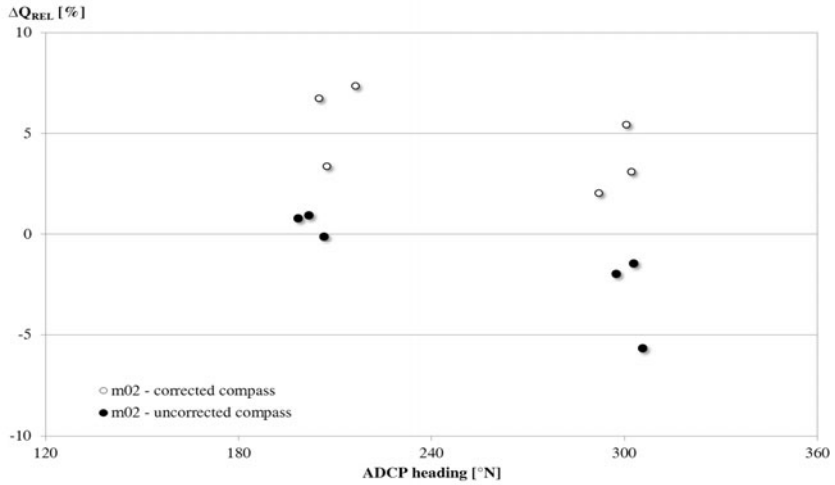

Fig. 6. Scatter plot of relative difference between measured discharges ΔQ_{REL} and instrument heading for location Osijek

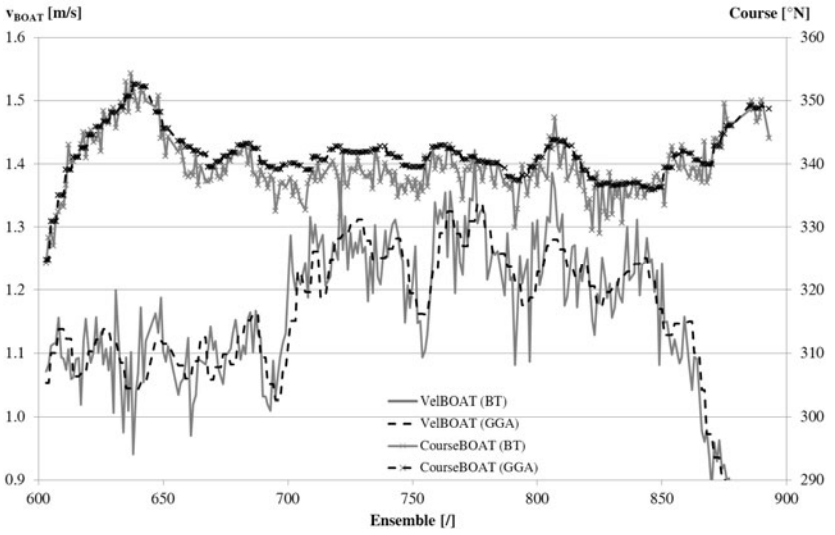

Fig. 7. Spatial distribution of boat speed and course data for transect 1 measured on *m*02

12.5. Conclusion

When conducting discharge measurements by using ADCP the best practice is to use built-in methods for boat speed reference. When measurements are made in natural watercourse there is often possibility of sediment movement on riverbed, i.e. occurrence of moving bottom. When moving bottom occurs ADCP's bottom tracking feature is biased and boat speed acquired with it is not accurate. In this case external device must be used for boat speed calculation, and most frequently used are GPS units. When external unit is used for boat speed and course, its data must be paired with appurtenant relative water velocity data from ADCP. This is done by water velocity data transformation into true earth coordinates which is done with ADCP's internal flux-gate compass information.

In order to acquire correct data from compass it must be calibrated on given location and boat mounting. In areas where there is no possibility of conducting correct compass calibration error up to ± 20 % can be introduced in discharge measurement. Even if there is no moving bottom on given location and compass calibration is not necessary for correct data acquisition, it is useful to properly calibrate compass so absolute water velocity data can be correctly displayed in true earth coordinate system on orthophoto images, for example.

References

[1] Bekić D., Kuspilić N., Gilja G.: Stability Assessment of the River Channel Bedform, Proceedings of the 8th international Conference on Hydro-Science and Engineering, Nagoya, Japan, 347–348, 2008.
[2] Faculty of Civil Engineering, Prokop Nemetin – Morfološka, hidrološka i hidraulička mjerenja. University of Zagreb: Zagreb 2007.
[3] Faculty of Civil Engineering, Prokop Nemetin – Morfološka, hidrološka i hidraulička mjerenja. University of Zagreb: Zagreb, 51, 2008.
[4] Faculty of Civil Engineering, Prokop Nemetin – Morfološka, hidrološka i hidraulička mjerenja. University of Zagreb: Zagreb, 29, 2009.
[5] Faculty of Civil Engineering, Prokop Nemetin – Morfološka, hidrološka i hidraulička mjerenja. University of Zagreb: Zagreb, 25, 2010.
[6] Gilcoto M., Jones E., Farina-Busto L.: Robust Estimations of Current Velocities with Four-Beam Broadband ADCPs. Journal of Atmospheric and Oceanic Technology (26): 2642–2654, 2009.
[7] Gilja G., Bekić D., Oskoruš, D.: Processing of Suspended Sediment Concentration Measurements on Drava River, Proceedings of International Symposium on Water Management and Hydraulic Engineering, Ohrid, Republic of Macedonia, 181–191, 2009.
[8] González-Castro J. A., Melching C. S., Oberg, K. A.: Analysis of open-channel velocity measurements collected with an acoustic Doppler current profiler, 1st International Conference On New/Emerging Concepts for Rivers Organized by the International Water Resources Association, Chicago, Illinois, USA, 1996.
[9] González-Castro J. A., Muste M.: Framework for Estimating Uncertainty of ADCP Measurements from a Moving Boat by Standardized Uncertainty Analysis. Journal of Hydraulic Engineering, 133(12): 1390–1410, 2007.
[10] Gordon R. L.: Acoustic Doppler Current Profiler: Principles of Operation – A Practical Primer, RD Instruments, San Diego, California, 1996.
[11] King B. A., Alderson S. G., Cromwell D.: Enhancement of shipboard ADCP data with DGPS position and GPS heading measurements Deep-Sea Research Part a-Oceanographic Research Papers, 43(6): 937–947, 1996.

[12] Kuspilić N., Bekić D., Carević D.: Channel stability assessment in a meander cut-off. In: M. Dohmen-Janssen (Editor), Proceedings of the 5th IAHR Symposium on River, Coastal and Estuarine Morphodynamics, Enschede, The Netherlands, 1135–1141, 2007.
[13] Mueller D. S., Wagner C. R.: Correcting Acoustic Doppler Current Profiler Discharge Measurements Biased by Sediment Transport. Journal of Hydraulic Engineering, 133(12): 1329–1336, 2007.
[14] Mueller D. S., Wagner C. R.: Measuring discharge with acoustic Doppler current profilers from a moving boat, U. S. Geological Survey Techniques and Methods 3A-22. USGS, Reston, Virginia, 72, 2009.
[15] National Geospatial-Intelligence Agency: Handbook of magnetic compass adjustment, Bethesda, Md. (formerly, publication No. 226, as originally published by Defense Mapping Agency, Hydrographic/Topographic Center, Washington, D.C., 1980), 2004.
[16] Osinski R.: The misalignment angle in vessel-mounted ADCP. Oceanologia, 42(3): 385–394, 2000.
[17] Rennie C. D., Rainville F.: Case Study of Precision of GPS Differential Correction Strategies: Influence on aDcp Velocity and Discharge Estimates. Journal of Hydraulic Engineering, 132(3): 225–234, 2006.
[18] Rennie C. D., Rainville F., Kashyap S.: Improved Estimation of ADCP Apparent Bed-Load Velocity Using a Real-Time Kalman Filter. Journal of Hydraulic Engineering, 133(12): 1337–1344, 2007.
[19] Simpson M. R.: Discharge Measurements Using a Broad-Band Acoustic Doppler Current Profiler, U.S. Geological Survey, Sacramento, California 2001.
[20] Teledyne RD Instruments. WinRiver user's guide, San Diego, CA, Teledyne RD Instruments, P/N 957–6096–00, 156, 2003.

.

13 Two Dimensional Simulation of Floods Caused by Dam Failures

Goran Gjetvaj, Marin Paladin (University of Zagreb,
Faculty of Civil Engineering, Croatia)

13.1. Introduction

Torrent Bliznec springs on Medvednica and from time to time causes floods in the city of Zagreb with significant damage. To protect the city from torrential waters, embankment dam and retention basin Jazbina was formed. In the case of a sudden collapse of the constructed dam, positive downstream wave (shock wave) will be formed. Areas downstream from the retention are densely populated but a hospital, some schools, kindergartens, crafts and police facilities are in the flooded area. In the case of a dam failure in the valley downstream, highly dynamical conditions prevail that can cause significant damage and loss of human life. The aim of developed hydraulic model is to determine flood wave parameters that can be used for the preparation of evacuation in the case of a dam failure as well as urban plans development.

The present paper offers a short description of the 2-dimensional numerical model developed for dam-break induced flood wave prediction. The description of the physical phenomena is based on MIKE 21 package, a very general software for computing hydrodynamics including highly transient shallow-water flow. The dam-break induced wave is computed farther downstream until there is no danger for the population.

13.2. Jazbina Dam

Jazbina dam is situated between south slopes of Medvednica mountain and the city of Zagreb (Fig. 1, 2). This embankment dam is 17.15 m high with the volume of V_{DAM} = 279 700 m^3. The dam forms retention of V_{RET} = 272 400 m^3. Average discharge of torrent Bliznec is Q_{sr} = 0.16 m^3/s, maximum discharge for 1000 year return period is Q_{1000}= 30 m^3/s and for the 10 000 year return period maximum discharge is Q_{10000} = 42 m^3/s.

Downstream from the dam is a valley whose topographical data are defined by digital terrain elevation model supplemented by detailed geodetic measurements of the channel. In the valley there are some pastures, forests as well as residential and commercial property. From the hydraulic point of view the flooded area can be divided into several parts with different hydraulic roughness coefficient. Manning roughness coefficient was adopted on the basis of the data from the literature [1, 2] and distributed as it is shown in Fig. 3.

13.2.1. Numerical Model

In the dam break process modelling we can distinguish two (more or less distinctive) physical processes. The basic process is formation of a breach in the embankment dam and

the belonging hydrograph in the profile of the dam. As a result of emptying the reservoir and a significant increase in the discharge in profile of the dam, a flood wave propagation occurs. In this research, these two processes are modelled separately.

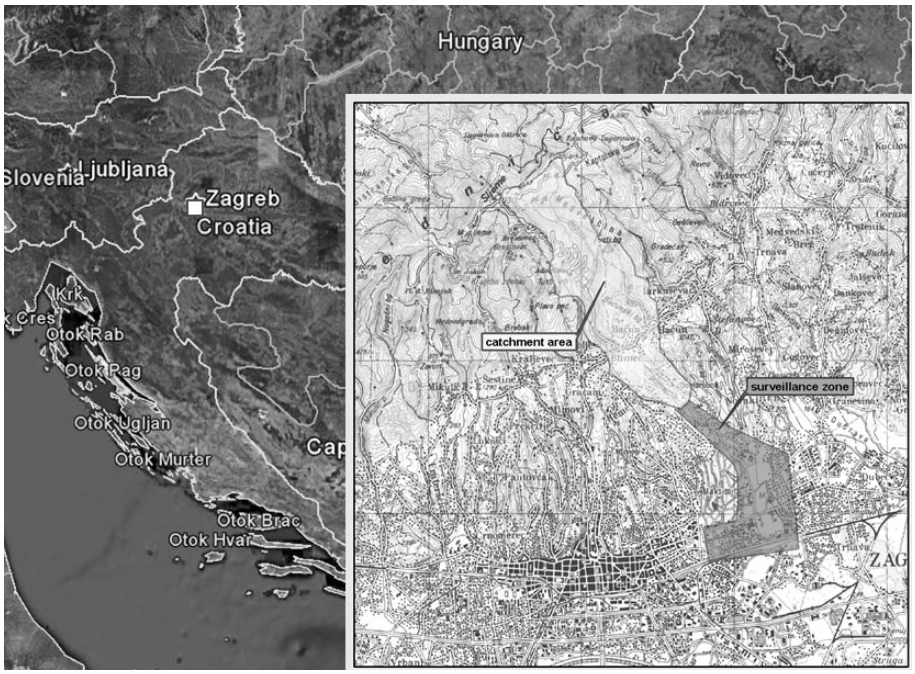

Fig. 1. Location of the dam and modeled area

Fig. 2. Jazbina Dam and retention basin

Fig. 3. Modeled area with the adopted roughness coefficient M (Manning's n = 1/M)

13.2.2. Dam Breaching Modelling Technology

Different levels of complexity can be distinguished in dam breaching modelling. The simplest and less general one is a non-physically based approach, which is mainly based on empirical and field data analysis. In the presented research this approach is used because there are no data on erodibility of the Jazbina dam and models based on physical approach would not have more reliable results.

To define the hydrograph produced by forming a breach in embankment dam it is assumed that the inflow in retention is produced by the rainfall of 1000 year return period. The breach is assumed to be trapezoidal in shape with bottom width B = 5 m and side slope 5:1 formed in the period of T = 0.1, 1, 2 and 3 hours. Output hydrograph is also calculated assuming that the breach is formed in a period of 1 hour, under the condition that the flood wave comes to a full retention basin (Fig. 4).

The maximum discharge that can occur due to dam breaching under the assumption that the breach is formed in 0.1 hour (6 minutes) is Q_{max} = 348 m^3/s which can be considered as the sudden dam collapse. The results obtained under this condition are presented in this paper.

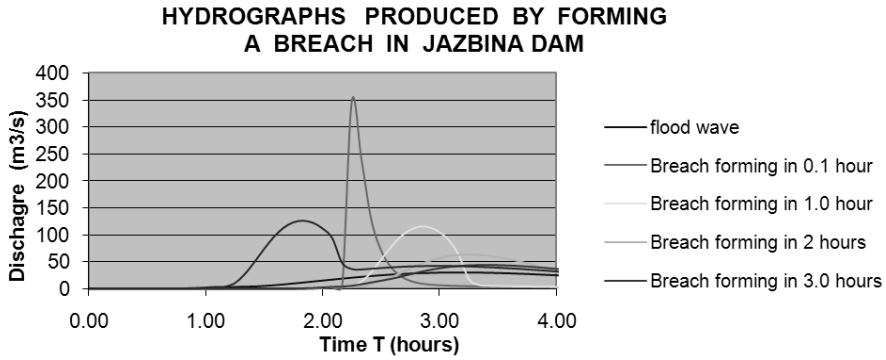

Fig. 4. Hydrograph as a result of a breach in Jazbina dam

13.2.3. Model of Flood Wave Propagation

Since there are significant velocity components perpendicular to the main direction of flood wave propagation, two-dimensional numerical model was chosen. Numerical model is based on the shallow water equations, derived from the three-dimensional Navier-Stokes equations. As the vertical components of velocity are weak enough in comparison with the horizontal ones, the pressure distribution is found to be hydrostatic and the shallow-water model is thus valid.

Recently, a few two-dimensional models of flood wave propagation have been developed [3, 4, 5, 6] and we decided to use MIKE 21 software package.

The mathematical model underlying the software packages is based upon the shallow water equations (SWE) in two dimensions. SWE are the most widely used mathematical frameworks in dam break simulation because they represent the conservation of water bulk mass and momentum.

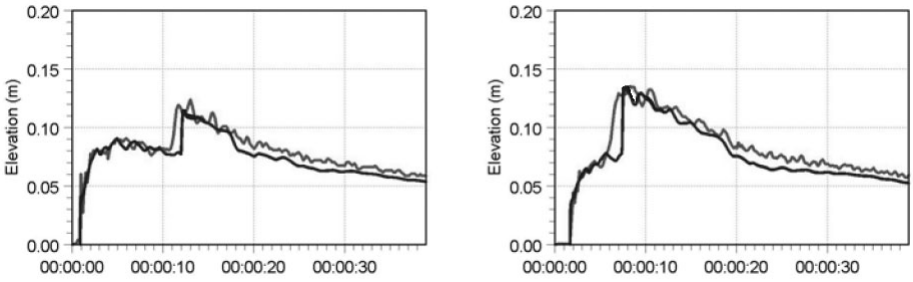

Fig. 5. Comparison of measured (red line) and calculated results (green line) for two characteristic measurements points

Since there is no a lot of experience with flood wave propagation after a dam collapse with MIKE 21 software package, verification of model was made. It is common to make verification of numerical model on real cases of dam break [1, 2] or on the results obtained on physical model. In this case, validation is based on comparing the results of numerical modeling of positive downstream wave propagation and the measurements obtained on the physical model.

Verification of used software package for propagation of flood waves resulting from dam collapse was used to model the physical model of 90° bent channel [4]. The physical model consists of a rectangular reservoir and a canal with 90° bend. Numerical results were compared with experimental data and the results showed that the numerical model described flood wave propagation very well (Fig. 5).

13.3. Results and Discussion

As an initial condition the average discharge torrent Bliznec was adopted. Boundary condition was defined by hydrograph obtained as a result of Jazbina dam break (Fig. 4). Downstream boundary condition for modeling extremely unsteady phenomena such as flood wave is very difficult to define and specify. Downstream boundary conditions in the presented work is defined by absorbent pools that are large enough and can accept the entire volume of water that passes through the spatial domain.

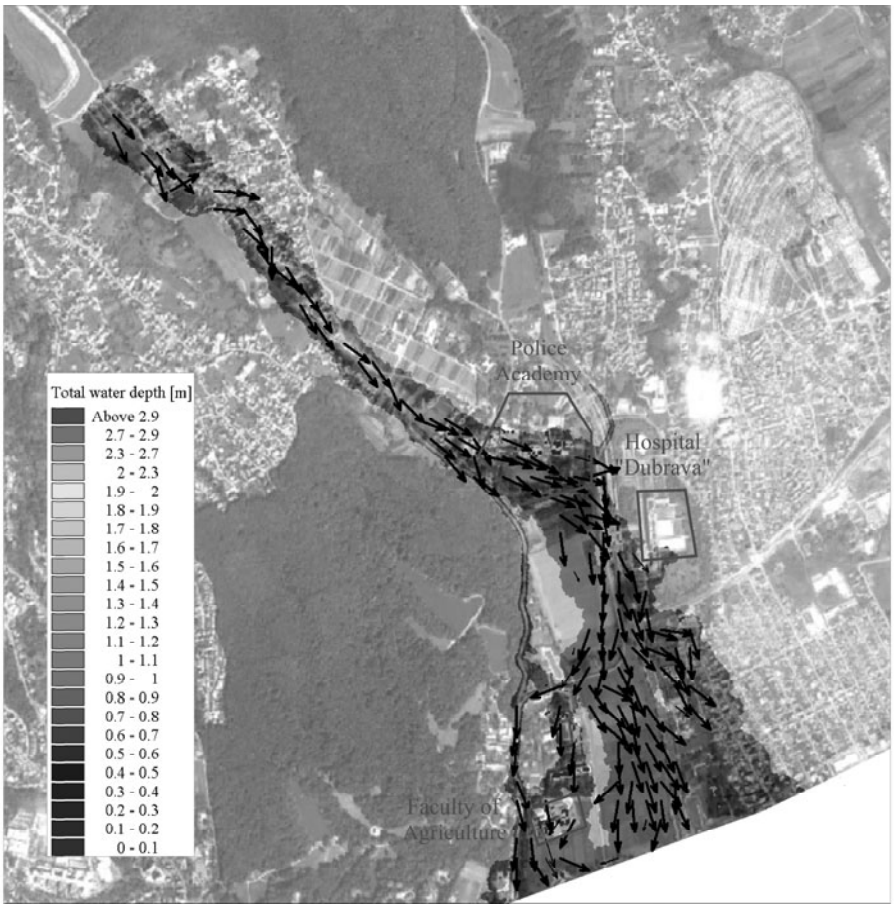

Fig. 6. Flooded area in case of a sudden dam failure

As a result we obtain inundation lines that delineate the areas that would be flooded in case of a sudden dam failure. Inundation maps are used both by the dam owner and emergency management officials to facilitate timely notification and evacuation of areas affected by a dam failure or flood condition. These maps significantly facilitate notification by graphically displaying flooded areas and showing travel times for wave front and flood peaks at critical locations.

The most interesting result in flood modeling is propagation of the front wave and the maximum possible flooded area. With this information emergency action can be developed. A risk map can be obtained by collecting the time elapsed between the moment of the dam breaching and the moment when a specified point of the domain is flooded (Fig. 5).

Fig. 7. Flooded area, water damage potential and travel times of wave front

13.4. Conclusion

A numerical model for determining hydraulic parameters of a flood wave after breaking a retention dam Jazbina that protects the city of Zagreb from the high water in creek Bliznec is described. Due to the lack of data on the material from which the dam was built, the way and speed the formation of breach was adopted on the basis of experiences with similar dams in the published literature.

Propagation of flood waves generated by breaching the Jazbina dam was calculated by us of the software package MIKE 21. Before using the package for flood wave propagation simulation, software package is verified by the results of measurements obtained on the hydraulic model. A comparison of results by numerical and hydraulic model showed that the software can well describe the hydraulic parameters of a produced flood wave.

As a result of the numerical simulations, size, maximum water velocities, the progress of the wave front as the maximum destructive potential in flooded area was obtained. The modeling results can be used to define hydraulic parameters in flooded area and develop evacuation plan for the population.

Model of breaching the dam and flood wave propagation is made assuming a linear increase of breach and flood wave propagation in an area where there is no change in shape due to riverbed erosion and deposition of sediment. To create a detailed model is needed to collect data on erodibility of material from which the dam was made and the factors associated with the erosion of the bed on which the flood wave propagates.

References

[1] Alcrudo F., Mulet F.: Description of Tous Dam break case study (Spain), Journal of Hydraulic Research, 45, 45–57, 2007.

[2] Frazao S. S., Alcrudo F., Goutal N.: Dam-break test cases summary, 4th CADAM meeting Zaragoza, Spain, November 1999 *http://www.hrwallingford.co.uk/projects/CADAM/ CADAM/ Zaragoza/Z3.pdf*.

[3] Caleffi V., Valian A., Zanni A.: Finite volume method for simulating extreme flood events in natural channels, J.of Hydraulic Research, 41, 167–177, 2003.

[4] Frazao S. S , Zech Y.: Dam Break in Channels with 90° Bend. Journal of Hydraulic Engineering, Vol. 128, No. 11, 956–968, 2002.

[5] Xinya Y., Sam S. Y. W., Khan A., A.: Numerical Simulation of Flood Inundation Due To Dam and Levee Breach, world water congress 2003.

[6] *http://www.asce.org/uploadedFiles/Communications-NEW/Hurricane/Numerical_Simulation_of_Flood_Inundation_Due_To_Dam_and_Levee_Breach.pdf.*

[7] Loukili Y., Soulaïmani A.: Numerical Tracking of Shallow Water Waves by the Unstructured Finite Volume WAF Approximation, International Journal for Computational Methods in Engineering Science and Mechanics 8, 1–14, 2007.

14 Flood Duration and Hydrograph Shape Impact on Scour Near Hydraulic Structures

Boriss Gjunsburgs, Gints Jaudzems, Elena Govsha (Riga Technical University, Department of Water Engineering and Technology, Latvia)

14.1. Introduction

The local scour developed during multiple floods is one of the major factors for failure or damage of hydraulic structures. According to the European Commission, there have been more than 100 large flood events in Europe during the last ten years [9].The EU Floods Directive 2007/60/EC aims to estimate, reduce and manage damaging floods in order to protect population, environment, cultural heritage and economic activity.

Most of the methods developed for estimating temporal or equilibrium depth of scour near hydraulic structures studied at steady flow conditions, but during flood events the flow loads on the engineering structures have the form of hydrograph, and hydraulic parameters are time-dependent [6]. The rain fall intensity, relief, soil type and other parameters affect the shape of the flood hydrograph and this influence the scour near hydraulic structures. The temporal impact of rising part of hydrograph on local scour depth at bridge piers was investigated by Lai et.al [5], duration of the floods and hydrograph shape influence on the local scour at bridge abutments, straight and elliptical guide banks was studied by Gjunsburgs et.al [3, 4], and the effect of flood recession time on the local scour at bed sills was examined by Tregnaghi et.al [7]. Lai et.al based his investigation on a theory that the recession period of hydrograph plays a minor role in the scouring process. However ,Tregnaghi et.al assumed an additional potential for scouring of a flood event with long recession compared to floods with symmetrical hydrographs. Such a difference in the conclusions can be explained by the fact that the phenomenon of relations between the triangle-shaped hydrograph and the time-dependent local scour has not been studied sufficiently .

In the present study, the impact of the floods with different triangle-shaped hydrographs on the local scour under clear-water conditions is investigated. Computer modeling based on the method for scour development with time [2] was made to perform this study. The method is confirmed by experimental results and enables to make time-dependent scour computing in our investigation.

Three types of triangle-shaped hydrographs with different time of rising and recession parts of it were modeled. For the first type the ratio between the time of rising and recession parts was similar, but duration of each part was different. For the second type the time of floods was fixed, but the time of recession part was changed; in this case,the ratio between the time of the rising and recession parts of the hydrograph varied. For the third type of hydrograph the total duration of rising and recession parts was similar, but the ratio between the times of both parts of hydrograph was changed.

14.2. Method

A method for computing the scour development with time was used to investigate the dependence of scour parameters on the floods duration and hydrograph shape. The method was confirmed by experimental results [2].

In the field conditions, the floods have the form of hydrograph and the scour is formed by floods with time-dependent parameters. The hydraulic characteristics, contraction rate of flow, the critical $V_{0,}$ and the local $V_{l,}$ velocities, the grain size in different layers of the bed, the sediment discharge, the depth, width and volume of a scour hole vary during the floods. Some intermediate values V_{lt} –the local velocity at any depth of the scour hole, V_{0t} – the critical velocity at any depth of the scour hole and h_m – the medium scour depth during the flood can be used in formulas to study the scour development in time.

According to the method described above, the flood hydrograph was divided into time steps, and each step in turn was divided into small time intervals (Fig.1). For each time step, the following parameters should be determined to start calculations: h_f – depth of water in the floodplain, Q/Q_b – contraction rate of the flow, Δh – maximum backwater value, d – grain size, H – thickness of the bed layer with d, and γ – specific weight of the bed material. As a result, V_{lt}, V_{0t}, and h_m were found at the end of time intervals and finally at the end of the time step. For the next time step, the flow parameters changed because of the flood and the scour developed during the previous time step.

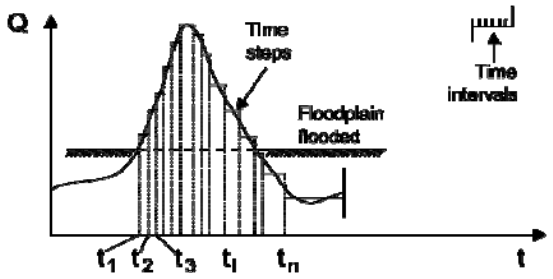

Fig. 1. Hydrograph divided in time steps and intervals

The calculation method is based on the differential equation of equilibrium for the bed sediment movement in clear-water conditions:

$$\frac{dw}{dt} = Q_s \tag{1}$$

where w = volume of the scour hole, which, according to the test results, is equal to 1⁄6 $\pi m^2 h_s^3$, t = time, and Q_s = sediment discharge out of the scour hole. After integration of time-dependent parameters the scour development during the floods was calculated by the formula:

$$N = \frac{t_i}{4D_i h_f{}^2} + N_{i-1} \tag{2}$$

where: N = 1⁄6$x_i^6$1–⁄5x,

t – time interval,
D_i – constant parameter in time step,
x_i – relative depth of scour.

Using $N = f(x)$ for calculated N_i, we found x_i and the scour at the end of time interval:

$$h_s = 2h_f\left(x-1\right) \tag{3}$$

The local scour rapidly develops at the start of the scour process ,and which is followed by a gradual reduction with time [2]. For the floods with different duration the scour development in time continues until the equilibrium stage is reached. In nature floods have the form of hydrograph and the time-dependent scour stops when the flood discharge reduces [3]. According to the method used, the scour stops when the local velocity V_{lt} becomes less then the critical velocity V_{0t} which causes sediment movement.

14.3. Modeling

Based on the method described, a computer modeling of the scour development with time during the floods was performed. The impact of the floods with different duration and shapes of hydrograph on the scour at engineering structures was studied.

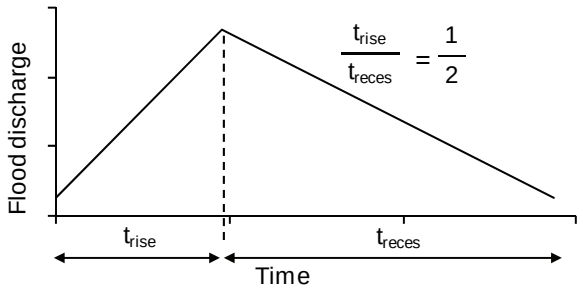

Fig. 2. Ratio between time periods of the rising and recession parts of hydrograph

The duration of floods t includes the time t_{rise}, when the flood discharge reaches its peak value, and the time t_{reces}, when the flood discharge decreases down to the low-water level; $t = t_{rise} + t_{reces}$. The form of the hydrograph is also characterized by the ratio between the time of the rising and recession parts of hydrograph (Fig. 2).

According to the method, the hydrograph was divided into time steps. The following parameters need to calculate the scour development in time: h_f = the depth of floodplain, Δh = maximum backwater value, Q/Q_b = flow contraction rate, Q = discharge of the floods, and t_n = the time of one step of the hydrograph.

The time of the rising or recession parts of the hydrograph was changed with the time of hydrograph steps. The time of the rising and recession parts of hydrograph had different ratios: 1:2, 1:3, 1:4, 1:6 and 1:8, where the first and second numbers are the rising part and recession part of hydrograph.

For the first type of hydrograph, the discharge and the ratio between times rising and recession parts were similar; however the duration of floods was changed by a proportional

increase in time for the rising and recession parts (Fig. 3).

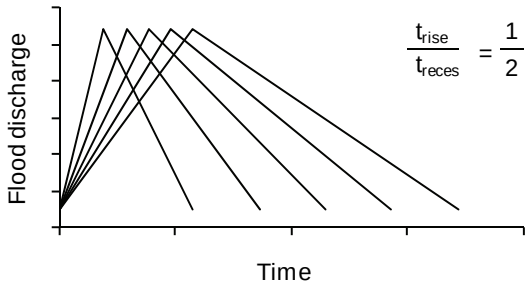

Fig. 3. Hydrographs with the same discharge and time ratio between rising and recession parts of hydrograph

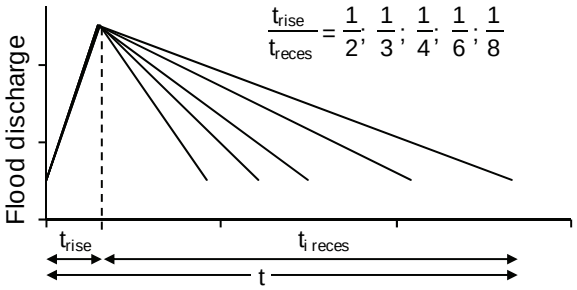

Fig. 4. Hydrographs with constant time of rising part of the flood

For the second type of hydrograph the rising time of the flood , were the same value, but the flood duration was different because of increase of recession time. The ratios between time of rising and recession parts of hydrograph were: 1:2, 1:3, 1:4, 1:6 and 1:8 (Fig. 4).

The flood duration were the same , but the slope of hydrograph was changed for the third type. Then ratios between the rising and recession time of the hydrograph were: 1:2, 1:3, 1:4, 1:6 and 1:8 (Fig. 5).

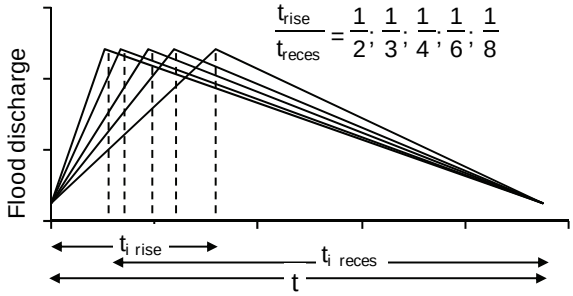

Fig. 5. Hydrographs with equal duration, but different time ratio between the rising and recession parts of flood

14.4. Results

According to the method employed [2], scour stops when the local velocity V_{lt} becomes less then the critical velocity βV_{0t}. The scour process usually stops just after the peak of the flood, therefore the scour development time T_s, when the maximum depth is reached, is less then the duration of the flood (Fig. 6).

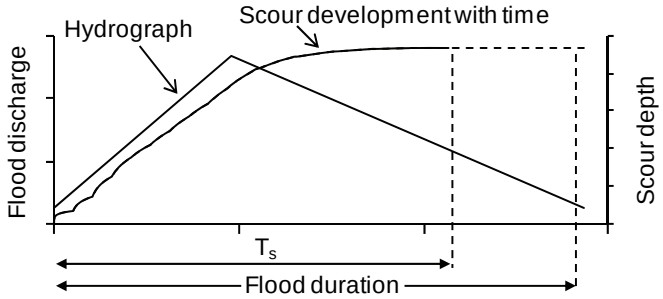

Fig. 6. Scour development with time. Comparison between the flood duration and scour development time T_s when the maximum scour depth is reached during a current flood event

For the floods – with equal peak discharge and hydrograph steepness (Fig. 3) it was found that the scour depth increases with increasing time of rising and recession parts of the hydrograph (Fig. 7). The results with similar tendency were obtained during modeling of hydrographs with different slopes of the rising and recession time of floods.

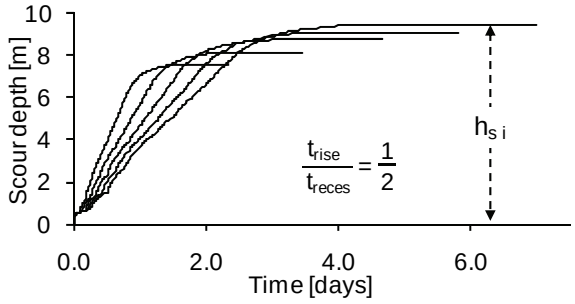

Fig. 7. Scour development with time for triangle-shaped hydrographs with the same discharge and ratio between the time of rising and recession parts of hydrograph

The time-dependent scour was modelled for the floods with the same discharge and time of the rising part of the flood. The flood duration was different because of the recession time of the floods was changed (Fig. 4). The scour development in time was similar for all the modes; however, the scour depth increases for with increase of recession time of the flood (Fig. 8).

In both models described, the flood duration changed because of the increasing time of the rising and the recession parts for the first type of the hydrograph, and the recession part varied only for the second type of hydrograph. The third type of hydrograph had a fixed

total duration; however , the time of the rising and recession of the flood was changed in the ratios: 1:2, 1:3, 1:4, 1:6 and 1:8 (Fig. 5). It was found that the maximum scour depth changes a little, but is developing more rapidly for floods with higher rising slope of the hydrograph (Fig. 9).

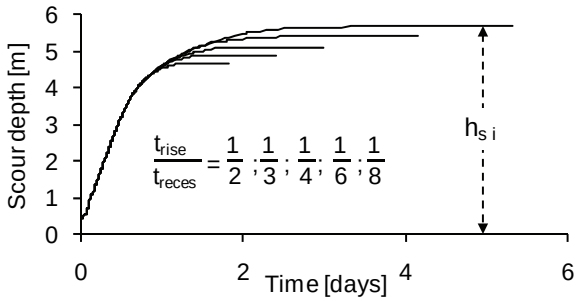

Fig. 8. Scour development with time for triangle-shaped hydrographs at constant time of the rising part

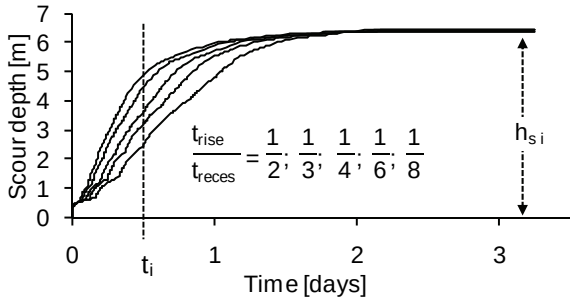

Fig. 9. Scour development with time for triangle-shaped hydrographs at an equal flood duration; ratio between the time of rising and recession parts is varied

14.5. Conclusions

A computer modeling of the scour development with time was performed to study the influence of a triangle-shaped hydrograph on the time-dependent local scour under clear-water conditions. Three shapes of flood hydrographs were studied. The flood duration was changed for the hydrograph with equal peak discharge and ratio between the time of the rising and recession parts of the hydrograph in the first case. The second type of hydrograph had a fixed time of the rising part, but the time of recession was changed according to the ratios 1:2, 1:3, 1:4, 1:6 and 1:8, thus the duration of the flood was increased. The third type of hydrograph had constant flood duration and discharge, but the shape of hydrograph was changed because of the ratio between the time of rising and recession parts. It was found that the shape of hydrograph affects the scour development with time and the flood duration increases the scour depth irrespective of the hydrograph steepness. For hydrographs with equal discharge and fixed time of the rising part, the scour

depth increases if time of recession of the flood becomes longer. The scour depth changes a little if the shape of hydrograph with a fixed duration is varied by the ratio between the times of the rise and recession. However, the time when the maximum scour depth is reached is less for floods with a higher slope of the rising limb. Similarly, the higher value of the scour is reached during the equal period of floods with a shorter time of the hydrograph rising limb.

It was determined that duration of the floods and hydrograph shape effect the results of a time-dependent scour depth near hydraulic structures and neglecting this fact can be reason for an sufficiently evaluated failure or damage risk of hydraulic structures because of the local scour.

References

[1] Gjunsburgs B., Neilands R.: Local velocity at bridge abutments on plain rivers. Proc. River Flow 2004, in Greco, Carravetta & Della Morte (eds), Napoli, Italy, Vol. 1, 443–448, 2004.
[2] Gjunsburgs B., Jaudzems G., Govsha E.: Assessment of Flood Damage Risk for Abutments in River Floodplains. Proceeding of the International Conference on Fluvial Hydraulics River Flow 2010, Germany, Braunschweig, Vol. 1, 1185–1192, 2010.
[3] Gjunsburgs B., Jaudzems G., Govsha E.: Hydrograph Shape Impact on the Scour Development with Time at Engineering Structures in River Flow. Scientific Journal of RTU. 2, series, Buvzinatne, Vol. 11, 6–12, 2010.
[4] Gjunsburgs B., Jaudzems G., Govsha J.: Influence of the Hydrograph Shape on the Scour Development. Hydrology: from Research to Water Management: the XXVI Nordic Hydrological Conference, Riga, Latvia, 196–198, 2010.
[5] Lai J. S., Chang W. Y., Yen C. L.: Maximum local scour depth at bridge piers under unsteady flow. Journal of Hydraulic Engineering, 135 (7), 609–614, 2009.
[6] Oliveto G., Hager W. H.: Further results to Time-Dependent Local Scour ar Bridge Elements. Journal of Hydraulic Engineering, 131 (2), 95–105, 2005.
[7] Tregnaghi M., Marion A., Coleman S., Tait S.: Effect of flood recession on scouring at bed sills. Journal of Hydraulic Engineering, 136 (4), 204–213, 2010.
[8] Oliveto G., Hager W. H.: Further results to Time-Dependent Local Scour ar Bridge Elements. Journal of Hydraulic Engineering, 131 (2), 95–105, 2005.
[9] http://ec.europa.eu/environment/water/flood_risk.

15 Proposal of the Second Hydraulic Project on Vistula River Downstream of Włocławek Project

Teresa Jarzębińska (Gdansk University of Technology,
Faculty of Civil and Environemtal Engineering, Poland),
Wojciech Majewski (Institute of Water Management, Poland)

15.1. Introduction

Vistula is the largest Polish River flowing from the south of Poland in the mountains to the Baltic Sea in the north. Length of Vistula is 1047 km and its catchment amounts to 194 thousand km^2. The catchment in Poland constitutes of 169 thousand km^2, thus occupying 54% of Polish territory. Water resources in relation to the population or country area are small. Similarly the volume of retention reservoirs and the hydro-energy potential are meager. At present the total volume of retention reservoirs amounts to about 6% of the average annual outflow from the Polish territory. Hydraulic power plants produce about 1.5% of the total electric energy produced mainly in thermal power plants.

There are, however, several locations where new retention reservoirs can be build and new hydraulic power plants installed. The area which includes such locations is the catchment of the upper Vistula including mainly mountain tributaries and along the section of the Lower Vistula, where estimated hydro-energy potential amounts to about of 30% of the total hydro potential of the country.

After the Second World War the project of establishing Lower Vistula Cascade (LVC) was put forward [2]. It consisted of 8 run-of-river hydraulic power plants of the total capacity1300 MW and annual energy production 4200 GWh. The main aim of the LVC was energy production and inland navigation. Ice phenomena and sediment transport were also taken into consideration.

In 1970 the first hydraulic project Włocławek was put into operation with power 160 MW and electric energy production in the average hydrological year 750 GWh. Till the present time Włocławek operates as a single project bringing a lot of advantages, but also a lot of drawbacks thus creating a lot of controversies. The most important problem of the operation of Włocławek project was the erosion downstream from the project. Another difficulties were created by ice phenomena and possibilities of ice jams. In 1982 a very important winter flood occurred on Włocławek reservoir. Now enterprise ENERGA wants to develop next hydraulic project downstream from Włocławek project.

15.2. Vistula River

Vistula is the largest river of Poland. Its length is 1047 km and the total catchment 194 000 km^2. 87% of the Vistula catchment is in Poland. The remaining part is in Bielarus, Ukraine and Slovakia. Vistula catchment which is in Poland amounts to 54% of the Polish territory. Vistula is the second largest, after Neva, river in the Baltic Sea basin. Vistula discharges about 7% of the total inflow of fresh water to the Baltic Sea.

Vistula can be divided into 3 distinctly different sections and sub-catchments. These are: Upper Vistula, Middle Vistula, and the Lover Vistula (Fig.1). Upper Vistula is from the source on Barania Mountain (1 116 m a.s.l.) up till the tributary San. Middle Vistula is from tributary San to the tributary Narew and the Lower Vistula is from tributary Narew to the outlet into Gdańsk Bay.

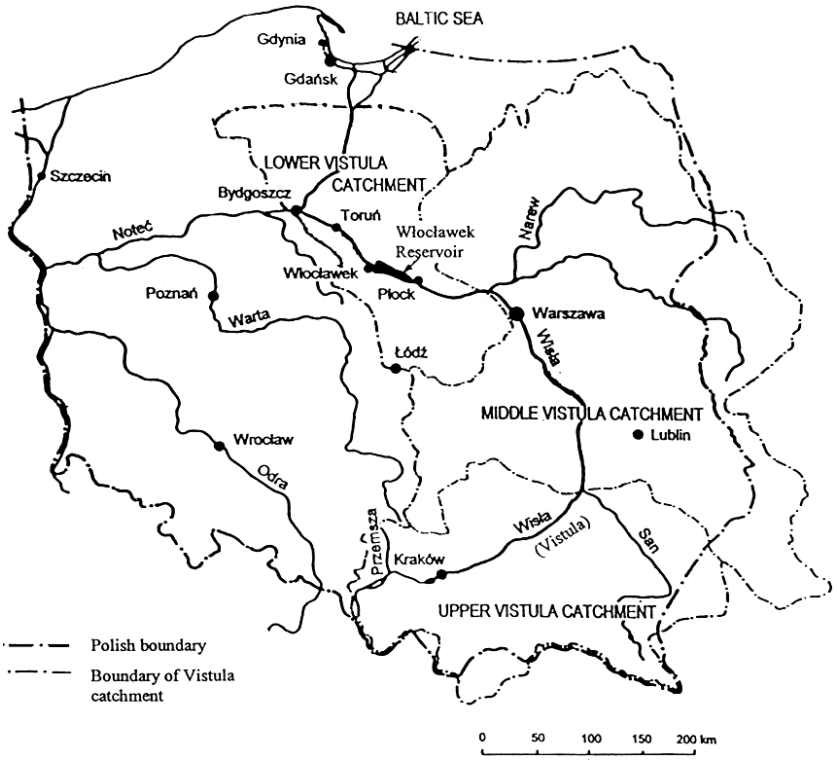

Fig. 1. Poland and the catchment of the Vistula River

Ecologists state that that Vistula is the only one wild, natural river (not trained) in Europe and should stay in the same state keeping to the maximum degree its ecological values. On the other hand water resources specialists consider the Vistula as the only one river of this size in Europe, which does not bring economical and social benefits to the country. In fact the Vistula is highly deteriorated and polluted river without any long term plan for management.

In the XVII century the Vistula was the most navigable river in Europe. Despite very primitive means of river transport, more than quarter million tons of goods and resources were transferred annually between Poland and the harbor Gdańsk, which at this time was

Poland window to the world. After partitioning of Poland the Vistula lost its significance and gradually deteriorated, while other European rivers developed very dynamically with respect to inland navigation, production of hydro-energy and forming important source of water supply for people, industry and agriculture.

15.3. Lower Vistula

Lower Vistula is the longest river section (391 km), but has the smallest catchment, without tributaries which have influence on the change of river discharge. The average multiannual discharge of the Vistula is 1080 m^3/s. The maximum recorded discharge at the mouth of the Vistula is 7840 m^3/s while the minimum discharge is 253 m^3/s. The average annual outflow of the Vistula to the sea is 34 km^3, while the minimum and maximum outflow are 20.5 and 50.8 km^3 respectively.

Along the Lower Vistula there are several important cities and industrial centers, which use the Vistula as the source of water. These are: Płock, Włocławek, Toruń, Bydgoszcz, Grudziądz, Tczew, Elbląg, and Gdańsk. Lower Vistula has high hydro energy potential, which is estimated as 30% of the total hydro energy potential of Poland.

Besides, this river section creates good navigation connection to European navigable network. It forms good navigable connection between the center of Poland and sea harbors Gdańsk and Gdynia.

15.4. Lower Vistula Cascade (LVC)

The idea of the LVC was proposed already in the sixties of past century [2]. The main purpose of the LVC was production of electric energy and formation of the navigable route of international class. The LVC is a very complex investment project which encompasses the economic, social and environmental aspects of previous 6 and present 3 vojvodeships. It will affect 12% of the Poland area and 14% of Poland population. The LVC will include 8 hydraulic impounding projects, including the present project Włocławek, which is in operation since 1970. The principal effect of the LVC is the production of environmentally sound and renewable electricity. Total annual production of electricity of LVC was estimated as 4200 GWh. with total power output 1300 MW, which can perform important regulation and peak-load functions in the energy supply system. The energy production is closely linked with the basic objectives of water management i.e. water supply, stabilizing of free surface and ground water levels, partial flood control, development of navigation, sport and recreation facilities.

The project will stimulate construction of additional road network associated with new crossings over the Vistula River, and will support significant economic growth, creating jobs for thousands of people and reducing unemployment in the area.

The LVC should be closely linked to a comprehensive program of the water quality improvement throughout the Vistula catchment thus reducing the pollution load carried to the Baltic Sea. The LVC will bring about many ecological changes, however, they will affect only the area between present flood dykes, which will be changed into side dams. The need to limit negative effects on nature to a minimum will require numerous interdisciplinary studies and close cooperation between experts from various fields. Similar problems have been solved in many places in Europe. The plan of the LVC is shown in Fig. 2 and longitudinal cross-section in Fig. 3.

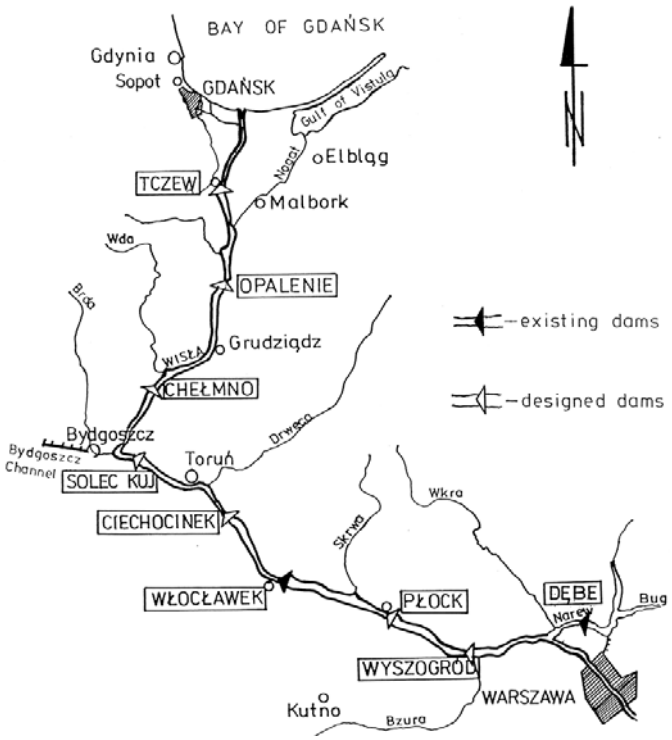

Fig. 2. Plan of the LVC

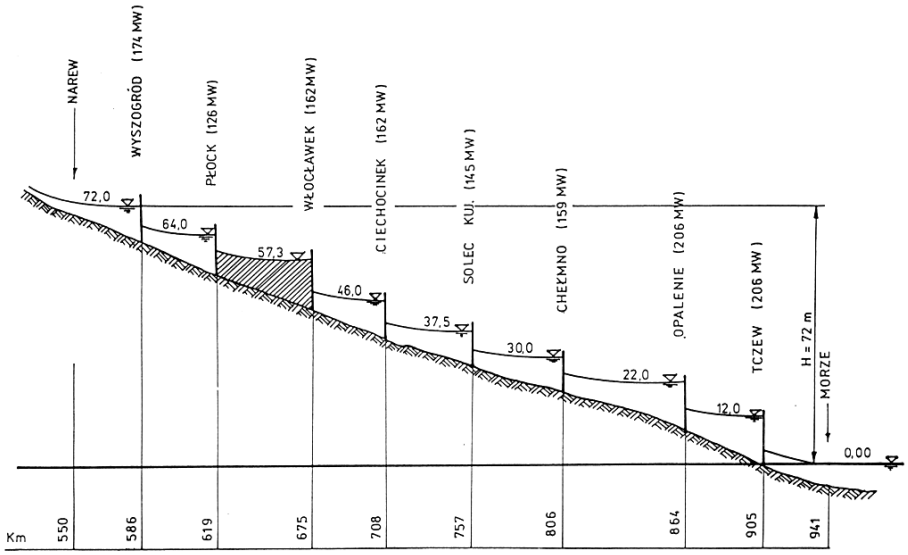

Fig. 3. Longitudinal cross-section of the LVC

15.5. Hydraulic Project Włocławek

In 1970 the first hydraulic project Włocławek of the LVC has been completed and put into operation. The project consists of earth dam, 10 bay weir with spillway for discharging water and ice, hydraulic power plant consisting of 6 units (Vertical Kaplan turbines), navigation lock and fish pass. The layout of the project is presented in Fig. 4. Włocławek project forms the run-of-river reservoir of the initial volume 400 hm^3. Over the crest of the project runs an important road connecting both banks of Vistula. The design of the project was done by Hydroproject. Chief Designer was Dr Eryk Bobiński. Construction and assembly work was completed by hydro-engineering enterprise Hydrobudowa.

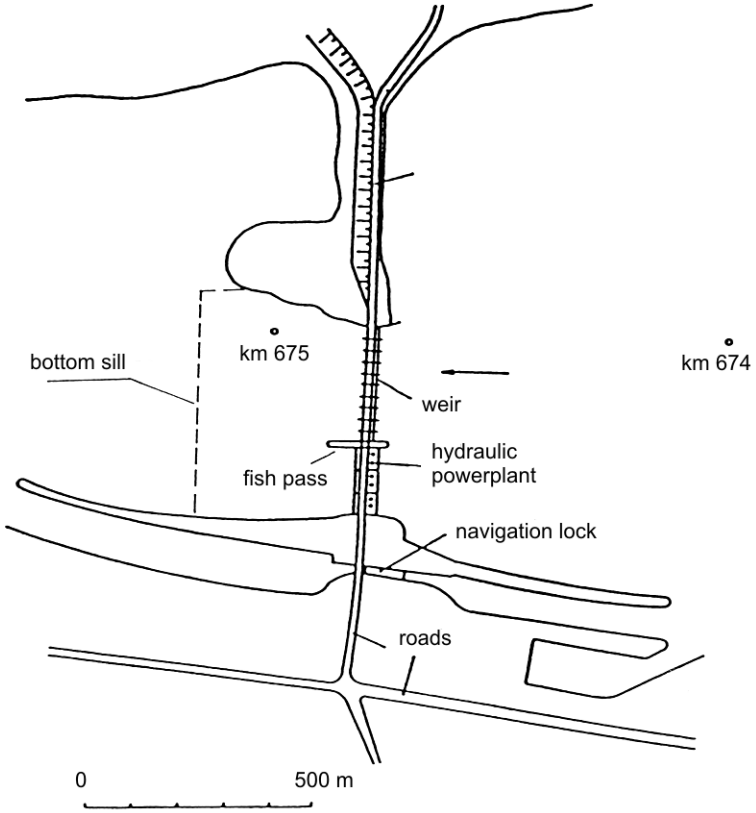

Fig. 4. Layout of hydraulic project Włocławek

The project was located in km 647.75 of the Vistula River. Normal water eleveation is 57.30 m, while maximum and minimum water levels are 58.50 and 56.50 m. Tail water level in case of the construction of next hydraulic project was assumed 46.00 m. This level guaranteed good performance of the weir and hydraulic power plant as well as stability of the whole project.

The average discharge in project cross-section is 890 m^3/s, the flow of 1% probability was calculated as 8700 m^3/s, and the control flow of the probability 0.3% was 10 280 m^3/s.

The biological flow was initially assumed as 350 m^3/s and later increased to 450 m^3/s. The maximum discharge at maximum water level (58.50 m) was estimated as 11 150 m^3/s. According to corrected later conveyance calculations this discharge is 9 590 m^3/s which is less than initially designed.

Navigation lock has the dimensions 12 × 115 m and was designed for the annual conveyance of 6 million tones. The bottom of the lock chamber is at the level 41.80 m. Upper gate is of the segment type while the lower gate is of the wicket type.

Hydraulic power plant is equipped with 6 Kaplan turbines of the total power 162 MW and energy production in the average hydrological year 750 GWh. Installed discharge of the power plant is 2190 m^3/s. The turbines can operate in the range of the head from 5.2 to 12.7 m.

15.6. Eksploitation of Włocławek Project

Hydraulic project was commissioned in 1970 and since that time for more than 40 years is operated not in conformity with the initial project. The fundamental drawback was the water level downstream from the project. This caused erosion, which resulted in decreasing tail water level and in consequence deteriorating the exploitation conditions. The main problem was the deterioration of working conditions of the power plant and performance of the spillway section. In order to improve this situation underwater bottom sill was constructed downstream from the power plant and the spillway section (Fig. 4). This, however, did not improve the stability of the dam and operation of the navigation lock. Now, especially during low discharges, the passage of the ships through the navigation lock is practically impossible.

Operation of Włocławek project caused also the change of ice regime on the reservoir but also downstream from the project. Important problem creates the river section upstream from the reservoir, where large amounts of frazil ice form. This ice is transferred to the reservoir, where surface ice cover already formed. In consequence frazil ice forms hanging dams, which deteriorates flow conditions and increases water levels. In order to improve this situation ice booms were installed every year in the upper part of the reservoir. It is generally indicated that the best solution to all problems of Włocławek Project will be the construction of the next project downstream form Włocławek [1].

15.7. Advantages of the Włocławek Project

The main advantage of the operation of hydraulic project Włocławek was the production of electric energy. On the average it was about 750 GWh per year. It varied due to hydrologic conditions from 550 to 1050 GWh per year.

Another advantage of the project was the stabilization of ground water levels in the vicinity of the reservoir. This had very important influence on the agriculture conditions as well as the state of forests.

Especially important influence of the reservoir was the improvement of water quality in the Vistula River downstream from the project. This resulted due to the deposition of many pollutants in the reservoir. Formation of the reservoir provided new recreational and water sport possibilities as well as possibilities of fish breading in the reservoir.

Quite recently arose also the possibility to decrease flood conditions downstream from the reservoir by very elastic operation of Włocławek project. This activity requires, however, very good record and forecast of hydrologic conditions upstream from the reservoir.

15.8. Next Hydraulic Project

After the completion of hydraulic project Włocławek first preparations were carried out to develop next projects downstream (Ciechocinek) and upstream (Wyszogród). As concerns the project in the localization Ciechocinek, technical design was completed and the preparation of grounds for the execution of the project were in progress. Unfortunately very bad economic conditions of the state resulted in the suspension of the project.

Afterwards many meetings and conferences were organized, which indicated the necessity of the construction of next hydraulic project. The government was not ready to fund this project because of bad financial situation of the country and also because of numerous protests of various ecological organizations. However, local consultations clearly indicated that all local communities are for the project, because of the decrease of unemployment due to construction as well as improvement of future economic situation of the region.

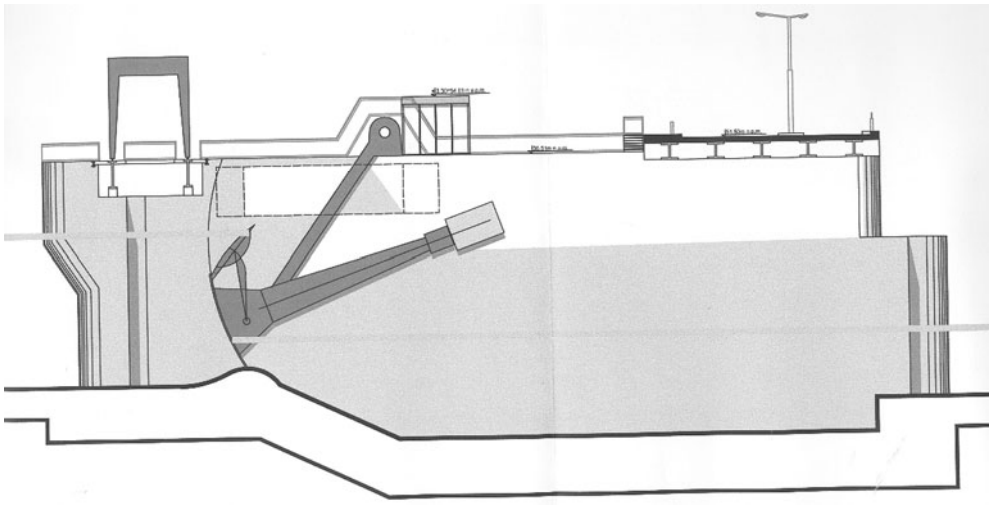

Fig. 5. Cross-section of the weir [3]

In 2005 Design Office Hydroproject Warsaw completed the concept of the new hydraulic project in the region Nieszawa-Ciechocinek [3]. This concept was prepared on the order of the Regional Board for Water Management in Warsaw.

This project was designed as a weir with 16 bays 20 meters long. The weir had low stable sill and segment gates with ice flaps. Cross-section of the weir is shown in Fig. 5. The normal water level in the reservoir was assumed at the elevation of 46 m.

Hydraulic power plant will consist of 6 units with bulb turbines of the total power 46.4 MW and design discharge 1150 m^3/s and the heads in the rage 4.80 to 7.15 m. Production

of electric energy in the average hydrological year was estimated as 276 GWh. Cross-section of the hydraulic power plant is shown in Fig. 6.

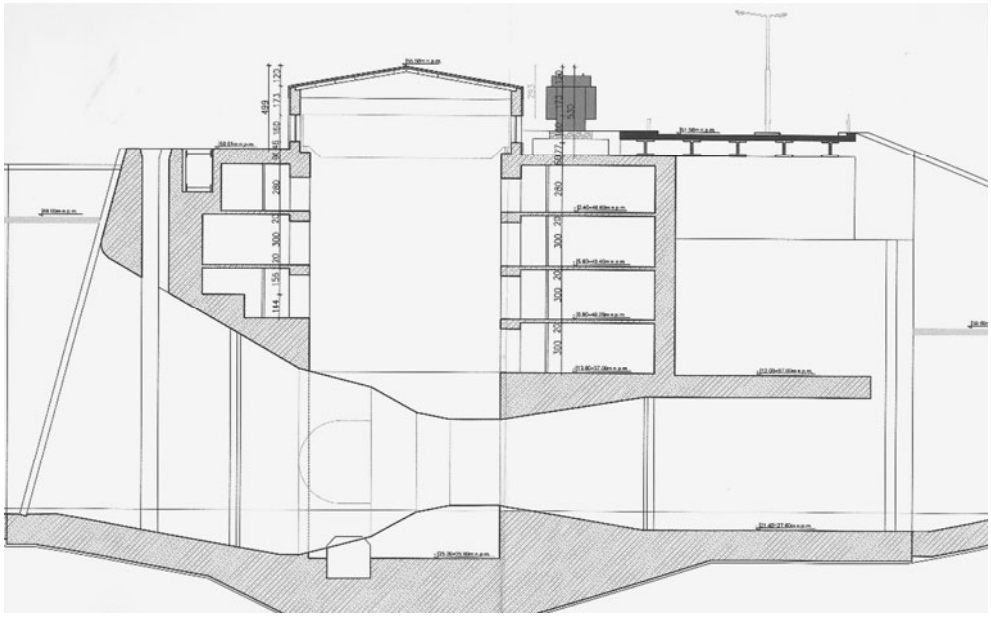

Fig. 6. Cross-section through the power plant [3]

The project will include also the navigation lock of the length 120 m and the width of loch chamber 12 m. Two fish passages were also designed. Technical fish pass was located in the pier between the weir and hydraulic power plant. The ecological fish pass is on the left hand bank and is very close to natural streams or mountain torrents.

The realization of the whole project was proposed during 60 months divided into 4 stages. In general it can be stated that new hydraulic project downstream from Włocławek is more ecological than the previous projects. The problem is whether present ecological requirements and especially Program NATURA 2000 will allow for the construction of this project.

15.9. Conclusions

1. The Vistula River always served numerous economical aims of Poland, however, the period of Poland's partition resulted in the deterioration of the river while other European river were developing rapidly.
2. Lower Vistula represents important hydro-energy potential and is suitable for the development of the river as a navigable route between center of Poland and the harbors Gdańsk, Gdynia.
3. After Second World War the idea of LVC was put forward. In 1970 first hydraulic project Włocławek was put into operation. Unfortunately till today it serves as a single project bringing important advantages but causing also several drawbacks.

4. Several times the construction of the new hydraulic project downstream from Włocławek was proposed, but unfortunately its realization always brings opposition from various ecological organizations.

References

[1] Hydraulic Project Ciechocinek on the Lower Vistula. Włocławek: Lower Vistula Cascade Foundation (in Polish), 1997.
[2] Lover Vistula Cascade. Warsaw: PROEKO, 1993.
[3] New hydraulic project in Nieszawa-Ciechocinek. Concept Design. Warsaw: Hydroproject (in Polish), 2005.

16 Slovakia Water Legislation Implementations

Jozef Kriš, Ivona Škultetyová, Stefan Stanko (Slovak University of Technology in Bratislava, Faculty of Civil Engineering)

16.1. Introduction

Implementation of new European countries policy in the field of the public water supplies moved the process from solving the partial problems to a comprehensive approach to protection and use of water regarding their quality and quantity [1]. The major objective of the Slovak Republic as a member of the European Union includes adopting and implementing EU legislation with respect to the Slovak environment [3]. This is a highly demanding task, in particular for those Slovak authorities and organizations responsible for meeting these requirements. The task is especially formidable since, besides resolving all major current problems, they are also expected to outline the future perspectives of Slovak water management.

Water supply resources are groundwater and surface water bodies currently used or intended for prospective use. Water used from identified water bodies shall meet relevant qualitative objectives and resulting requirements on water quality and quantity according to its purpose of use.

16.2. Water Framework Directive 2000/60/EC (WFD)

The new European Water Policy, and its operative tool, the WFD, are based on [3]:

— High level of protection,
— Precautionary principle,
— Preventive action,
— Rectification of pollution at the source,
— Polluter pays principle and
— Integration of environmental protection requirements into the definition and implementation of other,
— Community Policies – e.g. industry, agriculture, transport and energy,
— The promotion of sustainable development.

The resulting this directive thus reflects this new way of thinking and has the following particularly key objectives:

— the development of an integrated Community policy on and for the long-term sustainable use of water, and its application in accordance with the principle of subsidiarity;
— expanding the scope of water protection to all waters: surface waters, including coastal waters, and groundwater;

— achieving "good status" for all waters by a certain deadline, and preserving such status where it already exists;
— water management based on river basins, with a "combined approach" of emission limit values and quality standards, with appropriate coordination provisions for international river basin districts where river basins are located in more than one Member States and/or also involve non-Member States territory;
— setting prices for water use taking into account the principle of costs recovery and in accordance with the polluter pays principle;
— getting the citizen involved more closely involved; and
— streamlining legislation.

A number of new strategies will result from the implementation of the WFD. Specific issues that are important in formulating a sectoral strategy include the following [6].

— **River Basin Management** – The new approach to water management requires water to be managed on the basis of river basins, rather than according to geographical or political boundaries.
— **Programme of Measures** – Central to each river basin management plan will be a programme of measures to ensure that all waters in the river basin achieve good water status.
— **Combined Approach** – to pollution control (limiting pollution at source by setting emission limit values or other emission controls; establishing water quality objectives for water bodies; or providing for control of certain diffuse impacts).
— **Monitoring Programme** – The systematic monitoring of surface water and groundwater quality and quantity required is in several categories (surveillance monitoring; operational monitoring; investigative monitoring; and compliance monitoring)
— **Cost Recovery** Water is essential for a number of economic as well as environmental and health reasons such as the maintenance of drinking water supplies, the irrigation of crops and use in many industries. It is therefore essential to the viability of the population.
— **Public Consultation** – An important aspect of the development of river basin management plans is the need to involve the public.

16.3. Water Management Standardization, Legislation and International Cooperation

The Slovak legislation in the last period was aimed at meeting the obligations towards the EU related to new European water legislation adopted in 2006 and 2007 and at introducing common European currency – euro in the Slovak Republic. In 2009, the legislative process was focused mainly on finalizing the acts within their legislative approval process and on preparing the provisions to these acts [5, 7].

Standardization for water management sector of the Slovak Republic is conducted in the following technical committees (TC):

— TC 1 Water Supply and Sewerage Systems which cooperates with international standardisation committees (C150/TC 147, CEN TC164 etc.),
— TC 2 Melioration,

— TC 3 Hydraulic,
— TC 27 Water quality and protection,
— TC 64 Hydrology and Meteorology,
— TC 72 Environmental management.

The main activities were aimed at finalizing the process of Water Framework Directive (WFD) implementation through the development of final versions of river basin management plans in accordance with the Working and Time Schedule of Activities for Development of River Basin Management Plans and the National Strategy for WFD Implementation which fully respect the strategy of the European Commission and the International Commission for the Protection of the Danube River (ICPDR) [5].

Prior to this process the following core activities were carried out:

— publishing the proposal of the 1st version of the river basin management plans for comments, active participation and consultation of public;
— evaluation of the comments on the proposal of the 1st version of river basin management plans. An opportunity to comment on the published proposal of the 1st version of river basin management plans was taken by 11 entities. The final version of river basin management plans was published after evaluation of comments in December 2009;
— development of the final version of river basin management plans based on relevant comments and consultations of the involved parties. The Ministry of Environment submitted the Water Plan of Slovakia for comments in November 2009. The Water Plan should be a comprehensive document for water planning which consists of sub-basin management plans within the Danube and Vistula River Basin Districts. The Water Plan of Slovakia was approved in February 2010.

In addition, other significant works were done, especially within the assessment of ecological and chemical status of surface water bodies. The results were included in the final version of the Water Plan of the Slovak Republic and in the management plans of sub-basins. A part of activities within the WFD implementation included the preparation works for the second planning period 2015 – 2021.

These activities were aimed at updating the inventory of surface water types in Slovakia (reference localities), methodologies and determination of MEP and GEP for HMWB and AWB as well as classification schemes for the assessment of ecological status.

In 2009, the implementation of 26 EU directives and regulations together with reporting to EC on the process of their implementation was in the competence of the Ministry of Environment SR.

International cooperation continued under the intergovernmental agreements, international treaty and international conventions. International cooperation of the Slovak Republic in water management sector is done through cooperation on transboundary waters. This cooperation is in accordance with the Convention on the Protection and Use of Transboundary Watercourses and International Lakes UNECE (Helsinki Convention), the Convention on the Cooperation in Protection and Sustainable Use of the Danube River and many other agreements or conventions.

The Slovak Hydrometeorology Institute's (SHMI) conducts an assessment of surface water quality of the national river monitoring system based on the results of water analyses (basic physical-chemical parameters, biological parameters, micro-biological parameters, organic and inorganic micro-pollutants and in selected areas also radioactivity parameters) carried out in Slovak Water Management Enterprise (SWME) laboratories (physical-

chemical water analyses) and Water Research Institute Bratislava laboratories (biological analyses, analyses of specific organic substances and all analyses of samples from transboundary rivers with Austria, Hungary, Poland and Ukraine).

16.4. Monitoring

Monitoring is an essential part for implementation of the whole range of EU water legislation including in particular the WFD. Systematic monitoring of surface water and groundwater quality and quantity will arise in several categories – surveillance monitoring; operational monitoring; investigative monitoring; and compliance checking.

Summarising the water legislation, monitoring must be established for:

— surface waters, for ecological, physico-chemical and morphological parameters;
— groundwaters, for physico-chemical parameters;
— discharges of waste water, parameters depending on the particular case;
— bathing waters during the bathing season, for bacteriological and chemical parameters; and
— drinking water, for bacteriological and physico-chemical parameters.

16.4.1. Surface Water Monitoring

The Slovak Hydrometeorological Institute (SHMI) conducts an assessment of surface water quality of the national river monitoring system based on the results of water analyses (basic physical-chemical parameters, biological parameters, micro-biological parameters, organic and inorganic micro-pollutants and in selected areas also radioactivity parameters) carried out in SWME laboratories (physical-chemical water analyses) and WRI laboratories (biological analyses, analyses of specific organic substances and all analyses of samples from transboundary rivers with Austria, Hungary, Poland and Ukraine).

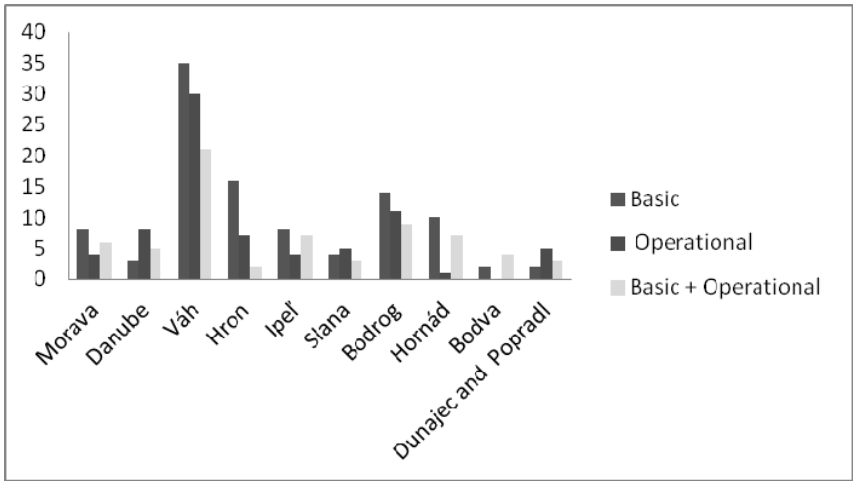

Fig. 1. The number of monitoring sites per sub-basin in 2009

Surface water quality parameters were monitored in accordance with the Programme of Monitoring of Water Quality and Quantity. The Programme includes 244 sites of basic and operational monitoring (for year 2009, see Fig. 1) [5].

The requirements for surface water quality defined under the Regulation of the Slovak Government 269/2010 were met at all monitoring sites in the following parameters:

— general parameters: total organic carbon, dissolved solids (dried and ignited), magnesium, sodium, fluorides, free ammonia, organic nitrogen, surface-active chemicals, selenium and dichlorobenzenes;
— radioactivity parameters: total volume alpha and beta activity, radium 226, tritium, strontium and caesium;
— hydrobiological and microbiological parameters: cultivable microorganisms at 22°C.

The limit values were exceeded most frequently regarding the following surface water quality parameters: general parameter – nitrite nitrogen (limit exceeded in all sub-basins), hydrobiological parameters – thermotolerant bacteria (exceeded in 7 sub-basins) and intestinal enterococci (exceeded in 8 sub-basins) [5].

16.4.2. Groundwater Monitoring

Groundwater, as one of important natural resources, represents invaluable, easily available and the most appropriate drinking water resource from quantitative, qualitative and economic viewpoints. Sufficient amount, better quality, low treatment costs and potentially low risk of contamination make groundwater a dominant resource of drinking water [1]. Assessment of relations between potential available groundwater quantity and used groundwater quantity is carried out through the annual water management balance developed by SHMI. Basic evaluation unit of groundwater balance is a hydrogeological region with its subsequent classification into sub-regions.

According to valid hydrogeological regionalization (1995) the territory of Slovakia was divided into 141 hydrogeological regions [5].

The Water Quality and Quantity Monitoring Programme for 2009 was developed in accordance with the strategy for implementation of the WFD in the Slovak Republic. This document includes the requirements for collecting all important information on water quality and quantity to be reported to the European Commission.

In 2009, the ground water quality was monitored in 136 sites of the basic monitoring. These sites are included in the national monitoring network of the Slovak Hydro-meteorological Institute or they are the springs not affected by point sources of pollution. Groundwater samples were taken once a year in 1 quaternary site, twice a year in 40 quaternary sites, once a year in 49 pre-quaternary sites and four times a year in 46 pre-quaternary karst sites.

The ground water quality was monitored in 298 sites (within the operational monitoring programme). The samples were taken 1–4 times a year in spring and autumn when the extreme condition of groundwater could be monitored.

Unfavourable oxidation-reduction conditions become an essential issue that is proved by the most frequently exceeded acceptable concentrations of the total Fe (58 times), Mn (53 times) and NH^{4+} (13 times). Besides these parameters, sporadic exceeding was observed in case of Cl^{-}, $SO^{4}{}_{2-}$, NO^{3-}, COD_{Mn} and soluble substances at 105°C. Increased concentrations of the followin g trace elements were recorded: Sb (8 times), As (6 times), Pb (5 times), Al (4 times), Ni (2 times), Hg (2 times) and Cr (1 time). The limit values for arsenic, lead and antimony were exceeded 4 times in the monitoring site Jasenie. Pollution

has only local impact. Most of specific organic substances were measured under the detection limit. No limit values were exceeded in this group. The limit for general organic substances was exceeded only for total organic carbon (3 times) [5].

16.4.3. Drinking Water Monitoring

Assessment of drinking water quality in public water supply systems is based on the results of the control of public water supply system operators – water companies and municipalities. Water quality is assessed on the basis of the number of determinations of individual drinking water quality parameters exceeding related hygienic limits.

In 2009 as many as 10,335 drinking water samples from sampling sites in water distribution network were analyzed in laboratories of water companies. In these laboratories 285.435 analyses were done concerning particular parameters of drinking water quality [5].

Not meeting the hygienic limits in drinking water in distribution network was mainly found out in the following parameters in 2009:

— microbiological and biological parameters (*Escherichia coli*, *coliform bacteria*, *Enterococci*, cultivated micro-organisms at 36°C, living micro-organisms, abioseston, *Clostrid* ium *perfringens*);
— inorganic and physical-chemical parameters (nitrates, nitrites, absorbance, colour, manganese, sulphates, turbidity, iron);
— radiological parameters (total volume activity alpha);
— disinfectants and their by-products (free chlorine, chlorites).

16.5. Conclusions

Water resource can be any part of water cycle in the nature where surface water or ground water is present in technically and economically usable form (e.g. watercourse, water reservoir, spring, well, etc.). Water is the most widespread substance on the Earth. The relationships among the number of population, development trends, hydrological cycle and actual available fresh water resources show the pressure that increases with demand for availability of water resources all over the world. Many of the mentioned problems can also be seen in our region of the Central Europe. The impact of anthropogenic activity (reducing forest areas, land use, urbanization, increase of impermeable surfaces, reduction of alluvial forests, wetlands, etc.) proves the fact that the trend to control water resources prevails over reasonable use of water also in our region.

The present conditions of drinking water supply, wastewater collection and treatment in Slovakia falls behind the level of developed countries in Europe and the world and it forces us to search for ways how to get closer to these trends and objectives.

References

[1] Act on Waters No.364/2004 Coll.
[2] Božíková J., Škultétyová I.: Groundwater-source of drinking water. In: Quality, environment, health protection and safety management development trends: Proceedings. International scientific conference. Neum, Bosnia and Herzegovina, 2.–6.9.2008. – Brno: Tribun EU, ISBN 978-80-7399-479-2, 34–39, 2008.

[3] Directive of the European Parliament and of the Council No. 2000/60/EC.
[4] Klinda J., Lieskovská Z. et all.: State of the Environment Report – Slovak Republic 2008, SEA, VKÚ, a.s., Harmanec, ISBN 978-80-88833-53-6, 308, 2008.
[5] Ministry of Environment of the Slovak Republic. Report on Water Management in the Slovak Republic in 2009, Water Research Institute Bratislava, 65, GLASS TRADING, spol. s r. o., Bratislava 2009.
[6] http://www.ewaonline.de/downloads/Bratislava_5_Kroiss.pdf
[7] http://www.unece.org/env/water/Protocol_reports/reports_pdf_web/Slovak Republic _ summary _report _en.pdf

Acknowledgements

The article was written with the support of the Scientific Grant Agency – projects VEGA no. 1/1143/11 and 1/0559/10 dealt with at the Department of Sanitary and Environmental Engineering of the Slovak University of Technology.

17 Development of Turbidity and Total Suspended Solids Relationship Based on Laboratory Subsamples

Laura Kusari (University of Prishtina, Faculty of Civil Engineering and Architecture, Kosovo)

17.1. Introduction

The anthropogenic activities taking place within a catchment have been altering our environment for many years. Large amount of sediments are delivered into our streams as land is cleared for construction. Our rivers, in particular urban ones, are being polluted with discharges from municipality wastewater, industrial wastewater discharge, mining activities, leachate from waste disposal areas as well as agricultural runoff. Urban river reaches are experiencing an increase in almost all constituents, as well as an increase of turbidity and Total Suspended Solids.

In order to have a clearer picture on the surface water quality of those rivers, many parameters have to be measured and also there are several factors that affect the reliability and the outcome of those measurements. Usually, monitoring of surface waters and the measurements of these constituents is within time frames that are previously determined and usually misses event discharges. It is a rather time consuming and resource intensive process. Therefore, a new approach of using one easy to measure parameter instead of another more expensive and time consuming one is a focus of this work. One component of water quality, total suspended solids is a significant indicator of physical and aesthetic degradation and a good indicator of other pollutants (particularly nutrients and metals). The aim of this work is to measure the values of TSS in urban streams through the measurements of turbidity. The turbidity is chosen as a surrogate for TSS because of the simplicity of its measurements. Turbidity also describes the changes in sediment concentration during precipitations and can be used in evaluating pollution loads attached to sediment particles. To achieve this, the relationship between turbidity and TSS must be developed.

Since there isn't a universal correlation between turbidity and TSS then the relationship is site specific. For the development of such a relationship in selected location, frequent sampling and measurement of turbidity and TSS is needed. However, because of the constraints in time, personnel and finances, different approach is used for the needs of this work. Laboratory subsamples are prepared, each of them with different turbidity and TSS concentrations. The results gained from the laboratory analysis of subsamples provide the data necessary for the development of the turbidity to TSS relationship.

The relationship, if such exists for selected location, will be developed by applying linear regression analysis.

The results gained would enable the use of turbidity as a water quality indicator. Monitoring the turbidity along a river would provide valuable information on the sediments quantity and at the same time would prevent the need of frequent sampling and conducting

expensive sediment analyses. The relationship may also be suitable for monitoring wastewater treatment effluent, dredging operations and dredged material disposal operations, discharges from mining activities and suspended sediments in storm water.

The prediction of pollutants entering a stream by conducting turbidity measurement, followed by the use of the relationship, would allow for a reliable, rapid and cost-effective water resources management.

17.2. Site Description

Selection of study site is one of the most important components of the research methodology. It is done carefully, after consideration of the suitability of the sites to conduct field investigations. Kosovo is a young country that is experiencing higher population growth and it is estimated that in the year 2000, about 2.4 million inhabitants were living here (”Assessment of number of population”, OSCE, 2000; Kosovo Spatial Planning, Spatial Development Strategy 2010 – 2020+, MESP, 2010). Besides, it ranks amongst the first countries in Europe, based on the population density, about 220 inhabitants / km^2. The higher density is in Prishtina, where over 900 inhabitants are living in one square kilometre (Fig. 1).

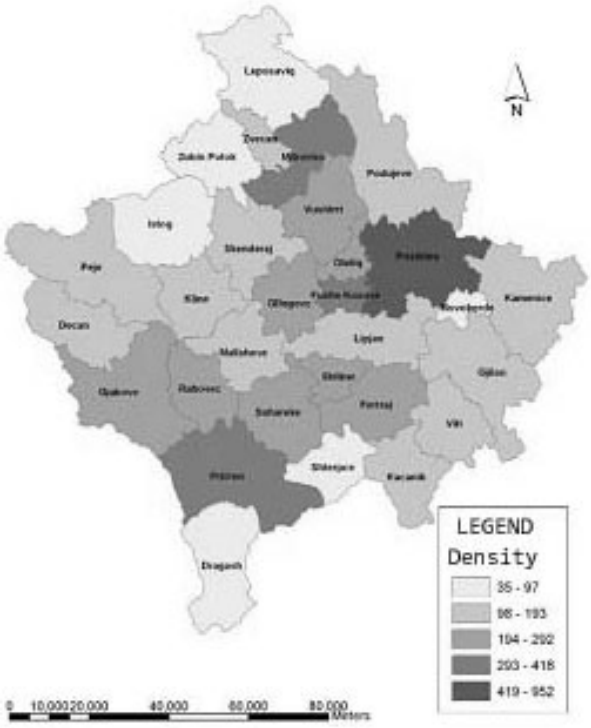

Source: Kosovo Spatial Plan 2010–2020+, Ministry of Environment and Spatial Planning (2010)

Fig. 1. Population density at municipalities

Due to the lack of infrastructure and the distance from education and health centres, the rural to urban migration is very evident. The higher number of citizens heading to urban areas imposes higher stress to receiving surface waters. This is associated with a large number of new constructions and changes in land use destination, often without the consent of urban planners. And the trend continues upward.

The urbanization's impact on the surface waters is going to be a huge environmental concern due to the fact that the actual health of streams is very low. It will continue to deteriorate, knowing the fact that according to the strategic plan 2010 – 2020+, this area is planned for industrial and economic growth, which will impose further stresses on surface waters.

Considering all the mentioned facts, the central part of Sitnica catchment was selected for this part of the research. The Sitnica catchment lies on the central part of Kosova and is characterized with medium – continental climate, with some impact of Aegean – Adriatic climate in this area. The average annual temperature is (10.2–10.4)ºC, minimal temperature is –26ºC while the maximum temperature reaches up to 37.4ºC (according to Hydro Meteorological Institute of Kosova).

The Sitnica catchment covers an area of 2931.71 km^2 with the catchment's average slope 4.4%. The average annual rainfall value is 691 mm and average annual flow is 16.6 m^3/s (source: Hydrologic station in Nedakovc, IHK).

The Sitnica catchment's vegetative cover (as shown in Fig. 2) comprises of arable land (1277.68 km^2), meadows (436.4 km^2), forests (339.9 km^2) and bushes (877.8 km^2).

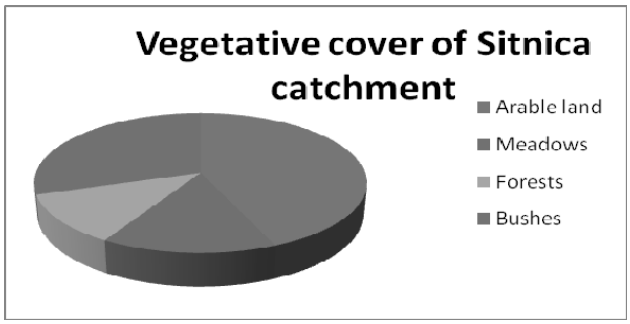

Fig. 2. Vegetative cover of Sitnica catchment

The main river is Sitnica, the longest river that flows completely within Kosovo, 167 km length and 13.62 m^3/s average annual flows. Since it has a relatively small longitudinal slope of 0.054%, Sitnica meanders a lot. It is located at the latitude and longitude coordinates of 42.901667 and 20.873889. Sitnica River originates from Sazlija pond, in the southern part of Kosovo and flows generally to the north, till its confluence into the Ibar River, as its right tributary.

The minimal and maximal values, as well as average annual flow for Sitnica River, measured at hydrometric station in Nedakovc, are as follows.

Sitnica flows through the Kosovo coal basin, west of Prishtina. In this area, Sitnica receives some of its most important tributaries, the Drenica River from the left and Prishtevka and Gracanka rivers from the right. The other tributaries that flow into Sitnica are also rivers Llapi, Shtimlanka and Sazlia and Matica, with their catchment's areas given in Tab. 1 and 2.

Table 1

Annual values of water flow (m^3/s)

STATION	RIVER	Q_{min} (m^3/s)	Q_{avg} (m^3/s)	Q_{max} (m^3/s)
NEDAKOVC	SITNICA	0.50	13.62	328.0

Table 2

Sitnica River's main tributaries

RIVER	MAIN TRIBUTARIES TRIBUTARIES	AREA (km^2)
SITNICA	Llap	1432.52
	Prishtevka	109.32
	Drenica	442.0
	Gracanka	180.93
	Shtimlanka	127.6
	Sazlia and Matica	141.5

Source: Kosovo Water Polluters Cadastre, Kosovo Environmental Protection Agency, KEPA (2000)

Fig. 3. Map of deployment sites

Sitnica River while flowing through the catchment is subject to many pollution sources. In urban reaches of this river, the untreated domestic and industrial waste waters are discharged directly into it. On the other hand, agriculture is a non point source contributor to those surface waters as well as direct dumping of solid waste in the vicinity of the river, erosion, mining activities as well as leachate from waste disposal areas.

Sitnica is the river with higher number of deployment sites in the Sitnica Catchment (Fig. 3), as it is known to be subject to at least 32 polluters (Kosovo Water Polluters Cadastre, Kosovo Environmental Protection Agency, KEPA). Except for the discharge of the domestic sewage in those rivers, they are endangered by the various industrial activities such as ironmongery, food and textile industry, slaughterhouse, metallurgical and chemical industry as well as energy industry. The map of deployment sites in Sitnica river is given

below. Considering all the mentioned facts and hydrological data, Sitnica river is selected for the development of turbidity to TSS relationship for this work. The selected sampling location was the reach of Sitnica River in Vragoli, after the outfalls of Prishtevka and Gracanka rivers.

17.3. Methods

17.3.1. Sampling

Water samples were collected in chosen locations during October, 2010. Due to the financial restrictions and the need for less personnel in the field, the most cost-effective method for sample collection was chosen. This is the main reason that the grab sampling was performed in this sampling site.

Samples were taken under stable environmental conditions, not following rainstorm or extremely high discharge event. Samples were collected manually in clean polyethylene bottles, volume 1000 ml, with the use of sampling rod, since it is proved to be the quickest procedure, needing less rinsing than the bailer and bucket combination. After the sample bottles were placed into the holders, they were inverted and half filled at 20 cm below the water surface. The lid was placed on sample bottles and they were shaken to ensure thoroughly rinsing of the lids and bottles. The content of the bottles was then discarded away from sampling site and this process was repeated three times.

The water samples collected were labelled with the time, date and site and placed in the cooler. For the determination of turbidity to TSS relationship, the sub sampling was done in a laboratory. Subsamples were prepared in order to have different values of turbidity and TSS, and after the preparation were preserved and refrigerated under a temperature of 4ºC (as specified in Standard Methods for the Examination of Water and Wastewater, APHA 2005). Those subsamples were then sent to the Hydro Meteorological Institute of Kosova (HIK) for the analyses of turbidity and TSS concentrations.

17.3.2. Statistical Analyses

It is well known that statistical methods are of a crucial importance in the successes of water quality monitoring. In general, water research studies require large data bases with a range of parameters. Therefore, clear mathematical relationships between key parameters and their surrogate parameters can improve the surface water quality monitoring. This is possible due to the fact that these relationships reduce the number of key water quality parameters that are to be monitored.

The objective of this work was to develop linear regression model between turbidity and total suspended solids based on the use of a statistical technique, known as linear regression analyses.

As shown in Fig. 4, the data from the laboratory analyses were plotted in Excel 2007 from which a linear regression equation was derived, for conversion of all recorded turbidity data to TSS values. In our case, the dependent variable Y is the total suspended solids, the TSS response variable, while independent variable X is turbidity.

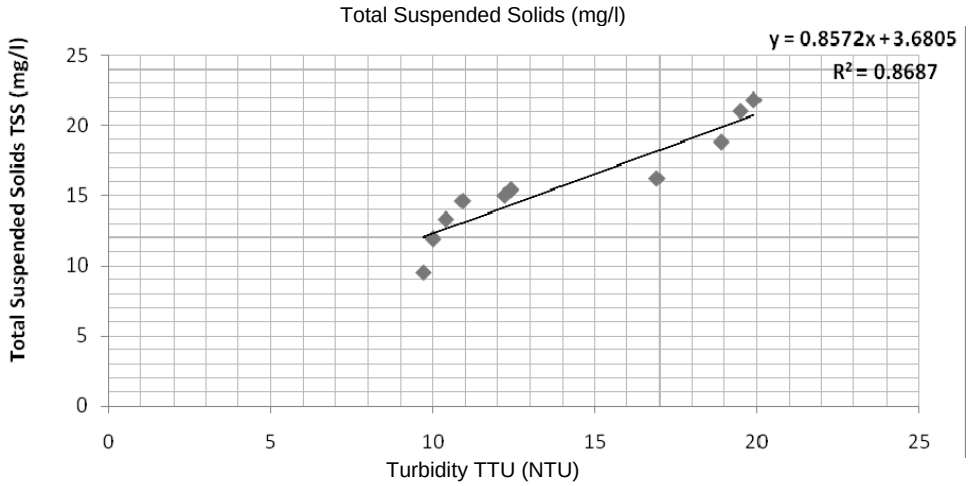

Fig. 4. Relationship between turbidity and Total Suspended Solids

17.4. Results and Discussions

As it can be noticed from the graph, the relationship between turbidity and total suspended solids (Tab. 3) for a study site is a positive relationship and it is as follows:

$$TSS\ (mg/l) = 0.8572\ TTU\ (NTU) + 3.6805$$

Table 3

Variable Description

Variable	Unit	Description
TTU	NTU	Turbidity
TSS	(mg/l)	Total Suspended Solids

An explanatory variable, such as turbidity in this relationship, can be used to compute the response variable Total Suspended Sediments.

Since the predictive ability of the relationship can be assessed based on the coefficient of determination (R^2), than for the selected location there is a strong correlation between turbidity and TSS (correlation coefficient of 0.868).

As it is evident in the same graph, we can conclude that the prediction of TSS based on turbidity readings, for a given site is quite reasonable.

17.5. Conclusions

Since the frequent sampling and laboratory analyses of the TSS are time consuming and require a considerable budget means, than the developed relationship would serve its best. The utility of this model will be in predicting TSS levels from a measured turbidity in a given location, when in fact the slight changes in TSS concentration have large effects on

turbidity reading. Also, the same relationship would be suitable for other sites in an event, where the coefficients for the developed models in each site are identical.

As an outcome of this study, this relationship can be used for measuring stream bank erosion, nutrient, contaminant transport and sediment loads.

The benefits of water quality measurements using this relationship include the ability for quick action in response to negative water quality changes. This will result in a reduction of overall monitoring costs. Additionally, when surface water quality criteria are exceeded then the immediate action can be taken.

The outcome of this research, the developed turbidity to TSS relationship can be used in many areas. The relationship can help in documenting the effectiveness of stream restoration projects. In agriculture, it can help in monitoring suspended solids, in order to reduce non – point source pollution. The data gained from this relationship can be used to identify water bodies impaired by suspended solids, to prioritize areas for additional monitoring and research, to detect trends of increasing or decreasing erosion in a watershed.

Finally, the positive value of this research is that the linear regression model relating turbidity to TSS may be a useful tool in hands of an engineer in controlling and regulating sediment Total Maximum Daily Loads in an urban stream. As a result, compliance with water quality standards and regulations that are based on concentration and load estimates can be determined with more certainty.

References

[1] Bartram J., Balance R.: A Practical Guide to the Design and Implementation of Freshwater Quality Studies and Monitoring Programs, Published on behalf of United Nations Environment Program and the World Health Organization, Taylor and Francis Group, 1996.

[2] Bilotta G. S., Brazier R. E.: Understanding the Influence of Suspended Solids on Water Quality and Aquatic Biota, Water Research, 42, Elsevier Publications, 2008.

[3] Christensen V.G., Rasmussen P. P., Ziegler A. G.: Comparison of Estimated Sediment Loads using Continuous Turbidity Measurements and Regression Analyses, Turbidity and Other Surrogates Workshop, Reno, Nevada, 2002.

[4] Christensen V.G., Ziegler A. G., Xiaodong J.: Continuous Turbidity Monitoring and Regression Analyses to Estimate Total Suspended Solids and Fecal Coliform Bacteria Loads in Real Time. Proceedings for Federal Interagency Sedimentation Conference, March 2001, Reno, Nevada, 2001.

[5] Glyson G. D., Gray J. R., Conge L. M.: Adjustment of Total Suspended Solids Data for use in Sediment Studies, U. S. Geological Survey, 2003.

[6] Glyson G. D., Gray J. R.: Total Suspended Solids Data for use in Sediment Studies, Proceedings of the Turbidity and Other Sediment Surrogates Workshop, Reno, Nevada, 2002.

[7] (2010): Spatial Plan of Kosovo – Spatial Development Strategy 2010–2020+, Ministry of Environment and Spatial Planning, The Institute for Spatial Planning, Prishtina, Kosovo.

[8] (2000): Kosovo Water Polluters Cadastre – Report, Regional Environmental Centre, Kosovo Environmental Protection Agency, Prishtina, Kosovo.

[9] (2010): The State of Water in Kosovo – Report, Ministry of Environment and Spatial Planning, Kosovo Environmental Protection Agency, Prishtina, Kosovo.

[10] Popovska C., Stavric V., Sekovski D.: Hydrology and Hydraulic Structures in Environmental Engineering. University of Ss Cyril and Methodius, Faculty of Civil Engineering, Skopje, Macedonia, 2011.

[11] Warner R., Sturn T.: Turbidity as a Surrogate to Estimate the Effluent Suspended Sediment Concentration of Sediment Controls at a Construction Site in the Southeastern United States, Turbidity and Other Surrogate Workshop, Reno, Nevada, 2002.

18 The Directive of Dam Break Modeling from the Hydraulic Structure and Two Dimensional Numerical Models

Radomil Květon, Peter Šulek, Martin Orfánus, Martin Mišík, Marián Kučera
(Slovak University of Technology in Bratislava, Faculty of Civil Engineering)

18.1. Introduction

The transition from 1D modeling of unsteady water flow with free surface to 2D mathematical modeling provides us to get better results. Flexible computing mesh (Fig. 1) allows us to generate refined mesh in key areas (inline structures, populated areas, etc. – characteristic dimension of a mesh element can be reduced to 2–5 m), where either we need more accurate results or expect a sudden change in water flow velocity. Flexible computing mesh is ideal for variation of rural zones (edge of computing elements is greater – 50–100 m) and urban zones (edge of computing element is of the order of tens of meters). Quantities characterizing the flow in 1D modeling are based on the modeling sections (the total flow through the profile, cross-sectional average velocity, water level in cross section). 2D modeling gives us spatially localized modeling results (water level in the modeling element, components of vertical averaged velocities in computation element). The total discharge through the specified selected profiles can be provided by integration of local transverse discharges. Water level (maximum and instantaneous) in the profile will always have a local character.

Because of much sizable result file in terms of 2D modeling in contrast to 1D as well as the changing character of the results from the cross to the local, forces us to change not only the methodology for retrieval but also the tools to accurately obtain the maximum instantaneous values as well (in a defined time step of storing results of a calculation) in the required site.

Working with 2D modeling results will put increased demands on the user, what will have to adapt the documentation required to calculate the dam break e.g. developing special-purpose user documentation.

18.2. Dam Break Modeling

The standard scenario assumes a simulated emergency incident of dam annihilated locally at steady discharge *Qa* (long-term average flow) conditions operated through the dam's outlet – the initial condition for calculating the simulation in the area under the construction. A breakthrough wave during the simulation is carried out into the distance, where the size of its maximum discharge has not exceeded the maximum discharge of average frequency once every 100 years – *Q*max100. In the case of a plane area, where

various branches of the proposed model does not join the flow in the channel under the construction, the simulation is provided up to a distance where the wave height falls below 0.5 m above existing ground level. Completion of modeling the discharge of *Q*100 is problematic, it is not possible to control the volume balance of dam break waves and hence the accuracy of the modeling process (choice of shape and density of computational mesh). Simulation of dam break waves under construction should cease when the discharge decrease in *Qa* or in terms of lowland areas where either water completely recedes or isolated water masses arise in the modeling space.

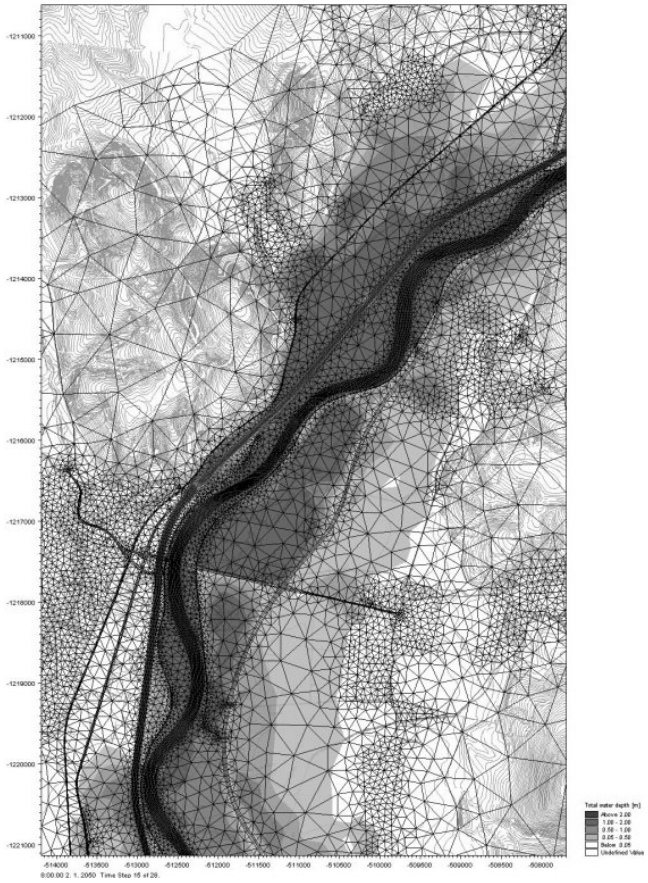

Fig. 1. Flexible mesh scheme layer on raster map

Decisive influence on the results of the simulation process has the definition of roughness conditions in the territory of the expected flooding. There is not to be an obligation to put these values in the documentation and custom roughness coefficients for the modeled area (part of the compilation model) is often referred as investigator's intellectual property (know-how). It is not therefore possible to re-check the calculation of another investigator. Tab. 1 and Fig. 2 are figuring out a possible way of documenting the roughness setting ratios in the modeling field [2].

Table 1

Manning's roughness coefficients used in 2D model

Cathegory	Landuse	Roughness "n"
1	Váh channel, intakes, inline structures	0.033
2	Derivation channel	0.025
3	Agriculture and undeffined areas	0.048
4	Towns and villages	0.077
5	Inundation 1 – upkeeped	0.063
6	Inundation 2 – less upkeeped	0.077
7	Inundation 3 – not upkeeped	0.09

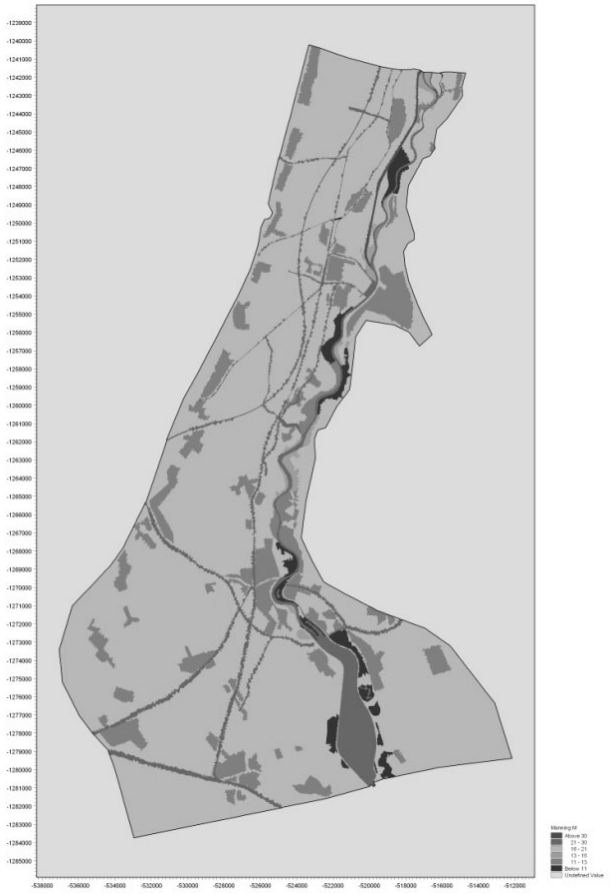

Fig. 2. The roughness coefficient map of modeled sector Drahovce – Králová

Surveying background

The quality and timeliness of geodetic documents largely affects the results of modeling process. Current digital terrain model (DTM) provided free by EUROSENSE, Ltd. was the basis for generating the computation mesh [3]. Raster maps provided by the client were applied to visualize the results of treatment only but were older dated therefore the investigator was forced to obtain some data or verification of http://maps.google.sk.

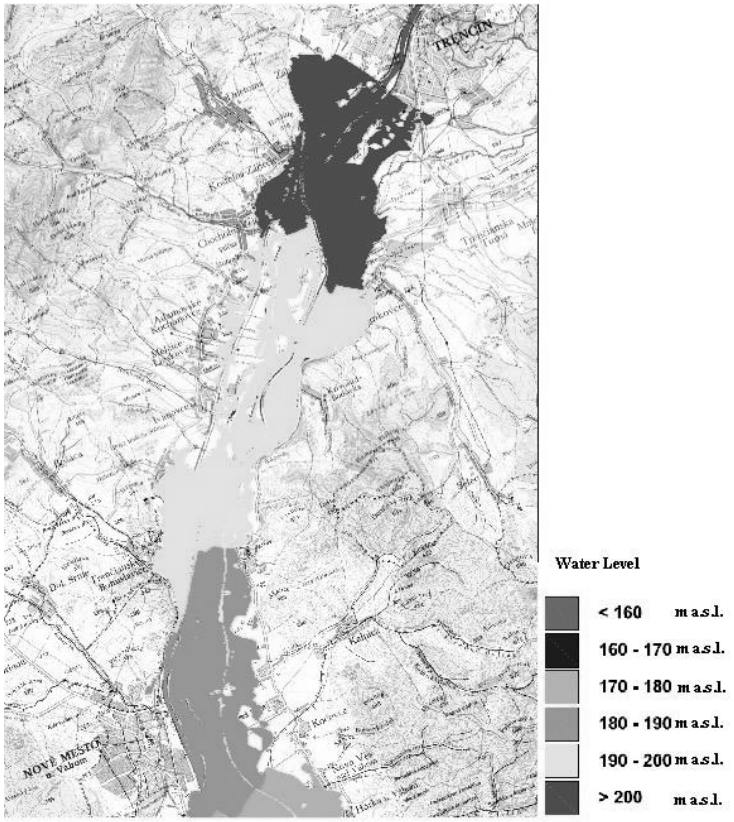

Fig. 3. Map reaching water levels peak in the sector T.Biskupice – Nové Mesto n.V.

Numeric results of parameters – tabs

The increase of the complexity area model and loss of simple orientation (irregular shape and size of elements of the model) will require new approaches to obtaining the numerical values. Increase in the number of the data shows the following comparison of the amount of data obtained from the modeling process [2]. The area between weir Trenčianske Biskupice and weir Drahovce were covered with computational mesh having 71 935 nodes and 101 777 elements (section length of 47 km), which represents the average number of 1530 nodes and 2165 elements per river kilometer. Comparable 1D model with 5 branches and the average distance between the profiles of 100 m has 50 sections and 55 computing nodes. It follows that the tabular data display can be calculated only for selected profiles

and the suitable treatment. Calculated data remain to be made available in the program in graphical environment, enabling easy selection and spatial orientation fore required data ([2] MIKE ZERO View).

Graphic representation of calculated variables

The Directive prescribes how the post-processing of the 2D model in graphic form should be formulized e.g. by situational pictures depicting the documented value (level, average vertical velocity) at each node computer mesh, with ranges of values displayed parameters is assigned a variety of colors.

In Fig. 3–5 are shown maps (situational pictures) achieved the maximum level values, depth of water and average size of velocities. Problematic is the color palette in the display of maximum levels. For long stretches (47 km [2]) is a display range of over 40 m and used scale colors must be very thick (Fig. 3).

Color scale (Fig. 4) must take into account water depth characteristic for evaluation during the dam break wave (0.5 m – limit decline in water levels) and should provide a basic orientation in determining the degree of damage to buildings or a threat to people in flooded areas by dam break wave.

Color scale at the maximum obtained velocity (Fig. 5) must take into account the velocity of water flow characteristics for determining the degree of damage to buildings or a threat to people in flooded areas by dam break wave. Boundary water velocities of $1\ m \cdot s^{-1}$ divide the area dominated by hydrostatic pressure of water and the area of the hydrodynamic action of the dam break wave.

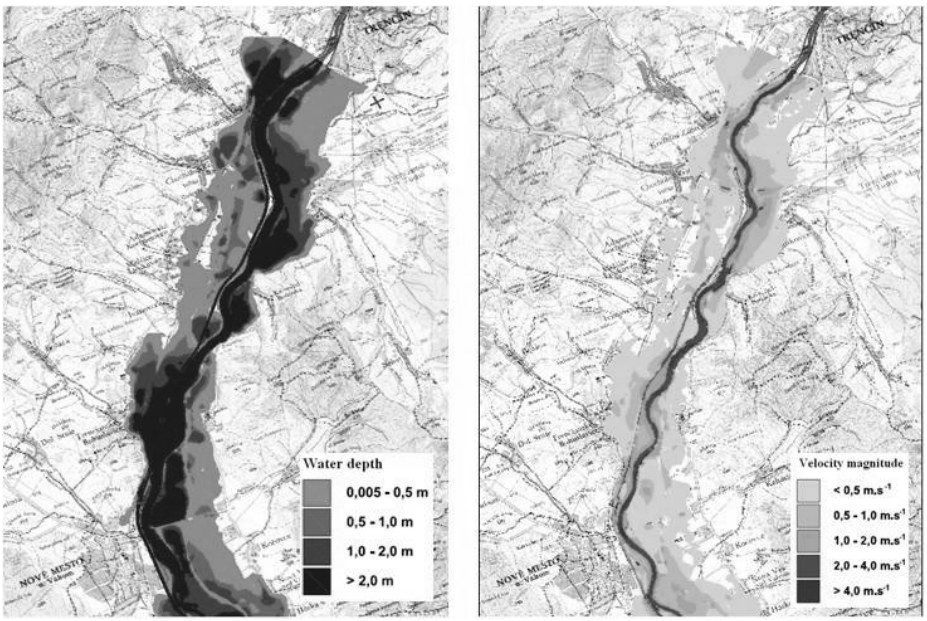

Fig. 4. Map of obtained maximum depths and velocities of water in the sector T. Biskupice-Nové Mesto nad Váhom

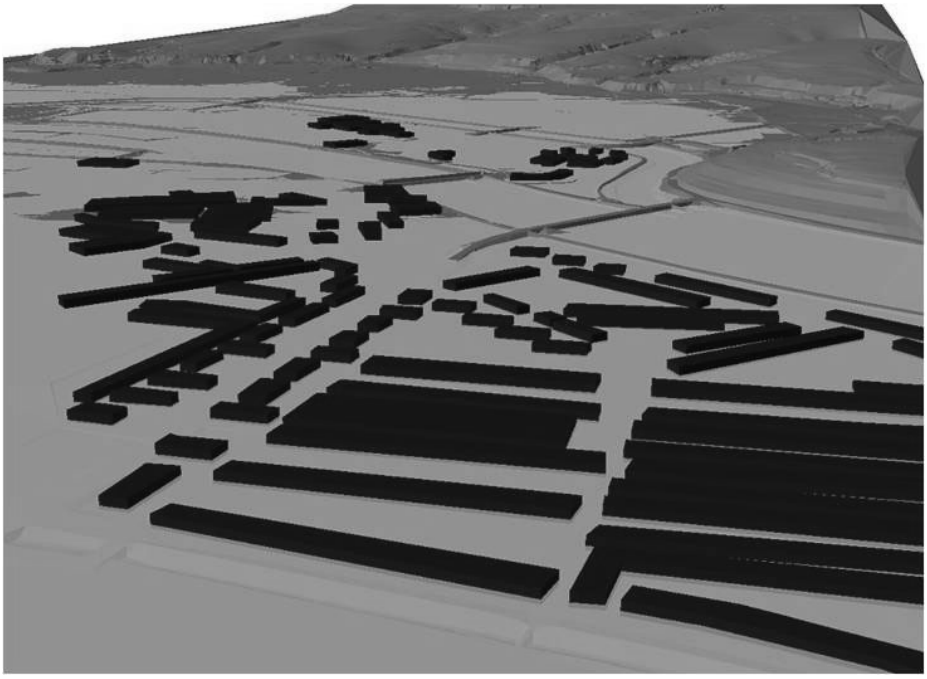

Fig. 5. Visualization of Piešťany town

Evaluation of the devastating effects of the dam break wave

The Directive [1] determines the evaluation process of the devastating effects of dam break wave in tabular form, which is needed to be defined for processing the results of 2D modeling data such as distance from the compromised water structure, time reduction discharge in analyzed area at the *Q*ma × 100 and degree of damage/destruction. As appropriate showed the utilization of risk analysis, flood plain, which develops in the process of flood modeling. The intensity of dam break wave should thus to be characterized as the intensity of the flood wave (IP) based on water depth h and velocity of the water in:

$IP = h$	for $h>0$ and $v<1\ m \cdot s^{-1}$	Hydrostatic pressure effect area
$IP = h \cdot v$	for $h>0$ and $v>1\ m \cdot s^{-1}$	Area of predominant hydrodynamic acts

With subsequent distribution at the areas with low, medium and high intensity of dam break wave. Length of exposure required for damage estimation from Damage curves may be calculated from information already monitored in terms of the current the directive.

18.3. Conclusion

The presented article at the above mentioned data and ideas sufficiently demonstrates the need for adjustments of the present Directive of the dam break wave calculation, so the modern means of mathematical modeling should be utilized and more accurate results obtained as well.

References

[1] Smernica Ministerstva Životného prostredia Slovenskej republiky z 30.apríla 2007 č.1/2007 – 1.5. pre výpočet prielomovej vlny z vodnej stavby.
[2] VD Liptovská Mara – Kompletná dokumentácia výpočtu prielomovej vlny, Dopočet od hate Trenčianske Biskupice, SvF STU v Bratislave, 08/2010.
[3] Digitálny model terénu dotknutej oblasti © EUROSENSE, s.r.o., www.eurosense.sk.

Acknowledgement

This paper was supported by the Grant agency VEGA under contract No.1/0578/11 and No.1/0281/10 and the Slovak Research and Development Agency under contract No.APVV-0680-10.

This paper was supported by the Grant agency VEGA under contract No.1/0894/10.

19 Review of Wind–Wave Generation

Eva Ocvirk, Marko Pršić, Dalibor Carević (University of Zagreb,
Faculty of Civil Engineering, Croatia)

19.1. Introduction

Wind waves feature the highest energy and produce the biggest impact on the structures. Due to their frequency they require most attention in dimensioning maritime structures. Wind waves belong to the group of duration limited oscillating waves.

The term wind-wave generation is used to define the growth of waves, increase in wave height and period, with respect to time and distance due to the action of wind on the water surface. The wind wave generation is an extremely difficult problem because it involves the modelling of a turbulent airflow over a surface that varies in space and time. Although there has been much progress in understanding turbulence over a flat plate in steady conditions, modelling attempts of turbulent flow over (nonlinear) gravity waves are only the beginning and there is still a considerable uncertainty regarding the validity of these models. From an experimental point of view it should be pointed out that it is not an easy task to measure growth rates of waves by wind. It is hard to measure growth rates by studying time series of the surface elevation since the time evolution of ocean waves is determined by a number of processes such as wind input, nonlinear interactions and dissipation. Because of the small air-water density ratio the growth rates are small, which means that a very accurate determination of amplitude and phase of the wave-induced pressure fluctuations is required.

In principle, a large number of variables may control wave growth. For example, in the idealised situation of duration-limited waves the following variables may be relevant: angular frequency, acceleration of gravity, viscosity, surface tension, air and water density, Coriolis parameter and a wind speed scale. In practice it is most convenient to select the wind speed scale at the height of 10 metres as this is nowadays the most common height at which the wind velocity is measured. However, this choice of the wind speed scale introduces a height scale, namely 10 m, which has no relevance to the problem of the generation of waves by wind, and therefore another wind speed scale, namely the one based on the friction velocity u^*, may be more appropriate, as this scale is related to the momentum transfer from air to water. There are a number of theories for deepwater wave generation and waves decay after generation.

19.2. The Mechanism of Wave Generation by Wind

The adopted mechanism of wave generation by wind is given in short due to the easier following of historical development and subsequent analyses.

Generally, wind waves are being generated through three phases. When the wind starts blowing over the sea the contact surface is flat and calm. In the first phase, which is the phase of initial generation the resonant mechanism emerges with pulsating pressure induced by the air turbulence on the sea surface. Due to this, the waves emerge out of the water surface, having the same frequency as pressure a pulsation, which leads to further increase of rollers due to the resonance (Fig. 1–1). Then follows the second phase, the phase of undulating air flow over wave profile without the separation of the streamline. The wind energy is being transferred on the waves over the air vortex towards the wave trough and over the resulting pressure field causing the wave height increase creating the young sea (Fig. 1–2). In the final phase the wave breaking takes place, when the small wavelengths break at the crests of long waves. The final phase features the highest waves. The short wave breaking at the long one adds the impulse of its displaced mass to the orbital motion's kinetic energy of particles of the long waves. The wave height increases with the growth of the long wave's energy, so that the wave energy transfers from the short waves to the long ones (Fig. 1–3).

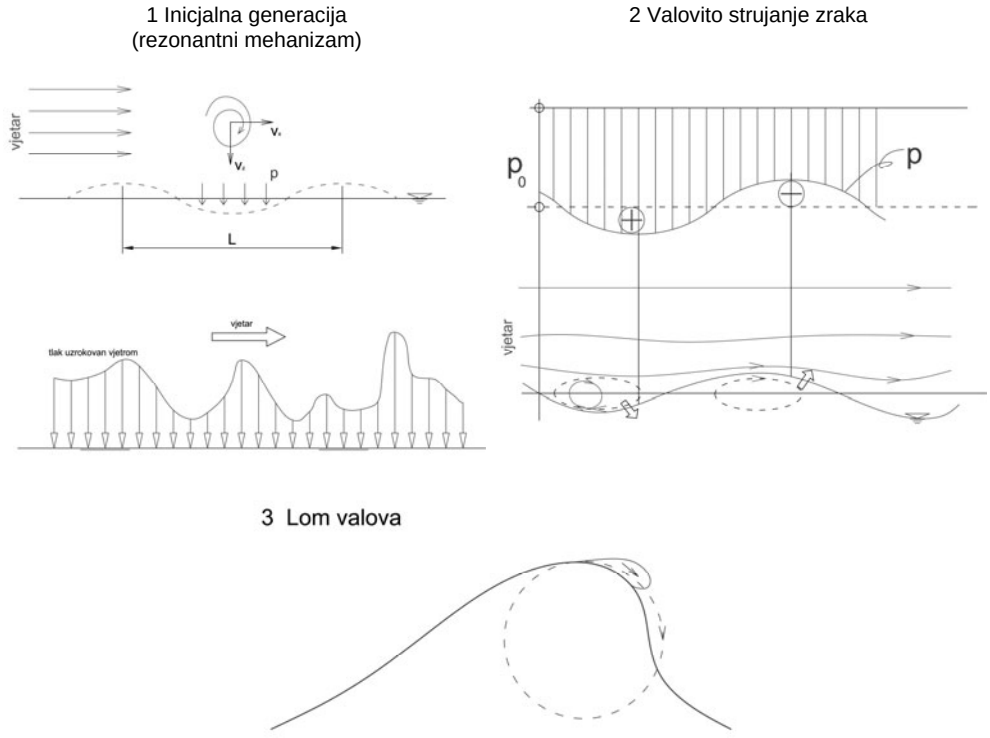

Fig. 1. Basic phases of the wind waves' generation mechanism: 1 – initial generation, 2 – air flow, 3 – waves breaking

The understanding of wind waves development is a very complex task. It is exceptionally challenging problem from the theoretical standpoint, as it involves the modelling of turbulent air flow, which is varying in space and time above the sea surface.

19.3. Theories on Wave Generation

19.3.1. Helmholtz's Theory

Helmholtz's theory is based on the study of the oscillations set up at the interface of two fluid media of mass densities ρ_1 and ρ_2 flowing with velocities u_1 and u_2 with respect to each other. The interface is a wave surface and the propagational velocity c is the speed at which the interface travels forward, and L is the distance between two successive peaks of the interface. Induced oscillation at the interface travelling at the velocity c such that

$$\rho_1(u_1 - c)^2 + \rho_2(u_2 - c)^2 = \left(\frac{g}{k}\right)(\rho_2 - \rho_1) \tag{1}$$

where g is acceleration of gravity and $k = 2\pi/L$ is wave number. In the case $u_1 = u_2 = 0$, Eq. (1) takes the form

$$c^2 = \frac{g}{k}\left(\frac{1 - \dfrac{\rho_1}{\rho_2}}{1 + \dfrac{\rho_1}{\rho_2}}\right) \tag{2}$$

If we consider the upper fluid to be air and the lower fluid water Eq. (2) takes the form $c^2 = g/k$, which is the classical equation for wave celerity obtained from linear wave theory.

Eq. (1) can be written as

$$c = \frac{\rho_2 u_2 + \rho_1 u_1}{\rho_1 + \rho_2} \pm \sqrt{\frac{g}{k}\left(\frac{\rho_2 - \rho_1}{\rho_1 + \rho_2}\right) - \left(\frac{\rho_1 \rho_2}{(\rho_1 + \rho_2)^2}\right)} \tag{3}$$

Using the equation above the instability condition of wave development can be determined (propagation) only when the term under the square root is negative. The instability condition for the assumed contact surface between water and air can be set as

$$\frac{\sqrt{\dfrac{g}{k}}}{u} < \frac{1}{28}.$$

As far as the above condition is fulfilled the waves are instable and keep growing according to the height and period.

It can be proved as well that the lowest speed of capillary waves propagation being 23.2 cm/s corresponds to the 1.7 cm wave length and the 0.073 s period. Providing that surface tension is included, according to Kelvin, the waves would be instable if the wind speed is > 6.5 m/s. Such velocity is called also the critical wind speed for gravity waves generation. According to measurements, the critical wind velocity can be determined within 4 do 6 m/s intervals. The wind flow over the water up to this speed is laminar, whereas the turbulence develops with the wind speed, and the surface becomes hydro dynamically rough. Therefore, the wave amplitudes increase in time and space.

19.3.2. Jeffreys' Theory

Jeffrey proposed that eddies on the leeward side of the waves resulted in a reduction of normal pressure as compared with the windward face and a consequent transfer of energy from wind to waves. Results suggested that the wind could add energy to waves only so long as the windspeed was equal or greater than the wave velocity, and when the wave celerity became equal to the wind speed the wave reached maximum height. The lowest wind speed required for the wave generation was on the order of 1m/s.

19.3.3. Svedrup and Munk Theory

Svedrup and Munk considered the transfer of energy by normal and tangential stresses. The energy of waves can increase only if the rate at which energy is added by normal and tangential stresses of the wind exceeds the rate at which energy is dissipated by viscosity. The energy added by the wind increases the wave height and thus the wave speed. During the very early stages of wave development energy is transmitted by normal stress, but at $c/u > 0.37$ the transmission by tangential stresses is dominant. When $c/u = 1$ energy is added by tangential stress, there is a small amount lost due to normal pressure. The fully developed sea state occurs, according to Breitschneider, when $c/u = 1.95$

19.3.4. Philips and Miles Theory

Both theories had in common that waves were generated by a resonance phenomenon: Phillips dealt with the resonant forcing of surface waves by turbulent pressure fluctuations, while Miles analysed the resonant interaction between the wave-induced pressure fluctuations and the free surface waves. Phillips' mechanism gives rise to a linear growth of the spectrum in time, but it turned out to be ineffective. This is because the effect is proportional to the variance spectrum of the turbulent pressure fluctuations at the resonant frequency, independent of the wave spectrum, and this is of the order of the square of the air-water density ratio. Miles' mechanism is proportional to the wave spectrum itself, which implies exponential growth, and it is of the order of the density ratio of air and water.

The main reason for the controversy was that Miles' theory oversimplified the problem by following the quasi-laminar approach. This approach assumes that the airflow is inviscid and that air turbulence does not play a role except in maintaining the shear flow. Miles also neglected nonlinear effects such as wave-mean flow interaction, which are expected to be important at the height where the phase speed of the surface waves matches the wind speed. The conducted experiments [5] provided the magnitudes of energy transfer from the wind to the waves, the order of magnitude higher than was suggested by Miles. Later measurements [14, 35, 36] showed the correspondence of order of magnitude with the Miles' theory. However, his theory implies lower energy transfer than the measured values, particularly with relatively low frequency waves with phase speed, which is nearly equal to the wind speed at the 10 m height above the surface.

Miles' theory implied the interactions between wind and waves to be linear enough, so that the wind impact on each spectral component can be independently observed. Especially Tsiming's investigations [39] focused on the interaction of two waves and air flow, which is the simplest case of the wave group. The resulting waves' growth of an individual spectral component depends now on the presence of other components. From the numerical point of view it is a small impact, as it is proportional to the ratio of air density and the sea and the square of wave spectrum. According to the models of big distortion, such as created

by Belcher and Hunt or Mastenbroek, the mechanism of the critical layer is relevant only with exceptionally quick waves. Belcher and Hunt [2] discovered two layers in the air flow over the waves. The turbulence in the layer closer to the surface, which they call the inner region, is in the balance with the local speed gradient. The second layer called the outer region, in which the turbulence can not be neglected, is being created above the first one. This mechanism is related to Jeffreys' protection hypothesis. According to Belcher and Hunt the waves' action is slow compared to the wind speed. The relevant waves in the models of waves forecast are the ones with the speed of the same order of magnitude for the wind speed, but this theory does not account for them. Their approach was upgraded by Mastenbroek [22] within his model of the second order of air turbulence. Lately, there have been proofs that Belcher and Hunt's approach overestimates vortices' impact on the waves' induced flow. Sullivan et al. [37] analysed the wind waves' generation in the context of solving numerical models of the vortices. Although the Reynold's number, in comparison with the natural one was lower within the order of magnitude, the direct proof of the critical layer presence was determined. While following the concept of the significant distortion, Belcher and Hunt stated that large vortices were too slow for the transmission of considerable energy during the individual wave period. Furthermore, there are nowadays more direct proofs for the presence and significance of the critical layer mechanism for in-situ observation [17].

For the given wind profile the quasilinear theory is rather satisfying in forecasting wind generated wave development. However, it ignores the possibility of wind profile modification during waves' development. The energy transfer onto the waves can be so high that corresponding stresses induced by wind reach a remarkable integral part in turbulent stresses [36]. The energy transfer from the air to the waves can be under the impact of sea state. The measurements ([7, 11, 24, 34]) showed that the wave drag coefficient depended on the sea state through the waves age. Janssen, 1982 [19] developed the theory of wind and waves interaction. Quasilinear theory of wind induced waves generation follows the slow development of the sea state and its impacts on the wind profile. The Miles' theory accounts for the dependency of air flow and the sea state at each individual moment. The resulting roughness parameterization, which is expressed by waves induced stresses, provides satisfying agreement with perceived roughness [19].

19.4. Numerical Formulation of the Problem

Generally the waves modelling theories were created through three time segments: the first segment includes purely empirical basic methods, the second phase implies half empirical spectral models and the third phase, still in development, includes numerical modelling.

Empirical data on ocean waves have been collected over the time. Most of recent observations on the sea state were collected on ships by means of visual inspection. On the base of these data empirical scaling laws were formed. Those laws had a defect that they were not dimensionally consistent. Stevenson (1874) suggested the relation between wave height in meter and fetch in kilometer

$$H_{\max} = \sqrt{F} / 3 .$$

Others such as Larisch (1925) and Cornish (1934) suggested that wave height would depend linearly on wind speed, e.g, $H = 0.48\ u_8$, where u_8 is the wind speed at about 8m height. Rossby and Montgomery (1935) suggested dimensionally consistent relation between wave height and the wind speed at about 10m above the sea, u_{10}, still in use today,

$$H_{\max} = 0{,}3u_{10}^2 / g\ .$$

Sverdrup and Munk (1946) made the first step in the more realistic modelling of wind generated waves by examining the waves development on the basis of energy, fetches and wind blowing duration observation, while introducing the concept of the significant wave amplitude H_s. Bretschneider (1952, 1958) extended their investigations with additional data, and developed generally accepted SMB (Sverdrup, Munk and Bretschneider) method.

The second phase started by introducing spectral analysis into waves' investigation in the early 1950 s, and by formulating Neumann spectrum. Pierson et al. developed in 1955 the waves forecast based on the spectral analysis method, PNJ (Pierson, Neumann and James). Finally in 1963, Hasselmann set up the framework for numerical modelling of wind induced waves when he established the law of wave spectrum energy conservation. The law presented the base of potentially precise dynamics theory of the wave spectrum in the form:

$$\frac{\partial E(\vec{k}, x, y, t)}{\partial t} + c_{g,x} \frac{\partial E(\vec{k}, x, y, t)}{\partial x} = S \tag{4}$$

where E is the wave spectrum energy in the vector function of the wave number $\vec{k}$, spreading direction (x, y) and time t, $c_{g,x}$ the speed of observed wave group in the x direction, and S is the total force coming in and out of the system.

1977 Donelan [6] noticed that the sea state is affected by the wind friction on its surface, so he connected the waves physics with the wind stresses on the surface. Donelan developed a simple model of waves forecast which bases on the concept of local balance of the momentum, and not on the energy balance. He was the first to introduce the angle of deviation between the wind blowing direction and the waves' propagation direction.

The process of generation, dissipation and waves' interaction in deep water was presented through three problem formulation generations, depending on the parameterization process level.

Schwab [33] upgraded the previous numerical framework to develop a half empirical parametric model, the first generation model where he completely neglected the non linear interaction. The representatives of the second model generation are SHALWV (shallow-water wave) and DWAVE (deep-water wave) models (1981 and 1986) related a lot in their structure to the WAM model – which is the third generation model. They differ in the fact that DWAVE does not include bottom friction. Their approach to parameterization of non linear interaction strictly dependent on beforehand defined spectral shape is the feature which classifies those two models as the second generation, and not the third one.

According to an extensive comparison study of first and second generation of wave models published in 1985 by an experts team forming the SWAMP group (Ocean wave modelling), both models shared some basic simplifications, which accounted for the models' lack of reality in extreme conditions (particularly at the sudden alteration of the wind field) [38].

The above mentioned study initiated the third phase, the period of numerical modelling, which meant the development of the third generation of wave models where the fourfold waves' interaction was explicitly expressed. The third generation model prototype

is the WAM model of ocean waves' generation of the WAMDI group [40]. In 1998 the third generation numerical model was developed for the application in coastal areas - Simulating Waves Nearshore – SWAN. The waves development in the SWAN model bases on the Euler's formulation of the balance of the equation of the spectral discrete wave action. The model discretises, the spectrum in the frequency domain and according to directions, while kinematic waves behaviour (including currents action) was described by using a linear theory of surface gravity waves. SWAN takes into consideration the following physical properties: the waves spreading in time and space, shoaling, refraction caused by currents and depth, frequency alteration induced by sea currents, variable depth, wind induced wave generation, non linear action: threefold and fourfold waves interaction, surface waves breaking, bottom friction and breaking induced by depth alteration, transmission through obstacles and reflexion from obstacles and diffraction. The numerical model MIKE 21/SW (DHI, 2009) applying the same process equations as the SWAN was used in this paper.

Energy balance equation

For a description of a wave model in a random case the elevation of the surface is suggested as the sum of a large number of independent linear wave components. Therefore the wave forecast bases on the forecast of each and every of those independent components, i.e. spectrum energy $E(f, \theta)$, where f is the wave frequency and θ a random direction of each individual component. As the spectrum energy varies over the time, t and space (x, y), the record $E(f, \theta) = E(f, \theta; x, y, t)$ is considered to be correct. The energy of each wave component in time (f, θ) can be determined by the integration of the equation of energy progress due to group's speed propagation in the wave direction:

$$\frac{dE(f,\theta;x,y,t)}{dt} = S(f,\theta;x,y,t) \tag{5}$$

– the left side of the equation is the speed alteration of the wave spectrum energy, and the right side presents a superposition of the functions describing different physical phenomena included into analysis, in the following form

$$S = S_{in} + S_{nl} + S_{ds} + S_{bot} + S_{surf} ,$$

(representing sources and abysses).

The energy source term $S(f, \theta; x, y, t)$, represents the superposition of source function describing various physical phenomena,

$$S = S_{in} + S_{nl} + S_{ds} + S_{bot} + S_{surf} ,$$

where S_{in} represents the wind induced energy generation, S_{nl} is the wave energy transfer due to non-linear wave-wave interaction, S_{ds} is the dissipation of wave energy due to whitecapping, S_{bot} is the dissipation due to bottom friction and S_{surf} is the dissipation of wave energy due to depth-induced breaking.

The waves' propagation, described on the equation's left side (5), considers identified refraction impacts, shoaling, diffraction and reflexion, which dominate in the alteration of the wave field. Wave propagation has been studied for centuries. Airy (1845) and Stokes (1847) developed an extensive theory of monochromatic linear and non linear waves, whereas Boussinesq (1872) analysed non linear impacts specific for a shallow area. 1955

Pierson [32] introduced the spectral analysis of wind waves in order to take into consideration the irregularity of sea waves into numerical analysis.

In this paper numerical model MIKE 21/SW (DHI, 2009) was used. The model simulates the growth, decay and transformation of wind-generated waves and swells in offshore and coastal areas.

The MIKE 21/SW provided a choice between two problem formulations, directional decoupled parametric formulation and fully spectral formulation. The directional decoupled parametric formulation is based on a parameterization of the wave action conservation equation. The parameterization is made in the frequency domain by introducing the zero and first moment of the wave action spectrum as dependent variables following Holthuijsen [15]. The fully spectral formulation is based on the wave action conservation equation [20, 42], where the directional-frequency wave action spectrum is the dependent variable. This formulation is more time consuming and provides the results with higher degree of accuracy, especially in larger spatial domains. The fully spectral formulation (instationary formulation) is used in the scope of performed numerical analysis.

The model includes the following physical phenomena: wave growth by the action of wind, non-linear wave-wave interaction, dissipation due to white-capping, dissipation due to bottom friction, dissipation due to depth-induced wave breaking, refraction and shoaling due to depth variations, wave-current interaction, and the effect of time-varying water depth.

The discretization of the governing equation in geographical and spectral space is performed using cell-cantered finite volume method. In the geographical domain, an unstructured mesh technique is used. The time integration is performed using a fractional step approach where a multi-sequence explicit method is applied for the propagation of wave action.

The governing equation is the wave action balance Eq. (4) formulated in either Cartesian or spherical coordinates [20, 42].

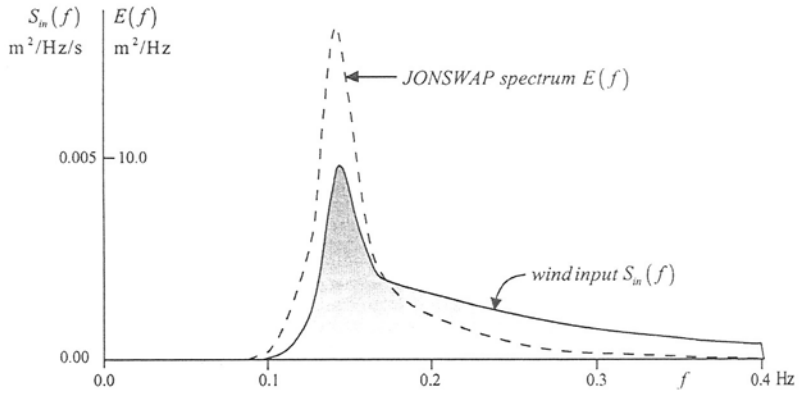

Fig. 2. The wind impact input for the JONSWAP spectrum in deep water (defined by the formulation of initial generation according to Cavalera and Malanotte-Rizzoli, 1981, and the Miles model, 1957, for H_{m0} = 3,5m, T_p = 7s and U_{10} = 20 m/s) [16]

The input source term S_{in} (4) which is the focus of this paper is defined according to [19] where is showed that the intensity of the wave generation depends on the time which passed from the wave's initialization according to the (Fig. 2):

$$S_{in}(f,\theta) = \gamma E(f,\theta) \tag{6}$$

where γ is the growth rate and $E(f, \theta)$ is energy density where $f = \omega/2\pi$ is wave frequency and θ wind direction.

The growth rate due to wind input can be calculated as [19]:

$$\gamma = \frac{\rho_a}{\rho_w}\left(\frac{1,2}{\kappa^2}\mu \ln^4 \mu\right)\left[\frac{u_*}{c}\cos(\theta-\theta_w)\right]^2 \quad \text{for} \quad \mu \le 1 \text{ for } \mu \le 1 \tag{7}$$
$$\gamma = 0 \quad \text{for} \quad \mu > 1$$

where: ρ_a/ρ_w is the ratio of density of air to water, κ is Karman's constant, $\kappa = 0.41$, μ is the dimensionless critical height defined as

$$\mu = kz_o \exp(\kappa / m) \tag{8}$$

where z_0 is sea roughness induced by the wind

$$z_0 = z_{0b} + z_{0w} \tag{9}$$

where z_{0b} models the effect of gravity-capillary waves and z_{0w} models the effect of short gravity waves. z_{0b} is parameterized as

$$z_{0b} = z_{Charnock} u_*^2 / g \tag{10}$$

where $z_{Charnock}$ is the Charnock parameter with the default value $z_{\text{Charnock}} = 0.01$. u_* is wind friction velocity and $c = \omega/k\, c = \omega / k$ is the phase speed, θ and θ_w are the wave and wind directions.

For a given wind speed and direction, the growth rate of waves of a given frequency and direction depends on the friction velocity u_*, and sea roughness z_0. In order to calculate friction velocity u_*, Janssen [19] assumed a logarithmic profile for the wind speed u:

$$u(z) = \frac{u_*}{\kappa} \ln \frac{z + z_{0w}}{z_{0b} + z_{0w}} \tag{11}$$

Usually, $z >> z_{0w}$ and in that case

$$u_* = \frac{\kappa u(z)}{\ln \dfrac{z}{z_0}} \tag{12}$$

Three different formulations for estimating u_* and z_0 have been implemented in the model:

Uncoupled model using a drag law

In this case the relation between the wind speed $u(z)$ at a level z and the wind friction velocity is given by a simple empirical formulation

$$u_*^2 = (\alpha + \beta u)u^2 \tag{13}$$

where α and β are constants with the default values, for $z = 10$ m, $\alpha = 6.3 \cdot 10^{-3}$ and $\beta = 6.6$

$\cdot 10^{-5}$ (Smith and Bank, 1975). Then the sea roughness is obtained using Eq. (11)

$$z_0 = z \exp(\kappa u / u_*) \tag{14}$$

Uncoupled model using Charnock

This model assumes that z_{0w} is small compared to z_{0b}, and the air roughness is given by

$$z_0 = z_{0b} = z_{Charnock} u_*^2 / g \tag{15}$$

For a given wind speed u at a level z it is possible to solve Eq. (12) and (15) iteratively to obtain the roughness length z_0 and the friction velocity u_*.

Coupled model

In this case the sea roughness is given by

$$z_0 = z_{0b} + z_{0w} = z_{0b}(1 - \frac{\tau_w}{\tau})^{-1/2} = \frac{z_{CHARNOCK} u_*^2}{g} \left(1 - \frac{\tau_w}{\rho_Z u_*^2}\right)^{-1/2} \tag{16}$$

where τ_w is the wave induced stress, and τ is the total stress $\tau = \rho_z u^2_*$. For a given wind speed u at the level z and the wave induced stress, it is possible to solve Eq. (11) and (15) iteratively to obtain the friction velocity u_*. The wave induced stress, τ_w, is calculated as

$$\tau_w = \int \left. \frac{\partial \vec{P}}{\partial t} \right|_{wind} df d\theta \tag{17}$$

where $\vec{P}$ is the wave momentum given by

$$\vec{P} = \rho_w \sigma E(f, \theta) \vec{k} / k \tag{18}$$

19.5. The Adriatic Model

Fig. 3 shows the spatial domain of numerical model of wave generation which includes the Adriatic area (AMST). Fig. 3 also shows the bathymetry synthesized on continuous raster grid of data with 7.5' (~200m) resolution in the longitudinal and latitudinal direction and model domain discretization with an unstructured grid of triangle finite volumes. Numerical distances between nodes set in the centres of finite volumes are variable, ranging from 160 m to 9.500 m. The model domain does not have open borders and all the rigid boundaries are completely absorbent (absence of reflection). The adoption of such assumptions about exclusion of open boundary, which are apparently inherent in the nature in the Otrant region, caused an initial error to enter the model generation of waves in winds blowing from the SE direction. Given the flatness of the coastline, it may be concluded that the error, which occured, had an impact on model results only in the vicinity of the Otrant region. Initial conditions were defined with a zero relevant range. It is assumed that there is the absence of the initial wave motion throughout the model spatial domain.

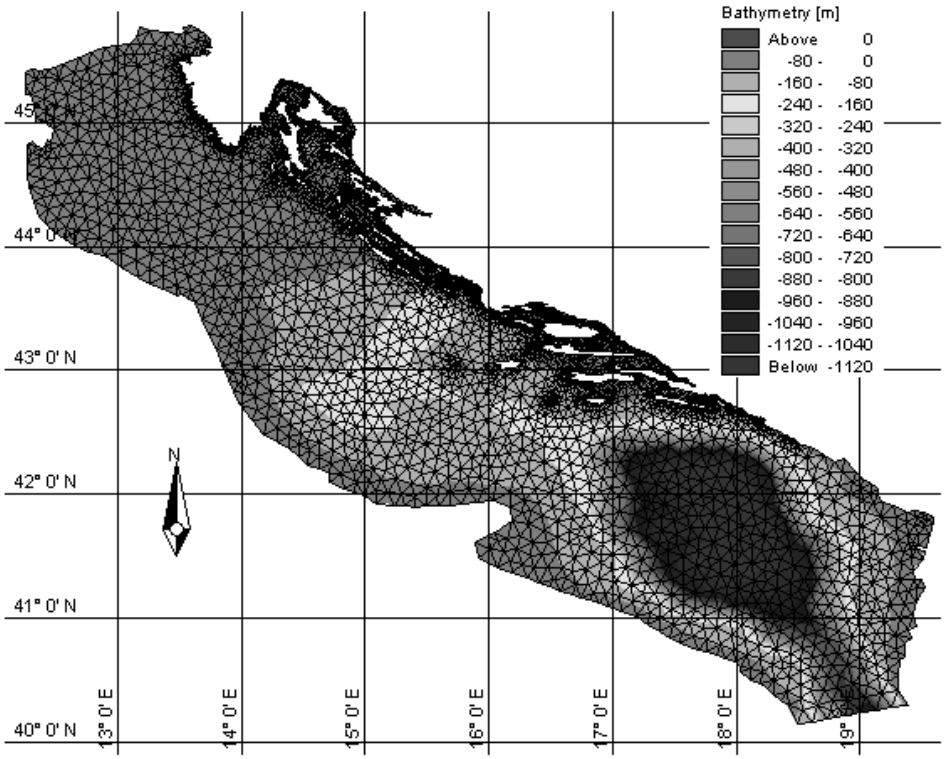

Fig. 3. Spatial domain of numerical model of wave generation with unstructured grid of triangle finite volumes

The applied wave generation model used the wind field obtained from Aladin atmospheric prognostic model with the spatial resolution of 4km and time step of 3 hours throughout the period from 1/11/2007 – 15/12/2008. The Aladin prognostic numerical atmospheric model is operationally used by the Croatian Meteorological and Hydrological Institute. The model was established in a hydrostatic version based on the primitive equations with a numerical implementation developed in cooperation with several national meteorological institutions. The model is derived from the global ARPEGE (Action de Recherche Petite Echelle Grande Echelle) model of Meteo-France [3, 4].

For the purposes of verification of the results obtained by the AMST numerical model, two waverider stations were used. Waverider V1 (φ = 44044,5'N and λ = 13010,2'E) was placed in open sea area in the north part of the Adriatic Sea, and the other one, waverider V2 (φ = 43029,3'N and λ = 16027,9'E) in front of Split. Measurements were carried out in the period from 1 November 2007 to 15 November 2008 during implementation of the Monitoring of the Adriatic Sea – Adriatic Project [1].

Further, the paper deals with the comparison of significant wave heights obtained by the application of different formulations, uncoupled model using a drag law, uncoupled model using Charnock and coupled model. Conducted analyses showed that the coupled model describes best higher wave heights, which are commonly heights in question. As for an illustration Fig. 4 shows one of some extreme situations. The paper deals further with the

coupled model used for a detailed analysis, i.e. in the MIKE21/SW model in this formulation a variable parameter $z_{Charnock}$.

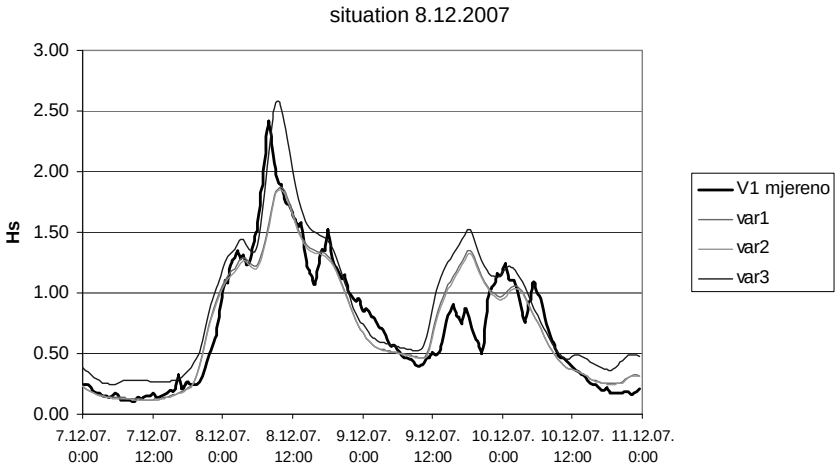

Fig. 4. Significant wave heights obtained by the application of different formulations

About Charnock parameter

Charnock (1955) suggested that the roughness length of airflow over ocean should depend on two parameters – acceleration of gravity, g, and the friction velocity, u_*. As a result, the expression for the roughness length over ocean waves becomes as in Eq. (14), and profile measurements resulted in an estimate of the Charnock constant $z_{Charnock}$ = 0.0112. Observation of the wind sea state obtained during the Joint North Sea Wave Project (JONSWAP [13]) suggested that the shape of the ocean wave spectrum depended on the stage of development of the sea state or the wave age. In the early stages of development, „young“sea, the wave spectrum showed a very sharp peak while the high frequency waves were steep. On the other hand, when the sea state approaches equilibrium the wind waves were less steep and the spectral peak was less pronounced. This led Stewart (1974) to suggest that the Charnock parameter is not a constant, but should depend on the stage of development of wind waves, i.e. the wave age. Steeper waves are associated with a rougher surface, so it is expected that the Charnock parameter will decrease with increasing wave age. The recent data sets show a more sensitive dependence of the Charnock parameter on the wave age than given by HEXOS [34]:

$$z_{Charnock} = 0.48\chi_*^{-1}, \qquad 5 < \chi_* < 25 \tag{19}$$

where χ_* is the wave age defined as

$$\chi_* = c_p / u_* \tag{20}$$

where c_p is the phase speed of the peak of the spectrum.

Yelland and Taylor [41] were unable to find a correlation between the sea state and the Charnock parameter based on data of the open ocean the Southern Atlantic. Janssen [19]

found by restricting to wind speed above 10m/s a similar relationship as Donelan et al. [9] and the Hexos group [34], Eq. (19).

The Charnock parameter is the key parameter that determines the surface stress for given wind. Many researchers have made attempts to measure surface stress and wind speed in order to obtain the Charnock parameter. But since the roughness length z_0 depends in an exponential way on these parameters, there are very high demands on the measurement accuracy of wind speed at a height of 10 meters, u_{10}, and the friction velocity, u_*. The roughness over the oceans is very small compared with that over land. As a consequence, the constant stress layer over the ocean is thin, and Donelan [8] finds that the assumption that the measured stress is the surface stress always introduces a systematic and wind speed dependent underestimation of the surface stress.

Table 1

Characteristic values for Charnock parameter defined in literature

Case number	Source	Charnock parameter
C1	DHI MIKE21/SW default value Smith (1980) Yelland and Taylor (1996)	0.01
C2	HEXOS in coastal areas	0.1
C3	Charnock (1955)	0.0112
C4	Battjes et al (1987)	0.0144

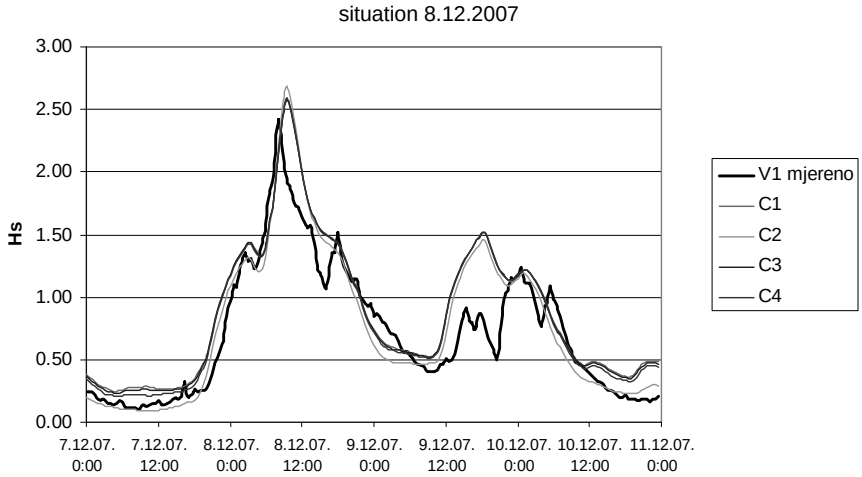

Fig. 5. Significant wave heights obtained by the application of different values for Charnock parameter (Tab. I, V1 – measurements)

In the weather forecasting it is usually assumed that the Charnock parameter is a constant. Open ocean observation of Smith [34] and Yelland and Taylor [41] gives values for the Charnock parameter about 0.01. In coastal areas or in rapidly varying circumstances young sea yields much larger values than the Charnock parameter, reaching even up to 0,1. This large variation of the Charnock parameter is captured by quasi-linear theory in a realistic manner.

The paper analysed some characteristic values for Charnock parameter defined in literature as shown in Tab. 1. Fig. 5 presents that the recommended value 0, 01 fully satisfies requirements of the numerical model. The differences, which are not considered as significant, are visible only when implementing ten times bigger values according to the literature specific for the shore area. In each case, presented results show that the error in the selection of Charnok's parameter in relationship to the possible error in the input data is up to 10% practically negligible. Generally seen, nowadays is the wind generated waves model accepted for implementation.

19.6. Conclusion

The Miles' quasi-laminar theory was the first model providing an acceptable explanation of wind waves' generation. The model was criticised as unrealistic because it ignored the waves induced turbulence in the flow. Nevertheless, the first attempts of introducing turbulence impacts in multi layered models were criticised, mostly because of vortices in the outer air layer, as being too slow to transfer a considerable energy amount during waves action.

Regardless of relatively satisfying quasi-linear theory, the issue of wind generated waves and waves response to wind is still not completely clarified, particularly with short waves, where there are currently no proofs on the waves' age impact. The quasi linear approach considers short waves to be linear, although they are relatively steep. Therefore, the non linear process of air flowing separation, related to Jeffrey's observation (1924, 1925), can have an impact with the energy transfer from the air to the waves, which can lead to alternative explanation of the sea state dependency on the resistance above waves [21]. Such an explanation requires that a significant part of the wave drag is defined by the separation of the boundary air layer above the dominant wave's crest.

Providing that prognostic wave model is included into weather forecasts system, it is possible for each time segment to determine which amount of energy is transmitted from the air onto the waves. The extended investigations of ECMWF have shown that the energy transfer dependent on the sea state provides improved results in the prognostics of waves and wind [19]. The paper put forward that the currently accepted formulation of numerical modelling of wind generated waves satisfyingly described a real condition. In the above applied model it was noticed that the modification of the Charnok's parameter had no significant impact on final results as far as it was within the boundaries recommended in presented investigations.

References

[1] Andročec V., Beg-Paklar G., Dadić V., Djakovac T., Grbec B., Janeković I., Krstulović N., Kušpilić G., Leder N., Lončar G., Marasović I., Precali R., Šolić M.: The Adriatic Sea Monitoring Program – Final Report, Zagreb, 2009.

[2] Belcher S. E., Hunt J. C. R.: Turbulent shear flow over slowly moving waves. Journal of Fluid Mechanics 251, 109–148, 1993.

[3] Cordoneanu E., Geleyn J. F.: Application to local circulation above the Carpathian Black Sea area of a NWP-type meso-scale model, Contributions to Atmospheric Physics, 71, 191–212, 1998.

[4] Courtier P. C., Freydier J. F., Geleyn F., Rochas M.: The ARPEGE project at METEO-FRANCE, Proceedings from the ECMWF workshop on numerical methods in atmospheric models, 193–231, 1991.
[5] Dobson F. W.: Measurements of atmospheric pressure on wind-generated sea waves. Journal of Fluid Mechanics 48, 91, 1971.
[6] Donelan M. A.: A simple numerical model for wave and wind stress prediction, National Water Research institute manuscript, Berlington, Canada, 28, 1977.
[7] Donelan M. A.: The dependence of the aerodynamic drag coefficient on wave parameters. Proceedings of the First International Conference on Meteorological and Air/sea Interaction of the Coastal Zone. American Meteorology Society, Boston, MA, 381–387, 1982.
[8] Donelan M. A., Hui W. H.: Mechanics of ocean surface waves, Surface Waves and Fluxes, Kluwert Academic Publishers, 381–387, 1990.
[9] Donelan M. A., Dobson F. W., Smith S. D., Anderson R. J.: On the dependence of sea-surface roughness on wave development, Journal of Physical Oceanography 23, 2143–2149, 1993.
[10] Donelan M. A., Yuan Y.: Wave dissipation by surface processes. In: Komen, G.J., Cavaleri, L., Donelan, M.A., Hasselmann K., Hasselmann S., Janssen P. A. E. M. (Eds.): Dynamics and Modelling of Ocean Waves. Cambridge University Press, 143–155, 1994.
[11] Drennan W. M., Graber H. C., Donelan M. A.: Evidence for the effects of swell and unsteady winds on marine wind stress. Journal of Physical Oceanography 29, 1853–1864, 1999.
[12] Drennan W. M., Kahma K. K., Donelan M. A.: On momentum flux and velocity spectra over waves. Boundary-Layer Meteorology 92, 489–515, 1999.
[13] Hasselmann K., Barnett T. P., Bouws E., Carlson H., Cartwright D. E., Enke K., Ewing J. I., Gienapp H., Hasselmann D. E., Kruseman P., Meerburg A., Müller P., Olbers D. J., Richter K., Sell W., Walden H.: Measurements of wind–wave growth and swell decay during the Joint North Sea Wave Project (JONSWAP). Deutsche Hydrographische Zeitschrift A 8 (12), 1–95, 1973.
[14] Hasselmann D. E., Bosenberg J.: Field measurements of wave-induced pressure over wind sea and swell. Journal of Fluid Mechanics 230, 391–428, 1991.
[15] Holthuijsen L. H., Booij N., Herbers T. H. C.: A prediction model for stationary, short-crested waves in shallow water with ambient currents, Coast. En.13, 23–54, 1989.
[16] Holthuijsen L. H.: Waves in Oceanic and Coastal Waters, Cambridge University Press 2007.
[17] Hristov T. S., Miller S. D., Friehe C. A.: Dynamical coupling of wind and ocean waves through wave-induced air flow. Nature 442, 55–58, 2003.
[18] Hsu T. -W., Ou S.-H., Liau J. -M.: Hindcasting nearshore wind waves using a FEM code for SWAN, Coastal Engineering, Vol. 52, Issue 2, 177–195, 2005.
[19] Janssen P. A. E. M.: The Interaction of Ocean Waves and Wind. Cambridge University Press, Cambridge, UK, 300, 2004.
[20] Komen, G.J., Cavaleri, L., Donelan, M., Hasselmann, K., Hasselmann, S., Janssen, P. (1994): Dynamics and Modelling of Ocean Waves. Cambridge University Press, 532.
[21] Makin V. K., Kudryavtsev V. N.: Impact of dominant waves on sea drag. Boundary-Layer Meteorology 103, 83–99, 2002.
[22] Mastenbroek C.: Wind-wave interaction. Ph.D. Thesis. Delft Techology University, 119, 1996.
[23] Miles J. W.: On the generation of surface waves by shear flows. Journal of Fluid Mechanics 3, 185–204, 1957.
[24] Oost W. A., Komen G. J., Jacobs C. M. J., van Oort C.: New evidence for a relation between wind stress and wave age from measurements during ASGAMAGE. Boundary-Layer Meteorology 103, 409–438, 2002.
[25] Phillips O. M.: On the generation of waves by turbulent wind. Journal of Fluid Mechanics 2, 417–445, 1957.
[26] Phillips O. M.: The equilibrium range in the spectrum of wind generated waves. Journal of Fluid Mechanics 4, 426–434, 1958.
[27] Phillips O. M.: On the dynamics of unsteady gravity waves of finite amplitude. Journal of Fluid Mechanics 9, 193–217, 1960.

[28] Phillips O. M.: On the attenuation of long gravity waves by short breaking waves. Journal of Fluid Mechanics 16, 321–332, 1963.
[29] Phillips O. M.: Wave interactions – The evolution of an idea. Journal of Fluid Mechanics 106, 5–227, 1981.
[30] Phillips O. M.: The dispersion of short wavelets in the presence of a dominant long wave. Journal of Fluid Mechanics 107, 465–485, 1981.
[31] Phillips O. M.: Spectral and statistical properties of the equilibrium range in wind-generated gravity waves. Journal of Fluid Mechanics 156, 505–531, 1985.
[32] Pierson W. J., Neumann G., James R. W.: Practical methods for observing and forecasting ocean waves by means of wave spectra and statistics. U.S. Navy Hydrographic Office Pub. No. 603, 1955.
[33] Schwab D. J., Bennett J. R., Liu P. C., Donelan M. A.: Application of a simple numerical wave prediction model to Lake Erie. J. Geophys. Res. 89: 3586–3592, 1984.
[34] Smith S. D., Anderson R. J., Oost W. A., Kraan C., Maat N., DeCosmo J., Katsaros K. B., Davidson K. L., Bumke K., Hasse,L., Chadwick H. M.: Sea surface wind stress and drag coeffcients: the HEXOS results. Boundary-Layer Meteorology 60, 109–142, 1992.
[35] Snyder R. L.: A field study of wave-induced pressure fluctuation above surface gravity waves. Journal of Marine Research 32, 497– 531, 1974.
[36] Snyder R. L., Dobson F. W., Elliott J. A., Long R. B.: Array measurements of atmospheric pressure fluctuations above surface gravity waves. Journal of Fluid Mechanics 102, 1–59, 1981.
[37] Sullivan P., McWilliams J., Moeng C.-H.: Simulation of turbulent flow over idealized water waves. Journal of Fluid Mechanics 404, 47–85, 2000.
[38] SWAMP Group: Ocean Wave Modeling. Plenum Press, New York, 266, 1985.
[39] Tsimring L. Sh.: Induced scattering of surface wind waves. Izvestiya Atmospheric and Oceanic Physics 19, 47–50, 1983.
[40] WAMDI Group: The WAM model – a third generation ocean wave prediction model. Journal of Physical Oceanography 18, 1775–1809, 1988.
[41] Yelland M. J., Taylor P. K.: Wind stress measurements from the open ocean. J. Phys. Oceanogr.,26, 541–558, 1996.
[42] Young I. R.: Wind generated ocean waves. Elsevier Ocean Engineering Book Series, Vol. 2, Elsevier 1999.

20 The State of the Rubble Mound Breakwaters' Primary Cover Layer in Istria

Eva Ocvirk, Marko Pršić, Vladimir Vlasac (University of Zagreb, Faculty of Civil Engineering, Croatia)

20.1. Introduction

The paper deals with the investigation conducted to define the condition of the armor layer on 6 breakwaters on the western shore of Istria (Fig. 1).

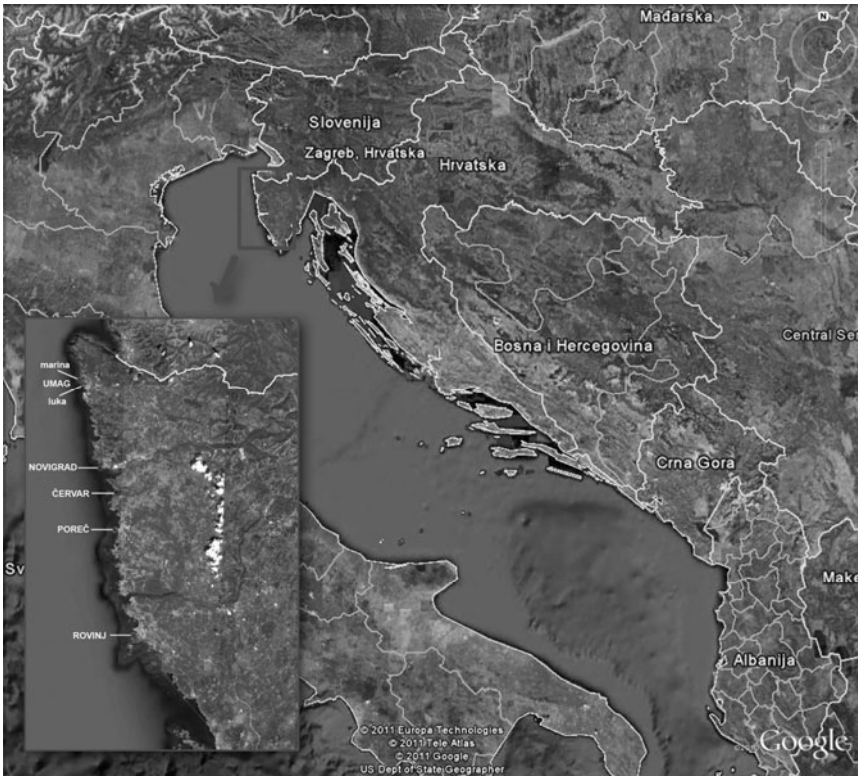

Fig. 1. The overview of recorded locations

A few characteristic profiles, 3.5 m wide, stretching from the crest to the sea level line on the slope were observed on each breakwater. Due to technical reasons the recording was

not conducted on the slope under the sea. The investigation comprised the measuring of all available blocks within the defined profile, whereas the dimensions of the rest of them were estimated. The granulometric curve of each profile was defined on the basis of recorded data, and the interlocking was estimated.

All breakwaters are located in the shallow water wave climate, which is determined from the deep water wave climate by means of wave deformations' calculations, shoaling and refraction (friction and reflexion are neglected). Refraction is interpreted by the refraction plan on the TK 1 : 25000, for all exposed directions, for different wave lengths using the method of orthogonality based on the linear theory. In this way the most inconvenient refraction coefficient was defined for each individual location according to exposed directions, while the shoaling coefficient was read from the chart.

The significant weave height was determined for each position according to Hudson's equation, with known mass of 50% of represented block and estimated interlocking of primary cover. In this way defined significant wave height should not affect the breakwater's stability. The shallow water wave height obtained in this way was transformed into equivalent deep water wave height considering wave deformations.

Return periods were matched to each location obtained in this way for wave heights according to the wave maps of the Adriatic defined in the thesis Ocvirk [4].

20.2. Recording and Data Processing

Several characteristic profiles, 3.5 m wide from the crest to the sea line on the slope were recorded on each breakwater. The recordings comprised the observation of stone blocks size above the sea (Tab. 1) and the observation of the contacts number between blocks (Tab. 2).

Table 1

The excerpt from the observation form for the stone blocks' size

The category of the stone block mass of the armour			Stone block's diameter: from $D_{toe\ lim.}$ to $D_{upp.lim.}$	The registration of the occurrence number of diameters' sizes	Number of pieces
PROFILE PPR1					
1	0.1–0.5 [t]	0.3 [t]	0.42 [m] do 0.72 [m]	IIIIIIIII	9
2	0.5–1 [t]	0.75[t]	0.73 [m] do 0.90 [m]	IIIIIIIIIIIII	14
3	1–2 [t]	1.5 [t]	0.91 [m] do 1.14 [m]	IIIIIIII	9
4	2–3 [t]	2.5 [t]	1.15 [m] do 1.30 [m]	IIIIII	6
5	3–4 [t]	3.5 [t]	1.31 [m] do 1.43 [m]	IIII	4
6	4–6 [t]	5.0 [t]	1.44 [m] do 1.64 [m]	I	1
7	6–8 [t]	7.0 [t]	1.65 [m] do 1.80 [m]	I	1
8	8–10 [t]	9.0 [t]	1.81 do 1.94	I	1
TOTAL NUMER OF PIECES:				Nr =	45

Table 2

The example of the observation form of the blocks' number with a defined contacts' number of adjacent blocks

Number of contacts with adjacent blocks	A number of blocks with determined number of contacts	Blocks in total
PPR 1		
0		
1	~~IIIIIIII~~ I	11
2	~~IIIIIIII~~ IIII	14
3	IIIIIIIII	9
4	IIIII	5
5 and more		
Average contacts' number Nk =		2.68

20.2.1. The structure of the Granulometric Curve

Tab. 1 presents an example of the observation form of stone blocks' sizes recorded according to profiles. The masses of stone blocks presented in the previous table were calculated according to the equation:

$$W = \rho_{stone} \cdot D^3 \cdot \frac{\pi}{6} = 0.524 \cdot \rho_{stone} \cdot D^3 \tag{1}$$

With the medium density of the stone block ρ_{stone} = 2.6 t/m^3.

Conforming to the examination presented in Tab. 1 the charts of grading curves in accordance with profile sections were drawn (an example shown in Fig. 2).

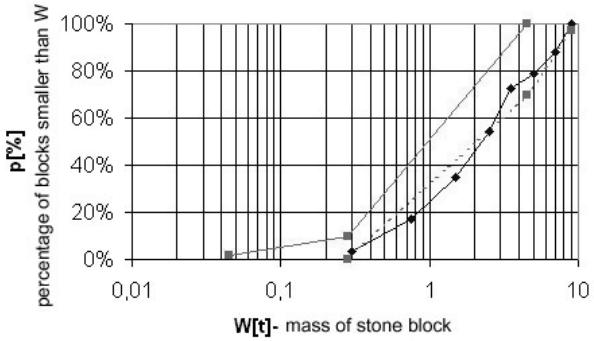

Fig. 2. An example of armour's granulometric curve according to profiles

In accordance with the rules for the quality of the armour granulometric curve the inspection of existing quality control can be undertaken. Firstly, it should be determined whether the existing armour is narrowly, widely or well graded of very wide range. The upper and lower limit for well graded armour is established for all cross sections according to recorded values $W_{50\%}$ from the granulometric curves.

The basic requirement is that the well-graded curve of the primary armour complies with the design area of granulation bordered by the upper and lower limit drawn into individual granulometric curves. (Fig. 2).

The blocks' masses $W_{85\%}$, $W_{50\%}$, $W_{15\%}$ are recorded for each granulometric curve, and nominal diameters of the blocks $D_{85\%}$, $D_{50\%}$, $D_{15\%}$ are calculated according to equation:

$$D_{x\%} = \left[\frac{6}{\pi}\cdot\left(\frac{W_X}{\rho_{stone}}\right)\right]^{1/3} = 1.24\cdot\left(\frac{W_X}{\rho_{stone}}\right)^{1/3} \tag{2}$$

The granulometric width parameter is then read for each granulometric curve:

$$pgw = \frac{D_{85\%}}{D_{15\%}} \tag{3}$$

The criteria for the choice of the granulometric curve's width are:

— narrow granulometry: pgw < 1.5,
— wide granulometry: 1.5 < pgw < 2.5,
— well-graded granulometry: 2.5 < pgw < 5.

According to current rules the embedded armour must be narrowly graded. As the armour on the observed breakwaters was constructed in the past, and was several times filled, the investigation proved that it was mostly well-graded.

20.2.2. Estimation of Porosity and Bulk Mass

On the basis of the data on the stone blocks' size given in the observation form (Tab. 1), and on the basis of the data from granulometric curves (Fig. 2) and the estimation of plan surface of individual profiles according to sections the porosity p[%] and the bulk density of mass $\gamma_{stone}^{\ bulk}$ [t/m^3] were defined on the basis of cross sections.

Porosity of the armour is determined:

$$p[\%] = 1 - \frac{N_r}{A\cdot n\cdot k_\Delta}\left(\frac{\rho_{stone}}{W_{50\%}}\right)^{2/3} \tag{4}$$

where p [%] is the armour's porosity, A [m^2] the section's slope surface, n = 1.5 the number of blocks in studied layer of the armour. As only the outer layer of embedded armour can be observed and counted, the reduction of all counted blocks' number onto the blocks' number in one armour's layer has been performed. Thus, for only one row of blocks n = 1.0 , and for two rows of blocks n = 2.0 (considering that N_r is known from both layers). In the case of armour 's wide grading the cross section is related to the one in Fig. 3 (centre), so the compromised value n = 1.5 is taken. Further, k_Δ = 1.1 is the layer's coefficient, ρ_{stone} = 2.6 [t/m^3] stone mass density, $W_{50\%}$ [t] mass of the 50% block from the granulometric curve and N_r a number of stone blocks counted on the surface founded on the > 0,4 m diameter blocks. The armour's average bulk mass as stated by rules should be $\gamma_{stone}^{bulk} = 1.6 \pm 0.1$ t/m^3. It is determined according to the equation:

$$\gamma_{stone}^{bulk} = \left(1 - \frac{p}{100}\right)\cdot\rho_{stone} \tag{5}$$

where γ_{stone}^{bulk} [t/m^3] armour's bulk mass and ρ_{stone} [t/m^3] armour's stone density.

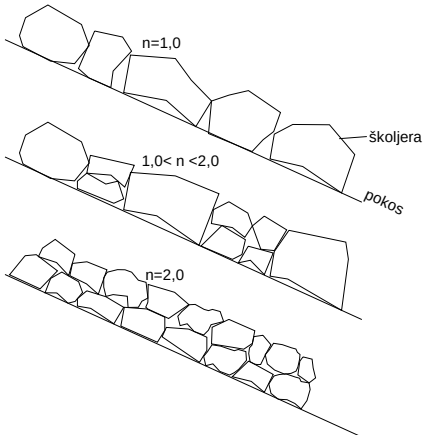

Fig. 3. The sketch which defines the coefficient of the number of blocks in the examined layer of the armour *"n"*

Those parameters are not precisely determined as the stone blocks' masses are approximate, and there is no information on subsurface layer of armour.

20.2.3. The evaluation of the Interlocking (Stability) of the Armour

Basing on the estimation of interlocking quality, the reduction of the stability coefficient of the existing armour K_D was subsequently conducted in relationship to the prescribed coefficient. To develop a theoretical fundament for such an analysis the starting point implies that armour is affected by the waves of the constant height ($H_d = H_{1/10}^{100year}$), while the interlocking of some blocks is satisfactory, of some not. The mass of the stable armour block is calculated according to Hudson:

$$W = \frac{\rho_{stone} g H_d^{\,3}}{K_D \left(\frac{\rho_{stone}}{\rho_{sea}} - 1 \right)^3 ctg\alpha} \tag{6}$$

Approved stability coefficient of the interlocked well graded armour $K_{D\,=\,0}$ is defined in Tab. 3 and does not refer to the top quality way of placing, but more to the standard "stone pile". That implies the random piling of individual stone blocks by the crane on the 1 : 1.5 slope or on the gentler slope, from the toe to the crest, without particular placing or diving directions. The blocks should be placed on the lower ones at 3 points at least. Embedded blocks should not tilt under wave load, they should not stand only due to friction; i.e. they have to be interlocked and should create a protective layer above other breakwater's layers, i.e. in terms of two blocks according to layer's thickness. With such an armour K_D provides an optimal size of armour block with 0 do 5% damage for a 100-year heavy sea design. Therefore such a stability coefficient of well graded armour is being determined as $K_{D=0}$.

The armour's damage is defined with a percentage of dropped blocks from the slope which have rolled down the slope to the sea's bottom.

Table 3

Nominal values of stability coefficient K_D of wide graded armour for the constant wave height, for different interlocking

WELL-GRADED ARMOUR	BREAKWATER'S TRUNK slope 1:1.5 non-breaking
$K_{D\ =\ 0}$ "prescribed" for fully interlocked well-graded CERC7-206	2.5
$K_{D\ >\ 0}$ for fully noninterlocked well-graded (calc. per Eq.)	1.65
$K_{D\ >>\ 0}$ with breakwater failure (filter on the slope)	→0

The analysis of stability coefficient K_D dependence of some embedded well graded armour starts from the assumption that the primary (cover) layer on the breakwater's slope has 2 rows of blocks, and that finer filter material or quite tiny core can not be observed on the slope. In this case the K_D can be reduced only due to weak interlocking. To evaluate the armour's stability hydrodynamically loaded by waves the interlocking of individual armour's blocks, i.e. of its cover layer should be estimated. The estimation of the interlocking is performed on defined profiles by estimating the number of armour's blocks' contacts with adjacent blocks of the same layer (slope's cover surface). The number of adjacent blocks in contact is estimated for each block within examined 3.5 m wide field. The blocks' contacts smaller than 0.4 m in diameter are not counted. The contact with the blocks' lower layer is not regarded as a touch [3].

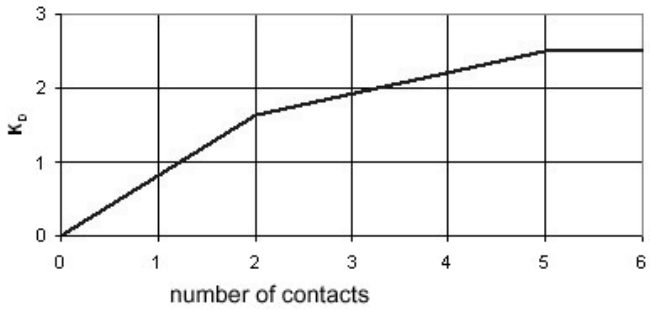

Fig. 4. The dependence of the stability coefficient K_D for well-graded interlocked armour on the breakwater's body with nonbreaking waves on the number of contacts with adjacent blocks

For the same size of the armour block the coefficient value $K_D = 0$ for interlocked armour of the same slope is bigger than $K_D > 0$ for non-interlocked armour; i.e. the non-interlocked block should be heavier than the interlocked one to reach the stability of the interlocked block. It is assumed that the complete interlocking has been achieved when the block has 5 and more contacts with adjacent ones. Then $K_D = 0$ is achieved which corresponds completely to the stable rock without damages. Armour block on the slope without any contacts, and of the same size as the interlocked one on that slope will be unstable. Such an armour block should be endlessly heavier than the interlocked one to

reach the same stability, and its K_D should tend to zero; i.e. $K_D > 0 \rightarrow 0$. Applying linear interpolations, a relationship chart "K_D – number of contacts" (shown in Fig. 4), was created on the basis of relations between stability coefficient K_D and the number of contacts with adjacent armour blocks.

Tab. 2 presents an example of the observation of the blocks' number with determined contacts' number with adjacent blocks. On the basis of the data on 2, 3, 4, 5 or more numbers of contacts an average contacts' number for each profile and individual section is going to be calculated. The average does not include 0 and1 contact, as they are not regarded as stable on the slope, and they do not contribute to the stability of the entire slope. The value of the coefficient K_D is being determined for each individual profile with determined number of contacts by means of the graph in Fig. 5. Accordingly, K_D can be equal or lower than the "prescribed" one in Tab. 3.

20.3. Wave Deformations in Front of Breakwater

A two-dimensional analysis of deformation of open sea waves from exposed directions reaching shallow sea with breakwaters was conducted to define deep-water wave climate under assumption of understanding well shallow water wave climate. The analysis of deformations from the deep sea area to the area close to breakwaters was conducted for previously assumed deep water wave climate. In this way the wave deformation coefficient was defined, applied then in the paper. The refraction was interpreted by the refraction plan on TK 1 : 25000, for all exposed directions, for different wave lengths by the orthogonal method based on linear theory. The most inconvenient refraction coefficient according to exposed directions was defined in this way for each individual position. The shoaling coefficient was recorded from the charts.

Defining of wave height of breakwater's "survival"

Basing on conducted investigations of the armour and calculations of waves' deformation the significant wave height, which corresponds to the dimensions of the breakwater's primary cover, was defined according to Hudson's formula (6).

The value of block's mass with 50% representation was defined as a mean value of masses obtained in all analysed cross section on each breakwater respectively, as well as the armor's coefficient which corresponds with the medium interlocking of each breakwater. On the basis of parameters, obtained in this way, the Hudson's equation defines pertaining wave height which should not put in danger breakwater's stability:

$$H_{1/10} = \sqrt[3]{\frac{W_{50\%} K_D (S_r - 1)^3 ctg\alpha}{\gamma_r}} \tag{7}$$

and

$$H_s = \frac{H_{1/10}}{1{,}27} \tag{8}$$

The significant wave height obtained in this way in the shallow area is then transformed into deep water area by previously defined coefficient. Results are presented in Tab. 4.

Table 4

Results of field investigation

UMAG marina	*W*		*SW*	
	Hs [m]	PR [god]	Hs [m]	PR [god]
	5.55	100	4.25	100
UMAG primarni lukobran	*W*		*SW*	
	Hs [m]	PR [god]	Hs [m]	PR [god]
	2.25	10	2.05	10
NOVIGRAD	*W*		*S*	
	Hs [m]	PR [god]	Hs [m]	PR [god]
	1.80	5	1.25	10
ČERVAR	*NW*			
	Hs [m]	PR [god]		
	2.05	100		
POREČ	*NW*			
	Hs [m]	PR [god]		
	2.55	100		
ROVINJ	*W*		*SW*	
	Hs [m]	PR [god]	Hs [m]	PR [god]
	3.60	100	3.60	100

20.4. Conclusion

The investigation was conducted to define the condition of the armour on 6 breakwaters on the western shore of Istria. The results given in Tab. 4 lead to the conclusion that the breakwaters in Rovinj, Poreč, Červar and the Umag marina traditionally dimensioned on the wave heights of 50–100 year return periods or even more, are in good condition. However, their cost-effectiveness is still the issue. On the other hand, the breakwater in Umag is in poor condition, which can be seen from the obtained results and the details in Fig. 5. The primary cover is in derelict condition sinking here and there down from the breakwater's crest for a few meters. Several cover elements are completely non-interlocked. Considering the new position of the primary cover beneath the sea, it is difficult to give an objective statement as the breakwater is very old and repaired several times. The same applies for the Novigrad's breakwater (Fig. 6) featuring some major damages.

The conducted analyses showed that the primary cover is to be replaced, or which is cheaper, a heavier armour should be added to the whole slope taking into account the nonexistence of annual maintenance. If we consider the absence of annual maintenance, there is the need for a larger armour whose size is determined by design wave height defined by $H_{design}=H_{1/10}^{100\ y}$, in view of future annual maintenance; i.e. the largness of the armour determined by design wave height and defined by $H_{des}=H_{1/10}^{3\ year}$, the structure could be repaired in places where the armour is of lower density, and where it is very largely graded.

Fig. 5. A view to the slope of the primary breakwater in Umag

Fig. 6. A detail of the damage on the breakwater's slope in Novigrad

References

[1] Case study: The state of the rubble mound primary layer on breakwater „Kaše“, Faculty of Civil Engineering Zagreb, 2004.
[2] Shore protection manual, Vol. II, Coastal Engineering Research Center, 1984.
[3] Pršić Marko, Kuspilić Neven, Kunštek Duška: Armour stability of constructed rubble breakwaters, Proceedings of the 7th International Symposium on Water Management and Hydraulic Engineering/ Gdansk, Poland, 2001, 269–276.
[4] Ocvirk, E. (2010): Optimization of the rubble mound protective structures in the terms of extreme wave climate of the Adriatic Sea, PhD Thesis.

21 Assessment of the Effect of the Floating Barrage on the Flow in the Intake Structure at Dobrohošt

Ján Rumann, Martin Orfánus (Slovak University of Technology in Bratislava, Faculty of Civil Engineering)

21.1. The Dobrohošť Water Structure and Small Hydropower Plant

Dobrohošť Water Structure is located within km 1.8 of the connecting dyke between the Hrušov Reservoir and the inlet channel of the Gabčíkovo HPP (Fig. 1). Its purpose is to ensure the water supply from the inlet channel to the left side inundation area in the old riverbed of the Danube River.

Fig. 1. The Dobrohošť Water Structure

This water structure consists of three weir fields. Each is 12 m wide with a radial gate of 3.6 m height. The capacity of the weir is 234 $m^3 \cdot s^{-1}$. The water supply into the river branches ranges from 6 to 150 $m^3 \cdot s^{-1}$, while the average water supply is 15 to 40 $m^3 \cdot s^{-1}$. According to appropriate conditions, the use of the available hydropower potential has been taken into account during the construction of this structure. Therefore, an intake structure of a small hydropower plant (SHPP) and an inlet conduit of rectangular cross section with dimensions of 4×3 m has been constructed. At present the construction of this small hydropower plants continues. The on-going construction builds on the existing objects of the intake structure and conduit (both objects are expected to be reconstructed). In the new SHPP one Kaplan turbine is planned, with the maximum discharge capacity of 25 $m^3 \cdot s^{-1}$ and the design gross head of 8.69 m. The SHPP designed this way has an installed capacity

of 1.800 kW and the estimated average annual power generation of 11.873 MWh [3].

The intake structure itself as well as the inlet into conduit of the small power plant is protected by a floating barrage. It is constructed from a steel pipe with a diameter of 1220 mm, with a steel plate of 840 mm height, which is welded to its down side. The floating barrage is submerged approximately 1.30 m beneath the water surface. The barrage consists of two parts with a length of 22.80 m and 28.72 meters, which are supported by a system of spurs from the weir piers at a distance of approximately 13 m in front of the piers (Fig. 2).

Fig. 2. Floating barrage at the Dobrohošť water structure

21.2. Floating Barrage at the Intake Structure of the Dobrohošť SHPP

In the preparation for the construction of the Dobrohošť small hydro power plant based on the requirements of the investor (Vodohospodárskej Výstavby š.p.), a physical research on the Dobrohošť small hydro power plant's inlet conduit had been conducted in the hydraulic laboratory of the Department of Hydraulic Engineering, Faculty of Civil Engineering in Bratislava. According the plans for the new SHPP the floating barrage should be a part of the structure as it is now without further adjustments in its construction. Therefore its possible effect was one of the tasks of the physical research to examine. Especially the effect of the barrage on the velocity fields in front of the intake to the conduit of the small hydro power plant.

Results of the physical research were then confronted with the results of mathematical modelling (simulation of the flow using a 3D model) to verify in detail the effect of the floating barrage on velocity fields of flowing water fields in front of the intake to the conduit of the small hydro power plant.

21.3. Measurement on the Physical Model of the Dobrohošť SHPP

A physical model of the inlet conduit of the Dobrohošť SHPP based on customer's provided design had been built in the hydraulic laboratory of the Department of Hydraulic

Engineering. The design of the model was based on the Froude model similarity criteria, with a scale lengths of M_l = 15. Such a scale considered the technical and spatial possibilities of the laboratory. For technical and mainly for the spatial reasons the geometric similarity could not be fully met. It was necessary to adjust some details so that, although they did not exactly correspond to the geometric reality, as a whole the model itself describes the reality (Fig. 3). Values obtained by measuring on the physical model, after multiplication by adequate scale, were identical to real values [3].

The measurements were divided according to scenarios that simulated normal operating conditions of the planned SHPP. These scenarios simulated the steady state (normal operation of small hydro power plant) as well as the unsteady state (sudden failure of small hydro power plant). Scenarios simulating normal operating conditions were defined by a combination of operational levels in the Gabčíkovo diversion channel from the minimum (130.10 m) to the maximum (131.10 m) and the discharge through the small hydro power plant (25 $m^3 \cdot s^{-1}$) or through the small hydro power plant and one of the weir fields (25 $m^3 \cdot s^{-1}$ + 25 $m^3 \cdot s^{-1}$) [3].

Fig. 3. View on the constructed physical model of the Dobrohošť SHPP in hydraulic laboratory

On the physical model were measured velocity fields in the profiles before and under the floating barrage, as well as the profile in the inlet structure of the SHPP's conduit. Visual observations of the effect of the barrage on the flow in the foreground of the intake were also made. These measurements and observations were designed to assess the effect of the floating barrage on the flow and velocity fields in front of the intake to the conduit of the small hydro power plant. The results of these measurements and observations are as follows [3]:

— in the area in front of the floating barrage were not recorded significant vortex areas in any series of experiments, in the area under the floating barrage and in front of the intake small surface vertexes with a short duration and without entrainment of more air into the conduit occurred,
— the floating barrage has no significant negative impact on the quality of the flow, the effect of the barrage partially shows in the hydraulic losses, the losses and therefore the velocities at a lower water level in the diversion channel are slightly higher, due to a reduction in the flow area under the floating barrage,
— in the area under the floating barrage, maximum velocities of 0.9 ÷ 1.70 $m \cdot s^{-1}$ were measured, depending on water level position.

21.4. Three Dimensional Mathematical Model

CFD (Computational Fluid Dynamics), a 3D modelling program, is modern tool of the computational simulating program group well known as the Computer-aided Engineering (CAE). The Computational Fluid Dynamics is based on theoretical fluid mechanics. The laws such as the momentum conservation law and the energy conservation law are formulized as the continuum equation, the energy equation and the motion equations also known as the Navier –Stokes partial differential equations. Simplification of these equations on so called Euler CFD equations for the non-viscous flow and by the space discretisation it is possible to solve the fluid flow on the field of computation technologies by iterative methods [5]. The solution scheme for the Dobrohošť SHPP was selected as explicit with finite difference method.

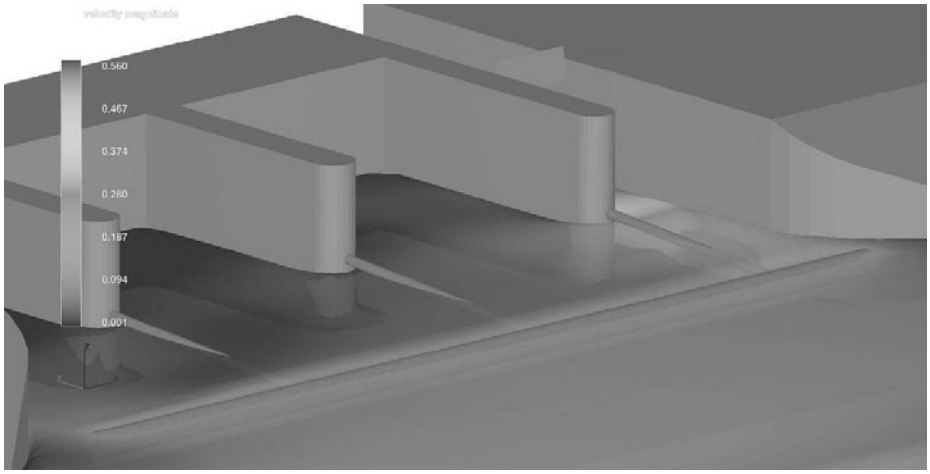

Fig. 4. The 3D modela – geometry overview

The model geometry is copying the geometry of the physical model. The precision of the geometry is specially aimed on the foreground area of the weir, the intake structure and the floating barrage (Fig. 4). All objects correspond to the physical model in terms of dimensions and disposition. The floating barrage is defined as a moving object with one degree of freedom: the rotation around X axis which intersects the anchoring of the floating barrage in weir piers. In simulation the floating barrage acts with full „fluid structure interaction".

Inlet boundary conditions of the mathematical model were simulating the steady flow scenario according to physical model conditions, with channel water level set on the maximum operational level of 131.10 m with an average cross sectional velocity on physical model of 0.6 $m \cdot s^{-1}$ (0.155 $m \cdot s^{-1}$ in real) [2]. The outlet boundary condition was defined as outflow.

Based on realized 3D simulations san be said that the velocity field deformation in area of the floating barrage has a local character and has no effect on the flow regime in area of the intake structure. There is a velocity pulsation effect occurring in the weir area, but it has no major effect on the flow regime in the intake structure as well.

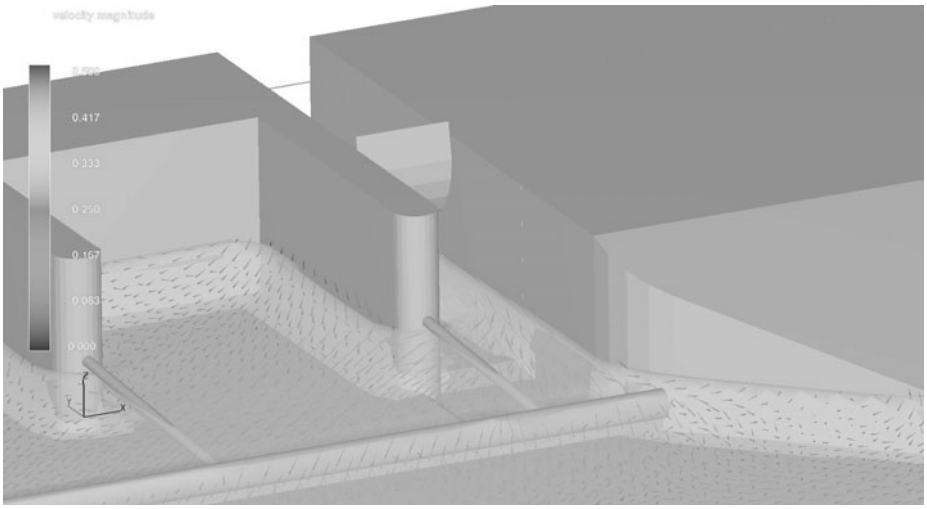

Fig. 5. An overview of the velocity field in the foreground of the intake structure

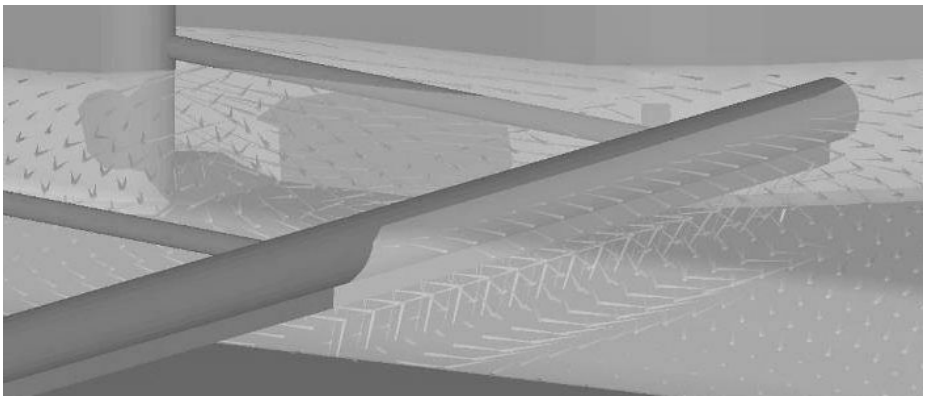

Fig. 6. A detailed overview of the velocity field near the floating barrage

Table 1

Comparison of physical measures and CFD simulation results

Velocity	Physical model	CFD simulation		Abberancennce
		last time step	velocity median*)	
	[m · s^{-1}]	[m · s^{-1}]	[m · s^{-1}]	
1	0.561	0.679	0.574	2.3%
2	0.573	0.683	0.596	3.9%
3	0.542	0.539	0.465	16.6%

*) Velocity median for all time steps after reaching required convergence

The main post-processing activities were focused on the intake structure area. Assumed deformation of velocity field caused by floating barrage is not as intensive to significantly affect the flow regime.

The measures of velocity vectors in the intake structure were used for comparing the simulation results (Tab. 1). Comparable results of the 3D simulation and physical model measurements confirm that the CFD models are an effective alternative and supplemental tool for physical models.

The results are confirming the local character of velocity field deformations in area of the floating barrage without any significant effect on character of the water flow regime in the intake structure (Fig. 5, 6, 7).

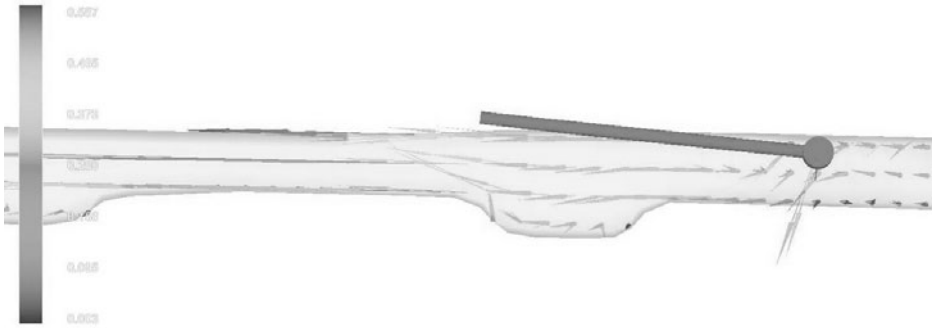

Fig. 7. Effect of the floating barrage on the velocity field in longitudinal section of the intake

21.5. Conclusion

Using modern methods of experimental hydraulics such as physical modelling and three dimensional mathematical modelling and their mutual combinations make it possible to reach required precision of examination of complicated hydraulic phenomena occurring at flow on water structures.

This approach was used for assessment of the effects of the floating barrage on the flow in the intake structure of the Dobrohošť small hydropower plant, which is presently under construction

The modelling methods had shown deformations and local velocity increase in the area under and behind the floating barrage. These deformations have no serious effect on water flow quality at intake structure of the SHPP.

References

[1] Ansys Inc.: Ansys Fluent 12.0/12.1 Documentation 2009.
[2] Dušička P. et al.: MVE Dobrohošť – štúdia, Katedra hydrotechniky. Stavebná fakulta STU v Bratislave, Bratislava 2007.
[3] Dušička P. et al.: MVE Dobrohošť – fyzikálny výskum vtokovej časti MVE. Záverečná správa, Katedra hydrotechniky, Stavebná fakulta STU v Bratislave, Bratislava 2008.

[4] Hulkó G.: Modelovanie a riadenie systémov s rozloženými parametrami v modernej technickej praxi. Ústav automatizácie, merania a aplikovanej informatiky SjF, STU v Bratislave, Bratislava 2007.
[5] Molnár V.: Počítačová dynamika tekutín. Bratislava, 2010.

Acknowledgement

This paper was supported by the Grant agency VEGA under contract No.1/0578/11 and No.1/0281/10 and the Slovak Research and Development Agency under contract No. APVV-0680-10.

22 Numerical Model for Two Phase Flow Through Porous Media

Todorka Samardzioska (Ss. Cyril and Methodius University,
Faculty of Civil Engineering, Skopje, Macedonia)

22.1. Introduction

Although it may seem that groundwater is more protected than surface water, it is still subjected to pollution, and when the latter occurs, the restoration to the original, unpolluted state, is usually more difficult and time-consuming process. Therefore, the interest in the mathematical and numerical treatment of multiphase flow in porous media, i.e. the necessity for sophisticated mathematical models and numerical tools capable of understanding, predicting and optimising all the physical phenomena occurring in this field, has been increasingly rising in many branches of science and engineering. Hydrologists, agricultural engineers, soil physicists have for many years been concerned with fluid movement in air-water porous media systems. In the most recent years, environmental concerns and search for secure atomic waste depositories and for remediation strategies for contaminated aquifers raised more interest in the movement of fluids in the so-called vadose or unsaturated zone interposed between the atmosphere and the groundwater (saturated zone). Many potential groundwater contaminants are introduced at or near the soil surface via atmospheric deposition, spills, leakage from underground tanks, subsurface waste disposal, etc. Soluble components may migrate in the aqueous phase through the vadose zone to groundwater. Furthermore, a wide class of environmental contaminants consists of organic compounds of low water solubility which can occur as a separate liquid phase in the soil. Such liquids include many widely used industrial solvents and automobile and jet fuels which unfortunately often enter the ground via surface spills or leaks from underground storage tanks. Historically, the greatest impetus for development of multiphase flow models was initiated by the commercial interest of the petroleum industry, induced by the lure of more efficient oil and gas recovery from reservoirs, see [1] – [4].

Most of the existing flow and transport models are single-phase models that describe the groundwater flow and the convective-dispersive spreading of one or more components entirely dissolved in water. On the contrary to the transport of dissolved contaminants, some substance groups very often used in industry, as petroleum products and halogenated hydrocarbons, represent an individual phase with characteristic flow law. The unsaturated zone is a multiphase system, consisted of wetting phase (water), air and non-wetting phase (for example, oil). The elimination of the equation of the gas phase is often referred to as Richard's approximation and it is the basis of conventional analyses of two-phase flow

The BE DRM-MD numerical scheme is used for the first time to solve a two-phase model. Verification of the complex numerical models is very difficult in absence of sufficient experimental measurements and accurate analytical solutions. Another objective is analysis of modelling two-phase flow in porous media, with complete insight in the complex nonlinear relationships between pressures, saturations and permeabilities. The

influences of the choice of boundary and initial condition, the heterogeneity of the domain, the temporal and space discretization, and some physical parameters on the fluid process are important to be determined in order to clarify the mathematical model and areas of existing uncertainty.

22.2. Two Phase Flow Model

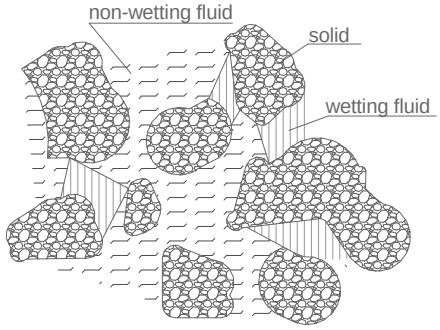

Fig. 1. Two-phase model

Two-phase flow consisted of two flowing fluids, which do not interchange mass and do not have reaction with the solid matrix, is the simplest multiphase flow, see Fig.1. It can describe very complex processes, such as: unsaturated flow in porous media, reservoir problems in petroleum engineering, salt-water intrusion in coastal aquifers, etc.

The equations governing the flow of fluids in a two-phase flow are special cases of general balance laws. The most common case is two-fluid flow, consisting of water (subscript W) and non-wetting phase (subscript O) and Darcy's law holds for both the phases:

$$\eta \frac{\partial}{\partial t}(S_W \rho_W) - \frac{\partial}{\partial x_i}\left[\rho_W \frac{1}{\mu_W} K_{W_{ij}}\left(\frac{\partial}{\partial x_i}(p_W) - \rho_W g_i\right)\right] - \rho_W q_W = 0 \tag{1}$$

$$\eta \frac{\partial}{\partial t}(S_O \rho_O) - \frac{\partial}{\partial x_i}\left[\rho_O \frac{1}{\mu_O} K_{O_{ij}}\left(\frac{\partial}{\partial x_i}(p_W) + \frac{\partial}{\partial x_i}(p_{COW}) - \rho_O g_i\right)\right] - \rho_O q_O = 0 \tag{2}$$

Equations (1) and (2) are not independent from each other, since they have to satisfy the condition that the fluids fill up the pore volume, i.e. the additional relations:

$$S_w + S_O = 1 \tag{3}$$

$$p_{COW} = p_O - p_W \tag{4}$$

where: η – porosity;
S_α – saturation of the fluid phase α,
ρ_α – density of the fluid phase α,
p_α – pressure head in the fluid phase α,
p_{COW} – capillary pressure;
μ_α – dynamic viscosity;
$g_i = g\delta_{i3}$ – vector of gravitational acceleration;
$K_{\alpha ij}$ – conductivity of the phase α,
$K_{\alpha ij} = K_{r\alpha} K_{ij}$,
$k_{r\alpha}$ – relative permeability of the fluid phase α,
K_{ij} – intrinsic permeability tensor (fluid independent).

The mobility of the fluid phase α is defined as $\lambda_\alpha = k_{r\alpha}/\mu_\alpha$. Therefore, mobility is a measure of the easiness with which a fluid will flow at particular saturation. The mobility ratio M is ratio between the mobility of the displacing phase and mobility of the displaced one, $M = \lambda_w/\lambda_o$. According the value of the mobility ratio, the mechanism of flow can be defined.

Darcy's law for the wetting and non-wetting phase can be formulated as follows:

$$v_{W_i} = -\lambda_W K_{ij}\left(\frac{\partial p_W}{\partial x_i} - \rho_W g_i\right) \tag{5}$$

$$v_{O_i} = -\lambda_O K_{ij}\left(\frac{\partial p_W}{\partial x_i} + \frac{\partial p_{COW}}{\partial x_i} - \rho_O g_i\right) \tag{6}$$

where: v_{α_i} – velocity of the fluid phase α.

Introducing (5) and (6) into equations (1) and (2) one can obtain shortened form:

$$\eta\frac{\partial(S_W\rho_W)}{\partial t} + \frac{\partial}{\partial x_i}(\rho_W v_{W_i}) - \rho_W q_W = 0 \tag{7}$$

$$\eta\frac{\partial(S_O\rho_O)}{\partial t} + \frac{\partial}{\partial x_i}(\rho_O v_{O_i}) - \rho_O q_O = 0 \tag{8}$$

Summing up the Eq. (7) and (8), and introducing (3):

$$v_{t_i} = v_{W_i} + v_{O_i}$$

$$\begin{aligned}\frac{\partial}{\partial x_i}v_{ti} = \frac{\partial}{\partial x_i}(v_{W_i} + v_{O_i}) = q_W + q_O - \frac{v_{O_i}}{\rho_O}\frac{\partial\rho_O}{\partial x_i} - \frac{v_{W_i}}{\rho_W}\frac{\partial\rho_W}{\partial x_i} - \\ -\eta\left[\frac{1-S_W}{\rho_O}\frac{\partial\rho_O}{\partial t} + \frac{S_W}{\rho_W}\frac{\partial\rho_W}{\partial t}\right] = 0\end{aligned} \tag{9}$$

Neglecting the compressibility of both phases, constant densities ρ_α yields to:

$$\frac{\partial}{\partial x_i}(v_{t_i}) = q_W + q_O = q_t \tag{10}$$

The combination of Eq. (5) and (6) when the first one is multiplied by λ_O, and the second one by λ_W, leads to:

$$v_{W_i}\lambda_O - v_{Oi}\lambda_W = \lambda_O\lambda_W K_{ij}\left[\frac{\partial p_{COW}}{\partial x_i} - \rho_O g_i + \rho_W g_i\right] \tag{11}$$

with $v_{W\,i} = v_{t\,i} - v_{O_i}$:

$$v_{O_i} = \frac{\lambda_O}{\lambda_O + \lambda_W}\left[v_{t_i} - \lambda_W K_{ij}\left(\frac{\partial p_{COW}}{\partial x_i} - \rho_O g_i + \rho_W g_i\right)\right] \tag{12}$$

After substituting Eq. (12) in Eq. (8), the resulting equation is:

$$\frac{\partial}{\partial x_i}\left[f_O v_{ti} - \bar{\lambda} K_{ij}\left(\frac{\partial p_{COW}}{\partial x_i} + \rho_W g_i - \rho_O g_i \right)\right] = \eta \frac{\partial S_W}{\partial t} + q_O \tag{13}$$

where:

$$f_O = \frac{\lambda_O}{\lambda_O + \lambda_W} \text{ is the fractional flow of oil} \tag{14}$$

$$f_w = \frac{\lambda_W}{\lambda_O + \lambda_W} \text{ is the fractional flow of water} \tag{15}$$

and

$$\bar{\lambda} = \frac{\lambda_W \lambda_O}{\lambda_O + \lambda_W} \tag{16}$$

All the unknowns in the Eq. (13) are functions of the saturation, thus one can use following expressions for the derivatives:

$$\frac{\partial p_{COW}}{\partial x_i} = \frac{dp_{COW}}{dS_W}\frac{\partial S_W}{\partial x_i} \tag{17}$$

$$\frac{\partial (f_O v_{ti})}{\partial x_i} = v_{ti}\frac{\partial f_O}{\partial x_i} + f_O \frac{\partial v_{ti}}{\partial x_i} = v_{ti}\frac{df_O}{dS_W}\frac{\partial S_W}{\partial x_i} + f_O q_t \tag{18}$$

$$\frac{\partial}{\partial x_i}\left[\bar{\lambda} K_{ij}(\rho_W g_i - \rho_O g_i)\right] = (\rho_W g_i - \rho_O g_i)\frac{d(\bar{\lambda} K_{ij})}{dS_W}\frac{\partial S_W}{\partial x_i} \tag{19}$$

Since $f_W + f_O = 1$, taking into consideration that

$$\frac{df_O}{dS_W} = -\frac{df_W}{dS_W} \text{ and } f_O q_t - q_O = q_W - f_W q_t,$$

and including Eq. (17), (18) and (19) into Eq. (13), the final equation is parabolic:

$$\begin{aligned} &\frac{\partial}{\partial x_i}\left[\bar{\lambda} K_{ij}\frac{dp_{COW}}{dS_W}\frac{\partial S_W}{\partial x_i}\right] + \left[v_{ti}\frac{df_W}{dS_W} + (\rho_W g_i - \rho_O g_i)\frac{d(\bar{\lambda} K_{ij})}{dS_W}\right]\frac{\partial S_W}{\partial x_i} + \\ &+ \eta\frac{\partial S_W}{\partial t} - q_W + f_W q_t = 0 \end{aligned} \tag{20}$$

The first term in the two-phase saturation Eq. (20) represents dispersive part, the second term is convective part, the third is mass storage term and last ones a source and sink terms. The equation is parabolic due to the presence of term that includes capillary pressure.

Neglecting only the gravitational effects and the source and sink term, for simplicity, and taking the significance of the capillary pressure gradient into account, one arrives to the so-called Mc Whorter problem:

$$\eta\frac{\partial S_W}{\partial t} + v_{t_i}\frac{df_W}{dS_W}\frac{\partial S_W}{\partial x_i} = -\frac{\partial}{\partial x_i}\left(D_{ij}\frac{\partial S_W}{\partial x_j}\right) \tag{21}$$

$$D_{ij}(S_W) = k_{ro} K_{ij} \frac{f_W}{\mu_O} \frac{dp_{COW}}{dS_W} \text{ – dispersion tensor} \tag{22}$$

The divergence of the dispersion tensor, Eq. (22), is

$$\frac{\partial}{\partial x_i}(D_{ij}) = \frac{\partial D}{\partial S_W} \frac{\partial S_W}{\partial x_i} = k_{ro} K_{ij} \frac{f_W}{\mu_O} \frac{d^2 p_{COW}}{dS_W{}^2} \frac{\partial S_W}{\partial x_i} \tag{23}$$

Therefore, for Mc Whorter Eq. (21), if

$$\frac{d^2 p_{COW}}{dS_W{}^2} << \frac{dp_{COW}}{dS_W}$$

and assuming that all the properties dependent on water saturation are constant in a particular time step over one single sub-domain, assuming that $D_{ij} \approx$ const and using the Laplace operator, Eq. (21) can be written as:

$$D \cdot \nabla^2 S_W = -\eta \frac{\partial S_W}{\partial t} - v_{t_i} \frac{df_W}{dS_W} \frac{\partial S_W}{\partial x_i} \tag{24}$$

22.2.1. Constitutive Models k – S – p

A critical component of predictive two-phase flow models is the mathematical description of the relative permeability, saturation and pressures relations (k–S–p), sometimes referred to as constitutive models. Reliable experimental measurements are difficult to obtain, they are time consuming, expensive and require advanced laboratory skills. A weakness of the experiments is that they typically involve only a limited set of boundary conditions for testing the predictive models and the employed constitutive relations.

The fraction of the total pore space occupied by the wetting phase is defined as saturation S, a quantity which varies from point to point in the domain. The points where saturation vanishes for both the phases are called residual or irreducible saturations S_{OR} and S_{WR}. A simultaneous flow of the two fluids is possible only if saturation in the wetting fluid is greater than the irreducible saturation S_{WR} and if saturation in non-wetting fluid is greater than the residual saturation ($1 - S_{WM}$). Therefore, the concept of relative permeability has meaning only on the interval of saturation in wetting fluid (fluid W), $S_{WR} \le S_W \le S_{WM}$.

The exact form of the curves relative permeability – saturation depends on the porous medium under consideration. The interesting fact is that the relative permeabilities do not depend on the characteristic dimension l of the pores. Therefore, two homothetic porous media must have the same relative permeability curves. The most common relations permeability-saturation are those of Brooks – Corey, van Genuchten, linear relation etc, and all of them are simplified, because in reality permeabilities exhibit significant hysteresis and the influence of compositional effects and presence of three or more phases is still not clear. A summary of different models for the relative permeability-saturation function is given e.g. by Ch. Marle [2] or R. Helmig [3]. Several authors worked on the determination of the relative permeability at the micro scale. Models to analyse this behaviour are e.g. network models, which describe the underground as a network of nodes and interconnecting capillary tubes. Those investigations confirmed the well known macro scale

relations between relative permeability and saturation of a phase in the medium. These functions can be hysteretic, i.e. the behaviour for draining and imbibition is differing. Furthermore they differ between the fluid with a higher affinity for the solid matrix ("wetting fluid") and other ones with a lower affinity ("non-wetting fluids"). These relationships must be defined to represent multiphase flow of fluids in the rock properly. Normally, they are measured in laboratory on rock samples from the reservoir under study.
The relative permeability $k_{R\alpha}$ varies from 0 when no phase α is present, to 1, when the medium is saturated with α phase. Darcy's law is a macroscopic equation which represents multiple fluids in porous media as overlapping continua occupying the same physical space. Darcy's equation is empirical in nature and invokes several implicit assumptions. A fundamental assumption is that flow of phase α is not directly affected by pressure gradients in other phases. Another critical assumption is the validity of the concept of intrinsic permeability which purports to separate fluid and porous medium dependent effects on fluid flow. The assumption that intrinsic permeability is a unique (tensorial) characteristic of the porous medium is reasonably justifiable for rigid granular soils which do not exhibit swelling or consolidation in response to interactions with fluids.

The most widely used empirical functions for representation of capillary retention data are the Brooks-Corey function and the van Genuchten function.

Brooks-Corey model

One of the most popular equations is the power-law function proposed by Brooks and Corey [4], who distinguished the non-wetting phase permeability k_{RO} from the wetting phase permeability k_{RW}. According it, the relative permeability for each phase is directly related to the corresponding phase saturation. Expression for the wetting phase is:

$$k_{RW} = \left(S_e\right)^{\frac{2+3\lambda}{\lambda}} \tag{25a}$$

Similarly for the non-wetting phase:

$$k_{RO} = \left(1-S_e\right)^2\left(1-S_e^{\frac{2+\lambda}{\lambda}}\right);\ k_{RO}=1 \text{ at } S_e = S_R \tag{25b}$$

$$p_{COW} = p_d\, S_e^{-1/\lambda} \tag{26}$$

The larger the value of λ (which means that the pore sizes in the soil are more uniform), the steeper the soil-water characteristics curve within the desaturation zone. It should be pointed out that values of $S_e < S_R$ can exist, but the theory can not apply in this range of saturations and may become inaccurate at saturations very close to S_R. The Brooks-Corey theory makes assumptions that k_{RW} is zero and k_{RO} is a maximum at S_R. Neither is actually true. However, k_{RW} appears to approach zero at the finite saturation S_R, when the curves of k_{RW} are extrapolated.

For the most often used values of $\lambda = 2$ the above equations obtain the following form (Fig. 2):

$$k_{RW} = S_e^{\,4} \tag{27}$$

$$k_{RO} = \left(1-S_e\right)^2\left(1-S_e^{\,2}\right) \tag{28}$$

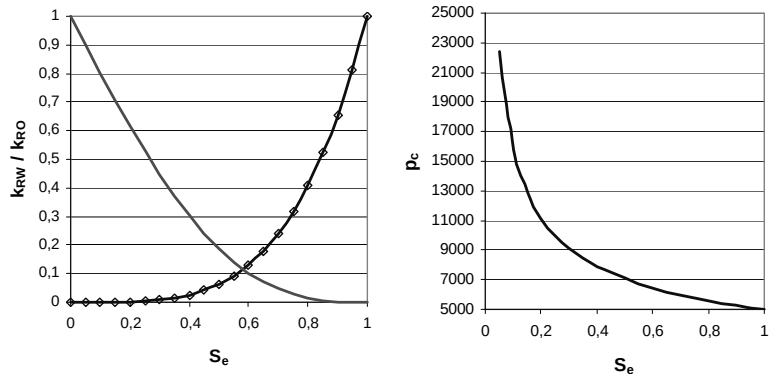

Fig. 2. Brooks – Corey model for values of $\lambda = 2$: a) relative permeabilities-saturation curves, b) capillary pressure – saturation curve

Van Genuchten model

This approach was derived by Van Genuchten [5], who made a modification with more accurate description of observed soil hydraulic data near saturation.

$$k_{RW} = S_e^{1/2}\left\{1-\left[1-S_e^{1/m}\right]^m\right\}^2 \tag{29}$$

$$k_{RO} = \left(1-S_e\right)^{1/3}\left[1-S_e^{1/m}\right]^{2m} \tag{30}$$

It uses three fitting parameters, namely, *a*, m and *n*:

— the parameter a is related to the inverse of the air entry value,

— the *n* parameter is related to the pore size distribution of the soil and

— the *m* parameter is related to asymmetry of the model and is assumed to be function of *n*.

The Brooks-Corey function has advantages in simplicity and produces acceptable results for coarse textured soils with narrow pore size distributions, whereas the van Genuchten function may be more applicable for fine textured soils with broad pore size distributions. Neither expression, however, is used exclusively in numerical models, and limited information is available on the influence of function selection on model predictions, especially in regards to two-phase flow systems involving long-term redistribution processes.

22.3. Numerical Implementation

The numerical technique that is used to solve the partial differential equation defined by the model is the Boundary Element Dual Reciprocity Method – Multi Domain scheme (BE DRM-MD) [6, 7, 11]. It has been used for the first time to solve a two-phase flow model. The method belongs to the boundary element techniques that transform the original partial differential equation into an equivalent integral equation by means of the corresponding Green's theorem and its fundamental solution. Simplicity, elegance of the formulation and its efficient solution extended the application of the BEM to a wide variety of time

dependent and non-linear problems. The general idea of the BEM is to transform the original partial differential equation (PDE), or set of PDEs that define a given physical problem, into an equivalent integral equation (or system) by means of the corresponding Green's theorem and its fundamental solution. In this way some or all of the field variables and their derivatives are necessary to be defined only on the boundary.

Applying the DRM (Dual Reciprocity Method) approach to the Eq. (21), according the detailed explanation in references [6, 7] and [11], yields:

$$HS_W - GQ = -\frac{S}{D}\left[\eta \frac{\partial S_W}{\partial t} + v_{t_i} \frac{df_W}{dS_W}\frac{\partial S_W}{\partial x_i}\right] \tag{31}$$

where:

$$S = \left(H\widehat{S_W} - G\widehat{Q}\right)F^{-1} \tag{32}$$

The two boundary element characteristic matrices H and G on both sides of the Eq. (31) are consisted of coefficients, which are calculated assuming the fundamental solution is applied at each node successively, and depending only on geometrical data, see [6, 7, 11].
Applying the following:

$$\frac{\partial S_W}{\partial x_i} = \frac{\partial F}{\partial x_i}F^{-1}S_W\ ;\ T = S\frac{1}{D}v_{t_i}\frac{df_W}{dS_W}\frac{\partial F}{\partial x_i}F^{-1};\ \varpi_{koef} = \frac{\eta}{D} \tag{33}$$

the main equation takes the following form:

$$HS_W - GQ = -S\varpi_{koef}\frac{\partial S_W}{\partial t} - T\,S_W \tag{34}$$

For the time marching scheme:

$$S_W = \left(1-\theta_s\right)\cdot {S_W}^n + \theta_s \cdot {S_W}^{n+1} \tag{35a}$$

$$q = \left(1-\theta_q\right)\cdot q^n + \theta_q \cdot q^{n+1} \tag{35b}$$

where θ_s and θ_q take values between 0 and 1. Time derivative is approximated using a finite-difference approximation:

$$\frac{\partial S_W}{\partial t} = \frac{1}{\Delta t}\cdot\left({S_W}^{n+1} - {S_W}^n\right) \tag{36}$$

Finally the equation for two-phase Mc Whorter flow is:

$$\begin{aligned}\left[\theta_S\left(H+T\right)+\frac{\varpi_{koef}\,S}{\Delta t}\right]{S_W}^{n+1} - G\,\theta_q\,Q^{n+1} = \\ = \left[\frac{\varpi_{koef}\,S}{\Delta t} - \left(1-\theta_S\right)\left(H+T\right)\right]{S_W}^n + G\left(1-\theta_q\right)Q^n\end{aligned} \tag{37}$$

The spatially discretized version of the Eq. (37) is solved for the increments in iteration for water saturation. Nonlinear coefficients such as the permeabilities, mobilities and fractional flow are represented using piecewise linear interpolation of their respective nodal values at each iteration. At each iteration step the saturation increments are used to

update the saturation of each phase, which are subsequently used to update all nonlinear coefficients. The system is then updated and solved, and the process repeated until the convergence is attained.

22.4. Model Verification

A variety of one and two dimensional two-phase numerical experiments are presented here to demonstrate the accuracy of the proposed BE DRM model with multi domains for predicting two-phase flow. The numerical performance of this algorithm is compared to others reported in the literature. Emphasis is directed toward examination certain physical phenomena of interest and understanding the complex flow processes. Analysis of the predicted results using grid systems of practical extent for use in large-scale simulations is given. The influence of numerical grid resolution, temporal discretization and the selection of constitutive relative permeability – saturation and capillary pressure – saturation models on the prediction of long term redistribution for two phase flow in homogeneous and heterogeneous domains was analysed.

22.4.1. One-Directional Two-Phase Flow; Mc Whorter Problem

In a one-dimensional set-up, water is entering the system on one side and the initial oil filling is extracted on the other side. For verification of the DRM MD code, numerical example that corresponds to the example in the book of R. Helmig, see [3] is analyzed. Domain is long $L = 2.6$ m, with width $w = 0.2$ m, as it is presented in Fig. 3. Dirichlet boundary conditions are imposed: for $x = 0.0$ m, $Sw = 1.0$ and for $x = 2.6$ m, $Sw = 0.01$, chosen for sake of having right boundary not influenced by the inflow. The oil pressure is $p_O = 2 \cdot 10^5$ Pa. Initial water saturation through the whole domain is $S_w = 0.01$. Densities are $\rho_w = \rho_o = 1000$ kg/m^3 and dynamic viscosities are $\mu_w = \mu_o = 0.001$ kg/(ms) for both fluids. The properties of the rock are: absolute permeability $K = 10^{-10}$ m^2, porosity $\eta = 0.3$. The Brooks-Corey model was employed for description of the k–s–p, equations (25), and (26). The entry pressure (bubbling, threshold pressure) is $p_d = 5000$ Pa. Residual saturations for the water and the oil are $S_{wr} = S_{or} = 0.0$.

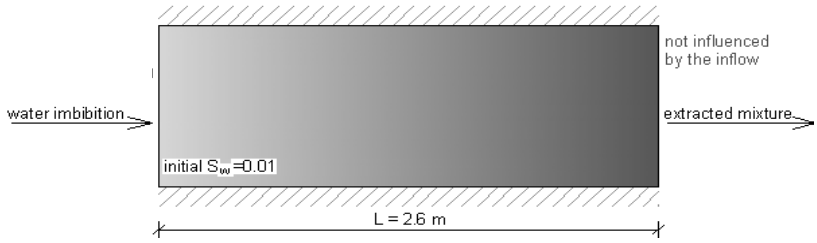

Fig. 3. Domain description for Mc Whorter problem; initially saturated with oil

The influence of the space discretization is analyzed with three meshes; the first one with 13 sub-domains of length 0.2 m, the second mesh with 26 sub-domains of length 0.1 m, and the third one is composed of 52 sub-domains $x = 0.05$ m. The results of the simulation with the grid with 52 sub-domains and time step $dt = 0.5$ sec are presented in Fig. 4. Even the

coarse grid simulation produces useable and acurate solution, though the results on the finer grids are considerably better. It is oscilation free and shows a good mass balance. Testing simulation with different time steps on each of these meshes showed that one should be extremely careful with the choice of the time step when rather coarse mesh is used for the domain.

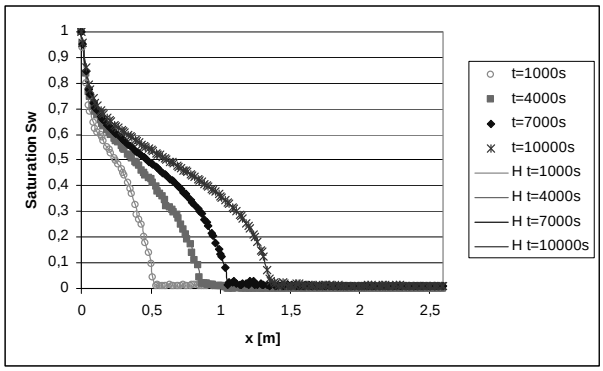

Fig. 4. Saturation profiles at four time steps (52sub-domains, dt = 0.5 sec)

Different time steps were analysed for all the grid meshes. The size of the time step practically does not have any influence on the final results for the mesh with 52 sub-domains. With larger time step $dt \geq 1.0$, the simulation overestimated the saturation change [11]. Acceptable saturation change used here is 1–5%. Using fully implicit formulation, even larger changes can be tolerated sometimes. It is difficult to specify general bounds for stability, that means, to control the oscillations of nonlinear processes. When stability limitation is exceeded, saturations and pressures may oscillate from time step to time step. The overshoot must be controlled, because negative saturations may be calculated. The truncation error can distort the results of the flow simulation, because it is approximately proportional to the change in saturation over a time step.

22.4.2. Two-Directional Two-Phase Flow; Five-Spot Example

Two-dimensional areal models are most commonly used models in reservoir studies, especially when areal flow patterns dominate reservoir performance, the influence of heterogeneity of the domain is of importance, or generally for studies of entire reservoirs. The so-called 'five-spot problem' is a two-dimensional test case, classical model problem from petroleum reservoir engineering. In order to exploit an oil reservoir, a large oil field is regarded. Water is pumped into the reservoir through injection wells and it displaces the oil.

The model configuration consists of a square in which's corners oil is produced. Water injection happens in the center of the square. The symmetry of the problem allows for the reduction of the problem to the right upper quadrant of the domain. Injection well is at lower left corner and production well at upper right. Both wells have constant rates $q = q_o$ and $q = -q_o$, respectively. Square mesh with dimensions 300 m × 300 m is analysed, see Fig. 5. The initial saturation of oil is assumed to be $So = 1.0$ and initial pressure is $Po = 2 \cdot 10^5$ Pa. Initial saturation through the whole domain is $S_w = 0.0$. Residual saturations for the water and the oil are assumed to be $S_{wr} = S_{or} = 0.0$. Densities are $\rho_w = \rho_o = 1000$ kg/m^3 and dynamic viscosities are $\mu_w = \mu_o = 0.001$ kg/(ms) for both the fluids. Properties of the rock

are: absolute permeability $K = 10^{-7}$ m^2, porosity $\lambda = 0.2$. Brooks and Corey approach has been employed with the following parameters: distribution index $\lambda = 2$ and entry pressure $p_d = 1350$Pa. Actually a Mc-Whorter case of saturation equation, (21) is solved for both cases. The example is solved with Neuman condition zero flux, $q = 0$, on all four sides, except in the two corners.

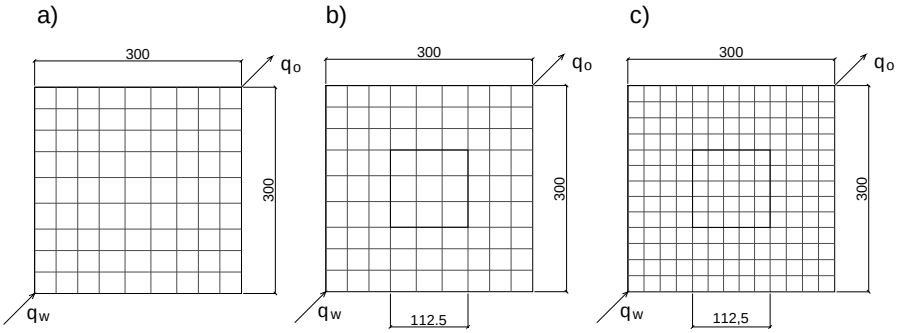

Fig. 5. Five-spot example: a) homogeneous domain, b) heterogeneous domain, grid mesh with 9×9 sub-domains, c) grid mesh with 13×13 sub-domains

The correct choice of boundary conditions is very important for these kind of problems. It was shown in the literature that, if the distribution of the injection rate along the boundary are strongly curved or only piecewise continuously differentiable, the oscillations in the infiltrating saturation occur, as a result of the not enough smooth distribution of the boundary fluxes. *Helmig* [3] has suggested distribution of the injection rate not on the corner nodes only, but on the neighbouring boundary nodes as well. Two cases are considered: homogeneous and heterogeneous domain.

Homogeneous domain

Applying all the abovementioned properties and conditions, the homogeneous domain is solved using grid mesh with 9×9 sub-domains, see Fig. 5a), and the distribution of the water saturation is presented in the Fig. 6.

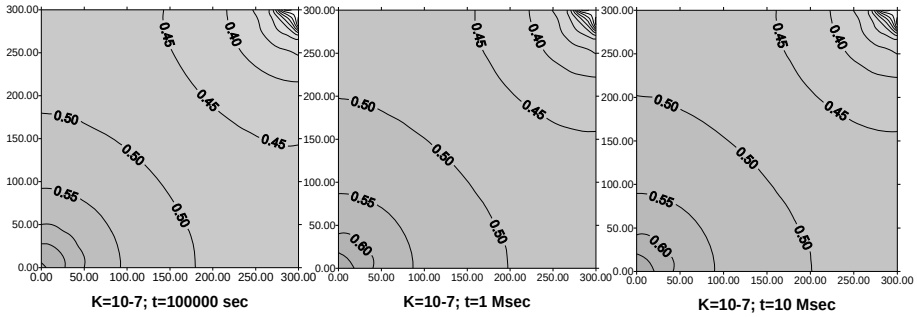

Fig. 6. Homogeneous five-spot example; mobility ratio $M = 1$

It can be noticed that the numerical five-spot experiment exhibits a very distinct front traversing the domain. Naturally, the modeller on the one hand tends to achieve stable results, while on the other the numerical results should not be smeared too much. **Todd et all.** [12] performed some numerical experiments using various upstream weighting techniques. In their experiments, the saturation distribution for a 9×9 grid (with single and two point approximation) was obviously diamond shaped and fallacious cusps are evident even for a grid mesh of 19×19, though predicted displacement fronts became more circular. In spite of that, here, with this model, the picture is more realistic and alike the natural scenario. At all times the flow is almost radial and the dispersion is equal in all directions out from the injection well.

As a grid dependency test, one finer mesh of 13×13 sub-domains is analyzed, see Fig. 5b). The residual saturations for this case were: $S_{wr} = 0.2$ and $S_{or} = 0.15$. Initial pressure is $Po = 10^4$ Pa. Initial saturation through the whole domain is $S_w = 0.2$.

The results of the simulations for both grid meshes along the diagonal of the domain are presented in Fig. 7. Even the coarse grid simulation produces a useable solution, though the results on the finer grids are considerably better. It is oscillation free and shows a good mass balance. The reproduction of the front steepness is considerably better on the finer grid.

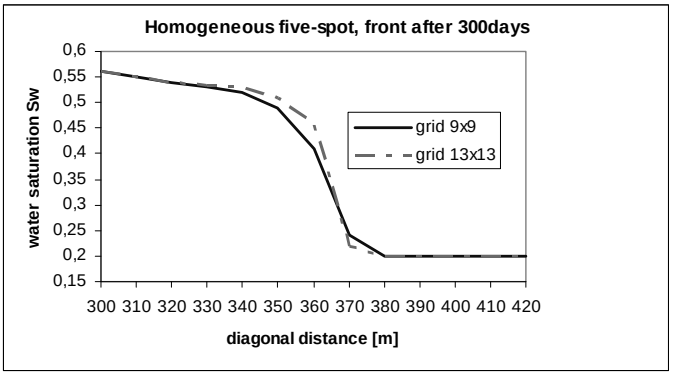

Fig. 7. Diagonal cut of homogeneous five-spot example; comparison between fronts with 2 mesh grids

Heterogeneous domain

If the permeability is not homogeneous throughout the domain, the front develops a complex shape. The heterogeneous permeability distribution shown in Fig. 5c) was used for the experiment. In the centre of the domain a zone of 112.5 m × 112.5 m with low permeability is assumed to exist ($K_2 = 10^{-10}$ m^2), three orders of magnitude less than in zone 1 ($K_1 = 10^{-7}$m^2).

The location of the low-permeable region is accurately positioned , clearly visible and is not smeared out between the wells, as it can be noticed in Fig. 8.

These results show the advantage that the current approach has in respect to the Finite Element Method, when contrasted to the statement of *Langlo & Espedal* [13]: “Modelling heterogeneous domain (with finite element model) is computing intensive, if not impossible. For instance, the model of *Damsleth* required 1–2 million permeability blocks. A high-resolution solution can only reflect one out of many probable flow patterns”.

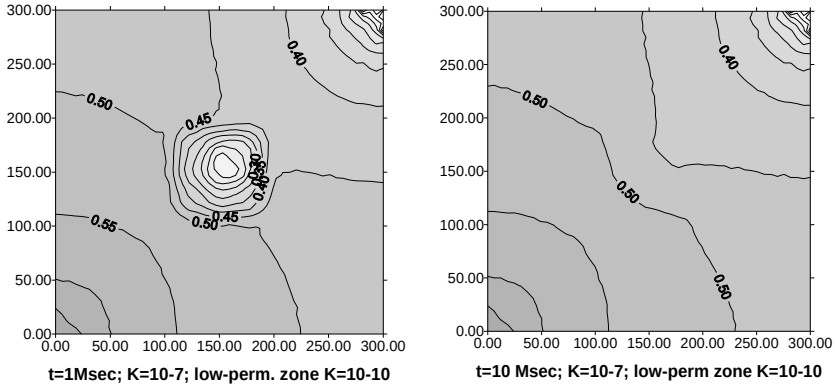

Fig. 8. Heterogeneous five-spot example; mobility ratio $M = 1$

22.5. Conclusions

For the two-phase flow, the fractional flow approach is used, or so-called Mc Whorter Eq. (21) was solved for all numerical examples. The fractional flow approach offers greater computational efficiency, because the two-phase system can be described with one nonlinear advection-diffusion equation only, and because the equation has a dominant hyperbolic part which can be treated with characteristic solution methods. Some conclusions are withdrawn from the analysis of different examples:

— Two-phase flow model was implemented using the boundary element DRM-MD scheme and tested on one-dimensional and two-dimensional examples. Application of DRM-MD scheme leads to solutions that are basically oscillation free, even in the presence of steep infiltrations fronts.

— Even the coarse grid simulation produces useable and accurate solution, though the results on the finer grids are considerably better. It is oscillation free and shows a good mass balance.

— Areas with different permeability and porosity can be treated and identified in numerical simulation. The DRM-MD scheme performs very well for non-homogeneous domains, even for great differences in the permeabilities.

— Testing simulation with different time steps on each of these meshes showed that one should be extremely careful with the choice of the time step when rather coarse mesh is used for the domain.

— Thinner domains showed more stable fronts and slightly slower breakthrough compared to wide fractured porous systems.

— Linear type of constitutive model $k - S - p$, as the simplest one, can be used for two-phase flow. The Brooks-Corey model appeared to be the most easiest and accurate at the same time, because it has two fitting parameters only and its derivative is easier to calculate. The Van Genuchten model overestimates the saturation and has more dispersive front.

It is important to point out that to assemble appropriate material relationships, and coherent set of boundary and initial conditions, in other words, to use the two-phase model

appropriately, in-depth understanding of the physical processes is required, because of the strong nonlinear coupling. Unfortunately, quantitative measurements of two-phase fluid flow are lacking in the literature. This work points to the necessity for further laboratory experiments designed to obtain the data necessary to verify numerical predictions of capillary dominated immiscible flow.

The examples showed that this BE formulation provides stable results and can be used successfully for solving flow processes in fractured porous media. The major reason why the BE DRM-MD can be attractive is that it is advantageous for modelling heterogeneous domains with different physical properties and it does not have the problems related to the coupling compatibility of the FEM – BEM hybrid methods.

References

[1] Hilfer R.: *Macroscopic equations of motion for two-phase flow in porous media*. Physical Review E., Vol. 58 (2), 2090–2096, August 1998.

[2] Marle Ch. M.: *Multiphase Flow in Porous Media*.Editions Technip, Paris 1981.

[3] Helmig R.: Multiphase Flow and Transport Processes in the Subsurface: A Contribution to the Modeling of Hydrosystems. Berlin, Heidelberg, New York: Springer-Verlag 1997.

[4] Brooks Royal H., Corey Arthur T.: Properties of porous media affecting fluid flow. Journal of the irrigation and drainage division, Proceedings of the American Society of Civil Engineers, June 1966, 61–68.

[5] Van Genuchten M. Th.: A Closed-form Equation for Predicting the Hydraulic Conductivity of Unsaturated Soils. Soil Sci. Soc. Am. J., Vol. 44, 892–898, 1980.

[6] Brebbia C. A., Dominguez J.: Boundary Elements, An Introductory Course. Second Edition, Southampton, UK: Computational Mechanics Publications 1992.

[7] Partridge P. W., Brebbia C. A., Wrobel L. C.: The dual reciprocity boundary element method. Southampton UK: Computational Mechanics Publications 1992.

[8] Abriola L. M., Rathfelder K.: Mass balance errors in modeling two-phase immiscible flows: causes and remedies. Advances in Water Resources. Vol. 16, 223–239, 1993.

[9] Parker J. C.: Multiphase Flow and Transport in Porous Media. Review of Geophysics, 27, 3/August, 311–328, 1989.

[10] Sillers W. Scot, Delwyn G. Fredlund, Noshin Zakarzadeh: Mathematical attributes of some soil-water characteristic curve models. Geotechnical and Geological Engineering, 19, 243–283, 2001.

[11] Samardzioska T.: Boundary Element Dual Reciprocity Method with Multi Domains for Modelling Fractured Porous Media: Single and Two-Phase Flow and Transport, PhD Thesis, Wessex Institute of Technology, University of Wales, UK 2006.

[12] Todd M. R., O'Dell P. M., Hirasaki G. J.: Methods for Increased Accuracy in Numerical Reservoir Simulators. Society of Petroleum Engineers Journal, December 1972, 515–530.

[13] Langlo P., Espedal M. S.: Macrodispersion for two-phase, immiscible flow in porous media. Advances in Water Resources. Vol. 17, 297–316, 1994.

23 The Riparian Corridor Concept – a Valuable Alternative to Traditional Riverbank Stabilization Techniques

Dimitrija Sekovski (Project Manager, UNDP/GEF Prespa Project, Republic of Macedonia)

23.1. Introduction

Healthy river ecosystems secure very important ecological and social functions and services which are of fundamental importance for the human well-being. They are complex ecosystems of structurally and functionally interrelated abiotic and biotic elements including humans. However, the river systems have always been subject to human modifications, motivated primarily by the exploitation of their potentials and achievement of short-term economic objectives.

In the variety of human induced alterations to river ecosystems, the conventional riverbank stabilization techniques are amongst the most widely spread. They are mainly used to prevent and/or control the negative effects associated with riverbank erosion processes. Because of the riverbed erosion impacts on the loss of land and associated resources, damages to property, infrastructure [4], the riverbed morphology and its flood conveyance capacity, it is often perceived as natural hazard, which historically have been managed mainly by applying technical/engineering measures.

However, the latest scientific concepts, increasingly acknowledging the importance of maintaining the structural and functional integrity of river ecosystems, recognize that besides its negative effects, riverbank erosion has also proven to be highly valuable for ecosysems. Moreover, the adverse ecosystem effects associated with applying the traditional riverbank stabilization techniques are now better understood. The growing knowledge on the benefits the naturally functioning river ecosystems provide has been stimulating the development of the river restoration science.

New riverbank management approaches are being developed as an integral part of the river restoration concept. These approaches, used as an alternative to the conventional riverbed stabilization techniques, are primarily based on the idea of minimizing the need for physical interventions in the riverbed and the riverbanks, thus allowing for free lateral migration of the river within a defined *river corridor*. In practical terms, applying this concept would mean avoiding engineering control of riverbank erosion within a defined corridor.

23.2. The Riparian Corridor Concept

The recently published river restoration work identifies a few main reasons motivating the change of approaches in controlling riverbank erosion, such as: a) high costs for building and maintaining the traditional riverbank stabilization structures; b) the importance

of erosion processes in maintaining the natural riverbed development dynamics; c) the unsustainable nature of some of the engineering stabilization techniques (e.g. reducing the downstream sediment supply stimulates riverbed incision processes); d) the importance of erosion processes in maintaining the beneficial ecosystem functions (e.g. habitats for important aquatic species), whose importance is now better recognized compared to the period of domination of purely river engineering techniques.

Because of the improved understanding of the positive attributes of riverbank erosion, and their contribution to the river restoration goals, the new management approaches are increasingly substituting or complementing the use of the conventional stabilization techniques.

These alternative riverbank management approaches are actually based on the idea of 'allowing' to rivers to migrate freely within a defined corridor where the land ownership related aspects will be specially regulated. This concept in the literature is called with different names, such as: **Riparian Corridor, Erodible Corridor Concept, Stream Corridor**, and other [4].

Although the discussions amongst researchers on the need for introducing such an approach as a river restoration measure are of older date, it is nowadays more widely used, and even incorporated in the national legal systems regulating the water and land-use management, primarily in the developed states. Based on that experience, this paper attempts to popularize the concept, especially in the EU accession countries, adopting the EU WFD as a guidance document for the design of the national river basin management systems.

There are a few definitions of the riparian corridor, calling it as 'space of freedom', or 'space of mobility'. It is actually 'the floodplain in which the active channel can naturally move in order to maintain coarse sediment supply and optimal terrestrial and aquatic ecosystem functioning' [3]. In order to integrate this 'zone of lateral mobility' of rivers into the water and land-use management systems, there is a need for it to be practically defined and incorporated in the respective legal framework.

Expectedly, because of the multitude of barriers and constraints for defining and enforcing the riparian corridor concept, it cannot always be considered as a full alternative to the traditional riverbank stabilization approaches. Therefore, in such situation (e.g. highly modified river systems) any attempt to introduce the concept cannot be in conflict with the existing measures. It should be rather complementing them, if more realistic restoration objectives are to be set and accomplished.

The possibility of applying this concept in practice would depend upon a few key factors such as the importance and value of the potentially enhanced ecosystem benefits (cost-benefit analysis), the nature of the river (e.g. its natural mobility), the need of controlling the erosion processes to protect important structures, and other. Therefore, it can be logically concluded that the viability and feasibility of such an approach is case specific. However, even in highly modified basins, there is still a possibility for limited restoration by adopting the river corridor concept.

23.2.1. Identifying the Possibilities for Applying the River Corridor Approach at a River Basin Scale

Because of the natural variability and interdependence of the elements comprising the river ecosystem, the restoration goals can be best achieved by adopting the river basin as the most appropriate scale for targeting priority action (Fig. 1). Therefore, the Integrated

River Basin Management (IRBM) principles are now widely integrated in national resource management systems (for e.g. through their harmonization with the EU Water Framework Directive). The IRBM concept provides an excellent opportunity for promoting the presented river corridor concept as a restoration approach.

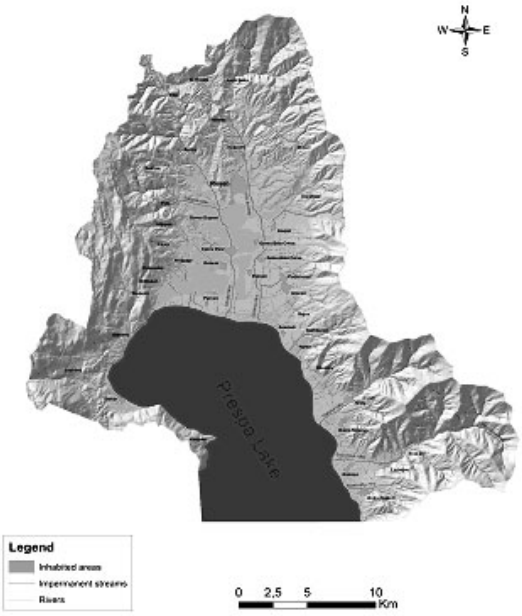

Fig. 1. The river basin is considered to be the most appropriate scale for evaluating the riverbank mobility and targeting restoration action; Example of the Prespa Lake Basin and its hydrological network (source: UNDP/GEF Prespa project)

The WFD based IRBM system establishes environmental objectives for different water bodies based on the evaluation of the divergence between the observed and the reference conditions. In the sense of the river corridor concept, this could be translated into identification of river sections with the greatest deviation from the previously established reference status (defined based on hydromorphological assessment, and by using historical data).

Such an approach allows for identification of river sections, within the basin, which are highly unstable by nature, and whose stabilization is dependent upon very expensive stabilization works. For such sections, a well structured cost-benefit analysis considering the ecosystem goods and services, may show that the removal of the existing stabilization structures is a viable management option. In that way progress toward the achievement of the restoration goals can be accomplished.

In the context of maintaining the natural levels of riverbank erosion, the primary goal is to identify the river sections, which are or may be potentially be unstable [4]. This can be analyzed by different models correlating the riverbed mobility with its slope, grain size, river flow, and the riverbank stability level.

Analyzing in further detail, at a river section scale, the level and the zone of riverbank instability can be determined (for the previously identified unstable sections at river basin scale). Identifying the spatial variability of the instable section is helpful in better planning

of certain developments (e.g. supporting a development at a more stable section, where less physical interventions will be required). The main question to be answered is the longitudinal variability of the riverbank erosion, which actually corresponds to the riparian corridor concept. A method for determining the riparian corridor based on historical analyses is presented below.

The purpose of such an effort would be to inform decisions on planning site selection for developments sensitive to erosion processes (similarly to the flood risk management). The effects of such an approach are twofold: a) better protection of the developments (infrastructure, man-made values) against erosion; b) restoration and/or maintenance of river ecosystem functions and more desirable levels.

The overlapping of the boundaries of the riparian corridor with the land-use/spatial plans, and/or the cadastral maps (land property maps), would provide particularly valuable information supporting the planning of future developments within the river systems.

23.2.2. Defining the Riparian Corridor Through Analysis of Historical Data

There are a wide variety of possible approaches for determining the boundaries of the riparian corridor, ranging from very simple equations to advanced simulation models. For the needs of this paper, only the approaches based on analysis of historical data are briefly elaborated. In an event of availability of historical data (aerial photographs, historical maps), this could be a very reliable approach in defining the zone of river's evolution and geomorphic activity, and consequently the riparian corridor.

For a more recent history of river mobility (10 – 20 years), subsequent aerial photographs can be used, while for longer periods, there is a need of using historical maps. Such an approach can be considered appropriate only when the riverbed is large enough, so that the movement of the riverbed can be captured with subsequent aerial surveys and/or determined with sufficient accuracy on historical topographic maps [9]. The approach is based on overlapping of the historical positions of the riverbed by applying GIS technology (Fig. 2).

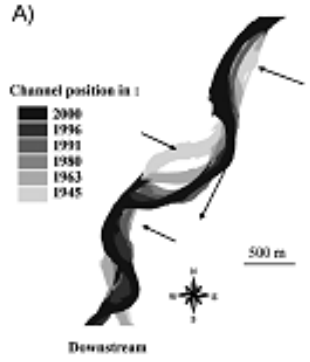

If sufficient number of aerial photographs exists for different time periods, they could provide a good estimate of the river corridor's boundaries. Normally, the information obtained by this approach should be complemented by a geomorphological analysis. Once established, the map derived by overlapping the historical positions of the riverbed, can be updated with the information obtained by the future aerial photographing.

Fig. 2. Example of information obtained by aerial photography; overlapping the historical positions of the riverbed is very helpful in establishing the extent of lateral movement for certain period [4]

In order to make the best use of the information acquired, mechanisms for integrating the riparian corridor into the river basin management system are required. An example of such a system is proposed within the next chapter. Understanding and integrating the zone of lateral migration of the riverbed into the legal framework, provides an excellent opportunity for informed decision-making on the land-use planning. This will allow for enhancing the role of the new riverbank management approaches and substituting and/or

supplementing the purely engineering stabilization works, hence promoting better development and targeting more effective restoration action.

23.3. Incorporating the River Corridor Concept in the Integrated River Basin Management Systems

Integrated river basin management (IRBM) is defined as 'the process of coordinating conservation, management and development of water, land and related resources across sectors within a given river basin, in order to maximize the economic and social benefits derived from water resources in an equitable manner while preserving and, where necessary, *restoring* freshwater ecosystems' [2].

This very generic definition on IRBM recognizes the importance of restoring freshwater ecosystems, including rivers. The restoration function of the IRBM concept provides the mechanism of integrating the river corridor approach as one of the important restoration measures in the national river basin management systems in the EU and accession countries (evolving as a result of the harmonization with the WFD). In addition, the WFD calls for protection, improvement and restoration of the artificial and the heavily modified water bodies aiming at reaching their 'good status' [1].

Although there may be variations in certain particularities of the country specific systems, still all of them, at least formally, are based on the general IRBM concept. Therefore, the next figure (Fig. 3) shows a generic proposal on the incorporation of the river corridor concept in the national IRBM systems, considering both the water (river basin) and land-use (spatial) management system.

The proposal contains practical steps and refers to the most suitable legal instruments (at policy and planning level) for incorporating the river corridor concept, thus providing the ground for the future restoration work. It actually gives an outline of an operational framework linking the riparian corridor concept, as a restoration management approach, to the IRBM's restoration functions.

The most suitable way of conducting the proposed work is to combine it with the process of preparation of integrated river basin management plans (as demanded by the WFD). The planning process requires that the water bodies are delineated in accordance to a set of criteria, including hydromorpological ones, which are relevant to the river corridor concept.

One of the first steps of the process would be to study the basin's hydrological network, including developing and inventory of existing stabilization works (erosion control structures) applied for different river sections. For the priority rivers / river sections, assessment of availability of historical data on the positions of the riverbed for different periods should be carried out (presence of historical maps and aerial photographs.

In order to identify the current positions of the riverbeds of the selected rivers, supplementary aerial photography may be conducted. The overlapping of the newly obtained positions of the riverbeds with the historical information (if available for a period of a few decades), is instrumental in determining the zone of lateral mobility – the riparian corridor. Such an assessment will provide valuable information to support the decisions on the possible removal of the existing stabilization works.

Another benefit of understanding the river corridor zone is to identify the reference conditions for the river sections, which may sometimes overlap with the delineated water

bodies. The divergence between the actual and the reference conditions is the basis for setting out the environmental objectives for the particular sections. Normally, providing free space of mobility of the riverbed within the river corridor would be one of the main restoration objectives.

However, the river corridor determined as such, considers only the geomorphic evolution aspects of the river system, and excludes the socio-economic and political dimensions, which are critical to its applicability potential.

Therefore, the next proposed steps is to overlap the river corridors of the priority sections with the land property maps (cadastral information), to identify the ownership structure within the corridor (size of private vs. state owned land). This information would be critical in assessing the level of constraints affecting the application of the concept. Other valuable information supporting the decision-making process regarding the implementation of the riparian corridor concept would be obtained by assessing the value of the 'affected' land based on its categorization (productivity potential, likely purpose and the like).

A well structured cost-benefit analysis considering the economic aspects of ecosystem goods and services would be particularly instrumental in defining the approach of involving the affected stakeholders in effectuating the river corridor concept. If considered feasible, the establishment of the river corridors within privately owned land can be achieved by negotiations and/or financial stimulations for owners to prevent certain types of development, allowing certain degree of riverbank erosion. Another option would be the state to purchase the private land, although this would normally be a more expensive option, not always practically feasible.

A comprehensive public participation process should be conducted to validate the proposed boundaries of the river corridor. Because of the constraints mentioned before, it is to be expected that the boundaries of the 'negotiated' corridor would be more narrow compared to the 'geomorphic' ones. However, only the negotiated and agreed boundaries can be considered feasible to enforce in practice. Therefore, the 'legal status' should be assigned to the 'agreed' river corridor only.

The integrated river basin management plan is one of the instruments, but in many legal systems in the region, the land-use (or spatial) plans are positioned higher in the national and regional planning hierarchy. Since the land-use plans set out the strategic development objectives for a region, the river corridor boundaries developed under the river basin management planning process should be incorporated in the spatial plan, to ensure strong legal basis for their implementation.

Considering the likely costs associated with the enforcement of this concept, long-term strategy should be developed and backed-up by appropriate financial mechanisms. The information from the cost-benefit analysis would be of a critical importance in establishing the financial mechanism.

Since the land-use plans are positioned at the top of the planning system's hierarchy, the incorporated river corridor boundaries will be taken up by the lower level plans (e.g. urban plans, rural development plans, area action plans, and other). In such a way, this integrated planning system, allows for gradual restructuring of the land-use patterns within the basin, including the river corridor. Even if the river corridor cannot be entirely enforced, still, these plans can define the types of permitted developments within the corridor, thus reducing the impact on the natural structure and functions of the river ecosystem.

The implementation of the river corridor concept should be subject to monitoring and evaluation. This monitoring can be integrated either in the overall monitoring of the implementation of the river basin management plans (controlling the achievement of the

ecological objectives, i.e. the reference conditions for each water body), or the implementation of the land-use/spatial plans. A well developed, cost-effective monitoring would allow for adaptive management of the restoration processes.

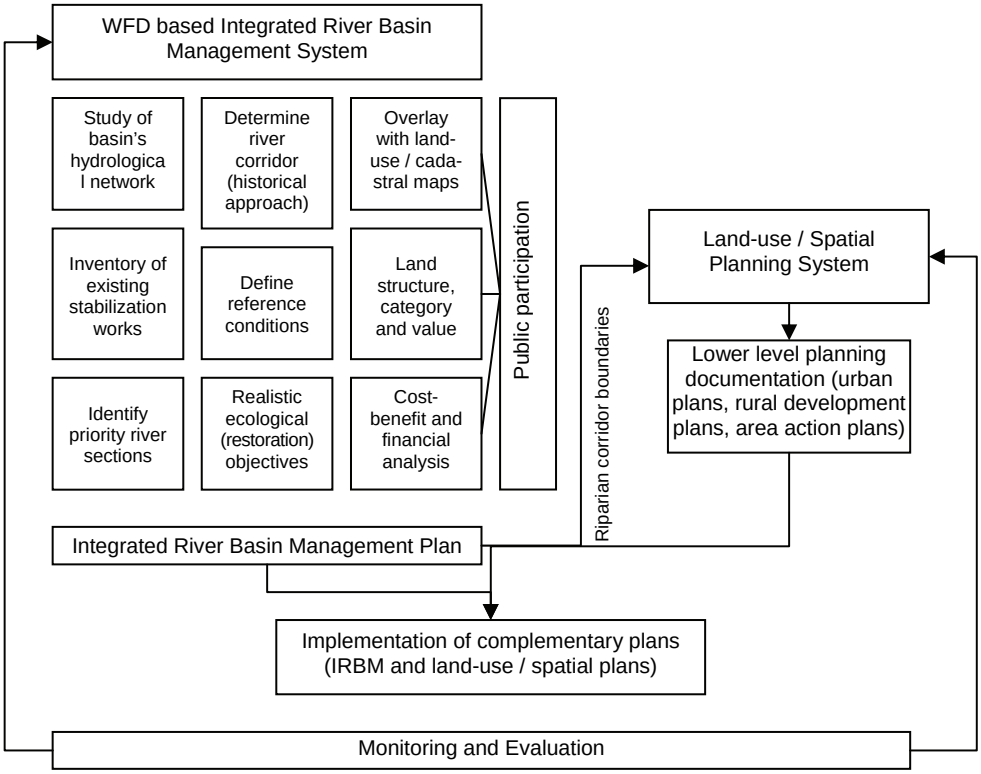

Fig. 3. The necessary steps for incorporating the river corridor concept in the IRBM; The legally defined River Basin Management Plans and the Land-Use / Spatial Plans provide the access points for the practical implementation of the concept

23.4. Conclusions

The riparian corridor concept can be a viable alternative to the conventional riverbank stabilization work. The concept actually attempts to maximize the combined benefits, both economic and environmental, of allowing certain degree of lateral mobility of the riverbed, and protecting the property and different types of development beyond the corridor's boundaries.

The cost-benefit analysis which considers the enhanced ecosystem goods and services as a result of the restoration work is a valuable instrument in support to the decisions on adopting this concept in specific basins. The river basin is the most appropriate scale for implementing restoration work. Therefore, the identification of the potential river sections

where the riparian corridor concept can be applied should be conducted as part of the process of developing the integrated river basin management plans.

In this way the concept can be integrated in the national river basin management systems. A very strong basis for the enforcement of the concept would be established if the boundaries defined under the river basin management systems are also replicated into the national/regional land-use/spatial plans.

However, in order to enhance the likelihood of enforcement of the riparian corridor concept, its boundaries should not only take into account the geomorphic and ecological considerations. The socio-economic, political and financial dimensions are of critical importance for the feasibility of the concept. Therefore, before assigning to it a legal status, the riparian corridor's boundaries should be subject to negotiations with the key stakeholders through a well structured participatory process.

References

[1] European Commission: Water Framework Directive 2000/60/EC, 2003.
[2] Global Water Partnership Technical Advisory Committee, Integrated Water Resources Management, GWP, Stockholm, Sweden, 2001.
[3] Malavoi J. R., Bravard J. P., Piégay H., Herouin E., Ramez P.: Détermination de l'espace de liberté des cours d'eau. Guide technique no. 2, SDAGE RMC 1998.
[4] Piégay H., Darby S. E., Mosselman S., Surian N.: A Review of Techniques Available for Delilmiting the Erodible corridor: A Sustainable Approach to managing Bakn Erosion. River Res. Applic. Vol. 21, 773–789, 2005.
[5] Popovska C., Krstic S.: River Restoration Manual, United Nations Development Programme, Skopje 2010.
[6] Popovska C., Sekovski D., Stavric V.: Problem Identification and Strategic Planning of River Restoration Projects. 4th International Conference on Water Observations and Information Systems for Decision Support-BALWOIS, Ohrid 2010.
[7] Sekovski D., Popovska C.: Restoration Measures and Practices in the Prespa Region. Eleventh International Symposium on Water Management and Hydraulic Engineering (WMHE 2009), Ohrid 2009.
[8] Surian N., Rinaldi M.: Channel adjustments in response to human alteration of sediment fluxes: examples from Italian rivers. Sediment Transfer through the Fluvial System Proceedings of a symposium held in Moscow, IAHS Publ. 288, 2004.
[9] Surian N., Ziliani L., Comiti F., Lenzi A. M., Mao L.: Channel Adjusstments and Alteration of Sediment Fluxes in Gravel-Bed Rivers of North-Eastern Italy: Potentials and Limitations for Channel Recovery. River. Res. Applic. 25: 551–567, 2009.
[10] Surian N.: River Channelization. Encyclopedia of Water Science DOI: 10.1081/E-EWS-120038046 by Taylor & Francis 2005.

24 Numerical and Physical Simulation of a River Bend Flow

Georg Schuster, Cedomil Josip Jugovic, Gerold Hepp, Thomas Pfaffenwimmer, Hans Peter Nachtnebel (University of Natural Resources and Life Sciences, Institute of Water Management, Vienna, Austria)

24.1. Introduction

In the field of hydraulic engineering, different jobs need a closely investigation by a hydraulic model. For this purpose two different methods of simulations are available. On the one hand, physical scale models, build up in special laboratories. On the other hand, numerical models, that can be used by every engineer on a computer. Physical scale models are often associated with high costs and extensive buildings works. Thus, in these days more often numerical models are used. To select and use a certain numerical model, the flow conditions in the simulated area respectively the numerical model must fulfill some preconditions. This paper is focused on the inundation of forelands of a river – a typically job for hydraulic engineers. The dimensions in length and width of a river-channel are much bigger than the depth. So we can consider the channel as a shallow water body. For these jobs, which include an essential interaction between the channel and the foreland, two-dimensional model can be used [7, 9]. Typically, two-dimensional hydraulic models use simplified equations which give only one mean velocity value and direction in every ground view cell, known as shallow water equations. Yet, the mainly horizontal expansion is not the only precondition for two-dimensional simulations. As well, both, a uniform vertical velocity distribution and a hydrostatic pressure conditions, are implied. Yet, in natural rivers always a three dimensional helicoidally flow occur. Within straight or stretched river section this three dimensional flows has no essential effect. However in both, river bends and in river diversions, these currents can get more important [6]. River bend flows are essential affected due to centrifugal forces and helicoidally flows. So, either a physical scale model or a sophisticated three-dimensional numerical model might be applied. If a three-dimensional numerical model should be used, the model must provide free water surface flow (which means a two-phase flow), an inhomogeneous vertical velocity distribution (usually no problem for a three dimensional model) and non-hydrostatical pressure approach (vertical momentum transfer). Mainly the first and the last precondition are sometimes not included in three-dimensional models. Thus the problem of a river bend flow can be solved correctly only by specific software with a high effort of computer power, which includes also long calculation times. Usually, for hydraulic engineering jobs this expenditure of work makes no sense. Therefrom software developers try to optimize their products, to improve simulation results also in river bend flow conditions. Nevertheless, due to the simplified reproduction of the real flow conditions, two-dimensional models will show always differences to the real flow.

This paper deals with HYDRO_AS-2D. It is a two-dimensional model and offers high calculation speed and stability. Furthermore also convective terms are used, whereby the velocity head is taken into account and the calculation of the water level in river bends is improved [4]. Thus HYDRO_AS-2D may be the missing link between difficult three-dimensional simulations and insufficient two-dimensional models.

24.2. Objective

To evaluate the results of numerical models, different studies have been conducted. Yet, in this paper a numerical two dimensional model was used for an exceeding challenge – modeling a river bend flow. Usually in river bends occur essential three dimensional flow conditions. Hence either physical or complex three dimensional models should be used. By the use of a comparable physical model, the verification of the numerical model was feasible. Despite the good performance of the software HYDRO_AS-2D it was expected, that essential differences between the numerical model and a physical model were measureable. Thus a comprehensive series of test runs where conducted, to illustrate the differences between the numerical and the physical model.

The objective of this paper is a comparison of a two-dimensional depth-averaged numerical simulation and a physical scale model. It should be observed, if a two-dimensional numerical simulation of a river bend can reproduce the helical flow situation basing on the centrifugal forces. The comparison of both models is founded on the following physical sizes:

— Water levels of both river banks measured in thirty profiles,
— Water levels of particular points in the river,
— Flow velocities in selected profiles.

This paper should show both, opportunities and limits of two-dimensional numerical simulations of river flows. More precisely, it should be proved, if it is possible to use two-dimensional models for simulations of river bends and river diversions. Yet, the result can support the selection of an adequate model for specific hydraulic engineering jobs.

24.3. Data Acquisition – Used Models

For the presented comparison of a two dimensional numerical model and a physical scale model was used. To obtain a good comparability of the models, the same scale and size was used for the numerical and the physical model. This means, that the numerical and the physical model operate under the same conditions. Thus, all measurements of the physical model can be compared directly to the results of the numerical model. Thereby it is possible to avoid any error by scaling the data from the physical model to the numerical model and vice versa.

In the area of hydraulic engineering often two types of basic parameter are collected on models: flow velocities and water levels. These basic parameters are used directly or for further calculation of other parameters. Flow velocities are important basic data to calculate sediment transport and identify regions of sediment aggradations or degradations. Water levels are needed to the dimension of flood water protection measures and to indicate

inundated areas during flood events. Thus flow velocities should be monitored over the whole cross section, but water levels are mainly interesting at the riverbanks. Basing on these fundamentals an adequate scheme of the control measurements was developed. So the flow velocity measurements were conducted in multiple cross sections. Specific attentions were on both areas, near the river diversion, and in the river bend. Thus the results of the numerical can be checked in areas with difficult flow conditions. The measurement of the flow velocities was conducted by electromagnetic sensors, which allow barely disturbed and multi-dimensional measurements. To receive comparable measurements in shallow water only one measurement and in deeper water an averaged two point measurement is used to check the model relations. The measurements were conducted in selected river profiles, which mean, that multiple measurements were done in each cross section. Yet, in the numerical simulation, the velocity distribution is displayed in ground view. The comparison of the flow velocities of both models is carried out in the gauged cross sections.

The measurement of the water levels in the physical model was accomplished by two different methods. On the one hand, the elevation of the edge of the water was gauged on both river banks; on the other hand the water level within the channel was detected by pressure measurement on selected points. The more interesting reference values are the gauged water levels on the river banks, because for hydraulic engineering issues mostly the point of the overflow is interesting. Yet, near the water´s edge also a lot of turbulence occurs mostly triggered by small unsteadiness of the surface of the river bank. Therefore it is difficult to get a representative value of the water level in these zones. Additionally you must keep in mind that these values of the water level are characteristic only for one local point and can change radically in space and time. Thus additionally pressure measurements within the channel on selected points were conducted. These measurements may be not so interesting for tasks of hydraulic engineering, but they afford convenient data for a reliable comparison of the models. So the captured data of the model gives the opportunity to make both, a very solid and a job-focused comparison of the water levels.

The data collection in the numerical model is much easier. Basing on the principles of numeric modeling, all calculated parameters can be saved at once in every time step over the whole model. This means, that we know all calculated values of every calculated point of the model. Vice versa, in the physical model, we can measure at a specific time usually only one point. Hence, in physical models is it necessary to keep a steady-state condition allow coherent data measurement series. Thus, also in the numerical model a steady-state flow is simulated. Due to the differences in the data collection in contrast to the physical model, in the numerical model the calculated data are visualized in a global plan view. Hence the data collection in the numerical model is more in two dimensional areas, where else in the physical model the measurements are conducted punctual. Thus the comparison of the parameters implemented only in the selected sections, as described above.

24.4. Method and Model Calibration

For the numerical simulation a state of the art two dimensional model, HYDRO-AS_2d, was chosen. The procedure integrated in HYDRO-AS-2D is based on the numerical solution of the 2D current equations with Finite-Volume-Discretisation [5]. By this method only horizontal flow processes can be calculated. Thus, formally the model is not suitable to simulate flow processes in river bends and diversons. Yet, by the use of the convective term also the velocity head can be taken into account, whereby the results of the water

levels are approved. The use of such improved two-dimensional models can be a great effort in practical use, because these programs have higher computation speed and they are easier to use. So, if this model can reproduce the flow in adequate accuracy, it can be used instead of high sophistic three-dimensional simulations or physical models.

24.4.1. Model Calibration

The most important challenge of developing a model is the calibration [3]. Thereby the intention is to minimize the differences between the measured and the modeled data. It is recommended to use a comparison of both, water levels and flow velocities [7, 8]. To optimize the numerical model in a way to reduce the differences between measured and calculated values, empirical parameters of the chosen numerical model are fitted [2]. Yet, it should be kept in mind that during this process the parameters are not determined by a physical process, but the whole model is calibrated. Thus the mathematical, physical, and geometrical characteristics of the model have an essential influence on the value of the parameters. Therefore the parameters are not only physical sizes which can be measured or compared directly to the reality. So the transfer to nature or other models is limited. Nevertheless it makes sense to use realistic values and stay in a confidence interval to avoid nonphysical phenomena in the numerical model. In the used model, HYDRO-AS_2d, the parameters of bed roughness and turbulence viscosity can be adjusted. The model which is used for this investigation used is influence mainly by bed turbulences [2]. Thus the calibration of the turbulence viscosity parameters is not used. In the numerical simulation as well as in the physical model a steady-state condition was simulated. Hence the simulated time in the numerical model must be chosen long enough, until this steady-state condition is reached.

24.4.2. Model Parameters

Basing on the physical model, areas of different roughness were used also in the numerical model (Fig. 1). Due to the fact, that the physical model was founded on a real nature problem, also the areas of different roughness were adapted to this natural example. In the physical model these different roughness were implemented by using different types of gravel or stones (Fig. 2). In the numerical model, the roughness parameter can be entered directly. At the beginning of the numerical simulation the parameters for the roughness were chosen by given values of the literature (Tab. 1).

Table 1

Starting values of the Strickler parameter k_{st} for the calibration (Strickler 1923, cit. [1])

Surface	Strickler parameter [$m^{1/3}$ / s]
Concrete, new, depending on surface	63 – 92.5
Coarse gravel	35
Middle gravel	40

By the calibration new parameters for the roughness were fitted. These roughness parameters used for the numerical model correspond only to physical scale model. Due to the scale, also the roughness parameters are different to common parameters in the nature.

In Tab. 2 all used roughness parameters are shown and converted to real scale. Yet, the real scale parameters are not used and only to give a better orientation.

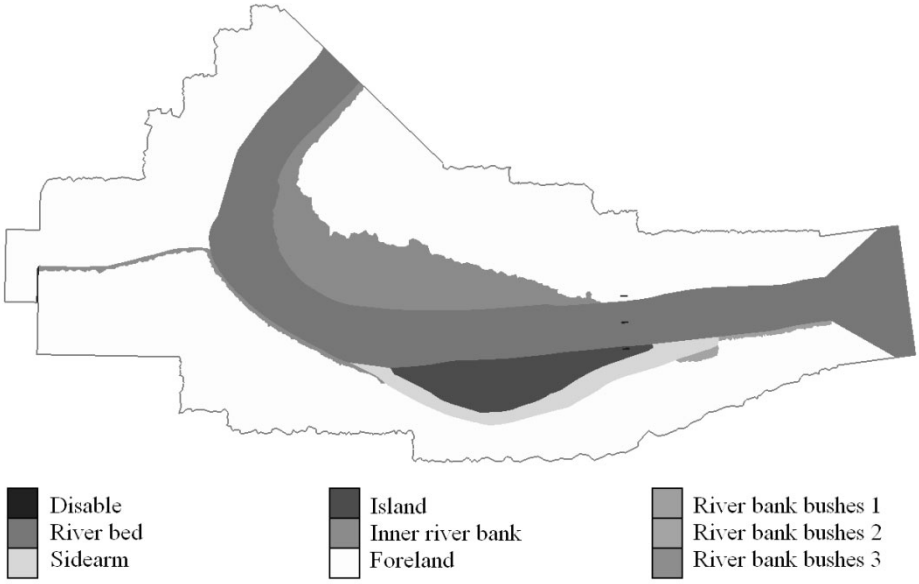

Fig. 1. Areas of different roughness in the numerical model. On the inner riverbank and the riverbank grow tree and bushes. In the areas described as “River bank bushes” mainly bushes are growing

Fig. 2. In the physical scale model, the roughness was implemented by using gravel and small stones

Due to the small water depths, the used values for the numerical model are in the lower range of the given values of Tab. 1. As can be seen in Tab. 2 with the comparable values in real scale, these values represent a realistic reproduction of the nature. But this

only a lateral effect of the intended idea – the test if a two dimensional model can reproduce the occurring flow conditions of river bends and river diversions.

Table 2

Strickler paramerter k_{st}: calibrated values, converted to real-scale, and comparable values in real scale from literature – all values in [$m^{1/3}/s$]

Region	k_{st} – calibration	k_{st} – converted	k_{st} – comparable values in reality
River bed	52.5	25.57	16.5 – 40.0
Sidearm	55.0	26.78	25.0 – 33.5
Island	15.0	7.30	6.0 – 14.5
Inner river bank	35.0	17.04	12.5 – 25.0
Foreland	65.0	31.65	–
River bank bushes 1	15.0	7.30	6.0 – 14.5
River bank bushes 2	15.0	7.30	6.0 – 14.5
River bank bushes 3	25.0	12.17	6.0 – 14.5

24.4.3. Quality of Calibration

For the comparison of the numerical and the physical model and to control the quality of the calibration water levels and flow velocities were used.

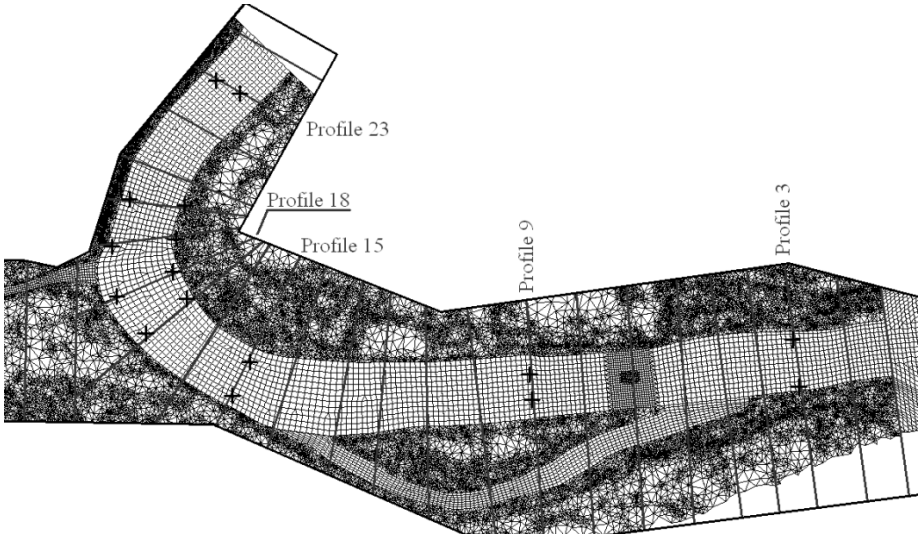

Fig. 3. Position of Profiles and pressure gauging points (crosses)

Water Level on River Banks. One part of the test of the quality of the calibration is the comparison of the water levels on the left and right river bank. Therefore the water levels were measured in 24 profiles in the physical model. Because of the turbulent flow the minimal as well as the maximal water level was recorded. These water levels are compared

to the results of the numerical model. Thus the water level in these points of the numerical model should be between the minimum and maximum value. In Fig. 3 the position of the 24 profiles is presented. Thereby the profiles near the inlet and the outlet are influenced essentially from the boundary conditions. Thus there are not suitable for an objective comparison. So the measured values of the first and the last profile are not shown and the values at profile 2 and 23 are not representative.

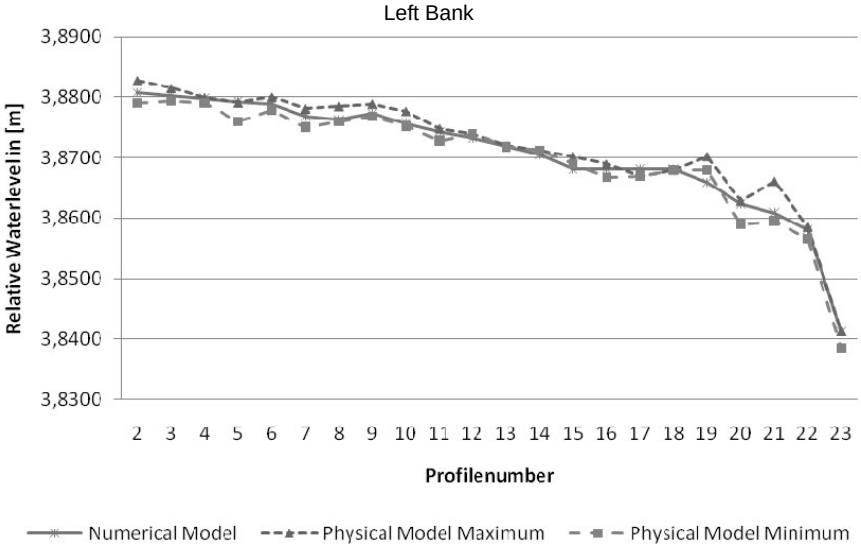

Fig. 4. Comparison of the water levels of numerical and physical model on the left river bank

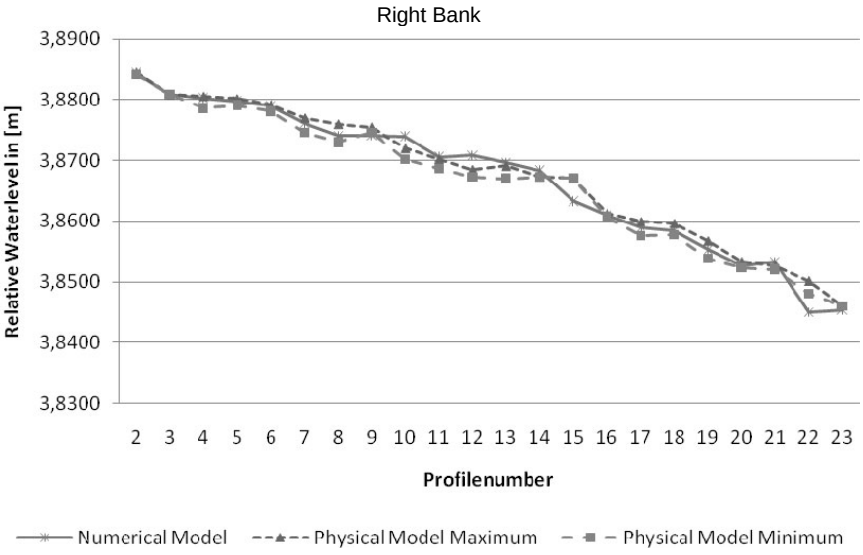

Fig. 5. Comparison of the water levels of numerical and physical model on the right river bank

A good similarity of the numerical and the physical model can be seen on both river banks (Fig. 4 and 5). Significant is the very good reproduction of the higher water level on the outer side of the river bend. A difference can be seen on the left bank in the region where a smaller channel flows into the river. On these spot high turbulences and mixture processes occur. Surprising are the differences on the right river bank facing the island, stream-up the river bend. Despite of all tries, the water level in this area could not be reproduced by the numerical model. That is as more interesting, as there seems to occur no critical three dimensional flows. These differences can only explained by turbulences and eddies which occur next to the bank.

Pressure Measuring on Selected Points. On selected points in the river bed the pressure was gauged. Contrary to the measured points on the river banks, these points are within the river channel. Due to the measuring method, the recorded values are not influence by turbulent flow processes and more stable. The comparison of the pressure measuring points gives a similar result, as by the measurements at the riverbank. The results of the numerical model show a good analogy to the measured water levels. Yet, on the left side of the river, where the sidearm (Profile 15) and the small channel (Profile 19 and 20) flows into the main river some discrepancies occur. These results show again, that small water level differences may occur, if turbulences or lateral flows must be taken into account.

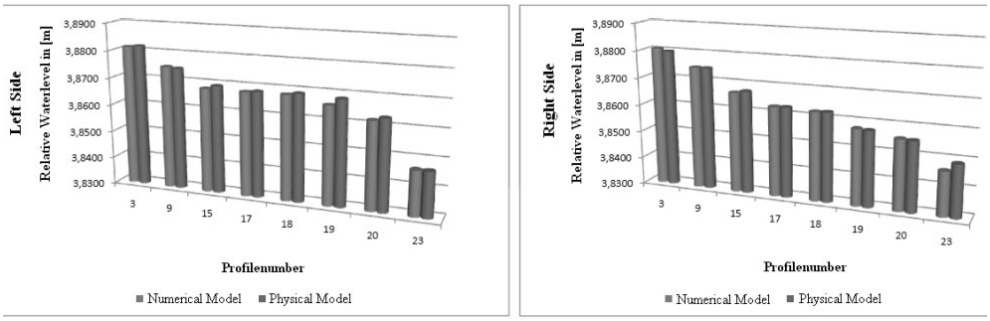

Fig. 6. Comparison of pressure measuring on selected points of numerical and physical model on the left (left figure) and on the right (right figure) river side

Flow Velocity Profiles. Additionally to the comparison of the water levels, also the flow velocities were controlled. The flow velocities were measured on severally profiles and realized by gauging with a two dimensional electro-magnetic sensor in the middle of the water depth. In Fig. 7 four selected profiles are presented. Due to the measurement in half of the depth, the bed-near flow velocities are not represented. Yet, the numerical model calculates a mean value of the whole flow velocities. Therefore the calculated mean flow velocities are always lower than the measured velocities. But it can be seen, that velocity distribution of the numerical model fit good to the measured data. However, on the left side of Profile 19 an error of the numerical model occur. Because of the small channel, which flows into the river, in this location higher turbulences occur. The numerical model underestimates the energy dissipation by the turbulences, by what means that the water level at this location is calculated to low and the flow velocity is calculated to high. Furthermore show the velocity profiles of the numerical model a more smooth distribution. The reason therefore can be found in the implemented simplifications of the numerical

model as well as in the roughness elements used in the physical model. The singular roughness elements of the physical model cause local differences in the flow velocity.

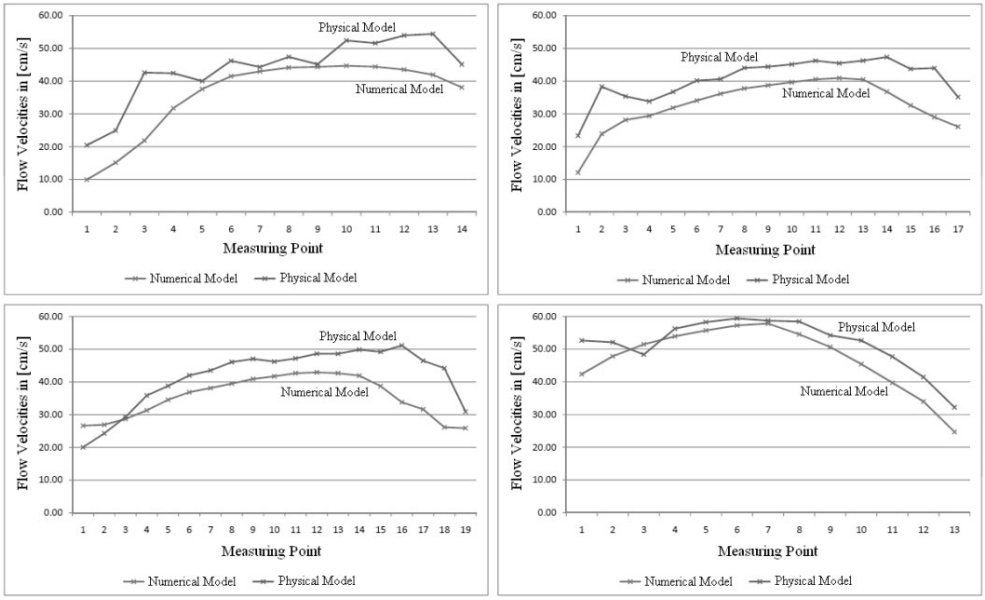

Fig. 7. Comparison of velocities in the profiles. (on top left: Profile 3; on top right: Profile 16; bottom left: Profile 19; bottom right: Profile 22)

24.5. Model Validation

By means of validation it the numerical model should be tested under different conditions. So it can be shown, that the numerical model is not only under the calibrated conditions reliable. Therefore also changed discharges were used for the simulation in the numerical as well as in physical model. The methodology of measurement and data acquisition are the same as during the calibration.

Water Level on River Banks. Over all, the results of the validation are quite similar to the calibration (Fig. 8 and 9). Actually the good similarity of the left bank is also given. As in the calibration also in the validation differences in the region of the inflow of the small channel (Profile 19) occur which is caused by the arising turbulences. Moreover in the other regions of higher turbulences, like in Profile 3 – 5 (bifurcation of the sidearm) and the inflow of the sidearm (Profile 13 and 14) also errors of the numerical model appear. On the right bank also a difference between the models in the region of the island can be seen.

Pressure Measuring on Selected Points (Fig. 10). During the compare process in the validation even better a better correlation of the left side between the models could be found. Yet in Profile 9 the result is not so good. Thus this difference is influenced by regional flow conditions. On the right side of the river, also a good similarity was achieved.

Flow Velocity Profiles. Also the measured velocities were used for the validation. Due to the fact, that are also here no significant changes occur, only two profiles are presented. In Profile 9 both, the numerical and the physical model, show lower flow

velocities on the right side. The velocity distribution of the numerical model is in Profile 9 similar to the physical model. In Profile 19 the differences on the left side between the numerical and the physical are smaller, which can been seen also in the water levels in this region. Yet, the underestimation of the numerical model on the right side of Profile 19 is still there.

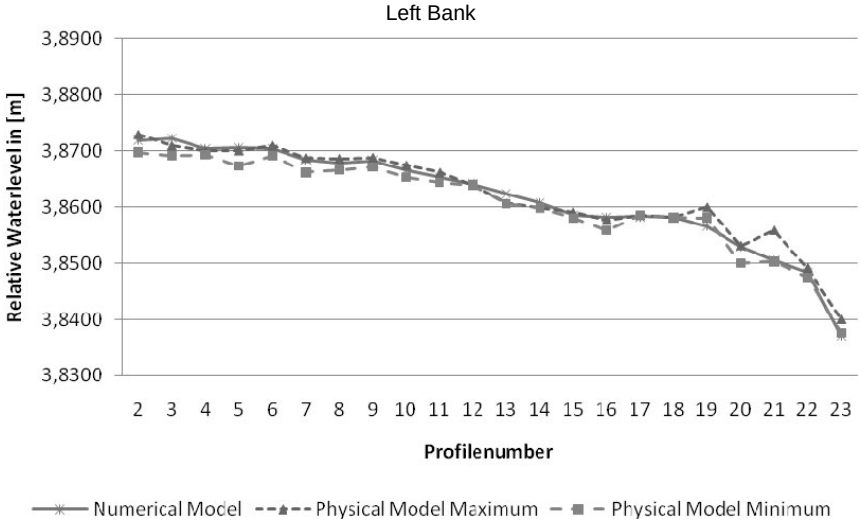

Fig. 8. Comparison of the water levels of numerical and physical model on the left river bank

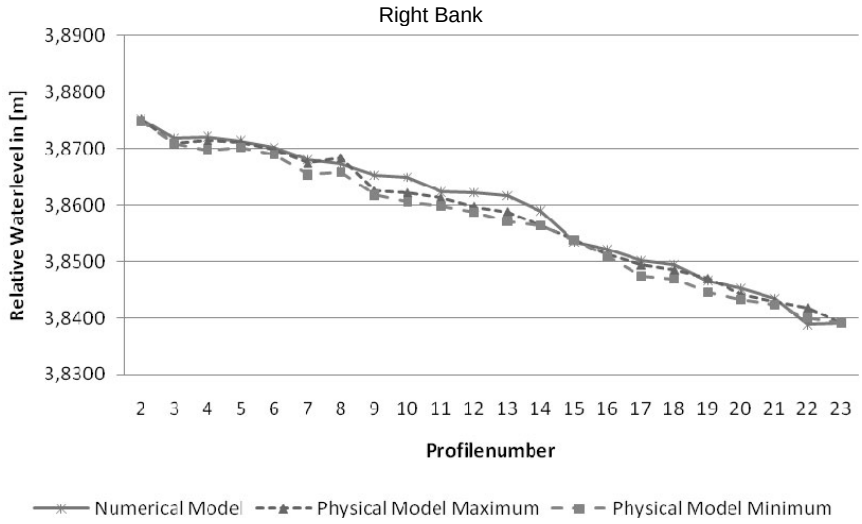

Fig. 9. Comparison of the water levels of numerical and physical model on the right river bank

The reason therefore is the influence of the small channel which discharges into the river. In the physical model was noticeable, that through the appearing turbulences by the inflow of the small channel the stream of the river was forced to the opposite bank. Thus near the confluence the flow velocities are smaller and on the facing bank they are higher. Since the

numerical model underestimates the turbulences, the flow velocities near the inflow of the small channel are higher and on the opposite right bank lower than in the physical model.

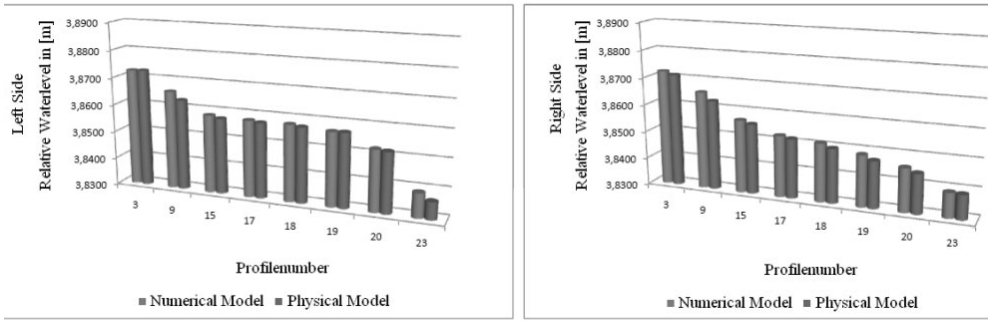

Fig. 10. Comparison of pressure measuring on selected points of numerical and physical model on the left (left figure) and on the right (right figure) river side

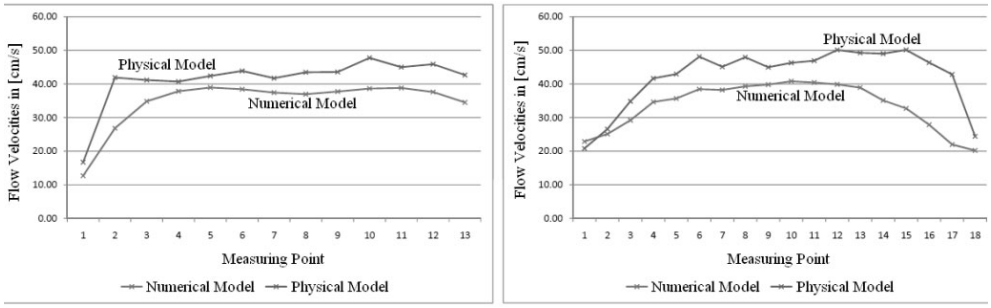

Fig. 11. Comparison of velocities in the profiles. (left: Profile 9; right: Profile 19)

24.6. Conclusion

The presented data show that also an improved two-dimensional numerical model can be used to compute the flow characteristics of a river bend reliable. Though it should be kept in mind that therefore only simplified equations are used. So the water level of also in river bend can be predicted very well. But the calculated flow velocity is a depth averaged value. This means, that the vertical velocity distribution is ignored. Thus differences of measured and calculated flow velocities can occur.

In regions of high turbulences like river diversions or estuaries the two dimensional model can underestimate the energy dissipation. Thus flow velocities may be too high and water levels to low. The explanation therefore is on the one hand the high fluctuation of water levels and flow velocities in time and on the other hand significant three dimensional progresses. If the river diversions or inflows are streamlined and smooth and only less turbulences occur, the two dimensional model can calculate the flow correct, as seen at the side arm. Yet, if a small channel flows perpendicular with an essential bed level gradient into a river, essential three dimensional turbulences occurs, which cannot be reproduced by

a two-dimensional model. Therefore three dimensional models with high spatial and temporal discretisition or a physical scale model are need.

The results are better than expected. but are based on an essential simplification of the occurring processes. Thus the used two-dimensional software is appropriate for tasks of flood prediction in river bends. Though, for the simulation of small local flow characteristics more sophisticated models are needed. Yet, such detailed information is only needed by habitat modeling or detailed bed load transport analysis. Hence a wide field of hydraulic engineering tasks can be done by two-dimensional simulation.

References

[1] DVWK: Hydraulische Methoden zur Erfassung von Rauheiten. Schriftenreihe des DeutschenVerbandes für Wasserwirtschaft und Kulturbau e. V., Heft 92; Hamburg Berlin: Verlag Paul Parey, 1990.

[2] DVWK: Numerische Modelle von Flüssen. Seen und Küstengewässern. Schriftenreihe des Deutschen Verbandes für Wasserwirtschaft und Kulturbau e. V. Heft 127; Bonn: Wirtschafts- und Verlagsgesellschaft Gas und Wasser mbH., 1999.

[3] Forkel Ch.: Numerische Modelle für die Wasserbaupraxis: Grundlagen. Anwendungen. Qualitätsaspekte. Mitteilungen des Instituts für Wasserbau und Was-serwirtschaft der Rheinisch-Westfälischen Technischen Hochschule Aachen. 130; Aachen: Shaker Verlag 2004.

[4] Nujic M. [Bearb.], Schwaller G. [Bearb.]: Wasserwirtschaftliche Rahmen-untersuchung Salzach. 2d-Abfluss-Simulation. Ständige Gewässerkommission nach dem Regensburger Vertrag. München 2000.

[5] Nujic M.: HYDRO_AS-2D. Ein zweidimensionales Strömungsmodell für die wasserwirtschaftliche Praxis. Benutzerhandbuch 2004.

[6] Hickin Edward J.: "Meandering Channels". In Middleton. Gerard V. Encyclopedia of Sediments and Sedimentary Rocks. New York: Springer, 432. ISBN 1 402 008724, 2003.

[7] Lfu: Hydraulik naturnaher Fließgewässer. Teil 4 – Numerische Modelle zur Strömungssimulation. Oberirdische Gewässer. Gewässerökologie 79. 1.Auflage 2003.

[8] Morvan H., Knight D., Wright N., Tang X., Crossley A.: The concept of roughness in fluvial hydraulics and its formulation in 1D, 2D and 3D numerical simulation models. Journal of Hydraulic Research, Vol. 46, No. 2, 191–208, 2008.

[9] Öwav: Fließgewässermodellierung – Arbeitsbehelf Hydrodynamik. Grund-lagen. Anwendung und Modelle für die Praxis. ÖWAV-Arbeitsbehelf 37, 2007.

25 Application of Rainfall – Runoff Model for the Analysis of Extreme Outflow from the Upper Strzyża Basin

Michał Szydłowski and Piotr Zima (Gdansk University of Technology, Faculty of Civil and Environmental Engineering, Poland)

25.1. Introduction

The purpose of the paper is to present the application of rainfall – runoff model for the analysis of extreme outflow from the upper Strzyża basin. The Strzyża Creek is a natural stream that flows from the Gdańsk moraine hills and which supplies the Dead Vistula and finally flows to the Baltic Sea (Fig. 1). The stream also performs the function of the rainwater and snowmelt collector. The intesive urban expansion in the direction of moraine hills is observed in the last half-century in the city of Gdańsk. The catchment transformation causes an acceleration of surface runoff, increase of discharge in the Strzyża Creek and its tributaries. The change of hydrological nature of the catchment has resulted with an increase of the flood risk in the city due to limits of stream conveyance and reservoirs capacity.

The very intense outflow was observed in Strzyża basin during rainfall event on September 2010. It has been resulted with dam break of Nowiec II reservoir and flood risk in the Gdańsk quarter called Matemblewo. The paper presents the hydrological model application used for the reconstruction of reservoir inflow hydrograph due to real precipitation observed before the dam failure. The aim of the study was to determine the runoff from the basin of the upper section of the stream during the real intensive rainfall. The entire episode of recorded rainfall lasted from 27 to 29 September 2010, and the aggregate amount of rainfall in this region reached a value of 90.2 to 150.4 mm. The intensive outflow from upper Strzyża basin has caused the failure of the earth dam of Nowiec II reservoir and sudden outflow in the Gdańsk Wrzeszcz quarter direction. As the model of rainfall – runoff transformation the SCS curve method and SCS unit hydrograph were used for estimation of precipitation loss rates and surface outflow, respectively. The HEC–HMS computer model was applied for numerical simulation of runoff from upper Strzyża drainage basin.

25.2. Strzyża Catchment Characteristic

The location of upper Strzyża basin is presented in Fig. 1. The total length of Strzyża Creek is 13.3 km, the catchment area is 35.15 km^2 and the average bottom slope is about 9.9‰. The average discharge at the mouth is 0.226 m^3/s. During the rain events the flow in the channel is increasing significantly as a consequence of the fact that this natural stream is

a collector of stormwater from urban areas. The water management in the catchment is possible due to reservoirs located along the creek. There are eight reservoirs located along the creek with a total area of 10.2 ha and the retention of about 80 thousand m^3. Moreover, there is the Jasień Lake of water storage about 138 thousand m^3 in the upper part of the Strzyża basin.

The Strzyża Creek is draining the Gdańsk moraine plateau. The relief is complex in this region as a result of the last glaciation. The hills reach 170 m above sea level. The glacier land consists here mainly of clay and silt. There are also observed sands and gravel materials in the upper part of the catchment. The lowlands of the catchment are covered with alluvial deposits like sands, organic parts with gravel or clay and the muds.

The Strzyża Creek runs for 8 km in a natural open channel in the upper part of the catchment. It can be defined here as a mountain stream with a significant slope and high flow velocity. In the lower part the stream flows into area becoming more urbanized and it often runs in the pipeline being a part of the stormwater channel system.

Fig. 1. System of streams in Gdańsk. Location of upper Strzyża catchment in circle

25.2.1. The Upper Strzyża Catchment

The outflow section of the analyzed upper Strzyża catchment is located upstream the Nowiec II reservoir and downstream the outlet of the Jasień Creek. The dam of the Nowiec II reservoir is placed at km 7 + 485 of the Strzyża Creek. The outlet of Jasień Creek is at km 7 + 800. At the beginning of the Strzyża Creek the Jasień Lake is located. The total length of Jasień Creek is about 3.5 km the slope is about 14.7‰.

In the upper part, the Strzyża flows through the forest area with the complex relief. Upstream the km 11+000 of the stream the Kiełpinek reservoir is located. The reservoir receives the water from catchments of the Strzyża springs, Matarnicki Creek and two small no-name inflows which convey stormwater from the "Auchan" commercial center and some housing estates.

In order to build the hydrological rainfall – runoff model for the upper Strzyża catchment the catchment area was split into six sub-basins. Sub-catchments boundaries and their names are shown in Fig. 2. There are three sub-basins for Strzyża Creek and three for the Jasień Creek called respecively: Potok Matarnicki, Potok Strzyża 1, Potok Strzyża 2, Jezioro Jasień, Potok Jasień 1 and Potok Jasień 2. The boundaries of the sub-basins were found using the topographic map on scale 1 : 10 000. The main geomorphological parameters for each sub-catchment are presented in the Tab. 1.

Table 1

Geomorphological parameters of the upper Strzyża sub-catchments

Sub-catchment	Area [km^2]	Length [m]	Slope [%]
Potok Matarnicki	1.431	2 060	2.18
Potok Strzyża 1	3.889	2 140	1.64
Potok Strzyża 2	2.627	2 585	1.55
Jezioro Jasień	3.380	1 865	1.61
Potok Jasień 1	1.304	1 695	1.77
Potok Jasień 2	2.570	1 715	2.33

25.3. The SCS Rainfall – Runoff Model

The SCS rainfall – runoff model was applied to prepare the hydrological model of upper Strzyża catchment. The model was built using the HEC–HMS software. The HEC–HMS system was created by U.S. Army Corps of Engineers (USACE) Hydrologic Engineering Center (HEC) [3]. The HEC–HMS is designed to simulate the precipitation-runoff processes of dendritic watershed systems. The program is a modeling system capable to represent many different watersheds. A model of the watershed is constructed by separating the hydrologic cycle into manageable pieces and constructing boundaries around the watershed of interest. Any mass or energy flux in the cycle can then be represented with a mathematical model. The program features a completely integrated work environment including a database, data entry utilities, computation engine, and results reporting tools. A graphical user interface ensures the easy usage of the model. The short characteristics of the method, based on the HEC–HMS Technical Reference Manual [3] is presented in this section.

25.3.1. Computing runoff volume – SCS Curve Number Loss Model

In 1972 the U.S. Soil Conservation Service (SCS) suggested an empirical model for rainfall abstractions which is based on the potential for the soil to absorb a certain amount of moisture. The basic assumption of the SCS curve number method is that, for a single storm, the ratio of actual soil retention after runoff begins to potential maximum retention is equal to the ratio of direct runoff to available rainfall.

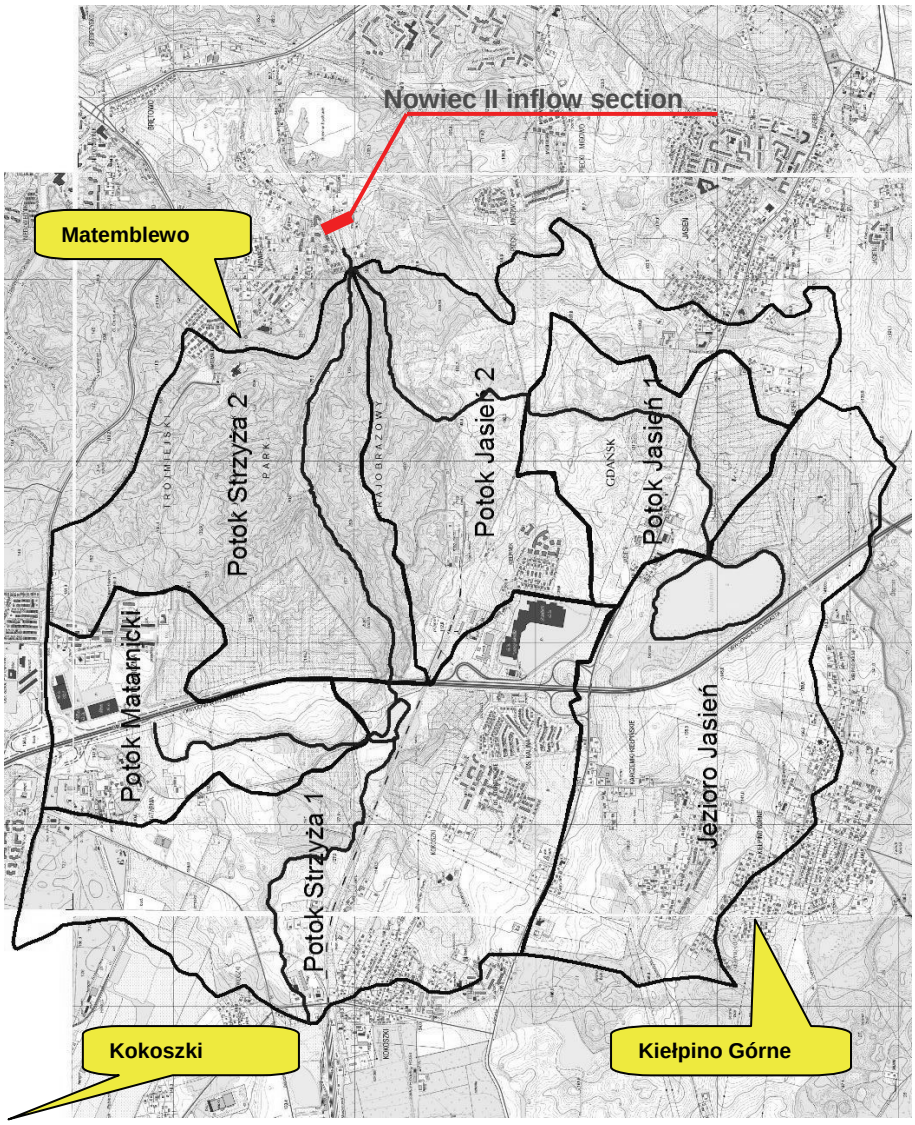

Fig. 2. The catchment and sub-basins of upper Strzyża and rainfall stations (hints)

This relationship (where curve number (*CN*) represents a convenient representation of the potential maximum soil retention *S*) represents the effective rainfall and can be computed by the equation:

$$Q(t) = \frac{(P(t) - I_a)^2}{(P(t) + S - I_a)} \tag{1}$$

where: $Q(t)$ – accumulated depth of effective rainfall to time t,
$P(t)$ – accumulated depth of rainfall to time t,

I_a – initial abstraction,
S – potential storage in the soil.

All of the terms in Eq. (1) are in units of millimeters. Note that the effective rainfall depth or runoff will be zero until the accumulated precipitation depth *P(t)* exceeds the initial abstraction I_a. From analysis of results from many small experimental watersheds, the SCS developed an empirical relationship of I_a and S:

$$I_a = 0.2 \cdot S \tag{2}$$

The potential storage S was related to a 'curve number' *CN* which is a characteristic of the soil type, land use and the initial degree of saturation known as the antecedent moisture condition. The value of S is defined by the empirical expression:

$$S = \frac{25400}{CN} - 254 \ \text{[mm]} \tag{3}$$

CN values range from 100 (for water bodies) to approximately 30 for permeable soils with high infiltration rates. The *CN* for a watershed can be estimated as a function of land use, soil type, and antecedent watershed moisture, using tables published by the SCS. HEC–HMS documentation includes *CN* tables developed by the SCS and published in Technical Report 55 (commonly known in literature as TR-55). With these tables and knowledge of the soil type and land use, the single-valued *CN* can be found. For a watershed that consists of several soil parts types and land uses, a composite *CN* can be calculated as:

$$CN_{composite} = \frac{\sum_{i=1}^{n} A_i \cdot CN_i}{\sum_{i=1}^{n} A_i} \tag{4}$$

25.3.2. Modeling direct runoff – SCS Unit Hydrograph Model

The Soil Conservation Service has also proposed a parametric Unit Hydrograph (UH) model. The model is based upon averages of UH derived from gauged rainfall and runoff for a large number of small agricultural watersheds throughout the US. The basic concept of the SCS UH model is a dimensionless, single-peaked UH. This dimensionless unit hydrograph, expresses the UH discharge U_t, as a ratio to the UH peak discharge U_p, for any time t, a fraction of the time to UH peak T_p (Fig. 3), where:

$$U_p = C\frac{A}{T_P} \tag{5}$$

$$T_p = \frac{\Delta t}{2} + t_{lag} \tag{6}$$

where: C – conversion constant C = 2.08,
Δt – the excess precipitation duration (computational interval),
t_{lag} – the basin lag time, defined as the time difference between the center of mass of rainfall excess and the peak of the UH.

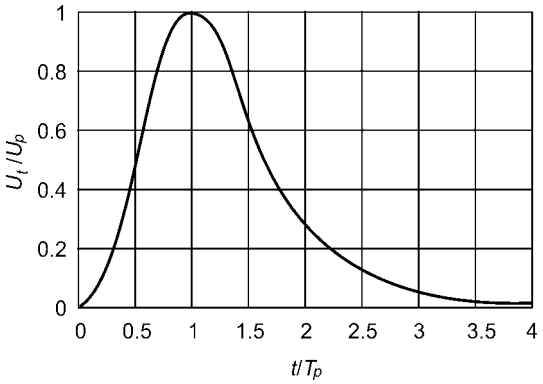

Fig. 3. SCS unit hydrograph [3]

The UH lag time is related to time of concentration t_c as follows:

$$t_{lag} = 0.6 \cdot t_c \tag{7}$$

$$t_c = t_{sheet} + t_{shallow} + t_{channel} \tag{8}$$

where: t_{sheet} – sum of travel time in sheet flow segments over the watershed land surface,
$t_{shallow}$ – sum of travel time in shallow flow segments,
$t_{channel}$ – sum of travel time in channel segments.

These above parameters (travel times) can be estimated by known methods. Details of the SCS UH are described in TR-55.

25.3.3. Modeling Channel Flow – Muskingum Model

The Muskingum routing model uses a simple finite difference approximation of the continuity equation:

$$\frac{(I_{t-1} - I_t)}{2} - \frac{(O_{t-1} - O_t)}{2} = \frac{(S_t - S_{t-1})}{\Delta t} \tag{9}$$

where: $I_{t,t-1}$ – inflow hydrograph ordinates at times t and t–1, respectively,
$O_{t,t-1}$ – outflow hydrograph ordinates at times t and t–1, respectively,
$S_{t,t-1}$ – storage in reach at times t and t–1, respectively.

In Muskingum model the storage S_t is defined:

$$S_t = K \cdot [x \cdot I_t - (1 - x) O_t] \tag{10}$$

where: K – travel time of the flood wave through routing reach,
x – dimensionless weight ($0 \le x \le 0.5$).

If Eq. (9) is substituted into Eq. (10) and the result is rearranged to isolate the unknown values at time t, the result is:

$$O_t = \left(\frac{\Delta t - 2 \cdot K \cdot x}{2 \cdot K \cdot (1-x) + \Delta t} \right) I_t + \left(\frac{\Delta t + 2 \cdot K \cdot x}{2 \cdot K \cdot (1-x) + \Delta t} \right) I_{t-1} + \left(\frac{2 \cdot K \cdot (1-x) - \Delta t}{2 \cdot K \cdot (1-x) + \Delta t} \right) O_{t-1} \quad (11)$$

In this paper, parameter x = 0.2 (typical value for natural streams) and time travel K was estimated from simple formula:

$$K = \frac{L}{V_w} \quad (12)$$

where: L – length of reach,
V_w – velocity of flow in reach.

25.4. Upper Strzyża Hydrological Model

In order to build the hydrological model of upper Strzyża catchment the basic parameters of the basin had to be estimated. As was mentioned before, the geometry of the sub-basins was analyzed using topographic maps of the region. The second group of parameters required the land cover and development analysis. In the process of the hydrological modeling of runoff caused by the rain, one of the main problems is the determination of effective rainfall. The effective rainfall is a part of the actual precipitation, which is involved in the formation of direct runoff from the catchment. The remaining part is treated as a kind of loss of precipitation, which includes infiltration, evaporation, retention, field interception.

Precise determination of individual losses, consisting of the detailed description of hydrological processes, is very complex and practically impossible. Hence, in hydrological models approximate modeling is usually used. In the present study the SCS–CN was used to determine the effective precipitation method. In this approach the curve number (*CN*) is assigned to each sub-basin, representing a potential retention of each part of the catchment. To determine the number of the curve, it is necessary to analyze the type of soil in the catchment area and to identify land cover and use of the watershed.

The analysis of soil types within the catchment area and categorization by their permeability were based on the hydrographic map. Finally the division into two types of soils was adopted – having a low or medium permeability. According to SCS classification sub-areas were assigned to the class B or C. The soils in areas of class B have a permeability above medium and the medium rate of filtration, whilst class C soil permeability is below medium. Such classification corresponds to the nature of glacier soils, which cover the upper Strzyża basin, dominated by clay, silt, and loamy sands.

In the second step the types of coverage and methods of land development were analyzed. In each sub-basin areas with different characteristics and land cover were isolated, and then their surface areas were calculated. The land cover and use analysis was prepared on the basis of topographic map on scale 1:10 000 and historical hydrological Strzyża catchment studies.

Catchment urbanization update was carried out using aerial photos of the basin. On this basis, the division of land into seven sub-basin types was defined: commercial and industrial areas, residential areas, streets and roads, meadows and pastures, open areas, forests and water. The final division of the catchment into homogeneous in terms of

permeability and land use and development areas are shown in Fig. 4. The final values of SCS curves numbers, calculated for each sub-basin respectively, are presented in the Tab. 2.

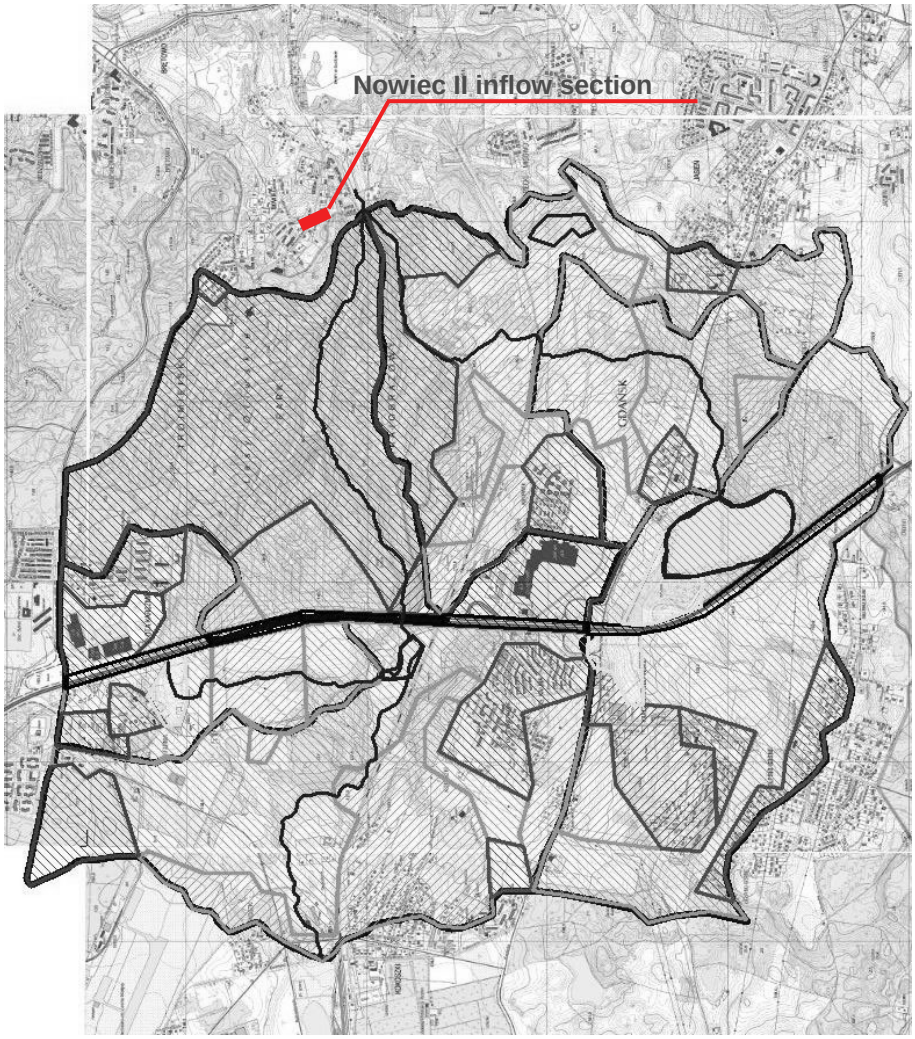

Fig. 4. Division of upper Strzyża catchment into homogeneous areas in the relation to types and land use. Colors: brown – commercial and industrial areas, red – urban area, black – streets and roads, yellow – meadows and pastures, light green – open spaces, dark green – forests, blue – water. The type of pattern is related to the soil class B or C

Table 2

SCS–CN values in upper Strzyża catchment

Sub-catchment	Curve Number (*CN*)
Potok Matarnicki	79.64
Potok Strzyża 1	76.75
Potok Strzyża 2	70.94
Jezioro Jasień	78.20
Potok Jasień 1	74.71
Potok Jasień 2	73.37

25.5. Outflow Simulation

The hydrological model of upper Strzyża catchment was used to simulate transformation of the recorded rain event resulting with the collapse of the Nowiec II dam. Actual precipitation from the period September 27–29, 2010 has been defined on the basis of pluviometric measurements. The measurement data were provided by the Gdańskie Melioracje ul. Łąkowa 35/38, 80-743 Gdańsk. The GM stormwater service in Gdańsk is the owner of the network of precipitation monitoring system composed of 15 rain stations.

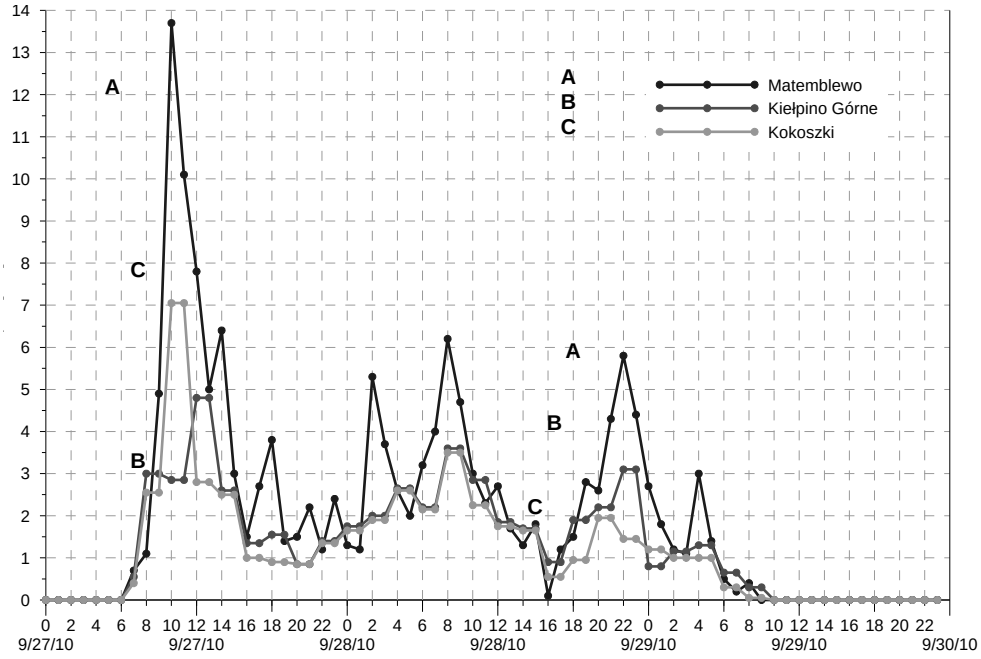

Fig. 5. Observed precipitation in [mm]

25.5.1. Precipitation Data

After analysis of the precipitation distribution three rainfall stations located within or near the catchment (Kokoszki, Kiełpino Górne and Matemblewo) were used for calculation of the runoff hydrograph. Location of stations in the catchment is shown in Fig. 2. The time history of the rainfall is presented in Fig. 5.

Maximum of the rainfall occurred on September 27 between 10 a.m. and 2 p.m.. In Kokoszki the rainfall was 19.7 mm, 15.3 mm in Kiełpino Górne and in Matemblewo up 37.6 mm. On September 28, the maximum rainfall was recorded between 8 and 10 a.m. and 10 – 12 p.m.. The total daily rainfall on September 27 and 28 amounted is respectively: in Kokoszki 38.4 and 44.7 mm, in Kiełpino Górne 37.9 and 44.7 mm, in Matemblewo 68.4 and 69.7 mm. After analysis of the distribution of the rainfall in the catchment the precipitation from the Kokoszki station was assumed in the Potok Matarnicki and Potok Strzyża 1 sub-basins, the rainfall from the Kiełpino Górne station in Jasień Lake and Potok Jasień 1 catchments and the rainfall from the Matemblewo station was chosen for Potok Strzyża 2 and potok Jasień 2 sub-basins.

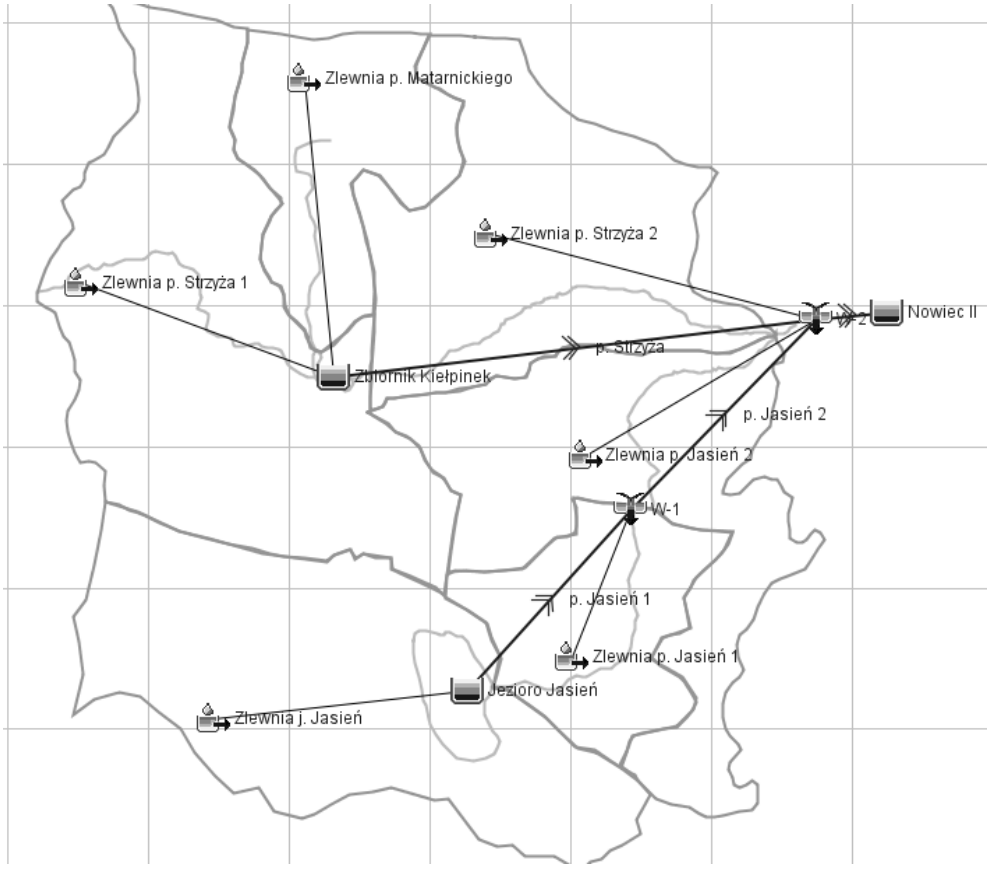

Fig. 6. Numerical model of the upper Strzyża catchment in HEC–HMS system

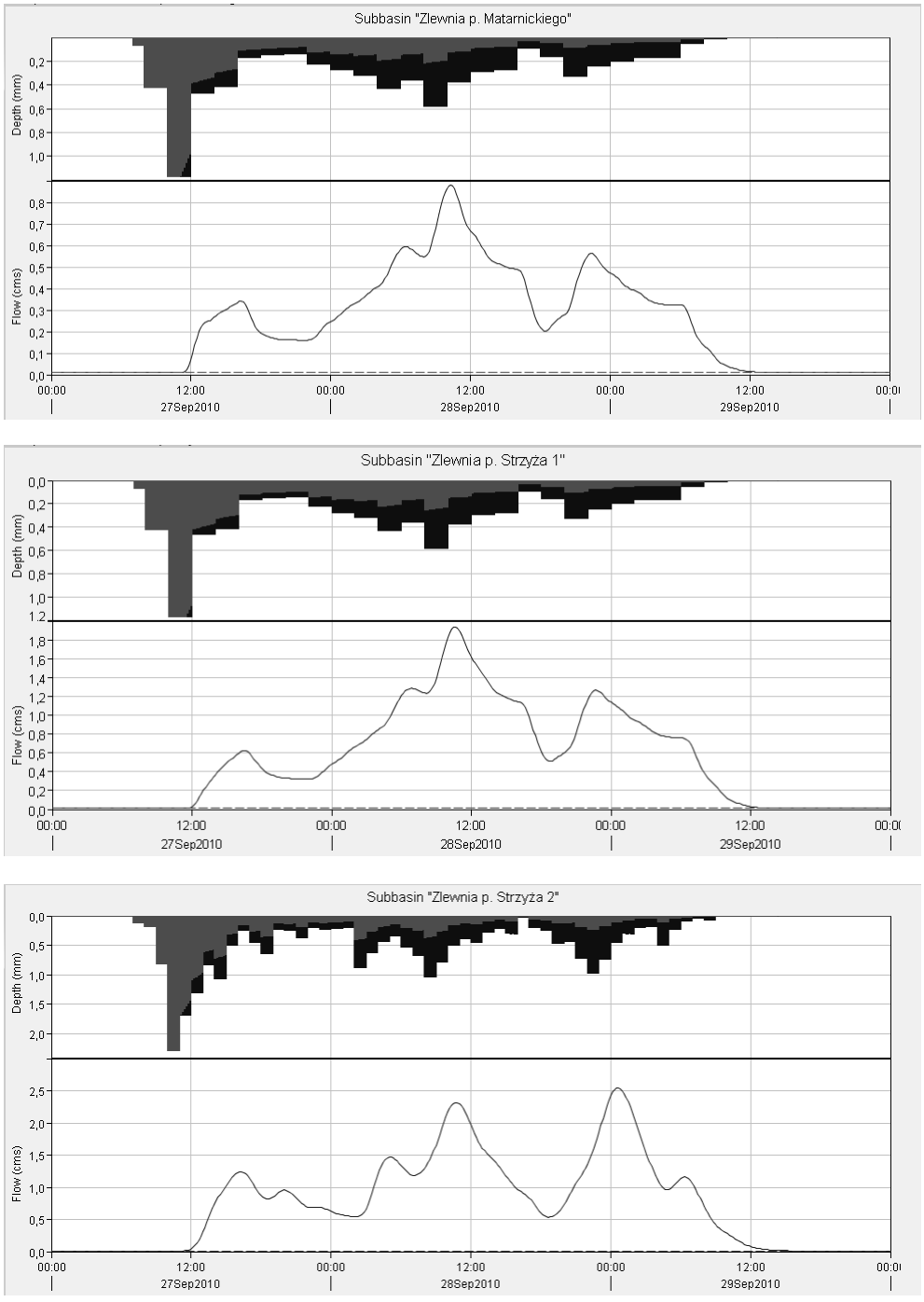

Fig. 7. Hyetographs of total and effective rainfall [mm] and outflow hydrographs [m^3/s] from the Matarnicki, Strzyża 1 and Strzyża 2 sub-basins

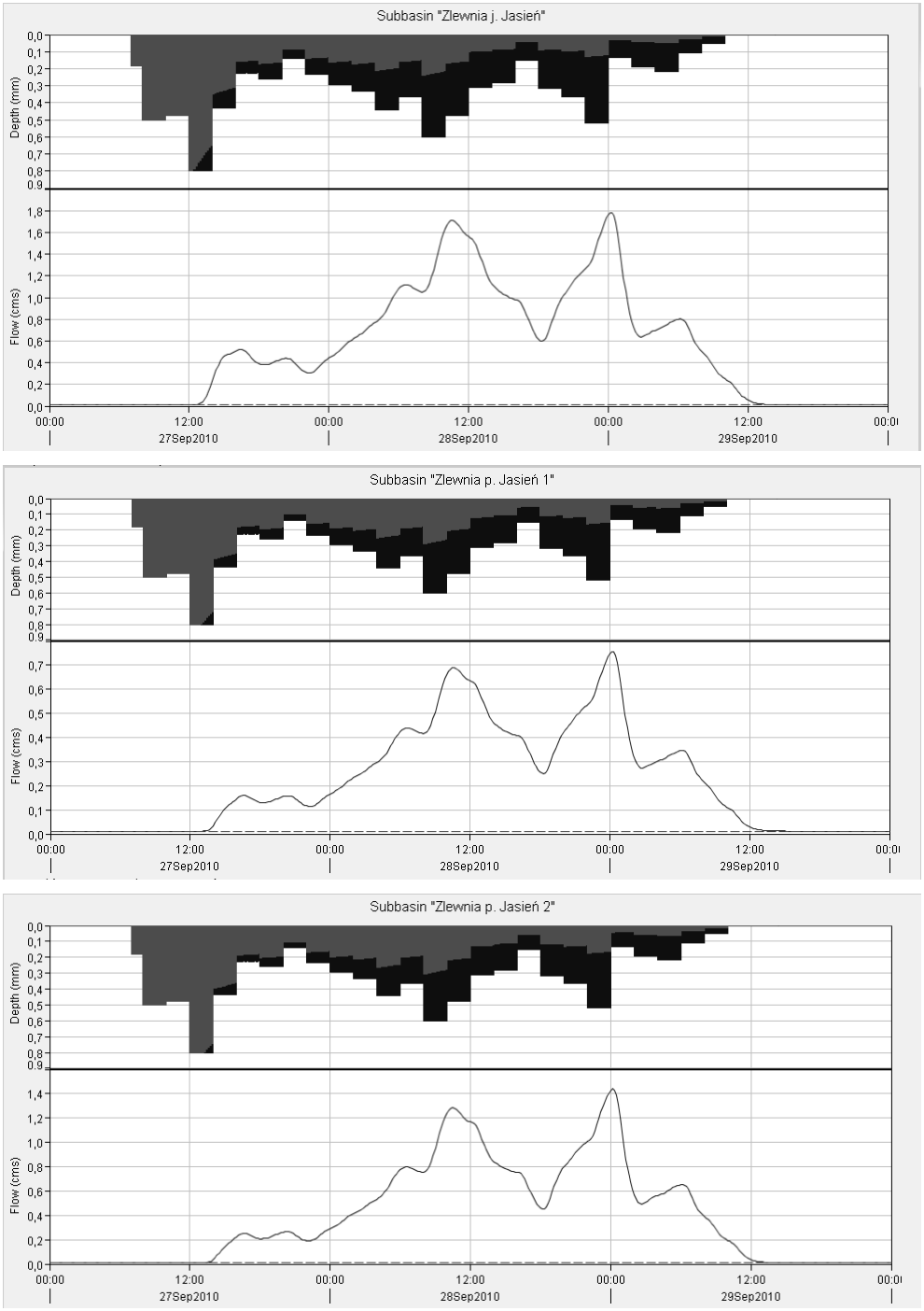

Fig. 8. Hyetographs of total and effective rainfall [mm] and outflow hydrographs [m^3/s] from the Jasień lake, Jasień 1 and Jasień 2 sub-basins

25.5.2. Outflow Calculation

Calculation of the flow hydrograph from the catchment located upstream the reservoir Nowiec II was performed using HEC–HMS software. In the first step the numerical model of the analyzed catchment has been prepared. The hydrological system has been composed of outflow sections from each sub-basin, existing storage reservoir Kiełpinek and the Jasień Lake, Jasień and Strzyża Creeks and the inlet into reservoir Nowiec II (Fig. 6).

Due to lack of flow measurements in the stream channels and reservoirs it was not possible to verify the hydrological model. Hence, calculations were made on the basis of general hydrological characteristics of the catchments, estimated using historical materials, literature and field observations.

In order to calculate the outflow several assumptions were done. For the reservoirs (Kiełpinek, Jasień Lake) the initial filling was assumed equal to minimal water level. For the catchment average soil moisture conditions (within 5 days before there was no precipitation) were assumed. Moreover it was decided to choose the constant supply the streams of groundwater.

Using the SCS–CN method for the estimation of the effective rainfall in each sub-basin and the corresponding outflow hydrographs from sub-basins (using the SCS UH) the total outflow at the sections were calculated. The obtained results are shown in Figs.7 and 8. In the upper part of each figure it was shown the actual hyetograph assigned to the basin in which red color has indicated hydrological losses (surface retention, infiltration and interception), and blue color has represented effective precipitation. At the bottom of the figure the outflow hydrograph for each sub-basin is shown.

The calculated total inflow into the reservoir Nowiec II is shown in the Fig. 9. There are clearly visible three extremes in the flow history. The significant increase of inflow is visible from 12 a.m. to 4 p.m. on September 27. At this time first discharge maximum about 2 m^3/s has occurred. The first peak is a result of extreme outflow from the catchment Strzyża 2 located in the vicinity of the analyzed cross section.

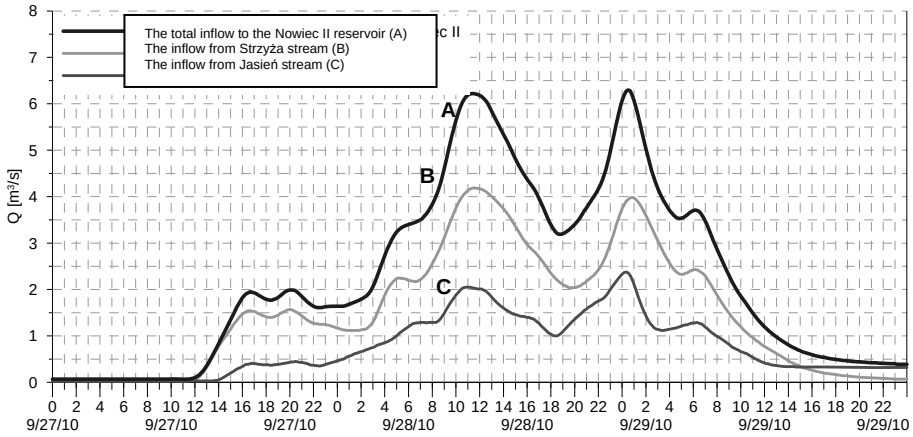

Fig. 9. The total inflow to the Nowiec II reservoir

The next flow increase is determined by the cumulative inflows from other sub-basins. At about 12:00 p.m. the flow has decreased down to 1.64 m^3/s, but then again gradually

increased and reached a maximum of 6.22 m^3/s on September 28 at 11:30 a.m. Maximum peak is the result of flood waves coming from all sub-catchments.

During the final part of rainfall event the inflow into the reservoir Nowiec II has decreased and reached a minimum value of 3.19 m^3/s at about 6:30 p.m. to rise again and reach the third maximum 6.29 m^3/s on September 29 at 0:30 a.m.. The maximum inflow is again the result of the overlap of the flood waves from all sub-catchments.

25.6. Conclusions

The mathematical model of rainfall-runoff transformation, based on the SCS methods was used for the calculation of the flow hydrograph on September 27–29, 2010 at the Nowiec II reservoir inlet section. The simulation was done using the precipitation data for the almost 51 hours of intense rainfall. Rainfall recorded on September 27–29, 2010 has resulted with significant increase of flow and it was a reason of flood risk in this region.

The calculations have shown that there were three flood waves with three peaks of 1.99, 6.22, 6.29 m^3/s during the rain event. They have occurred on September 27 at 4 p.m., September 28 at 11:30 a.m. and on September 29 at 00:30 a.m. The highest of these peaks has exceeded the maximum 10% flow rate, estimated for Strzyża Creek equal to 5.67 m^3/s.

The total outflow from the upper Strzyża basin was about 586 thousand m^3. Referring this value to the total volume of water that has felled onto the surface of the analyzed catchment (1597 thousand m^3), the average rate of outflow can be estimated about 0.367. It can be found that outflow from the basin has exceeded the storage parameters of Nowiec II reservoir and could be the reason of collapse of the dam.

It should be underlined here that the hydrological model of the upper Strzyża catchment was not identified and verified. These very important and crucial elements of hydrological modeling will be an aim of the next project for monitoring, modeling and analysis of flood risk in the Strzyża catchment which has just been started in co-operation between Gdańskie Melioracje and Gdańsk University of Technology.

References

[1] Banasik K.: Estimation of flood waves In small urbanized catchments. SGGW 2009 (in Polish).
[2] Byczkowski A.: Hydrology. Warszawa: PWN 1999 (in Polish).
[3] HEC–HMS Technical Reference Manual. US Army Corps of Engineers Hydrologic Engineering Center 609 Second Street Davis, CA 95616-4687 USA 2000.
[4] Soczyńska U.: Dynamic Hydrology. Warszawa: PWN 1997 (in Polish).

Acknowledgements

This paper presents some results obtained in a framework of the project “Hydrological analysis of stormwater runoff from the Strzyża Creek catchment upstream the reservoir Nowiec II in Gdańsk” which has been financed by the Gdańskie Melioracje, ul. Łąkowa 35/38, 80-743 Gdańsk, Poland. The work is also a part of the research project No. RX-03/12/2011 “Monitoring, modeling and analysis of flood risk in a small urban basin on the example of Strzyża catchment in Gdańsk”, subsidized by the Regional Fund for Environmental Protection and Water Management in Gdańsk.

26 Minimalization of Solid Waste Landfilling Base on Waste Analyses

Ivona Škultetyová, Štefan Stanko, Kristína Galbová (Slovak University of Technology in Bratislava, Faculty of Civil Engineering)

26.1. Introduction

There is a demand for the flow of information, from the international level down to the individual level, across all areas of life. This is also true for the issue of waste, as waste is a necessary by-product of human existence.

Recently we have been observing the continuing trend of growth in the production of communal waste, as well as corresponding growth in the costs related to its disposal. Growth in the amount of waste produced is especially affected by the rising degree of economic growth, which highlights the need for solving the problem of dealing with waste.

The waste landfilling is the worst alternative of waste disposal. We can say, that this is not the waste disposal, but only the moving the problem solving into the future. If we want to dispose the wastes, we must take consider on waste specific, we must respect the waste material. The way out of this problem solution must be base on system waste analyses, which is not easy.

26.2. Waste Management System

In the past, when it came to designing waste management facilities, generally the only parameter taken into account was the size of the population producing waste, neglecting to consider other parameters that affect waste creation [2]. Additionally, waste management was analyzed as an independent subsystem without considering its other ties to individual spheres of the environment. However, the production of waste is dependent on various parameters that interact with each other. Being aware of these parameters, as well as the methods for evaluating their effects on one another, helps to identify the condition and the designation of development trends in the field of waste management. It is possible to point out the limitations in this field, which will be possible to improve on or remove in the future.

The necessity of being well informed, from the international level to the individual level, is broadly manifested in every sphere of life. It is also tied to the field of waste management because wastes are an accompanying feature of the existence of mankind. With an increasing degree of economic development the production of waste also increases, which highlights the need of solving this problem [3]. The basis for proper waste management and for the design of facilities dedicated to dealing with waste is the prediction of the quantity and composition of the waste, based on various prognostic models. One of the most important parameters influencing the size of the new future waste management system is waste flow forecast. All design, technical solutions in a feasibility study and, at the end, final costs and tariffs crucially depend on future waste flows. Waste flow forecast, which helps with the creation

of prognostic models usually is based on present waste management situation (statistical data on waste generation, waste quantity and composition), waste generation sources (rural and urban population, industry, businesses), demographic trends (rural and urban population growth, migration), economic activity (GDP growth), waste management policy developments (increased sorting, recycling, separate, treatment of certain waste types (end-of-life vehicles), waste prevention, increased coverage of territory and population).

26.3. The Production of Waste

In terms of modeling, in concentrating on the analysis of parameters that influence the processes of waste creation we can apply factor models [1], which when predicting waste production (in terms of quantity and composition of waste) focus on various parameters, for example economic and demographic. We can predict individual parameters with considerable precision on longer timeframes. When identifying and rating the degree of their influence on waste production it is necessary to consider their interaction on one another, because waste production is not dependent on just one of these parameters.

Parameters that influence the production of waste include especially:

— Environmental parameters,
— Demographic,
— Economic,
— Social,
— Institutional.

26.3.1. Environmental Parameters

Environmental parameters characterize indicators, for example:

— Global warming,
— Emissions,
— Urbanization,
— Agriculture,
— Forestry ....

26.3.2. Demographic Parameters

Demographic parameters characterize indicators, for example:

— Population size

The number of inhabitants significantly affects the total quantitative production of waste of a specific regional entity. When estimating the amount of waste produced, if we take into account just the population size, we could reach an incorrect estimate because the creation of waste is affected by other factors.

— Population increase

This is an indicator that characterizes the average annual degree of change in the size of the population of a given regional entity. The meaning of this degree is characterized by the relationship to social, economic and environmental factors of the region’s development.

— Inhabitants of urban centers.

A factor conveying the degree of urbanization – the percentage of the population living in areas that are characterized by a heightened environmental weight and developmental problems (including waste production). In developing countries the percentage of inhabitants living in urban centers is under 50 percent, in some cases under 10 percent. On the other hand, in developed countries this percentage represents more than 75 percent of the population. In Slovakia, 57,3 percent of the population lives in urban centers.

26.3.3. Economic Parameters

Economic parameters are characterized:

— Gross domestic product per inhabitant

The total economic performance of a given regional entity is conveyed by the gross product, while its value in USD per inhabitant in the majority of developing countries ranges from 1000 to 1500 USD and in economically developed countries ranges from 12000 to 14000 USD.

— Proportion of investments in GDP

In Slovakia the value of investments as a percentage of GDP is cca 41 percent (in most countries it is 20 percent to 25 percent).

— Economic balance of goods and services

This indicator shows the difference between the nominal value of export and import. An unfavorable economic balance is embodied by many countries, which represents values of this indicator in a range of 20 percent to 40 percent. A positive balance of some countries is over 10 percent; others embody a level economic balance. Slovakia has a negative balance – cca 10.4 percent.

— Debt in proportion to GDP

This indicator represents a brake on the development of a region, especially in regards to less-developed countries (debt is over 50 percent of to several times GDP). The debt of developed countries is 5 percent to 30 percent of GDP.

Indicators of the economy's dependence on natural and other resources, as well as on burdening the environment with the manufacture and creation of waste, include:

— Intensity of the use of materials,
— Annual consumption of energy per inhabitant,
— Proportion of use of renewable sources of energy,
— Energetic intensity,
— Recycling and secondary use of waste,
— Prosperity of the country.

Various economic indicators are together folded into an indicator of the country's prosperity.

26.3.4. Social Parameters

— Percentage of inhabitants living below the poverty threshold,
— Unemployment,
— Ratio of average income of women to men.

Social parameters include indicators focused on the health and existential aspect of mankind, for example:

— Measure of mortality of children under 5,
— Surface area per person.

26.3.5. Institutional Parameters

Currently, access to information and being informed are considered to be important aspects of human existence. Institutional parameters include:

— Number of radios,
— Number of internet connections,
— Number of telephone lines, mobile phones, etc.

and also indicators tied more closely to economic parameters:

— Spending on research and development as a percentage of GDP
— Economic and human costs caused by natural disasters, as well as by fires, floods, and so on

and also, for example:

— Legislative factors,
— Application of permanently sustainable development.

26.4. Conclusions

To guarantee progress in the management of the waste industry and to reach positive results in the waste sector in Slovakia, we have established certain rules and goals concerning the planned development of individual flows of waste, divided into commodities and categories of waste. This presents the base for a properly functioning and effective system of waste management [5, 6].

To create such systems it is necessary to ensure the availability of sorted waste collection in cities and towns. This will lead to, for example, the appropriate choice of how to process organic waste. New methods will improve the use of waste in all aspects – material, energy and safety. In order to construct an optimal and effectively functioning system, it it necessary to have objective data about the volume and contents of communal waste, as well as the prognosis for its volume and contents. Waste analysis has been a key issue for a long time, given that it is very complicated to get a representative sample of waste, given its heterogeneity.

Many authors had prepared individual methodical rules that were later recommended for general use. This led to the creation of various types of analyses, whose results are in certain ways different and are in general not comparable.

It is characteristic of current times that the increase in waste produced is leading to growth in waste management costs. This in turn leads to a decrease in the prosperity of the waste industry and an ineffective connection between sorted and unsorted waste collection. The results of analyzing the contents of communal waste – finding out the volume of each category and its quality – is helping with optimalization of waste industry at an efficient level. So is the prognosis of the development of the waste industry with the help of prognostic and evaluative models leading to a long-term economic and environmental tenability.

The scientific goal of this work is to characterize the current situation and future prognosis for the production of communal waste. Based on available resources, we aim to prepare a methodical analysis of the storage of communal waste, and seek an overview of available models of analyzing the contents of communal waste as well as new systems of evaluation of communal waste management at home and abroad.

Our goal is to perform an analysis of communal waste in a selected area, taking into account the locality´s size, the composition of waste produced and the make-up of the population. This helped us collect data for the LCA-IWM model for determining the prognosis of waste production. We will be able to create and evaluate different scenarios for the waste industry, as well as offer suggestions for various technologies and equipment for working with waste materials, taking into account the social, environmental and economic impact involved [4].

References

[1] Plánovanie a optimalizácia odpadového hospodárstva – Príručka na vypracovanie prognózy množstva komunálneho odpadu a trvalo udržateľného systému odpadového hospodárstva, Projekt "Použitie programu odhadu životného cyklu pre rozvoj stratégie integrovaného odpadového hospodárstva pre mestá a regióny s rýchlym rastom hospodárstva EVK4–CT–2002–0087, 304, Bratislava 2005.

[2] Čermák O., Čermáková M.: Integrated approach to the solution of the infrastructure of an urbanised area. In 8th Conference on Environment and Mineral Processing, VŠB TU Ostrava, 67–72.

[3] Jankovičová, K., Parráková, E.: Odpadové hospodárstvo v Bratislave. In: Zborník medzinárodnej konferencie TOP 2004, Účelové zariadenie Kancelárie NR SR, Častá-Papiernička, 291–296, ISBN 80-227-2058-5, 2004.

[4] www.lca–iwm.net

[5] Škultétyová I.: Vvyužitie LCA v rozhodovacom procese integrovaného odpadového hospodárstva, 127, STU v Bratislave, 2011.

[6] Škultétyová I.: Solid Waste Production. 9th Conference on Environment and Mineral Processing: Part I – Ostrava 2005.

Acknowledgements

The article was written with the support of the Scientific Grant Agency – project VEGA no. 1/0559/10 dealt with at the Department of Sanitary and Environmental Engineering of the Slovak University of Technology.

27 Heuristic Optimization Methods for Hydro Plants Generation Scheduling

Peter Šulek, Katarína Cipovová (Slovak University of Technology in Bratislava, Faculty of Civil Engineering)

27.1. Introduction

The efficient scheduling of available energy resources for satisfying load demand has became an important task in modern power systems. For hydrothermal systems, the limited energy storage capability of water reservoirs, make its solution a more difficult job than for purely systems. The hydrothermal generation scheduling problem, also called hydrothermal coordination problem, is a non-linear problem with high dimensionality, continuous and discrete variables, a non-explicit objective function, with many constraints. The solution of the problem has been approached by conventional (traditional) or heuristic optimization techniques. The use of both approaches is often associated with difficulties. The article describes the possibility to solve this problem by combination of both numerical and heuristic approach.

27.2. Materials and methods

The objective of the hydrothermal coordination (HTC) is to determine the optimal operation schedule of thermal units and hydro plants that minimizes the total system operation cost during the scheduling horizon, subject to many system and units constraints. The HTC problem can be formulated as a mathematical optimization problem as follows:

$$C = C = \sum_{i=1}^{T} \sum_{j=1}^{NT} CC_{j,i}(P_{T\,j,i}) \rightarrow \min \tag{1}$$

It has been assumed that hydro plants have zero operating cost.

C – total system operation cost,
i – time interval (hour) index,
T – total number of time intervals (scheduling horizon),
j – thermal unit index,
NT – number of thermal units,
$CC_i(\ )$ – fuel cost function of thermal unit j during hour i, a function of $P_{T\,j,i}$
$P_{T\,j,i}$ – power output of thermal unit j during hour i,

$$\sum_{j=1}^{NT} P_{T\,j,i} = Dem_i - \sum_{k=1}^{NH} P_{k,i}$$

Dem_i – total load demand of hydrothermal power system during hour i,
NH – number of hydro plants,
$P_{k,i}$ – power output of hydro plant k during hour i,
k – hydro plant index.

Optimal scheduling of a hydrothermal power system is a complex mixed-integer non-linear optimization problem. The solution of the problem above has been approached by many optimization techniques such as peak shaving [13, 15, 16]; linear programming [11, 12]; dynamic programming [14, 17]; mixed-integer programming [5, 9] and genetic algorithms [3, 18]. Many of the above mentioned methods make various simplifying assumptions in order to reduce the complexity of the optimization problem which arises from simultaneous consideration of thermal and hydro plants. Oftentimes, the original problem is decomposed into smaller hydro and thermal sub-problems which are solved independently. The decomposition of the problem allows the detailed formulation of each sub-problem, without making major simplifying assumptions.

The typical example of decomposition method is the **peak shaving (PS)** method. The PS method is based on an idea that the hydroelectric generation should be allocated in the higher part of the system load curve which corresponds to the system peak loads (Fig.1). The solution of the hydro sub-problem by PS method is described below.

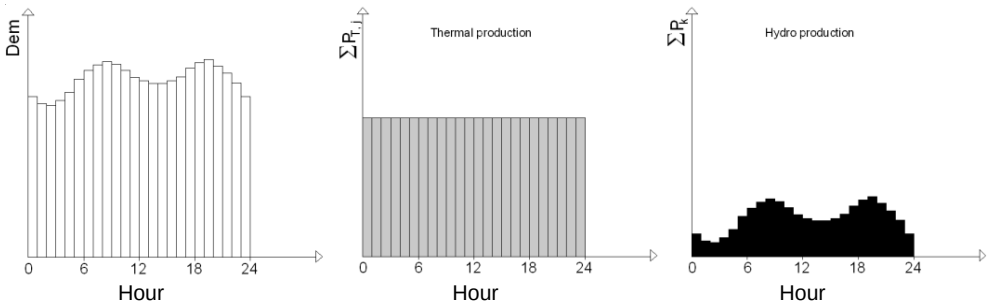

Fig. 1. Peak-shaved load curve

27.2.1. Hydro Sub-problem Formulation

The hydro sub-problem can be defined by the following function

$$F = \sum_{i=1}^{T}\left(Dem_i - \sum_{k=1}^{NH}(ST_{k,i}.P_{k,i})\right)^2 = \sum_{i=1}^{T}\left(Dem_i - \sum_{k=1}^{NH}(ST_{k,i}.9.81.Q_{k,i}.H_{k,i}.\eta_{k,i}.10^{-3})\right)^2 \quad (2)$$

$\rightarrow \min,\ k \in [1, NH]; \in [1, T]$

subject to:

— hydro plant operation limits $\forall k \in [1, NH], \forall i \in [1, T]$

$$ST_{k,i} \,.\, (P_{min,k} + {}^{RSV-}P_{k,i}) <= P_{k,i} <= ST_{k,i} \,.\, (P_{max,k} - {}^{RSV+}P_{k,i}) \quad (3)$$

$$ST_{k,i} \,.\, (Q_{min,k} + {}^{RSV-}Q_{k,i}) <= Q_{k,i} <= ST_{k,i} \,.\, (Q_{max,k} - {}^{RSV+}Q_{k,i}) \quad (4)$$

— reservoir storage capacity limits $\forall k \in [1, NH], \forall i \in [1,T]$

$$V_{min,k} <= V_{k,i} <= V_{max,k} \tag{5}$$

$$V_{k,0} = V_{in,k} \quad \text{and} \quad V_{k,T} = V_{fin,k} \tag{6}$$

where: $ST_{k,i}$ – operating state of hydro plant (**variables**), (1 – if the plant is ON and 0 – if the plant is OFF),

$P_{k,i}$ – power output of hydro plant [MW]

$$P_{k,i} = 9.81.Q_{k,i}.H_{k,i}.\eta_{k,i}.10^{-3}$$

$Q_{k,i}$ – discharge of hydro plant [m^3/s] **(variables)**,
$H_{k,i}$ – average net head of hydro plant [m],
$\eta_{k,i}$ – efficiency of hydro plant [–]
$\eta_{k,i}$ – is function of $Q_{k,i}$ and $H_{k,i}$,
$P_{min,k}$ – minimum power output of hydro plant [MW],
$P_{max,k}$ – maximum power output of hydro plant [MW],
$^{RSV+}P_{k,i}$ – plus spinning reserve of hydro plant [MW],
$^{RSV-}P_{k,i}$ – minus spinning reserve of hydro plant [MW],
$Q_{min,k}$ – minimum discharge of hydro plant [m^3/s],
$Q_{max,k}$ – maximum discharge of hydro plant [m^3/s],
$^{RSV+}Q_{k,i}$ – discharge equivalent of the plus spinning reserve of hydro plant [MW],
$^{RSV-}Q_{k,i}$ – discharge equivalent of the minus spinning reserve of hydro plant [MW],
$V_{min,k}$ – reservoir minimum storage volume [m^3],
$V_{max,k}$ – reservoir maximum storage volume [m^3].
$V_{in,k}$ – reservoir initial storage volume [m^3],
$V_{fin,k}$ – reservoir final **(target)** storage volume [m^3].

The water balance for each reservoir of hydro plant k during hour i is given by

$$V_{k,i} = V_{k,i-1} - 3600.Q_{k,i} + I_{k,i} \tag{7}$$

where: $V_{k,i}$ – reservoir storage volume in the end of hour i [m^3],
$I_{k,i}$ – inflow rate including the evaporation losses, leakage and other not energetic withdrawals [m^3].

The solution of problem (2) is represented by matrix ***S*.**

$$\boldsymbol{S} = \left[\begin{array}{cccc|cccc} Q_{1,1} & Q_{1,2} & ..... & Q_{1,T} & ST_{1,1} & ST_{1,2} & ..... & ST_{1,T} \\ Q_{2,1} & Q_{2,2} & ..... & Q_{2,T} & ST_{2,1} & ST_{2,2} & ..... & ST_{2,T} \\ : & : & ..... & : & : & : & ..... & : \\ Q_{NH,1} & Q_{NH,2} & ..... & Q_{NH,T} & ST_{NH,1} & ST_{NH,2} & ..... & ST_{NH,T} \end{array}\right]$$

27.2.2. Hydro Sub-problem Solution Methods

The optimization problem (2) with limits (3) – (6) is a complex mixed-integer non-linear optimization problem with non-linear constraints. The problem is all the more complicated if it's taken into account also the water travel time between the cascaded hydro

plants. Consequently, the course of objective function is the complexity with many local extremes.

27.2.2.1. Traditional Numerical Optimization Methods

The solution of the above mentioned problem using traditional numerical optimization methods (e.g. non-linear programming, dynamic programming) is associated with many difficulties (e.g. "curse of dimensionality"). The most of the traditional methods is unable to produce near-optimal solution for this kind of a problem.

The problem must be decomposed into several smaller problems to decrease number of variables. The objective function F is decomposed into partial functions F_K for each hydro plant. It can be written:

$$F = \sum_{k=1}^{NH} F_K = \sum_{k=1}^{NH} \sum_{i=1}^{T} \left(\left(Dem_i - \sum_{k=1}^{k-1} (ST_{k-1,i}.P_{k-1,i}) \right) - ST_{k,i}.P_{k,i} \right)^2 \rightarrow min, \tag{8}$$

The solution of a problem (8) is represented by vectors $\boldsymbol{s_k}$.

$$\boldsymbol{s_k} = \left[Q_{k,1} \quad Q_{k,2} \quad ..... \quad Q_{k,T} \mid ST_{k,1} \quad ST_{k,2} \quad ..... \quad ST_{k,T} \right] \qquad k \in [1, NH]$$

The value of the objective function F is obtained by sequential (downstream) solution of the sub-objective functions F_K. That's how the number of variables is decreased from $2*T*NH$ to $2*T$. The sub-objective functions F_K are solved using traditional numerical optimization methods for mixed-integer nonlinear problem (MINLP). However, in many cases the value of objective function F (as the sum of the values F_K) may not be the global extreme function F.

27.2.2.2. Heuristic Optimization Methods

In addition to traditional numerical optimization methods, heuristic optimization methods (e.g. local search, tabu search, harmony search, simulated annealing, genetic algorithms) are used. There is a significant representative of heuristic methods – so called genetic algorithms (GA). GA are searching algorithms based on the mechanics of natural selections and natural genetics. Detailed description of the method can be found in [2]. For the use of the GA, the objective function of the hydro sub-problem (2) must be modify to

$$\begin{aligned} F = & \sum_{i=1}^{T} \left(Dem_i - \sum_{k=1}^{NH} ST_{k,i}.P_{k,i} \right)^2 + \sum_{k=1}^{NH} pen_1(V_{k,T}, V_{fin,k}) + \sum_{k=1}^{NH} \sum_{i=1}^{T-1} pen_2(V_{k,i}, V_{\min,k}) \\ & + \sum_{k=1}^{NH} \sum_{i=1}^{T} pen_3(ST_{k,i}, P_{k,i}, P_{\max,k}) + \sum_{k=1}^{NH} \sum_{i=1}^{T} pen_4(ST_{k,i}, P_{k,i}, P_{\min,k}) \\ & + \sum_{k=1}^{NH} \sum_{i=1}^{T} pen_5(ST_{k,i}, Q_{k,i}, Q_{\max,k}) + \sum_{k=1}^{NH} \sum_{i=1}^{T} pen_6(ST_{k,i}, Q_{k,i}, Q_{\min,k}) \\ & \rightarrow \min, \quad \forall k \in [1, NH]; \quad \forall i \in [1, T] \end{aligned} \tag{9}$$

The *pen*1(), *pen*2(), *pen*3(), *pen*4(), *pen*5(), *pen*6() are penalty functions.

$$pen_1(V_{k,T}, V_{k,\,fin}) = \begin{cases} K_1(V_{k,T} - V_{fin,k})^2 & V_{k,T} < V_{fin,k} \\ 0 & V_{k,T} \geq V_{fin,k} \end{cases} \tag{10}$$

$$pen_2(V_{k,T}, V_{\min,k}) = \begin{cases} K_2(V_{k,i} - V_{\min,k})^2 & V_{k,\,j} < V_{\min,i} \\ 0 & V_{k,\,j} \geq V_{\min,i} \end{cases} \tag{11}$$

$$pen_3(ST_{k,i}, P_{k,i}, P_{\max,k}) = \begin{cases} K_3\left[(P_{\max,k} - {}^{RSV+}P_{k,i}) - ST_{k,i}.P_{k,i})\right]^2 \\ 0 \end{cases} \tag{12}$$

$$ST_{k,i}.P_{k,i} > (P_{\max,i} - {}^{RSV+}P_{k,i})$$

$$ST_{k,i}.P_{k,i} \leq (P_{\max,i} - {}^{RSV+}P_{k,i})$$

$$pen_4(ST_{k,i}, P_{k,i}, P_{\min,k}) = \begin{cases} K_4\left[(ST_{k,i}.P_{k,i} - (P_{\min,k} + {}^{RSV-}P_{k,i})\right]^2 \\ 0 \end{cases} \tag{13}$$

$$ST_{k,i}.P_{k,i} < (P_{\min,i} + {}^{RSV-}P_{k,i})$$

$$ST_{k,i}.P_{k,i} \geq (P_{\min,i} + {}^{RSV-}P_{k,i})$$

$$pen_5(ST_{k,i}, Q_{k,i}, Q_{\max,k}) =$$

$$= \begin{cases} K_5\left[(Q_{\max,k} - {}^{RSV+}Q_{k,i}) - ST_{k,i}.Q_{k,i})\right]^2 & ST_{k,i}.Q_{k,i} > (Q_{\max,i} - {}^{RSV+}Q_{k,i}) \\ 0 & ST_{k,i}.Q_{k,i} \leq (Q_{\max,i} - {}^{RSV+}Q_{k,i}) \end{cases} \tag{14}$$

$$pen_6(ST_{k,i}, Q_{k,i}, Q_{\min,k}) = \begin{cases} K_6\left[(ST_{k,i}.Q_{k,i} - (Q_{\min,k} + {}^{RSV-}Q_{k,i})\right]^2 \\ 0 \end{cases} \tag{15}$$

$$ST_{k,i}.Q_{k,i} < (Q_{\min,i} + {}^{RSV-}Q_{k,i})$$

$$ST_{k,i}.Q_{k,i} \geq (Q_{\min,i} + {}^{RSV-}Q_{k,i})$$

where: K_1, K_2, K_3, K_4, K_5 and K_6 are weight factors of the penalty functions.

The solution of the problem (9) is represented by best chromosome ${}^{FIN}\boldsymbol{S}$ from final generation (the chromosome with best fitness, *fitness* = – *F*). Despite many benefits (e.g. non-explicit the objective function acceptability) GA have a number of disadvantages:

— high risk of being trapped in local extreme of the *F*,

— it's relatively difficult to define the weight of the penalty functions.

Furthermore, we describe possibility of eliminating these disadvantages using the proposed method.

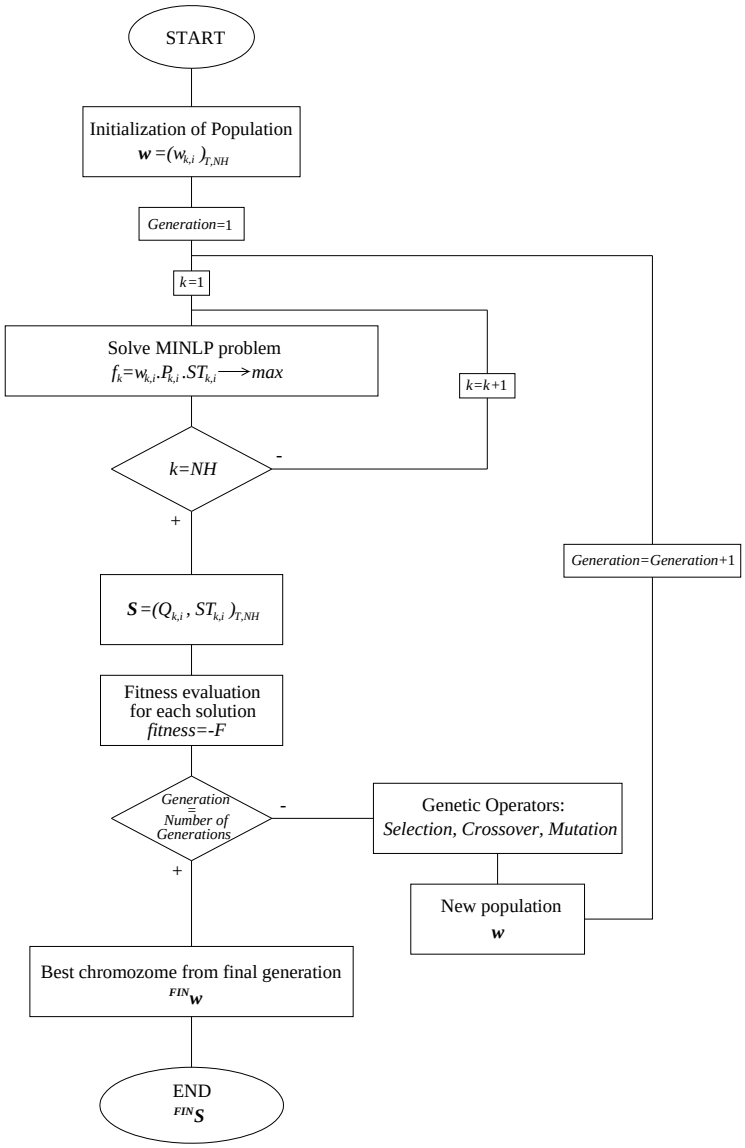

Fig. 2. Block diagram of the proposed hybrid method GA-MINLP

27.2.2.3. Hybrid Optimization Methods

According [10] one way to eliminate the disadvantages of GA is a combination of the genetic algorithms with the traditional numerical optimization methods. The objective function (9) can be written in stand-alone form (16) without penalty functions.

$$F = \sum_{i=1}^{T}\left(Dem_i - \sum_{k=1}^{NH}(ST_{k,i}.P_{k,i}) \right)^2 \rightarrow min,\ \forall k \in [1, NH]; \forall i \in [1, T] \quad (16)$$

The fact that the GA searching space includes just feasible solutions $\boldsymbol{S}=(Q_{k,i}|ST_{k,i})_{T,NH}$ is ensured by numerical optimization methods, which is directly implanted in the fitness function. The chromosomes $\boldsymbol{S}$ are replaced with the chromosomes $\boldsymbol{w}=(w_{k,i})_{T,NH}$. The $w_{k,i}$ value is the weight factor of the objective functions f_K.

$$f_k = \sum_{i=1}^{T} w_{k,i}.ST_{k,i}.P_{k,i} \rightarrow max,\ \forall k \in [1, NH]; \forall i \in [1, T] \quad (17)$$

The optimization problem (17) with constraints (3) – (6) is solved using traditional numerical methods for mixed-integer nonlinear problem. If the matrix ${}^{FIN}_{w}$ is the best chromosome from final generation (the chromosome with best fitness, *fitness* = $-F$), the solution of problem (16) is represented by matrix ${}^{FIN}_{S}$. The block diagram of the proposed hybrid optimization method **GA-MINLP** (combining GA and traditional numerical method for mixed-integer nonlinear problem) is shown in Fig. 2.

27.3. Results and Discussion

The proposed hybrid method GA-MINLP was applied to the HTC problem of the Slovak power system (operated by ENEL SE, Inc.). This hydrothermal system consists of 20 hydro plants (three of them are pumped-storage) and 2 thermal plants.

The hourly load demand system of September 20, 2010 is given in Tab. 1. System imports, small, run-of-river hydro plants production and nuclear production have been subtracted from the actual load demand.

Hydro system configuration with input data is presented in Fig. 4. It can be seen that two of the hydro plants are independent, but the rest are hydraulically coupled in a cascade. The computer code (developed in Visual Basic) has been designed to model a complex network of rivers with time delays between hydro plants and reservoirs.

Table 1

Hourly load demand of September 20, 2010 [MW]

Hour	Load	Hour	Load	Hour	Load	Hour	Load
1	731	7	781	13	991	19	1013
2	720	8	831	14	969	20	1000
3	720	9	881	15	954	21	950
4	720	10	931	16	950	22	900
5	720	11	980	17	951	23	850
6	731	12	1002	18	964	24	801

The proposed hybrid approach solution was applied to the hydro sub-problem. The traditional numerical optimization with decomposition **MINLP Decomp** (described in 2.2.1) was applied to the same hydro sub-problem too.

Tab. 2 summarizes the test parameters and results obtained from each method. The results of the GA-MINLP and MINLP Decomp are compared in terms of their minimum *F* value. The difference *F* value of the best GA-MINLP and MINLP Decomp runs was 0.12% (in favour of GA-MINLP method). The decrease of total system operation costs of the best GA-MINLP run could be determined by calculation of thermal units fuel cost function (not available).

Fig. 3 illustrates the power production of the hydro and thermal plants solved using both approaches. As expected, the operation of the hydro plants focuses on the peak load hours, resulting in a peak shaved load curve which is supplied by the thermal units.

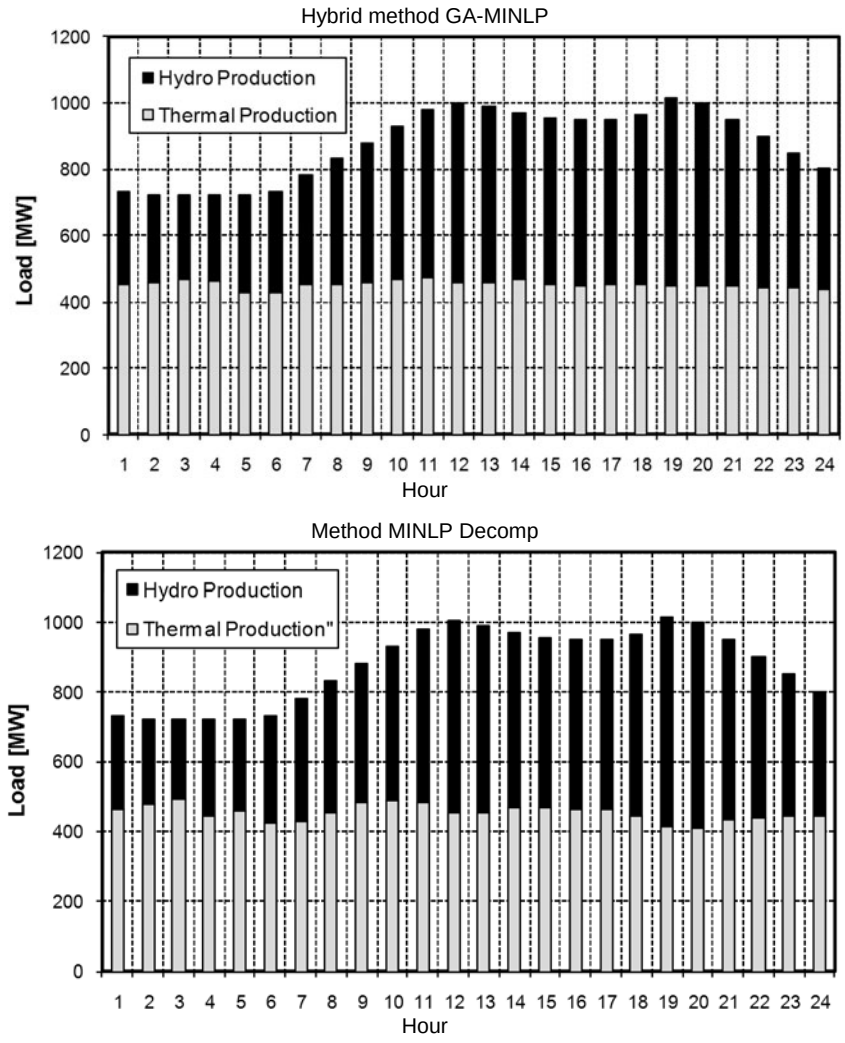

Fig. 3. Power generation from hydro and thermal plants

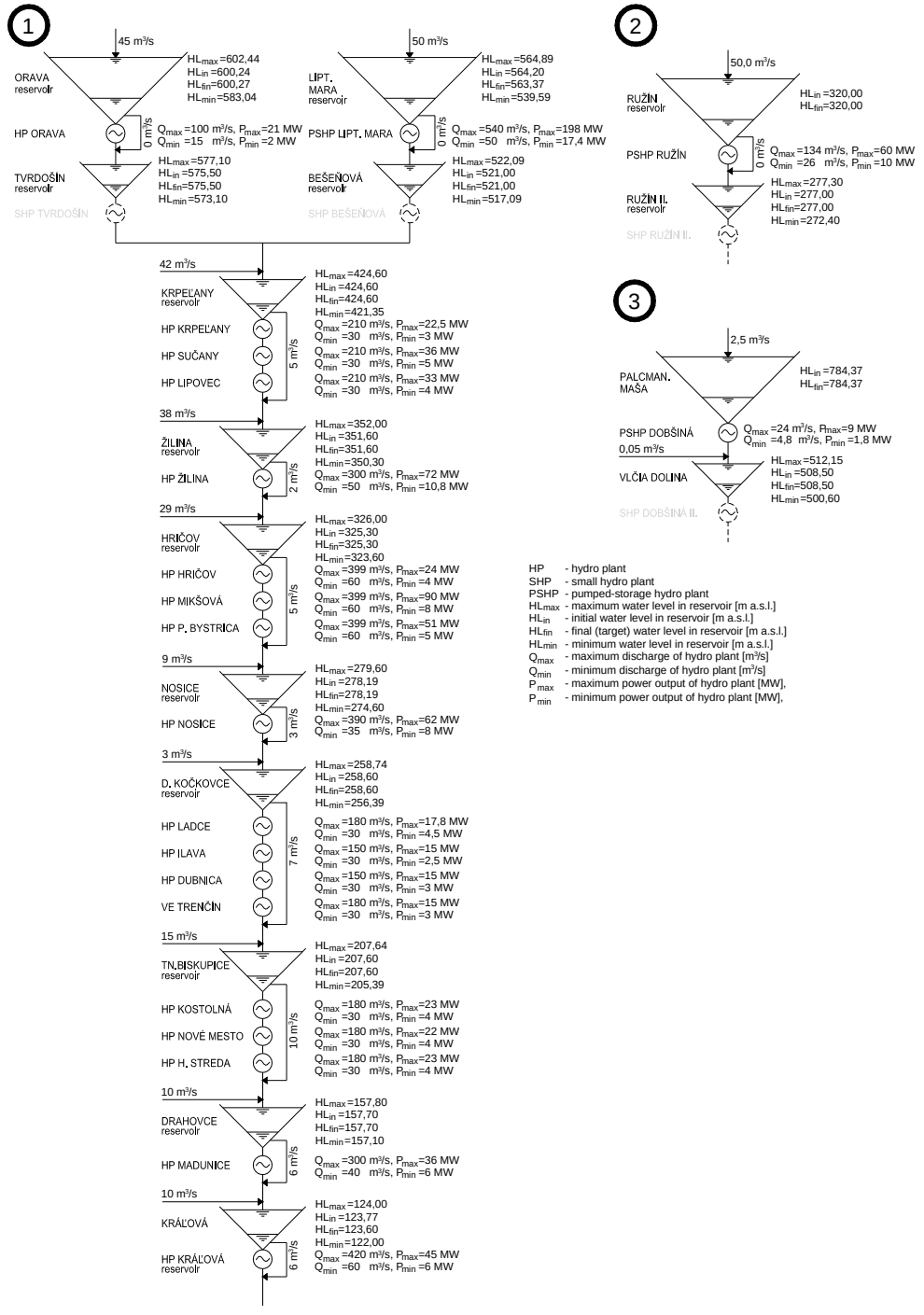

Fig. 4. Hydro system configuration with input data from September 20, 2010

Table 2

Test parameters and results

Method		GA-MINLP	MINLP Decomp
Number of HP		20	
Number of Variables (in one-step of solution)		576	48
Population size		50	–
Number of Generation		500	–
Minimum *F* Value	Best run	4 957 082	4 963 015
	Worst run	5 395 882	–
	% Difference	8.852	–

27.4. Conclusion

A hybrid method for the solution of the hydro sub-problem using a combination of GA and MINLP has been presented. The proposed method has been tested on a real power system, the Slovak power system, consisting of 20 hydro plants and 2 thermal plants. The results prove the effectiveness of the method. The disadvantage of the hybrid GA-MINLP methods is still remaining relatively "long" execution time and high demands on hardware equipments.

References

[1] Čistý M., Bajtek Z.: Hybrid method for the design of the water distribution systems. Bratislava: Journal of Hydrology and Hydromechanics. 57(2). SAP. 130–141, 2009.

[2] Goldberg D. E.: Genetic Algorithms in Search. Optimization and Machine Learning. New York: Addison-Wesley, 1989.

[3] Gil E., Bustos J., Rudnick H.: Short-term hydrothermal generation scheduling model using a genetic algorithm. IEEE Trans Power Syst. 18(4): 1256–64, 2003.

[4] Heredia F. J., Nabona N.: Optimum short-term hydrothermal scheduling with spinning reserve through network flows. IEEE Trans Power Syst. 10(3): 1642–51, 1995.

[5] Chang G. W., Aganagic M., Waight J. G., Medina J., Burton T., Reeves S. et al.: Experiences with mixed integer linear programming based approaches on short-term hydro scheduling. IEEE Trans Power Syst. 16(4): 743–9 2001.

[6] Joyce L., Ponnambalam K.: Hydro energy management optimization in a deregulated electricity market, Kolcun, M. a kol. (2001): Riadenie prevádzky elektrizačných sústav. Bratislava 2006.

[7] Li C., Jap P. J., Streiffert D. L.: Implementation of network flow programming to the hydrothermal coordination in an energy management system. IEEE Trans Power Syst. 8(3): 1045–53, 1993.

[8] Nacházel K., Toman M.: Perspective of the genetic algorithms in the theory of reservoirs water resources systems. Bratislava: Journal of Hydrology and Hydromechanics 43(3). SAP, 1995.

[9] Nilsson O., Sjelvgren D.: Mixed-integer programming applied to short-term planning of a hydro-thermal system. IEEE Trans Power Syst. 11(1): 281–6, 1996.

[10] Reis L. F. R., Bessler F. T., Walters G. A., Savic D.: Water Supply Reservoir Operation by Combined Genetic Algorithm – Linear Programming Approach. Water Resources Management.20: 227–255, 2006.

[11] Seewald V.: Operating of hydro power system in Slovakia. Bratislava: Journal of electronics and energy 1(3): 17–20, 1997.
[12] Šulek P., Dušička P.: The proposed algorithms of hydromodeling for SW Operating model of hydro power system. Technical documentation. STU Bratislava 2006.
[13] Simopoulos D., Kavatza S., Vournas C.: An enhanced peak shaving method for short term hydrothermal scheduling. Energy Conversion and Management 48/2007: 3018–3024, 2007.
[14] Tang J., Luh P. B.: Hydrothermal scheduling via extended differential dynamic programming and mixed coordination. IEEE Trans Power Syst. 10(4): 2021–8, 1995.
[15] Wu R. N., Lee T. H., Hill E. F.: An investigation of the accuracy and the characteristics of the peak-shaving method applied to production cost calculations. IEEE Trans Power Syst, 4(3): 1043–9, 1989.
[16] Wu R. N., Lee T. H., Hill E., F.: Effect of interchange on short-term hydrothermal scheduling. IEEE Trans Power Syst. 6(3): 1217–23, 1991.
[17] yang j., chen N.: Short term hydrothermal coordination using multipass dynamic programming. IEEE Trans Power Syst. 4(3): 1050–6, 1989.
[18] Zoumas C. E., Bakirtzis A. G., Theocharis J. B., Petridis V.: A genetic algorithm solution approach to the hydrothermal coordination problem. IEEE Trans Power Syst. 19(2): 1356–64, 2004.
[19] NeuroDimension, Inc.: Genetic Server, http://www.nd.com
[20] Frontline Systems, Inc.: Frontline Systems Solver Engines, http://www.solver.com

Acknowledgements

This paper was supported by the Grant agency VEGA under contract No.1/0578/11 and No.1/0281/10 and the Slovak Research and Development Agency under contract No.APVV-0680-10.

28 Analysis of the Bearing Structures of Diversion Tunnel

Zlatko Zafirovski, Darko Moslavac, Milorad Jovanovski, Marijana Lazarevska
(Ss. Cyril and Methodius University, Faculty of Civil Engineering, Skopje, Macedonia)

28.1. Introduction

The tailing dams are specific structures with high level of risks on the environment. The risks are connected with possible contamination of the ground water, air pollution and extreme consequences in cases of eventual failure.

This paper presents one specific case where a partial collapse of diversion tunnel bellow system of tailing dams which is a part of all structures in a frame of lead and zinc mine "Sasa" in Makedonska Kamenica. Formerly, tree tailing dams were constructed, and they are used for deposition of the waste material obtained by the technological process of flotation of lead and zinc minerals till present moment (Fig. 1).

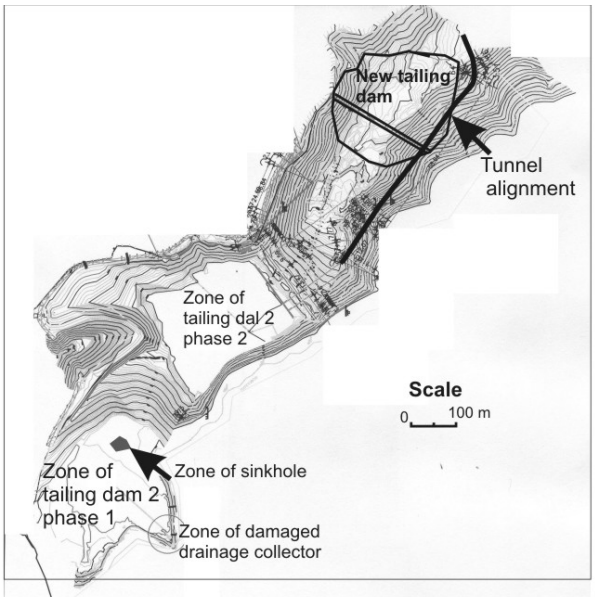

Fig. 1. General layout of tailing dams for the lead and zinc mine “Sasa”

During 2005, a specific collapse at the area of Dam Lake had happened, connected with destruction of the diversion tunnel, occurence of the sinkhole at the waste area and partial contamination along river Kamenicka. (Fig. 2 and 3).

a) b)

Fig. 2. Partial collapse of diversion tunnel and occurrence of sinkhole for the waste surface area of tailing dam 2

Fig. 3. Contamination along Kamenicka river with waste material

Having in mind this specific case, after that, starting from 2007, the tailing dam 3 was designed and with all necesary remedial mesaures for future safe exploitation. It is insured with remediation of the old and construction of new section a new diversion tunnel.

Now, the process of design of tailing dam no 4 is in progress, so some elements of the technical solutions are given in a frame of this article. Briefly, geological and geotechnical elements of the environment are explained.

28.2. Geometric Parameters of the Diversion Tunnel

On the larger part of the length (≈70%), the tunnel is cut through gneisses that are jointed into blocks with dimensions from decimeters up to meters. The Rock Mass Rating for this sections belongs to so called III-category according to Bieniawski RMR classification. On the other part of the length of the tunnel's route (≈30%), the tunnel passes through gneisses that are cracked into smaller block and in a III–IV category according to Bieniawski. The input parameters for numerical analyses is given in a Tab. 1.

Table 1

Input parameters for the Hoek-Brown classification

Rock category according to Bieniawski	σ_{ci} (MPa)	GSI	mi	D
III	50	47	10	0.8
IV	50	30	10	0.8

Using the input parameters that are given in Tab. 1 and the equations used for the calculation of the strength-deformability rock parameters, according to the Hoek-Brown's failure criteria, the global strength of the rock material (σ_{cm}), cohesion (C), angle of the internal friction (φ) and the deformability module of the rock (E_{rm}) are given in Tab. 2.

Table 2

Estimated values of the strength-deformability rock characteristics

Rock category according to Bieniawski	σ_{cm} (MPa)	C (MPa)	$\varphi^{(0)}$	E_{rm} (MPa)
III	4.2	0.246	43	3400
IV	2.3	0.135	34	1480

Based on this assumption, the designed procedure is briefly explained bellow.

28.3. Static and Dynamic Analyses for the Diversion Tunnel's Lining

28.3.1. Numerical Model

Numerical model of the continuum, as well as the primary and secondary lining of the diversion tunnel, were made using the finite element method (FEM) which is also implemented as a part of the software package PHASE 2 (www.rocscience.com). Using the failure criteria of Hoek-Brown and the assumption that the surrounding rock material is elastic-plastic, numerical analyses were performed. A range of five diameters (5D) of the continuum, left, right and under the tunnel, was analyzed. The upper edge of the model is included in the analyses as it is the real terrain in the section with the maximal above layer. The following boundary conditions were adopted for the numerical model: flexible bearings in vertical direction on the left and right boundary, fixed bearings on the bottom boundary and free (without displacement limitations) upper boundary of the model. The numerical model is shown in Fig. 4.

The tunnel construction is a process that happens during some period of time, so the analyses were performed in few phases as follows:

— **Phase–1:** the primary condition of the stresses in the massif, before any intervention;
— **Phase–2:** tunnel excavation;
— **Phase–3:** support placement;
— **Phase–4:** earthquake influences during the tunnel exploitation.

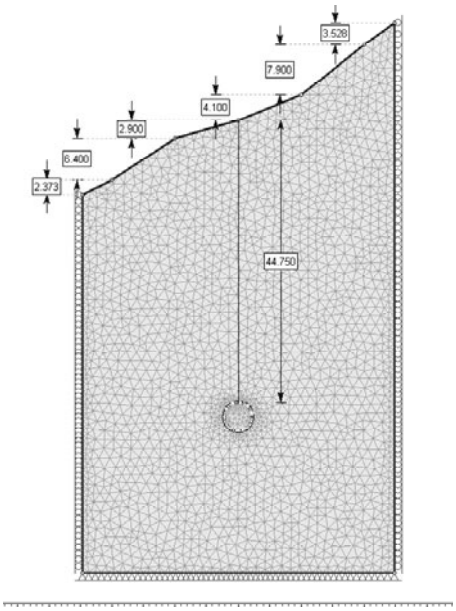

Fig. 4. Numerical model

28.3.2. Loads

The most unfavorable section, aka the section where the largest primary stresses in the rock are expected, is the section of the route of the diversion tunnel extension that has a maximal above layer. The value of the above layer's height in that section is *Hnmax* = 44.75 m (Fig. 4).

When the diversion tunnel's profile is excavated, it is expected that the primary stress condition of the surrounding rock mass will be disturbed, and that a concentrated stresses will occur in the opening area, which will lead to deformations appearance. In order to prevent large deformations in the walls of the tunnel excavation and uncontrolled increasing of the plastic zone around the unsupported tunnel excavation, as well as for the prevention of potential unstable blocks falling, the tunnel excavation has to be stabilized. The predicted stabilization, in this case, is formed of shotcrete support and anchors. Apart from the basic loads, that come from the size of the above layer mountainous material, analyses also include an earthquake influence (through the inertial forces) that occur when the earth's acceleration in horizontal direction is a_H = 0.3 g and when the earth's acceleration in vertical direction is a_V = ±0.15 g.

28.3.3. Results from the Numerical Analyses

Tunnel TYPE-3 is applied in the sections of the extension of the diversion tunnel where the rock mass falls into category III, according to the Bienawski classification. The primary support, made of shotcrete *d* = 15 cm; MB-25 (calotte +abutments) reinforced with a net reinforcement in the calotte *Q*–196 and "SN" anchors Ø22–25 mm; *La* = 2.5 m; *ap*/*an* = 1.25/1.5 m, completely ensures the tunnel stability. A complete reinforced concrete lining is not predicted for these parts, but construction of a base arch that is shaped as a channel (the side's height is *h* = 185 cm) which will enable the river flow during the tunnel exploitation (Fig. 5).

On these tunnel sections, the capacity of the primary supporting (the thickness of the shotcrete and the anchors disposition) should be proven according to the basic principles of the New Austrian Tunneling Method (NATM). This means that the tunnel convergences have to be permanently measured during the whole exploitation time period.

Diagrams and intensity of the axial forces, bending moments and transversal forces that occur in the primary support, are shown in Fig. 6, 7 and 8.

Measuring units: MN, m, MPa
Sign convention
(+*N*) = pressure axial force; (–*N*) = tension axial force;
(+*M*) = tension stress from the inner lining side, pressure stress from the outer lining side;

(–*M*) = tension stress from the outer lining side, pressure stress from the inner lining side; (+σ) = normal pressure stress; (–σ) = normal tension stress.

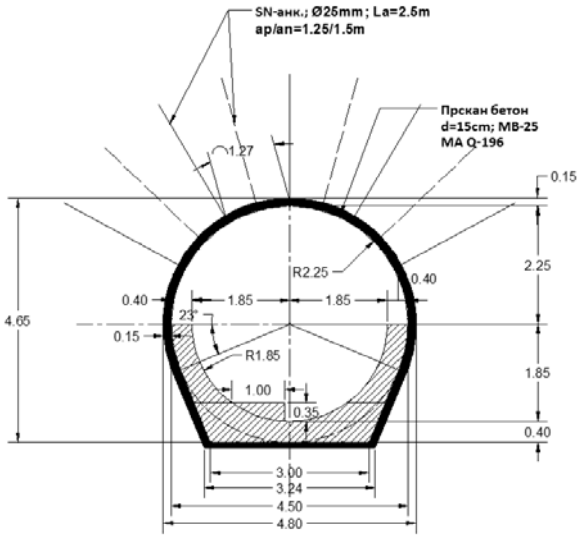

Fig. 5. Tunnel TYPE-3 in materials of III-rd category according to Bieinawski

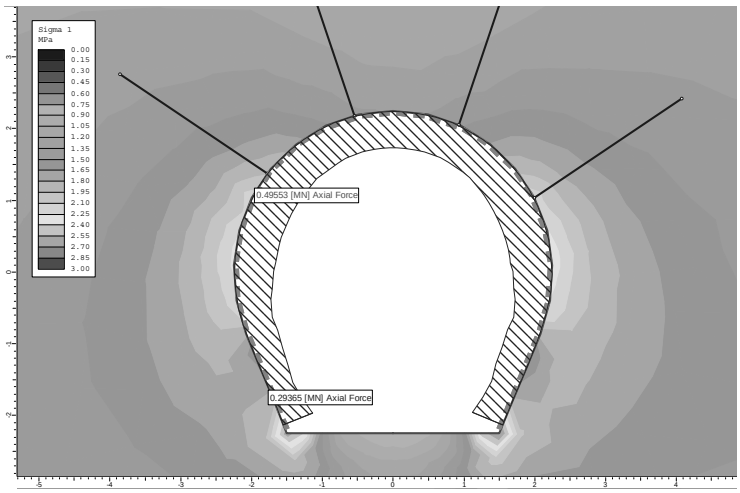

Fig. 6. Diagram of the axial forces in the shotcrete in tunnel TYPE-3
Nmax = 0.496 MN; Nmin = 0.294 MN

The diagrams for static units that occur in the shotcrete lining show that the axial forces are dominant compared to the bending moment which are relatively smaller. The primary support made of shotcrete and anchors, for the tunnel TYPE-3, is also its final (permanent) supporting, because the concrete support has no load-bearing capacity and it is used only as a erosion protection of the tunnel's bottom in case of the water seepage through the tunnel.

Because of this, we analyzed the influence of earthquake on the primary support, an earthquake with horizontal acceleration of a_H = 0.3 g and vertical acceleration of a_V = ±0.15 g.

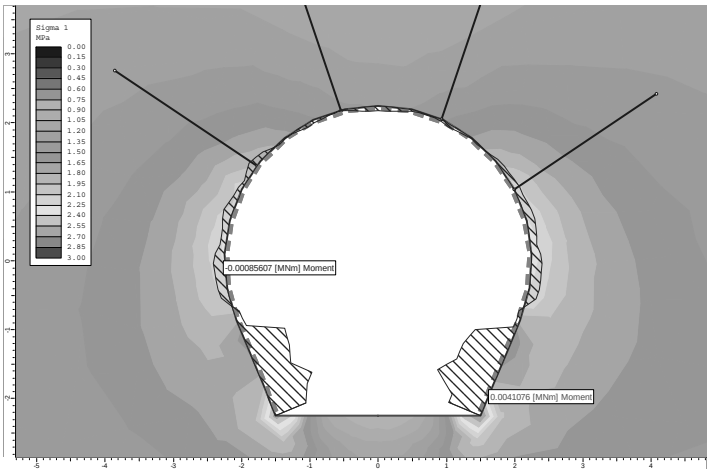

Fig. 7. Diagram of the bending moments in the shotcrete in tunnel TYPE-3
Mmax = 0.004 MNm; Nmin = –0.0008 MNm

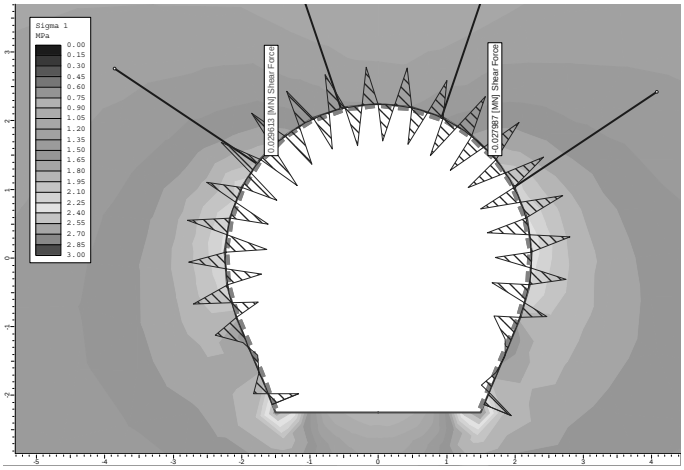

Fig. 8. Diagram of the transversal forces in the shotcrete in tunnel TYPE-3
Qmax = 0.0296 MN; Qmin = –0.028 MN

Fig. 9 and 10 show the occurred static units in the shotcrete support when there is an earthquake influence. It is noticeable that the value of the maximal axial force is increased for (0.759/0.496) 53% when there is an influence of an earthquake that has a horizontal acceleration of a_H = 0.3 g and vertical acceleration of a_V = – 0.15 g (downwards). When the vertical acceleration is a_V = +0.15 g and has an upper direction, the axial forces in the shotcrete have lower values, and this case is not adequate for dimension calculations. Bending moments remain insignificantly small, even with the influence of an earthquake.

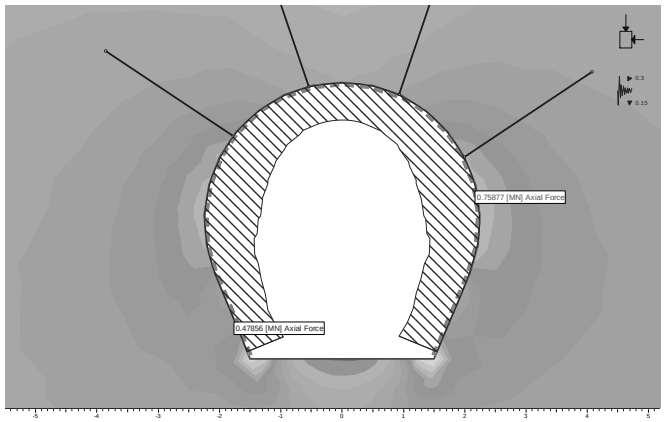

Fig. 9. Diagram of the axial forces in the shotcrete with an earthquake influence
Nmax = 0.759 MN; Nmin = 0.478 MN

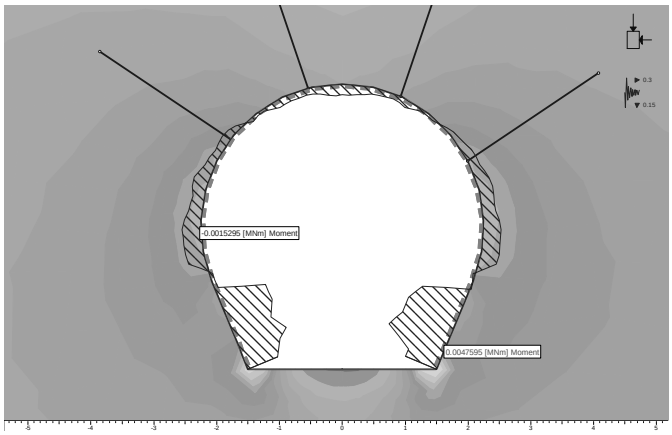

Fig. 10. Diagram of moments in the shotcrete with an earthquake influence
Mmax = 0.0048 MNm; Nmin = –0.0015 MNm

Dimensioning of the primary support for the tunnel TYPE-3

Diagrams of the support's load-bearing capacity give the opportunity for determination of the safety factor for some reinforced-concrete support. For the given safety factor, it is possible to draw the envelopes of the load-bearing capacity, as a function of axial force and moment, as well as the envelopes of the load-bearing capacity as a function of axial and transverse force. The values of the axial force, moment and transverse force that occur in the support are compared to the load-bearing capacity envelopes. If the calculated values of the static units in the support (*N*, *M*, *Q*) are inside the envelopes, than the support has a safety factor which is larger than the envelope's value. If all calculated values of the static units in the support are inside the load-bearing envelope that has the designed safety factor, then the safety factor of the support exceeds the value of the needed safety factor (**Fs = 1.4** for temporal support; **Fs = 2.0** for permanent support). Load-bearing

diagrams for shotcrete (thickness d = 15cm and concrete strength 25 MPa are shown in Fig. 11.

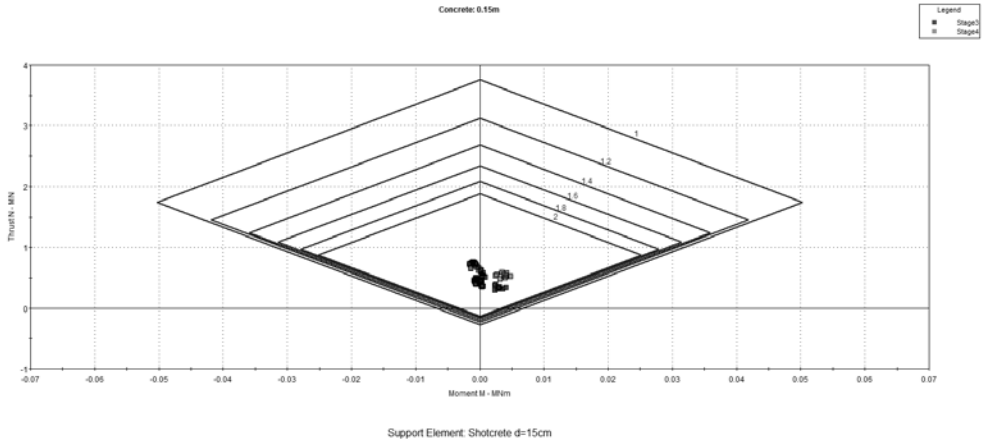

Fig. 11. Load-bearing capacity envelope as a function of moments and axial forces, for shotcrete that has a thickness of *d* = 15cm, MB-25

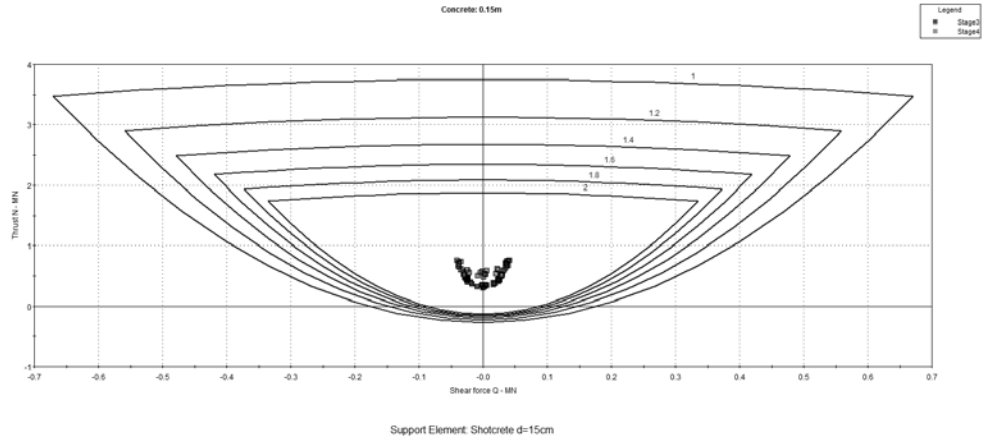

Fig. 12. Load-bearing capacity envelope as a function of transverse and axial forces, for shotcrete that has a thickness of *d* = 15 cm

Analyzing Fig. 11 and 12, it can be concluded that in every finite element of the shotcrete, the calculated static unit's values (*N*, *M*, *Q*) during an excavation phase (red spots Stage3), as well as for the stage that contains an earthquake influence (green spots Stage 4), are inside the envelope that has a safety factor of **Fs** = 2.0, which means that the value of the safety factor for shotcrete support is **Fs** > 2. The shotcrete should be reinforced using a constructive reinforcement *Q* – 196. Fig. 13 illustrates the tunnel's deformed condition during an exploitation phase and the intensity of the resulted displacements. Horizontal convergence is in a range of 1.25 mm, while the convergence is about 0,028%. Vertical convergence ia about 2.1 mm and convergence 0.047%.

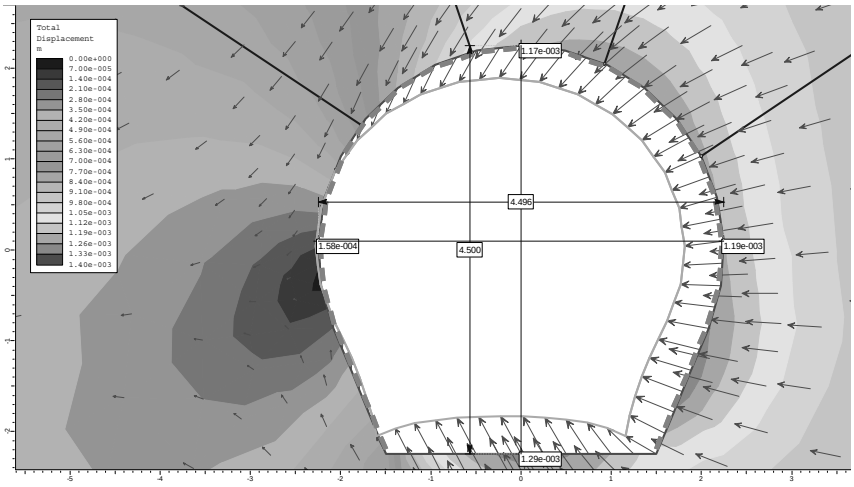

Fig. 13 Total displacement of the shotcrete support for tunnel TYPE-3

From the values of the convergences and in accordance with the Sakurai and Charn [1] recommendations, we can conclude that the tunnel excavation will be safe and the tunnel will be stable. The final lining on the sections of tunnel TYPE-3 has no load-bearing capacity function and it will be constructed just to enable the freely water seepage from the river Saska. This tunnel lining will be reinforced with constructive reinforcement Φ12/20 cm in both zones. According to Eurocode-2;

$$A_{s,\,\min} = 0.002 \cdot Ac = 0.002 \cdot 100 \cdot 40 = 8\ \text{cm}^2/\text{m}'$$

$$A_s = 2 \cdot 5.66 = 11.3\ \text{cm}^2/\text{m}' \rightarrow OK$$

28.4. Conclusions

The exploitation of the tailing dams is connected with is with high level of risks on the environment. This indicates that design of diversion structures must be done with a great attention, in order to insure safe work during operational phase. The important step in the design is to obtain reliable input parameters for the geological elements along diversion structures, which is basic prerequisite for numerical analyses. Authors believe that the given analyses can be illustrative for similar cases in the practice.

References

[1] Hoek E., Carranza-Tores, Corcum B.: Hoek-Brown failure criterion – 2002 Edition.
[2] Petkovski Lj., Moslavac D., Jovanovski M.: Design for new tailing dam for the lead and zinc mine Sasa 2007.

29 Presentation in the Applied Hydraulics

Marija Vukelic-Sutoska (Ss. Cyril and Methodius University,
Faculty of Agriculture and Food, Skopje, Macedonia) Ivica Vukelic
(Enterprise “Cesta”), Zvonimir Vukelic (Prof. emeritus)

29.1. Function of the Communication

No one would talk much in society if they knew how often they misunderstood others (Johann Wolfgang von Goethe). Nothing is so simple that it cannot be misunderstood (Freeman Teague, Jr.). When you know something, say what you know. When you do not know something, say that you do not know. That is knowledge (Kung Fu Tzu-Confucius).Without knowing the force of words it is impossible to knew men (Confucios). Speak comfortable words (William Shakespeare). Trying to speak of something as messy as communication in technical terms seems to be another, that is, math and science and technology are the answer to all of our problems.

Successful active listening is: Listen to the other person, stop your own thinking, support with non-verbal signs/sounds, if necessary, interrupt (friendly way) to grasp point, summarize briefly + value free and use their own words, structure the discussion or, add/build your own point on top. In Fig. (1) is shown a message from a speaker to a receiver.

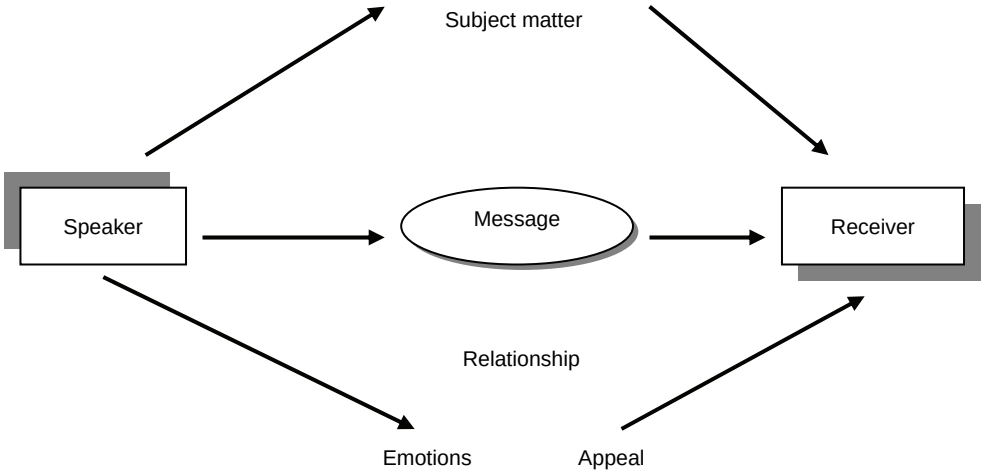

Fig. 1. From Speaker to Receiver

In contact with people, the outside world, our mind always follows this simple pattern (Fig. 2):

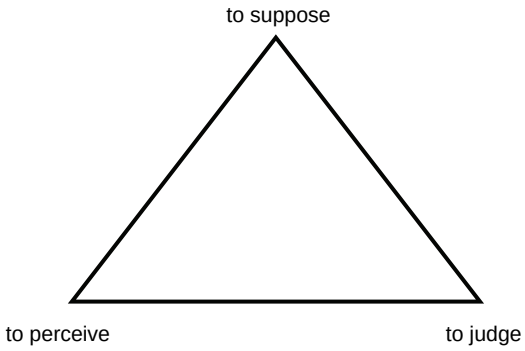

Fig. 2. Contact with people

Table 1

Feedback and Criticism

Feedback	Criticism
Constructive	Destructive
Positive sense for improvement	Negative sense
For future actions	On the past actions
Behaviour	Character, personal
Action + change	Passive + standstill
Needs of receiver	Needs of sender
Helping	Judgement
Observation upon request	
Dialogue	Monologue

29.2. Presentation

Due to Tab. 2 it is possible to basic elements of presentation.

Graphical display media are: Blackboard, daylight projector, flip chart, pin-board, worksheets, model, poster, photo, film.

Visual aids: Should never be used without first being tried out, should promote, not hinder, understanding, should be used systematically, need a clear view by all the audience, should be allowed to work, must be supported with a loud voice.

There is a model, the "explanation structure in four steps"

MILTZ (1971) trained 30 teachers in this technique. The teachers achieved the following cores on a scale from 10very poor to 5 = excellen.

	Before	After
Structure	2.92	3.62
Clarity	2.79	3.59
Quality	2.84	3.68

Table 2

Reaction to poor explanation

Speaker **"I can't explain things"** Possible consequences: I will have to improve	**Listener** **"I'm too stupid"** Possible consequences: Resignation
"The listeners don't want to understand or can't understand!" Typical request: "Listen more closely!"	**"The speaker can't or won't explain!"** Typical request: "Explain that again!"

What is the model like?

1. What is the question? Define the question yourself?
2. Identify the things – the elements, the variables – that matter.
3. What is the relationship between the things?
4. What is the principle involved?

The Explanation Structure in Four Steps

An example from the field of

Step 1 The question you have to reformulate could be as follows:
Step 2 Which elements have to be explained?
Step 3 What relationships exist between these elements?
Step 4 What general principle the listener already know can be named her.

The purpose of a brief presentation is to inform a certain number of staff or interested parties about subject matter and circumstances. It differs from an address in that the appeal is not to the listeners' emotions, but to their intellect. The brief presentation is not, therefore, intended to impress, convince influence or motivate, but systematically to disseminate knowledge and facts. Its major disadvantage is that the listeners are only passively involved. As a rule, there is no feedback between the speaker and listener.

It is therefore particularly important to make use of the following **structuring elements**: **Guides** (Pre-structuring), **Frames** (Transition signals), **Bridges** (Back and cross references), **Markers** (Accentuation)

The motivating elements are just as important:

— Examples,
— Persons,
— Figures,
— Questions.

Use a clear structure Say what you are going to say – Say it – Then say what you have said, provide a summary and find a (gripping concluding formula.

Use short sentences: Use telling words, use verbs rather than nouns, avoid abstractions, avoid negatives, avoid "imaginary subjects".

29.3. Facilitation

Facilitation is a type and method of group discussion. The aim is to involve the participants actively and to focus them on their objectives.

The **Facilitation Method** is a system of techniques and individual methods for the implementation of facilitation and info-markets. The main elements are: Visualisation, group question techniques, work in plenary and small groups.

29.4. The Factors to be Considered When Preparing a Meeting or a Workshop

There are the following factors:Type and objective of the workshop, available budget / who sponsors (might sponsor) the conference? / ceiling allowances, souvenirs, conferences fees, official permission to hold the workshop, selection of participants (if possible use criteria), consider all related institutions, groups and persons (to select from), consider that often participants have to be nominated by their institution, time (date), location and duration, select the facilitator, if needed, chair person etc., select and contact the experts who (should) present papers, prepare related documents for the participants (and facilitator), prepare a time table/topics (prioritisation) (preferably in co-operation with the facilitator), reservation of suitable meeting/workshop rooms, accommodation for participants, transportation, send invitations to the participants together with relevant information and material handouts, tourist information, presentation of the country to participants, give a deadline for their response and follow up, secretarial services and support staff, translation services, treatment for special guests, seating arrangements, security, name tags and flags, logo of the conference, official meetings (outside the workshop), meetings with interested parties (private sector), cultural and special considerations, facilities, such as typing, printing, photocopying, needed visualisation material, public relations (press, radio, TV), lunch refreshments etc. social event, spouse programme, “by order” shopping, evaluation of the workshop and follow-up activities, proceedings and funding.

Good facilitation involves proper time management, taking into account local customs and the type and duration of the event. The plan should include regular changes in techniques and exercises. If you plan three card collections, one after the other, people will get bored and become less motivated. Methodological changes make an event more interesting and the participants will be eager to know what comes next. There are no fixed rules for timetables. It is recommended that there should be a programme in the evening. However, the evening programme may be optional and more informal, sometimes for small groups work such as preparing a presentation for the next day’s plenary showing a film or slides concerning a case study on the theme of the workshop. An informal session may also be scheduled to facilitate social contacts.

Whilst facilitating you are dealing with groups and your task as facilitator is to activate your group. Each group is a new group and each participant is there with his individual expectations, wishes and fears. As facilitator you are the one who brings life into this gathering of people. Every group has to be born. To make this difficult job “easy” here are some hints for activating participants and how to organise group work.

Every participant is a resource person and every resource person is a participant, everyone helps everyone, every idea counts, conflicts and controversial points of view should be visualised and dealt with at an appropriate time, uncomfortable feelings must be dealt with promptly, use the “yellow card” technique to stop people from talking too long and use FacilitationTechniques as a learning process for making people more tolerant and receptive for other opinions.

29.5. Basin Wide Holistic Integrated Water Assessment Model

As a part of CPSP (Country Policy Support Program), a Basin Wide Holistic integrated Water Assessment (BHIWA) model was developed (Fig. 3, 4, 5). The model has seven computation modules:

1) actual evapotranspiration, quick runoff and natural recharge,
2) irrigation withdrawal,
3) irrigation returns,
4) evapotranspiration (ET) by sector,
5) domestic and industrial withdrawals,
6) river water balance and
7) groundwater balance.

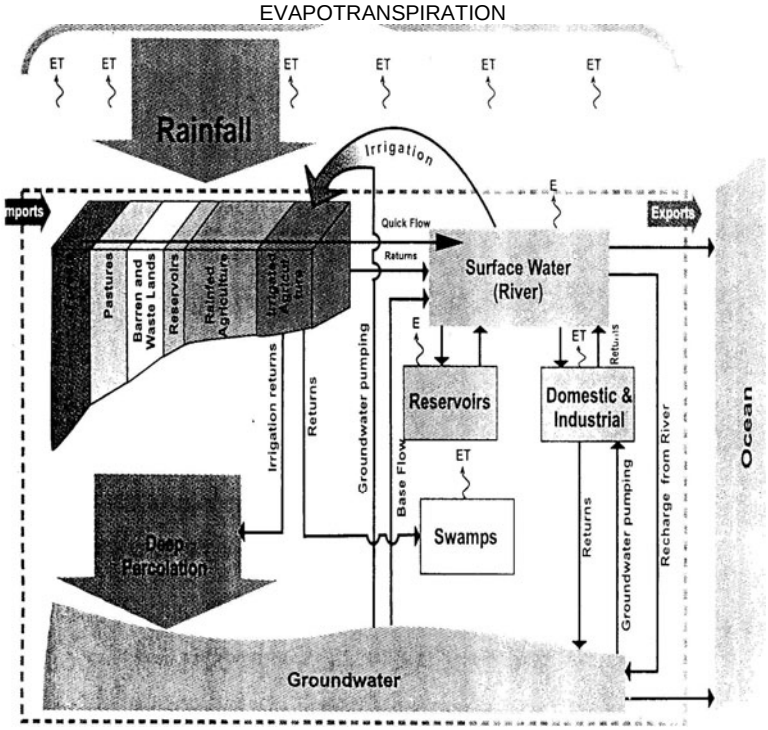

Fig. 3. Diagram of BHIWA model (After ICID newsletter 2002)

In addition to these moules, there are worksheets to facilitate data inputs, and generation of aggregated results in the form of tables and charts.

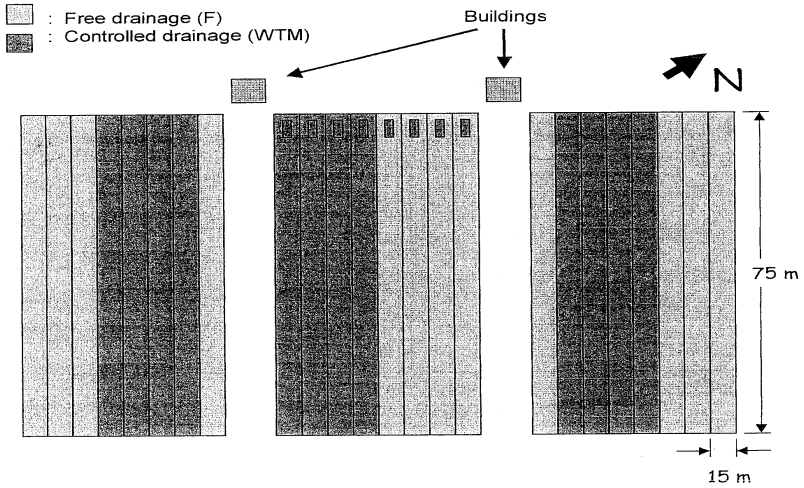

Fig. 4. Layot of one field (after N. Stampfli and A. Madramootoo 2002)

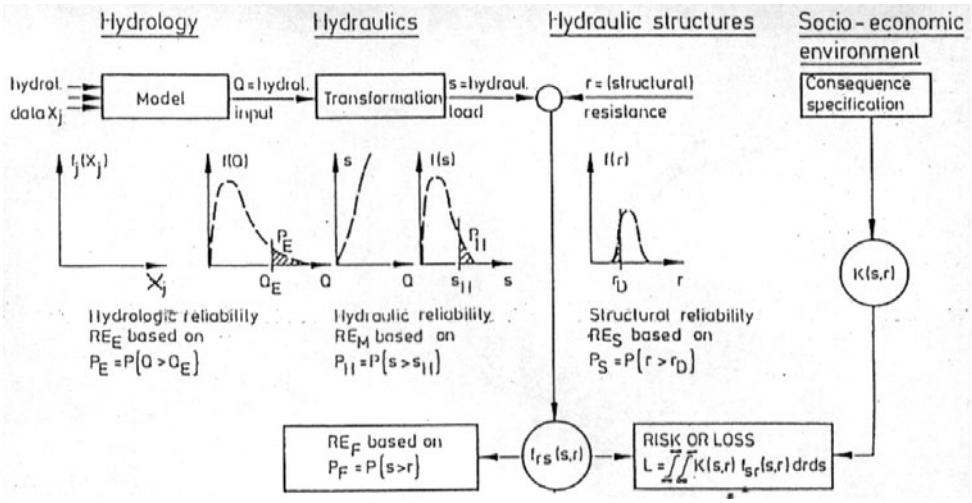

Fig. 5. Hydraulic structures

29.6. Irrigation – Gas Exchange – Drainage Model

The optimised solution for a lasting cost reduction and quality improvement featuring the following integrated functions: Irrigation and liquid fertiliser application, Oxygen supply and gas exchange, Active suction drainage, Pollutant degradation, soil

decontamination, leaching, Water extraction by condensation, Soil heating and temperature control.

References

[1] Butler Gillian, Hope Tony: Managing Your Mind. New York: Oxford University Press 1996.
[2] Meherabian Albert and Morton Wiener: Decoding of Inconsistent Communications, Journal of Personality and Social Psychology 6: 109–114, 1967.
[3] Neubauer Ewald: Facilitation techniques, training course in Skopje 2005.
[4] Pearson J.: Interpersonal communivation. Glenview, Illinois: Scott Foreman and company 1983.
[5] Pinker S.: How the mind works. New York: w. W. Norton and company 1997.
[6] Vukelic Z., Zileska-Pancevska V., Donevska K.: Public presentation of the irrigation system project in the republic of macedonia.- Montreal, the 18 th Congress and the 53 rd Confernce food production under conditions of water scarsity, increasing population and environmental pressures, proceedings Q. 51, P. 4.O3, 174–177, 2002.
[7] Vukelic Z., Cukaliev O., Vukelic-Sutoska M., Trajanovska L.: Watershed modelling as a part of ecological concepts in hydrology.-ohrid. Conference on water observation and information systems for decision support, proceedings 1–10, 2004.
[8] Vukelic Z.: Teknika e komunikimit dhe prezentimit. University in Tetovo, Faculty of Civil Emgeeneriring 2009.

30 Basic Indicators of University Studies of Civil Engineering in the Hydraulic Engineering Department at the Faculty of Civil Engineering, University of Zagreb

Josip Marušić, Damir Bekić (University of Zagreb,
Faculty of Civil Engineering, Croatia)

30.1. Introduction

Following the suggestion of the *National Council of Higher Education and the DECREE of the Ministry of Science, Education and Sports*, the APPROVAL was issued on June 2, 2005 to the *Faculty of Civil Engineering, University of Zagreb,* to conduct the pre-graduate and graduate university course in civil engineering, starting from the academic year 2005/06. The post-graduate doctoral and specialist courses program was initiated in the academic year 2006/07. The university curriculum in civil engineering is in agreement with the principles and guidelines of the *Bologna Declaration,* signed on June 19, 1999, by representatives of 29 European countries, for the purpose of reforming of higher education in Europe. By 2001, the Bologna Declaration was signed by 40 countries, including the Republic of Croatia.

In formulation of study programs, experience on pre-graduate and graduate civil engineering studies was used, acquired by renowned universities in European Union countries: Delft, Zürich, Hannover, Stuttgart, Trieste, London and Glasgow. Also, recommendations were used for formulation of teaching programs resulting from important European projects defining of the objectives of higher education in civil engineering SOCRATES and ERASMUS – European Civil Engineering Education and Training and E4 – Enhancing Engineering Education in Europe, as well as suggestions of the German association of agencies for accreditation of higher education teaching programs in civil engineering.

30.2. Primary Objectives of the Bologna Process of Higher Education

Achievemnt of joint European system of higher education is planned through the following objectives of the *Bologna Declaration:*

a. Adoptation of the system of easily recognizable and comparable academic and professional degrees and introduction of diploma supplements for easier and rapid employment and international competitiveness. *Upon completion of the course, along*

with the final document, a Diploma Supplement is issued, which contains the list of all passed exams and their value in ECTS points. The supplement contains provisions which are not mentioned in the final document but are important for understanding of the program of the final study and achieved level of education, for easier comparison of final studies.

b. *Adoptation of the uniform system of three educational cycles: undergraduate* (*bachelor*) *– three years, graduate* (*master's*) *– two years, and post-graduate* (*doctoral*) *– three years.*
c. Introduction of European system of ECTS points expresses the amount of students' effort required to process and complete a given unit – subject of the program. *In the ECTS point system, one academic year is worth* 60 *points, which is the total working load during the year, and one semester is equal to* 30 *ECTS points.* A student's engagement during the academic year is 1,500 to 1,800 working hours, which means that one ECTS point is worth 25 to 30 student's working hours.
d. Promotion of mobility, overcoming of obstacles to free movement of students and teaching staff, both by horizontal mobility (student studying a part of time on another university in the country or abroad), and vertical mobility (student completing the whole study abroad)
e. Establishment of the national system of monitoring and guaranteeing the quality, and promotion of European cooperation for permanent monitoring and improvement of study programs during the academic year.
f. Promotiion of required European dimension in the field of higher education, which may be achiedved by inauguration of the European space in development of teaching programs, inter-institutional co-operation, mobility programs and integrated study programs, upgrading and research.

The above objectives may be materialized by higher financial investment in higher education, both by Croatia and by using special funds of the European Union.

30.3. University Undergraduate Course of Civil Engineering

The undergraduate course lasts three years, i.e. six semesters, and is valued by 180 *ECTS points.* The instruction plan is based on students' engagement of 40 hours per week – which includes lectures, field work, practice, and field instructions. The academic year lasts 44 working weeks, out of which 30 weeks of instruction. In one semester, students register 25 to 35 ECTS points. *The sub graduate course finishes by passing the final exam in civil engineering subject from the study program* before a board of three members nominated by the *Committee for graduate and final exams* of the Faculty of Civil Engineering.

In the sub graduate course of university education, the number of subjects per semester is the following:

1st semester: 4 mandatory and 6 optional, out of which 2.30 ECTS points registered (15+10 hours),
2nd semester: 6 mandatory subjects, 30 ECTS points (14+11 hours),
3rd semester: 5 mandatory and 2 optional, out of which 1.30 points are registered (14+10),
4th semester: 4 mandatory and 4 optional, out of which 2.30 points registered (16+8),
5th semester: 4 mandatory and 4 optional, out of which 2.31 points registered (16+9),
6th semester: 5 mandatory and 2 optional, out of which 1.29 points registered (12+9).

From 1st to 6th semester, students register 28 mandatory subjects (147 ECTS points), and out of 18 optional subjects they register 8 subjects (30 ECTS points. *In* 6*th semester the final exam is worth* 3 *ECTS points. In the sub graduate course of civil engineering the students register the following hydrotechnical programs*:

Fluid Mechanics (6 ECTS points), Hydrology (3.0), Water Supply and Sewerage I or Water Protection (4) and Hydrotechnical Structures (4). *Total* 3 *mandatory* (13 *ECTS points*) *and two optional hydrotechnical subjects out of which one is registered*(4 *points*), *or together* 4 *hydrotechnical subjects valued* 17 *ECTS points* – out of the total of 180 ECTS points from 1st to 6th semester of the sub graduate course in civil engineering.

30.4. Graduate Course of University Study of Civil Engineering, Hydrotechnical Branch

Starting from the academic year 2005/06, *the program of the graduate university course in civil engineering is conducted in the following branches:* GEOTECHNOLOGY, **HYDRAULIC ENGINEERING,** STRUCTURES, ORGANIZATION OF CONSTRUCTION, MATERIALS, COMMUNICATIONS and THEORY AND MODELING OF STRUCTURES. *The graduate course takes two years, i.e. four semesters worth* 120 *ECTS points.* The instruction plan is based on students' engagement of 40 hours per week, which includes lectures, practice, field instruction and time required for preparations for exams. The academic year lasts 44 weeks, out of which 30 instructional weeks and 14 weeks for consultations, preparing for exams and exams (during these weeks there are neither lectures nor practice).

The number of subjects of the graduate course in the hydrotechnical branch of civil engineering in the separate semesters is as follows:

1st semester: 4 mandatory (22.5 points), out of which 3 *hydrotechnical* (21 *points*) and 1 subject from other branches (1.5), and 2 optional out of which students select one (7.5 points). *Hydrotechnical subjects are the following:* **Hydraulics (7.5 points), Hydrology 2 (6.0) and Regulation of Watercourses (7.5 points) – total 21 ECTS points.**

2nd semester: 3 mandatory subjects (23.0 points), out of which 2 *hydrotechnical* (17.0 points) and 4 optional out of which students select 2 (7 points). *The mandatory hydrotechnical subjects are:* **Waterways and Ports (9.0), Hydrotechnical Land Reclamation (8.0),** and optional subjects are **Water Supply and Sewerage 1** and **Water Protection (4.0). Hydrotechnical subjects are worth 21 points,** *and the others* 9 *points*, among which Environmental Protection is worth 3.0 ECTS points.

3rd semester: 2 mandatory *hydrotechnical subjects***: Hydrotechnical Systems (6.0 points) and Water Supply and Sewerage 2 (6.0) – total 12.0 points,** *and* 3 *out of the following* 5 *optional subjects***: Urban Hydrology (6.0 points), Water Treatment (6.0), Modelling in Hydraulic Engineering (6.0), Hydrotechnical Land Reclamation 2 (6.0) and Practice in Protection from Water (6.0) – total 18 ECTS points,** or 30 ECTS points, two mandatory and three optional hydrotechnical subjects. There is also a possibility of selecting two optional subjects from programs of other branches.

4th semester: One mandatory *hydrotechnical subject* – **Utilization of Water Power (6.0 points)** and *one optional subject out of the following six hydrotechnical subjects:* **Hydraulic Engineering Design (6.0), Biological Waterworks (6.0), Hydrotechnical Protection of Communications (6.0), Experimental Hydraulics (6.0), Special Hydropower Systems (6.0), and Maritime Structures (6.0).** Students register one mandatory and one optional subject which are worth 12 ECTS points. There is also a possibility of selecting one of 4 optional subjects from programs of other branches. *In the* 4*th semester, preparing of the GRADUATION THESIS* is planned on one of *Sub-graduate* the *hydrotechnical subjects, which is worth* 18 *ECTS points.*

According to the program of UNIVERSITY GRADUATE COURSE IN HYDROTECHNICAL BRANCH OF CIVIL ENGINEERING, the students during four semesters register for and undergo exams on 8 *mandatory hydrotechnical subjects which are worth* 56.0 *ECTS points, and* 5 *optional* (*out of total* 12) *hydrotechnical subjects worth* 28.0 *points, or* ***total*** 84**.**0 ***ECTS points*** (70.0 *percent*). The students separately register for 2 mandatory subjects from other branches (7.5 points) and 2 optional subjects from other branches (10.5 points) – total 18 points (15.0 percent). *The graduation thesis on hydrotechnical subjects is prepared during the* 4*th semester and is worth* 18 *points* (15.0 *percent*).

30.5. Conclusion Regarding Undergraduate and Graduate Course in Civil Engineering

Under the program of UNDERGRADUATE UNIVERSITY COURSE IN CIVIL ENGINEERING the students from 1st to 6th semester register for and undergo exams on 28 mandatory subjects worth 147 ECTS points. Out of 18 optional subjects, the students register for and undergo exams in 8 subjects which are worth 30 points. The final thesis is prepared after 6th semester, worth 3.0 ECTS points. *Out of the total of* 28 *mandatory, there are* 3 *hydrotechnical subjects with the total of* 13.0 *ECTS points, and out of* 18 *optional subjects, there are* 2 *hydrotechnical subjects, out of which the students register for one worth* 4.0 *ECTS points. Totally,* 4 *hydrotechnical subjects of the sub graduate course are worth* 17.0 *ECTS points.*

Under the program of UNIVERSITY GRADUATE COURSE IN HYDROTECHNICAL BRANCH OF CIVIL ENGINEERING the students from 1st to 4th semester register for and undergo exams in 17 subjects worth 102 ECTS points. **There are 8 mandatory hydrotechnical subjects (56.0 points) and 5 optional subjects (out of 12, 28.0 points). The total of 13 hydrotechnical subjects is worth 84 ECTS points.** Two mandatory subjects from other branches are worth 7.5 and two optional 10.5 points, i.e. they together contribute 18 ECTS points. *The students submit the application for the graduate thesis at the beginning of* 4*th semester, and the period for preparing of graduation thesis is* 45 *to* 90 *days. Scholarship or credit holders may get the subject of the thesis in accordance with the requirements of the company or legal entity awarding the scholarship or credit.*

30.6. Post-Graduate Doctoral Course of Civil Engineering

30.6.1. Organization and Conducting of Post-Graduate Doctoral Course Since Academic Year 2006/07

The post-graduate doctoral course is conducted in the domain of technical science, scientific field of civil engineering, in the following branches: GEOTECHNOLOGY, **HYDRAULIC ENGINEERING,** ENGINEERING STRUCTURES, MATERIALS IN CIVIL ENGINEERING, CONSTRUCTION MECHANICS, ORGANIZATION OF CONSTRUCTION and COMMUNICATIONS.

Doctoral course is carried out through lecturing and research work, practical research, laboratory work and work on research project which is the frame of the subject of the doctoral thesis of the candidate. The course may be full-time, lasting 3 years, or part-time lasting 4 years. The lecturing period is the same for full time and part-time course (two semesters), and in the part-time course the period of research work is longer. In agreement with the tutor and with the permission of the *Scientific Board*, the student may temporarily stay, i.e. spend one semester on another faculty in the country or abroad. *The student and the Board tutor* suggest the research program on another faculty.
The program may include only research work and/or examinations.

Doctoral course is available to persons who have completed the graduate course and achieved 300 *ECTS points, out of which* 60 *ECTS points from the subjects belonging to the domain of civil engineering, with minimum* 30 *ECTS points from the branch for which the student is registered.* The student's duties include attending post-graduate lectures, examinations, research work and work on preparing of the doctoral thesis. The plan of research contains the list of subjects registered for, the way of achieving ECTS points through research work, the schedule of exams and time of registration of the thesis. Total weekly engagement of the student in post-graduate course may be up to 12 hours. Students, depending on the branch, register for subjects consisting of the group of mandatory and optional subjects. In the first semester, students register for mandatory subjects and research work with total engagement of minimum 30 ECTS points. In the second semester, students register for optional subjects with total engagement of minimum 30 ECTS points.

The second and the third year are scheduled for preparing of the doctoral thesis. Full-time students must be present at the Faculty during the entire semester for 8 *hours in a working day* – throughout all three years of the course. Part-time students must be present for 8 hours in a working day during at least two semesters of the second and/or third year, during preparing of the thesis. At the time of registration, each student gets a tutor until the approval of the subject of the thesis. The tutor's name is put forward by the branch leader, with the tutor's consent, and the tutor is appointed by the *Scientific Board.* The tutor assists the student in his studies, supervises his work and gives suggestions regarding fulfilment of his duties. Conducting of the study is monitored by the *Scientific Board* which submits the report to the *Faculty Council* at least once a year.

The doctoral thesis is prepared during the second and third year of the course, and by completion and defending of the thesis the student acquires 120 *ECTS points. The post-graduate study for achieving of the grade of doctor of science is completed by working out and defending of the doctoral thesis* (*dissertation*)*. The doctoral thesis* must be an original scientific work which must contain the following chapters – the general hypothesis, relevant review of present knowledge in the field of research, description of methods used by the candidate, description of the candidate's research and presentation of results,

conclusion showing recognizable and undisputable scientific contribution, and the reference bibliography. After successful defending of the thesis, the student must within 60 days submit the final version of the work in printed and electronic form. *Completing the study, the candidate is awarded the academic title – doctor of technical science in the field of civil engineering.*

30.6.2. List of Subjects in the Hydrotechnical Branch of Post-Graduate Doctoral Course

According to the program of post-graduate doctoral course in hydrotechnical branch, the students must in the first semester register for the following mandatory subjects:

— *Methodology of Scientific Research* (6 *ECTS points*), *Applied Mathematics or Applied Statistics* (8), **Hydrology – selected chapters or Methodology of balanced modelling (10) and Research Work (6-12) – total 30 ECTS points.**

In the second semester the students register for 5 out of the total 11 optional hydrotechnical subjects worth 30 ECTS points. According to the curriculum, the optional subjects are the following:

— *Water Management, Systematic Analysis in Hydraulic Engineering, Ecohydraulics, Chemistry in Hydraulic Engineering, Interaction of Sea and Structures, Hydrotechnical Land Reclamation III, River Engineering, Control of Non-point Sources of Pollution, Water Supply Systems for Sustainable Development, Scientific Research in Sanitary Hydroengineering, Ecohydrology.*

The number of lecture hours for all optional subjects is 30 hours, valued by 6 ECTS points. There is a possibility of registering one subject from other branches of post-graduate doctoral course. The student must have at least 48 ECTS points from passed exams and 6 to 12 ECTS points from research work. The students must collect 60 ECTS points from exams and research work. *The post-graduate doctoral course ends by collecting the total of* 180 *ECTS points.*

30.7. Post-Graduate Specialist Course of Civil Engineering

The post-graduate specialist course of civil engineering is done in the domain of technical science, in the field of civil engineering, in the following branches:

— **HYDRAULIC ENGINEERING,** STRUCTURES, BRIDGES, FIRE-FIGHTING ENGINEERING, NUMERIC AND EXPERIMENTAL ANALYSIS OF STRUCTURES and ORGANIZATION AND MANAGEMENT IN CIVIL ENGINEERING.

Completing the specialist study the student achieves the academic title of master specialist in the field of civil engineering, with mentioning one of the above six branches. The persons eligible for registering are students who have completed the Graduate course (and undergraduate course under the program valid until the academic year 2004/05), and who have achieved at least 60 ECTS points from the subjects belonging to the field of civil engineering, out of which at least 30 ECTS points from the field of the branch the student registers for. The students' duties include attending post-graduate lectures, exams and working on the specialist thesis. The study is conducted as part-time, lasting for one year in

two semesters. The first semester includes lectures in mandatory and optional subjects, valued with minimum 30 ECTS points.

In the first semester, the students register for the mandatory module **Basic Hydroengineering,** *which is worth* 8 *ECTS points.* The remaining 22 points in the first semester are achieved by registering one of the following five optional modules – *Engineering Modelling, River Hydroengineering, Ecological Engineering, Ports and Waterways, and Land Reclamation Systems.* Total average weekly engagement of students may be up to 12 hours.

In the second semester the students prepare the specialist thesis, which is worth 30 ECTS points.

The student applies for the topic of the specialist thesis on registering for the second semester. The application must give the proposed title of the thesis in Croatian and in English, explanation of the topic, basic objective and plan of research, methodology of research and expected contribution of the thesis. The students are compelled to complete the course within three years from the day of registration. The condition for approval of the specialist thesis is at least 12 points from exams, and the topic accepted by the Scientific Board is valued 4 ECTS points, and successful defending of the thesis 6 points.

30.8. Conclusion for the Post-Graduate Course in Civil Engineering

The post-graduate doctoral course in civil engineering under the present program has been conducted since the academic year 2006/07, *and its duration is three years.* In the first semester the students register for *mandatory subjects and research work,* which are worth 30 ECTS points. In the second semester the students register *optional hydrotechnical subjects,* also with 30 ECTS points. The second and the third year are scheduled for preparing of the doctoral thesis. *Full-time students must be present at the Faculty during the entire doctoral course, and part-time students for at least two semesters of the second and third year* – with the commitment to complete the doctoral thesis within four years from the date of registration. The post-graduate doctoral course is completed with achieved 180 ECTS points. Completing the doctoral study, the candidate is *awarded the academic title of doctor of technical science in the field of civil engineering.*

The post-graduate specialist study of civil engineering is conducted as part-time course lasting one year, i.e. two semesters. In the first semester, students register the mandatory module Basic Hydroengineering, which is worth 8 ECTS points, and the remaining 22 points are achieved by registering and passing of the exam in one of five hydrotechnical subjects. In the second semester, students prepare the specialist thesis (30 points). Completing the post-graduate specialist course, the student is awarded the title *master specialist in civil engineering, hydrotechnical branch.*

References

[1] Law on Scientific Activity and Higher Education, Ministry of Science, Education and Sport, Zagreb, 2003–2004.
[2] Statute of University of Zagreb Faculty of Civil Engineering, Zagreb 2005.

[3] Antun Szavits-Nossan: Bolonjska deklaracija i novi studiji građevinarstva u Hrvatskoj; (Bologna Declaration and New Study of Civil Engineering in Croatia) Građevinar 58, 5, Zagreb, 2006, 357–366.
[4] Undergraduate and graduate university course in civil engineering – Curriculum, University of Zagreb, Faculty of Civil Engineering, Zagreb, February 2007, 1–174.
[5] Post-graduate course in civil engineering, Doctoral course and Special course – Curriculum, University of Zagreb, Faculty of Civil Engineering, February 2007, 1–101.
[6] Marušić J.: University Education in Hydrotechnical Branch of the Faculty of Civil Engineering, University of Zagreb (Sveučilišni studij na Hidrotehničkom smjeru Građevinskog fakulteta Sveučilišta u Zagrebu); 4th Croatian Conference on Water with international participation, Hrvatske vode and European Union – challenges and possibilities, Miscellany, Opatija, 961–970, 2007.

TECHNICAL PROGRESS IN SANITARY ENGINEERING

Editors
Jerzy M. Sawicki
Katarzyna Weinerowska-Bords

Gdańsk 2011

PRZEWODNICZĄCY KOMITETU REDAKCYJNEGO
WYDAWNICTWA POLITECHNIKI GDAŃSKIEJ
Romuald Szymkiewicz

REDAKTOR PUBLIKACJI NAUKOWYCH
Janusz T. Cieśliński

RECENZENCI
Kazimierz Burzyński
Janusz Kubrak

PROJEKT OKŁADKI
Miriam Artichowicz
Zdjęcie na okładce: *materiały źródłowe GIWK Sp. z o.o*

Wydano za zgodą
Rektora Politechniki Gdańskiej

Oferta wydawnicza Politechniki Gdańskiej jest dostępna pod adresem
http://www.pg.gda.pl/WydawnictwoPG

ISBN 978–83–7348–374–3

CONTENTS

1 Sewer System of Public Sewerage in Slovakia

Monika Bronišová, Dušan Rusnák (Slovak University of Technology, Faculty of Civil Engineering, Department of Sanitary and Environmental Engineering, Bratislava, Slovak Republic)

1.1. INTRODUCTION

By increasing awareness among the general public in recent years gets the essence and importance of municipal sewerage for everyday life. This is the result of increased attention towards ensuring the protection of the environment gradually improved and more stringent enforcement of legislative regulations. Implementation of legislation is for sewerage operators increasingly challenging. The cause of the aging buildings and facilities operated in conditions of worsening economic situation. Another reason is the tightening of permitted pollution limits as required by the EU, which requires continuous improvement of the operation of sewer system and wastewater treatment plants. The paper contains basic information about the development of public sewerage in Slovakia, primary documents, legal regulations and guidelines aimed at the development of sewerage structures.

1.2. THE HISTORY OF CONSTRUCTION OF SEWERAGE

In Slovakia, the public sewerage (PS) started to build mass in the late 19th and early 20th century. The beginnings of construction of sewer systems (SS) without a consistent approach, according to [11]:

a) in the second half of the 19th century: Dobšiná (1850), Bratislava (1886), Špišská Nová Ves (1900);
b) early 20th century: Komarno (1902), Levoča (1905), Prešov (1908), Košice (1906), Rim. Sobota (1912), Kežmarok (1912), Žilina (1913), Partizánske (1919);
c) to II. World War: Lučnec (1930), Nitra (1930), Poprad (1932), Dolný Kubín (1934), Liptovský Mikuláš (1935), Humenné (1936), Martin (1939), Krupina (1940), Skalica (1944).

Significant development PS was recorded in the 60´s years wastewater treatment plant (WWTP) and the 70's years sewer system (SS) at the last century, when the rate of construction of sewer reached according to Pašek [8] over 150 km sewer system annually. Summary of basic details about development PS is in the Table 1.

According to [11] the first sewers were built in Slovakia as masonry, most of the bricks. Later were built of monolithic concrete and gradually from concrete and reinforced concrete pipes, used from the beginning in smaller shapes, and later over DN 1500. Often

technology in the construction of monolithic concrete sewer was first inflatable formwork applied to small profiles, then up to DN 2200. The sewers to remove chemically contaminated water with a diameter to DN 500 were built of clay pipes. Term in the development of sewers was use of plastics pipes. Except smooth socket pipes from PVC up to DN 400 mm are also used fibreglass profiles of DN 800 to DN 2200. Durability of pipes is increased by coatings and in the industrial water by the padding of plastic concrete (Berol). Newer pipe materials (ductile iron, plastic pipes with profiled walls, PP) became applicable up in 90's years. Cushioning material to protect the sewer against aggression wastewater (WW) were fused basalt and pottery, today were added also plastics (PVC, PE, fibreglass, polymer concrete and ductile iron) and sprayed cement mortar and a polymer mortar.

Table 1

Overview of the development of public sewerage in Slovakia

Item	MU	Year							
		1950	1960	1970	1980	1990	2000	2005	2008
Portion canalized population	%	12.4[a)]	19.6[a)]	28.2[a)]	40.6[a)]	46.2[b)]	54.7[b)]	57.1[c)]	59.06[d)]
Municipality with PS	piece	52[a)]	116[a)]	208[a)]	311[a)]	-)	461[f)]	631[c)]	806[d)]
Length PS	km	590[a)]	1237[a)]	2527[a)]	3951[a)]	5122[b)]	6329[b)]	7690[c)]	9265[d)]
Number WWTP	piece	8[a)]	23[a)]	82[a)]	127[a)]	179[b)]	340[b)]	465[g)]	577[d)]
Purified WW	%	2.9	2	41.6	64.5	–	94.4	96.6[c)]	97.9
Specific production WW	l/day	274[a)]	293[a)]	402[a)]	475[a)]	425.2[e)]	260.2[e)]	204.7[e)]	189.7[d)]

Shortcuts: [a)] Building Industry [11], [b)] Official publication of water management 2000, [c)] Data about WM investment construction and operation in SR (DWMICP SR) to 31.XII.2005, VÚVH, [d)] DWMICP SR to 31.XII.2008, VÚVH, [e)]Administration about WM in SR in 2007, [f)] according to Belica and col. [1] to 1999, [g)] Official publication of water management 2005, [-)] details unknown

Wastewater treatment plants (WWTPs) were built in connection the construction of SS in large cities. For WWTP in the 60´s years it was typical that, when they were put into service metabolism and hydraulic surcharged. Classic structure was applied to WWTP: mechanical and biological level, sludge management. The most common technology was medium to highly loaded activation with medium bubble aeration or biological filters filled with stone.

In the 70´s years the pressure companies pushed to construction to build a simple object shapes (rectangular floor plans), which weren´t hydraulically most suitable.

In the 80´s years started to put emphasis on the capacity ensure of WWTP to the forward looking-state to 20 to 30 years, due to plans to build new urban area and high consumption of water. WWTP was proposed on the principle of medium-loaded activation. There is a development of fine-bubble aeration; in sludge management (SM) gone from the sludge fields to mechanical sludge dewatering. WWTP put into operation in the 80's years and early 90´s years was typical that the capacity was suitable, but their construction solution and mechanical devices did not regulate and optimize the cleaning processes.

Significant changes in the sewerage have occurred after changing social establishment after year 1989. Dramatic reduction in industrial production and associated reduced production of pollution had a positive impact on the load for WWTP, quality treated water and the environment. Construction of sewer systems kept pace with new construction (apartments, houses, community amenities, industrial restructuring and construction of industrial parks).

In the treatment WW was introduced an obligation eliminate also forms of nitrogen and phosphor addition removal of organic pollution (COD_{cr}, BOD_5 and suspended solid). This with connection the statement the whole territory of the SR as a sensitive area resulted that all of the WWTP treatment WW from agglomerations (AG) greater than 10 000 equivalent inhabitants (EI) had to (must) go through extensive reconstruction. Construction of SS is also implemented in the outskirts of the cities and moves into the rural areas. Currently runs extensive construction of small profiles SS, reconstruction and capacitance completion of existing feeders, trunk sewer and WWTP.

Acceptance of the obligations SR toward EU in the Treaty on the accession SR to the EU [17] about the quantities suitably diverted and treatment WW from the AG over 2000 EI in concrete terms had resulted the necessity incurring very high financial cost of carrying out sewerage structures in a relatively short timescale (from entering to EU to year 2015). In cities and municipalities in Slovakia is built and operated a combined system. Separate system (exceptionally the pressure or vacuum) is typical for small communities respectively small WWTPs. Serious problems of existing SS is their quality manufacturing, what is often connected to a high proportion of infiltrating water. In 90´s years became current rating building condition of SS, when relatively large proportion operated sewer was getting progressively to limit its life, which according to Pašek [8] estimated at 60 years (generally, without material differentiation).

The need to rehabilitation sewers (replacements, renovations) at the end of 1995 had the same length like the sewer system in Slovakia in 1935 according to the survey. It was considered that the operation the need for rehabilitation sewer will copy rate their construction with the movement 60 years. It is anticipated that the need for rehabilitation sewer will increase and the surge should occur around 2020, given the accelerated pace of construction of SS in Slovakia after 1960. In this context, the projected growths in importance of various technologies for the rehabilitation sewer without open excavation as an important sector construction activity. This is confirmed by recent development these technologies as a natural response to a real need for comprehensive rehabilitation PS.

1.3. IMPORTANT DOCUMENTS RELATED TO THE DEVELOPMENT OF MUNICIPAL SEWERAGE

The basic document is **Directive 91/271/EEC concerning urban waste water treatment** [12]. The aims of directive are to protect the environment from the adverse effects of untreated or inadequately treated municipal wastewater (WW).

Emission requirements of directive about loading with municipal WW are complemented by qualitative – immission requirements for protection of waters, in directives: 76/160/EEC concerning the quality of bathing water, 75/440/EEC concerning the quality required of surface water intended for the abstraction of drinking water and 78/659/EEC on the quality of fresh waters needing protection or improvement in order to support fish life

and natural reproduction of fish. Under directive [12] member states of EU ensure sewerage all agglomerations according to certain principles and terms. Design, construction and operation of sewerage constructions must be carried out in accordance with the latest technical knowledge, if cost is not excessive, especially with regard to: a) the amount of pollution and urban WW, b) prevent leaching, c) reduction of pollution receiving water discharging mixed waters during rain flurry.

Legal framework European water policy creates the **Framework Directive about Water (FDW) 2000/60/EC** [10]. The purpose of the directive is to establish conditions for an effective system of protection of inland surface waters, transitional waters, coastal waters and ground water. WFD determines the principles of direction in the individual activities and practices of water policy, including the WW.

In connection with the preparation of Slovakia for entry to the EU was necessary to prepare documents related to securing the implementation of EU directives into legislation in Slovakia. The development of sewerage has been gradually:

1. **The Concept of water management policy SR until 2005** [5] contains proposals for the objectives and principles of solutions how to develop WMP SR. For the area towns and municipalities Concept [3] assumed:
   a) reduce the development gap in the development PS behind the development public water supply system (PWSS) in 2005 with aim to reach 57% share of population living in houses sewerage,
   b) providing treatment WW at all sites of urban character with PS without WWTP,
   c) after 2005 gradually align with the operation of existing PS with requirements of current legislation and the EU.

Concept [5] based on the principles of the document "Strategy, principles and priorities of state environmental policy" from 1993 and anticipated expending high funds, in particular to harmonization treatment WW with requirements of the directive 91/271/EEC concerning urban WWTP.

High investments should be made to: 1) on the reconstruction existing WWTPs and SS, 2) for the construction of WWTP and SS in municipalities over 2000 EI, 3) for the construction of WWTP and SS in the sensitive water management areas, 4) and to remove surface and drainage water from PS and for other measures.

By the year 2005 on the reconstruction and construction of sewerage is anticipated amount of 37 mld. Sk. Sources of funding should be from the pre-accession financial assistance from the programs from ISPA, PHARE, loans, and funds, from local authorities and public participation and input of foreign capital and similar.

2. **Treaty of accession SR to the EU** [17], in which the EU has accepted transitional period until year 2015, that was requesting SR for to meet the criteria of council Directive Nr. 91/271/EEC [12].

Slovakia´s commitments set in the Treaty [17] and others, arising from the Directive [12] for the PS are:

— 31. 12. 2004 to reach compliance with directive for 83% of the total biodegradable pollution;
— 31. 12. 2008 to comply with [12] for 91% of the total biodegradable pollution;
— 31. 12. 2010 to comply with [12] for AG with more than 10 000 EI (to ensure drainage WW and their treatment, including removal of nutrients);
— 31. 12. 2012 to comply with [12] for 97% of the total biodegradable pollution;

— the end of 2015 to ensure drainage and biological treatment WW in accordance [12] in the AG over 2000 EI;
— ensure appropriate treatment WW in the AG under 2000 EI, which have built SS.

All municipal WW produced in the AG over 2000 EI should be treated in accordance with the requirements of article 4 of the directive – the removal of organic pollution. All municipal WW produced in the AG over 10 000 EI have to be cleaned in accordance with the requirements of article 5 of the directive - nutrient removal.

Between 2004 – 2006 was carried out analysis state of PS, as a basis for parallel development Concept WP SR until 2015 [6] and Development Plan PS SR [9].
According to the analysis of the state PS to the year 2004 raised the proportion of people living in houses connected to the PS to 56.3% (the intended target Concept [5] until 2005 was necessary to increased to at least 57%).

Analyses were identified in the SS the following *shortcomings* and *problems*:
— frequent flue larger profiles of sewer into smaller profiles, due to additional construction of conduit to the WWTP,
— oversized profiles collectors due to the generous projections of urban development,
— dilution of WW, the cooling due to drainage area by combined sewerage (flue drainages, springs, streams, etc..), non solution of water draining from the extra region,
— high proportion of extraneous water (in the year 2003 to 30.54%), uneven loading and operation of WW streams through WWTP – the result of poor quality materials and construction,
— poor layout and construction solutions to WWTPs, old and energy consuming equipment of machine, usually poor current conditions;
— high proportion of industrial WW purified at the municipal WWTPs, insufficient attention devoted to maintenance and repair services, often are solved to emergencies on the SS.

Table 2

Evaluation WWTP under Directive 91/271/EEC in 2003, according to [9]

Capacity WWTP (EI)	Number WWTP	From that		U WWTP (%)	Frequency of non-compliance limits
		S	U		
until 2 000	88	49	39	44.3	COD-18, BOD-38, suspended solid-23
2 000 – 10 000	60	45	15	25.0	COD-2, BOD-15, suspended solid-6
10 000 – 100 000	52	10	42	80.8	COD-2, BOD-11, s.s.-7, N_T-31, P_T-37
over 100 000	10	1	9	90.0	COD-1, BOD-3, s.s.-1, N_T-9, P_T-8
∑	210	105	105	50.0	COD-23, BOD-67, s.s.-37, N_T-40, P_T-45

Shortcuts: S– satisfactory, U – unsatisfactory, U WWTP – unsatisfactory WWTP

In Table 2 are the results of the WWTP under Directive 91/271 EEC. As seen from the table, for larger WWTPs is problematic indicators of nitrogen (N) and phosphor (P). Of total 395 municipal WWTPs recorded in Slovakia was evaluated only 210 WWTPs, which have the necessary data. The vast majority of WWTPs, which were not included in the present analysis fall within the size category of the 2000 EI, possibly the category from 2000 to 10000 PI. Ensuring alignment of real opportunities existing WWTP with the qual-

ity requirements of current legislation required the most complete reconstruction, respectively construction of new WWTPs.

3. **The concept of water management policy SR until 2015** [6] builds on the Concept [5] and was prepared for the period after the entry SR to the EU. The strategic objective of the Concept [6] until the year 2015 in field the sewerage is to create conditions for the smooth supply of the population with quality drinking water and effective disposal of WW, without negative impacts on the environment. In Table 3 is a given initial state in 2004 and projected forward-looking states share of inhabitants living in houses connected to sewerage.

Table 3

Proportion of population living in houses connected to the PS under Concept [6]

Year	Region							
	BA	TT	TN	NR	ZA	BB	PO	KE
2004	61.55	49.91	54.48	41.00	49.29	54.56	52.24	46.29
2010	64.10	65.40	64.75	56.47	71.67	55.77	54.11	48.01
2015	87.46	89.44	80.25	81.76	85.57	72.84	71.61	72.42

Shortcuts: BA- Bratislava, TT- Trnava, TN – Trenčín, NR – Nitra, ZA – Žilina, BB – Banská Bystrica, PO – Prešov, KE – Košice

Concept WMP SR [6] in accordance with the Law Nr. 442/2002 collective of law about the PWSS and PS [13] identified draw up Development plans PWSS and PS, where on the section of public sewer has set targets:

1. by 2010 to ensure:
   - satisfactory drainage and adequate treatment WW in all AG over 100 000 EI;
   - satisfactory drainage and adequate treatment WW in all AG from 10 000 to 100 000 EI;
   - reconstruction and extension of SS in AG over 10 000 EI;
   - reconstruction of WWTPs in AG with the production pollution from the 10 000 EI, as a priority in areas with impaired water quality in receiving water in the group "nutrients";
   - completion of unfinished buildings in AG over 2000 EI situated in protected water management areas and in the catchment of water supply flow above the exemption profile;
   - preparation for reconstruction, construction of WWTP and extend SS in the AG with production of pollution over 2000 EI (in areas with high potential for eutrophication and the need for enhanced protection of habitat);
   - to solve drainage water from surface runoff water in AG over 100 000 EI in accordance with the requirements of the legislation.
2. by 2015 to ensure:
   - suitable drainage water and adequate treatment WW in all AG over 2000 EI;
   - continuously in AG below 2000 EI, where is built SS, adequate treatment WW;
   - to solve drainage water from surface runoff water in AG in accordance with the requirements of the legislation;
   - technically, organizationally and economically prepare the solutions treatment WW for the highest number of AG under 2000 EI.

Table 4

Planned sources of financing structures of PS – by Concept WMP SR in 2015 [6]

Sources of financing to implement the Concept WMP SR till 2015						
Programs	Sources of financing [mil. €]					∑
	SB	OR	M	EU	L	
Drainage and treatment WW Together	779 25%	468 15%	156 5%	1247 40%	468 15%	31167 100%
Construction and reconstr. SS	586	351	117	937	351	2343
Intensification WWTP	98	59	20	158	59	394
Construction WWTP	95	57	19	152	57	380

Shortcuts: B – state budget, OR – own recourses, M – municipalities, EU – funds from EU, L loans (including foreign capital)

Based on the analysis of the state sewerage and the needs for achieving strategic objectives were planned sources of financing sewerage construction are given in Table 4.

4. **Development Plan PS SR** [9] was prepared based on the requirements EU and national legislation. The aim of meeting the development plans PWSS and PS is bringing about the development of municipal infrastructure (upgrading of sanitation, housing comfort and standard of living of the population), while increased protection and improvement of water resources, aquatic ecosystems and human health. The development plan was processed concurrently with the Concept of WMP SR till 2015 and is closely linked. Development Plan PS SR [9] in terms of differentiated requirements of Directive 91/271/EEC [12] by size category of pollution sources divided agglomerations – Table 5.

Table 5

Overview of data on planned agglomerations according to [9]

Agglomeration	< 2000 EI	2001 – 10 000 EI	> 10 001 EI	∑ SR
number inhabitants	1073732	1002065	3304256	5380053
number municipalities	1859	527	542	2928
number agglomerations	1703	277	93	2073
nr. inhabit. in average municip.	577.6	1901.5	6096.4	1873.4
nr. inhabit. in average agglom.	630.5	3617.6	35529.6	2595.3
nr. municip. in average aggl.	1.1	1.9	5.8	1.4

From the data listed in Table 5 clear that by 2010 it was necessary to ensure the required sewerage and treatment WW from 93 AG, thus resolving sewerage 542 municipalities SR with a total of 3 304 256 inhabitants. The average AG in this size category has approximately 35 530 inhabitants. By 2015, subsequently has to solve sewerage and treatment WW in the next 277 AG, which cover 527 municipalities in Slovakia with 1 002 065 inhabitants and in the size category from 2 001 to 10 000 EI.

The main aims defined in the Development plan PS [9]:

- to ensure appropriate levels of drainage and treatment of urban WW with the removal of nutrients from the AG with the production of organic pollution more than 10 000 EI in the term to 31. 12. 2010;
- to ensure appropriate levels of drainage and secondary (biological) treatment of municipal WW from the AG with the production of organic pollution from 2 000 EI to 10 000 EI in the term to 31. 12. 2015;
- if in the AG with size under 2000 EI is built SS, with aim to ensure an adequate level of treatment municipal WW or domestic WW, so as to ensure the required measure of protection for the receiving water;
- to ensure implementation of measures to mitigate the negative impact of overflow and drainage water from surface runoff on ecosystem receiving water;
- to eliminate the discharge of sewage sludge and content septic to the surface water and groundwater;
- to ensure that into the PS were discharged only those industrial WW which contain especially harmful substances, which not cause:
  - damage to the SS and WWTPs and threat health of employees in their operation,
  - threat to the operation of WWTP, treatment sludge and its further use or safe disposal,
  - overrun the limit values of pollution determinate for the discharge of WW from PS and threat quality aims.

Plan sewerage SR [9] was further made specified in the plans sewerage large territorial units (regions), from which solutions were evaluated more detailed estimated the necessary technical measures. In Table 6 shows the planned investment funds according to [9] necessary for the development of PS that are aligned to the requirements of the basic document of Directive 91/271/EEC [12].

Table 6

Planned development PS and investment costs according to [9] (price index to 1.1.2005)

AG	MU	< 2000 EI	2001–10 000 EI	>10 001 EI	∑
population	to 31.12.2003	1 026 711	1 032 675	3 320 667	5 380 053
reconstr. SS	km	33	77	738	848
extension SS	km	5 310	2 538	3 116	10 964
costs for SS	mil. Sk	25 890	15 257	29 434	70 581
recon. WWTP	mil. Sk	439	1 879	9 544	11 862
constr. WWTP	mil. Sk	7 252	2 861	1 341	11 454
Costs together	mil. Sk	33 581	19 997	40 319	93 897

1.4. SOURCES OF FUNDING FOR DEVELOPMENT OF SEWERAGE

Before entering SR to the EU (2000 – 2004) was able to use the funds for water management infrastructure development from EU funds (ISPA, Phare, Interreg). By joining the EU in 2004 received the SR approach to draw money from the Structural and Cohesion Funds in the environmental area.

Table 7

Summary of drawing financial resources (mil.) from funds EU by [2, 3, 4]

FUNDS	Year										Σ
	2000	2001	2002	2003	2004	2005	2006	2007	2008	2009	
ISPA	31	34	80	–	–	–	–	–	–	–	145.0
Cohesion	–	–	–	–	52	24	–	–	–	–	76.0
Structural	–	–	–	–	–	32	9	7	0.1	–	48.1
OPE	–	–	–	–	–	–	–	–	112.0	103	215.0
∑	31	34	80	–	52	56	9	7	112.1	103	484.1

There are currently drawn in the operating program environment (OPE) of EU funds for the environmental sector for the years 2007 – 2013, which is funded by the European Regional Development Fund (ERDF) and Cohesion Fund (CF). In Ttable 7 shows the indication of the spending on construction of PS.

Data are not accurate and complete, are drawn from open sources and are not in them in all the necessary information to compare spending over years. Data are about means for the construction of sewer, WWTP, reconstruction and intensification WWTP, but also PWSS.

1.5. LEGISLATIVE REGULATIONS AND TECHNICAL STANDARDS

Principles of Directive 91/271/EEC [12] have been introduced gradually in our legislation, first in Law Nr 184/2002 collection of law about waters and in Government Regulation (GR) SR Nr. 249/2003 coll. of law defining the whole country as a sensitive area, then defining and specifying the vulnerable areas in GR SR Nr. 617/2004 coll. of law [4]. Further implementation was carried out by successive modifications and the adoption of improved version of the waters law as well as government regulation SR.

Important for the operation of PS is Law Nr. 442/2002 coll. of law [13], later complemented for certain areas Law Nr. 230/2005 coll. of law and Law Nr. 394/2009 coll. of law [15].

At present, the issue of sewerage in Slovakia governed by applicable Law Nr. 364/2004 coll. of law about the water [14] as later amended and Law Nr. 442/2002 coll. of law [13] as other regulations. Qualitative requirements asked for surface water with their different determination and limits values of pollution indicators of different types of purified WW discharged into surface waters at the present is governed by GR SR Nr. 269/2010 [7].

Laws Nr. 364/2004 collection of law about the waters [14] and Nr. 442/2002 collection of law about PWWS and PS [13] as modified for PS are spelled out in a more of decrees issued by the Ministry of Environment SR (MoE SR) and Ministry of Agriculture SR (MoA SR) as:

— Decree of the MoE SR Nr. 100/2005 collection of law, which provides details on the handling of dangerous substances, about the requisites of the emergency plan and about the procedure at resolving the extraordinary worsening of water;

— Decree of the MoE SR Nr. 211/2005 collection of law, which establishing a list of water management important water course and water supply water course;
— Decree of the MoE SR Nr. 124/2003 collection of law, which provides details of professional qualifications to operate PWSS and PS;
— Decree of the MoE SR Nr. 397/2003 collection of law, which provides details on the measurement of the quantity of water supplied by PWSS and quantity of discharged water, about the method of calculating the amount of discharged WW and water from surface runoff and about the guide numbers of water consumption;
— Decree of the MoE SR Nr. 55/2004 collection of law which establishing the requisites operational rules of public water supply systems and public sewerage;
— Decree of the MoE SR Nr. 315/2004 collection of law, which establishing the scope and frequency of sampling and requirements for the scope and implementation of analysis WW;
— Decree of the MoE SR Nr. 605/2005 collection of law about the details of provision data from property register and operating register about objects and equipment PWSS and PS;
— Decree of the MoE SR Nr. 684/2006 collection of law, which laying down details on technical requirements for design, project documentation and construction of PWSS and PS;
— Decree of the MoE SR Nr. 262/2010 collection of law, which establishing content of the plan of rehabilitation PWSS, plan of rehabilitation PS and procedure at their elaboration.

At present in the area PS is very current task resulting from Law Nr. 394/2009 collection of law [15], which identifies the owner of PS ensure its development in terms of development plan PS [9] and a minimum of 10 years to develop a rehabilitation plan for sewerage, together with its financial security. The rehabilitation plan must be prepared to 30 9. 2011. Details of the contents of the rehabilitation plan clarify Decree Ministry of the Environment 262/2010 coll. of law [16]. At present are rehabilitation plans in the stage of preparation, their implementation must begin no later than 30.06.2015.

Design, construction, operation and service of PS in the SR are specified in the recommendations of Slovak technical standards (STN) and EU standards taken to the STN system (STN EN).

For sewer systems are the main recommendations of standards:
— STN EN 752: 2008 Sewer systems and drain system outside the building,
— STN 75 6101: 2002 Sewer systems and branches drain,
— STN EN 1610: 1999 Construction and testing of drain and sewer,
— STN EN 14654-1: 2006 Management and control operation of drain and sewers,
— STN EN 13508-1 & 2: 2004 Determination of the state system of drain system outside the building,
— STN 75 6221: 1993 Pumping station waste water,
— STN 75 6261: 1997 Storm water tank.

For treatment WW are most important valid standards:
— STN 75 6401: 1999 WWTPs for more than 500 EI,
— STN 75 6402: 1992 Small WWTPs,
— STN EN 12566-1 to 5: 2001 Small WWTPs to 50 EI,
— STN EN 12255-1 to 16: 2003 WWTPs,
— STN 75 6601: 1990 Machine-technological equipment of WWTPs.

1.6. THE CURRENT STATE SEWERAGE OF MUNICIPAL

At present the area of sewerage is a primary responsibility to ensure SR drainage and treatment WW from AG above 2000 EI. In the commitments SR towards EU [17] are defined specific terms and for belonging the amounts the biodegradable pollution, which have to be suitable way transferred and purified.

Complex valuation compliance drainage and treatment municipal WW with the requirements of council Directive 91/271/EEC [12] was to year 2008, was made to year 2010 [19, 20].

In SR is 2434 AG, from that the AG under 2000 EI is 2078. Size structure of AG above 2000 EI is in the following Table 8.

Table 8

Division AG over 2000 EI in SR according to categories, count and capacity of SS for collection and drainage municipal WW "which are regard to satisfied" to 31.12.2008

Size category AG	2 000 – 10 000 EI	10 001 – 15 000 EI	15 001 – 150 000 EI	Vver 150 000 EI	Together over 2 000 EI
Produced pollution					
number EI	1 106 510	267410	2 183 850	1 701 600	5 259 370
number AG	276	21	54	5	356
Transferred pollution					
number EI	462 371	183 455	1 796 114	1 571 358	4 013 298
number AG	201	21	54	5	281

In the year 2008 the total amount of pollution produced by the AG above 2000 EI amounted 5 259 370 EI. This number also served as a basis for assessing the state of the drainage and treatment WW.

The quantity of transferred pollution (built SS and WWTP) in 356 AG over 2000 EI in Slovakia was evaluated at 4 013 298 EI (Table 8).

From Table 8 is seen that in accordance with article nr. 3 of Directive [12] has been transferred pollution corresponding 4013.298 EI which is 76.31% of the total pollution produced in the AG above 2000 EI. Amount of pollution remains at the number 1 246 072.

EI which is not drainage by sewer systems – more than 1.2 million inhabitants living in houses not connected to the PS in the AG greater than 2000 EI.

The evaluation level of treatment municipal WW is in the Table 9.

From Table No. 9 is seen that in the year 2008 was in accordance with the requirements of article nr. 4 Directive [12] removed pollution corresponding 3 726 385 EI, which is 70.85% of the total pollution produced from the AG above 2000 EI and overall quality of purified WW satisfied the requirements of article 4 in 225 municipal WWTP. To 31. December 2008 was necessary to comply with article nr. 4 of Directive [12] for 91% of the total biodegradable pollution produced in the AG above 2000 EI. From the comparing the figures show SR delay in fulfilling the obligations under article 4 of Directive [12].

Currently on going very intensive reconstructions of WWTP, but the number of reconstruction and construction of WWTP delays behind the needs under obligations from the accession treaty SR to the EU [17].

In the year 2008 was in accordance with article nr. 5 removed the pollution from 1 766 091 EI, which was 42.53% of the total pollution produced from the AG above 10 000

EI. Overall the requirements of article 5 suited 41 WWTP. Summary results according size categories AG are listed in Table 9**.**

Table 9

Count and capacity of WWTP suitable article 4 (removal organic pollution – BOD_5, COD_{cr}) and suitable article 5 (removal N a P) to 31. 12. 2008

Quantitative category AG	2 000-10 000 EO	10 001 - 15 000 EO	15 001 - 150 000 EO	> 1 50 000 EO	Together over 2 000 EO
Removal organic pollution (article 4 Directive)					
number EI	356180	156298	1 659 406	1 554 501	3 726 385
number WWTP	176	24	60	7	225*)
Removal N a P (article 5 Directive)					
number EI		80 497	884 717	800 877	1 766 091
number WWTP		13	25	4	41*)

*) count several WWTP – if WWTP treats more AG in the different quantitative category, is at total of count inclusive only once (summary count WWTP is not given sum WWTP for individual quantitative category AG)

According to Belica and col. [18] lived toward to 31.12.2009 in houses connected to the PS 3 224 966 inhabitants, which was 59.45% (of total population SR), from that the PS with WWTP 3 141 698 inhabitants. In the year 2009 overall length of sewers in the SR reached 9658 km. There is a discrepancy between the length of newly constructed sewers and a population living in houses connected to the PS. The cause is often a reluctance to connect at PS and paying sewerage charges.

1.7. CONCLUSION

In recent years in the SR was significant progress in the drainage and treatment municipal WW. At present is devoted especially attention to ensuring sewerage of AG over 2000 EI categories but still engaged in parallel work on several buildings PS belonging to the category AG over 10 000 EI, which according to the requirements of Directive 91/271/EEC [12] should be discontinued at the end 2010.

Attention is focused on reconstruction WWTPs and in the necessary extent also SS mainly the construction of new WWTP and SS. Draining and treatment of industrial WW is resolved and considered individually. Little attention is devoted to the concept and functions of the final SS (after connecting AG under 2000 EI) waters from surface runoff, protection sewerage system against water from intravilan, overflow waters, infiltration of rainwater and similarly.

Toward year 31.12.2008 was compliance with article nr. 3 of Directive [12] transferred pollution representing 76.31% of the total amount of pollution produced in the AG above 2000 EI. In compliance with the requirements of article 4 of Directive [12] (secondary treatment) was removed pollution representing 70.85% of the total pollution produced from the AG over 2000 EI (toward 31. 12. 2008 was necessary to achieve compliance for up to 91%).

In the year 2008 was in compliance with article nr. 5 (removal of nutrients) removed pollution representing 42.53% of the total biodegradable pollution produced in AG with size over 10 000 EI (to 31.12.2010 should be 100%).

Estimate of financial claims to achieve comply in the drainage and treatment municipal WW in the AG over 2000 EI is in the range of 2 to 2.24 mld. . To meet commitments SR by accession treaty SR to the EU under Directive [12] is necessary to provide and invest about 1.5 mld. .

References

[1] Belica P. and col.: Situation in the Urban Wastewater Treatment in Slovakia II. Section Water Management 5/2001.
[2] http://www.enviro.gov.sk/servlets/page/868?c_id=2937.
[3] http://www.enviro.gov.sk/servlets/page/868?c_id=2291.
[4] http://www.opzp.sk/20/projekty-do-25-mil.-eur/zoznam-schvalenych-ziadosti-o-nfp.
[5] The Concept of water management policy SR until 2005, Bratislava 2001.
[6] The Concept of water management policy SR until 2015, Bratislava 2006.
[7] GR SR Nr. 269/2010 collection of law, which determines the requirements to achieve good state water.
[8] Pašek J.: Rehabilitation underground lines PWSS and PS modern technologies with regards for protection environment and application domestic products, Bratislava 1998.
[9] Development plan of public sewerage for area Slovak Republic, Bratislava 2006.
[10] Framework Directive about Water 2000/60/EC
[11] Building Industry in Slovakia, Water management buildings, Bratislava 1991.
[12] Directive 91/271/EEC concerning urban waste water treatment 1991.
[13] Law Nr. 442/2002 collection of law about PWSS and PS and about changes and complement Law Nr. 276/2001 collection of law.
[14] Law Nr. 364/2004 collection of law about waters and about changes and complement law SR NL Nr. 372/1990 coll.
[15] Law Nr. 394/2009 which changes and complement Law Nr. 442/2002 collection of law about PWSS and PS.
[16] Decree MoE SR Nr. 262/2010 collection of law, which determines contents rehabilitation plan of PWSS, rehabilitation plan of PS and method on their elaborating.
[17] Treaty of accession Slovak Republic to the EU, Athens, 16.4.2003.
[18] Belica P. and col.: Sewerage municipal areas. Contribution on the conference “World-wide day of water”, Bratislava, 22.03.2011
[19] Michniaková B. and col.: Details for filling reporting duties result from membership in EU according to Directive 91/271/EEC, VUVH Bratislava 2010.
[20] National program SR for performance Directive 91/271/EEC concerning treatment municipal WW amend Directive Committee 98/15/ES and regulations EP and Layer 1882/20/ES, VUVH Bratislava, MoE SR 2010.

Acknowledgement

The article was written within the Project KEGA Nr. 3/7452/09 “Urban Area Drainage” conducted at the Department of Sanitary and Environmental Engineering, Faculty of Civil Engineering of the Slovak University of Technology in Bratislava.

2 From a Manure to Energy and a Clean Environment

Stanislava Dodeva, Aleksa Tomovski (Swiss Cooperation Office Macedonia BAR E.C.E.)

2.1. INTRODUCTION

In the accession process towards the European Union, the Republic of Macedonia took over the obligation for harmonization of the national with the European legislation in all areas of the society. New laws concerning the environment require change in the way of thinking and acting of the state and of individuals as well, and have financial implications which it would be rather difficult to fulfill. But, on the other hand, these laws create pre-conditions for improvement of the status of the environment and the quality of life and also support the sustainable development that will ensure safe and healthy environment for the coming generations. Regarding the global processes, the Republic of Macedonia is also active in the area of climate change, actually in reduction of emissions of the greenhouse gases and mitigation of the effects of the climate change through implementation of the planned measures.

The development and research project [1]: Comparative analysis of possible solutions for preventing pollution of the River Temisnica with utilization of the energetic potential of the manure from the pig farm “Edinstvo”, elaborates the problem of pollution of the water from the River Temisnica and analyzes the manners for its protection through application of adequate technology for manure treatment from the farm. In the same time, it tackles the problem of the climate change, due to significant emissions of methane that are generated during the treatment of the manure of the swine farm.

According to Water Law, the operators that generate wastewater during their operation process must treat the wastewater before it is discharged into sewerage system or any other recipient. This development and research project gives recommendations for the manner of the treatment of the wastewater from the pig farm “Edinstvo” in accordance to the requirements of the European Directives for discharging treated wastewater into recipients, but also offers solutions that will valorize biogas – a product of the manure and wastewater treatment that would bring benefits not only for the operators, but also for the environment, including water, soil and air.

2.2. DESCRIPTION OF THE EXISTING SYSTEM FOR TREATMENT OF THE MANURE

The pig farm “Edinstvo” is located close to the village Chelopek and near city of Tetovo. The total capacity of the farm is 15.000 pigs, while the annual production of the manure is 10.250 t or 28 t/day.

The existing system for treatment of the manure and the wastewater is composed of:

— channels for collection of the manure,
— main collector of the manure,
— collecting pool,
— separation unit,
— aeration pool,
— discharge channel,
— controlling point,
— auxiliary structures: access road, fence atc.

The manure starts its fermentation in the channels for collection of the manure. The capacity of the channels is about 1.200 m^3, which means that their emptying can be done every 34 days, if the pig farm operates with a full capacity. The main collector is a transporting channel that connects the channels for collection of the manure and the collecting pool. This pool has a capacity of 56 m^3 and the manure stays there until the separation. The separation unit separates the solid part of the manure that is stored close by and later transported to the fields as a fertilizer. The liquid part of the manure continues in the aeration pool where the organic matters ferment and the process of mineralization occurs. After the treatment in the aeration pool, the wastewater is discharged into a channel with length of 2 km, and from there to the river Temisnica.

2.3. QUALITY OF THE WASTEWATER FROM THE PIG FARM "EDINSTVO"

In order to define the efficiency of the treatment of the manure and wastewater, in June 2009, samples from five different points of the treatment process were taken and analysis of the wastewater were made. The samples were taken from the (1) stalls, (2) collecting pool (3) separation unit (4) aeration pool and (5) discharge channel. The analysis presented the physical-chemical indicators: total residuals from evaporation at 378.16 K and suspended matters SM, and chemical indicators: bio-chemical oxygen demand BOD_5, dry residual from filtrated water and chemical oxygen demand COD. The results of the three most important indicators are given in the following Figure 1.

According to the opinion of the Public Institute for Health-Skopje, the quality of the wastewater from all five sample points is classified as V^{th} class, actually the worst class of quality. It was very clear that the treatment efficiency is very low and it is not fulfilling the legal requirements for the quality of the effluent discharged into the river Temisnica.

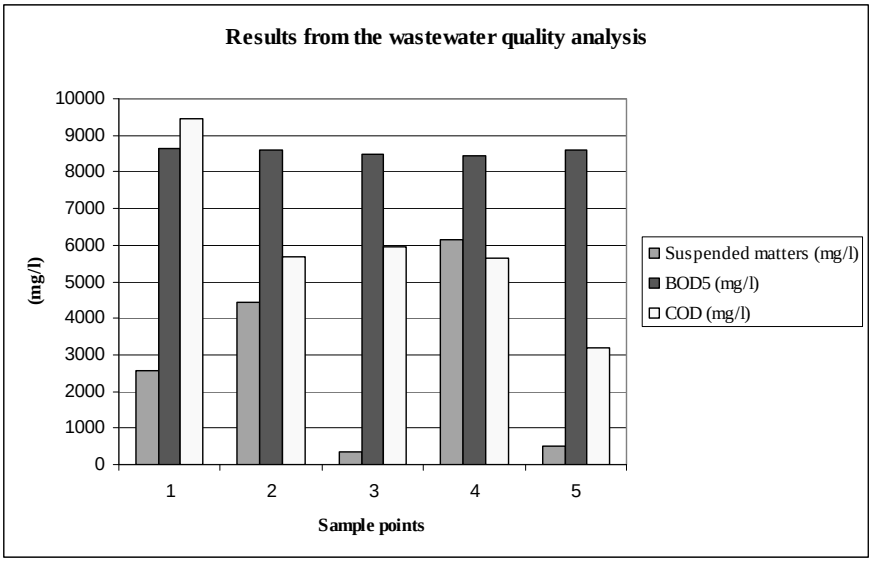

Fig. 1. Quality of the wastewater defined by SM, BOD_5 and COD

2.4. WATER QUALITY OF THE RIVER TEMISHNICA

The main geomorphologic features of the River Temisnica are as following:

— Area of the river basin 23.32 km^2,
— Length of the river basin 11.80 km,
— Perimeter of the river basin 24.90 km,
— Erosion coefficient 0.44,
— Annual sediment production 19.870 m^3.

This river is the main water source for the people from the village G. Palciste, who are using the water for water supply and in the vegetation period for irrigation. Therefore, in the summer period, the quantity of water in the river is significantly reduced. Downstream, the pig farm "Edinstvo" discharges the wastewater directly into the river, which provokes high pollution of the water in the river, destroys the aquatic and costal life systems and endangers the ground water. The water downstream is used for irrigation of the Polog valley, so if the water is contaminated, the quality of the irrigated crops, mainly vegetables and maize could be questioned. Considering that the local population depends mainly on agriculture, the quality of the water for irrigation is of crucial importance.

In order to define the quality of the River Temisnica, a sample of the water was taken in June 2009 and in the following table, the results of the analysis are presented, together with the legal requirements according to the Decree on categorization of rivers, lakes, reservoirs and groundwater (Official Gazette of the Republic of Macedonia 18/99).

The presence of high BOD_5 indicates strong organic pollution that is a result of the discharged partially treated wastewater from the pig farm, as well as from other potential

polluters upstream. According to the categorization of the water quality, the sample from the River Temisnica is of V^{th} class.

Table 1

Water Quality of the River Temisnica compared with the legal requirements

Parameters	According to the Decree	According to the analysis in June 2009
Phisical-chemical indicators:		
1. Total dry residuals of evaporation at 378.16 K		333 mg/l
2. Suspended Matters	10.0 – 30 mg/l	10 mg/l
Chemical indicators:		
1. BOD_5	2.01 – 4.0 mg/l	2.160 mg/l
2. Dry residual from filtrated water	500.0 mg/l	323 mg/l
3. COD	2.51 – 5.00 mg/l	3.0 mg/l

2.5. PROPOSAL FOR TREATMENT OF THE MANURE AND WASTEWATER FROM THE PIG FARM

According to the world wide experiences, the anaerobic process is recommended as the most suitable one for treatment of the manure from the pig farms. The advantages of this method are numerous:

— the emission of disagreeable odor is significantly reduced,
— produced biogas can be used as a fuel or for generation of heat/electricity which economically valorize the process,
— the composition of the nutrients in the stabilized fertilizer is almost the same as the row waste,
— the fertilizer is biologically stable and it can be stored for a longer period without problems or disagreeable odor,
— emissions of methane are reduced.

Considering the possible and applied solutions as well as the experiences from the treatment of the manure and the wastewater from the pig farms in Europe [2, 3, 4] and all over the world [5], on one hand, and respecting the local and specific features of the pig farm “Edinstvo”, on the other hand, the existing system for the treatment of the manure and wastewater was analyzed and a new solution was proposed. In the elaboration of the solution, important request was to consider the existing situation and structures and to plan inclusion and upgrading of those structures. It was decided to apply a technology with anaerobic digestion and biogas production that can be used for energy generation. The figure 2 presents the scheme of the system for treatment of the manure and wastewater including an anaerobic digester.

In order to enable the process of anaerobic digestion and utilization of the produced biogas, new investments are needed. At the moment, only part of the structures presented on the Fig. 2, exists at the farm: separation unit, pumping station and the sedimentation

tank. Additional technical modification and adaptations will be needed for these structures, but still their value is an important amount from the total investment needed.

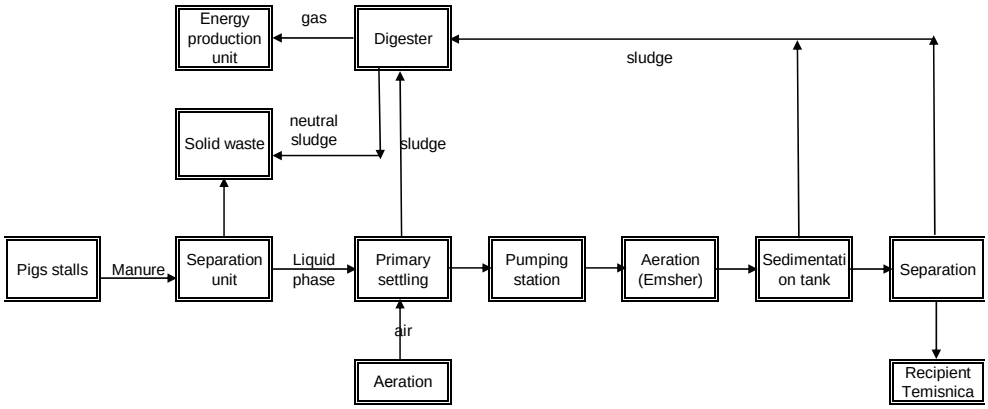

Fig. 2. Scheme of the system for treatment of the manure and wastewater from the pig farm "Edinstvo"

In order to transform the existing structures in the required condition so that they can treat successfully the manure and wastewater, and to produce biogas, the investments are needed for:

— primary sedimentation tank as recipient of the liquid phase from the separation unit,
— reorganization of the existing sedimentation tank and collecting pool in order to enable additional aeration, sedimentation and abstraction of the sludge from the sedimentation tank,
— installation of sedimentation tank with lamellas integrated into the existing sedimentation tank,
— pumps for abstraction and transport of the sludge,
— digester with installed devices for maintaining the process,
— reservoir for gas with adequate safety and regulation devices,
— aggregate for electricity production composed of gas engine, generator of electricity, electro-regulation of the produced energy,
— connection with the existing transformer-station with necessary components for fitting the produced energy with the public electricity network.

The treatment of the manure starts with separation of the liquid and the solid part. The liquid part continues to the primary sedimentation tank where the sludge additionally settles. After that, the sludge goes to thickening and after that is pumped into the digester. In the digester the process of anaerobic digestion takes place and as a result, the biogas is generated. The sludge from the digester goes again to thickening, stabilization and depositing. After this treatment, the sludge can be used for many purposes, but mainly it is used as natural fertilizer in agriculture or as a material for soil remediation.

The liquid part from the primary sedimentation tank flows into the aeration pool In this pool the sedimentation process continues facilitated with the low velocity of the water through the labyrinth part and as well as through the part with lamellas. The sludge that will be settled at the bottom will be additionally removed by mechanical tools.

With this technology, the wastewater will be treated up to the legally required level and it can be discharged into the river Temisnica.

The biogas from the digester is filtrated, dried and compressed, so that later can be used to generate heat for the parts of the farm where the heat is needed, or to generate electricity. In order to use the energetic potential of the gas, a distribution network shall be constructed.

As next step, it is planned to elaborate a detailed technical design for the treatment of the manure and the wastewater and for the utilization of the generated biogas.

2.6. QUANTITIES OF THE PRODUCED BIOGAS AND MODALITIES FOR ITS USE

The quantities of the produced biogas depend on many parameters like, type of the animals and their number, actually the quantity of the waste, type of the reactor, temperature of the anaerobic process etc. Methane as a main component of the biogas (40-75%) generated from the anaerobic digestion is very similar to the natural gas that is abstracted from the ground. But, due to components like ethane, propane and butane, the natural gas has higher calorific value than the pure methane. The biogas generated by the anaerobic digestion has calorific value of 15 000 to 18 000 kJ/Nm^3. Using gas engines of the type Jenbacher, from 1 Nm^3 biogas can be produced 2.5 kWh and 3.3 kWh thermal energy. This biogas can be used in the following manner:

a) to be combusted and the generated energy to be used for heating, cooling or other purposes,
b) to produce electric energy (with use of generator) that can be used at the site or to be sold to energy distribution companies,
c) can be stored and sold and d) after additional purification, the biogas can be used as fuel for cars, machines for agriculture etc.

In the pig farm “Edinstvo”, daily production of the manure amounts around 28 t, out of which 6 702 kg is a solid waste, while 21 363 kg is a liquid phase. If we use a density of the liquid phase as ρ = 1.4 kg/m³, then the daily discharge of the liquid waste from the farm will be:

$$21\ 363\ \text{kg} / 1.4\ \text{kg/m}^3 = 15\ 259.3\ \text{m}^3\text{/day or } 636\ \text{kg/h}$$

With equivalent of generation of biogas of V_e = 65 m^3/t, the potential for generation of gas is:

$$L = G\ V_e = 28\ \text{t/day} \times 65\ \text{m}^3\text{/t} = 1\ 820\ \text{m}^3\text{/day}$$

According to the general recommendations, the efficient use of the biogas is 80%:

$$1\ 820 \times 0.8 = 1\ 456\ \text{m}^3\text{/day biogas}$$

The purpose of the generated biogas and its use depend on the technological process at the farm and the needs for energy. The produced biogas can be used for the:

— Heating of part of the stalls, that will substitute the use of the liquid fuel, and it will improve the quality and the productivity,
— Heating and maintaining of the temperature of the activated sludge necessary for the process in the anaerobic digester,
— Generation of the electric energy by combusting in a generator.

With application of the contemporary technology, 1 m^3 biogas usually generates 2 kWh electric energy. According to these data, the pig farm "Edinstvo" can daily generate energy of 2 912 kWh or at annual level 1 062 880 kWh.

2.7. ECONOMIC ANALYSIS

Elaboration of a technical and economical analysis of the profitability of the system for biogas generation and its utilization covers a macro-economic and a micro-economic analysis. The macro-economic analysis compares the costs of the system for biogas generation and the benefits for the state or the society, while the micro-economic analysis gives an assessment of the profitability of the system for biogas production from the aspects of the operator. The focus in this paper will be the micro-analysis, since the macro-economic analysis requires additional socio-economic, macro-economic and institutional analysis and research.

The required investments for implementation of the system for treatment of the manure and wastewater from the pig farm "Edinstvo", including facilities for production of electricity from the biogas amount Euro 225 000. Additionally, operational costs of about Euro 40 000 per year should be planned for personnel for monitoring and management of the processes at the plant (2 staff members), technical personnel for maintenance, operation and daily interventions (3 staff members), materials, chemicals, spare parts, third party services, assurance etc. Considering that some of these costs are covered at the actual status of the farm, they can be reduced to 70% of the planned, which led to Euro 28 000 per year.

Cost regarding the bank interest depend on financial arrangements, but can be calculated as 10% at annual level (credit for investment of Euro 225 000 for 10 years), actually Euro 22 500. This is rather pessimistic amount, since if the investment is categorized as Clean Development Mechanism (CDM) project, the financial support could be much more favorable. According to the calculations, the total costs at annual level are:

Investments + operational & maintenance costs + interest

$$22\,500 + 28\,000 + 22\,500 = 63\,000 \text{ Euro}$$

The annual production of biogas is:

$$1\,500 \text{ m}^3/\text{day} \times 365 \text{ days} = 547\,500 \text{ m}^3$$

This amount should be reduced for equivalent amount of 30.000 l heating fuel which is now used for heating of the farm. The energetic equivalent of $1m^3$ gas for 1 l of liquid fuel is 1.47:

$$30\,000 \text{ l/year} \times 1.47 = 44\,000 \text{ m}^3/\text{year biogas}$$

In round figures, the total annual available quantity of biogas is 500 000 m^3. The designing of the unit for generation of the electricity will be done for the whole available capacity of the biogas, since the heating with biogas is done only in the winter period, while in the summer, the unit should be able to process the whole amount of biogas.

With the amount of 500 000 m^3 of biogas, the economic benefits of the farm are the following:

30 000 l of liquid fuel will be substituted. The price of this fuel is 0.6 Euro/l:

$$30\,000\ \text{l} \times 0.6\ \text{Euro/l} = 18\,000\ \text{Euro/year}.$$

From 500.000 m^3 biogas can be generated 1 million kWh of electricity. This amount is reduced for 20% due to amount that is spent at the facility, which means 800 000 kWh. If that amount is multiplied with the unit costs of 1 kWh = 0.09 Euro, than the income is Euro 72 000. It is not planned that the farm sells that energy, because there are facilities at the farm that are large consumers of energy, so it can be used at the site.

At annual level, the benefit is Euro 90 000, without the income from the sold fertilizer (the solid part of the waste).

If a comparison is made between the costs and benefits at annual level for the system of treatment of the manure and wastewater, including the generation of the electricity and substitution of liquid fuel, it can be concluded that the return period of the investment is 7 years.

This short period is possible due to the existing infrastructure and other installed mechanical equipment that is already in operation and which reduces significantly the investment costs. If entire infrastructure should be constructed, then the return period is much longer. For this type of specific operators, the real possibilities for so called “soft” financing shall be taken under consideration. That kind of financing enables positive results during elaboration of possible scenarios for profitability and return of the investment. This is confirmed by large number of farms in Europe [2] and USA [6, 7] that successfully manage the manure treatment in sustainable manner from all aspects: technically, economically and regarding the environment protection.

2.8. CONCLUSIONS

— According to the obtained results, it can be concluded that there are good conditions for profitability and fast return of the investments. It is recommended to the operator of the pig farm “Edinstvo” to continue with the activities for implementation of the system for treatment of the manure and wastewater, including the unit for generation of the electricity from the biogas.
— This solution can be replicated or adapted accordingly to other pig or animal farms in the Republic of Macedonia. The proposed solution shall be treated as a basis that can be modified following the specific conditions of each farm.
— The future scientific and development research shall be directed towards the analysis of the parameters that influence the anaerobic process and their optimization in the local conditions of the country, as well as depending on the practices of breading pigs in local farms.
— Also, the research can be focused on looking for a regional solution of the treatment of the manure from bigger number of animal farms and slaughterhouses in one regional center for treatment of the waste and production of energy from the biogas. There are already existing examples in developed European countries and in USA.
— It is very important that the state enables farmers to have access to favorable financing mechanisms for this type of investments, considering the benefits for the environment, nature and economy from anaerobic treatment of the manure.

References

[1] Dodeva S., Tomovski A., Beska P., Jankovska S.: Comparative analysis of possible solutions for preventing pollution of the River Temisnica with utilization of the energetic potential of the manure from the swine farm “Edinstvo”. Development and Research Project, Skopje 2009.
[2] Held J., Mathiasson A., Nylander A.: Biogas from Manure and Waste Products Swedish Case Studies. SBGF, SGC, Gasforeningen 2008.
[3] Brent A. Gloy: Creating Renewable Energy from Livestock Waste: Overcoming Barriers to Adoption. Department of Applied Economics and management, College of Agriculture and Life Sciences, Cornell University, Ithaca, New York 2008.
[4] Poels J., G., Neukermans van Assche P., Debruychere P., Verstraete W.: Performance, operations, and benefits of an anaerobic digestion system on a closed piggery farm. AgricWastes 8: 233–249, 1983.
[5] Sullivan H., Peters N., Ostrand C. M.: A methane production feasibility model for central anaerobic digesters. Resource Recovery Conserv. 5: 319–331, 1981.
[6] Ernst M., Rodecker J., Luvaga E., Alexander T., Kliebenstein J., Miranowski J.: Viability of Methane Production by Anaerobic Digestion on Iowa Swine Farms. Iowa State University, Department of Economics, ASL-R1693.
[7] Powers W. J., Burns R. T.: Energy and Nutrient Recovery from Swine Manures, Fact sheet, Pork Information Gateway 2001.

3 Corrosion Tests at the Pernek Water Resource

Vanda Dubová, Ján Ilavský, Danka Barloková (Slovak University of Technology Bratislava, Slovakia)

3.1. INTRODUCTION

Water distribution systems are often constructed of metal pipes having besides good mainly mechanical properties also a tendency to corrode. Inner corrosion of metal pipes is more or less experienced by all operators of water supply systems. Unwanted corrosion effects are always reflected in financial loss and they can be divided into the following groups according to their impact [1, 2]:

— causing water quality deterioration,

— having an adverse effect on hydraulic flow conditions, increasing water loss, increasing frequency of failures and decreasing service life of the pipes. Closing the pipes during repairs can increase the pressure in other parts of the system and cause further failures of old corroding pipes. Higher water leaks increase not only financial loss but also demands for water resource and its capacity.

3.2. STUDY OF CORROSIVE EFFECTS OF WATER AND OPTIONS FOR THEIR REDUCTION

Corrosive effects of water can be identified on the base chemical water analyses, using the test of solid $CaCO_3$ (Heyer test), various calculation relationships and tables or corrosion tests.

Determination of corrosive effects of water has its advantages and disadvantages. The advantage is that the results of chemical analyses are available within a relatively short period of time and the analyses can be carried out on a regular basis. This allows continual monitoring of water quality and its changes along with the comparison of parameter values. The disadvantage is that the calculations of water corrosion potential by various authors take into account only the corrosive effects of water due to aggressive CO_2. Despite the fact that the concentration of dissolved oxygen can be dominating factor and the flow velocity has a significant effect on the corrosion process, these calculations do not take these parameters into consideration.

Since the calculations of calcium-carbonate balance do not include other effects influencing the balance (complex effect of some organic and inorganic substances, effect of chemicals inhibiting $CaCO_3$ crystallization such as magnesium, presence of extraneous

substances, dissolved chlorine concentration, etc.), the results do not always correspond with practical experience.

A corrosion test is another method for determining the corrosive effect of water [3]. The test methodology is included in the Slovak Technical Standard STN 75 7151 "Requirements for Quality of Water in Piping Systems" and it is based on measuring the difference in weight loss of a sample material on the 30th and 60th day after its exposure to flowing water. Weight loss is a measure of corrosion rates, which indicate the difference in measured thickness in comparison to the original thickness of pipe material. Based on the corrosion rate (μm/year = 10^{-6}m/year) between the 30th and 60th day, the water is evaluated and categorized according to the level of corrosive effect. STN 75 7151 defines three levels of the corrosive effects of water (Table 1).

Table 1

Water categories according to the level of corrosive effect

Corrosive effect	Corrosion velocity (μm/year = 10^{-6}m /year)	Category
I.	under 50	mild corrosive
II.	from 50 to 150	moderate corrosive
III.	over 150	strong corrosive

No corrosion protection measures are needed for the 1st level of corrosive effect. The measures for the 2nd level of corrosive effect are applied based on the results of technical-economical analysis taking into account the required service life of pipes. The 3rd level requires implementation of corrosion protection measures.

The corrosion test is relatively difficult and time consuming. In case you want to identify also the type of corrosion, i.e. whether the pipe corrosion is uniform (general) or non-uniform (point) or what type of corrosion sediments is present, the test will last up to one year. The advantage of the test is the effect of water on a sample material is the same as the effect on pipe. The effect of dissolved oxygen can be present – whether it is dominating corrosive factor or it has a positive role regarding metal passivation by forming a protective layer that separates water from the pipe surface.

3.3. CORROSION REDUCTION METHODS

One of the methods of how to reduce corrosion is a selection of appropriate water resource. Water quality should be in balance regarding physical-chemical aspects (calcium-carbonate balance).

It is practically impossible to completely prevent corrosion. There are three basic methods for corrosion reduction:

— treatment of corrosive properties of water with respect to pipe material,
— creation of protective barrier between water and material,
— using corrosion resistant materials.

Combination of all three approaches is often applicated in practice, whereby the treatment for limitation of corrosive properties of water is usually the basic condition for stabilization of water intended for transport.

Behaviour of steel and other metals in water is influenced by the presence of HCO^{3-} ions and calcium. In favourable conditions, these create adhesive protection films on the surface, consisting of the corrosive products of iron and calcium carbonate. The existence of balance between HCO^{3-} ions, calcium and free carbon dioxide is a basic assumption for occurrence of these films. Sufficient concentration of hydrogen carbonate (by reducing CO_2) in water is important to prevent corrosion. Hydrogen carbonate acts as corrosion inhibitor, increases buffering capacity of water and thus keeps the pH stable.

Higher concentrations of chlorides and sulphates have adverse effect on formation of protection film in metal pipes. In the presence of these chemicals, unstable iron oxides are formed on the surface of metals. The reduction of iron oxides at a lower oxygen concentration leads to the release of iron and continuing corrosion. On the other hand, hydrogen carbonates reduce adverse effect of sulphates and chlorides through competitive adsorption. Adding inhibitors to water (inhibitors on the basis of phosphates are used in water distribution systems) should help form protection film on inner metal surface of pipes.

3.3.1. Galvanic water treatment

The new trend in water treatment includes galvanic water treatment, appropriate pressure for scale removal as well as protection against corrosion [5].
The effect of this method is based on the electro-galvanic principle, which is generated by flowing water between zinc anode and copper-alloy cover of column (Figure 1) where the difference of potentials is generated (voltage 0.7 to 1 V).

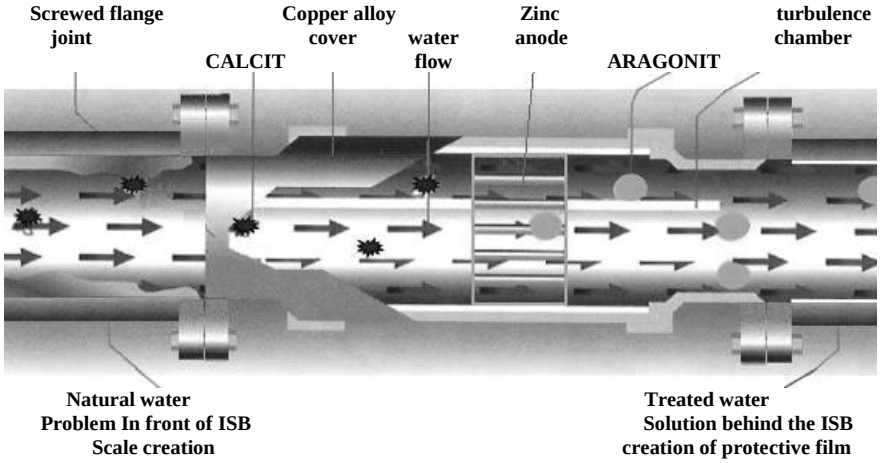

Fig. 1. ISB-ION SCALEBUSTER Device

Galvanic process releases the microscopic particles of zinc from the anode (they work as a crystallizing core). Zinc ions (Zn+2) in water create a strong bond with anions (HCO^{3-}, SO_4^{2-}, Cl^-, etc.). Consequently more cations are bound (Ca^{+2}, Mg^{+2}, Na^{+2}, Al^{+2}). This way the spherical form of calcium (aragonite $CaCO_3$) is generated from the original acicular form of calcium crystal (calcite $CaCO_3$) while the volume of spherical form increases 15 times. Generated molecule of the ions changes 7 μm acicular forms to 110 μm spherical

forms which cannot create sediments in the pipes and therefore they are easily washed away by water.

Zinc ions have reduction effect on the surface layers of the metal which stops the process of oxidation/rust formation in protected system. Passivated layer of magnetite (Fe_3O_4) is created and it protects the whole system.

The amount of zinc supports the cathodic protection of the pipes. Electrons released from the zinc react with the rust (Fe_2O_3) which changes slowly into magnetite (Fe_3O_4). This completely stops the formation of rust.

3.4. CORROSION TESTS AT WATER RESOURCE

Our department, in cooperation with BVS, a.s. (Bratislava Water Company), currently performs the corrosion tests at the Pernek water resource containing corrosive water. This water resource is currently used for supplying the municipalities of Jablonové and Pernek. The corrosion tests have been running since April 2010.

The experiments have shown the following ranges of groundwater parameters regarding calcium-carbonate balance:

Saturation index	–0.52 to –0.74,
Free CO_2	6.60 to 10.12 mg · l^{-1},
Balanced CO_2	2.19 to 4.52 mg · l^{-1},
Corrosive CO_2 on Fe	4.41 to 5.60 mg · l^{-1},
Corrosive CO_2 on $CaCO_3$	2.58 to 3.24 mg · l^{-1}.

The pH value of groundwater was in the range from 7.30 to 7.42; water temperature from 9.8 to 10.5°C; ANC4.5 from 2.10 to 2.43 mmol · l^{-1}; BNC 8.3 from 0.15 to 0.23 mmol · l^{-1}; Fe below 0.03 mg · l^{-1}; Mn below 0.01 mg · l^{-1}; Ca^{2+} from 69 to 74 mg · l^{-1}; NH^{4+} below 0,02 mg · l^{-1}; NO^{3-} from 18 to 22 mg · l^{-1}; SO_4^{2-} from 74 to 78 mg · l^{-1}; and Cl^- from 10 to 14 mg · l^{-1}.

Two 1.5 m long test units (columns) are placed in the well HL–1. Both columns contain 6 stands with test samples. Each stand includes 5 samples separated by non-conductive strip. Test samples were made of steel sheet: class 11, thickness 1mm and size 42 × 42 mm. Water is pumped into the testing columns from the well using one Grundfos pump. The pipes are divided into two directions and water flows separately into each column. The test devices are placed parallel to each other. After passing through the columns, water flows back into the well.

The ISB-ION SCALEBUSTER device, which has been used in our country mainly for service water treatment, is mounted to one of these units. In addition to testing the performance of the device there is evaluated also the suitability of the used methodology, since such methodology of corrosive tests has been not yet used for evaluation of the device efficiency. To prevent potential distortion of the results obtained by using the mentioned methodology, we have placed 15 cm long steel pipes DN 3/4’ to be evaluated after completing the tests.

Loss of material due to corrosion, corrosion rates, amount of sediments and water flow rate in the testing units are evaluated for both columns.

Two uppermost stands with samples are used in the 60-day measurements. These stands are replaced by new ones immediately after they are taken out. Five 60-day meas-

urements have been completed and they indicate that the corrosive effect water is in the second and third category. The results of measurements are shown in the charts 1 and 2.

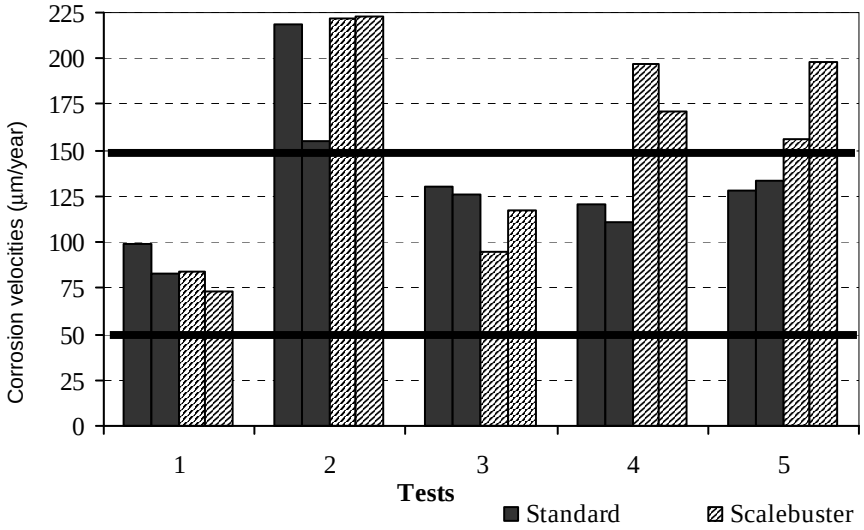

Chart 1. Corrosion velocities obtained in the 1st – 5th 60-day cycles

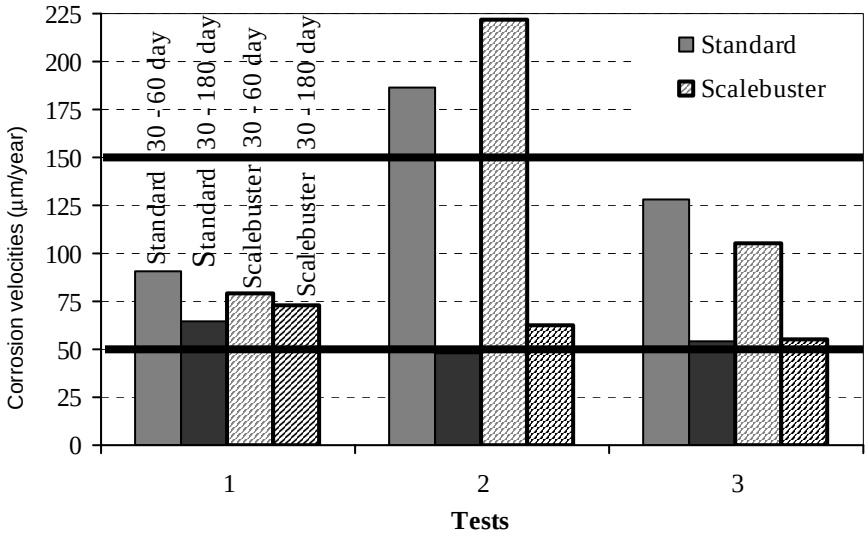

Chart 2. Comparison of corrosion rates obtained in individual trials between 30th and 60th day of the cycle and 30th and 189th day of the cycle

The chart 1 shows the changes in corrosive properties of water during the monitored period. Corrosive rates considerably increased especially in the second 60-day trial probably due to a significant rise in groundwater level caused by a long-lasting heavy rainfall.

To find out how the corrosive effect of water on test samples changes during a longer period, the third series of PVC frames with samples were taken from the test columns after half a year. The remaining frames will be used for the 1-year and 2-year measurements [4]. A comparison of the values of corrosive rates obtained in a half-year measurement is shown in chart 2. The chart indicates that the corrosion rates in a longer half-year trial were considerably lower than those in short standardized 30-day and 60-days trials. The rates are slightly above the lower limit of the 2nd level of water corrosive effect.

In addition to material loss due to corrosion, we also evaluate the amount of sediments for every test sample. The chart 3 shows the loss caused by corrosion and the amount of sediments measured during four 60-day trials. Each 60-day trial consists of two 30-day and one 60-day measurements. The correlation between sediments and corrosive declines can be more precisely assessed after the completion of all tests.

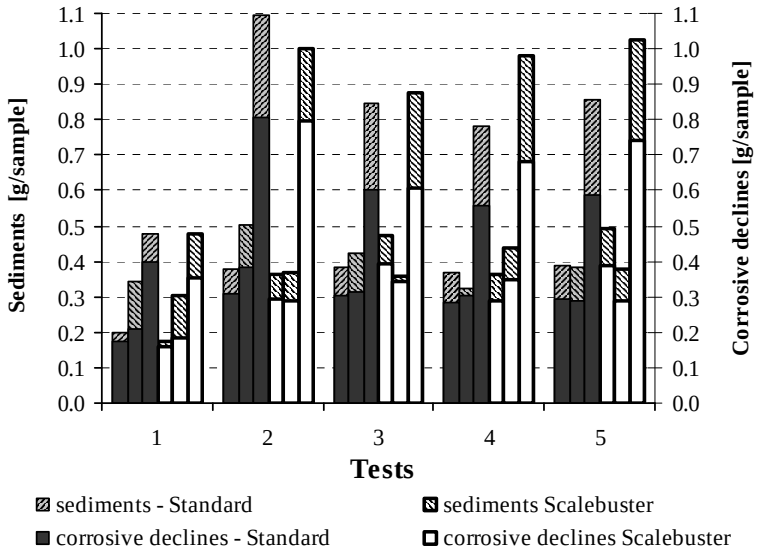

Chart 3. Comparison of the amount of sediments and corrosive declines obtained by using a standard device during 30-day and 60-day measurements

3.5. CONCLUSION

The article presents partial results of the model tests evaluating corrosive effects of water on steel and the comparison with ISB-ION SCALEBUSTER device. The obtained results indicate a decrease in corrosion rates in long-term trials (30-day up to 189-day trials) in comparison with standard trials (30-day up to 60-day trials). The corrosion rates in standard trials were in the range from 83 to 218 μm/year (it corresponds to 2nd and 3rd level of corrosive effect), while the corrosion rates in the half-year trials experienced significant decrease with the values ranged from 49 to 65 μm/year. Visual evaluation of samples indicates the change in corrosion and sediment types. The 1-year measurements will be finished in April and they will more precisely define the level of corrosive effect, efficiency of de-

vices used in trials as well as the change in corrosive effect of water during one year depending on precipitation intensity having an effect on groundwater level fluctuation.

Experimental measurements were conducted with the financial support for the Project APVV-0379-07 and in cooperation with BVS, a.s. (Bratislava Water Company) and water production company in Malacky.

References

[1] Dubová V.: Lifetimes of Pipes. In: Proceedings of International Conference on New Trends in Water Supply, Sewerage and Solid Waste Treatment, Žiar, September 2006, pp. 21–28. ISBN 80-227-2469-6.

[2] Dubová V., Kriš J.: Effect of Transported Water on a Steel Pipeline. In: Proceedings of Conference on Topical Problems of Water Management of Human Habitats, Banská Bystrica, May 2006, pp. 31–34, ISBN 80-227-2402-5.

[3] Dubová V., Kriš J.: Corrosion tests of a steel pipeline water distribution system. In: Slovak Journal of Civil Engineering, 2004/ 1, vol. XII, pp. 18–22, ISSN 1210-3896.

[4] Dubová V., Kriš J., Ilavský J.: Corrosion of steel pipeline of Long-distance Water Supply System. In: Proceedings of 6th International Conference on Water Zlín 2002, Zlín, 26.-27.3.2002, pp. 49–54.

[5] Ilavský J., Barloková D.: Galvanic Water Treatment. In: Proceedings of 12th International Conference on Water Zlín 2008, Zlín, March 2008, ISBN 978-80-254-1348-7, pp. 131–136, 2008.

4 Appearance of the Risk Contamination of Drinking Water Supply Sources at Rainfall and Vegetation Periods

Nuriddin Fayz, Inom Normatov, Makhmadrezbon Idiev, Obid Bokiev
(Institute of Water problems, Hydropower and Ecology Academy of Sciences Republic of Tajikistan)

4.1. INTRODUCTION

Tajikistan is a mountainous country located at altitudes from 300 up to 7000 m above the sea level. Cities, settlements and kishlak (villages) are located in valleys of the rivers, where the anthropogenic loading of contaminants in surface waters reaches a maximum. According to the results of water control analyses during storm rainfall, the bacterial pollution of the rivers measured by a contamination index can reach numerous amounts of intestine sticks in 1 liter of water (Varzob River – 3800 intestine sticks in 1 liter of water). The basic importance of infection transfer by waterways is especially evident in the dynamics of typhoid spreading, which is always characterized as very high. Thus between maximum (1984–69.0 on 100 thousand population) and minimum (1992–16.9 on 100 thousand population) number of cases, there is large variability (4 and more times), which is reflective of the fluctuations of epidemic activity due to waterway transfer through different territories. In particular, because of lack of means to maintain good water supply quality and sanitation, we expect a further increase in epidemic activity and typhoid case rate at the high levels of past years, equal to other widely spread intestinal diseases. In connection with these conditions, the likelihood of cases of typhoid in a village population is 2 and more times higher than in an urban area. The greatest levels are recorded in valleys, where they are 2.5 to 150 times higher than in foothills and mountainous zones. In many districts of the valley zone, first of all in cotton planting areas, the case rate of typhoid was extremely high in the period 1994–2000. As a rule, it exceeded state-wide parameters caused by the high activity of waterway transfer and extremely potent fecal pollution of sources due to agriculture. A significant number of diseases by typhoid (41–82%) are attributed to acute water epidemic flashes.

4.2. INFLUENCE OF THE IRRIGATION ON THE GROUNDWATER MINERALIZATION

Groundwater plays an important role in the potable water supply of the population of Tajikistan. Water as a dynamical component of the ecosystem, possesses the ability to promptly transfer various pollution and infectious diseases to greater areas. Although this concern mostly surface waters, groundwaters are not an exception. First of all the reason is that surface and groundwaters are constantly in dynamic interaction, and thus a penetration and diffusion of pollution into the groundwater aquifers takes place. Previous studies have shown a significant seasonal difference in the concentration of nitrates in groundwater: during the drought periods the concentration of nitrates was low, while during rains it reached 18 mg/dm^3. Tajikistan is an agrarian country, with cotton as the basic agricultural product. To achieve a good harvest many farmers break the established norms by applying excessive amounts of mineral fertilizers and pesticides. It is necessary to note that the majority of sources of mass water delivery to the rural population are near to the irrigated fields and it is not excluded that during rains the mineral fertilizers and pesticides enter the groundwater reservoirs. In the Central Asian Region and in the basins of the two great transboundary rivers of Aral Sea basin, Syrdarya and Amudarya, the use of water up to 339 deposits is recommended and has been approved. The general regional groundwater volumes are estimated 43.49 km^3/year (Table 1): Amudarya River basin – 25.09 km^3/year; Syrdarya River Basin – 18.40 km^3/year.

Table 1

Groundwater stocks in Aral Sea basin (km^3/year) (Source: SIC ICWC, 2000)

State	Estimate of regional yield	Approved pumping rates	Actual pumping rates in 1999 year	Water use			
				Drinking	Industry	Agriculture	Vertical drainage
Kazakhstan	1.846	1.270	0.293	0.200	0.081	0.000	0.000
Kyrgyzstan	1.595	0.632	0.244	0.043	0.056	0.145	0.000
Tajikistan	18.700	6.020	2.294	0.485	0.200	0.428	0.018
Turkmenistan	3.360	1.220	0.457	0.210	0.036	0.150	0.060
Uzbekistan	18.455	7.796	7.749	3.369	0.715	2.156	1.349

The groundwater bodies have an appreciable hydraulic interrelation with a superficial vertical drain. This is shown by the reduction of the flow rate in the superficial vertical drain at excessive pumping. In view of this, the national state commissions approved operational groundwater pumping rates 11.04 km^3/year. The increased groundwater pumping rates require an expansion of the international cooperation on the regulation of groundwater use and quality control.

Water is one of the dynamic components of an ecosystem and is able to transfer pollution and infectious diseases in the big catchments studied. This is mainly of concern for surface water but can also be of importance for groundwater. Since surface waters and groundwater are in a dynamic interaction, surface waters can also contaminate groundwaters and vice versa. The groundwater resources supply an appreciable part of the population of Tajikistan with potable water. Earlier, a considerable seasonal change in groundwater nitrate concentration was detected: during drought periods, the concentration of nitrates did

not exceed standards, while in rainy periods it reached 18 mg/dm^3. The Republic of Tajikistan is an agrarian country, and cotton is the basic agricultural production. For good harvest reception, many farmers apply considerable quantities of mineral fertilizers and pesticides, thereby exceeding the established standards. Most wells of the rural population are near irrigated lands. The pollution of groundwater at storm rains and during the irrigation of lands is an unexpected experience [1].

In the Republic of Tajikistan more 90% of agricultural crops (730 000 ha) are produced on irrigated lands. For keeping groundwater levels at a depth of 3.0–3.5 m, more than 325 000 ha are supplied with a collector-drainage network. This is mainly the case in the Kurgantube Region (Sogd and Khatlon). Other irrigated lands are located in the foothill areas that are drained naturally and have deep groundwater levels. In 2002 the irrigated lands of the Kurgantube zone of the Republic of Tajikistan extended to 238 005 ha. These lands are subdivided into >50 areas that extend to 1000–20 000 ha. These areas are found in cones of intermountain valleys and along rivers. The start of the production of cotton, rice and lucerne on these lands with an irrigation of more than 20 000 m^3/ha, has sharply altered the depth of the water table. With the current irrigation technology (e.g. onto furrows), the water loss made up >40%. These water losses influence the water table and lead to the salting of the soil profile. In Table 2, we present loss of infiltration water for the period of 1995–2002, in the irrigated lands of the Kurgantube zone.

Table 2

Loss of irrigation waters during infiltration

Name	Unit	1995	1996	1997	1998	1999	2000	2001	2002
Total irrigation	10^6 m^3	5215	5612	5795	5356	5484	4999	5008	4413
Total water loss	10^6 m^3	1870	2258	2260	2098	2098	2084	1907	1860

The main water sources for the irrigation of the lands of the Kurgantube zone are the Pyanj, Vakhsh and Kafernigan rivers, whose mineralization fluctuates from 0.23 to 0.5–1.0 g/l total dissolved solids. The chemical composition of the waters of the Pyanj and Kafernigan rivers is mainly of a hydrocarbonate-calcium type, and that of the waters of the River Vakhsh is of a calcium-sodium and sulfate-hydrocarbonate-chloride type. The mineralization of ground waters in the Kurgantube zone is from 0.5 to 3.0 g/l and more (total dissolved solids). The increase of the area of irrigated lands with high groundwater mineralization over time is shown in Table 3.

Table 3

Distribution of irrigated lands ($\times 10^3$ ha) on the degree of the groundwater mineralization

Mineralization [g/l]	1995	1996	1997	1998	1999	2000	2001	2002
<1.0	75.2	66.6	68.83	71.30	73.89	72.02	72.03	72.57
1.0–3.0	146.8	157.3	157.36	152.45	149.64	150.10	151.44	151.74

The present work is devoted to research of the change in chemical compounds of groundwater of Tajikistan in dependence on the period of the year and the quantity of precipitation. For this purpose two sources of underground waters have been chosen: 1 – Kafarniganski and 2 – East unit. Results of the research are presented in Fig. 1.

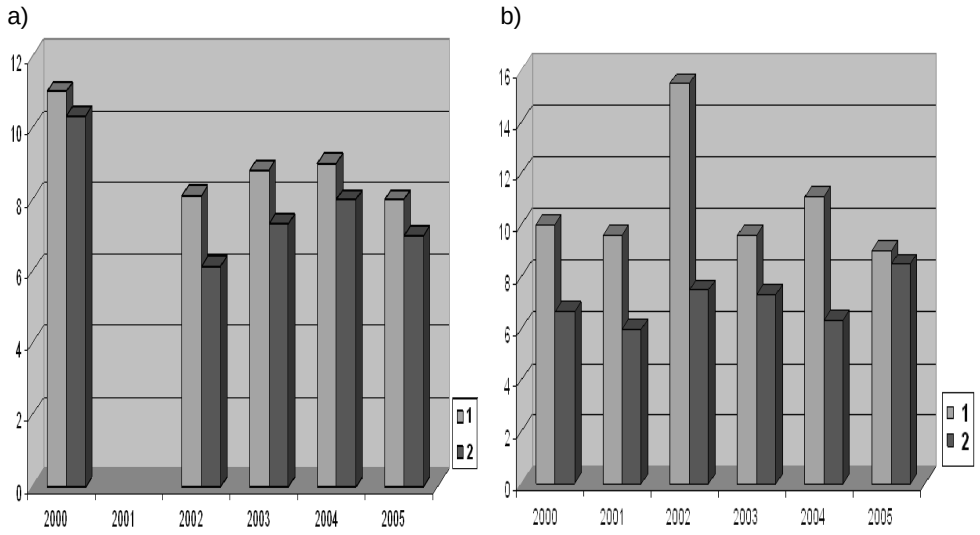

Fig 1. Average annual chloride concentration (mg/l) in groundwater sources in summer (a) and autumn (b): 1 – Kofarnigansk, 2 – East unit

The presented figures are demonstrating that in the summer, during insignificant quantities of atmospheric precipitation, the concentrations of chlorides in sources 1 and 2 strongly differ. In the autumn, when atmospheric precipitation is higher, the chloride concentrations in these sources are almost equal. A similar picture was found for nitrates, sulfates and other chemical compounds.

The problem of studying the water quality change and development of mechanisms of its control is still actual and concerns not only the separately taken country of Central Asia, but all the states of the region.

Nowadays one of the most polluted rivers of Central Asia is Zeravshan River. The capacity of this water is changed under the influence of collector drainage water of irrigating basin zone and wastewater of Samarqand, Kattakurgan, Navoi and Bukhara cities. Mineralization of water exceeds from origin to estuary from 0.27–0.30 g/l to 1.5–1.6 g/l [2].

Results of chemical analysis indicate that mineralization of river's water changes within surveyed area from 0.3 to 2.7 g/1. Down the stream from mountains to Navoi meridian mineralization increases from 0.3 to 1 g/1 and then up to Bukhara oasis it reaches 2.6 g/1According to the results of atomic absorption method the chemical contents of Zeravshan waters is closely related to the collecting points and varies extensively (mg.eqv.%): HCO_3–: 15.0–28.0; Cl^-: 11.74–27.0; SO_4^{2-}: 55.0–69.72; Ca^{2+}: 27.0–36.79; Mg^{2+}: 24.0–45.00; Na+K: 28.0–36.82. It was defined that the HCO_3– content is decreasing and the Cl^- and SO_4^{2-} are generally increasing from Navoi to Bukhara [3]. In most cases the problem of water quality of the Zeravshan River consider in organic communication with activity of the Anzob Mountain-concentrating Industrial Complex (AMCIC). AMCIC is the mining enterprise for extraction and enrichment of complex mercury-antimony ores of the Dzhizhikrut deposit. It is located in a right-bank part the rivers Dzhizhikrut which are the left inflow of the river Jagnob (the river Jagnob is the right inflow of the river Fondarja which in turn is the left inflow of the river Zeravshan). The main ore minerals are antimonite. Since 1966 to 1970 reconstruction of industrial complex was spent and for the purpose of

prevention of hit of sewage of industrial complex in the river Dzhizhikrut in village of Ravot (8–10 km from industrial complex) on left to river bank Jagnob was are built waste-water dams (WWD). With 1970 on 1994 pipelines of sewage functioned normally and from 1994 years a result of heavy rains pipeline pieces has been destroyed. In 2009 the industrial complex has completely restored pipelines and now dams in the complete set and works in the established mode.

For definition influence of the AMCIC on qualities of waters of the river Zeravshan were made sampling of water from the river in two points – on Fondarya and Pete Rivers is located accordingly before and after wastewater dams of AMCIC [4]. Results of analyses are presented in tables 4 and 5.

Table 4

Chemical analyses of the Zeravshan river waters from point above WWD

Date	T, C	pH	NO_3	NH_4	PO_4	Cr(VI)	Cr(IV)	Hg	Sb	Cd	Zn
06.03.10	14.2	7.96	27.78	0	102.0	0.030	0	0	0	0	0.020
17.04.10	15.3	8.17	11.74	0	147.0	0.00	0	0	0	0	0.019
22.05.10	15.9	8.30	10.95	0	110.0	0.009	0	0	0	0	0.014
11.06.10	16.4	8.19	9.74	0	87.40	0.014	0	0	0	0	0.013
31.07.10	16.8	8.29	8.04	0	127.0	0.025	0	0	0	0	0.020

Table 5

Chemical analyses of the Zeravshan river waters sampling from point down WWD

Date	T, C	pH	NO_3	NH_4	PO_4	Cr(VI)	Cr(IV)	Hg	Sb	Cd	Zn
06.03.10	14.4	7.96	30.72	0	103.15	0.029	0	0	0	0	0.019
17.04.10	15.5	8.17	12.10	0	146.60	0.014	0	0	0	0	0.017
22.05.10	16.2	8.30	11.17	0	112.00	0.010	0	0	0	0	0.015
11.06.10	16.6	8.19	10.64	0	88.10	0.015	0	0	0	0	0.014
31.07.10	17.0	8.29	7.73	0	129.20	0.029	0	0	0	0	0.021

Comparison of results chemical analyses have shown about absence of the factor of pollution of the river Zeravshan by wastewaters of industrial complex.

4.3. CONCLUSION

By carrying out of the chemical analysis of underground waters it is established that at vegetation of farmlands essential infiltration of irrigation water in sources of underground waters is observed. Results of comparison of the analysis of waters have shown about absence of essential pollution of waters of the Zeravshan River by wastewaters of the Anzob mountain-concentrating industrial complex.

References

[1] Obid S. B., Nurkhon S. K., Nuriddin F.: Influence of the irrigation on the groundwater quality. Proc. IV Intern. Sci. Conference of the Young Scientist and Talented Students, 2010, Moscow, P. 175–176.
[2] Chembarisov E. I.: Modern hydrological problems of water resources of Central Asia and ways of their decision. Water and steady development. Bishkek. Publ. Center FPOI, 82, 2001.
[3] Toderich K. N., Tsukatani T., Mardonov B. K., Gintzburger G. and et al.: Discussion Paper No. 553, Water Quality, Cropping and Small Ruminants: A Challenge for the Future Agriculture in Dry Areas of Uzbekistan October 2002, Kyoto Institute of Economic Research Kyoto University, Japan 2002.
[4] Nuriddin Fayz, Obid Bokiev. Environmental, water and energy problems of the Zeravshan River Basin and perspective their development. Proc. IV Intern. Sci. Conference of the Young Scientist and Talented Students, 2010, Moscow, p. 21–24.

Acknowledgements

In the paper are used results of work is executed in framework of the project financed by Fund Volkswagen. Authors express gratitude to the Fund Volkswagen.

5 Study of Rotational Separators Operation and Design

Marlena A. Gronowska, Jerzy M. Sawicki (Gdańsk University of Technology, Faculty of Civil and Environmental Engineering)

5.1. ROLE OF CIRCULATION IN ROTATIONAL SEPARATORS

Rotational separators comprise a special category of devices (e.g. grit chambers, clarifying tanks or settling tanks) employed for gravitational removal of suspensions from liquids (storm sewage, domestic sewage or industrial effluents). The design of such a device enforces the flow of the liquid to be circular. As a result, by rotation around a vertical axis, liquid flow generates centrifugal force that acts on a suspended particle by retarding its motion. Particle detention time within the object is elongated what increases the probability of particle separation from the feed liquid stream in the process of sedimentation or flotation. The principle of rotational separator operation is analogical to that of dust removal process in a cyclone, where the centrifugal force generated by rotating gas stream pushes dust particles towards the outside wall of the cyclone. Particles approach this wall moving towards the bottom of the object (Fig. 1).

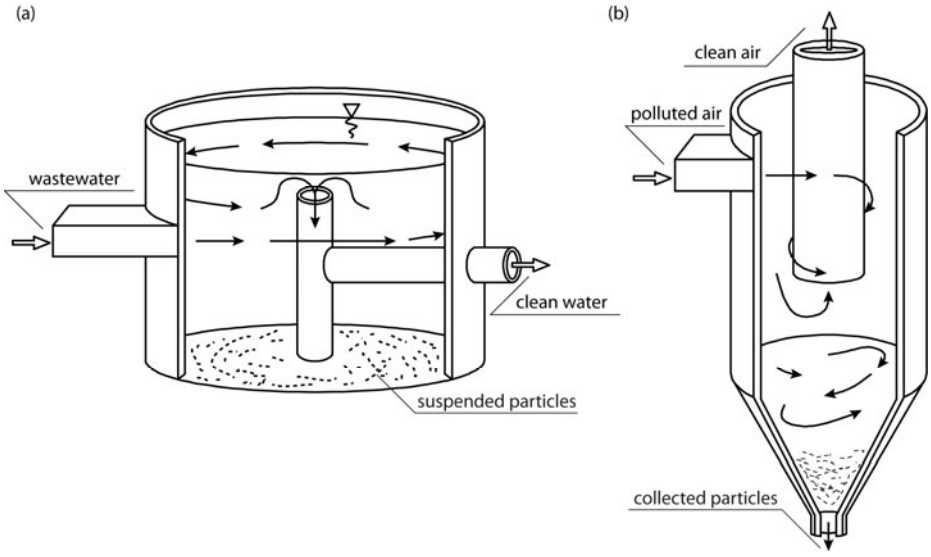

Fig. 1. Schematic diagrams of main types of circulative separators: a) rotational separator, b) cyclone

5.2. GRAVITATIONAL SEPARATORS OPERATION AND DESIGN

5.2.1. General remarks

Mathematical description of gravitational separators operation requires employment of structural method in analysis of occurring effects. In this method, trajectory of particle characteristic for device operation comprises the fundamental tool. The trajectory is expressed by a function $\mathbf{r}_p(t)$ that can be determined from the relation:

$$\frac{d\mathbf{r}_p(t)}{dt} = \mathbf{v}_p \tag{1}$$

as long as velocity of the particle $\boldsymbol{v}_p(t)$ is known. Particle's velocity is defined by Newton's second law (for a particle of constant mass m_p):

$$m_p \frac{d\mathbf{v}_p}{dt} = \mathbf{F}_M + \mathbf{F}_S \tag{2}$$

Particular components of body force $\mathbf{F}_M$ may be easily specified depending on the character of analyzed device. In majority of cases gravity force **G** is present, in case of curvilinear motion – centrifugal force $\mathbf{F}_C$, and also, in specific situations – electromagnetic force.

On the other hand, resultant surface force is defined by the relation:

$$\mathbf{F}_S = \int_S \boldsymbol{\tau} dS \tag{3}$$

where: $\boldsymbol{\tau}$ – stress on interfacial surface S between particle and liquid.

In order to determine stress $\boldsymbol{\tau}$ in accordance with Newton's hypothesis, one needs to describe liquid's velocity **u** and pressure **p** distributions around surface *S*. However, in general case determination of velocity and pressure distributions is impossible as this problem is formally too complex. Consequently, in practical issues only specific situations are considered.

5.2.2. Dynamic interactions between particle and fluid

Specific relations describing particular components of the surface force that acts on a suspended particle may be found in literature on the topic (e.g. [4, 5]). In order to reach better understanding of the problem it is convenient to specify fundamental aspects expressed by the force components. The aspects are [3, 4]:

— time dependence (steady components, denoted by index "S"; and unsteady components, denoted by "U");
— scale of variability in space (general variability, denoted by "G", connected with conditions of liquid motion; and local variability, denoted by "L", generated by suspended particle motion);
— physical effects (disturbance of velocity, denoted by "V" or disturbance of pressure, denoted as "P").

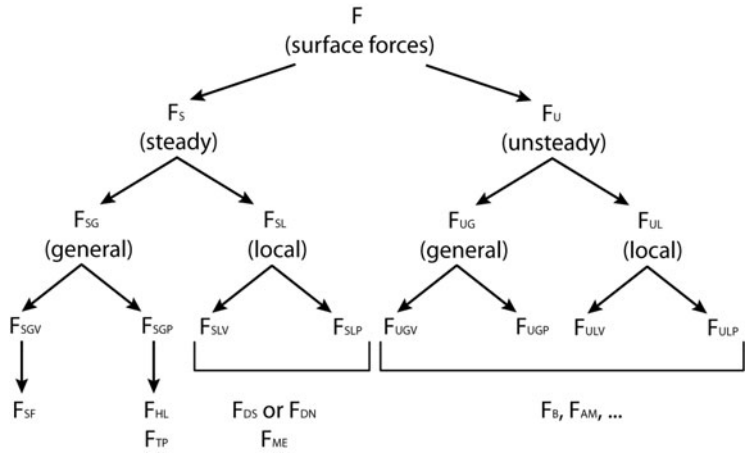

Fig. 2. Mechanical aspects defining surface forces acting on suspended particles

Particular combinations of situations defined by abovementioned aspects are presented in (Fig. 2). It must be emphasized that the scheme is ideological in character as forces employed practically comprise simultaneously of several aspects, especially in case of unsteady elements (Basset force FB, mass associated force F_{MA}, resistance force forms varying in time). However, the scheme underlines the physical essence of individual forces; in particular – resistance force, defined by Stoke's formula (F_{DS}) in laminar flow or Newton's formula (F_{DN}) in turbulent flow; Magnus' effect (FME) generated by rotation of a body; Saffman's force (F_{SF}) and even forces generated by pressure diversification. In case of devices used for separation of suspension, two forces play a significant role – buoyant force (FHL) generated by vertical pressure diversification and transverse force (FTP) (transversal pressure effect) related to change of pressure in curvilinear motion.

5.2.3. Design criterion

Analysis of characteristic trajectories of suspended particles (Eq. (1)) does not always prove to be a convenient tool while designing devices under consideration. Therefore, some methods make use of specific situations or states representative for device operation. These serve as design criteria. When analyzing present or developing new methods one should pay attention to the issue of clarity, coherence and accuracy of applied criteria.

5.3. EXISTING METHODS OF DESIGNING ROTATIONAL SEPARATORS

5.3.1. Presentation of existing methods

Proper design of a rotational separator proves to be a complex issue due to object specific construction and nature of the circular water flow. In general, literature on the topic of wastewater treatment facilities provides two methods with different approaches.

The first method [7, 8] is based upon the following characteristic state: a particle, motionless relative to a horizontal plane, is subjected to force F_{DS} of the liquid flowing radially from the outside wall to the central pipe with velocity u_R. The stress is balanced by the centrifugal force F_C. Transversal pressure effect F_{TP} is also included (Fig. 3).

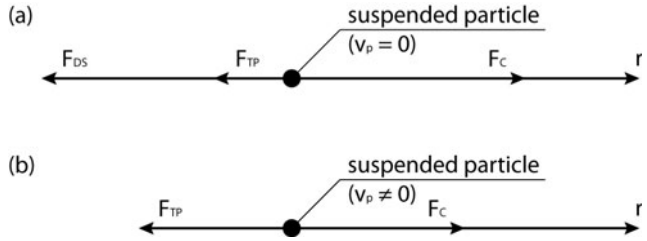

Fig. 3. Balance of characteristic forces: a) immovable particle; b) movable particle

It is assumed that the critical particle is the smallest one from particles that are to be removed due to separation. With design criterion defined by the relation:

$$F_C = F_{DS} + F_{TP} \tag{4}$$

all the particles bigger and heavier that the critical one will be pushed towards the outside wall simultaneously descending towards the bottom due to the gravity force. In this way particles are removed from the suspension. On the contrary, particles smaller than the critical one are carried away from the device with the flowing liquid stream. Individual forces present in the first method are described as follows [8]:

— centrifugal force:

$$F_C = m_p \omega^2 r \tag{5}$$

— Stoke's stress force:

$$F_{DS} = 3\pi \mu d_p u_R \tag{6}$$

— "buoyancy effect":

$$F_{TP} = m_d \omega^2 r \tag{7}$$

where: m_d – mass of liquid displaced by a particle.

Distribution of maximum values of abovementioned forces seems to be problematic, as the maximum value of F_{DS} occurs near the outflow pipe ($r = r_w$), contrary to remaining two forces whose maximum values are found near the outside wall ($r = R$). In order to prevent the design expression from taking the form of a radius r function, Eq. (4) is analyzed with maximum values of all the forces. Transformation of this equation yields a formula for critical particle's diameter (particle is immovable):

$$d_{ci} = \sqrt{9 \frac{\mu R Q}{\Delta \rho r_w \pi H u_S^2}} \tag{8}$$

It is assumed that liquids angular velocity ω is constant and defined by velocity in the inflow pipe:

$$\omega = \frac{u_S}{R} \tag{9}$$

The second method [2] is derived from another characteristic state. Initially, the critical particle is located near the outflow pipe. The particle is pushed towards the outside wall by the centrifugal force F_C (horizontal motion of liquid is neglected). Thus, the resisting force also acts on the particle. Additionally, transversal pressure effects F_{TP} is neglected. As a result, force balance looks as follows:

$$F_C = F_{DS} \tag{10}$$

By substituting Eq. (5) and Eq. (6) into Eq. (10) one obtains:

$$v_r = \frac{dr}{dt} = \frac{\omega^2 d_p{}^2 \rho_p}{18\mu} r \tag{11}$$

Integration of Eq. (11) from $r = r_w$ to $r = R$ gives the time which the particle requires to reach the outside wall:

$$t_r = \frac{18\mu}{\omega^2 d_p{}^2 \rho_p} \ln \frac{R}{r_w} \tag{12}$$

The chosen design criterion requires that the time of particle's horizontal displacement t_r and the time in which the particle reaches the bottom t_s are equal.

The original version of this method, that was developed for cyclones (Fig. 1b), neglects sedimentation of a dust particle and time t_s is the time of advection of dust towards the bottom:

$$t_s = \frac{H}{u_z} = \frac{\pi \left(R^2 - r_w{}^2 \right) H}{Q} \tag{13}$$

Comparison of Eq. (12) and Eq. (13), with inclusion of Eq. (9), yields a formula for diameter of the suspended critical particle:

$$d_{cc} = \sqrt{\frac{18\mu Q R^2}{\pi \rho_p u_s{}^2 H \left(R^2 - r_w{}^2 \right)} \ln \frac{R}{r_w}} \tag{14}$$

In order to design rotational separators according to the abovementioned concept, relation (13) should be replaced by an expression describing the time of particle's vertical displacement upon action of the gravity force. Denoting free sedimentation velocity as v_{so}, this time equals:

$$t_s = \frac{H}{v_{so}} \tag{15}$$

Taking into account the formula for velocity v_{so} [4, 5]:

$$v_{so} = \sqrt{\frac{4\Delta\rho g d_c}{3C_D\rho}} \tag{16}$$

instead of Eq. (14) one obtains:

$$d_{cm} = \left[\frac{36\mu\sqrt{g}R^2}{Hv_s^{\,2}\sqrt{3C_D\rho\,\Delta\rho}} \ln\frac{R}{r_w} \right]^{2/3} \tag{17}$$

It should be noted that when the value of dc is equal to 1.0 mm, velocity v_{so} equals 0.2 m/s and *Re* for laminar flow equals 200. Thus, Stoke's formula, that is valid up to *Re* = 1, should be replaced by Newton's formula. Relation (17) includes also the transversal pressure force F_{TP}, what seems to be a rational addition to the method under consideration.

5.3.2. Verification of existing methods

At present, producers of devices for local waste-water treatment are becoming more and more interested in rotational separators. As a result, there appeared a need for an efficient method for separator design. Although the existing methods, as already provided, were developed for cyclones, the authors decided on trying to apply these methods in designing rotational separators.

Table 1

Data and results of verification calculations for a series of rotational separators designed and manufactured by ECOL-UNICON

Device type	Q [m^3/s]	H [m]	R [m]	r_w [m]	u_s [m/s]	d_{ci} [mm]	d_{cm} [mm]
DOW 25/250	0.025	1.81	0.60	0.20	0.20	1.33	4.00
PDOW 35/350	0.035	1.85	0.75	0.25	0.18	1.73	6.14
PDOW 60/600	0.060	2.19	1.00	0.30	0.21	1.85	6.78
PDOW 100/1000	0.100	2.47	1.25	0.40	0.20	2.32	8.86
PDOW 140/1400	0.140	2.75	1.50	0.50	0.18	2.85	11.88
PDOW 350/1600	0.350	4.03	2.50	0.60	0.31	2.52	10.38
PDOW 550/1600	0.550	4.03	3.00	0.60	0.49	2.20	7.85

for: μ = 0.001 kg/ms; ρ = 2700 kg/m^3; C_D = 0.44

Possibility of application was verified by control calculations made for a series of rotational separators designed and manufactured by ECOL-UNICON, Gdansk, Poland [1]. Separators were designed using a classical "volumetric" method, based on a plug-flow model, for particles with critical diameter d_c = 0.1 mm. Circumferential flow of waste-water introduced in devices is acknowledged as a support of the process of sedimentation. This flow should additionally improve the efficiency of devices under consideration (lower the value of d_c), even without being included in the design calculus. Consequently, diameters of particles critical for analyzed devices calculated using Eq. (8) ("immovable particle

method") or Eq. (17) ("movable particle method") should be smaller than 0.1 mm. Calculations were made for PDOW series of separators [1]. Data together with results of calculations are listed in Table 1. It can be seen that critical particles diameters as determined by described methods are more than two orders of magnitude larger than the basic value d_c = 0.1 mm. The results obtained indicate that the methods for rotational separators design presented in literature should be thoroughly discussed.

5.4. PHYSICAL ANALYSIS OF EXISTING METHODS

First of all, the design criteria chosen within the analyzed methods should be discussed. The criteria are unquestionable in themselves, however, adoption of extreme values of the thrust force and the centrifugal force in the first method (Eq. (4)) seems to be a too cautious approach that lowers calculated efficiency of the device. On the other hand, in the second method, once the correction (Eq. (13) replaced by Eq. (15)) has been implemented, the employed design criterion can be acknowledged as typical of devices designed for gravitational separation. In case of force balance, first to be noted is the fact that application of Stoke's formula (Eq. (6)) for description of the resisting force is improper. One should remember that the issue under consideration is the process of separation of suspension occurring in a flowing liquid. In such a case, liquid motion is turbulent (with circumferential velocity of the order of 0.1 m/s and chamber diameter of the order of 1.0 m Reynolds number is of the order of 100 000), thus, Newton's formula should be applied:

$$F_{DN} = C_D A \frac{\rho\left(v_c - v_D\right)^2}{2} \tag{18}$$

However, as this correction is not fundamental in character, it cannot justify the discrepancy between calculations (Table 1) and the efficiency of actual devices.

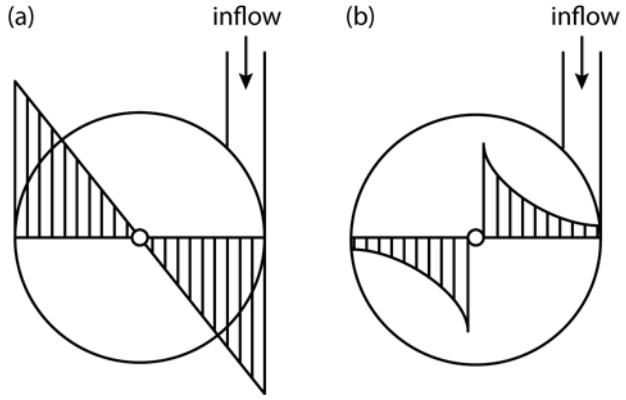

Fig. 4. Flow velocity distributions in: a) rotating separator, b) rotational separator

A detailed study of relations used in both methods indicate that they were developed on the assumption that angular velocity in the chamber is constant:

$$\omega = \text{constant} \tag{19}$$

Being excluded from discussions in literature, the assumption is treated as an evident one. Meanwhile, it evokes the main uncertainty resulting from relations between velocity tangential to trajectory of mass u_T, mass trajectory's radius of curvature and angular velocity ω:

$$\omega = \frac{u_T}{r} \tag{20}$$

Making such an assumption means that the circumferential velocity profile along separator radius is a linear function (Fig. 4a):

$$u_T(r) = \omega r \tag{21}$$

This situation corresponds to velocity of the Couette's flow in a rotating cylinder with a vertical axis what comprises a model of flow in a centrifuge instead of centrifugal separators (cyclones and rotational separators).

5.5. POSSIBILITIES OF CORRECTIONS OF EXISTING METHODS OF CENTRIFUGAL SEPARATORS DESIGN

In literature on the topic abovementioned divergence of velocity fields can be observed. According to Stairmand maximum value of circumferential velocity is found near the outflow pipe. Velocity decreases approximately exponentially towards the outside wall according to the quality relation (Fig. 4b):

$$u_T r = \text{constant} \tag{22}$$

Nonetheless, this information hasn't been so far used in designing separators. Replacement of velocity profile according to Eq. (21) by Eq. (22), as well as variability of angular velocity along the radius:

$$\omega(r) = \text{constant} / r^2 \tag{23}$$

will change the character of the centrifugal force. Change of radial pressure distribution– value of transversal pressure effect F_{TP} (Fig. 2) will be the second consequence of velocity field alteration. Change of pressure distribution may be estimated basing on the fact that, in case of free surface flow, radial pressure profile is portrayed by the shape of free surface. In a rotating chamber liquids' surface is specifically bent (Fig. 5a) convex down (in accordance with classical rules of hydromechanics [5]).

In order to obtain a quality description of the shape of water free surface in a tank supplied by a tangential liquid flow, a simple experiment was conducted. A transparent cylinder was supplied by an elastic hose mounted into the outside wall. Liquid exited the chamber through a pipe located in tank's axis. Liquid circulated around the axis and shape of the free surface was described by a curve convex up (Fig 5b). The same effect may be observed while water flows out of a bathtub through a bottom in the bottom. Comparison of the two situations provides interesting conclusions. One should remember that transversal

pressure effect F_{TP} is a result of pressure difference between opposite sides of a body (a suspended particle). In the first case highest pressure diversification (highest value of F_{TP}) is found near the outside wall, the fact described by a known relation (Eq. (7)). On the contrary, in the second case, highest value of F_{TP} is found near the outflow pipe. It seems that the two described factors – radial velocity and pressure profiles that influence the centrifugal force and the "buoyancy effect" – constitute the main reason of calculus divergences. This issue is the subject of further research.

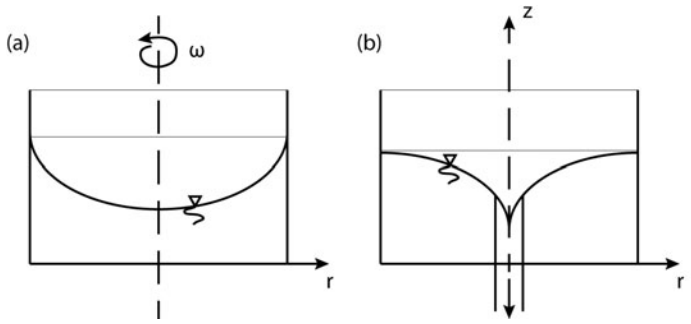

Fig. 5. Water free surface profiles: a) rotating tank; b) centrifugal tank

Notation: A – particle active cross section, C_D – drag coefficient, d_{cc} – critical particle diameter, d_P – particle diameter, $\mathbf{F}$ – force, g – gravity acceleration, H – chamber depth, m_p – particle mass, m_d – displaced fluid mass, Q – discharge, r – radial coordinate, $\mathbf{r}_p$ – particle radius vector, r_w – inlet radius, R – chamber radius, t – time, t_s – time of sedimentation, u_R, u_S, u_Z – radial, tangential and vertical flui velocity, $\mathbf{v}_p$ – particle velocity, μ – liquid viscosity, ω – liquid angular velocity, ρ – density, τ – stress

REFERENCES

[1] Ecol Unicon: Catalogue of products. Gdańsk 2010.
[2] Mitosek M.: Mechanika płynów w inżynierii środowiska. Warszawa: Oficyna Wydawnicza Politechniki Warszawskiej 1997.
[3] Prandtl L.: Fuehrer durch die Stroemungslehre, Braunschweig: F. Vieweg u. Sohn 1949.
[4] Soo L.: Fluid dynamics of multiphase systems. London: Blaisdale Publ. Comp. 1966.
[5] Sawicki J.M.: Migration of pollutants (in Polish). Gdańsk: GUT Publishing House 2003.
[6] Stairmand C.J.: The design and performance of cyclone separators. Trans. Inst. Chem. Eng. Vol. 29, 1951.
[7] Warych J.: Gas purification (in Polish). Warsaw: WNT 1998.
[8] Wikipedia. The Free Encyclopedia: http://en.wikipedia.org/wiki/Cyclonic separation.

ACKNOWLEDGEMENTS

Scientific research has been carried out as a part of the Project "Innovative resources and effective methods of safety improvement and durability of buildings and transport infrastructure in the sustainable development" financed by the European Union from the European Fund of Regional Development based on the Operational Program of the Innovative Economy.

6 Adsorption and Removal of Antimony from Drinking Water by Oxihydroxide Iron

Ján Ilavský, Danka Barloková (Slovak University of Technology Bratislava, Slovakia), Karol Munka (Water Research Institute, Bratislava, Slovakia)

6.1. INTRODUCTION

The chemistry of antimony and its natural occurrence in some water resources combine to create a potent, widespread human health risk, requiring management and removal from drinking water [1, 2].

The Dúbrava water supply resource is situated in the western part of the Low Tatras Mountain Range. Geological and hydrogeological conditions of this region are very complex where the water of crystalline and Mesozoic basements is interconnected. Higher antimony concentration in the springs of Močidlo, Brdáre and Škripeň occur mainly due to existence of the antimony deposit in Dúbrava and its higher content in granitoids of this part of the Low Tatras Region. Moreover, the concentration of antimony in mining water was considerably increased at relatively high capacities of wells. Adverse effect comes from the mine tailing piles and sludge lagoon where the rocks rich in antimony were continually washed by the rainwater infiltrating into the groundwater resources or flowing into to the surface stream of Križianky. Contaminated water of the Križianka River and water of its alluvial deposits has deteriorated water quality in the springs of Močidlo and Brdáre [3, 4, 5]. In the past, three springs of the Dúbrava water resource (Brdáre, Močidlo, Škripeň) were used for supplying population with drinking water, but today only one spring is used for this purpose (spring Škripeň that does not contain antimony).

6.1.1. Quality of Water in the Dúbrava Water Supply Resource

According to the data from operational monitoring of water quality provided by the Water Company of the Liptov Region, the selected quality parameters of water from the wells of the Dúbrava water supply resource for 2000–2005 are presented in Table 1. The most significant contamination by antimony was observed in water from the spring of Brdáre where the antimony concentrations were in the range from 80.3 to 91.3 µg/l.

Table 1

Water quality of the Dúbrava water supply resource according to selected parameters for the period 2000 – 2005

Parameter	Dúbrava – springs		
	Močidlo	Škripeň	Brdáre
pH	7.65–7.90	7.55–7.95	7.75–7.95
$ANC_{4,5}$ [mmol/l]	1.7–3.8	1.8–3.8	1.7–2.2
Conductivity [mS/m]	23.1–38.6	23.0–42.6	22.5–28.7
Ca^{2+} [mg/l]	30.0–54	48–52	28–32
Mg^{2+} [mg/l]	8.5–28.0	15.8–24.3	9.7–15.8
Sb [µg/l]	70.6–82.0	< 1.0	80.3–91.3

6.2. EXPERIMENTAL PART

The model tests of antimony removal were carried out at the Dúbrava chlorination plant. Today, only water from the Škripeň well is transported to the storage reservoir of the chlorination plant and after chlorination it is distributed to the consumption point. For the purpose of model antimony removal tests, there was a need to transport the water from the Brdáre well to chlorination plant through a separate pipe in order to avoid mixing with the water from the Škripeň well because the water from the Škripeň well is free of antimony.

Table 2

Physical and chemical properties of selected sorption materials [6, 7, 8]

Parameter	Bayoxide E33	GEH	CFH12
Matrix/Active agent	Fe_2O_3>70% and 90.1% α -FeOOH)	52-57% $Fe(OH)_3$ and β-FeOOH	FeOOH Fe^{3+} >40%
Physical Form	Dry granular media	Moist granular media	Dry granular media
Color	Amber	Dark brown	Brown – murrey
Bulk Density [g/cm^3]	0.45	1.12–1.19	1.12–1.2
Specific Surface Area [m^2/g]	120–200	250-300	120
Grain Porosity [%]	85	75-80	72–80
Operating pH Range	6.0 to 8.0	5.5 to 9.0	6.5–7.5

The objective of the study was to verify sorption properties of some new sorption materials (Bayoxide E33, GEH, CFH12 and CFH18) for removal of antimony from selected water resource and compare their efficiency. These materials are very efficient in removal of arsenic from water. Their basic physical and chemical properties and chemical composition are listed in Table 2 and 3.

Fig.1. Dúbrava chlorination plant and model filtration columns

Table 3

Chemical composition of selected sorption materials [9]

Material	Compound in mass [%]						
	MgO	Al_2O_3	SiO_2	SO_x	CaO	TiO_2	Fe_2O_3 (FeOOH)
Bayoxide E33	0.97	6.59	12.75	0.31	2.01	0.91	75.28
CFH12	3.75	0.45	1.18	8.49	2.72	0.50	82.65
GEH	–	1.74	3.05	0.54	0.18	–	91.92

6.3. RESULTS AND DISCUSSION

The model tests of antimony removal were divided into two parts.

Model Tests – 06.2010

To verify the efficiency of antimony elimination process three adsorption columns filled with the sorption material (Bayoxide E33, GEH, CFH12) were used. Adsorption column was made of glass material with a diameter of 5.0 cm and medium height from 50 to 52 cm.

Water flew through the column from the top to the bottom. Water discharge was measured continually and the filtration rate reached approximately 5 m/h. Amount of water flowing through the column was monitored using water meter placed in front of the column inlet.

In first stage of model tests was monitored efficiency of sorption materials GEH, CFH12 and Bayoxide E33 in removal of antimony from water. During the model tests, the antimony concentrations in raw water were in the range from 55 to 62 µg/l. Filtration rates in experimental columns were 12, Bayoxide E33) were 4.3 – 5.3 m/h.

The figure 2 shows the antimony concentrations measured at the outlets of columns depending on the ratio V/V_0 (Bed volume). The figure 3 presents the values of V/V_0 ratios for particular adsorption materials when meeting the limit concentration of antimony

(5 µg/l) at the outlets of adsorbent media. Moreover, the figure indicates the adsorption capacity for the above-mentioned values of V/V_0 ratios. Considering the minimum differences in filtration rates and the results obtained in tests, it can be concluded that GEH is the most suitable material for antimony removal compared to other adsorbents used in the test. The following ratios V/V_0 (Bed volume) were measured for the antimony concentration of 5 µg/l at the outlet of 50 cm high adsorbent media: V/V_0 = 1700 for GEH, V/V_0 = 790 for CFH 12 and V/V_0 = 715. GEH adsorption capacity is 83.6 µg/g, Bayoxide E33 adsorption capacity is 91.4 µg/g and CFH 12 adsorption capacity is 42.4 µg/g.

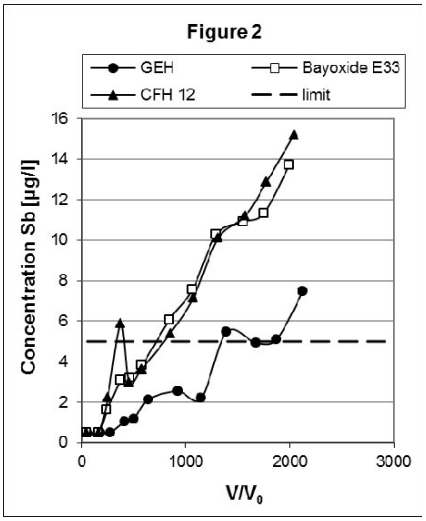

Fig. 2. Concentrations measured at the outlets of columns depending on the ratio V/V_0

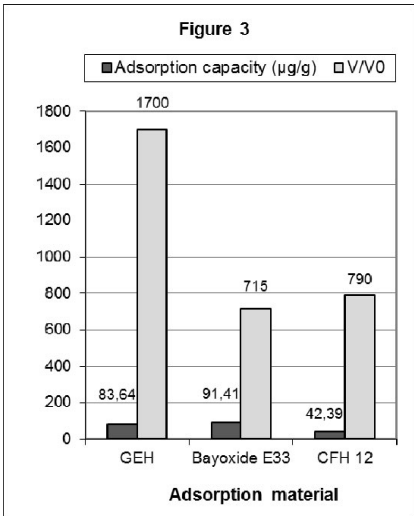

Fig. 3. Adsorption capacity and values of V/V_0 ratios for particular adsorption materials when meeting the limit concentration of antimony

Model Tests – 08.2010

The antimony concentrations in raw water during the model tests were in the range from 69 to 77 µg/l. This indicates an increase in antimony concentration by 15 µg/l compared to the previous trials. Filtration rates in three glass columns were in the interval from 5.0 to 5.8 m/h (GEH, Bayoxide E33, CFH 12). The figure 4 shows the concentrations of antimony in treated water (height of adsorbent media was 52 cm) depending on the ratio V/V_0. As it can be seen in this figure, Bayoxide E33 was not efficient in antimony removal because the concentration of antimony at the outlet of the adsorbent medium reached the value of 20 µg/l already in the first sampling (after 22 hours of operation). The antimony concentration for the ratio V/V_0 = 2750 at the outlet of the Bayoxide E33 medium was nearly the same as in raw water. According to these results and comparison with the results of the model tests 06.2010, it was clear that despite the same labelling of both products as Bayoxide E33 these materials were different to a certain extent (different colour and grain size). The figure 5 shows the relationship between adsorbed amount of antimony in adsorbent media and the ratio V/V_0. Very low adsorption of antimony by using this material can be expected when assessing the above-mentioned dependency for Bayoxide E33. Only

100 000 µg of antimony was adsorbed by Bayoxide E33 at V/V_0 = 4000, while for CFH12 and GEH it was 2.1 and 2.5 times higher amount respectively.

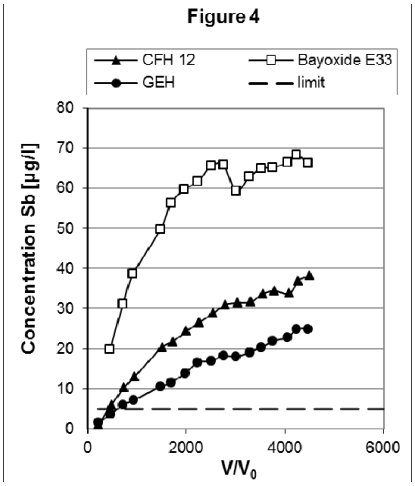

Fig. 4. Concentrations of antimony in treated water depending on the ratio V/V_0

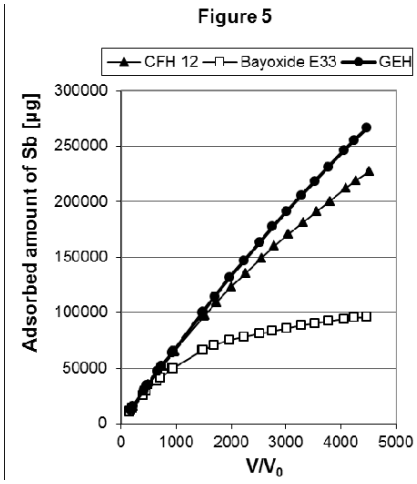

Fig. 5. Relationship between adsorbed amount of antimony in adsorbent media and the ratio V/V_0

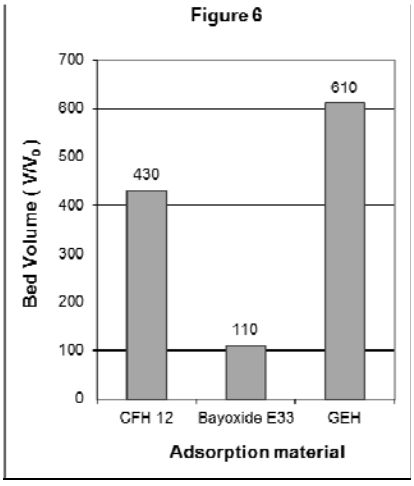

Fig. 6. Values of the V/V_0 when meeting the limit concentration of antimony (5 µg/l) at the outlet of adsorbent media

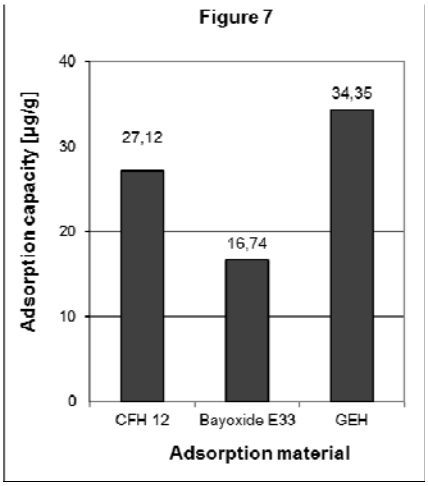

Fig. 7. Adsorption capacity of materials and the limit concentration of antimony at the outlets

Higher mass and hydraulic loadings of adsorbent media than in the model test 06.2010 resulted in lower values of the V/V_0 when meeting the limit concentration of antimony (5 µg/l) at the outlet of adsorbent media (see figure 6). The ratios V/V_0 were as follows: Bayoxide E33 V/V_0 = 110, CFH12 V/V_0 = 430 and GEH V/V_0 = 610.

The relationship between the adsorption capacity of materials and the limit concentration of antimony at the outlets of adsorbent media is shown in figure 7. The highest adsorption capacity was measured for GEH, lower for CFH 12 (27.12 µg/l) and the lowest for Bayoxide E33 (16.74 µg/). Also these model tests proved that the best results related to antimony removal were obtained by using the adsorption material GEH.

6.4. CONCLUSION

According to the results obtained in the model tests of antimony removal using selected adsorption materials, it can be concluded that GEH is the most suitable adsorption material for antimony removal.

Acknowledgement

Experimental measurements were done with the financial support within the Project APVV-0379-07. This paper was written with the support of the scientific grant agency VEGA in terms of solving the grant task no. 1/1143/1.

References

[1] Drinking Water Directive 80/778/EEC, COM(94) 612 Final.
[2] Ilavský J., Barloková D., Munka, K.: Heavy Metals in Water – Health Risk and Removal by Sorption Materials. In: Water Management and Hydraulic Engineering. Proceedings of 10th International Symposium. Croatia, Šibenik, September 2007. Zagreb, Faculty of Civil Engineering, 2007. ISBN 978-953-6272-21-1-II-02, 2007.
[3] Cahlíková Z., Cahlík A.: Dúbrava − water monitoring regime. Water Resources Holešov. Final Report 1993.
[4] Munka K., et al.: Design of antimony removal technology from water resources SKV Dúbrava and Partizánska Ľupča (in Slovak). Final Report, Water Research Institute Bratislava 1999.
[5] Sokáč M.: Simulation of influence of discontinuous resources of pollution to surface water (in Slovak). Bratislava, STU Bratislava, pp. 104. ISBN 978-80-227-3328-1, 2010.
[6] Driehaus W., Jekel M., Hildebrandt U.: "Granular Ferric Hydroxide – A New Adsorbent for the Removal of Arsenic from Natural Water." J. Water Supply Res. and Technol.-Aqua 47, 1998, pp. 30–35, 1998.
[7] Severn Trent Services: DWI Statement of Qualifications – SORB 33™ Arsenic Removal and Bayoxide® E33 media. Brochure.
[8] EPA/600/R-10/012 by Lipps, J. P., et al. Arsenic Removal from Drinking Water by Adsorptive Media. U.S. EPA Demonstration Project at Spring Brook Mobile Home Park in Wales, ME Final Performance Evaluation Report, March 2010.
[9] Ilavský J., et al.: Adsorption properties of materials used to remove heavy metals from water (in Slovak). In: Proceedings of the II. Conference Modernization and optimization of treatment plants. Stará Lesná, March 2011, pp. 33–40, ISBN 978-80-969974-4-2, 2011.

7 Approach in Preparation of Groundwater Vulnerability Maps in Republic of Macedonia

Zlatko Ilijoski (Civil Engineering Instutute "Makedonija", Macedonia"),
Igor Peshevski, Cvetanka Popovska, Milorad Jovanovski (University of Ss Cyril and Methodius)

7.1. INTRODUCTION

Aquifer vulnerability has been a topic of international concern for more than a decade. During this time, technology advancements have made the difficult process of analyzing data regarding aquifer vulnerability increasingly easier. More potential ground water pollution sources can now be located on a map using computer software. The ground water quality data collected by various agencies can be collated into a database and plotted on a map. Having this in mind, the most important step in preparation of aquifer vulnerability mass is to choose adequate parameters which are of primary interest for possible groundwater contamination.

There is a lot of assessment method in the practice which defines vulnerability with a quantitative index as an output, but in general, they can be classified as **coverage** and **grid** methods.

The coverage methods are based on a selection of limited number of parameters, and define a rating system for each parameter so that each parameter has several classes. Then next steps are creation of coverage map for each parameter, and then creation of a map of intersection of all coverage maps. The result can be presented as a coverage map with attributes of vulnerability.

In grid method, more parameters are used than in the method described above, since the map is handled as a grid rather than a coverage. An array of ratings of each parameter is prepared for each grid point on the map. The elements of the array are then used to calculate the vulnerability at the grid point by predefined arithmetic calculations. A parameter would be assigned with a larger weighting than others, based on its importance in determining vulnerability. Carrying out the calculation for each grid point, we have a grid map having a vulnerability index assigned to each grid point.

In the practice, several methods are widely used, but so-called GOD and DRASTIC methods are dominant.

This GOD method presented by Foster, 1987 is described as an empirical ranking system for the rapid assessment of aquifer vulnerability to contamination [2]. The reference mentioned this method as having a simple and pragmatic structure. It accounts only three properties that are: Type of aquifer, Grade of consolidation and lithological character and Depth of groundwater

The DRASTIC method is developed for the USEPA by Aller *et al* (1987). It incorporates following properties in its assessment: **D**epth of water table from the surface, Net **R**echarge, Lithology of the **A**quifer, **S**oil texture, **T**opography (slope), Lithology of vadose zone and Hydraulic **C**onductivity of aquifer [1].

Sets of weighting factors are prescribed for specific objective of the analysis. So many variables are factored into the final number (vulnerability index) that critical parameters in the groundwater vulnerability may be subdued any other parameters that have no bearing on vulnerability for a particular setting.

Having in mind these basic notes, in the frame of this article, we will explain the basic assumptions for the developing methodology in preparation of vulnerability maps in R.Macedonia.

7.2. ANALYZED AREA

The region of Republic of Macedonia is situated in the central part of Balkan Peninsula (Figure 1).

Fig. 1. Key map, position of R.Macedonia in Balkan Peninsula and Europe

This is a mountainous country with many lowlands. The average altitude of the whole territory is 850 meters. According to the Spatial Plan of the Country, 1.9% of the territory is covered by water (lakes), 19.1% are plains and valleys, and the biggest parts of 79% are hills and mountains. Plains and valleys in Macedonia occupy a total area of 4 900 km^2 throughout the country (Table 1).

Table 1

Main data about the range of elevations in R.Macedonia

Level of elevation	Area (km^2)	Percentage (%)
Up to 200 m	744.10	2.89
200–500 m	5769.10	22.44
500–1000 m	11317.32	44.01
1000–1500 m	1786.54	22.33
1500–2000 m	354.26	6.95
Over 2000 m	354.26	1.38
Total from 44–2764	25713.00	100.00

7.3. BASIC HYDROGEOLOGICAL CHARACTERISTICS OF THE COUNTRY

The nature of occurrence, quantity and quality of groundwaters depends on topographic, geological and morphological characteristics of the relief, connected with the runoff and infiltration of surface waters from one side, as well as on the type of porosity and other geological characteristics of the area. Beside other important aspects, we will add that some areas in Republic of Macedonia have unique geological and hydrogeological characteristics. Differentiation in different hydrogeological classes is according to transmissivity of the aquifer zones, which is in direct or indirect correlation with structural type of porosity [5, 7]. All rocks are classified in several classes according criteria in a Table 2.

Table 2

Criteria for classification of hydrogeological classes for permeable rocks with intergranular porosity

Description of permeability	Transmissivity coefficient T(m^2/day)	Specific yield Q (1/s/m)	Maximal yield Qv (1/s)
Low	15 – 50	0.1 – 0.3	0.5 – 2
Middle	50 – 300	0.3 – 2	2 – 10
High	300 – 1500	2 – 10	10 – 50
Extremely high	> 1500	> 10	> 50

When there are no quantitatively measured data, the rocks with intergranular and fissured type of porosity can be divided in classes with low transmissivity to middle transmissivity, according to the measured spring yield (*Qn*). For a class of low transmissivity *Qn* = 0.05 – 5 l/s, while for the class of middle transmissivity *Qn* > 5 l/s.

Carbonate rocks with karsts phenomenon, are divided in 3 (three) main classes according to the degree of karstification, as follows:

— Class with low degree of karstification with karsts occurrences (approximately 1 occurrence/1 km^2).

— Class with middle degree of karstification with karsts occurrences mainly on a surface (approximately 10 occurrence/1 km^2).

Class with high degree of karstification at surface and underground (>10 occurrence/1 km$^{2)}$.

— Practically impermeable formations (aquiclude) with intergranular or fissured porosity are classified as different classes.

The general presentation of main hydrogeological complexes is presented in Figure 2.

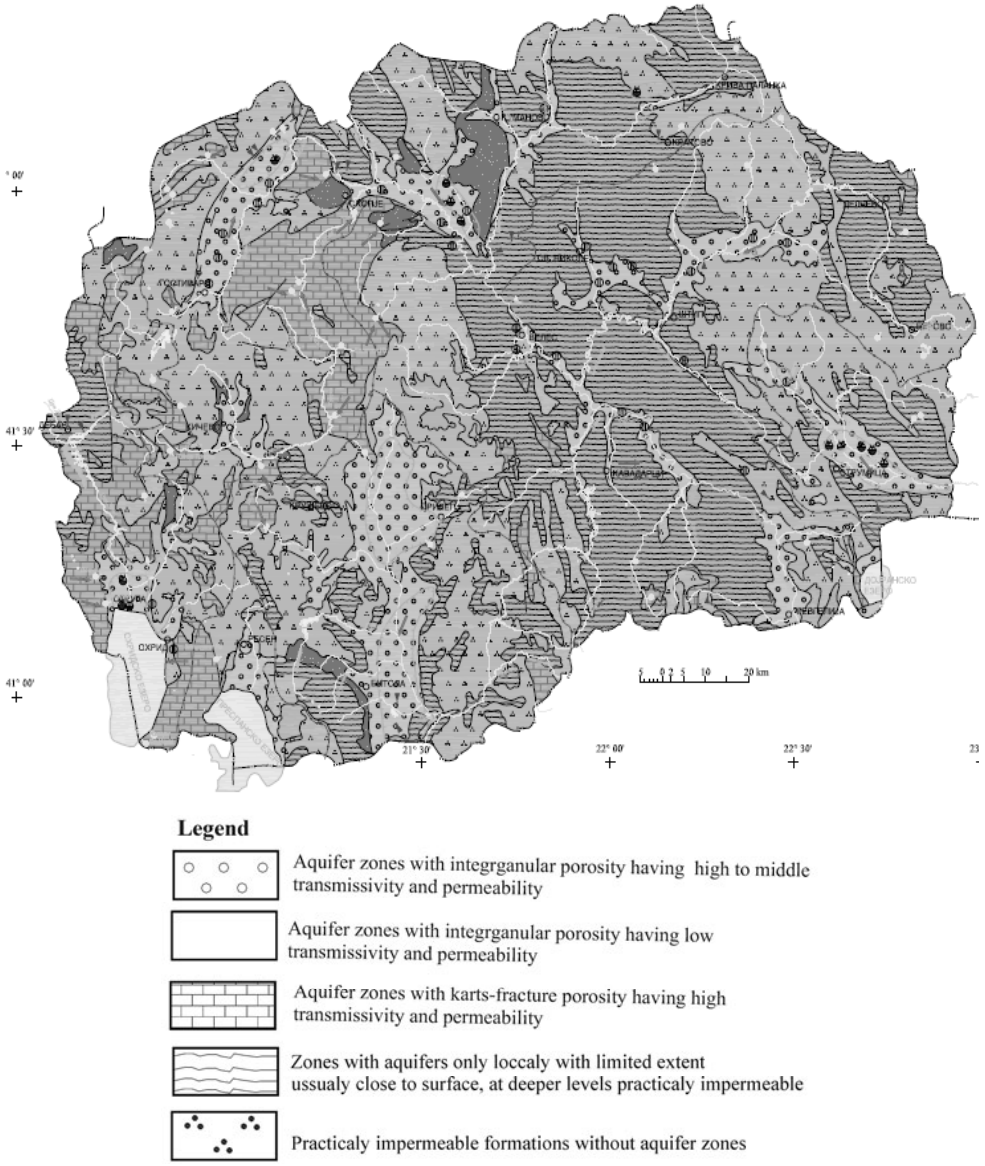

Fig.2. Synoptic Hydrogeological Map of Republic of Macedonia

This hydrogeological map is in fact basic document for further preparation on vulnerability map in the country.

7.4. PRESENT PRACTICES IN PREPARATION OF GROUNDWATER VULNERABILITY MAPS IN REPUBLIC OF MACEDONIA

Methodology for preparation of vulnerability maps in the country mainly use criteria connected with a permeability and transmissivity of the media [3, 4]. This is so-called first approximation in prognosis of conditions for possible ground water contamination. Four main vulnerability classes are defined:
Class of non vulnerable zones;
Class of lowly vulnerable zones;
Class with middle vulnerable zones;
Class with highly vulnerable zones.

Vulnerability Map according to such methodology is presented in Figure 3.

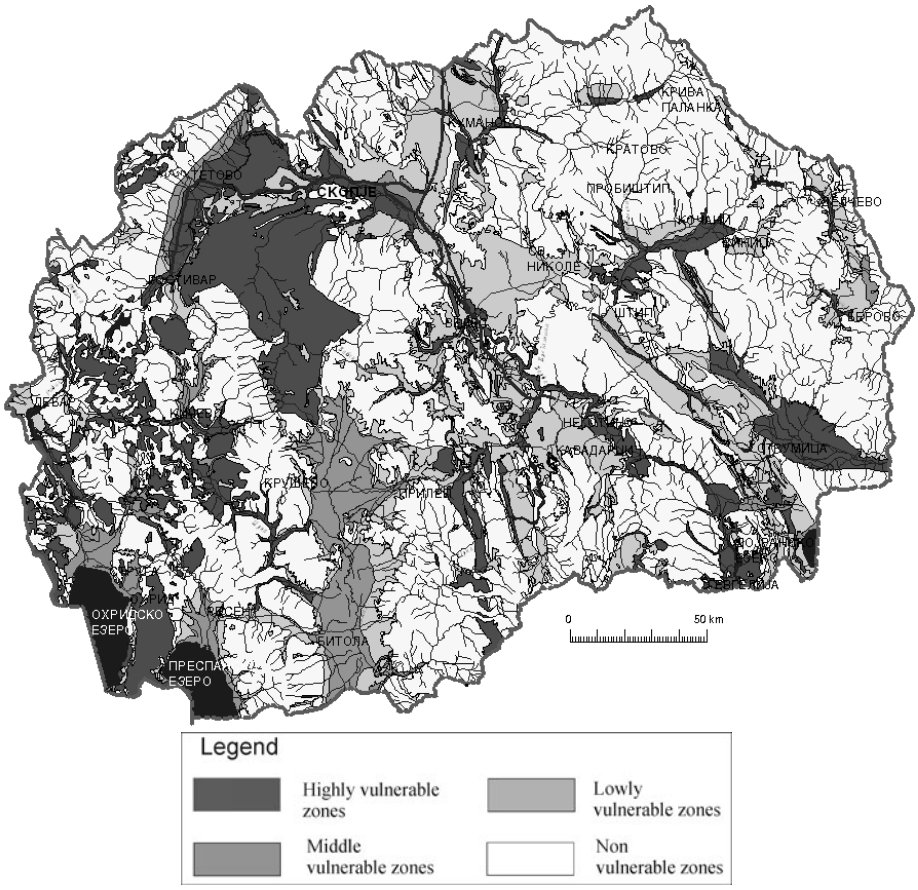

Fig. 3. Vulnerability Map of R.Macedonia according to criteria in Manual for Preparation of Hydrogeological maps [6]

Highly vulnerable zones are mainly connected with karts formations and gravel-like sediments without coverage, while middle vulnerable zones are defined mainly with alluvial and valley areas composed of classes with middle transmissivity (Table 2).
Lowly vulnerable zones are mainly connected with class of low permeability, while non-vulnerable zones with impermeable formations. Any how, it is obvious that this methodology has limitation because it doesn't use external factors important for vulnerability of the area. That is one of the main reasons, why a new developing methodology is suggested for future analyses, briefly explained in a frame of this article.

7.5. MULTI PARAMETER VULNERABILITY CLASSIFICATION RATING SYSTEM

Based on longer time investigations during preparation of Hydrogeological maps in the country, multi parameter classification is developed, which is called VCRS (Vulnerability Classification Rating System). The development of the classification is mainly according to known criteria given in DRASTIC or GOD methodology. The system is based on scoring, where for each range of values for classification parameters; an adequate rating is given in Table 3.

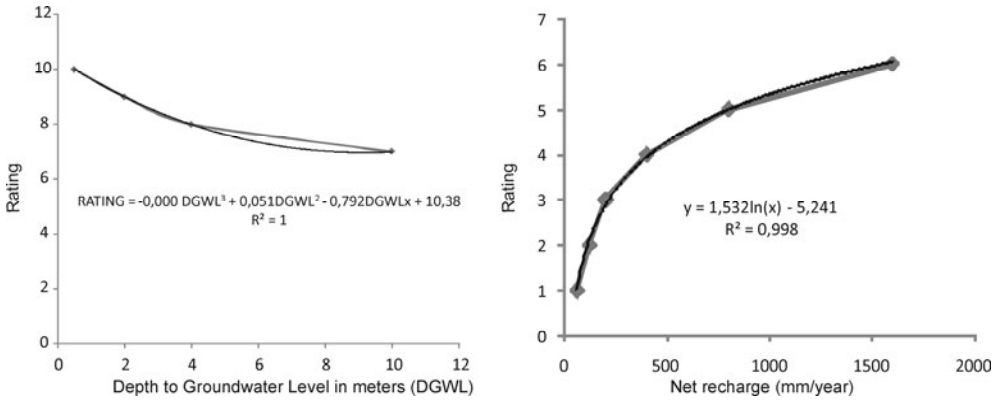

Fig. 4. Ratings for Depth to Ground Water Level (DGWL) and Net Rechargeusing polynomial or power law interpolation

All hydrogeological zones according this system are divided in five basic classes as follows:
Class 1 is for Very Low Vulnerable zones with rating lower than 25;
Class 2 is for Vulnerable zones with rating from 26–30;
Class 3 is for Middle Vulnerable zones with rating from 31–35;
Class 4 is for Highly Vulnerable zones with rating from 36–40;
Class 5 is for Very High Vulnerable zones with rating from 41–50.

Table 3

Multi-parameter vulnerability classification rating system **(VCRS)**

Classification parameter	Range of values for each classification parameter				
1. Depth to Groundwater level (m)	>10	5-10	3.1–5	1.1–3	<1
Rating	6	7	8	9	10
2. Net recharge (mm/year)	50–100	101–200	201–400	401–800	800–1600
Rating	1	2	3	4	6
3. Lithology of the aquifer zone (*)	Claylike sands, silts Flysch formations	Sandy loam, sands, schist formations	Sands, lowly fractured igneous and metamorphic rocks	Sandy gravels, highly fractured igneous and metamorphic rocks	Gravels Karts formations
Lithological type (**)	1	2	3	4	5
Rating	2	3	4	6	8
4. Lithology of the unsaturated zone or soil debris over hard rocks	Clay,	Sandy loam, sands,	Sands, lowly fractured igneous and metamorphic rocks	Sandy gravels, highly fractured igneous and metamor-phic rocks	Sands, gravels
Lithological type (**)	1	2	3	4	5
Rating	2	3	4	6	8
5. Topography (Slope in %)	>4	2.5–3	1.6–2.5	1–1.5	0–1
Rating	6	7	8	9	10
6. Hydraulic conductivity (m/day)	<4	5–20	21–30	31–80	>80
Rating	1	2	4	6	8
Total Rating (VCR)	<25	25–20	31–35	36–40	41–50
Vulnerability Class Description	Very low	Low	Medium	High	Very high

*) The Lythological type is defined for mathematical calculation for which arbitrated value from 1 to 6 is assigned

**) The description is partially modified in relation to Aller et all, 1987 from DRASTIC criterion

For all classification parameters, a correlative polynomial or power law curves are defined in order to have possibility to assign an adequate rating for all range of values given in Table 3.

For Lythological Types, an arbitrary value from 1 to 6 is used as a basis for correlation with ratings. The charts are helpful for borderline cases and remove impression that abrupt changes in rating occur between evaluation categories.

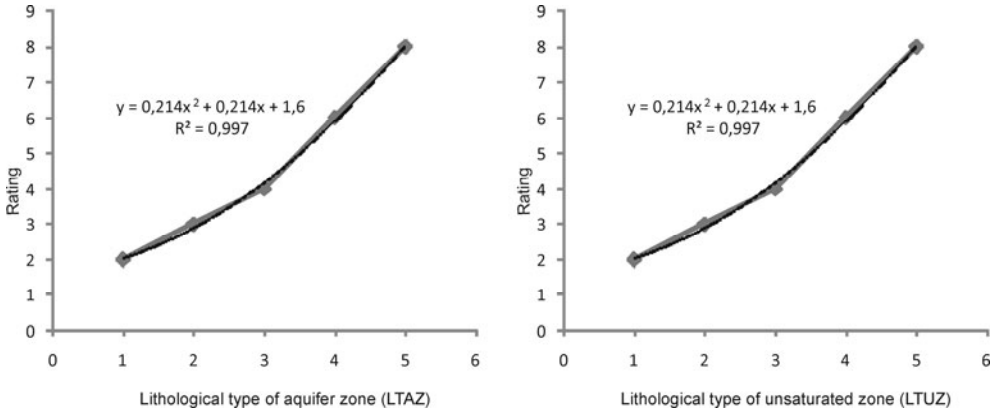

Fig. 5. Ratings for Lythological types using polynomial interpolation

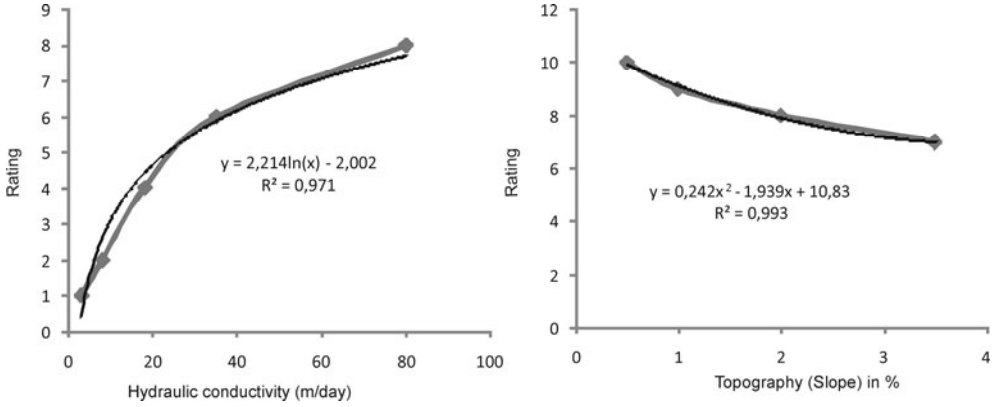

Fig. 6. Ratings for Hydraulic conductivity and topography using polynomial or power law interpolation

7.6. CONCLUSIONS

According to longer time analyses during preparation of vulnerability maps in Republic of Macedonia, the new developing methodology for preparation of ground water vulnerability maps named as Vulnerability Class Rating System (VCRM) is presented. An analysis of the problems is also related to the existing groundwater management situation in Macedonia.

This approach can serve as a basis for preparation of Vulnerability Zonation Maps. Unique condition units was developed by combination of geological map (lithological units), slope angle map, map with thickness of soil debris and groundwater conditions. The resulting total score contains the essential elements regarding the evaluation of the degree of the exposition to the risk for the analysed area.

Having in mind that this is empirical methods based on certain level of experience, the philosophy of the methodology presumes dynamical, critical and development period, relatively it should be subjected to critical reviewing in time, and should be used in combination with other methods developed for this problem. Further, this methodology will be developed in order to prepare correlation with known DRASTIC or GOD indexes, combination with Risk maps etc.

References

[1] Aller L., Bennett T., Lehr J. H., PettyR. J., Hacket G.: DRASTIC: A standardized system for evaluating groundwater pollution potential using hydrogeological settings, US-EPA Report 600/2-87-035, Washington DC, USA 1987.
[2] Foster S.S.D.: Fundamental concepts in aquifer vulnerability, pollution risk and protection strategy, International Conference VSPG. Noordwijk, The Nederland 1987.
[3] Ilijovski Z., Jovanovski M., Peshevski I., An overview on the methodology for preparation of vulnerability maps, First Geological Congress of Macedonia, Ohrid 2008.
[4] Ilijovski Z., Pesovska S., Nikolovska D.: Vulnerability map of Republic of Macedonia, 3 rd Symposium of Geotechnics, Struga 2010.
[5] Jovanovski M.: Groundwater Study in The Republic of Macedonia, Report supported by German Development Cooperation (GTZ), Coordination Office in Macedonia 2009.
[6] Manual for preparation of Basic Hydrogeological map of SFRJ at a scale 1:100 000, Geological Department, Belgrade 1988.
[7] Popovska C.: Surface Water Study in The Republic of Macedonia, Report supported by German Development Cooperation (GTZ), Coordination Office in Macedonia 2009.

8 Influence of Characteristic of Ball Valve Closing on Water Hammer Run

Apoloniusz Kodura (Warsaw University of Technology, Environmental Engineering Faculty)

8.1. INTRODUCTION

The water hammer is one of examples of transient flow in pressure pipelines. This phenomenon is described as pressure wave which was created by rapid change of velocity. That wave spreads in pipeline with high celerity and can lead to dangerous conditions of pipeline work due to significant increase pressure as well as high wave frequency [9]. The celerity of pressure wave is a function of the fluid's precise bulk modulus, friction forces, inertia forces, and characteristics of the pipe wall including its material composition, thickness, and geometry [5, 10].

The results of water hammer occurring can be one of the major problems for pipelines maintenance. According to data [2] a number of breakdowns in water supply systems due to water hammer phenomenon can be significant. A good description of water hammer run would be very useful for scientists and engineers. This is a reason of large number of different models and equations which are used to calculate the extreme values of pressure, wave frequency and others parameters of transient flow. One of the significant problems is lack of experimental data measuring this phenomenon. This is a reason of many theoretical solutions during more than 100 years of the water hammer phenomenon history.

The existing literature describes two situations [8, 10, 11] – rapid water hammer, when the gate closure's duration time is shorter than one wave period and complex water hammer (or slow gate closure) when the time of gate's closure is longer than one wave period. The maximum pressure increase of rapid water hammer is still being calculated using Joukowsky's equation (1898). However, many numerical methods were introduced and developed [1, 4, 6, 7, 13]. In a hydraulic system the second case – complex water hammer – is very common and is still being calculated today using equations from Michaud (1878) and Wood and Jones (1966) [11]. The slow gate closure is used as one of the ways to protect a pipeline system from the potential damage caused by rapid water hammer, particularly at pumps and pump stations where the water hammer phenomenon often emerges [11]. However, this seemingly simple solution is complicated by the existence of many different kinds of gates and valves. This study will address to one type of common use of gate closure – ball valve. The main target is to compare theoretical methods of the maximum pressure increase with experimental results for fully closing ball valve for two kinds of pipeline – made from steel and PE.

8.2. COMMON USED EQUATIONS TO CALCULATE PRESSURE INCREASE DUE TO COMPLEX WATER HAMMER

As it was mentioned, the characteristic of valve closure can have important influence on water hammer run. The rapid water hammer leads to the largest increase of pressure. For longer times of gates closure, the lowest increases of pressure are expected. The most common use of equation for calculation the pressure increase can be a good starting point to the next analysis. This is Joukowsky's formula which describes the increase of pressure due to water hammer [7, 10]:

$$\Delta p = \Delta \upsilon \cdot \rho \cdot a \tag{1}$$

where: $\Delta\upsilon$ – water velocity change,
ρ – liquid density,
a – wave propagation celerity.

The phenomenon can be called a positive water hammer, if it consists of fluid impede. Otherwise it is called a negative water hammer. During positive water hammer, when equals to 0 $\upsilon_e = 0$, that is $\Delta\upsilon = \upsilon_0$, equation (1) expressed the maximum increase of pressure due to total exchange of kinetic energy into potential energy.
The pressure wave can be expressed by the celerity of disturbance propagation a which is given by the equation [7, 10]:

$$a = 2L/T \tag{2}$$

where: T – wave period,
L – pipeline length,
a – wave propagation celerity.

A comparison between time period from equation (2) and time of gate closure is the important classification of the phenomenon. For rapid water hammer, a valve at the downstream end of a pipeline is closed in a time less than the wave period. When the valve closure is longer than the wave period during the gate closing, a deflected wave of the opposite sign is created. This returning wave reduces the pressure increase that resulted from the valve closure. If liquid velocity change is linear and the total pressure increase is less than 220% of pressure in steady condition before the water hammer phenomenon gives effect, then generated value of pressure increase can be calculated using Michaud's equation [5]:

$$\Delta p = \frac{2 \cdot \rho \cdot \upsilon_0 \cdot L}{T_c} \tag{3}$$

where: ρ – liquid density,
υ_0 – velocity in steady condition before water hammer run,
L – pipeline length,
T_c – time of gate closure.

In comparison to Joukowsky's equation, the value of wave propagation celerity in Michaud's equation was substituted by quotient $2L/T_c$ [3]. This equation assumes a linear change of liquid velocity, which cannot ever be achieved.

The next improvement on Michaud's model was introduced by Wood and Jones [11], [12]. It was an idea to introduce dimensionless valve closure time and dimensionless maximum transient pressure change. The calculation of the maximum increase of pressure can be done in few steps by using charts for each kind of valves. These charts based on theoretical analysis express a relationship between dimensionless valve closure time, dimen-

sionless maximum transient pressure change and coefficient α which describes a gate. The α is a parameter which applies to the most commonly used types of valves (circular gate, globe, needle, square gate, butterfly, and ball valves). This parameter is defined as [12]:

$$\alpha = \frac{g \cdot h_0}{\Delta \upsilon \cdot a} \tag{4}$$

where: h_0 – the head drop across the valve under the initial steady flow conditions, which can be observed just before a water hammer phenomenon occurs,
a – wave propagation celerity,
g – acceleration due to gravity,
$\Delta\upsilon$ – water velocity change.

To use Wood and Jones method α parameter from equation (4) has to be calculated. The next step is finding the value of the dimensionless valve closure time [12]:

$$t_c = T_c \Big/ \frac{2 \cdot L}{a} \tag{5}$$

where: t_c – dimensionless valve closure time,
T_c – valve closure time,
L – pipeline length,
a – wave propagation celerity.

That both values – α parameter and dimensionless valve closure time are needed to estimate dimensionless maximum transient pressure change which is given by equation [12]:

$$\Delta p_m = \frac{\Delta p_{\max}}{\Delta \upsilon \cdot \rho \cdot a} \tag{6}$$

where: Δp_m – dimensionless maximum pressure change,
$\Delta p_{\max}$ – maximum pressure head,
$\Delta\upsilon$ – liquid speed change,
ρ – liquid density,
a – wave propagation celerity.

By considering gate type, Wood's and Jones' method offers a significant advantage over using Michaud's equations. However, Wood's and Jones' is limited in application; it assumes the introduction of a resistance value in initial steady conditions and applies the same resistance coefficient in transient flow. As a result, this model has no impact on the characteristics of gate closure. The method also excludes friction resistance in dynamic unsteady conditions of water hammer run. [3].

8.3. EXPERIMENTS

8.3.1. Model

The model which was used during experiments is shown at the Fig. 1. in two cases – each was made for different material of pipeline. Two different pipelines (1) were used – steel pipeline 177 m long and 32 mm internal diameter and PE pipeline 240 m long and 35 mm internal diameter.

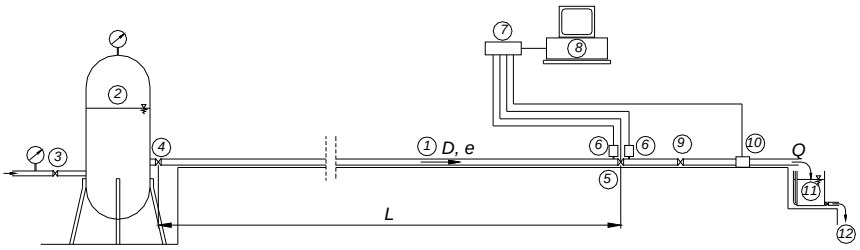

Fig. 1. Schema of model

Model was supplied by pressure tank (2) from city network (3). Downstream ball valve (5) was equipped by a unique system to register an angle of closing. Two pressure transducers (6) were connected to the pipeline to register pressure before and after ball valve. Pressure transducers and valve were connected to a computer via an analog-digital card to store experimental data. During a steady flow, just before starting a water hammer phenomenon, a value of discharge was measured by using electro-magnetic water-meter (10). Additional container (11) was used to control indications of water-meter.

For each pipeline at least 40 different measurements of water hammer were collected. The idea was to close the ball valve completely with linear function.

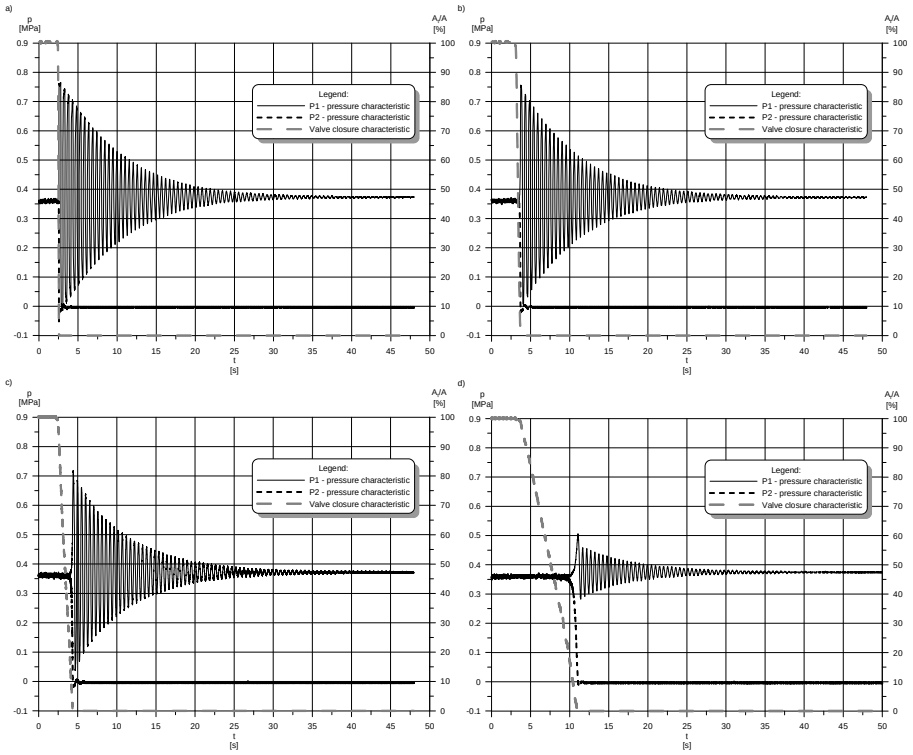

Fig. 2. Characteristics of pressures for steel pipeline, wave period $T = 0.26$ s.: a) ball valve closure time $T_c = 0.16$ s < T, b) $T_c = 0.64$ s > T, c) $T_c = 2.04$ s > T, d) $T_c = 7.7$ s > T

8.3.2. Results

The results of experiments were stored as pressure characteristics (Fig. 2 and 3). From each characteristic a wave period, wave propagation celerity and maximum pressure values are calculated.

The results for steel pipeline are shown at fig. 2. There are four cases presented. For each velocity during steady condition was comparable and equaled 0.31 m/s. The value of wave period was calculated by using pressure characteristic and equaled 0.26 s. Ball valve was closed by using linear relationship between ratio of current available cross-section area to full area cross-section and time. This value is illustrated by a grey doted line. There is a visible relationship between time of closure and the pressure increase. For the longest time shorter time of phenomenon duration can be observed.

Fig. 3 presented similar characteristics for PE pipeline. For that series velocity during steady condition was comparable and equaled 0.68 m/s. The wave period calculated by using pressure characteristic equals 1.32 s. Similarly, characteristic of ball valve closure is linear and expressed by ratio of current available cross-section area to full area cross-section. A similar influence of valve closure time on maximum values of pressure can be observed.

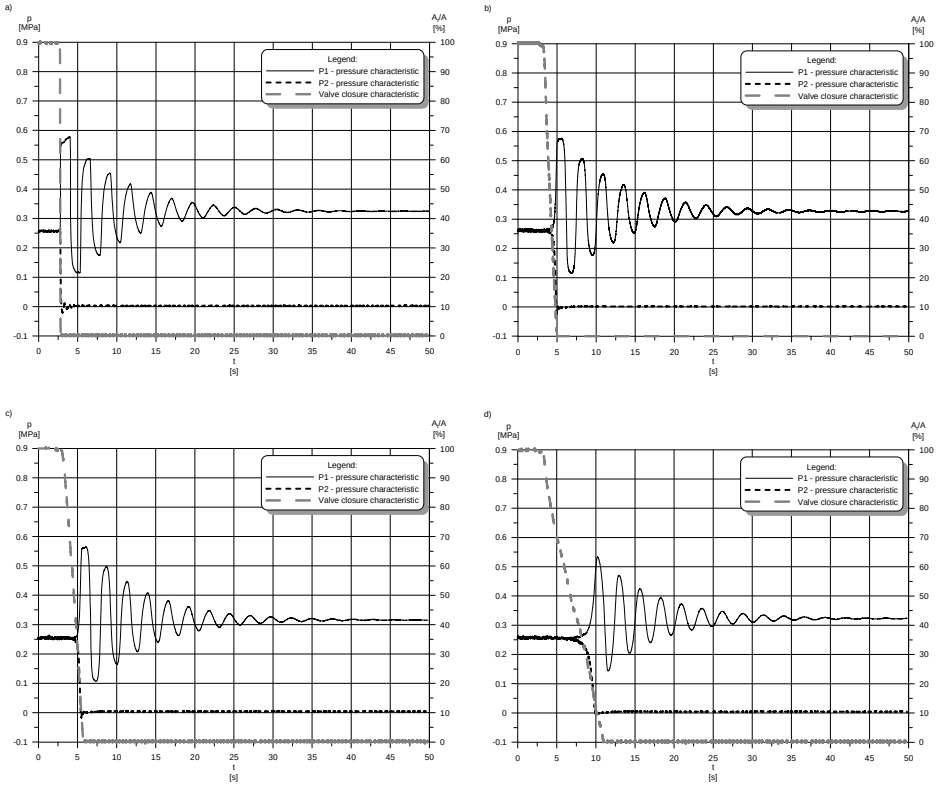

Fig. 3. Characteristics of pressures for PE pipeline, wave period T = 1.32 s. a) ball valve closure time Tc = 0.105 s < T, b) T_c = 1.8 s > T, c) T_c = 3.55 s > T, d) T_c = 7.0 s > T

The next step was to compare the results of the experiment to theoretical methods. Proper calculations to find pressure increase from Michaud's equation were made by using equation (3). Next, by using equation (4) the values of α parameter were calculated. This parameter expressed head drop across the valve. The measured value of head losses across the valve leads to calculate the α parameter for each experimental series. For the steel pipeline these α parameters ware higher than 0.002 and lower than 0.005. For the PE pipeline the α parameters were lower than 0.01. Higher values of head losses across the ball valve is the reason of different values of α parameter for PE pipelines.

8.3.3. Comparison with Michaud's and Wood and Jones' methods

The main idea of Wood and Jones method is to build a valve closing charts and to calculate a value of maximum pressure increase from that charts. This theoretical assumption takes the initial head losses across the valve during steady condition and a kind of valve. The aim of that paper was to compare experimental results to theoretical calculations. Fig 4 and 5 present that comparison. There are charts according to Wood and Jones' idea – *X* axis represents dimensionless valve closure time and *Y* axis expresses dimensionless maximum pressure changes. Two charts are built due to different values of α parameter for the steel and PE pipeline. In both cases by using curves the characteristics by Wood and Jones were presented. The results from Michaud's equation were expressed by empty circles. The filled circles present measured values of pressure increase in ratio to Joukowsky's formula.

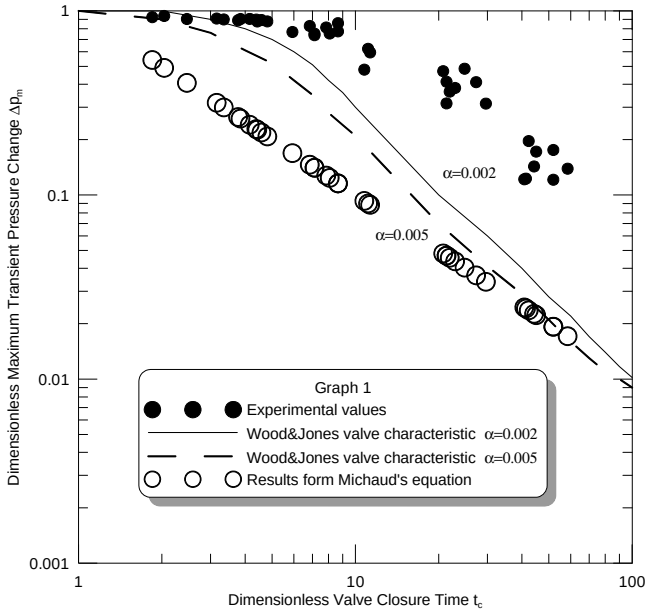

Fig. 4. Comparison results of experiments with Michaud's equation and Wood and Jones method – steel pipeline

A comparison between results leads to important remarks – in both cases a strong relationship between time of closure and maximum pressure increase can be observed. However, this relationship is different for experimental data and theoretical results. First of all, Michaud equation leads to significantly lower values of maximum pressure increase in comparison to Wood and Jones results and experimental data for the steel and PE pipeline. This is quite an important statement – this equation should not be used for calculation influence of valve closure time on pressure increase.

The second important remark is that applying Wood and Jones method leads to too small values of maximum pressure increase. The difference between calculated data and results of experiments can be very significant both for steel and PE pipelines.

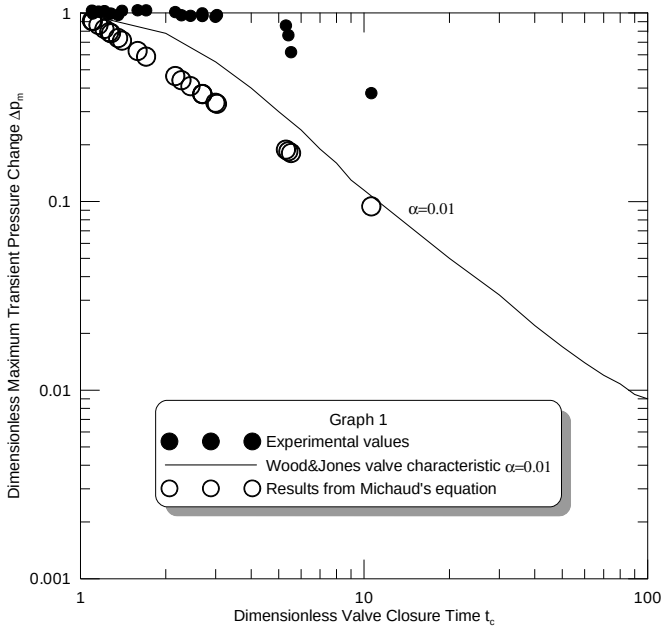

Fig. 5. Comparison results of experiments with Michaud's equation and Wood and Jones method – PE pipeline

8.4. CONCLUSIONS

In this paper experimental data for full closing ball valve was compared to theoretical methods: Michaud and Wood and Jones. The strong influence of valve closure time on maximum pressure increase was observed. The maximum pressure values were obtained for experimental data. The maximum pressure increases calculated by using Michaud's are significantly smaller than experimental. Due to too big difference this equation should not be used for calculation of the influence of valve closure time on pressure increase.

Wood and Jones method, analyzed in the paper, gives too small pressure increase in comparison to experimental results. Taking a kind of valve and initial steady head losses across the valve as the only factors under consideration is not satisfying. The character of

the influence of valve closure characteristic is more complex. A fact of high similarity between the results of PE and steel pipeline should be underlined. The problem of closure time influence on maximum pressure increase should be developed by analysis of experimental results. Making only theoretical investigation can lead to improper process description.

The presented results give an advise for practical calculations – the maximum pressure increase can be calculated from the Joukowsky's formula for times of closure shortest than 3 periods of wave as well as for steel pipelines as PE pipelines.

References

[1] Evett J. B., Liu C.: 2500 Solved Problems in Fluid Mechanics and Hydraulics, McGraw-Hill (1989).

[2] Ilin Jo. A.: Rasczet nadzieżnosti podaczi wody, Stroizdat, Moscow (in Russish) 1987).

[3] Kodura A.: Influence of valve closure characteristic on pressure increase during water hammer run, Environmental Engineering III, CRC Press (2010) Pages 463–472.

[4] Marcinkiewicz J., Adamowski A., Lewandowski M.: Experimental evaluation of ability of Relap5, Drako®, Flowmaster2™ and program using unsteady wall friction model to calculate water hammer loadings on pipelines, Nucl Eng Des, doi:10.1016/j.nucengdes.2007.10.027, 2008.

[5] Mitosek M.: Mechanika Płynów w Inżynierii i Ochronie Środowiska. Warsaw: WNT (in Polish) 2007.

[6] Niełacny M.: Uderzenia hydrauliczne w systemach wodociągowych. Poznan: WPP (in Polish) 2005.

[7] Parmakian J.: Water hammer analysis. New York: Prentice-Hall Inc., 1955.

[8] Pires L. F. G., Laidea R. C. C., Baretto C. V.: Transient Flow Analysis of Fast Valve Closure in Short Pipelines, Proceedings of International Pipeline Conference, October 4–8, 2004, Calgary, Alberta, Canada 2004.

[9] Ramos H., de Almeida B. A.: Parametric Analysis of Water Hammer Effects in Small Hydro Schemes, Journal of Hydraulic Engineering, Vol. 128, No 7, pp. 689–696, 2002.

[10] Streeter V. L., Wylie B. E., Bedford K. W.: Fluid Mechanics. New York: WCB McGraw-Hill 1998.

[11] Thorley A. R. D.: Fluid transients in pipeline system: a guide to the control land suppression of fluid transients in liquids in closed conduits. New York, ASME Press 2004.

[12] Wood, D. J., Jones, S. E.: Water-hammer charts for various types of valves. Journal of Hydraulic Division, Vol. 99, No 1, pp. 167–178, 1973.

[13] Wylie B. E., Streeter V. L., Suo L.: Fluid Transients in Systems. Englewood Hills New Jersey, Prentice Hall 1993.

9 Numerical Modeling of Rectangular Settling Tank Efficiency

Goran Lončar, Marin Paladin, Vladimir Andročec (Water Research Department, Faculty of Civil Engineering – University of Zagreb)

9.1. INTRODUCTION

Sedimentation tanks are hydro technical objects used for deposition of solid particles due to increased gravity forcing. Primer effect is achieved through average flow velocity decrease, caused by lateral expansion of solid boundaries (Fig. 1). During the deposition solid particles accelerate until drag force and buoyancy force becomes equal. After that, the particle reaches a constant sinking velocity, mostly in the region of Stokes law validity. In practice, the design solution also should take into account the reduction of deposition due to particle interactions and flow in the zone of deposition caused by a variety of "external" influences (circulation due to density difference, the wind influence on uncovered sedimentation tank water surface...). Although sedimentation tank could be designed in wide range of geometry configuration, undertaken research and results presented in this paper are focused on rectangular sedimentation tank with horizontal flow. Like all other hydro technical structure, sedimentation tank must simultaneously meet the requirement of functionality and economy. In this sense, optimization procedure also includes modeling implementation with the aim of defining the connection between lowest possible costs and assumed settling efficiency.

Variation of sedimentation tank basic geometry parameters (Fig. 1) will affect the overall deposition process and settling efficiency. According to the engineering recommendations and guidelines [10] depth of rectangular sedimentation tank H should be in the range 2 – 3 m, width B should not exceed 5 m and length L should not exceed 50 m. Many studies have been conducted with the aim of flow classification in dependence on geometrical parameters and of determining the optimum geometry for maximum sediment removal.

Already back in 1944 Dobbins provides the first empirical and semi empirical expressions for the efficiency of deposition in rectangular sedimentation tanks. Abbot and Kline (1962) [1] explored the phenomenon of asymmetric flow depending on the geometry of the basin and marked the existence of two symmetrically recirculation zones in case of expansion ratio $\Delta b/b<0.25$ (Δb lateral expansion; b inflow channel width). Garde et al. (1990) [6] experimentally analyzed the efficiency of settling with the purpose of finding an analytical expression for geometry elements calculation according to the imposed value of deposition efficiency. Sediment concentration (mass flux) that one finds in outflow channel is given with following functional relationship [6]:

$$q_{out} = f\left(L, H, \Delta h, b, B, U, u_*, g, w_s, q_{in}\right) \tag{1}$$

where: L length of sedimentation tank, H water depth in the sedimentation tank, Δh height of bottom expansion, b inflow channel width at the water table level, B width of sedimentation tank cross section at the water table level, U mean flow velocity through sedimentation tank cross-section, u_* shear velocity in sedimentation tank profile, w_s sediment sinking velocity, q_{in} mass flux of solid phase through the vertical cross section of incoming channel, q_{out} mass flux of solid phase through the vertical cross section of outgoing channel.

Equation (1) can be represented in dimensionless form as follows:

$$\eta = \frac{q_{in} - q_{out}}{q_{in}} = f\left(\frac{L}{H}, F_r, C, \frac{w_s}{u_*}, \frac{\Delta h}{L}, \frac{b}{B}, \frac{B}{H}\right) \tag{2}$$

where: η sedimentation tank efficiency, C average concentration of solid phase for incoming flow $C = q_{in} / (uhb)$, u average velocity in cross section of incoming channel, Fr – Froude number within sedimentation tank $U / (gH)^{1/2}$.

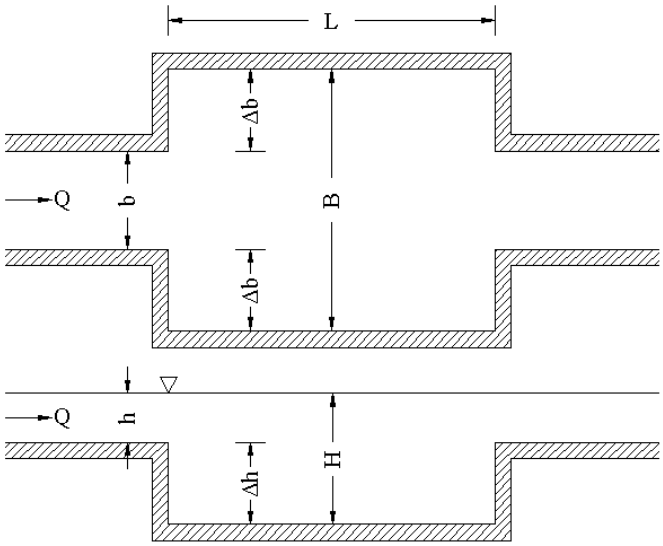

Fig. 1. Basic geometry parameters of rectangular sedimentation tank

The dependence of particulate matter sinking velocity on their concentration was analyzed by Hetsroni [7] and Garde et al. [6]. Results of experimental studies have shown that sinking velocities, in a wide range of analyzed concentrations, differ only by 15% from the sinking velocities defined by Stokes' law. Afterwards, implementation of experimental research [6] have shown that certain parameters specified in equation (2) have only minor influence in the deposition process, what gives a rise to the simplification of the equation (2) into the following relation:

$$\eta = f\left(\frac{L}{H}, \frac{w_s}{u_*}\right) \tag{3}$$

Conducted experimental research and related results [6] enabled determination of interdependence of the remaining relevant non-dimensional parameters, which is shown by the equation:

$$\eta = \eta_0 \left(1 - e^{-kL/H}\right) \tag{4}$$

where: η_0 marginal efficiency of observed (w_s/u_*) at high values of (L / H), k dimensionless coefficient.

In order to define the dependence of η_0 and k on (w_s / u_*), Garde et. al. [6] defined functional relation in the form of η_0, $k = f(w_s / u_*)$, which for an assumed value of efficiency η_0 determines the value of (w_s / u_*) and k. Using the equation 4 it is possible to define the expected efficiency η for the sedimentation tank of arbitrary dimensions. Verification using the expression 4 in the range L / H = 2–50 and d = 0.082–1.67 mm was achieved through experimental studies conducted by Ranga Raju [9]. Based on a wide range of referenced and published results of laboratory studies Dongre [3] suggested an empirical relationship that includes expanded number of constitutive geometric variables:

$$\eta = 102.5\left(1 - \exp\left(-0.3\frac{A}{A_{in}}\right)\right)\left(1 - \exp\left(-0.1\frac{L}{H}\right)\right)\left(1 - \exp\left(-0.42\frac{w_s}{u_*}\right)\right) \tag{5}$$

where: $A = BH$ cross-sectional area of sedimentation tank, $A_{in}=bh$ cross-sectional area of rectangular incoming channel.

Equation (5) can be used for determination of sedimentation tank efficiency η with a maximum error of about ± 25%.

9.2. NUMERICAL MODEL IMPLEMENTATION

We conducted a numerical analysis of the efficiency of settling tanks, depending on its geometrical parameters. Sedimentation tank length L, width B and depth H are varied within model spatial domain (Table 1). Incoming channel geometry is set with constant values of b = 1 m and h = 0.5 m. Constant and stationary inflow discharge of Q = 0.25 m^3/s is used in all model simulations. 2D numerical model MIKE 21 (www.dhigroup.com) was used for the implementation of numerical analysis. The model analyzes incompressible fluid flow and convective-dispersion of suspended sediment in one homogeneous vertical layer with assumption of hydrostatic pressure distribution. System of shallow water equations contains of a vertically integrated continuity equation and momentum conservation equations within Cartesian coordinate system [1].

The model spatial domain was discretized using a structured finite difference mesh with equidistant spacing in the horizontal direction $\Delta x = \Delta y$ = 0.25 m.

The calculation time step used in the numerical integration was set to Δt = 0.05 s. Turbulence closure scheme for resolving vertically and sub-incremental spatial fluctuations is realized using the Smagorinsky formulation. Smagorinsky constant, as the time-varying function of local gradients in the velocity field is adopted with the value of 0.4. Bottom roughness is expressed as a homogeneous in space with the adopted Manning's coefficient of 0.015 for all conducted numerical simulations.

Table 1

Nomenclature of conducted numerical simulations with related geometry and hydraulic properties

	code	B (m)	H (m)	L (m)	h_p (m)	$\Delta b/b$ (1)	$L/\Delta b$ (1)	U (m/s)	u_* (m/s)	$Dx=Dy$ (m^2/s)	Re (1)	τ_{CR} (N/m^2)
1	1	5	2	10	1.5	2	5.0	0.025	0.0013	0.029	2.0	0.092
	2	5	2	15	1.5	2	7.5	0.025	0.0013	0.029	2.0	0.092
	3	5	2	20	1.5	2	10.0	0.025	0.0013	0.029	2.0	0.092
	4	5	3	10	2.5	2	5.0	0.017	0.0008	0.029	1.3	0.141
	5	5	3	15	2.5	2	7.5	0.017	0.0008	0.029	1.3	0.141
	6	5	3	20	2.5	2	10.0	0.017	0.0008	0.029	1.3	0.141
2	7	4	2	10	1.5	1.5	6.7	0.031	0.0016	0.036	2.5	0.071
	8	4	2	15	1.5	1.5	10.8	0.031	0.0016	0.036	2.5	0.071
	9	4	2	20	1.5	1.5	13.3	0.031	0.0016	0.036	2.5	0.071
	10	4	3	10	2.5	1.5	6.7	0.021	0.0010	0.036	1.7	0.099
	11	4	3	15	2.5	1.5	10.8	0.021	0.0010	0.036	1.7	0.099
	12	4	3	20	2.5	1.5	13.3	0.021	0.0010	0.036	1.7	0.099
3	13	3	2	10	1.5	1	10.0	0.042	0.0021	0.048	3.3	0.064
	14	3	2	15	1.5	1	15.0	0.042	0.0021	0.048	3.3	0.064
	15	3	2	20	1.5	1	20.0	0.042	0.0021	0.048	3.3	0.064
	16	3	3	10	2.5	1	10.0	0.028	0.0014	0.048	2.2	0.082
	17	3	3	15	2.5	1	15.0	0.028	0.0014	0.048	2.2	0.082
	18	3	3	20	2.5	1	20.0	0.028	0.0014	0.048	2.2	0.082

Boundary conditions for suspended sediment at model open boundaries are expressed by the mass flux of 0.1 kg/m^3 of fine sand with grain diameter d = 0.09 mm. Turbulent dispersion coefficient values given in Table 1 were adopted as equal in x and y direction with the values calculated according to [5] $D_x=D_y= 0.57UH$. Sinking velocity of suspended sediment particles is determined by Stokes's law $w_s= 1.65\, gd^2/(18\nu) = 0.006$ m/s. Erosion is defined according to the methodology given in [8] with the adopted value of erosion coefficient and erosion exponent of 8.3 and 0.00005, respectively. Critical stress is defined using the Shields diagram with the values τ_{CR} shown in Table 1.

9.3. NUMERICAL AND ANALYTICAL MODEL RESULTS COMPARISON

Fig. 2 shows the stationary velocity fields obtained by models 1, 2 and 3 (see Table 1) and fig. 3 shows the corresponding fields of stationary suspended sediment mass fluxes. The comparison of sedimentation tank efficiency obtained with numerical and analytical models is given in fig. 4. Given analytical model results are directly calculated with the aim of equation (5), while processing of numerical model results is based upon relation within equation (2).

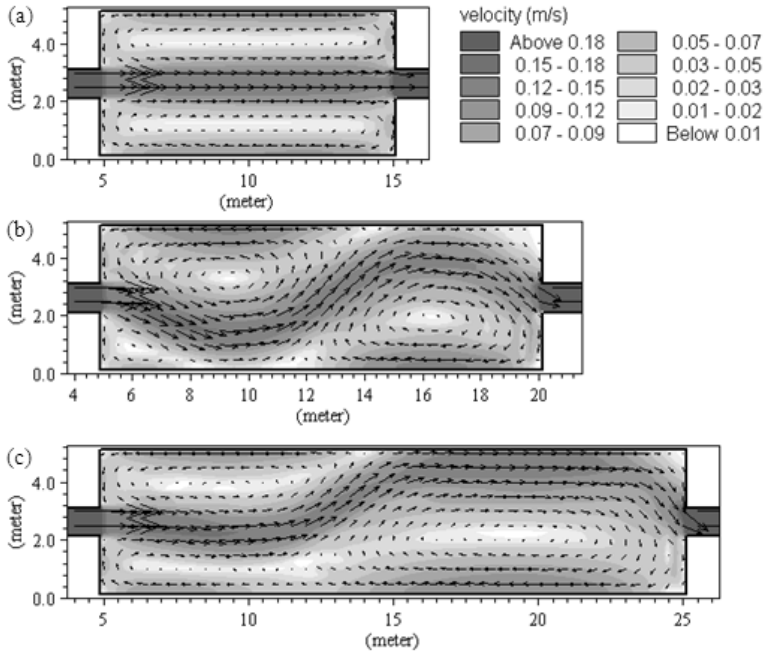

Fig. 2. Stationary velocity fields for numerical models 1 (a), 2 (b) and 3 (c)

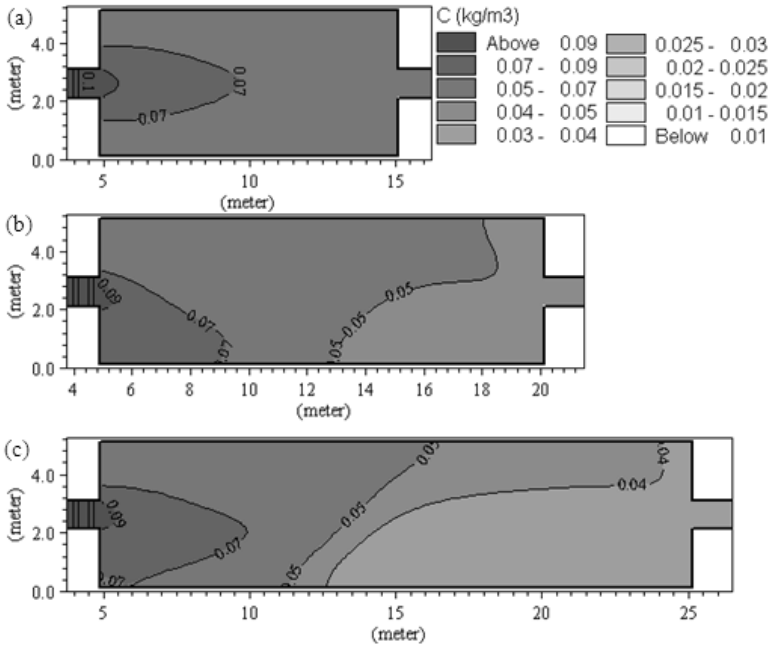

Fig. 3. Suspended sediment mass flux fields for numerical models 1 (a), 2 (b) and 3 (c)

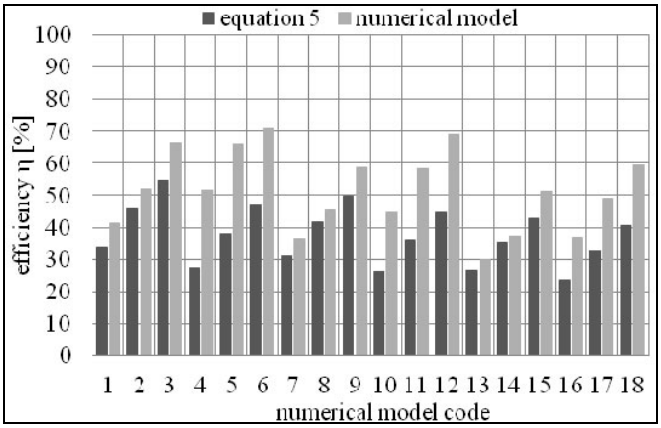

Fig. 4. Comparison of sedimentation tank efficiency obtained with analytical model (equation (5)) and numerical model (results processed according equation (2))

Model results show that symmetrical flow occurs only in short sedimentation tanks (in this case $B/L = 0.5$). For $B/L < 0.5$ asymmetrical flow is noticed. Velocity fields presented in fig. 2 show a satisfactory degree of correlation with flow patterns highlighted by Dufresne et.al. (2010) [4].

Fig. 4 shows the comparison of settling efficiency calculated by equation (5) and gained by numerical model. Longest settling tanks have the largest values of efficiency, like expected. All the numerical model efficiency results exceed analytical results. Greatest difference is 28.1%, and smallest one is 1.6%. Average difference in all 18 experiments is 13.8%. Results of numerical models for short tanks correspond more to analytical results then the results of long tank. Efficiency of sedimentation tank depends on three parameters A / A_{in}, L / H and w_s / u_*. It is interesting to find out which one of these three ratios has the biggest influence on value of efficiency. For this purpose we used code 1 model values and increased each ratio value separately by 50% and 100% respectively. Corresponding increase of efficiency was then calculated by equation 5 and determined by numerical model. Comparison of those values is presented in Table 2.

Table 2

Determination of most influential parameter in efficiency calculations

A/A_{in}	L/H	w_s/u_*		η–eq. 5	Increase of η[%]	η-numerical model	Increase of η[%]
20	5	4.48		34.108		41.24	
30	5	4.48	A/A_{in} (+50%)	34.188	0.24	45.73	10.88
40	5	4.48	A/A_{in} (+100%)	34.192	0.25	49.28	19.50
20	5	4.48		34.108		41.24	
20	7.5	4.48	L/H (+50%)	45.738	34.10	52.24	26.66
20	10	4.48	L/H (+100%)	54.795	60.65	66.33	60.84
20	5	4.48		34.108		41.24	
20	5	6.72	w_s / u_* (+50%)	50.740	48.76	69.18	67.75
20	5	8.96	w_s / u_* (+100%)	63.132	85.09	85.07	106.27

Both numerical model and equation 5 show that the most significant parameter in efficiency calculation is w_s/u_* ratio.

9.4. CONCLUSION

Numerical models of sediment transport trough rectangular shaped sedimentation tank that are presented in this paper were calculated using finite difference method. Sediment grain was uniform. Result of numerical models were velocity and sediment mass flux fields. The efficiency of sedimentation tank was then determined as described in equation 2. The main goal was to compare the tank efficiency gained by numerical model to one calculated by equation suggested by Dongre (2002) and verified by Ranga Raju (2004). The velocity fields in sedimentation tanks were also compared to flow patterns highlighted by Dufresne et.al. (2010). The results of numerical models qualitatively show very good correlation with results from referenced literature. This paper shows that numerical modeling can be successfully implemented in process of designing sedimentation tanks because it gives good insight in velocity field in area of the tank, and also it's efficiency.

References

[1] Abbott D. E., Kline S. J.: Experimental investigation of subsonic turbulent flow over single and double backward facing steps. Journal of Basic Engineering 84, 317–325, 1962.
[2] Abbott M. B., McCowan A., Warren I. R.: Numerical modelling of free surface flows that are two-dimensional in plan, Transport models for inland and coastal waters. London: Academic Press 1981.
[3] Dongre N. B.: Settling basin design, M. Tech Thesis. Department of Civil Engineering, Indian Institute of Technology, Roorkee, India 2002.
[4] Dufresne M., Dewals B. J., Erpicum S., Archembeau P., Pirotton M.: Classificaton of flow patterns in rectangular shallow reservoirs, Journal of Hydraulic Research, 48(2), 197–204, 2010.
[5] Fischer H. B., List E. J., Koh R. C. Y., Imberger J., Brooks N. H.: Mixing in Inland and Coastal Waters. New York: Academic Press 1979.
[6] Garde R. J., Ranga Raju K. G., Sujudi A. W. R.: Design of settling basins. Journal of Hydraulic Research, 28(1), 81–91, 1990.
[7] Hetsroni G.: Handbook of multiphase systems. New York: McGraw-Hill Book Co., 9–118; 9–121, 1982.
[8] Mehta A. J., Hayter E. J., Parker W. R., Krone R. B., Teeter A. M.: Cohesive Sediment Transport. I: Process Description. Journal of Hydraulic Engineering 115 (8), 1076–1093, 1989.
[9] Ranga Raju K. G., Kothayari U. C.: Sediment management in hydroelectric projects. Proceedings of the Ninth Interantional Symposium on River Sedimentation, Yichang, China 2004.
[10] Tedeschi S.: Zaštita voda, udžbenik sveučilišta u Zagrebu, Zagreb 1997.

10 Influence of Operation Parameters of Water Treatment Plant Exploitation on Trihalomethane Concentration in Chlorinated Water

Ewa Łobos (Silesian University of Technology; Institute of Mathematics),
Izabela Zimoch (Silesian University of Technology, Institute of Water and Sewage Engineering)

10.1. INTRODUCTION

The directive of European Union 98/83/EC of 3 November 1998 [1] which concerns drinking water quality, defines maximal permissible concentrations of disinfection by products (mainly trihalometanes) in water delivered directly to consumers. It is strictly connected with WHO recommendations [2] because numerous research confirm that trihalometanes (THMs) have carcinogenic and mutagenic character and they are dangerous for human health [3, 4, 5]. Trihalometanes formation is the result of chemical reaction between organic matter and chlorine used to disinfection. The harmfulness of THM and other disinfection by products forces the necessity of complex technological processes of water treatment such as preliminary oxidation, ozonization, sorption on activated carbon, and double disinfection process using chlorine and chlorine dioxide. All these processes together with standard water treatment (coagulation, filtration) guarantee the production of high quality drinking water.

However, highly efficient technological processes which are applied in current water treatment plants not always eliminate all difficulties in disinfection by chlorine process. It is connected with the fact that water treatment arrangements are not adjusted to high efficient removal of THM precursors. The concentration of THM precursors in surface water is high and it continuously increases as the result of anthropogenic environment pollution. Therefore it is very important to adapt just existing water treatment arrangement to changing conditions of raw water quality, which decreases the risk of too high concentration of THM generated in drinking water. It is essential because DBP are generated not only in water treatment process but also (mainly) in wide distribution water pipe network. Since it is impossible to completely remove the THM precursors, the monitoring of DBP concentration in water supply systems is necessary. On the other hand, the precise monitoring of THM is expensive so it is limited to indispensable minimal range.

The process of THM formation is a complicated chemical reaction which depends on many factors such as organic substance concentration, chlorine dose, reaction time, temperature, pH, and other. This chemical process is intensively studied but still it is not com-

pletely explored. One of possible method of characterizing the THM formation is the statistical depiction. Numerous difficulties in statistical application of data and then the interpretation of obtained results explain the fact that there were only a few attempts made in order to define a mathematical model which describes changes of level of THM formation in time. Models defined until now base mainly on data generated during laboratory research in fixed conditions. Only several of them were specified in research conducted in real water distributions systems, however they differ depending on their location [6, 7, 8, 9, 10].

The statistical analysis of data collected in real water supply systems in Krakow and Wroclaw resulted in very good mathematical models [11, 12, 13, 14] which explain dependencies between THM formation and unstable water quality or exploitation conditions in both production and distribution subsystems. Of course obtained models are different. The natural consequence of these studies was to ask searching question: does there exist one universal model that includes condition of THM formation in different water supply systems? The first step to answer this question is common statistical analysis of two water treatment plants for which high determination coefficients were obtained when systems were considered separately.

10.2. CHARACTERISTICS OF WATER TREATMENT PLANTS IN KRAKOW AND WROCLAW

Water supply systems (WSS) in Krakow and Wroclaw came into being in the 13th century and they were successively developed. Nowadays they have diverse structures of water production subsystems as well as distribution subsystems. Average daily water demand of these systems is 120–160.000 m^3.

Krakow WSS has five independent water supply arrangements (WSA). Four of them intake surface water, one – underground water. The most important WSA is Raba water treatment plant (WTP) which works with water from Dobczyce reservoir. The reservoir is an unstable and nonhomogeneous system. Its waters undergo typical qualitative and quantitative changes during the year which result in eutrophication process. There are in the reservoir 120 identified kinds of algae. The domination of green algae diatomaceous phytoplankton is observed. Green algae intensively develop from the spring to the late autumn. Phytoplankton is also represented by blue-green algae Woronichinia nageliana i Microcistis sp. Water bloom effects cause exploitation difficulties in WTP Raba. Moreover, the water pollution hazard by the toxic substances produced by some algae increases. The daily water production of WTP Raba is about 40–60% of daily water demand in Krakow and simultaneously, in accidental situations, it secures required water quantity for all consumers.

Drinking water in Wroclaw city is produced in three independent WSAs: Mokry Dwor, Na Grobli, and Lesnica. Only WTP Mokry Dwor intakes surface water from Olawa River. Water in Olawa is characterized by high turbidity and suspended matter, it contains chemical substances (iron and nitrogen compounds), organic fouling (bacteria, phytoplankton), which changes during the year. WTP Mokry Dwor produces on average 50% of daily water demand in Wroclaw. Actually its possible maximal productivity guarantee almost 100% of daily water requirement in the city.

Water production subsystems in both cities exploit surface water intakes and comparable technological processes (classic coagulation using aluminum compounds, sedimenta-

tion, rapid filtration on sand bed, intermediate ozonization, sorption on activated carbon, and disinfection using chlorine or chlorine dioxide). Above facts justify the selection of WTPs to statistical research. It was also important that in WTP times of contact between chlorine and organic compound are comparable and determined by disinfection process.

10.3. EXPERIMENTAL PROCEDURES AND METHODS

During the normal exploitation process, the Krakow and Wroclaw Water Companies regularly control the parameters of treated water such as chlorine and THM concentrations, UV, chemical oxygen demand, total organic carbon, pH, temperature, and others. These parameters are tested in the water treatment plants as well in different characteristic points of distribution network. Laboratory analyses of water quality made during 2000 – 2006 by Central Water Quality Laboratories in Krakow and Wroclaw formed the sample which was statistically worked out. Although there were many collected data, the final sample was not large one because of numerous missing data.

Water samples at WTP Raba in Krakow and WTP Mokry Dwor in Wroclaw were collected according to the PN-87/C-04632/01-04 norm. The following variables were considered (in parentheses the procedures according to which water samples' quality was specified are given):

— *pH* [dimensionless] (PN-90/C-04540.01, multifunction apparatus inoLab MultiLevel1),
— *T* [°C] – temperature (PN-77/C-04584, mercury thermometer),
— *TD_Cl*2 [mg Cl_2/dm^3] – the total chlorine dose (PN-ISO 7393-2:1997, photometer PC Compact Chlor),
— *R_Cl*2 [mg Cl_2/dm^3] – residual chlorine (PN-ISO 7393-2:1997, photometer PC Compact Chlor),
— *C_Cl*2 [mg Cl_2/dm^3] – the consumption of chlorine (*C_Cl*2=*TD_Cl*2 – *R_Cl*2),
— *UV* [cm^{-1}] – absorbance UV_{254} (PN-84/C-05472, spectrophotometer HACH DR 4000U),
— *COD* [mg O_2/dm^3] – chemical oxygen demand (PB-NJL-W-15, spectrophotometer HACH DR 4000U),
— *TOC* [mg C/dm^3] – total organic carbon (PN-EN-1484-1999, analyzer TOC 5050 Shimadzu),
— *THM* [µg/dm^3] – the concentration of trihalometanes (75-PB-NJL-W-06, gas chromatograph HP-5890GC/5970MSD).

In the research concerning the statistical models of THM concentrations in treated water the basic is the following formula:

$$THM = 0.00309(UV \cdot TOC)^{0,440}(TD\_Cl2)^{0.409} t^{0.205} \cdot \cdot T^{1.06}(pH - 2.6)^{0.715}(Br + 1)^{0.0356} \quad (1)$$

which was obtained in 1987 [6]. In this model predicted concentrations of THMs [µmol/dm^3] are expressed as the function of content of organic compounds (*TOC* [mg C/dm^3] and *UV*–254 nm), total chlorine dose *TD_Cl*2 [mgCl_2/dm^3], contact time of water and chlorine *t* [h], the temperature of water *T* [°C], *pH*, and the concentration of bromide *Br* [mg Br/dm^3] in water. Above model was obtained in laboratory studies and it was based on standard solutions that contained humic maters. This is the reason why this model can not

be directly applied in a real exploitation water supply system; every time it has to be necessarily verified.

Model (1) suggest that for multiple regression in further research the natural logarithms of considered variables should be used. Thus we will look for a linear function f which minimizes the sum of squares of differences between observed and predicted values (by the method of least squares), and the general form of the model is

$$\ln(THM) = f(\ln(pH), \ln(T), \ln(UV), \ln(TOC), \ln(COD), \ln(TD\_Cl2), \ln(R\_Cl2), \ln(C\_Cl2)).$$

Tested models were obtained by standard methods, i.e.: multiple regression, forward selection, and backward elimination [15]. All statistical hypotheses were tested at the level of significance $\alpha = 0.05$.

10.4. RESULTS OF STATISTICAL ANALYSES

We start with basic descriptive statistics (number of cases *N*, mean value, standard deviation, minimal and maximal values) of all variables selected in Krakow and Wroclaw. These statistics are given in Tables 1 and 2.

Table 1

Basic descriptive statistics for WTP Raba in Krakow

Variable	N	Mean	Standard deviation	Minimum	Maximum
TD_Cl2	50	1.15	0.41	0.60	2.41
R_Cl2	44	0.39	0.17	0.06	0.80
C_Cl2	44	0.76	0.45	0.13	2.35
pH	58	7.85	0.16	7.40	8.20
T	43	12.02	6.44	2.70	23.90
COD	58	1.67	0.59	0.70	3.20
TOC	58	2.18	0.69	1.20	5.00
UV	58	0.02	0.01	0.01	0.04
THM	58	6.51	5.10	0.00	22.20

It seems that realizations of variables in most cases are taken from different populations. This presumption is confirmed by box-whiskers plots for variables *TD_Cl*2 and *C_Cl*2 in Fig. 1 (the central tendency in the plot is median, 50% of observations are contained in the box, whiskers stand for inner fences). Such simple conclusion is impossible e.g. for *pH* and THM ANOVA tests indicate that means are different in Krakow and Wroclaw, except variables: *pH*, ln(*pH*), *T*, ln(*T*), and ln(*THM*). The important fact is that the null hypothesis on equality of means is not rejected in the case of ln(*THM*) because it justifies the search for a model of this variable, common for both cities.

The variability of ln(*THM*) at WTP Mokry Dwor is given in [12] by

$$\begin{aligned} \ln(THM) &= 0.858140 + 0.375259\ln(C\_Cl2) + \\ &+ 0.246148\ln(T) + 0.717789\ln(UV/COD) \pm 0.40899 \end{aligned} \tag{2}$$

with $R = 0{,}799$ and $R_a^2 = 0.5969$. The same variable at WTP Raba is modeled in [13] by

$$\ln(THM) = 4.711219 + 0.311819\ln(R\_Cl2) + \\ + 0.616570\ln(T) + 0.917731\ln(UV/TOC) \pm 0.49779 \quad (3)$$

with R = 0.761 and R^2_a = 0.5468. Both models have rather small standard errors of estimation and their adjusted multiple coefficients of determination are greater than 0.5, which means that they explain over 50% of the variability of ln (*THM*). However, no one of these model fits to the data from Krakow and Wroclaw considered commonly. For example, Fig. 2 presents the histogram of differences between observed values of THM and values that were predicted using model (2). For good models such differences should be normally distributed with mean equal to 0. The application of model (3) gives even worse results – there appear a few differences that are less than –300.

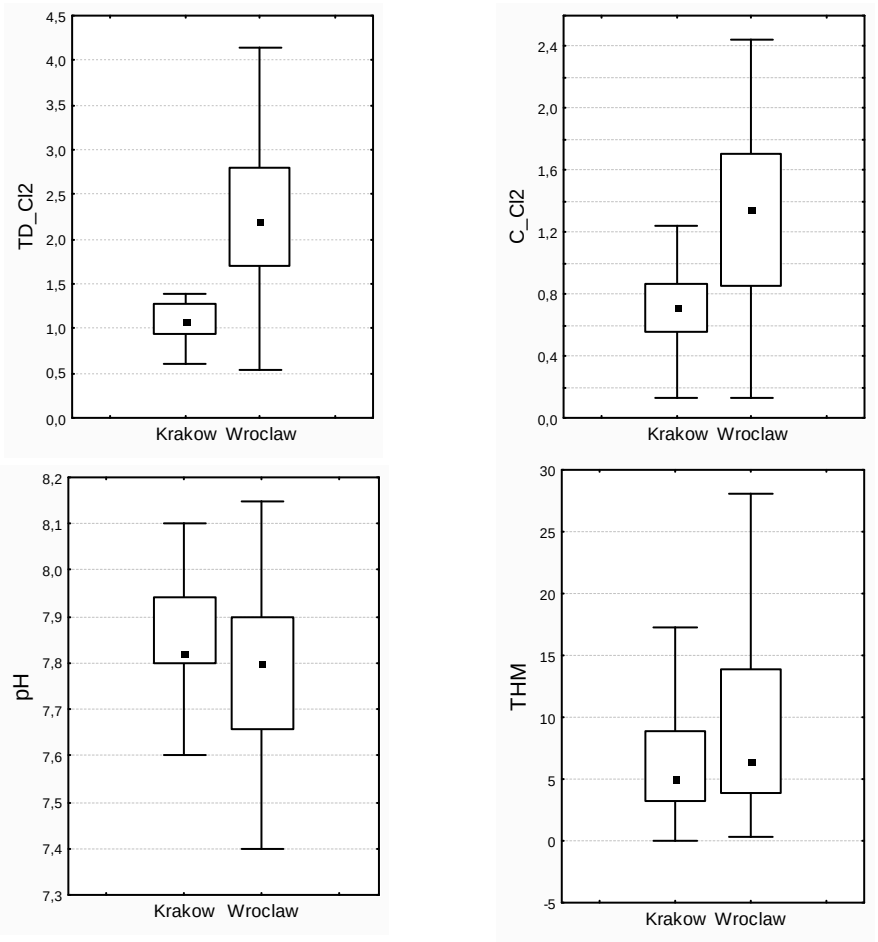

Fig. 1. Box-whiskers plots for comparison of selected variables in WTP Raba (Krakow) and WTP Mokry Dwor (Wroclaw) with median as central tendency

Table 2

Basic descriptive statistics for WTP Mokry Dwor in Wroclaw

Variable	N	Mean	Standard deviation	Minimum	Maximum
TD_Cl2	51	2.21	0.91	0.53	4.13
R_Cl2	51	0.89	0.43	0.11	1.83
C_Cl2	51	1.32	0.68	0.14	3.30
pH	52	7.77	0.18	7.40	8.15
T	52	10.98	8.35	0.50	23.67
COD	52	2.44	0.58	1.31	3.90
TOC	10	3.18	0.92	1.92	4.71
UV	30	3.96	1.79	0.63	7.86
THM	52	11.93	12.70	0.40	58.10

Next, an attempt to build new model, good for the two cities, was made. The standard multiple regression gave result not satisfactory statistically which explained only 30% of the variability of ln(*THM*). The better model was obtained by forward selection with F_{enter} = 4 and F_{remove} = 3:

$$\ln(THM) = 1.49213 + 1.15684\ln(TD\_Cl2) + \\ + 0.35298\ln(T) - 1.11861\ln(TOC) \pm 0.6214. \tag{4}$$

For this model R = 0.755 and R^2_a = 0.5419. The model is acceptable because it predicts greater values of *THM* if greater are values of *TD_Cl*2 or *T* (such situations are observed in practice).

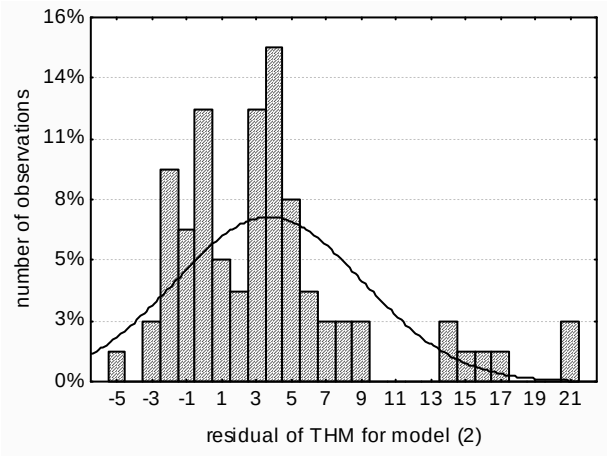

Fig. 2. Histogram of residuals of THM obtained from model (2) applied to all data collected in Wroclaw and Krakow

There were also built models using backward elimination with different sets of independent variables (there were considered also variables ln(*UV/TOC*), ln(*UV/COD*), ln (*UV* · *TOC*) that have appeared in other models). For backward elimination, as previously, values

F_{enter} = 4 and F_{remove} = 3 were accepted. The best model obtained by this method has $R = 0.784$ and $R^2_a = 0.5887$. It is given by formula

$$\ln(THM) = -0.84769 + 4.27359\ln(TD\_Cl2) - \\ -1.98770\ln(C\_Cl2) - 0.35531\ln(UV) \pm 0.5888. \tag{5}$$

Model (5) has standard error of estimation ± 0.5888 which is less than the error for model (4). Simultaneously, (5) explains 58.87% of variability of ln(*THM*) while (4) explains 54.19%.

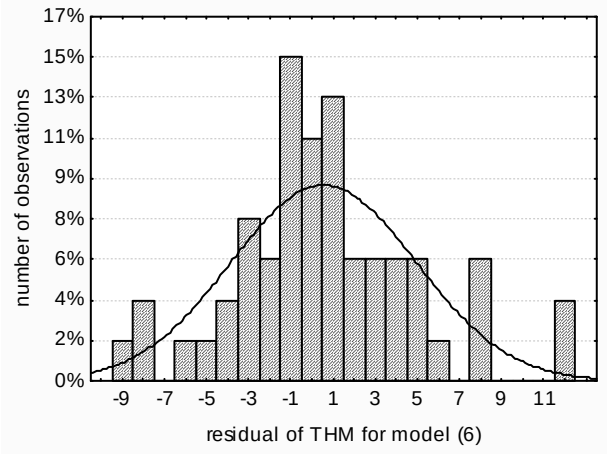

Fig. 3. Residuals of THM obtained from model (6)

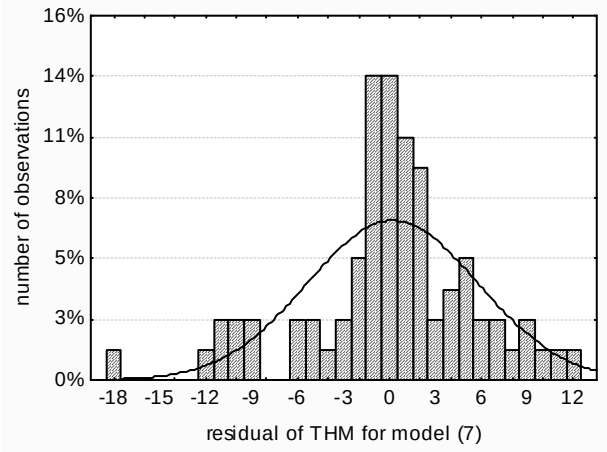

Fig. 4. Residuals of THM obtained from model (7)

Although models (4) and (5) have both small standard estimation errors and small residuals (i.e. differences between observed and predicted values), one can not be sure that the direct estimation of variable *THM* will be good. It follows from properties of logarithms

– small difference between logarithms may produce greater difference between original variables, especially if the original variable is large. The direct formulas for the THM concentration obtained from (4) and (5) are respectively:

$$THM = 4.446557\,(TD\_Cl2)^{1.15684}\,T^{0.35298}\,(TOC)^{-1.11861} \tag{6}$$

and

$$THM = 0.428403(TD\_Cl2)^{4.27359}\,(C\_Cl2)^{-1.98770}\,(UV)^{-0.35531}. \tag{7}$$

In Fig. 3 and 4 the residuals of THM that follow from models (6) and (7) are presented. In general, model (6) looks better than (7) – its residuals lie in shorter interval and they are more concentrated about zero. For example, 65% of residuals from (6) and 59% of residuals from (7) is contained in the interval $\langle -3,3\rangle$.

The next argument follows from Fig. 5 where residuals of THMs obtained from (6) and (7) are grouped with respect to the city. There is only one mild outlier (in Krakow) resulting from (6) whereas there are more mild and extreme outliers (in both cities) resulting from (7).

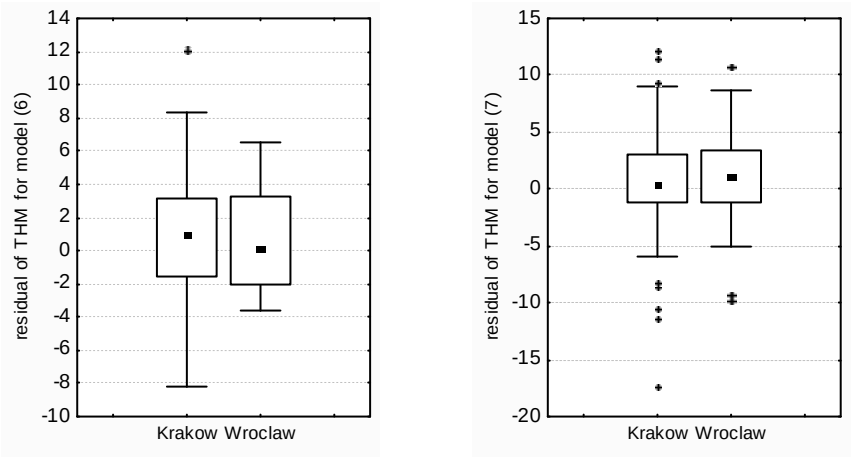

Fig. 5. Comparison of models (6) and (7): box-whiskers plots with respect to median for THM residuals obtained from these models

10.5. CONCLUSIONS

Results presented in this paper have shown that that the application of statistical analysis to build dynamic model of changes of water quality parameters in the production subsystems is an important research method which is also a convenient practicable tool. Such a model makes it possible to predict the range of changes of significant water quality parameters such as trihalomethanes in order to develop rational disinfection. Disinfection should minimize the risk microbiological contamination of water as well as and the level of DBP forming. Control of THMs concentration in treated water by using mathematical model can significantly reduce operating cost of water supply system. Hence mathematical models

will make easier water managements in the optimization and safety aspects.

It should be stressed that both models described above have to be precisely verified on greater samples before they will be applied in real systems. Therefore it is worth to continue statistical research concerning influence of operation parameters of water treatment plants exploitation (such as chlorine dose, temperature, the content of organic compounds, etc.) on THM concentration in chlorinated water. It is possible that one can find one mathematical model which will be good for some similar water supply systems.

References

[1] Council Directive 98/83/EC of 3 November 1998 on the quality of water intended for human consumption, Official Journal of the European Communities no. L 330.5.12.98, 32–54.

[2] WHO Guideline for drinking water quality, 3rd edition, Geneva 2004.

[3] Cantor K. P., Hoover R., Mason T. J., Mc Cabe L. J.: Association of cancer mortality with halometanes in drinking water. Journal of the National Cancer Institute. Vol. 61 (1978), 979–985.

[4] Cantor K. P., Lynch Ch. F., Hildesheim M. E., Dosemeci M., Lubin J., Alavanja M., Craun G.: Drinking water source and chlorination by products in Iowa. III. Risk of brain cancer. American Journal of Epidemiology. Vol. 150, No. 6 552–560, 1999.

[5] Kuo H. W., Tiao M. M.,Wu T. N., Yang C. Y.: Does calcium in drinking water modify the association between trihalomethanes and risk of death from colon cancer. Journal of Toxicology and Environmental Heath Part A. Vol. 73, No. 10, 657–668, 2010.

[6] Amy G. L., Chadik P. A., Chowdhury Z. K.: Developing models for predicting trihalomethane formation – potential and kinetics. Research & Technology 7, 89–97, 1987.

[7] Baribeau H., Prevost M., Desjardins R., Lafrance P.: Changes in chlorine and DOX concentration in distribution system. Journal AWWA. Vol. 93, No. 12, 102–114, 2001.

[8] Amy G. et al.: Empirical based models for predicting chlorination and coronation by-products: halo acetic acids, chloral hydrate and bromated. EPA report CX 819579, 1998.

[9] Gallard H., Von-Gunten U.: Chlorination of natural organic matter: kinetics of chlorination and of THM formation. Water Research, Vol. 36, 65–74, 2002.

[10] Elshorbagy W. E. et al.: Simulation of THM species in water distribution systems. Water Research, Vol. 34, 3431–3439, 2000.

[11] Zimoch I., Łobos E.: Analysis of Spatial Water Quality Changes in Water Pipe Network as a Function that Describes THM Formation. Polish Journal of Environmental Studies, Vol.17, No. 3A, 627–631, 2008.

[12] Zimoch I., Łobos E.: Szacowanie poziomu stężenia trihalometanów w wodzie jako parametr operacyjny eksploatacji zakładu uzdatniania wody. INSTAL, No. 6, 50–53, 2008.

[13] Zimoch I., Łobos E.: Statistical Approach to the THMs Formation Process in Water Treatment Arrangements, Białystok (2011) – in print.

[14] Zimoch I.: Opracowanie modelu niezawodności funkcjonowania systemu zaopatrzenia w wodę (SZW) w aspekcie wtórnego zanieczyszczenia wody w sieci wodociągowej. Final realization report of the research project PB no. 5 T07E 044 25, Gliwice 2007.

[15] Stanisz A.: Przystępny kurs statystyki z zastosowaniem STATISTICA PL na przykładach z medycyny. Vol. II, StatSoft, Krakow, 59–166, 271–306 2007.

Acknowledgements

Scientific work was financed from the measures of National Center of Research and Development as a development research project No N R14 0006 10: “Development of comprehensive methodology for the assessment of the reliability and safety of water supply to consumers” in the years 2010–2013.

11 Fire Fighting Standards in Rural Areas in Croatia

Davor Malus, Drazen Vouk (University of Zagreb), Dejan Kovacevic (IGH – Zagreb)

11.1. INTRODUCTION

According to the data of 2006, water supply covers, on average, 80 percent of the Republic of Croatia [1]. The supply is best in large urban centers, and the coverage is lower in rural areas distant from towns and larger supply systems. Unit costs of construction, operation and maintenance in rural areas are very high, because of the long water supply network and high power costs. This means that providing of water supply for the remaining potential users is very costly and comprises large portions of planned investments in county long-term plans.

In the Republic of Croatia, rural settlements are numerous (more than 40 percent of the population live in settlements of less than 2000 inhabitants), and the economic potential of their population is limited. Respecting the principle of recovery of operating costs from final users, the price of water supply is highly important to final users. Regardless of the source of funds – direct investments by the local community, government investments, EU (pre)accession funds or various combinations of sources, the available funds must be directed into projects involving as the largest possible number of users.

Fire fighting in urban settlements in Croatia is regulated by the Regulations on Hydrant Networks (hereinafter: the Regulations). Implementation of the Regulations is the responsibility of the Ministry of Internal Affairs, through its department.

11.2. TECHNICAL CONDITIONS FOR HYDRANT NETWORK

The minimum water flow that should be provided for fire fighting is determined according to specific fire load in MJ/m^2 and the area of the building. For residential buildings, fire fighting should be done with 10 l/s, simultaneously with two hydrants of 5 l/s each, for minimum two hours, which implies a reserved volume in the storage of at least 72 m^3. At the same time, it is necessary to provide minimum pressure of 2.5 bar on each hydrant, and the supply pipelines must be sized to maximum hourly consumption plus firefighting requirements.

In densely populated areas the maximum spacing between hydrants is 150 m, and in settlements with individual freestanding buildings the spacing may be up to 300 m.

In designing of each public water supply system special technical conditions regarding fire fighting prescribed by the Ministry must be respected, and formally it is impossi-

ble to obtain the construction permit for the project that does not apply all provisions of the Regulations.

11.3. THE PROBLEM

In small settlements, distant from larger centers, the criterion for sizing of supply pipelines is the discharge prescribed by the Regulations, and not the discharge of maximum hourly consumption, and consequently the minimum pipe diameter is 110 mm. At the least favorably positioned hydrant, the pressure must be 2.5 bars, which often implies installing of booster stations. The required water quantity must be provided in the storage, and therefore the minimum storage capacity is 100 m^3. In spite of the permitted spacing of 300 m between hydrants, their number is rather high due to great total length of supply pipelines.

Looking from the standpoint of potential health hazards, the problem is staleness of water in the pipes and discontinued bactericide action of the disinfectant, usually chlorine-based. Low flow velocities favor sedimentation and scaling of pipes. Stale water has a bad taste, and its temperature may be higher if pipes have not been buried deep enough.

Meeting of the conditions from the Regulation considerably affects the costs of construction, operation and maintenance of small water supply systems and, as shown above, sanitary and operating conditions are not optimum either.

Although the professional circles have frequently pointed out the unfavorable influence of the Regulations on small rural water supply systems, such warnings were never supported by sound evidence showing the real extent of the influence of the Regulations on increasing of water supply costs.

In the Water Research Department of the Faculty of Civil Engineering, University of Zagreb, four students with tutorship of their professors, in the framework of preparing their graduation theses worked out the water supply projects for actual rural settlements in the continental part of the Republic of Croatia [2, 3, 4, 5]. The designs were made in two alternatives, one with full application of the Regulations, and the other with selective application.

In the alternative with selective application of the Regulations, in all settlements or parts of settlements where social and economic facilities existed, the Regulations were applied fully, and in villages and hamlets where there were no such facilities, only population requirements for water were met. In designing the minimum nominal pipe diameter of 50 mm was used.

The studied areas were the territories of the municipality Vojnic (20 settlements), municipality Hum na Sutli (18 settlements) and high water supply zone of the municipality Desinic (11 settlements).

In short lines, the results may be described as follows: in projects with selective application of the Regulations, the savings in construction costs were in the range of 40 to 50 percent. Operation and maintenance costs have not been compared, but undoubtedly the comparison would show further savings.

This fact should be sufficient to initiate serious consideration of the possibility of modifying and amending the Regulations.

11.3.1. Suggestion

With regard to the above, the authors suggest reconsidering the contents of the Regulations and, for the purpose of cost reduction, and allowing of solving of water supply issues without meeting of the criteria from the Regulations in all locations where this is justified. This does not mean that fire fighting is neglected; it is only delayed, solved separately or in an alternative way. This would considerably shorten the period of achieving the planned level of water supply and relieve the pressure on increasing of the price of water supply.

11.3.2. Alternative Methods of Fire Fighting

Regardless of the high costs of fire protection, negotiation between the local community and the Ministry in order to find a compromise solution is not possible. Solving of the problem by compromise or by agreement is practiced in some countries (in cases when it is obvious that meeting of the prescribed criteria regarding water quantity, pressure and discharge is a large financial burden on the utility running or owning the water supply system [6, 7]. Fire protection may be delayed or organized beside the public water supply system.

The fire statistics in Croatia, available to the public refers to the total number of fires in the counties and in the country as a whole, to material damages and number of causalities. It is impossible to get information about rural settlements, separately for settlements that have got or have not got public water supply and hydrant network. In the total damages, the largest part consists of summer forest fires on the Adriatic coast. Such fires usually start outside the settlements and can rarely be extinguished using water from the hydrant network, but fire trucks, helicopters and specialized planes are used instead.

In rural settlements in Croatia the prevailing type is the freestanding family house of non-combustible materials (concrete, bricks, stone), with roof truss of wood. The spacing between buildings is such that there is little probability of fire transfer from one house to another. In the continental part of the country there is still a considerable number of farm buildings (granaries, stables, barns) built mostly of wood. When fire occurs on such buildings, chances for successful extinguishing are minimum, in particular if that involves waiting for professional or volunteer firemen.

In Croatia there is a well-developed network of professional and volunteer fire brigades. Such units are equipped with technical means, the most important being self-propelled fire engines capable of autonomous operation, because they have the storage capacity and pumps to provide the necessary pressure. They can extinguish minor fires without the need for additional water.

The basic problem in fire fighting with water is providing of the required quantity and pressure. Water may be provided by construction of water storages in the settlement, to which the fire engines will be connected. There is the possibility of procuring ready-made tanks of plastic, steel sheet, or construction of storages of reinforced concrete or earth ponds [8]. The storages may be filled by rainfall or from the water supply network. Fire trucks and other fire engines are equipped with pumps to achieve the pressure. Such pumps may be portable or installed at the water storage.

Fires may be efficiently fought using handy fire extinguishing household devices (fire extinguishers, fire detection sensors), because almost any fire may be extinguished at the beginning by early intervention. It is a pity that the law does not prescribe owning of such devices in households.

11.3.3. Measures for Reduction of Fire Risk

The fire risk is not increased by construction of water supply that does not meet the criteria from the Regulations. It may be only reduced, in spite of inadequate insufficient pressures, discharges, quantities and pressures, but such water supply may fully meet alternative methods of fire fighting by providing sufficient water quantities for all alternatives where water is stored in various ways.

The fact is that the population, on average, is inadequately educated about actions and measures to reduce the fire risk, as well as about prevention of fire propagation once it occurs. Very few households own fire detection devices, as well as fire extinguishers for household use. A short education and equipping of each household with a portable fire extinguisher would do more to reduce the damage than installation of water supply with hydrants. In this respect the government and the local communities have not done anything. The only initiative worth mentioning is that by the government firm managing the Croatian forests warning the population and tourists not to make fires and to handle potential fires sources with care.

11.4. CONCLUSION

With regard to exceptionally high unit prices of construction, operation and maintenance of rural public water supply systems, which are increased by 40 to 50 percent by the application of the Regulations, it seems logical that the Regulations should be modified, allowing solving of water supply issues separately from fire protection, for rural settlements without social and industrial facilities. This would make it possible to reach the planned level of water supply in a comparatively short time, and relieve the budgets of local communities.

Fire protection could be solved in one of many unconventional ways, for which there already exist real conditions.

The request for modification of the Regulations should be supported by the analysis of fire risk and fire damages based on statistics of fire occurrence and damages in rural settlements with and without hydrant networks.

In this context, it is necessary to separate the area along the Adriatic coast where there is fire risk in forests and macchia around urban centers.

In general, it is necessary to do more in education of the population in prevention of fires and fighting at the moment of outbreak using fire detectors and portable fire extinguishers.

References

[1] Hrvatske vode: Strategija upravljanja vodama. Hrvatske vode, Zagreb 2009.
[2] Franjić M.: Istraživanje zakonitosti vodoopskrbe na vodoopskrbnom sustavu općine Hum na Sutli. Diplomski rad, Sveučilište u Zagrebu. Građevinski fakultet 2010.
[3] Grljak A.: Idejni projekt opskrbe vodom visoke zone općine Desinić, Diplomski rad, Sveučilište u Zagrebu, Građevinski fakultet 2010.
[4] Kvartuč I.: Istraživanje zakonitosti troškova vodoopskrbe na vodo-opskrbnom sustavu općine Hum na Sutli, Diplomski rad, Sveučilište u Zagrebu, Građevinski fakultet 2011.

[5] Mudrić H.: Gubici vode na vodoopskrbnim sustavima. Diplomski rad, Sveučilište u Zagrebu, Građevinski fakultet 2010.
[6] AWWA: Manual M31-Distribution System Requirements for Fire Protection. The American Water Works Association 1998.
[7] LGA & Water UK: National guidance document on the provision of water for fire fighting, Local Government Association and Water UK 2002.
[8] NFPA 1142: Standard on Water Supplies for Suburban and Rural Fire Fighting. National Fire Protection Association 1999.

12 Development of Models for Nitrogen-Removal Processes in Subsurface Flow Constructed Wetlands

Marcin J. Marcinkowski, Hanna Obarska-Pempkowiak, Magdalena Gajewska (Gdańsk University of Technology, Faculty of Civil and Environmental Engineering)

12.1. INTRODUCTION

Wastewater treatment systems based on constructed wetlands (CW) technology are nowadays commonly used not only for treatment of municipal wastewater, but also for stormwater treatment systems as well as industrial wastewater treatment (e.g. landfill leachate). CWs are complex systems designed and build to create best treatment conditions found in natural environment. Using physical, chemical and biological processes occurring in natural wetland ecosystems – but in a controlled environment created in CWs – high rate removal processes of organic matter (including hardly degradable organic matter such as PAHs and pesticides) and nitrogen compounds can be achieved. These processes are dynamically taking place next to each other, therefore influencing the main process of wastewater treatment.

The growing potential of this technology, together with strict effluent standards, demands the necessity for optimization of CWs design and operation. Most commonly used approach for design of CWs is based on a minimum necessary area per person equivalent [2] or simple models, using first-order kinetic equations [9]. However, approach to understanding the process of wastewater purification is often considered as "black box" due to complexity of the processes active in parallel and mutually influencing each other in engineered systems such as CWs [19]. This paper summarizes recent progress in modelling approach of subsurface flow constructed wetlands (SSF CWs), focusing on nitrogen removal processes.

12.2. FIRST-ORDER MODELS

In temperate conditions of Europe and USA the CWs with subsurface flow are used more frequently for wastewater treatment. In order to prevent clogging of porous filter media (sand and gravel), low content of total suspended solids (TSS) is required. Therefore, pre-treated wastewater with low TSS concentration is mostly suitable for subsurface flow CWs. Subsurface constructed wetlands can work as a horizontal flow (HSSF) or vertical

flow (VSSF) systems depending on water flow direction in the filter media [18]. According to many reports[13, 19, 24] there are only few models able to describe treatment processes in SS CWs. Most of the available models are applicable for SS HF beds and are based on simple first-order decay models or define the CWs as a "black box" (Fig. 1). Several individual wetland processes are first-order, such as mass transport, volatilization, sedimentation and sorption.

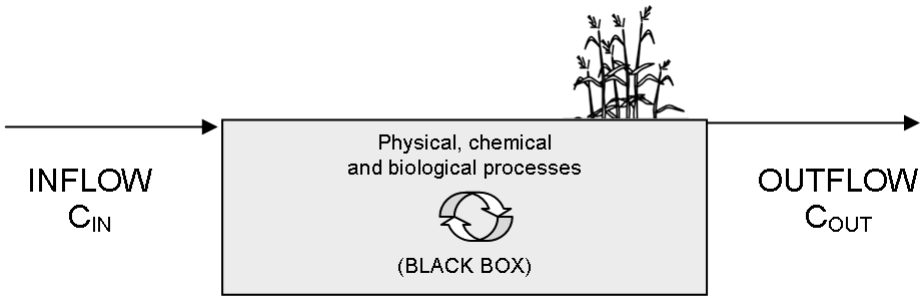

Fig. 1. Schematic illustration of a wetland "black box" processes
(adopted in part from [26])

First-order models are commonly used for the design of treatment CWs using hydraulic retention time and decomposition constant and follow either Eq. (1) or Eq. (2):

$$\frac{C_{OUT}}{C_{IN}} = e^{\frac{k_A}{q}} \tag{1}$$

where k_A is the real decomposition constant [$m \cdot d^{-1}$]

$$\frac{C_{out}}{C_{in}} = e^{-k_V t} \tag{2}$$

where: t is hydraulic retention time (HRT) in days,
k_v is the volumetric decomposition constant [$m \cdot d^{-1}$] [9].

This approach can be used to forecast mostly all major pollutants such as organic matter, suspended solids and nitrogen [10, 11, 25]. While these models were reported insufficient due to variable input flow and concentrations, they are still a useful "tool" in design of pollutants removal. The origin of these simple models is based on fundamental laws governing water flow and solute transport (e.g. advection-dispersion equation). The governing equations are simplified and reduced to simple formulas by defining correct boundary conditions and system geometrical performance. Such models have an evident benefit that no advanced mathematical handling is required to solve the equations. The incapability of the traditional first order models, for capturing the variety encountered in wetland systems [16], could be attributed to their over simplified postulations such as: the concentration of reactant is limited (i.e. pollutant) and wastewater is assumed to have plug flow behaviour in these systems. Basic assumptions of first order models often do not fit the complex conditions of SSF CWs. Classic denitrification and its pathway, with complicated dependency between denitrifying microorganisms, availability of substrate (NO_3–N) and organic carbon, represents the major nitrogen removing mechanism in wetland systems. However, the sig-

nificant interdependency between limiting reactants (i.e. nitrates and organic carbon) and the catalyst (i.e. biomass) shows that presence of excess denitrifying biomass may not be the established condition in these engineered systems for nitrogen removal, especially at limiting conditions [20, 21].

Additionally, the hypothesis of idealized plug flow condition may not be suitable for VSSF. Such systems are usually fed with batch load of wastewater (pumped inflow), which is probably divided over the filter media (in unsaturated conditions) during downward flow. Water travels in wetlands through "fast" and "slow" tracks due to vegetation, topography and other environmental factors.

In order to overcome the insufficiency of first-order models, some mechanistic models were developed [14]. Effective performance of these models above all depends on two crucial factors linked together: kinetics of biological degradation and hydrodynamic behaviour. These two factors are believed to play the major role in pollutant removal processes in CWs. It is important to note several authors who point out that assumptions connected with flow can be in some way simplified to one-dimensional behaviour, and the effects of dispersion, heterogeneity and so called "dead zones" are placed together in the hydrodynamic dispersivity term. Such an approach may produce a significant computation error of e.g. the effective residence time, and therefore have a remarkable impact on estimation of the degradation efficiency [9]. Even though first-order models look simple, they correspond to the highest level of complexity that can generally be calibrated with wetland data and provide an adequate approximation of performance for an extensive range of pollutants in CWs.

12.3. PROCESS BASED MODELS

Models incorporating Monod kinetics [17], considering bacterial growth as a method for the study of bacterial physiology and biochemistry, could be another choice for developing a more reasonable wetland predictive model by a well known expression (Eq. (2)):

$$r = k_{0,v} V \frac{C}{K_{HSC} + C} \tag{3}$$

where r [mg $\cdot$ d^{-1}] is the rate of biological degradation and K_{HSC} [mg $\cdot$ m^{-3}] is the so called half-saturation constant, C is pollutant concentration [mg$\cdot$m^{-3}], $k_{0,v}$ is zero-order volumetric rate constant [mg$\cdot$m^{-3} $\cdot$ d^{-1}]. When $C << K_{HSC}$, kinetics is first-order and as concentration C increases, the kinetics become saturated. Process rates in these models are based on the biochemical elimination and transformation processes described by Monod-type expressions. All process rates and diffusion coefficients are temperature dependant. Some of the processes considered are hydrolysis, mineralization of organic matter, nitrification (modelled as a two-step process), denitrification, and a lysis process for the microorganisms (decay and loss processes).

Example of such a model is the multi-component reactive transport module CW2D [12, 14] incorporated into HYDRUS 2D/3D software (a finite element model to simulate movement of water and multiple solutes in variably saturated media). CW2D takes for assumption a constant concentration of biomass and other compounds in each finite element. Also, the thickness of the biofilm is not considered. The mathematical formulation of CW2D is based on the Activated Sludge Models (ASMs) by IWA [7]. In comparison to

ASMs, the CW2D module considers 12 components and 9 processes. The components are: dissolved oxygen, organic matter (inert, readily- and slowly-biodegradable), ammonium, nitrite, nitrate, and nitrogen gas, inorganic phosphorus, and heterotrophic plus two species of autotrophic microorganisms. Organic nitrogen and organic phosphorus are modelled as nutrient content of the organic matter (percentage of COD).

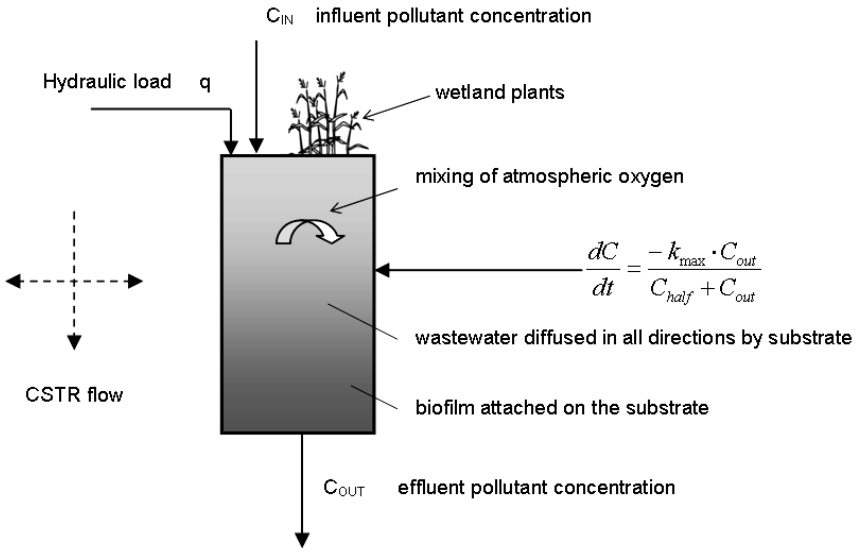

Fig. 2. Modelling approach with Monod kinetics for predicting pollutant dynamics in VSSF bed (adopted in part from [21])

Monod models can be described as the expression of the transition from first- to zero-order biological degradation kinetics. Monod kinetics shows that the loading rate and the zero-order degradation rate constant are essential parameters for efficient wetland design and removal of organic carbon in subsurface flow CWs. While Monod type model can better describe the variability of the data than first-order model, it cannot be evaluated without combination of two different hydrodynamic patterns: continuously stirred tank reactor (CSTR) and plug flow pattern, respectively in VSSF and HSSF CWs [21]. Focusing mainly on the hydraulic behaviour of CWs one must notice that there is a need for a comparative assessment between first order and Monod kinetics combined with two different hydrodynamic patterns: CSTR for VF wetlands and plug flow for HF wetlands. Recent investigations show that such a study should have a double objective: exploration of precision of the Monod approach for modelling the dynamics of nitrogen and organics removal in VSSF and HF wetland systems, and observation of performance variation in the two systems based on kinetic modelling [23].

Process based model category has only some numerical models able to simulate CWs [3]. Most of these models can simulate horizontal subsurface flow constructed wetlands (HSSF CWs), but only few can simulate vertical subsurface flow constructed wetlands (VSSF CWs). A short summary of the existing numerical modelling software used for CWs is presented in Table 1.

Model developed by Giraldi et al. (2010) [6] called FITOVERT can simulate the hydraulic pathways of HSSF in both saturated and unsaturated conditions, with organic matter

and nitrogen species biodegradation following ASM 1 [7]. Additionally, FITOVERT can also describe the clogging process as an effect of pore size reduction on the hydraulic conductivity of the simulated system (due to bacterial activity and particulate components accumulation).

Also, the CW2D implementation in HSSF CWs modeling is a good estimation of biochemical transformations, where flow and single solute transport was described using HYDRUS-2D software. The main disadvantage of CW2D until now is that only dissolved substances are considered and it is crucial for future development of the realistic model to consider particulate wastewater constituents [14]. Authors also suggest that other processes including the influence of plants, adsorption and desorption processes and physical reaeration must be considered for the formulation of a full model for CWs.

According to modeling tool presented by Brovelli et al. (2009) [4] able to simulate the clogging process (in 1, 2 and 3D), it is possible to forecast the effect of biomass growth on the hydraulic properties of saturated porous media, i.e. biological clogging of filter media. It is based on a numerical model PHWAT (evolved from numerical model called PHT3D). The PHWAT model was developed at macro-scale, and includes the effect of flow-induced shear stress on biofilms. Due to nature of this model for reactive transport in variable-density saturated flow, it has large flexibility because of e.g. multiple components inducing pore clogging. The simulation results also demonstrate that the rate and pattern of biological clogging progress are sensitive to the initial biomass distribution in CW system.

Table 1

Summary of the existing modeling software

Modelling software name	Origin
CW2D (Hydrus)	PC Progress, Czech Republic
FITOVERT	University of Pisa, Italy
PHWAT	Ecole Polytechnique Federale De Lausanne (EPFL), Switzerland
CWM1	University of Natural Resources and Applied Life Sciences, Vienna, Austria
2D Mechanistic Model	Technical University of Catalonia, Spain
STELLA	Isee systems inc. (former High Performance Systems), USA

12.4. ALTERNATIVE KINETIC MODELS FOR VF WETLANDS

The study by Saeed et al. (2011) [21] presented a combination of models to connect the inlet and outlet concentrations of nitrogen (NH_4–N, NO_3–N), BOD_5 and COD across a VSSF bed. These models have been build up on combination of first order, Monod and multiple Monod kinetics with continuously stirred tank reactor (CSTR) flow behaviour.
First order kinetics in a wetland "reactor" is expressed as Eq. (4):

$$\frac{dC}{dt} = -k_v Cout \tag{4}$$

where: C_{out} is outlet pollutant concentration [mg · L^{-1}],
k_v is volumetric rate constant [d^{-1}].

CSTR flow scheme in the reactor can be expressed as Eq. (5):

$$\frac{dC}{dt} + \frac{1}{\tau} C_{in} = \frac{1}{\tau} C_{out} \tag{5}$$

where C_{in} is inlet pollutant concentration [mg · L^{-1}], τ is hydraulic retention time [days]. Combination of Eqs. 4 and 5 gives a simplified first order kinetics combined with CSTR flow pattern in terms of area rate constant K_1 [m · d^{-1}].

Correlation of influent and effluent nitrogen and organics values in the VF CWs is expressed in Eq. (6):

$$K_1 = \frac{q(C_{in} - C_{out})}{C_{out}} \tag{6}$$

where q is hydraulic loading rate (m · d^{-1}).
Monod kinetics which includes parameters such as substrate concentration, half saturation constant of limiting substrate and maximum volumetric pollutant removal rates can be expressed as Eq. (7):

$$\frac{dC}{dt} = -K_{\max} \frac{C_{out}}{C_{half} + C_{out}} \tag{7}$$

here C_{out} is substrate concentration, C_{half} is half saturation constant of limiting substrate (mg · L^{-1}), and $K_{\max}$ is maximum volumetric pollutant removal rate (g · m^{-3} · d^{-1}). Including CSTR flow pattern (Eq. (5)) with Monod kinetics (Eq. (7)) gives Eq. (8), which links inlet and outlet pollutant concentrations:

$$\frac{C_{in} - C_{out}}{\tau} = K_{\max} \frac{C_{out}}{C_{half} - C_{out}} \tag{8}$$

The above equation (different notation of Eq. (2)) is expressed in terms of hydraulic retention time τ (units in days), and $K_{\max}$ represents maximum pollutant mass removal per m^3 of wetland volume per day. The relation between HRT, area (A, m^2), depth (h, m), porosity of packed filter media (ϵ) and inlet discharge (Q, m^3 ·d^{-1}) can be expressed in Eq. (9):

$$\tau = \frac{Ah\varepsilon}{Q} \tag{9}$$

Combination of volumetric pollutant removal rates ($K_{\max}$) with h and ϵ results areal maximum pollutant removal rates (K_2, g · m^{-2} ·d^{-1}), expressed by Eq. (10) correlating inlet and outlet pollutant concentrations [21].

$$K_2 = \frac{q(C_{in} - C_{out})(C_{half} + C_{out})}{C_{out}} \tag{10}$$

Prediction of nitrogen and organics degradation in VSSF wetland systems can be done using Eq. (10). First step of NH_4–N transformation during nitrification (i.e. from NH_4–N to NO_2–N) should use half saturation constant for *Nitrosomonas* (C_{half}) as half saturation con-

stant value in Eq. (10) for nitrification. Following this pathway, saturation constants in the Monod kinetics for denitrification, heterotrophic biodegradable organics removal (BOD_5), and COD can be taken from existing studies found in literature [7, 15].

Multiple Monod kinetics assumes that more than one substrate is limiting the rate of pollutants degradation. The multiple Monod kinetics were previously expressed by several authors [8] and can be expressed in the following equation:

$$\frac{dC}{dt} = -K \frac{C_{out1}}{C_{half1} + C_{out1}} \frac{C_{out2}}{C_{half2} + C_{out2}} \tag{11}$$

C_{out1} and C_{out2} in the Eq. (11) represent the outlet concentrations [mg · L^{-1}] of two substrates that may limit the biodegradation rate of target pollutant. Half saturation constants for these substrates are expressed as C_{half1} and C_{half2} [mg·L^{-1}]. Combining CSTR flow pattern equation (Eq. (5)) and multiple Monod kinetics equation (Eq. (11)) links inlet and outlet pollutant concentration, and K_3 value (maximum areal pollutant removal rate K_3, g · m^{-2} · d^{-1}) in equation presented below (Eq. (12)):

$$K_3 = \frac{q(C_{in} - C_{out})(C_{out1} + C_{half1})(C_{out2} + C_{half2})}{C_{out1} C_{out2}} \tag{12}$$

Following the above scheme of Monod kinetics, one can setup equations for e.g. nitrification (NH_4–N removal) or denitrification (NO_3–N removal). When Eq. (12) is used to model nitrification or denitrification rate in VSSF CWs the limiting factors could be ammonium concentration and dissolved oxygen value, or nitrate availability and presence of anoxic and aerobic conditions, respectively. In addition, denitrification can have third limiting factor which is availability of organic carbon (e.g. indicated by COD presence).

12.5. DISCUSSION

The presented efforts of CWs modelling were divided in either simple first-order or process-based models. This paper aimed at showing complexity of processes taking place in constructed wetlands treatment systems and approach to simulate effluent concentrations.
Most of the literature focuses on modelling of CW systems using simplified equations. Fundamental statements of such models are based on water flow which is hypothetically homogenous and one dimensional, often simplified to plug flow criteria. Some hydrodynamic analysis of Giraldi et al. (2009) [5] found that mono-dimensional plug flow with dispersion can be accurate to simulate both saturated and unsaturated conditions in VSSF CWs. It was also pointed out that dependency between dispersivity and saturation in the flow model is needed for a successful modelling of VSSF CWs. The first order degradation model was shown to be practical in describing removal of organic matter in HSSF CWs [19]. Applications of the first order models found in literature are also studied, with close focus on temperature dependency of the model parameters in COD and ammonium nitrogen removal (e.g. [24]).

Rousseau [19] and Langergraber [13] used mathematical structure of the ASMs presented in matrix notation to describe organic matter and nitrogen transformation processes in mechanistic models of commercially available modelling software. Described models

use both saturated and unsaturated conditions to present these processes during flow through porous media.

Compared to first order kinetics, process based models (following Monod kinetics) increase understanding occurring in the "black box" CWs. It shows clearly the need for a precise biochemical model simulating both saturated and unsaturated conditions of VSSF CWs. However, since process based models are highly sensitive and dependant on temperature (mostly for nitrogen transformations) a temperature dependency for half-saturation constant must be introduced.

This review shows clearly that CW modelling should focus on the individual processes occurring in the system to give better information to the designers on efficient design of CW systems. Until now, research carried out by several authors demonstrates that a part of organic nitrogen is trapped in the CW filter bed and does not undergo rapid transformation processes. The concentration of this part of nitrogen is considered to be the background concentration (C^*) and using Eq. (2) it can be presented as following (Eq. (13)):

$$\frac{C_{out} - C^*}{C_{in} - C^*} = e^{-k_V t} \tag{13}$$

Kadlec [10] refers also to apparent (C_a^*) and true background (C_b^*) concentration for initial presence of pollutants in the wetland systems. It was noted that after first pass of water flow through CW a "short-circuit" effect takes place influencing the treatment process. Reaction constants (k and C^*) are derived from the wetland characteristics and operating conditions such as dispersion coefficient, free water depth, precipitation and evapotranspiration. The background concentration C^* in this model is explained by processes, mainly autochthonous production and/or sediment release [19]. Literature values of C^* are in the range between 10 and 20 [mg N $\cdot$ L^{-1}]. Shepherd et al. (2001) [22] presented a time dependent model that allows a constant decrease in pollutant concentration. Compared with first-order model, the time-dependant retardation model turned out to be more appropriate for CWs design because it has more reliable parameters for pollutant concentration across the CW filter bed.

Short-circuiting effect as a common phenomenon in SSF CW systems makes the so-called reaction rate "constants" dependable on influent concentrations, hydraulic retention time and water depth in the CW, thus making difficult to set universal rate constants. Taking into consideration the above statements and the complex network of interactions and processes in a constructed wetland it builds a list of difficulties for designers to choose a proper CW model.

References

[1] Akratos C. S., Papaspyros J. N. E., Tsihrintzis V. A.: Total Nitrogen and Ammonia Removal Prediction in Horizontal Subsurface Flow Constructed Wetlands: Use of Artificial Neural Networks and Development of a Design Equation, Biores. Technol. 100: 586–596, 2009.

[2] Brix H., Johansen N. H.: Guidelines for Vertical Flow Constructed Wetland System up to 30PE. No. 52. Denmark, Copenhagen 2004.

[3] Brovelli A., Baechler S., Rossi L., Langergraber G., Barry D. A.: Coupled flow and hydrogeochemical modelling for design and optimization of horizontal flow constructed wetlands. In: Mander Ü., Kóiv, M., Vohla C., editors. 2nd International Symposium on "Wetland pollutant dynamics and control WETPOL 2007" – extended abstracts, Tartu, Estonia, vol. II, p. 393–395, 2007.

[4] Brovelli A., Malaguerra F., Barry D. A.: Bioclogging in porous media: model development and sensitivity to initial conditions. Environmental Modelling and Software 24(5), 611–626, 2009.
[5] Giraldi D., de'Michieli Vitturi M., Zaramella M., Marion A., Iannelli R. : Hydrodynamics of vertical subsurface flow constructed wetlands: tracer tests with rhodamine WT and numerical modelling. Ecological Engineering 35, 265–273, 2009.
[6] Giraldi D., de'Michieli Vitturi M., Iannelli R. : FITOVERT: a dynamic numerical model of subsurface vertical flow constructed wetlands. Environmental Modelling and Software 25, 633–640, 2010.
[7] Henze M., Gujer W., Mino T., von Loosdrecht M. C. M.: Activated sludge models ASM1, ASM2, ASM2D, and ASM3. IWA Scientific and technical report no. 9, IWA Publishing, London, UK, 2000.
[8] Henze M., Harremoes P., Jansen J. L. C., Arvin E.: Wastewater Treatment: biological and chemical processes. Berlin, Heidelberg, New York: Springer-Verlag 1995.
[9] Kadlec R. H., Knight, R.L., 1996. Treatment Wetlands. CRC Press, Boca Raton, FL, USA.
[10] Kadlec R. H., 2000. The inadequancy of first-order treatment kinetic models. Ecological Engineering 20(1), 1–16.
[11] Knight R. L., Payne Jr., V. W. E., Borer R. E., Clark Jr., R. A., Pries J. H.: Constructed wetland for livestock wastewater 2000.
[12] Langergraber G.: Development of simulation tool for subsurface flow constructed wetlands. Wiener Mitteilungen 169, p. 207, Vienna 2001.
[13] Lagergraber G.: Modelling of processes in subsurface flow constructed wetlands – A review. Vadoze Zone Journal 7(2), 830–842, 2008.
[14] Langergraber G., Šimůnek J.: Modeling variably saturated water flow and multi component reactive transport in constructed wetlands. Vadoze Zone J 4(4), 924–938, 2005.
[15] Metcalf and Eddy: Wastewater Engineering, Treatment and Reuse. 4th Edition. McGraw – Hill Publishing, USA 2003.
[16] Mitchell C., McNevin D.: Alternative analysis of BOD removal in subsurface flow constructed wetlands employing Monod Kinetics. Water Research 35(5), 1295–1303, 2001.
[17] Monod J.: The growth of bacterial cultures. Annual Rev. Microbiology 3, 371–394, 1949.
[18] Obarska-Pempkowiak H., Gajewska M., Wojciechowska E.: Hydrofitowe oczyszczanie wód i ścieków. Warszawa: Wydawnictwo Naukowe PWN 2010.
[19] Rousseau D. P. L., Vanrollegham P. A., Pauw N. D.: Model based design of horizontal subsurface flow constructed wetlands: a review. Water Research 38, 1484–1493, 2004.
[20] Saeed T., Sun G.: Enhanced denitrification and organics removal in hybrid wetland columns: comparative experiments. Bioresource Technology 102(2), 967–974, 2011.
[21] Saeed T., Sun G.: The removal of nitrogen and organics in vertical flow wetland reactors: predictive models. Bioresource Technology 102(2), 1205–1213, 2011.
[22] Shepherd H. L., Tchobanogolous G., Grismer M. E.: Time-dependant retardation model for chemical oxygen demand removal in a subsurface-flow constructed wetland for winery wastewater treatment. Water Environ Res 73(5) 597-606, 2001.
[23] Saeed T., Sun G.: Kinetic modelling of nitrogen and organics removal in vertical and horizontal flow wetlands. Water Research 2011 (Article in press), 1–16, 2011.
[24] Stein O. R., Biederman J. A., Hook P. B.: Plant species and temperature effects on the k – C* first order model for COD removal in batch-loaded SSF wetlands. Ecological Engineering 26(2), 100–112, 2006.
[25] Stone K. C., Poach M. E., Hunt P. G., Reddy G. B.: Marsh-pond-marsh constructed wetland design analysis for swine lagoon waste water treatment. Ecological Engineering 23, 127–133, 2004.
[26] Zhao Y. Q., Kumar J. L. G.: A review on numerous modeling approaches for effective, economical and ecological treatment wetlands. Journal of Environmental Management 92, 400–406, 2011.

13 The Newest Researches and Applications of Treatment Wetlands in Sewage Sludge Management

Hanna Obarska-Pempkowiak, Magdalena Gajewska, Ewa Wojciechowska, Marzena Stosik (Gdańsk University of Technology, Faculty of Civil and Environmental Engineering)

13.1. INTRODUCTION

In the recent years the awareness of environmental hazards is growing. In the 1992 the Stockholm Conference outlined the necessity of decentralization of large sewerage systems in the agglomerations. Smaller, local sewerage systems and local wastewater treatment plants (WWTPs) also have smaller environmental impact. The access to effective but cheaper methods of wastewater treatment has been increasing since 1990s. Also constructed wetlands (CW) are gaining popularity. This method perfectly solves the problem of sewage treatment at the rural areas. Recently, new applications of constructed wetlands are introduced. Hybrid constructed wetlands are used for treatment of industrial wastewater, stormwater runoff and landfill leachate. CW systems can also be used at the second or third stage of multi-stage sewage treatment. The latest solutions for rural areas propose closing of water and nutrients circulation, with application of CWs. Constructed wetlands are also an effective and economical solution of utilization of sewage sludge in rural communitites.

In the article, the latest research and appplications of constructed wetlands performed at the Faculty of Civil and Environmental Engineering are presented. The research covers application of constructed wetlands for treatment of high strength wastewater (landfill leachate and reject waters from sewage sludge dewatering process) and treatment of urban drainage waters. Implementation of constructed wetlands at individual households at rural areas, without possibility of building sewarage systems and central WWTP is presented. Finally, the quality of conventional and constructed wetlands outflows in terms of recalcitrant organic matter (hummic acids) presence was assessed.

13.2. APPLICATION OF CONSTRUCTED WETLAND FOR TREATMENT OF HIGHLY POLLUTED WASTEWATER

One of the up-to-date problems in municipal management is treatment of landfill leachate and reject waters from sewage sludge dewatering. Due to significant quantitative and qualitative changes, presence of toxic micropollutants and low BOD/COD ratio, treatment of these types of wastewater is difficult and usually requires high tech-solutions and

high financial expenditures in terms of investment and later operation.

Within the research project "New methods of emission reduction of selected pollutants and application of by-products from sewage treatment plants" financed by Norwegian Financial Mechanism and Ministry of Science and Higher Education PL 0085 E007/P01/2007/01 application of sequentially operated VF beds for treatment of highly polluted wastewater: reject water from sewage sludge dewatering (RW) as well as municipal landfill leachate (LL), was analysed. Reject waters from centrifugation of digested sewage sludge from WWTP in Gdańsk and the leachate from municipal landfill in Chlewnica (Pommerania Region) were analysed. The analysis of LL and RW composition showed that both types of wastewater contain very high concentrations of total nitrogen (N_{tot}), present mostly in the form of Kjeldahl nitrogen. RW also contains enormously high concentrations of recalcitrant organic matter (COD). In the Fig. 1, the concentrations of pollutants in LL and RW were compared to the composition of raw sewage discharged to the municipal WWTP in Gdańsk. Average N_{tot} concentration in LL and RW was, respectively, 9 and 15 times higher than in raw sewage.The BOD_5/COD ratio of RW and LL is very low, indicating low bioavailability of organic substance.

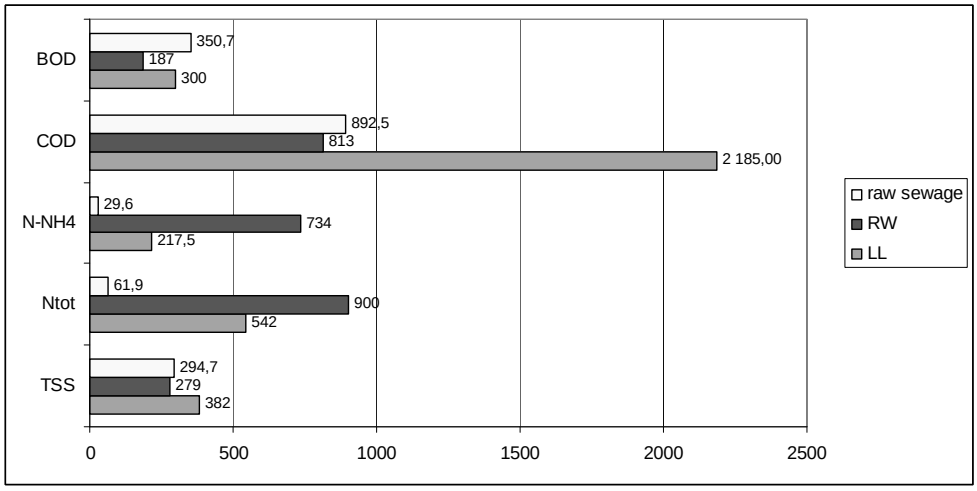

Fig. 1. Concentrations of contaminants in LL, RW and raw sewage from municipal WWTP „Wschód" in Gdańsk

In summer 2008 two pilot constructed wetlands were constructed: at the municipal WWTP "Wschód" in Gdańsk – for RW treatment and at the municipal landfill in Chlewnica (Pommerania Region) – for LL treatment. Each pilot CW consisted of three beds: two sequential vertical subsurface flow beds (VSSF I – 7.84 m^2 and VSSF II – 5.29 m^2), followed by a horizontal subsurface flow bed HSSF (3.91 m^2). Pre-treatment was realized in sedimentation tanks – in case of CW for LL treatment one tank with 1 m^3 volume; in case of RW – two tanks 1 m^3 volume each, working in series. Pre-treatment role is to even up the flow and composition of wastewater entering the beds, as well as to provide primary sedimentation. At VSSF beds good environment for the mineralization of organic compounds and oxidation of nitrogen compounds is developed. During resting periods, accumulated organic matter is decomposed, which protects the beds against clogging [1, 3,

7]. On the other hand, long retention time and anoxic conditions in HSSF beds favour the degradation of even hardly degradable organic matter [16].

The pilot CWs were planted with common reed (*P. australis*). The start-up of the CWs took place in autumn 2008. The analyses of treatment performance were carried out at both pilot CWs in 2009 and 2010.

In the Fig. 2 and 3 the concentrations of selected pollutants: COD, BOD_5, total nitrogen (N_{tot}), ammonia nitrogen ($N–NH_4^+$) and total suspended solids (TSS), after subsequent treatment stages at pilot CWs for RW and LL treatment is presented. In Table 1, the values of BOD_5/COD ratios after subsequent beds, are presented.

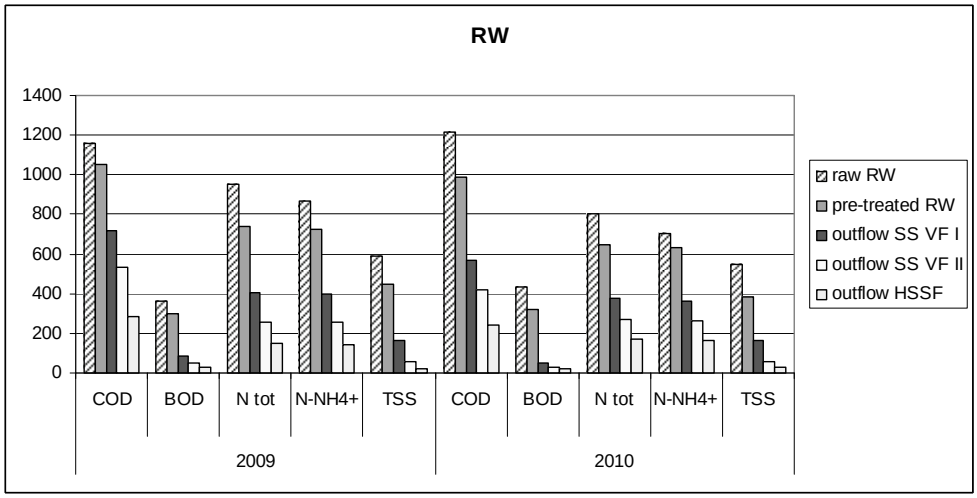

Fig. 2. The concentrations of selected pollutants in RW after subsequent treatment stages at pilot CW

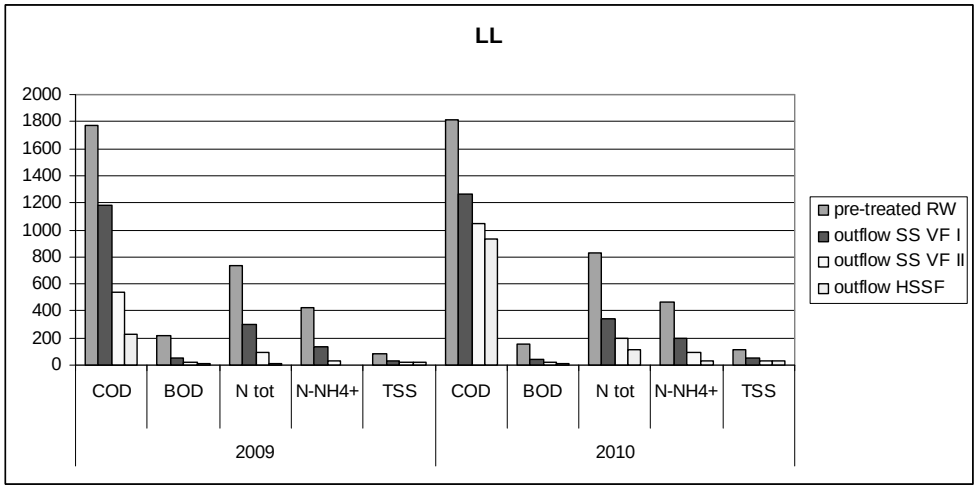

Fig. 3. The concentrations of selected pollutants in LL after subsequent treatment stages at pilot CW

At both pilot CWs treatment performance was relatively high, in spite of unfavourable composition of treated wastewater. At the CW for RW treatment, treatment effectiveness was equal to 96% for TSS, 70% for COD and over 90% for BOD_5. The low BOD_5/COD ratio (Table 1), decreasing after subsequent treatment stages, indicates that recalcitrant organic mater, i.e., in the form of humic acids, is present in RW. The concentration of total nitrogen in treated RW was still quite high. At the outflow, the main form of nitrogen was ammonia nitrogen, with concentrations varing from 99.6 to 198.6 mg/l. Since the average concentration of nitrogen at the inflow to WWTP "Wschód" is 90 mg/l, it can be reckoned that recirculation of treated RW will not disturb the WWTP performance.

In case of pilot CW for LL treatment, in 2009 very high treatment efficiencies were achieved: 87% for COD, 95.4% for BOD_5, over 99% for ammnia nitrogen, 98% for total nitrogen and 72% for TSS. In 2010 the treatment efficiencies decreased. The most significant decrease was observed for COD (48.5%). Ammonia nitrogen treatment efficiency decreased to 94%. The denitrification process at HSSF bed was stopped, resulting in the decrease of treatment efficiency of total nitrogen to 86.5%.The anaysis of BOD_5/COD ratios after subsequent treatment stages (Table 1) indicates that easily biodegradable carbon was almost completely consumed. The organic substance remaining as COD was unavailable for biological decomposition (humic substances). The low BOD_5/COD ratio also explain the inhibition of denitrifcation, which requires easily degradable carbon source [7].

Table 1

The values of BOD_5/COD ratios in RW/LL after subsequent stages of treatment at pilot CWs

BOD_5/COD	Year	Raw RW/LL	After pre-treatment	Outflow from VSSF I	Outflow from VSSF II	Outflow from HSSF
RW	2009	0.29	0.25	0.11	0.09	0.09
	2010	0.35	0.32	0.09	0.06	0.07
LL	2009		0.12	0.04	0.04	0.04
	2010		0.09	0.03	0.02	0.01

13.3. INNOVATIVE SANITARY SYSTEM FOR AN INDIVIDUAL HOUSEHOLD

The latest report of Environmental Protection Inspection regarding the condition of Polish waters indicates that the protection of waters against eutrophication is one of the most significant issues. In order to solve the problem of the eutrophication of waters in Poland, strategies not only for big agglomerations but, first of all, for rural areas with dispersed farms and buildings have to be developed. Surface waters are especially exposed to eutrophication due to the way land is used in rural areas.

The idea of an innovative sanitary system for individual hosueholdis based upon a closed circulation of matter in the environment. The nutrient elements N, P and K from sewage should be re-used for soil fertilization.

Within the research project *Innovative Solutions for Wastewater Management in Rural Areas* (financed by Polish Ministry of Science and Higher Education E033/P01/2008/02

and EOG Financial Mechanism and Norwegian Financial Mechanism PL0271) the conception of sewage treatment and sewage sludge utilization at the CWs for individual households in a rural area was worked out. The project has been launched in the catchment area of the river Borucinka in the Municipality of Stezyca, Pommerania Region. The idea was to prepare a ready-to-implement solution for community in a rural area. Three configurations of constructed wetlands were proposed: two with vertical flow(VF) beds and the third one with a horizontal flow (HF) bed preceded by a prefilter (Fig. 4) [15]:

— Configuration I: primary sedimentation tank with elongated detention time (5–6 days), followed by a single VF bed (the unit area of 4 m^2/PE) and a pond,
— Configuration II: existing primary sedimentation tank (with short retention time up to two days), then two sequential VF beds followed by a pond,
— Configuration III: primary sedimentation tank, prefilter (pre-treatment), HF bed.

Nine CW facilities (three per each configuration) were constructed in summer 2009.

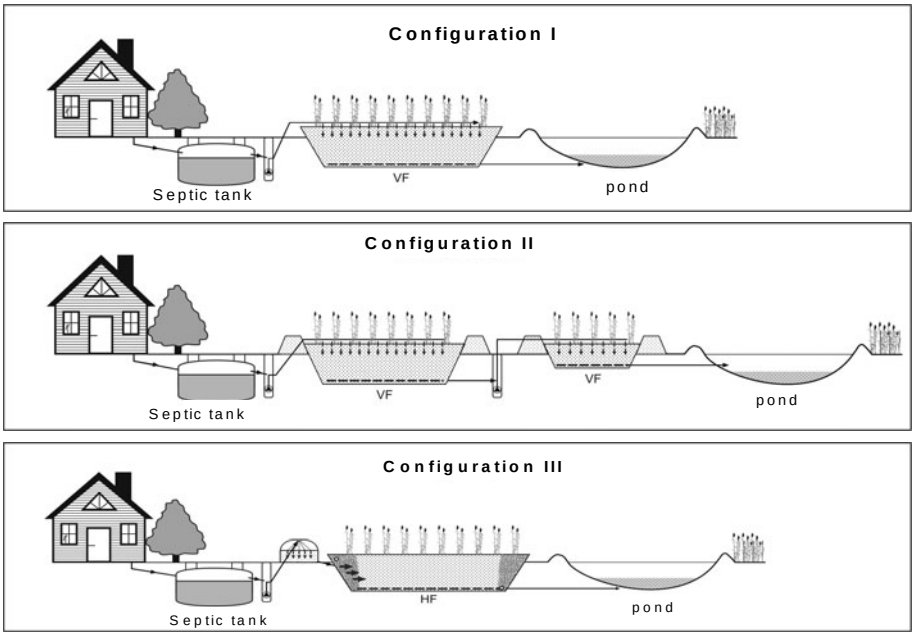

Fig. 4. Layout of three single-farm TW configurations, according to Paruch et al. (2011)

One of the aims of the project was comparison of three CW configurations in terms of treatment effectiveness.

The average concentrations of pollutants in sewage (inflow and outflow), treated at three CW configurations, are presented in Table 2. The analyses of concentrations of characteristic pollutants and treatment performance lead to the following observations and conclusions:

a) Very high concentrations of pollutants were present at the inflow (after septic tanks); especially organics (COD and BOD_5). At 4 farms COD was exceeding 1000 mg/l and at another farm it was 970 mg/l. Concentrations of N_{tot} varied from 85 to 170 mg/l. So

high inflow concentrations could be caused either by improper maintenance and operation of septic tanks or the inflow of high strength wastewater (manure, run-off from the fields or leakages from farmyard).

b) Despite so high inflow pollutants concentrations, quite effective removal of pollutants was observed at most TWs. The organis removal effectiveness in 2010 varied from 56 to 83% (COD) and 64% to 92% (BOD_5). The effectiveness of total nitrogen removal varied from 44 to 77%. Removal effectiveness of phosphorus varied from 24 to 66%.
c) The best performance was achieved in configuration II with two sequentially working VSSF beds. Since the contact time in sequentially working beds is twice as long as in a single bed, it can be concluded that elongation of the contact time has more positive impact on treatment results than application of larger unit area of a single VSSF bed.
d) Although the concentration of pollutants decreased, however the sewage samples collected from the last stage of treatment (the pond) did not fulfil the requirements of the Regulation of Environmental Ministry from 24th July 2006. Relatively low quality of the treated effluent is likely be a result of short period of operation (low development of roots and rizhomes as well as biofilms) and short period of sewage retention in the pond.

Table 2

Average concentrations of pollutants at individual household CWs, mg/l

Parameter	Configuration					
	I		II		III	
	influent	effluent	influent	effluent	influent	effluent
TSS	289.7	69.9	178.3	37.2	269.4	100.3
SS org.	236.9	52.7	137.5	30.5	221.5	91.4
BOD_5	236.0	46.8	328.3	36.0	558.1	69.5
COD	537.3	170.3	745.3	165.9	1140.9	204.5
TN	107.9	39.9	134.1	42.4	115.7	48.0
$N–NH_4^+$	76.6	17.7	78.5	15.4	61.4	16.8
TP	11.2	4.3	15.5	5.5	14.3	6.6

13.4. WASTEWATER RENATURALIZATION – ANALYSES OF PROPERTIES OF RECALCITRANT SUBSTANCES (HUMIC ACIDS) IN SEWAGE TREATED IN CONVENTIONAL AND CONSTRUCTED WETLANDS FACILITIES

Recently, it was pointed out that in the wastewater treatment process organic compounds characterized by properties similar to humic acids are formed [5]. The chemical features of wastewater indicate that they can influence the form of trace metals, the salts concentrations as well as concentrations of organic substances, including humic acids. The concentrations of these substances are higher in sewage than in surface waters. Moreover, the complexing abilities of the humic acids originating in wastewater treatment process are stronger than the naturally occurring humic substances [4]. The humic acids formed in

wastewater treatment process can be also responsible for trace metals transport and increase of their bioavailability in the ecosystem.

The objective of undertaken research was evaluation of the impact of conventional and natural (constructed wetlands) wastewater treatment on organic matter speciation with special regard to retention of recalcitrant organic matter. Quantitative and qualitative comparison of humic acids formed during conventional and natural (CW) wastewater treatment was performed. The research was conducted within research project N 523 080 32/2926, financed by Ministry of Sicence and Higher Education.. The quality of effluent from three highly-effective WWTPs (Jamno near Koszalin, Unieście and "Wschód" Gdańsk and two CWs (Darżlubie and Wiklino) was investigated and compared to the quality of humic acids present in the water of Vistula river (in the section near Gdańsk). Humic substances were isolated from treated sewage in order to analyze their properties: elemental composition, absorption spectrum in the visible light (VIS), ultraviolet (UV) and infrared (IR).

The research results proved that humic acids (HA) in the analysed treated wastewater have similar elemental composition and infrared spectra, although this is not the evidence of similar composition of particles.

The $A_{4/6}$ and C/H ratios bring useful information concerning humic acids origin and composition. The values of these ratios for HA isolated from treated wastewater and water from Vistula River differ from each other due to the presence of aromatic rings in HA from treated wastewater. Thus, their potential role in the environment may also be different.
The concentration of HA in treated wastewater is similar to the concentration in surface waters. Thus, treated wastewater can be a potential source of HA, especially in case of smaller streams [14].

13.5. POTENTIAL OF CW SYSTEMS FOR TREATMENT OF URBAN RUNOFF

In Poland, stormwater collected by drainage systems is usually discharged directly to the receiver, without treatment [13]. This practice has a significant impact on surface waters quality, especially in case of smaller streams flowing through urbanized area [6].

According to the Regulation of Environment Ministry (2006) [11], stormwater collected from polluted non-permeable areas can be discharged to surface waters, if concentrations of pollutants do not exceed the admissible values. The necessity of adequate treatment of drainage water is stressed, for example through infiltration to ground in order to improve water balance of urbanized areas [2]. Infiltration allows for evening up and decrease of the outflow as well as for decrease of pollutant loads discharged to surface receivers. According to foreign [8, 10, 12] and Polish experiences [9], constructed wetlands can be applied for treatment of drainage waters from urban areas and motorways. Apart from effective treatment, CWs can also create additional retention of drainage waters. CWs for stormwater treatment should consist of several treatment stages. At least one of them should be a surface flow CW (SF-CW) – for example a pond with adequate retention volume in case of storm events.

Constructed wetland system for treatment of urban runoff was constructed on Swelina Stream in Sopot in 1994, in order to protect the Stream against pollution. The Swelina Stream discharges its waters directly to the Gulf of Gdańsk, near popular bathing places. The Stream receives drainage waters from surrounding area. The system consists of sedi-

mentation-retention tank and gravel-filled bed planted with common reed (*P. australis*).

The treated water is collected by drainage pipes, outflows to a control well and then it is discharged back to the stream. During intensive rainfall, the first, most polluted part of drainage is collected in a retention reservoir, while the rest of water is discharged through an overflow to the stream (without treatment). The system was built in order to remove the nutrients, mainly phosphorus, and faecal bacteria discharged with drainage. After the CW was constructed, a significant improvement of the Stream quality was observed [9]. The analyses carried out by the Regional Inspection of Environment Protection in Gdańsk indicated that Swelina Stream waters fulfil criteria of the first class waters.

Monitoring of Swelina Stream quality downstream and upstream the CW system during rainfall events is planned within the research project „Innovative resources and effective methods of safety improvement and durability of buildings and transport infrastructure in the sustainable development" financed by the European Union from the European Fund of Regional Development based on the Operational Program of the Innovative Economy.

Urban drainage contains high concentrations of TSS. The size of solids is a crucial parameter, determining sorption abilities and the way the solids settle. Smaller fractions, which are difficult to remove during conventional treatment processes, are responsible for migration of pollutants in aquatic environment, since they act as carriers of hydrophobic organic micropollutants, ntrogen and phosphorus compounds and heavy metals. Within the project, it is planned to analyze the granulometry of TSS present at the inflow and at the outflow of CW system on Swelina Stream to find the ability of the system to retain different fractions of suspended solids.

13.6. CONCLUSIONS

The results of research and CWs implementation from the last 5 years, the following conclusions can be drawn:

1. CW systems are an ecological, easy-to-implement and close to nature solution to wastewater treatment and sewage sludge utilization at the rural areas, where sewarage systems cannot be built
2. The latest applications confirm that CWs can be used for treatment of high strength wastewater, like landfill leachate and reject waters from mechanical dewatering of sewage sludge at conventional WWTPs.
3. Constructed wetlands minimize the ingerention in the environment and are a classical example of ecological engineering.

References

[1] Gajewska M., Tuszyńska A., Obarska-Pempkowiak H.: Influence of Configuration of the Beds on Contaminations Removal in Hybrid Constructed Wetlands, Polish Journal of Environmental Studies. 13: 149–153, 2004.

[2] Geiger W., Dreiseitl H.: Nowe sposoby odprowadzania wód deszczowych. Neue Wege für das Regenwasser. Oficyna Wydawnicza Projprzem-EKO Bydgoszcz 1999.

[3] Kayser K., Kunst S., Fehr G., Voermanek H.: Nitrification in reed beds-capacity and potential control methods, World water congress, published at the IWA, Berlin, Germany, October 2001, s. 126–138, 2001.

[4] Nissinen T., Miettinen I., Martikainen P., Vartiainen T.: Molecular size distribution of natural organic matter in row and drinking waters. Chemosphere, 45: 865–873, 2001.
[5] Obarska-Pempkowiak H., Gajewska M., Pempkowiak J.: Quantitatively and qualitatively characteristic of organic matter in sewage after treatment in constructed wetlands. Wetland Systems for Water Pollution Control: 10th International Conference, Lisbon, Portugal, September 23-29, 2006, s. 771–776, 2006.
[6] Królikowski A., Grabarczyk K.: Uwarunkowania techniczne i eksploatacyjne prawidłowego funkcjonowania systemu kanalizacji deszczowej. II Ogólnopolska Konferencja Naukowo-Techniczna nt. Bezpieczeństwo, niezawodność, diagnostyka urządzeń i systemów gazowych, wodociągowych, kanalizacyjnych i grzewczych, Zakopane- Kościelisko: 129–141, 2001.
[7] Molle P, Lienard A, Boutin C, Merlin G, Iwema A.: How to treat raw sewage with constructed wetlands: An overview of the French systems, (Proceedings) 9th International Conference on Wetland System for Water Pollution Control, 2004, Avignon, France: 11–20.
[8] Mungur A.S., Shutes R.B.E., Revitt D.M., House M. A.: An assessment of metal removal from highway runoff by a natural wetland. Wat.SciTech. 92 (3): 169–175, 1995.
[9] Obarska-Pempkowiak H., Gajewska M., Wojciechowska E.: Hydrofitowe oczyszczanie wód i ścieków, Constructed wetlands for water and wastewater treatment. Wydawnictwo Naukowe PWN, Warszawa 2010, p. 307 [in Polish], 2010.
[10] Revitt D.M., Shutes R.B.E., Jones R.H., Forshaw M., Winter B.: The performances of vegetative treatment systems for highway runoff during dry and wet conditions. The science of the total environment 334-335 (2004). 262–270, 2004.
[11] Rozporządzenie Ministra Środowiska z 24 lipca 2006 r.(DzU nr 137, poz. 984).
[12] Shutes R.B.E., Revitt D.M., Lagerberg I.M., Barraud V.C.E.: The design of vegetative constructed wetlands for the treatment of highway runoff. The Science of the Total Environment 235 (1999): 189–197, 1999.
[13] Suligowski Z.: Alternatywa dla wód opadowych. Wodociągi i Kanalizacja 4/2008:54–55, 2008.
[14] Pempkowiak J., Obarska-Pempkowiak H., Gajewska M., Wojciechowska E.: The influence of humic substances in treated sewage on the quality of surface waters Polish Journal of Environmental Studies, 3: 27–33, 2009.
[15] Paruch A., Mæhlum T., Obarska-Pempkowiak H., Gajewska M., Wojciechowska E., Ostojski A.: Rural domestic wastewater treatment in Norway and Poland: experiences, cooperation and concepts on the improvement of constructed wetland technology. Wat Sci Tech. 63/4 (2011): 776–781, 2011.
[16] Vymazal J.: Horizontal sub-surface flow and hybrid constructed wetland systems for wastewater treatment Ecol. Eng. 25: 478–490, 2005.

Acknowledgments

Financial support from the following research projects is gratefully acknowledged:

— research project “New methods of emission reduction of selected pollutants and application of by-products from sewage treatment plants” financed by Norwegian Financial Mechanism and Ministry of Science and Higher Education PL 0085 E007/P01/2007/01,
— research project “Innovative Solutions for Wastewater Management in Rural Areas”, financed by Polish Ministry of Science and Higher Education E033/P01/2008/02 and EOG Financial Mechanism and Norwegian Financial Mechanism Nr PL0271,
— research project „Innovative resources and effective methods of safety improvement and durability of buildings and transport infrastructure in the sustainable development” financed by the European Union from the European Fund of Regional Development based on the Operational Program of the Innovative Economy.

14 The EIS Method and Z-Meter III Device

Jana Pařílková, Marie Fejfarová, Jaroslav Veselý, Zbyněk Zachoval,
Pavel Šmíra (Brno University of Technology, Faculty of Civil Engineering

14.1. INTRODUCTION

Electrical impedance spectrometry (EIS) enables the detection of the distribution of impedance or other electrical variables arising from it (resistivity, conductivity, etc.) [1, 2], inside a monitored (homogeneous and heterogeneous) object, and thus the observation of its inner structure and its changes. Due to the electrodes used and the way of their location in a monitored object, it is possible to use the method as non-destructive invasive or non-invasive. The method ranks among indirect electrical methods [3] and is used in measuring the properties of organic and inorganic substances. It constitutes a very sensitive tool for monitoring phenomena that take place in objects (e.g. changes occurring in earth-fill dams when loaded by water, in wet masonry when being dried, in sewerage systems during the transport of water with sediments), electrokinetic phenomena at boundaries (e.g. electrode/soil grain, between soil grains) or for describing basic ideas about the structure of an inter-phase boundary (e.g. electrode/water). The EIS method is based on the periodic driving signal – the alternating signal. If the low amplitude of the alternating signal is used, concentration changes of charge are minimal at the surface of an electrode connected with measurement, which is very important in systems sensitive to so-called concentration polarization. The range of frequencies used of the driving signal enables the characterization of systems comprising more interconnected processes with different kinetics.

In the Laboratory of Water-Management Research of the Institute of Water Structures at the Civil Engineering Faculty of Brno University of Technology, a measuring instrument with a Z-meter III device has been developed within the solution of the international project E!4981 of the programme EUREKA (a part of the Czech researcher of the project bears the designation OE 10002). This instrument is verified in laboratory experiments and measurements on objects *in situ*. Phenomena identifiable by changes in impedance, which take place in a porous environment (soil, stone masonry), are investigated.

14.2. IMPEDANCE

Impedance Z can be considered as generalized electrical resistance [4]. The electrical resistance of an element can be encountered in the form of Ohm's relation defined by the German physicist George Simon Ohm on the basis of his experimental measurements in 1827.

$$R = \frac{U}{I} \tag{1}$$

where R is the ohmic resistance to the passage of an electric current, I is the electric current flowing through a system and U is the electric voltage on the electric resistance. However, it has been found that the given relationship has certain limitations of validity. It holds solely for conductors of the first kind, i.e. electron conductors, and during the passage of the alternating current it holds only if changes of the alternating current are "sufficiently slow". The maximum allowable velocity of changes depends on the characteristics of the system used. In the case of conductors of the first kind (electron conductors), the allowable velocity of changes of the alternating current is chiefly defined by their length, the geometric arrangement, and shielding, if any. However, if more kinds of conductors occur in a studied system, the situation becomes complicated, particularly in relation to the passages of charge between individual phases. It is necessary to describe phenomena in a more complex approach, which electrical engineering solves by defining three basic variables describing the response of the system exposed to the effects of the alternating electric field. This concerns the ohmic resistance R, the capacitance C and the inductance L. The term 'alternating signal' can designate every signal (harmonic, triangular, sawtooth, oblong, pulse, etc.), the direction of which periodically alternates. Further on, the harmonic alternating signal is assumed, the ideal time pattern of which can be described by a sine function. The alternating current is generated in a circuit which is connected to a source of an alternating voltage. The alternating voltage is harmonic electromagnetic oscillation, the instantaneous value of which is determined by the relation

$$u = u(t) = U_m \sin(\omega t + \varphi_0) \tag{2}$$

where U_m is the amplitude of voltage oscillations, ω is the angular frequency and φ_0 is the initial phase of the alternating voltage. The alternating current is also harmonic electromagnetic oscillation that has the same period but is not always in phase with voltage. The ideal pattern of the alternating current is a harmonic alternating current, the instantaneous value of which changes in time according to a sine function

$$i = i(t) = I_m \sin(\omega t + \varphi_0 + \varphi) \tag{3}$$

where I_m is the amplitude of the current, ω is the angular frequency, φ_0 is the initial phase of the alternating current and φ is the phase difference or the phase displacement, shortly the phase between voltage and current. In terms (2) and (3), t is the time and the angular frequency (the angular velocity) ω of harmonic oscillation [rads^{-1}] or, also only [s^{-1}], is expressed by the relation

$$\omega = 2\pi\ f = \frac{2\pi}{T} \tag{4}$$

where f is the frequency of the rotational motion [Hz] and T is its period. The amplitude I_m, or U_m respectively, and the phase difference φ are determined by the frequency and the properties of elements connected in the circuit, i.e. the properties of the measured porous environment (in our case this concerns soil and masonry).

By the size of the amplitude, the ohmic resistance expresses the response of the studied system to the insertion signal, the harmonic alternating electric current I of the given

frequency *f*, and the presence of capacitance and inductance in the electric circuit results in the phase displacement φ against the driving signal.

In a complex plane (Fig. 1), the phasor of the current is graphically depicted by a vector which rotates counterclockwise at an angular velocity ω around the origin. The rotating phasor of the current at the time $t = 0$ s, when the initial angle of the phase φ_0' is expressed by the relation

$$i(t) = \mathrm{Re}(I_m) + j\,\mathrm{Im}(I_m) \tag{5}$$

$$\mathrm{Re}(I_m) = I_m \cos(\omega t + \varphi_0) \;\text{ and }\; \mathrm{Im}(I_m) = I_m \sin(\omega t + \varphi_0) \tag{6}$$

Substituting (6) into (5), it can be written the trigonometric formula

$$i(t) = I_m\left[\cos(\omega t + \varphi_0) + j\sin(\omega t + \varphi_0)\right] \tag{7}$$

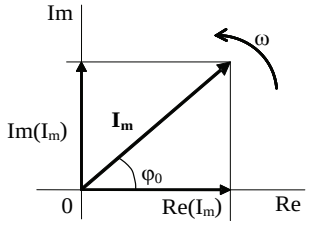

Fig. 1. Phasor of the current in a complex plane

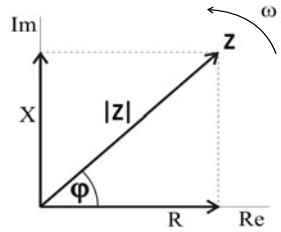

Fig. 2. Phasor of impedance

That is similarly as the electric resistance *R* characterizes the properties of an element or a system for the direct current (1), the impedance *Z* characterizes the properties of an element for the alternating current (8). In contrast to the electrical resistance where the voltage is in phase with the current, the voltage and the current in impedance can be phase-displaced according to the character of the reactance.

Impedance can be expressed using Ohm's relation for alternating-current circuits, i.e. using the ratio of the phasor of the electric voltage **U** to the phasor of the electric current **I**:

$$Z = \frac{U}{I} \;\text{ or }\; Z = \frac{\mathrm{Re}(U_m) + j\,\mathrm{Im}(U_m)}{\mathrm{Re}(I_m) + j\,\mathrm{Im}(I_m)} \tag{8}$$

The values of impedance are, just as the values of the resistance R in the case of direct-current circuits, expressed in ohms [Ω].

The frequency characteristic of impedance (Fig. 2) can be expressed as a function of a complex variable in the algebraic (component) form

$$Z = R + jX \tag{9}$$

$$|Z| = \sqrt{R^2 + X^2}, \quad \varphi = \arctan\left(\frac{X}{R}\right) \tag{10}$$

where *R* is the electrical resistance forming the real part of impedance independent of frequency, and the imaginary component of the impedance *X* is the reactance that changes with frequency. The modulus of impedance (10) can be detected by commonly available measuring instruments (voltmeter, amperemeter, ohmmeter, etc.); to measure the phase

displacement, it is necessary to have specialized instrument equipment. If it is a system which contains a transition between phases, it is possible to use direct measurement in a very limited number of cases in which the properties of the system approach the ideal ones. Electrochemical processes, however, are heterogeneous by their essence of transmission of charge across a phase boundary, which means that they are connected with transmission features at the electrode/monitored porous material boundary, and thus with limitations determined by their kinetics. The electrical description of the system thus begins to complicate, also due to the fact that relationships that hold true at the boundary are usually nonlinear.

The first marked limitation is the amplitude of the driving electric voltage, which must be so much low so that the relationships between the electric current flowing through a system and the voltage can be considered as linear in a given area (as experience shows, the amplitude should not exceed a value of 10 mV). The given condition lays relatively great demands on instrument equipment. Another, not less serious problem is the separation of those phenomena on electrodes which are not the subject of study. The given problem solves different methods of connecting driving and measuring circuits when measuring the unknown impedance of a system (two-, three-, four-, five- and more-terminal connection). Measurement takes place in a wide range of frequencies of the driving signal, which will enable the efficient separation of individual mechanisms involved in the transmission of charge and thus the provision of information about their significance for the description of kinetic parameters of a monitored system.

The exact approach to the solution consists in a design corresponding to a kinetic model, the parameters of which are optimized on the basis of detected experimental data [5, 6, 7, 8]. However, for most real systems, the given procedure of the solution is not realistic without significant simplified assumptions. Therefore, in practice, the approach of a physical model is used when a studied system is described by a substitute electric circuit, in which electrical elements replace the real process at the phase boundary. The largest problem in this approach, of course, is the definition of the physical justification of each element of the circuit and the optimization of its parameters with the aim to achieve the least possible number of settable parameters.

14.3. THE Z-METER III DEVICE AND PROBES USED

The requirement of achieving a greater comfort in measurement in the field while retaining the higher and, at the same time, optional number of measuring points has led to the minimization of the Z-meter III device [9], which, however, required certain limitations. For the implementation, a signal processor of the latest development line of impedance meters of the company “ST Microelectronics” was chosen. Its 32-bit processor enables only two-terminal measurement. The record of measurement is solved by logging in a text file to a portable medium – a SD card, and it is also possible to connect the Z-meter III device through the USB interface to a PC. Parameters of measurement are entered directly into the device, are depicted on a LCD display and, when switched to the measuring mode, the device will display the value of unknown measured impedance in the form of its real and imaginary components.

The device is battery-powered, with the assumed time of operation being 8 hours and with an option to recharge it from a 12 V source. The basic parameters are given in Tab. 1, and the structural design of the device in Fig. 3.

Table 1

Parameters of Z-meter III device

Parameter	Z-meter III	Parameter	Z-meter III
Impedance range	50 Ω – 1 MΩ	Communication interface	USB SD card
Frequency range	100 Hz – 100 kHz	Number of measuring points	1, 8, 16, 32, 64, 128
Accuracy of modulus *Z* measurement	±2% of the range	Switch	Internal, external
Accuracy of phase measurement	±2°	Power supply	Batteries

Fig. 3. Structural design of a Z-meter III device with an adapter for measurement on one rod (Karolinka, 2011)

The system consists of a modular design of the device designated Z-meter III, which also contains a source unit, a display unit and a unit for data backup. Part of the device is software enabling communication between the user and the Z-meter III device. For obtaining information about the monitored system, passive probes have been constructed (usually vertically divided rod-shaped paired probes, but it is also possible to use divided unit arrangement).

14.3.1. Connection of measuring probes

From the physical point of view, the probes of the electrical impedance spectrometry (EIS) methods can be characterized as passive sensors that change their characteristic property during the action of the measured variable. This property will then influence the flow of electric energy. The change in the property is thus the degree of the value of the measured non-electrical variable. In terms of connection, a two-terminal connection was used in measurement, while obeying the principle of the tight contact of the probe sensor with the surrounding environment. The two-terminal connection does not eliminate the effect of voltage drops on the resistance of lead-in cables and on contact resistances between sensors

and the measured environment, but it is sufficiently sensitive and accurate for changes in the monitored impedance caused by a change in the soil profile moisture.

The impedance meter contains a source of an exciting current *Ic* and a unit *Z* of the meter. In addition to the detected impedance Z_x, the evaluated impedance measured between the terminals 1 and 2 also comprises parasitic impedances Z_c of the lead-in cables and contact impedances Z_t between the electrode and the measured environment (Fig. 4).
In the case of the two-terminal measurement, the measured impedance expresses the sum of all impedances (including parasitic ones) that occur in the measuring route

$$Z = Z_x + Z_{C1} + Z_{C2} + Z_{T1} + Z_{T2} \tag{11}$$

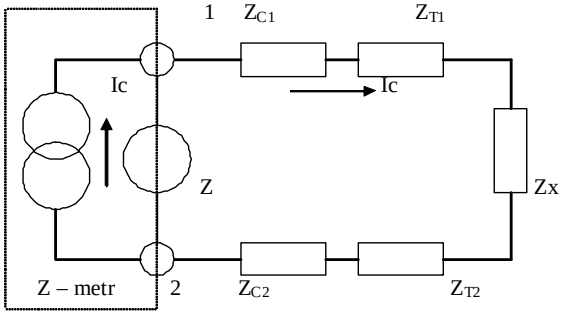

Fig. 4. Scheme of the two-terminal principle of measurement

The basic knowledge of the measured environment, based on engineering-geological and hydrogeological surveys, can be extended by information on a qualitatively higher level of possibilities of a modified design of the measuring set by the application of the EIS method.

14.4. EXAMPLES OF APPLICATION

The examples of application EIS method and Z-meter III device, which are shown in this paper, are from monitoring of porous environment with quite different parameters.

14.4.1. The Karolinka Water Reservoir

The Karolinka Water Reservoir (Fig. 2) on the River Stanovnice is used for supplying the Town of Vsetin and its vicinity with drinking water. It has a retention effect for flood control, and improves the discharge. The reservoir lies near the town of the same name with almost three thousand inhabitants; it is about 6 km away from Novy Hrozenkov and from Velke Karlovice. It falls into the area of the CHKO (Protected Landscape Area) Beskydy and is in the wooded frontier region between the Czech and Slovak Republics, relatively little populated but recreationally used, with many cottages, and yet, in a relatively ecologically clean area attracting tourists.

The River Stanovnice, Strahler Stream Order No. 4-11-01-018, springs near Bukovina at an altitude of about 970 m a.s.l. (above sea level), and has a fan-like basin. The river has the length L = 8.9 km, and the area of the basin is A = 23.18 km^2. It empties into the River Vsetinska Becva at the river kilometre 105.5 near the Town of Karolinka at an altitude of 480 m a.s.l. The average discharge at the confluence is 0.34 m^3 · s^{-1}. The River Stanovnice is characterized by a great slope because its average slope is $\bar{i} = 5.5\%$. The coefficient of the shape of the basin is also high and acquires a value of

$$\alpha = \frac{A}{L^2} \approx \frac{23.2}{8.9^2} = 0.29 \tag{12}$$

It is noted for a relatively large amount of material transported by the river. The prevailing amount of these bed-load sediments is entrained just in the Karolinka Reservoir.

The reservoir dam is a rock-fill embankment dam with a central loam core. The elevation of the dam crest 5 m wide is 522.7 m a.s.l., its length is 391.5 m and is 38.2 m high above the ground surface. It is equipped with 2 bottom outlets of a diameter of D = 0.8 m, each with a capacity of up to 4.1 m^3·s^{-1}, and a shaft emergency spillway of a capacity of up to 104 m^3·s^{-1} (the discharge Q_{100} = 87.4 m^3·s^{-1}). Electric power is generated using two META turbines of installed outputs of 0.01 + 0.04 MW and a total maximum usable flow of 0.15 m^3·s^{-1} with the head H = 22 m to 42 m. The dam was constructed in the years 1975 to 1985.

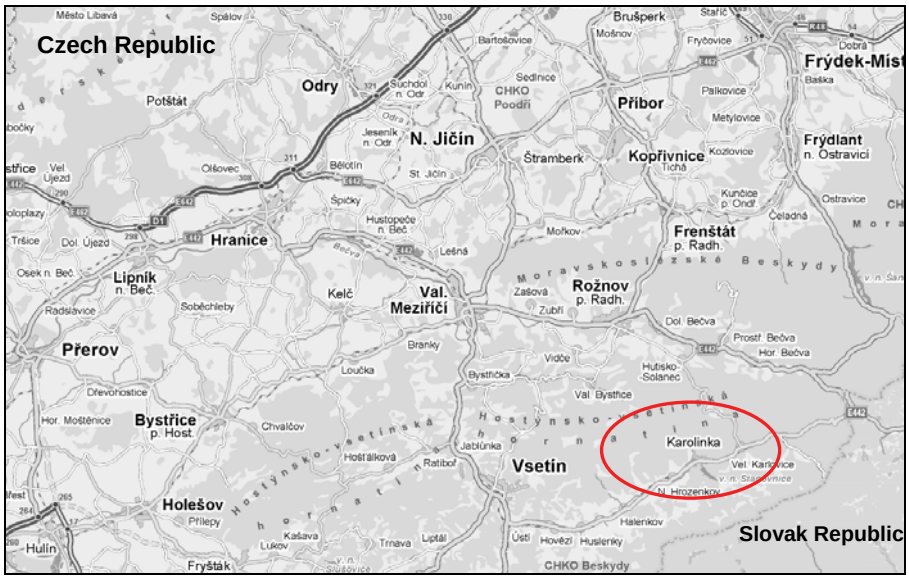

Fig. 5. Situation of the Karolinka Dam

The reservoir has a constant capacity of 0.96 mil. m^3, its storage capacity is 6 008 m^3 and the total capacity is 7 571 m^3. The length of the backwater is 1.94 km, the maximum level is at 521.20 m a.s.l. and the water area is 50.5 ha.

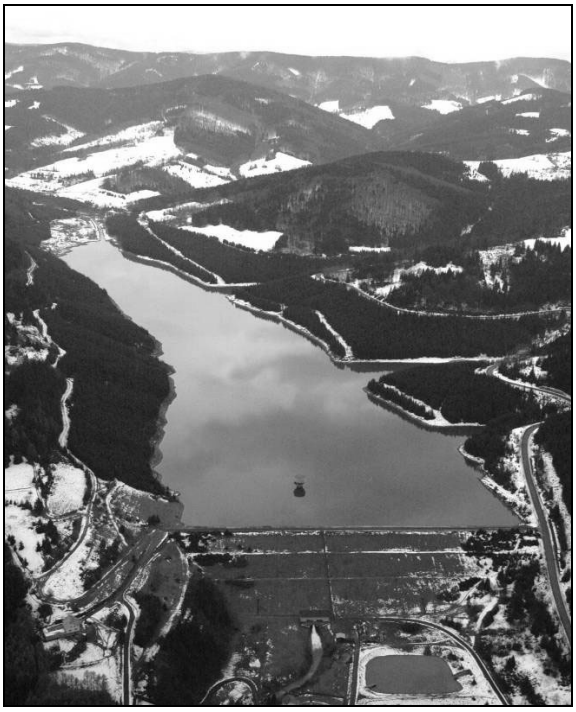

Fig. 6. View of the Karolinka Dam and Reservoir

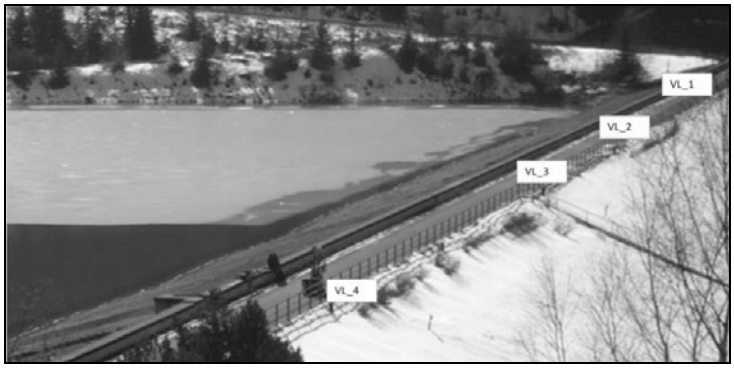

Fig. 7. Location of probes of the EIS method in the crest of the Karolinka Dam

The just increased seepage detected by the VD-TBD (Dam Safety Surveillance and Supervision) has led to the need of the remediation of the central loam core and its monitoring, where the EIS method has been used as one of methods.

The installed passive probes of a special construction have been designed as vertically divided (a total of 20 measuring points), with irregular lengths, and linked to the monitoring system of the dam. Their total length was 13 m; data reading was made with a two-terminal connection of the measuring instrument on one rod. In all, four measuring rods were

mounted into the dam core from the dam crest in pre-defined positions (Fig. 7), using a static penetration set PAGANI (GEO*test*, a.s.) (Fig. 8). They will enable the monitoring of changes in the electrical conductivity $G = 1/R$ of soils of the dam core, and hence indirectly changes in moisture.

Fig. 8. Installing of probe of the EIS method into sealing core dam

14.4.2. The Rychvald Castle

The second experiment was carried out on the object of Rychvald Castle being reconstructed (Fig. 9). At that site, it concerned the verification of the sensitivity of the measuring apparatus (including the special construction of passive measuring electrodes) for transmission phenomena that occur at the electrode/masonry boundary when applying microwave heating (Fig. 10).

Fig. 9. Rychvald Castle under reconstruction

Divided probes with a total length of 1 m were installed into stone masonry, using microwave radiation of an output of 1 kW for the duration of 240 s in one point and moni-

toring changes in conductivity $\sigma = l/(R \cdot A)$, where l is the length of a fictitious conductor made by applying an electromagnetic field and A is its cross section, whereby indirectly monitoring also changes in moisture at individual depth levels of masonry. 10 measuring points regularly spaced apart were on one rod; the connection was two-electrode; the arrangement of data readers during measurement was single-rod as well as paired; the measurement was made at the fixed frequency f = 8000 Hz and in a frequency spectrum of f = 1000 Hz to 100 000 Hz.

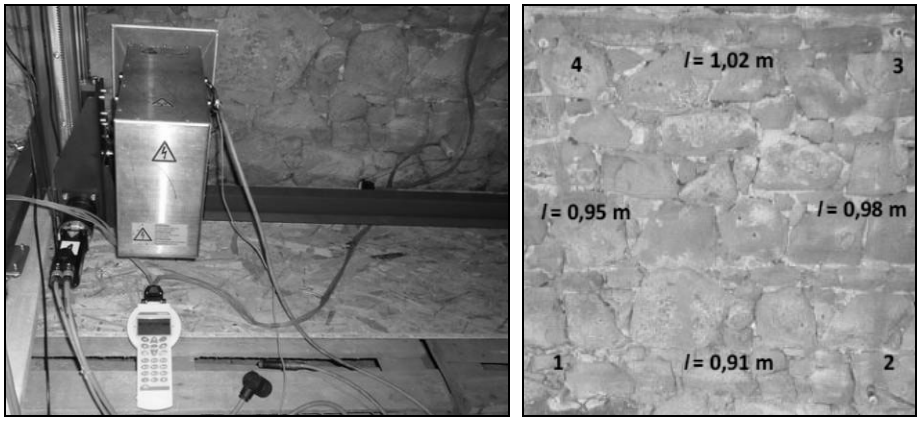

Fig. 10. Microwave radiation apparatus with a Z-meter III device (left), stone masonry with probes (right)

14.5. SELECTED RESULTS

Monitoring by the Z-meter III device on the Karolinka Dam was commenced on 23.3.2011. The measuring rod-shaped EIS probes with electrodes, together with the probes of static penetration and the readers of pore pressures, were mounted from the dam crest spaced 50.00 m, 45.12 m and 69.13 m apart. The time pattern of changes in the electrical conductivity G with the increasing depth h is evident in Fig. 11. The map of conductivity is shown in Fig. 12, monitoring days are March 23 and 31, April 29 and May 19, 2011.

Fig. 13 shows the pattern of conductivity measured during the application of microwave radiation to a sandstone wall. The measurement was made on 25.2.2011, the air temperature was −10°C, weak snow showers occurred and the wind blew; the monitored part of masonry was exposed to weather effects. Fig. 9 (right) shows that not all probes were successfully installed into masonry at the same spacing, therefore changes in conductivity were evaluated, while already taking account of the length of the fictitious electrical conductor generated by transferring the driving signal to the paired electrode placed in the monitoring area. Fig. 14 shows maps of conductivity at different times of radiation and at three depths.

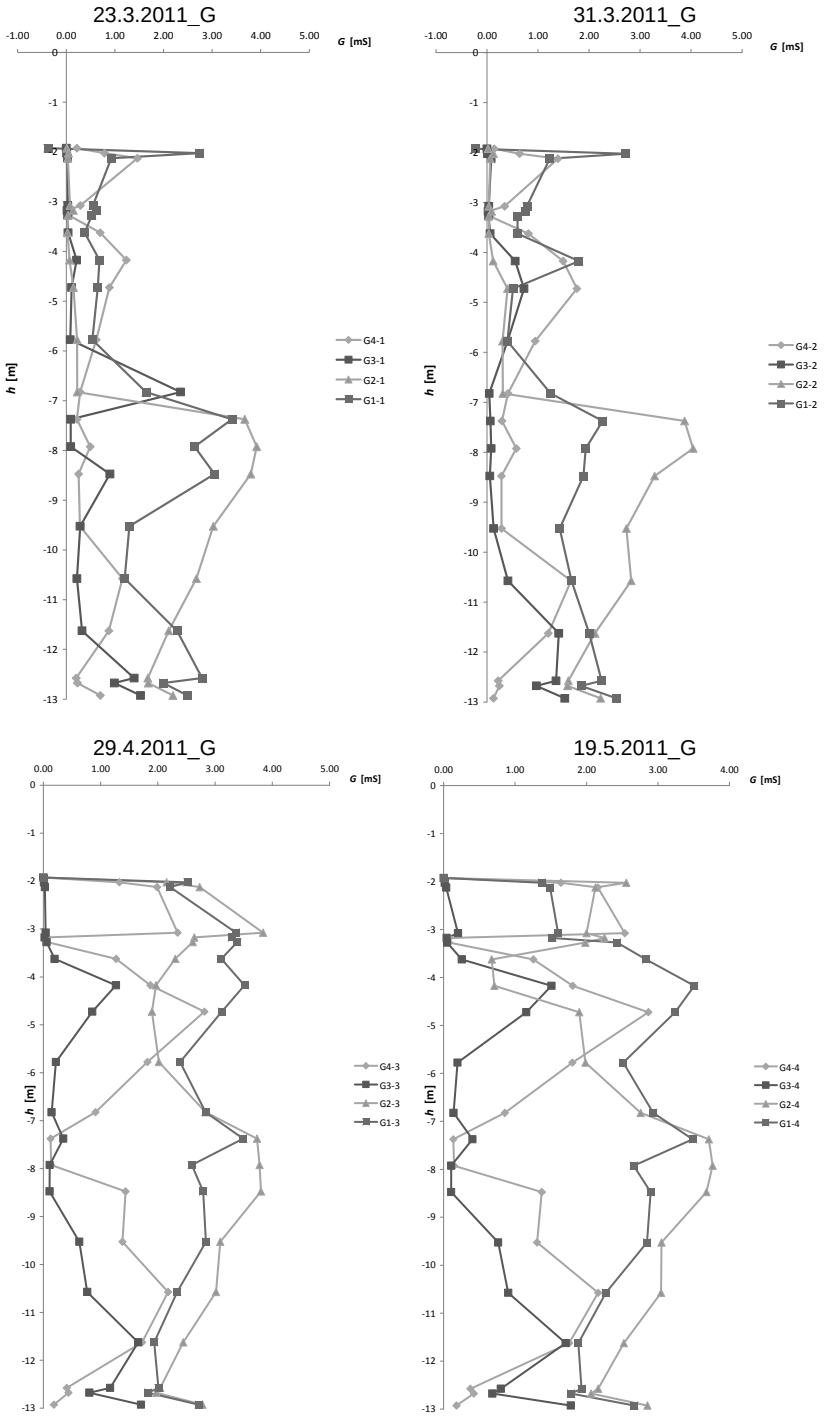

Fig. 11. Pattern of conductivity on individual rod-shaped probes

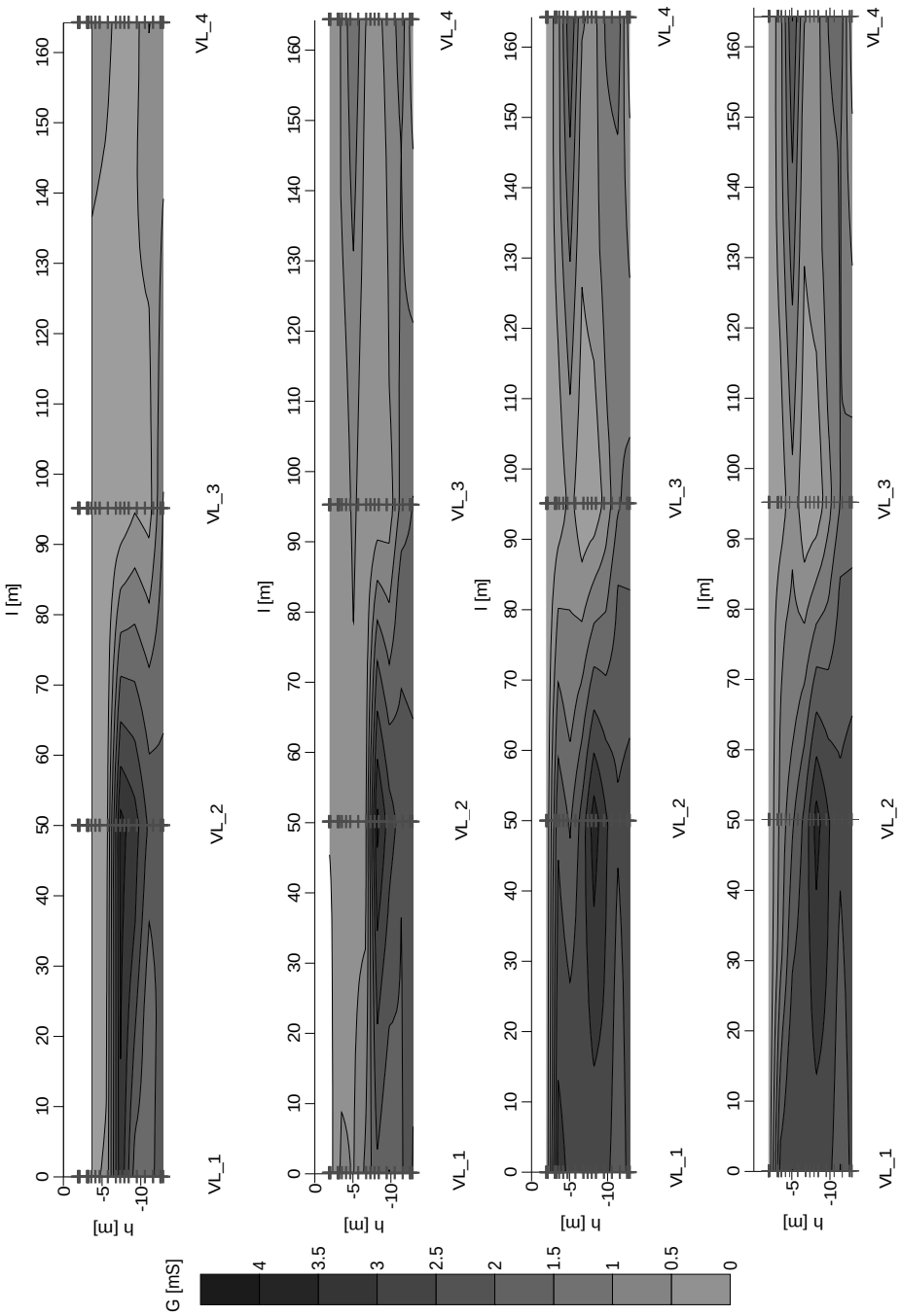

Fig. 12. Map of electrical conductivity in the area of interest, measurements made on 23.3., 31.3., 29.4. and 19.5.2011 (from top to bottom)

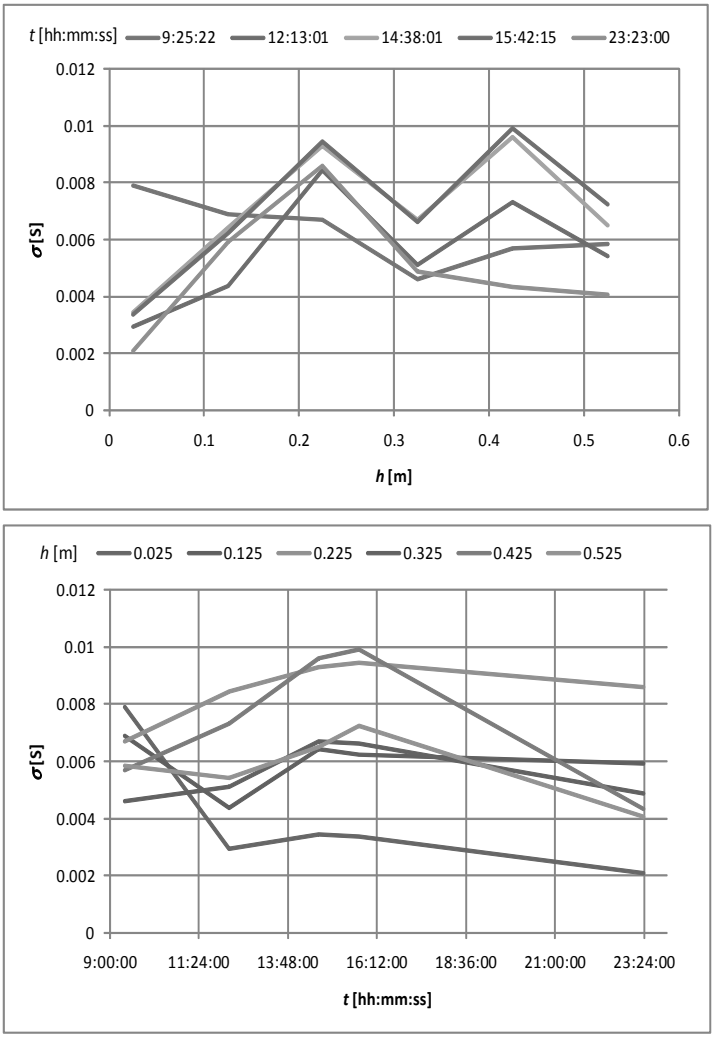

Fig. 13. Patterns of changes in conductivity in time and depth, profile 1_2 marked in Fig. 5

14.6. CONCLUSION

Measurements at both sites have confirmed the possibility of applying the EIS method to the monitoring of processes occurring in porous materials identifiable by the change in their impedance or electrical conductivity, including the use of the Z-meter III device.

Measurements at both sites were specific by the construction of the measuring probes. At the Karolinka Dam, measuring rods 13 m long were installed for the first time, which required the preparation of special procedures for their construction and installation. They were implemented as irretrievable because the condition of the proper function of the appa-

ratus was to secure the contact of the probe with the monitored environment and, moreover, the same position of the reader was thus achieved over the whole duration of monitoring. The measurements made can be considered as pilot ones at the given site, and the evaluation of monitoring in relationship to the other monitored variables will certainly be interesting.

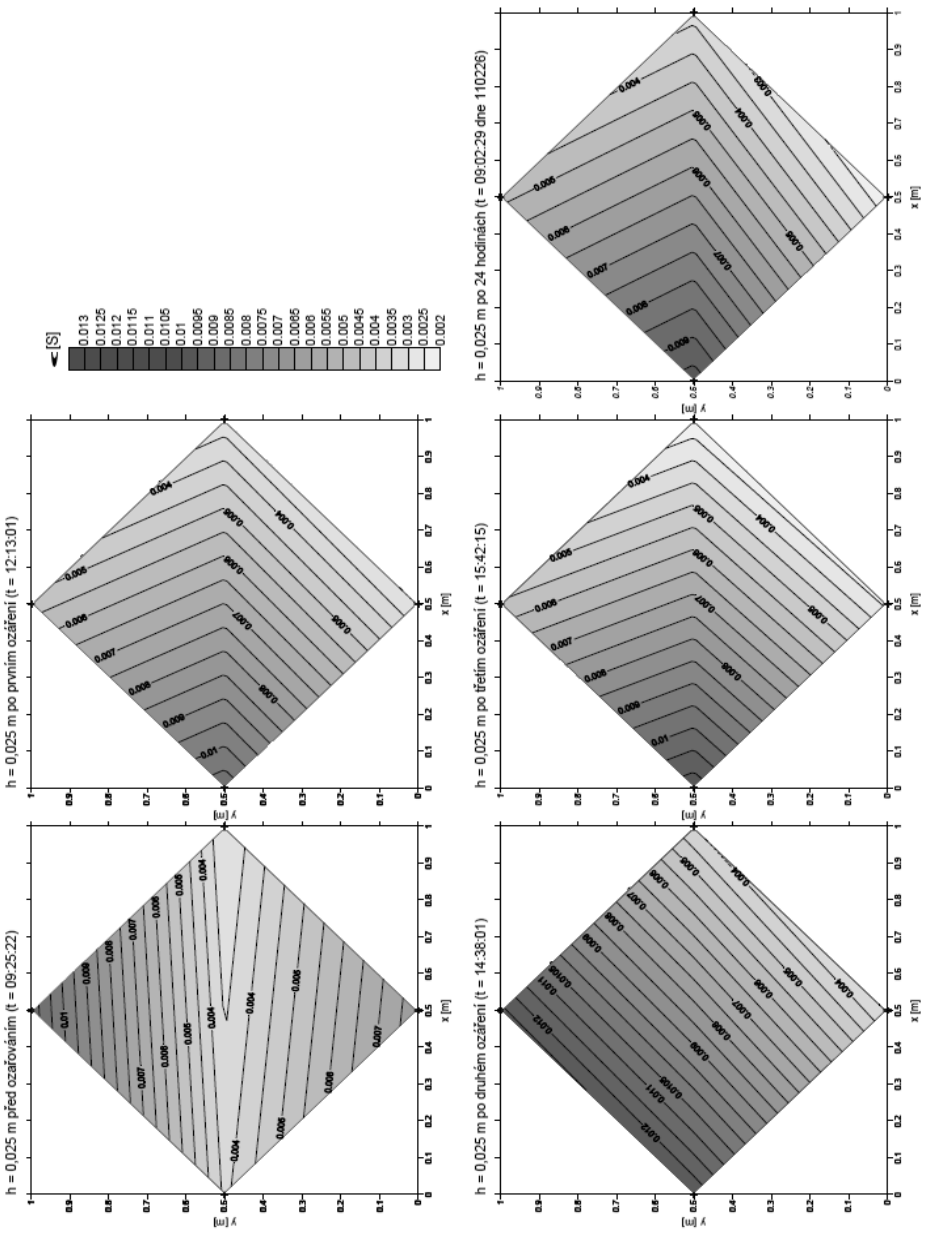

changes of the conductivity in the depth h = 0.025 m below the surface in different time

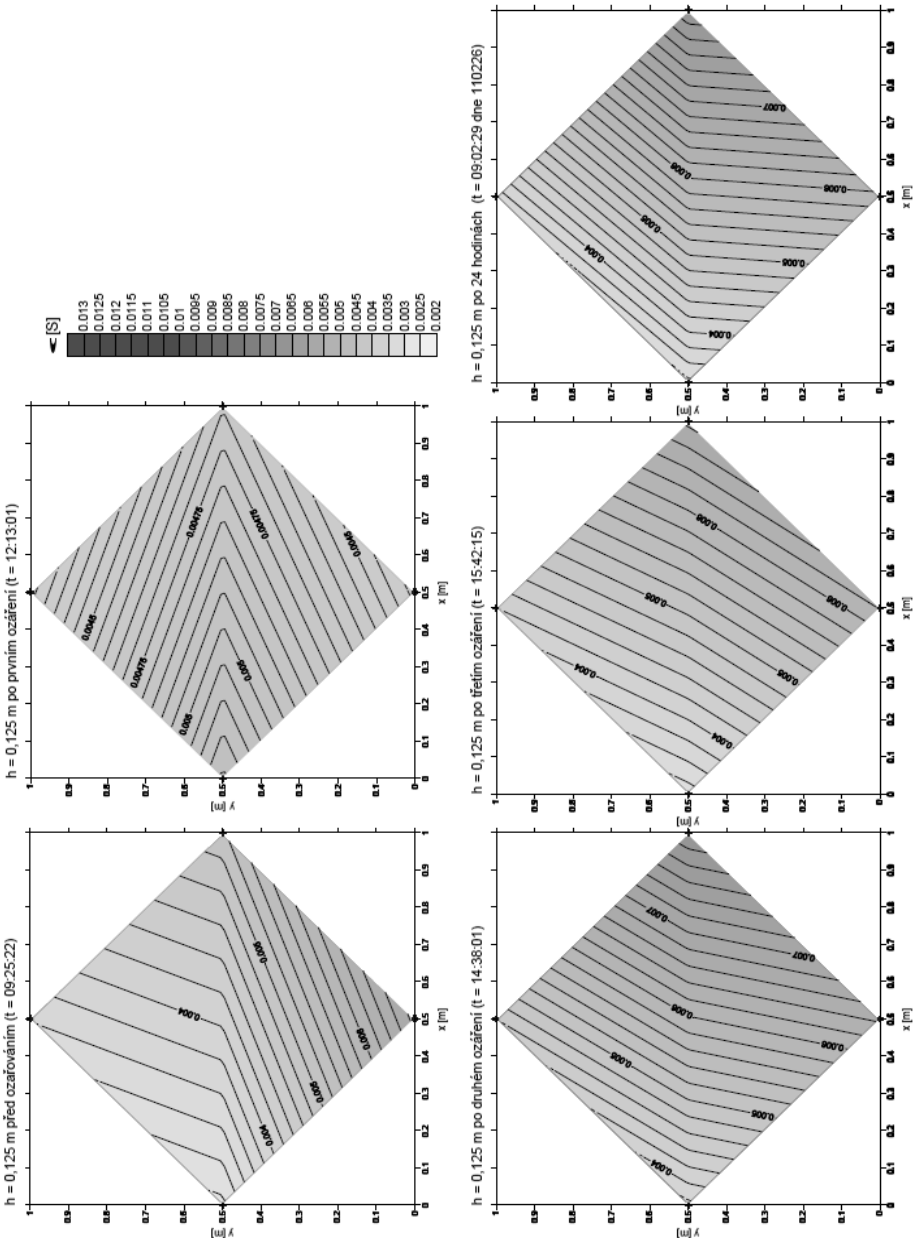

changes of the conductivity in the depth h = 0.125 m below the surface in different time

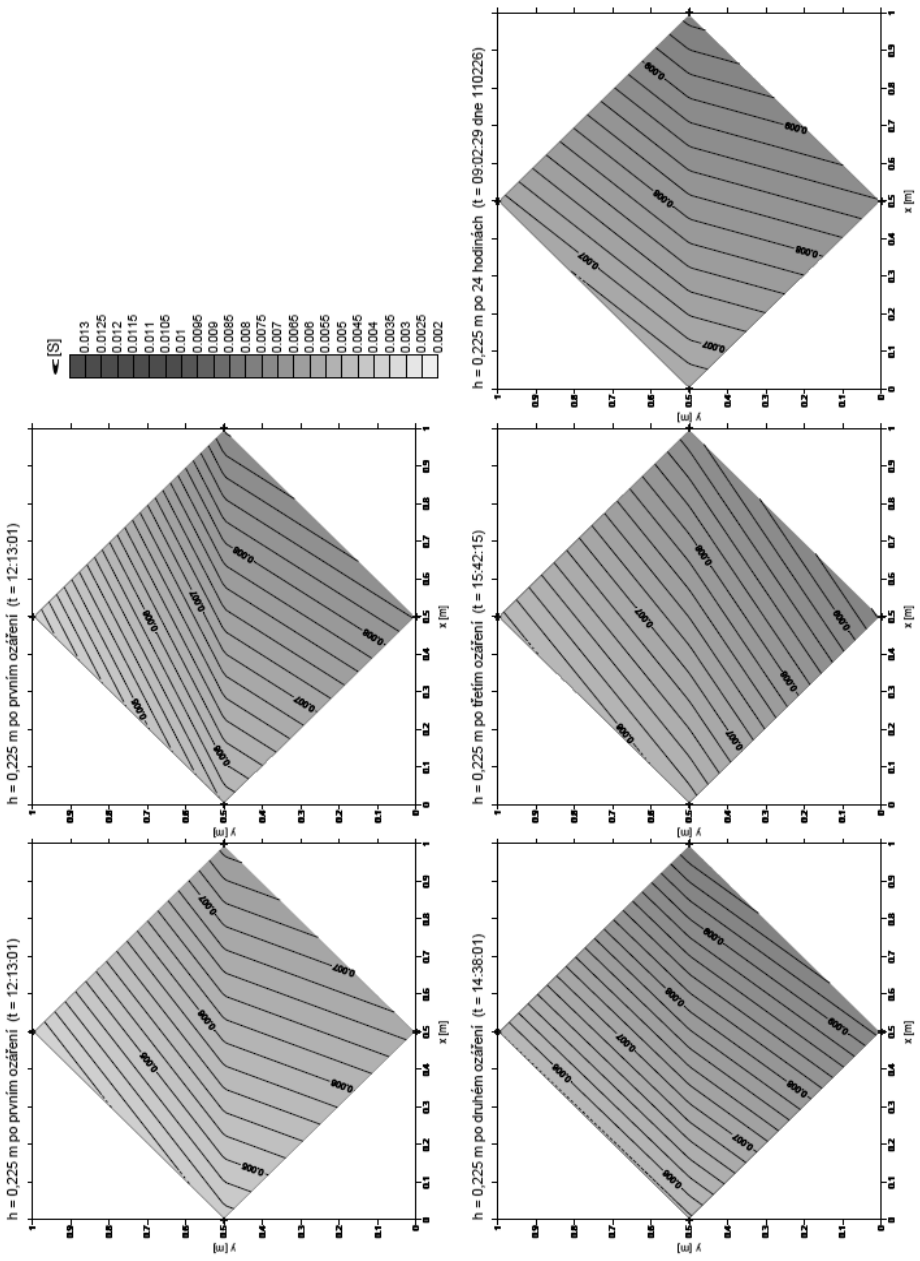

Fig. 14. Maps of conductivity with increasing depth

The probes for the indirect monitoring of changes in moisture of the stone masonry also required a special construction and particularly quite different procedures in their installation. They were implemented as removable but remained in one position over the whole duration of measurement (repeatability of measurements). The evaluated results

show, and it is also likely due to weather effects, that microwave heating caused the little crystals of water in sandstone to dissolve, which is recorded by the increased conductivity in the layer at a depth of 0.025 m. Due to the fact that the heating was made as point heating (in all, 16 points in the area of interest) and the displacement between the points was controlled by a PC, it is also possible to monitor these changes in the maps of conductivity.

References

[1] Davis J. L., Topp G. C., Annan P.: Measuring soil water content in situ using time-domain reflectometry techniques. Geol. Surv. of Canada, Pap. 77-1Bpp. 33–36, 1977.

[2] Fenton G. A., Griffiths D. V., and Cavers W.: Resistance factors for settlement design, Canadian Geotechnical Journal, 42(5), pp. 1422–1436, 2005.

[3] Beneš V.: Geofyzikální metody vhodné pro rychlý průzkum stavu zemních hrází (Geophysical methods suitable for a quick survey of the state of earth-fill dams). Firemní materiál dostupný na (Company material available at) www. gimpuls.cz. 2009.

[4] Pařílková J. a kol.: Optimalizace metod monitorování volné hladiny a jejího působení v zemních hrázích (Optimization of methods for monitoring the unconfined water table and its action in earth-fill dams). Dílčí zpráva projektu GA ČR (Sub-report of a project of the Grant Agency of the CR) 103/04/0741, LVV ÚVST FAST VUT v Brně, (Laboratory of Water-Management Research of the Institute of Water Structures at the Faculty of Civil Engineering of Brno University of Technology) 2005.

[5] Gomboš M., Tall A., Kandra B., Pařílková J.: Calibration of Z-meter device for measurement of volumetric moisture of soils. EUREKA 2009. ISBN 978-80-214-3969-6, pp. 77–87, 2009.

[6] Šoltész A., Baroková D.: Analysis, prognosis and design of control measures of ground water level regime using numerical modelling, Podzemná voda, XII, SAH, Bratislava 2006, No.2, pp.113–123, 2006.

[7] Šoltész A., Baroková D., Hašková L.: Optimalizácia vodného režimu na Medzibodroží (Optimization of the water regime in the Medzibodrog Basin). Acta hydrologica slovaca 8. 2: pp. 173–181, 2007.

[8] Štekauerová V., Nagy V., Šútor J., Milics G., Neményi M.: Influence of groundwater level on soil water regime of Žitný ostrov. In V. Növénytermesztési Tudományos Nap – Növénytermesztés: Gazdálkodás – Klimaváltozás – Társadalom. Budapest: Akadémiai Kiadó, ISBN 978-963-05-8804-1, pp. 197–200, 2009.

[9] Pařílková J., Pavlík J.: Automatizovaný systém pro analýzu vybraných charakteristik a procesů v porézním prostředí metodou EIS. Dílčí oponovaná zpráva projektu za rok 2010 (An Automated System for Analysis of Selected Characteristics and Processes in a Porous Environment Using the EIS Method. A partial report of the Project OE10002 for the year 2010 externally examined), Brno 2010.

Acknowledgements (if necessary)

Thanks are due to the project E!4981 “An Automated System for Analysis of Selected Characteristics and Processes in a Porous Environment Using the EIS Method”, to the Cluster CREA and the Company Thermo Sanace, Ltd.

Appendix:

Fig. 15. View of the downstream face of Karolinka embankment Dam

Next philosophy of the monitoring is to show the relation of electrical conductivity with free water level in dam, temperature and others measured parameters. From the crown of the dam were carried out four penetrating probes using the Marchetti dilatometer for verify the homogeneity of the kernel. Furthermore, into the sealing core of the dam in 4 core holes, which were dug to a depth of 20.0 meters, were stored in the levels of 13.0 m and 20.0 m piezometer equipped for long-term monitoring of pore pressures.

As well as other building materials are tested for suitability of the EIS method for measurement of moisture changes.

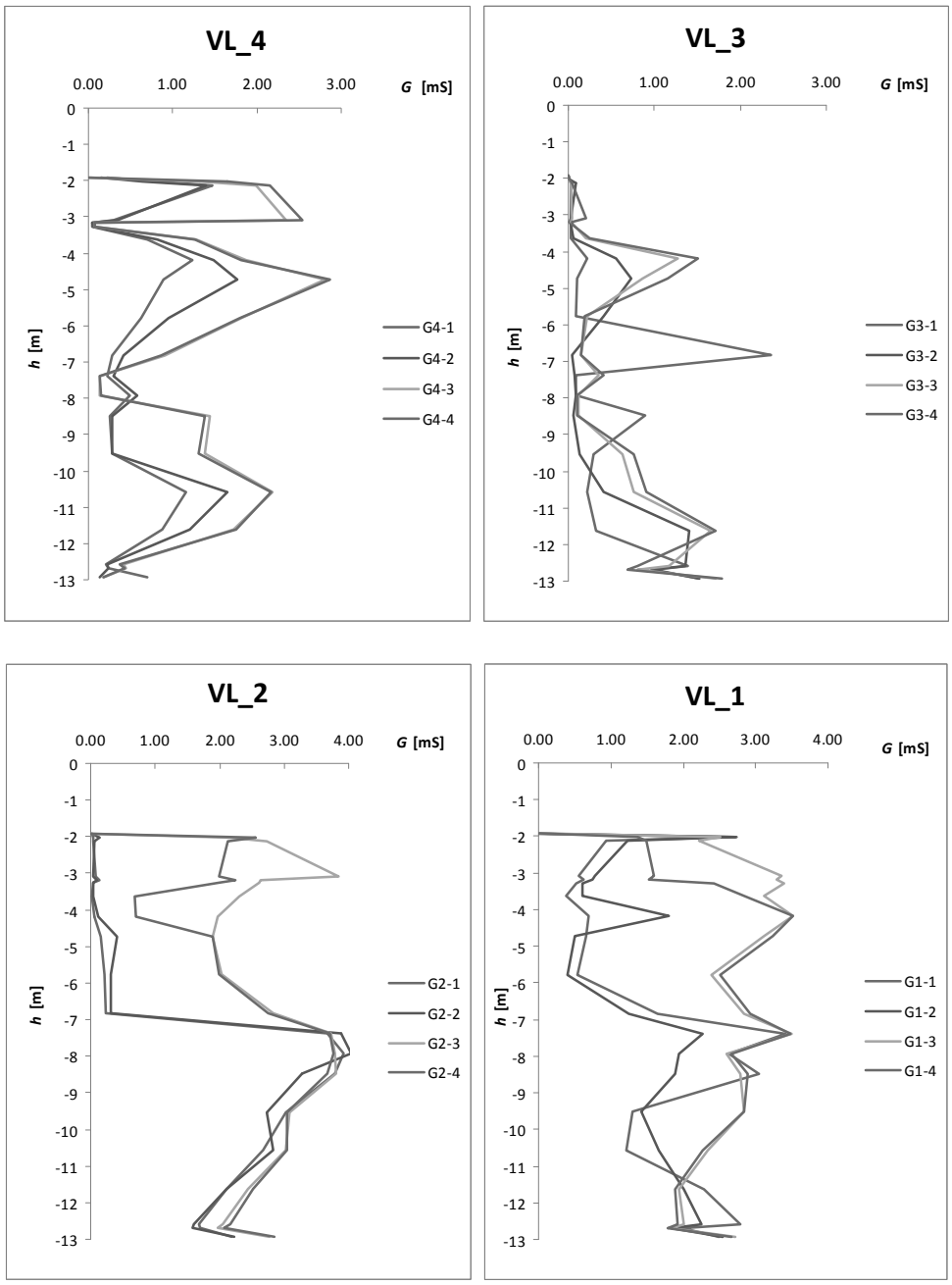

Fig. 16. The changes of conductivity measured in time on each rod probes (Karolinka Dam)

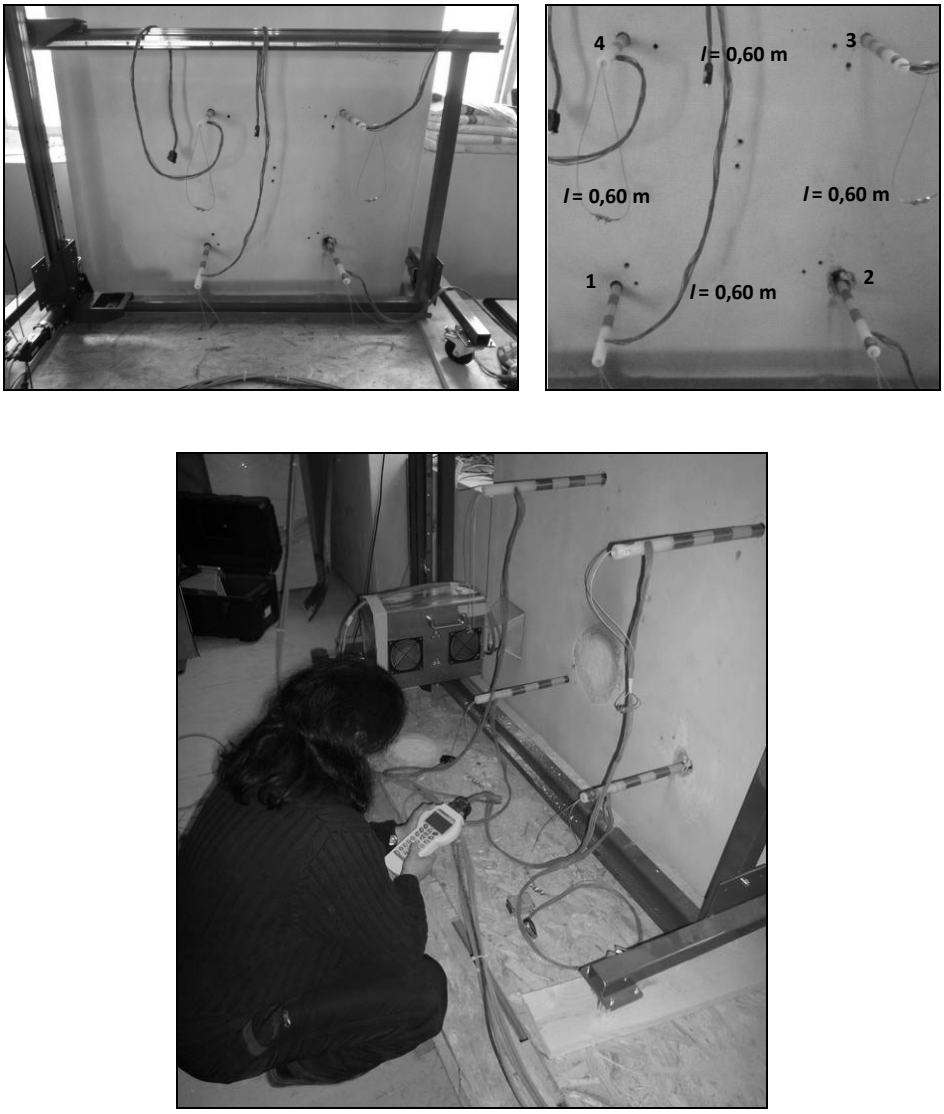

Fig. 17. The impedance measurement (damage to the wall during the application of microwave radiation to a mixed masonry)

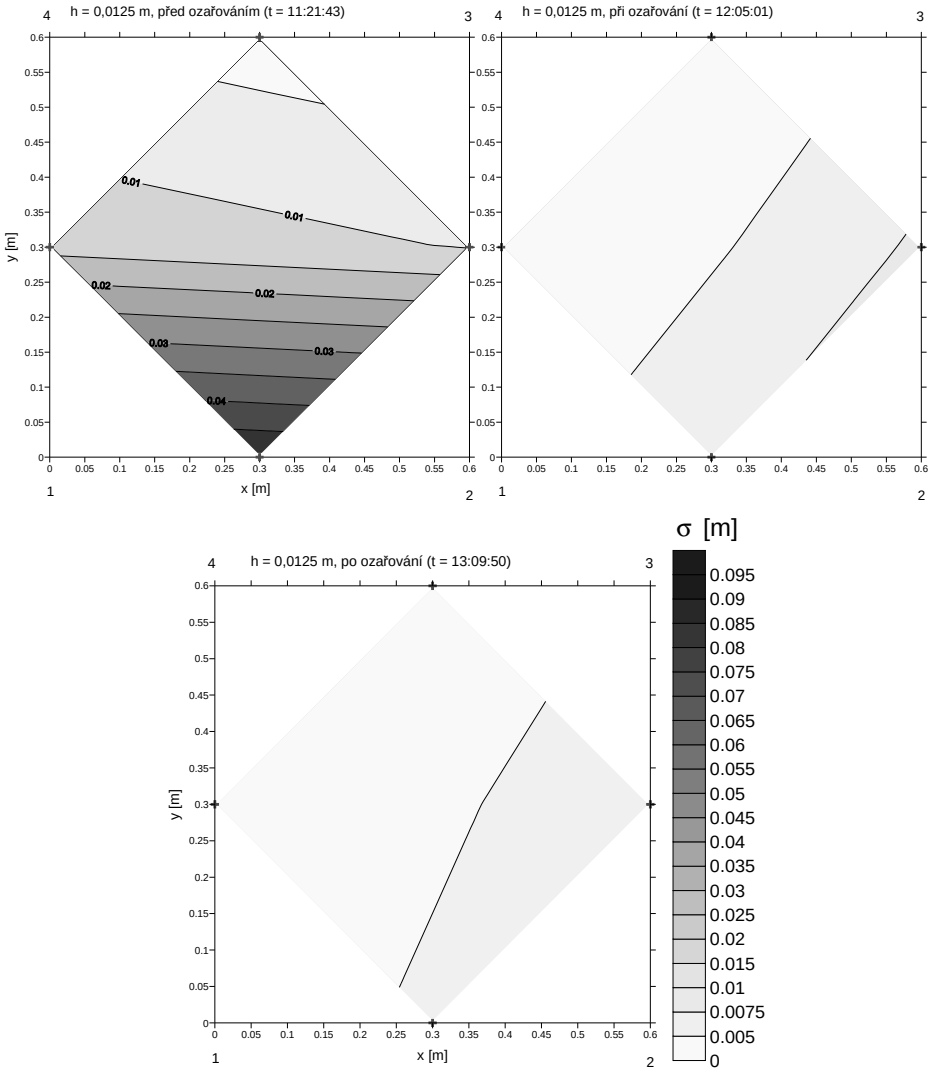

Fig. 18. Maps of the conductivity in depth h = 0.0125 m (mixed masonry)

15 Method for Determining the Optimal Solution for Disposing of Wastewater in the Upper Course of River Treska

Petko Pelivanoski, Zivko Veljanovski, Goce Taseski (University "Ss. Cyril and Methodius", Faculty of Civil Engineering – Skopje)

15.1. INTRODUCTION

As a candidate for the European Union Republic of Macedonia has an obligation to develop national action plan for natural environment protection. So the main purpose of this text is capturing and treating waste waters in the communities in the Kicevo region in order to obtain relevant inputs for protection of the environment which are necessary for strategic plan for regional development of this places, and also better water quality in river Treska in her upper part, because this is main resource for filling the accumulations "Kozjak" and "Matka" which in the future may be the main water suppliers for big part of the country.

In this paper are being analyzed three possible conceptions for developing a sewer system for this region. In all three possible conceptions for developing a sewer system, for rising ground places that are farther away from the rivers "Treska", "Zajaska" and "Temnica" no difference how big there are, it is being planned construction of local sewer systems with purifying station for waste waters only for one settlement or more of them combined together.

For the other communities nearby rivers "Treska", "Zajaska" and "Temnica", there are three possible conceptions for sewer system.

This paper should give the answer which of these possible conceptions for developing sewer system is optimal considering many of the analyzed standards. Besides technical and technological solution, the positive influence of the quality of the water in river "Treska" well is measured by national standards and European directives for that part.

The technical solution well be followed by technical economical analysis.

Main gold of this paper is to found the basic concept of sewer systems in Kicevo region which is consisted of six municipalities in witch according to the census in 2002, there was 61.300 citizens and according the evaluation in 2060 there well be 110 000 citizens. In this paper every community in Kicevo region is being analyzed and that should give the answer how accepting, taking away and purification of waste water should be done, before giving it to the recipients.

15.2. PRESENT CONDITION OF SEWER SYSTEMS IN THE REGION

Up until now, in Kicevo region, and other places in the country there is not much done on this subject. The waste waters in the communities, in most of the chases are let directly in the pipes without any purification. Figure 1.

Having this in mind and how it effects the quality of the water and flora – fauna in the water it is necessary to take appropriate measures to make the present situation better meaning to significantly reduce the permanent emission of waste water on a daily bases.

Fig. 1. Direct flowing of waste waters

Fig. 2. Kicevo River flowing through the waste

City of Kicevo as the biggest community has a partly develop sewer system, just for fecal waste waters, and for the other communities in the region the construction of sewer systems is just starting. Waste waters from homes are directly distributed to the recipients.

Subject of this paper, as it was said is capturing and treating waste waters in the communities of this region, but it is important to mention that the condition of treatment of solid waste is chaotic which can be seen from Figure 2.

From the figure it can be seen that solid waste without any treatment is storing nearby Kicevo River which directly influence the quality of the water in the river. Therefore our recommendation is urgent dislocation of the waste in order to reduce the effect on the quality of the water.

15.3. CONCEPTION OF SEWER SYSTEMS

Whit this paper it should be determent optimal solution for treating waste waters from communities in Kicevo region (Communities: Kicevo, Zajas, Oslomej, Drugovo, Vranesnica, Plasnica) with collector systems, treating, purifying and sending water to the recipients.

The system well cover communities relatively close one to another for which there is engineer purport and economic justification to be linked with one sewer system for purifying waste water. There are three developed variants for two systems (Kicevo and Plasnica):

Variant 1

Centralized sewer system. In this variant two big waste water treatment stations should be building. First waste water treatment station is near Kicevo for waste water of communities: Zajas, Oslomej, Kicevo and Drugovo. Second waste water treatment station is located near village Plasnica for waste water of communities Vranesnica and Plasnica. Figure 3.

Variant 2

Group decentralized sewer system. In this variant there should be build several group sewer systems with suitable waste water treatment stations. In Zajas there should be two sewer systems with two waste water treatment stations. In Oslomej there shoul be three sewer systems with three waste water treatment stations. Kicevo well merge with the sewer system in Drugovo in one waste water treatment station. In Vranesnica and Plasnica there should be one sewer system with suitable purification station.

Variant 3

Great number of local sewer systems. With this variant there should be maximum decentralization of the sewer systems. That means approaching the locations of waste water treatment stations to the communities. With this variant there should be one bigger, and great number of smaller waste water treatment stations. In this variant the length of the sewer collectors should be minimal.

Fig. 3. Conception for sewer system (Variant 3)

15.4. CRITERIONS FOR SELECTING THE BEST CONCEPTION

Defining the optimal conception for sewer system, centralized, group decentralized and fully decentralized is based on the following criterions:

Investment cost for building the system

The investment necessary for building the collectors is planed with previous analysis of cost for sewer system based on the diameter of sewer pipe. Whit this price we get the total necessary investments for building the collectors. From the analysis we can conclude that centralized system has the biggest investment cost for building sewer collectors and that the smallest investment is for fully decentralized system. For waste water treatment stations necessary investment is planed according the number of citizens for whom this waste water treatment station is build. Estimated cost of WWTP for equivalent citizen is based on experience of cost for stations that are already build in Macedonia and in the region. WWTP investment cost is opposite of the one for collectors, smallest for centralized system and biggest for decentralized system. With the investment cost for collectors and WWTP we can determent total investment cost for all three variants. In the Table 1 display the total investment costs for the system for all variants.

Table 1

Total investment cost for all variants

WWTP	Variant	Investment costs [€]
KICEVO	VARIANT 1	17 000 000
	VARIANT 2	16 800 000
	VARIANT 3	17 500 000
PLASNICA	VARIANT 1	2 600 000
	VARIANT 2	2 400 000
	VARIANT 3	2 100 000

Operating (Annual) costs

Operating costs for collectors are: maintenance of collectors and pump stations, spending for staff – employers, amortization, and unanticipated costs and paying bank credits. Operating costs for WWTP are: maintenance, staff – employers, spending energy, amortization, chemical costs, unanticipated costs and bank credits.

The same way investment cost is calculated for collectors and WWTP. Operating costs is being planned and also total operative cost for the system in all three variants. Further on, economic analyses have been made for the operating costs for collectors and water treatment plants for all the alternative solutions of the system. The following three variants are studied in this analysis:

I. Using a Bank Loan Including Depreciation;
II. Donation Funds Including Depreciation and
III. Donation Funds without Depreciation.

In continuation, the total operating costs for the variants are given in the next tables for all the analysed variants of the system.

Table 2

Total operating costs with a bank loan including depreciation

WWTP	Variant	Operating costs [€]
KICEVO	VARIANT 1	2 600.000
	VARIANT 2	2 700.000
	VARIANT 3	2 850.000
PLASNICA	VARIANT 1	400 000
	VARIANT 2	410 000
	VARIANT 3	400 000

Table 3

Total operating costs with donation founds including depreciation

WWTP	Variant	Operating costs [€]
KICEVO	VARIANT 1	1 100 000
	VARIANT 2	1 200 000
	VARIANT 3	1 350 000
PLASNICA	VARIANT 1	165 000
	VARIANT 2	190 000
	VARIANT 3	210 000

Table 4

Total operating costs with donation founds without depreciation

WWTP	Variant	Operating costs [€]
KICEVO	VARIANT 1	470 000
	VARIANT 2	570 000
	VARIANT 3	630 000
PLASNICA	VARIANT 1	75 000
	VARIANT 2	105 000
	VARIANT 3	130 000

Net present value (NPV_{30}) after thirty years

Net present value is most frequently used method to determent present value of future investment in order to find alternative solutions for systems of capital importance.

The *NPV* is determined in tables and the final results from the estimates made are given in this paper for all the analysed variants for net present value of the system after 30 years that are shown in the following tables.

Table 5

NPV_{30} of the system with a bank loan including depreciation

WWTP	Variant	NPV_{30} [€]
KICEVO	VARIANT 1	52 000 000
	VARIANT 2	53 000 000
	VARIANT 3	56 000 000
PLASNICA	VARIANT 1	8 000 000
	VARIANT 2	8 000 000
	VARIANT 3	7 500 000

Table 6

NPV_{30} of the system with donation founds including depreciation

WWTP	Variant	NPV_{30} [€]
KICEVO	VARIANT 1	33 000 000
	VARIANT 2	34 000 000
	VARIANT 3	36 500 000
PLASNICA	VARIANT 1	5 100 000
	VARIANT 2	5 250 000
	VARIANT 3	5 200 000

Table 7

NPV_{30} of the system with donation founds without depreciation

WWTP	Variant	NPV_{30} [€]
KICEVO	VARIANT 1	24 000 000
	VARIANT 2	25 000 000
	VARIANT 3	27 500 000
PLASNICA	VARIANT 1	3 800 000
	VARIANT 2	4 000 000
	VARIANT 3	4 000 000

Cost – Benefit analysis

Cost – Benefit analysis was used to predict the price of m^3 purified waste water which is paid by the users of the system and the public company managing the system well work with minimum profitability. According to this analysis, smallest price of m^3 purified waste water is for the centralized sewer system and the highest price for decentralized system.

Regional range of the system

In the future it is thought that every system of this tip well have the tendency for regional range. Having this fact in mind we give advantage to centralized systems before decentralized systems.

Managing the system

This systems well be managed for a long period of time, they are also very complex so they should be made in a way in which the management well be easier. In this paper it's predicted that centralized system with smallest number of WWTP stations is much easier to manage than decentralized system with many WWTP stations.

Flexibility of hydraulic capacity of the purification station

With this component we value the opportunity for future expansion of the purification station meaning expending its capacity. It is predicted that larger purification stations have a better chance of expending its capacity comparing to smaller WWTP.

Processing sludge in purification station

In this paper it's predicted that only larger WWTP have treatment of sludge. The sludge from other purification stations well be transported to the station that has capacity for this kind of treatment.

Effect on the natural environment

There are no negative effects on natural environment during construction of collectors and WWTP stations because this is a short-term condition. Benefits of building the system in terms of protection of human environment are grand. Biggest protection of natural environment is made with centralized systems with small number of WWTP, meaning that during exploitation of the system probability of defects is smaller. All waste waters are accepted opposed to the recipients and distributed in one location and there is a very small chance of uncontrolled flowing of waste water in many locations.

15.5. SELECTION OF THE OPTIMAL SOLUTION

Watercourse regional protection optimal solution selection in a situation of several elaborated alternative solutions can be made through the multi-criteria ranking method. This method ranks the considered alternatives (a_1, a_2, a_3 … a_j) and on the basis of determined measures and criteria (f_1, f_2, f_3 … f_i). Each alternative should be evaluated in terms of all the considered criteria. If the value of the i-criterion related to the alternative a_j is marked as f_{ij}, in that case the alternative a_j will be better than the alternative a_k according the i-criterion if $f_{ij} > f_{ik}$:

$$a_j > a_k;\ f_{ij} > f_{ik}, \text{ where } i = 1, 2, 3 \ldots N\ \ j = 1, 2, 3 \ldots J$$

The method of interactive compromise optimal ranking „ICOR" related to the multi-criteria ranking of the alternative solutions is developed on the basis of compromise programming. Multi-criteria ranking by means of this method is made on the basis of the following expression:

$$Q_j = v_1 \cdot (S_j - S^*)/(S^- - S^*) + v_2 \cdot (R_j - R^*)/(R^- - R^*)$$

Where:

$$S_j = \sum W_i \cdot (f_i^* - f_{ij})/(f_i^* - f_i^-)$$

$$Rj = \max W_i \cdot (f_i^* - f_{ij})/(f_i^* - f_i^-)$$

$$S^* = \min S_j;\ S^- = max\ S_j;\ R^* = min\ R_j;\ R^- = \max R_j$$

$$f^* = \max f_{ij}\ \ and\ \ f^- = \min f_{ij}$$

In the above expression the index $j = 1, 2, 3 \ldots J$ is the number of elaborated alternatives and the index $i = 1, 2, 3 \ldots N$ is the number of elaborated criteria.

It is assumed that the alternative a_j will be better than the alternative a_k according to the i- criterion if $f_{ij} > f_{ik}$. With the multi-criteria ranking by the ICOR method the alternative a_j will be better than the alternative a_k if $Q_j < Q_k$ that is $q(a_j) < q(a_k)$. The position $q(a_j)$ on the rank list depends on the values of f_{ij}, f_i^* and f_i^-. The values of f_i^* and f_i^- are the values of the worst and the best alternative according to the elaborated criterion.

Table 8

Weighted impact matrix for the best Variant 1) – WWTP Kicevo

No	Criteria	Value	Unit	Classification										Σ
				1	2	3	4	5	6	7	8	9	10	
1	Number of population covered by the system	86 000	population											
2	Length	47 0	km			x								3
3	Investmen cost for collectors	5 100 000				x								3
4	Operating costs for the collector	160 000	/year				x							4
5	Pump stations	1	number		x									2
6	nvestmen cost for WWTP	12 000 000									x			8
7	Operating costs for WWTP	930 000	/year									x		9
8	NPV 2040	33 000 000								x				7
9	Flexibility of the hydraulic capacity of the WWTP										x			8
10	Flexibility of the capacity for eliminating the pollution of WWTP											x		9
11	Sludge processing in WWTP											x		9
12	Proportion of investments of collector/WWTP	43	%					x						5
13	Regional coverage of the system											x		9
14	Energy consumption	2 400 000	kWh								x			8
15	Energy production							x						5
16	System management											x		9
17	Environmental impact										x			8
18	Total													106

Depending on the meaning we can introduce various weight factors of particular criteria ($w_1, w_2, w_3 \ldots w_n$). The weight factor values should be $\sum W_i = 1$ and ($w_i > 0$).

The ICOR method makes possible for the decision making strategy to be more signifi-

cant v_1 and v_2 (where $v_2 = 1 - v_1$). We take $v_1 > v_2$ when we want to give advantage to the meeting more criteria and not taking into account that one criterion is not met. If we don't allow complete unsatisfying according to any criterion, we should add bigger value to v_2 in the expression Q_j.

Table 9

Weighted impact matrix for the best Variant (1) – WWTP Plasnica

No	Criteria	Value	Unit	Classification										Σ
				1	2	3	4	5	6	7	8	9	10	
1	Number of population covered by the system	8 800	population											
2	Length	14 5	km			x								3
3	Investmen cost for collectors	1 000 000				x								3
4	Operating costs for the collector	40 000	/year							x				7
5	Pump stations	2	number	x										1
6	nvestmen cost for WWTP	1 600 00									x			8
7	Operating costs for WWTP	130 000	/year									x		9
8	NPV 2040	5 100 000								x				7
9	Flexibility of the hydraulic capacity of the WWTP										x			8
10	Flexibility of the capacity for eliminating the pollution of WWTP											x		9
11	Sludge processing in WWTP									x				7
12	Proportion of investments of collector/WWTP	68	%		x									2
13	Regional coverage of the system											x		9
14	Energy consumption	310 000	kWh								x			8
15	Energy production							x						5
16	System management											x		9
17	Environmental impact										x			8
18	Total													103

Giving various values to the weight factors (particularly for each criterion) and changing various decision making strategies (group or individual favor) we can analyze the stability of position of individual alternative on the multi-criteria rank list. The analysis of these criteria has been done in the form of severity matrices where the criteria are assessed with the advantages and disadvantages, with indicators from 1 (in red) to 10 (in green) depending on the impact of the component. Indicator 1 is the weakest, i.e. the most negative

indicator, and indicator 10 is the best, i.e. the most favourable indicator. The indicator between 1 and 10 are indicators with impacts between the most severe and the most favourable impact. In the next table display the weighted impact matrix for assessment of the criteria for selecting the most favourable solution.

15.6. CONCLUSION

Choosing the optimal conception of sewer system for protection of southwest region of Macedonia, in the upper course of river Treska should be made by analyzing many criterions, not just by one – investment value of the system. One of the ways of choosing the best conception is the method of multi criterion optimization.

We can conclude that best conception for protection of this region from waste waters from homes is centralized sewer system with two waste water treatment stations – WWTP Kicevo and WWTP Plasnica.

Collector system that gravitates towards WWTP Kichevo collects and drains the waste waters from the settlements: Bigor, Dolenci, Srbjani, Drugovo, Kichevo, Osoj, Rashtani, Mamudovci, Lazorovci, Trapchin Dol, Strelci, Garani, Crvivci, Shutovo, Premka, Oslomej, Srbica, Zhubrino, Arangel, Tuin, Dlapkin Dol, Kolibari, Greshnica, Zajas, Dolno Strogomishte, Gorno Strogomishte and Colari. The total capacity of WWTP Kichevo is a total of 86 000 PE, and the total length of the collector system is 47 km. The collector system is almost entirely gravitational, and only one pump station is provided for the surrounding of the settlement Srbjani with Q = 5.0 l/s and N_{man} – 8 m.

The water treatment plant under Kichevo (WWTP Kichevo) is located near the mouth of Kicevo River in the river Treska.. Advanced technology has been proposed for the reduction of nitrogen and phosphorus (pre-anoxic denitrification – modified method of Ludzack – Ettinger) with anaerobic stabilisation of the sludge and usage of the methane for covering part of the energy needs of the water treatment plant.

Smaller water treatment plants which will be constructed in the settlements not connected to the centralized sewerage system will perform waste water treatment. The sludge which will be removed through the processes of the plants will be transported to WWTP “Kichevo”.

Waste waters form the settlements Vraneshtica, Atishta, Lisichani, Chelopeci, Dvorci, Preglovo and Plasnica are accepted and drained to one common waste water treatment plant located downriver to the settlement Plasnica – WWTP Plasnica. The total length of this system collectors amounts 14.5 km; two pump stations are planned in the downriver direction from the settlement Lisichani with Q = 27.0 l/s and H_{man} = 8 m, the number of citizens covered by this system is 8.800 PE, and a waste water treatment plant from the type II R-D-N (regeneration, denitrification, nitrification) is planned for this number of citizens.

Reference

[1] Feasibility study for waste water drainage from the Kicevo Micro-region, 2011.
[2] Syed R. Qasim, Wastewater Treatment Plants – Planning, Design, and Operation. London, New York, Washington, D. C.: CRC Press LLC 2000.
[3] Metclaf & Eddy, Wastewater Engineering – Treatment and Reuse, International fourth edition, by McGraw – Hill Higher Education 2003.
[4] Zivko Veljanovski: Vodovod I kanalizacija 2009.

16 Impacts from Waste Disposal Sites to Surface Waters

Cvetanka Popovska, Milorad Jovanovski (University of Ss Cyril and Methodius, Faculty of Civil Engineering, Skopje, Macedonia

16.1. INTRODUCTION

Collection, transport and landfill are the main methods for final disposal of almost each waste fraction. For obtaining healthy environment and human life identification of waste and current waste streams is very important. In Macedonia only approximately 70% of the population is involved in public municipal waste collection system. Collection of non-separated municipal and non-hazardous industrial waste, as well as non-separated non-hazardous and hazardous waste fractions is common practice. Scrap metals represent the biggest part of the collected recyclable materials. There are no formal collection systems for construction and demolition waste as well as for high-risk animal tissues from slaughterhouses and animal breeding farms. The level of management of hazardous and non0hazardous medical waste within the hospitals is generally low.

Table 1

Yearly-generated waste quantity

Type of waste	Estimated quantity (t/year)
Municipal waste	420 000
Commercial waste*)	150 000
Waste from healthcare institutions	1 000
Construction and demolition waste	500 000
Industrial non-hazardous waste	2 120 000
Industrial hazardous waste	77 500
Waste from mining	17 300 000
Waste from agriculture-animal by-products	4 900 000
Waste from agriculture-plant by-products	550 000
Used tyres	5 000
Used mineral oils	8 000
End-of-life vehicles	17 500
Used car batteries	3 500
Total	26 000 000

*) Waste constituents to those in household waste
Source: Waste Management Strategy of the Republic of Macedonia, Government of RM, 2008

Roughly estimated quantities of yearly-generated waste, including waste from mining, is shown in Table 1. Regarding quantities of generated municipal waste, one may expect waste quantities to rise by the rate of 1.7% per year depending on the dynamic of economic development in the country.

Estimated total amount of generated waste, inclusive of waste from mining amounts app. 26.0 million t/year. The main waste fractions arise from mineral excavation and ore processing (17.3 million t/year). This group of waste contains significant amount of hazardous constituents and improper landfills cause the most evident impacts on the environment. Wastes from agriculture represent the second biggest waste fraction manly addressed as by-products i.e. these types of waste represent "recyclable" fractions in agricultural activities. The management of animal by-products from slaughterhouses and dead animals on breeding farms is far from the requirements of EU regulations.

Municipal solid waste is one of the main generated waste streams (app. 570 000 t/year with prognosis of rising up-to 700 000 t/year in 2020 that is 285–350 kg/capita annually). This waste is consist of household wastes, street sweepings and green park wastes, commercial-institutional waste and wastes generated in industry with a household-like character. A small proportion of the household waste stream has hazardous properties (batteries with heavy metals and acids, oil-based paints). An important proportion of the general waste stream is contributed to by spent goods and of a variety of end-of-life products such as construction and demolition waste (app. 500 000 t/year), used tyres, end-of-life vehicles, electrical/electronic waste (app. 40 000 t/year).

Power plants, thermal metallurgical and inorganic chemical processes generate an additional group of non-hazardous waste with quantity of 2.0 million t/year. The main quantity of hazardous waste (app. 77 500 t/year) is generated by the two main metallurgical industries and is disposed on industrial landfill. They also represent environmental "hot-spots" regarding their impact on the environment.

16.2. GENERATED WASTE PROJECTION

Waste projection is performed in [7] National Waste Management Plan (NWMP) in the Republic of Macedonia (2009–2015) and in [10] Waste Management Strategy (WMS) of the Republic of Macedonia (2008–2020). The analysis is performed for four scenarios with methodology applied in most EU countries. A rise of generated waste is based on population growth and GDP projection. The effect of waste amount rise per capita on annual level is presented in Figure 1. The scenario "zero" growth considers waste production to grow proportional to population increase only. The scenario "low" growth is based on waste generation increase of 50%, population growth and 3% GDP increase. The scenario "medium" is as the previous one, only with 5% GDP growth. The scenario "high" growth is based on 5% GDP growth, but with proportional increase in waste generation per capita.

16.2.1. Landfills

In the Republic of Macedonia there are 55 active municipal landfills operating without permits. Only the landfill DRISLA that covers the region of Skopje (590 000 inhabitants) has the operational permit and is the only waste site compliant with national requirements.

However, even this waste site doesn't comply with contemporary technical standards or with the requirements of the EU Landfill Directive. Map of the existing municipal landfills with risk categorization is presented in Figure 2.

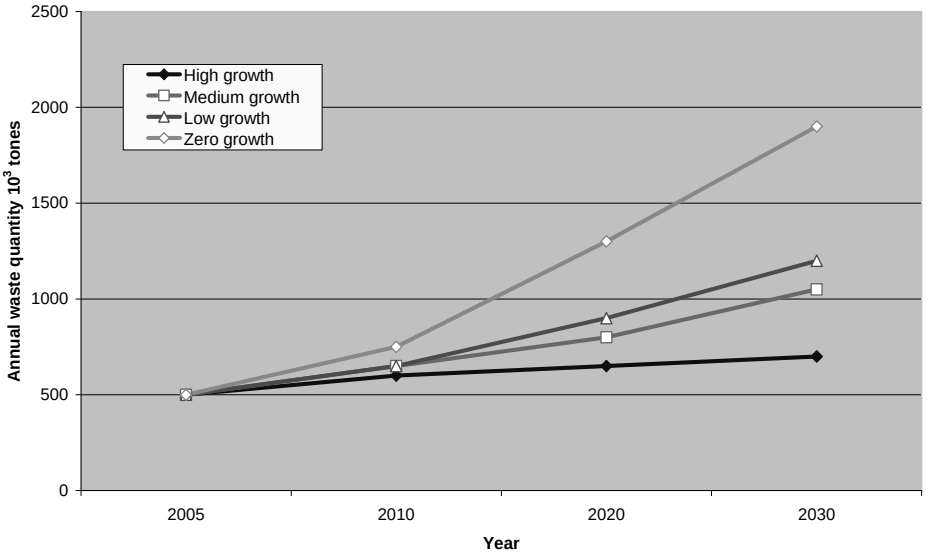

Fig. 1. Annual waste generation growth, Source: NWMP, (2008)

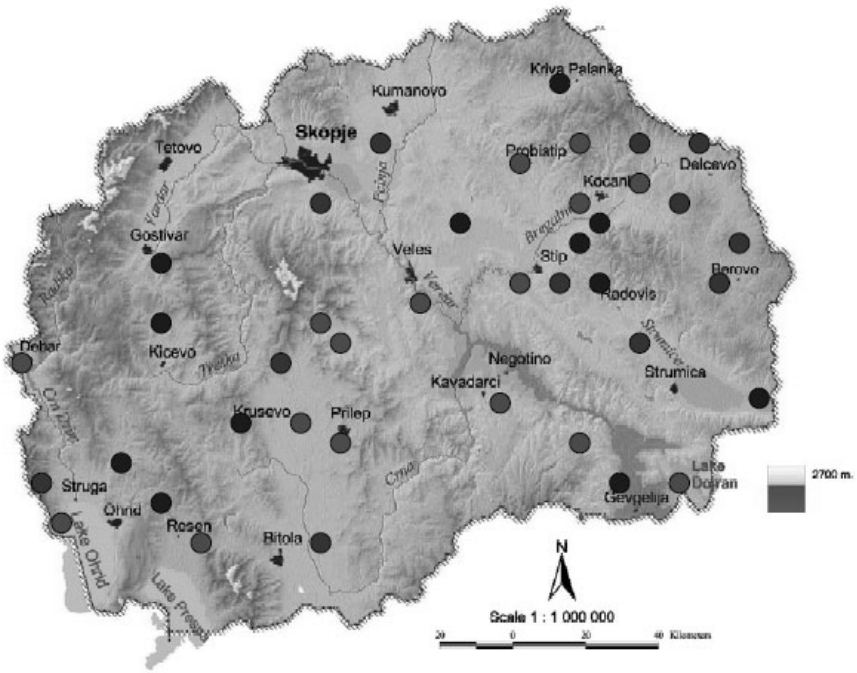

Fig. 2. Municipal landfills with risk categorization on the environment. Legend: red-high risk assessment, violet-medium risk assessment, green-low risk assessment

16.2.2. Impacts

Municipal landfills and wild dumps represent risk for the pollution of air, soil, surface water and groundwater, as well as potential risk for biodiversity, agricultural land and human health. An additional environmental problem is represented by the traditional burning on open air fires of municipal waste, plant tissue waste and plastics originating from greenhouses or silage coverage.

Existing waste disposal practices do not comply with any technical and/or environmental standards. Most of the existing municipal dump sites need to be closed since the site conditions and environmental impact do not allow them to be upgraded economically, to be harmonized with the EU standards.

Active municipal waste landfills are categorized according to the assessment of their environmental risk shown in Figure 1. According to this categorization 16 landfills are ranked with high risk, 16 with medium, and 19 with low environmental risk.

Table 2

Mining environmental hot-spots

Mining Environmental Hot Spot	Current status	Landfill waste quantity (m^3)	Landfill area (m^2)
BUCHIM (copper mine) – Radovis Open pit; Waste Rock Dump; Tailings	In operation	250 000000	900 000
MHK Zletovo (lead and zinc smelter) – Veles Tailings; Dumps	Out of operation	1 115 00	95 000
LOJANE (chromium, arsenic, antimony mine) – Kumanovo	Abandoned	1 000 000	95 000
SASA (lead and zinc mine) – Makedonska Kamenica	In operation	30 000 000	285 000
SILMAK (ferro-silicon plant, former HEK Jugohrom) – Jegunovce Tailings (Cr6)	Out of operation	851 000	80 000
Toranica (lead and zinc mine) – Kriva Palanka	Out of operation	3 000 000	25 000
ZLETOVO (lead and zinc mine) – Probistip	In operation	14 000 000	280 000
REK Bitola (thermal power plant and lignite mine) – Bitola.	In operation	11 000 000	100 000
FENI Industry (ferro-nickel smelter) – Kavadrci	In operation	2 200 000	167 000
REK Oslomej (thermal power plant and coal mine) – Kicevo	In operation	2 000 000	280 000

Source: NWMP, (2005)

The hazardous waste generated by Macedonian mining and processing industries faced severe problems during the transition period and many have stopped their activities, with no chance of being restarted in the near future. Their on-site process waste dumps were abandoned as well, and little or no information is available on the history of these dump sites. In

the frame of CARDS 2001 project for development of National Waste Management Plan (NWMP) with Feasibility Studies in total the following 16 Industrial Contaminated Sites – "hotspots" were identified and evaluated. Out of those, historical mining waste is presented in Table 2, including current status of operation.

Landfills, collection and disposal of all type of waste, and landfills management are a week point in environmental practices in Macedonia. Therefore, the impact of dump sites by having no construction and no control is a major problem for surface water pollution. Many of illegal dump sites are along the watercourses and in most cases the basic river channel is actually waste water and solid waste recipient, Figure 3.

Fig. 3. Solid waste disposal in Upper Vardar River in Gostivar (*Popovska*, October 2009)

A review and analysis of the key problems related to the existing waste management situation in Macedonia show that the main problems and constrains are focused almost on all areas, and may be summarized as it follows: policy and legislative framework; institutional framework, organisational arrangements; human resources and capacity building; financing, cost recovery and investments; stakeholder awareness and communication; data availability and reporting; waste avoidance and reduction; waste recovery and recycling; waste segregation, storage, collection and transport; waste treatment and processing.

16.3. SURFACE WATER QUALITY MONITORING

Surface water quality monitoring is performed by Hydro-Meteorological Administration (HMA) in Skopje (rivers, reservoirs and groundwater) and Hydro-Biological Institute (HBI) in Ohrid (natural lakes). Based on the Law on waters (Official Gazette of RM, No. 4/98), the Government of the Republic of Macedonia brought a "Regulation for Classification of Water" (Official Gazette of the Republic of Macedonia No. 18/99). Surface waters,

rivers, natural and man-made lakes and groundwater are classified within five classes. This Regulation doesn't apply to mineral and thermal waters. Short description of the quality classification is as follows: very clean, oligotrophic water, which in its natural state, with possible disinfecting, can be used for drinking, production and processing of food product and is suitable for mating and cultivation of noble types of fish (Class I); very clean, mesotrophic water, which in its natural state can be used for bathing and recreation, water sports, production of other types of fish (cyprinid species), or which can be used, after usual methods of purification (coagulation, filtration, disinfections etc.), for drinking, production and processing of food products (Class II); moderately eutrophic water, which in its natural state can be used for irrigation, and after usual purification methods (conditioning) for industries, which do not need drinking water quality (Class III); strongly polluted (euthrophic) water, which in its natural state can be used for other purposes only after certain processing (Class IV); very polluted (hypertrophy) water, which in its natural state could not be used for any purposes and the water has no buffer capacity (Class V). Legally required water quality as well as estimated water quality for the period (1996–2025) is obtained by JICA [4] (1999).

Water quality monitoring and analysis is performed within the River Monitoring System (RIMSYS) that started in 2000 and funded by the Swiss Agency for Development and Cooperation. The aim of this project is to support the Macedonian authorities in strengthening their capacity to document long-term changes in water pollution and the hydrological regime of the major rivers. RYMSIS's first phase in 2000 had the objective of improving the monitoring system on rivers with installation of 18 river monitoring stations and the environmental laboratory at HMA. The location of RIMSYS stations is presented in Figure 4. The following indicators are worked out: physical, chemical, oxygenic, eutrophication and dangerous substances. Following the Annual Report on surface water quality (HMA, 2006) the following percentage of the classes is obtained: 81% of the waters are in Class II, 11% are in Class III, and only 8% are classified in Class I.

The most polluted rivers are: Crna (Skochivir), Vardar (Taor), Strumica (Novo Selo) and Lepenec (Zlokukani). Permanent high value of the saprobic value is monitored for the River Lepenec at Zlokukani. Higher values of saprobic index within the most of the sampling points have been recorded in autumn (September, October) and in summer period (July). It means that the quality of surface waters trough the whole year is most critical in the summer and fall seasons.

According to the Report on Water Quality for Rivers and Lakes in the Republic of Macedonia in 2002, prepared by the Macedonian Environmental Information Centre (MEIC) at the MEPP, concentration of Fe was highest in Crna Reka-Skochivir and in Eleshka River. The recorded Fe concentration values classified these waters in Class IV. For the same measuring point Crna Reka-Skochivir, dissolved oxygen had lowest value, so according to this parameter the water is classified in Class V.

On the sampling point at Vardar-Taor downstream of Skopje, the Biochemical Oxygen Demand (BOD) has value allowed for Class V. Concentration of Cu was highest at the sampling point Vardar-Radusha upstream of Skopje and according to that parameter the water was classified as class III-IV.

Regarding Chemical Oxygen Demand (COD) highest values were recorded in Crna Reka at Skochivir, which put the water in Class IV and in Vardar at Taor where COD value corresponds to eutrophic water.

Fig. 4. Location of RIMSYS stations, Source: HMA, (2006)

16.4. CONCLUSIONS

Landfills, collection and disposal of all type of waste, and landfills management are a week point in environmental practices in Macedonia. Therefore, the impact of dump sites by having no construction and no control is a major problem for surface water pollution. Many of illegal dump sites are along the watercourses and in most cases the basic river channel is actually waste water and solid waste recipient.

A review and analysis of the key problems related to the existing waste management situation in Macedonia and surface water continuous degradation show that the main problems and constrains are focused almost on all areas, and may be summarized as it follows: policy and legislative framework; institutional framework, organisational arrangements; human resources and capacity building; financing, cost recovery and investments; stakeholder awareness and communication; data availability and reporting; waste avoidance and reduction; waste recovery and recycling; waste segregation, storage, collection and transport; waste treatment and processing.

References

[1] An overview of the physical-chemical, geomorphologic and biological quality elements on inland surface waters and monitoring actions in The Republic of Macedonia, Transboundary Cooperation on Waters according to Water Framework Directive (2000/60/EC), (2006): BIOECO-Skopje, Hellenic Ministry of Foreign Affairs-Athens.

[2] Annual Report on Water: Hydro Meteorological Administration (HMA) of The Republic of Macedonia (www.meteo.gov.mk), 2006.
[3] Biodiversity Strategy and Action Plan of the Republic of Macedonia: Ministry of Environment and Physical Planning of RM 2004.
[4] Directive Specific Implementation Plan for Framework Directive on Water Quality (2000/60/EC): SOFRECO & Carl Bro, European Agency for Reconstruction, Ministry of Environment and Physical Planning of RM 2007.
[5] National Capacity Self Assessment for Global Environment Management, Cross-Cutting Assessment: UNDP Project, Ministry of Environment and Physical Planning of RM
[6] National Waste Management Plan (NWMP) of The Republic of Macedonia, (2008): Ministry of Environment and Physical Planning of RM 2004.
[7] Popovska C.: Surface Water Study in The Republic of Macedonia, Report supported by German Development Cooperation (GTZ), Coordination Office in Macedonia 2009.
[8] Spatial Plan of The Republic of Macedonia. Draft Report: Public Enterprise for Spatial Planning, Skopje 1998.
[9] Study on Integrated Water Resources Development and Management Master Plan in The Republic of Macedonia-Final Report: Japan International Cooperation Agency (JICA) and Ministry of Development of RM 1999.
[10] Waste Management Strategy of The Republic of Macedonia 2008–2020: Government of RM 2008.

17 Design of Sewer Tanks and Related Calculations in the Conditions of Slovakia

Dušan Rusnák (Slovak University of Technology in Bratislava, Faculty of Civil Engineering)

17.1. INTRODUCTION

Sewer tanks play an important role in sewerage systems. There are several types of these structures according to the type of sewerage system and their function. Sewer tanks generally serve the purpose of collecting pollution carried by mixed rain water (RW) and wastewater (WW) and this way they protect the quality of water courses. Further function of tanks is temporary accumulation of RW and WW for the purpose of transformation of maximum discharge waves of waters conveyed into waste water treatment plants (WWTPs). Some types of tanks are used for infiltration of slightly polluted RW (surface runoff water) into ground water. Slovak Republic adopted the provisions from EU directives related to protection of water resources against pollution into legislation. New and more stringent criteria were introduced in connection with the design and function of sewerage systems as well as protection of recipients against pollution contained in WW discharged from WWTPs and in mixed waters discharged from stormwater overflows (SO) which are often constructed together with sewer tanks.

The paper introduces the basic categorization and characteristics of sewer tanks, methods recommended according to the Slovak Technical Standards for dimensioning and design of different types of these tanks as well as new published approaches to dimensioning of sewer tanks in Slovakia, especially with the focus on small drainage areas of a catchment.

17.2. TYPES OF SEWER TANKS AND PRINCIPLES OF CALCULATING THEIR VOLUME

Sewer tanks can be designed within WWTPs (settling tanks – ST) to capture settleable and floating solids or they can be built at sewerage systems.

17.2.1. Types of sewer tanks

Detention tanks (DT) are designed for sewers to capture temporarily some water and decrease maximum discharge to required value. The captured volume of water flows from of the tanks into sewerage system. Detention tanks are designed for combined sewer system (CSS) as well as for separate sewer system (SSS) – they are either watertight covered ones (for CSS) or open ones (for SSS). The detention tanks are required when expanding the existing sewerage system with already limited capacity.

Retention tanks (RT) can be designed only for SSS storm sewers. They are intended for capturing the whole collected volume of slightly polluted water from surface runoff and their consequent infiltration. They are one of several possibilities how to apply a modern method of slightly polluted water treatment from surface runoff. Suitable subsoil geological properties and sufficient depth of ground water level under the bottom of the tank are the conditions for their design.

Tanks associated with stormwater overflows are designed for CSS sewers to protect the quality of water in receiving body against pollution discharged from stormwater overflows during heavy rain. Besides the above-mentioned these tanks have also accumulation function. According to the size of catchment belonging to the tank (runoff travel time is a criterion) we distinguish between *catch basins* (CB) (small tanks, runoff travel time not longer than 15 – 20 minutes) and *flow tanks* (FT) (larger catchments, runoff travel time over 20 minutes).

Storm water overflow is designed at supply sewer before CB (FT). In the catch basin there is accumulation of initial (the most polluted) part of mixed water which cannot flow through storm water overflow. Captured part of the discharge is conveyed into WWTP biological stage as limit discharge $Q_{WWTP.}$ For this reason the outflow controller is installed on the tank outflow pipe. Stormwater overflow starts to be active after catch basin is filled.
In flow tanks a part of mixed waste water is treated using sedimentation process. Regulated discharge from the flow tank is at the value Q_{WWTP} and it is also equipped with the weir (aperture) through which the mixed wastewater treated through sedimentation is discharged into the receiving water after the tank is filled. Stormwater overflow starts to be active after exceeding the discharge $2 \times Q_{WWTP}$ through the tank.

17.2.2. Calculation principles

Calculation of necessary volumes of tanks depends on their type and size of the drainage area. Modern calculation methods use the rainfall-runoff models based on long-term simulation of runoff in sewers in related drainage area. This technique of calculating the volume of tanks in small drainage areas is quite expensive and it is also technically difficult due to required calibration and verification of the model. Therefore, graphic or simple modifications of rational method with the application of block rainfalls with certain periodicity (DT and RT) or with the application of critical rain (CB and FT) are used to design the tanks in small urban catchments.

Calculations of tank volume are based on rainfall periodicity with enhanced safety (for example $p = 0.2$ or $p = 0.1$ for open tanks) unlike the calculation of design discharges for dimensioning the profiles of sewers. The calculation is based on block rainfalls regardless the travel time of surface runoff into storm drains (time of concentration equals the travel time of runoff into sewerage system). A safety of design is provided through applying the

enlargement factor f_z = 1.1 up to 1.2 as compared to simulation. Concerning large and significant tanks, the volume calculated according to block rainfalls using modified rational method must be assessed by long-term runoff simulation.

In the paper there are calculations of the volumes of detention and retention tanks using simple calculation methods based on rational method following design block rainfalls and critical rains (for DT and RT). There is also a new design method based on the principle of permissible annual overflow rate applied for the conditions of Slovakia (CB and FT).

17.3. DETENTION TANKS

17.3.1. Calculation of volume using iteration

Currently, the Slovak technical Standard STN 75 6261 [1] applies in designing sewer tanks in Slovakia. Before the amendment in 1997 this standard recommended to apply block rainfalls for the calculation of the volume of detention tank for small catchments (similar to the recommendations according to ČSN 75 6261 [2] for the Czech Republic at present) and the equation derived from trapezoidal rainfall runoff hydrograph for the calculation of the tank volume V (m^3):

$$V = 0.06\,[Q_c \cdot t_c - Q_o\,(t_c + t_s - t_s \cdot Q_o \cdot Q_c^{-1})]\,f_z \tag{1}$$

where: Q_o – permissible runoff from the tank ($l \cdot s^{-1}$),
t_s – runoff travel time through sewer into DT (min),
f_z – enlargement factor (f_z = 1.1 to 1.2),
Q_c – value of design discharge ($l \cdot s^{-1}$).

$$Q_c = S_r \cdot q_c \tag{2}$$

S_r – reduced area of catchment related to relevant tank (ha),
t_c – duration of block rainfall (min), which gives its maximum value in the calculation of tank volume,
q_c – intensity of block rainfall ($l \cdot s^{-1} \cdot ha^{-1}$) with time of duration t_c.

Parameters of design hydrograph are calculated using the method „trial and error“ by consequent substitution of elected values t into the equation (2) and consequently by substitution of values t and calculated discharges Q according to the equation (2) into the basic equation (1) for the calculation of volume (V). Maximum calculated value V according to the equation (1) is then the volume of detention reservoir.

17.3.2. Direct calculation of the volume

In Slovak conditions it is possible to calculate the rain intensity ($l \cdot s^{-1} \cdot ha^{-1}$) also in the following way

$$q = K_{(p)}\,(t + B_{(p)})^{-1} \tag{3}$$

$K_{(p)}$ a $B_{(p)}$ – local parameters (–) dependent on the periodicity of block rainfalls and they are published for 68 localities in the Slovak Republic in STN 75 6101 [3].

If we apply the form of equation (3) in calculations, we can directly calculate the critical period of block rainfall duration t_c (min) which leads to maximum volume of detention tank

$$t_c = K_{(p)} \{(B_{(p)} \cdot [q_o (K_{(p)} - q_o \cdot t_s)]^{-1}\}^{0.5} - B_{(p)} \quad (4)$$

q_{dr} – acceptable specific rain runoff from the tank ($l \cdot s^{-1} \cdot ha^{-1}$).

Detailed calculation method was published in SOVAK 11/2002 [4].

17.3.3. Calculation according to STN 75 6261

In 1997, the STN 75 6261 [1] was amended in the Slovak Republic and it recommends the calculation of the DT volume based on the reference locality of Sliač. For other localities in the Slovak Republic the DT volume calculated for Sliač is modified by the parameter of geographical longitude. Specific *DT* volume v_T (m^3/ha^{-1}) for repeating T = 1 up to 10 years

$$v_T = v_1 + (v_{10} - v_1) \cdot \log T \quad (5)$$

T – repetition period (y), $v_1(v_{10})$ – specific volume for T = 1(10) years (m^3/ha^{-1}) .
Specific volumes for the locality of Sliač:

$$v_1 = 249 - (62 + 10{,}8\, t_p^{0.51}) \cdot \log q_o \ (m^3/ha^{-1}) \quad (6)$$

$$v_{10} = 727 - (484 - 12\,463\, t_p^{-1.27}) \cdot \log q_o \quad (m^3/ha^{-1}) \quad (7)$$

t_p is the runoff travel time into the tank (min), q_o – specific runoff of rain water from DT ($l \cdot s^{-1} \cdot ha^{-1}$)

$$q_0 = Q_o \cdot S_p^{-1} \cdot \psi^{-1} = Q_o \cdot S_r^{-1} \quad (8)$$

Q_o – rainwater runoff from DT ($l \cdot s^{-1}$), S_p – drainage area related to DT (ha), ψ – runoff factor (–), S_r – reduced basin area (ha).
Required volume of detention tank V (m^3) for the locality of Sliač

$$V = v_T \cdot S_r \quad (9)$$

For optional locality „*L*“in Slovakia the necessary volume of the tank $V(L)$ (m^3) is modified by the parameter Kret (–)

$$V(L) = V \cdot K_{ret} \quad (10)$$

$$K_{ret} = H_z(L) \cdot 736^{-1} \cdot (A + B \cdot ZD) \cdot I^{-1} \quad (11)$$

$H_z(L)$ – annual precipitation total in the locality “*L*“ (mm), *ZD* – geographical longitude of the locality (°), *A*, *B* and *I* – factors; their calculation is defined under STN 75 6261 [1] in dependence on *A*, *B*, $I = f(q_o)$.

17.4. RETENTION TANKS WITH INFILTRATION

In the Slovak technical standards there are no recommendations for calculation of retention tanks. However, it is possible to use the recommended calculation for the volume of detention tanks, when rain water runoff from the tank Q_o in equation (1) is replaced by infiltration discharge Q_v. Volume V (m^3) of retention tank with infiltration function is then calculated using the modified equation (1)

$$V = 0.06\,[Q \cdot t - Q_v\,(t + t_k - t_k\,Q_v\,Q^{-1})]\,f_z \tag{12}$$

$$Q_v = k_v\,S_{vs} \tag{13}$$

Q_v – infiltration discharge (l/s^{-1}), k_v – coefficient of infiltration intensity ($l \cdot s^{-1}ha^{-1}$), for unsaturated soil it is derived from filtration coefficient k_f (m/s^{-1}) applied in the Darcy equation $v = k_f\,I$

$$k_v = 0.5\,k_f\,10^7 \tag{14}$$

The values of the coefficient k_f and k_v are put in tables for different types of soil.

Infiltration „runoff" from retention tank depends on actual effective infiltration area. Therefore it is necessary when calculating the volume of RT to have estimated geometrical dimensions of related retention tank and derived estimated values of maximum infiltration area $S_{v\max}$ at the beginning of calculation. Mentioned procedure has to be therefore performed by using iteration.

Flow Q (l/s^{-1}) into the tank is calculated as follows:

$$Q = (\psi\,S + S_{v\max})\,q_{(t,\,p\,=\,0.2)} = (S_r + S_{v\max})\,q_{(t,\,p\,=\,0.2)} \tag{15}$$

ψ – runoff coefficient (–),
S – catchment area drained into the tank (ha),
$S_{v\max}$ – maximum infiltration area (ha),
S_r – reduced catchment area (ha),
$q_{(t,\,p\,=\,0,2)}$ – intensity of block rain ($l \cdot s^{-1}\,ha^{-1}$) with time of duration t (min) and periodicity $p = 0.2$ according to the data of the Slovak Hydro-Meteorological Institute (SHMI).

When the form $q = K_{0.2}\,(t + B_{0.2})^{-1}$ is applied for the calculation of block rain, then the inflow Q ($l \cdot s^{-1}$) into recharging tank will be

$$Q = q\,(\psi\,S + S_{v\max}) = K_{0.2}\,(S_r + S_{v\max})\,(t_{\max} + B_{0.2})^{-1} \tag{16}$$

$t_{\max}$ – critical time of block rain duration (min) according to the equation (17) corresponding with the maximum retention volume of the tank

$$t_{\max} = B_{0.2}\,K_{0.2}\,(S_r + S_{v\max})\,[B_{0.2} \cdot Q_v\,K_{0.2}\,(S_r + S_{v\max}) - B_{0.2} \cdot Q_v^{\,2}\,t_s\,]^{-0.5} - B \tag{17}$$

t_s – maximum travel time of flow through storm sewer to stormwater tank (min).

Detailed calculation method was published in [4].

17.5. TANKS ASSOCIATED WITH STORMWATER OVERFLOWS IN COMBINED SEWERS

Simple methods (concerning regular emission requirements for protection of receiving water) or more complex rainfall – runoff models (concerning special requirements for protection of receiving water) are used for dimensioning and design of tanks associated with stormwater overflows. In case of special requirements the attention is paid to pollution effects of rain water after mixing with minimum flows in a receiving river. The method of critical rain and the method applying permissible annual overflow rate (PAOR) are among the simplest ones.

17.5.1. Calculation according to the method of critical rain

The method of critical rain used for calculation of the capacity of tanks in the Czech Republic is recommended under the Czech Technical Standard 75 6261 [2] and this method was also applied in Slovakia until 1997 in accordance with the Slovak Technical Standard 75 6261 [1].

The critical flow of wastewater mixed with rainwater Q_{wwtp} (l/s^{-1}) is conveyed from the system of stormwater overflows (SO) + catch basins (CB) (stormwater overflows + flow tank) to WWTP:

$$Q_{wwtp} = Q_{b24} + Q_m + \Sigma\, Q_m^* = Q_{b24} + q_m\, S_p\, \psi + \Sigma\, Q_m^* \qquad (18)$$

Q_m – critical flow ($l \cdot s^{-1}$) from the catchment of flow tank (catch basins) with an area S_p (ha) and runoff coefficient ψ (–), q_m – intensity of critical rain ($l \cdot s^{-1} \cdot ha^{-1}$), $\Sigma\, Q_m^*$ – the sum of critical flows (l/s^{-1}) from SO situated upstream of the FT (CB) catchment, Q_{b24} – average dry weather flow to FT (CB) (l/s^{-1}).

The volume V (m^3) of catch basin or flow tank

$$V = \gamma\, V_s\, S_r \qquad (19)$$

V_s – specific volume of CB (FT) ($m^3\, ha^{-1}$) is obtained from the graph (it is a function of critical rain q_m ($l \cdot s^{-1} \cdot ha^{-1}$)) and specific rainwater runoff q_o ($l \cdot s^{-1} \cdot ha^{-1}$) from CB (FT) into WWTP, S_r – reduced drainage area related to CB (FT) (ha), γ – coefficient defining the runoff travel time from drainage area to tank/reservoir (–).

17.5.2. Calculation using the Method of Permissible Annual Overflow Rate (PAOR)

dard ATV A 128 [6]. The condition of calculation is that the sum of pollution load carried by overflowed water and treated rainwater into receiving water from the entire area connected to sewer system should be lower according to annual balance than the pollution load conveyed into receiving water through the storm sewer system from the same area.

17.5.2.1. Calculation according to STN 75 6261 (Slovak Technical Standard)

Using the principle of PAOR, the approach to dimensioning of CB and FT was drawn up in accordance with STN 75 6261 [1]. This method is based on the results obtained from the simulation of runoff using the long-term precipitation data in three localities of Slovakia (Bratislava, Sliač and Košice).

BOD_5 is used as the distinguishing parameter of water pollution where the characteristic concentrations of BOD_5 pollution are assumed for different types of water: rainwater c_d = 35 mg/l^{-1}, WWTP effluent c_V = 20 mg/l^{-1}, mixed water from stormwater overflows c_{od} = 55.6 mg/l^{-1} and dry-weather water c_b = 200 mg/l^{-1}.

A concentration of pollution of wastewater c_{bv} (mg · l^{-1}) is calculated using the correction factors according to actual (measured) pollution concentration of wastewater c_b (mg l^{-1}), annual precipitation height H_z (mm) and average slope of surface i_t).

The annual runoff of rainwater from the area connected to sewer system Q_z (m^3/year)

$$Q_z = 10\, S_p\, H_z\, \varphi \tag{20}$$

S_p (ha) – catchment area,
φ – volumetric runoff coefficient (–),
H_z – annual precipitation height (mm).

The annual discharge of water from stormwater overflows (m^3/year)

$$Q_{od} = Q_z \times P_{od}\, 100^{-1} \tag{21}$$

P_{od} (%) – percentage of overflow water, it is recommended to select P_{odzv} = 60 up to 70% at the beginning of calculation.

Time of overflowing (hour/year)

$$T = (1.45 - 0.1\, q_o + 0.01\, t_d)\, P_{odzv} - 17 \tag{22}$$

t_d – runoff travel time to SO (min.),
q_o – specific runoff of rainwater into WWTP (l s ha^{-1}).

Mix (dilution) ratio in overflow water (–).

$$n = Q_{od}\, Q_{b24}{}^{-1} \tag{23}$$

If $n < 7$ according to the equation (23), then the value $n = 7$ is assumed for further calculations.

The average BOD_5 concentration in overflow water (mg/l)

$$c_{od} = (n\, c_d + c_{bv})\, (n + 1)^{-1} \tag{24}$$

Permissible percentage of overflow water (%)

$$P_{odp} = 100\, (c_d - c_v)(c_{od} - c_v)^{-1} \tag{25}$$

If $(P_{odp} - P_{odzv}) > \pm 3\%$, the calculation is repeated using approximation according to the equation (21).

Required specific volume of tank (m^{3}ha^{-1}) for the conditions of Bratislava

$$v_s = (\, J + L \cdot t_d\,) \tag{26}$$

J, L – parameters calculated according to the equations (27), (28) and (29):

$$J = 79{,}2 + (-0{,}92 - 0.25\ q_o)\ P_{od}(B) \tag{27}$$

$$L = M\ P_{od}(B) - 0{,}01\ q_o^{1{,}57} \tag{28}$$

$$M = (\ 7.6 - 25.5\ q_o)\ 10^{-4} \tag{29}$$

$P_{od}(B)$ – percentage of overflow water calculated for the conditions of Bratislava using the percentage of overflow water in a particular locality P_{od}(L) (%)

$$P_{od}(B) = P_{od}(L)\ K_{pz}^{-1} \tag{30}$$

K_{pz} – calculation coefficient (–).

$$K_{pz} = A + B\ .\ ZD \tag{31}$$

ZD – locality geographical longitude (°); A, B – parameters

$$A = 0.036\ q_m - 0.31 \tag{32}$$

$$B = 0.076 - 0.002\ q_m \tag{33}$$

q_m (q_o) – intensity of critical rain (runoff of rainwater from tank/reservoir into WWTP) (l s ha^{-1}).

The values of P_{od} (B) (%) for selected intensity of critical rain q_m (q_o) and runoff travel times t_d (min.) are listed in Slovak Technical Standard STN 75 6261[2].

Required volume of stormwater catch basin or flow tank V (m^3)

$$V = v_s\ S_r \tag{34}$$

17.5.2.2. Calculation using the modification of PAOR for the territory of Slovakia

The method applies the annual loading of receiving body expressed through the COD parameter, average annual precipitation H_z = 700 mm and average COD concentrations: a) in dry-weather wastewater c = 600 mg/l, b) in rainwater effluent from WWTP c_v = 70 mg/l.

The average annual concentration of COD in rainwater runoff from the surface of urban catchment will be $c_d = 100\ L\ \varphi^{-1}\ H_z^{-1} = 100 \cdot 600 \cdot 0.7^{-1} \cdot 700^{-1} = 122.5$ mg/l COD, where the annual runoff coefficient φ = 0.7 is assumed.

The receiving river discharge, which affects the requirements for designing the capacity of stormwater catch basins and flow tanks, is calculated through $Q_{270} \cdot Q_{m24}^{-1}$ (Q_{270} – 270-day discharge of receiving river (l/s), Q_{m24} – average discharge of urban wastewater from the entire area connected to sewer system (l/s).

The effect of discharge ratio $Q_{270} \cdot Q_{m24}^{-1}$ can be expressed through the parameter f (–) calculated according to the equation

$$f = 1.0 + 0.024 \ln (Q_{270}\ .\ Q_{m24}^{-1}) \tag{35}$$

if f < 1.0 according to the equation (35), then f = 1.0 is applied to further calculation; if f < 1.15, then f = 1.15 is applied to further calculation.

The discharges of wastewater measured at WWTP or obtained from calculations are assumed when calculating the volumes.

The following discharges are important for calculations:

a) average discharge of urban wastewater (sewage and industrial) Q_{m24} (l/s),

b) average discharge of dry-weather wastewater (urban and ballast) Q_{b24} (l/s),
c) maximum hourly discharge of urban wastewater $Q_{m\max}$ (l/s),
d) maximum hourly discharge of dry-weather wastewater $Q_{b\max}$ (l/s),
e) flow of rainwater into sewer systems during rain Q_{dD24} (l/s)

$$Q_{dD24} = Q_{mD24} = M_D \; q_{sD} \, 86400^{-1} + \Sigma \, Q_{pD24} \tag{36}$$

Q_{mD24} – urban wastewater discharge in a sewer system (l/s),
M_D – the number of population in the catchment of sewer system,
q_{sD} – production of wastewater in sewer systems ($l \cdot pop^{-1}d^{-1}$),
ΣQ_{pD24} – average discharge of industrial wastewater in the catchment of sewer systems (l/s).

Permissible discharge of mixed wastewater Q_{wwtp} (l/s) conveyed from the tank into WWTP (biological stage of WWTP is dimensioned according to this discharge) is calculated in accordance with ATW A 128 [6]:

$$Q_{wwtp} = N_d \, Q_{mmax} + Q_B + Q_{dD24} \tag{37}$$

N_d – portion of rainwater treated in the biological stage of WWTP, $N_d \geq 2.0$ is recommended.

Rainwater discharge Q_{d24} (l/s) in the section from storm water tank/catch basin to biological stage of WWTP:

$$Q_{d24} = Q_{\acute{c}ov} - Q_{m24} - Q_B - Q_{dD24} \tag{38}$$

$$q_d = Q_{d24} \; S_s^{-1} \tag{39}$$

S_s – paved area of catchment (ha),
q_d – specific runoff of rainwater from the tank/basin ($ls^{-1}ha^{-1}$).

According to ATV A128 [6] the runoff q_d should be in the range $0.2 \leq q_d \leq 2 \; l \cdot s^{-1} \; ha^{-1}$. Ratio n (–) of rainwater and dry-weather runoff during overflowing

$$n = (2.78 \, H_z \, S_z \, T_{od}^{-1} + Q_{dD24}) \, Q_{b24}^{-1} \tag{40}$$

$$T_{od} = t_s^{-0.087} \, [42(p)^{-0.62} \, (q_d + 1.4)^{-1}]^c \tag{41}$$

$$p = 1463 \; 10^4 \, (H_z + 200)^{-2.674} \tag{42}$$

H_z – average annual precipitation (mm),
T_{od} – time of overflowing (y^{-1}),
t_s – maximum travel time of flow through sewers to tank (min),
$c = 1.8 \, p^{0.077}$,
p – parameter (–).

If $n < 7.0$, then $n = 7.0$ will be applied to further calculation according to ATV A128 [6]. The equation (40) applies to $q_d \leq 2 \; l \cdot s^{-1} \cdot ha^{-1}$.

The concentration of COD in dry weather discharge c_b (mg/l COD) is determined through the direct measurement at WWTP or by calculation:

$$c_b = (Q_{s24} \, c_s + \Sigma \, Q_{p24} \, c_p) \, (Q_{s24} + \Sigma \, Q_{p24} + Q_B)^{-1} \tag{43}$$

c_s – COD concentration in sewage water $c_s = 120 \cdot 10^3 \, q_s^{-1}$ (mg/l),
q_s – specific production of sewage water ($l \cdot pop^{-1}d^{-1}$),
Q_{p24} – average discharge of industrial wastewater (l/s),
c_p – concentration of industrial wastewater (mg/l),
Q_B – ballast water discharge (l/s).

Calculated value of the ratio n according to the equation (40) shall comply with the conditions:

if $c_b \leq 600$ mg/l CHSK then $n_{\min} \geq 7$,

if $c_b > 600$ mg/l CHSK then $n \geq (c_b - 180)\, 60^{-1}$.

The COD concentration in dry weather flow c_{bv} (mg/l COD) according to ATV A128 [6] depends of the following factors: a) a_c – actual concentration of COD in dry-weather discharge c_b; b) a_H – average local precipitation total H_z; c) a_n – sediments in a sewer system during the increasing discharge:

$$c_{bv} = 600\ (a_c + a_H + a_n) \tag{44}$$

Details about the calculation of the values of particular factors were published in [8, 9].
The COD concentration in overflow water c_{od} (mg l^{-1} COD)

$$c_{od} = (n \cdot c_d + c_{bv})\ (n + 1)^{-1} \tag{45}$$

The PAOR condition can be formulated using the equation

$$Z_{od} + Z_{wwtp} \leq Z_d \tag{46}$$

Z_{od} – stream pollution load (COD) in water from the combined sewer overflows (kg/y),
Z_{wwtp} – stream load in treated rain water effluent from WWTP (kg/y),
Z_d – load flushed by precipitation from urban surface (kg/y).

The condition of the equation (46) can be formulated as follows:

$$V_{Qd} \cdot P_{od} \cdot c_{od} + V_{Qd}\ (1 - P_{od})\ c_v \leq V_{Qd} \cdot c_d \tag{47}$$

V_{Qd} – volume of rainfall runoff in an average year (m^3),
c_{od} – COD concentration of water from the overflows according to the equation (45),
c_v – concentration in rain water effluent from WWTP $c_v = 70$ mg/l COD,
c_d – concentration in the runoff from the surface of urban catchment for Slovakia $c_d = 122.5$ mg/l COD,
P_{od} – percentage of the volume of water from the overflows and the volume of rainfall runoff in an average year (%).

According to the equations (35), (44), (47) and by applying the concentration $c_d = 122.5$ mg/l COD, the percentage of water from the overflows P_{od} (%) will be in the range $25\% \leq P_{od} \leq 75\%$

$$P_{od} = 52.5\ f\ (n + 1)\ [\ 6\ (a_c + a_H + a_n) + 0.525\ n - 0.7\ ]^{-1} \tag{48}$$

Required specific volume of storm water tank v_s ($m^3 ha^{-1}$)

$$v_s = [3893\ q_d^{0.028} - (P_{od} + 6)(36.8 + 13.5\ q_d)] \cdot (P_{od} + 6)^{-1}(0.5 + q_d)^{-1} \tag{49}$$

q_d – specific runoff from the tank according to the equation (39) ($l \cdot s^{-1} \cdot ha^{-1}$).
The value v_s of the equation (49) is used in the next calculation providing that the following condition is met:

$$v_{smin} \leq v_s \leq 40\ m^3/ha \tag{50}$$

if
$$v_{smin} = 3.6 + 3.84\ q_d \tag{51}$$

If $Q_{wwtp} > 2\ Q_{b\max}$, q_d (l s^{-1} ha^{-1}) in the equation (51) is calculated as

$$q_d = (2\ Q_{b\max} - Q_{b24} - Q_{dD24})\ S_z^{-1} \tag{52}$$

Required volume of flow tank (catch basin) V (m^3) will be

$$V = v_s \; S_z \tag{53}$$

If $v_s < v_{smin}$ applies according to the equation (49), then the volume of stormwater tank V (m^3) will be calculated for v_{smin}

$$V = v_{smin} \, S_z \tag{54}$$

The calculation of stormwater catch basins, flow tanks and accumulation sewers is performed in four steps:

1. Required total volume of one fictive flow tank for the entire drainage area belonging to WWTP (fictive tank located in WWTP) will be calculated.
2. The volumes of tanks V_N and volumes of accumulation sewers V_{AS} included in the sewerage system in particular sub-catchments will be calculated.
3. Particular stormwater overflows with high weir edges will be dimensioned and then the accumulation volume V_{OK} in collecting sewers with increased water level flowing into the stormwater overflows will be calculated
4. Required (remaining) volume of the tank V_{wwtp} (m^3) located in WWTP will be calculated

$$V_{wwtp} = V_c - \Sigma \, V_N - \Sigma \, V_{ASH} - 0{,}7 \, (\Sigma \, V_{ASD} + \Sigma \, V_{OK}) \tag{55}$$

ΣV_N – the sum of the volume of stormwater catch basins and flow tanks in sub-catchments of sewerage system,

ΣV_{ASH}, ΣV_{ASD} – the volume of accumulation sewers with combined sewer overflows at the lower and upper ends of sewers,

ΣV_{OK} – is a volume of combined sewer overflows and flow distribution chambers including the accumulation volumes of collecting sewers with increased water level.

The detailed calculation procedure using the PAOR method for the conditions of Slovakia together with the particular calculation were published in the journal "Vodní hospodářství" [8] and [9].

17.6. CONCLUSION

Different functions of sewer tanks require various methods of their dimensioning. The article presents the methods recommended in accordance with the Slovak Technical Standard STN 75 6261 [1] together with other approaches used in the past (Slovakia) or currently applied (Czech Republic). The calculations of tanks/basins according to the current Slovak Technical Standard STN 75 6261 [1] often give quite different results for localities with the same conditions. Urcikán and Rusnák [10] compared specific volumes of detention tanks calculated by using simple methods according to several authors and STN 75 6261 [1] for 6 localities of Slovakia with the same conditions S_r = 10 ha, t_k = 14 min and Q_o = 260 l/s. All the volumes according to STN 75 6261 [1] are considerably larger. The largest ones are in the region of Central Slovakia (B. Bystrica and L. Hrádok)

The comments on the method recommended in accordance with STN 75 6261 were published by Urcikán [7]. Practical example of calculating the required volume of flow tanks for urban areas of the same size situated in different regions of Slovakia proved quite different results when using the calculation method recommended in accordance with STN 75 6261 [1]. The factor of geographical longitude of a given locality is the cause. The men-

tioned problem was discussed in more detail and the modification of ATV A128 method [6] was developed for the conditions of Slovakia and published in [8] and [9].

The above-mentioned simple methods take into account in more comprehensive way every local factor having an effect on the volumes of tanks required to retain an inflow wave regarding detention and retention tanks or to protect water quality in streams against pollution coming from combined sewer systems.

References

[1] STN 75 6261 Dažďové nádrže, 1997.
[2] ČSN 75 6261 Dešťové nádrže, 1997.
[3] STN 75 6101 Stokové siete a kanalizačné prípojky, 2002.
[4] Urcikán P., Rusnák D.: Navrhovanie detenčných a retenčných kanalizačných nádrží v mestských oblastiach. SOVAK, 11/2002.
[5] Urcikán P., Rusnák D.: Dimenzovanie dažďových nádrží na stokách delenej sústavy. Hydrosphere 2003, Optimalizace návrhu a provozu stokových sítí a ČOV, Břeclav, október 2003.
[6] ATV A128 Richtlinien für die Bemessung u. Gestaltung von Regentlastungsanlagen in Mischwasserkanälen, april 1992.
[7] Urcikán P.: Problémy s používaním STN 75 6261 Dažďové nádrže“. Vodohospodársky spravodajca č.4/2001 s. 7–8.
[8] Urcikán P., Rusnák D.: K navrhovaniu prietočných a záchytných dažďových nádrží. Vodní hospodářství, 12/2003.
[9] Urcikán P., Rusnák D.: Aplikácia modifikovanej metódy na dimenzovanie prietočných a záchytných dažďových nádrží. Vodní hospodářství, 1/2004.
[10] Urcikán P., Rusnák D.: K návrhu objemu detenčných dažďových nádrží na malých povodiach. J. Hydrol. Hydromech., 49, 2001, 5, 301–323.

Acknowledgements

The article was written within the Project KEGA No. 3/7452/09 “Urban Area Drainage” conducted at the Department of Sanitary and Environmental Engineering, Faculty of Civil Engineering of the Slovak University of Technology in Bratislava.

18 Minimalization of Solid Waste Landfilling Base on Waste Analyses

Ivona Škultetyová, Štefan Stanko, Kristína Galbová (Faculty of Civil Engineering of the Slovak University of Technology in Bratislava, Department of Sanitary and Environmental Engineering)

18.1. INTRODUCTION

There is a demand for the flow of information, from the international level down to the individual level, across all areas of life. This is also true for the issue of waste, as waste is a necessary by-product of human existence.

Recently we have been observing the continuing trend of growth in the production of communal waste, as well as corresponding growth in the costs related to its disposal. Growth in the amount of waste produced is especially affected by the rising degree of economic growth, which highlights the need for solving the problem of dealing with waste.

The waste landfilling is the worst alternative of waste disposal. We can say, that this is not the waste disposal, but only the moving the problem solving into the future. If we want to dispose the wastes, we must take consider on waste specific, we must respect the waste material. The way out of this problem solution must be base on system waste analyses, which is not easy.

18.2. WASTE MANAGEMENT SYSTEM

In the past, when it came to designing waste management facilities, generally the only parameter taken into account was the size of the population producing waste, neglecting to consider other parameters that affect waste creation [2]. Additionally, waste management was analyzed as an independent subsystem without considering its other ties to individual spheres of the environment. However, the production of waste is dependent on various parameters that interact with each other. Being aware of these parameters, as well as the methods for evaluating their effects on one another, helps to identify the condition and the designation of development trends in the field of waste management. It is possible to point out the limitations in this field, which will be possible to improve on or remove in the future. The necessity of being well informed, from the international level to the individual level, is broadly manifested in every sphere of life. It is also tied to the field of waste management because wastes are an accompanying feature of the existence of mankind. With an increasing degree of economic development the production of waste also increases, which highlights the need of solving this problem [3]. The basis for proper waste management and for the design of facilities dedicated to dealing with waste is the prediction of the quantity and composition of the waste, based on various prognostic models.

One of the most important parameters influencing the size of the new future waste management system is waste flow forecast. All design, technical solutions in a feasibility study and, at the end, final costs and tariffs crucially depend on future waste flows. Waste flow forecast, which helps with the creation of prognostic models usually is based on present waste management situation (statistical data on waste generation, waste quantity and composition), waste generation sources (rural and urban population, industry, businesses), demographic trends (rural and urban population growth, migration), economic activity (GDP growth), waste management policy developments (increased sorting, recycling, separate, treatment of certain waste types (end-of-life vehicles), waste prevention, increased coverage of territory and population).

18.3. THE PRODUCTION OF WASTE

In terms of modeling, in concentrating on the analysis of parameters that influence the processes of waste creation we can apply factor models [1], which when predicting waste production (in terms of quantity and composition of waste) focus on various parameters, for example economic and demographic. We can predict individual parameters with considerable precision on longer timeframes. When identifying and rating the degree of their influence on waste production it is necessary to consider their interaction on one another, because waste production is not dependent on just one of these parameters.

Parameters that influence the production of waste include especially:

— Environmental parameters,
— Demographic,
— Economic,
— Social,
— Institutional.

18.3.1. Environmental parameters

Environmental parameters characterize indicators, for example:

— Global warming,
— Emissions,
— Urbanization,
— Agriculture,
— Forestry.

18.3.2. Demographic parameters

Demographic parameters characterize indicators, for example:

— Population size

The number of inhabitants significantly affects the total quantitative production of waste of a specific regional entity. When estimating the amount of waste produced, if we

take into account just the population size, we could reach an incorrect estimate because the creation of waste is affected by other factors.

— Population increase
  This is an indicator that characterizes the average annual degree of change in the size of the population of a given regional entity. The meaning of this degree is characterized by the relationship to social, economic and environmental factors of the region's development.

— Inhabitants of urban centers
  A factor conveying the degree of urbanization – the percentage of the population living in areas that are characterized by a heightened environmental weight and developmental problems (including waste production). In developing countries the percentage of inhabitants living in urban centers is under 50 percent, in some cases under 10 percent. On the other hand, in developed countries this percentage represents more than 75 percent of the population. In Slovakia, 57.3 percent of the population lives in urban centers.

18.3.3. Economic parameters

Economic parameters are characterized:

— Gross domestic product per inhabitant
  The total economic performance of a given regional entity is conveyed by the gross product, while its value in USD per inhabitant in the majority of developing countries ranges from 1000 to 1500 USD and in economically developed countries ranges from 12000 to 14000 USD.

— Proportion of investments in GDP
  In Slovakia the value of investments as a percentage of GDP is cca 41 percent. (In most countries it is 20 percent to 25 percent.).

— Economic balance of goods and services
  This indicator shows the difference between the nominal value of export and import. An unfavorable economic balance is embodied by many countries, which represents values of this indicator in a range of 20 percent to 40 percent. A positive balance of some countries is over 10 percent; others embody a level economic balance. Slovakia has a negative balance – cca 10,4 percent.

— Debt in proportion to GDP
  This indicator represents a brake on the development of a region, especially in regards to less-developed countries (debt is over 50 percent of to several times GDP). The debt of developed countries is 5 percent to 30 percent of GDP.

Indicators of the economy's dependence on natural and other resources, as well as on burdening the environment with the manufacture and creation of waste, include:

— Intensity of the use of materials,
— Annual consumption of energy per inhabitant,
— Proportion of use of renewable sources of energy,
— Energetic intensity,
— Recycling and secondary use of waste,
— Prosperity of the country.

Various economic indicators are together folded into an indicator of the country's prosperity.

18.3.4. Social parameters

— Percentage of inhabitants living below the poverty threshold,
— Unemployment,
— Ratio of average income of women to men.

Social parameters include indicators focused on the health and existential aspect of mankind, for example:
— Measure of mortality of children under 5,
— Surface area per person.

18.3.5. Institutional parameters

Currently, access to information and being informed are considered to be important aspects of human existence. Institutional parameters include:
— Number of radios,
— Number of internet connections,
— Number of telephone lines, mobile phones, etc.,
and also indicators tied more closely to economic parameters:
— Spending on research and development as a percentage of GDP,
— Economic and human costs caused by natural disasters, as well as by fires, floods, and so on
and also, for example:
— Legislative factors,
— Application of permanently sustainable development.

18.4. CONCLUSIONS

To guarantee progress in the management of the waste industry and to reach positive results in the waste sector in Slovakia, we have established certain rules and goals concerning the planned development of individual flows of waste, divided into commodities and categories of waste. This presents the base for a properly functioning and effective system of waste management [5, 6].

To create such systems it is necessary to ensure the availability of sorted waste collection in cities and towns. This will lead to, for example, the appropriate choice of how to process organic waste. New methods will improve the use of waste in all aspects – material, energy and safety. In order to construct an optimal and effectively functioning system, it it necessary to have objective data about the volume and contents of communal waste, as well as the prognosis for its volume and contents. Waste analysis has been a key issue for a long time, given that it is very complicated to get a representative sample of waste, given its heterogeneity.

Many authors had prepared individual methodical rules that were later recommended for general use. This led to the creation of various types of analyses, whose results are in certain ways different and are in general not comparable.

It is characteristic of current times that the increase in waste produced is leading to growth in waste management costs. This in turn leads to a decrease in the prosperity of the waste industry and an ineffective connection between sorted and unsorted waste collection. The results of analyzing the contents of communal waste – finding out the volume of each category and its quality – is helping with optimalization of waste industry at an efficient level. So is the prognosis of the development of the waste industry with the help of prognostic and evaluative models leading to a long-term economic and environmental tenability.

The scientific goal of this work is to characterize the current situation and future prognosis for the production of communal waste. Based on available resources, we aim to prepare a methodical analysis of the storage of communal waste, and seek an overview of available models of analyzing the contents of communal waste as well as new systems of evaluation of communal waste management at home and abroad.

Our goal is to perform an analysis of communal waste in a selected area, taking into account the locality´s size, the composition of waste produced and the make-up of the population. This helped us collect data for the LCA-IWM model for determining the prognosis of waste production. We will be able to create and evaluate different scenarios for the waste industry, as well as offer suggestions for various technologies and equipment for working with waste materials, taking into account the social, environmental and economic impact involved [4].

References

[1] Plánovanie a optimalizácia odpadového hospodárstva – Príručka na vypracovanie prognózy množstva komunálneho odpadu a trvalo udržateľného systému odpadového hospodárstva, Projekt "Použitie programu odhadu životného cyklu pre rozvoj stratégie integrovaného odpadového hospodárstva pre mestá a regióny s rýchlym rastom hospodárstva EVK4–CT–2002–0087, p.304, Bratislava2005.

[2] Čermák O., Čermáková M.: Integrated approach to the solution of the infrastructure of an urbanised area . In 8thConference on Environment and Mineral Processing. VŠB TU Ostrava, pp. 67–72.

[3] Jankovičová K., Parráková E.: Odpadové hospodárstvo v Bratislave. In: Zborník medzinárodnej konferencie TOP 2004, Účelové zariadenie, Kancelárie NR SR, Častá-Papiernička 2004, pp. 291–296, ISBN 80-227-2058-5.

[4] www.lca–iwm.net

[5] Škultétyová I.: Vvyužitie LCA v rozhodovacom procese integrovaného odpadového hospodárstva, 127s. STU v Bratislave 2011.

[6] Škultétyová I.: Solid Waste Production. 9th Conference on Environment and Mineral Processing: Part I – Ostrava 2005.

Acknowledgements

The article was written with the support of the Scientific Grant Agency – project VEGA no. 1/0559/10 dealt with at the Department of Sanitary and Environmental Engineering of the Slovak University of Technology.

19 Computational Advances in Sewer System Appraisal

Štefan Stanko (Slovak University of Technology, Faculty of Civil Engineering, Bratislava, Slovakia)

19.1. INTRODUCTION

The Slovakian advances in sewer system design and build could be defined on experiences base. The extensive sewer system built up in last years was orientated to build up mainly the separated sewer system. The combined sewer system became very expensive and concerning the arrangements didn't fulfill the extensive requirements for the general covering of the sewer system in Slovakia. The newest information about public sewer system covering show us, that only build up the domestic waste water sewer system can fulfill the EU promised to dewater municipalities more than 2 thousand and less than 10 thousand inhabitants till year 2015 and municipalities with agglomeration more than 10 thousand inhabitants till 2010. This is the Slovakia's obligation. The failure of this obligation will be affected by the penalty. Comparable EU countries, the Slovakia is lag behind the inhabitants connection on public sewer system. Now this is about 60%. The highly-developed EU countries such as Germany, France, Finland, Spanish, Netherland and Austria it represent about 85%.

19.2. SEWER SYSTEM APPRAISAL

The appraisal of sewer system is very important rule of hydraulic and hydrologic engineering field. Every fault in sewer system disrupts the life activities in the touched municipality. If the fault takes longer than short certain time, it could involve the health hazard concerned inhabitants. The repeating density of fault is interesting too. Only sewer system appraisal and early malfunction investigation could prevent the people against uncomfortable life and stopped the health risk. The many items have an influence on sewer system condition, such as build state and capacity of the sewer pipe. In the case of combined sewer system, which is used mainly in urban city areas, the periodicity of flooding is important. Our cities contain combined sewer system, which is now relatively old. It means, that the probability of malfunction reaches higher percentage and sewer system extension, involving the houses build up extension, can absolutely change the sewer behavior. We need to know the sewer system behavior and it can be reached by using appraisal procedures of sewer system. In the Slovakia we use the hydrodynamical computer mathematical models, which are very accurate, but need to much accurate data for obtaining the real appraisal results. The other way how to reach very fast required results are using the computer model

based on rational method, which recalculate the old sewer system with the same method, how was used in the historical design, but with actual data. This way can very fast answer for required questions, whether the sewer capacity is or will be enough.

To manage the appraisal computation we need to know the rule of separated and combined sewer system.

19.3. THE RULE OF SEPARATED SEWER SYSTEM

Separated sewer system used separate dewatering of sanitary waste water and storm-water. The sanitary waste water dewatering becomes the most important. The main role of the separated sewer system is dewatering the domestic waste water from residences to waste water treatment plant – WWTP through the sewer system. The people, who live in their residences, are not very often informed, which sewer system dewaters their waste water to WWTP. This illiteracy cause the problems with storm water dewater, mainly in residence areas, where the people connect their roofs and pavement areas to the sewer system in some cases, which is designated only for the domestic waste waters. People assert, that they pay the waste waters, so they have accrue dewater the roofs and pavement areas from their residence. This misunderstanding cause the problem mainly with the capacity and energy consumption of separated pumping stations, and consequently in WWTP. The standard for determining the domestic waste water amount uses the follow design formula (1):

$$Q_{dwf} = I_{no} \cdot q_{wwp} \cdot k_h \tag{1}$$

where: Q_{dwf} – amount of domestic waste waters,
I_{no} – number of inhabitants connected to the actual computed point,
k_h – maximum hourly coefficient, which depends on the inhabitants number I_{no}.

Equation (1) computes only the amount of domestic wastewaters, but it is determined for the sewer pipe diameter design. The pipe profile design depends on the computed amount of waste water Q_{d-dwf}, and this value is twice more Q_{dwf} (2)

$$Q_{d-dwf} = 2 \cdot Q_{dwf} \tag{2}$$

The multiplication factor 2 shows, that the pipe exploitation is 50%. The rest 50% of capacity represents the volume, which is exploiting for the annual sewer cleaning under sewer operation.

19.4. WHY COMBINED SEWER SYSTEM

Combined sewer system dewaters together domestic waste waters and storm waters. This type of sewage is historical; it was built in the history in many towns. The historical principle was to provide the self cleaning service for sediments of dry weather flow without equipment exploitation. The waste waters were drain directly to recipient, with only the dewatering interest. The idea about the waste water treating was not interested.

Present era showed us, that the non-treated waters cause the various problems in the recipients. The huge recipients, such as big rivers, have the self cleaning ability concerning waste waters. But the population density increasing, together with living standard, causes the enormous amount of pollution increasing. Many rivers lose the self cleaning ability. It was the one reason for waste water treatment plant building.

The combined sewer system, dewatering the waters to the waste water treatment plants, causes the non-uniformity flow to the WWTP. That means, in dry periods the pollution goes directly to the WWTP. In wet period, the municipal waste waters are mixed with the storm waters. And this is the problem, because the WWTP is designed only for the municipality waste water treating and some polluted parts of storm water, mean first flush. The other storm waters needs to separate and send directly to the recipient, because the WWTP capacity and the technology process doesn't allow treat all waste water from the watershed.

This storm water separation is executed through the combined sewer overflow – CSO structure, which is designed for the specific amount of storm waters separation.
The Slovak big cities uses the combined sewer system for dewater the storm and municipality waste waters [6].

The basic principle, how to determine the amount of storm and municipality waste waters is based on basic rational formula.

$$Q_{sw} = S \cdot \mathrm{q}_{sw} \cdot \psi \tag{3}$$

where: Q_{sw} – amount of storm water,
q_{sw} – specific rainfall capacity (similar on specific storm/rainfall intensity) ($\mathrm{l \cdot ha^{-1}s^{-1}}$) (6),
ψ – runoff coefficient (range 0–1).

Specific rainfall intensity q_{sw} represented by capacity-duration-frequency – CDF curves are determined for 68 rain stations in Slovakia [8], which measure the rainfall intensity. The CDF curves are used mainly for periodicity/frequency 0.5 or 1.0, depends on locality size [5]. The elaboration of rainfall intensity produces the block rains, through the CDF curves. This block rains, depends on storm duration is used for determining the storm water flow [5]. Formula (3) determines only the storm waters amount. For total design flow determining for combined sewer system, we use the follow formula (4)

$$Q_{d-css} = Q_{sw} + Q_{dwf} + Q_b \tag{4}$$

where: Q_{dwf} – represents dry weather flow – municipal waste water,
Q_b – ballast waters.

The amount of Q_{dwf} is neglected under the condition, when the Q_{dwf} is less than 10% of Q_{sw}. The ballast water Q_b is included, because the sewer system is very often untightness.

The formula (4) shows, that in dry weather period, only amount of municipal waste water flows into the sewer system. This flow must be drain into the WWTP.

In the wet weather, when the storm start, the specific amount of waste waters are dewater to the WWTP and rest to the recipient through the CSO structure. The determination, which part will be dewatering to the WWTP is not easy for determining, because this determination influences the WWTP pollution and capacity loading or recipient pollution. The CSO structure is the very risk factor on CSS, concerning environment protection and cleaning process optimization. Slovakia uses two ways for the waste water flow determination: a) method of the dilution ratio and b) method of the boundary rain.

The dilution ration method defines as the ration between domestic waste water and storm water. Usually this ratio represents 1 to 4 or 1 to 8 in last time. The more dilution mean, that the larger waste water flow will be dewater into the WWTP for treating, and it means the greater recipient protection against pollution.

Determine the WWTP flow by using the Boundary rain method is base on watershed size and this is defined by formula (5):

$$Q_{boundary} = S \cdot \psi \cdot q_b \tag{5}$$

where: q_b – represents the specific capacity of boundary storm, range <from 10 to 25 l/s/ha>.

This value depends on self-cleaning recipient ability. Generally the larger recipient, with the more self-cleaning ability, uses the smaller specific boundary rainfall capacity and vice-versa.

19.5. DESIGN THE COMBINED AND STORM SEWER SYSTEM THROUGH THE SEWACAD

The many Slovak sewer system were designed and recalculated by the SeWaCAD – computational software system, which can design and recalculate existing sewer systems, combined and separated, by the rational formula. This system is a user friendly and with huge computer capacity. The goal of this system is to design the longitudinal profiles of sewer pipes, which is useful for build the sewers. The system works very dynamic, and the hydro-technical computation is directly transferred into the graphical representation. This software offers to solve the separated and combined sewer system. Because the combined sewer system design is more complicated when the domestic waste water sewer system; system contains the rainfall tool with the rainfall database from 68 Slovak rainfall stations.

$$q_{sw} = \frac{K}{t^a + B} \tag{6}$$

The formula (6) shows the basic principle of the q_{sw} designation, where the K, B, a represent the parameters which represents the specific rainfall station, where the measurement data were elaborated, t – represents the time of the rainfall duration.

The Fig. 1 and Fig. 2 show the existing sewer system [7] and indicate the overload of this part of the sewer pipes. The color lines shows the percentage of overload of the combined sewer system, and the number in brackets shows the value of existing diameter and the other the design diameter of the sewer pipe [3].

The design of the longitudinal profiles represents difficult work for designers; because it needs be careful in the same time with the hydro-technical and graphical solutions. Repeat process computation could fulfill the requirement results. The system SeWaCAD can design the slopes, which can design the slopes for the designed pipes. Base on slope design, there is possibility of diameter change and vice-versa.

The recommendation for minimal profile of public sewer system is 250 mm diameter. In the past it was 300 mm in diameter for the sewer pipes design. Concerning the minimal slope computation the 250 mm has the worse influence on excavation depth and over-

charge the investment costs. But on the other hand, the operational conditions are improved by using the new design conditions.

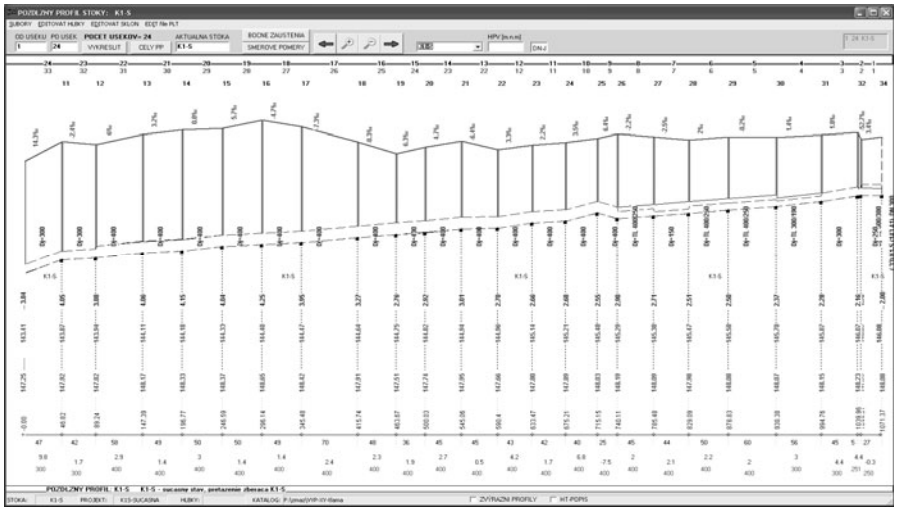

Fig. 1. The longitudinal profiles for the sewer system design – example of the existing sewer system

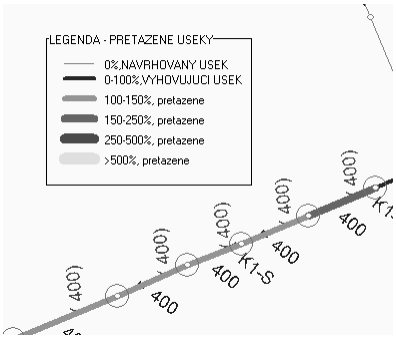

Fig. 2. Example of sewer system overloading

19.6. CONCLUSION

The present time is represented with various system of sewer system appraisal. Every system is specific. We very often give us the question, why we need to much mathematical computer models. Why we don't use one, the best one. The answer is, that the best one system is the system, which is understandable for us, which is accessible from the financing possibilities. That's why in Slovakia we use the commercial system such as MOUSE, or SWMM, SeWaCAD but the difference is evident in price, in using, in results offering. We need to know that we need to declare our goal and use the system, which fulfill our expectations. From this view the recommendation of sewer system appraisal model depends on

us and recommendation is: Use the system, which is clear for you and which fulfill your requirements!

References

[1] Ghawi Ali Hadi, Kriš J.: "Separate Treatment And Reuse Of Grey Water In Iraq Villages" The 3rd IWA-ASPIRE 2009, Taipei. October 18–22, 2009.
[2] Mahríková I.: Waste water from small urban areas – impact of environment in Slovakia, In: Risk management of water supply and sanitation systems impaired by operational failures, natural disasters and war conflicts. ISBN 978-90-481-2364-3. Published by Springer 2009, The Netherlands. Book, pp. 37–45 2009.
[3] Mahríková I.: Waste Water Treatment from Small Urban Areas. In: Dangerous Pollutants (Xenobiotics) in Urban Water Cycle, ISBN 978-1-4020-6800-3. Published by Springer 2008, The Netherlands. Book, pp. 71–81.
[4] McCuen R. H.: Hydrologic Analysis and Design, Pearson. New Jersey: Prentice Hall 2007.
[5] Šamaj F., Valovič Š.: Intenzity krátkodobých dažďov na Slovensku. Zborník prác SHMÚ č. 5. SHMÚ, Bratislava 1973.
[6] Šerek M., Šálek J., Mičín J.: Stokování a odvodnění – Vodohospodářské tabulky (Praha 1985).
[7] Stanko Š, Sirák I.: Implementation of trench-less methods on Slovak conditions. In: WMHE 2009. Vol. I.: Eleventh International Symposium on Water Management and Hydralic Engineering.Ohrid,Macedonia, 1–5.9.2009. – Skopje: University Ss. Cyril and Methodius, 2009. – ISBN 978-9989-2469-6-8. - S. 553-561, 2009.
[8] Urcikán P., Imriška L.: Stokovanie a čistenie odpadových vôd. Tabuľky na výpočet stôk. SNT, ALFA, Praha, Bratislava 1986.

Acknowledgement

The article was written with the support of the Scientific Grant Agency – projects KEGA No. 3/7452/09 dealt with at the Department of Sanitary and Environmental Engineering of the Slovak University of Technology.

20 The Alternative Sewer System Design in Flat Areas Considering Sewer Type

Štefan Stanko (Slovak University of Technology, Faculty of Civil Engineering, Bratislava 81368, Slovakia), Borys Skip (Chernivtsi National University by Yuriy Fedkovich, Chemistry Department, Ukraine)

20.1. INTRODUCTION

The Slovakia landscape, especially east East-Slovakian Lowland and west part – Danube Lowland, allows realize the sewage networks by various principles. The investment process needs to revalue the approaches, needs to take the consideration, that the building sewage will be operated under the municipalities, which will be want to operate it without non wanted operational costs involved by the improper design, or no adequate cheap investment. The European financing by the EU budget looks very interesting for the investors. The tendering process chooses the lowest investment solution, and the impact will be evident after the few years, after the operational experiences. The question is: What is the important?: The fast building, the proper operational, saving the investment or what? The answer is relatively clear by the clever approach, but in real life, these few questions produce very often non clever answers, concerning the various subject interests.

Using the alternative, mean gravitational, pressure or vacuum sewage system very often decides the financial conception solution. Specially the flat areas allows to use these alternative solutions, which very often saving the money, but the relevancy mirror could be not clear.

20.2. FLAT AREA OFFER MINIMAL LANDSCAPE SLOPE

The present Slovakia sewage state, when the greatest problem of the build is non design documentation, but the investment gaining and the fastest building process, shunts the technical, especially operational conditions on the minor side. The sewage alleviation is no discussed, only quantitative aspects are important. It concerns to the gravitational solution. The problem will be significant in the future when no only operational costs will increase, but rehabilitation and reconstruction will be necessary, too, together with the increasing financing.

The present minimal slope recommended in Slovakia sewage design is defined by the empirical equation:

$$i_{\min} = 1500/D \tag{1}$$

where D is the sewer diameter in millimeters. The minimal slope define the build-technical slope, which is possible to observe in building process and this slope has no elegible value concerning sewage alleviation, where the sewer slope we need to define regarding the amount and quality of waste water. The minimal slope were defined till few years ago and through more than 50 years by the equation

$$i_{\text{min–historical}} = 1000/D \tag{2}$$

It was more advantage in the design process, especially when the minimal allowed sewer diameter were DN 300 mm against present recommended DN250. The historical design saved the excavation and together the investment costs and allowed more sewer capacity reservation and in the flat areas saved the number of pumping stations.

The present value of minimal slope is insufficient – despite of slope increasing. This opinion is supported by the authors Stránsky D. et all. [2], which are interested about the question of alleviation and related problems of the odor. They recommend the minimal slopes, which are mentioned in the table 1. The columns (3) and (5) are the multiplication of the columns (1) × (2) and (1) × (4). These aspects clear the situation and we can say, that there is no empirical influence between the recommended slope and sewer diameter. Mentioned values of minimal slope were determined by the influence of minimal recommended transportation waste water velocity v_t, at which the dry weather sewage recommended for the $Q_{h\max}$ 0.6 m/s. In the case of combined sewer system, the 0.75 m/s is recommended and in the case of stormwater sewage this value is represented 0.75 m/s where the flow is Q_p – average flow.

20.3. SELF-CLEANING SLOPE

The EN752 recommendation for the design of dewatering and sewer systems are explicitness and wants to prevent the sewers against the permanent drift deposition, which increasing the risk of the flooding involving by the sewer system and follow environmental pollution.

The sewers bedded in the minimal slope are drifted and we need to clean it. Čížek [1] in the 1953 advised to compute the sewer slope of the combined sewage with the exploitation of the equation for critical tangential tension near the wall of the sewer pipe by the equation

$$\tau = \rho\, g\, R\, io \ (\text{N/m}^2) \tag{3}$$

where: τ – tangential tension [Pa],
g – gravitational acceleration [m/s^2],
R – hydraulic radius [m],
i_o – slope.

When we put $\tau_{critical}$ = 4.0 Pa for combined sewer system, after self-cleaning velocity is defined by the equation.

$$v_s = 0.02 \cdot R \cdot 0.167 \cdot n^{-1} \ (\text{m} \cdot \text{s}^{-1}) \tag{4}$$

where: n – Manning's roughness coefficient.

In the case of dry-weather sewage we choose the $\tau_{critical}$ = 2.0 Pa [3]. The sewer bottom slope is equal i_s = 0.00204/R, and the R is relative to the average dry-weather flow Q_{b24}.

Table 1

Recommended values of minimal slopes in dependency on sewage type

Indicators	Recommended values				
	(1) DN	(2) Sanitary sewage	(3) x/D	(4) Combined sewage	(5) x/D
Minimal recommended slope	[mm]	[‰]	x	[‰]	x
	250	18	4500	12	3000
	300	14	4200	9	2700
	400	9	3600	6	2400
	500	7	3500	5	2500
	600	6	3600	4	2400
	800	5	4000	3	2400

20.4. FLAT AREA – SOFTWARE EXPLOITATION

The design software exploitation in the flat areas is the effective tool for the alternative sewer system design. The hand calculation of sewer system take too much time, this is maybe inaccurate and very difficult. The software using offer the chance in a short time to investigate more alternatives of design, the using of more diameters of sewers and solve the conception of sewer pumping station.

The Department of Sanitary and Environmental Engineering use offer the solution, through the computational system SeWaCAD, which offer to design alternative solutions with the possibility of alternatives comparing. The using minimal diameter DN250 against DN300 in older period bring the saving the profile diameter, but not excavation and number of pumping stations. To elaborate of alternatives could clear us the effective solution, and answer the question, what is effective. For example the historical approach uses the minimal slope 3.33‰ with the profile DN300 against present minimal slope 6‰ together with the DN250 diameter using. It caused the lost of elevation 60 cm – 33 cm = 27 cm for every 100 meters, which represent total lost of elevation 2.7 meters per 1 km of sewer length. So we can very easy assert, that we need to build 2x more pumping stations against older principles. If is it effective or no, we find this answer through the alternative design evaluation, from technical and economical view, with the respecting the operational conditions and operational costs. We can say, that influence of terrain composition play the important role in sewer system design. Evaluation of many sewer system design in various conditions offer for us declaration, that saving profile diameters DN250 is not in every case the clever solution, but in many cases legitimate. And we can declarate, that only complex alternative solution could give answer this question.

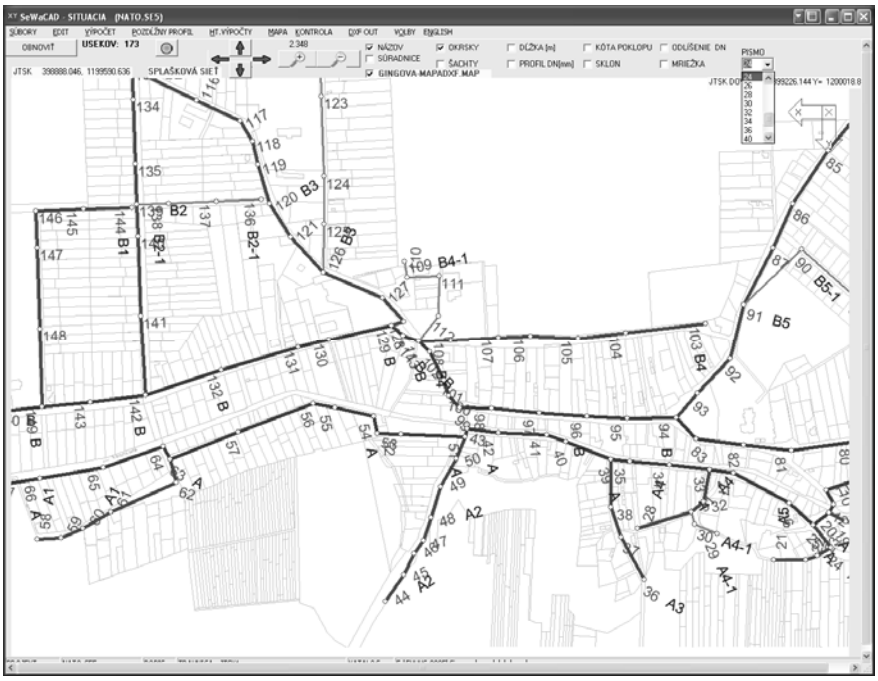

Fig. 1. Computational example of sewer system design in the flat area (SeWaCAD)

Under-pressure or vacuum sewage

Is the alternative way of sewage concerning only for sanitary waste waters in the locations, where is the problem to build the gravitational sewer system from the technical or investment view.

This system we can use in location, where the storm water dewatering system is done and where we want to save the environment against the excavation together with the saving of building works, and where we want to save a relative financial costs. The word relative is for discussing, because investment costs saving with the excavation and profiles, which are from DN50 do DN200, against gravitational sewer system which start from DN250 are become evident, when we need to build the vacuum station with the relatively high operational costs concerning energy, which is needed for making the vacuum in the pipes. The under-pressure range is usually from 400 to 500 mm of quicksilver column, minimum 175 mm from the maximum 760 mm, which represent theoretically max. 7.5 m of water column. Under-pressure 400–500 mm allow to overrun the elevation differences approximately from 4 to 5 m.

The main part of this sewage becomes the vacuum station, which produces the under-pressure. This part is very demanding for the energy, which could cause the operational of this system economically intolerable.

Sewage waters are collected throught the system of pipes in the collection container, from this there are transported to the WWTP. The advantage of such sewage is a minimum depth of the bedding, the ease exploitation by user and groundwater protection.

Its use is appropriate when we have a problem to build a gravity sewer system in places where there are no suitable geological conditions such as high groundwater level, soil inconsistency – sands (Slovakia – Záhorie).

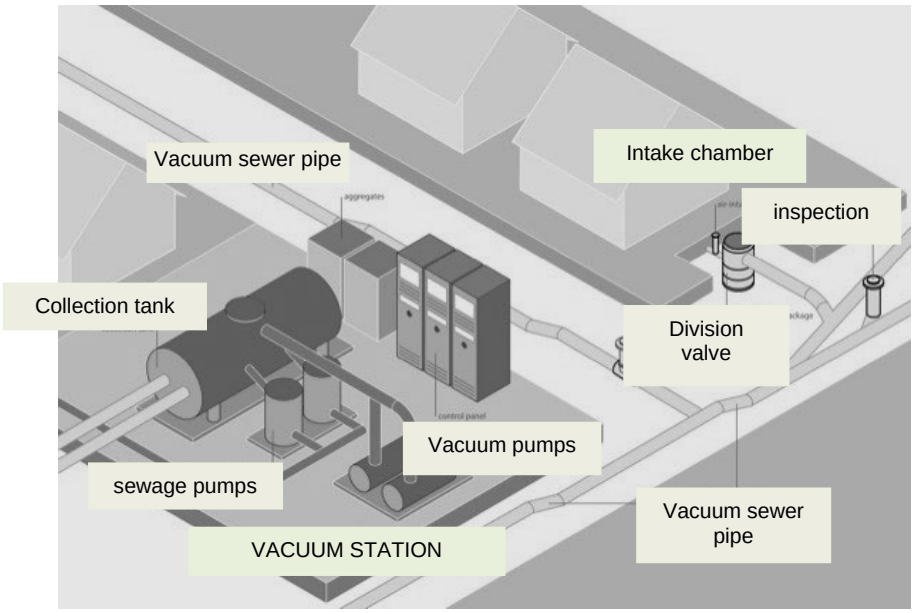

Fig. 2. The scheme of vacuum sewage [7]

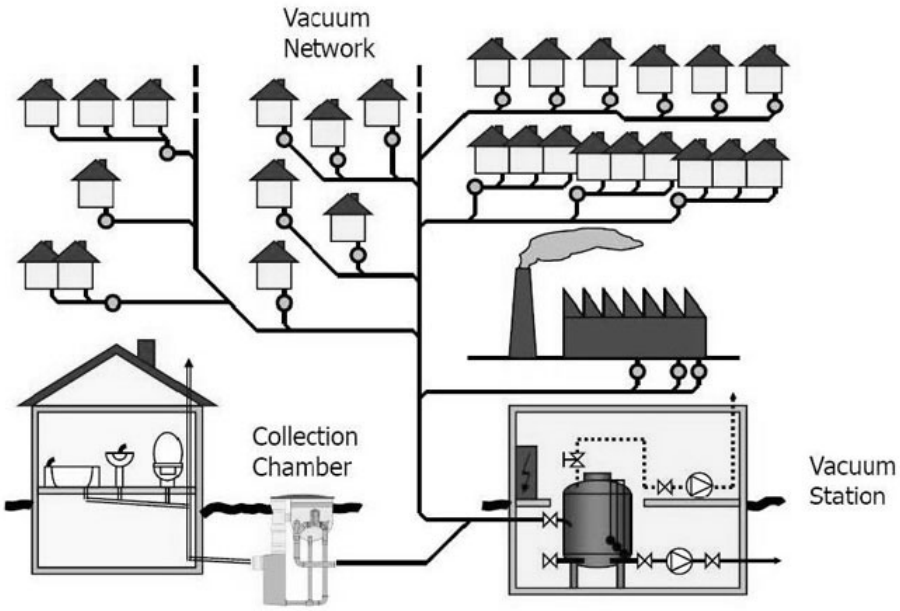

Fig. 3. Logical scheme of vacuum system [9]

The application vacuum sewer system requires the build management base on the assumption of construction quality.

The insufficiency of this type of sewage is noted by the residents in the village Vajnory in Slovak republic, when was implemented [6] this type of sewage, and there was published the instruction article in the local newspaper, how to exploit this sewage, and after the state is unsatisfied [5].

Pressure sewage

The idea of pressure sewer system started up as alternative dewatering of small residential areas, small municipalities in flat areas, resp. on the terrain with the low elevation differences with the aim to save an investment costs. The greatest influence have investors. The operational quality depends on equipment, mainly on end pressure stations, on tide gate. Results from the operational experiences of pressure sewage say that this sewage alternative can be favorable. The build of pressure sewer system is suitable in spread areas, in recreational zones. From the financial demand, this type of sewage is the most competitive, considering the argument, that the pumping stations are situated on the residential owners, which are financing and operating the pressure pumping stations. From the operational company this is an advantage, but on the other side it could generate the complex problems concerning the faults cause by this pressure pumping stations.

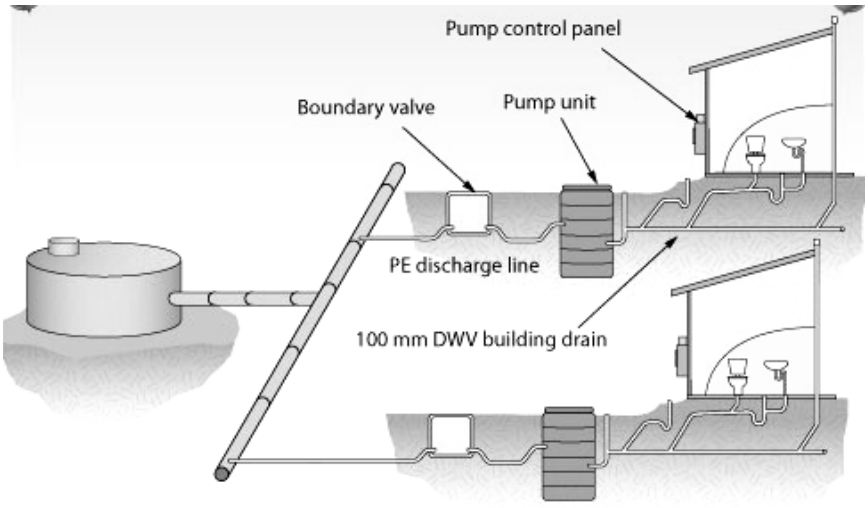

Fig. 4. The system of low pressure sewer system [8] with pumping units, ground pipe, collecting pipes

How to make a decision

In EU contries every designer must consider, which type of sewer system will be designed, base on investment costs, operational costs and from the technical opportunities. In the places, where is the slope of terrain enough, the gravitational is more effective than in flat areas. We reflect the vacuum system designing in the next cases:

— Inadequate nature slope,

— Isolated or rare build-up area,

— No quality underbed,
— Zone of hygienical water supply protection,
— Barries in the way of build – other engineering networks, water streams,
— Seasonal operation – touristic zones,
— In the places where we need to eliminate excavation works.

The vacuum sewage design consists from the network design, longitudinal profiles designing, the separate branches designing and the location of collection manholes. The main criteria of design is the appraisal of total pressure loses on separate branches of the system, where are the losses involved by friction – mixture of water-air in the velocity 6 $m.s^{-1}$ and local losses which are involved by the flow direction – refractivity. The determining item is the energy demand needed for vacuum station air-pump engine and pumping stations. The specific demand of energy for air-pump power drive increases with increased length of main sewer branches.

20.5. CONCLUSION

The buil-up of sewage in flat areas is the intersection of investor interest and operator. The decision which type of sewage we will build up, and how we will solve this problem absolutely belong under expert decision, and this is very incorrect, if this decision is accepted by the investor, without expert and operator discussing.

The experiences show, that investment interests have the highest priority for decision and it mean the saving investment costs without interest on the operational experiences. The final problem is transferred on operational company, on users of the sewage. The start decision, which sewer type we will build up, have a longtime impact and this could be very negative in the horizon of more years, could have a impacts on lifetime of sewage, to transfer the problems into the future. Eighty percent of a municipality's problems are caused by twenty percent of its sanitary sewers and storm water drainage systems. The best way to avoid the majority of future problems is to pay greater attention to them during the design phase.

Only clever and expert approach of main decision, supported by expert could have an effective, optimal impact on dewatering the area from waste waters.

References

[1] Čížek P.: Hydrologie stokových sítí, Stokování, 1.část, SNTL, 1961.
[2] Stránsky D., Havlík V., Kabelková I., Metelka T., Sýkora P., Dolejš M., Haloun R., Mucha A., Pryl K.: Posouzení stokových systému urbanizovaných povodí, část III. – řešení balastních vod a výskytu sedimentú ve stokové sítí, Vodní hospodářství 08/2010.
[3] STN 75 61 01 Stokové siete a kanalizačné prípojky.
[4] STN EN 752 Stokové siete a systémy kanalizačných potrubí mimo budov.
[5] Grič J.: Pokyny pre občanov k vypúšťaniu odpadových vôd do podtlakových šácht a tým do podtlakovej kanalizácie Vajnory, Vajnorské novinky, ročník XIV 9/2008.
[6] Mrva J.: Vákuová kanalizácia Pod Válkom spôsobuje problémy. Vajnorské novinky, ročník XVI 3/2010.
[7] sewagetreatmentss.com/2011/05/21/vacuum-sewage/ (2011).
[8] zephyr.cit.act.edu.au/toolboxes/licensed_to_plumb_12.01/toolbox12_01 /units/cpcpdr4001a_sanitary/00_groundwork/page_002.htm
[9] www.lce.com.na/projects_ongoing.html

Acknowledgement

The article was written with the support of the Scientific Grant Agency – projects KEGA No. 3/7452/09 dealt with at the Department of Sanitary and Environmental Engineering of the Slovak University of Technology.

21 Numerical Modeling of Combined Sewer Systems

Drazen Vouk, Davor Malus, Vladimir Poljak (University of Zagreb, Faculty of Civil Engineering, Water Research Department)

21.1. INTRODUCTION

Dimensioning of combined sewer systems in Croatian engineering practice is still influenced by the established practice using simple conventional methods. Simplicity of application and results guaranteeing high safety, and long-term habit in engineering practice resist changes and novelties requiring additional efforts and investments.

With present possibilities reflected by the wide use of sophisticated numerical models with high-quality computer support, further insisting on the conventional approach cannot be considered reasonable and justified. The present trend of strict rationalization of costs in all segments of social and economic development, including municipal water management, results in unavoidable need to use numerical models in dimensioning of combined sewer systems. Numerical models allow rapid and simple simulation of complex hydraulic problems typical for combined sewer systems, while the conventional method of solving is extremely complex and most frequently results in oversized solutions [1, 2]. In this context, designing of new systems is not the only topic, but it includes also remodeling and optimization of the existing systems.

The paper shows the way of defining of the basic parameters describing the runoff of rainfall inflow, as the key segment of the analysis of inflow into the combined sewer systems. It points out the method of defining of catchment areas, including the relevant descriptive parameters. In practice, a larger number of typical sub-catchment areas is enlarged and substituted by an integrated larger catchment area with averaged values of key parameters (runoff coefficient, infiltration, etc.). The reason of such practice is simplifying of the entire calculation. The paper will demonstrate the justification of enlarging of catchment areas, or the influence of enlarging on the quality of presentation of basic hydraulic and operational circumstances within a closed sewerage network.

The problem is analyzed on an actual example describing real hydraulic and operational flow conditions. Numerical modeling has been done using the model EPASWMM, version 5.0.021 [3]. On the same example, model calibration has been carried out in relation to results of field research in the form of measuring the discharge, flow velocity and height of the water table within the pipeline, and records of real rainfall events coinciding with the other measurements.

21.2. METHODOLOGY

Numerical modeling implies estimating of hydraulic properties of the system by means of the numeric algorithm which describes dynamically all relevant flow regularities. Simplicity of their use and speed in conduction of complex numerical operations make them an unavoidable tool of modern way of solving the engineering problems. So far, numerous numerical models have been developed; however, the process of their development continues, and they are undergoing constant improvement.

Using of numerical models greatly facilitates the entire process of calculation and dimensioning of sewer systems, both separated and combined, with presentation of real flow conditions and the additional possibility of testing a great number of complex scenarios for maximum optimization. Problem complexity refers to:

— simulation of dynamic conditions in unlimited time period
— testing of various dynamics of system loading through arbitrary time periods (monthly, daily or hourly inflow irregularities) and for actual rainfall events in unlimited time period,
— respecting of system languidity
— estimate of backwater and checking of the height of sewer filling by wastewater
— checking of sections where pressure flow is occurring, and duration of pressure conditions
— comparison of results with differently defined dynamics of pumping station operation
— comparison of results with differently defined properties of combined sewer overflows, etc.

Among other things, models offer high-quality graphic presentation of results, which facilitates their review and proof.

Although most numerical models are of commercial nature, availability of some of them does not present a problem, because they can be, as free tools, taken off from the Internet. One of such models is EPASWMM (Environmental Protection Agency – Storm Water Management Model). It was developed in the early seventies of the past century, and has been constantly improved ever since, with several basic versions. New versions are suited to the users of Windows interface, which facilitates introduction of input parameters and overview of results. The model allows simulation of stationary and dynamic runoff conditions of dry, rainy or combined inflow within closed or open sewer systems. The possibility of simulation of rainfall inflow runoff in catchment areas, with generating of waste substances and their discharge through the sewerage network, and statistic processing of input and output parameters contribute to the quality of the model and its worldwide acceptance.

As regards defining of the relevant rainfall intensity, EPASWMM offers the possibility of defining real values. If real rainfall records are available, numerical algorithm of the model automatically calculates the rainfall intensity and resulting values of other hydraulic parameters. If the influence of relevant rainfall, obtained from IDF relation, is analyzed on the model, a series of iterative steps helps to determine very simply and quickly the relevant concentration time and intensity of rainfall to which the new system is dimensioned, or the existing system optimized.

An important step in the entire procedure of analysis of existing combined sewer systems on the numerical model is successful calibration of the model. Calibration is carried out in relation to measurement of separate hydraulic parameters in characteristic points of

the system, and to later comparison with the results obtained on the model. It is important to carry out simultaneously rainfall measuring, to enable the model to describe also the flow during rainfall events with equal reliability. With successful calibration, the model automatically determines the real values of runoff coefficients, for each component of the system as well as for the system as a whole.

When the model has been successfully calibrated, i.e. when it is determined that the model describes the existing conditions with adequate quality, it can be applied in analyses of planned situations and making of sound and reliable conclusions.

21.3. ANALYSIS OF THE PROBLEM

The entire problem was analyzed on the actual example created for the purpose of this paper. The system selected was the combined sewer system of the city of Djakovo, in which framework a part of the entire system was singled out (north-eastern part of the city of Djakovo), shown in Fig. 1. and Fig. 2.

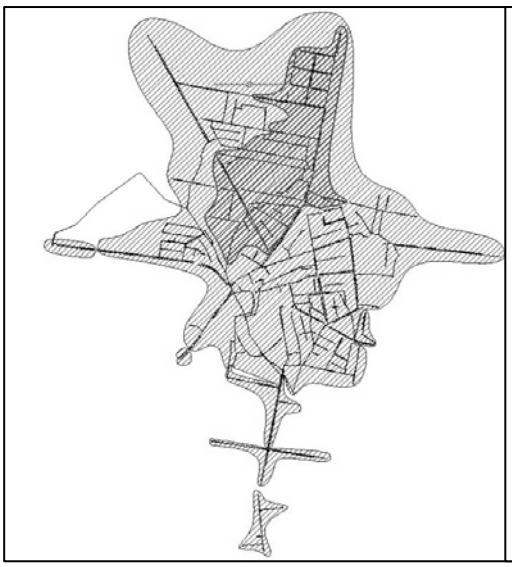

Fig. 1. Sewerage system of the city Djakovo with project area

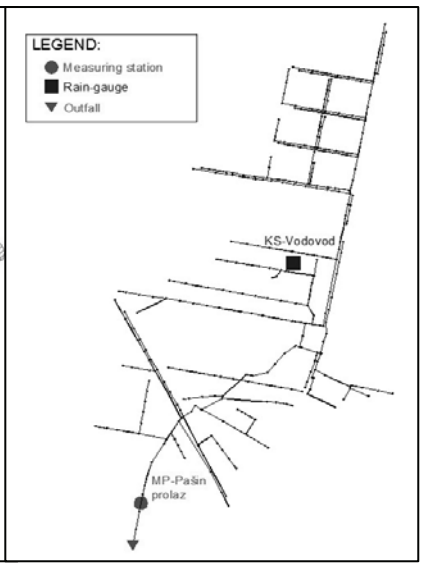

Fig. 2. Hydraulic scheme of the project area

21.3.1. Defining of input parameters on the model

The entire encompassed area is defined on the numerical model using EPASWMM. The area serving the population of about 7000 is characterized by the total length of the sewerage network of approx. 20 km. The entire sewerage network is built of concrete pipes of circular profile with diameters ranging from DN 300 to DN 1000 mm. The wastewater

flow in the separated area is gravitational. The catchment area from which rain water is drained is 140 ha.

Geometry of the pipeline network

The basic geometry of the system consists of point and linear elements. Point elements are, as a rule, nodes representing manholes, horizontal and vertical sharp turns of the pipeline route, connecting points of several pipes, lock shafts, etc. The nodes define the initial and final points of the pipe, altitude and depth of the pipe gradient. In addition to the above geometric properties, it is important to note that the nodes determine the inflow of wastewater into the system, by direct defining of the dry inflow, while the relevant rain inflow is calculated within the numerical algorithm of the model, in relation to the properties of the catchment area connected to the corresponding node and rainfall intensity (rainfall records or separate rain event).

Linear elements in the created model are the pipes, of circular cross-section. All pipes are made of concrete, with calibrated mean value of Manning roughness coefficient n = 0.0145. It is important to note that 4 different scenarios of the system have been defined, with identical pipe network geometry with 330 nodes, 330 pipes and 1 outlet.

Catchment areas

Catchment areas are hydrological terrain units whose relevant characteristics must be defined by the user, and the resulting rainfall inflow is automatically calculated in the numerical algorithm of the model. The designer is requested to divide the project area into a number of catchment areas and determine their properties. The elements where the rainfall inflow from the corresponding catchment area is introduced may be nodes or neighboring catchment areas. The size of the entire catchment area analyzed on the example in this paper is approx. 140 ha. The basic characteristics of catchment areas are, as follows:

— *Area* – in hectares
— *Width* – calculated by dividing the catchment area by the maximum length of the surface flow. A change of the catchment area width influences the change of the time of concentration. The larger the width of the analyzed catchment area, the concentration time is less, and the resulting peak discharge increases.
— *Imperviousness* – the share of impervious surfaces in the catchment area, i.e. the surface where the rainfall cannot infiltrate into the soil, but requires a system to conduct it into the sewerage network.
— *Roughness Coefficient* – Manning roughness coefficient n. In the model, the Manning roughness coefficient should be determined separately for pervious and impervious surfaces (e.g. for thick forest areas n = 0.8, and for smooth asphalt surface n = 0.012).
— *Depression storage* – corresponds to the volume that has to be filled before the runoff starts. Various values may be defined for pervious and impervious surfaces.
— *Percent of Impervious Area Without Depression Storage* – This parameter represents runoff that starts simultaneously with the beginning of the rain, before the depression storage condition is attained. It represents the pavement close to the sink, where there is no surface retention, slanting roof drained directly into the sink, etc.

— *Infiltration Mode* – Modeling of infiltration in pervious parts of the catchment area may be done in three ways, by Horton's method. Green-Ampt method of by the Curve Number method. In the actual example described in this paper, the Horton model of infiltration was used.

Inflow

The sewer system in question may be described as a combined system, which means that in addition to rainfall inflow it is also necessary to define the inflow of wastewater from the population and industry. In the actual case, the measurements determined the specific inflow of wastewater from the population of 125 l/PE-day. The coefficient of overall irregularity of wastewater inflow is 2.25, while the hourly irregularity within the whole-day regime is defined on the basis of field tests.

Industrial wastewater has been defined for only one industrial plant working in whole-day regime with maximum hourly discharge of 10 l/s with equal daily distribution as defined for household wastewater.

Rainfall data were obtained by several months of ombrographic measurements with 5 minute time increment, on the location "KS-Vodovod" (Fig. 2).

21.3.2. Model calibration

The model simulated the flow in the time period of 17 days, as for this period the results of measurements of separate hydraulic parameters at the most downstream point of the system ("MP – Pasin prolaz") were available, as well as the rainfall record of the rain-gauge station situated in the central part of the system ("KS – Vodovod").
In the given case, on the basis of the results of numerical model calibration, it may be concluded that the model gives high-quality description of real conditions, both for dry inflow and for combined inflow with rainfall of varying intensity and duration (Fig. 3).

21.3.3. Effect of enlargement of catchment areas

Defining of catchment areas and their parameters is one of the most complex and time-consuming problems in numerical modeling of combined sewer systems. Therefore, in practice a larger number of typical sub-catchment areas is often enlarged and replaced by a larger integrated catchment area with averaged values of key parameters of rainfall runoff (runoff coefficient, infiltration, etc.). The reason for such practice is simplification of the entire procedure. Therefore, the paper tries to assess justification of enlargement of catchment areas, and the effect of enlargement on the quality of presentation of the basic hydraulic and operational situations in a combined sewer network.

Three alternatives of the system were created, in relation to the method of defining of catchment areas – irregular catchment areas of 0.1 – 6.57 ha (Fig. 4A), square catchment areas of 1 ha (Fig. 4B), and irregular enlarged catchment areas 4 – 6 ha (Fig. 4C). The idea of enlargement was to cover the area of several catchment areas by a catchment area of 4 – 6 ha, and to connect it to the node conducting the inflow from replaced catchment areas.

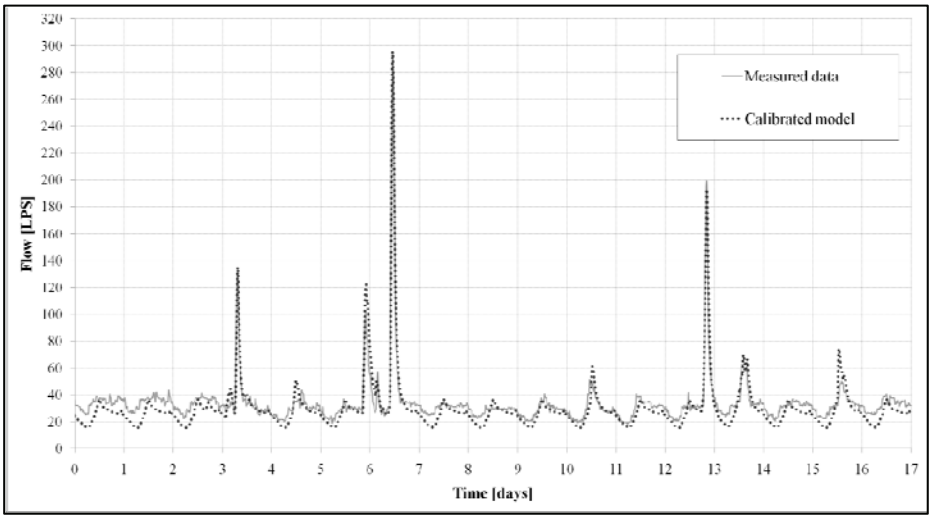

Fig. 3. Parallel presentation of measured and calibrated hydrograph on the gauge profile (outfall)

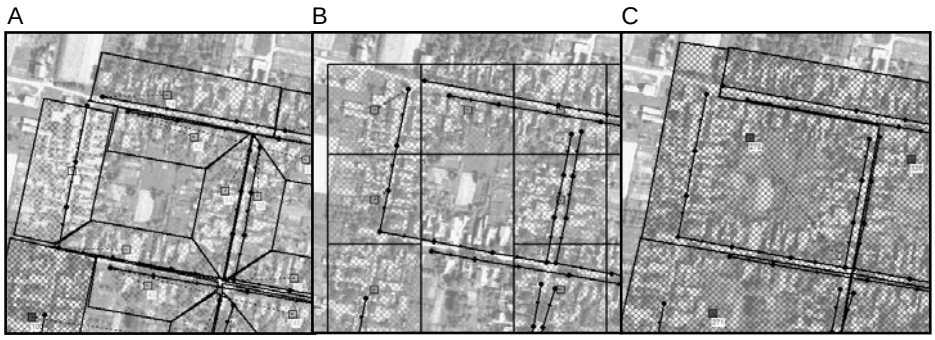

Fig. 4. Scheme of alternative solutions: A – standard, B – square, C – large catchment areas

The analysis of the results will include comparison in relation to concentrations, form of the resulting hydrograph and matching of peak discharges. The model geometry (pipes and nodes) is identical in all the alternatives. The alternatives differ in the number of catchment areas and in the way they were defined. Most parameters describing the catchment areas are identical in all alternatives, except the catchment area size, share of impervious surfaces, and the width of the catchment area. The catchment areas vary in each alternative, except with square catchments where all areas are identical, 1 ha. The parameter *width* is identical for all catchment areas in the second alternative, and varies in the first and the third alternative, but it is important to note that the parameter *width* is directly dependent on the size of the catchment area, because all values of this parameter are obtained by dividing the area by the maximum length of the surface flow. Catchment area characteristics that are equal, common to all alternatives, are shown in Table 1.

Table 1

Characteristics of catchment areas and infiltration model

Parameter	Catchment characteristics						
	Slope	Imperv	n-Imperv	n-perv	Dstore-imperv	Dstore-perv	Zero-imperv
Unit	[%]	[%]	[–]	[–]	[mm]	[mm]	[%]
Value	0,5	28	0,02	0,4	2	25	25

Parameter	Infiltration				
	Max-infil rate	Min-infil rate	Decay const	Drying time	Max. volume
Unit	[mm/h]	[mm/h]	[1/h]	[days]	[mm]
Value	40	3	3	6	0

Alternative 1 (standard) – The number of catchment areas is 103. The areas vary from 0.1 to 6.57 ha. The total catchment area is 140 ha. Each catchment area is connected only to one node. The problem in such defining of catchment areas is comparatively time consuming process, but large diversity of areas is obtained which may be more efficiently used in model calibration.

Alternative 2 (square) – The number of catchment areas is 140, 1 ha each. The data on boundaries, locations and nodes are determined automatically (by computer algorithm analyzing the geometry of the network, and with defining of certain marginal conditions the result is the network of catchment areas) and integrated in the input file. The total area of all catchments is 140 ha. Connecting of each catchment area is done to the closest node, so that two or more catchment areas may be connected to one node. The advantage of this way is considerably faster process of model defining, with better quality results in relation to other alternatives. However, due to generating of a comparatively large number of catchment areas, the calibration process may be difficult and time-consuming.

Alternative 3 (large catchment areas 4-6 ha) – The number of catchment areas is 29. The catchment areas are of irregular shapes and defined manually over the graphic interface. The size of catchment areas ranges from 4 to 6 ha. The total catchment area is 140 ha. The boundaries are selected in the way to encompass the areas that would be enclosed in several minor catchment areas (like in Alternative 1), and are connected to the most downstream node of the encompassed part of the system. The advantage of this method is faster defining of the model and simple model calibration due to a smaller number of catchment areas. However, in the first iteration there is a higher probability of error in the choice of the time of concentration. Also, with larger catchment areas and rainfall events of higher intensity there is the possibility of flooding of inlet nodes in peripheral parts of the system.

21.4. RESULTS

Results obtained on the numerical model show that all three alternative solutions, independently from differences regarding the way the catchment areas were defined, describe the real hydraulic and operational flow conditions with approximately equal quality, which was proved in relation to measured values of discharge, velocity and depth of flow in the check profile. Detailed presentation of the results obtained on the model in comparison with the measured values is shown in Table 2. Additionally, graphic comparison of results is shown in Fig. 5. On the basis of the results it may be concluded that all three ways of defining of catchment areas can be applied with equal success. However, analyzing the advantages and drawbacks of catchment area defining and later model calibration, the authors recommend the use of the combination of Alternative 1 and Alternative 3, where in marginal parts of the system it is desirable to define a larger number of smaller catchment areas.

Table 2

Results of models of alternative solutions

Alternative	Alternative 1 square	Alternative 2 standard	Alternative 3 large catchments	Measured values
Time of concentration	104 min	103 min	93 min	140 min
Runoff coefficient	0.256	0.261	0.261	–
Peak discharge	300.37 l/s	309.36 l/s	303.93 l/s	292.26

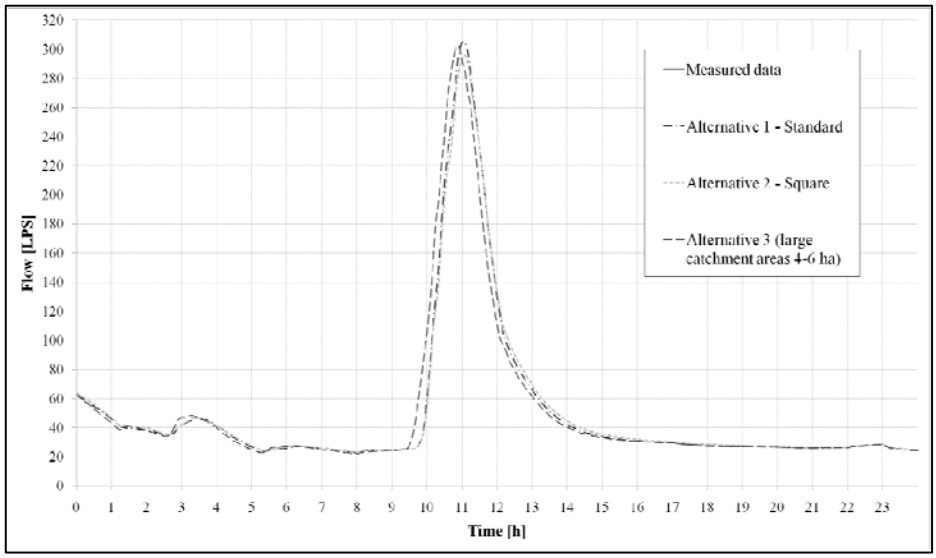

Fig. 5. Runoff hydrograph by variants for rain event

21.5. CONCLUSION

Although the use of numerical models in the analysis of combined sewer systems is becoming frequent, there are numerous cases where their use is connected exclusively to accelerate the procedure of calculation according to conventional principles, or as a means to confirm the results obtained by conventional methods. The paper points out the possibilities and importance of the use of numerical models, which greatly accelerate and simplify the entire analysis, both in dimensioning of new and optimization of existing combined sewer systems.

As regards the way of defining of catchment areas on the calibrated numerical model, the analyses show that enlarging of catchment areas (defining of a smaller number of larger catchment areas) for the purpose of simpler and faster creating of the model and its subsequent calibration, does not disrupt the quality of output results.

References

[1] Malus D., Vouk D.; Tadic Z., Leko-Kos M., Sibalic L., Garic I., Radeljak I.: Vaznost Numerickog Modeliranja pri Optimalizaciji Razdjelnih Sustava Odvodnje. Razdjelni sustavi odvodnje. Ban, Dario (ur.). Rijeka: Venerus, Rijeka 2006.

[2] Vouk D., Malus D.: Numerical Modelling in Wastewater Collection Systems Optimization. Book of Abstracts & Proceedings on CD, Petras, Josip (ur.), Velika Gorica: Gradjevinski fakultet Sveucilista u Zagrebu 2007.

[3] Lewis A. Rossman: Storm Water Management Model – User's Manual, Version 5.0, Water Supply and Water Resources Division, National Risk Management Research Laboratory, Cincinnati, OH, SAD, 2004.

22 NPSH for Centrifugal Pumps

Živko Vuković, Ivan Halkijević (University of Zagreb,
Faculty of Civil Engineering)

22.1. INTRODUCTION

Pumps which operate by rotary action are called rotodynamic pumps and the centrifugal pumps are the first type to be considered. Other types of pumps still have their uses, but the centrifugal pumps are the most commonly used for pumping liquid (water) because of the wide range of duties possible and the comparatively high efficiency and low cost [1].

Centrifugal pumps are machines in which liquids are conveyed in rotors (impellers) fitted with one or more blades by a moment of momentum so that pressure is gained in a continuous flow, Fig. 1. The rotating impeller transmits the mechanical work from the driving machine to the liquid in the impeller channels. Centrifugal forces are generated by the rotation which forces the pumped liquid out of the impeller channels, thus creating a low pressure zone at the start of the blade into which liquid continuously flows due to the steady atmospheric or tank pressure on the surface of the inlet liquid [2].

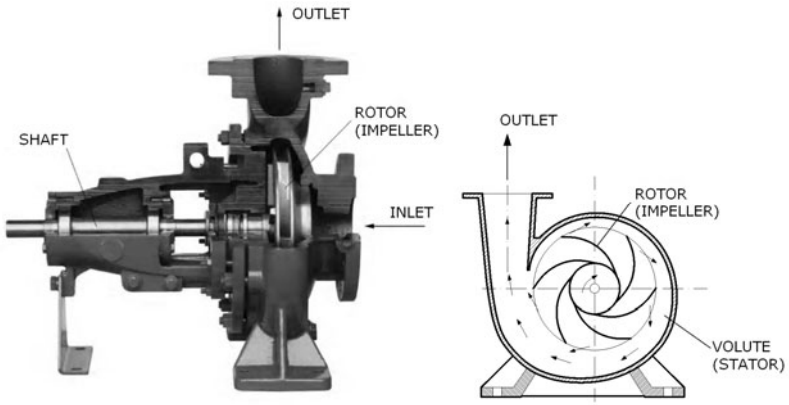

Fig. 1. Cross-sections of centrifugal pumps [2]

Large sums have to be paid each year for the repair of centrifugal pumps because a large number of these machines are not correctly installed. A key factor in this is cavitation, a type of malfunction in pumps due to insufficient vapour pressure in the flowing liquid because the pump has not been correctly installed.

In centrifugal pumps cavitation usually starts at the entry of the impeller blade, but it can be also found in other locations such as the leading edge of diffuser vanes, or wear rings, for example.

Cavitation may destroy impeller, shaft seal or motor bearings after less than 100 hours operation. Furthermore, cavitation results in increased noise and vibration, which can also consequently damage bearings, shaft seals and weldings. Cavitation may also lower the pump flow/head, Q/H, curve and efficiency, η. Finally, the degree of cavitation can increase up to complete breakdown of the flow [3].

The aim of this paper is to give an overview of current scientific research that describes the phenomenon of cavitation in centrifugal pumps. It will also bring knowledge whose application establishes the cavitation-free operation of centrifugal pumps, and thus eliminates the problems noted above.

22.2. CAVITATION

Cavitation is caused by the formation and collapse of vapour bubbles in a liquid. Vapour bubbles form when the local pressure in a flowing liquid decreases to or falls below its vapour pressure at ambient temperature. When a bubble, or void, moves with the flow to an area with a higher pressure, it will rapidly collapse (implode). The implosion causes a transitory, extremely high local shock wave in the liquid. If the implosion takes place near a surface, the pressure shock will, if occurring repeatedly, eventually erode the surface material. This effect is known as cavitation erosion and cavitation corrosion, respectively [1, 2, 4]. Wear marks from cavitation erosion typically occur locally and consist of deep pittings with sharp edges. The pittings can be several millimetres deep.

As mentioned above, the cavitation phenomenon will usually occur in centrifugal pumps at a location close to the impeller vane leading edge, Fig. 2, when the pressure on the suction side drops below the vapour pressure of the liquid and small vapour bubbles form. These bubbles implode when the pressure rises and release shock waves.

Normally pump curves published for submersible pumps are drawn so that a pump in normal submerged installation will not cavitate as long as the duty point is on the allowed section of the Q/H curve [7].

However, if the centrifugal pump is installed dry with a suction pipe, the installation must be checked for cavitation.

Fig. 2. Typical cavitation pitting in impeller [5, 6]

Fig. 3 shows the principle of liquid pressure distribution in the suction pipe, pump and pressure pipe of a dry pump installation.

In order to avoid cavitation, the absolute minimum pressure in the pump, $p_{abs,min}$ [Pa], must be larger than the liquid vapour pressure at prevailing temperature, p_v [Pa], or:

$$p_{abs,min} > p_v \tag{1}$$

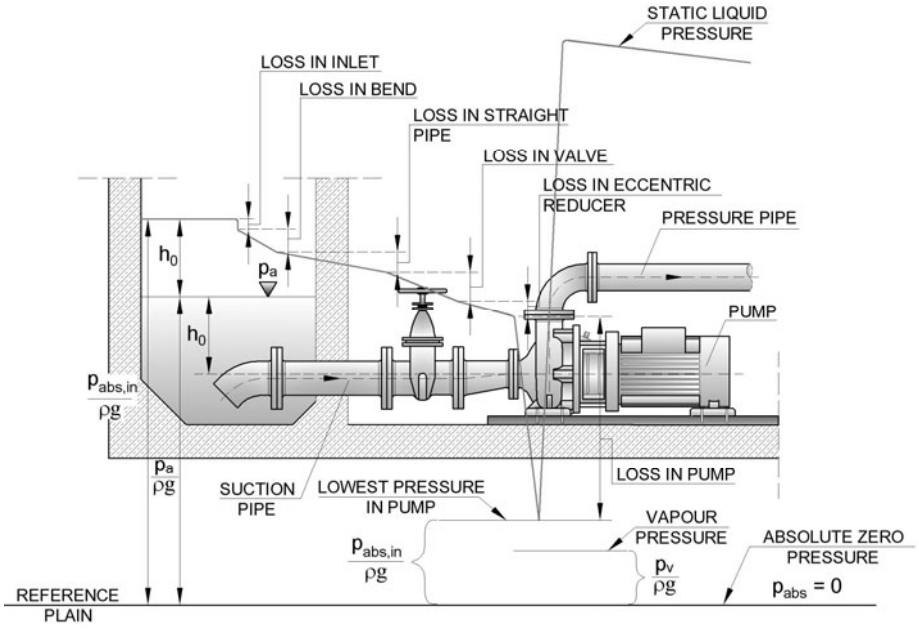

Fig. 3. Pressure variation in a dry pump installation. Distribution of liquid pressure in suction pipe, pump and pressure pipe [8]

22.3. NET POSITIVE SUCTION HEAD

The concept of the net positive suction head (*NPSH*) was developed for the purpose of taking into account the parameters affecting the pump's cavitation behaviour [14].

Let us now assume a typical pump system with a dry installed pump under positive head i.e. with the liquid (water) level in the wet well above the reference plane, and the liquid in the wet well under atmospheric pressure, p_a [Pa], as shown in Fig. 4(a). The reference plane is a horizontal plane through the centreline of the pump suction nozzle.

According to Bernoulli´s energy equation between the two reference cross sections 0–0 and 1–1, we get:

$$z_0 + \frac{p_{abs,0}}{\rho g} + \alpha_0 \frac{v_0^2}{2g} = z_1 + \frac{p_{abs,1}}{\rho g} + \alpha_1 \frac{v_1^2}{2g} + \Delta H_{0-1} \tag{2}$$

where z_0, z_1 [m] is static elevation of the liquid above the datum point, $p_{abs,0}$, $p_{abs,1}$ [Pa] is absolute pressure at the datum point, v_0, v_1 [m/s] is flow velocity at the datum point, α_0, α_1 [1] is Coriolis coefficient at the datum point, ρ [kg/m^3] is liquid density, g [m/s^2] is gravity acceleration and ΔH_{0-1} [m] are head losses (friction and local) between cross section 0-0 and cross section 1–1.

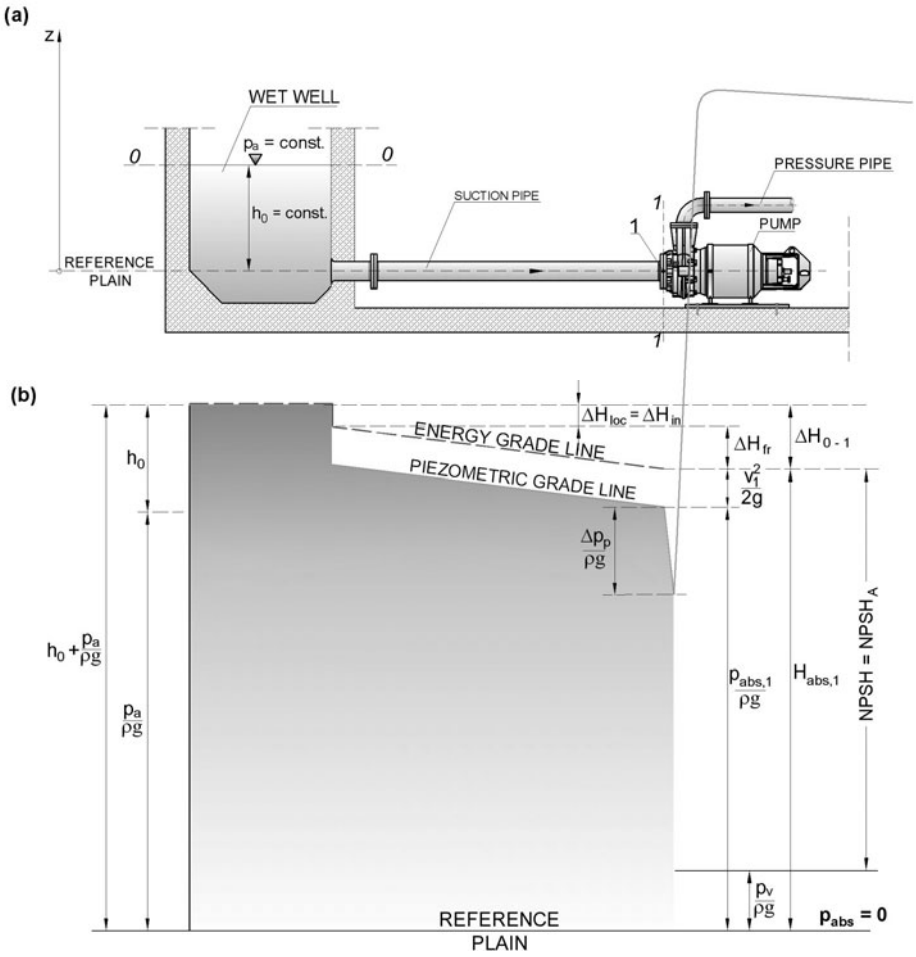

Fig. 4. *NPSH* for a pump with the liquid level above the reference plane and the liquid under atmospheric pressure: (a) suction of pump system; (b) pressure variation and *NPSH*

Substituting $z_0 = h_0$, $p_{abs,0} = p_a$, $\alpha_0 = \alpha_1 = 1.0$, $v_0 = 0$ and $z_1 = 0$, we obtain:

$$h_0 + \frac{p_a}{\rho g} = \frac{p_{abs,1}}{\rho g} + \frac{v_1^2}{2g} + \Delta H_{0-1} \tag{3}$$

which is illustrated graphically by Fig. 4(b).

According to a reference guide of the *European Association of Pump Manufactures*, the net positive suction head, *NPSH* [m], is defined as [9]:

$$NPSH = \frac{p_{abs,1}}{\rho g} + \frac{v_1^2}{2g} - \frac{p_v}{\rho g} \tag{4a}$$

For convenience, we define:

$$H_{abs,1} = \frac{p_{abs,1}}{\rho g} + \frac{v_1^2}{2g} \tag{4b}$$

With this definition, Eq. (4b) becomes:

$$NPSH = H_{abs,1} - \frac{p_v}{\rho g} \tag{4c}$$

where $H_{abs,1}$ [m] is absolute head in point 1.
Multiplying both sides of the above equation by g, yields:

$$g(NPSH) = gH_{abs,1} - \frac{p_v}{\rho} \tag{4d}$$

which represents the liquid specific energy above the vapour pressure at the pump inlet.

The value of *NPSH* calculated by Eq. (4a) is by definition called the net positive suction head available, $NPSH_A$. The *NPSH* available is determined by the pumping station designer.

This quantity can be calculated using the Bernoulli equation. As shown in Fig. 4(b), we can write:

$$h_0 + \frac{p_a}{\rho g} = \Delta H_{0-1} + NPSH_A + \frac{p_v}{\rho g} \tag{5a}$$

or:

$$NPSH_A = h_0 + \frac{p_a - p_v}{\rho g} - \Delta H_{0-1} \tag{5b}$$

A typical $NPSH_A$ curve for a centrifugal pump is shown in Fig 5, where Q [m^3/s] is flow rate and H [m] is pump head.

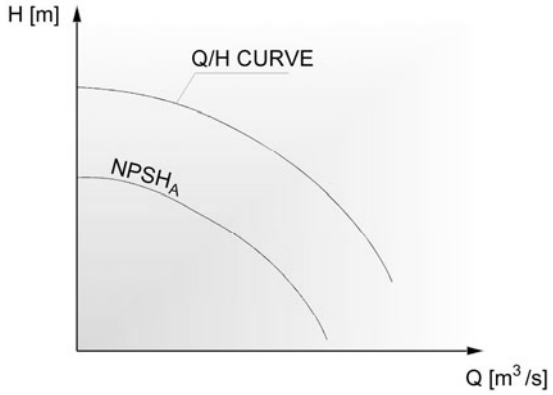

Fig. 5. Typical $NPSH_A$ curve in the Q/H diagram [2, 7]

In the case of a pump system with a dry installed pump under negative head, i.e. with the liquid (water) level in the wet well below the reference plane and the liquid in the wet well under atmospheric pressure, Fig. 6, Eq. (5b) becomes:

$$NPSH_A = -h_0 + \frac{p_a - p_v}{\rho g} - \Delta H_{0-1} \tag{5c}$$

Finally, in the case that $h_0 = 0$, i.e. when the liquid level in the wet well coincides with the reference plane, then:

$$NPSH_A = \frac{p_a - p_v}{\rho g} - \Delta H_{0-1} \tag{5d}$$

As we can see from Eq. (5b) and Eq. (5c), the term h_0 is positive when the reference plane is below the liquid level in the wet well and negative if it is above it.

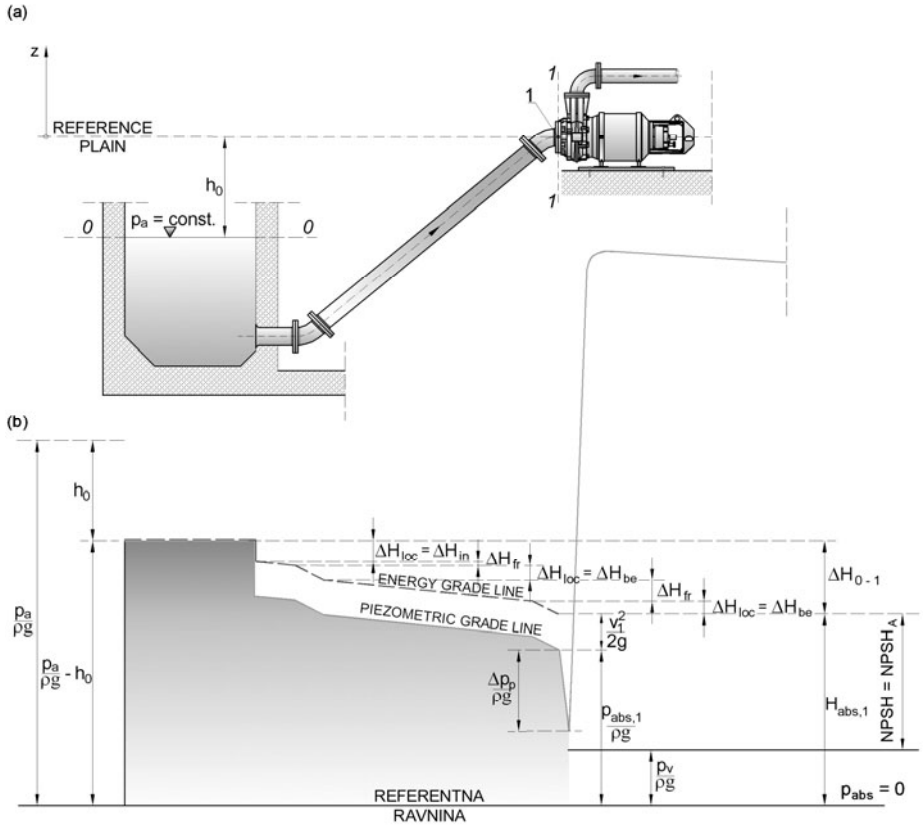

Fig. 6. *NPSH* for pump with the liquid level below the reference plane and the liquid under atmospheric pressure: (a) suction of pump system; (b) pressure variation and *NPSH*

According to the previous analysis, it is obvious that in order to avoid cavitation in centrifugal pumps, the pressure of the liquid at all points within the pump must remain

above the liquid vapour pressure at prevailing temperature. This practically means that, inter alia, taking into account the pressure drop in the pump, Δp_p [Pa], the pumping system must ensure the minimum value of absolute pressure greater than vapour pressure.
This requirement is ensured by introducing the concept of the net positive suction head required, $NPSH_R$. The *NPSH* required, Fig. 7, is defined as [7]:

$$NPSH_R = h_A + \frac{v_0^2}{2g} + \Delta h \tag{6}$$

where h_A [m] is height difference between reference plane and tip of vane leading edge, v_0 [m/s] is inlet velocity and Δh [m] is local pressure head drop at vane leading edge.

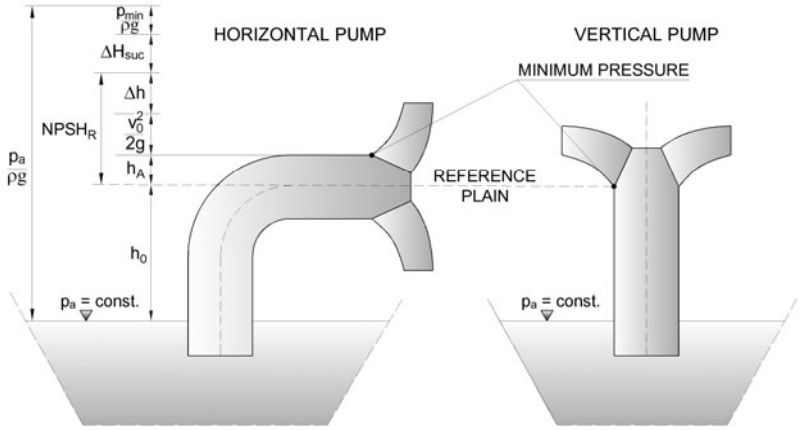

Fig. 7. Dimensions and reference pressures for $NPSH_R$ calculations [7]

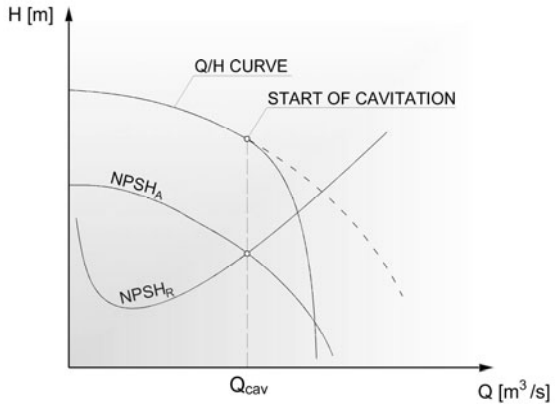

Fig. 8. $NPSH_A$ and $NPSH_R$ curve in the *Q*/*H* diagram [2, 7]

For horizontal pumps the reference plane coincides with the shaft centre line. For vertical pumps the location of the reference plane is stated by the pump manufacturer.

$NPSH_R$ is determined through testing by the pump manufacturer and depends upon factors including type of impeller inlet, impeller design, pump flow rate, impeller rotational speed and the type of liquid being pumped [10]. The manufacturer typically supplies curves of $NPSH_R$ as a function of pump flow rate for a particular liquid (usually water) in the vendor manual for the pump, Fig. 8.

By convention, the pump industry has defined a criterion to quantify $NPSH_R$. $NPSH_R$ quantified by this criterion will be referred to as $NPSH_3$. Basically, it correspondents to the degree of cavitation where the associated drop of pump total differential head in the first stage is equal to 3 [%] of the normal total differential head.

Fig. 9(a) shows how the $NPSH_3$ is determined for a given flow rate, Q_a [m^3/s], and for the pump being operated under constant speed and flow rate. Fig. 9(b) shows a typical $NPSH_A$ and $NPSH_3$ curve in the Q/H diagram.

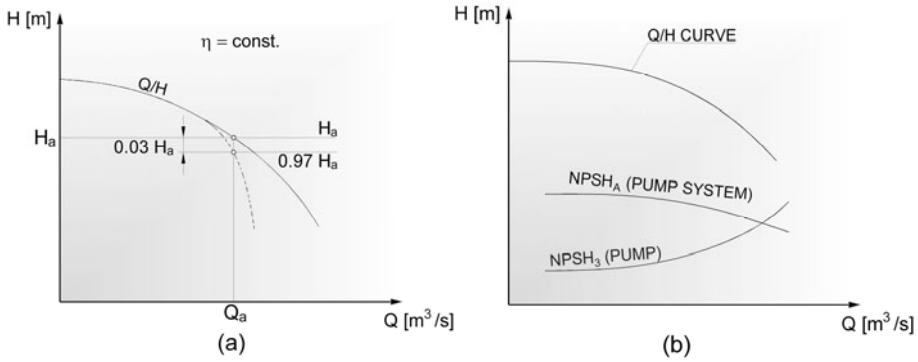

Fig. 9. $NPSH_A$ and $NPSH_3$: (a) practical determination of $NPSH_3$; (b) typical $NPSH_A$ and $NPSH_3$ curve in the Q/H diagram [9]

22.4. CAVITATION-FREE OPERATION OF CENTRIFUGAL PUMPS

Cavitation-free operation, Fig. 10, is present if the following condition is met:

$$NPSH_A > NPSH_R \tag{7a}$$

or:

$$NPSH_A > NPSH_3 \tag{7b}$$

Therefore, the $NPSH_A$ must be always greater than the $NPSH_3$ if cavitation-free operation is to be guaranteed.

As shown in Fig. 10, this condition can be expressed as:

$$NPSH_A = NPSH_R + \Delta NPSH_A \tag{8a}$$

or:

$$NPSH_A = NPSH_3 + \Delta NPSH_A \tag{8b}$$

Safety margin, $\Delta NPSH_A$ [m], must be sufficient to allow for variations in a situation when the real conditions may differ from those theoretically calculated.

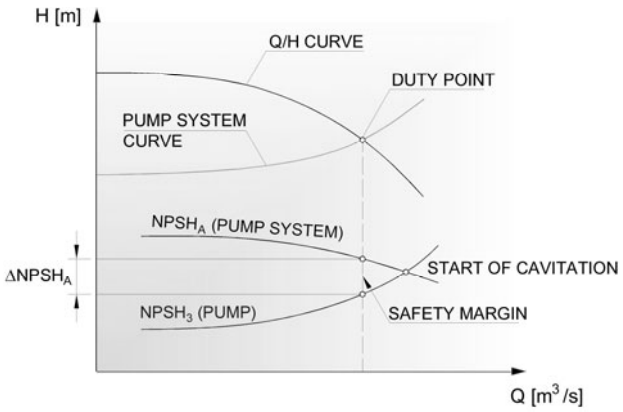

Fig. 10. $NPSH_A$ safety margin with respect to $NPSH_3$ in the Q/H diagram [2]

One rule of thumb followed by several standards, and by the pump industry generally, is that the site conditions should be at least such that [9]:

$$NPSH_A \geq NPSH_3 + 0.5 \text{ [m]} \tag{9}$$

that is, there should be at least a 0.5 [m] margin between $NPSH_3$ and $NPSH_A$.
Some sources [11], [12] recommend a safety margin of 1.5 [m].

The pump manufacturer *Grundfos* [7] recommends for safety margin as follows:

— For Horizontally Installed Pumps With Straight Suction Pipes, A Safety Margin Of 1.0 To 1.5 [M],
— for vertically installed pumps the safety margin should be set at 2.0 to 2.5 [m].

In any case, the condition that must exist to avoid cavitation is that $NPSH_A$ must be greater than or equal to $NPSH_R$. That practically means that several changes in the system design or operation may be necessary to increase the $NPSH_A$ above the $NPSH_R$ [13].

Various methods used to increase the $NPSH_A$ include:

— increasing the pressure at the suction of the pump; for example, if a pump is taking suction from an enclosed tank, either raising the level of the liquid in the tank or increasing the pressure in the space above the liquid increases suction pressure,
— decreasing the temperature of the liquid being pumped; decreasing the temperature of the liquid decreases the saturation pressure, causing $NPSH_A$ to increase,
— reducing head losses in the pump suction pipe; the methods for reducing head losses include increasing the pipe diameter, reducing the number of elbows, valves and fittings in the pipe, and decreasing the length of the pipe.

It may also be possible to reduce the $NPSH_R$ for the pump. Some methods for achieving this include:

— decreasing the flow rate through a pump by throttling a discharge valve,
— decreasing the centrifugal pump speed.

22.5. NUMERICAL EXAMPLE

In order to illustrate the previous analysis, a numerical example of calculation of $NPSH_A$ is presented. The following example is representative for most situations likely to occur.

The calculation results are shown in Table 1.

Table 1

The calculation results of $NPSH_A$

Atmospheric pressure p_a [Pa]	Gravity acceleration g [m/s^2]	Head losses ΔH_{0-1} [m]	Water level above the centerline of the pump h_0 [m]	Water temperature T [°]	Water density ρ [kg/m^3]	Vapour pressure p_v [Pa]	$NPSH_A$ [m]
01	02	03	04	05	06	07	08
10^5	9.81	1.2	2.0	10	999.7	$1.2 \cdot 10^3$	10.9
				30	995.7	$4.3 \cdot 10^3$	10.6
			0.0	10	999.7	$1.2 \cdot 10^3$	8.9
				30	995.7	$4.3 \cdot 10^3$	8.6
			–2.0	10	999.7	$1.2 \cdot 10^3$	6.9
				30	995.7	$4.3 \cdot 10^3$	6.6

From the calculation results it is obviously that:

(a) $NPSH_A$ decreases as temperature of the liquid (water) increases,

(b) $NPSH_A$ decreases as liquid (water) level above the centerline of the pump decreases.

22.6. CONCLUSION

The cavitation phenomenon may damage or destroy centrifugal pumps, lower the pump flow/head curve and efficiency, and result in increased noise and vibration.

The condition that must exist to avoid cavitation is that the net positive suction head available must be greater than or equal to the net positive suction head required.

If a centrifugal pump is cavitating, several changes in the system design or operation may be necessary to increase the net positive suction head available above the net positive suction head required and stop the cavitation.

The possibilities for increasing the net positive suction head available are:

— to increase the pressure at the suction of the pump,

— to decrease the temperature of the liquid being pumped,

— to reduce the head losses in the pump suction pipe.

The changes in the system design and operation for decreasing the net positive suction head required are:

— to reduce the flow rate through a pump,

— to reduce the pump speed.

References

[1] Johnson M.; Ratnayaka D. D., Brandt M. J.: Twort's Water Supply, 6th edn, Burlington-Oxford: Butterworth-Heinemann 2009.
[2] Neumaier R.: Hermetic Pumps. Sulbach: Verlag und Bildarchiv 1994.
[3] Paugh J. J.: How to Compute Net Positive Suction Head for Centrifugal Pumps. Richmond: Warren Pumps 2001.
[4] Mackay R.: The Practical Pumping Handbook. Oxford-New York-Tokyo: Elsevier 2004.
[5] Björk J., Erickson, B.: Centrifugal Pumps. Flowserve Corp., Irving 2005.
[6] Arndt R. E. A.: Cavitation in Depth. St. Anthony Falls Laboratory, University of Minnesota, 2001.
[7] Grundfos: The Sewage Pumping Handbook, Grundfos DK A/S, Bjerringbro 2007.
[8] Grundfos: Wastewater Pumps, 3rd edn, Grundfos DK A/S, Bjerringbro 2002.
[9] European Association of Pump Manufacturers: NPSH for Rotodynamic Pumps: A Reference Guide. Oxford-New York-Tokyo: Elsevier 1999.
[10] Engineers Edge: Preventing Cavitation in Centrifugal Pump 2010.
[11] www.engineersedge.com
[12] Bachus L., Custodio A.: Know and Understand Centrifugal Pumps. Oxford-New York-Tokyo: Elsevier 2003.
[13] Jones G. M. (edit): Pumping Station Design, 3rd edn, Butterworth-Heinemann, Burlington-Oxford 2008.
[14] Schiavello B., Visser F. C.: Pump Cavitation – Various NPSHR Criteria, NPSHA Margins and Impeller Life Expectancy. Proceedings of the 25th International Pump Users Symposium, Houston, 2009, pp. 113–144.

23 Theoretical and Experimental Analysis of Corrugated Gravity Pipes

Živko Vuković, Joško Krolo, Ivan Halkijević (University of Zagreb, Faculty of Civil Engineering)

23.1. INTRODUCTION

The structural design of buried (underground) pipes, according to the installation type, the soil group and the elastic property of the pipe material, includes the following:

— deformation (deflection) analysis,
— stress analysis,
— stability analysis.

A basic parameter to be determined in these analyses is the bearing capacity of the pipes. This capability of the pipe to resist external forces can be expressed by the pipe ring stiffness, which is a function of the modulus of elasticity of the pipe material, the moment of inertia of the pipe wall section and the mean pipe diameter.

Methods of structural design of buried pipes, like the European ones, in their original form have been developed for smooth pipes, i.e. for pipes with constant wall thickness. However, today corrugated thermoplastics pipes are being increasingly used, especially in gravity sewage. Therefore, the existing calculation methods need to be upgraded for this type of pipes.

The aim of this paper is to express the pipe ring stiffness for corrugated pipes, i.e. to define the moment of inertia of the pipe wall section and the mean pipe diameter for corrugated pipes. The analysis will be based on the German ATV-127 method. Also, the theoretical analysis will be compared with the experimental results.

23.2. THEORETICAL ANALYSIS

23.2.1. European Calculation Methods for Buried Pipes

Within the European Committee for Standardization CEN (Comité Européen de Normalisation) an extensive work started in 1990 with the goal to create a common calculation method (or model) for all types of buried pipes independent of material (rigid, semi-rigid or flexible) and field of application (pressure or gravity). Initially some established national calculation methods were collected and evaluated as a basis for this development work. The idea was to extract the best of each of the national methods and bring about such a new and

common model, which would simulate documented field experience better than any of the established ones [1].

Whilst there are differences between some of the established national design procedures, there are no differences in respect of the fundamental basis of design, which is an interactive system consisting of the pipe and the surrounding soil.

It was then found that all methods could be recognised as having the same structural base as the classical Spangler formula [2], although with various degree of modifications. These modifications are mainly the result of assessments of assumed soil pressure distribution particularly in the horizontal direction, but also on assumed bedding angles and vertical load factors expressed as the relation between vertical pressure against the pipe and the same pressure in natural soil without the pipe present.

As the practical behaviour of a flexible buried pipe is easy to define and measure in terms of pipe deflection, a natural starting point was to discuss the various national calculation methods used for determining this deflection.

Due to the inability of general consensus about a feasible common method of design, the CEN in 1997 issued the standard *Structural design of buried pipelines under various conditions of loading – Part* 1*: General requirements* (EN 1295–1:1997), and then in 2005 the standard *Structural design of buried pipelines under various conditions of loading – Part* 2*: Summary of nationally established methods of design* (CEN/TR 1295-2:2005). Two years later the CEN issued the third standard *Structural design of buried pipelines under various conditions of loading – Part* 3*: Common method* (CEN/TR 1295-3:2007).

The second standard includes summaries of Austrian, Belgian, Danish, French, German, Dutch, Norwegian, Swedish and British methods. According to the third standard, there are two options for methods of calculation: *Option* 1 and *Option* 2. *Option* 1 was developed on the basis of the German ATV-A127 [3] and the Austrian ÖNORM B5012 [4] standards. *Option* 2 consists of an interactive model which is able to describe the behaviour of the soil-structure system from rigid to flexible in a continuous way.

23.2.2. German Method

The calculation method given in the ATV-A127 standard applies for the structural calculation of buried pipes of all standardised pipe materials. The method is applicable for rigid and flexible pipes with different pipe stiffness and installation conditions with a smooth transition from trench to embankment, in which the loading of the pipes is dependent on the deformation properties of the pipe and soil and their mutual influence.

Note that the definition of pipes as rigid and flexible is essentially based on consideration of the structural performance of the pipe cross-section under external loads. The pressure distribution is assumed as in Fig. 1 with the vertical support angle, $\alpha_v = 120$ [°].

The spectrum of the existing soils and their deformation moduli is mostly represented by 4 groups of soil (non-cohesive, slightly cohesive, cohesive mixed and cohesive soils), characterised through different friction angles and grades of compaction. Solutions for the influence of traffic loads (road, railway and airplane) are given.

Different installation methods on site, trench shapes, installation and earth fill condition depending on trench sheeting or embankment, soil compaction and ground water influence are considered.

The analysis and its verification is made by calculating bearing capacity, stresses, strains and pipe deformation.

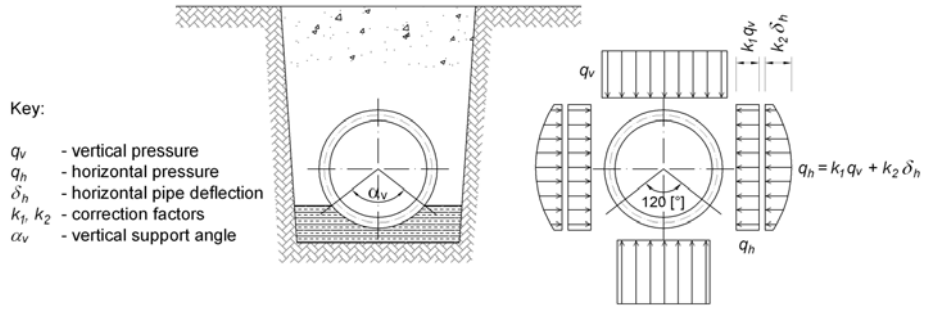

Fig. 1. Soil pressure distribution for pipe supported on soil according to the ATV method [3]

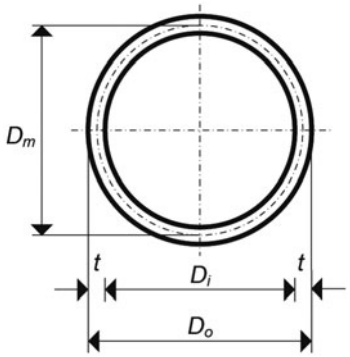

Fig. 2. Cross-section of smooth circular pipe

The ATV method applies for smooth circular pipes; it can be applied analogously for other cross-sections. Prerequisite is that the initial assumptions taken for the structural calculation are in agreement with the construction method.

Also, according to this method, the design can be performed for short-term and long-term conditions of the pipeline. Short-term analyses are being performed using the initial or short-term properties of the soil and pipe material. When analysing the long-term performance of the buried pipe, traffic loads are always treated as short-term loading, however for all sustained loads the appropriate long-term analyses shall be performed using the two-year material and the long-term soil properties.

According to the ATV method, the relative vertical deflection of the pipe, δ_v [%], is given as:

$$\delta_v = -\frac{100\ c_v^*(q_v - q_h)}{8S_{RP}} \tag{1}$$

where S_{RP} [kN/m^2] is pipe ring stiffness per unit length of pipe, c_v^* [1] is vertical deflection coefficient, q_v [kN/m^2] is resulting vertical pressure acting on the pipe and q_h [kN/m^2] is resulting horizontal pressure acting on the pipe due to vertical loads.

• *The pipe ring stiffness, S_{RP}*, is defined as:

$$S_{RP} = \frac{E_p\ I}{D_m^3} \tag{2}$$

where E_p [kN/m^2] is modulus of elasticity of the pipe material, I [m^4/m] is moment of inertia of the pipe wall per unit length of the pipe and D_m [m] is mean pipe diameter.

In its original form, the pipe ring stiffness in the ATV method is based on the mean radius of the circular pipe, r_m [m] ($r_m = D_m/2$), and not as above on the mean diameter. This means a unit which is 8 times larger than the ring stiffness defined according to Eq. (2).
For smooth circular pipe, Fig. 2, the moment of inertia is:

$$I = \frac{t^3}{12} \tag{3}$$

which inserted in Eq. (3) gives:

$$S_{RP} = \frac{E_p}{12}\left(\frac{t}{D_m}\right)^3 \tag{4}$$

where t [m] is the pipe wall thickness.
The mean pipe diameter is:

$$D_m = \frac{D_o + D_i}{2} \tag{5}$$

where D_o [m] and D_i [m] are outside and inside pipe diameter, respectively.

For a corrugated circular pipe, Fig. 3, the moment of inertia and the mean pipe diameter can be expressed as follows:

$$I = I_y^{(1)}\frac{1}{a} \tag{6}$$

$$D_m = D_i + 2z_T \tag{7}$$

where:

$$I_y^{(1)} = at_1\left[\frac{t_1^2}{12} + \left(z_T - \frac{t_1}{1}\right)^2\right] + 2bt_2\left[\frac{t_2^2}{12} + \left(z_T - t_1 - \frac{t_2}{2}\right)^2\right] + \\ + 2dt_3\left[\frac{d^3}{12} + \left(t_0 + \frac{d}{2} - z_T\right)^2\right] + ct_4\left[\frac{t_4^2}{12} + \left(t_0 + d - z_T\right)^2\right] \tag{8}$$

$$t_0 = t_1 + t_2 \tag{9}$$

$$b = \frac{1}{2}\left(a - c - 2d\ tg\ \alpha\right) \tag{10}$$

$$z_T = \frac{1}{A^{(1)}}\left[a\frac{t_1^2}{2} + 2bt_2\left(t_1 + \frac{t_2}{2}\right) + 2dt_3\left(t_0 + \frac{d}{2}\right) + ct_4\left(t_0 + d\right)\right] \tag{11}$$

$$A^{(1)} = at_1 + 2bt_2 + ct_4 + 2dt_3 \tag{12}$$

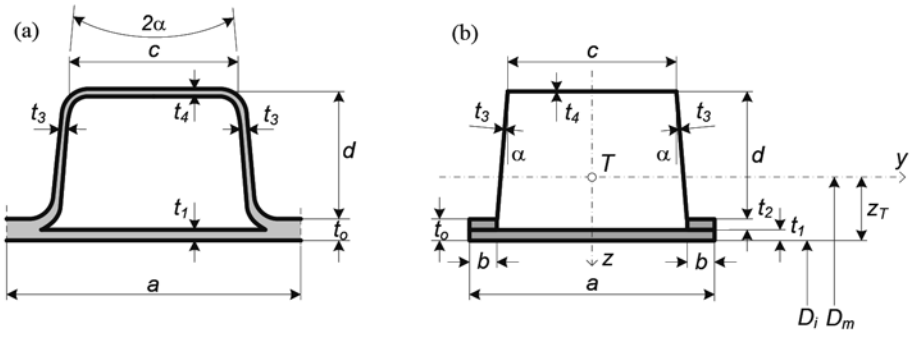

Fig. 3. One corrugated longitudinal section: (a) cross-section; (b) calculated model

Here, according to Fig. 3(b), $I_y^{(1)}$ [m^4] is moment of inertia of one corrugated section, a, b, c, d, t_i [m] are dimensions of pipe cross section, z_T [m] is barycenter position of the area section and $A^{(1)}$ [m^2] is sectional area.

• *The vertical deflection coefficient,* c_v^*, is defined as:

$$c_v^* = c_{v1} + c_{v2}\ K^* \tag{13}$$

where:

$$\Delta f = \frac{b/D_o - 1}{1.154 + 0.444\ (b/D_o - 1)} \le 1.44 \tag{14}$$

$$\alpha_B = 1 - \frac{(4 - b/D_o)(1 - \alpha_{Bi})}{3} \le 1 \tag{15}$$

$$E_2 = f_1 f_2 \alpha_B E_{20} \tag{16}$$

$$f_2 = \frac{D_{pr} - 75}{20} \le 1 \tag{17}$$

$$\zeta = \frac{1.44}{\Delta f + (1.44 - \Delta f)\dfrac{E_2}{E_3}} \tag{18}$$

$$S_{Bh} = 0.6\ \zeta\ E_2 \tag{19}$$

$$V_{RB} = \frac{8 S_{RP}}{S_{Bh}} \tag{20}$$

$$K^* = \frac{c_{h1}}{V_{RB} - c_{h2}} \tag{21}$$

Here, according to Fig. 4, c_{v1}, c_{h1} [1] is vertical and horizontal deflection coefficient (soil support) due to vertical loads, respectively, depending on vertical support angle, α_v [°], c_{v2}, c_{h2} [1] is vertical and horizontal deflection coefficient (soil support) due to horizontal loads, depending on vertical support angle, α_v [°], K^* [1] is reaction pressure coefficient, V_{RB} [1] is system stiffness, S_{Bh} [kN/m^2] is horizontal soil bedding stiffness, ζ [1] is correction factor for the horizontal soil bedding stiffness, Δf [1] is correction factor, depending on trench width, E_1 [kN/m^2] is soil modulus for the backfill over the top of the pipe, depending on the soil group, E_2 [kN/m^2] is soil modulus for the sidefill material, after various reduction, see Eq. (16), E_3 [kN/m^2] is soil modulus for the native soil to the side of the pipe, E_4 [kN/m^2] is soil modulus for the native soil under the pipe bedding, E_{20} [kN/m^2] is calculative soil modulus, depending on the group of soil, f_1 [1] is soil modulus reduction factor, f_2 [1] is soil modulus reduction factor due to ground water table, α_B [1] is soil modulus reduction factor due to trench width, b [m] is trench width at the top of the pipe between the native soil, h [m] is depth of cover, h_w [m] is height of ground water table above pipe crown, β [°] is trench angle, α_{Bi} [1] is correction factor related to the compaction class and D_{pr} [%] is percentage of full compaction used for design purpose.

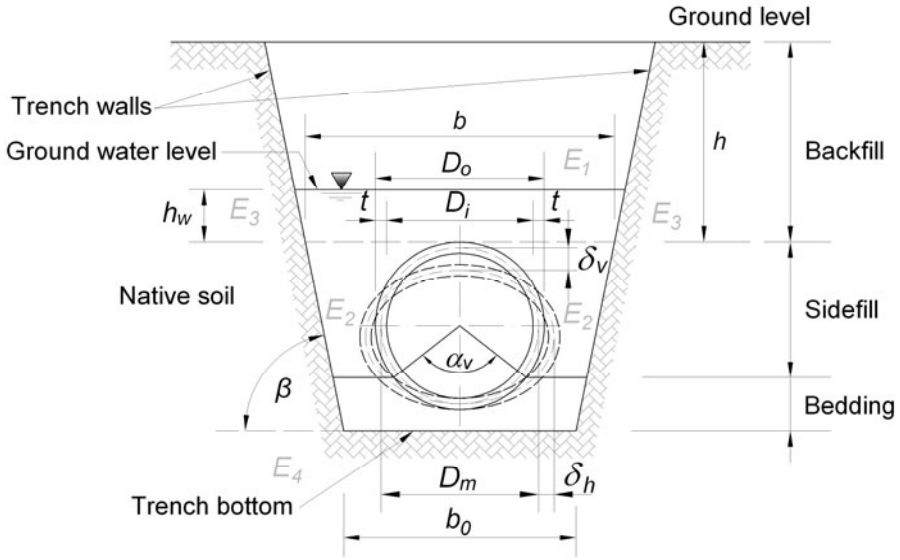

Fig. 4. General installation and pipe deflection terms

• *The vertical total load*, q_v, of the pipe is:

$$q_v = \lambda_{RG}\ \ p_e + p_v \tag{22}$$

where:

$$V_S = \frac{8S_{RP}}{\left|c_v^*\right|E_2} \tag{23}$$

$$\lambda_{\max} = 1 + \frac{\dfrac{h}{D_o}}{\dfrac{3.5}{\dfrac{E_1}{E_2}} + \dfrac{2.2}{\dfrac{E_4}{E_2}\left(\dfrac{E_1}{E_2} - 0.25\right)} + \dfrac{h}{D_o}\left[\dfrac{0.62}{\dfrac{E_1}{E_2}} + \dfrac{1.6}{\dfrac{E_4}{E_2}\left(\dfrac{E_1}{E_2} - 0.25\right)}\right]} \tag{24}$$

$$\lambda_R = \frac{\lambda_{\max}\ V_S + \dfrac{E_1}{E_2}\dfrac{4K_2}{3}\dfrac{\lambda_{\max} - 1}{E_1/E_2 - 0.25}}{V_S + \dfrac{E_1}{E_2}\dfrac{3 + K_2}{3}\dfrac{\lambda_{\max} - 1}{E_1/E_2 - 0.25}} \le 4 \tag{25}$$

$$\lambda_{RG} = \frac{\lambda_R - 1}{3}\frac{b}{D_o} + \frac{4 - \lambda_R}{3} \quad for\ 1 \le \frac{b}{D_o} \le 4 \tag{26}$$

$$\chi_\beta = 1 - \frac{\beta}{90} + \frac{\beta}{90}\left[\frac{1 - e^{-2(h/b)K_1\ \tan\ \delta}}{2(h/b)K_1 \tan\ \delta}\right] \tag{27}$$

$$p_e = \chi_\beta \left[\gamma_s (h - h_w) + \gamma_{sw} h_w\right] \tag{28}$$

$$p_F = \frac{F_A}{r_A^2 \pi}\left\{1 - \left[\frac{1}{1+(r_A/h)^2}\right]^{3/2}\right\} + \frac{3F_E}{2\pi h^2}\left[\frac{1}{1+(r_E/h)^2}\right]^{5/2} \tag{29}$$

$$a_F = 1 - \left[\frac{0.9}{0.9 + (4h^2 + h^6)/1.1\ D_m^{2/3}}\right] \quad for\ h \geq 0.5\ [m]\ and\ D_m \leq 5.0\ [m] \tag{30}$$

$$p_v = \varphi'\ a_F\ p_F \tag{31}$$

Here p_e [kN/m^2] is vertical pressure from soil load in a trench in the absence of a pipe, p_v [kN/m^2] is vertical load resulting from road traffic loading, λ_R, λ_{RG}, λ_{max} [1] are load concentration factors above the pipe, V_S [1] is stiffness ratio, K_1 [1] is lateral soil pressure ratio in the backfill above the pipe, K_2 [1] is lateral soil pressure ratio in the sidefill, $\chi_ß$ [1] is coefficient for silo effect with sloping trench sides, δ [°] is trench friction angle, depending on installation condition, φ [°] is internal friction angle, depending on the soil group, γ_s [kN/m^3] is unit weight of soil, depending on the soil group, γ_{sw} [kN/m^3] is submerged unit weight of soil, depending on the soil group, φ' [1] is impact coefficient for road traffic loads, depending on standard vehicle (SLW 60, SLW 30, LKW 12), p_F [kN/m^2] is effective traffic load at a depth h below the ground level, a_F [1] is correction factor related to road traffic load which takes into account the load distribution over the pipe, F_A, F_E [kN] are auxiliary traffic loads, depending on standard vehicle, and r_A, r_E [m] are auxiliary radii, depending on standard vehicle.

• *The horizontal total load*, q_h, can be calculated using the following equation:

$$q_h = K_2\left(\lambda_B\ p_e + \gamma_s \frac{D_v}{2}\right) \tag{32}$$

where λ_B [1] is the load concentration factor to the side of the pipe, defined as:

$$\lambda_B = \frac{4 - \lambda_R}{3} \tag{33}$$

23.2.3. Numerical Examples

Numerical example 1: The calculation of moment of inertia, I, mean pipe diameter, D_m, and pipe ring stiffness, S_{RP}, for a corrugated HDPE pipe, DN 400, type VARGON. The input and output data (calculation results) are shown in Table 1.

Numerical example 2: The calculation of vertical pipe deflection, δ_v, for a smooth PVC pipe, DN 400 and S_{RP} = 4.00 [kN/m^2]. Calculation results are shown in Table 2.

Table 1

Input and output data for the calculation of moment of inertia, mean pipe diameter and pipe ring stiffness for a corrugated HDPE pipe, DN 400, type VARGON

INPUT DATA		OUTPUT DATA		
Pipe material:	Thermoplastics (HDPE)	Symbol, unit	Equation	Value
Symbol, unit	Value	t_o, [m]	(09)	0.0046000
D_i, [m]	0.3438	b, [m]	(10)	0.0005644
a, [m]	0.0434	$A^{(1)}$, [m^2]	(12)	0.0002580
c, [m]	0.0280	z_T, [m]	(11)	0.011338
d, [m]	0.0235	$I_y^{(1)}$ [m^4]*	(08)	$2.7634 \cdot 10^{-8}$
α, [°]	5	I [m^4/m]	(06)	$6.367 \cdot 10^{-7}$
t_1, [m]	0.0023	D_m [m]	(07)	0.36648
t_2, [m]	0.0023	r_m [m]	$D_m/2$	0.18324
t_3, [m]	0.0018	S_{RP} [kN/m^2]	(02)	9.18
t_4, [m]	0.0017			

*) exactly value $I_y^{(1)} = 2.8165 \cdot 10^{-8}$ [m^4] (error 1.9 [%])

Table 2

Input and output data for the calculation of vertical pipe deflection for a smooth PVC pipe, DN 400, $S_{RP} = 4.00$ [kN/m^2]

INPUT DATA		OUTPUT DATA		
Pipe material:	Thermoplastics (PVC)	Symbol, unit	Equation	Value
Soil group:	G1 (GE, GW)	Δf, [1]	(14)	0.824
Symbol, unit	Value	α_B, [1]	(15)	0.667
S_{RP}, [kN/m^2]	4.00	f_2, [1]	(17)	1.00
b, [m]	1.00	E_2, [kN/m^2]	(16)	2 667.0
h, [m]	2.00	ζ, [1]	(18)	0.875
h_w, [m]	0.00	S_{Bh},[kN/m^2]	(19)	2 667.0
D_o, [m]	0.40	V_{RB}, [1]	(20)	0.02285
D_i, [m]	0.38	K*, [1]	(21)	0,94
f_1, [1]	2/3	c_v*, [1]	(13)	–0.0232
α_{Bi}, [1]	1/3	V_S, [1]	(23)	0.5181
E_{20}, [kN/m^2]	6 000	λ_{max}, [1]	(24)	1.461
α_v, [°]	180	λ_R, [1]	(25)	0.865
c_{h1}, [1]	0.0833	λ_{RG}, [1]	(26)	0.932
c_{h2}, [1]	–0.0658	χ_β, [1]	(27)	0.819
c_{v1}, [1]	–0.0833	p_e, [kN/m^2]	(28)	32.77
c_{v2}, [1]	0.0640	p_F, [kN/m^2]	(29)	24.92
E_1, [kN/m^2]	2 000	D_m, [m]	(05)	0.39

cont. Table 2

INPUT DATA		OUTPUT DATA			
Pipe material:	Thermoplastics (PVC)	Symbol, unit		Equation	Value
E_3, [kN/m^2]	2 000	a_F, [1]		(30)	0.993
E_4, [kN/m^2]	20 000	p_v, [kN/m^2]		(31)	29.70
K_1, [1]	0.5	q_v, [kN/m^2]		(22)	60.26
K_2, [1]	0.4	λ_B, [1]		(33)	1.045
γ_s, [kN/m^3]	20	q_h, [kN/m^2]		(32)	60.26
φ, [°]	35	δ_v	[%]	(01)	3.25
β, [°]	90		[mm]		13.00
δ, [°]	35/3				
F_A, [kN]	100				
F_E, [kN]	500				
r_A, [m]	0.25				
r_E, [m]	1.82				
φ', [1]	1.2				

23.3. EXPERIMENTAL ANALYSIS

As a verification of the theoretical analysis of the moment of inertia and the mean pipe diameter of the corrugated pipe, experimental analysis was carried out. The HDPE corrugated pipe, type VARGON, DN 400, with the inside diameter, D_i = 343.8 [mm], the outside diameter, D_o = 400.0 [mm], and the length of the tested specimen, L = 300.0 [mm], was chosen for testing. Longitudinal cross-section for one corrugated section is shown in Fig. 3(a).

Table 3

Physico-mechanical properties of the HDPE pipe material

Physico-mechanical properties	Symbol, unit	Value
Density	g [g/cm^3]	950
Modulus of elasticity	E [MPa]	> 700
Ultimate tensile strength	[MPa]	20
Coefficient of thermal expansion	[1/K]	$(1.3 – 2.0)\cdot 10^{-4}$
Heat of thermal conductivity (20 [◦C])	[W/mK]	0.40

Physico-mechanical properties of the HDPE pipe material are shown in Table 3. Testing of the pipe was carried out on a universal testing machine Zwick&Roell in the Laboratory for Testing of Structures, Department for Technical Mechanics, University of Zagreb, Faculty of Civil Engineering. Testing was performed by applying concentrated load. Force, F [kN], and vertical deflection of pipe vertex, δ_v^{exp} [mm], were measured during the testing. Vertical deflection was measured by an LVDT sensor. Load was applied by

displacement control with deformation speed 10 [mm/min]. A schematic presentation and a picture of the testing of the corrugated pipe are shown in Fig. 5.

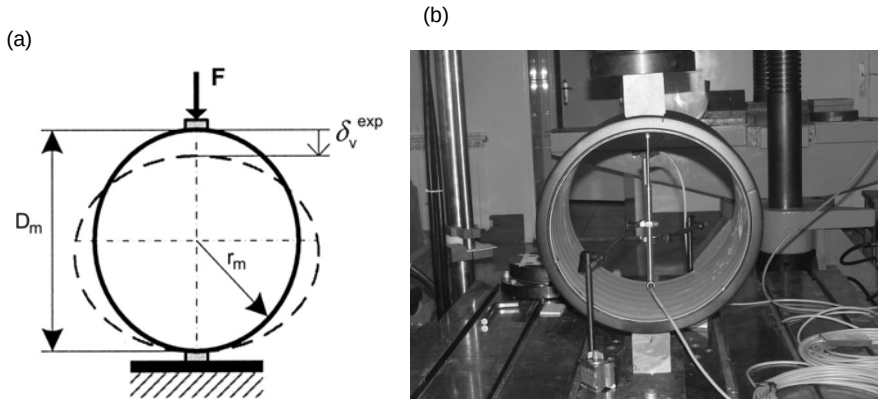

Fig. 5. Schematic presentation of testing (a), testing of the corrugated pipe in the laboratory (b)

Results of the testing are shown in Fig. 6.

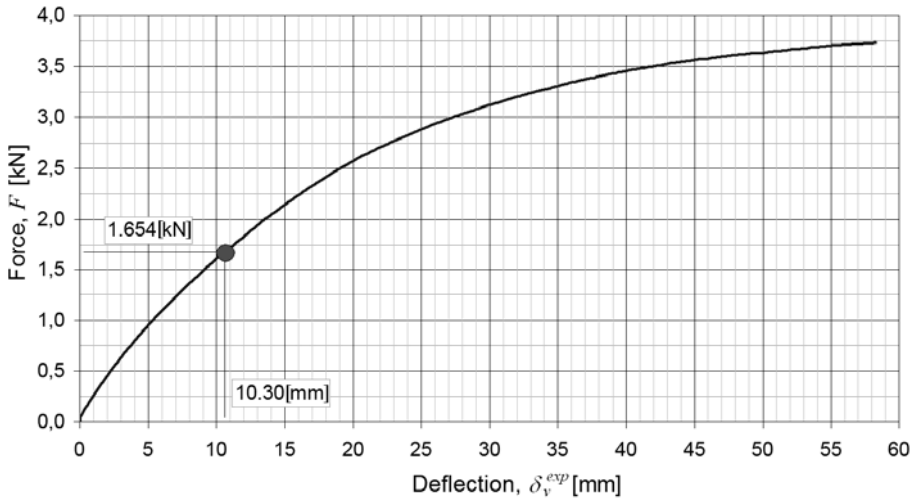

Fig. 6. Force-deflection diagram

Using the experimentally obtained force-deflection diagram shown in Fig. 6, the force corresponding to the inside diameter decrease of 3 [%], δ_v^{exp} = 10.30 [mm], was determined.

For this value of the force, F = 1.654 [kN], we can estimate theoretical vertical pipe deflection, δ_v^{th} [5] using modulus of elasticity for high density polyethylene, E_p = 700 [MPa] (Table 3), moment of inertia, $I = 6.367 \cdot 10^{-7}$ [m^4/m], and mean pipe radius, r_m = 183.24 [mm] (Table 1), as:

$$\delta_v^{th} = 0.1488 \frac{F\ r_m{}^3}{E_p\ I} \cdot \frac{1\ [m]}{L\ [m]} = 0.1488 \cdot \frac{1654 \cdot 183.24^3}{700 \cdot 6.367 \cdot 10^{-7} \cdot 10^{12}} \cdot \frac{1}{0.30} = 11.32[mm] \tag{34}$$

According to Fig. 6, for F = 1.654 [kN] the experimentally obtained vertical deflection, δ_v^{exp} = 10.30 [mm], which is approximately 10 [%] less than the theoretically obtained value, δ_v^{th} = 11.32 [mm].

In addition, the ring stiffness of the corrugated pipe, S_R^{exp} [kN/m^2], was estimated based on the results of the testing and in conformity with the standard EN ISO 9969 [6] as:

$$\begin{aligned} S_R^{\exp} &= \left(0.0186 + 0.025\ \frac{\delta_v^{\exp}}{D_i} \right) \frac{F}{L\ \delta_v^{\exp}} = \\ &= \left(0.0186 + 0.025 \cdot \frac{0.0103}{0.3438} \right) \cdot \frac{1.654}{0.30 \cdot 0.0103} = 10.35[\mathrm{kN/m^2}] \end{aligned} \tag{35}$$

We can see that the pipe ring stiffness, S_{RP} = 9.18 [kN/m^2] (Table 1), estimated using Eq. (2), is slightly smaller than the stiffness, S_R^{exp} = 10.35 [kN/m^2], which was determined from the experimental results. On the basis of these results we can conclude that the modulus of elasticity, E_p, is higher than it was previously taken (E_p = 700 [MPa]).

If we assume that the experimentally obtained deflection, δ_v^{exp} = 10.30 [mm] is an exact value, we can estimate the modulus of elasticity from the expression for δ_v^{th}, which is then E_p = 769.7 [MPa]. Using this value of the modulus of elasticity, the estimated pipe ring stiffness obtained from Eq. (2) is S_R = 9.96 [kN/m^2]. This value is approximately 3.5 [%] lower than S_R^{exp} = 10.35 [kN/m^2]. The experimentally obtained results of the pipe ring stiffness are in good correlation with the characteristics declared by the manufacturer of the corrugated pipe.

23.4. CONCLUSION

A basic parameter to be determined in the structural design of buried pipes is the pipe ring stiffness, which is a function of the modulus of elasticity of the pipe material, the moment of inertia of the pipe wall section and the mean pipe diameter. Methods for the structural design of buried pipes, such as the German ATV method in its original form, have been developed for smooth pipes. In this paper the existing calculation methods are upgraded for corrugated thermoplastics pipes type VARGON. The verification of the theoretical analysis is made by experimental analysis. Experimentally obtained results of the pipe ring stiffness are in good correlation with the theoretical analysis and with the pipe characteristics declared by the corrugated pipe manufacturer.

References

[1] Janson L. E.: Plastics Pipes for Water Supply and Sewage Disposal, Borealis. Stockholm 1999.
[2] Spangler M. G.: The Structural Design of Flexible Pipe Culverts. Iowa Eng. Exp. Stat. Bull. 153, 1941.

[3] ATV Regelwerk: Richtlinie für die statische Berechnung von Entwässerunkanälen und-leitungen, Arbeitsblatt A127, Abwassertechnischen Vereinigung (ATV), 1988.
[4] Standards NÖNORM B 5012, Part 1(1990), Part 2 (1995), Österreichisches Normunginstitut, Vienna.
[5] Šimić V.: Otpornost materijala II, Školska knjiga. Zagreb 2002.
[6] European Standard EN ISO 9969: Thermoplastics Pipes – Determination of Ring Stiffness 2000.

24 Relativity of the Simplified Runoff Calculations for Rainwater Drainage Systems

Katarzyna Weinerowska-Bords (Gdańsk University of Technology, Faculty of Civil and Environmental Engineering)

24.1. INTRODUCTION

The basis for engineering calculations of different drainage systems (both – artificial stormwater sewer systems, and natural channels which are permanent or temporary storm water receivers) – is the transformation of rainfall to runoff. The effect of such transformation is the result of many complex processes, which include mainly rainfall, infiltration, evapotranspiration, surface and subsurface runoff. Each of these processes for the proper quantitative characterization require advanced mathematical notation, and full and accurate mathematical representation of their complicated structure is – for many reasons – in practice impossible ([3, 6] et al.). As a result, a necessary and unavoidable procedure enabling solution to this problem is to reduce the minuteness if the mathematical description, leading consequently to more or less simplified models of rainfall-runoff type. However, the *relatively high complexity* of the problem is not the only reason of this suitable simplifications in calculations. Additional causes that determine mentioned simplifications in solutions are: necessity of representation in the system *quantities of random character* (e.g. precipitation) that very often determine stochastic attitude to the problem, *lack or limited access to full and reliable data* (e.g. historical rainfall events, catchment characteristics etc.) and *economical* or *practical aspects* [7]. Thus, in practice one always deals with only a simplified description of real processes that determine the final amount of rainwater, and as a well as follows – with only a rough estimate of this quantity, which from the engineering point of view, is crucial. It can be thus concluded, that any assessment of the volume of rainwater is burdened with a certain degree of *relativity* and *conventionality*, which has many very important consequences – not only computational, but also of formal, economical and sometimes even legal nature. Vivid examples are: a relatively wide range of possible values of chosen coefficients of formulas (which in consequence leads to the calculation result from a wide range of values), lack of homogeneous procedures of solutions resulting in potential arbitrariness and the possibility of adjusting the choice of computational methods for calculating the desired results and difficulties in comparing and interpretation of different solutions obtained by use of different schemes and assumptions.

The facts presented above make us conclude that the result of estimating the amount of rainwater strongly depends on the calculation method used in each particular case and the simplifications applied in solution procedure. In general, rainfall-runoff model can be illustrated by specifying in its structure three main sub-models: model of rainfall (in which

on the basis of historical or synthetic precipitation events so called "computational rain" is determined), runoff model (in which "computational rain" is transformed into the channel inflow) and the model of flow routing in channels (which ultimately leads to the computational discharges in channels) (Fig. 1).

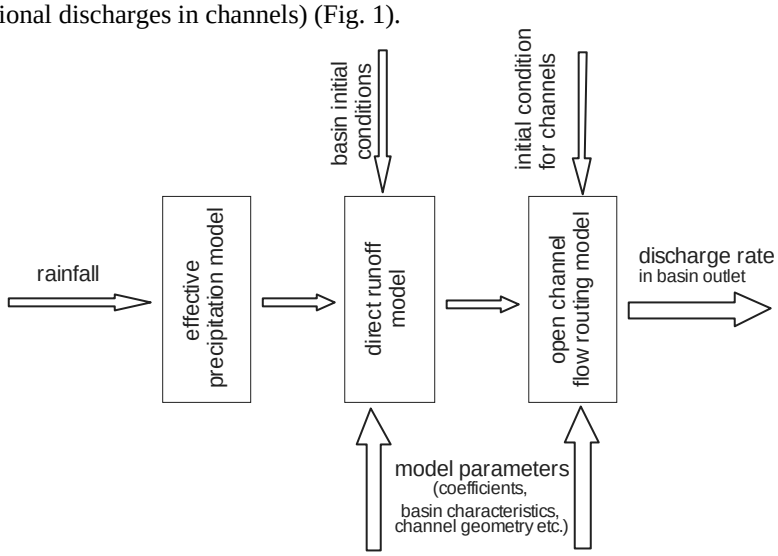

Fig.1. Schematic structure of raifall-runoff model

However, not in every practical application the sub-models mentioned above can be explicitly distinguished. In the simplest mathematical rainfall-runoff models the physical structure of the phenomena is not studied in such detailed way, and very often the rainfall is "directly" transformed into the outflow through specific, often very simply formulas [2, 7]. The example of such attitude are many variants of so-called rational method or its modifications [1, 2]. In these simplest – but very often applied – methods, the information of the maximum flow rate in the analyzed cross-sections is considered to be sufficient, while the shape of the flow hydrograph, the time of the appearance of the flow peak or more advanced analyses are often regarded as secondary or irrelevant (Fig. 2). Commonly applied, simplified methods of calculation of outflow discharge Q (understood as a maximum value – Fig. 2b) may be written in general form as:

$$Q = C \cdot I \cdot A \tag{1}$$

where Q is maximal (so-called: "computational") discharge rate, A – is catchment area and I is "computational" rainfall intensity. The coefficient C, often called "rational method coefficient", is the value dependent on climate features of the analyzed region and catchment characteristics. Very popular in Poland version of (1), called "constant rainfall intensity method", can be expressed by the formula:

$$Q = \psi \cdot \varphi \cdot q \cdot A \tag{2}$$

where Q is maximal discharge rate in m^3/s, A – is catchment area [ha], q is "computational" rainfall intensity [$dm^3/(s \cdot ha)$], φ is runoff coefficient [–] and ψ is the lag coefficient, representing the delay in time resulting from basin reaction for rainfall episode. Apart from (2) there are also several other versions or modifications of (1).

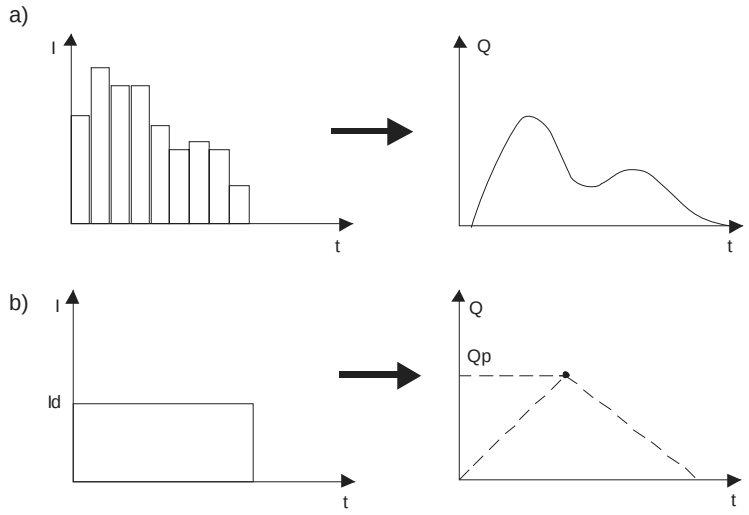

Fig. 2. Scheme of rainfall-runoff transformation in models: a) unsteady, b) steady (I – rainfall intensity, Q – discharge rate, t – time)

In such simplified representation of rainfall-runoff processes, seemingly very easy in application, there are many "practical" problems and computational aspects very strongly determining the quality of the solution. The paper presents in more detailed way several of them.

24.2. RUNOFF COEFFICIENT IN SIMPLIFIED CALCULATIONS OF RUNOFF

Basic input data necessary to estimate the amount of rainwater is information about rainfall and at least basic characteristics of the catchment, describing its size, shape, height variation (surface elevation), land cover, land use, water retention capacity, etc. Practice shows, however, that in the most common simplified computational methods the information about the catchment is reduced to a minimum. In the case of the most widely used approach in Poland – the method of constant rainfall intensity (CRI) (and also the method of limiting rainfall intensity (LRI), modified limiting rainfall intensity (MLRI) etc)), all information about the basin specificity is included in the values of catchment area, and one or two factors: the coefficient of runoff and the coefficient representing delay in basin. The role of these factors can not be overstated. Their values have a major impact on the obtained results of calculations. This is particularly clear in the case of the coefficient of runoff.

The runoff coefficient ψ, as it is known, is a measure of the ability of land to form surface runoff, and is defined as the ratio of the volume of surface runoff (expressed in units of flow rate, Q_s) to the volume of precipitation intensity Q_o (expressed in the same units):

$$\psi = \frac{Q_S}{Q_O} \tag{3}$$

Runoff coefficient in a global way takes into account the total influence on the runoff from the catchment area of such factors as infiltration, retention, evapotranspiration, etc. The values of runoff coefficients thus depend on many factors, the main of which is the type of land cover. In addition, these coefficients depend on the surface slope, the geological structure of the upper layers of soil but also from the rain intensity, rain duration, initial soil moisture (or dehydration, or frost), land surface temperature and the degree of filling with water of local surface hollows. Thus it is obvious that exact determination of the value of this ratio is therefore an impossible task, especially since it varies during runoff. Although there are empirical formulas that allow to estimate runoff coefficients on the basis of rainfall intensity, rainfall duration and type of land cover, the attitude mostly used in practice is to determine the value of ψ on the basis of its typical values presented in tables [2].

The number of sources in which one can find the tables enabling to determine the coefficient of runoff is very high. These are primarily the documents presenting engineering standards, engineering guide-books, technical papers, books etc. Unfortunately, the use of tables – despite the significant convenience of this approach – is a source of potential errors and inconsistencies in the results, resulting in a large conventionality and the relativity of the solution.

The first reason for this is the fact that the values of the coefficients reported in various sources for the same category of land are not always identical. This is crucial for the results of calculations. Another reason is a big influence of the surface elevation and catchment slope on the value of runoff coefficient. The larger slope, the faster and more intensive runoff, which is reflected in the flow-rates in the storm water drainage channels. Taking into account that the formulas of the most “engineering” methods do not consider basin slope in a direct way, its impact should be taken into account by proper adjusting the runoff coefficient. However, only several sources provide the values of runoff coefficients related to land slope.

Another problem in runoff coefficient determining may be the classification of the terrain to the particular category of land use. For example, the question of determining the density (or otherwise: the degree of compactness) of building, the distinction of category of green areas or classification of undeveloped land, wasteland, etc.

Another very important problem is to adopt the value of runoff coefficient for a given category. As mentioned, even for the same type of land cover different authors give different ranges of values. Moreover, within the same range it is possible to select different values, sometimes of a quite large range. Can thus be seen, that the choice of the value of runoff coefficient is characterized by high subjectivity. What makes things worse, the , but decisions taken at this stage, have a major impact on the results of calculations.

24.2.1. Example

To illustrate the problem the simple example of three hypothetical urban catchments A, B and C may be presented. Let us assume that the three basins are located in the same region (e.g. the same town). Basin A is a small catchment from which the rain water is drained to the local sewer, while B and C are larger basins, that drain the rainfall water

from the several districts of the town to the local streams. The basin B is characterized by a large share of forest and green terrains in the total basin area, while the basin C is characterized by a larger share of industrial and built-up areas. Percentage shares of different types of land cover for these catchments are shown in Table 1 [7]. Assuming that the basins are flat areas, for each of them the resultant runoff coefficient is determined on the basis of typical values of such coefficients presented in tables in literature.

Table 1

Land cover characteristics for hypothetical catchments A, B and C [7]

Land use characteristics	Catchment		
	A	B	C
Basin area [ha]: in this:	16.47	216.0	460.9
Forests [%]	10.0	51.0	20.0
Other green terrains [%]	20.0	15.0	5.0
Building of villa-type [%]	35.0	14.0	18.5
Dispersed building [%]	35.0	2.0	13.5
Undeveloped terrain [%]	0.0	14.0	13.5
Industrial and store terrain [%]	0.0	4.0	29.0

In order to assess the impact of the chosen values on the results obtained, it was assumed that for each catchment three cases will be considered. As the literature sources present the values of ψ of a several range for each category (not just a single value for each category), in the first case the lowest possible values of coefficients will be considered. In the second case – the average value (from the middle of the possible range, which in fact is the most common engineering attitude to this question, if there are no additional requirements). Finally, in the third case – the highest values from the suggested range in the tables is taken into consideration. The chosen values of ψ for different categories of land use taken to calculations are presented in Table 2. Final results of the ψ calculation for each catchment are presented in Table. 3.

Table 2

Values of runoff coefficient taken to calculations [7]

Basin land-use characteristics	Runoff coefficient		
	min.	av.	max.
Forests	0.01	0.05	0.15
Other green terrains	0.05	0.20	0.40
Building of villa-type	0.20	0.30	0.40
Dispersed building	0.30	0.50	0.80
Undeveloped terrain	0.10	0.15	0.20
Industrial and store terrain	0.50	0.70	0.90

This simple example shows how big and important influence to the calculation results has the subjective choice of the values of runoff coefficients. It is worth noting that the differences in the results of calculations, which – let us stress this fact – are the consequences of the choice of one factor only, reach up to 250%. Taking into account the fact that in most engineering methods for calculating flows in the sewers, runoff coefficient is the coefficient of linear proportionality between the flow rate in the channel and a rainfall intensity and catchment area, it is clear that the resulting flow can vary significantly (even 2.5 times), depending on the chosen values of ψ, while each of the results is "correct" in the sense of engineering art. This fact is of significant meaning in doing and/or interpreting calculations.

Table 3

Calculated values of runoff coefficient [7]

Basin	Runoff coefficient		
	min.	av.	max.
Forests	0.186	0.325	0.515
Other green terrains	0.080	0.156	0.272
Building of villa-type	0.240	0.370	0.520

24.3. TIME OF CONCENTRATION IN SIMPLIFIED MODELS

In the tasks related to the basin runoff calculation (including the cases of urban catchments) the very important element is the proper choice of the "computational rainfall" (also known as "model rainfall", "project rainfall" or "design rainfall"), which is the rainfall that – for the particular analyzed case – represents the typical, authoritative rainfall conditions. It can have a character of genuine precipitation episode or the hypothetical rain, obtained in a synthetic way, e.g. project storm (a project frequency-based storm), or finally the extremely simplified form, which is so-called "block storm". Regardless of the assumed general form of project rainfall, one of the essential elements is to determine its duration.

From the computational point of view, the most dangerous (and therefore also authoritative) is the rainfall of such duration, during which the largest outflow from the basin occurs. The duration of such precipitation is called the critical duration of rain. In general, this time can take different values for the same catchment, depending on the intensity of time-varying runoff conditions in the basin ([1, 3]). In typical engineering calculations in Poland considering the analysis of runoff from the urban catchment, the most common type of project rainfall is so-called "*block rainfall*", which is the precipitation of the unlimited scope, covering the entire basin, of the intensity constant in time and equal in the whole area of the basin, occurring with some frequency, and limited in time. In such a situation, if one also assumes the constant in time value of the runoff coefficient, critical duration of rain is equal to the time of concentration ([1, 2, 3]). Thus, the time of concentration is very important in runoff calculations as very often it is equal to the duration of the project rainfall.

Depending on the method of calculation, time of concentration is determined in a explicit manner, or its determination is an integral part of runoff calculation procedure, thus it can be indirect (often implicit) step of whole runoff calculations. The first of the

mentioned approaches is typical for the simplest “engineering” models, including the method of constant rainfall intensity (CRI). The second is characteristic for more complex computational models (eg. hydrodynamic models), as well as some of the modified versions of “engineering” models, e.g. modified method of limiting rainfall intensity (MLRI) [6, 7].

The most common approaches in determining time of concentration in the urbanized catchments are:

— *a priori* assumption of the rainfall duration, on the basis of the “typical” values, derived from various kinds of guidelines or of the earlier calculations of similar nature,
— equating time of concentration with travel time in the channel (excluding the processes of concentration and retention), calculated on the basis of the length of the channel and the “average” velocity in the channel during the culmination of the flood,
— use of empirical formulas,
— more thorough analysis of the subsequent stages of the runoff formation in the basin and the summing up of the individual specific times of runoff for the various stages (so-called *segment method*),
— detailed analysis of the processes determining runoff and flow in channels (complex hydrological models).

For obvious reasons, the most controversial are the first two approaches. Paradoxically, they are most often prescribed methods for determining the duration of rain in a typical engineering calculations. In Poland, it has been adopted for many years to dimension the sewer systems on the basis of calculations for the rainfall of 10 minutes or 15 minutes duration, without any detailed analysis of the actual conditions of the catchment runoff. Consequently, the results of calculations differ significantly from the real, and hence – have value only of a rough estimate in a narrow scope of applications.

Another, slightly better, although rarely used in Poland, method is to use empirical formulas. World literature supplies of many such formulas, including, among others formulas of Kerby, Kirpich, FFA, English, various modifications of the kinematic wave model, et al. [4]. Most of these formulas has been developed for natural catchments (mainly agricultural), although some of them are also recommended to be used in the case of urban catchments, including Kirpich and FFA formulas. The example of determining the time of concentration on the basis of this method and conclusions from the analysis are presented later in this article.

The best of the relatively simple methods for determining time of concentration is the segment method, in which the longest flow path in the basin is divided into segments (sections) representing the different forms of runoff and/or different nature of the catchment. The total time of concentration is the sum of the times of runoff in particular segments [1, 3]. In the most popular version of segment method (SCS method), three general stages in runoff formation can be distinguished:

— sheet flow – the very first stage of runoff, in which the water flows on the relatively smooth surface of the terrain, forming the very thin layer, without concentration in streams;
— shallow concentrated flow – flow in grooves and other longitudinal cavings on the basin surface;
— channel flow – concentrated flow in streams, channels, sewers etc.

Sheet flow is usually described with the kinematic wave equation, thus the time of such flow may be determined from the formula:

$$t_s = \frac{84.87}{I_d^{0.4}} \cdot \left(\frac{n \cdot L_s}{\sqrt{i_s}} \right)^{0.6} \tag{4}$$

where: L_s – is the length of the flow path [km],
n – is Manning roughness coefficient for the basin surface,
i_s – is the average slope of flow path [–], and
I_d – is the rainfall intensity [mm/min].

The duration time of the second stage of the runoff (shallow concentrated flow) is usually calculated on the basis of the average velocity of surface runoff and the length of flow path. Runoff velocity v [m/s] can be estimated from the empirical equation [3]:

$$v = 10 \cdot k \cdot i_s^{0.5} \tag{5}$$

where i_s is the average slope of shallow flow path [–], and k is a parameter characterizing land cover, with the values varying from 0.076 for the forests to 0.619 for the paved surfaces [3]. This form of runoff can also be described by the Manning's equation [1, 4], which is more general approach than applying of formula (5).

The last stage of runoff is the flow in open channels (streams, sewers, ditches etc.), which can be also described by Manning's equation:

$$v = \frac{1}{n} \cdot R_h^{2/3} \cdot i_s^{1/2} \tag{6}$$

where n is Manning channel roughness coefficient, and R_h [m] is the length of hydraulic radius, determined for the maximal fill of the channel.

In order to illustrate the influence of the chosen method of time of concentration determination to the obtained calculation results, the case study example is presented.

24.3.1. Example

Let us consider the Kolibkowski stream in Gdynia (Poland), which is one of many streams being the receivers of rainwater from different districts of this town. The channel length is 2.337 km, the catchment area is 216.6 ha, maximal catchment length is 2.860 km, basin width is 0.760 km, average slope of the catchment 71.5‰ and average slope of the channel is 22‰. Land-use of the basin surface is very diverse: more than 60% of the basin area are green terrains, approximately 16% is undeveloped land, about 2% – the industrial area, while the remaining area is the urban terrain, with a predominance of residential building. The urbanized part of the basin is equipped with stormwater drainage system, leading rainwater to the Kolibkowski stream. Rainwater from the undeveloped areas also flow into the stream, which eventually becomes a receiver of total amount of water forming runoff from the analyzed catchment.

For the basin presented above, time of concentration was calculated with use of chosen empirical formulas and the segment method. For the purposes of the latter, the representative path of runoff was divided into five segments with different values of characteristics and/or different form of runoff. Due to the forest nature of the upper part of the catchment (relatively high roughness of the surface), it was assumed that the sheet flow in the analyzed basin is neglected. The shape of the cross-sections of the channel was

approximated by trapezoidal one, with bottom width B and wall slope 1 : m. The values of the channel characteristics are presented in Table 4 (F – cross section area, O_z – wetted perimeter, R_h – hydraulic radius, H – maximal depth of the channel). The table also contains the values of time of concentration t_c calculated with use of segment method. The values of the time of concentration determined on the basis of selected empirical equations are presented in Table 5. To compare – the time of concentration obtained with use of more complex model – the kinematic wave model for direct runoff and reservoir model for channel flow – was approximately 130 min [7].

Table 4

Characteristics of the flow path segments and calculated time of concentration for the basin of Kolibkowski stream [7]

Section	k [–]	Channel characteristics									Results	
		L [m]	i_s [–]	n [–]	B [m]	m [–	H [m]	F [m^2]	O_z [m]	R_h [m]	v [m/s]	tc [min]
A – B	0,076	523	0,083	–	–	–	–	–	–	–	0.06	145
B – C	–	732	0.013	0.40	1.0	0.59	1.7	3.40	4.94	0.69	0.22	55
C – D	–	685	0.013	0.17	1.0	0.59	1.7	3.40	4.94	0.69	0.52	22
D – E	–	450	0.013	0.04	1.0	1.50	1.0	2.50	4.60	0.54	1.89	4
E –F	–	470	0.037	0.04	1.0	1.50	1.0	2.50	4.60	0.54	3.18	2.5

Table 5

Time of concentration in the basin of Kolibkowski stream calculated with empirical formulas [7]

Formula	Time of concentration [min]
Kerby's eq.	94.49
Kirpich's eq.	97.17
English eq.	100.94
Giandotti's eq.	105.24
Izzard's eq.	93.36
Bransby-Williams' eq.	67.55
kinematic wave eq.	91.65
FFA formula	127.225

24.4. FURTHER ANALYSIS

To assess the impact of a value of t_c to the value of the maximum intensity of outflow from catchment area, the calculations of the maximal flow rate were run. Four methods from the group of simplified "engineering" models were compared: the most often used in Poland method of constant rainfall intensity (CRI), the modified method of limiting rainfall intensity (MLRI) and the popular methods in Germany – the method of runoff delay coefficient (RDC) and the method of variable runoff coefficient (VRC). In the example the

two values of time of concentration were considered: 90 min – which is a value close to those obtained with empirical formulas, and 130 min which was obtained with use of FFA formula and the kinematic wave model and tank model as it was already mentioned. Additionally, for the CRI method (in which the time of rainfall duration can be assumed *a priori*) also two typical for Polish calculations values were taken into account: 10 min and 20 min.

The values of the computational flow rate obtained as a result of the study are presented in Table 6.

Table 6

Computational flow rate in the basin of Kolibkowski stream [7]

Method of calculation	Raifall duration t_d [min]	Project rainfall intensity q [$dm^3/(s \cdot ha)$]	Discharge rate in basin outlet Q [m^3/s]
MSND	10	173.2	2.32
	20	109.1	1.46
	90	39.4	0.53
	130	30.8	0.51
ZMNG-S.	130	30.9	1.01
MWOO	90	43.3	2.81
	130	30.8	2.00
MZWS	90	21.5	1.40
	130	15.5	1.00

24.5. CONCLUSIONS

The paper presented only a few chosen aspects of estimating the amount of runoff in the urban catchment. Each of the elements, such as project rainfall estimation, determination of time of concentration, the choice of values of runoff coefficients, the choice of calculation method and others, may be a potential source of errors, inaccuracies in estimates, and significant relativity of calculation results. Unfortunately, in general, divergence of results is relatively high. The examples presented in the paper shown that - due to the choice of runoff coefficient only – the obtained values of basin outflow may differ more than 200%. The same effect may be obtained if different formulas for rainfall duration (time of concentration) are considered. Taking into account that the both effects may superimpose and the number of coefficients and different characteristics taken to calculations may be greater, in consequence the results of such calculations suffer very much from uncertainty and relativity. This is a very important conclusion, questioning the accuracy of any simplified computations of runoff. It is very difficult to determine reliably and unambiguously which method is “correct” and how to proceed, especially in the case of lack of sufficiently reliable data (in rainfall and catchment characteristics), which – as it is known – is a common situation. The examples presented in the paper prove, that each solution result obtained with simplified methods should be treated as the rough estimation

only. However, very often the mentioned methods are the only one taken into account in engineering approach.

References

[1] Akan A. O., Houghtalen R. J.: Urban Hydrology, Hydraulics and Stormwater Quality. Engineering Applications and Computer Modeling. John Wiley and Sons, Inc. 2003.
[2] Chow V. T.: Handbook of Applied Hydrology. New York: McGraw Hill Book Company 1964.
[3] McCuen R. H.: Hydrologican Analysis and Design. New Jersey: Practice Hall, Englewood Cliffs 2005.
[4] Roussel M. C., Thompson D. B., Fang X., Cleveland T. G., Garcia C. A.: Time-Parameter Estimation for Applicable Texas Watersheds. Dep. of Civil Eng., College of Engineering, Lamar University, Beaumont, Texas, USA, Research Rep. 0-4696-2, 2005.
[5] Sawicka D., Sawicki J. M.: Hydraulic aspects of the storage reservoirs design. Mat.: International Symposium on Water Management and Hydraulic Engineering, Dubrownik, 14–19 September 1998, Paper No. 3.10. pp. 117–125, 1998.
[6] Soczyńska U.: Hydrologia dynamiczna. Warszawa: PWN 1997 (in Polish).
[7] Weinerowska-Bords K.: Influence of Simplifications on Calculation of Runoff in Urban Catchment. Publ. of Gdansk University of Technology, Gdansk, Poland 2010 (in Polish).

25 Mathematical Modeling of Dissolved Matter Transport with Biodegradation in Activated-Sludge Systems

Piotr Zima (Gdańsk University of Technology, Faculty of Civil and Environmental Engineering)

25.1. INTRODUCTION

Water as an essential element of the ecosystem of the planet, always contains some admixture of various substances and microorganisms. If the additives are in abundance, we can talk about the pollution, which can be disposed of in a process called purging. This phenomenon may be either natural or artificial. As it occurs naturally in rivers, where at low load of pollutants we are dealing with self-cleaning process. It is mainly a distribution, dilution and detention by the environment of substances contained in water. Through this process, small portions of impurities are removed in a natural way, without causing harm to the environment. Purification processes may also be forced artificially by humans and relate to contaminated water, or sewage.

Ability to perform the simulation of solute transport with biodegradation involves the potential use of mathematical models and computational methods. On the one hand there are models describing the hydrodynamics of a carrier of pollutants (water) and advective-dispersive transport of dissolved matter – that are physical processes. On the other hand there are models describing biodegradation processes of that substance – that are biochemical processes. In the first case, which is in hydromechanics, the existing equations of mathematical physics describing these processes are well known and widely used in practice. For the description of the pollutants decay, the problem is more complex and as far as getting to know the nature of these processes, new models are created. Widely used and are currently being developed deterministic models of a new generation – ASM (Activated Sludge Models). These models describe the biochemical changes in the factors determining the stoichiometric ratios of substrates and products of various biochemical reactions and kinetic parameters describing the speed of the processes. These models have been developed to mathematical description of the wastewater treatment processes used in bioreactors for the biological stage of wastewater treatment plants, and can be used to describe the phenomena occurring in the canals and rivers. These models are used as a source terms in solute transport equation to describe processes of biodegradation.

25.2. MATERIALS AND METHODS

According to the latest global trends, mathematical modeling become an integral part of designing and operating wastewater treatment systems, particularly with the use of activated sludge systems [1]. Application of mathematical models allows analysis in a short time and low financial effort many technological solutions and to simulate events in a typical real systems [2, 3].

25.2.1. Solute Transport Modeling

The equation of unsteady solute transport in a general case can be presented in the following form (Sawicki, 2003):

$$\frac{\partial C_j}{\partial t} + \nabla(\mathbf{u}C_j) = \nabla(\mathbf{D}_j \nabla C_j) + \sum_{i=1}^{I} S_{ij} \tag{1}$$

where: C_j – concentration of the j-th substance,
t – time coordinate,
∇ – nabla operator,

$$\nabla = \left(\frac{\partial}{\partial x}, \frac{\partial}{\partial y}, \frac{\partial}{\partial z} \right) \tag{2}$$

$\mathbf{u}$ – velocity vector,
$\mathbf{D}_j$ – tensor diffusion coefficient of the j-th substance,
$\sum_{i=1}^{I} S_{ij}$ – sum of source terms (i = 1, I).

Equation (1) describes three additive processes: advection, diffusion (dispersion in the spatially averaged models) and external factors causing the increase or loss of substance. The last process, in this case, have a biochemical character and can be express by source terms in following form:

$$S_{ij} = k_i \prod_{i=1}^{I} C_i^{W_i} \tag{3}$$

where: k_i – reaction coefficient,
$\prod_{i=1}^{I}$ – multiple components of the product,
w_i – order of reaction.

25.2.2. Models of Kinetics of Bacterial Growth Rate

The kinetics of bacterial growth rate can be described by equation (3). In this case Equation (3) takes the form:

$$S_i = \mu X \tag{4}$$

where: X – bacteria concentration,
μ – term of the kinetics of bacterial growth,

$$\mu = \mu_{\max}\left(\frac{S}{S + K_S}\right) \tag{5}$$

where: $\mu_{\max}$ – maximum value of the constant growth kinetics of bacteria,
S – substrate concentration,
K_S – half saturation constant, which corresponds to the substrate concentration at half maximum of the reaction kinetics.

The right side of equation (5) defines the approximation of the Monod [5], called Monod factor (term) limiting. Be the first to Jacques Monod [6] suggested that the relationship between reaction rate and concentration of the substance has a hyperbolic form. This factor allows for limiting the reaction rate of substrate deficiency (reaction of the 1^{st} – order) and the complete response rate with an excess of substrate (reaction of the 0^{th} – order). This term also provide a smooth transition between these two states. Graphical interpretation of the Monod term is shown in Fig. 1.

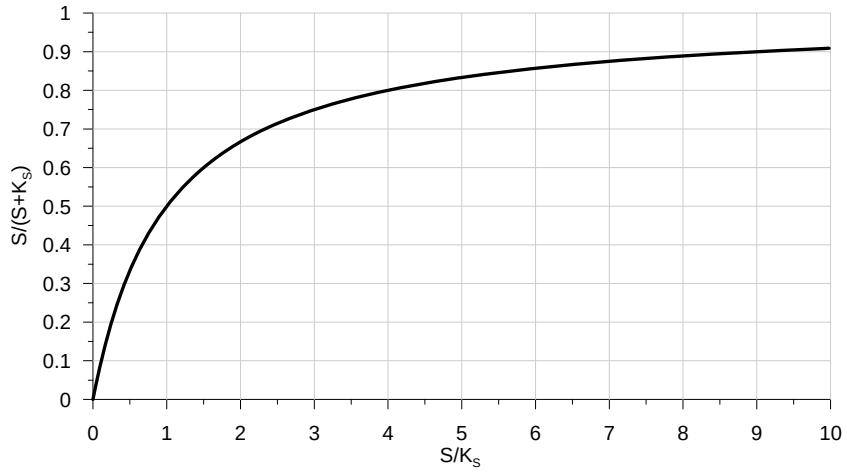

Fig. 1. Graphical interpretation of the Monod term

The concentration of biomass present in wastewater can be reduced to the total of its decay, or until to the transition into a state of endogenous respiration (in the absence of food microorganisms consume their own mass of the cell). Disappearance is proportional to the concentration of biomass and is often described by linear model and can take the form as follows:

$$S_i = k_d X \tag{6}$$

where: k_d – biomass decay rate constant.

	(j)	Component (i) / Process	S_{O_2} (1)	S_F (2)	S_A (3)	S_{NH_4} (4)	S_{NO_3} (5)	S_{PO_4} (6)	S_I (7)	S_{ALK} (8)	S_{N_2} (9)	X_I (10)	X_S (11)	X_H (12)	X_{PAO} (13)	X_{PP} (14)	X_{PHA} (15)	X_{AUT} (16)	X_{TSS} (17)	X_{MeOH} (18)	X_{MeP} (19)	Process rate equations r_j
Hydrolysis processes	(1)	Aerobic hydrolysis		$1-f_{S_I}$		ϑ_{1,NH_4}		ϑ_{1,PO_4}	f_{S_I}	$\vartheta_{1,ALK}$			-1						$\vartheta_{1,TSS}$			$K_h \cdot \frac{S_{O_2}}{K_{O_2}+S_{O_2}} \cdot \frac{X_S/X_H}{K_X+X_S/X_H} \cdot X_H$
	(2)	Anoxic hydrolysis		$1-f_{S_I}$		ϑ_{2,NH_4}		ϑ_{2,PO_4}	f_{S_I}	$\vartheta_{2,ALK}$			-1						$\vartheta_{2,TSS}$			$K_h \cdot \eta_{NO_3} \frac{K_{O_2}}{K_{O_2}+S_{O_2}} \frac{S_{NO_3}}{K_{NO_3}+S_{NO_3}} \frac{X_S/X_H}{K_X+X_S/X_H} \cdot X_H$
	(3)	Anaerobic hydrolysis		$1-f_{S_I}$		ϑ_{3,NH_4}		ϑ_{3,PO_4}	f_{S_I}	$\vartheta_{3,ALK}$			-1						$\vartheta_{3,TSS}$			$K_h \cdot \eta_{fe} \frac{K_{O_2}}{K_{O_2}+S_{O_2}} \frac{K_{NO_3}}{K_{NO_3}+S_{NO_3}} \frac{X_S/X_H}{K_X+X_S/X_H} \cdot X_H$
Heterotrophic organisms X_H	(4)	Aerobic growth on S_F	$1-\frac{1}{Y_H}$	$-\frac{1}{Y_H}$		ϑ_{4,NH_4}		ϑ_{4,PO_4}		$\vartheta_{4,ALK}$				1					$\vartheta_{4,TSS}$			$\mu_H \frac{S_{O_2}}{K_{O_2}+S_{O_2}} \frac{S_F}{K_F+S_F} \frac{S_F}{S_F+S_A} \frac{S_{NH_4}}{K_{NH_4}+S_{NH_4}} \frac{S_{PO_4}}{K_P+S_{PO_4}} \frac{S_{ALK}}{K_{ALK}+S_{ALK}} \cdot X_H$
	(5)	Aerobic growth on S_A	$1-\frac{1}{Y_H}$		$-\frac{1}{Y_H}$	ϑ_{5,NH_4}		ϑ_{5,PO_4}		$\vartheta_{5,ALK}$				1					$\vartheta_{5,TSS}$			$\mu_H \frac{S_{O_2}}{K_{O_2}+S_{O_2}} \frac{S_A}{K_A+S_A} \frac{S_A}{S_F+S_A} \frac{S_{NH_4}}{K_{NH_4}+S_{NH_4}} \frac{S_{PO_4}}{K_P+S_{PO_4}} \frac{S_{ALK}}{K_{ALK}+S_{ALK}} \cdot X_H$
	(6)	Anoxic growth on S_F		$-\frac{1}{Y_H}$		ϑ_{6,NH_4}	$-\frac{1-Y_H}{2.86 \cdot Y_H}$	ϑ_{6,PO_4}		$\vartheta_{6,ALK}$	$\frac{1-Y_H}{2.86 \cdot Y_H}$			1					$\vartheta_{6,TSS}$			$\mu_H \cdot \eta_{NO_3} \frac{K_{O_2}}{K_{O_2}+S_{O_2}} \frac{K_{NO_3}}{K_{NO_3}+S_{NO_3}} \frac{S_F}{K_F+S_F} \frac{S_F}{S_F+S_A} \frac{S_{NH_4}}{K_{NH_4}+S_{NH_4}} \frac{S_{PO_4}}{K_P+S_{PO_4}} \frac{S_{ALK}}{K_{ALK}+S_{ALK}} \cdot X_H$
	(7)	Anoxic growth on S_A Denitrification			$-\frac{1}{Y_H}$	ϑ_{7,NH_4}	$-\frac{1-Y_H}{2.86 \cdot Y_H}$	ϑ_{7,PO_4}		$\vartheta_{7,ALK}$	$-\frac{1-Y_H}{2.86 \cdot Y_H}$			1					$\vartheta_{7,TSS}$			$\mu_H \cdot \eta_{NO_3} \frac{K_{O_2}}{K_{O_2}+S_{O_2}} \frac{K_{NO_3}}{K_{NO_3}+S_{NO_3}} \frac{S_A}{K_A+S_A} \frac{S_A}{S_F+S_A} \frac{S_{NH_4}}{K_{NH_4}+S_{NH_4}} \frac{S_{PO_4}}{K_P+S_{PO_4}} \frac{S_{ALK}}{K_{ALK}+S_{ALK}} \cdot X_H$
	(8)	Fermentation		-1	1	ϑ_{8,NH_4}		ϑ_{8,PO_4}		$\vartheta_{8,ALK}$									$\vartheta_{8,TSS}$			$q_{fe} \frac{K_{O_2}}{K_{O_2}+S_{O_2}} \frac{K_{NO_3}}{K_{NO_3}+S_{NO_3}} \frac{S_F}{K_F+S_F} \frac{S_{ALK}}{K_{ALK}+S_{ALK}} \cdot X_H$
	(9)	Lysis				ϑ_{9,NH_4}		ϑ_{9,PO_4}		$\vartheta_{9,ALK}$		f_{X_I}	$1-f_{X_I}$	-1					$\vartheta_{9,TSS}$			$b_H \cdot X_H$
Phosphorus-accumulating organisms X_{PAO}	(10)	Storage of X_{PHA}			-1	ϑ_{10,NH_4}		ϑ_{10,PO_4}		$\vartheta_{10,ALK}$						$-Y_{PO_4}$	1		$\vartheta_{10,TSS}$			$q_{PHA} \cdot \frac{S_A}{K_A+S_A} \frac{S_{ALK}}{K_{ALK}+S_{ALK}} \frac{X_{PP}/X_{PAO}}{K_{PP}+X_{PP}/X_{PAO}} \cdot X_{PAO}$
	(11)	Aerobic storage of X_{PP}	$-Y_{PHA}$			ϑ_{11,NH_4}		ϑ_{11,PO_4}		$\vartheta_{11,ALK}$						1	$-Y_{PHA}$		$\vartheta_{11,TSS}$			$q_{PP} \cdot \frac{S_{O_2}}{K_{O_2}+S_{O_2}} \frac{S_{PO_4}}{K_{PO_4}+S_{PO_4}} \frac{S_{ALK}}{K_{ALK}+S_{ALK}} \frac{X_{PHA}/X_{PAO}}{K_{PHA}+X_{PHA}/X_{PAO}} \frac{K_{MAX}-X_{PP}/X_{PAO}}{K_{PP}+K_{MAX}-X_{PP}/X_{PAO}} \cdot X_{PAO}$
	(12)	Anoxic storage of X_{PP}				ϑ_{12,NH_4}	ϑ_{12,NO_3}	ϑ_{12,PO_4}		$\vartheta_{12,ALK}$	$-\vartheta_{12,NO_3}$					1	$-Y_{PHA}$		$\vartheta_{12,TSS}$			$r_{12} = r_{11} \cdot \eta_{NO_3} \frac{K_{O_2}}{K_{O_2}+S_{O_2}} \frac{S_{NO_3}}{K_{NO_3}+S_{NO_3}}$
	(13)	Aerobic growth of X_{PHA}	ϑ_{13,O_2}			ϑ_{13,NH_4}		ϑ_{13,PO_4}		$\vartheta_{13,ALK}$					1		$-\frac{1}{Y_H}$		$\vartheta_{13,TSS}$			$\mu_{PAO} \cdot \frac{S_{O_2}}{K_{O_2}+S_{O_2}} \frac{S_{NH_4}}{K_{NH_4}+S_{NH_4}} \frac{S_{PO_4}}{K_P+S_{PO_4}} \frac{S_{ALK}}{K_{ALK}+S_{ALK}} \frac{X_{PHA}/X_{PAO}}{K_{PHA}+X_{PHA}/X_{PAO}} \cdot X_{PAO}$
	(14)	Anoxic growth of X_{PP}				ϑ_{14,NH_4}	ϑ_{14,NO_3}	ϑ_{14,PO_4}		$\vartheta_{14,ALK}$	$-\vartheta_{14,NO_3}$				1		$-\frac{1}{Y_H}$		$\vartheta_{14,TSS}$			$r_{14} = r_{13} \cdot \eta_{NO_3} \frac{K_{O_2}}{K_{O_2}+S_{O_2}} \frac{S_{NO_3}}{K_{NO_3}+S_{NO_3}}$
	(15)	Lysis of X_{PAO}				ϑ_{15,NH_4}		ϑ_{15,PO_4}		$\vartheta_{15,ALK}$		f_{X_I}	$1-f_{X_I}$		-1				$\vartheta_{15,TSS}$			$b_{PAO} \cdot \frac{S_{ALK}}{K_{ALK}+S_{ALK}} \cdot X_{PAO}$
	(16)	Lysis of X_{PP}				ϑ_{16,NH_4}		ϑ_{16,PO_4}		$\vartheta_{16,ALK}$						-1			$\vartheta_{16,TSS}$			$b_{PP} \cdot \frac{S_{ALK}}{K_{ALK}+S_{ALK}} \cdot X_{PP}$
	(17)	Lysis of X_{PHA}			1	ϑ_{17,NH_4}		ϑ_{17,PO_4}		$\vartheta_{17,ALK}$							-1		$\vartheta_{17,TSS}$			$b_{PHA} \cdot \frac{S_{ALK}}{K_{ALK}+S_{ALK}} \cdot X_{PHA}$
Nitrifying organisms X_{AUT}	(18)	Aerobic growth of X_{AUT}	$-\frac{4.57-Y_A}{Y_A}$			ϑ_{18,NH_4}	$\frac{1}{Y_A}$	ϑ_{18,PO_4}		$\vartheta_{18,ALK}$								1	$\vartheta_{18,TSS}$			$\mu_{AUT} \cdot \frac{S_{O_2}}{K_{O_2}+S_{O_2}} \frac{S_{NH_4}}{K_{NH_4}+S_{NH_4}} \frac{S_{PO_4}}{K_P+S_{PO_4}} \frac{S_{ALK}}{K_{ALK}+S_{ALK}} \cdot X_{AUT}$
	(19)	Lysis of X_{AUT}				ϑ_{19,NH_4}		ϑ_{19,PO_4}		$\vartheta_{19,ALK}$		f_{X_I}	$1-f_{X_I}$					-1	$\vartheta_{19,TSS}$			$b_{AUT} \cdot X_{AUT}$
Precipitation of phosphorus	(20)	Precipitation						ϑ_{20,PO_4}		$\vartheta_{20,ALK}$									$\vartheta_{20,TSS}$	-3.45	4.87	$k_{PRE} \cdot S_{PO_4} \cdot X_{MeOH}$
	(21)	Redissolution						ϑ_{21,PO_4}		$\vartheta_{21,ALK}$									$\vartheta_{21,TSS}$	3.45	-4.87	$k_{RED} \cdot \frac{S_{ALK}}{K_{ALK}+S_{ALK}} \cdot X_{MeP}$

Fig. 2. Petersen matrix in ASM2d model

25.2.3. Activated Sludge Models

Biochemical mathematical model ASM (Activated Sludge Model) describes the transformation of organic compounds and nitrogen [7]. In its original form was presented in a report on the activities of the Working Group IAWPRC (International Association on Water Pollution Research and Control), working on practical use of models in the design and operation of systems for biological wastewater treatment [1]. The basis of the model are pre-developed concepts [1]. In its original form it consisted of eight equations describing the kinetics of change with 13 state variables, using the nomenclature recommended by IAWPRC. Matrix form was used for the mathematical description, allowing a clear link between kinetics of the rate changes in concentration of the model fractions. The model is based on mass balance equations and the stoichiometric and kinetic dependencies. Kinetic equation is based on assumptions about the kinetics of Monod [6].

In the next years, the model underwent modifications and extensions [2, 8, 9]. From its original form differs mainly the denitrification, assimilation and a more complex form of equations of kinetics [3, 10]. Model included also unreactive fraction, primarily due to more accurate models and possibilities to combine them with other processes [2].

25.2.4. Activated Sludge Model No 2d

Like all ASM models, the ASM2d model has matrix structure. The basis is the Petersen matrix [11] and the state variables which can be defined as a state vector. ASM2d model is characterized by two types of components: soluble (marked *S* with the appropriate index) and particulate matter (indicated by *X* with the appropriate index). Finally, the Petersen matrix for ASM2d model can be written in the form presented in Fig. 2 [2]. There are 21 ordinary differential equations and 19 parameters. To solve the resulting system of equations was used procedure, which is a part of the program (written by the author of this paper) for the simulation of solute transport with biodegradation. In this procedure, the Runge-Kutta method (second order) was used.

25.2.5. Simulation Studies of Reactors with Activated Sludge System

A guideline for simulation studies of wastewater treatment plants was developed by the Working Group HSG (Hochschulgruppe) [12]. Flowchart of a simulation study according to the HSG guideline is presented in Fig. 3.

In Fig. 3 is selected phase, which deals with the problem of model parameters estimation discussed in this paper. The ASM2d was calibrated using the results of a series of batch tests with the Gdańsk "Wschód" WWTP (nortern Poland) mixed liquor presented by Swiniarski et. al. (2011) [13]. The first was a conventional nitrate uptake rate (NUR) measurement, in which the nitrate (KNO_3) were added at the beginning of a 4-hour test. In the second batch test procedure (so-called phosphate release rate (PRR)/anoxic phosphorus uptake rate (PUR)), a mixture of WWTP mixed liquor and settled wastewater was contacted for 2.5 hours under anaerobic conditions.

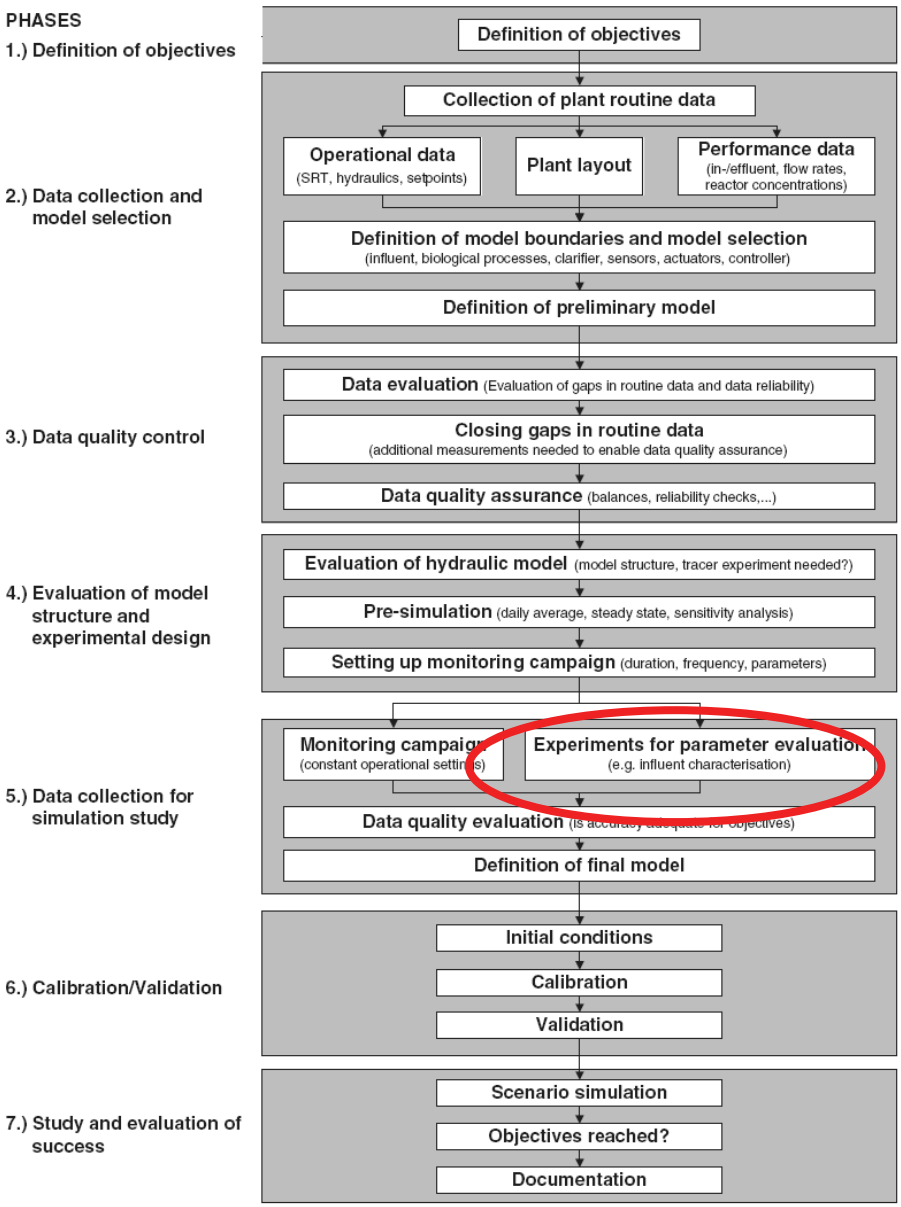

Fig. 3. Flowchart of a simulation study according to the HSG guideline [12]

After that time, the nitrate were added and the test continued for 4.5–5 hours. The aerobic PURs and ammonia utilization rates (AURs) were measured in two-phase experiment, in which the anoxic conditions in the second phase were replaced by aerobic conditions (no KNO_3 added, a DO concentration set point of 6 g O_2/m^3). In addition, three-phase experiment with the settled wastewater were also carried out including anaerobic conditions (2 h), anoxic conditions (4 h, after addition of KNO_3) and aerobic conditions (6 h, at a DO con-

centration set point of 6 g O_2/m^3). These experiments were described in detail by Mąkinia et al. (2010) [14].

Table 1

Kinetic Parameters Adjusted in the ASM2d [13]

Definition	Symbol	Unit	ASM2d default	Calibrated value
Heterotrophic organisms (X_H):				
Max. growth rate of X_H on S_A and S_F	μ_H	d^{-1}	6.0	3.0
Autotrophic organisms (X_A):				
Maximum growth rate of X_A	μ_A	d^{-1}	1.0	1.35
Saturation coefficient for NH_4–N	$K_{NH4,A}$	g N/m^3	1.0	1.3
Saturation coefficient for PO_4–P (nutrient)	$K_{PO4,A}$	g P/m^3	0.01	0.001
Phosphorus Accumulating Organisms (X_{PAO}):				
Rate constant for storage of X_{PHA}	q_{PHA}	d^{-1}	3.0	6.0
Rate constant for storage of X_{PP}	q_{PP}	d^{-1}	1.5	4.5
Reduction factor for anoxic activity of X_{PAO}	$\eta_{NO3,PAO}$	–	0.6	0.5
Saturation coefficient for S_A	$K_{SA,PAO}$	g COD/m^3	4.0	1.0
Saturation coefficient for NH_4–N (nutrient)	$K_{NH4,PAO}$	g N/m^3	0.05	0.01
Saturation coefficient for PO_4–P (nutrient)	$K_{PO4,PAO}$	g P/m^3	0.01	0.001
Saturation coefficient for X_{PP}	K_{PP}	g P/g COD	0.01	0.02
Inhibition coefficient for X_{PP} storage	K_{IPP}	g P/g COD	0.02	0.05
Saturation coefficient for X_{PHA}	K_{PHA}	g COD/g COD	0.01	0.1
Hydrolysis of particulate substrate (X_S):				
Hydrolysis rate constant	k_{hyd}	d^{-1}	3.0	2.5

Table 2

Stoichiometric Parameters Adjusted in the ASM2d [13]

Definition	Symbol	Unit	ASM2d default	Calibrated value
Heterotrophic organisms (X_H):				
Yield coefficient	Y_H	g COD/g COD	0.625	0.67
Phosphorus Accumulating Organisms (X_{PAO}):				
PP requirement (PO_4–P release) for S_{A1}	Y_{PO4}	g P/g COD	0.4	0.34

The NUR measurements with the external carbon sources were conducted in a glass beaker with the maximum working volume of 4.0 dm^3, whereas the other experiments were conducted under well-controlled conditions in an apparatus consisting of two parallel batch reactors (max. volume of 4.0 dm^3). The reactors were equipped with electrodes and probes for monitoring of pH, ORP, temperature, and DO concentration. The automated control system maintained DO concentration and temperature around set points in the reactors. Batch test temperatures were in the range of 13 to 22°C. The results of these experiments

and computer simulations are presented in Fig.4 – 7. Computer simulations was carried out with ASM2d standard parameters [2] and some parameters with new values estimated by Swiniarski et. al. [13]. The new parameters (kinetic and stochiometric) are presented in Tab. 1 and 2.

25.3. NUMERICAL SIMULATIONS

Presented ASM2d model was verified for the above tests in batch reactors in laboratory tests by Swinarski et al. [13]. The results (measurements and calculations) for all tests are shown in Figures 4 – 7.

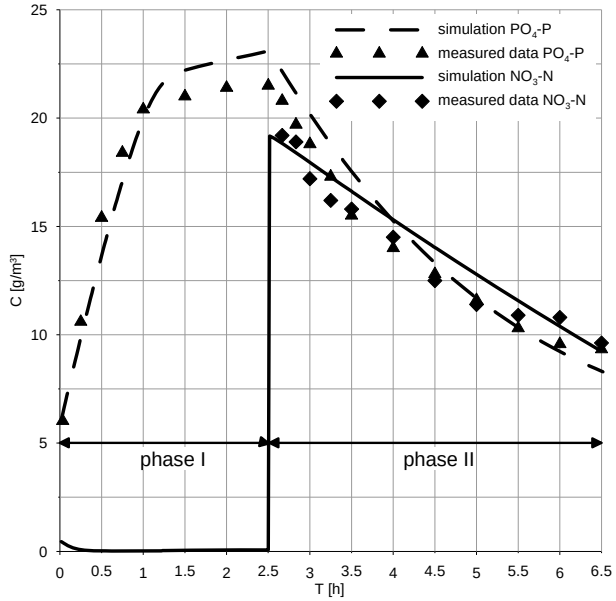

Fig. 4. Measured data vs. ASM2d simulations for batch experiment with WWTP mixed liquor and settled wastewater: NO_3–N and PO_4–P during the Anaerobic P release (phase I) and Anoxic P Uptake (phase II) (MLSS = 1.88 kg/m^3, T = 19.8°C)

25.4. SUMMARY

Description of the transformation of nutrients under the influence of activated sludge system requires the determination of the source functions in transport equation. In this paper, to describe these transformations was applied one of the most widely used biokinetic models – Activated Sludge Model No. 2d. Using the full model (19 parameters, 21 processes) computer simulations was carried out reproducing the purification processes taking place in the wastewater during the tests in batch reactors.

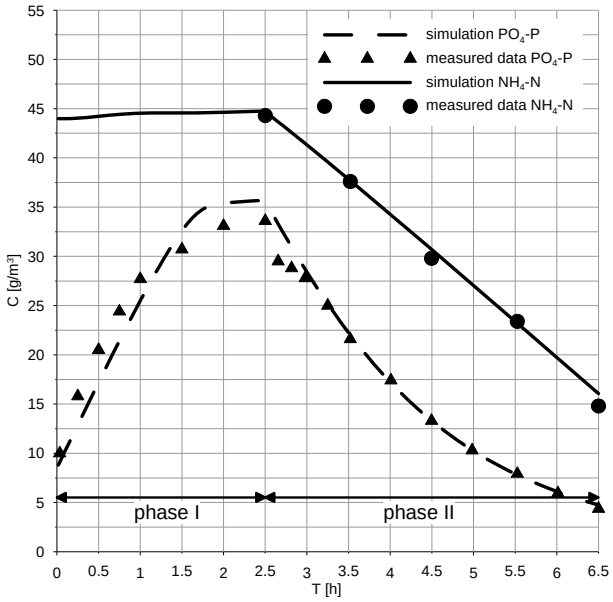

Fig. 5. Measured data vs. ASM2d simulations for batch experiment with WWTP mixed liquor and settled wastewater: NH_4–N and PO_4–P during the anaerobic P release (phase I) and aerobic P uptake (MLSS = 2.17 kg/m^3, T = 18.9°C)

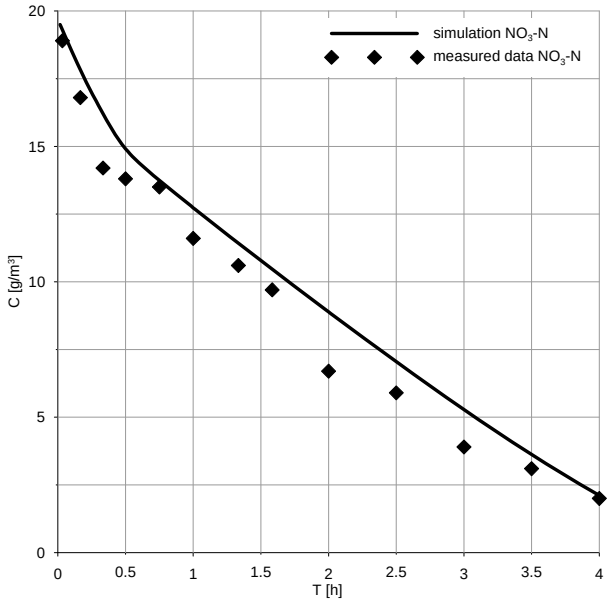

Fig. 6. Measured data vs. ASM2d simulations for batch experiment with WWTP mixed liquor and settled wastewater: NO_3–N during the "conventional" denitrification (MLSS = 3.17 kg/m^3, T = 20.5°C)

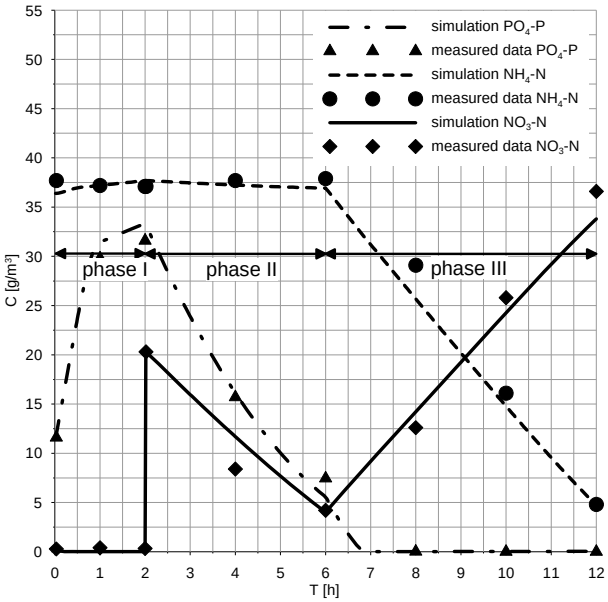

Fig. 7. Measured data vs. ASM2d simulations for batch experiment with WWTP mixed liquor and settled wastewater: NO_3–N, NH_4–N and PO_4–P during a 3-Phase (phase I – anaerobic/phase II – anoxic/phase III – aerobic) experiment (MLSS = 3.54 kg/m^3, T = 13.2°C)

To solve the various equations the second order Runge-Kutta method was used. The simulations verified the correctness of the source terms in the transport equation in the form of a full Petersen matrix. The obtained results of computer simulations are in accordance with the results obtained during the test measurements in a batch reactor and allowed to verify the created by the author of this paper a ASM2d model with a full Petersen matrix.

References

[1] Henze M., Grady C. P. L. Jr., Gujer W., Marais G. v. R. and Matsuo T.: Activated Sludge Model No. 1. Scientific and Technical Report No. 1, IAWPRC, London 1987.
[2] Henze M., Gujer W., Mino T., Van Loosdrecht M. (eds.): Activated Sludge Models ASM1, ASM2d and ASM3. Scientific and Technical Report No. 9. IWA, London 2000.
[3] Henze M., Gujer W., Mino T., van Loosdrecht M.: Activated sludge models ASM1, ASM2, ASM2d and ASM3 IWA Task Group on Mathematical Modelling for Design and Operation of Biological Wastewater Treatment. London: IWA Publishing 2002.
[4] Sawicki J. M.: Migration of pollutants. Gdańsk: Wyd. Politechniki Gdańskiej 2003. ISBN 83-7348-052-8 (in polish) 2003.
[5] Orhon D., Sözen S., Ubayo E.: Assessment of Nitrification-Denitrification Potential of Istanbul Domestic Wastewaters. Wat. Sci. Tech., 30 (6), 21–30, 1994.
[6] Monod J.: The growth of microbial cultures. Ann. Rev. Microbiol., 3, 371–394, 1949.
[7] Batstone D. J., Keller J., Angelidaki I., Kalyuzhnyi S. V., Pavlostathis S. G., Rozzi A., Sanders W. T. M., Siegrist H., Vavilin V. A.: Anaerobic Digestion Model No. 1 (ADM1). IWA Scientific and Technical Report #13. London: IWA Publishing, 2002.
[8] Henze M.: Characterisation of wastewater for modelling of activated sludge processes. Wat. Sci. Tech., 25 (6), 1–15, 1992.

[9] Henze M., Gujer W., Mino T., Matsuo T., Wentzel M. C., Marais G. V. R., van Loos-drecht M.: Activated Sludge Model No. 2d. Wat. Sci. Tech., 39 (1), p. 165–182, 1999.
[10] Gernaey K. V., van Loosdrecht M. C. M, Henze M., Lind M., Jorgensen S. B.: Activated sludge wastewater treatment plant modelling and simulation: state of the art. Env. Model. Soft., 19, 763–783, 2004.
[11] Petersen E. E.: Chemical Reaction Analysis. Engelwood Cliffs, NJ: Prentice Hall 1965.
[12] Langergraber G., Rieger L., Winkler S., Alex J., Wiese J., Owerdieck C., Ahnert M., Simon and Maurer M.: A guideline for simulation studies of wastewater treatment plants. Wat. Sci. Tech., 50 (7), 131–138, 2004.
[13] Swinarski M., Mąkinia J., Stensel H. D., Czerwionka K., Drewnowski J.: Modeling External Carbon Addition in Combined N–P Activated Sludge Systems with an Extension of the IWA Activated Sludge Models. Proc. the WEF Specialty Conference "Nutrient Recovery and Management 2011", Miami, Florida, January, 9–12, 2011, Water Environment Federation: Alexandria, Virginia, USA.
[14] Mąkinia J., Pagilla K., Czerwionka K., Stensel H. D.: Modeling Organic Nitrogen Conversions in Activated Sludge Bioreactors. Water. Sci. Technol. (2011); 63(7): 1418–26, 2010.

WYDAWNICTWO POLITECHNIKI GDAŃSKIEJ

Wydanie I. Ark. wyd. 14,8, ark. druku 14,75, 103/666

Druk i oprawa: *EXPOL* P. Rybiński, J. Dąbek, Sp. Jawna
ul. Brzeska 4, 87-800 Włocławek, tel. 54 232 37 23

ECOHYDROLOGICAL METHODS IN WATER MANAGEMENT

Editors:
Jerzy M. Sawicki
Wojciech Szpakowski

Gdańsk 2011

PRZEWODNICZĄCY KOMITETU REDAKCYJNEGO
WYDAWNICTWA POLITECHNIKI GDAŃSKIEJ
Romuald Szymkiewicz

REDAKTOR PUBLIKACJI NAUKOWYCH
Janusz T. Cieśliński

RECENZENCI
Artur Magnuszewski
Michał Szydłowski

PROJEKT OKŁADKI
Miriam Artichowicz

Wydano za zgodą
Rektora Politechniki Gdańskiej

Oferta wydawnicza Politechniki Gdańskiej jest dostępna pod adresem
http://www.pg.gda.pl/WydawnictwoPG

ISBN 978–83–7348–376–7

CONTENTS

1 Climatic Influence on Surface Water Resources in the Republic of Macedonia

Donevska Katerina (University Sts Cyril and Methodius, Faculty of Civil Engineering in Skopje, Republic of Macedonia), Gorsevski Peter (School of Earth, Environment and Society, Bowling Green State University, Bowling Green, OH, USA)

1.1. INTRODUCTION

Spatial and temporal variability of precipitation and temperature requires the use of many tools to estimate their mean values in time and space. Both variables are important in many natural resources and water resources studies, in predicting extreme events like droughts and floods, hydrological modeling, etc. However, the network of measuring stations is often not sufficiently dense for adequate presentation of their spatial distribution. For example, there are many difficulties associated with the measurement of the precipitation in mountainous areas. Therefore, for such data poor areas, precipitation data should be estimated using measured data from the existing weather stations. Also, precipitation and temperature data are not measured in all points of a territory, but only in measurement stations. Consequently, many interpolation methods are used to transform point data into a continuous grid of information. Among them, kriging is a sophisticated geostatistical method often used for spatial interpolation of data. Many authors have described different kriging methods [1] and applied them into a meteorological data analyses [3]. The first part of the paper involves simple linear regressions and spatial interpolation kriging methods for modeling of the monthly temperature and precipitation data for the whole territory of the country. Spatial distribution of temperature and precipitation is used for defining the water resources vulnerability.

The second part of the paper studies the variability of the surface water resources throughout the country. Macedonia's total water resources per year are: 18.8×10^9 m^3 from rainfall (with a 733 mm average rainfall); 6.36×10^9 m^3 run-off from the river basin areas; 0.52×10^9 m^3 groundwater; and 0.42×10^9 m^3 from the largest springs. The annual water resources per capita are about 3.150 m^3 y^{-1}, which categorize the country in the middle category of the European countries upon the available water resources per capita. The surface waters depend mainly on the appearance, intensity and duration of precipitation. Due to the morphological, hydro-geographical and hydro-geological structure of the terrain for the major part of the country (with the exception of the karst areas), the storage is limited.

Total water demands including: population, tourists, irrigation, industry, fisheries and minimum accepted flows are estimated on $2.227.891.1 \times 10^3$ m^3 y^{-1} in nowadays. The major user of the water is the irrigation which consumes about 40% of the total water demands in the country. Industry consumes 12% and water supply of population about 10% of the country's total water demands [6].

The aim of the paper is to analyze the climatic impact on surface water resources and to define the regions that are mostly influenced by the climate variations. Basic data about water resources, analyses of the climate data and data about surface water quantity for

twelve hydrological stations located on the three major river basins are used to identify the most vulnerable regions.

1.2. MATERIALS AND METHODS

The data set used in the analysis in the first part of the paper is consisted of two recorded variables: temperature and precipitation. Data for average temperature are used from 32 temperature stations recorded between 1961 and 1990. The precipitation data are the averages of monthly precipitation recorded at 160 precipitation stations for the same time period as the temperature series. Spatial distribution of the control points (measurement stations) covers the whole territory of the country. Simple regression analyses were carried out to quantify the relationship between monthly temperature variation and elevation, while universal kriging method is used for spatial distribution of precipitation. The calculations are carried out by ARC GIS –ESRI software. Analyses of the climatic influence on water resources can be considered as an extension of the former research activities performed within the Macedonia's First National Communication under the United Nations Framework Convention on Climate Change (2003). Further research activities are performed for the Second National Communication on Climate Change [5]. Some of them are presented within the second part of the paper. Analyses of the climatic influence on the water resources quantity has been carried out for the whole territory of the country, represented by twelve hydrological stations located on the three major river basins (Vardar, Crn Drim, Strumica) and sub-basins (Figure 1). The main criteria for selection of the hydrological stations were the station location, i.e. stations were selected where the anthropogenic impact on the discharge is minimal and presence of meteorological station (records about climate and meteorological data) in the nearby vicinity.

Hydrological Stations:

1. Radusa – Vardar
2. Skopje – Vardar
3. Demir Kapija – Vardar
4. Mak. Brod – Treska
5. Katlanovska b. – Pcinja
6. Oci Pale – Bregalnica
7. Stip – Bregalnica
8. Dolenci – Crna Reka
9. Skocivir – Crna Reka
10. Susevo – Strumica
11. Novo Selo Strumica
12. Boskov Most – Radika

Fig. 1. Hydrological stations

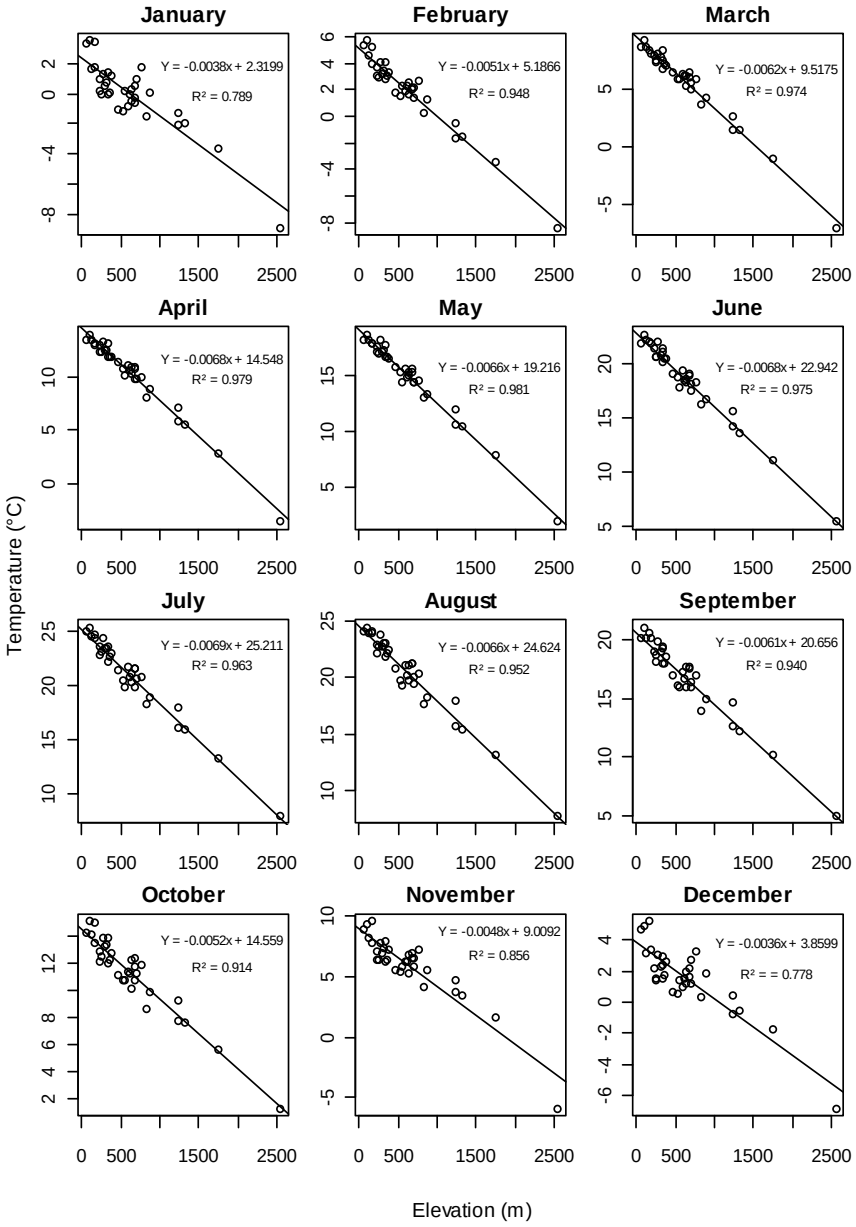

Fig. 2. Correlation between average temperatures (°C) obtained from 32 weather station for the period 1961 – 1990 versus elevation

The analyses of climatic influence on water resources are based on historical data of annual values of the minimal annual, maximum annual and average annual discharges for the period 1961–2003, as well as the average monthly values. Assessment of the influence of the climate factors on the available water resources in the Republic of Macedonia is done

applying standard methodology used in stochastic hydrology [7, 8]. The applied methodology for vulnerability assessment of water resources is consisted of analysis of data variability of the historical series and trend lines, analysis of homogeneity, independence of subsequent members and autocorrelation graph. The analysis of the homogeneity was carried out to test whether the data are homogeneous or there is a non homogeneity as a result of the climatic influence or human activities. Any forecast for the future based on the historical features of the hydrological variables demands the conclusions to be made upon homogeneous series. Due to this fact, only the series that are considered to be homogeneous are included into the subsequent analyses of climatic influence on water resources and are used in presenting the variations and trend lines of annual discharges till 2003.

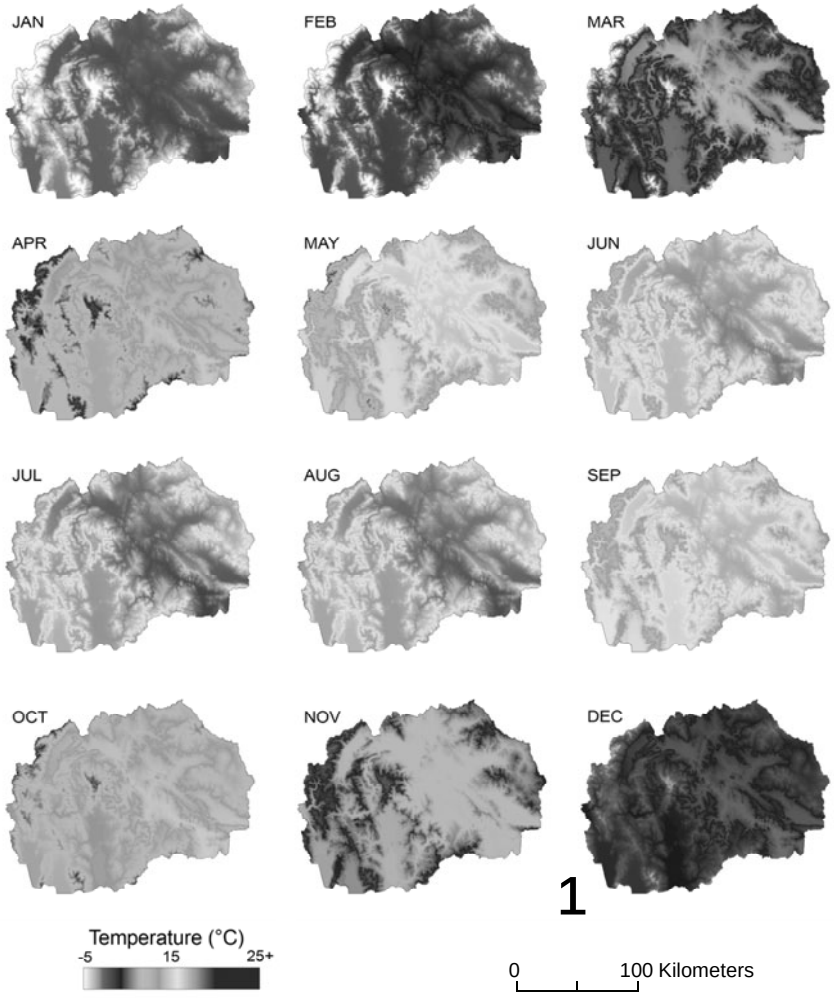

Fig. 3. Modeled monthly temperatures

1.3. RESULTS

The results of the climatic analyses are presented on Figures 2 – 4. Results of the linear correlation analyses of the temperature and elevation for the 32 temperature stations are presented on Figure 2, while Figure 3 presents spatial distribution of average monthly temperatures. Modeled quantities of monthly precipitation are derived by applying spatial interpolation using universal kriging method are shown on Figure 4.

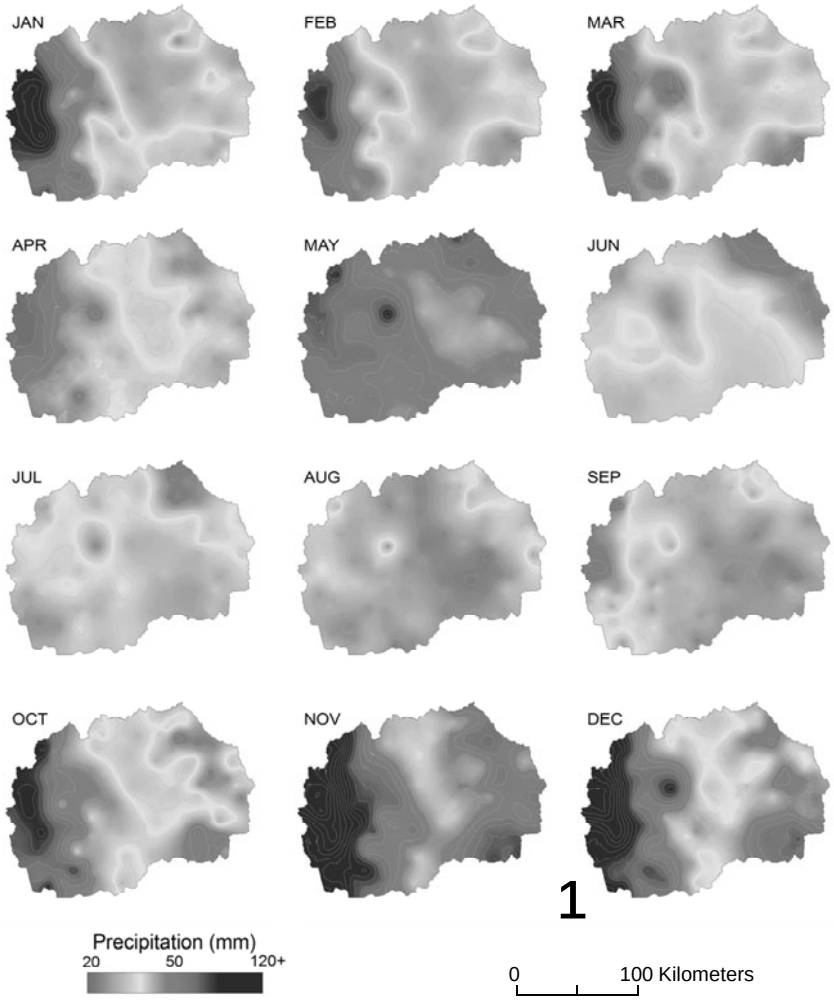

Fig. 4. Modeled monthly precipitation

Some of the results of the second part analyses are presented on Figures 5 – 7 [5].

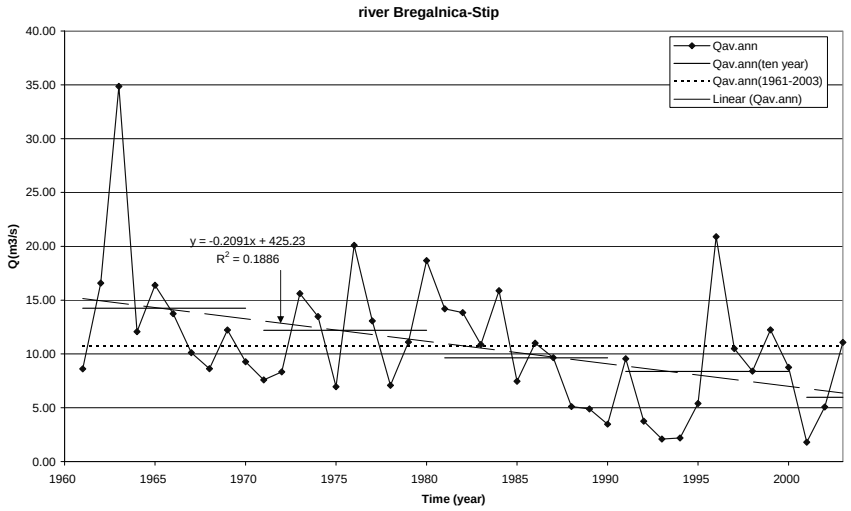

Fig. 5. Annual values of average discharges for the river Bregalnica at Stip

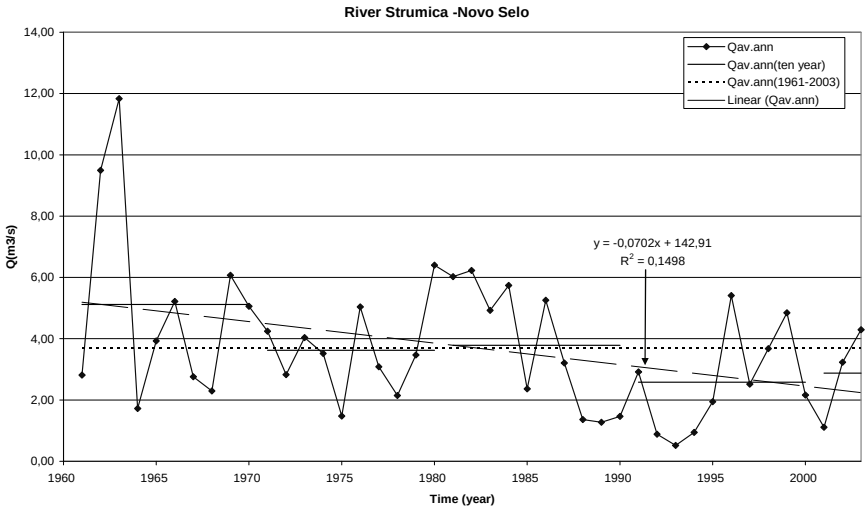

Fig. 6. Annual values of average discharges for the river Strumica at Novo Selo

Regarding surface water resources, analyses of the variations and trend lines of the minimal, average and maximal annual discharges for all river basins in the country are showing that there is a general trend of reduction of all discharges. Also, the results are indicating that the reduction of the average annual discharges is mostly expressed for the region with moderate-continental-sub-Mediterranean climate, i.e. for the river Bregalnica at hydrological station Stip and for the river Strumica at hydrological station Novo Selo. Therefore, only these results are being presented in the paper.

For the river Bregalnica at hydrological station Oci Pale, the series of average annual discharges is characterized with descending linear trend. Maximal value of decade discharge is recorded for the decade 1961–1970, and minimal for the decade 1981–1990. Reduction of the decade discharges for the period 2000–2003 compared with the decade discharges for the period 1961–1970 is 36%. More severe reduction of the average annual discharges is noticed at downstream hydrological station Stip (Fig. 5) in the central part of the country. The reduction ratio for the period 2000–2003, compared with the decade 1961–1970 is 58%.

For river Strumica at hydrological station Susevo, the series of the minimal annual discharges are showing that the river has very low water discharges or even there is no water at all during summer period. At the downstream hydrological station Novo Selo (south eastern part of the country), for the series of average annual discharges (Fig. 6) percentage of reduction of the discharges for the period 2000–2003 compared with the decade 1961–1970 is 43.7%.

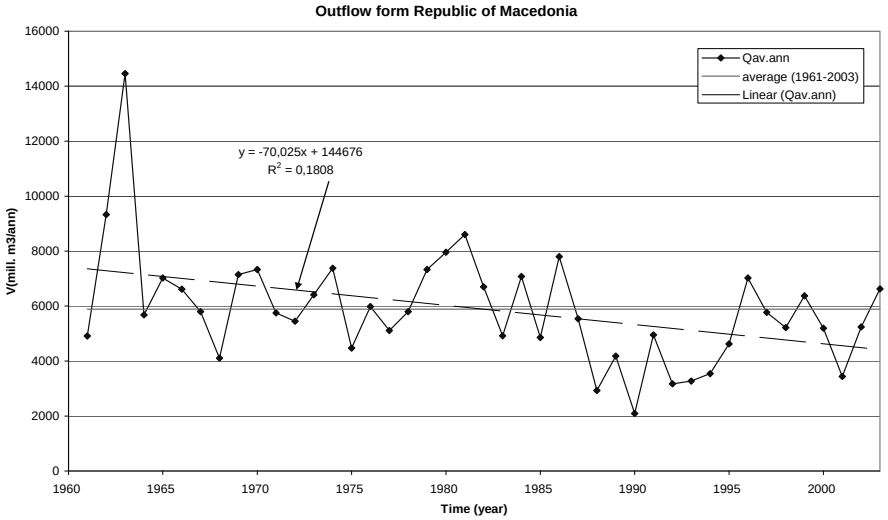

Fig. 7. Annual outflow from the Republic of Macedonia (x 10^6 m^3)

Climate influence on water resources has been considered also through analyses of variations of the water quantities which outflow from Macedonia. The linear descending trend of the water quantities which outflow from the country, with a drop of around 70 x 10^6 m^3 on annual level is presented on Figure 7. Minimal values of outflow water quantities are recorded for the period 1987–1995, and after 2001, there is a light increase of the water quantities. The variation of the outflow water quantities has been compared to the precipitations variability. A decrease of precipitation during last twenty years compared with the period 1961–90 at annual level is recorded, especially in 1988–1990, 1992–1994, 2000 and 2001 [5]. On the contrary, average annual temperature during last ten years is continuously higher than the long-range average. Data about consumed water for industry are showing that the consumption has decreased after 1996 [6]. Also permanent decrease of the presently irrigated areas has been recorded after 1992 indicating decrease of the major water use in the country, i.e. water for irrigation [2]. Consequently, reduction of the water quantities

which outflow from the country is not only due to increased use of the water resources (anthropogenic impact), but primarily due to the changed climate conditions.

1.4. CONCLUSIONS

This paper considers the climatic impact on surface water resources in the Republic of Macedonia. Analyzes of the climate parameters for the territory of the country presents the first phase of the analyses, that includes simple linear regressions and spatial interpolation kriging methods. Climate elements as air temperature and precipitations are analyzed and spatially interpolated to create maps of monthly precipitation and temperature. Spatial distribution of modeled monthly precipitation and temperature is presented.

Further analyses include analyses of surface water resources presented by variations and trend lines of the minimal, average and maximal annual discharges for all river basins in the country. The homogeneity analyses of the series is tested, indicating that the sample size is not large. However, the results are providing good directions for accepting or rejecting the null hypothesis for homogeneity of the data, and therefore making statement that there are or there are no significant modifications in examined samples during the analysed period. In the cases of homogeneous series, it can be stated that there are no significant modifications of the mean values and of the variances during the time and that all data belong to the same population. Variations and trend lines of these series are subsequently analysed.

The analysis of the minimal, maximal and average annual discharge indicates continuous reduction in annual amounts of discharge for all river basins in the country. The reduction of the average annual discharge is the most expressed in the central and south-eastern part of the country, i.e., in the region with highest temperatures and lowest precipitation. These areas are presented with moderate-continental-sub-Mediterranean climate.

Analyses of variations of the water quantities which outflow from Macedonia are characterized with linear descending trend. Analyses of the series of: water quantities which outflow from the country, precipitation and also water consumption variation indicate that the reduction of the water quantities which outflow from the country is influenced mainly by the climate variation.

References

[1] Chang K. T.: Introduction to Geographic Information Systems, fourth ed. New York: McGraw-Hill 2008.
[2] Donevska K.: Report on Second Communication on Climate and Climate Changes and Adaptation in the Republic of Macedonia, Section: Vulnerability Assessment and Adaptation for Water Resources Sector, (Ministry of Environment and Physical Planning/ UNDP) 2006.
[3] Hunter R. D., Meentemeyer Ross K.: Climatologically Aided Mapping of Daily Precipitation and Temperature, Journal of Applied Meteorology, Vol. 44, 1501–1510, 2005.
[4] Ministry of Environment and Physical Planning of the Republic of Macedonia/ UNDP, 2003, Macedonia's First National Communication under the United Nations Framework Convention on Climate Change.
[5] Ministry of Environment and Physical Planning of the Republic of Macedonia, 2008, Second National Communication on Climate Change.
[6] NEAP 2 – DPSIR Report on Water 2004.
[7] Popovska C., Gesovska V., Donevska K.: Hydrology, Faculty of Civil Engineering, Skopje.
[8] Yevjevic, V.: Stochastic Processes in Hydrology, Fort Collins, Colorado 2004.

Acknowledgments

The first author gratefully acknowledges the support from the Fulbright Program for providing the opportunity to perform the climate data research in the USA. Gratitude is extended to the host institution, the Bowling Green State University, School of Earth, Environment and Society where the research was performed.

2 Flood Risk Analysis Methods Used in the Czech Republic

Aleš Dráb, Jaromír Říha (Brno University of Technology, Faculty of Civil Engineering Water Structures Institute)

2.1. INTRODUCTION

The flood risk analysis methods are currently used in the flood management procedures worldwide. Directive 2007/60/EC [1] commonly known as Flood Risk Directive (FRD) signifies that flood risk analysis methods are gaining ground in EC Member States and thus also in the Czech Republic. Procedures of flood risk analysis have been developed in the Czech Republic since the catastrophic floods of 1997 in line with worldwide trends and have been tested and applied in hundreds of case studies to date. Currently, the Directive 2007/60/EC [1] commonly known as Flood Risk Directive (FRD) Guideline based on past experience with flood risk analysis applications is being processed.

In the text flood risk analysis procedures and specially developed techniques for the assembly of flood hazard, danger and flood risk maps are presented, methods related to flood risk management plans are mentioned as well. The particular problems like an application and extension of the "danger matrix" approach, the definition of residual danger, the formulation of efficiency criteria and preliminary multi-criteria flood risk assessment are also discussed. Present experience provides evidence that the flood risk analysis methods used in the Czech Republic (CR) are in harm with the requirements of the FRD. The proposed and applied methods are based primarily on existing available data such as flood extent maps, cadastral maps and data provided by the Czech Statistical Institute.

The objectives of the paper are also to introduce the philosophy of FRD implementation in the Czech Republic and to present the way in which the general requirements have been met. More information is given about the preliminary flood risk assessment method, flood hazard and risk map compilation for the given set of flood return periods, and also about the development of flood risk management plans using economic efficiency criteria and multi-criteria assessment techniques. The procedures are demonstrated in a case study within the municipal area at the city of Moravské Budějovice.

2.2. THE DIRECTIVE 2007/60/EC (FRD)

The Directive 2007/60/EC [1] is calling for the development of effective tools for appointing priorities for the taking of technical, financial and political decisions in flood risk management. The FRD requires three stages of flood risk management:

— Preliminary flood risk assessment.
— Creation of flood hazard and risk maps for various scenarios.
— Development of flood risk management plans.

The FRD only defines general requirements for these three stages. Member states themselves decide the appropriate methods needed for its implementation as geographical, hydrological and social differences demand specific approaches. Therefore, the working group on floods (WGF) was established in 2007 primarily to support the implementation of the Flood Risk Directive. The WGF provides a platform for information exchange through a series of thematic workshops addressing particular issues of the Flood Risk Directive to help member states with the implementation process.

The terminology of flood risk analysis is still not uniform worldwide and also not within Europe. In this paper, terminology according to [1] and [2] has been used. The authors of this text follow the concepts of hazard, exposure and vulnerability as components of flood risk. However, a few additional terms have been introduced and defined, namely in the context of the matrix for the "danger" classification [3, 4]. At this context *danger* is understood as a convolution of hazard and exposure and is expressed by means of danger maps.

In the paper we focus on the process of implementing the FRD in the Czech Republic. It is essential that the flood risk assessment methods in the Czech Republic are founded on existing and well-established data and procedures. This prerequisite principle has resulted in the necessity of modifying and adapting existing techniques, e.g. the "danger matrix" approach, to define residual danger and to formulate efficiency criteria.

2.2.1. Preliminary flood risk assessment

The aim of preliminary flood risk assessment is the definition of areas where more detailed risk-based methods should be applied. Logically it was proposed, that the initial basis for preliminary flood risk assessment would be existing documentation, namely flood extent maps. These contain flood scenarios corresponding to return periods of 5. 20 and 100 years, extreme historical flood extents and the extents of dam break floods are displayed on the maps as well. In some cases, so-called "active zones" are demarcated in the existing floodplain documentation according to [5]. These sub-areas in the floodplain represent zones with high hazard and extensive flood damage potential (high flow velocity, water depth, etc.). These documents provide a starting point for preliminary risk assessment in the area of interest and for the demarcation of watercourses in the Czech Republic with potential significant flood risk. The following aspects have been considered:

— The number of residents in the floodplain area.
— The property in the urbanised areas.
— Pollution sources.
— Transport infrastructure.

The necessary data were taken from the Register of Census Districts and Structures and ZABAGED [6]. By combining the aforementioned aspects using GIS techniques it was possible to preliminarily estimate the endangered property and the number of affected inhabitants in existing areas with the potential for flooding [7]. The procedure resulted in the identification of 2 494 km of watercourses in the Czech Republic (CR) which have high flood risk potential and for which more detailed evaluation is proposed (Fig. 1).

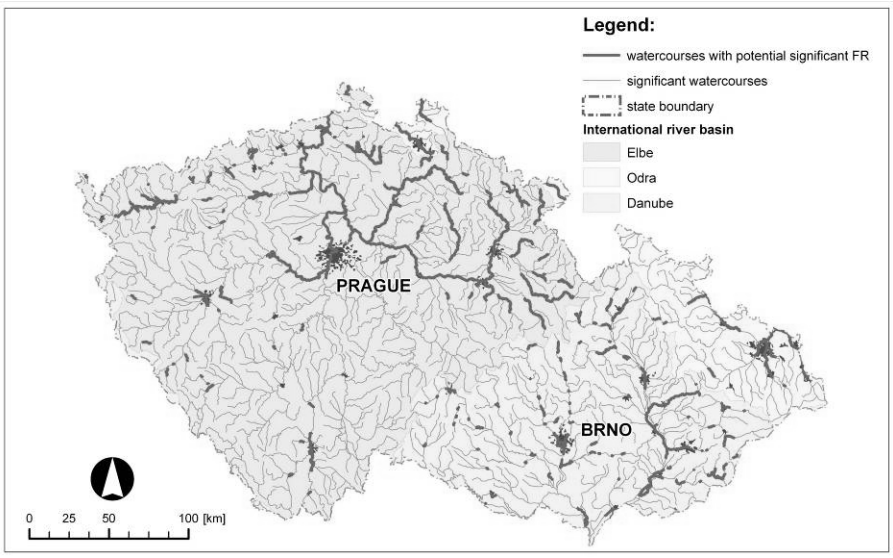

Fig. 1. Selected watercourses in the CR with high flood risk potential [7]

2.2.2. Flood Hazard Maps and Flood Risk Mmaps

The second stage in the FRD implementation is the creation of flood hazard and risk maps. For the construction of the danger and risk maps a semi-quantitative method has been proposed based on a matrix for the determination of the danger level [3]. The procedure originates from [4], which was adapted for the conditions in the Czech Republic. In the context of the matrix approach the concept "flood danger" – exposure to hazard – has been adopted using the following steps:

— The quantification of flood hazard via hydraulic calculations and the evaluation of flood intensity *IP* [4].
— Determination of exposure to flood hazard using the "danger matrix" [3].
— The construction of flood risk maps by combining flood danger with the vulnerability of the area.

At the first step the flood hazard is expressed in terms of flood intensity *IP* which is a measure of the destructive ability of a flood and is defined as a function of water depth *h* and velocity *v* as follows [4]:

$$IP(h,v)=\begin{Bmatrix} 0, & h=0 \\ h, & h>0\,\text{m},\ v\le 1\,\text{m/s} \\ h,v, & v>1\,\text{m/s} \end{Bmatrix} \tag{1}$$

The flood hazard maps have to be developed using existing flood extent maps based on previously performed hydraulic calculations. The majority of older studies used a 1D hydraulic model; only a few were performed with the use of 2D simulations. The crucial problems with the use of existing flood extent maps are as follows:

— Existing flood extent maps have been prepared for flood scenarios corresponding with return periods of 5, 20 and 100 years as required by current Czech legislation [8] and do not include the scenario defined by [1] for floods with a low probability or extreme event scenarios. In the CR this scenario is defined as the Q_{500} discharge, for which further hydraulic calculations are required.
— Flood extent maps do not generally contain information on water depth, which has to be subsequently evaluated using GIS tools. Usually, the information about flow velocity is not adequate or is completely missing.

Solving the above-mentioned problems is easier in cases where an updated hydrodynamic model is available. This allows the additional calculation of the Q_{500} scenario, and also the completion of missing data on water depths and velocities. For more significant watercourses in the CR hydrodynamic models maintained by river authorities are available. Based on the calculated flood intensity *IP* from Eq. (1) the flood danger is evaluated using the so-called "danger matrix". Recommendations according to Table 1 are taken into account during the determination of such derived hazard values. In the Czech Republic the method described is applied for the relevant flood scenarios: Q_5, Q_{20}, Q_{100}, Q_{500}. The resulting danger level is assumed to be the maximum danger level obtained in individual flood scenarios according to Eq. (4).

Table 1

Danger classification and verbal description consistent with [3, 4]

Danger *R* - Eq. (2)	Danger level	Recommendation
$R \geq 0.1$ *or* $IP \geq 3$	(4) High (red)	Do not permit new built up areas. It is necessary to put forward designs for flood protection measures for existing buildings.
$0.01 < R \leq 0.1$	(3) Medium (blue)	New construction is possible with restrictions. The location of sensitive structures such as hospitals, fire departments, etc. is unsuitable.
$R < 0.01$	(2) Low (orange)	Construction is possible but land parcel owners must be warned of the potential flood hazard. It is necessary to employ special flood measures for sensitive buildings.
$p < 0.0033$ ($N > 300$)	(1) Residual (yellow)	Questions associated with flooding should be solved by means of urban planning, taking into account sensitive structures.

The corresponding maps then express the flood danger across the whole floodplain regardless of the land use.

The flood danger R_i for a flood scenario i with the exceedance probability p_i and a return period of N_i years is obtained from the following formula [9]:

$$R_i = (0.3 + 1.35 \cdot IP_i) \cdot p_i \tag{2}$$

where the exceedance probability p of flood scenario i can be expressed as follows:

$$p_i = 1 - e^{1/N_i/} \approx \frac{1}{N_i} \tag{3}$$

The resulting danger R is expressed as the maximum value of the individual dangers R_i corresponding to flood scenarios represented by the return period N_i:

$$R = \max_{i=1}^{n} R_i \tag{4}$$

where n is number of assessed flood scenarios. The obtained flood danger values R are classified according to Table 1. The specific problem was the definition and delimitation of sub-regions corresponding to "residual danger". The extent of real past extreme floods with high return periods (e.g. $N > 300$) was the basis for the estimation of the residual danger area. Furthermore, the extent of alluvial loams in the area and the surface inundated by a potential dam break flood were also taken into account. The outer envelope of the flood extents mentioned above was defined as the "residual danger" zone in danger maps.

The results of the described analysis in the area of interest are maps of flood danger (Fig. 3). The categorisation of danger enables the assessment of the suitability of existing or planned land use and the recommendation of restrictions on activities or on the development of corresponding areas with higher danger rates (Tab. 2). The method described can be used in the process of urban planning, during the preliminary proposals for flood protection measures, etc. Risk maps combine data about danger and vulnerability in the exposed area. The vulnerability data can be derived from urban plans and maps, and should be verified by site investigation. Based on the available urban plans, it is possible to define classes of land use (Table 2 – column ''Land use'').

Table 2

An example of selected land use zones

Land use	Acceptable risk
Residential	(2) Low
Public services	
Transportation and utility	
Industrial and manufacturing	
Agriculture	
Sport and recreation	(3) Medium
Water area	(4) High
Parks and open spaces, gardens, woods	
Arable land, meadows, pasture land	

A value of maximum acceptable risk is assigned to each class according to Table 2 - column "Acceptable risk". The maps of the areas thus classified according to land use (vulnerability maps) are ''overlaid'' by danger maps and are processed by GIS analytical tools into risk maps in which existing or anticipated areas with exceeded acceptable risk are highlighted using a spectrum corresponding to Table 1. The following logical step is a more detailed analysis of ''risky areas'' from the point of view of risk management and risk attenuation to an acceptable level. The described method using tailor-made software tools for GIS applications has been elaborated, tested and applied in the CR since the year 2001 at about 25 municipalities which contain more than 400 km of watercourses.

2.2.3. Flood Risk Management Plans

The FRD requires that Member States shall establish flood risk management plans on the basis of hazard and risk maps. Flood risk management plans are primarily focused on prevention, protection and preparedness. During the development of flood risk management plans, existing hydraulic and feasibility studies are used as basic documents. To date, the following risk-based methods have been implemented in the CR in the studies mentioned:

— The matrix for danger level determination [3, 4] is being used for the assessment of floodplains from the viewpoint of flood hazard, vulnerability and risk. The method enables the general identification of areas and structures where the acceptable risk has been exceeded.
— The method based on flood loss estimates described below serves for an assessment of the economic efficiency of structural FPMs. For the estimation of flood losses the available geographical data and data from the Census District and Building Register are employed.

In accordance with the requirements of the FRD, the processing of flood risk management plans stems from the results of spatial analysis using the matrix method (Sect. 2.2) in which recommendations for further analysis and flood protection in areas with exceeded acceptable risk are introduced. For the complex assessment of FPM variants according to [1], economic, environmental and social viewpoints are taken into account. For this purpose, multi-criteria analysis is frequently used. At present the evaluation of the economic effectiveness of FPMs is elaborated in detail while the risk-based analysis related to other loss categories is still subject to research activities. In the case of the evaluation of the economic effectiveness of FPMs, the following steps are followed:

— estimate of the extent of endangered property in the floodplain,
— estimation of material flood losses and quantification of economic risk,
— determination of quantitative economic criteria using cost benefit analysis.

The endangered property in the floodplain is estimated for the existing state and for the state after the implementation of flood protection measures. Firstly, the processing of flood hazards is carried out for flood scenarios corresponding with at least the Q_5, Q_{20} and Q_{100} discharges.

The estimate of flood damage to property in the floodplain is performed using so-called damage functions which express the relation between water depth and the percentage of damage. The damage functions were developed and tested for the floods in the years 1997, 1998 and 2002 for residential buildings, service buildings, industrial buildings, roads, railways, bridges, paved areas, infrastructure, sport and recreation areas, farmland, forest land. For these elements the economic value of assets was estimated based on official census data. Material flood losses in monetary units are obtained by multiplying the economic value of assets and the corresponding percentage of damage. The total potential economic flood loss D for a given flood scenario with exceedance probability p is calculated by summarizing the losses across all elements in the analysed flooded area. Based on the potential flood losses D the economic flood risk is expressed as follows:

$$RI = \int_0^{p_H} D(p)\,\mathrm{d}p \tag{5}$$

where RI is the annual economic flood risk in monetary units, p is the exceedance probability of the corresponding peak flood discharge determined by Eq. (3), $D(p)$ is the dependence

of potential losses on flood exceedance probability p and p_H is the exceedance probability of harmless discharge corresponding to the flood protection level in the area. The dependence (5) is derived from the potential losses estimated for individual flood scenarios (Fig. 2).

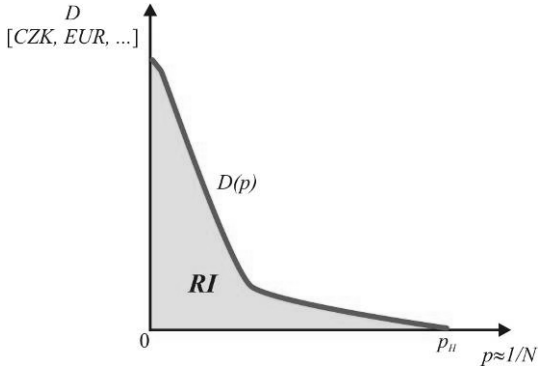

Fig. 2. Schematic interpretation of a flood loss exceedance curve $D(p)$

A practical procedure for the average annual economic risk estimate is as follows:

— The exceedance probability for individual flood scenarios represented by selected N-year flood discharges is estimated using Eq. (3).
— The hydraulic characteristics of the flood, namely water depth, are determined by hydraulic modelling (1D, 2D).
— The direct economic losses in the area of interest are derived using the damage curves and water depth for selected flood scenarios. A graphical interpretation of the obtained function $D(p)$ can be seen in Fig. 2.
— Eq. (5) is figured out by the numerical integration. It gives an estimate of the annual average risk.

The method described was implemented into GIS using a tailor-made application eliminating the routine manual re-running of individual procedures.
The final value of RI serves for the evaluation of the economic efficiency of proposed variants of structural flood protection measures. Primarily the relative efficiency RE was used for the cost – benefit analysis [10]:

$$RE = \frac{RI_{ORIG} - RI_{NEW}}{I \cdot DR} \tag{6}$$

where RI_{ORIG} and RI_{NEW} are average annual economic risks before and after the application of flood protection measures, I is the investment cost and DR is the discount rate. The flood protection arrangements are profitable if $RE > 1$.

The method described has been widely applied in the assessment of hundreds of anticipated flood protection measures in the CR financed from the funds of the European Investment Bank. During this assessment the economic risk was the only criterion.

According to [1], the flood protection measures and their sub-sections related to individual areas should be prioritised using multi-criteria analysis during which other important partial risks are taken into account. For the flood risk management plans in the Czech Republic the partial risks RI_i are related to the following loss categories:

— RI_1 – annual average loss – economic risk (see Eq. (5)) (CZK/yr.).
— RI_2 – annual average affected population (inhabitants/yr.).
— RI_3 – annual average number of affected sensitive buildings (buildings/yr.).
— RI_4 – annual average affected area with historical monuments (m^2/yr.).
— RI_5 – annual average number of affected potential pollution sources (sources/yr.).

Quantification of partial risk RI_i can be performed using the modified Eq. (5):

$$RI_i = \int_0^{p_H} D_i(p)\, dp \tag{7}$$

where RI_i is the risk for loss category i and $D_i(p)$ represents the functional dependence of corresponding potential loss on flood exceedance probability p.
The final assessment is usually done using multicriterial analysis. A more detailed description of these methods is outside the scope of this paper [11, 12].

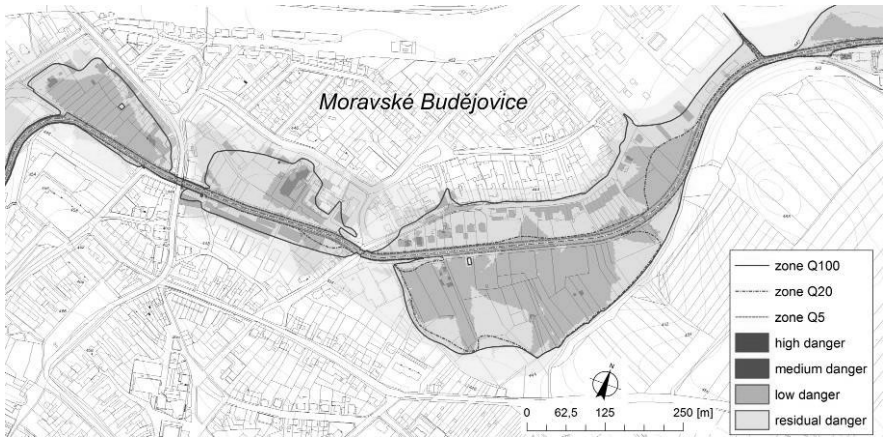

Fig. 3. Example of a flood danger map for Moravské Budějovice (original scale 1 : 5 000)

2.3. CASE STUDY

The procedures mentioned above were applied in numerous localities in the CR like cities of Brno, Šumperk, Litoměřice, Děčín, Moravské Budějovice etc. In this section an example from the city of Moravské Budějovice is shown.
The study comprises an assessment of the Rokytka river with total length of about 4,5 km within the area of the city, which has a population of over 7 700 inhabitants. Part of the solution was the proposal of structural flood protection measures based on danger and risk maps (Fig. 3 and Fig. 4).

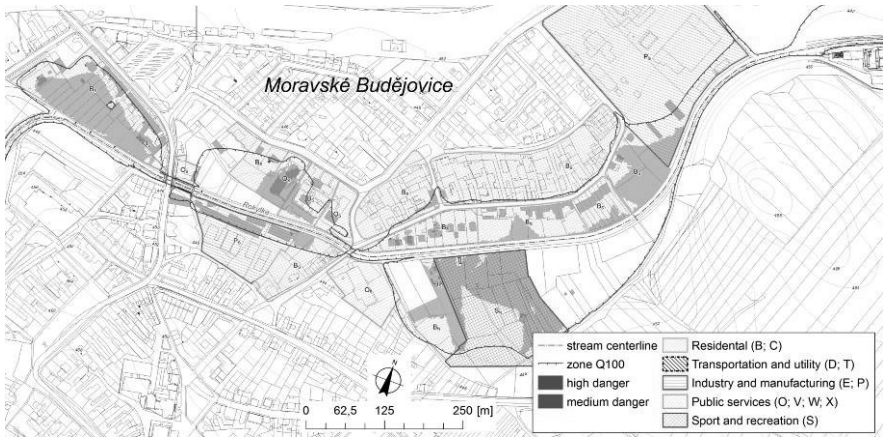

Fig. 4. Example of a flood risk map for Moravské Budějovice – areas with exceeded acceptable risk (original scale 1 : 5 000)

The conceptual proposal for structural flood protection measures was implemented for the areas with exceeded levels of acceptable risk. To establish priorities for the realization of flood protection measures the efficiency indicator defined by equation (6) was calculated. At this point, the aim was to assess partial risks in the sub-sections in terms of potential material losses. At sub-sections for which $RE < 1$ the flood protection measures were rejected as uneconomical. For those sub-sections with $RE \geq 1$ a descending sequence according to the value of RE was elaborated.

2.4. DISCUSSION AND CONCLUSIONS

In this paper the flood risk techniques corresponding to [1] are discussed in the context of implementing the FRD in the CR. The procedures used for the development of flood hazard and flood risk maps are described together with the development of danger and vulnerability maps or residual risk assessment. The assessment of economic efficiency should be a necessary part of flood risk management plans.

The present methods of flood risk analysis in the CR are generally in accordance with the FRD. From this viewpoint the Czech Republic is well prepared for the implementation of the FRD and long-term experience from numerous practical applications has been integrated into the National Guidelines to the FRD.

However further research into flood risk analysis needs to be carried out to improve and refine individual techniques and outputs. It should be focused on the topics like more detailed multi-criteria flood risk assessment, non-structural flood protection measures and the evaluation of their effectiveness and efficiency, inclusion of risks from the exposure of inhabitants to flood hazards, assessment of environmental risks, assessment of risks due to the flooding of sensitive facilities and historical monuments, estimation of indirect losses, more comprehensive uncertainty analysis in risk management.

The process culminates in the design and construction of risk attenuation measures. At present, quantitative risk analysis methods are dominantly based on the assessment of direct

economic losses; the other aspects, such as human, social and environmental losses, are not taken into account in the Czech Republic.

References

[1] ES.: Directive 2007/60/EC of the European Parliament and of the Council of 23 October 2007 on the assessment and management of flood risks, 2007.

[2] Gouldby, B. and Samuels, P.: Language of Risk. Report T32-04-01. FLOODsite Consortium, 2005.

[3] Zimmerman, M., Pozzi, A. and Stoessel, F.: Vademecum – Hazard Maps and Related Instruments, The Swiss System and its Application Abroad, PLANAT, Bern, Switzerland, 2005.

[4] FOWM.: Empfehlungen: Berücksichtigung der Hochwassergefahren bei raumwirksamen Tätigkeiten. EDMZ, CH-3000. Federal Office for Water Management, Bern, 1997.

[5] Act No. 254/2001 Sb. (Water Act).

[6] COSMC.: Fundamental basis of geographical data (ZABAGED). Czech office for surveying, mapping and cadastre. Prague. 2009.

[7] Drbal, K. and Stepankova, P.: Preliminary Flood Risk Assessment in the Czech Republic. In Das Magdeburger Gewässerschutzseminar 2008. Magdeburg. pp. 97–99, 2008.

[8] Decree No. 236/2002 Sb. regarding methods of floodplain documentation processing. 2002.

[9] Beffa, C.: A Statistical Approach for Spatial Analysis of Flood Prone Areas. International Symposium on Flood Defence, Kassel, Germany, 2000.

[10] Riha, J. et al.: Flood risk analysis. Monographs of the Water Structures Institute, FCE Brno University of Technology, Issue 7, CERM, 2005, 286 p., ISBN 80-7204-404-4, 2005.

[11] Brans, J.P. and Mareschal, B.: PROMETHEE methods. In: Figueira, J., Greco, S., and Ehrgott, M., (Eds.), Multiple Criteria Decision Analysis: State of the Art Surveys, Springer, New York, 2005, ISBN 0-387-23067 –X, pp. 163–195, 2005.

[12] Meyer, V. et al.: GIS-based Multicriteria Analysis as Decision Support in Flood Risk Management. Report T10-07-06. FLOODsite Consortium, 2007.

Acknowledgements

The paper contains results from the research project CEframe (Central European Flood Risk Assessment and Management in Centrope) implemented through the CENTRAL EUROPE programme co-financed by the European Regional Development Fund (ERDF) and from the project of Specific Research at Brno University of Technology No. FAST-S-11-64/1415 “Assessment of uncertainties in flood risk analysis”.

3 Estimation of Rainfall Parameter Values Within Sediment Production Model Rusle in Istria

Danko Holjević (Croatian Waters, Zagreb, Croatia), Josip Petraš (Faculty of Civil Engineering, Zagreb, Croatia), Danko Biondić (Croatian Waters, Zagreb, Croatia)

3.1. INTRODUCTION

Water impact on soil initiates erosion process, which influences many human activities and facilities built and used by people in everyday life. Erosion processes, i.e. sediment production and sediment transfer, significantly impact the state of vegetation cover of our planet, water regime of watercourses within catchment areas, potential and future use of agricultural surfaces, stability, functionality and duration of hydrotechnical structures and other infrastructure facilities (roads, bridges, etc.). The problem of qualitative and quantitative forecasting of soil erosion and sediment transfer in engineering practice is mostly solved by empirical methods for parameter estimation, which are based on the results of systematic long-term investigations and field measurements. In such and similar methods, physical factors of erosion and sediment transfer are represented by different parameters, and the selected values of these parameters directly reflect on the results of estimated sediment transfer. For selection of parameter values which are prominent in these methods, method authors recommend certain evaluation systems, mostly in the form of evaluation tables, where recommended parameter values are determined in investigations based on measurements of production and transfer of eroded sediment in precisely determined climate, topographic, hydrographic, geological, biological and other conditions. Therefore, to apply any formula for the value of an individual parameter within a selected method in conditions which always to some extent differ from conditions for which the formula was created, it is important to have the possibility to compare the results obtained by application of selected formula with the results obtained by measurements in specific natural conditions in pilot catchment areas. This gives us the possibility to calibrate the recommended parameter evaluation system of a selected method for the area in which investigations are conducted, or other areas with identical or similar conditions.

3.2. INVESTIGATION AREA ABRAMI

In the procedure of determining erosion parameters, we frequently use the results of long-term field investigations and measurements. In this way, we achieve reliability of each methodology with given limitations, primarily for individual locations, areas and regions as well as for climate type and rainfall regime. This fact lead to the idea of implementation of complex, long-term field investigations in Istria aimed at establishing a base of measured data related to sediment production as a consequence of erosion caused by rainfall. In the framework of the new research in the investigation area Abrami, investigations were carried out in the duration of 7 years, of which the first 3 years were used for establishment of procedures and methods of measurement first on 6, and since 2005 on 7 typical plots. Fig. 1

gives the overview of an investigation plot (No. 5), which at the time of establishment (1971) was represented by old-growth pine culture. It has a reduced plan view surface of F = 98.57 m^2, with the slope of 30%. The amelioration of this degraded, erosion-affected surface was carried out only by planting pines in pits. The land was without grass cover, and belongs to brown carbonate soils with uncovered C horizon. Afforestation that was carried out with black pine in pits did not have expected results in view of production and increase of wood volume, but contributed to subsiding of erosion. The main characteristics of other investigation plots (soil, surface, slope, type of work and vegetation state) are given in Table 1. In 1961, a meteorological station was established inside the investigation area Abrami, since when uninterrupted measurements have been conducted of precipitation quantity, humidity, evaporation and air temperature. During the establishment of pilot plots for measurements of erosion production in the investigation area Abrami, the methodology of cumulative measurement of water runoff and eroded sediment was adopted for each test plot.

Fig. 1. Investigation plot No. 5

This means that for each rain event the entire inflow of water together with eroded sediment from the plot is collected into relatively large detention basins and/or rain barrels through a steel-plate down pipe placed in a gutter at the base station of each plot. Measurements of inflown water with sediment are carried out in the field through measurements of water levels in detention basins and/or rain barrels and calculations of volume of collected water in relation to measured water levels and dimensions of detention basins and/or rain barrels. The total quantity of eroded sediment in collected water is determined according to the Standard HRN ISO 4365, i.e. after complete settling of sediment in detention basins (rain barrels) clear water is removed, the remaining content is filtered and dried in a laboratory and the total sediment mass determined by weighing. Rain events are registered by ombrograph located within the meteorological station Abrami. In practice, measurements of runoff and quantity of eroded sediment are divided into two phases: immediately after rain at the location in the investigation area and after settling and filtration of the sample in the laboratory. The measured results are entered manually into previously prepared forms and later digitalized by computer entry. This is how the data base was generated, on which basis the procedure of calibration and optimization of parameters was carried out within parameter estima-

tion methods for calculation of eroded sediment. The results of measurements conducted at Abrami for the period 2003 – 2007 are given in Table 2.

Table 1

Basic characteristics of investigation plots (soil, surface, slope, type of work and vegetation state)

Plot	Soil	Plan view surface (m^2)	Slope (%)	Treatment	Vegetation status
1	uncovered flysch	15.08	185	untreated	no plant cover
2	regosol	84.75	62	untreated	slow-growth pine and interrupted plant spacing
3	eutric cambisol	93.25	44	untreated	hop hornbeam and oriental hornbeam underbrush
4	rendzina	102.4	59	dry stone wall crown and planting of black pine	combined stands of black pine
5	eroded eutric cambisol	98.57	30	traditional planting of pines in pits	slow-growth pine culture
6	rendzina	122.7	27	planting of black pine	combined stands of black pine
7	eutric cambisol	93.25	44	hop hornbeam and oriental hornbeam underbrush	predominantly grass covered surface

Table2

Summary overview of measurement results for sediment production in the period 2003 – 2007 in m^3/km^2

Plot	2003	2004	2005	2006	2007
2	28.31	43.13	47.92	65.75	58.21
3	1.38	2.06	2.2	2.8	1.9
4	0.45	0.69	0.5	0.8	0.46
5	1.36	1.73	1.48	3.49	1.91
6	0.17	0.27	0.09	0.13	0.25
7			0.97	2.53	0.95

3.3. ESTIMATION OF RAINFALL PARAMETER OF SOIL EROSION

In parameter estimation of soil erosion, erosion factors are represented by parameters of:

— rainfall,
— soil,
— vegetation cover,
— relief,
— human impact.

Within the selected parameter estimation method RUSLE [11], the value of erosion production is obtained with the following formula:

$$A = R\,K\,LS\,C\,P \text{ in } (10^3 \text{ kg ac}^{-1}\text{ y}^{-1}) \text{ or } (10^3 \text{ kg ha}^{-1}\text{ y}^{-1}) \quad (1)$$

where: A – annual sediment production,
R – parameter of rainfall erosivity,
K – parameter of soil erodibility,
L – parameter of length of terrain with ongoing erosion,
S – parameter of terrain slope,
C – parameter of vegetation cover,
P – parameter of terrain utilization and cultivation method.

Each parameter can be determined by application of formulas proposed by different researchers, thus the parameter of rainfall erosivity can be determined in different ways, as follows:
According to Renard [11]:

$$R = E \cdot I_{30} \quad (2)$$

Where E is rainfall energy (total rainfall energy), which is calculated by application of the formula:

$$E = \sum_k e_k \cdot P_k \quad (3)$$

Where e_k represents specific rainfall energy in the time interval k, while P_k represents rainfall amount in the time interval k, expressed in [mm]. Specific energy e can be calculated according to the formula by Brown and Foster [1], as follows:

$$e = 0.29 \cdot \left[1 - 0.72 \cdot \exp(-0.05 \cdot i^*)\right] \quad (4)$$

Where i^* represents the rainfall intensity per 5-minute time intervals, but expressed in mm h^{-1}.

To determine the erosion parameter, according to these authors it is necessary to have 5-minute intensities available for each rainfall, i.e. registered rain event, and develop adequate computer software for easier processing of numerous data. When calculating the parameter R, rain events with rainfall amount of less than 12.25 mm are excluded, except if 6.12 mm or more rain fell in less than 15 minutes. For separation of two rain events, in the period of 6 hours the rainfall must equal less than 1.2 mm.
According to Fournier [2]:

$$R = \left(\Sigma \frac{p^2}{P} \right) \tag{5}$$

Where p is mean monthly rainfall in [mm], where P is total annual amount of rainfall in [mm].
According to Schwertman et al. [12]:

$$R = 0.083 * N - 1.77 \tag{6}$$

Where N represents total annual amount of rainfall in mm.

By using the above formulas for determination of rainfall parameter value of soil erosion (R) within the parameter estimation method RUSLE for the observed period 2003 – 2007, the values were obtained as shown in Table 3.

Table 3

Results of parameter R estimation per year

Year	2003	2004	2005	2006	2007
R_{Renar}	69.98	45.78	74.65	80.63	82.46
$R_{Furnier}$	104.11	98.98	109.54	137.18	102.35
$R_{Schwertman}$	67.59	84.71	84.99	94.73	74.66

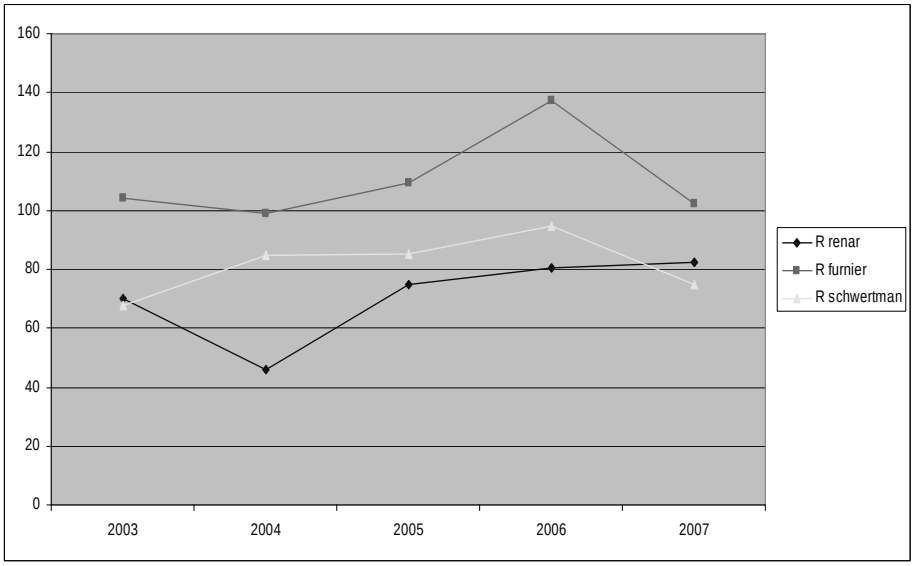

Fig. 2. Rainfall parameter values of soil erosion per year

With regards to other erosion parameters within the applied method (RUSLE), only values of rainfall parameter can significantly differ within an observed year. The illustration of dynamics of rainfall parameter values per year and per formula by different authors is

given in Fig. 2. By the use of standard calculation formulas for other erosion parameters within the selected RUSLE method and by comparison of calculated annual quantities of sediment production with measured values, the possible application of a selected method with acceptable level of result accuracy was confirmed. The results of conducted calculations of annual sediment production with use of rainfall parameter (R) values according to different authors for Table 5 are given in Fig. 3.

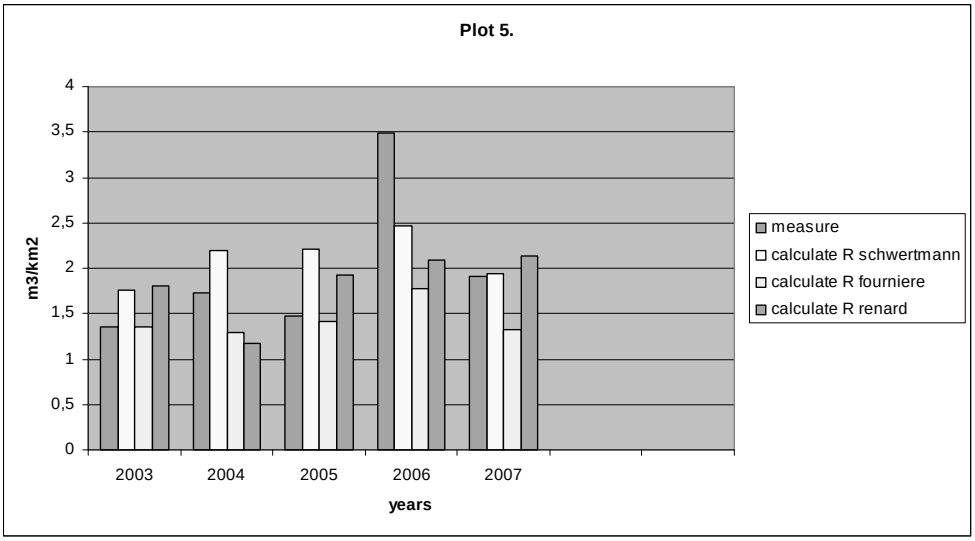

Fig. 3. Measured and calculated annual sediment production (m^3 km^{-2}) in Plot 5 as function of calculation method for rainfall parameter of soil erosion within the RUSLE method

3.4. CONCLUSION

Conducted calculations of annual sediment production on the test plots by application of the modified USLE model (RUSLE), with calculation of rainfall parameter by application of empirical formulas according to various authors gave results which generally follow the variation dynamics of annual sediment production within measured values. By conducting comparative analysis of calculated and measured values at the annual level, an existing empirical formula for calculation of rainfall parameter value can be selected which will result in the best results of calculated annual sediment production as compared with field measurement results. In case of conducted measurements and calculations of production for the majority test plots within the investigation area Abrami, this is the formula for calculation of rainfall parameter (R) according to Schwertman et al. In case of calculations of other model parameters within the conducted estimation procedure, standard procedures for determination of individual values of model parameters, which had already been in use in Croatia, were adopted. Based on the conducted field investigations and comparative analyses of measured and calculated values, on condition that estimation of other model parameters is conducted according to to-date practice in Croatia, it can be concluded that in case of application of the modified USLE (RUSLE) model in Istria and coastal and island areas in

Croatia with similar climate, relief and pedological characteristics, best results are obtained by application of the rainfall parameter formula according to Schwertman.

References

[1] Brown L.C., Foster G. G.: Storm erosivity using idealized intensity distributions. Trans. ASAE 30; 379–386, 1987.

[2] Fournier F.: Climat et erosion; La relation entre l erosion, du sol par l ean et les precipitations atmosferiques, Presses Univertsitaces de France, Paris 1960.

[3] Holjević D.: Procjena erozije tla i pronosa nanosa primjenom GIS-tehnologije, Magistarski rad. (Estimation of soil erosion and sediment transfer with application of GIS technology, Master's thesis.) 2002.

[4] Holjević D.:Vrednovanje prametara erozije genetskim algoritmom, Disertacija, Građevinski fakultet Zagreb, Zagreb. (Evaluation of erosion parameters with genetic algorithm, Thesis, Faculty of Civil Engineering, Zagreb, Zagreb) 2011.

[5] Kisić I.: Utjecaj načina obrade na eroziju tla vodom na pseudogleju središnje Hrvatske, dizertacija, Zagreb. (Impact of cultivation method on soil erosion by water on pseudogley in central Croatia, A thesis, Zagreb) 1998.

[6] Kisić I., Bašić F., Butorac A., Mesić M., Nestroy O., Sabolić M.: Erozija tla vodom pri različitim načinima obrade, Udžbenik sveučilišta u Zagrebu, Agronomski fakultet. (Soil erosion by water at different cultivation methods, Texbook, University of Zagreb – Faculty of Agriculture) 2005.

[7] Petraš J.: Prikaz istraživačke i demonstracijske plohe "Abrami" u Istri i prijedlog obnove istraživanja, elaborat, Građevinski fakultet sveučilišta u Zagrebu. (Overview of investigation and demonstration plots Abrami in Istria and proposal for renewed investigations, Study, Faculty of Civil Engineering – University of Zagreb) 1997.

[8] Petraš J., Bašić F.: Metode istraživanja erozije tla vodom i zaštita voda, "Hrvatske vode", br. 2, 99 – 105. (Investigation methods for soil erosion by water and water protection, Hrvatske vode magazine No. 2, pp. 99–105) 1993.

[9] Petraš J., Holjević D., Kunstek D.: Measurements Of Soil Erosion Production on the Investigation Plots "Abrami" On Flysch In Central Istria /Croatia/, 10th International Symposium on Water Management and Hydraulic Engineering, 04-09.09.2007 Šibenik, Croatia, Book of Abstract & Proceedings on CD, Građevinski fakultet Sveučilišta u Zagrebu (Faculty of Civil Engineering – University of Zagreb) 2007.

[10] Pernar N., Bakšić D., Perković I., Holjević D.: Odraz sanacije erodiranog terena na svojstva tla na flišu – slučajevi Abrami i Butoniga u Istri, Šumarski list no 5–6. (Impact of rehabilitation of eroded terrain on soil characteristics in flysch – Cases Abrami and Butoniga in Istria, Journal of Forestry No. 5–6) 2010.

[11] Renard K. G., Foster G. R., Weesies G. A., Mccool D. K., Yoder D. C.: Predicting soil erosion by water: a guide to conservation planning with the revised universal soil loss equation (RUSLE).USDA, Agricultural Habdbook No 703, 1977.

[12] Schwertmann U., Vogel W., Kainz M.: Bodenerosion durch Waser, Vorhersage des Auftragas und Bewertung von gegenmassnahmen, Stuttgart 1987.

4 Groundwater Quality in the Gdansk Aquifer System

Beata Jaworska-Szulc, Małgorzata Pruszkowska-Caceres, Maria Przewłócka
(Gdansk University of Technology, Faculty of Civil and Environmental Engineering)

4.1. HYDROGEOLOGY OF GDANSK AQUIFER SYSTEM

The area of the Gdańsk hydrogeological system covers about 2800 km^2 (Fig. 1). The recharge zone is situated on the glacial upland of the Kashubian Lake District. Its average elevation is 200 m a.s.l. The discharge zones, separated from the upland by a steep edge, include: Reda Ice Marginal Valley, marine terrace, western part of Vistula River Delta and the coastal areas of the Bay of Gdańsk, where under-sea discharge occurs, a very distinctive feature of the system. The Gdańsk hydrogeological system consists of three main aquifers: Cretaceous, Paleogene-Neogene and Pleistocene.

The main usable water bearing bed in the Cretaceous aquifer is built of upper Cretaceous Coniacian-Santoniam glauconitic sands. This widespread hydrogeological structure is called the Gdansk Artesian Basin [22]. The roof of the horizon lies about 150 m b.s.l (Fig. 2), its thickness in the Gdansk reaches 110 m b.s.l., and transmissivity is about 600 m^2/day. Analysis of the original piezometric surface of the basin indicates that it is recharged upon the moraine hills of the Kashubian Lake District. The recharge indicates an indirect character and is proceeding by leakage through Paleogene and Neogene sediments. The original piezometric surface in the areas of the costal plains and the western part of the Vistula River Delta reached 18 m above sea level. Before the period of intensive exploitation there was a great recharge of upper aquifers by leakage from the Cretaceous aquifer [6]. In the 80-ties, which was the period of the most intensive usage, total output from Cretaceous aquifer achieved over 70 000 m^3/day. In consequence on marine lowlands area there was created a vast cone of depression in the center of which the piezometric level was 5 to 10 meters below the sea level. The leakage from the bottom to top changed its direction. Consequently the upper aquifers recharge decrease has caused deterioration of water quality [6]. In the nineties the total output from Cretaceous aquifer was lowered to 43 000 m^3/day. The decreased output resulted in the rise of piezometric pressure. The process is still being observed, the piezometric surface now is only up to 2 meters lower than original piezometric surface [4]. Above the Coniacian-Santoniam aquifer, a limestone and marl Campanian-Maastrichtian aquifer occurs (Fig. 2). It is of main importance for water supply only in the eastern part of the region, in the Vistula River delta.

In the Paleogene and Neogene sediments groundwater has been found in the Eocene-Oligocene glauconite sands and Miocene sands, which are separated by layers of silts and clays with brown coal-dust [6]. The Oligocene-Eocene aquifer is being exploited mainly in the marine lowlands area. It consists of varigrained sands, in places with gravel and phosphate concretions. The roof of the Oligocene-Eocene aquifer is about 60 – 90 m b.s.l and its thickness does not exceed 20 m. Groundwater surface is of subartesian character and stabilizes at 120–160 m a.s.l. in the upland center and it lowers to 20 m a.s.l. in the zone of the upland edge and finaly reach about 5 m a.s.l. along the sea shoreline. The Oligocene-Eocene aquifer is locally in direct contact with the Pleistocene aquifer through erosional

channels cutting the Miocene deposits. The Miocene material of ligniferous formation is composed of alternating sand and clay strata of total thickness reaching 100 m [6]. The Miocene aquifer consists of fine grained sands with coal. The aquifer's top elevation is 30–40 m b.s.l., and its thickness is about 20 m.

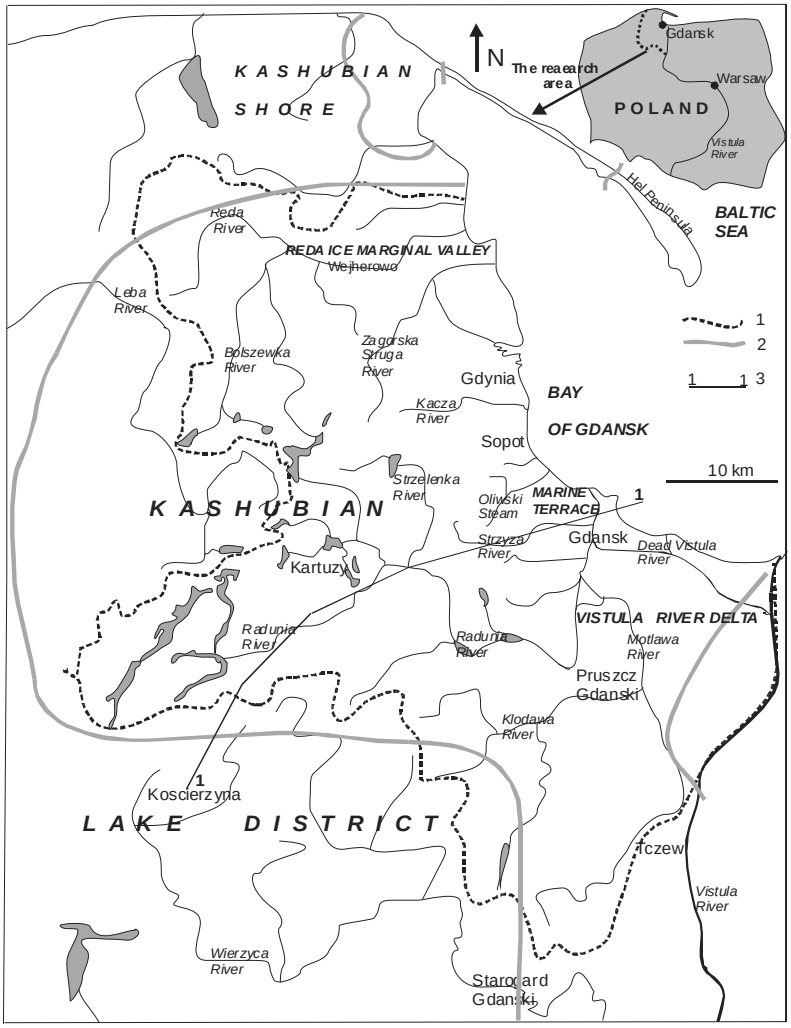

Fig. 1. The boundaries of Gdansk hydrogeological system, according to Kozerski et al. [10]:
1 – watershed of surface waters – the boundary of the Gdansk aquifer system,
2 – reach of the Cretaceous aquifer, 3 – cross-section line (Fig. 2)

The diversified topography and geological structure have had an impact upon differentiation of conditions of groundwater occurrence in Pleistocene formation in different morphologic units [6].

In the upland the Pleistocene aquifer consists of several water bearing beds. The water-bearing horizons are most frequently separated with tills, silts and clays (Fig. 2). Some of

water bearing beds are of local range, others are in contact with the water of deep lakes and the Miocene formation [6]. The deeper ones are the basis for water supply for numerous towns and villages. The shallow aquifers occur only locally, and they are composed of sandy sediments of alluvial plains, of river and lake valleys (Fig. 2). Locally it has direct contact through erosional channels with older Pleistocene aquifers.

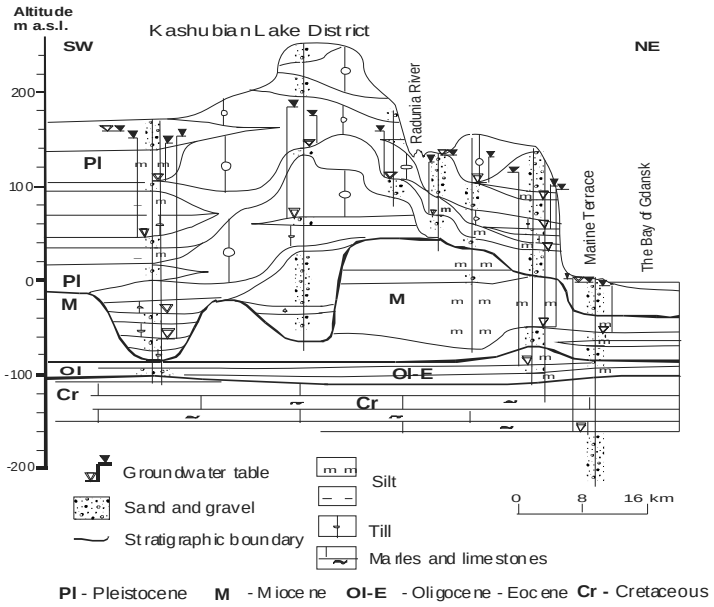

Fig. 2. The hydrogeological cross section (line 1–1 on Fig. 1), according to Kozerski et al. [10]

The deeper aquifers occur regionally in inter-moraine Pleistocene sediments, isolated from the surface (Fig. 2). They are recharged laterally or by indirect seepage from the overlying layers. Commonly, especially in the area of deep glacial channel valleys, the Pleistocene aquifer is in direct contact with the Miocene aquifer, and together they create main useful aquifer. The groundwater piezometric surface is at the highest level in the central part of the moraine hills of the Kashubian Lake District (160–180 m a.s.l.). The piezometric surface lowers in the east and northern direction to 20 meters above sea level in the zone of upland egde and to 1–5 meters above sea level in the lowland of the Marine Terrace and in the Vistula River Delta.

The Pleistocene water bearing beds in the Reda Ice Marginal Valley, in the marine terrace, and in the western part of the Vistula River delta have high transmissivity: 2900 – 4300 $m^2 d^{-1}$. Superficial deposits of the Vistula River delta are composed of peat and mud lying on fine-grained sand. The thickness of these Holocene sediments is about 30 m, below them there appear medium and the coarse-grained sand of Pleistocene age. The sand series of the Pleistocene together with the permeable deposit of the Holocene create one aquifer. The water-table rests at the height of several meters near the edge and descends below sea level in depressions. Most often it is about 1 m above sea level. The best conditions of groundwater occurrence exist in the western part of delta near Gdansk. The Pleistocene aquifer is recharged by the inflow of water both from the moraine hill aquifers and the leakage from the Cretaceous basin. The transmissivity varies between 500–2000 $m^2 d^{-1}$ [6].

The marine terrace stretches upon relatively small area about 15 square kilometers between Gdansk and Sopot. It is a plain situated from several to over ten meters above sea level composed of fluvioglacial sand covered by loam. Among the sandy formation the thickness of which reaches up to 50 m there appears quite commonly a layer of glacial till and clay. The Pleistocene sandy series constitutes a very valuable aquifer, the transmissivity is to 1000 $m^2\ d^{-1}$. The groundwater table lowers its level from the moraine hills towards the sea shore. The original piezometric surface reached 2 m a.s.l. along the coastline.

The Reda Ice Marginal Valley is the dominating geomorphological unit in the Gdansk region and is of great hydrogeological importance. The surface of the terrain varies from 15 m in the western part to 3 m a.s.l. at the sea shore. It is an erosive form. Over vast area of the valley glacial deposits are removed so that the bottom of the valley is now made of fluvioglacial sediments composed of sand and gravel of thickness reaching up to 40 m. The fluvioglacial sediments are covered at some places with peat, mud, and alluvial sand of Reda River. The sand series occurring at the bottom of the ice marginal valley create a very valuable Pleistocene aquifer. The groundwater table or piezometric surface drops towards the valley mouth. In the confined part of the aquifer at the sea shore it was originally about 5 m a.s.l.. The inflow to the Pleistocene aquifer of The Reda Ice Marginal Valley is mainly lateral, from the Kashubian Lake District and also comes from the ascension of water from the Eocene-Oligocene formation [6].

4.2. GROUNDWATER QUALITY OF THE GDANSK AQUIFER SYSTEM

Chemical composition of groundwater in the Gdansk aquifer system varies between water-bearing beds, although water from Pleistocene and Paleogene-Neogene aquifers shows much similarities. The vertical hydrogeochemical zoning is strictly connected with groundwater flow conditions, especially with the flow velocity and also with the chemical processes occurring between aquifer media and water. Groundwater quality shows horizontal zoning as well. This concerns mainly Cretaceous and Pleistocene aquifers. The differences are visible especially between recharge and discharge zones.

Groundwater from **Cretaceous aquifer** in the recharge zone is of HCO_3–Ca type, locally of HCO_3–Ca–Na and HCO_3–Na–Ca type. The mineralization varies between 170 and 550 mg dm^{-3}, pH 7.0 to 8.9. Total hardness is low 0.1–2.0 mval dm^{-3}, alkalinity: 1.0–6.0 mval dm^{-3}. Characteristic feature of the water is lack of oxygen or it's very low concentrations and lack of free carbon dioxide [15, 16, 21, 23].

Chloride ion concentration doesn't exceed 43.0 mg Cl dm^{-3} and the hydrogeochemical background for this ion varies from 0 to 30 mg Cl dm^{-3} (Tab. 1). The amount of sulphates is also low: 1–30 mg $SO_4\ dm^{-3}$. Iron and manganese occur in trace amounts only, although iron concentration increases locally to 2.4 mg Fe dm^{-3} (Kępa Oksywska) with the range of hydrogeochemical background: 0 – 0.3 mg Fe dm^{-3}. Considering nitrogen compounds, nitrate and nitrite nitrogen concentrations are very small, but ammonia nitrogen increases in the edge zone of the Kashubian Lake District upland, reaching the highest amount 1.7 mg $NH_4\ dm^{-3}$ in Gdańsk Chełm [16]. High concentrations of ammonia is a natural feature of groundwater from deep confined aquifers of low redox potential [24]. In the same area (edge zone of the upland) hydrogen sulphide together with the ions HS^- and S^{2-} were detected. Concentrations of hydrogen sulphide varies from 0.006 to 0.039 mg dm^{-3} resulting in a disagreeable odour and taste of the water. Low concentrations of

sulphates together with hydrogen sulphide presence is the effect of sulphate reducing bacteria (SRB) activity [12, 13]. In the absence of oxygen, microbiological oxidation of organic matter takes place due to the use of successive acceptors, for example SO_4 or NO_3. In the Cretaceous aquifer this process has led to gradual depletion of nitrates and nitrites and to decrease of sulphates concentration. As a result of the microbiological processes ammonia and hydrogen sulphide appeared and also pH increased because of depletion of free carbon dioxide concentration [13].

Table 1

Concentrations of main hydrogeochemical parameters and hydrogeochemical background of the Cretaceous aquifer

Hydrogeochemical parameter		Recharge zone	Discharge zone	Hydrogeochemical background (Kozerski et all. 1987)
Total hardness	[mval dm^{-3}]	0.1–2.0	0.1–5	0.1–2.0
Alkalinity	[mval dm^{-3}]	1.0–6.0	1.0–6.0	5.0–6.0
pH		7.0–8.9	7.0–8.9	7.2–8.3
Color	[mg Pt dm^{-3}]	5.0–10.0	5–17	–
Mineralization	[mg dm^{-3}]	170–550	200–1000	200–500
Chlorides	[mg Cl dm^{-3}]	0–43	10–548	0–30
Sulphates	[mg SO4 dm^{-3}]	1–30	1–30	0–25
Calcium	[mg Ca dm^{-3}]	1.6–36.8	1.6–66.5	–
Magnesium	[mg Mg dm^{-3}]	0.7–11.8	0.49–18.7	–
Sodium	[mg Na dm^{-3}]	49.5–190	8.9–487	–
Potassium	[mg K dm^{-3}]	2.2–8.2	2.9–18.8	–
Iron	[mg Fe dm^{-3}]	0–2.4	trace	0–0.3
Manganese	[mg Mn dm^{-3}]	trace	trace	–
Ammonia	[mg NH4 dm^{-3}]	0–1.7	0–2.1	–
Fluorides	[mg F dm^{-3}]	0–5.5	0–5.5	0–1.5

Locally, in the southern part of the edge zone, groundwater from Cretaceous aquifer contains elevated concentrations of fluoride ion, reaching the value 5.5 mg F dm^{-3}. The origin of such high amounts of fluorides is probably connected with ion exchange processes or with local leaching of fluoride minerals from Cretaceous rocks by soft water of HCO_3–Na type. Elevated concentration of fluoride ion is observed only in the type of bicarbonate – sodium water, while harder, bicarbonate – calcium water contains small amounts of this ion [7].

In the discharge zone, groundwater from Cretaceous aquifer is mainly of HCO_3–Na type (marine terrace, north – east part of the Vistula river delta) and HCO_3–Na–Ca (western part of the Vistula river delta), although in Reda ice marginal valley it shows HCO_3–Ca type. The mineralization is higher than in recharge zone, reaching 1000 mg dm^{-3} in places. Sulphates and nitrogen compounds concentrations are very low, like in the recharge zone (Tab. 1). Only locally, ammonia ion increases to 0.64 mg NH_4 dm^{-3} (Błotnik, Cedry Małe, Lipce and Grodza Kamienna) and 2.1 mg NH_4 dm^{-3} in Pruszcz Gdański. Ammonia nitrogen presence in groundwater is typical for reducing environment (Eh around 50 mS or less).

Low amount of sulphate ions in the groundwater and hydrogen sulphide odour observed in many wells also prove reduction conditions in the aquifer. Sulphate reducing bacteria and nitrate reducing bacteria were also detected in the groundwater [13].

The considered groundwater show variable concentrations of chloride ion. In the area of Reda ice-marginal valley, marine terrace and a part of Vistula river delta the concentrations don't exceed 20 mg dm^{-3} and the mineralization of the water is less than 500 mg dm^{-3}. However, in the eastern and northern part of the Vistula river delta the amount of chlorides increase up to 500 Cl dm^{-3} (Długie Pole, Tczew) and the mineralization reaches 1000 mg dm^{-3}. In Osice, Błotnik and Cedry Małe chlorides concentration is around 100 mg Cl dm^{-3}. This results in the change of groundwater type to Cl-HCO_3–Na and Cl–Na. Moreover the groundwater shows elevated values of boron (above 2 mg B dm^{-3}), and total hardness reaches 5 mval dm^{-3}. Regarding groundwater dynamics, the area of elevated salinity can be qualified as intermediate between intensive exchange and the zone of hydrogeological stagnancy. According to Sadurski [21], the origin of brackish water occurance in the Cretaceous aquifer is complex. Partially it is the effect of saline water ascent from older formations (Jurassic, Triassic) and on the other hand is the result of fossil connate waters reminded sealed in the aquifer.

Another specific compound of the groundwater is fluoride ion; it's concentration reaches 4–2 mg F dm^{-3} in Trutnowy and 5–48 mg F dm^{-3} in Długie Pole. The hydrogeochemical fluoride anomaly zone, specified by Kozerski et al. [7] spreads along the line: Przegalina, Długie Pole, Suchy Dąb and continues to the edge of the upland reaching Mieścin and Żelisławki, where concentration reach the maximum value 5–5 mg F dm^{-3}. The limit for drinking water (1–5 mg F dm^{-3}) is exceeded in all wells there. Nevertheless in the western part of the delta, where Lipce groundwater intake is situated and also in the area of marine terrace and Reda ice-marginal valley the concentrations are less than 0–5 mg F dm^{-3}. This can be explained by higher specific capacity in the mentioned areas and consequently shorter time for interaction between aquifer media and groundwater [7].

Groundwater occurring in **Paleogene – Neogene deposits** is similar in recharge and discharge zones. Slight changes of physico-chemical composition occur only locally and result from differences in groundwater flow conditions. The dominant type of water is HCO_3-Ca, although locally in the area of Tczew there occur also HCO3–Ca–Na type. Total hardness varies from 1.0 to 8.0 mval dm^{-3}, alkalinity from 1.0 to 6.8 mval dm^{-3} and pH value between 6.5 and 8.3.

The colour of the groundwater is higher than in Cretaceous aquifer; maximum value is 65 mg Pt dm^{-3}. Calcium and magnesium ions predominate over sodium and potassium, however in the Tczew area (discharge zone) sodium concentration in groundwater from oligocene deposits increases to 107 mg Na dm^{-3} (Tab. 2).

Together with sodium, chloride ion is elevated up to 283 mg Cl dm^{-3}. Beyond the mentioned area, chlorides occur in small amounts; the range of hydrogeochemical background is 0 to 25 mg Cl dm^{-3}. Sulphate ion concentrations are also low, the background range is 0–25 mg SO_4 dm^{-3}; however locally concentrations increase to 95 mg SO_4 dm^{-3}.

Table 2

Chemical composition of groundwater from Paleogene-Neogene aquifer in the recharge and discharge zone

Hydrogeo-chemical parameter	Recharge zone				Discharge zone			
	Neogene series		Paleogene series		Neogene series		Paleogene series	
	number of data	min-max background	number of data	min-max background	number of data	min-max background	number of data	min-max background
Total hardness [mval dm^{-3}]	302	$\frac{1.0-8.0}{3.2-4.4}$	298	$\frac{1.0-7.6}{3.4-5.4}$	127	$\frac{1.0-7.8}{3.2-4.4}$	114	$\frac{1.0-7.8}{3.4-4.4}$
Alkalinity [mval dm^{-3}]	227	$\frac{1.0-6.8}{3.4-4.6}$	233	$\frac{1.4-6.8}{3.2-4.8}$	63	$\frac{2.4-6.8}{3.2-4.2}$	68	$\frac{2.2-6.8}{3.0-4.0}$
pH [-]	219	$\frac{6.5-8.2}{7.2-7.8}$	215	$\frac{6.5-8.2}{7.2-7.8}$	297	$\frac{6.8-8.2}{7.2-7.9}$	121	$\frac{6.9-8.3}{7.1-7.6}$
Mineralization [mg dm^{-3}]	199	$\frac{140-598}{200-360}$	224	$\frac{140-560}{240-380}$	66	$\frac{182-479}{260-380}$	59	$\frac{160-580}{260-380}$
Colour [mp Pt dm^{-3}]	199	$\frac{1-50}{0-20}$	209	$\frac{1-65}{0-25}$	124	$\frac{1-50}{0-20}$	85	$\frac{1-44}{0-20}$
Chlorides [mg Cl dm^{-3}]	220	$\frac{0-60}{0-20}$	240	$\frac{0-88}{0-25}$	207	$\frac{0-77}{0-25}$	114	$\frac{0-74}{0-15}$
Sulphates [mg SO_4dm^{-3}]	111	$\frac{0-95}{0-25}$	125	$\frac{0-75}{0-25}$	111	$\frac{0-84}{0-20}$	47	$\frac{0-50}{0-20}$
Calcium [mg Ca dm^{-3}]	110	$\frac{10-140}{40-90}$	146	$\frac{30-130}{40-90}$	121	$\frac{10-119}{40-70}$	47	$\frac{21-130}{40-90}$
Magnezium [mg Mg dm^{-3}]	109	$\frac{0-40}{0-12}$	134	$\frac{0-40}{0-12}$	103	$\frac{0-27}{8-16}$	46	$\frac{0-26}{8-16}$
Sodium [mg Na dm^{-3}]	46	$\frac{0-10{,}1}{-}$	54	$\frac{0-11{,}2}{-}$	78	$\frac{0.39-107}{-}$	25	$\frac{0-9.8}{-}$
Potassium [mg K dm^{-3}]	46	$\frac{0-2{,}9}{-}$	54	$\frac{0-3{,}6}{-}$	78	$\frac{0-5{,}8}{-}$	25	$\frac{0-3{,}1}{-}$
Iron [mg Fe dm^{-3}]	239	$\frac{0-4.0}{0-1.8}$	318	$\frac{0-4.0}{0-1.2}$	240	$\frac{0-4.0}{0-1.8}$	114	$\frac{0-4.0}{0-1.2}$
Manganease [mg Mn dm^{-3}]	192	$\frac{0-0.46}{0.08-0.16}$	186	$\frac{0.02-0.46}{0.06-0.2}$	215	$\frac{0-0.3}{0.08-0.16}$	77	$\frac{0-0.3}{0.08-0.18}$
Ammonia [mg NH_4 dm^{-3}]	158	$\frac{0-0.58}{0-0.04}$	177	$\frac{0-0.58}{0-0.01}$	113	$\frac{0-0.93}{0-0.08}$	93	$\frac{0-0.58}{0-0.04}$
Nitrates [mg NO_3 dm^{-3}]	152	$\frac{0-0.2}{0-0.04}$	175	$\frac{0-0.3}{0-0.05}$	198	$\frac{0-0.3}{0-0.05}$	60	$\frac{0-0.28}{0-0.04}$
Nitrites [mg NO_2 dm^{-}]	120	$\frac{0-0.03}{0-0.05}$	182	$\frac{0-0.034}{0-0.008}$	187	$\frac{0-0.034}{0-0.008}$	62	$\frac{0-0.02}{0-0.006}$

Nitrogen compounds are generally of trace amount; nevertheless ammonia sporadically occur in elevated concentrations: 0.58 mg NH_4 dm^{-3} in Otomin and 0.93 mg NH_4 dm^{-3} in Tczew. Low level of sulphates, nitrates, nitrites and the presence of hydrogen sulphide together with elevated ammonia concentrations result from microbiological processes taking place in the conditions of decreased oxygen level [14]. Iron concentration ranges 0–1.8 mg Fe dm^{-3} and manganease 0.08–0.2 mg Mn dm^{-3}. Fluorides don't exceed the value 0.8 mg F dm^{-3} except for Tczew, where the level increases to 2.0 mg F dm^{-3} in groundwater from Paleogene deposits.

Groundwater quality from **Pleistocene aquifer** will be characterized in reference to the diversified topography and geological structure which have an impact upon the conditions of groundwater occurrence. The upland **of Kashubian Lake District** constitutes the vast recharge zone for the whole system. In this unit physico-chemical properties of groundwater are not very diverse. Major ions in the two distinguished water bearing strata are presented in the Piper diagram (Fig. 3).

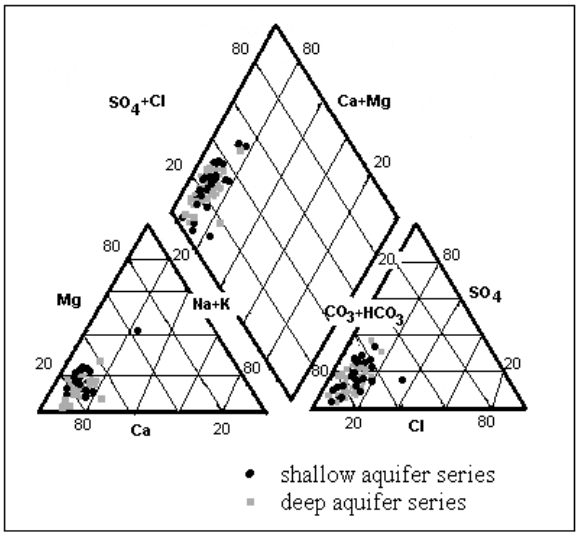

Fig. 3. Piper diagram showing major ions distribution in the Pleistocene aquifer, with the division to shallower and deeper aquifer, according to Pruszkowska (2004)

The water is mainly of HCO_3–Ca type, however the types HCO_3–Ca–Mg and HCO_3–SO_4–Ca also appear locally. The comparison of the two water bearing beds, regarding hydrogeochemical background and extreme values is presented in the Table 3.

The data presented above indicate hydrogeochemical anomalies occuring in the upper aquifer of the Kashubian Lake District. Elevated values of such parameters as chlorides, sulphates, nitrogen compounds, zinc, mineralization in the shallow aquifer, are evidences of pollution sources influencing groundwater (farms, landfills, sewage treatment plants, plants of timber and food industry). However, the sulphate anomalies in the deeper aquifer are of geogenic origin. Increased concentrations of the ions derive from silts and clays of ice dam lakes overlying the aquifer. The deposits are rich in organic matter containing S^{2-} which oxidizes and appears in groundwater in the form of sulphate ion [2].

Table 3

Groundwater composition in the area of Kashubian Lake District upland

Hydrogeo chemical parameter	Shallow horizon		Deeper horizon	
	number of data	min-max / background	number of data	min-max / background
Total hardness [mval dm^{-3}]	54	1.6 – 8.1 / 2.0 – 4.5	138	1.5 – 8.1 / 2.0 – 5.2
Alkalinity [mval dm^{-3}]	55	1.1 – 7.4 / 1.6 – 5.1	113	1.2 – 7.1 / 1.6 – 5.1
pH [-]	188	6.7 – 8.2 / 6.9 – 7.7	359	6.6 – 8.2 / 6.9 – 7.9
Mineralization [mg dm^{-3}]	152	90 – 625 / 110 – 350	246	94 – 580 / 110 – 350
Chlorides [mg Cl dm^{-3}]	70	0.1 – 177 / 0 – 23	148	0.2 – 100 / 0 – 20
Colour [mp Pt/dm^3]	52	0 – 30	67	0 – 30
Sulphates [mg SO_4 dm^{-3}]	73	5 – 178 / 8 – 42	75	0.1 – 58 / 10 – 42
Calcium [mg Ca dm^{-3}]	42	20.8 – 183.2 / 25 – 105	41	24.3 – 142 / 30 – 88
Magnease [mg Mg dm^{-3}]	42	0.1 – 19.7 / 0 – 12	42	0.1 – 28.2 / 0 – 15
Sodium [mg Na dm^{-3}]	87	0.3 – 48.8	76	0.4 – 16
Potassium [mg K dm^{-3}]	86	0.6 – 18.4	78	0.6 – 6.0
Iron [mg Fe dm^{-3}]	99	0.01 – 8.5 / 0 – 0.9	181	0.01 – 5.4 / 0 – 1.3
Manganease [mg Mn dm^{-3}]	98	0.01 – 0.7 / 0 – 0.12	126	0.01 – 1.0 / 0 – 0.18
Ammonia [mg NH_4 dm^{-3}]	68	0.019 – 1.29 / 0 – 0.45	125	0.019 – 2.58 / 0 – 0.36
Nitrates [mg NO_3 dm^{-3}]	48	0.004 – 83.2 / 0.035 – 2.22	87	0.004 – 47.0 / 0.18 – 2.21
Nitrites [mg NO_2 dm^{-3}]	80	0.003 – 0.92 / 0 – 0.16	79	0.003 – 10.5 / 0 – 0.16

The origin of elevated concentrations of iron and manganease is also geogenic. According to Ratajczak and Witczak [20] high amounts of the ions are typical for groundwater from Quaternary deposits, where the compounds are leached from glacial tills.

In the discharge zone the hydrogeochemical conditions are more complex. Groundwater of **Reda ice-marginal valley** is generally of HCO_3–Ca type, but locally in areas of antropopression, or where peat overlies the aquifer, the type of water changes into HCO_3–SO_4–Ca. In some places, especially in the zone of ash landfill in Rewa and in harbour wharf surroundings chlorides are elevated up to 100–200 mg Cl dm^{-3}. In the region between Rumia and Gdynia chloride ion concentrations are elevated to 20–50 mg Cl dm^{-3} or even 50–100 mg Cl dm^{-3} [11], exceeding the natural hydrogeochemical background range. Besides the mentioned zones, the concentrations are up to 20 mg Cl dm^{-3}. The distribution of chloride ion is an example of groundwater diversity between Kashubian ice-marginal valley and the rest of Reda ice-marginal valley. The western part of the reservoir is of good quality, characteristic for natural conditions. The water is soft and semi-hard (3–4 mval dm^{-3}). Sulphate concentrations don't exceed 40 mg SO_4 dm^{-3}. There are areas (e.g. Strzebielino, Bolszewo) where groundwater doesn't need any treatment [1]. The biggest intake in this region is „Cedron" in Wejherowo, exploiting the reservoir in the valley of Cedron – Reda's tributary. Groundwater quality from 17 wells of the intake is shown in Table 4. The quality is typical for this part of Reda ice-marginal valley. It should be added, that besides the parameters shown in Table 4, groundwater from the intake was sampled for lead, cadmium, nickel, mercury, chromium, benzo(a)piren, PAH and the micro-compounds were not detected; nitrites and nitrates concentrations were close to zero.

Table 4

Chemical composition of groundwater of „Cedron" intake in 2004

Hydrogeochemical parameter	Min. – max	Mediane	Hydrogeochemical parameter	Min. – max	Mediane
Total hardness [mval dm^{-3}]	3.3–4.1	3.6	Iron [mg Fe dm^{-3}]	0.044–1.32	0.5
Alkalinity [mval dm^{-3}]	3.0–3.6	3.4	Manganease [mg Mn dm^{-3}]	0.03–0.15	0.08
Chlorides [mg Cl dm^{-3}]	5.3–3.1	8.2	Ammonia [mg NH_4 dm^{-3}]	0.019–0.447	0.1
Sulphates [mg SO_4 dm^{-3}]	<10–33.6	15.6	Dry residue [mg dm^{-3}]	273–346	309

However, in Kashubian ice-marginal valley groundwater composition differs from natural, especially between Reda and Gdynia, where two big municipal intakes and many industrial intakes are situated. The cause of the quality changes is intensive exploiation on one hand, but on the other hand - numerous pollution sources, such as sewage treatment plant, heat and power plant, ash landfill, fuel base, shipyard and also roads of high traffic. Additionaly, the aquifer is vulnerable to contamination because of lack of overlying aquitards or aquicludes. All of that caused groundwater quality deterioration. In 60-ties and 70-ties chemical composition of groundwater was close to natural [11]. Table 5 compares hydrogeochemical backgrounds determined for periods 1965–1975 and 1991–1997. The most visible changes concern nitrates, chlorides and lead.

Table 5

Comparison of hydrogeochemical background of Kashubian ice-marginal valley in periods: 1965–75 and 1991–97

Hydrogeochemical parameter		Hydrogeochemical background 1965–1975	Hydrogeochemical background 1991–1997
Dry residue	[mg dm^{-3}]	220–320	250–490
Total hardness	[mval dm^{-3}]	3.4–5.6	3.3–7.6
Alkalinity	[mval dm^{-3}]	3.1–4.4	3.5–5.0
Cl^-	[mg Cl dm^{-3}]	5–28	16–48
SO_4^{2-}	[mg SO_4 dm^{-3}]	20–80	20–100
Fe^{2+}	[mg Fe dm^{-3}]	0.2–2.0	0.4–2.4
Mn^{2+}	[mg Mn dm^{-3}]	0.05–0.16	0.06–0.24
NO_3^-	[mg NO_3 dm^{-3}]	~0–0.44	0.44–11.1
NH_4^+	[mg NH_4 dm^{-3}]	0.01–0.026	0.026–0.19
Pb	[mg Pb dm^{-3}]		0.01–0.04

In spite of evident changes in groundwater composition, the water is of good quality; only iron and manganease concentrations exceed the limits determined for drinking water. Table 6 presents groundwater composition from two intakes: Reda II and Rumia. In groundwater taken from Reda II intake, sulphate concentrations are elevated, probably because of peats overlying the aquifer. Together with sulphates, total hardness and dry residue is elevated. Besides hydrochemical parameters presented in Table 6, nitrate and nitrite compounds were determined with concentrations close to zero. Lead, cadmium, nickel, mercury, chromium, benzo(a)piren and PAH were not detected.

Much worse quality is in the shallow part of the aquifer, 6 – 10 m below ground level. Chlorides, sulphites, nitrogen compounds, dry residue occur in elevated concentrations [11]. It is an effect of geogenic processes, but mainly is the result of antropopression. The shallow groundwater can be a danger for the main useful aquifer.

On the **marine terrace**, Quaternary aquifer is exploited by three big municipal intakes: Czarny Dwór, Zaspa and Bitwy pod Płowcami. The aquifer is unconfined and vulnerable to contamination. Intensive exploitation and the influence of pollution sources have caused undesirable changes of groundwater quality. Table 7 presents natural and current hydrogeochemical background determined for the marine terrace by Przewłócka [18]. The values are compared with the background for Kashubian Lake District according to Pruszkowska [16]. It is worth emphasising, that even in natural conditions groundwater composition on marine terrace differs from that of recharge area – Kashubian Lake District. Natural background for sulphates ranges from 10 to 110 mg SO_4 dm^{-3} and for chlorides 5–40 mg Cl dm^{-3}. Because of antropopression, concentrations of the ions increased and diversified – current hydrogeochemical background for sulphtes is: 40–160 mg SO_4 dm^{-3}, and for chlorides: 18–70 mg Cl dm^{-3}. Besides, ammonia amount increased from 0–0.26 mg NH_4 dm^{-3} in natural conditions to 0–0.077 mg NH_4 dm^{-3} currently (Tab. 7).

Table 6

Groundwater composition of „Rumia" and „Reda II" intakes in the year 2004

Hydrogeochemical parameter		Rumia intake		Reda II intake	
		min. – max	mediane	min. – max	mediane
Total hardness	[mval dm^{-3}]	3.9–5.5	5.0	4.2–9.2	5.8
Alkalinity	[mval dm^{-3}]	3.22–4.1	3.7	3.5–4.73	3.99
Chlorides	[mg Cl dm^{-3}]	8.1–30.1	14.4	11.5–36	19.1
Sulphates	[mg SO_4 dm^{-3}]	17.4–93.5	39.6	50.2–211	95.4
Iron	[mg Fe dm^{-3}]	0.79–10.1	1.25	0.65–6.09	1.27
Manganease	[mg Mn dm^{-3}]	0.08–1.0	0.16	0.07–0.25	0.18
Ammonia	[mg H_4 dm^{-3}]	0–0.53	0.35	0.02–0.81	0.47
Dry residue	[mg dm^{-3}]	334–496	410	281–656	409

Table 7

Current and natural hydrogeochemical background for Quaternary deposits of marine terrace in comparison with the background for Kashubian Lake District

Hydrogeochemical parameter	Natural conditions, marine terrace		Current conditions, marine terrace		Kashubian Lake District, natural background (> 30 m)
	number of data	min. – max / mediane background	number of data	min. – max / mediane background	
Total hardness [mval dm^{-3}]	65	3.2–8.1 / 5.2 **3.5–7.2**	239	4,1–10,2 / 7,1 **5.6–8.5**	**2.0–4.5**
Alkalinity mval dm^{-3}]	101	3.1–6.41 / 4.4 **3.3–5.7**	238	3.8–5.9 / 4.8 **4.0–5.7**	**1.6–5.1**
Chlorides [mg Cl dm^{-3}]	104	2.8–74.4 / 21.2 **5–40**	239	16.7–148 / 42.2 **18–70**	**0.0–20**
Sulphates [mg SO_4 dm^{-3}]	50	0–133.7 / 62.9 **10–110**	238	11.2–213.7 / 95.6 **40–160**	**10–42**
Iron [Mg Fe dm^{-3}]	101	0.05–10.0 / 1.0 **0.2–2.4**	239	0.1–5.94 / 1.24 **0.3–3.0**	**0.0–1.3**
Manganease [mg Mn dm^{-3}]	58	0 – 1.5 / 0.15 **0–0.3**	239	0.07–1.27 / 0.18 **0.07–0.35**	**0.0–0.18**
Ammonia [mg NH_4 dm^{-3}]	79	0–1.11 / 0.04 **0–0.26**	239	0.01–1.23 / 0.34 **0–0.77**	**0.0–0.36**
Nitrates [mg NO_3 dm^{-3}]	72	0–15.51 / 0.09 **0–0.89**	239	0–16.52 / 0.44 **0–0.89**	**0.18–0.8**

Groundwater from Pleistocene aquifer on the marine terrace is hard and semi-hard; the background for total hardness ranges from 5.6 to 8.5 mval dm^{-3}. Alkalinity background values are between 4.0 and 5.7 mval/dm^3. The groundwater type is predominantly HCO_3–SO_4–Ca and HCO_3–SO_4–Cl–Ca. Only in Sopot and Jelitkowo surroundings, where intensive lateral recharge from Kashubian Lake District takes place, it is of HCO_3–Ca type. Increased amount of sulphates in groundwater from marine terrace is an effect of both, natural conditions – hydrogeochemical and hydrodynamic and also antropopression [19]. As to the natural agents influencing sulphates concentrations, lithology of the aquifer and of overlying layer should be indicated. The aquifer of the marine terrace is polygenetic, consisting of fluvioglacial sands, marine sands and sands of alluvial fans.

According to Górski [2] natural diversity of aquifer media often results in groundwater quality changes. The aquifer is covered by discontinuous layer of peat consisting of organic matter rich in sulphur compounds, which may cause sulphate anomalies in groundwater [5]. Groundwater from Kashubian Lake District inflowing laterally to the aquifer of marine terrace loose flow velocity, because of drop of hydraulic gradient and thus the time of contact between groundwater and the diverse geochemical environment water extends. As to the human impact on groundwater quality, an important factor is uneven output from wells, especially switching off and switching on pumping which results in fluctuation of groundwater level and consequently changes in red-ox conditions. There are also pollution sources influencing groundwater quality, especially in the area of Zaspa groundwater intake. As a result sulphates concentration observed in some wells reached 100–120 mg SO_4 dm^{-3}; also nitrates concentrations increased to 8–13 mg NO_3 dm^{-3}. The ifluence of pollutions resulted also in elevated concentrations of chloride ion; the range of hydrogeochemical background moved from 5–40 mg Cl dm^{-3} in natural condition to 18–70 mg Cl dm^{-3} currently. The pollution sources that should be mentioned are: sewage disposal plant, roads of heavy traffic, allotment gardens. However the sources are of minor importance in comparison with the main cause of chlorine ion increase in groundwater of marine terrace, that is salt water intrusion to the aquifer, which took place in 80-ties and 90-ties of the previous century. The intrusion was caused by overexploitation of Pleistocene aquifer and took place in the middle part of the marine terrace. Maximum concentration of chloride ion: 700–1000 mg Cl dm^{-3}, was measured in 1992 in water taken from piezometers located between the line of wells and the sea shore. The amount of chlorides measured in wells was comparatively low, only sporadically exceeded 100 mg Cl dm^{-3} and predominantly was between 40 and 60 mg Cl dm^{-3}. Such low concentrations in water taken from wells can be explained by intensive lateral recharge from the upland of Kashubian Lake District and as a result diluting the intruded salt water [17]. Reduction of exploitation has stopped salt water intrusion. Currently the amount of Cl^- in the groundwater from the piezometers mantioned above is 20–50 mg Cl^- dm^{-3}. The stop of salt water intrusion was confirmed by geophysical investigations led by the team of hydrogeologists and students from Royal Technical University of Stockholm and from Gdańsk University of Technology, in years 2002–2004 [3].

Summing up, groundwater from Pleistocene aquifer of marine terrace, in spite of some symptoms of antropopression, is generally of good quality. The limits for drinking water are exceeded only in case of iron (hydrogeochemical background: 0.3–3.0 mg Fe dm^{-3}) and manganease (hydrogeochemical background: 0.07–0.35 mg Mn dm^{-3}), also colour in some cases. The exploited water undergo typical treatment leading to reduction of iron and manganease concentrations. The aquifer vulnerability however, requires high protection and monitoring of groundwater quality, especially with regard to micro-compounds. Previous

analyses proved that lead, chromium, cadmium, mercury, arsenic, aluminium were not detected; zinc, boron and barium occurred in amounts typical for clear water. PCB, pesticides and PAH were not detected or close to zero. The only concern is benzene detected in a few wells: 1.25 and 0.47 μg dm^{-3} [18] and also Trichloroethene and Tetrachloroethane that appeared several wells in the middle sector of Czarny Dwór groundwater intake. The investigations and monitoring of the intake focused especially on micro-compounds is being continued.

Pleistocene aquifer in the **Vistula River Delta** shows variable quality. The dominant type of the main usable aquifer is HCO_3–Ca, but the ascent from Cretaceous aquifer changes the water type in some areas to HCO_3–Na. Locally saline water of young fossil connate type occur increasing concentrations of chlorides. The shallow Holocene water shows elevated concentrations of sulphates, nitrates, decreased pH value and the presence of organic gases: hydrogen sulphide and methane. It can be stated, that groundwater in the Vistula River Delta is of moderate quality, especially due to high concentration of iron compounds. The highest quality is observed in western part of the delta, close to the edge of the upland, and also in the southern part. Groundwater is of HCO_3-Ca and HCO_3-Ca-Na type.

Table 8

Concentrations of chosen hydrogeochemical parameters and ranges of hydrogeochemical background in groundwater from Pleistocene aquifer in Vistula River Delta

Hydrogeochemical parameter		Concentrations range	Hydrogeochemical background
Total hardness	[mval dm^{-3}]	0.5–5.7	3–5
pH	[–]	7.2–8.4	7.3–8.0
Sulphates	[mg SO_4 dm^{-3}]	0–100	5–50
Chlorides	[mg Cl dm^{-3}]	0–120	2–20
Iron	[mg Fe dm^{-3}]	0–9.1	0.5–3.0
Manganease	[mg Mn dm^{-3}]	0–0.2	0.05–0.15
Fluorides	[mg F dm^{-3}]	0–4.58	0–0.6
Ammonia	[mg NH_4 dm^{-3}]	0–8.7	0.1–0.75
Nitrates	[mg NO_3 dm^{-3}]	0–0.23	0–0.1

Characteristic feature of the groundwater is high iron compounds concentration. Hydrogeochemical background was determined as 0.5–3.0 mg Fe dm^{-3}, but the maximum values reach 9.1 mg Fe dm^{-3} in Roszkowo and 8.5 mg Fe dm^{-3} in Przegalina and Wocławy. Manganease concentrations are also high: up to 0.2 mg Mn dm^{-3} in Przegalina, Roszkowo and Lipce.

In longitudinal zone running from Tczew to the Bay of Gdańsk, fluride ion concentrations are increased. In some places the amount of fluorides reaches 4.58 mg F dm^{-3} in Suchy Dąb and 2.8 mg F dm^{-3} in Cedry Wielkie. In this zone, a few kilometers wide, the ascent from Creatceous aquifer takes place [7]. Total hardess of the groundwater decreases to 0.5–1.5 mval dm^{-3}, so does calcium concentration; instead, sodium ammount increases up to 233 mg Na dm^{-3}. Elevated amounts of fluoride ions are strictly connected with fluoride anomaly occurring in Cretaceous aquifer. Hydrogeochemical background for fluorides has been determined as 0–0.6 mg F dm^{-3}.

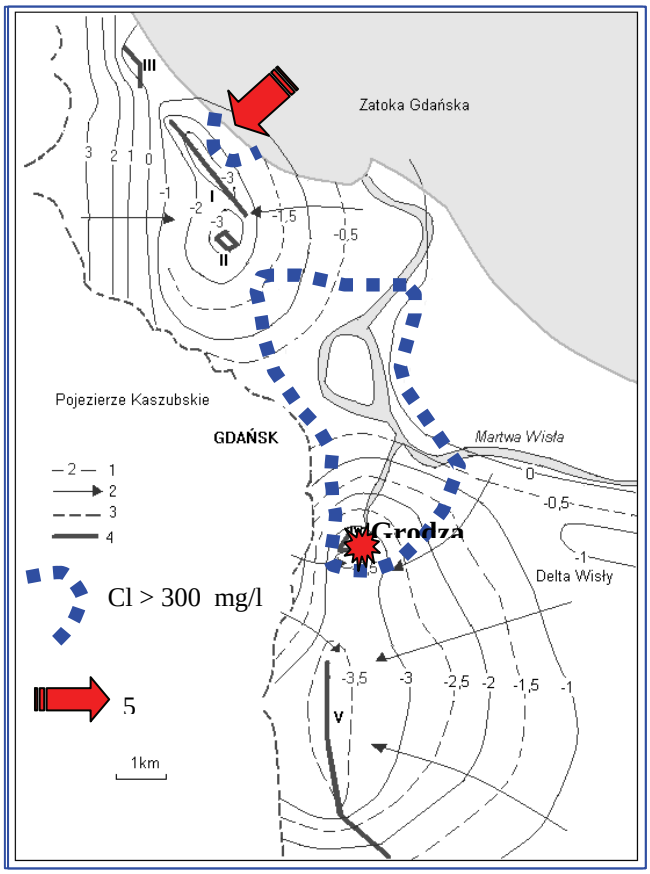

Fig. 4. Map of groundwater contour lines in 1985 with marked zones of salt water intrusion [8]:
1 – hydroizohipsies, 2 – directions of groundwater flow,
3 – upland edge, 4 – groundwater intakes, 5 – directions of salt water intrusion

In northern and north–eastern part of the Vistula River Delta elevated concentrations of chlorides are observed, reaching values about 100 mg Cl/dm^3 (Przegalina, Cedry Wielkie and Kiezmark). The origin of the chlorides is connected with the period of delta forming and remaining of young fossil water in the aquifer. Describing chloride ion concentrations in the Pleistocene aquifer of Vistula River Delta it is necessary to remind a past problem of salt water intrusion. In 70-ties and 80-ties of the previous century salt water from Martwa Wisła River and port channels intruded to the main usable aquifer exploited by wells of Grodza Kamienna intake. The salinity reached the concentration 2000 mg Cl dm^{-3}; in consequence the groundwater intake had to stop exploitation. The reason of the intrusion was overexploitation of the aquifer lasting for many years. In the period 1972–1982 the intake output exceeded the admissible volume of extracted groundwater determined as 800 m^3 h^{-1}. Fig. 4 shows ranges of depression cones developed in the period of the highest exploitation (1985) both on the area of Vistula River Delta and also on the marine terrace. It is clearly

visible, that the hydrodynamic conditions could have provoked salt water intrusion to the aquifers.

It should be added, that northword from Grodza Kamienna, numerous industrial intakes exploiting water from Pleistocene aquifer, had to be stopped because of high amounts of chloride ion appearing in the extracted water. Even before 1970, concentrations were 500–700 mg Cl dm^{-3} (meat plant, fish plant, dockyard, grease plant etc.) and in some places (e.g. intake for gas-works) reached the value 2000 mg Cl dm^{-3}. Consecutive excluding the intakes from exploitation resulted in quick flow of the saline water towards the wells of Grodza Kamienna. At the beginning of 90-ties of XX century the exploitation in the whole region has been considerably lowered, which resulted in recovery of the aquifer. Current analysis of groundwater taken from observation wells surrounding Grodza Kamienna intake show low concentrations of chlorides: 40–50 mg dm^{-3}. This can be evidence of high groundwater renewal in the Gdańsk region.

4.3. CONCLUSIONS

Groundwater in the Gdansk aquifer system is generally of good quality. The hydrochemical types differ between the aquifers, but HCO_3–Ca type is dominant. This type is characteristic for Pleistocene deposits in the Kashubian Lake District where natural chemical composition is preserved and also for Paleogene-Neogene aquifer. Groundwater from Cretaceous deposits in part of the region is also HCO_3–Ca but the dominant type seems to be HCO_3–Na. An increased amount of chlorine ion causes change of type into Cl–HCO_3–Na or Cl–Na in some places. A specific component occurring in water from Cretaceous aquifer is fluoride ion. Its concentration in western part of Vistula River Delta reaches the value 4–5 mg dm^{-3}. In some areas an increased amount of ammonia nitrogen and hydrogen sulphide is also observed.

Pleistocene aquifer in the discharge zone is often changed due to antropopression and the type HCO_3–SO_4–Ca and HCO_3–SO_4–Cl–Ca appears there. The main reason for the changes is connected with the processes provoked by uneven and intensive exploitation and also with salt water intrusion. In some places contamination from the surface appears. As a result an increased amount of sulphates, chlorides, ammonia nitrogen and sometimes nitrate nitrogen is observed. Occasionally organic micro–compounds and other trace contaminants appear in groundwater. Generally the water is of good quality and meets the standards for drinking water. Only iron and manganese concentrations and also in the Vistula River Delta – ammonia nitrogen, exceed the limits. In order to preserve good quality of groundwater it is very important to exploit it in a rational way, protect the aquifer from contamination, especially on the marine terrace, where the Pleistocene aquifer is unconfined and also to maintain groundwater monitoring. The quality monitoring must include investigations of microcompounds, appearing sporadically in the discharge zone of the Pleistocene aquifer.

References

[1] Balcer M., Jankowski M., Walczak M.: Dokumentacja zasobów dyspozycyjnych wód podziemnych zlewni Redy, Zagórskiej Strugi i Piaśnicy. Przedsiębiorstwo Geologiczne POLGEOL w Warszawie, Zakład w Gdańsku, p. 149 (maszynopis), 2004.

[2] Górski J.: Kształtowanie się jakości wód podziemnych utworów czwartorzędowych w warunkach naturalnych oraz wymuszonych eksploatacją. Instytut Kształtowania Środowiska Warszawa, p. 142, 1981.
[3] Jaworska-Szulc B., Pruszkowska M., Przewłócka M.: The Changes of Groundwater Quality on the „Czarny Dwór"Intake in the Light of Polish-Swedish Investigations. VII Int. Symp. Wtar Management and Hydraulic Engineering, 2003, Podbanske, Slovakia, p. 151–158, 2003.
[4] Jaworska-Szulc B.: Odnowa zasobów górnokredowego piętra wodonośnego w rejonie Gdańska [Groundwater resources regeneration in Cretaceous aquifer – Gdansk region] Inzynieria Morska i Geotechnika, r. 28 no 1/2007.
[5] Kleczkowski A. S.: Kształtowanie chemizmu czwartorzędowych wód podziemnych Krakowa 1870–2002; Tendencje dalszych zmian. AGH Kraków, p. 131, 2003.
[6] Kozerski B.: Groundwater resources of Gdansk region. Groundwater resources utilization and contaminant hydrogeology. International Groundwater Symposium. Montreal, Quebec, p. 116–124, 1984.
[7] Kozerski B., Macioszczyk A., Pazdro Z., Sadurski A.: Fluor w wodach podziemnych w rejonie Gdańska. Ann. Societ. Geol. Poloniae, vol. 57, p. 349–374, 1987.
[8] Kozerski B., Kwaterkiewicz A.: O zmianach zasolenia wód podziemnych czwartorzędu Gdańska. W: Współczesne Problemy Hydrogeologii, T. VIII, WIND-J Wojewoda Wrocław, p. 345–347, 1997.
[9] Kozerski B., Jaworska-Szulc B., Pruszkowska M., Przewłócka M.: Wysladzanie sie wod podziemnych w pietrze czwartorzedowym Gdanska jako rezultat zmniejszonego poboru [The groundwater desalinization in the quaternary aquifer in Gdansk as a result of decreasing exploitation]. In: Wspolczesne problemy hydrogeologii. T. XII Torun: Wydaw. UMK [in Polish] 2005.
[10] Kozerski B., Jaworska-Szulc B., Pruszkowska M., Przewłócka M.: Gdański system wodonośny, Wyd. Politechniki Gdańskiej 2007.
[11] Lidzbarski M.: Chemizm wód podziemnych Pradoliny Kaszubskiej. W: Współczesne Problemy Hydrogrologii, T. IX, Kielce 1999.
[12] Olańczuk-Neyman K., Prejzner J., Bray R., Mierzejewska K., Tarkowska D., Wargin A.: Opracowanie o przyczynach pojawienia się siarkowodoru i jonu amonowego w wodach piętra kredowego Subniecki Gdańskiej. Arch. Wydz. Inżynierii Środowiska Polit. Gdańskiej (maszynopis), 1996.
[13] Olańczuk-Neyman K., Pruszkowska M., Wargin A.: Chemical and bacteriological quality of ground water of Cretaceous formation in Gdańsk region. W: Proceedings International Symposium „Water Management and Hydraulic Engineering". Dubrownik, Croatia, vol. 2, p. 349–358, 1998.
[14] Olańczuk-Neyman K.: Mikroorganizmy w kształtowaniu jakości i uzdatnianiu wód podziemnych. Monografie Komitetu Inż. Środowiska PAN, vol. 1. Gdańsk: Wyd. Politechniki Gdańskiej 2001.
[15] Pruszkowska M., Wargin A.: Ocena przyczyn zmian jakości wód podziemnych z utworów kredowych w regionie gdańskim. W: Współczesne Problemy Hydrogeologii, T. XI, cz. 2, Gdańsk, p. 265–271, 2003.
[16] Pruszkowska M.: Hydrochemia wód podziemnych z utworów czwartorzędu Pojezierza Kaszubskiego [Hydrochemistry of Quaternary groundwater in Kashubian Lake District]. Seria Monografie Politechniki Gdanskiej, nr 51, 2004.
[17] Przewłócka M.: Zmiany zasolenia na ujęciu „Czarny Dwór" w świetle eksploatacji czwartorzędowego poziomu wodonośnego. Współczesne Problemy Hydrogeologii, t XI, cz. 2, Gdańsk, p. 273 – 280, 2003.
[18] Przewłócka M.: Ocena zmian jakości wód podziemnych piętra czwartorzędowego Gdańska w świetle ich poboru [Evaluation of groundwater quality changes in Quaternary aquifer in the region of Gdańsk] Gdansk University of Technology, p. 207, 2004.

[19] Przewłócka M.: Zmiany stężeń siarczanów w wodach podziemnych piętra czwartorzędowego Gdańska na Tarasie Nadmorskim. W: Współczesne Problemy Hydrogeologii, T. XII, Toruń 2005, p. 563–568, 2005.
[20] Ratajczak T., Witczak S.: Mineralogia i hydrogeochemia żelaza w kolmatacji filtrów studziennych ujmujących wody czwartorzędowe. Zesz. Nauk. AGH, Kraków, nr 29, p. 129, 1983.
[21] Sadurski A.: Warunki hydrogeochemiczne utworów kredowych w rejonie Gdańska. Kwartalnik Geologiczny, T. 29, no 2, p. 405–418, 1985.
[22] Sadurski A.: Hydrogeological evolution of the Upper Cretaceous artesian basin of the Gdansk region. Ann.Soc. Geol. Pol. vol. 56, p. 143–161, 1986.
[23] Sadurski A.: Górnokredowy system wód podziemnych Pomorza Wschodniego. Zesz. Nauk. AGH, Kraków, nr 46, p. 140, 1989.
[24] Witczak S., Adamczyk A.: Katalog wybranych fizycznych i chemicznych wskaźników zanieczyszczeń wód podziemnych i metod ich oznaczania. T. II, Bibl. Monitoringu Środowiska, PIOŚ, Warszawa. 448 s, 1995.

5 The Relationships and Interactions of Transboundary

Jozef Kriš, Ivona Škultetyová, Stefan Stanko (Faculty of Civil Engineering of the Slovak University of Technology in Bratislava, Department of Sanitary and Environmental Engineering)

5.1. INTRODUCTION

Water is one of the most important elements of landscape and it is essential for human society. Water is the most widespread substance in the nature and fundamental for life on the Earth. A significant feature is that the water is renewable resource dependent on water cycle in the nature (in contrast to other resources such as fossil fuels which is non-renewable). Water resource can be any part of water cycle in the nature where surface water or ground water is present in technically and economically usable form (e.g. watercourse, water reservoir, spring, well, etc.). Concerning occurrence, usability, protection and assessment we distinguish between surface water and ground water resources. The relationships among the number of population, development trends, hydrological cycle and actual available fresh water resources show the pressure that increases with demand for availability of water resources all over the world. In many regions of the world the demand for water and available water resources can lead to political conflicts.

Water does not recognize state borders and as a shared resource it requires international cooperation. Water resource management should be implemented within the natural river basins and not within the political boundaries.

Mentioned problem can also be seen in our region of the Central Europe. The impact of anthropogenic activity (reducing forest areas, land use, urbanization, increase of impermeable surfaces, reduction of alluvial forests, wetlands, etc.) proves the fact that the trend to control water resources prevails over reasonable use of water also in our region. The present conditions of drinking water supply, wastewater collection and treatment in Slovakia falls behind the level of developed countries in Europe and the world and it forces us to search for ways how to get closer to these trends and objectives.

5.2. RIVER BASIN DISTRICTS IN SLOVAKIA

The area covering 96% of the Slovak territory belongs to the Black Sea Basin. The area of the Danube River Basin in Slovakia is 47 064 km^2 including sub-basins of lower Morava (2 282 km^2), Danube (1 138 km^2), Váh (14 268 km^2), Nitra (4 501 km^2), Hron (5 465 km^2), Ipeľ (3 649 km^2), Slaná (3 217 km^2), Bodva (858 km^2), Bodrog and Tisa (7 272 km^2) and Hornád (4 414 km^2). Water flows from the rest of the territory (4%) into the Baltic Sea. The total area of the Poprad and Dunajec sub-basin is 1 950 km^2. The total length of streams in Slovakia is 49 775 km. The average density of river system is 1.1 km km^{-2}.

The state borders of Slovakia with five neighbouring countries mostly do not pass along the boundaries of hydrological units (watershed divides, fall lines, streams) in most cases. Some large rivers, namely Danube (flows from Austria), Tisa (from Hungary), Morava (from the Czech Republic) and Dunajec (from Poland), flow through the boundary regions of our country. Long-term average discharge of rivers in Slovakia is approximately 3 328 $m^3 s^{-1}$ (including tributaries from neighbouring countries) where only 398 $m^3 s^{-1}$ rises in our territory (12 %).

The following water volumes (expressed as long-term average discharge) flow into the territory of Slovakia through the inflow boundary profiles:

— from the territory of Poland – about 39 $m^3 s^{-1}$ by the Dunajec and Poprad rivers and their tributaries,
— from Ukraine – about 58 $m^3 s^{-1}$ by the Uh and Latorica rivers,
— from Hungary – about 379 $m^3 s^{-1}$ mainly by the Tisa River and left tributaries of the Ipel' River,
— largest volumes flow by the Danube River from Austria – about 1 976 $m^3 s^{-1}$ in total,
— from the Czech Republic – about 62 $m^3 s^{-1}$ mainly by the Morava River and other smaller rivers.

The total discharge is 2 514 $m^3 s^{-1}$, i.e. 86 percent.

The long-term average run – off from the territory of Slovakia (expressed as discharge) is 2 912 $m^3 s^{-1}$.

5.3. SPATIAL AND TEMPORAL DISTRIBUTION OF GROUNDWATER RESOURCES IN THE SLOVAK REPUBLIC

Groundwater resources of Slovakia are distributed very unevenly. Their quality and possibility to exploit them are given by the characteristics of geological formations, their surface distribution, thickness and permeability of rocks that create more or less favourable conditions of hydro-geological structure for occurrence and accumulation of groundwater. Available volumes of groundwater represent maximum amount of groundwater that can be abstracted from a given water system for water supply during whole planned period of exploitation. The use of groundwater resources is considered at acceptable ecological, technical and economic conditions without the influence of natural runoff that can be regarded as unacceptable and without unacceptable water quality deterioration.

The qualitative assessment of natural groundwater serving as a basis for determining available supplies is a fundamental problem in assessment of available groundwater resources. Natural groundwater resources are 146.7 $m^3 s^{-1}$ in average (source: Slovak Hydrometeorological Institute, 2010), out of which documented available resources represent 51.6%. Available groundwater resources are located mainly in the areas with large permeable aquifers where significant amounts of groundwater can be abstracted by smaller number of intake structures. These are usually alluvial deposits of large rivers with thick layers of gravel-sands and very good porosity and permeability. In mountain regions there are many available resources located in zones with crevice-carstic permeability of main aquifer. These are zones formed by limestone and dolomites. More than 80 percent of all available resources are found in Quaternary and Mesozoic structures of Slovakia.

On the other hand, zones with poor permeability of aquifers have low number of available resources. These are zones formed mainly by paleogenic flysch sediments, neogenic

clay sediments, crystallinic formations, vulcanites and some mesozoic rocks of low permeability such as claystone. Unfavourable situation is improved in some locations by drainage of tectonic zones where higher accumulation of groundwater occurs and significant resources are formed. Most of resources are diffused and suitable only for local use.

The total available groundwater resources of Slovakia are represented by the total number of resources approved by the Sub-committee for Classification of Resources and Supplies. This number is defined based on documented amounts resulting from hydrological researches and surveys. Available groundwater resources of Slovakia were 76 748 l s^{-1} according to data of the Slovak Water Management Balance as of December 31, 2006.

The total capacity of groundwater resources managed by water companies and municipal authorities was 27 713 l s^{-1} in 2000. However, only 42% out of this capacity is used for drinking water supply.

5.4. WATER QUALITY

Industrial and agricultural activities on both sides of the borders give rise to long-lasting problems with quality of water resources. There are localities known for the presence of contaminants such as NO_3, NH_4, PO_4, pesticides and other. It is important to solve these problems in a short-time perspective to eliminate further contamination of water resources on both sides of the border.

There are several guidelines for protection and management of these water resources, e.g. Directive on the protection of groundwater against pollution (2006/118/EC), Directive 91/676/EEC concerning the protection of groundwater against pollution caused by nitrates and the Directive 91/414/ECC concerning the placing of plant protection products on the market. Many other directives provide instructions for users for example how to use the areas inside the protection zones of water-supply resources, etc.

Basic measures for protection of water resources are as follows:

— preservation of unspoiled environment,
— regulation of groundwater abstraction,
— increase in retention capacity and erosion protection measures,
— change of land use pattern in catchment area,
— protection of infiltration areas,
— increase in retention capacity of forest ecosystems,
— other measures.

5.5. INTERNATIONAL COOPERATION IN WATER MANAGEMENT SECTOR

5.5.1. Cooperation on Transboundary Rivers

International cooperation of the Slovak Republic in water management sector is done through cooperation on transboundary waters. This cooperation is in accordance with the Convention on the Protection and Use of Transboundary Watercourses and International Lakes UNECE (Helsinki Convention), the Convention on the Cooperation in Protection and Sustainable Use of the Danube River and many other agreements or conventions. The cooperation with neighbouring countries results from agreements and treaties concerning the

cooperation on transboundary waters. The treaties were signed also in the past. Later they were reviewed and followed by new treaties and agreements with regard to establishment of new countries (Slovakia, Czech Republic) and changes in approach to given problems.

Bilateral agreements were signed with neighbouring countries (with Poland, Ukraine, Hungary, Austria and the Czech Republic). In the region of the Poprad and Dunajec River Basin, the Agreement between the Government of the Czechoslovak Socialistic Republic and the Government of the Peoples Republic of Poland of October 3, 1986 on fisheries in transboundary waters is still in effect and it was recognized within the succession of international treaties. In 2001, the new Agreement between the Slovak Republic and Poland on fisheries in transboundary waters was signed.

The Joint Committees on Transboundary Waters were established in accordance with the treaties and agreements. These committees discuss all water management measures implemented in transboundary waters at annual meetings. The committees carry out measurements, marking and identification of the state borders. Moreover, they cooperate in regulation of stream channels to prevent shift and change of the state borders as well as damage of signs used for demarcation of the state border. International cooperation is mainly aimed at the following:

— warning and forecasting hydrological service,
— maintenance and training of watercourses, change of water regime,
— stabilization of state borders,
— protection against floods, risen levels of reservoir water and dangerous ice run,
— construction of hydraulic structures affecting changes in runoff ratios,
— use of transboundary waters – abstraction for economic purposes, utilization of water for navigation, use of hydropower potential and use of water for recreation and sports,
— ecologization of water resources including water quality monitoring and measures for protection of water from accidental pollution,
— emergency information service,
— measures for emergency water quality deterioration and emergency hydrological events, including warning system,
— abstraction of surface water and groundwater,
— discharge of wastewater and other types of water,
— protection of surface water and groundwater against pollution; maintenance and improvement of their quality,
— protection zones of water-supply resources,
— amelioration measures,
— use of water power,
— exploitation of sands, gravel sands, stones and other materials from river beds,
— measurements and monitoring, their evaluation and result Exchange,
— water management planning and balance,
— protection of aquatic and litoral habitats,
— protection of transboundary waters as a part of environment,
— other water management measures.

The committees on transboundary waters carry out the monitoring of quality and quantity of transboundary groundwater resources.

Experience in this field is not sufficient compared to surface waters. Moreover, no bilateral agreements on groundwater use are signed between neighbouring countries. Today,

the solutions to problems such as declared areas (bodies) are sought. These problems also include the following:

— use of dynamic water resources (water flow direction, regulations for sampling, etc.),
— potential impact on use of these waters (protection, pollution, methods of contamination removal etc.),
— regulations for their use,
— information exchange methods,
— ecologization of water resources (quality monitoring) and measures in case of accidents,
— emergency information service etc.

Another problem is geothermal water located in transboundary bodies (for instance the Slovak-Hungarian Region). Geothermal water can have larger zone (area) compared to surface and ground water resources. The official talks in this field have begun with the Czech Republic and Hungary.

5.5.2. Present activities of the Slovak Republic Related to use of Transboundary Groundwater Resources

Transboundary activities also include the development of case studies within the cooperation between Slovakia and Poland. For groundwater monitoring in the boundary region between Slovakia and Poland, the experts from both countries provide performance of the tasks under the WFD requirements.

At present, the assessment of quantitative status and chemical status of the groundwater bodies is carried out for the river basin management plans by 2010. Unless the mentioned plans are completed, no transboundary groundwater body will be identified in the boundary region of Slovakia and Poland.

The following activities are in progress:

— localization of sites for groundwater quality and quantity monitoring in 2007 including cartographic coordinates of monitoring objects and depth of wells;
— monthly averages of groundwater quantity monitoring for 2007;
— complete analyses of groundwater quality monitoring carried out in 2007;
— localization of sites for groundwater quality and quantity monitoring in 2008 including cartographic coordinates of monitoring objects.

The first programmes and experience exchange from the cooperation on transboundary groundwater supporting the use of transboundary zones of groundwater have begun in 2006 within the INTERREG Programme. These waters are of interest to Slovakia, Hungary and Ukraine. The activities within the ENWAT programme with participation of the Hungarian Geological Institute and the Geological Institute of the Slovak Republic include development of several documents such as hydrological maps, characteristics of groundwater and aquifers, contamination index, groundwater pH value, total mineralization, and distribution of arsenic, chlorides, hydrogen carbonates, nitrogen, sodium, nitrates and pesticides. The Slovak experts make an effort to achieve similar objectives for all transboundary waters. The general objective of the project is to improve qualitative and quantitative parameters of groundwater in transboundary bodies by 2015. The main goal was aimed at the development of integrated geological, hydro-geological and environmental geo-information system, which should serve as useful and supporting tool in the WFD implementation in both countries and it should be the basis for further activities in respective regions related to ground-

water and environment. Detailed information on the project is available on the website (www.enwat.eu). The activities with Austria are currently focused on the assessment of groundwater in the Hlideboden groundwater body in the region of Pama. These activities include monitoring of hydro-geological structures of bedrock, measurement of well capacity together with short-term pumping for identification of biochemical composition of groundwater. In addition, there are activities aimed at monitoring of groundwater quality and quantity in the right boundary region of the Danube River between Wolfstahl and Petržalka near the municipality of Berg. This groundwater resource is influenced by water levels of the Danube River and other factors. The survey in particular regions provides relevant and the most current information on quality and quantity of groundwater bodies and helps experts and public in decision-making process. The results of the joint project should improve the quality of life in assessed transboundary regions. The effort of the projects is to solve all problems related to water management in particular regions. The project results will be useful in protection and efficient management of groundwater to assure the resources for public water supply. Moreover, groundwater resources will be important element of protected areas. The outcomes can be also used as a basis for other projects with similar scope providing that the plans for groundwater quality exchange will be observed. Finally, the results of the project should be used in proper monitoring and use of groundwater resources and relevant groundwater bodies in transboundary regions.

5.6. CASE STUDY

The case study deals with the training of certain stretch of the Morava River which forms the state border between Slovakia and Austria. Although this study solves the problem with discharges, sediments and river bank regulation, it also has direct influence on the quality of water along the river banks on both sides of state border.

The name of the project is „Measures for regulation of river banks and cross sections as well as measures for connecting the meanders of the Morava River at the river stretch Marchegg (rkm 15 –25).

The objectives of the project submitted for approval are as follows:

— increase in smooth development, reduction of vertical alignment gradient,
— increase in occurrence of bank overflows,
— support of groundwater recovery (groundwater production),
— recovery (production) of side waters (= trenches improving conections with the Morava River),
— improvement of hydrology of side waters,
— formation of bank structures in accordance with natural channel patterns,
— increase in bank slopes with compact riparian stands,
— structures for low water levels.

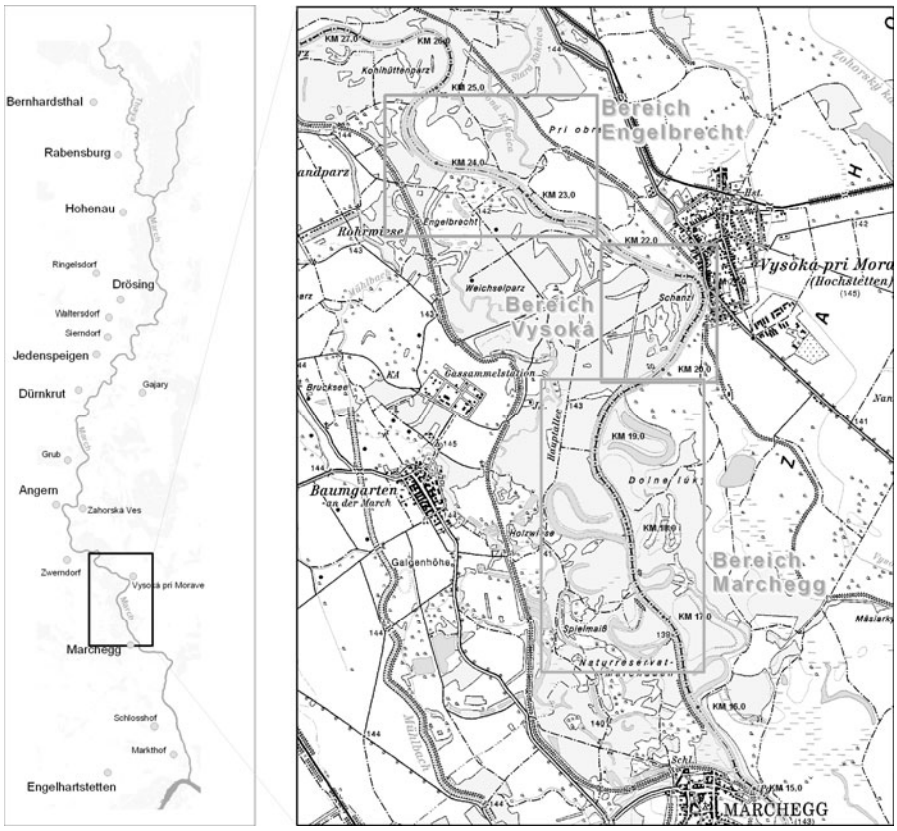

Fig. 1. Map of structure location

Time interval for construction works in the area of Austrian river bank was planned from the half of June to the end of September 2002. Flood caused that construction works had to be interrupted from the half of August to the beginning of September 2002. Already implemented measures were not affected by the flood. Deadline for finishing the construction works (30 March 2003) given by water legal decision was met. Construction works were smooth and the weather was favourable in July and September 2002 and therefore most construction sections were completed sooner than it had been planned while roads and land properties were disturbed minimally. After completion of construction works the disturbed areas were returned into original condition in line with the order. Tree selection for cutting down as well as specification of most suitable access roads and transport roads were made in cooperation with the water legal building supervision. The emphasis was put on showing as much consideration as possible towards surrounding territory of floodplain forest. In connection with individual measures it is necessary to say that construction works at both banks of river were basically implemented in line with the project with legal permission. Tiny deviations originated mostly due to more practical construction or optimal adjustment to local conditions and were discussed among water legal, local and ecological building inspectors.

It can be said that during construction works in line with the project the water legal conditions were satisfied and the expected result was achieved through taken measures.

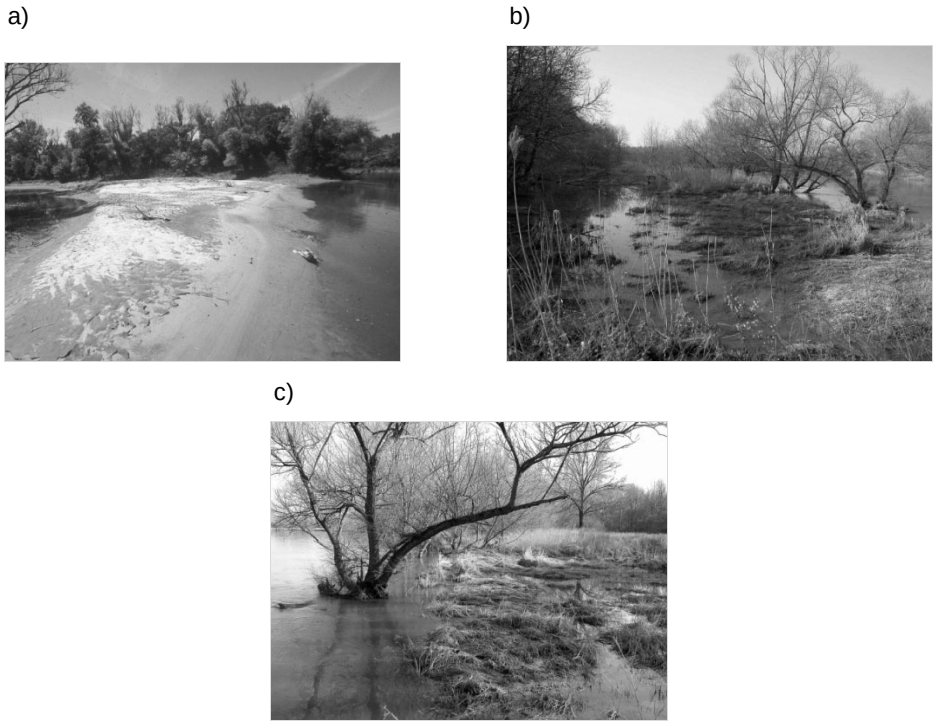

Fig. 2. Views on the interest territory: a) view on the river bank, b) meander mouth, c) decrease of the river bank line – flooded mould

5.7. CONCLUSION

Waters do not respect the borders of countries. They had been created according to their own logic long time before the states with their borders were established. Establishment of new states is an ongoing process and we are also witnesses of dividing larger states in smaller ones with all attributes that sovereign state should have. Water as a fundamental element of life may also give rise to conflicts and tension between neighbouring countries mainly due to water shortage. Therefore, it is important to foresee and solve such problems to prevent the risk of international conflicts.

Issues related to use of transboundary waters are very topical and important. The world's 263 transboundary lake and river basins cover 45 percent of the Earth's land surface including 40 percent of the world's population. Many of them are situated on the territory of more than two countries. The Danube River flows through 18 countries and in each border area it creates natural surface and ground water environment which can become the source of conflict between countries in utilizing these waters. It is high time to solve also these problems; otherwise, they can lead to different kinds of crises.

Slovakia experienced some problems related to transboundary waters. Currently, this issue is very important in negotiations on use of groundwater in transboundary regions. It is

very important to foresee and solve problems to the satisfaction of all involved countries. Transboundary groundwater quantity and quality monitoring together with surface waters is in the competence of the committees on transboundary waters. The experience in the field of groundwater is not such considerable compared to surface water. So far, no bilateral agreements on transboundary groundwater use have been signed.

References

[1] Good Ground Water Quality and Quantity www.vuvh.sk/rsv/docs/dobry_stav_vod.pdf (in Slovak).
[2] General Plan of Protection and Rational Use of Water, 2nd Edition, Bratislava 2002 (in Slovak).
[3] Quantitative Water Management Balance in 2006 – Part "Groundwater", Bratislava 2007 (in Slovak).
[4] Proposal – A Plan of Public Water Supply Systems for the Region of Prešov (in Slovak).
[5] Proposal of River Basin Management Plan – Water Act ww.vuvh.sk/rsv/docs/vec.cas.harm (in Slovak).
[6] Overview of Significant Water Management Problems/Implementation of the Directive 2000/60/EC of the European Parliament and of the Council establishing a framework for the Community action in the field of water policy. WRI Bratislava, August 2008 (in Slovak).
[7] Projekt der Wasserstraßendirektion "Measures for Regulation of River Banks and Cross Sections as well as Measures for Connecting the Meanders of the Morava River at the river stretch Marchegg (rkm 15 – 25)" The Report of Water Legal Building Inspection, September 2008 (in Slovak).
[8] WFD – Water Framework Directive www.vuvh.sk/rsv/ (in Slovak).
[9] Report on Water Management in the Slovak Republic in 2009, Bratislava 2010 (in Slovak).
[10] www.inwater.org/worldwaterday/
[11] www.unwater.org/worldwaterday/about.html
[12] www.unwater.org/worldwaterday/fags.html
[13] www.all-/n.sk/enwat/dvd/kras.html

Acknowledgements

The article was written with the support of the Scientific Grant Agency – project VEGA no. 1/1143/11 dealt with at the Department of Sanitary and Environmental Engineering of the Slovak University of Technology.

6 Elaboration of CRR model for Saturated Soil on the Example of Flood Wave on Botonega Catchment

Duška Kunštek, Kristina Potočki, Ivana Carević (University of Zagreb, Faculty of Civil Engineering, Department for Hydraulic Engineering and Water Resources, Zagreb)

6.1. INTRODUCTION

Engineering practice often requires assessment of catchment runoff for which the water gauging data do not exist or are insufficient. For that purpose the conceptual parameter models are used with input – rainfall and output-runoff, generally called CRR models ("Conceptual Rainfall – Runoff Models"). CRR models are characterized by many climatic, physical and geographic parameters, which describe and modify the description of the runoff process with the value modification [1]. The relationship between precipitation and runoff is defined by a system where physical processes mostly affect the input values transforming them into the output values. In mathematical terms, it refers to the equation system and appertaining algorithm describing the structure and behavior of the system. The limitations of the CRR model are connected to the lack of knowledge of hydrologic system operation and the complexity of calculations within the hydrologic field. Therefore, the CRR models use many simplifications for the purpose of presentation of the catchment hydrology [2, 3].

The CRR mathematical model for water runoff in thin layer over the water saturated catchment surface is made for the catchment of the Botonega storage basin in Istria. When a flood wave occurs on saturated catchment due to heavy and long precipitations, the peak runoff occurs fast, i.e. catchment lag time is short and retention effect is small (almost none). This hypothetical state considered by the CRR mathematical model is the closest to the state when the extreme flood waves occur. The model calibration is conducted by comparison with the HEC-HMS model, which was made precisely for such climatic state – the state of complete soil saturation, minimum losses and occurrence of short-lasting extreme precipitations. The model validation is made on the example of the flood wave which occurred on 21–24 October, 1993. In all other cases of flood wave occurrence in different climatological conditions, when the dry period with the soil partly or completely unsaturated preceded the event, the retention effect of the catchment cannot be neglected. For such purposes, the model was corrected so that the catchment retention effect is covered by the coefficient of the reduced water flow velocity in the initial hydraulic flow description over the catchment surface on one hand (applying the Chezy equation), and with the element of the water wave volume reduction by nonlinear reservoir on the other hand [4].

6.2. DATA

Conceptual parameter model is performed on the numerical example of the torrential stream of the Botonega catchment located in the central part of Istria for which there is a small data base regarding precipitations and catchment runoff hydrographs required for calibration and control of model operation. At the catchment outflow multipurpose surface

storage reservoir Botonega is situated (Fig. 1). The catchment area of the storage reservoir spreads on the area of 73.04 km^2, with height difference from 20 to 503 m a.s.l. Average catchment slope is about 16%. Relief is indented with a dense network of torrential streams flowing into the valleys: Dragućki, Grdoselski, Podmerišće and Račićki streams [4].

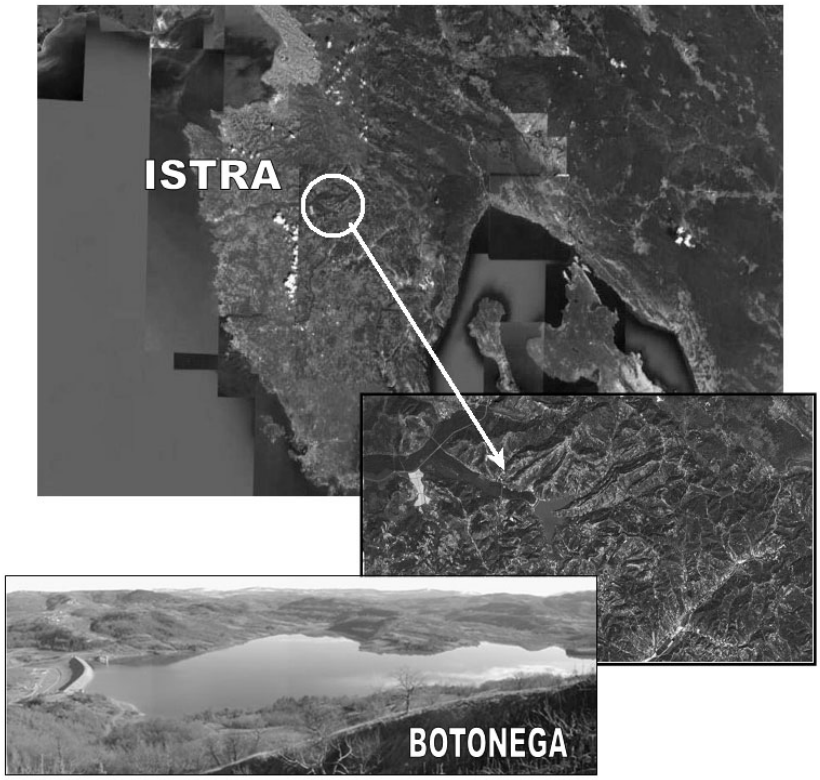

Fig. 1. Location of Botonega catchment and reservoir

For the purposes of model calibration, 8 rain events were taken. Measurements of water wave are provided on the barrier of the Botonega storage reservoir for the rain events. Pluviometric database has been provided for the Botonega station for relevant events in form of 5 minute precipitation by the Meteorological and Hydrological Service of Croatia. These precipitation events fall on the following dates:
21 – 24 October1993,
05 – 09 October 1998,
25 – 29 November 1990,
03 – 08 May 1987,
27 – 30 August 1989,
30 October – 11 November 2000,
07 –11 June 2002,
02 – 03 June 2003.

It should be mentioned that the measured inflow in the storage reservoir is in fact the result of water balance estimation and the reservoir storage. Therefore, the values of inflow

into the storage reservoir have been obtained based on the storage-elevation-discharge curves of reservoir, spillway and outlet. Five minute hyetographs for these precipitation events, for the 20–30% longer period than the duration of the event itself, i.e. 10–15% before and 10–15% after the duration of the event, were requested from the Meteorological and Hydrological Service of Croatia. Precipitation on the mentioned dates thus represents the input data for the CRR model, while the measured hydrographs are used for calibration of the hydrograph obtained through the CRR model.

6.3. CRR MODEL CONCEPT

With the purpose of determining hydrologic and hydraulic elements, the basin surface is defined in GIS through DEM model and it is covered with a discretization grid of 112 818 nodes at the distance of 25 m. Node carries all information about the catchments, which is contained in the field of 25 × 25 m and with the center point in the node. The CRR mathematical model concept consists of hydrological and hydraulic elements. Hydraulic elements of model determinate flow velocity on the ground surface. Hydrologic elements of model estimate water balance in each node of the discretization grid [4, 5].

6.3.1. Hydraulic Model of Surface Flow

Hydraulic elements of model determinate flow velocity on the ground surface. The flow on the terrain surface consists of a thin water layer covering a vast area while the flow in the bed consists of a very narrow water stream along the limited way.

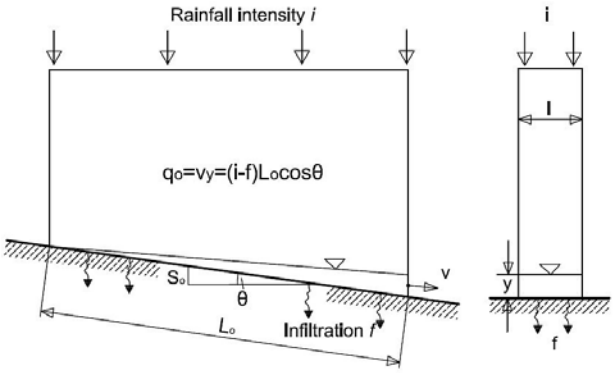

Fig. 2. Steady state flow over a homogenous surface of rainfall intensity *i*

Surface flow in the hypothetical water layer of shallow depth along the endlessly wide bed is idealized in the way so that the flat flow surface is superposed with a uniform fall vertically on isohypses [6]. Average water velocity can be then determined with the hydraulic expressions: continuity equation for incompressible steady state and dynamic equation.
Continuity equation for incompressible steady state flow along the catchment surface is equal to:

$$\iint_{c.s.} \mathrm{v}\,\mathrm{d}A = f \cdot L_o \cdot \cos\theta + \mathrm{v} \cdot y - i \cdot L_o \cdot \cos\theta = 0 \tag{1}$$

Where: i – rainfall intensity [mm/min],
f – infiltration [mm/min],
v – water velocity [m s^{-1}],
dA – area differential,
c.s. – control surface,
y – water column height [m].
θ – surface inclination angle,
L – surface flow path [m].

Discharge for the unit width q_o is equal to:

$$q_o = v \cdot y = (i - f) \cdot L_o \cdot \cos\theta \tag{2}$$

Supposing that the stream is uniform laminar flow on an inclined plane, from dynamic equation can be shown that the average velocity is equal to:

$$\mathrm{v} = \frac{g \cdot I_o \cdot y^2}{3 \cdot v} \tag{3}$$

Where: v – water velocity [m s^{-1}],
g – gravitational acceleration [m s^{-2}],
v – kinematic viscosity of fluids [ ],
I_o – bed bottom slope [%],
y – height of water column (water depth) [m].

Field studies of overland flow indicate that the flow is laminar but that the flow resistance is about ten times larger than for laboratory studies on uniform planes (Darcy-Weisbach friction factor for overland flow is in the range 20–200). The increase in flow resistance results primarily from the unevenness in topography and surface vegetation. When discharge turns into turbulent motion, the friction factor becomes independent of the Reynolds number and depends only on the surface roughness [6].
Manning's equation is used for turbulent flow and for infinite water bed:

$$\mathrm{v}_X = \frac{1}{n} \cdot y^{2/3} \cdot I^{1/2} \tag{4}$$

Where: v – water velocity [m s^{-}],
y – hydraulic radius (approximately equal to the depth of water layer) [m],
I – catchment surface slope [%],
n – Manning's roughness coefficient [m$^{-1/3}$s].

6.3.2. Hydrological Model of Surface Flow

Hydrological model is solved with water balance model for each individual cell [7]:

$$\frac{\Delta V(t)}{\Delta t} = Q_u(t) - Q_i(t) \tag{5}$$

where: $\Delta V(t)$ – state of the system or the volume of accumulated water in the interval t,

$Q_u(t)$ – water inflow into the system in the interval *t*,
$Q_i(t)$ – water outflow the system in the interval *t*.

Water balance is calculated for 1 minute time intervals: $t_1, t_2, \ldots, t_n$

When t_i is the observed time interval, then $t + \Delta t = t_{i+1}$ is the next time interval. Calculation of the height of water column in each cell of the discretion space in each interval is:

$$h_{new}(t + \Delta t) = h_{old}(t) - h_{runoff}(t + \Delta t) + h_{\inf low}(t + \Delta t) + h_{precip.}(t + \Delta t) \quad (6)$$

Where: $h_{new}(t + \Delta t)$ – height of water column in the interval $t + \Delta t$ in the observed cell of the discretion space,
$h_{old}(t)$ – height of water column representing the remaining water in the observed cell of the discretion space from the previous interval *t*,
$h_{runoff}(t + \Delta t)$ – height of water column that runs off from the cell of the discretion space in the interval $t + \Delta t$,
$h_{inflow}(t + \Delta t)$ – height of water column that inflows into the observed cell from the neighboring cells of the discretization space in the interval $t + \Delta t$,
$h_{precip.}(t + \Delta t)$ – height of water column of rain that falls on the cells of the discretion space in the interval $t + \Delta t$.

6.4. MATHEMATICAL RUNOFF MODEL

The states of hydrological system are described by state matrices while the physical processes that are active within the hydrological system are presented by transformations of matrix elements. The procedure of matrix transformation is presented by a non-linear algorithm, which describes the structure and behavior of the system at any moment and it is based on iterative procedure of meeting hydrological balance relations. Algorithm is written in the C++ language and some important parts of program routines are presented in the "pseudocode" record, which is recognizable and the same in all programming languages.

For the purpose of easier and more realistic presentation of the system of model matrices and their transformation on the non-linear algorithms, the matrices as to their structure are divided into two groups: matrices of model constants and matrices of model variables. Model constant matrices are: *incidence matrix* (spatial position of the cell in the discretion grid), *direction matrix* (shows the direction of runoff, Fig. 3), r*oughness coefficient matrix*, *surface slope matrix*, *flowpath length matrix* [4].

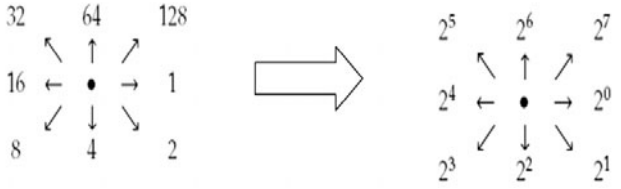

Fig. 3. Scheme of runoff direction from the observed point into the neighboring point

When determining matrix *models variables*, the procedure is carried out in several phases supposing that each cell (*i*, *j*) belongs to the catchment and that all above mentioned matrices of model constants are defined in the following sequence:

1. The height of water column (equation 6) is calculated within the observed computed time interval for each cell (i, j).
2. For each cell (i, j) for the first time increment, the value of the inflow (i, j) matrix is set to zero.
3. Based on the height of water column of the cell (i, j), *velocity* shall be computed applying the following formula:

$$velocity(i,\ j) = \frac{\sqrt{\left(\frac{h(i,\ j)}{1000}\right)^3} \cdot \sqrt{slope(i,\ j)}}{kh(i,\ j)} \tag{7}$$

4. Using previously computed *velocity* (step 3) and the methodology for obtaining the matrix *outflow* (i, j), over the *ratio* (i, j), for each cell the quantity of water that flows out of the cell (i, j) can be calculated.

$$ratio(i,\ j) = \begin{cases} 1, & \frac{path(i,\ j)}{s(i,\ j)} > 1 \\ \frac{path(i,\ j)}{s(i,\ j)}, & \frac{path(i,\ j)}{s(i,\ j)} \le 1 \end{cases} \tag{8}$$

$$\text{outflow}\ (i,\ j) = \text{ratio}\ (i,\ j) \cdot h(i,\ j) \tag{9}$$

5. There are two possible situations:
   a) If the cell is not on the border with the lake and if the flow direction from the cell (i, j) is into (r, s), then the quantity of water inflow (r, s) is increased by the amount of runoff (i, j).
   b) If the cell (i, j) is a part of the border with the lake, then the hydrograph ordinate of the previous moment is increased by the runoff (i, j) in the observed computing moment.
6. Return to the first step [4].

6.5. HEC – HMS MODEL

HEC – HMS model was developed with the HEC – GeoHMS model extension involving all essential physical characteristics of the catchment from GIS [8]. The Botonega catchment model in HEC – HMS is divided into 16 sub-catchments (Fig. 4).

The HEC – HMS uses separate calculation models for each runoff process component:

— model that compute runoff volume,
— models of direct runoff (overland flow and interflow),
— baseflow models,
— models of channel flow [9].

Computing method used in each model depends on available input data.

SCS Curve Number method is used for the runoff volume model. The previously obtained curve number taken over from the GIS spatial model for the mean soil moisture conditions, the so called BCN is used as input.

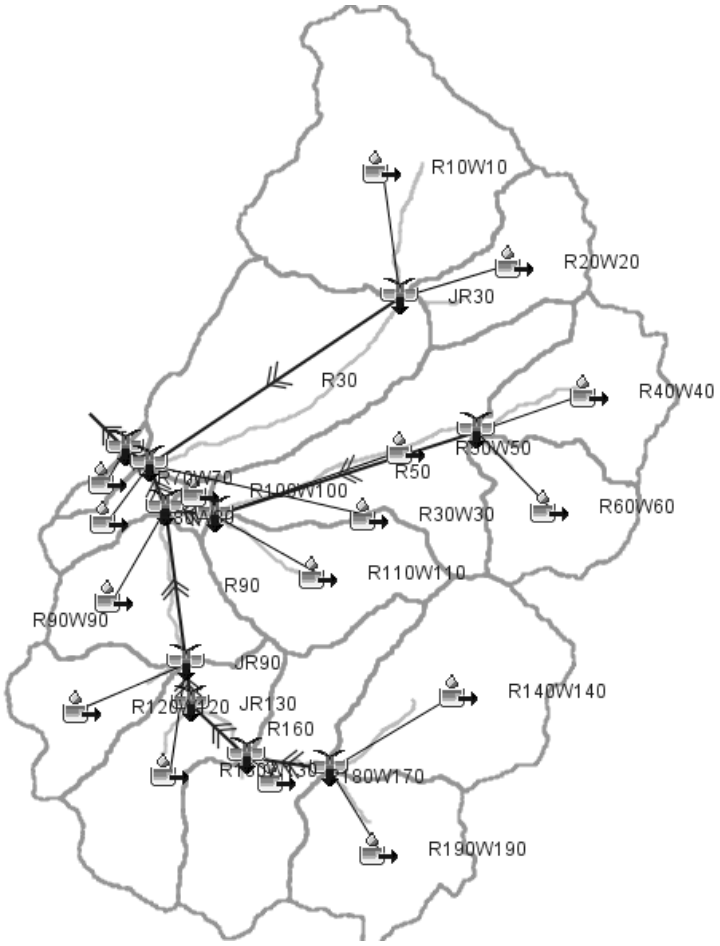

Fig. 4. The scheme of the Botonega catchment in HEC – HMS

The general idea is that the hydrological model obtained by the HEC–HMS be compared with the CRR mathematical model output i.e. – gross hydrograph in order to examine the reliability of its output results. Since the mathematical model was conceptually elaborated to compute the surface runoff without taking into consideration the previous moisture state of the soil and the losses, the BCN numbers (Table 1) which have been set according to the mean soil moisture, should be adjusted to the state of complete soil saturation. The CN number correction regarding antecedent soil moisture conditions was determined according to [10] and [11]:

$$_{SAT}CN = \frac{23 \cdot BCN}{10 + 0.13 \cdot BCN} \tag{10}$$

Where: BCN – curve number for average soil conditions (condition II),
$_{SAT}CN$ – curve number for the previous state of complete soil saturation (condition III).

Table 1

Input data for HEC–HMS runoff volume model

Sub-catchment	BCN	$_{SAT}$ CN
R100W100	75	87
R10W10	78	89
R110W110	87	94
R120W120	74	87
R130W130	73	86
R140W140	92	96
R180W170	80	90
R190W190	78	89
R20W20	78	89
R30W30	80	90
R40W40	74	87
R50W50	74	87
R60W60	73	86
R70W70	75	87
R80W80	78	89
R90W90	70	84

In this way, the loss calculation in the surface runoff of the hydrological model HEC–HMS is minimized, but does not equal zero, meaning that the rainfall from HEC–HMS model is real precipitation with minimum losses of gross precipitation. Consequently, the output hydrograph has a net value and the runoff volumes of HEC–HMS model output are always smaller than the volumes of output model hydrographs of CRR model, which use gross precipitations in calculations. Such a procedure is characteristic to all commercial specialist programs and cannot be changed structurally.

The direct runoff model uses the SCS unit hydrograph method. The catchment lag time (T_1) is used as the input parameter in the method. The lag time for the rain event is specified as time difference between the maximum measured hydrograph and the weight of hyetograph of the fallen gross precipitation, so that the model calibration was conducted considering the measured T_1 for each rain event (Table 2).

The Muskingum Cunge method is used for channel flow model. It is defined by the length of watercourse bed, Manning coefficient, bed bottom fall, and bed cross-section characteristics. The mentioned data were taken over into the model from the catchment spatial model.

The model of base runoff was not calculated due to unavailability of data necessary for its definition.

6.6. REVIEW AND ANALYSIS OF RESULTS OF CRR AND HEC–HMS MODELS FOR SATURATED SOIL

In addition to all of the above mentioned, the gross precipitation in the form of a hyetograph of rain events, for which model hydrographs have previously been calculated in the elaborated conceptual parameter model, is also entered into the HEC–HMS hydrological model as an input datum. The output hydrographs of the HEC–HMS model for the boundary points of the storage reservoir are compared to the CRR model hydrographs. Some of the results obtained through this comparison are presented (Fig. 5 to Fig. 10).

It can be concluded from the comparison of CRR model hydrograph and HEC–HMS model that the outputs from the models are comparable and very similar. Physical description of the runoff process is considered from the point of view of the maximum flow occurrence for the observed time base of total duration of runoff from 35 hours (02–03 June, 2003) to 80 hours (25–29 November, 1990). The maximum difference in occurrence of maximum flow is 2 hours. That means that the initial time of catchment concentration, the catchment time lag, the time of hydrograph rising and the flood wave duration are well modeled in CRR mathematical model. These are hydrological parameters calculated for the complete soil saturation, without the impact of previous saturation state or the catchment meteorological history. Consequently, determination of these parameters with CRR mathematical model could be applied to any other catchment.

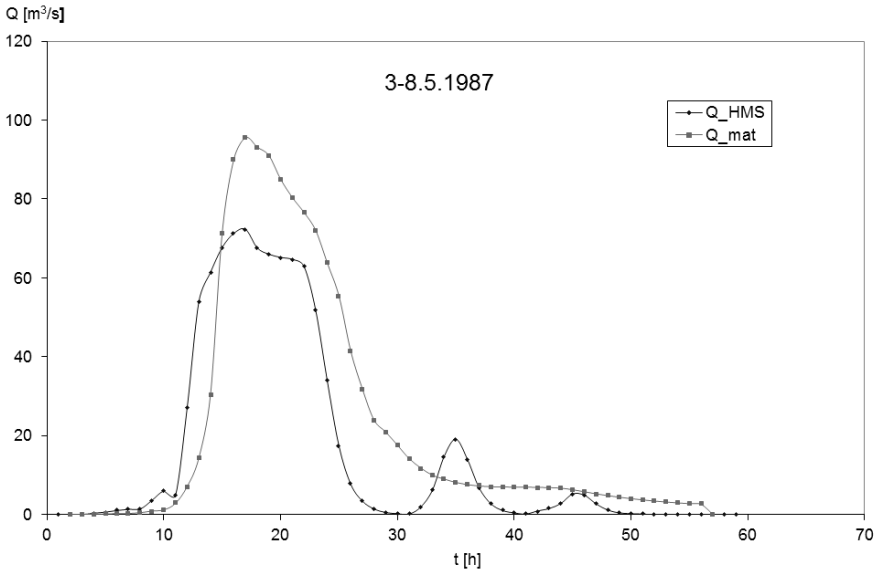

Fig. 5. Comparison of the CRR mathematical model hydrograph (QMAT) with the HEC–HMS hydrograph (QHMS) for the rain event from 3rd May to 8th May1987

Runoff volumes obtained by HEC–HMS model (V_{HMS}) and that obtained by the mathematical CRR model (V_{MAT}) have also been compared (Table 2). The reasons for occurrence of lower volume values of HEC–HMS hydrographs in relation to the CRR mathematical model hydrographs should be mentioned. The volume reduction of HEC–HMS model is the measure

of runoff coefficient used in the model calculation, and the coefficient was lower than 1 for all rain events. As opposed to the CRR model which uses the runoff coefficient of 1. The volume reduction of output CRR hydrographs can be made in model extension with nonlinear reservoir for case of unsaturated soil and more dominant catchment retention effect.

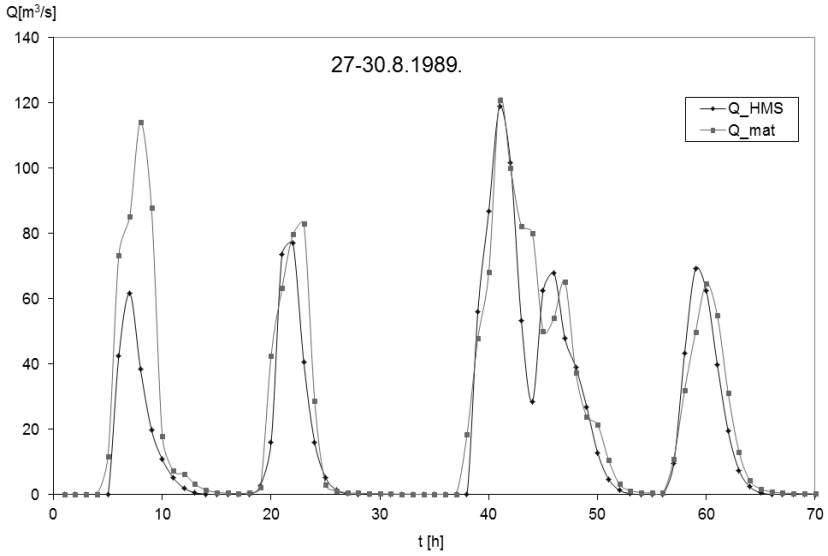

Fig. 6. Comparison of the CRR mathematical model hydrograph (Q_{MAT}) with the HEC–HMS hydrograph (Q_{HMS}) for the rain event from 27th August to 30th August 1989

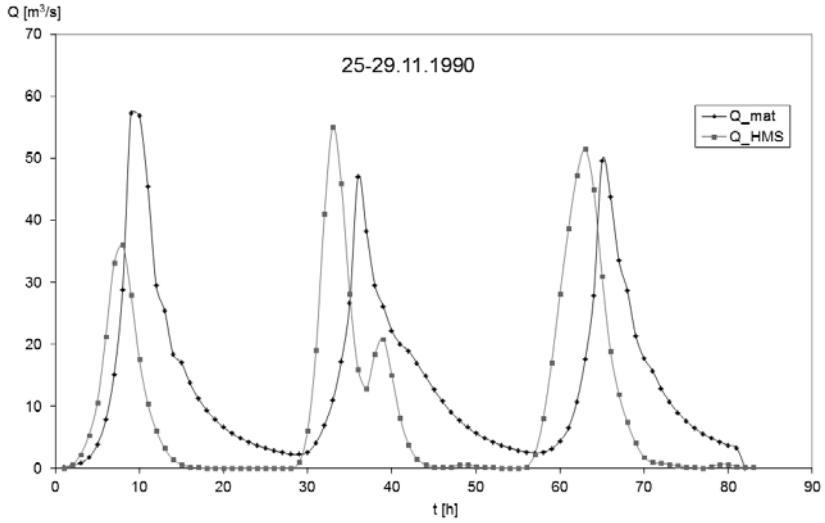

Fig. 7. Comparison of the CRR mathematical model hydrograph (Q_{MAT}) with the HEC–HMS hydrograph (Q_{HMS}) for the rain event from 25th November to 29th November 1990

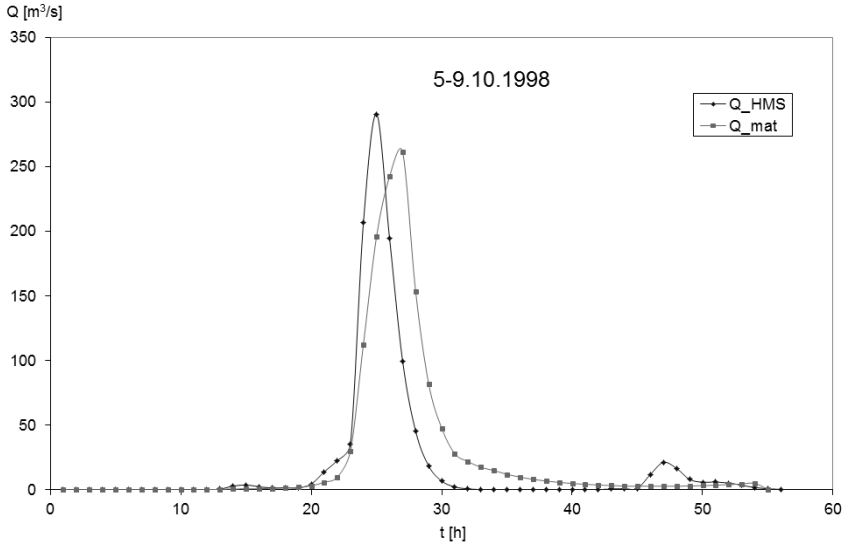

Fig. 8. Comparison of the CRR mathematical model hydrograph (Q_{MAT}) with the HEC–HMS hydrograph (Q_{HMS}) for the rain event from 5th October to 9th October 1998

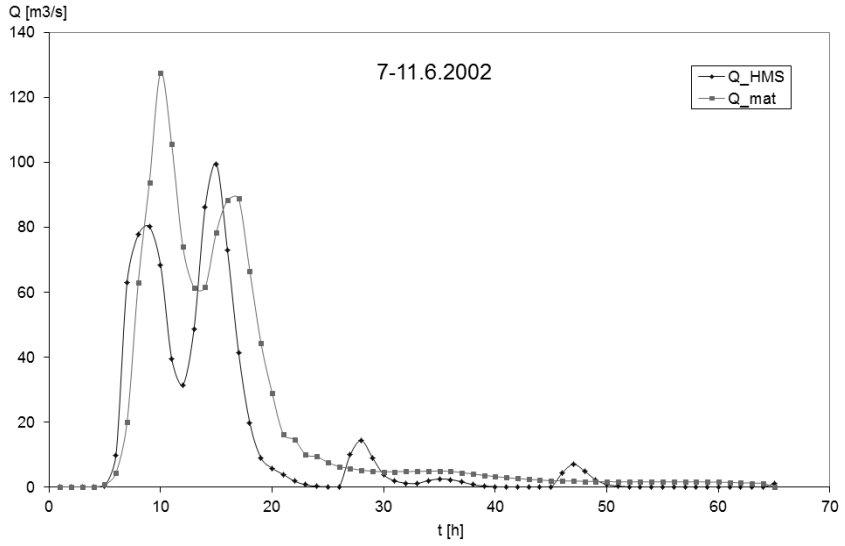

Fig. 9. Comparison of the CRR mathematical model hydrograph (QMAT) with the HEC–HMS hydrograph (QHMS) for the rain event from 7th June to 11th June 2002

The CRR mathematical model validation was elaborated for an extreme flood wave recorded on 21st–24th Oct, 1993. This flood wave presents an extreme flood wave generated by long lasting and strong precipitation events, which caused numerous floods not only in Istria and Croatia, but also in Europe. In this case rainy period lasted long enough before the occurrence of a water wave and soil saturation was considerable. The impact of evapotran-

spiration, interception, water remaining in the valleys, infiltration and other processes of the hydrological cycle were not dominant. Furthermore, the impact of catchment retention was also negligible because the water was practically pouring down directly from the catchment surface without considerable time lag (T_l = 1.5 *h*). This resulted in the occurrence of a steep hydrograph, the concentration time between 3 and 4 hours, close to the concentration time established according to the concentration time analysis of the measured wave of 3.5 h from [12].

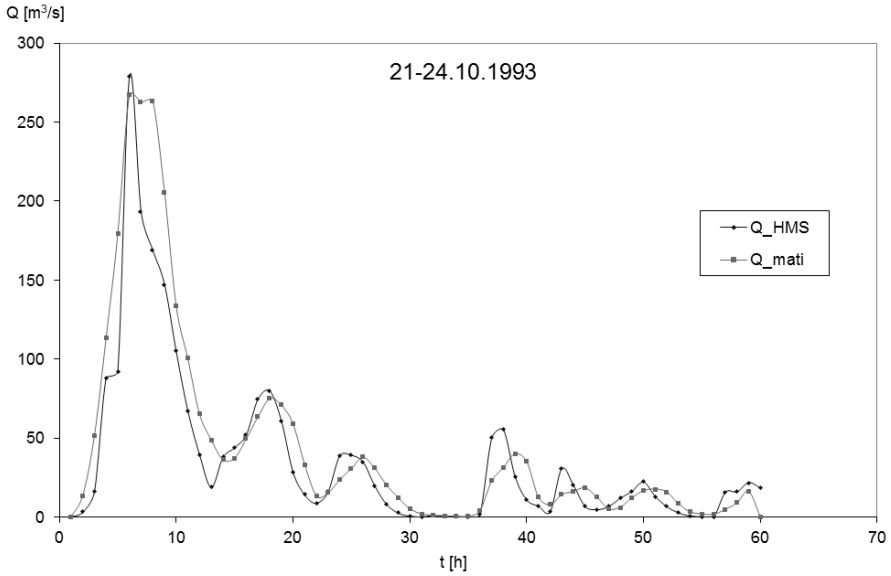

Fig. 10. Comparison of the CRR mathematical model hydrograph (Q_{MAT}) with the HEC–HMS hydrograph (Q_{HMS}) for the rain event from 21st October to 24th October 1993

Table 2

Comparison of the runoff volume from HEC–HMS model (V_{HMS}) and CRR mathematical model (V_{MAT}) together with lag time for every precipitation event

Precipitation event	Tlag [hour]	$V_{,HMS}$ [m^3*10^6]	$V_{,MAT}$ [m^3*10^6]
3.–8.5.1987	14,6	3,25	4,44
7.–11.6.2002.	9,53	2,99	4,24
5.–9.10.1998	13,4	3,72	4,76
2.–3.6.2003.	7,5	1,48	2,53
30.10.–11.11.2000.	8,0	6,52	7,78
27.–30.8.1989.	4,8	4,95	6,36
25.–29.11.1990	13,6	2,84	4,03
21.–24.10.1993.	1,5	7,70	9,58

The hypothetical state of the saturated soil, neglected retention properties of the catchment and minimum losses presented through CRR mathematical model hydrograph closely corresponds to the conditions in measured extreme flood wave (Fig. 11).

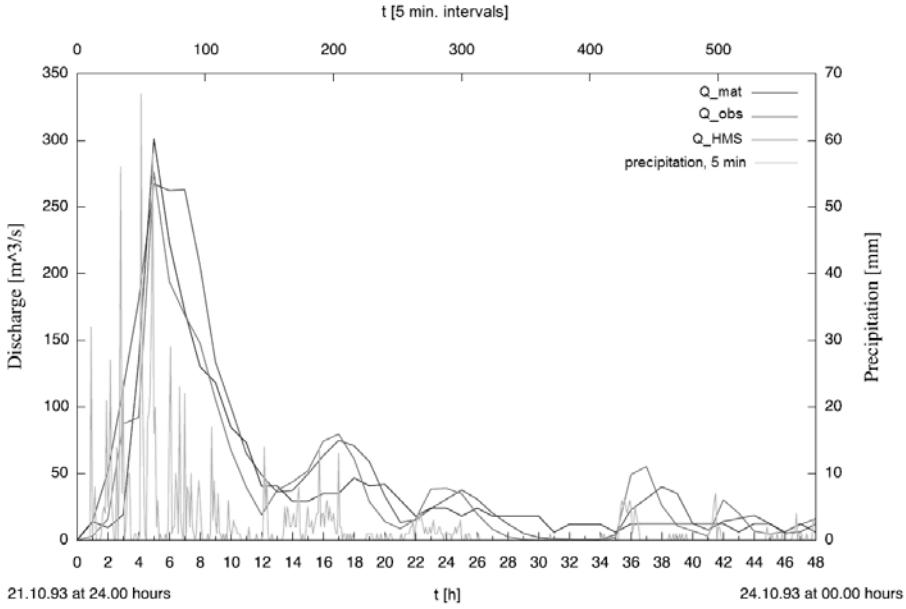

Fig. 11. Precipitation and discharge for extreme flood from 21.10–24.10.1993. Comparison of CRR mathematical model hydrograph (*Q_mat*) and HEC–HMS model hydrograph (*Q_HMS*) with measured hydrograph (*Q_obs*).

Performance and comparison of the HEC–HMS and CRR mathematical model for that event is evaluated through visual inspection and presented by coefficient of correlation (R) and Root Mean Square Error (RMSE). RMSE emphasizes high flow simulations [13].

The difference in RMSE for the mathematical model and the HEC–HMS model is 5 m^3/s, which is 2% from observed peak flow (301 m^3/s). The results confirm that the mathematical model for saturated soil with small lag time of 1.5 hour is well conceived in comparison with the HEC–HMS model.

6.7. CRR MODEL EXTENSION

Analysis of water waves, which are not described as extreme flood waves, was subsequently conducted, so that output model hydrographs for the analyzed rain events are computed according to the methodology described in this paper. At the end of conceptual model procedure, the output model hydrograph was compared with the measured one for each of the remaining 7 non-flood cases, and in general the following was observed:

— soil saturation at the moment of water wave was negligible, system losses are considerable,

— important retention impact is noticed, so there is a considerable lag in the occurrence of the measured hydrograph in relation to the time of rain occurrence. (Table 2).

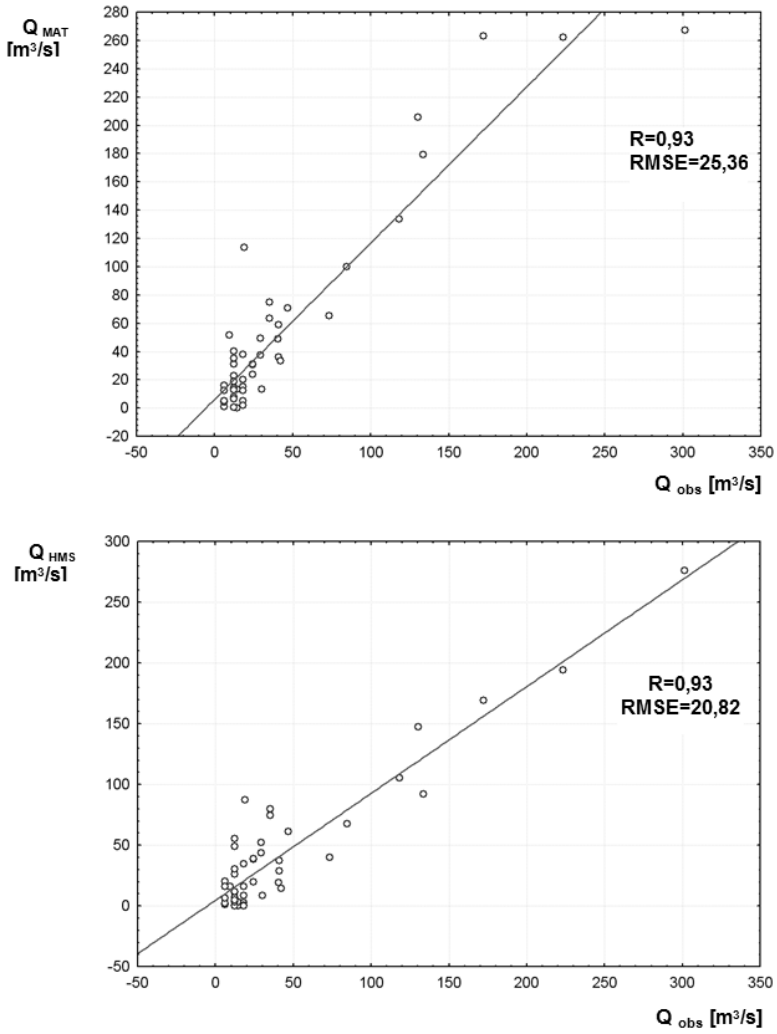

Fig. 12. Scatterplots of observed flows (Q_{obs}) against simulated flows with introduced mathematical CRR model (Q_{MAT}) for storm hydrograph in October 1993. Flows are simulated with introduced mathematical (Q_{MAT}) CRR model (above) and with SCS UH method (Q_{HMS}) in HEC HMS (below)

The impact of the lag time on the form of the computed hydrograph at the outlet of the Botonega catchment is given in mathematical model by the correction of velocity equation (Eq. (4)) with coefficient ($1/t_{lag}$):

$$v_X = \frac{1}{t_{lag}} \cdot \frac{1}{n} \cdot y^{2/3} \cdot I^{1/2} \tag{11}$$

where t_{lag} – catchment lag time as a dimensionless magnitude.

The function of the coefficient is to slow down the water flow over the catchment surface; it is dimensionless and from its origin comes out the magnitude measure or catchment time delay.

The method of nonlinear reservoir has been applied to each calculated kinematic runoff hydrograph in the conceptual model in which the effect of the catchment retention basin has not been considered. The final formula of the hydrograph transformation reads as follows:

$$\left| \frac{Q_{i-1} + Q_i}{2} \cdot \Delta t - \frac{q_{i-1} + q_i}{2} \cdot \Delta t \right| = K \left| q_i - q_{i-1} \right|^k \tag{12}$$

where: Q_i – ordinate of original hydrograph at the moment t_i,
Q_{i-1} – ordinate of original hydrograph at the moment t_{i-1},
q_i – ordinate of transformed hydrograph at the moment t_i,
q_{i-1} – ordinate of transformed hydrograph at the moment t_{i-1},
K – transformation coefficient,
k – transformation exponent (transformation effects of the reservoir).

Coefficients of nonlinear reservoir were calculated applying the optimization method using the genetic algorithm (GA), in the procedure with defined fitness and condition function.

For each K and k a series of transformed data q_1, q_2, …, q_m is calcualted by using nonlinear reservoir (Eq. (12)) and the "distance" of transformed and measured data is calculated as a "goodness of fit function":

$$\sqrt{\sum_{i=1}^{m} \left(q_i - I_i \right)^2} \tag{13}$$

where: q_i – ordinate of transformed hydrograph at the moment t_i [m ^{3} s^{-1}],
I_i – ordinate of measured hydrograph at the moment t_i [m^3 s^{-1}].

The "condition" function is defined so that the runoff volume from the transformed hydrograph is equal or approximately equal to the runoff volume from the measured hydrograph for the same event. Pairs of K and k coefficient are sought for which the "distance" between transformed magnitudes q_i and measured magnitudes I_i is minimum. Objective of the calculation in the genetic algorithm is to determine the constants K and k, so that the "goodness of fit function" reaches the minimum, provided that the function value "condition" is approximately equal to zero [4]. Since the conceptual model is elaborated with gross precipitation, this condition presents the reduction of hydrograph to the value of effective precipitation. In this way, the final computed hydrographs, i.e. model outputs were made comparable with the measured ones.

Further on, some examples of comparison between computed hydrograph, transformed hydrograph and measured hydrograph for the cases of non-flooding water waves and unsaturated soil are given (Fig. 13 and Fig. 14).

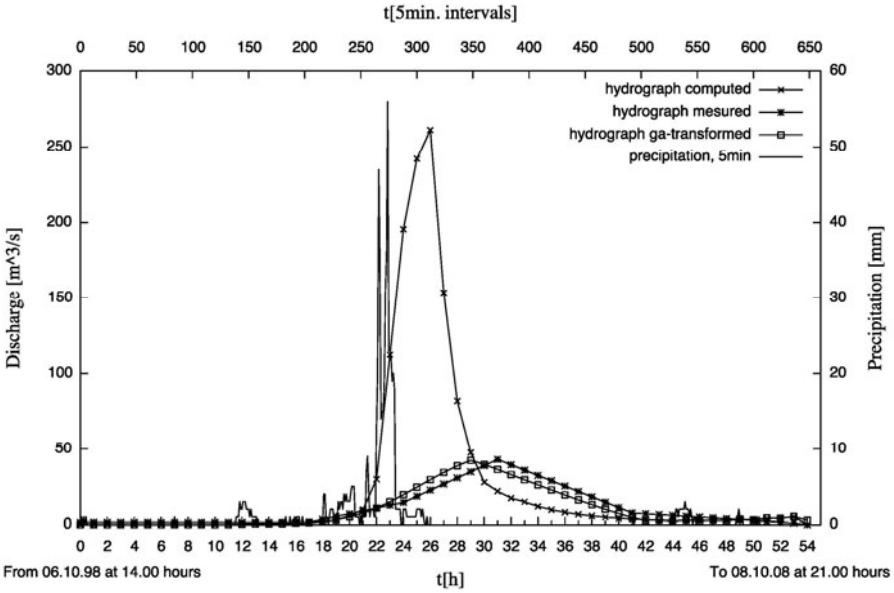

Fig. 13. Comparison of computed hydrograph, transformed hydrograph and measured hydrograph for the rainfall event from 06–08.10.1998

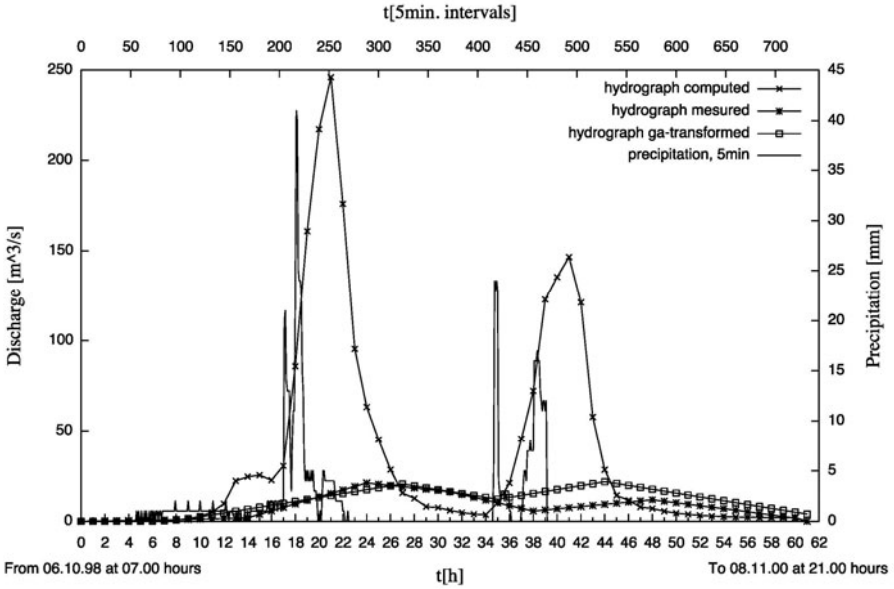

Fig. 14. Comparison of computed hydrograph, transformed hydrograph and measured hydrograph for the rainfall event from 06–08.11.2000

6.8. CONCLUSION

CRR model of Botonega catchment in Istria is presented. First part of mathematical model presents flow on saturated soil with small lag time and shows good flow simulation results in comparison with conventional HEC–HMS model. Considering the physical description of the runoff process, and from the standpoint of occurrence of maximum flow in the observed time base for the total duration of runoff, the maximum occurrence at parallel hydrographs differs very little (max 2 hours). That means that the initial time of catchment concentration, catchment lag, time of hydrograph rising and the duration of the water wave are well modeled and model can be applied to other catchments.

The second part shows possible extension of model with taking retention property of the catchment into consideration. The correction of the Manning equation for the calculation of velocity in the coefficient domain by which the Manning roughness coefficient is multiplied, is therefore introduced as a possible improvement of this approach. The measure of that correction is the reciprocal value of t_{lag} value. Such a solution does not have any other justification except the fact that the more the catchment retention is expressed, the smaller the velocity of water flow over the surface and vice versa. Such a solution could be particularly important if the time of catchment concentration as a special case of delay time is interconnected with the surface flow velocity, i.e. occurrence of output hydrograph. The reliability of this solution certainly lies in the reliability of hydrological data measurment and the knowledge about the terrain.

References

[1] "Primijenjena hidrologija", stručni seminar. 2002: Zagreb.

[2] Jeniček M.: Rainfall-runoff modeling in small and middle-large catchment – an overvew. Geografie – Sbornik ČGS, 2007. 111: p. 305–313.

[3] Murphy C., et al.: Catering for uncertainty in a conceptual rainfall runoff model: Model preparation for climate change impact assessment and the application of GLUE using Latin Hypercube Sampling. 2006: Citeseer.

[4] Kunštek D.: Unapređenje parametarskih metoda za proračun otjecanja informatičkom tehnologijom. 2010, Phd thesis, Građevinski fakultet Sveučilišta u Zagrebu: Zagreb.

[5] Kunštek D., Petraš J., Potočki K.: Elaboration of CRRS models using GIS and GA technology calibrated at Botonega catchment. Technical Gazette, 2010. 17(4): p. 425–433.

[6] Chow V. T., Maidment D. R., Mays L. W.: Applied hydrology. New York: McGraw-Hill. 1988.

[7] Hrelja H.: Inženjerska hidrologija. Građevinski fakultet u Sarajevu 2007.

[8] Kunštek D., et al.: Implementacija znanja i tehnika informatičke znanosti u CRRS modele. in 4. hrvatska konferencija o vodama. 2007. Opatija.

[9] Feldman A. D., C.: Hydrologic Engineering, Hydrologic Modeling System HEC–HMS: Technical Reference Manual. 2000: US Army Corps of Engineers, Hydrologic Engineering Center.

[10] McCuen R. H.: Hydrologie analysis and design. Prentice Hall. Englewood Cliffs, New Jersey, 1989. 16: p. 17.

[11] Mark A., Marek P. E.: Hydraulic Design Manual. 2009, Texas Department of Transportation, Design Division, Texas.

[12] Rubinić J., Kukuljan I.: Poplave na području Istre (22–23.10.1993), elaborat broj H. 1993, JVP „Hrvatska vodoprivreda“ OJ Rijeka: Labin.

[13] Khakbaz B., et al.: From lumped to distributed via semi-distributed: Calibration strategies for semi-distributed hydrologic models. Journal of Hydrology, 2009.

7 Estimation of the Monthly Rainfall Intensity Design Values in the Western Part of Slovakia

Jana Látečková, Silvia Kohnová, Ladislav Gaál, Ján Szolgay, Kamila Hlavčová (Slovak University of Technology, Faculty of Civil Engineering, Bratislava, Slovak Republic)

7.1. INTRODUCTION

In engineering hydrology, information about rainfall intensities is often used for an estimation of design rainfall values.

Rainfall intensity-duration-frequency curves (IDF) were first established in the 1930s [4]. Since then, many forms of these relationships for several regions all over the world have been defined. For estimating design values for shorter periods (hours, minutes) and a selected return period, the simple scaling method is often used. The characterization of the scaling properties of point precipitation is an important theoretical and practical issue in precipitation analysis [7, 12].

In the scientific literature, there are many articles dealing with the methodological aspects and practical implementation of the simple scaling of rainfall [8, 10, 11, 13] which will be presented in more details in the following parts of this article.

Menabde, et al. [8] demonstrated that the cumulative distribution function (CDF) for annual maximum rainfall intensities has scaling properties over a range of 30 minutes to 24 hours. The authors analyzed data sets from two different climatic regions (Melbourne, Australia and Warmbaths, South Africa) and investigated the scaling properties of statistical moments. They fitted the observed data with the cumulative distribution function EV1 (Extreme Value 1, i.e., the Gumbel distribution) for the verification of the scaling properties for the different durations. It was shown that the scaling exponents, which were obtained by two different methods (using the scaling of statistical moments and the methods of the direct fitting of the CDF), have approximately the same value.

Yu, et al. [13] used regional IDF formulas for estimating scaling exponents for non-recording rain gauge stations. The data set consisted of 46 rain gauge stations in Northern Taiwan. Firstly, the authors investigated the scaling properties of the annual maximum rainfall intensities for various durations (1, 2, 3, and up to 24 hours). Then, three groups were divided based on the scaling properties of rainfall. According to this selection, three homogenous regions were created; the differences between each region were in the small variability of the scaling exponents.

Molnar and Burlando [10] examined the variability of the scaling properties from 62 rain gauge stations in Switzerland. The experimental data consisted of 21 complete years of observations in the period 1978−2003. They applied the simple scaling theory to the data set from a range of 1 day to 10 minutes. The rain gauge stations were pooled into four climatologically and geographically similar regions. The authors came to the conclusion that the seasonal variability was dominant.

Özger, et al. [11] investigated the scaling properties of rainfall on 43 rain gauge stations in Texas. They used the monthly maximum precipitation totals from the years 1925–2005 and applied the simple scaling method of the statistical moments. They determined that scaling properties do not depend on climatic regions.

The scaling properties of extreme short-term rainfall were also examined in Slovakia [1, 2, 3]. Generally, these studies were aimed at adopting the simple scaling method of the rainfall intensities on the non-recording rain gauge stations. The presented study was aimed at applying the simple scaling theory to experimental data consisting of the monthly maximum rainfall intensities in selected rain gauge stations in Slovakia and comparing the resulting design values with those derived by [3], which were estimated for the entire warm season using a regional (i.e, a regionally averaged) scaling exponent.

7.2. METHODOLOGY

The methodology applied in this study follows the one presented in [8] and [13].
Let I_d and $I_{\lambda d}$ denote the annual maximum rainfall intensity series for the time durations d and λd, respectively. The two random variables I_d and $I_{\lambda d}$ are said to have the following scaling property [13] if

$$I_d \overset{dist}{=} \lambda^{-\beta} I_{\lambda d} , \tag{1}$$

where the equality $\overset{dist}{=}$ is understood in the sense of the equality of the probability distributions, and β represents the scaling exponent. This property is usually referred to as "simple scaling in a strict sense" [5].

If $I_{\lambda d}$ has finite moments $E[I_{\lambda d}^q]$ of order q, then in the strict sense, the simple scaling in Eq. (1) implies that $I_{\lambda d}^q$ and $(\lambda^{\beta} I_d)^q$ have the same probability distribution. Therefore, they have the same moments:

$$E\left(I_{\lambda d}^q\right) = \lambda^{\beta_q} E\left(I_d^q\right) \tag{2}$$

where β_q represents the scaling exponent of order n. For obtaining the values of β_q, Eq. (2) can be transformed as:

$$\log E[I_{\lambda d}^q] = \log E[I_d^q] + \beta_q \log \lambda . \tag{3}$$

For more details see for example [5, 6, 9].

7.3. DATA ANALYSIS

For this study, observed data of the short-term rainfall intensities (in a one-minute step) from the three selected rain gauge stations in the western part of Slovakia were used (Tab. 1). Generally, the periods of observation in our dataset ranged from 1996 to 2008.

After selecting the time series of the monthly maximum intensities for the selected durations from 5 up to 1440 minutes in each rain gauge station, we decided to analyze the following rainfall intensities: (a) for the months of April and May separately, (b) June to-

gether with July, and (c) August together with September, which should better represent the rainfall generation properties during the warm season.

Table 1

List of rain gauge stations used in this study

Rain gauge station	Record length	Observation period
Bratislava	13	1996−2008
Kuchyňa – Nový Dvor	11	1998−2008
Myjava	13	1996−2008

7.4. RESULTS AND DISCUSSION

The simple scaling of rainfall intensities was demonstrated for the three sample stations. Firstly, the scaling exponents were derived for all the durations of rainfall analyzed (5, 10, 20, 30, 40, 50, 60, 90, 120, 180 and 1440 minutes). Figs. 1 and 2 show the relationships between the log-transformed values of the moments of various orders against the various rainfall durations at the Kuchyňa – Nový Dvor rain gauge station.

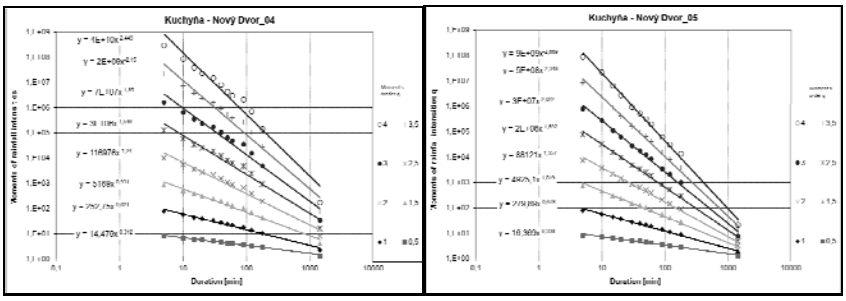

Fig. 1. The scaling of the moments of the rainfall intensities at the Kuchyňa – Nový Dvor station, for the periods of April (04, left) and May (05, right)

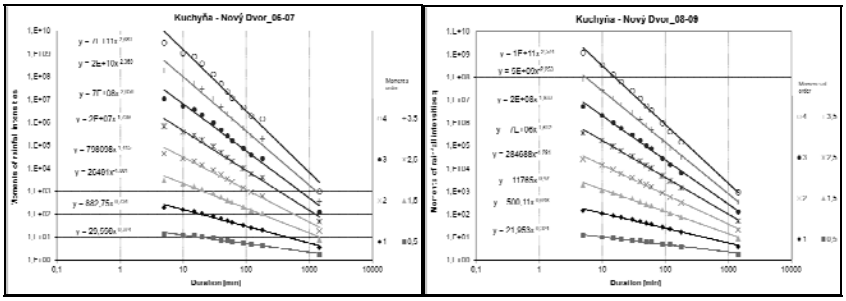

Fig. 2. The scaling of the moments of rainfall intensities at the Kuchyňa – Nový Dvor station, for the periods of June-July (06–07, left), and August-September (08–09, right)

According to Eq. (3), we estimated the scaling exponents for the Kuchyňa – Nový Dvor station. Figs. 3 and 4 show the relationship between the scaling exponents of the moments and the orders of the moments at the Kuchyňa – Nový Dvor station. The fact that the fitted straight line matched the individual points really close (indicated also by the high correlation coefficient close or equal to 1.0) confirmed that the property of simple scaling exists.

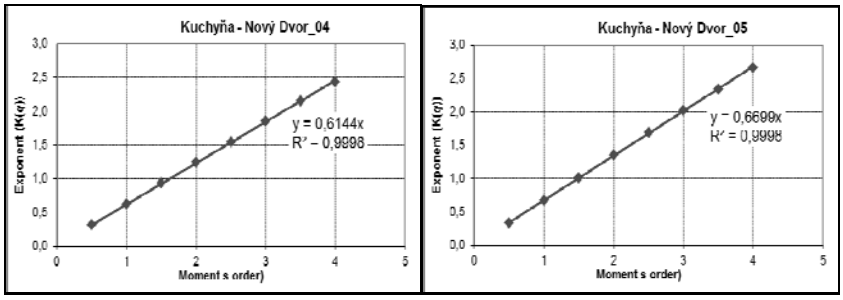

Fig. 3. The relationship between the slope of the equations and the order of moments *q* at the Kuchyňa – Nový Dvor station, for the periods of April (04, left) and May (05, right)

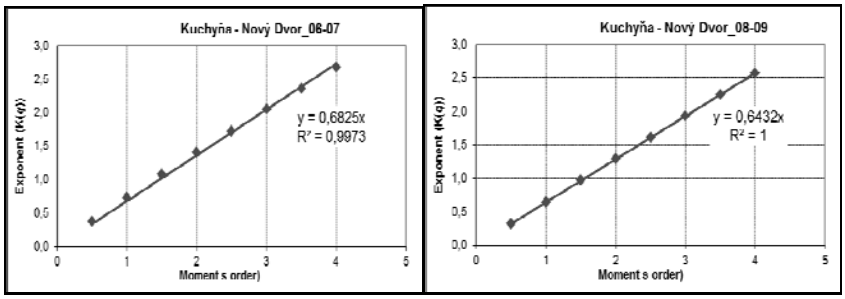

Fig. 4. The relationship between the slope of the equations and the order of moments *q* at the Kuchyňa – Nový Dvor station, for the periods of June-July (06–07, left), and August-September (08–09, right)

For the Kuchyňa – Nový Dvor station, the derived values of the scaling exponent was 0.614 for April, 0.669 for May, 0.682 for June and July, and 0.643 for August and September.

Table 2 presents the estimation of the scaling exponents in each of the selected rain gauge stations. The lowest values appear in April for all of the rain gauge stations. First, it is likely that this is an effect of the relatively short observation periods (only 13 years). The second reason of odd figures for April may be the fact that the measurements at the rain gauge stations usually start in the middle of April (sometimes even later), thus the estimation of the scaling exponent is only based on relatively few data.

To test the applicability of the derived scaling exponents in engineering practice, we applied steps as follows: (i) according to the study of [5], we estimated the design rainfall for the duration of 1 day for the summer season; (ii) we downscaled the design daily rainfall using the highest scaling exponents for each station from Tab. 2; and (iii) we compared the obtained design values for shorter durations with the IDF curves derived by means of the

regionally averaged scaling exponent of 0.738 estimated for the western region of Slovakia in [3]. The value of the regional scaling exponent was comparable to the highest scaling exponent derived by means of the simple scaling method for the warm season or separate months.

Tables 3 to 5 present a comparison of the design values derived by the simple scaling and design values by [3], using the regional scaling exponent at the three test stations.

Table 2

The scaling exponents derived by the simple scaling method, shown separately for the one-month or two-month periods and for the whole warm season.

Raingauge station	Period	Scaling exponent β
Bratislava	April (4)	0.459
	May (5)	0.619
	June-July (6-7)	0.722
	August-Sept. (8-9)	0.678
	Warm period	0.710
Kuchyňa – Nový Dvor	April (4)	0.614
	May (5)	0.669
	June-July (6-7)	0.682
	August-Sept. (8-9)	0.643
	Warm period	0.719
Myjava	April (4)	0.522
	May (5)	0.715
	June-July (6-7)	0.694
	August-Sept. (8-9)	0.714
	Warm period	0.754

Table 3

Comparison of the design values of the rainfall intensities [l s^{-1} ha^{-1}] obtained by means of the simple scaling method and based on the study of [3], respectively, at the Kuchyňa – Nový Dvor station for the period June – July

Method	Periodicity	Scaling exponent	Duration of rainfall intensity [min]							
			5	10	20	40	60	90	120	180
scaling	0.1	0.719	394	239	145	88	66	49	40	30
study [3]	0.1	0.738	439	263	158	94	70	52	42	31
scaling	0.05	0.719	450	273	166	101	75	56	45	34
study [3]	0.05	0.738	502	301	180	108	80	59	48	35

Table 4

Comparison of the design values of the rainfall intensities [l s^{-1} ha^{-1}] obtained by means of the simple scaling method and based on the regional analysis [3], respectively, at the Myjava station for the period June – July

Method	Periodicity	Scaling exponent	Duration of rainfall intensity [min]							
			5	10	20	40	60	90	120	180
scaling	0.1	0.754	437	259	153	91	67	49	39	29
study [3]	0.1	0.738	400	239	143	86	63	47	38	28
scaling	0.05	0.754	497	295	174	103	76	56	45	33
study [3]	0.05	0.738	454	272	163	98	72	53	43	32

Table 5

Comparison of the design values of the rainfall intensities [l s^{-1} ha^{-1}] obtained by means of the simple scaling method and based on the regional analysis [3], respectively, at the Bratislava – Koliba station for the period June – July

Method	Periodicity	Scaling exponent	Duration of rainfall intensity [min]							
			5	10	20	40	60	90	120	180
scaling	0.1	0.722	370	226	138	84	63	47	38	29
study [3]	0.1	0.738	434	260	156	93	69	51	41	30
scaling	0.05	0.722	413	253	154	94	70	53	43	32
study [3]	0.05	0.738	485	290	174	104	77	57	46	34

From the results at the Kuchyňa – Nový Dvor and Bratislava – Koliba stations, it can be seen that the design values obtained by the simple scaling method are underestimated for all the durations compared to the design values derived by using the regional scaling exponent [3].

7.5. SUMMARY AND CONCLUSIONS

This study was aimed at applying the simple scaling theory to the observed data of the annual maximum rainfall intensities at selected rain gauge stations in the western part of Slovakia. The scaling exponents were derived according to the simple scaling method used by [8] and [13].

The scaling exponents were derived on a monthly or bimonthly basis, and were then compared with the scaling exponents derived for the whole season. Both the highest (0.722) and the lowest (0.459) scaling exponent derived on a monthly basis was estimated at the Bratislava – Koliba station. The study showed high variability of the scaling exponents for separate months as well as for the whole season. The highest values, which were estimated for the whole warm season (Myjava and Kuchyňa – Nový Dvor stations) and at the Bratislava station for the June-July months were subsequently used for the estimation of IDF curves. The IDF curves were compared with IDF curves derived by means of the regional scaling exponent [3]. The results show that IDF curves estimated by the simple scaling

method are higher for the durations 5−40 min., while for the durations 40–180 min. are comparable with the values derived by using the regional scaling exponent [3].
The study proved that the derived scaling exponents can be used in engineering practice by estimating IDF curves.

References

[1] Bara M.: The analysis of rainfall intensities in Slovakia. Dissertation thesis. Slovak University of Technology, Bratislava (in Slovak), 2010.
[2] Bara M., Gaál L., Kohnová S., Szolgay J., Hlavčová K.: Simple scaling of extreme rainfall in Slovakia, a case study. Meteorological Journal, Vol. 11, No. 4, 153−157, 2009.
[3] Bara M., Kohnová S., Gaál L., Szolgay J., Hlavčová K.: Scaling of short-term rainfall intensities in Slovakia. Key Publishing, Ostrava (in Slovak), 2010.
[4] Bernard M. M.: Formulas for rainfall intensities of long durations. Transactions of the American Society of Civil Engineers, Vol. 96, 592–624, 1932.
[5] Gupta V.K., Waymire E.: Multiscaling properties of spatial and river flow distributions. Journal of Geophysical Research, 95 D3, (1990), 1999–2009.
[6] Koutsoyiannis D., Kozonis D., Manetas A.: A mathematical framework for studying rainfall intensity-duration-frequency relationships. Journal of Hydrology, Vol. 206, (1998), 118−135.
[7] Marani M.: On the correlation structure of continuous and discrete point rainfall. Water Resources Research, Vol. 39, No. 5, 1128−1136, 2003.
[8] Menabde M., Seed A., Pegram G.: A simple scaling model for extreme rainfall. Water Resources Research, Vol. 35, No. 1, 335−339, 1999.
[9] Molnar P., Burlando P.: Preservation of rainfall properties in stochastic disaggregation by a simple random cascade model. Atmospheric Research, Vol. 77, 137–151, 2005.
[10] Molnar P., Burlando P.: Variability in the scaling properties of high resolution precipitation data in the Alpine climate of Switzerland. Water Resources Research, Vol. 44, No. 10, 2007.
[11] Özger M., Mishra A. K., Singh V. P.: Scaling characteristics of precipitation data in conjunction with wavelet analysis. Journal of Hydrology, Vol. 395, 279−288, 2010.
[12] Rodriguez-Iturbe I., Gupta V. K., Waymire E. C.: Scale considerations in the modeling of temporal rainfall. Water Resources Research, Vol. 20, No. 11,1611−1619, 1984.
[13] Yu P.-Sh., Yang T.-Ch., Lin Ch.-Sh.: Regional rainfall intensity formulas based on scaling property of rainfall. Journal of Hydrology, Vol. 295, No. 1–4, 108−123, 2004.

Acknowledgements

The study was supported by the Slovak Grant Agency VEGA under the Project No. 1/0103/10 and by the Slovak Research and Development Agency under the contract No. APVV-0015-10. The support is gratefully acknowledged.

8 Occurrence of Antimicrobial Resistant Bacteria in Environment and the Statistical Analysis of this Phenomenon

Aneta Łuczkiewicz, Wojciech Artichowicz (Faculty of Civil and Environmental Engineering, Gdańsk University of Technology)

8.1. BACKGROUND INFORMATION

It is no doubt that application of antimicrobial agents (antibiotics and synthetic antimicrobials) in human medicine at concentrations much higher than found in natural ecosystems led to the revolution in bacterial infections treatment (Fig. 1). Antimicrobial agents inhibit the bacterial growth or disrupt the essential functions of bacterial cells (inhibition of DNA replication, inhibition of the production of proteins or cell wall materials, disruption of cell membrane activities that maintain chemical activity). Before antimicrobial agents were used for infection treatment, the human-associated bacteria were regarded as susceptible to them, but now all regions of the world are facing the problem of increasing antimicrobial resistance among human isolates [3].

Since most of the antibiotics are produced by environmental bacteria, it is suggested that the phenotype of intrinsic antimicrobial resistance (low susceptibility to antibiotics) evolved originally in natural ecosystems, mainly soils [10]. In contrast to intrinsic, acquired antibiotic resistance is considered to have been driven by selective pressure of antimicrobial agents used in human therapy. Thus it is suspected that human-associated bacteria acquired the resistance from environmental populations due to the horizontal gene transfer. In this process bacteria present in human commensal flora can be regarded as vectors for the gene transmition between pathogenic and environmental populations.

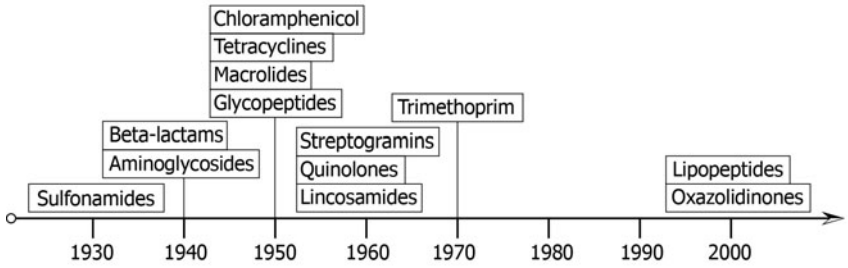

Fig. 1. Introduction of antimicrobial agents on the markets (adapted from [4])

Among human-associated bacteria *Escherichia coli* and *Enterococcus* spp. play an important role. They are regarded as indicators of fecal contamination in environment and additionally can be used as model organisms in the study of antibiotic resistance evolution due to their dual role in human ecology. *E. coli* is the predominant facultative microorganism

in the human colonic flora and, on the other hand, an important foodborne pathogen as well as frequent cause of community and hospital acquired urinary tract infections. Among several identified enterococci, *E. faecium* and *E. faecalis* are of clinically significance. That two species are common commensal in the intestines, but also opportunistic pathogens, known as the most frequent cause of surgical-site infections in intensive care units and prevalent pathogens of bloodstream infections [12].

8.2. CLINICAL AND ENVIRONMENTAL STUDIES

In clinics, the emergence of antimicrobial resistance is regarded as a complex problem driven by many interconnected factors (Fig. 2). The usage of antimicrobial agents creates a selective pressure on microorganisms and may promote the survival of mutant (resistant) strains in antimicrobial-sensitive population of the treated host. Consequently, due to the die off of the sensitive strains, the resistant ones may become clinically manifested 10]. Moreover, also in natural ecosystems, where antimicrobial agents (used in human and animal therapy) and their metabolites are discharged with treated wastewater, manure and others, the positive selection of resistant strains can be expected.

In bacterial cells resistance determinants are usually located on mobile genetic elements such as conjugative plasmids or conjugative transposons, thus except mutation, the dissemination of antimicrobial resistance can be also a consequence of horizontal gene transfer [13, 2]. The lateral transfer of resistance genes poses serious health problems [2]. Based on the current data provided by European Antimicrobial Resistance Surveillance Network [3] as well as by local surveillance networks it is expected that in the coming years particular problems will arise due to the lack of new agents to treat bacteria resistant to three or more different chemical classes of antimicrobial agents (MAR). Also vancomycin-resistant (VR) and high-level aminoglycoside-resistant (HLAR) enterococci as well as extended-spectrum beta-lactamase-producing *E. coli* are regarded as clinically relevant [3].

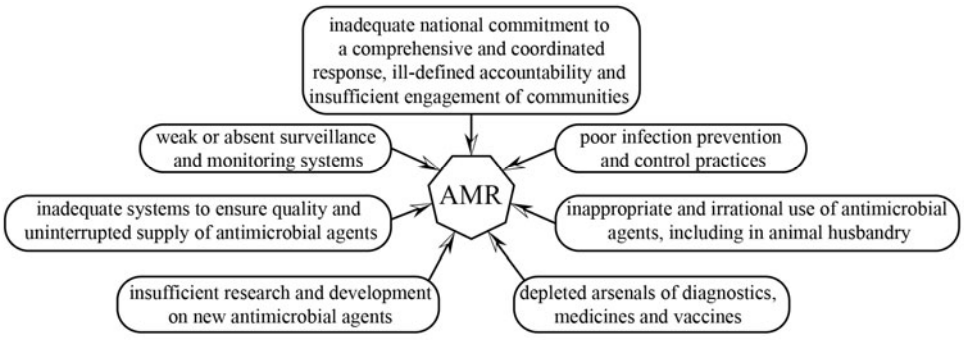

Fig. 2. Factors of antimicrobial resistance (AMR) in clinics

Till now, little or no attention is paid to natural ecosystems as reservoirs of resistance determinants as well as to dissemination of clinically important resistance genes among environmental bacterial population. Thus, from the environmental as well as public health perspective, the understanding of the global trends in antibiotic resistance is needed.

8.3. CASE STUDY

Fecal contamination of recreational waters and drinking-water sources is one of the most important problems connected with the anthropogenic impact on the environment. The specific location of Gulf of Gdansk and the nearby multifunctional agglomeration (Gdansk – Sopot – Gdynia – Rumia – Reda – Wejherowo) implies a variety of actions connected with urban, industrial as well as recreational activity concentrated in this area. Fecal degradation of the gulf coastal water was previously observed [11] and lead to beach closures and sea-bathing prohibition. Numerous direct tributes as well as effluents of local wastewater treatment plants were recognized as main sources of fecal contamination of Gulf of Gdansk.

Nowadays, dissemination of fecal bacteria in coastal water is often linked to the potential dissemination of resistance determinants. Thus, in the presented study the fecal indicators, *E. coli* and enterococci, isolated from the local wastewater treatment plant as well as from two local watercourses, were subjected for the antimicrobial susceptibility. The selected watercourses, Oliwski Stream and Reda River, cover mixed land usage, including urban, agricultural as well as forestry area with no direct discharge of wastewater treatment plant effluent. The samples of the wastewater were collected from WWTP Gdansk-Wschod ($Q_{av.}$ 96 000 m^3 per day, population equivalent – 700 000), which treats mainly the municipal wastewater including wastewater from local industry (5%) and undisinfected wastewater from local hospitals (0.17%). During the study isolation and identification of fecal bacteria were carried out using conventional cultivation methods [6, 7, 9]. The susceptibility tests of the isolates were carried out against antimicrobial agents important in treating *E. coli* and enterococci infections.

According to the obtained data, the resistance rate observed among the isolates of wastewater origin was higher then that observed among the riverine strains. For *E. coli*, 48% of wastewater and 36% of riverine isolates were resistant to at least one of the tested antimicrobial agents, while for enterococci the resistance rate was equal to 78% and 73%, respectively. A general tendency was observed, regardless of the isolate origin, that among *E. coli* the antimicrobial resistance was detected mainly to penicillins (ampicillin and piperacillin), tetracycline, fluoroquinolones and trimethoprim/sulfamethoxazole (Fig. 3a). Enterococci were resistant mainly to erythromycin, nitrofuration, followed by the fluoroquinolones and tetracycline (Fig. 3b).

An important aspect of the undertaken study was that isolates with clinically relevant resistance patterns were found in both environments. Extended-spectrum beta-lactamase–producing *E. coli* was detected once in the wastewater samples and two times in Oliwski Stream, at the sampling point situated just below the fish farm. Additionally, 9% of all riverine and all wastewater isolates were resistant to three or more different chemical classes of antimicrobial agents (MAR). In case of enterococci, 10% of riverine and twenty nine of wastewater isolates were regarded as MARs. Vancomycin-resistant (VR) and high-level aminoglycoside-resistant (HLAR) enterococci were also detected in both environments (below 5% of isolates).

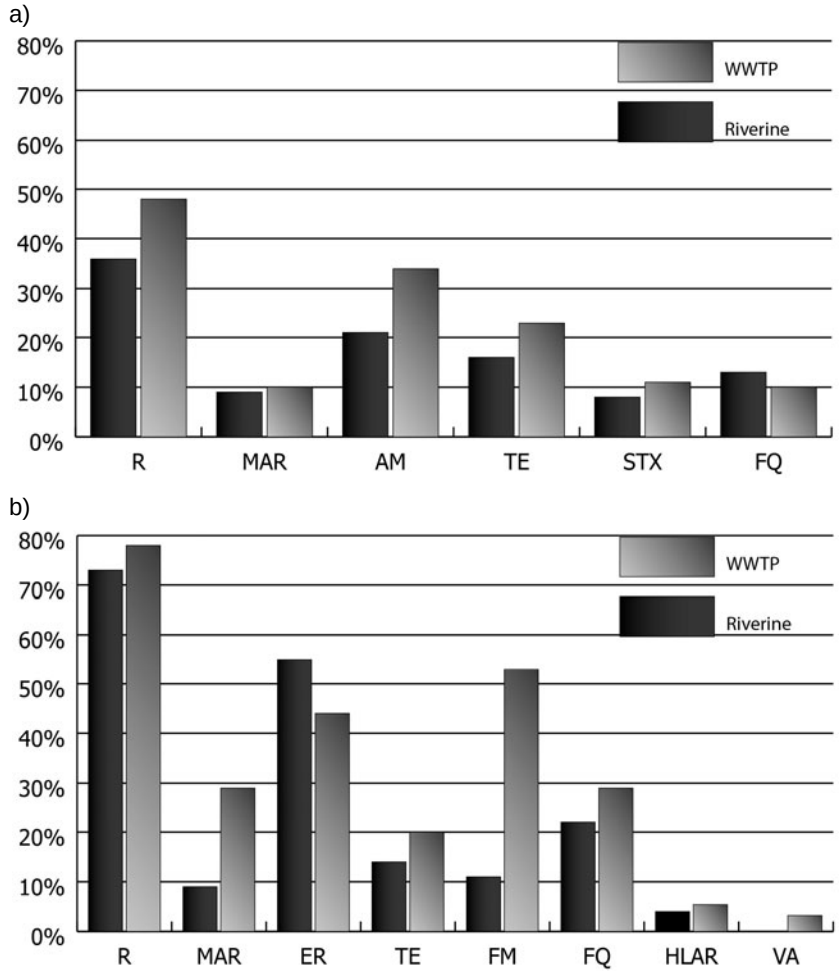

Fig. 3. Antimicrobial resistance of: a) *Escherichia coli* b) *enterococci*; Ratio of bacteria resistant: R – to at least one agent; MAR - to three or more different chemical classes of antimicrobial agents; AM – to ampicillin; ER – to erythromycin; FM – to nitrofurantoin; FQ – to fluoroquinolones; HLAR – to high – level aminoglycoside resistance; STX – to trimethoprim/sulfamethoxazole; TE – to tetracycline; VA – to vancomycin; WWTP – wastewater treatment plant

8.4. STATISTICAL ANALYSIS

In order to analyze the importance of a phenomenon and its significance critical statistical analysis is required. In antibiotic resistance analysis, basic statistical methods are widely used for example in: [5, 8, 14, 15]. Basic statistical analyses provide simple algorithms for hypotheses testing and give results that are easy to interpret. In practice, due to insufficient sample size, it is often impossible to check, whether the collected data fulfills all assumptions required by statistical analyses (f.ex. normality of sample distribution). In

such a case, only the assumption about sample characteristics can be made. The more sophisticated methods are used, the more difficult it becomes to find out how strongly the differences between real sample properties and assumed sample properties influence the results. Therefore basic statistical methods are very helpful, although they do not give such comprehensive answers as advanced statistical methods.

In the present study basic statistical methods were used to answer if antimicrobial resistance patterns are independent of the location of sample collection place as well as to analyzed the significance of positive selection of antimicrobial resistant strains during the wastewater treatment [6, 7, 8, 9].

For the fecal bacteria of riverine origin, Chi square independence test and linear regression were used to estimate the trend of antimicrobial resistance. Knowing the characteristics of area surrounding the sample collection place, it was possible to make a strong assumption, which sources of contamination are responsible for increase in antimicrobial resistance.

In case of Oliwski Stream the ratio of *E. coli* with resistance patterns to all tested *E. coli* isolates against the monitoring points suggested positive correlation downstream. In this watercourse, resistance rate increased downstream for: gentamicin, penicillins (ampicillin and piperacillin), fluoroquinolones (ciprofloxacin and levofloxacin) as well as for tetracycline. It should be additionally noted that the clinically relevant *E. coli* isolates with MAR patterns were mainly detected in the mouth area of the stream during the bathing season (May to August). In Reda River such association was not observed. The fecal pollutants were brought to the river body probably with surface runoff and soil leaching processes. *E. coli* with MAR patterns were isolated from the Reda River mainly during long-lasting spring rainfalls. In case of enterococci, for both watercourses the explicit correlation between the antimicrobial resistance rate against sampling points was not confirmed. It should be noted that the linear regression coefficients estimated for each of studied indicator bacteria were very similar among the antimicrobials belonging to the same chemical classes, however, differ for each watercourse.

In case of wastewater, to evaluate the influence of wastewater treatment processes on the presence of antimicrobial resistance patterns and the potential positive selection of antimicrobial resistant strains a two-sided z-test for two proportions ($p < 0.05$) was used. In wastewater the selective pressure of subinhibitory concentration of antimicrobial agents, their residues as well as other contaminants like heavy metals, can select the bacterial population with resistance patterns. Additionally, wastewater treatment processes based on activated sludge with high concentration of bacterial cells have the potential to increase horizontal gene transfer and this way dissemination of antimicrobial resistance genes (Beaber, et al., 2004). Among studied *E. coli* the wastewater treatment processes selected the penicillins, fluoroquinolones, tetracycline and trimethoprim-sulfamethoxazole resistant isolates, but the increase in resistance rate was not statistically significant. In case of enterococci significant increase ($p < 0.05$) was observed only for isolates resistant to fluoroquinolones, however, the nitrofurantoin, erythromycin and tetracycline resistant isolates were also selected. It should be stressed that fecal bacteria isolated from the studied treated wastewater were periodically found to consist of 90% of isolates with antimicrobial resistance patterns.

In highly effective wastewater processes the bacterial reduction reaches up to 99.9%, but even then the number of remaining strains may vary from 10^4 to 10^6 CFU *E. coli* in 100 ml of treated wastewater. It should be stressed that bacterial number in treated wastewater is not regulated by the Urban Waste Water Treatment Directive or any other regulatory. Ac-

cording to the obtained data and since the bacterial elimination is not a priority in wastewater treatment plant policy, the final disinfection should be considered.

8.5. CONCLUSION

The presented studies confirmed, that treatment processes favor survival of resistant bacteria and that similar antibiotic resistance patterns were observed among the fecal bacteria isolated from the clinical and environmental sources. Since antimicrobial resistance is an important health problem future research should develop the better methods of data aggregation in order to assess how the resistance determinants are progressing in clinic and in natural environment. Special attention should be given to the selection and dissemination of clinically relevant resistance determinants.

References

[1] Beaber J. W., Hochhut B., Waldor M. K.: SOS response promotes horizontal dissemination of antibiotic resistance genes. Nature, 427: 72–74, 2004.

[2] Dröge M., Pühler A., Selbitschka W.: Phenotypic and molecular characterization of conjugative antibiotic resistance plasmids isolated from bacterial communities of activated sludge. Mol. Gen. Genet., 263(3): 471–82, 2000.

[3] EARS-Net 2009. European Antimicrobial Resistance Surveillance Network Annual report on Antimicrobial resistance surveillance in Europe 2009. http://www.ecdc.europa.eu/en/ publications/Publications/1011_SUR_annual_EARS_Net_2009.pdf, last access March 2011.

[4] ECDC-EMEA Technical Raport http://www.ema.europa.eu/docs/en_GB/document_library/Report/2009/11/WC500008770.pdf 2009.

[5] Isenbarger D. W., Hoge C. W., Srijan A., Pitarangsi C., Vithayasai N., Bodhidatta L., Hickey K. W., Dac Cam P.: Comparative antibiotic resistance of diarrheal pathogens from Vietnam and Thailand, 1996–1999, Emerg. Infect. Dis., 8 (2): 175–80, 2002.

[6] Luczkiewicz A., Fudala-Książek S., Jankowska K., Olanczuk-Neyman K.: Antimicrobial resistance of fecal indicators in municipal wastewater treatment plant. Wat. Res., 44(17): 5089–5097, 2010a.

[7] Luczkiewicz A., Jankowska K., Kurlenda J., Olańczuk-Neyman K.: Identification and antimicrobial resistance of *Enterococcus* spp. isolated from surface water. Water Sci. Technol. 62 (2), 466–473, 2010b.

[8] Łuczkiewicz A., Artichowicz W., Kalicki M.: Analysis of antibiotic resistance in *Escherichia coli* isolated from the Reda River and the Oliwski Stream using basic statistical methods. Monografie Komitetu Inżynierii Środowiska PAN, Ed. K. Olańczuk-Neyman, H. Mazur-Marzec, vol. 64, 115–125, 2010c.

[9] Łuczkiewicz, A., Jankowska, K., Kurlenda, J., Olańczuk-Neyman, K.: Identification and antimicrobial susceptibility of fecal coliforms isolated from surface water. Polish J. Environ. Stud, in press 2011.

[10] Martinez J. L.: The role of natural environments in the evolution of resistance traits in pathogenic bacteria. Proc. R. Soc. B, 276: 2521–2530, 2009.

[11] Olanczuk-Neyman, K., Geneja, M., Quant, B., Dembinska, M., Kruczalak, K., Kulbat, E., Kulik-Kuziemska, I., Miko1ajski, S., Gielert, M.: Microbiological and biological aspects of the wastewater treatment plant "Wschod" in Gdansk. Polish J. Environ. Stud. 12 (6): 747–757, 2003.

[12] Richards M. J., Edwards J. R., Culver D. H., Gaynes R. P.: Nosocomial infections in combined medical-surgical intensive care units in the United States. Infect Control Hosp Epidemiol 21: 510–515, 2000.

[13] Tennstedt T., Szczepanowski R., Braun S., Pühler A., Schlüter A.: Occurrence of integron-associated resistance gene cassettes located on antibiotic resistance plasmids isolated from a wastewater treatment plant, FEMS Microbiol. Ecol. 45: 239–252, 2003.

[14] Sauer P, Andrew S. E., Lassaline M., Gelatt K. N., Denis H. M.: Changes In antibiotic resistance In equine bacterial ulcerative keratitis (1991–2000): 65 horses. Vet. Ophthalmol., 6(4), 309–313, 2003.

[15] Sørum M., Johansen P. J., Aasnes B., Rosvoll T., Kruse H., Sundsfjord A., Simonsen G. S.: Prevalence, persistence, and molecular characterization of glycopeptide-resistant Enterococci in Norwegian poultry and Poultry farmers 3 to 8 years after the ban on Avoparcin, Appl. Environ. Microbiol., 72 (1): 516–521, 2006.

9 Importance of Reservoir Turček in the Flood Protection

Andrea Marikovičová, Marian Minárik (Slovak University of Technology, Faculty of Civil Engineering)

9.1. INTRODUCTION

In the year 2010 in eastern and central part of Slovakia occurred several storm rainfalls which caused floods mainly on upper parts of basins. These floods were accompanied by high material losses. From the flood protection measures one of the most efficient are reservoirs. In august 2010 village Turček situated on river Turiec was also stricken by flood. Above this village is situated fresh water supply reservoir Turček. Besides its main function one of supplement purpose is flood protection. During flood the flood discharges were accumulated in this reservoir. Unfortunately only part of the basin above village Turček is protected by reservoir; tributaries of the river Turiec are not regulated. Flood discharges from these tributaries caused damage of several houses. If the reservoir Turček would not be constructed consequences of flood could be significantly higher. In this paper is analyzing contribution of reservoir Turček to the flood protection of the land under this reservoir.

9.2. DESCRIPTION OF LOCALITY

Village Turček is situated in Central Slovakia on the north root of the Kremnica Mountain in the source region of the stream Turiec. Above village is constructed hydraulic structure Turček, which is situated under the confluence of the river Turiec with its right-bank tributary from Ružová dolina. Its main purpose is to accumulate water for the purification plant in Turček and to supply the towns of Žiar nad Hronom, Prievidza and Handlová with drinking water. The reservoir also contributes to the flood protection of the area under the dam and it utilizes the hydro power potential in three small hydro power plants. Total volume of reservoir is 10.8 million m^3, from which represents 9.094 million m^3 storage volume, dead volume 0.288 million m^3 and retention volume 1.413 million m^3 (1.013 million m^3 controlled a 0.40 million m^3 uncontrolled). The dam was constructed in extremely complex geological conditions, in a rock subsoil of volcanic origin. The dam is a rock-fill one, with an asphalt-concrete sealing blanket. The height of the dam above the terrain is 59 m. The inclination of the upstream slope is 1 : 2, the inclination of the downstream slope, 1 : 1.65. The subsoil of the dam is tightened by a grout curtain of a depth ranging from 30 to 60 m. This hydraulic structure was the first one drinking water supply reservoir in Slovakia in the construction of which the asphalt-concrete sealing blanket was used.

Basin of stream Turiec above village Turček can be divided into two subbasins. Runoff from sub-basin SB1 of streams Ružová, Štrich and Turiec is regulated by reservoir Turček, sub-basin SB2 of stream Turček is not regulated (Fig. 1). Village Turček is therefore only partly protected against floods. Area of sub-basin SB1 is 31.05 km^2; it is more than two times bigger than unregulated area of sub-basin SB2 – 14.14 km^2.

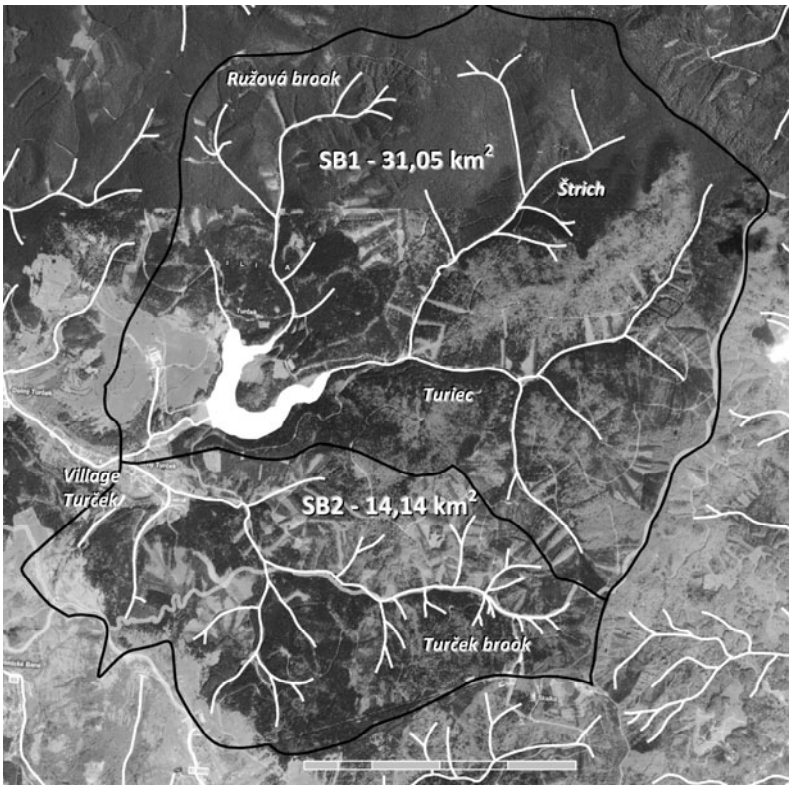

Fig. 1. Basin of stream Turiec above village Turček

9.3. FLOOD IN AUGUST 2010

After observation of Slovak hydrometeorology institute precipitation recorded in year 2010 were highest in the history of observation, from the year 1871. Average annual precipitation amount in Slovakia is 743 mm, in year 2010 was recorded precipitation amount approximately 1200 mm. Especially the rainfalls in May and June 2010 were characterized by theirs exceptional intensity and overall quantity. During this period occurred many floods especially in the eastern and southern part of Slovakia. The second wave of floods occurred after rainstorms on 15th and 16th august, when towns in Horná Nitra and in Turiec valley were stricken. That time most of these catchments had been sufficiently water-saturated by previous precipitation events.

On the Fig. 2 are presented hourly precipitation registered in rain gauge station situated near village Turček. From this graph results, that extreme precipitation occurred in two phases. First storm started 15th of August at 6:00 AM and finished at 10:00 AM. During these four hours total precipitation amount was 33 mm, strongest rain was recorded during first hour, when fell 18.27 mm of rainfall. Second storm started 16th of August at 11:00 AM, finished after 5 hours at 4:00 PM, total precipitation amount of this storm was 49 mm. Rainfall was very intensive especially during first hour, when was recorded 29.17 mm of rainfall.

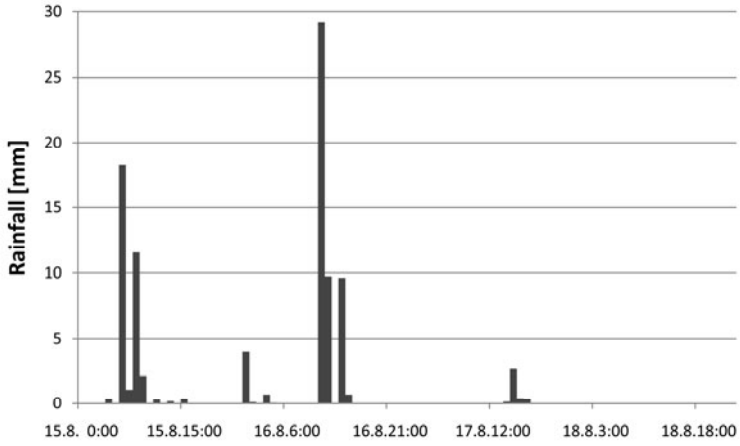

Fig. 2. Hourly precipitation registered in rain gauge station near village Turček

Fig. 3. Consequences of flood

Because village Turček is situated in the upper part of Turiec river basin, runoff from these two storms caused rapid increase of water level on all streams in this region. Consequently, river Turiec flooded village Turček. Mainly the lower part of village was affected (Fig. 3). The flood came very quickly; inhabitants could not save any property. Several houses have been damaged, the road and gas pipelines were destroyed, the houses stricken by water did not have electricity, mud seeped into houses etc. Proportion of the residents presumed that the village was flooded due to releases of water from the reservoir Turček. These opinions are in conflict with the purpose of the reservoir; through the medium of retention volume protect land against floods. Effect of reservoir Turček on discharges in river Turiec under reservoir during flood is analysed below.

9.4. EFFECT OF RESERVOIR TURČEK ON DISCHARGES IN TURIEC RIVER DURING FLOOD IN AUGUST 2010

Discharges in streams around village and dam Turček are observed in four stream gauging stations (Fig. 4). Gauging station S1 is situated on brook Ružová above reservoir Turček, gauging station S2 is situated on stream Turiec above reservoir. Sum of discharges measured in these two gauging station represent inflow to the reservoir Turček. Stream gauging station S3 is placed under reservoir, thus the discharges measured in this station represent outflow from reservoir. Station S4 is situated inside the village Turček under confluence of river Turiec with brook Turček.

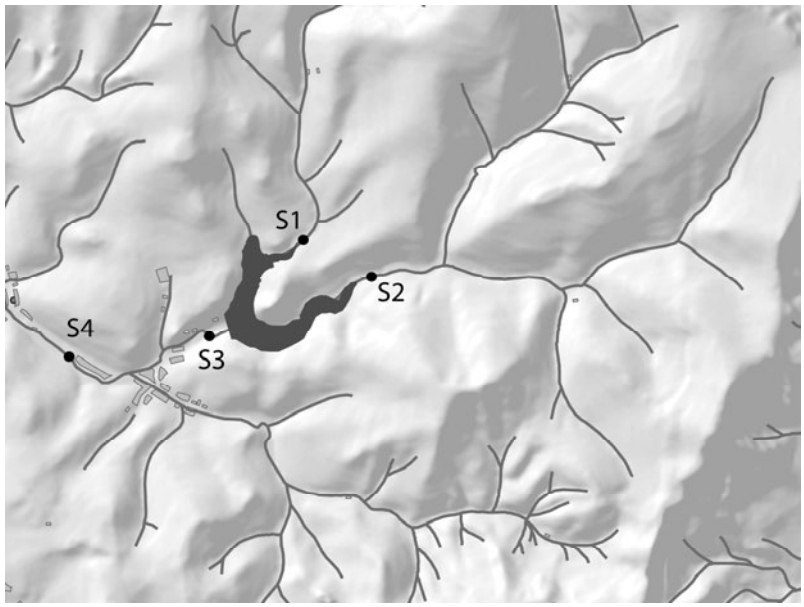

Fig. 4. Position of the stream gauging stations

To evaluate how hydraulic structure Turček affected discharges in river Turiec it is necessary to evaluate inflows to (stations S1+S2) and outflows from (station S3) reservoir (Fig. 5).

From presented graph results, that during first wave of flood natural unregulated discharge (inflow) culminated at 2240 l s^{-1}, while at the same time outflow was only 670 l s^{-1}. Second wave of flood brought much higher discharges as the first one. Culmination discharge on 16th of August at 5:15 PM reached value 4000 l s^{-1}. That time by manipulation on hydraulic structure outflows decreases to only 250 l s^{-1}. Retention volume of reservoir Turček accumulated the whole volume of flood wave; later the reservoir was safely released. Reservoir Turček positively affected discharge conditions under the dam.

Based on mentioned fact the flood in the village Turček was caused by water flowing from sub-basin of stream Turček, which is not regulated. Discharges under confluence of streams flowing from both sub-basins are measured in stream gauging station S4 (Fig. 6). Flood wave which originated from first storm had relatively low culmination – 1780 l s^{-1}, flood wave from second storm event had very steep shape and high culmination – 5850

l s^{-1}. Discharge almost 6 000 l s^{-1} exceed the capacity of water course Turiec and caused disastrous flood in village.

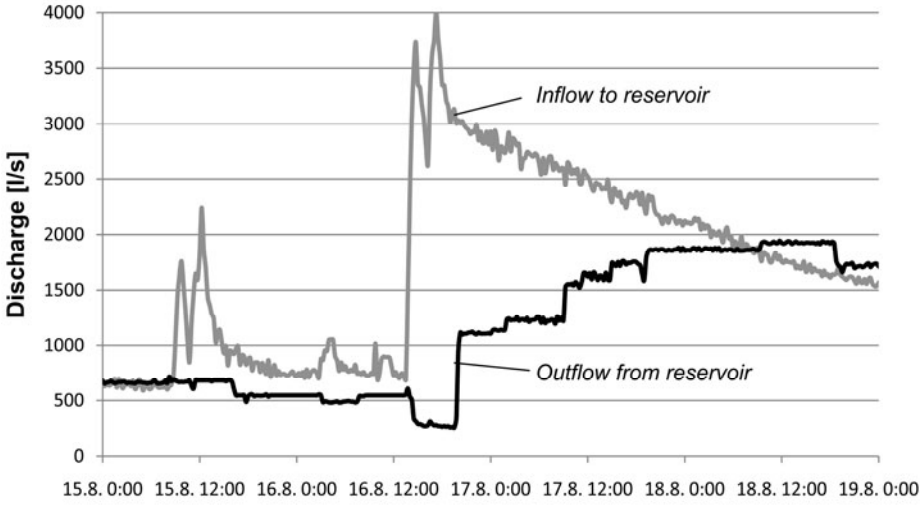

Fig. 5. Inflow and outflow from reservoir Turček

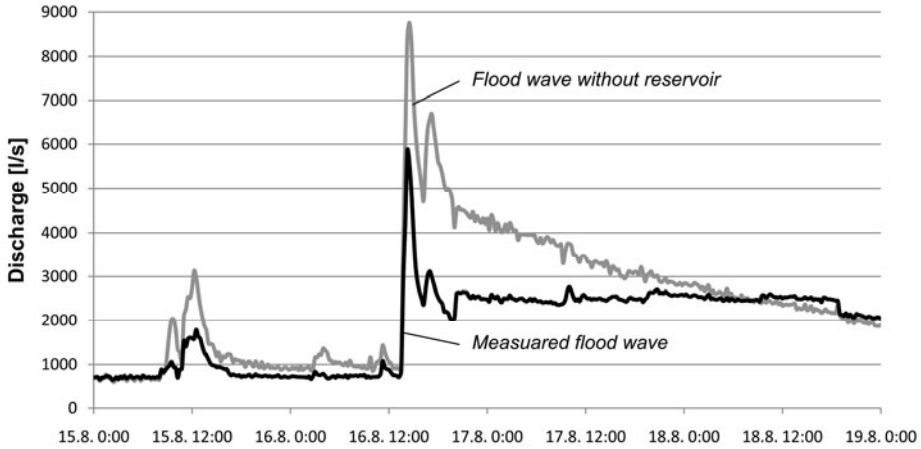

Fig. 6. Comparison of observed flood wave and assumed flood wave without reservoir in stream gauging station S4

Based on these facts the question arises, what would happen if the reservoir Turček not existed. Because both sub-basins are located in close vicinity to each other and their characteristics are similar, the flood wave would be combined and under confluence the culmination grew to a higher level. After calculation the culmination would increase to almost 9 000 l s^{-1} (Fig. 6). Such high discharge would result to much higher losses in the village Turček. Thankfully, due to presence of reservoir maximal discharges were reduced by 50 percent.

9.5. CONCLUSION

Protecting of land against flash floods is very demanding. These floods can be characterised by their accidental character, short duration and disastrous consequences. In August 2010 two extreme rainfalls stroked country around village Turček. Water reservoirs belong to the most effective measures protecting land against floods. However the main purpose of reservoir Turček is supplying inhabitants with fresh water, it was analysed, that this resevoir (with its retention volume 1.413 million m^3), significantly contributed to reduction of discharges in river Turiec during above mentioned events. Flow discharges were in the stream below the dam reduced by 50 percent. Nevertheless, the flood wave that originated from unregulated tributaries caused extensive material losses. But, if the reservoir Turček would not be constructed consequences of flood could be significantly higher.

References

[1] Bednárová E. et. al.: Dam Construction in Slovakia. Originalities, Milestones, Highlights. Kuskus, Bratislava, Slovakia, 206 pp., 2010.
[2] Hydrologic Data Obtained from Slovak Hydrometeorology Institute and Slovak Water Management Enterprise.

Acknowledgements

This paper was supported by grant project VEGA No. 1/0704/09.

10 The Assessment and Forecasting of Sedimentation at the Nove Mlyny Reservoirs

Jaromír Říha, Zbyněk Zachoval (Brno University of Technology,
Faculty of Civil Engineering, Institute of Water Structures)

10.1. INTRODUCTION

The issues connected with dam reservoir sedimentation are becoming more and more topical. The estimation of current sedimentation and the forecasting of future decreases in reservoir volume and of locations affected by sedimentation are routine procedures performed by dam owners. In this paper a method of sedimentation progress assessment is demonstrated for the middle reservoir of the Nove Mlyny (NM) water reservoir system.

The Nove Mlyny dams and reservoirs are located in the South Moravian region in the Czech Republic. The system was completed in the year 1989. The scheme consists of three reservoirs with a total reservoir volume of approx. 134 mil. m^3. The reservoirs are situated at the junction of three significant Moravian rivers – the Dyje, Svratka and Jihlava (Fig. 1), which contribute a considerable amount of sediment mostly to the middle reservoir. The most significant sediment deposits are therefore located in the middle reservoir downstream of the confluence of the Svratka and Jihlava Rivers. During extensive floods and high entrance velocities in the estuarine area the sediments are transferred further into the reservoir. A small portion of suspended sediments is flushed down to the lower reservoir, where the water level is normally maintained at approximately the same level as in the middle reservoir.

In the paper the present sediment volume has been estimated with the use of data obtained from echo-sounder measurements carried out in the years 1994 and 2004 and processed by GIS techniques. To obtain the real values of sediment load during the period 1981 to 2004 a 1D sediment transport model of the lower reaches at the mouths of the Jihlava and Svratka Rivers and a model of sedimentation in the upper reservoir (where the Dyje River inflows) were calibrated. The forecast of future reservoir sedimentation includes a comparison of results obtained from methods developed by Brune, Churchill and Borland. The results obtained by Churchill and Borland's approaches show relatively good agreement; the difference is about 20%. The technique developed by Brune gives an approximately two times smaller annual average sediment input into the middle reservoir. The analysis shows that for the present normal water level (170 m a.s.l.) at the middle reservoir, the total reservoir volume will decrease by one half during about 120 years.

10.2. DESCRIPTION OF THE LOCALITY

The Nove Mlyny dams and reservoirs are located about 40 km to the south-west of Brno, the second largest city in the Czech Republic. The scheme was constructed during the period 1975 to 1989 and consists of three reservoirs with a total reservoir volume of approx. 130×10^6 m^3. The main purposes of the scheme are water storage for extensive irrigation,

flood attenuation, hydropower generation, fish production and recreation. The basic data regarding the scheme are shown in Table 1.

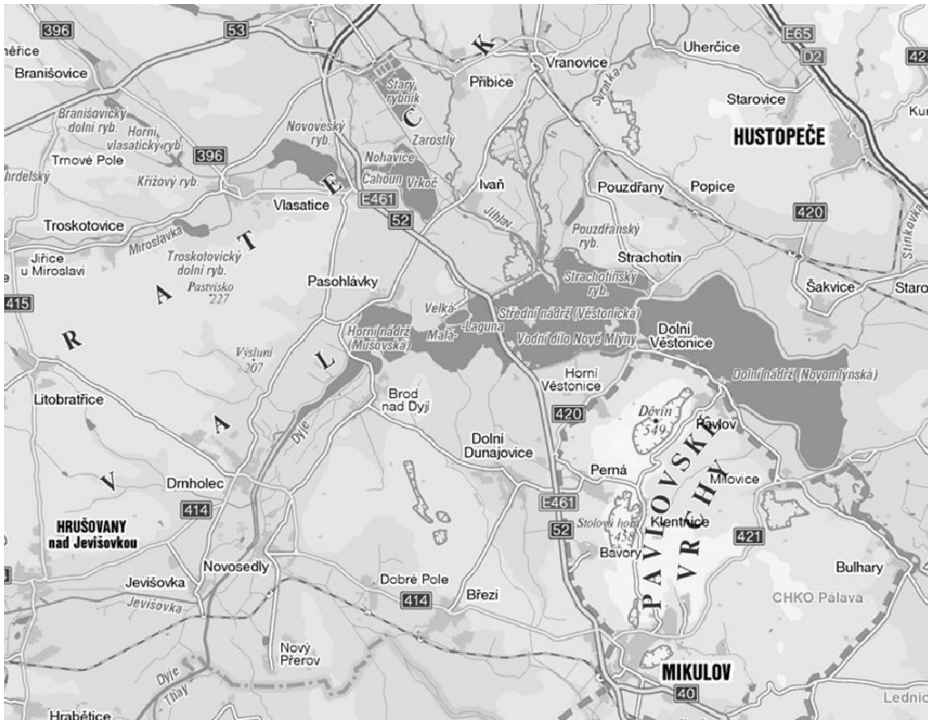

Fig. 1. The Nove Mlyny reservoir scheme

Table 1

Main parameters of the Nove Mlyny reservoirs

Reservoir	Lower (LR)	Middle (MR)	Upper (UR)
Year of completion	1989	1981	1978
Permanent reservoir volume [10^6 m^3]	23.685	17.545	9.769
Active reservoir volume [10^6 m^3]	45.776	3.517	3.914
Total reservoir volume [10^6 m^3]	83.961	32.062	14.313
Flooded area [ha]	1668.0	1033.0	575.0
Catchment area [km^2]	11853.0	11713.0	4599.0

The reservoirs are situated at the junction of three significant Moravian rivers – the Dyje, Svratka and Jihlava (Fig. 1), which contribute a considerable amount of sediment to the scheme, especially to the middle reservoir. Therefore, this reservoir is subject to the most intensive siltation and loss of reservoir volume. In our paper we have focused on the analysis of sedimentation processes in the middle reservoir only.

10.3. ESTIMATE OF THE ACTUAL SEDIMENT AMOUNT IN THE MIDDLE RESERVOIR

The present sediment volume in the middle reservoir corresponding to the period of operation since 1981 has been estimated with the use of data obtained from echo-sounder measurements carried out in the years 1994 and 2004. The original reservoir terrain level was derived from historical maps and land surveying data. The surface of the sediment in the reservoir and its volume were processed by GIS techniques. The data obtained were compared with photographic data derived from aerial photogrammetry. Using GIS techniques, a map of differences in the reservoir bottom corresponding to the period 1981–2004 was compiled (Fig. 2).

Fig. 2. Differences in the bottom of the middle reservoir – for the years 1981 – 2004

The resulting volume of sediment in the middle reservoir for the period 1981 to 2004 is about 980 000 m^3, with an average sediment thickness of 0.095 m and a maximum identified thickness of 0.4 m. The maximum thickness is situated at the area downstream of the confluence of the Svratka and Jihlava Rivers. The corresponding mass of sediment deposited during the period of 23 years (1981–2004) is about 1.25 10^6 tons. Annual sedimentation mass is about 54 000 t y^{-1}.

10.4. SEDIMENT TRANSPORT

10.4.1. Past sediment Transport into the Middle Reservoir

The obtained data about the sediment volume during a period of about 14 years were used for the calibration of the sediment transport model for the Jihlava and Svratka Rivers and the model of sedimentation in the NM upper reservoir (into which the Dyje River flows). The crucial amount of sediments enters the middle reservoir from two tributaries – the Svratka and Jihlava Rivers. Therefore, special attention was paid to the assessment of suspended sediments and bed load transported via these rivers.

The analysis of suspended sediment load was carried out by the comparison of methods summarized in Tab. 2. The results of the analysis for the Jihlava River can be seen in Fig. 3.

Table 2

Methods and data sources for the estimation of suspended sediment load

Method	No.	Author / source of data
Former research	1a)	Kališ [1, 2]
	1b)	Kališ [3, 4]
Recalculated data from 1b)	2)	Actual daily discharges and the grain sizes of suspended sediments.
Measured suspended sediment load	3a)	Czech Hydrometeorological Institute
	3b)	Morava River Agency, state enterprise
Dimensional analysis applied to measured data	4a)	Czech Hydrometeorological Institute
	4b)	Morava River Agency, state enterprise
Empirical formulae for Czech rivers [5]	5a)	Szolgay
	5b)	BSBA (Austrian standard [5])
	5c)	Bogárdi
Method of analogy	6a)	All Czech rivers
	6b)	similar Czech rivers
	6c)	Slovak rivers

Table 3

Methods and data sources for the estimate of bed load

Method	No.	Author / source of data
Former research	1a)	Kališ [1, 2]
	1b)	Kališ [3, 4]
1D steady simulations (HEC-RAS software) [6, 7, 8, 9]	2a)	Ackers-White
	2b)	Meyer-Peter and Müller
	2c)	Yang
1D steady uniform flow applied to typical cross sections of the Svratka and Jihlava Rivers [7, 8, 9]	3a)	Ackers-White
	3b)	Meyer-Peter and Müller
	3c)	Yang

The analysis of the bed load was carried out by the comparison of data summarized in Tab. 3. The results of the bed load analysis for the Jihlava River can be seen in Fig. 4.

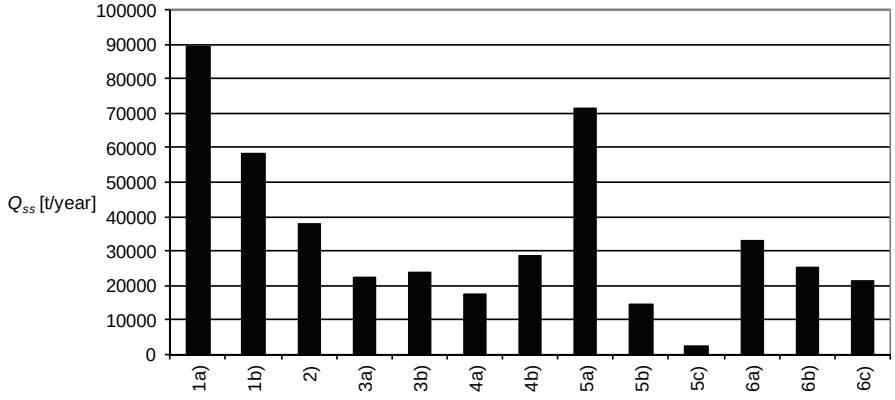

Fig. 3. Comparison of average annual suspended sediment load Q_{ss} [t y^{-1}] at the Jihlava river estuary entering the NM middle reservoir, determined by various methods

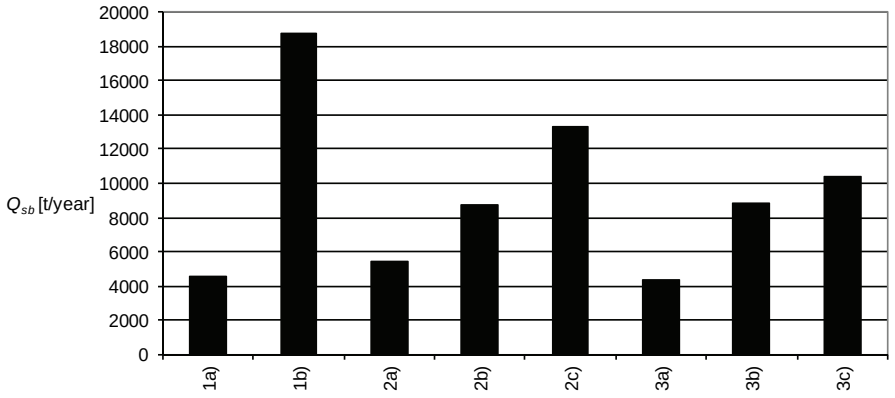

Fig. 4. Comparison of average bed load Q_{ss} [t y^{-1}] at the Jihlava estuary entering the NM middle reservoir, determined by various methods

The goal of the assessment of sedimentation in the NM upper reservoir was to estimate the amount of suspended sediments trapped by the upper reservoir and the amount entering the middle reservoir. For this purpose older results of aerodynamic modelling of transition flow in the upper reservoir were taken into account [3]. The sedimentation rate was related to the size of grains, flow velocity in the reservoir and density [10], which indicated the mass flow of suspended sediments. The analysis showed that all bed load transported by the Dyje River is trapped in the upper reservoir; the annual average amount of suspended sediments was estimated at 2000 t y^{-1}.

The overall balance summarizes the results mentioned above. Values of annual average suspended sediment Q_{ss}, bed load Q_{sb} and total load Q_s are shown in Table 4. The total load at individual localities can be seen from Fig. 5. For the estimate the most reliable methods

were taken into account, namely 3) and 4) in the case of suspended sediments (Table 2) and 2) in the case of bed load (Table 3).

Table 4

Summarized estimated sediment load entering the middle reservoir

River	Suspended load Q_{ss} [t y^{-1}]	Bed load Q_{sb} [t y^{-1}]	Total load Q_s [t y^{-1}]
Dyje	20 000	10 000	30 000
Jihlava	23 000	8 000	31 000
Svratka	41 000	7 000	48 000
Dyje UR to MR	2 000	0	2 000
Dyje MR to DR	10 000	0	10 000

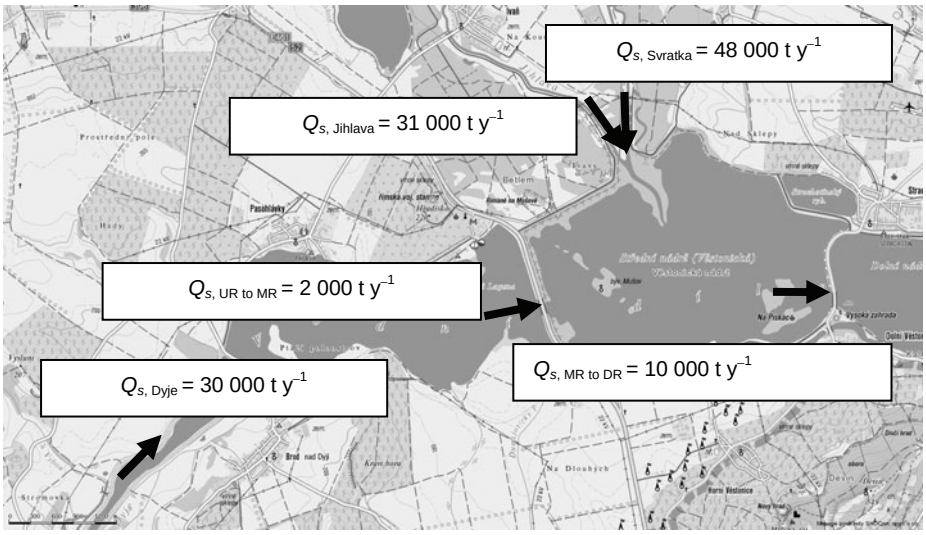

Fig. 5. Overall balance of total load

The obtained sediment volume in the middle reservoir was compared with the amount estimated from the reservoir bed survey described in section 3. The comparison proved there was a relatively good agreement between modelled and measured values, with the difference about 30%.

10.4.2. Sediment Transport Forecasting

The forecasting of the future siltation of the middle reservoir was carried out by comparing several methods according to their authors – Brune, Churchill and Borland [5, 9, 11]. As the real process is rather complicated, the following set of simplifying assumptions was taken into account:

— the siltation is uniform over the reservoir area,
— the sediment bulk density and grain size distribution is constant with time,
— reservoir water level does not change with time,

— the particle inflow to the middle reservoir is not influenced by its siltation,
— the particle inflow is estimated as an average annual amount based on the "calibrated" amounts derived in section 4.1,
— particles are only transported by the Svratka and Jihlava Rivers.

The method according to Brune

Based on measurements at real reservoirs, Brune proposed a dependence between the proportion V_t / V_{in} of the volume of settled particles V_t to the volume V_{in} of all particles entering the reservoir and the ratio V_r / V_a, where V_r is the permanent reservoir volume (Tab. 1) and V_a is the annual volume of water entering the reservoir. Three curves are plotted in Fig. 6 [9], namely average, upper and lower envelope curves.

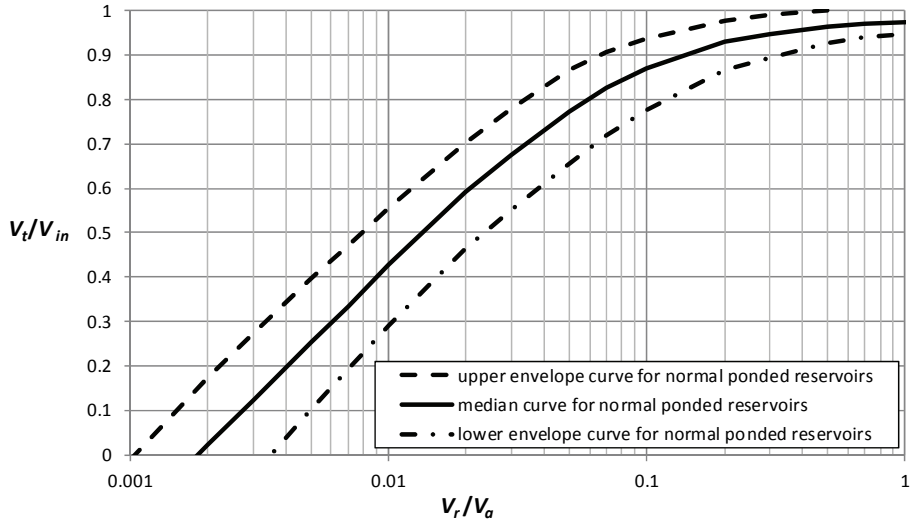

Fig. 6. Trap efficiency curves according to Brune

For all three curves the siltation of the middle reservoir was calculated and plotted in Fig. 8.

The method according to Churchill

The method is analogous to Brune´s method; the governing dependence is defined between V_t / V_{in} and t / v, where t is the detention time and v is the mean velocity along the reservoir (Fig. 7). The method enables segmentation of the reservoir and quantification of the sedimentation process. Because of the mixing due to macrovortices in the middle reservoir this procedure was not fully applied.

The results of the calculation expressed as temporal progression of the siltation are shown in Fig. 8.

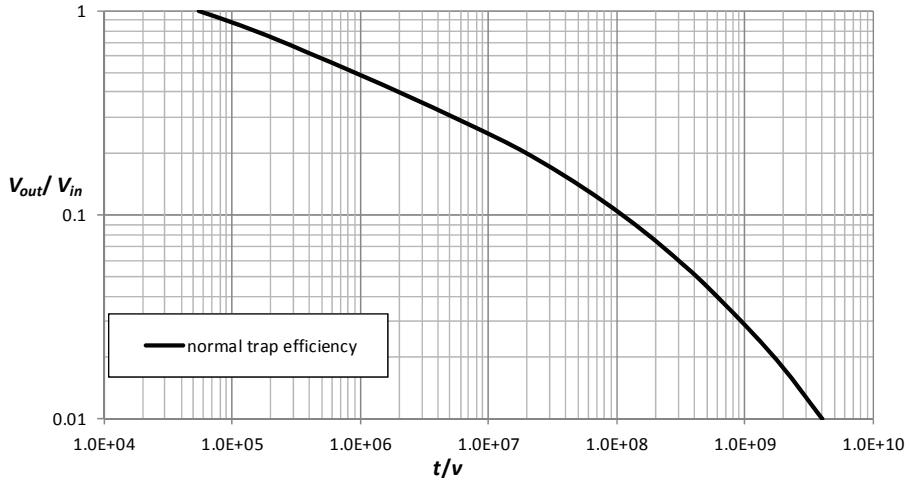

Fig. 7. Trap efficiency curve by Churchill

Siltation according to Borland

Borland [11] employed the methods mentioned above and developed his own method based on the following formula:

$$r = 1 - e^{-\frac{1{,}055 \cdot L \cdot w}{v \cdot h}} \tag{1}$$

where r is the ratio between the mass of settled and inflow particles to the reservoir, L is the reservoir length, h is the reservoir depth, w is the settling velocity and v is the mean velocity in the reservoir cross section.

Table 5

The assessment of permanent volume reduction in the reservoir from the year 2004

Method	Time [years] to the reduction of the permanent volume of the middle NM reservoir by one half from 2004
Brune – upper envelope	147
Brune – medium	189
Brune – lower envelope	277
Churchill	100
Borland	84

The results of the forecasts

Using the methods mentioned above the necessary time for siltation of 1/2 of the permanent storage capacity of the middle reservoir was estimated (Tab. 5). The temporal progression of sedimentation in the middle reservoir and the reduction of its available permanent storage volume can be seen from Fig. 8.

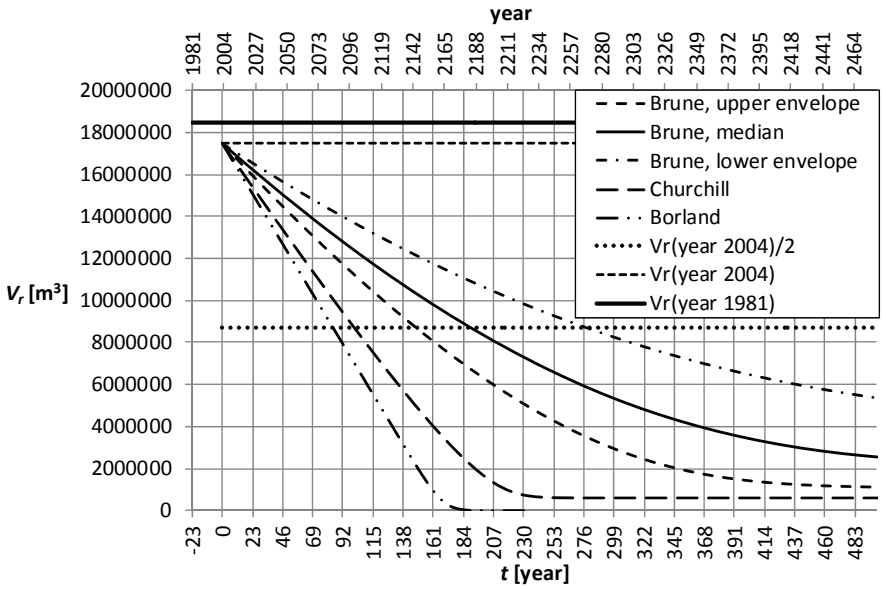

Fig. 8. Temporal progression of permanent volume reduction in the NM middle reservoir from the year 1981

10.5. DISCUSSION AND CONCLUSIONS

In this study the sediment volume in the Nove Mlyny middle reservoir was estimated from the measurements for the period of reservoir operation from 1981 to 2004. Data from echo-sounder measurements were used in the calculation. The resulting sediment volume for the mentioned period is about 980 000 m^3, which represents approximately 3.1% of total reservoir volume. The annual average sedimentation volume is about 43 600 $m^3 y^{-1}$. When extrapolated, it indicates that today the most exposed, middle reservoir of the NM scheme is silted by approximately 4%.

The estimation of future reservoir sedimentation was carried out by comparing results obtained from methods developed by Brune, Churchill and Borland (Fig. 8). It can be seen that the results obtained by various authors differ significantly; in the case of Brune's lower envelope and Borland's method the former forecast in years is more than three times greater than the latter prediction. The estimated time to the reduction of reservoir volume varies from 85 to 280 years; the trustworthy period can be assumed to be about 120 years of reservoir operation.

References

[1] Kališ J.: Suspended and bed load sediments in Nové Mlýny reservoirs and the forecast of the siltation process. Study. VVÚVSH, BUT Brno, 1967.

[2] Kališ J.: Siltation of Nové Mlýny reservoirs and in the estuaries of the Dyje, Svratka and Jihlava rivers. Study. VVÚVSH, BUT Brno, 1969.

[3] Kališ J.: Suspended and bed load sediments in upper and middle Nové Mlýny reservoirs and in the estuaries of the Svratka and Jihlava rivers. VVÚVSH, BUT Brno, 1970.
[4] Kališ J.: The excavation of sediments in the Nové Mlýny reservoirs: The forecast of bed load sediments in the estuaries of the Dyje, Svratka and Jihlava rivers. Study. VVÚVSH, BUT Brno, 1970.
[5] Bačík M., Kališ J., Klučovská J.: Modelovanie zanášania nádrží. VÚVH Bratislava. Bratislava, 1985.
[6] US Army Corps of Engineers, Hydrologic Engineering Center: HEC-RAS. Version 4.1.
[7] Yalin S.: Mechanics of Sediment Transport. Oxford: Pergamon Press, 1972. 290 p. ISBN 08-016646-6.
[8] Graf W. H.: Hydraulics of Sediment Transport. New York: McGraw-Hill Book Company, 1971. 513 p. ISBN 07-023900-2.
[9] García M. H.: Sedimentation Engineering. Processes, Measurements, Modeling, and Practice. ASCE Manuals and Reports on Engineering Practice No. 110. ASCE 2008. ISBN 13: 978-0-7844-0814-8.
[10] Veselý J., Pařílková J., Weiglová K.: The middle reservoir of the Nové Mlýny scheme. Artificial island – volumetric changes in sediments. Final report. LVV ÚVST, BUT Brno, 1998.
[11] Borland W.M.: Reservoir sedimentation. In: River Mechanics (ed. H. Shen). Water Resources Publications, Fort Collins, Colorado, 1970.

Acknowledgements

The paper contains results of Czech Ministry of Agriculture project QI92A139.

11 Anthropogenic Influences on Water Balance in Urban Area

Marek Sokáč, Vanda Dubová (Slovak University of Technology, Bratislava,
Dpt. of Sanitary and Environmental Engineering)

11.1. INTRODUCTION

Human activity significantly disturbs not only quantitative but also qualitative parameters of the natural hydrological cycle. This concerns not only the environment of cities, but also the wider area. In the cities result in high proportion of impervious surfaces prevent natural infiltration of rainwater, but also reduce evaporation (evapotranspiration). Storm water runoff from paved surfaces, flows in most cases to the public sewer network and water is transferred and discharged by a network out of urbanized area. Rapid runoff, however, leads to an extreme increase of the discharge, so part of this water hydraulically overflows to the recipients.

11.2. BACKGROUND

The urbanization process changes the hydrological balance of an natural catchment [4]. An overview of the balance is described on Fig. 1.

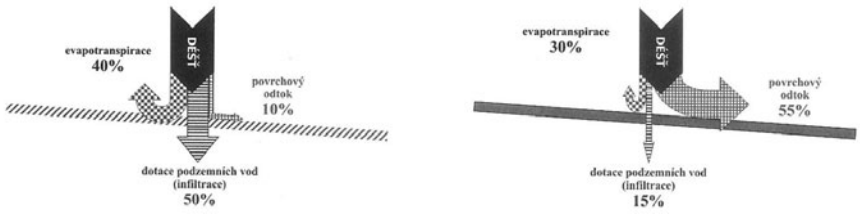

Fig. 1. The annual volumetric hydrological balance of a natural catchment (with vegetation cover) and an urbanized catchment (central part of the city) (déšť – precipitation, povrchový odtok – surface runoff, evapotranspirace – evapotranspiration, dotace podzemních vod – underground water recharge) [4]

The various studies of the hydrological balance of urbanized areas can be found in paper [3]. According to the results reported, for example evaporation in different locations can reach values from 17 to 71% of the annual total volume of water in the examined urbanized catchment, surface runoff from 29 to 76%, infiltration from 0 to 28%. An interesting study is an analysis of the hydrological balance of the urban water cycle, published by Carlsson and Falk [1] for the territory of urban areas in Sweden.

The foreign studies mentioned above are certainly interesting documents, however in the specific conditions of the Slovak Republic can be the hydrological balance in urbanized catchment significantly different. As a significant factor, which may cause substantial differences we particularly consider the infiltration into sewer systems, as well as water discharge of extraneous water (private water wells, drainage systems) into the sewer network.

In the literature we could find many studies and scientific articles dealing with issues of urbanized area hydrology. Almost all papers without exception refer to the long term strategic objective, which is to approach the hydrological characteristics of urban catchment to the natural catchment.

Interesting paper is the study [6], which was performed on relatively extensive Ebi river basin (27 km^2). It has been analysed two scenarios of urbanization: with and without the infiltration trenches focusing on the hydrological regime of the river network and with regard to the occurrence of maximum flows and flooding risk. The scenarios are built on assumptions of urbanization in the basin since 2035, and the technical rainwater infiltration feasibility was taken into account. The results of this study according the authors clearly demonstrate the need, respectively advantages of drainage facilities. This approach also will allow a sustainable development preserving the hydrological characteristics of the original river before urbanisation, despite of a relatively significant urbanization increase.

11.3. CASE STUDY PEZINOK

For a complex analysis of the hydrological balance, within the framework of the scientific research project VEGA no. 1/1143/11 we decided to perform an analysis of the hydrological balance of a city in Slovakia. The town of Pezinok was chosen, because of very interesting solutions regarding the water balance and sewerage disposal.

The river network around the town of Pezinok consists of streams running down the eastern side of the Small Carpathian mountains. Their runoff conditions are characterized by irregularities during the year and also in the course of the longer hydrological period. The quantity and the areal distribution of precipitation are subject to the altitude and orientation. In most areas of the district, the average precipitation ranges from 600 to 700 mm y^{-1}.

The most significant creek in the area of interest is the Blatina creek. This creek is in hydrological order 4-21-15-002, its catchment area has 18.8 km^2 and the total catchment area of 37.9 km^2. The Blatina creek in river chainage 11.30 – station Pezinok had in 2008 the average annual discharge Q_a = 0.079 $m^3 s^{-1}$. Minimum monthly flow was recorded in August (0.028 $m^3 s^{-1}$) and maximal in December (0.219 $m^3 s^{-1}$).

Rated territory belongs to the hydrogeological area MG 055 – crystalline and mesozoic area of the south-east part of the Pezinok's part of the Carpathian Mountains, and subregion, of quaternary alluvial deposits. The alluvial cone has a continuous horizon of groundwater. The groundwater level is mainly dependent on rainfall and the permeability of the ground. The direction of groundwater flow corresponds to the neogene bedrock surface gradient, and is drained directly to Blatina creek, but the direction of flow is a stream which flows to the creek, which flows out from the dam, situated above the city. Based on empirical relationships we can assume the coefficient of permeability value of the gravel soils of the order of 1.10^{-5} to 1.10^{-6} m s^{-1}.

In the City of Pezinok water supply system provides drinking water to almost the entire territory of the city. For the water supply purposes are fully used the available local resources. Because of the insufficient volume of these water sources the city of Pezinok has to be supplied by the water sources, located at relatively far outside of the city area (water resources Šamorín, Podunajské Biskupice, approx. 20 – 28 km). Connection rate the area is according to the operator around 96%, which is more than the national average (about 86%) and there are total 20,865 inhabitants served with water supply. Problem of the existing water supply network is relatively high age of the network pipes (mainly steel pipes), frequent high failures occurrence and resulting high water losses rate in the supply network [5].

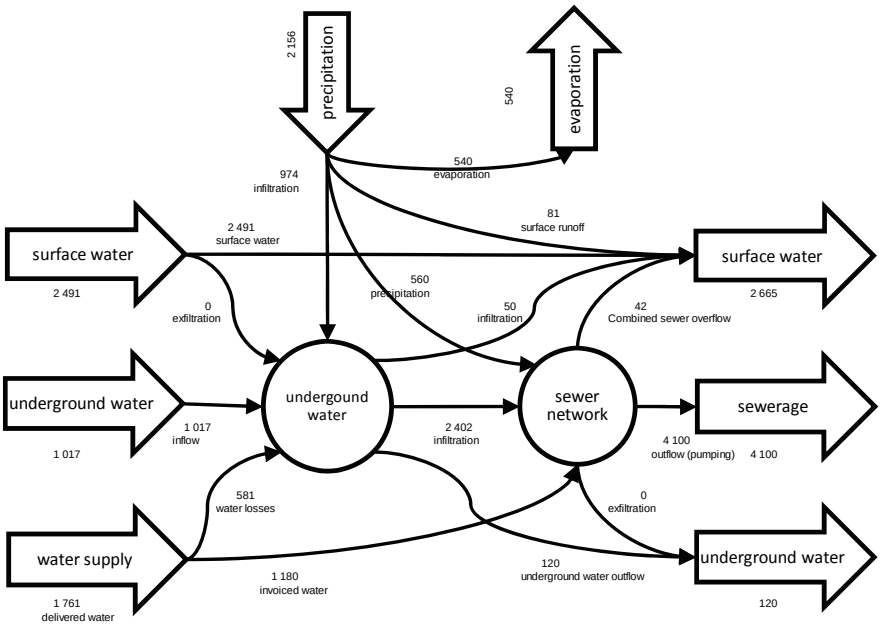

Fig. 2. Water balance of Pezinok town area (in 10^3 m^3 y^{-1})

In the City of Pezinok combined sewerage network with an existing wastewater treatment plant (WWTP) exists since 1970. The WWTP was located in the southern outskirts of the city. The problem of the sewer network in the city is also its relatively high age and high proportion of infiltration water into the sewer network [2, 5]. A significant change in the sewerage system come into being at the end of May 2009: The operator discontinued work of the existing WWTP in the town of Pezinok and all sewage water is pumped by pressure main to the central wastewater treatment plant in Bratislava – Vrakuňa (about 18 km), which has currently quite large unused capacity. Instead of the WWTP there is currently only sewage pumping station and a temporary accumulation tank for the waste water for the storm water storage or for the event of pump failure. Removal of the old, overloaded and malfunctioning wastewater treatment plant will probably improve water quality in the recipient Blatina in the near future. On the other hand the mentioned WWTP was not only pollution source, but also substantial tributary for the creek Blatina (average annual flow in

2008 was in the creek about 79 l s^{-1}, the flow of treated water from WWTP Pezinok was about 100 – 130 l s^{-1}).

Based on available data, we created a detailed scheme of the hydrological balance and water transfers in the town of Pezinok, which includes also volumes of water transported in and out of the city area by the water infrastructure (water supply, sewerage). This balance is shown on Fig. 2. At this point it should be noted that we received the water volumes from the water infrastructure operator (Bratislava waterworks company, a.s.) and for the quantities of water from natural sources we used available and accurate hydrological data. Where no such data were available, water volumes were determined on the basis of expert estimates. Of course, we assume data accuracy improvement during the project performance.

11.4. RISKS

The principle of water balance is the rule of mass conserving. If part of the water from surface runoff will be transferred into the infiltration facilities, a reduction of surface runoff will be achieved. However the implied question will be: what happens with the increased amount of underground water? Logical answer is, that there will be groundwater flow increase towards the surface water, which acts in urban catchments as underground drainage, but only in cases where the basin is with a sloping surface and surface water (creeks, rivers) are present in the urbanized area.

However, if the urbanized area is relatively flat and there is a sparse hydrographical network, it can be assumed that in the urban areas a relatively stable level of groundwater is established, particularly stabilized by leaky sewer systems, which acts in the urbanized area as a drain system. This level of groundwater was considered for many years as a natural level and lot of constructions were adjusted to this underground level on the site, particularly in terms of waterproof insulation of underground spaces, buildings and other infrastructure. Groundwater level rise, which may be due to the increased surface runoff infiltration, will probably result in the increase of infiltration into the sewer network.

Logical step of the sewer network operator is a rehabilitation of the sewer network and its sealing, in aim to reduce the water infiltration into the sewer network, but this will also increase the groundwater level, since the sewer network will be sealed and will no longer work as a drainage system for the underground water. This may be followed by further infiltration increase into the sewer network at the upstream sewer network sections and in particular on household connections, but probably also by unauthorized water inflows – particularly small drainage systems, built to protect the objects and buildings against the groundwater because of higher groundwater levels.

The above scenario looks in some respects very unlikely, but the cause of increased groundwater levels may not only be increased surface runoff water infiltration, it can also be due to increased precipitation (this happens indeed in the extremely wet years) and the fact is that certain aspects and events described above are already happened in the past at various locations.

11.5. SOLUTIONS

The solution of this difficult situation can be technical measures aimed to achieve the original hydrological conditions. These measures may be aimed in two directions:

1. In cases where it is necessary, it is appropriate to reduce the amount of infiltrated water by using other means of surface water runoff disposal, e.g. evaporation support measures (green roofs, detention tanks), elimination of illegal outlets, the drainage.
2. groundwater level decrease by other means, than infiltration into leaky sewer network, for example with other drainage systems.

In the first case we have to ensure, where necessary, that we will infiltrate to the underground water only such quantity of surface runoff water, which does not negative affect the water balance and groundwater will not endanger buildings located in urban areas. The solution may be to support the evaporation with green roofs. It may be also the storage of runoff water and its re-use, e.g. for irrigation of urban green areas, recharge water in fountains, and watering the streets. It is also possible to use rainwater as process (service) water in industry, respectively also in households (toilets flushing or washing). A separate group of measures to evaporation support in cities is to establish water bodies, which may serve as an open air stormwater tanks.

Naturally, there must be also effort of the infrastructure operator to eliminate illegal drainage inlets to public sewer system, even though this is quite tedious and difficult task, requiring household's connection inspection in combination with monitoring of the drinking water consumption and wastewater production in dry weather period.

The second group of measures (in aim to decrease groundwater level in urban areas) may include measures to reduce groundwater levels by point, line or area drainage. Construction and operation of new drainage facilities for the underground water decrease will be probably financially very expensive and will require different restrictions for residents; therefore, this method is appropriate only in specific parts of the cities. However, we believe that in some cases it would be possible to use the existing drainage systems were built, e.g. during the construction of buildings or the construction of certain utilities.

An interesting way how to resolve this situation was shown in the town of Liptovský Hrádok within the project "Environmental improvement of the Liptov region", co-funded by the EU Cohesion Fund (former ISPA). In the city a new sanitary sewer system was build, and the old and leaky combined sewer system was reclassified to a storm sewer network, so a complete separated system was established. Thus, old and leaky sewer system diverts water from surface runoff, and because it was not sealed, it works as a drainage system for groundwater.

Infiltrated underground water has typically very low pollution level, so we can assume that in most cases, that the state water authorities will not have objections to their direct discharge into surface water (recipients) without further treatment (but some mechanical pre-treatment will be required for rainwaters).

11.6. CONCLUSION

The paper deals with the quantitative water balance of an urban catchment. The overall objective of surface runoff management is to achieve such hydrological characteristics of the urbanized catchment, which are similar or equal to the natural catchment. It is mainly an effort to reduce the velocity and volume of surface runoff and the effort to increase the

groundwater build-up, in other words to increase infiltration of surface runoff by disconnection of paved surfaces in urban areas and infiltration of the surface runoff water into the groundwater. The question is if such an increase of groundwater volume, which also leads to groundwater levels increase is acceptable and appropriate for urban catchment area. On the one hand, it represents an approximation to the natural conditions, but on the other hand it partially changes long-term steady hydrogeological regime of groundwater flow, which can cause considerable problems for all buildings, located on urbanized area. Moreover, it is likely to be assumed that the increased amount of underground water ends in the sewer network, whether as infiltrated water, or as illegal inflow of the drainage water.

References

[1] Carlsson L. Falk J.: Urban hydrology in Sweden – an inventory of the problems and their costs. IAHS-AISH Publ. No. 123, 1977.
[2] Stanovenie nočných prietokov a prietokov podzemných vôd v jednotnej stokovej sieti v meste Pezinok. (Determination of night flows and groundwater inflows in a combined sewer network in the town of Pezinok). Department of Sanitary Engineering, Faculty of Civil Engineering, Bratislava, 1996.
[3] Stephenson D.: Comparison of the water balance for an undeveloped and a suburban catchment. In: Sciences-Journal – des Sciences Hydrologiques, 39, 4, August, 1994.
[4] Stránský D. et al.: Posouzení stokových systémů urbanizovaných povodí. část II. – Řešení odtoku v povodí a stavebně – technický stav stokové sítě. (Assessment of drainage systems in urban catchments. Part II. – Runoff management in urban catchment and structural and technical status of the sewer system) In: Vodní hospodářství, ISSN 1211-0760, Vol. 60, No. 7/2010, pp. 184–186.
[5] ÚPN mesta Pezinok (Land use and territorial plan), AUREX, s.r.o. Bratislava, r. 2010.
[6] Yangwen Jia, Guangheng Ni, Yoshihisa Kawahara, Tadashi Suetsugi: Simulation of hydrological cycle in an urbanized watershed and effect evaluation of infiltration facilities with wep model. In: Journal of Hydro science and Hydraulic Engineering Vol. 19, No. 1 May, 2001, 43–52.

Acknowledgement

This paper was written with the support of the scientific grant agency VEGA in terms of solving the grant task no. 1/1143/1 „Integrované riešenie obnovy zdravotno-technickej infraštruktúry urbanizovaných sídiel, jej spoľahlivosť a vplyv na životné prostredie“. (“Integrated rehabilitation solution of sanitary infrastructure of urban settlements, its reliability and environmental impacts”).

12 Sensitivity Analysis of Numerical Water Quality Model Considering to the Dispersion Coefficient Values

Marek Sokáč (Slovak University of Technology, Bratislava,
Dpt. of Sanitary and Environmental Engineering), Yvetta Velísková
(Institute of Hydrology, Slovak Academy of Science, Bratislava)

12.1. INTRODUCTION

The article is aimed at the study of how the values of dispersion coefficients, used as model input data, affect the results of water quality numerical simulation. This paper is partly based on the results obtained within previous project conducted in cooperation with the Institute of Hydrology of the Slovak Academy of Science and the Department of Sanitary and Environmental Engineering of the Slovak University of Technology in Bratislava. The objective of the project was to improve reliability and increase applicability of existing model tools for simulation of transport of water and dissolved substances in complex natural conditions and different hydrological situations. Numerical simulation of any area is based on detailed, complete and updated input data set. A dispersion coefficient is one of the crucial input parameters of transport processes. The previous research within the mentioned project [5] was aimed at determining these coefficients and obtained results have been applied to this study. A one-dimensional model applying longitudinal dispersion coefficient as an input dispersion parameter is used for numerical simulation in this study.

12.2. THEORETICAL BASIS

In this chapter we are going to discuss the basic theoretical terms and relationships related to dispersion in open streams only to the extent important in relation to the scope of the article.

One-dimensional advection-diffusion equation is the simplest mathematical formulation of dispersion:

$$\frac{\partial AC}{\partial t} + \frac{\partial QC}{\partial x} - \frac{\partial}{\partial x}\left(AD\frac{\partial C}{\partial x} \right) = -AKC + C_2.q \qquad (1)$$

Where: C is concentration of relevant substance (mg l^{-1}), D is dispersion coefficient (m^2 s^{-1}), A is flow area (m^2), K is a coefficient expressing the effect of chemical and biological processes on dissolved substance (s^{-1}), C_2 is concentration of resource, q discharge of resource, x is a length (m) and t is time.

This equation includes two basic transport mechanisms:

1) advective (or convective) transport caused by fluid flow,
2) dispersion transport caused by concentration gradient.

Advection-diffusion equation is based on the following assumptions:

— a substance under consideration is homogenously distributed over the cross section and an ideal mixing (immediate homogenisation in cross section) is taken into account even for resource/abstraction of substance,

— a substance is conservative (is not subject to chemical and biological processes) or its interaction with environment can be described using the first order differential equation

$$\frac{dC}{dt} = K, C \tag{2}$$

— Fick's law of diffusion is applied, i.e. dispersion transport is proportional to the concentration gradient.

The first assumption, namely ideal mixing and homogenous distribution of substances in cross section, is a result of one-dimensional description of model area using the MIKE 11 model. Such description is applicable where one dimension predominates over other (for example the river where the length is a determining dimension and the phase of cross-sectional mixing can be neglected). However, this assumption cannot be applied to water reservoirs in any case where distribution of hydraulic parameters over the depth and width of flow cross section plays a significant role (this situation requires at least two or three-dimensional simulation).

12.3. MODEL MIKE

MIKE 11, developed by the Danish Hydraulic Institute, is a set of programmes for simulation of flow, water quality and sediment transport in rivers, channels, river mouths, irrigation systems and other surface water resources.

It is a dynamic one-dimensional modelling tool for detailed proposal and management of simple and complex river and channel systems. Simulation results can be used in engineering, water management, water quality management and planning applications.

MIKE 11 consists of several modules for: hydrodynamics (basic module), hydrology, cohesive sediment transport, water quality and non-cohesive sediment transport. In this study only the basic hydrodynamic and advection-dispersion transport modules are used for simulation. Generally, a module structure of the model offers great flexibility: each of modules can be processed separately; data transfer among modules is automated; coupling of physical processes is easier; quick and simple application and development of new modules is possible.

The type of database technology used in the model provides efficient data storage and retrieval. Data organization and handling is unified within the whole model system. MIKE 11 is operated through the interactive control menu system.

Hydrodynamic module is a basic computational module required to run other computational modules. The module simulates unsteady flow in streams through the finite difference method by using implicit computational scheme. The computational scheme is applicable to vertically homogenous stream in conditions of subcritical and supercritical flows. The hydrodynamic module requires the most data from all modules that are used. The data are stored in several datasets and in some cases it is possible to import data from other formats (text files). The data can be categorized into two large groups:

1) geometric data (describing stream channel geometry, dimensions and topology) and
2) hydraulic parameters (hydraulic roughness of stream channel etc.).

Advection-dispersion module is based on the one-dimensional equation of mass conservation of dissolved and suspended solids (e.g. salts or cohesive sediments). This module requires the outputs of hydrodynamic module in time and space (discharges, water levels, hydraulic radius and flow areas). Advection-dispersion equation (see equation (1)) is solved numerically using implicit scheme with the finite differences. Suddenly changed concentrations can be simulated in this way. For advection-dispersion module, it is important to specify the substances considered in simulation and the value of dispersion coefficient. This value can be specified according to the equation:

$$D = a.v^b \tag{3}$$

Where a is a dispersion factor and v is a flow velocity. The resulting value of dispersion coefficient can be defined by setting the minimum and maximum values.

Simulation of pollution transport in the Hron River for the study of the effect of dispersion coefficient and pollutant concentrations along the river were carried out using the numerical model of the Hron River in the section from Slovenská Ľupča (river km 183.84) up to the river mouth (river km 0.0). Numerical simulations were performed using the abovementioned MIKE 11 model. For all alternatives of simulation we took into consideration a uniform load of receiving body (the same concentration of pollutant). The ammonia pollution was taken into account in simulation and it was specified as a concentration of ammonia nitrogen $N–NH_4$ in the model. The modelled way of getting the pollution into the river is similar to accidental pollution of river, i.e. discharge (release) of larger wastewater volumes with relatively high concentrations of ammonia nitrogen (800 mg l^{-1}) during two hours. It is clear that these inputs to the numerical model represent extreme emergency situation. However, our objective is to analyse the sensitivity of simulation results to data used as model inputs regardless of the impacts of accident on water quality in a stream. To clarify this issue it is important to note that the decrease in concentrations (see charts of this article) is caused not only by the dispersion but also by mixing the water in the Hron River with its tributaries (dilution) and by biological oxidation processes that are included in the MIKE 11 model (water quality module – WQ). The objective of this article is to determine the sensitivity of numerical models to input values of the dispersion coefficient while maintaining other processes having an effect on changes in quality of water in stream (physical, chemical and biological processes of water self-purification).

The value of dispersion coefficient D was selected through the dispersion factor a and exponent b according to the equation (3). The values in the range from 5 to 50 were used for dispersion factor a. Two series of numerical simulations were performed in order to eliminate the effect of flow velocity on pollution dispersion from the results of simulation. One series was done using the exponent value in the equation (3) $b = 0$, and thus the value of dispersion coefficient did not depend on flow velocity. The value of exponent in the second series of trials was $b = 1$ and the dispersion coefficient was a function of flow velocity according to the equation (3).

All the mentioned simulations were carried out in two alternatives – hydrological conditions: average annual discharge Q_a in particular cross sections along the whole length of river, and the discharge close to the minimum value – Q_{355}.

12.4. OUTCOMES AND DISCUSSION

We have obtained a number of curves showing the distribution of concentration along the whole length of the monitored section of river. Then the curves were analysed. The analysis was aimed at the change in distribution of concentrations at different values of the dispersion coefficient while eliminating the effect of flow velocity (b = 0). One of such cases is shown in figure 1 (for Q_a and Q_{355}). It is apparent that the time-concentration curves in considered cross section differ in dispersion coefficient value from each other. The model responds to the changed value of dispersion characteristics. The values of maximum concentrations also differ from each other regarding the value D and definitely the discharge condition applied to particular model situation.

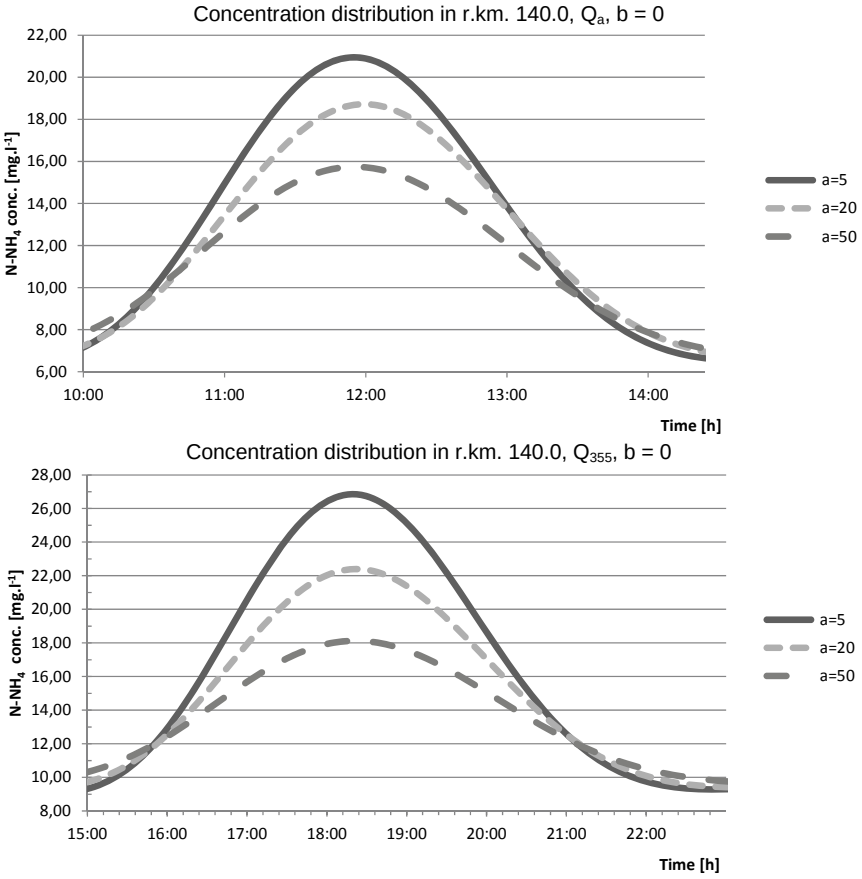

Fig. 1. Concentration curves at river kilometre 140.0 and Q_a and Q_{355} (b = 0)

Other two figures – figures 2 and 3 – show the comparison of simulation results proving the effect of dispersion coefficient, whether it is the function of flow velocity in a given river section or not. According to the equation (3), when b equals 0, than the value of dispersion coefficient D taken into account in simulation is not affected by the flow velocity.

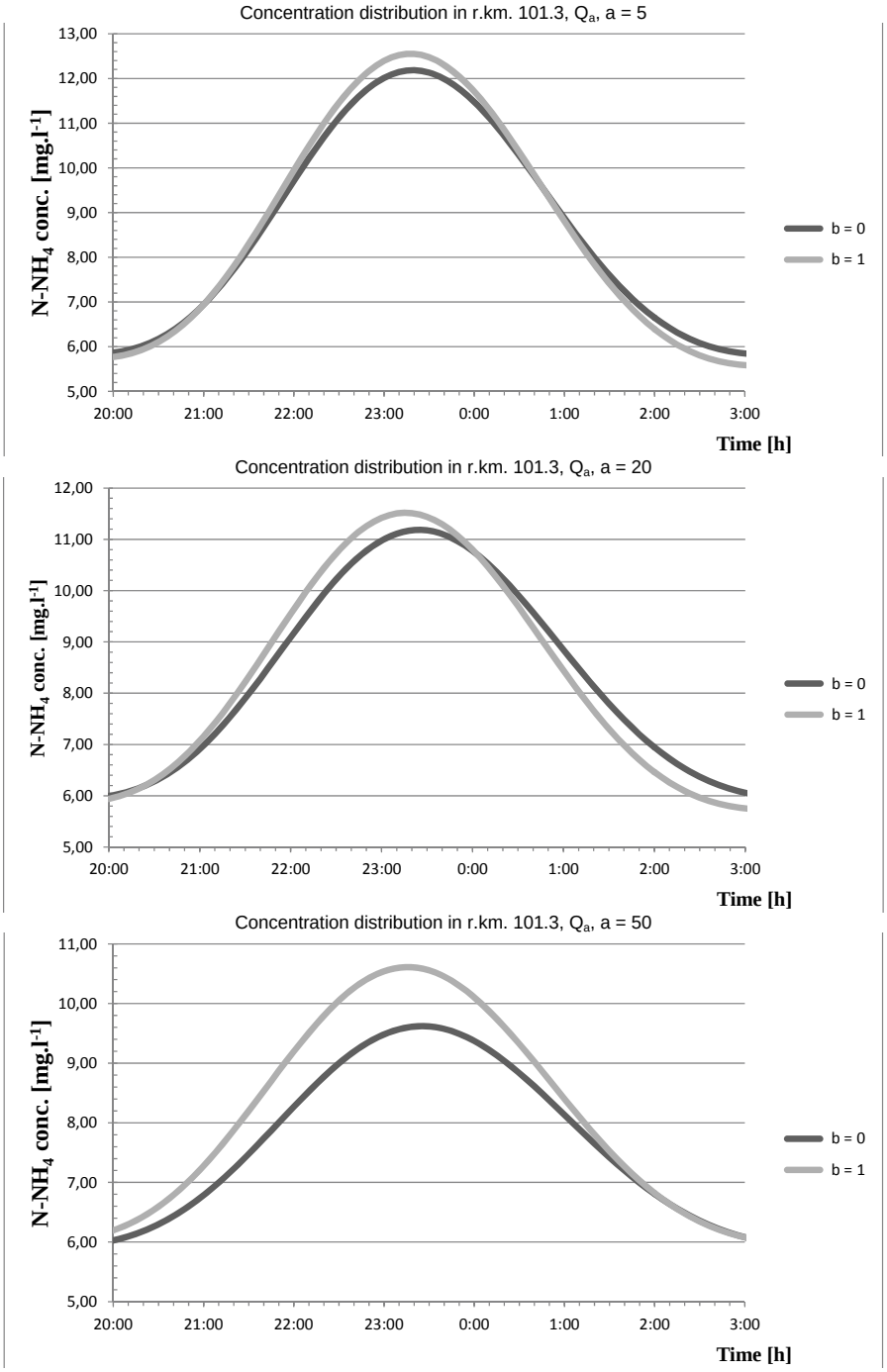

Fig. 2. Concentration curve at river kilometre 101.3 for different values of coefficient *a* (equation (3)) (considering the effect of flow velocity $b = 1$ or without the effect of flow velocity $b = 0$) – discharge Q_a

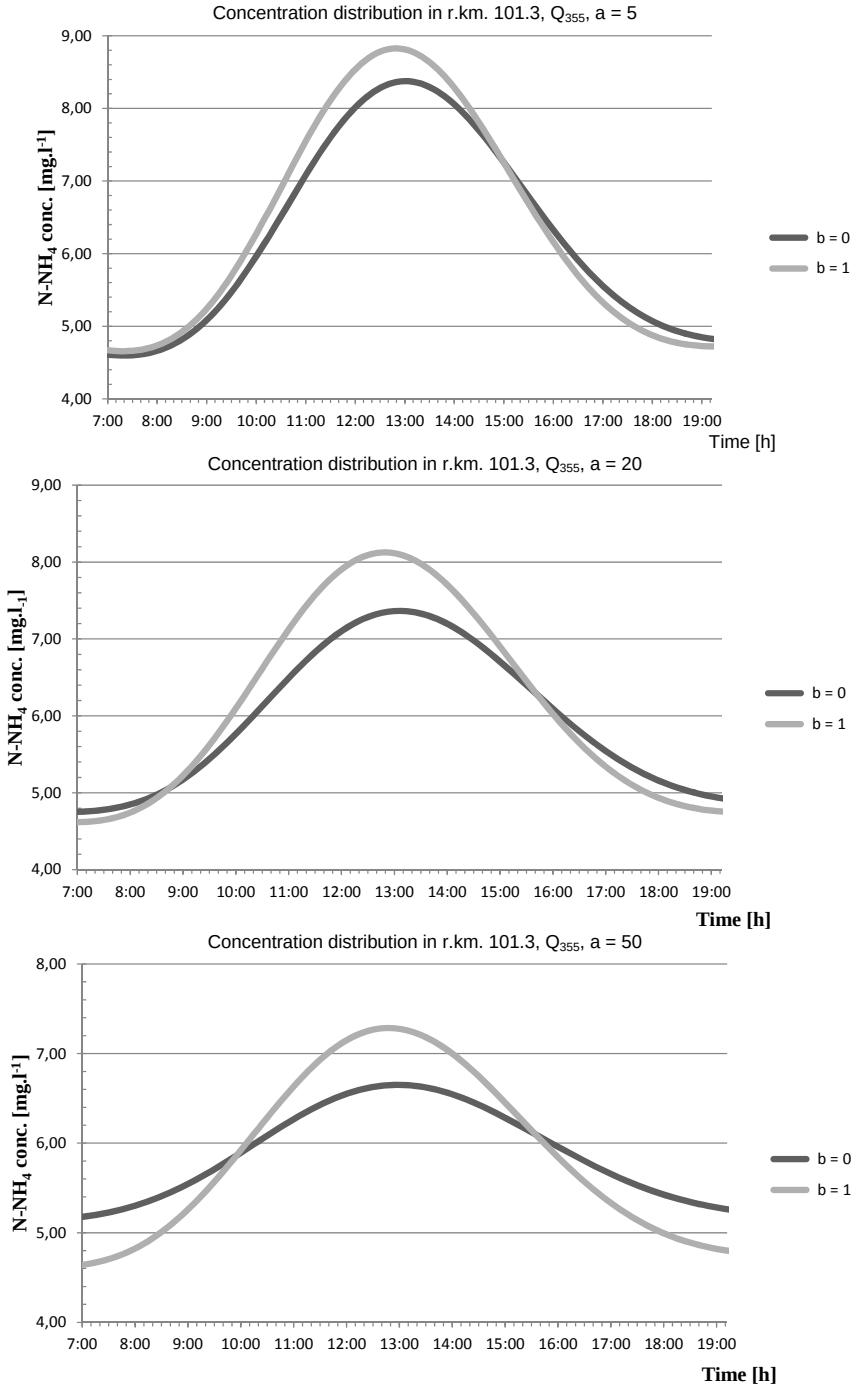

Fig. 3. Concentration curve at river kilometre 101.3 for different values of coefficient *a* (Eq. (3)) (considering the effect of flow velocity b = 1 or without the effect of flow velocity b = 0) – discharge Q_{355}

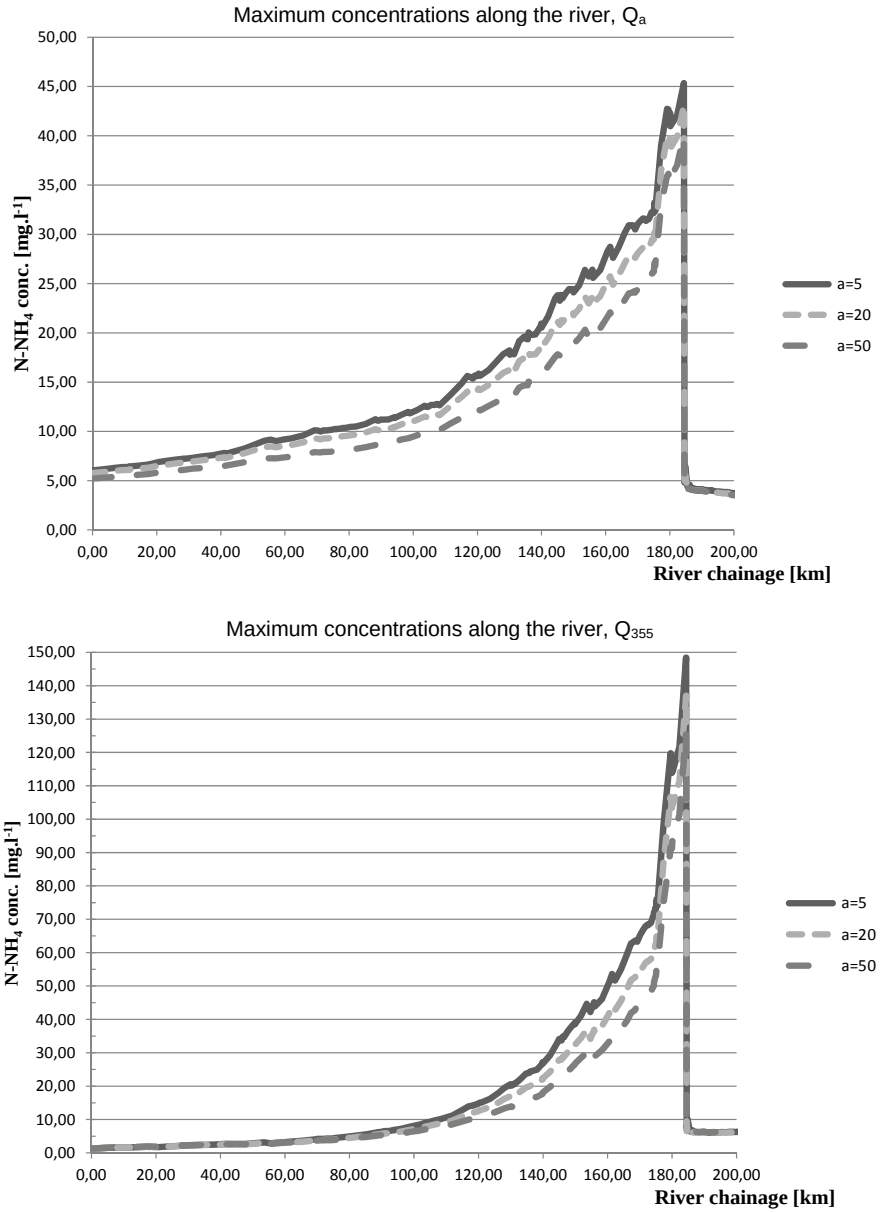

Fig. 4. Maximum concentration curve along the simulated section of the Hron River

On the contrary, if $b \neq 0$, than the value of dispersion coefficient becomes the function of flow velocity and thus it is influenced by this parameter. The results of the simulations show (see figure) that such method of setting the values has an effect on distribution of pollutant concentration in stream – maximum concentration values and concentration distribution curve shape are changed. These differences are less significant for Q_a ($Q_a > Q_{355}$) than for Q_{355}. That is due to the fact that flow velocity in stream at Q_a is higher and close to

the value of 1 m s^{-1} compared to Q_{355} where the velocities are considerably lower. However, it is important to take into account the effect of dispersion factor *a* of the equation (3) on the value of dispersion coefficient *D*.

Another output of the series of simulations was the distribution of maximum concentrations along the simulated section of the Hron River. This graphical output has a great significance in the assessment of the change in water quality due to potential accidental pollution. The figure 4 indicates the distribution of concentrations for both simulated discharges (Q_a and Q_{355}) as well as for different values of dispersion coefficient *D* (5; 20; 50). As shown in the figure, the effect of selected value for dispersion coefficient is evident. Despite the fact that this case is a theoretical simulation of accidental pollutant discharge into a stream and the concentrations indicated in the charts are also only theoretical (illustrative), it is important to be aware of the differences in maximum concentrations at particular river kilometre for different dispersion coefficient values. Such differences could be of crucial importance to river biota in a real situation.

12.5. CONCLUSION

The article deals with the sensitivity of MIKE numerical model outputs to used values of dispersion coefficients. These coefficients are one of the main characteristics affecting the dispersion phenomenon in a stream. Figure 1 clearly shows how this phenomenon affects pollution transport – when the value of dispersion coefficient is low, the dispersion phenomenon is minimal and concentrations of transported substance are higher than in case when the dispersion is applied in a larger extent.

As it was stated previously, if the real situation in stream is assessed, the differences in the values of maximum concentrations at particular river kilometres for different values of dispersion could be of crucial importance to river biota. Therefore, it is important to select the value of dispersion coefficients in simulation model very precisely which is also confirmed by the results of this study.

We expected more explicit result when we firstly intended to find out the sensitivity of water quality numerical model to used values of dispersion coefficients. As the outcomes of simulations indicate, it is necessary to continue with the analysis because there are still many factors entering the assessment and affecting the explicitness of effects.

References

[1] Kosorin K.: Disperzný koeficient pre prirodzené profily povrchových tokov. (Dispersion coefficient for natural cross-sections of surface watercourses) J. Hydrol. Hydromech., 43, 1995, 1–2, 93–101.

[2] Říha J. et al.: Jakost vody v povrchových tocích a její matematické modelování. (Water quality and its modeling) NOEL, 2000, Brno, 269 p.

[3] Sokáč M.: The influence of discontinuous pollution sources on the receiving water body (in Slovak). Slovak University of Technology, Bratislava, Faculty of Civil Engineering, Edition of scientific works, sheet 87, ISBN 978-80-227-3328-1, 104 p.

[4] Swamee P. K.; Pathak S. K., Sohrab M.: Empirical relations for longitudinal dispersion in streams. Journal of Environmental Engineering 126 (11), 2000, pp. 1056–1062.

[5] Velísková Y., Dulovičová R., Sokáč M.: Determination of the Size of the Longitudinal Dispersion of the Flow with a Free Water Surface in a Prismatic Channel. Part 1: Straight Stretch of Route. (in Slovak) Acta Hydrologica Slovaca, 1, 35–43 (2009a).
[6] Velísková Y., Dulovičová R., Sokáč M.: Determination of the Size of the Longitudinal Dispersion of the Flow with a Free Water Surface in a Prismatic Channel. Part 2: Straight Curved line. (in Slovak) Acta Hydrologica Slovaca, 2, pp. 328–335 (2009b).
[7] Velísková Y., Sokáč M., Dulovičová R.: Determination of longitudinal dispersion coefficient in sewer networks. WMHE 2009. Vol. I.: Eleventh International Symposium on Water Management and Hydralic Engineering. Ohrid, Macedonia, 1.-5.9.2009, Skopje, University Ss. Cyril and Methodius, 2009., ISBN 978-9989-2469-6-8., S. 493-498. (2009c)
[8] Velísková Y., Sokáč M.: Sensitivity of Water Quality Numerical Model for Used Dispersion Coefficient Values (in Slovak) Acta Hydrologica Slovaca, 2, pp. 210–218, 2010.

Acknowledgement

This article was prepared with the support of the Scientific Grant Agency APVV within the implementation of the project no. APVV-0274-10 „Kvantifikácia vplyvu vstupných údajov a parametrov modelového prostriedku na presnosť výstupov simulačných modelov disperzie v povrchových tokoch“ (Quantification of input data and model parameters influences on correctness of outputs of dispersion models for surface water).

13 Variable Patterns of Evapotranspiration in a Protected Wetland Catchment Inferred from MODIS Data

Urszula Somorowska (University of Warsaw, Faculty of Geography and Regional Studies, Department of Hydrology, Warsaw, Poland)

13.1. INTRODUCTION

A quantification of water resources available for ecosystems is a prerequisite for any water management practices. In case of water sensitive environments this issue is of the primary importance. In temperate regions where precipitation recharging the soil water and groundwater resources is highly variable in space and time, the quantification of water available for ecosystems remains an important issue. Given the importance of green and white water fluxes for the maintenance of natural ecosystems, a fundamental understanding of their quantities and dynamics is required.

The question asked in this study was to identify seasonal and inter-annual variability of evapotranspiration (ET) in a protected wetland catchment of the Łasica Channel (Fig. 1). This catchment is located in the central part of Poland (N 52°13' – N 52°26' and E 20°15' – E 20°57'), on the Mazovian Lowland, within boundaries of the Kampinos National Park (KPN). It covers the area of about 363 km^2. There are wetlands of international importance belonging to the UNESCO Biosphere Reserves requiring protection and regeneration. Such ecosystems need environmentally oriented water management approach one of which is sustaining or restoring the water regime [1]. Elaboration of reconstruction methods of former water conditions in the catchment requires the identification of current hydrological processes, in them the ET, as a starting point for implementation of restoration measures. While quantifying the ET at a point is relatively achievable e.g. through lysimeters and tower flux measurements, characterizing it at a catchment scale is still a challenging opportunity.

For catchment studies high-resolution satellite images are applicable to derive averages of land characteristics over the specific region. Simultaneously, estimation of terrestrial ET from earth land surface by using satellite remote sensing data requires special algorithms. Recently developed algorithm to estimate ET using the Penman-Montheith was developed by the Numerical Terradynamic Simulation Group at the University of Montana [2, 3, 4]. It has enabled estimation of actual levels of ET across the globe, using imagery collected by the Moderate Resolution Imaging Spectroradiometer (MODIS) instrument aboard the NASA satellite Terra. Successive improvements to a MODIS Global Terrestrial Evapotranspiration Algorithm has resulted in preparation of monthly-averaged estimates with 1 km resolution for the entire globe [5]. In this study the ET estimates from the MODIS Global ET Project (MOD16) were acquired for years 2001–2008 from the NASA Land Measurement Portal.

The specific objectives of this study were the following: (1) to provide an assessment of the water participating in the evapotranspiration process under different land use in the protected catchment using MODIS estimates of the ET, (2) to track monthly ET rate related

to the depletion and recharge patterns of the soil moisture conditions and dynamic groundwater storage, (3) to display the interactions between the ET and vegetation. The study yields unique data of ET estimates across the protected catchment as for the incorporation into the water balance. Variable ET patterns are referred to the changes in the subsurface water storage inferred from the monitoring system of groundwater levels and soil moisture.

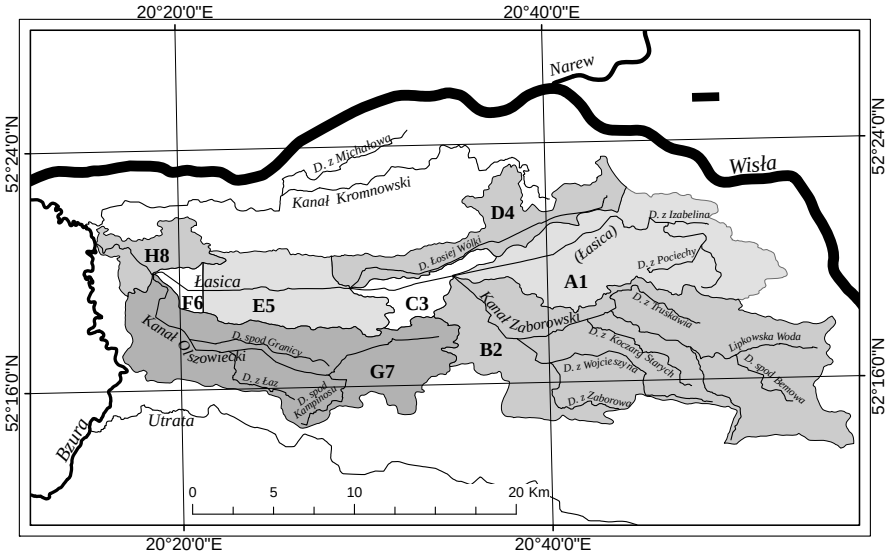

Fig. 1. Location of the Łasica catchment and its sub-catchments

13.2. DATA AND IMAGE PROCESSING

Evapotranspiration estimates produced with the Moderate Resolution Imaging Spectroradiometer (MODIS) sensor were acquired at a spatial resolution of 1 km and temporal resolution of 1 month in years 2001–2008. The MODIS data product labeled 'MOD16A2' stored in sinusoidal grid tiling system in HDF format was acquired to extract the subdata set of the ET. Data were extracted and processed in the ArcGIS version 9.3.1 for horizontal tile number 19 and vertical tile number 03 (h19v03). In the analysis of the interaction between ET and vegetation, the Normalized Difference Vegetation Index (NDVI) was applied using the MODIS data product labeled '13A3'. Additionally, the MODIS Terra/Aqua Land Cover product labeled '12Q1' was acquired for the land use evaluation. This land cover scheme identifies 17 land cover classes defined by the International Geosphere Biosphere Programme (IGBP), which includes 11 natural vegetation classes, 3 developed and mosaic land classes, and three non-vegetated land classes (https://lpdaac.usgs.gov/lpdaac/products/). Within the analyzed catchment there are five land use classes distinguished. Evergreen needle leaf forest covers 10% of the catchment area, deciduous broad leaf forest – 5%, mixed forest – 42%, agricultural land – 56%, mosaic of natural vegetation and cropland – 6% and urban and built up areas – 9%. Grasslands and croplands occupy accordingly 44% and 56% of the agricultural land. Protected ecosystems of special ecological importance are situated within the lowland wet-

land strips that belong to the grassland, deciduous forest and mosaic classes. Besides groundwater records from the monitoring system of the KPN as well as soil moisture in situ data were utilized [6].

13.3. TEMPORAL AND SPATIAL VARIABILITY OF EVAPOTRANSPIRATION

Temporal and spatial patterns of ET were determined for the catchment scale, within dominant land use types and for main sub-catchments.

13.3.1. Evapotranspiration at a Catchment Scale

Temporal variability of monthly ET is displayed in Figure 2 whereas spatial distribution of annual ET is presented in Figures 3 and 4.

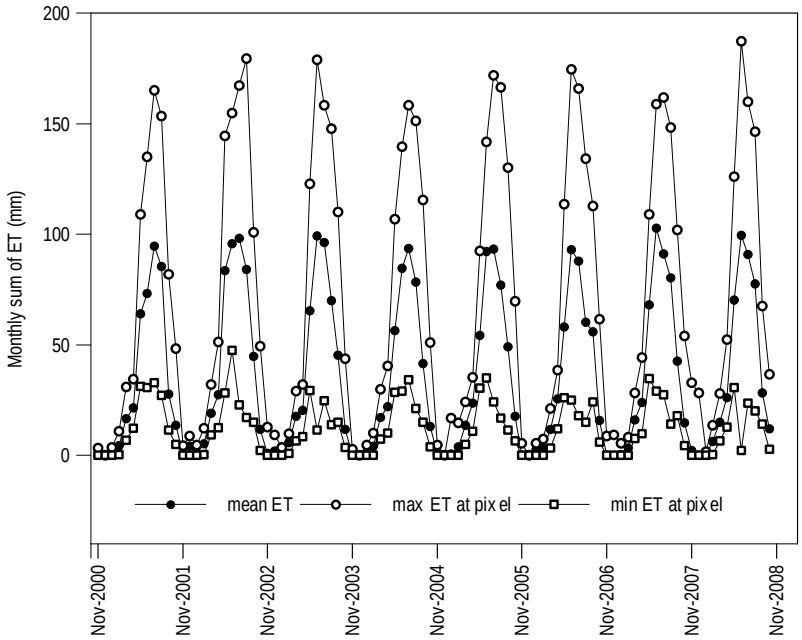

Fig. 2. Mean monthly sums of ET in the Lasica catchment in years 2001–2008. Maximum and minimum sums of ET for particular month display the range of ET variability

In months November-April the ET is the lowest. In summer half of the year the maximum ET of approximately 90 mm/month appear in months June-July. From July on, the ET gradually decreases to 77 mm/month in August, 42 mm/month in September and 14 mm/month in October. The maximum monthly pixel ET reached the value of 187 mm (June 2008). Maximum annual sums of the catchment ET appeared in 2002 (475 mm) and in 2007 (444 mm). Although maximum pixel values of annual ET reached 757 mm in 2008 (Fig. 4).

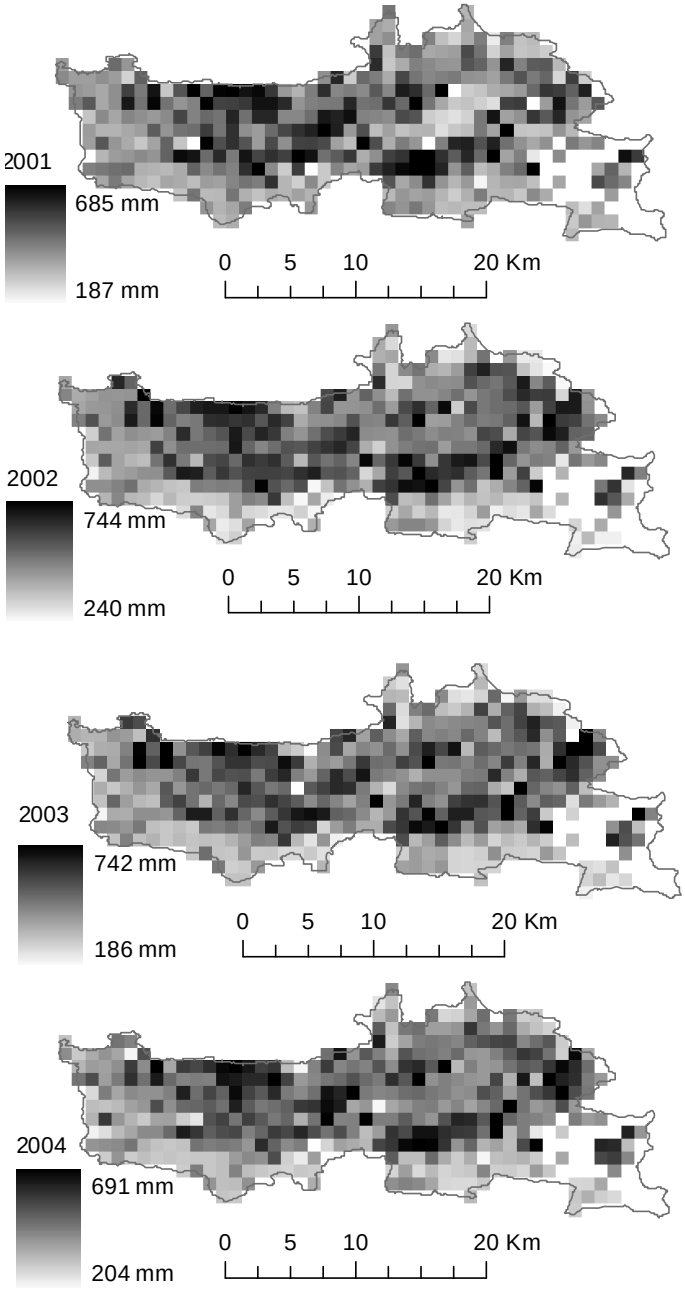

Fig. 3. Spatial patterns of ET annual sums in the Łasica catchment in years 2001–2004

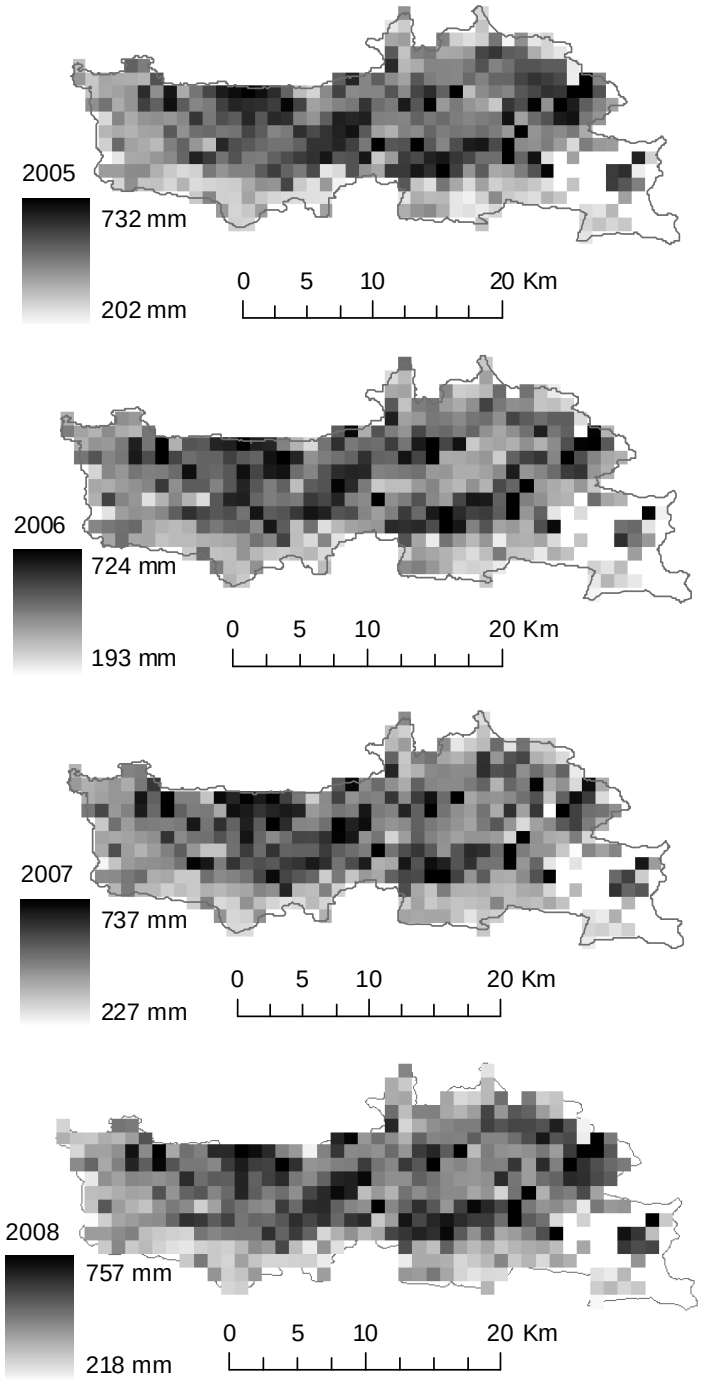

Fig. 4. Spatial patterns of ET annual sums in the Łasica catchment in years 2005–2008

13.3.2. Evapotranspiration Across Different Land Use

Temporal variability of monthly ET for different land use categories are presented in Figures 5 and 6. For all land use classes the regular rhythm of low ET values in winter followed by gradually increasing values in summer is observed every year. The highest monthly ET across all vegetation types are observed from June to July. The highest values concern deciduous forest; in July the ET is approximately 130 mm on average whereas across coniferous forest it is approximately 95 mm and 109 mm across mixed forest (Fig. 7a). In areas of mosaic vegetation consisting of grasslands and cropland the ET in July is relatively high reaching 109 mm in July (Fig. 7b). Across cropland areas the ET values are within the range of 70–78 mm in June and July.

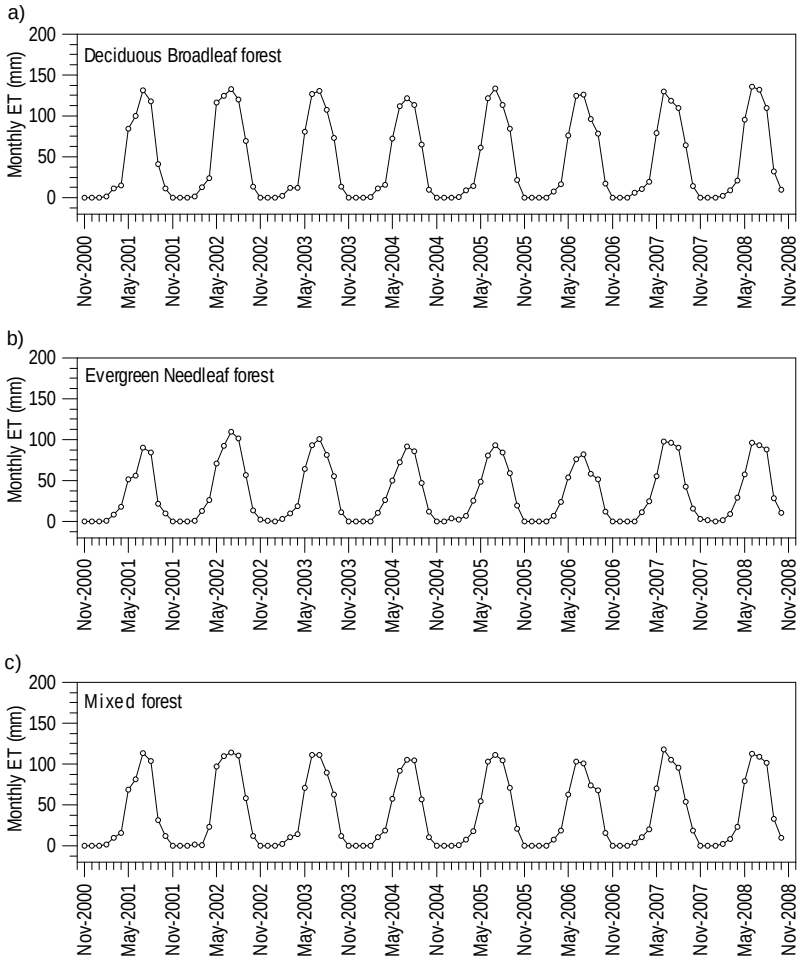

Fig. 5. Monthly ET time series in the Łasica catchment for deciduous (a), coniferous (b) and mixed forests (c), on average in landuse class, in hydrological years 2001–2008

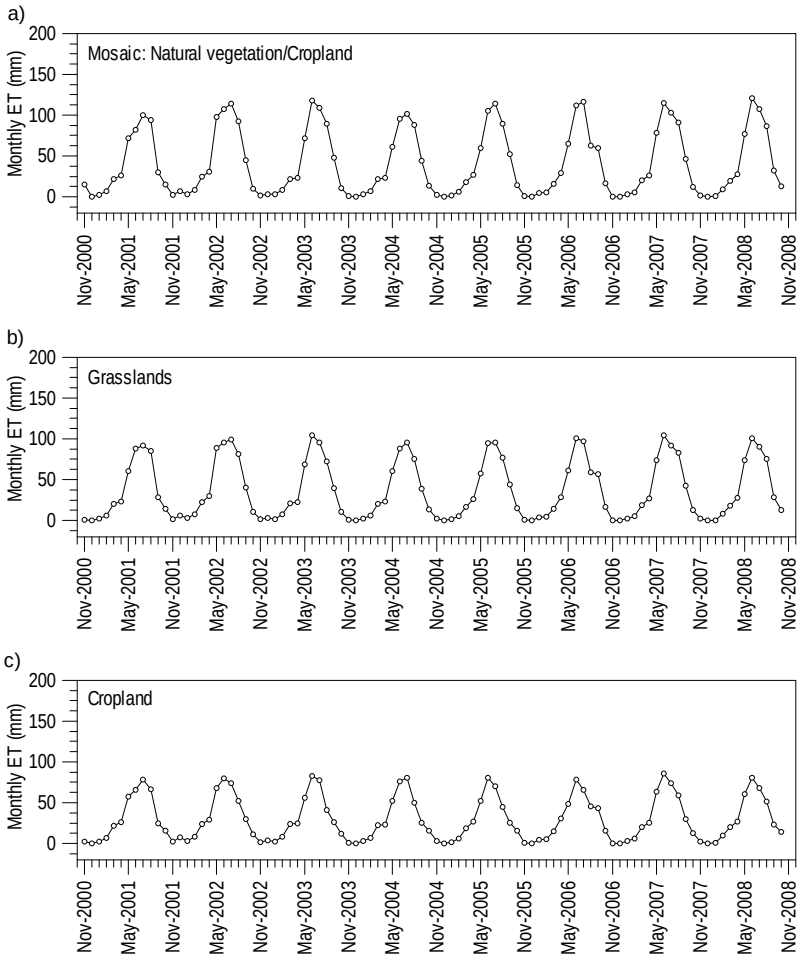

Fig. 6. Monthly ET time series in the Lasica catchment for mosaic vegetation: natural and cropland (a), grasslands (b) and croplands (c), on average in land use class, in hydrological years 2001–2008

The above mentioned values are averages across different land use classes. In particular cases the pixel values within each land use class differ significantly from the mean values depending on local land surface characteristics.

13.3.3. Mean Evapotranspiration in the Sub-catchments

Mean, maximum and minimum values of the annual ET in the sub-catchments are presented in Table 1. The highest annual ET are observed in the sub-catchment E5 located in the middle west part of the Łasica catchment (Fig. 1). Most of the area (60%) is covered with lowland wetland strips of special ecological importance. Approximately 60% of the area is covered by deciduous and coniferous forest, and approximately 30% by grasslands and mosaic vegetation. Mean annual ET is 492 mm.

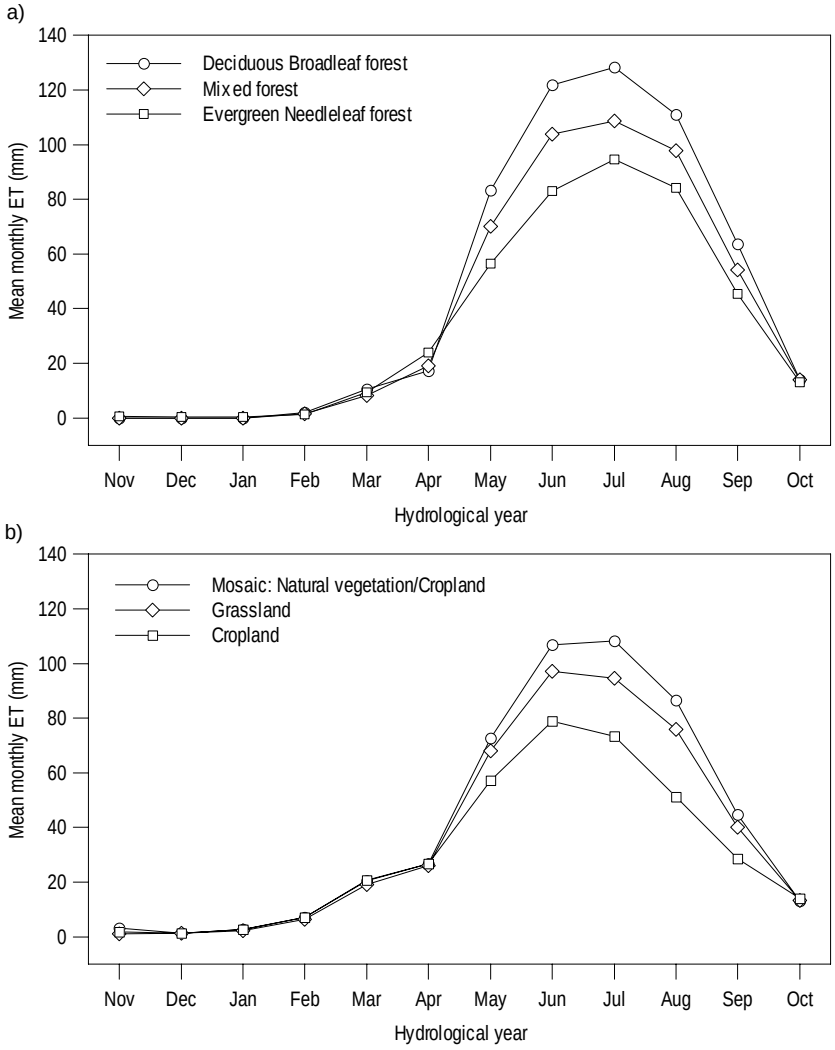

Fig. 7. Mean monthly values of ET in hydrological year in deciduous, coniferous and mixed forests (a) and in mosaic, grassland and cropland (b). Mean values derived from monthly values in years 2001–2008

Higher values then the mean appeared here in 2002 (560 mm) and in 2007 (508 mm). Relatively similar annual values are observed in the sub-catchment C3 where forests, grasslands and mosaic vegetation are also dominant. The lowest annual values concern the sub-catchment D4. The reason is the high contribution of agricultural land with dominant class of cropland. The highest differences within sub-catchment due to differentiation in land use appeared in the sub-catchment A1 and reached on average 220 mm y^{-1}. The smallest differences are characteristic for the sub-catchment F6 (61 mm y^{-1}) and C3 (89 mm y^{-1}). In these sub-catchments the land use is the most uniform.

Table 1

Annual sums of ET (mm) in the sub-catchments of the Łasica catchment in years 2001–2008. Minimum and maximum of ET represent extreme values at pixel in the sub-catchment. Sub-catchments division is presented in Fig. 1

Year		A1	B2	C3	D4	E5	F6	G7	H8
2001	Min	231	187	383	297	313	359	204	298
	Max	685	617	553	538	574	521	577	523
	Mean	394	393	448	397	443	406	382	391
2002	Min	265	240	380	302	429	405	274	401
	Max	744	698	601	632	735	642	682	697
	Mean	499	466	499	444	560	482	437	494
2003	Min	234	259	388	237	186	370	249	324
	Max	742	721	572	615	699	662	613	657
	Mean	458	431	469	399	497	469	404	437
2004	Min	226	238	344	254	360	379	204	255
	Max	691	644	559	592	658	511	597	573
	Mean	431	403	455	407	469	418	372	394
2005	Min	228	239	389	255	352	367	202	307
	Max	732	661	578	620	727	527	593	589
	Mean	455	417	481	403	492	422	378	399
2006	Min	193	200	401	272	319	400	197	328
	Max	724	659	593	621	699	557	566	598
	Mean	418	395	477	408	478	448	383	402
2007	Min	227	256	420	290	337	415	266	362
	Max	737	691	628	618	730	584	618	657
	Mean	449	427	496	428	508	465	412	443
2008	Min	218	237	398	245	363	366	230	285
	Max	730	724	608	687	757	569	559	626
	Mean	457	424	488	411	485	444	382	403

13.3.4. Temporal Patterns of Interactions Between the Subsurface Water Storage and Evapotranspiration

In Fig. 8 it is seen that during summer months with high values of ET, significant decrease in the subsurface water storage is present. Decrease in the subsurface water storage concerns both the soil water storage and the groundwater storage. Increasing values of the ET are followed by gradual decrease in the subsurface water storage during summer. During winter, when ET is limited to the minimum, recharge of the soil water storage and groundwater take place.

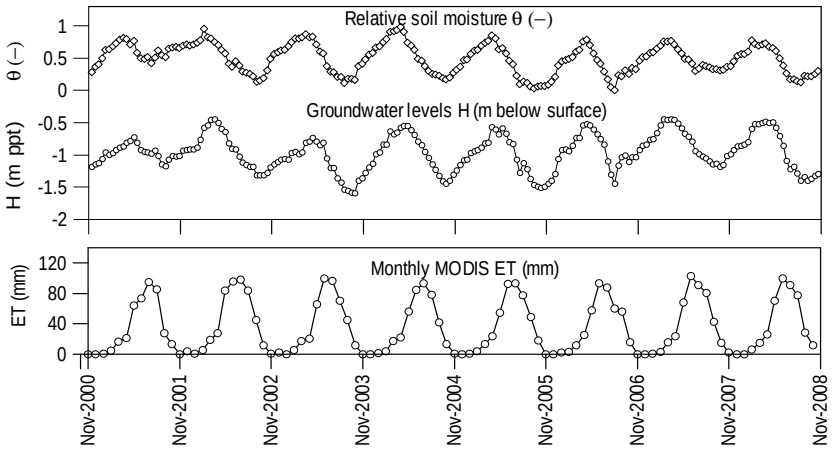

Fig. 8. Temporal patterns of soil moisture, groundwater levels and ET in years 2001–2008 in the Łasica catchment

13.3.5. Interactions Between Evapotranspiration and Vegetation

Relation between the Normalized Difference Vegetation Index (NDVI) and monthly ET, averaged for the catchment area, is displayed in Fig. 9. High values of NDVI are related with high photosynthetic activity and good conditions of plants. For NDVI-s equal to 0.7–0.8, the values of ET reach the level of approximately 80–100 mm.

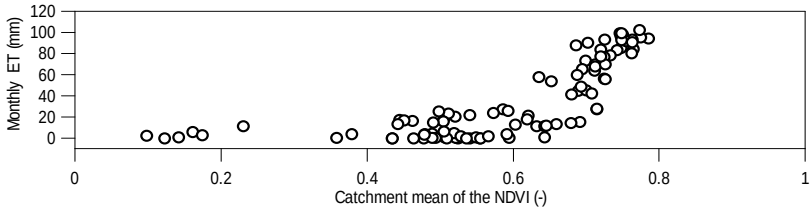

Fig. 9. Monthly values of ET versus NDVI averaged for the Łasica catchment

13.4. CONCLUSIONS

The study has provided basic understanding of the evapotranspiration rates at seasonal and inter-annual time scales over the lowland catchment within which protected ecosystems are present. Using satellite-derived MODIS data spatial and temporal variation of the evapotranspiration was identified in the catchment and sub-catchments detecting the range of monthly evapotranspiration in years 2001–2008. Enhanced understanding of temporal dynamics of evapotranspiration across the catchment is revealed through the consideration of different land use and links with vegetation conditions and subsurface water storage. Investigated relationships reveal the substantial dynamics of the green water fluxes.

References

[1] Somorowska U.: Perspectives of Water Management in a Protected Area of the Kampinos National Park. Miscellanea Geographica 10 (2002) 167–174.
[2] Cleugh H. A., Leuning R., Mu Q., Running S. W.: Regional evaporation estimates from flux tower and MODIS satellite data. Remote Sensing of Environment 106 (2007) 285–304 (doi:10.1016/j.rse.2006.07.007).
[3] Mu Q., Heinsch F.A., Zhao M., Running S. W.: Development of a global evapotranspiration algorithm based on MODIS and global meteorology data. Remote Sensing of Environment 111 (2007) 519–536 (doi:10.1016/j.rse.2007.04.015).
[4] Mu Q., Jones L. A., Kimball J. S., McDonald K. C., Running, S. W.: Satellite assessment of land surface evapotranspiration for the pan-Arctic domain. Water Resources Research 45 (2009) W09420 (doi:10.1029/2008WR007189).
[5] Mu Q., Zhao M., Running S. W.: Improvements to a MODIS Global Terrestrial Evapotranspiration Algorithm (in press). Remote Sensing of Environment (2011) (doi: 10.1016/ j.rse.2011.02.019).
[6] Somorowska U.: Changes in the soil moisture regime in lowland basin in current and future climate conditions. In: Siwek J., Chełmicki W. (eds.): Hydrological extremes in small basins. Proceedings of the XII Biennal International Conference of the European Network of Representative and Experimental Basins, 18–20 September 2008, Kraków. Technical Documents in Hydrology, No. 84. UNESCO, Paris (2009) 157–164.

Acknowledgements

The research is supported by the Norwegian Financial Mechanism, the European Economic Area (EEA) grant No. PL0268: “Development of the method for reconstruction of primary hydrological conditions in Kampinos National Park in order to restrain nature degradation and improvement of biodiversity status”. Research project financed from resources allocated for science in years 2008–2011.

14 Influence of Meteorological Hazards on the Hydrological Network in Respect to UEFA Euro 2012 Football Tournament in Gdansk

Wojciech Szpakowski (Gdansk University of Technology, Faculty of Civil and Environmental Engineering)

14.1. INTRODUCTION

The entire Gdansk agglomeration is involved in the organization of the final tournament of Euro 2012 championships. This agglomeration consists of three main cities of the region (Gdansk, Gdynia, Sopot). To the Gdansk agglomeration belong also the small Kashubian Tricity (Rumia, Reda Wejherowo) from the northern side and also Pruszcz Gdanski and Tczew situated on the south of Gdansk. The fundamental communication system used during the Euro 2012 includes Tricity and Pruszcz Gdanski (Fig. 1).

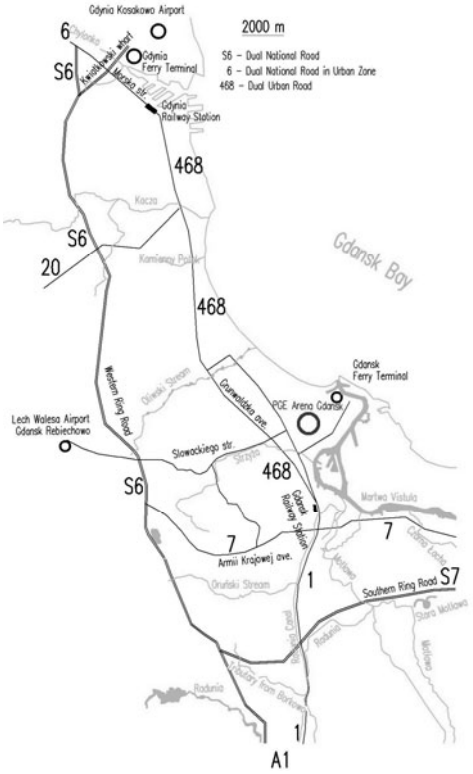

Fig. 1. Communication network of Gdansk agglomeration during Euro 2012 football tournament

It consists of two dual carriageways (S6 – Tricity west ring road, S7 – south Gdańsk ring road) and of internal communication arterial roads (No. 7 – departure to Warsaw, No. 6 – departure to Berlin, No. 468 Gdańsk – Gdynia). Roads to ferry Terminals and airports in Gdańsk and Gdynia are supplementing the road system of Gdansk agglomeration.

Western districts of Gdańsk and Gdynia with the Lech Walesa Gdansk airport located in Gdansk Rebiechowo are situated on moraine hills at more than 100 meters asl (upper terrace). City centres and the PGE Arena Gdansk are located only a little higher than the sea level (lower terrace). Between these two geomorphologic forms on the northern side forest areas are located which are hampering the communication. Between the Kwiatkowski fly-over in Gdynia and Slowacki road in Gdansk, the upper and lower terraces of the urbanized area are connected with only three municipal dual roads. The PGE Arena Gdansk is situated not far from the centre of Gdansk (5 km) and from the ferry terminal in Gdansk (2 km).

To the south of the Slowacki road an area of intensive building development is situated. From the year 1975 practically all housing investments of Gdansk are being located in the south of Gdansk. The greatest urban expansions of south districts of Gdansk have started 15 years ago, in contrast to the road system which is still under construction. This situation is creating tremendous transport problems which seems to be solved for the moment by the new Armii Krajowej Ave (dual road nr 7) and a southern ring road of Gdansk (S7).

14.2. HYDROGRAPHICAL NETWORK

In the northern part of the Tricity urbanized area, the hydrographical network is creating the first order streams. To the north of Gdynia, Reda river is flowing into the Gdansk bay and the Baltic sea. In the area of Gdynia, Sopot and north districts of Gdansk, little stream river basins are situated near the sea shore, the greatest of which are Kacza river (14.8 km long) and Oliwski stream (9.9 km long) (Fig. 2). The centre and southern districts of Gdańsk belong to the Vistula river basin. The majority of streams flowing eastward into the Martwa Vistula and the Radunia Channel. The Radunia channel, Radunia and Motlawa rivers are reaching Martwa Vistula from the south.

Streams flowing from west to east are characterized by large declines resulting from the natural surface area. In recent years the retention capacity of existing storage reservoirs was restored (mainly on Oliwski stream and Strzyza river). New storage reservoirs were constructed mainly on Orunski Stream. In intensive development areas situated mainly on the lower terrace of Gdansk, Sopot and Gdynia, streams are integrated in the open or closed artificial systems. Therefore, streams have limited bandwidth in these areas.

In the case of high-intensity rainfall, there are moments when the water is poured from the main riverbed causing temporary flooding the adjacent land. The most dangerous urban flood occurs in streams Strzyza (13.5 km in length and average slope of 1%) and Orunski (7.5 km in length and average slope of 1%).

Fig. 2. Gdansk agglomeration hydrographical network on the basis of [6]

14.3. GDANSK CLIMATE OVERVIEW

Gdansk is located in the southern part of the Baltic Sea. In this region the exchange of air masses is mainly connected with the western circulation. Depending on the season, temperature conditions and air humidity, the area of Gdansk is reached by different air masses: maritime polar, continental polar, tropic and arctic. Therefore, Gdansk region is characterized by dynamic weather variations resulting from air masse changes. In the analysis of the basic elements of Gdansk climate, the available scientific literature papers were used extensively [1, 2, 3].

14.3.1. Barometric Pressure

The average value of atmospheric pressure reduced to sea level in Gdansk is 1015 hPa. The lowest pressure – 967.2 hPa, was noted on February 26 1989, while the highest one occurred on January 3 1993 – 1050.7 hPa. Larger fluctuations in atmospheric pressure occur in the cool half of the year (from October to March) which indicates a greater variability of the weather in this part of the year [1].

14.3.2. Wind Conditions

Gdansk is located in the zone of prevailing westerly winds which derive from the general circulation of the atmosphere. Local winds are also important because of the existing buildings and area cover. Finally, Gdansk has complicated wind conditions. In the coastal zone, south and south-west winds dominate in the autumn and winter months. In the spring and summer months, north-western and western winds dominate.

The monthly average wind speed is about 5 meters per second in winter months and 4 meters per second in the summer months. Strong winds with daily average speed higher than 17 meters per second occur occasionally mostly in winter and spring. The highest wind speed recorded in Gdansk exceeds 20 meters per second, with wind gusts up to 36 meters per second. In the summer months, wind gusts over 15 meters per second occur occasionally and last for a short period of time [1].

14.3.3. Air Temperature

Gdansk is characterized by high spatial variability in air temperature depending on terrain elevation. Average annual air temperature in Gdansk in the years 1881–1995 ranged from 7.2°C at Lech Walesa Airport meteorological station (upper terrace) to 9.0°C in the northern seaport meteorological station (lower terrace) [1]. The average air temperature in the winter months was –0.7°C, and in the summer months, 16.5°C. Average temperatures in the autumn months (8.6°C) are higher than in the spring months (6.5°C). This is resulting from the summer heat accumulation in the seawater in the Bay of Gdansk. The increase in air temperature in 100 years is estimated to 0.7°C [2]. The highest yearly mean air temperature occurred between 1989 and 1990 (9.5–10.0°C). The lowest average annual temperature occurred during the Second World War, falling even below 6°C.

Results of observations of air temperature in the period 1987–2005 indicate a large temperature change in Gdansk. On the average, there are two days each year with maximum temperature above 30°C, mostly in the month of July [1, 2].

14.3.4. Precipitation

The analysis of precipitation in Gdansk Wrzeszcz is based on the collected weather data from the years 1951–2010. Full meteorological observations in such a long period of time were collected only on the Gdansk Wrzeszcz airport station which was moved to the current localization in 1974.

The precipitation data in the years 1991–2010 were collected at the Gdansk University of Technology climate station and the data contained in papers [1, 3, 5].

Mean annual sum of precipitation in Gdansk Wrzeszcz is estimated on 553 mm (1951–2010). In 1981–2005 mean annual sum of precipitation is equal to 583 mm (Gdansk Rebiechowo – upper terrace) and 478 mm (Northern seaport – lower terrace) [1]. Analyzing monthly and annual totals of precipitation, we can conclude that the period 1951–2010 was very variable (Fig. 3). In the driest years (1951, 1953, 1964) annual rainfall does not exceed 350 mm. Not much more was recorded in 1982. In the wettest years, rainfalls of 750 mm were recorded (1970, 1980, 2001) and even over 800 mm precipitation in 2010. The general precipitation trend is upward in the whole period. In the years 1982–1992, downward trend of average annual rainfall can be distinguished. In the years 1993–2001, precipi-

tation trend is strongly upward. In the last decade, only three years have the annual rainfall not higher than the long-term average. The highest value of the entire analyzed period of 60 years was in 2010.

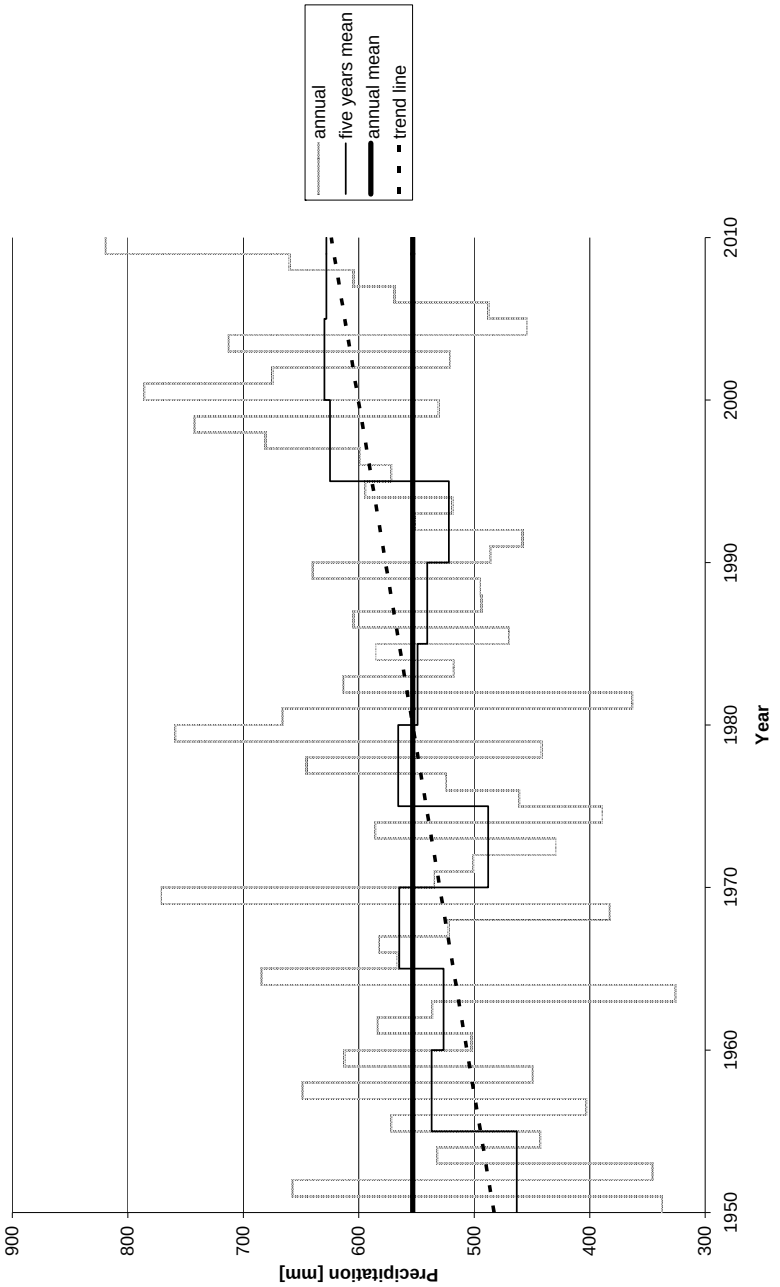

Fig. 3. Precipitation collected in Gdansk Wrzeszcz during the 60 years period of time (1951 – 2010)

Analysis of the total monthly rainfall during 60 years period of time shows that the highest monthly total rainfall is noted in the summer months (Fig. 4). Precipitation in the period from May to October represents almost 65% of the total annual precipitation.

According to the present analysis, precipitations are the greatest threat during the final tournament of Euro 2012 in Gdańsk. As a result, runoff from the hydrological network may provoke temporary flooding in various districts localized in lower part of Gdansk agglomeration.

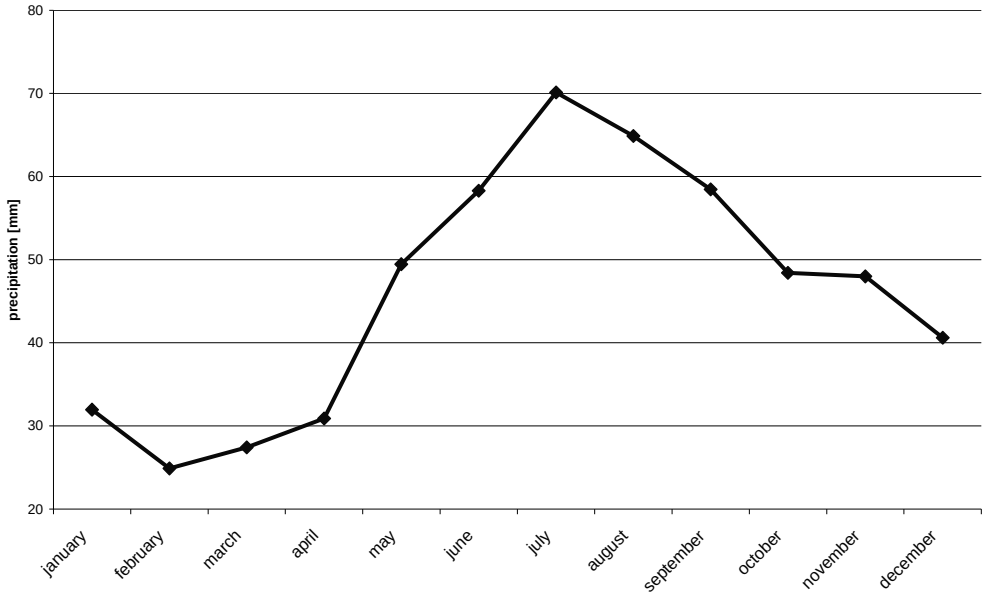

Fig. 4. Mean monthly sum of rainfall in years 1950–2010

14.4. EFFECTS OF SUMMER STORMS IN THE HYDROGRAPHICAL NETWORK

Storms are the main reason of floods in the lower terrace of Gdansk hydrographic system. One of the characteristic parameters of storms is the number of days with precipitation above 10 mm. In an average year rainfalls exceeding 10 mm were recorded from 10 to 13 days. These showers occur most frequently in the summer months (May to September), statistically between 1.5 and 2 times a month [1]. Maximum daily precipitation sums are much higher in summer than in winter. The maximum daily amount of precipitation in an average year occur most often in July.

The average maximum daily precipitation in June and August was around 20mm and in July of more than 24mm (years 1954–2007). Daily rainfall can have more than 70% of the total monthly precipitation in the summer months. In some years, the amount of monthly precipitation is realized in one day resulting from one single storm [4].

The frequency of daily precipitation was also analyzed in years 1954–2007 [4]. The daily sum of precipitation above 10 mm has occurred on the average 1.7 days per year in June and July. Strong rainfall over 20 mm daily sum of precipitation constitute about 50%

of the events. Storms with total daily rainfall exceeding 50 mm occurred three times in July. During the whole day of 9th of July 2001, 123.5 mm of precipitation was recorded in Gdansk Wrzeszcz. This amount is the highest recorded rainfall value in the history of weather measurements at the Gdansk University of Technology.

In the decade 2001–2010, eleven summer storms occurred in Tricity agglomeration which brought about a temporary flood of the hydrographical network in the Gdansk region (Table 1). Most of these storms fell on a small urban area. Therefore, the Gdansk University of Technology climate station registered often no rainfall. The exception is the huge storm of 9th of July 2001, which occurred around the area of Gdansk, Sopot and Gdynia. The sum of daily rainfall on this day ranged from about 40 mm in Gdynia to about 160 mm in Straszyn barrage. The daily sum of precipitation recorded in Gdansk Rębiechowo was 127 mm and 118 mm in the northern seaport of Gdansk. Only 71.5 mm of daily precipitation was recorded near the Vistula River estuary in Swibno [1].

The storm of the 9th of July 2001 was the worst natural catastrophe in Gdansk after the Second World War. One person died in his own car at the Grunwaldzka Ave. – Slowackiego str. intersection when the flood wave was created after interruption of the Strzyza storage reservoir. In centre of Gdansk, a rail trackway was filled by mud, sand and clay, which flowed rapidly with flood wave. Traffic on the most important rail track (Gdansk – Warsaw) was suspended for one week. The southward traffic road on national road no. 1 (Gdansk – Pruszcz Gdanski) was suspended for more than two weeks. The reason was a disruption at six localizations of the higher situated Radunia Channel's right side embankment. A huge volume of land masses flowed into the road and sheet erosion of water flowed by the Radunia Channel breaches destroyed road construction [5]. On the remaining part of Gdansk, traffic returned back to normal situation after a day.

Storm of the 1st of June 2009 has caused also damage in railway infrastructure. Rail traffic on the same rail trackway as eight years earlier was suspended, but "only" for 5 hours. The reason was a sheet erosion on the extension of the Kartuska street when rain water flowed into rail trackway. Road traffic was suspended for two hours in the whole region of centre of Gdansk.

Other storm events had resulted in temporary traffic suspensions at a far smaller scale. There were also strong rainfalls in the decade 2001–2010, which are not indicated in Table 1. In the moments of rainfall the traffic was congested for a few hours in not enlarged areas situated in different localizations of Gdansk agglomeration.

Summer storms provoke periodic inundations on some part of lower terrace. Four areas listed in this paper are most vulnerable to flooding:

I area – Gdansk main town nearby the railway station. This area is urbanized. Rain water flows directly or carried by Orunski stream into the Radunia canal and Martwa Vistula river. Eight storms causing inundations of this area were included. Road traffic was suspended for a period of several hours. Communication was impossible on Kartuska street as well as on the lower terrace of Gdansk. After the storm of the 9th of July 2001, the railway and road (road No. 1) tracks in the southern direction (towards Tczew) have been suspended for two weeks.

II area – Gdansk Wrzeszcz – stream Strzyza neighborhood in the lower part of the city. This area includes Grunwaldzka ave. – Slowackiego str. intersection and Strzyza river mouth not far from the PGE Arena Gdańsk. In this region Strzyza stream is fully canalized and it flows partially in open artificial channel. In the lower terrace, Strzyza has the minimum slope of water surface. Blocking the road communication within Grunwaldzka Ave. (road No. 468) even for a few tens of min-

utes resulted always in the several hours traffic perturbations in the whole Gdansk Wrzeszcz area.

Table 1

Summer storms in the decade 2001 – 2010 which provoked temporary urban inundations (flooded area see Fig. 5, GUT – Gdansk University of Technology)

	Date	Flood area	Precipitation	Losses due to storm
1	July 9, 2001	I, II, III, IV	from 40mm (24h IV) to 127mm (24h II)	One fatality; Radunia Channel interrupted at six localizations; Strzyza storage reservoir disrupted; rail traffic suspended (one week southward Gdansk); road traffic suspended (1 day – I, II, 2 weeks road nr 1 southward Gdansk)
2	July 1, 2003	I	36mm (24h GUT)	rail traffic suspended (2 hours), road traffic suspended (I – 1 hour)
3	July 3,2004	IV	0 mm (GUT)	rail and road traffic suspended (1 hour)
4	July 24, 2004	I, II	35mm (24h GUT)	road traffic suspended (I – 2 hours)
5	June 21, 2006	III	21mm (3h GUT)	rail traffic suspended (3 hours)
6	August 12, 2007	I, II	24mm (1h GUT)	road traffic suspended (2 hours)
7	August 13, 2008	I, II	16mm (0,3h GUT)	road traffic suspended (3 hours)
8	May 18, 2009	IV	0 mm (GUT)	road traffic suspended (2 hours)
9	July 1, 2009	I, II	18mm (0,3h GUT)	The lower ground on the rail network Damage to the tramway line rail traffic suspended (over than 5 hours), road traffic suspended (2 hours)
10	July 24, 2010	I	17mm (1h GUT) 10mm (10min GUT)	road traffic suspended (1 hour)
11	August 3, 2010	I,II	26mm (0,6h GUT) 14mm (10min GUT)	road traffic suspended (2 hours)

III Area – Oliwa stream in the vicinity of Grunwaldzka Ave. (road No. 468). While the Oliwski stream is well protected against urban flood, rainwater runoff from the Oliwa and Zabianka districts cause flooding of roads on railway overpass (Pomorska and Piastowska Street) and along the Grunwaldzka Ave. (road number 468).

IV area – Gdynia city centre. Water flowing from the upper lying areas in the urbanized part of city flows rapidly down to the railway station locality and one of the main streets of the city (Morska Street). In flood period the movement of passengers in the train station tunnel is impossible what provoke instability of the railway network.

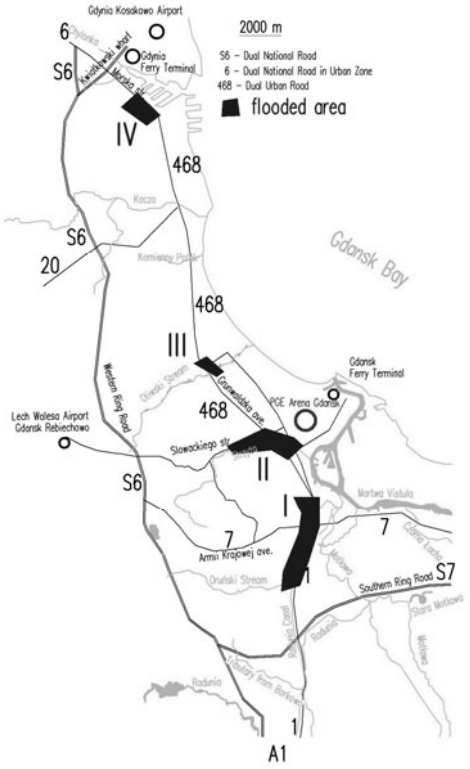

Fig. 5. Area of possible flooding: I – Gdansk centre, II – Gdansk Wrzeszcz, III – Gdańsk Oliwa, IV – Gdynia centre

14.5. SUMMARY

Storms are the greatest threat during the final tournament of Euro 2012 in Gdańsk. As a result, runoff from the hydrological network may provoke temporary flooding in various districts localized in lower part of Gdansk agglomeration. This event has not so high probability since the analysis of existing data in the decade 2001–2010 shows that it can occur once or twice in a summer season. What is worrying is the fact that the trend of precipitation is upward. From year to year, more storm events and local inundations are noted in Poland.

In the last ten years, many investments were devoted for improving flood safety in Gdansk. The most important are:

— construction of flood storage reservoirs on the Strzyza river. The main zone of Gdansk Wrzeszcz should have more safty during storm epizodes;
— construction of flood storage reservoirs on the Orunski stream what should help the flood management on the Radunia Channel and centre of Gdansk;
— construction of water trap in the rain water canalization situated above the rail trackway in the centre of Gdansk. This device should prevent from the sheet erosion of water

flowing from the upper terrace. Unfortunately, the water trap was still under construction during the storm of the 1st of June 2009;

— construction of special hydraulic by-passes from Radunia Channel to Radunia River situated on Vistula delta plain. These devices should protect the Radunia Channel embankment.

PGE Arena Gdansk is also well protected from the storm events. Rainwater and groundwater from the stadium and its neighbourhood will be discharged into the Martwa Vistula. Drainage network will be equipped with pumps for collection of water during high water levels in the Dead Vistula. Currently, the investment is made and the work should be finished end of 2011.

At the same time, the Gdansk is covered with a new road infrastructure. Additionally, the upper terrace has more and more residential areas of compact settlement. Drainage water and rainfall are collected by artificial canalization systems. The time of rain concentration is also shorter. This situation can provoke additional flood risk on the lower situated part of Gdansk.

It seems that the agglomeration of Gdansk is well prepared to violent rainfalls, similar to these which occurred in the last ten years. Difficulties in road and railway transport should disappear within a few hours. However, in the case where a storm comparable to that in the 9th of June, 2001 would occur, there will be inevitably a rain traffic suspension even for a few days. Also, some roads on the lower terrace of Tricity may be closed for a longer period of time.

Let us hope that the Euro 2012 in Gdansk will take place under favourable weather conditions. The days of matches will be the feast of football fans and not the practical exam of the services of Gdansk crisis management.

References

[1] Owczarek M., Jakusik E., Wojtkiewicz A., Malik P.: Klimat Gdańska, 1981–2005. W: 200 lat regularnych pomiarów i obserwacji meteorologicznych w Gdańsku. IMGW UG GTN 2007.

[2] Marosz M., Malinowska M.: Zmienność temperatury powietrza w Gdańsku na tle wieloletniej zmienności typów cyrkulacji atmosferycznej w regionie atlantycko-europejskim. W: 200 lat regularnych pomiarów i obserwacji meteorologicznych w Gdańsku. IMGW UG GTN 2007.

[3] Szpakowski W.: Działania firm w organizacji EURO 2012 w rejonie Gdańska a środowisko naturalne w: Partnerstwo publiczno-prywatne w kontekście EURO 2012, Euro 2012 szanse i zagrożenia dla Pomorza. WZiE, Gdańsk 2010.

[4] Wołoszyn E.: Zmiana opadów maksymalnych w Gdańsku. Wodociągi – Kanalizacja, 51511/2008, s. 70–73.

[5] Bednarczyk S., Jarzębińska T., Majewski W., Wołoszyn E.: Vademecum ochrony przeciwpowodziowej. Warszawa: KZGW 2006.

[6] Rastrowa Mapa Podziału hydrograficznego Polski, http://www.kzgw.gov.pl/pl/Rastrowa-Mapa-Podzialu-Hydrograficznego-Polski.html KZGW, Warszawa, obtained 03/2001.

15 Efficient Use of GIS Applications in Waterworks Sector

Branislav Štefanec (Bratislava Waterworks Company, Slovak University of Technology, Bratislava), Marek Sokáč (Slovak University of Technology, Bratislava)

15.1. INTRODUCTION

The human view often generalizes the real world to objects and classifies them in the spatial context. Of course, there is a demand for information with a relation to a specific place. The GIS systems have been developed for viewing, manipulation, and editing, compiling and analysing this kind of data.

Definition of an information system (IS) could be following: „An information data file associated with instruments and rules which allow processing the data entered by the given method" [1]. In other words, an information system consists of a controlled management process built on well-defined principles, aimed at the collection, compilation, presentation, analysis (in case of GIS) georeferenced data.

15.2. DATA MODEL IN THE CONDITIONS OF WATER COMPANIES

Regarding to the advantages and disadvantages of different data models types, there is no clear choice of the best data model for the water companies. The choice depends on:

— data collection method,
— accuracy required,
— expected data analysis methods,
— data storage device capacity,
— editing data tools.

If necessary, the mutual conversion of vector and raster data into the opposite forms could be secured. The ideal solution is then the data transfer and analysis in the form corresponding to the data presentation and data analysis. In general, for the water companies seems to be the vector model more suitable. Primary and wide quantitative data element in the water companies are the supply water and drainage networks. The vector model provides greater accuracy and is suitable for network analysis.

15.3. DATA RANGE EXTENT AND THEIR ACQUIRING POSSIBILITIES

Location information is an essential component of data which can gradually be connected with other data. Data on water company's pipelines can be obtained by several ways. Data source maybe a direct measurement, using of data in digital form from external sources, transposing the data in analogue form or the completion of cartographic base layer.

The different forms of data varies considerably on financial requirements, difficulty of obtaining, data verification, and of course of data accuracy and suitability for use without substantial modification needs.

Table 1

Methods of data acquisition for GIS

Acquisition method/data parameters	Direct survey		Usage of external data in digital form	Data take-over in analogue form	Completion of cartographic base layer
	Conventional	GPS			
Financial requirements	Very large	Large	Small	Small	Very small
Difficulty of obtaining	Very large	Large	Small	Very large	Very small
Data verification requirements	Small	Small	Large	Large	Very large
Additional data modification requirements	Small	Small – Very small	Small – Large	Very large	Small
Data accuracy	Very large	Very large – Large	Small	Small	Very small

Direct measurement by using conventional methods like a total station is a relatively accurate method of data collection. It is expensive because of its time demands, the need for additional processing in the office, a higher number of workers needed during the measurements and because of the necessary technical equipment. Office work may affect the accuracy of the measured data and increase error occurrence in the processing of measured points in the data model. Additional processing outside the field carries a risk of incorrect point identification, creation of incorrect topology links etc.

In data acquisition process on new construction works can the investor or the future works operator require a geodetic survey in digital form as part of the works takeover process. This method of data collection is only applicable to new construction and reconstruction. The financial requirements for this type are typically very low. Usually, the demands on finance and labour to obtain necessary data are transferred to the investor. Verification of the data in this method of obtaining data is very easy. Necessary additional data adjustment range could be affected by strong instructions for measurement processing. With available good instructions, explaining how to process the measured data and about the output form, could be the time required for adjustments minimized to zero. Typically the only need is to connect the new data to the existing one. It is one of the ways of obtaining high-quality, inexpensive and accurate data. Drawback is the application to the existing sections. The advantages of this mapping method make it suitable for mapping of the newly constructed sections not only in conditions of water companies.

Data in digital form also serves as an exchange platform between the different institutions. By exchanging or purchasing data from other institutions, it is irrelevant to evaluate the financial needs, difficulty of data obtaining, data verification or their accuracy. All of these features could be considered as adequate for the purpose of the data use in an internal GIS system. The remaining question is the extent of necessary arrangements for data

implementation into the new GIS. Difficulty matter in this case relates to data exchange format.

Data in the analogue format are used if there is no better, or equivalent digital dataset available. Even classic paper map can have a great informative value. The accuracy is expressed in the scale of what documents have been made and for what purpose they were created. An example could be the cadastral maps. In Slovakia the majority of data was taken from older cadastral maps at a scale of 1:2880. In some places, the data has been verified, digitalised and edited on digitizing equipment from analogue maps. Only few areas have been newly mapped and are in a different scale than 1:2880. The accuracy of digitized data depends on the ability of mapmakers, which performs the digitization, but it is clear that an error of ±1 mm (which means in real world ± 2.8 m) will be not enough. The last form of data acquisition process could be a combination of digital datasets (orthophotomap, cadastral map, layout map) and knowledge of the location of the object related to the digital layout data. An example could be a drawing of the water main by using the surface signs related to the edge of sidewalk, road, house etc. Such data are typically of low accuracy, but their acquisition is very fast and cheap.

15.4. TOPOLOGICAL DATA

The topological data can be collected by the direct detection in the field, or data derivation from other documents and their verification. Data on new objects could be taken from design plans updated after construction, or from post-construction geodetic survey. For existing objects, where are no relevant documents available, it is necessary to perform direct survey in the field. Problems are mainly old sewers built in various periods. There are sections of the sewer system where are 2 or 3 interconnected or disconnected sewer, or vice versa (unused) sewer. If it is not possible to check the sections directly from the surface, small flowing objects (such as pieces of styrofoam) can be used for place them into sewer and follow the flow. It is necessary to determine all unclear connections preferably with entry into the sewer network (if possible). For objects without possibility of visual control could be the camcorder inspection applicable, but this is relatively expensive way to detect the network topology. Only some of the water companies have the technology to CCTV survey of sewer systems, although the operation of such a service would be profitable for the company. Equipment for CCTV survey camera with standard equipment costs around 50 000. Professional delivery of services including CCTV survey handed with the protocol, digital media record and other matters, costs around 70–120 per hour.

Verification of a water supply network is more complicated than it is in case of a sewer network. If there are no relevant documents, it is necessary to manipulate the valves and to monitor the consequences of the manipulation. Closing a network section is an uncomfortable issue for the customer in affected areas, so these operations should be performed in a minimal extent. Complications occur with valves malfunction or their leakage.

15.5. DATA ATTRIBUTES

Data attributes represents added value to the GIS system. Data can be downloaded from the already existing digital documents or obtained directly in the field. In water companies GIS systems are of particular interest this multimedia:

- Construction drawings:
  - layout plans and schemes,
  - longitudinal and cross sections,
  - layouts,
  - technologic schemes,
  - pressure schemes.
- Photo documentation,
- CCTV survey,
- Documents:
  - About the construction:
    - works placement permit,
    - construction permit,
    - construction documentation,
    - post-construction documents,
- Contracts:
  - Operational:
    - About the operation,
    - Donation contracts,
    - Purchase contracts.
  - Client contracts:
    - water supply contracts,
    - sewerage contracts,
  - Company decisions and positions:
    - connection possibility (households, industry etc.),
    - new objects construction close of the existing water infrastructure (protection zones).

  Economic data:
    - operating costs
    - investment costs,
    - service costs.

15.6. GIS UTILIZATION

A major reason for the GIS implementation is the collection of information at one place. The aim of the GIS use is to limit the number of information sources to the minimum, respectively to completely replace the several sources with GIS. If there is no users' confidence in the data filled into the GIS system, the advantage of one information source is lost.

GIS systems are also designed to decision making support in case of problems with significant geographical dimension. In order to support a decision making the GIS should be able to produce outputs from the databases in various forms. All attribute data stored

in the database serve as potential sources for a system analysis. Integration of proprietary and business data, active and passive elements of infrastructure and land ownership in GIS, are necessary assumptions to the elimination of risks of infrastructure investment or maintenance, renovation or construction on foreign territory without an agreement with the owner of the property.

One of the most important tasks for water companies today is to create the rehabilitation plans for public water and sewer systems. Such a role has a very close connection to the GIS systems. Where a high-quality database is not available, for the needs of the rehabilitation plan it is necessary to create it in a very short time. In this context, one of the basic questions is: will be the available functionality and GIS data sufficient to create a recovery plan? If the answer is no, than the degree of complexity of GIS is probably not at the full GIS level, but only at the level of a digital map. The output of the rehabilitation plan is expected in tabular form. The object database can be hence made for one purpose or in a broader scope and may be applicable to other GIS applications as well.

The geodatabase output combined with attribute data can be used to assess the hydraulic network function (capacity). Sophisticated systems support two-way link, i.e. details for hydraulic assessment are exported to the hydraulic model and outputs from the hydraulic assessment are stored as metadata of the modelled objects.

Daily inspection of a network and the related objects, their structural condition, all this can be gradually collected and also used for the rehabilitation plan, or for an own assessment of objects structural status or in the aim to improve the operation effectiveness, e.g. decrease the sewer infiltration or decrease the water losses in supply network [5].

Company positions to the proposed construction can be fast and the positions will be uniform for all applicants. Sufficient assumption is to have a link with the document databases and GIS. The positions may be a common document, for example a positions about the protection zones, positions (permits) about the connection to public water supply network (public sewer system) or positions on various territorial plans.

Various network analysis are very effective as well. The GIS systems can be deployed to detect problems such as unauthorized connection of drinking water from public water supply network and detect unauthorized discharges into public sewer system. GIS offers integration function of the visual presentation of georeferenced data from other information systems.

15.7. ANALYSIS

Obviously, there are currently expert systems focused primarily on the mathematical models of hydraulic pipe networks, which is a task out of the GIS analytical tools capabilities. The network analysis tools are designed primarily for vector models. The network is represented by a series of interconnected sections, which may pass through the transported medium from source to destination. Water companies may be interested to use the network analysis with the aim to get the answers to such questions:

— which streets (houses) will be affected by the failure and following valve closure on A site?
— how many of inhabitants will be without water supply?
— if in place A water quality will be lower, will it affect also B?
— how to disconnect the water supply on the street A and minimise the number of disconnected inhabitants?

15.8. GIS OPERATION PROBLEMS

The basic problem is to convince the water company top management of necessity to implement a GIS system because of following issues:

— lack of investment funds,
— lack of staff dealing with the issue,
— lack of equipment,
— out-of-date software products,
— out-of-date data and support data,
— incomplete knowledge and skills of GIS technology among technical (infrastructure) staff,
— lack of confidence in the possibilities and tools that GIS could provide and insufficient knowledge among employees,
— overloading of the technical staff with administration, which causes a smaller opportunity to put the data into a GIS system, as well as to check or complete GIS data,
— inappropriate definition of the operation procedures,
— insufficient or no access to the GIS relevant data.

15.9. CONCLUSION

We need to realize, that the GIS system could perform only the same things a man is able to do, but much faster. Also, each GIS handle the data, which were collected by a man, so there is a high risk of errors. No GIS can automatically fill all necessary data itself, and cannot automatically update the data. The speed advantage in GIS system is a relatively long and difficult data entry, but once is the database complete, the maintenance and update of such database is considerably easier. The cost-effectiveness and ability to analyse and summarize data in a GIS environment are an added value and powerful tool for the sewer and water networks operation.

References

[1] Tuček J.: Geografické informační systémy – Principy a praxe (GIS – principles and practice) Computer Press, ISBN: 807226091X, 438 s., 1998.
[2] ATV A 145 Aufbau und Anwendung einer Kanaldatenbank. (Establishment and use of sewer database systems). Abwassertechnische Vereinigung e.V., Gesellschaft zur Förderung der Abwassertechnik e.V., St. Augustin, (1991).
[3] ITWH Hannover: Entwässerungsplanung. Datenbanken in der Stadtentwässerung. (Urban drainage planning. Database systems in urban sewerage.) Institut für Technisch – Wissenschaftliche Hydrologie, Engelbosteller Damm, Hannover 1991.
[4] Hlásny T.: Geografické informačné systémy – Priestorové analýzy. (GIS – spatial analyse) Zvolen: Zephyros, NLC, 2007, 160 s, 2007.
[5] Tóthová K., Dubová V., Barloková D.: Benchmarking of Water Supply Systems – Water Losses Assessment. Integrated Urban Water Resources Management, NATO Security through Science Series – C: Environmental Security. Springer 2006 printed in Netherland, p. 111–118, ISBN-10 1-4020-4684-7, 2006.
[6] Hofierka J.:Geografické informačné systémy a diaľkový prieskum Zeme. (GIS and Earth remote sensing). University textbook. FHPV PU, Prešov, 106 p., 2003.

[7] Harmon J. E., Anderson S. J.: The Design and Implementation of Geographic Information Systems. Hoboken, New Jersey: John Wiley & Sons, ISBN 0-471-20488-9. 264 p., 2003.
[8] Bratislavská vodárenská spoločnosť, a. s. súhrnné správy. (Waterworks company of the city Bratislava, summary reports) 2004–2009.

Acknowledgement

This paper was written with the support of the grant agency KEGA in terms of solving the grant task no. 3/7452/09 „Odkanalizovanie urbanizovaných území“ (“Sewerage in urban areas”).

16 Comparison of Summer Low Flow Regime Regionalization Schemes in Slovakia

Andrea Ševkova, Silvia Kohnová, Kamila Hlavčová (Slovak University of Technology, Department of Land and Water Resources Management, Faculty of Civil Engineering)

16.1. INTRODUCTION

Hydrological regionalization, or pooling, is a procedure for locating groups of catchments with homogeneous hydrological responses. During recent years regionalization methods have had many applications in the hydrological design, planning and management of water resources systems [7].

Estimating low flows is of great importance to assess the availability of water resources, but not many studies have been published in recent years that deal with the seasonal characteristics of the regionalization of low flows.

Among the interesting studies on this topic belongs the study of Laaha and Blöschl [5], who applied four catchment grouping methods using the data from 325 catchments in Austria. They compared the results in terms of their performance in predicting specific low flow discharges q_{95}. The grouping methods consisted of the residual pattern approach, a weighted cluster analysis, regression trees and an approach based on seasonality data. Kahay [4] used hierarchical clustering to create regional types of monthly low flows in Turkey. Among the recently published studies dealing with low flow regionalization belongs the study of Castiglioni, et. al. [1], where the authors investigated the applicability of physiographic space-based interpolation techniques for the prediction of low flow indices in ungauged basins. The study analysed 51 catchments located in a wide region of central Italy, for which several geomorphological and climatic descriptions are available. The analysis applies deterministic and geostatistical techniques for interpolating low flow indices in a physiographic space. Castiglioni, et. al. [2] compares two innovative interpolation techniques for the prediction of low flows in ungauged catchments. The first one used was Physiographic-Space Based Information (PSBI), which performs the spatial interpolation of the desired streamflow index, and the second technique was Top-Kriging. PSBI and Top Kriging were applied for the regionalization of discharge Q_{355} over a broad geographical region in central Italy containing 51 gauged catchments.

The aim of our study was to apply hierarchical and non-hierarchical clustering methods to derive regionalization groups of summer low flow regimes in Slovakia. As hierarchical clustering pooling methods, the Average, Centroid and Ward methods were selected; for the non-hierarchical methods, the K-means clustering method was used. For determining the correct number clusters, a statistical Silhouette coefficient and Root Mean Square Standard Deviation (RMSSTD) were used. Finally, the derived pooling groups were compared.

16.2. METHODS

16.2.1. Cluster Analysis

Cluster analysis is the generic name for a variety of multivariate statistical procedures that are used to investigate, interpret and classify given data into similar groups or clusters, which may or may not overlap. The data points within a cluster should be as similar as possible, and the data points of different clusters should be as dissimilar as possible [7]. In our study, we used hierarchical and non-hierarchical clustering methods for classifying the pooling groups.

16.2.2. Non-hierarchical Clustering – K-means Method

The K-means clustering method is a non-hierarchical method of cluster analysis. The prototype – based clustering techniques create a one-level partitioning of the data objects. The K-means defines a prototype in terms of a centroid, which is usually the mean of a group of points and is typically applied to objects in a continuous n-dimensional space.

In the k-means clustering technique each point is assigned to the closest centroid, and each collection of points is assigned to a centroid, around which a cluster is built. The centroid of each cluster is then updated, based on the points assigned to the cluster. These steps are repeated and updated until the centroids remain unchanged [9].

For determining the correct number of clusters, we used a Silhouette coefficient [8].

For each object i we calculated the value $s(i)$ from the following formula [8]:

$$s(i) = \frac{b(i) - a(i)}{\max\{a(i), b(i)\}} \tag{1}$$

where a_i is the average value of the dissimilarities on the object i with respect to the other objects in the cluster; b_i is the minimum value of the dissimilarities on the object i and all the objects in the other clusters.

From the above definition we can see that for each object i [6]:

$$-1 \le s(i) \le 1 \tag{2}$$

For determining the correct number of clusters, the average silhouette value was defined and the highest average silhouette value was used for the final selection of the correct number of clusters.

16.2.3. Hierarchical Clustering

Hierarchical clustering algorithms provide a nested sequence of partitions, whereas partitioned clustering algorithms generate a single partition of the data to recover the natural grouping present in it.

Hierarchical clustering can be divided into two categories: agglomerative and divisive clustering [7].

In this study average, centroid and ward clustering methods were used.

Average method – the distance between two clusters is defined as the average distance between them. There are several methods available for computing the average distance [7].

Centroid method – the cluster to be merged is the one with the smallest sum of distances between the cluster means (centroids) for all the variables [3].

Ward method – it is based on the assumption that if two clusters are merged, the resulting loss of information or change in the value of the objective function will depend only on the relationship between the two merged clusters and not on the relationships with any other clusters [7].

For determining the correct number of clusters, we used the *Root Mean Square Standard Deviation* (*RMSSTD*). The RMSSTD of a new clustering scheme defined at the level of a clustering hierarchy is the square root of the variance of all the variables (the attributes used in the clustering process). This index measures the homogeneity of the formed clusters at each step of the hierarchical algorithm. Since the objective of cluster analysis is to form homogeneous groups, the RMSSTD of a cluster should be as small as possible. Where the values of the RMSSTD are higher than the values of the previous step, we have an indication that the new clustering scheme is worse [10].

The dissimilarity measure between the clusters was derived using Euclidean and Minkowski distances.

16.3. INPUT DATA

For this study 205 small and mid-sized catchments from the whole territory of Slovakia with observation periods longer than 20 years were used. The spatial distribution of the analysed catchments is shown at Fig.1.

Fig. 1. Map of the locations of the analyzed catchments in Slovakia

The number of low-flow days lower than the Q_{95} occurrence was calculated in each catchment. Subsequently, the relative frequency of low-flow occurrences for the months of May until November was estimated and used as a pooling variable in the clustering methods.

16.4. RESULTS

The analysed catchments were pooled into clusters using hierarchical and non-hierarchical cluster analyses. For determining the final number of clusters, a Silhouette coefficient and the RMSSTD method as an additional method for hierarchical clustering was used as well. Table 1 gives an overview of the clustering methods and the number of catchments in the selected clusters.

Table 1

Overview of the clustering methods and number of catchments in the selected clusters

Cluster analysis – metrics	Methods for determining the correct number of clusters	The highest average silhouette value	Number of clusters	Number of catchments in clusters
				1 cluster/2 cluster/…
K-means	Silhouette –squared Euclidean distance	0.510	2	103/102
Average – Euclidean distance	RMSSTD		3	166/31/8
	Silhouette –squared Euclidean distance	0.546	2	8/197
Centroid – Euclidean distance	RMSSTD		8	1/160/1/31/9/1/1/1
	Silhouette –squared Euclidean distance	0.461	3	1/203/1
Ward – Euclidean distance	RMSSTD		3	31/84/90
	Silhouette –squared Euclidean distance	0.457	2	90/115

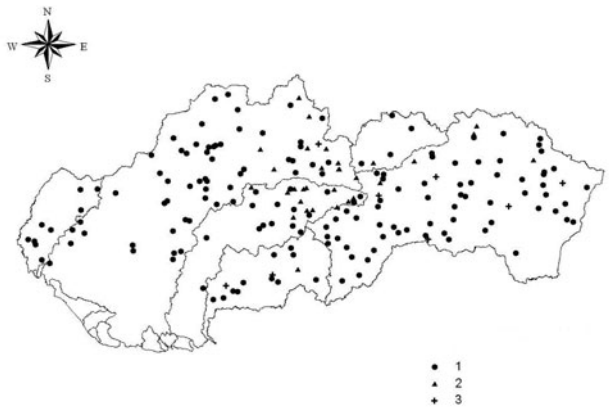

Fig. 2. Visualization of the pooling of the catchments into 3 groups, based on the relative frequency of the occurrence of low flows lower than Q_{95} during the summer season, using the Average clustering method

As presented in Table 1, the clustering methods classified the catchments into various numbers of clusters, but all of them are very similar according to the results of the Silhouette validation test. Those classification schemes where only one catchment was estimated

in the cluster were apriori rejected. The best grouping was achieved by the Average and K-means clustering methods according to the Silhouette validation method. According to the results, pooling method similar to the K-means clustering method was the hierarchical Ward clustering method. This method classified the catchments into two (2) clusters. The Centroid method classified our catchments into three (3) clusters. Using the RMSSTD testing method we obtained a greater number of clusters in all the pooling schemes than by using the Silhouette validation method.

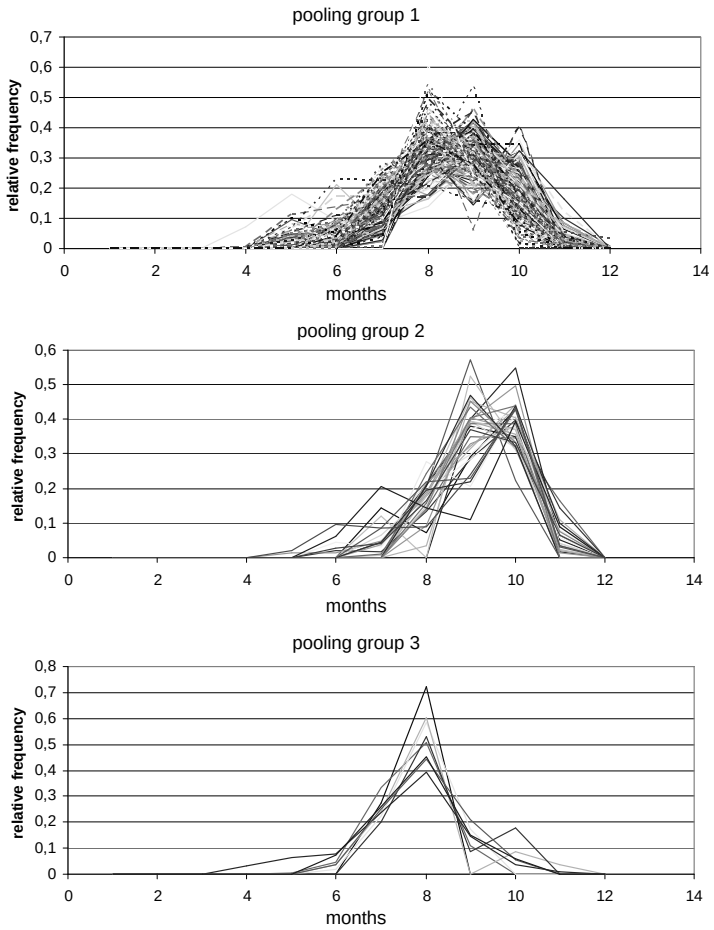

Fig. 3. Visualization of the summer low flow regimes for analysed catchments in the derived pooling groups, using the Average clustering method

For a final decision about the most suitable pooling scheme, we tested the similarity in summer low flow regimes in the derived pooling schemes. From this comparison the pooling scheme from the Average hierarchical clustering method with three (3) pooling groups was selected as the best, Fig. 2. This scheme is very similar to the Ward clustering and K-means clustering methods, especially in the pooling group No. 2. This pooling group No. 2 represents summer low flow regime for catchments located in the High and Low Tatras, the Levočské Mountains, and the Ondavská Mountains. Pooling group No.1 represents a typical regime for

catchments in Slovakia, which are mostly located in the Javorníky, Small and High Fatra Mountains, the White Carpathians, the Slovenské Rudohorie, the Small Carpathians and the Strážovské Mountains. The third pooling group is quite different from the previous ones and comprises only eight (8) catchments with low flow occurrences prevailing in August, Fig. 3.

16.5. CONCLUSION

In this study various clustering methods for pooling summer low flow regimes in Slovakia were tested. Various hierarchical and non-hierarchical clustering methods were tested. For determining the correct cluster number, the Silhouette coefficient and RMSSTD methods were used. The results show that the clustering methods classified the analysed catchments into different numbers of clusters. The best classification was reached using the hierarchical average clustering method. This method divided the analysed catchments into three groups. The derived pooling groups can also be used subsequently for the undirected estimation of design minimum discharges in ungauged catchments.

References

[1] Castiglioni S., Castellarin A., Montanari A.: Prediction of low-flow indices in ungauged basins through physiographical space-based interpolation. Journal of Hydrology 378 (272–280), 2009.
[2] Castiglioni S., Castellarin A., Montanari A., Skoien, J. O., Laaha G., Bloschl G.: Smooth regional estimation of low flow indices: physiographical space-based interpolation and top-kriging. Hydrol. Earth Syst. Sci., 15 715–727, 2011.
[3] Gan Guojun, Chaoqun Ma, Jianhong Wu: Data Clustering: Theory, Algorithms, and Applications, ASA-SIAM Series on Statistics and Applied Probability, SIAM, Philadelphia, ASA, Alexandria, VA, 2007.
[4] Kahya E., Demirel M. C.: A Comparison of Low-Flow Clustering Methods: Streamflow Grouping. Journal of Engineering and Applied Sciences 2 (3), 524 – 530, 2007.
[5] Laaha G., Blöschl G.: A comparison of low flow regionalisation methods-catchment grouping. Journal of Hydrology 323 193–214, 2006.
[6] Meloun M., Militký J., Hill M.: Computer analysis of multidimensional data in the examples. (Počítačová analýza vícerozměrných dat v příkladech), Academia Prague. In Czech, 2005.
[7] Rao A., R., Srinivas V., V.: Regionalization of Watersheds: An Approach Based on Cluster Analysis. Springer Science+Business Media B.V. 241, 2008.
[8] Rousseeuw P. J.: Silhouettes: a graphical aid to the interpretation and validation of cluster analysis. Journal of Computation and Applied Mathematics 20 (1987), 53 – 65, 1987.
[9] Tan P. N., Steinbach M., Kumar V.: Introduction to data mining. Addison-Wesley 2006.
[10] Vazirgiannis M., Halkidi M., Gunopulos D.: Uncertainty Handling and Quality Assessment in Data Mining. Springer-Verlag London Limited 2003, 223, 2003.

Acknowledgement

This work was supported by the Slovak Research and Development Agency under the contract No. APVV-0015-10 and the Slovak VEGA Grant Agency under the project No. 1/0103/10.

17 Small Watersheds – Comparison of Different Methods for Calculation of High Water Hydrographs

Diana Šustić, Zdenko Tadić, Lidija Tadić (Civil Engineering Hidroing LTD., Osijek, Zagreb, Croatia)

17.1. INTRODUCTION

In the hydrological practice frequently occurring with the necessary calculates the water wave by hydrological ungaged or insufficiently ungaged watershed, known physical characteristic and data about the precipitation. In the work is presented the determining of maximal flow using the hydrological model (the HEC−HMS) and using the regional model. For the determining real precipitation uses SCS method, and prepares data are made using the GIS tool.

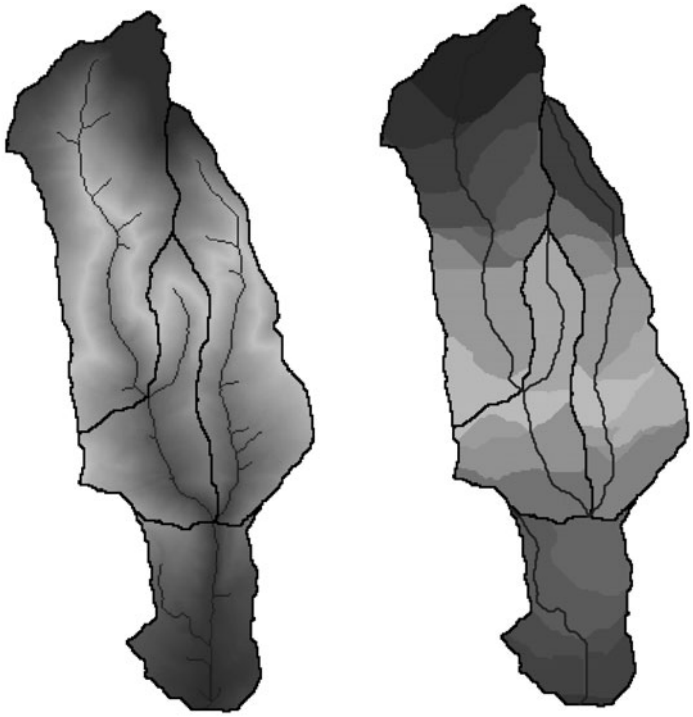

Fig. 1. Terrain preprocessing

17.2. PREPARATION OF DATA

Processing of physical and geographic characteristics of watershed and preparation of spatial data related to geometry of river valleys and waterways are simplified by using digital elevation models and GIS tools. HEC–GeoHMS is a set of ArcGIS tools specifically designed to process geospatial data and create input files for the Hydrologic Engineering Center – Hydrologic Modeling System (HEC–HMS). HEC–GeoHMS provides the connection for translating GIS spatial information into model files for HEC–HMS. It operates on the DEM to derive subbasin delineation and to prepare a number of hydrologic inputs. HEC–HMS accepts these hydrologic inputs as a starting point for hydrologic modeling.

17.2.1. Meteorological Model

Meteorological model – the rain model, which defines precipitation events with basic meteorological data: precipitation – definition of applicable rain event on each observed runoff element, evapotranspiration, snow.

For the use of the regulation of the mountain watershed precipitation data from main meteorological station Zagreb–Maksimir were analyzed for the period 1955–2005.

17.3. HYDROLOGICAL MODELS

The hydrologic analysis was made with the two different hydrological models. One from them is kinematic wave model, a part of HEC HMS 3.5., mathematical modeling software and other is the regional hydrological model.

17.3.1. Kinematic-Wave Model

HEC–HMS is a numerical model for watershed modeling that includes a large set of methods to simulate watershed, channel, and water-control structure behavior, thus predicting flow, stage, and timing. The chosen methods of calculation are:

— Transformation of surface runoff using kinematic-wave method,
— Infiltration losses using SCS (Soil Conservation Service curve number loss model).

Kinematic wave model represents a watershed as an open channel (a very wide, open channel), with inflow to the channel equal to the excess precipitation. Then it solves the equations that simulate unsteady shallow water flow in an open channel to compute the watershed runoff hydrograph.

Figure 1 (left) shows a simple watershed for which runoff is to be computed for design, planning, or regulating. For kinematic wave routing, the watershed and its channels are conceptualized as shown in Figure 1 (right). This represents the watershed as two plane surfaces over which water runs until it reaches the channel. The water then flows down the channel to the outlet.

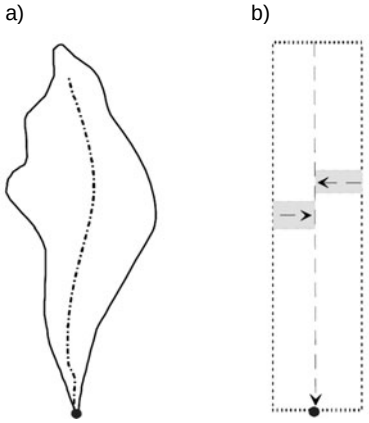

Fig. 2. Simple watershed with kinematic-wave model representation

At the heart of the overland model are the fundamental equations of open channel flow: the momentum equation and the continuity equation. Flow over the plane surfaces is primarily one-dimensional flow. In one dimension, the momentum equation after [1]:

$$S_f = S_0 - \frac{\partial y}{\partial x} - \frac{v}{g}\frac{\partial y}{\partial x} - \frac{1}{g}\frac{\partial v}{\partial t} \tag{1}$$

S_f – energy gradient,
S_0 – bottom slope,
v – velocity,
y – hydraulic depth,
x – distance along the flow path,
t – time,
g – acceleration due to gravity.

The energy gradient can be estimated with Manning's equation (2), which can be written as:

$$Q = \frac{CR^{2/3}S_f^{1/2}}{N}A \tag{2}$$

Q – flow,
R – hydraulic radius,
A – cross-sectional area,
N – a resistance factor that depends on the cover of the slopes (note that this is not Manning's n).

For shallow flow, bottom slope and the energy gradient are approximately equal and acceleration effects are negligible, so the momentum equation simplifies to:

$$Q = \alpha A^m \tag{3}$$

Where α and m are parameters related to flow geometry and surface roughness.

The second critical equation, the one-dimensional representation of the continuity equation, is:

$$A\frac{\partial v}{\partial x} + vB\frac{\partial y}{\partial x} - B\frac{\partial y}{\partial t} = q \tag{4}$$

B – water surface width,
q – lateral inflow per unit length of channel.

Again, the equation, the terms, and the basic concepts are described in detail in [1], and other texts.

With simplification appropriate for shallow flow over a plane, the continuity equation reduces to:

$$\frac{\partial A}{\partial t} + \frac{\partial Q}{\partial x} = q \tag{5}$$

Combining the continuity and the momentum equation as a result follow the equation:

$$\frac{\partial A}{\partial t} + \alpha m A^{(m-1)}\frac{\partial A}{\partial x} = q \tag{6}$$

This equation is a kinematic-wave approximation of the equations of motion. HEC–HMS represents the overland flow element as a wide rectangular channel of unit width; $\alpha = 1.486\, S^{1/2}/N$ and $m = 5/3$.

For certain classes of channel flow, conditions are such that the momentum equation can be simplified. In those cases, the kinematic-wave approximation of early mentioned equation is an appropriate model of channel flow. Values for α and m for different types of section channel shapes used in HEC–HMS could be defined. The Kinematic wave equation for the trapezoidal section is given below (7):

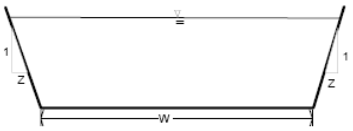

$$Q = \frac{1.49}{n} S^{1/2} A^{5/3} \left(\frac{1}{W + 2Y\sqrt{1+Z^2}} \right)^{2/3} \tag{7}$$

The kinematic-wave approximation is solved in the same manner for either overland or channel flow:

— the partial differential equation is approximated with a finite-difference scheme,
— initial and boundary conditions are assigned,
— the resulting algebraic equations are solved to find unknown hydrograph ordinates.

In the early mentioned equation, A is the only dependent variable, as α and m are constants, so solution requires only finding values of A at different times and locations. To do so, the partial difference scheme approximates with finite difference scheme using a scheme proposed by Leclerc and Schaake (1973). The resulting algebraic equation is:

$$\frac{A_i^j - A_i^{j-1}}{\Delta t} + \alpha m \left[\frac{A_i^{j-1} + A_{i-1}^{j-1}}{2} \right]^{m-1} \left[\frac{A_i^{j-1} - A_{i-1}^{j-1}}{\Delta x} \right] = \frac{q_i^j + q_i^{j-1}}{2} \tag{8}$$

To estimate runoff with the kinematic-wave model, the watershed is described as a set of elements that include:

Overland flow planes	Main channel
— Typical length L (km), — Representative slope S (‰), — Overland-flow roughness coefficient, — Area represented by plane, — Loss model parameters	— Channel length, — Channel slope, — Representative Manning's roughness coefficient, — Principle dimensions of channel cross section)

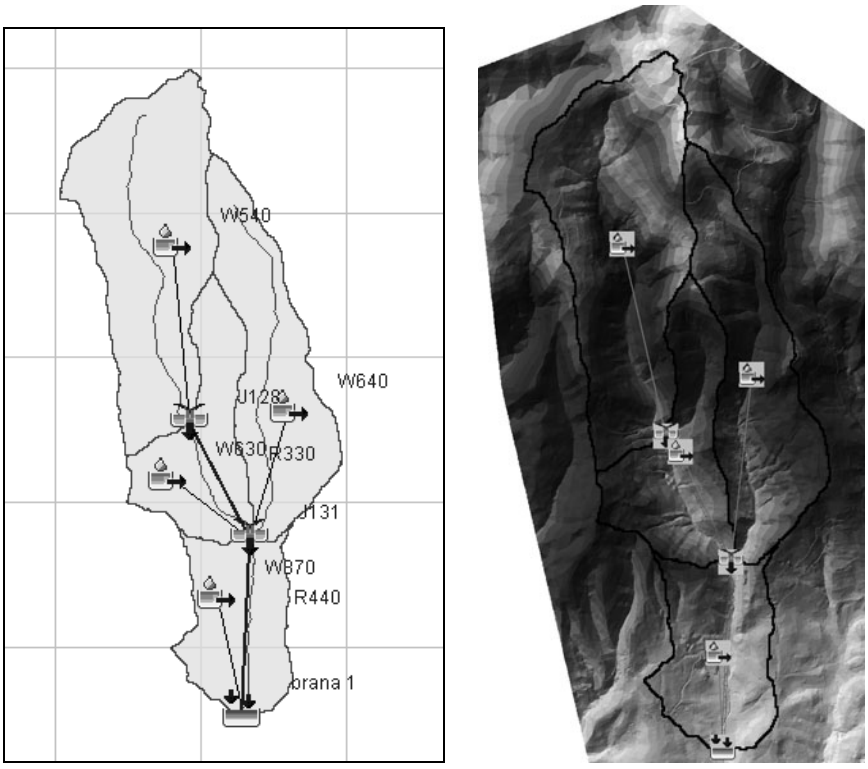

Fig. 3. HEC–HMS Basin model

17.3.1.1. Basin Model

The physical representation of a watershed is accomplished with a basin model. Hydrologic elements are connected in a dendrite network to simulate runoff processes. Available elements are: subbasin, reach, junction, reservoir, diversion, source, and sink. A GIS companion product has been developed to aid in the creation of basin models. It is called the Geospatial Hydrologic Modeling Extension (HEC–GeoHMS) and can be used to create basin models for use with the program.

17.3.2. Regional Hydrological Model

The regional hydrological model is developed inside Water Management Master Plan of Zagreb City. In the model for defining effective runoff the SCS method is applied. After that, the maximum discharge is defined using Ven Te Chow's expression [1]:

$$Q_{max}=F * i * y * K * 16.6 \ \ (m^3 s^{-1}) \tag{9}$$

F – watershed area in [km^2],
i – net precipitation intensity [mm min^{-1}],
y – climatic factor (for Zagreb area y = 1 is accepted),
K – hydrograph-peak reduction factor,
16.6 dimensional factor.

The core of this procedure is determined by factor K**.** For estimation this factor Ven Te Chow recommends the expression:

$$K = -0{,}00303 + 0{,}849\frac{t}{t_p} - 0{,}177\left(\frac{t}{t_p}\right)^2 \tag{10}$$

for $t/t_p \le 2.13$,
for $t/t_p > 2.13$ $K = 1$.

In regional model for estimation lag time t_p**,** the next expression is recommended, according to Srebrenovic [2]:

$$t_p = C \cdot \left(\frac{LU}{\sqrt{S}}\right)^{0{,}38} \text{ (hour)} \tag{11}$$

where is: $L = \sqrt{\frac{F(2-k)}{k}}$ – typical length, length of the fictive rectangle slope in km,

k – watershed concentration coefficient $k = \frac{2F}{OU}$,
U – distance of the reference profile of water channel from the watershed center [km],
O – watershed perimeter [km],
S – representative slope of the watershed [‰].

In the WMMP are performed regional analyses of parameters K and t_p. On the basis of the flood waves observed on the available water-gauge, precipitation and flow, obtained is unit hydrograph. For the every station is acquired one representative hydrograph on the basis of who is determined really are noted lag time. On the basis of this result possible defines the ratio of $K = f\,(t/t_p)$ for different durations entry precipitation for certain water-gauge. The whole area is divided in the hydrological unit which is the associated ratio of of $K = f\,(t/t_p)$.

For the defining complete hydrograph, Srebrenovic expression is recommended [2]:

$$Q_t = Q_{max}\left(\frac{t}{T_c}\right)^m e^{m\left(1-\frac{t}{T_c}\right)} \tag{12}$$

where: Q_t – discharge in time t [m^3 s^{-1}],
Q_{max} – maximum discharge [m^3 s^{-1}],
t – time [h],

$T_c = -0.5\ t_k + t_p$ time of concentration [h],
m – coefficient of shape of flood wave which calculates from the expression:

$$\gamma = 9450 * m^{-0.515}, \quad \gamma = \frac{V}{Q_{\max} T_c} \tag{13}$$

17.4. THE MODELING RESULTS

Calculation of hydrographs of high waters on small, insufficiently analyzed, mountain watershed using different methods can conclude:

- the each model necessary calibrates, and for the model of kinematic wave calibrates the overland-flow roughness coefficient (N)**.**

Result modeling is presented in Fig. 4 and 5 where can see hydrographs of high water waves calculated in two different models.

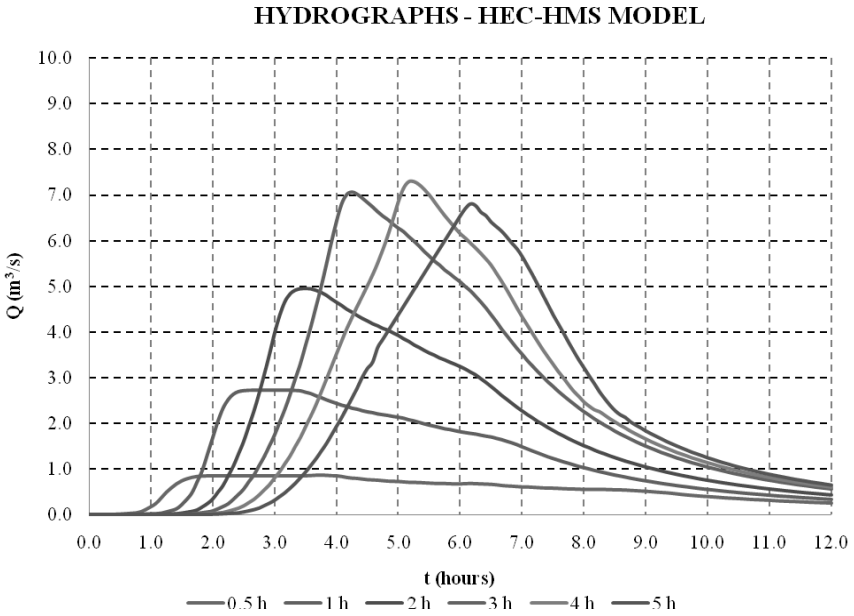

Fig. 4. Hydrographs calculated with HEC–HMS

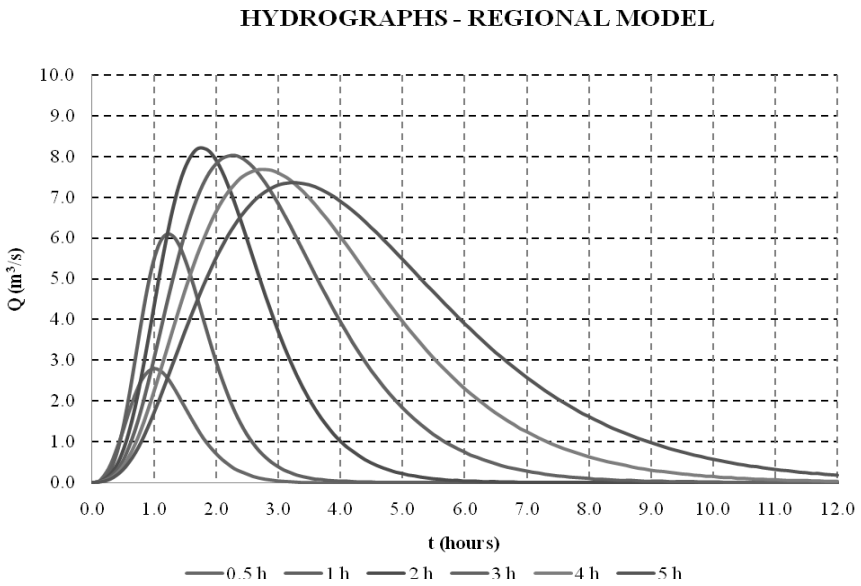

Fig. 5. Hydrographs calculated with REGIONAL MODEL

17.5. CONCLUSION

The ungauged problem is currently an area of extensive research and it can be expected that considerable progress will be made during the coming years. The complexity of the problem requires a holistic approach that can be provided only by a wide variety of hydrologists working on different topics. However, the potential value of the scientific outcome is very high. Current predictions in ungauged watersheds have to be considered as very uncertain though and must be used carefully in decisionmaking.

References

[1] Chow W. T.: Open–Channel Hydraulics. Singapore: McGraw-Hill 1986.
[2] Srebrenovic D.: Primjenjena Hidrologija. Zagreb: Tehnicka knjiga, 509 pp., 1986.
[3] Hydrologic Modeling System HEC–HMS, Technical Reference Manual, US Army Corps of Engeneering.
[4] Bonacci O., Roglic S.: Hidroloski proracun osnovne kanalske mreze za povrsinsku odvodnju; Društvo za Odvodnju i navodnjavanje Hrvatske. Zagreb: Prirucnik za hidrotehnicke melioracije, I kolo; Knjga 3, pp 63–88, 1985.
[5] Vodoprivredna osnova Zagreba – izmjene i dopune; Hrvatske vode 1992.

18 Risks of Danube Sources Exploitation in Context of Rapidly Developing Capital City and its Environment

Tóthová Katarína, Kriš Jozef (Slovak University of Technology, Faculty of Civil Engineering, Bratislava)

18.1. INTRODUCTION

The task to ensure a higher level of water supply is closely linked with issues of exploitation and protection of water sources, particularly in terms of their uneven surface distribution. Slovakia has high quality water resources of groundwater in the alluvial area of the river Danube, which has a cross-border character. These waters are used to supply a wide deficit area out of Danube basin. Bratislava Water Works, which operates on a wide territory around the capital city, executes strategically most important abstractions of drinking water from this area. Large-scale water sources of alluvial Danube area are used not only for the capital city, but they are also considered to be a possible water source which can be used in the whole region, outstretching to several districts.

18.2. ORGANIZATION OF THE WATER SECTOR IN THE SLOVAK REPUBLIC

Until 1997 the unique utility was entirely state-owned by the State Water Works Company. In 1997 the government began the process of transforming the sector from a state monopoly into municipal utility companies. However, due to a lack of leadership and because of political divisions, the process was vague and confusing and as a result only three districts obtained the control of a water utility. These districts were the Trencin district (48 municipalities), Komárno district (33 municipalities) and the city of Hlohovec. Only Trencin has chosen to delegate its water utilities to a private foreign company. After an open-call, the Lyonnaise des Eaux (nowadays SUEZ ENVIRONMENT) took over the utilities and has been operating them in a joint-stock agreement with the municipal association. By year 2000, only 736 of the 1815 municipalities had applied for the transfer of assets and only a small number had actually completed the negotiation process. In year 2000 a new government reformed the process in an attempt to add clarity and to accelerate the pace of change. It was agreed that State Water Company had to transfer its control of water utility property – free of charge – to those municipal authorities wishing to establish their own water companies. Thus, in theory, the municipal authorities were free to manage utilities in the way most suited to their area and to involve private companies. The state company was then divided into 5 regional organizations, according to the existing main water networks. Since May 2003, the new companies have been created from the split of this into more units.

Currently in Slovakia there are 14 territorially greater water groups, whose property is in the hands of municipalities. Three of them have charged with operation the private companies with external share – SUEZ ENVIRONNEMENT in Trencin and Veolia Voda in the

center of Slovakia (the Banska Bystrica district) and in the North of the country (the Poprad district). In addition to these previously mentioned large companies there are over 100 small municipality companies that operate local water supplies for small communities; usually with their own sources of water.

18.3. WATER SUPPLY IN SLOVAKIA IN FIGURES

The total number of inhabitants connected to public water supply network in SR is 86.3% of all inhabitants (in common 4.67 million inhabitants). From the 2.883 municipalities in Slovakia about 2.170 of them are connected to public water supply systems; in 110 municipalities is water supply system under construction; without the public water supply system are 710 municipalities. Without the public water supply system is mainly smaller villages with number of inhabitants 200–2.000.

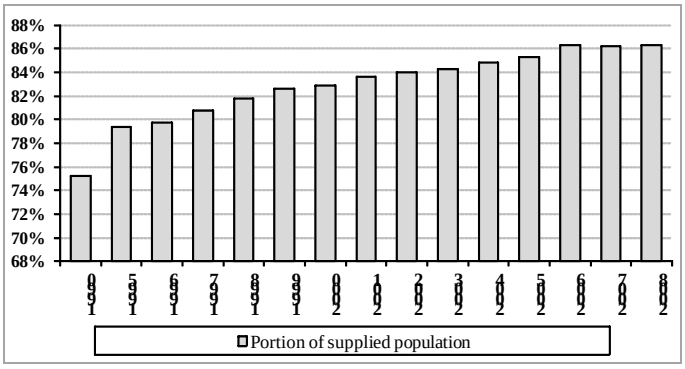

Fig. 1. Number of inhabitants supplied with drinking water from public water supply network out of total population

The volume of not invoiced water is 103.0×10^6 m^3 which is 31.8% of water intended for supply. The measures for reduction of water loss in pipes to acceptable level corresponding with European trends should be adopted and implemented.

18.4. SIGNIFICANT WATER SOURCES

Non-uniform occurrence of water in time and space in the different regions of the country has led in the past to development of large-scale water supply systems. Due to this, there are 47 regional water supply networks currently supplying some 70% of the inhabitants with good quality drinking water (i.e. 80% of all produced water in the country). Interconnections of the regional systems have resulted in the formation of supra-regional systems (long-distribution systems), such as the Western Slovakian, Central Slovakian or Eastern Slovakian Water Supply Systems, based on combined use of several large mostly ground water resources. The concept of forming supra-regional systems currently depends on and is limited by the territory of water companies.

Within the Danube bank territory, wells – as more significant water sources – are located there, which serve approximately 1 million people with high – quality drinking water. The largest quantities available are associated with the mesozoic and quaternary hydrogeological structures or zones. Absolutely the greatest amount (24.8 $m^3 s^{-1}$) regarding the quality of groundwater documented in Europe is found in a unique structure of Danube Plain Žitný ostrov (Rye Island), represented by a powerful Pliocene-Quaternary formations of gravel and sand, where the largest withdrawals for drinking water are registered. The water from this region supplies the population through a large-scale pipeline up to central and west Slovakia. Žitný ostrov is the biggest river island in Europe located between the river Danube and Danube's left arms; as these are marked as the most fertile grounds in the region of Slovakia and the island is the biggest reservoir of high quality drinking water in central Europe. BVS Water Company, as well as The West Slovak Water Company use Žitny ostrov water sources and Water Company of the city of Komárno uses another significant Danube water source in addition to those, as well.

Recently, water sources especially for the city of Bratislava and its wide surroundings are being strategically discussed, as conceptually large water systems should be formed. Various reports on investment interests in protected areas of water resources, which could mean a real risk of deterioration of water resources, are a reason for recent professional and political discussions.

18.5. WATER SOURCES AND RISKS OF THEIR FUTURE EXPLOITATION

Strategic point of water supply in the region is the question of future use of water sources. Climate changes, environmental and economical pressures lead towards increased use of large-scale resources of Žitný Ostrov in the City of Bratislava (Sihoť, Sedlacek Ostrov, Pečniansky les, Rusovce-ROL) or in its immediate surroundings (Šamorín, Kalinkovo). These significant water sources consist of dozens of wells with high quality water, which don't need any other treatment except for the hygienic security treatment. This water is prospectively determined for long water transport to deficient areas located over 100 km from sources.

Main water sources of a large currently-forming water system are becoming water sources listed in Table 1, where the minimum capacity of source means limited capacity as of high or low water levels of Danube and groundwater subsequently affected by the river Danube. Maximum capacity of water source is considered in two ways (Tables 1 and 2):

— maximum capacity limited by technical equipment and water resources state;
— maximum capacity limited by hydrogeological area water source options.

Calculations for future water supply demand for was carried out and the usage of given water sources was determined. Proposals for the years 2010, 2020 and 2030 are summarized in Table 2.

The proposal for future water balance usage of sources summarized in Table 1 are closer to the real maximum use of all water sources because of safety representation of each water source for respective critical states. There are indications that current natural and anthropogenic activities in the Danube alluvial zone and the water quality in river may affect the quality of just about any water source.

Table 1

Proposals for the use of Bratislava water sources

Water source WS	Source capacity [l s^{-1}]			2006	2010	2020	2030
				use of WS			
	min	max*)	max**)	[l s^{-1}]	[l s^{-1}]	[l s^{-1}]	[l s^{-1}]
WS Sihoť	300	700	700	561	700	700	700
WS Sedláčkov Ostrov	0	90.5	90.5	12.1	6	7	8
WS Pečnian. Les	300	600	900	358.5	400	600	600
WS ROL	1400	2650	2650	567.6	1400	2000	2000
WS Kalinkovo	70	70	850	53.4	70	70	70
WS Šamorin	600	970	1210	212.7	600	970	1210
Total [l/s]	2670	5081	6401	1765	3176	4347	4588
			Water demand 2030:	1771	2036	2543	3272

*) maximum capacity is limited by technical equipment and water resources` state. This value represents a really achievable capacity confirmed by an official approval and achievable under existing technical construction, considering small interventions into the existing situation, modernization or technological supplement,

**) maximum capacity is limited by hydro-geological area water-source options. To ensure this capacity, a greater investment to modification of constructions (new wells or their equipment, or reconstruction of wells) is required

Table 2 shows that all of the Bratislava water sources and surrounding water sources are strategically necessary to be maintained so that they can be used for maximum capacity. Due to emergency backup and strategic functions of water sources they have to be maintained also at the time they are not utilized in order to ensure achievement of their maximum capacity.

Petroleum Pipeline Topic

In relation to Danube water sources the topic of petroleum pipeline that would pass through Žitný ostrov and should supply the Austrian oil refinery is discussed. The government was already considering this proposal of the Ministry of Economy to connect Slovakia and Austria by such a pipeline, or Transpetrol company with OMV in 2005. The Ministry of Environment did not recommend the construction of such a pipeline in 2005, as technical measures, which would completely eliminate the risk of oil spills to the groundwater in the protected water area of Žitný ostrov and Danube water were not satisfactorily met. Currently, it seems that this topic is still alive. Responsible government representatives have been talking about 100% security against leakage of the oil into groundwater, but a disaster can never be avoided with 100% certainty. Penetration of oil into the water sources would cause a catastrophe which could take nature decades to bounce back. In addition, drinking water supply would collapse, and the demands of inhabitants of Bratislava and its surroundings would have to be satisfied by water from cisterns that would bring water from great distances.

Table 2

The combination of water sources´ representation

Water source WS	Source capacity [l s^{-1}]			Critical combination of water sources condition			
				1	2	3	4
	min	max*)	max**)	[l s^{-1}]	[l s^{-1}]	[l s^{-1}]	[l s^{-1}]
WS Sihoť	300	700	700	300	700	700	700
WS Sedláčkov Ostrov	0	90,5	90,5	0	85	700	700
WS Pečnian. Les	300	600	900	300	600	85	85
WS ROL	1400	2650	2650	2000	1400	600	600
WS Kalinkovo	70	70	850	70	70	2000	0
WS Šamorin	600	970	1210	1210	600	70	70
Total [l/s]	2670	5081	6401	3880	3455	0	1210
Water demand 2030:				4588	4588	4588	4588

*), **) – see description below the Table 1.
1 – limiting capacity of water sources Sihoť, Sedlacek ostrov and Pečniansky les during high or low water levels in the Danube. Listed water sources are located above the Danube dam and therefore they are limited in an equal scope at the same time, assuming that other water sources will not be limited by the river Danube conditions within the same time period;
2 – achieving the minimum capacity of water sources under the Danube dam ROL, Kalinkovo, Šamorín;
3 – failure of the Šamorín water source;
4 – failure of the ROL water source.

Bratislava already has such a bitter experience in its past. Oil spilt from Bratislava refinery in 1971 caused an irreversible deterioration of ground water source quality in Podunajske Biskupice, which was used to supply the eastern part of Bratislava by drinking water. The water source built in 1966, with capacity of 1200 l s^{-1}, had to be closed down after 6 years. Permanent disposal of this water source meant shutdown nearly 95 thousand people of drinking water. It took almost a year before residents of east city could again use water from public water supply system. One year after this collapse 2 new water sources in Kalinkovo and later also in Šamorin were readily put into operation and a new connecting pipeline of 800 mm profile with the length of more than 15 km was built. Because the oil spill in the underground was spreading south, towards the area of Žitný Ostrov, dynamic water wall had to be built in order to stop it. This wall consists of 21 wells and more than 600 observation objects that are continuously monitored by a dispatching center. In present, respective wells pump 1 000 l s^{-1} of water. Its role is to prevent oil pollution transport and this function must be preserved, even after any termination of production at the Slovnaft refinery.

Danube water dams topic

A water dam on the river Danube located in profile above the city could cause fundamental changes in the evolution of quality parameters, particularly of groundwater sources in the territory of Bratislava. Since the implementation of Wolfsthal water dam on the Aus-

trian side of the river was refused by the Austrian government, there have been on-going discussions regarding building a replacement water work in the river profile at the water source Pečniansky Les. Arguments in favour of such building include talks about deepening of the Danube riverbed and ensuring the fairway, which is threatened by fouling. On the other hand, there are serious concerns about the negative effects imposed on the water source of Pečniansky Les. This water source is irreplaceable for the city not only due to its excellent quality but also for its core position in relation to the consumption area.

18.6. CONCLUSION

Increasing of water supply level and its quality are the ultimate goals of the Slovak Republic after its accession into the Euro Zone. As for the uneven distribution of water sources; the task of to increasing the share of public water can be solved only by a comprehensive review of the utilization of matching sources´ capacity. On one hand the issues of securing the quantity of water sources are addressed preferentially. On the other hand the security of water supply, including the risk of covering the future needs is often neglected. The Bratislava example of usage and potential impact of a depreciation of any strategic water resources of Žitný Ostrov – the largest reservoir of drinking water in Central Europe – is specifically used to visualize the seriousness of a problem in this strategic region. Experience from the water source collapse clearly supports the fact that contamination of water resources is irreversible. The Danube region, which is under the operation of BVS, is moving towards large developments despite the current economic crisis and it seems that the development shall not stop in the near future. The potential of large-scale water resources of the Danube basin in Žitný Ostrov is therefore strategically important for the future. The reserves in the water sources´ balance – as of the optimistic variant of an increased supply connection and future water demand are minimal, and as it can be seen from the above-mentioned factors, a failure of any of these strategic sources could mean a serious threat to coverage of our future needs.

References

[1] Ministry of the Environment of the Slovak Republic. Report: State of the Environment Report Slovak Republic 2008.
[2] BVS a.s. ANNUAL REPORT 2009, www.bvsas.sk.
[3] VUVH Bratislava: What we know about drinking water in the Slovak Republic. www.vuvh.sk.
[4] Tóthová K. Analyze of processes and elements of water supply systems BVS. Study BVS, 2007.

Acknowledgement

The article has been supported by project „Operational Programme Research and Development – Excellence Centre of Integral Territory Flood Protection (Centrum excelentnosti integrálnej protipovodňovej ochrany územia)", code ITMS 26240120004 dealt with at the Department of Sanitary and Environmental Engineering, Faculty of Civil Engineering, Slovak University of Technology in Bratislava.

This work was supported by Science and Technology Assistance Agency under the contract no. APVT-20-031804.

WYDAWNICTWO POLITECHNIKI GDAŃSKIEJ

Wydanie I. Ark. wyd. 10,5, ark. druku 10,5, 105/665

Druk i oprawa: *EXPOL* P. Rybiński, J. Dąbek, Sp. Jawna
ul. Brzeska 4, 87-800 Włocławek, tel. 54 232 37 23